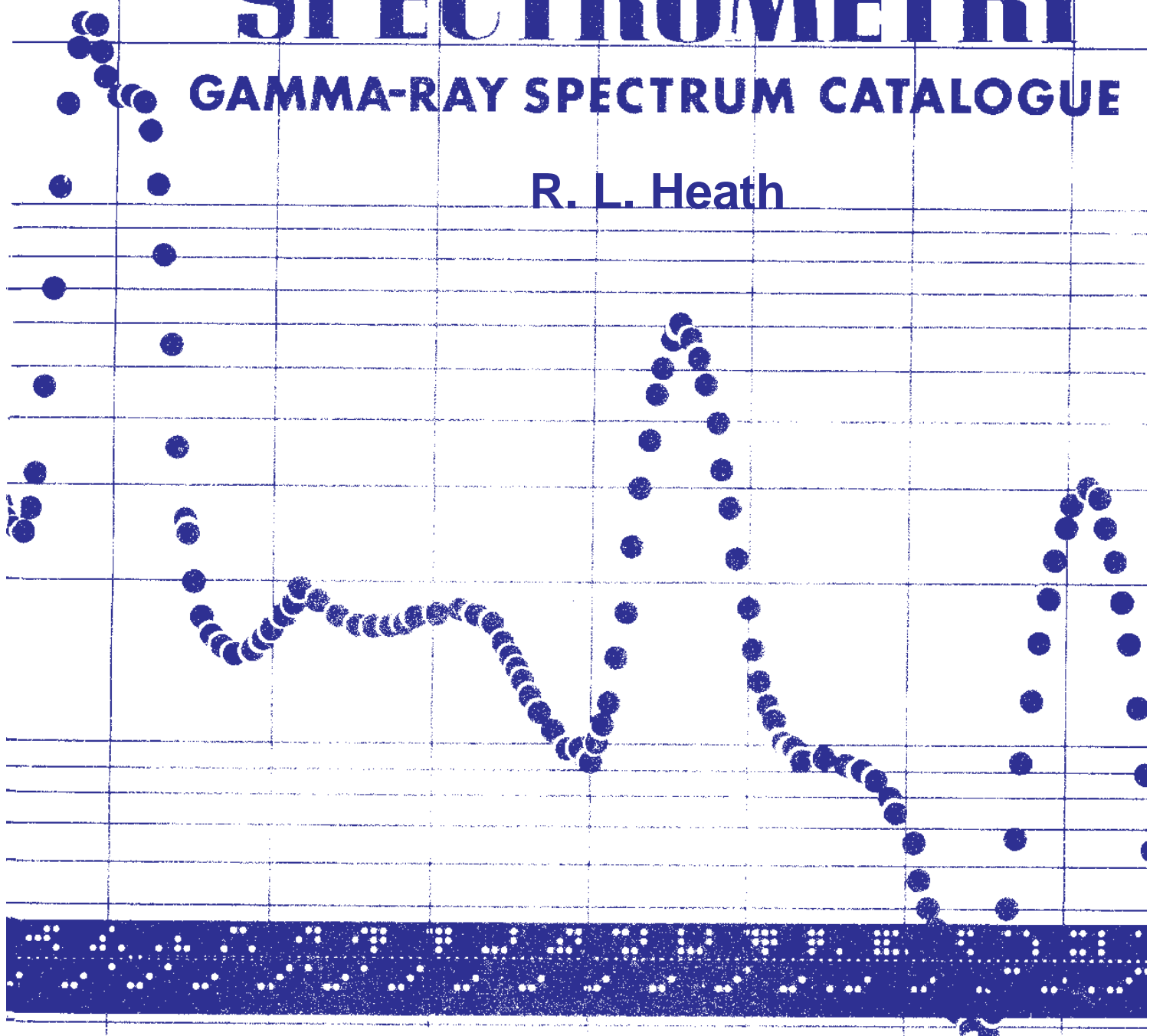


Reissue of IDO-16880
2nd Edition - Vol. 1 (Rev.)
Tutorial Text

SCINTILLATION SPECTROMETRY

GAMMA-RAY SPECTRUM CATALOGUE

R. L. Heath



REVISED EDITION OF REPORT IDO - 16880 - 1
ORIGINAL ISSUED: AUGUST 1964
REV. ELECTRONIC UPDATE:: FEBRUARY 1997

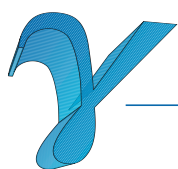
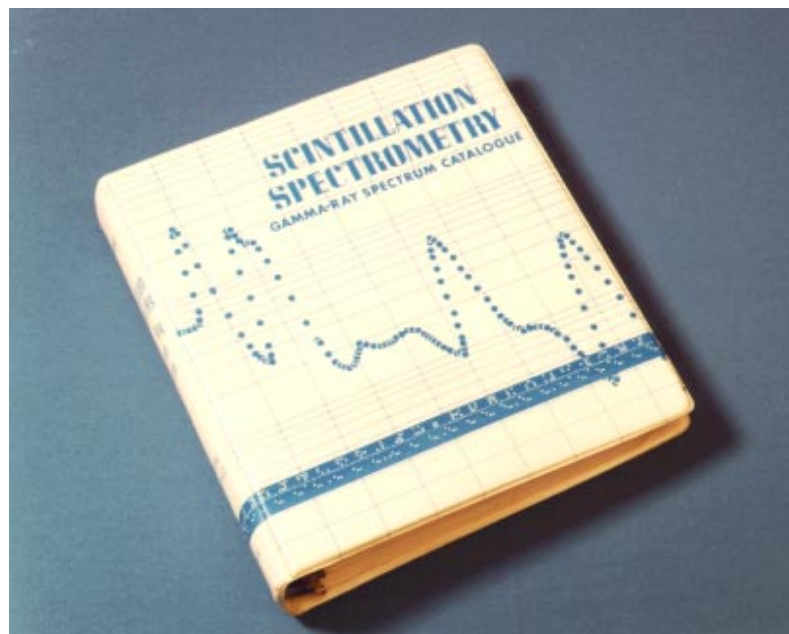
SCINTILLATION SPECTROMETRY

GAMMA-RAY SPECTRUM CATALOGUE

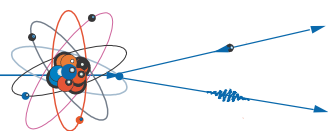
NEW VERSION OF 2ND EDITION
COMPILATION OF GAMMA-RAY SPECTRA
AND RELATED NUCLEAR DECAY DATA
VOLUME 1 OF 2

BY

R. L. HEATH



-RAY SPECTROMETRY CENTER
Idaho National Engineering & Environmental Laboratory



CONTENTS

Volume I

I.	Acknowledgement	2
II.	Introduction	3
III.	Detector Response	4
	A. Interaction of Gamma Rays with Matter	4
	1. Photoelectric Effect	4
	2. Compton Scattering	4
	3. Pair Production	4
	B. The Pulse-height Spectrum	6
	1. Spectrum Shape vs Gamma-ray Energy	6
	2. Variation in Spectrum with Detector Size	7
	3. Detector Resolution	8
IV.	Effects Due to Reactor Environment	11
	A. X-ray Escape	11
	B. Scattering from Surrounding Material	11
	1. Backscatter Spectrum	13
	2. X-ray Production in Shield	14
	C. Effect of Beta Absorber	14
	D. Annihilation Radiation	16
V.	Summation Effects	17
	A. Coincidence Sum Spectrum	17
	1. Coincident Gamma Rays	17
	2. Annihilation Radiation	18
	B. Random Sum Spectrum	18
VI.	Bremsstrahlung	19
VII.	Quantitative Analysis of Scintillation Gamma-ray Spectra	20
	A. Detector Efficiency	2
	B. Concept of Photopeak Efficiency	20
	1. Peak-to-Total Ratio	22
	2. Absolute Emission Rate Determination	22
VIII.	Experimental Measurements	26
	A. Laboratory Scintillation Spectrometer	26
	1. Detector	26
	2. Detector Shield	29
	3. Electronics	29
	4. Source Preparation	29
	5. Data Preparation	31



CONTENTS (Cont.)

B. Energy Calibration	32
1. Zero Convention for Pulse height Scale	32
2. Non-linear Energy Response of NaI	33
3. Method for Energy,Pulse-height Calibration	34
4. Gain Shift Program	34
IX. Computer Techniques for Data Analysis.....	35
A.Computer Program for Generation of Detector Responce to Monoenergetic Gamma Rays	35
B. Sum Spectrum Program	38
C. Linear Least-squares Program	39

Appendices

I. Index of Gamma Rays Ordered by Z, A, Photon Energy, Method of Production, and Half-Life	
II. Intrinsic Efficiencies for NaI Detectors	
III. Photopeak Efficiency and Other Data for Analysis of Gamma-ray Spectra	
IV. Numerical Data Used in Compilation of Gamma-ray Spectra	

TABLES

1. Measured Values of dL/dE as a Function of Gamma-ray Energy	34
11. Table of Energy Calibration Sources	34

FIGURES

Fig. I - Absorption coefficient for NaI(Tl) as a function of gamma-ray energy. Results using the total absorption cross section and the total minus coherent scattering are shown for comparison	5
Fig. 2 - Theoretical electron energy distribution (single events) for Compton and photoelectric interaction in a NaI detector compared with an experimental pulse-height distribution obtained on a 3" x 3" NaIDetector (0.50 MeV)	6
Fig. 3 - Pulse-height distributions obtained with a 3" x 3" NaI scintillation detector .. from monoenergetic gamma ray sources of 0.060, 0.32, 0.83, and 1.92 MeV. Pertinent features of these spectra are noted	7
Fig. 4 - Comparison of pulse,heiheight spectra of Cs ¹³⁷ obtained with different sized NaI detectors. All spectra are normalized in gain and area of photopeak	8
Fig. 5 - Effect of detector resolution on pulse-height spectrum.....	8
Fig. 6 - Plot of detector resolution (FWHM) as a function of gamma- ray energy for detectors used to measure catalogue spectra	9
Fig. 7 -Illustration representing a NaI scintillation detector showing sequence of events producing output from electron multiplier and various processes which contribute to response of detector to a gamma-ray source	10

FIGURES (Cont.)

- Fig. 8 - Pulse-height spectrum of 0.068-MeV gamma ray emitted in the decay of 3.3-hr Co⁶¹ illustrating iodine K -x-ray escape phenomena 11
- Fig. 9 - Probability for escape of the iodine K x-ray following photo-electric interaction in a 3" x 3" NaI detector. Data are plotted as the fraction of the total photo electric response to a pointsource at 10 cm as a function of gamma,ray energy. Shown for comparison is the calculated escape fraction for a ll/z" x I" detector in a similar geometry 12
- Fig. 10 The pulse-height spectrum representing the response of a 3" x 3" NaI detector to the 0.478-MeV gamma ray emitted in the decay of Be⁷. The contribution to the spectrum from photons scattered from the shield and beta absorber are shown together with the random summation spectrum. 13
- Fig. 11 - The energy of Compton scattered photons as a function of scattering angle for various primary gamma-ray energies 13
- Fig. 12 - Detector shield configurations used to demonstrate effect of Compton scattering of response of detector to monoenergetic gamma radiation 14
- Fig. 13 - Effect of detector shield configuration on scattered component of pulse-height spectrum obtained from monoenergetic source 14
- Fig. 14 - Illustration showing the effect of Pb x-rays produced by photo-electric interaction in the shield and the use of critical absorption techniques in "arading" shield to reduce this effect 15
- Fig. 15 - Effect of beta absorber on observed spectrum and use of absorber cap over detector to reduce beta rays scattered into side of detector 15
- Fig. 16 - Standard laboratory source mounting geometry 15
- Fig. 17 - Illustration showing absorber cap over detector used to prevent scatter of electrons into side of detector 16
- Fig. 18 - Effect of absorber thickness on monoenergetic response of detector 16
- Fig. 19 - Spectrum of Nb⁹⁴ showing coincidence sum spectrum and effect of source-detector geometry on intensity of sum spectrum 17
- Fig. 20 - Pulse-height spectrum of 3.08-hr Ti⁴⁵ showing coincidence summing of annihilation radiation with 180°-scattered photons from the other annihilation quantum 17
- Fig. 21 - Illustration of the effect of superposition of two pulses within the sampling time of the analogue-to-digital converter. Variations in overlap will result in smearing of the random coincidence summation spectrum 18
- Fig. 22 - Intensity of random sum spectrum vs source intensity 19
- Fig. 23 - Typical bremsstrahlung spectra on 3" x 3" NaI detector. All spectra are normalized in intensity to 10⁷ disintegrations 19
- Fig. 24 - Pulse-height spectrum of radiations emitted by source of 58-day Y⁹¹ showing contribution to spectrum from bremsstrahlung continuum 20
- Fig. 25 - Expression for calculation of detector efficiency for point source of radiation and cylindrical detector 21

FIGURES (Cont.)

Fig. 26 - Expression for calculation of detector efficiency for disk source of radiation and cylindrical detector	21
Fig. 27 - Error in detection efficiency vs error in absorption coefficient for 3" x 1/4" NaI detector (h = 10 cm)	22
Fig. 28 - Error in detection efficiency vs error in absorption coefficient for 3" x 3" NaI detector (h = 10 cm)	22
Fig. 29 - Detection efficiency for a 3" x 3" detector (662 keV) as a function of source radius and distance from the detector.	22
Fig. 30 - Illustration of Peak-to-Total Ratio concept for NaI pulse-height spectrum	23
Fig. 33 - Gaussian fit to experimental photopeak of Cs ¹³⁷ (0.662 MeV) showing deviation from functional form	25
Fig. 34 - Variation of the experimental parameter α_1 with gamma-ray energy for the 10 keV/channel gain scale	25
Fig. 35 - Variation of the experimental parameter α_1 with gamma-ray energy for the 5 keV/channel gain scale	25
Fig. 36 - Variation of the experimental parameter α_2 with gamma-ray energy for both the 5 and 10 keV/channel gain scales	26
Fig. 31 - Peak-to-total ratio for a 3" x 3" NaI detector	23
Fig. 32 - Results of experimental determination of photopeak attenuation for Be beta absorbers. These measurements were made for point sources of radiation at 10 cm distance from the detector. Absorbers positioned on top of cylindrical detector	24
 Fig. 37 - Least-squares polynomial fit to experimental values for EpA for 3"x3" NaI detector	27
Fig. 38 - Laboratory scintillation detector packaged in 0.005" Al can.	28
Fig. 39 - Typical commercial scintillation detector (3" x 3") showing details of packaging technique. The increased mass of material used in the packaging of these .. detectors will produce some distortion of the spectrum due to scattering .	28
Fig. 40 - X-ray photograph of commercial 3" x 3" Nal detector illustrating method used to locate position of crystal inside container. Recently, manufacturers have taken steps to provide this information with each detector	28
Fig. 41 - Photograph of standard laboratory detector showing source holder used to .. minimize scattering geometry	28
Fig. 42 - Standard laboratory detector shield used for experimental measurement of all spectra in the Spectrum Catalogue	29
Fig. 43 - Output waveform from double-differentiated linear pulse	29
Fig. 44 - Photograph of one of the scintillation spectrometers used to obtain data for the Spectrum Catalogue.	30
Fig. 45 - Examples of source mounti ig arrangements used	30
Fig. 46 - Effect of scattering from source mount and source holder	31
Fig. 47 - Punched-card format for all computer data processing programs	32

FIGURES (Cont.)

Fig. 48 - 8-level perforated tape code used at this laboratory. This code is one of the standard IBM codes with odd parity in the 5th level. All spectra in the Catalogue are on file in this format	32
Fig. 49 - Histogram of pulse-height scale illustrating procedure for establishing zero position of pulse analyzer	33
 Fig. 50 - Pulse@height vs gamma-ray energy response of 3" x 3" NaI detector.. To correspond with the energy scale adopted, all data are normalized to unit light output at 0.66162 MeV (Cs^{137})	33
Fig. 51 - Example of energy calibration procedure using Cs^{137} gamma ray. Data were taken on a gain scale approximating 5 keV/channel. Peak channel positions indicated are result of least-squares fit of modified gaussian shape to each photo-line. Figure shows calibration of Lu^{177} peaks due to 0.11297, and 0.20836-MeV gamma rays	34
Fig. 52 - Illustration of results of gain shifting program. Closed circles represent Cs^{137} spectrum on 5 keV/channel gain scale. Open circles show spectrum taken on 10 keV/channel gain scale shifted by a factor of two to match 5 keV experimental shape -	35
Fig. 53 - The response of a 3"x3" NaI detector to monoenergetic gamma rays from 0.335 to 2.75 MeV. All spectra are for a point source mounted 10 cm from the detector and have been normalized in intensity to 10^7 photons emitted from the source.	36
Fig. 54 - Three-dimensional model of the response of a 3"x3" NaI detector to monoenergetic gamma radiation. This model illustrates the interpolation scheme used to obtain the energy response of a given detector	37
Fig. 55 - Comparison of computed detector response to experimental spectrum (0.335 MeV)	38
Fig. 56 - Comparison of computed detector response to experimental spectrum (1.114 MeV)	38
Fig. 57 - Comparison of the experimental spectrum obtained from a source of 42-day Pm^{148} on a 3" x 3" detector with a spectrum calculated using the computer programs described for the generation of gamma-ray shapes, summation spectra, and a knowledge of the decay scheme of this nuclide	40
Fig. 58 - Example of least-squares analysis of a five-component pulse-height spectrum containing ten gamma rays. Residuals are shown for each channel	41
Fig. 59 - Results of least-squares analysis of Nb^{94} spectrum. The Analysis used calculated shapes for the two gamma rays and the coincidence sum spectrum. The residuals are shown plotted at the bottom of the figure	41

Volume II

Master Index of Gamma-ray Spectra

Compilation of Gamma-ray Spectra

ABSTRACT

This is a new electronic format edition of the Scintillation Spectrometry Gamma-ray Spectrum Catalogue. This edition is a revision of the original data compilation, which was issued as an AEC R & D Report (IDO-16880) in 1964. As in the original catalogue, this edition contains a collection of spectra representing the response of a scintillation spectrometer to individual radioactive nuclides. In addition to the graphs representing the response of a 3"x 3" NaI detector in a standard geometrical arrangement, current nuclear data are presented which are based on the 1996 ENSDF data file. Each spectrum is accompanied by a decay scheme and a listing of gamma ray energies and intensities currently associated with the decay of that nuclide.

The original version of the 2nd edition was prepared in two loose-leaf volumes and containing data for almost 300 isotopes. All spectra are normalized to a standard set of gain scales and a text is presented which describes the fundamentals of gamma-ray spectrometry. This includes a discussion of spectrometer design, electronics, instrumental calibration, and data processing as it was practiced at the time this version was published..

To facilitate the use of these data, tables of detector efficiency, photopeak efficiency, and other information useful for quantitative data analysis have been included. An extensive index has also been added with separate tables of data listed according to gamma-ray energy, half-life, method of source production, and other specialized categories.

I - ACKNOWLEDGEMENT

The development of techniques and the collection and preparation of all data presented in the Second Edition of the Scintillation Spectrometry Gamma-ray Spectrum Catalogue represent the combined efforts of many people on the laboratory staff. The preparation of this Edition and the original Catalogue has been a part of the program of Radioactivity and level schemes studies supported by the Reactor Development Division of the U. S. Atomic Energy Commission. Work necessary to extend the new Edition to include spectra of accelerator, produced neutron-deficient isotopes was supported by the Division of Isotopes Development.

Experimental Measurements

Radioactivity and Decay Schemes Group

C. W. Reich	G. O. English
J. E. Cline	C. H. Hogg
R. G. Helmer	L. D. Weber
W. W. Black	D. F. Crouch
L. D. McIsaac	E. L. Murri

Source Preparation and Chemistry

L. D. McIsaac	R. P. Schuman
S. D. Reeder	A. L. Erickson
E. H. Turk	W. J. Maeck
S. F. Marsh	

The author acknowledges with pleasure the support of the individuals listed below who have contributed the very complex task of preparing data for a compilation of this magnitude. Each individual spectrum is the result of considerable experimental effort in many areas. Among these are source preparation, chemical purification, calibration and maintenance of equipment, experimental measurements, data reduction, and graphic arts. Without the cooperation and understanding of specialists in these fields it would not have been possible to produce the uniformity and quality of the data which have been obtained.

Data Reduction and Preparation of Manuscript

Patricia Chase	Carol Ball
----------------	------------

Computer Services and Programming

L.A. Schmittroth	G. A. Cazier
D. D. Metcalf	G. A. Jayne

Statistical Drafting and Graphic Arts

D. W. Elison	D. V. Jenson
G. Hammer	M. Wheelwright,
L. Peterson	Wheelwright Lithographing Co.
G. Bybee	

The program to develop and produce the new editions of the Spectrum Catalogues in electronic format was established at the INEL in 1995. Major contributors to this effort include R. G. Helmer, J. R. Davidson, and R. J. Gehrke. This Program is currently supported by the Office of Science and Technology, Office of Environmental Management and the Division of Nuclear Physics, Office of High Energy and Nuclear Physics, U.S. Department of Energy under DOE Idaho Operations Contract DE-AC07-94ID13223 with Lockheed-Martin Idaho Technologies Co.

II. INTRODUCTION

Since the publication of the original edition of the Gamma-ray Spectrum Catalogue, the experimental techniques and electronic apparatus have undergone a significant improvement. To a great extent this has been the result of the use of solid-state circuitry in the design of more reliable and versatile multichannel pulse height analyzers. The improved stability and linearity of equipment now available has made possible the application of more sophisticated methods to the analysis of data using digital computers.

In view of the expanded application of nuclear spectrometry and the acceptance of the original version of the spectrum catalogue as a useful laboratory reference, it was felt that there would be a need for additional information of this type. The second edition of the catalogue, which has been in preparation for the past three years, is offered as an aid to the experimentalist for the application of the NaI scintillation detector as a gamma-ray spectrometer. The new edition has been completely revised. With few exceptions, all spectra included in the compilation were prepared from new data, using improved equipment, experimental techniques, and methods of data presentation and analysis. Because of the increased use of neutron, deficient nuclides, this addition has been expanded to include a large number of these isotopes. In addition, a number of isotopes produced by (n,p), (n, α), and double neutron capture reactions have been included.

Beginning with the publication of this edition, supplementary material will be made available. To obtain this material as it becomes available, the user should address a request to the author at the address shown below. It should be noted that the spectra included in the first printing of the new edition are only a small fraction of the total number presently on file. Spectra are available of many nuclides measured using detectors of various size, resolution, and source-detector geometry. In the interest of promoting a standard detector geometry for laboratory use, these spectra were not included in the catalogue but are available on special request. The data collection also includes spectra of gross fission products as a function of decay time, spectra of neutron-irradiated chemical elements, and gamma-ray spectra of isotopes measured using germanium semi-conductor detectors.

1. R. L. Heath, AEC Report, IDO-16408 (1958).

To make the catalogue more useful as a laboratory tool, special loose-leaf binders are available which permit the removal of individual spectra for use in the interpretation of data. If these binders are desired, arrangements have been made to purchase them from the supplier. Included with the binders are index tabs and page lifters to make the catalogue more durable.

A brief description of the important considerations in the use of the scintillation spectrometer for the quantitative and qualitative measurement of gamma-ray spectra is given in the following sections. This includes a discussion of the factors which influence detector response, the experimental techniques used in the compilation of gamma ray spectra for the catalogue, and recently developed computer techniques for analysis of gamma-ray spectra.

The text is intended to be a summary of the current state-of-the-art in experimental techniques developed for the application of the scintillation spectrometer to quantitative gamma-ray spectrometry. Numerical tables of detector efficiency, photpeak efficiency, and other experimental variables are presented as appendices. The numerical data used to prepare the graphs of all gamma-ray spectra are also included to permit the user to prepare reference libraries of spectra on perforated tape, punched cards, or magnetic tape for use with pulse analyzers equipped with digital read-in devices. Spectra in this form can be very useful in the interpretation of data by visual comparison and simple subtraction procedures using arithmetic circuitry provided as a feature on many modern pulse-height analyzers.

It is the sincere desire of the author that this compilation will be a useful laboratory reference. Suggestions for improvement of the data collection are invited.

All inquiries concerning the catalogue or the additional services listed above should be directed to:

Gamma-ray Spectrometry Center
Idaho National Engineering Laboratory
P. O. Box 1625
Idaho Falls, Idaho 83415-2211

ATTN: R. L. Heath

III. DETECTOR RESPONSE

A. Interaction of Gamma Rays with Matter

A knowledge of the basic processes by which a photon interacts with matter is essential to an understanding of the response of a scintillation detector. Although many processes are involved in the chain of events which produce an electrical impulse at the output of the electron multiplier, the major features of the differential pulseheight spectrum resulting from the detection of gamma rays may be interpreted in terms of the basic interactions which occur within the detector. There are three main processes, all continuous functions of photon energy, by which photons may interact with matter giving up all or part of their energy in single events. These are (1) the photoelectric effect, (2) Compton scattering by electrons in the atoms of the material, and (3) the production of a positron-electron pair in the electric field of an atom. Although a detailed treatment of these processes is beyond the scope of this work, a brief discussion of the characteristics essential to an understanding of the response of a NaI scintillation detector is included in this section.

Before proceeding with this discussion it should be stated that a review of the theory of inorganic scintillators will not be included. For this, the reader is referred to the early work of Hofstadter² and to the extensive publications of Van Sciver^{3,4,5}, who has been responsible for much of the fundamental work on NaI. For a detailed presentation of the present state of the theory of scintillators, an excellent review of this subject has been published by Murray.⁶

1. Photoelectric Effect

In the photoelectric process all of the energy of the incident photon is absorbed by a bound electron of an atom, appearing as kinetic energy of this electron as it is ejected from the atom. The energy of the ejected electron will then be equal to the difference between the energy of the incident photon and the binding energy of the shell from which the electron was ejected. Although some energy is absorbed by recoil of the nucleus of the atom, this is negligible compared with the energy of the gamma ray and photoelectron. If the incident gamma-ray photon exceeds the binding energy of the K shell, interaction will be principally with electrons in that shell of the atom. As a result of this process the atom is left with a vacancy in the shell from which the electron was ejected, resulting in the emission of x-rays or Auger electrons. This series of events occurs within a time short relative to other time-dependent processes in a scintillator. The result is that the x-rays from the initial photoelectric event are generally absorbed by a second photoelectric event and the total energy of the incident photon is absorbed within the detector. The important characteristic of the photoelectric effect in a scintillation detector is that monoenergetic photons which interact by the photo process

² R. Hofstadter and J. A. McIntyre, Phys. Rev., 78, 619 (1950), also 74, IOC (1948).

³ W. J. Van Sciver and R. Hofstadter, Phys. Rev., 87, 522 (1952).

⁴ W. J. Van Sciver, HEPL Report No. 38, Stanford University (1955).

⁵ W. J. Van Sciver and L. Bogart, IRE Trans. Nuclear Sci., NS-5, 90 (1958).

⁶ R. B. Murray, Nuclear Instruments and their Uses, Chap. 2, A. H. Snell, Ed..., (Wiley, New York, 1962).

will produce a monoenergetic electron energy distribution within the volume of the detector. If this were the only process for energy loss, the response of a detector capable of indicating the energy of these individual photoelectrons, would be quite simple.

2. Compton Scattering

In the Compton process incident photons are scattered by the electrons with a partial energy loss. In this process scattering generally occurs with electrons that are considered essentially free and the energy of the incoming photon is shared between the electron and the scattered quantum. At low energies a gamma ray may be scattered from a bound electron with the atom remaining in its initial state. In this case there is negligible energy loss and only a change in direction. Since this process does not result in an energy change it is an important consideration in the calculation of the efficiency of a detector. The cross section for this process (Coherent Scattering) must not be included since events of this type leave no energy in the detector.

In the Compton process the energy of the scattered photon and electron are given by the following relationships:

$$E_{\gamma} = \frac{E_{\gamma}}{1 + E_o(1 - \cos \theta)} \quad (1)$$

$$E_e = E_{\gamma} - \frac{E_{\gamma}}{1 + E_o(1 - \cos \theta)} \quad (2)$$

where E_{γ} is the incident gamma-ray energy, E_e is the scattered electron energy, E_o is E_{γ}/mc^2 and ϕ is the angle between the direction of the primary and scattered photons. From these relationships it may be deduced that a Compton electron energy spectrum will result which extends from zero energy ($\theta=0^\circ$) up to a maximum energy ($\theta=180^\circ$) which is somewhat less than the energy of the incident photon. The energy of the scattered photon then extends from the original photon energy down to a minimum value which is always less than $m_q c^2/2$ (0.257 MeV). Fig. 2 shows a Compton electron energy distribution obtained by integrating the differential scattering cross section over all angles from a primary photon energy of 0.5 MeV. A monoenergetic source of gamma radiation will produce such an energy distribution of electrons as a result of interaction by the Compton process.

3. Pair Production

If the incident photon has an energy in excess of the rest mass of a positron-electron pair (1.02 MeV) then pair production is possible. In this process, which occurs in the presence of the Coulomb field of a nucleus, the gamma ray disappears and a positron-electron pair is created. The total energy of the pair of particles will be equal to the energy of the primary photon and their kinetic energy will be equal to the total energy minus the rest energy of the two particles ($2mc^2$). Since the positron is unstable, as it comes to rest in the field of an electron, annihilation of

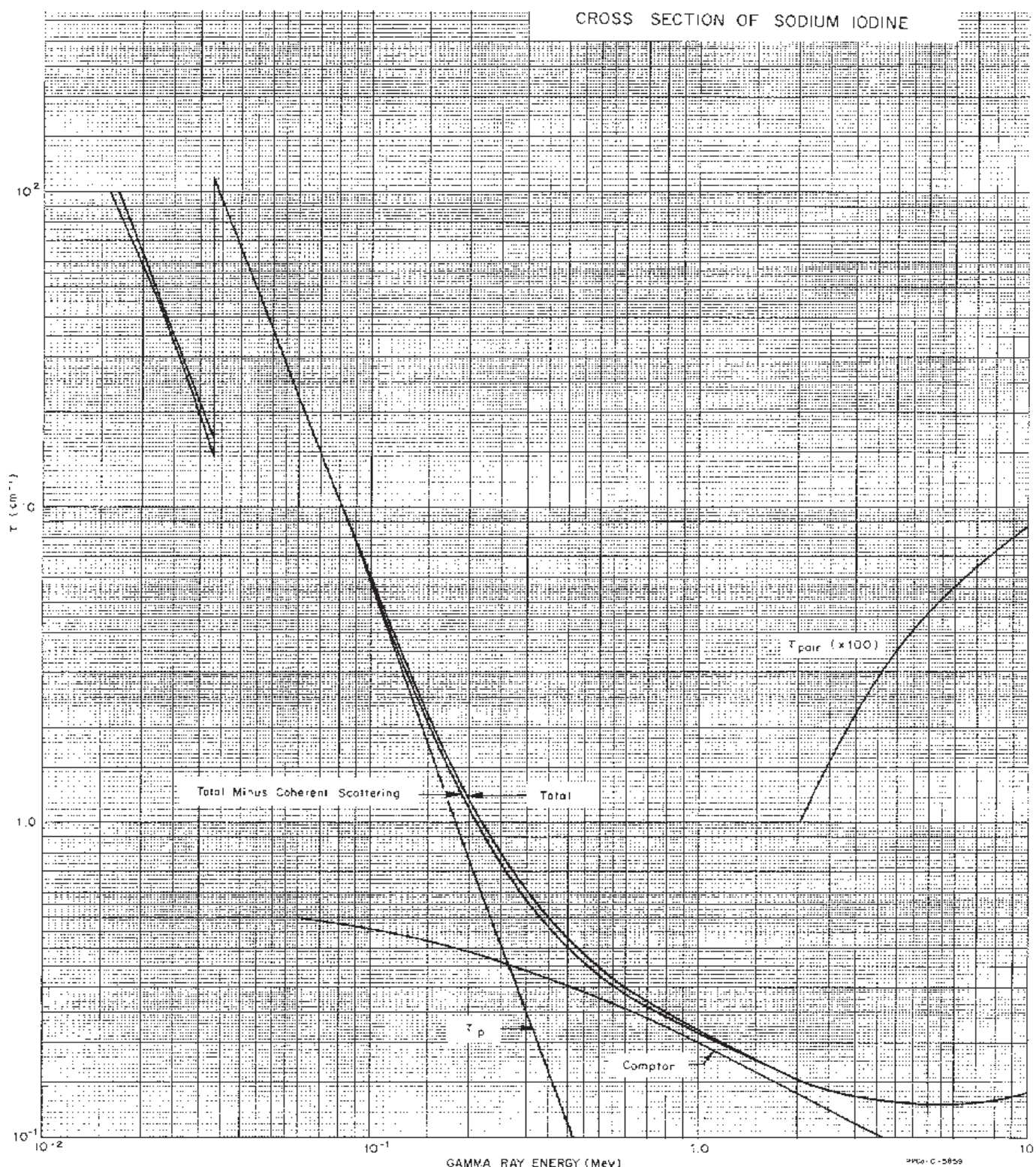


Fig. 1 - Absorption coefficient for NaI(Tl) as a function of gamma-ray energy. Results using the total absorption cross section and the total minus coherent scattering are shown for comparison.

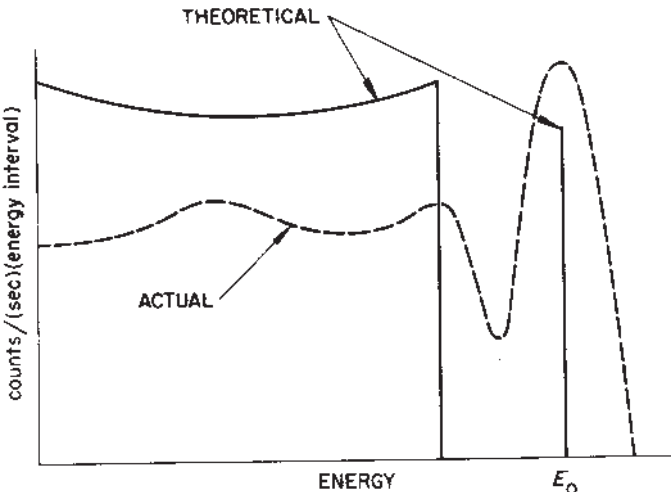


FIG.2 - Theoretical electron energy distribution (single events) for Compton and photoelectric interaction in a NaI detector compared with an experimental pulse-height distribution obtained on a 3"x3" NaI detector (0.50 MeV).

the two particles occurs with the emission of two photons equal in energy to the rest mass of the particles (0.511 MeV). Interaction by the idair process in a detector will therefore result in an energy loss equal to the primary photon energy minus 1.02 MeV. As will be discussed below, the possibility also exists of detecting one or both of the annihilation quanta by either the photoelectric or Compton process. These alternatives result in a complex electron energy distribution for the pair process. A series of events can result in an energy loss to the detector of any energy from $E_g - 1.02$ MeV up to the full energy of the primary photon.

The total probability for detection of a gamma ray (expressed as the total absorption coefficient) will then be given by:

$$\tau = \tau_{\text{phot}} + \tau_{\text{compt}} + \tau_{\text{pair}} \quad (3)$$

The total absorption coefficient for NaI(Tl) and the contribution from the photoelectric, Compton, and pair processes is shown in **Fig. 1**. The total absorption coefficient is plotted as a function of incident gamma-ray energy using data from Gladys White Grodstein.⁷ Examination of this figure will give an indication of the relative importance of each type of interaction as the energy of the incoming gamma ray is varied. In the energy region up to a few hundred kilovolts, the photoelectric process dominates. At higher energies, Compton scattering dominates while pair production becomes important at higher energies. In the discussion of the detector response which follows, frequent reference will be made to this figure in describing the response of a NaI scintillation detector to monoenergetic gamma radiation.

⁷ Gladys White Grodstein, *NBS Circular 583* (1956).

B. The Pulse-amplitude Spectrum

1. Spectrum Shape vs Gamma-ray Energy

To provide a basis for describing a pulse amplitude distribution observed at the anode of the electron multiplier tube in terms of the basic processes described above, let us briefly review the succession of events which produce it. Assume that a monoenergetic source of gamma radiation of approximately 0.50 MeV is incident upon the NaI crystal-phototube combination. Inspection of the absorption cross section of NaI shown in **Fig.1** indicates that these gamma rays will interact with the NaI detector by both Compton scattering and the photoelectric effect in the ratio of about 6 : 1. If a sufficient number of gamma rays are detected to give a reasonable statistical sample, an electron energy distribution similar to that portrayed by the solid line in Fig. 2 will be produced within the volume of the NaI detector. We see a monoenergetic line of photoelectrons and a continuous distribution of Compton electrons from zero energy up to a sharp cut-off at an energy somewhat below the photoline. Shown for comparison is the pulse-height distribution from a 3"x3" NaI detector obtained with a differential pulse-height analyzer. Although the pulse,amplitude spectrum is similar in character, we observe that the energy distribution has been smeared by what appears to be a gaussian function. This is due to flunctuations in the light output from the phosphor and to the statistical nature of the processes occurring in the electron multiplier.

The peak resulting from total energy loss (photopeak) is the distinguishing characteristic of all spectra. The amplitude of this peak and its intensity are used to determine the energy and intensity of gamma rays producing a given pulse height distribution. The width of this peak is a measure of the energy resolution of the detector - a subject which will be treated in more detail in a later section.

In addition to the amplitude smearing of the original electron spectrum it is apparent that a much larger fraction of the total number of events have appeared in the "photopeak" than would be predicted from the ratio of the photoelectric and Compton cross sections. In a detector of this size, the probability that a Compton-scattered gamma ray will escape the volume of the detector is somewhat reduced and many multiple events (e.g., Compton scattering followed by a photo event) can occur resulting in total energy loss. Since this chain of events occurs well within the lifetime of the phosphor, the energy loss from all events will sum to produce a pulse in the full-energy peak. As will be shown later, the relative probability for total energy loss in the detector due to the occurrence of multiple events will increase as the dimensions of the detector are increased.

The complicated pulse-height spectrum produced from monoenergetic photons incident upon a detector presents a basic problem in the interpretation and analysis of data obtained with a scintillation spectrometer. Let us now examine variations in the shape of the pulse-height spectrum as the incident gamma-ray energy is varied. **Fig. 3** shows the energy positions of four gamma rays of 0.060, 0.320, 0.830, and 1.92 MeV incident energy, all of equal intensity. Above

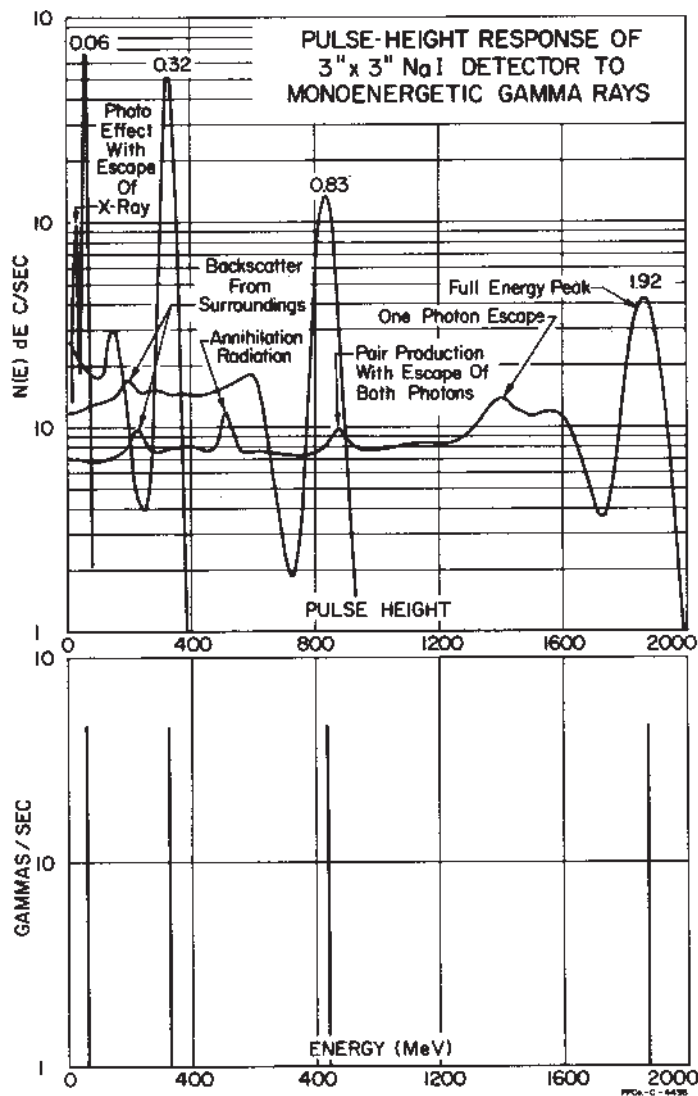


FIG. 3 - Pulse-height distributions obtained with a 3"x3" NaI scintillation detector from monoenergetic gamma-ray sources of 0.060, 0.32, 0.83, and 1.92 MeV. Pertinent features of these spectra are noted.

this are the pulse amplitude spectra for each of these gamma rays obtained with a 3"x3" NaI detector. At 0.060 MeV, gamma rays interact with the detector almost entirely by the photo process and the detector response is essentially a single peak - nearly Gaussian in shape. The peak of lesser intensity on the lowenergy side of the full-energy peak is attributed to escape of iodine x-rays from the surface of the detector following a photoelectric interaction. This effect will be discussed in more detail in a later section. As the gamma-ray energy increases, the pulse,height distribution becomes more complicated. In addition to the photopeak we see the continuous distribution of pulses resulting from the detection of Compton electrons. As the gamma-ray energy increases, the fraction of pulses in the photopeak is reduced as the Compton cross section becomes more dominant. At 1.92 MeV, the pulse,height distribution becomes more compli- cated. In addition to the Compton electron distribution and the full-energy peak, several satellite peaks are superimposed upon the Compton

distribution as a result of interaction by the pair process. As previously indicated, all energy in excess of the 1.02 MeV threshold for this process, will appear as kinetic energy of the positron-electron pair. This results in the peak which appears at an amplitude equal to the energy of the incident gamma ray minus 1.02 MeV. Subsequent annihilation of the positron will create two 0.511 MeV photons within the volume of the detector. If both of these annihilation quanta escape detection in the crystal only the energy of the positron- electron pair will be lost to the detector. If one of the annihilation quanta is detected in the crystal by the photo process, or by any combination of multiple processes which result in total energy loss, then a peak will appear at an energy corresponding to 0.511 MeV less than that of the incident photon. If both annihilation quanta are detected with total energy loss, the addition of the energy left in the detector by all processes for one pair event will pr duce pulses in the full-energy peak. The total result interaction by the pair process will then be a distribution of pulses ranging from the full-energy peak to 1.02 MeV less than the photopeak, including the three prominent peaks just described. Further examination of the spectrum for the 1.92 MeV gamma ray indicates the presence of a peak with an amplitude corresponding to 0.511 MeV. This peak is due to the detection of annihilation quanta resulting from pair production external to the NaI crystal. The escape and subsequent detection of annihilation quanta from these events represents a background effect for gamma rays above the pair threshold. This peak does not result from the detection of primary photons included in the cone of solid angle intercepted by the detector and should not be considered a part of the detector response to gamma rays originating in the source, but an extraneous effect due to detector environment. Such effects are discussed in detail in Section IV. Further examples of the response of a NaI scintillation detector to monoenergetic radiation are given in **Fig. 53**.

If we now consider the change in shape of the pulse amplitude spectrum as the energy of the incident gamma ray increases, it is apparent that the interpretation of spectra containing more than one gamma ray presents many problems. At low energies the pulse spectrum is characterized by a single symmetrical peak which is nearly Gaussian in shape and the response may be said to be unique. Information representing both the energy and intensity of the photons incident upon the detector is contained in a relatively few pulse-height channels of the analyzer. As the gamma-ray energy increases, this uniqueness between energy, intensity, and pulse amplitude rapidly disappears. Although the essential information about energy and intensity still exists in the presence of the full energy peak as a distinct feature of the pulse spectrum, any channel of a given pulse-height distribution may have contributions from gamma rays whose full-energy peaks are above that channel. This is a major source of difficulty in the analysis of complex gamma-ray spectra.

2. Variations in Pulse-height Distribution with Detector Size

As previously mentioned, the pulse-amplitude spectrum results from both primary and secondary events which haveoccurred in

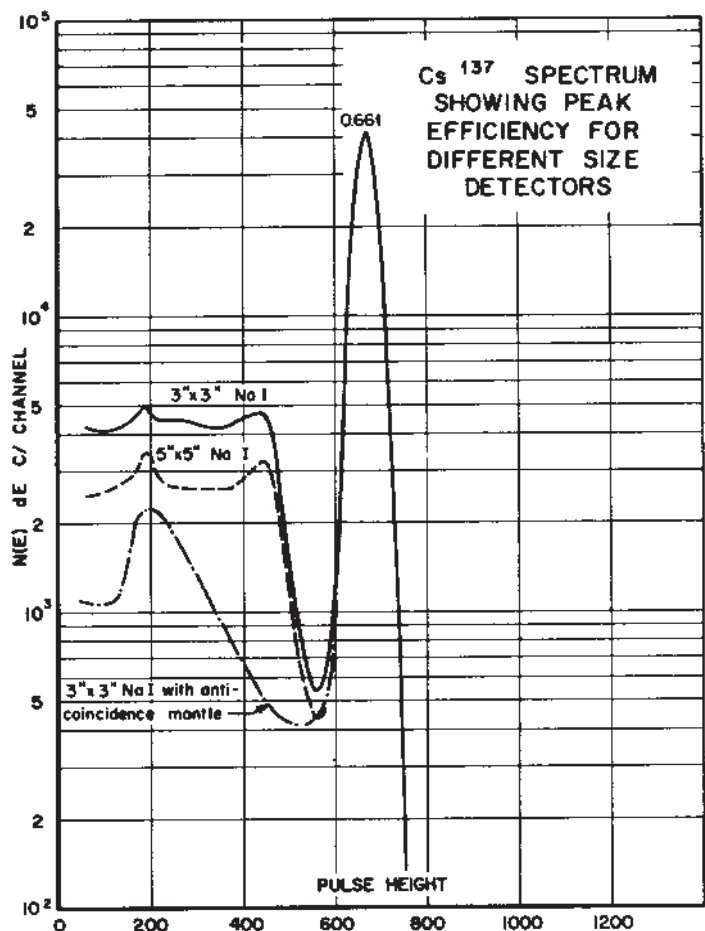


Fig. 4 Comparison of pulse-height spectra of ¹³⁷Cs obtained with different sized NaI detectors. All spectra are normalized in gain and area of photopeak.

the crystal. The result of a series of successive interactions is a single pulse whose amplitude will be proportional to the sum of the energy loss from each interaction. Since the probability for interaction of a photon within the volume of the detector will be proportional to the path length traversed in passing through the detector, the relative number of secondary processes following an initial Compton scattering will increase with the dimensions of the detector. The increase in the fraction of events which result in total energy loss realized by increasing the size of the detector is demonstrated in Fig 4. This figure illustrates the pulse-height distributions obtained from ¹³⁷Cs gamma rays detected with cylindrical crystals of NaI measuring 3" diameter by 3" high, and 5" diameter by 5" high. Also shown for comparison is the spectrum obtained with a 3"x 3" detector surrounded by an anti-coincidence mantle such as that described by Raboy and Trail.⁸ In a detector arrangement of this type, if a gamma-ray experiences a Compton scattering event in the central crystal and the scattered photon is detected in the surrounding mantle detector, an anticoincidence circuit rejects the pulse from the central detector.

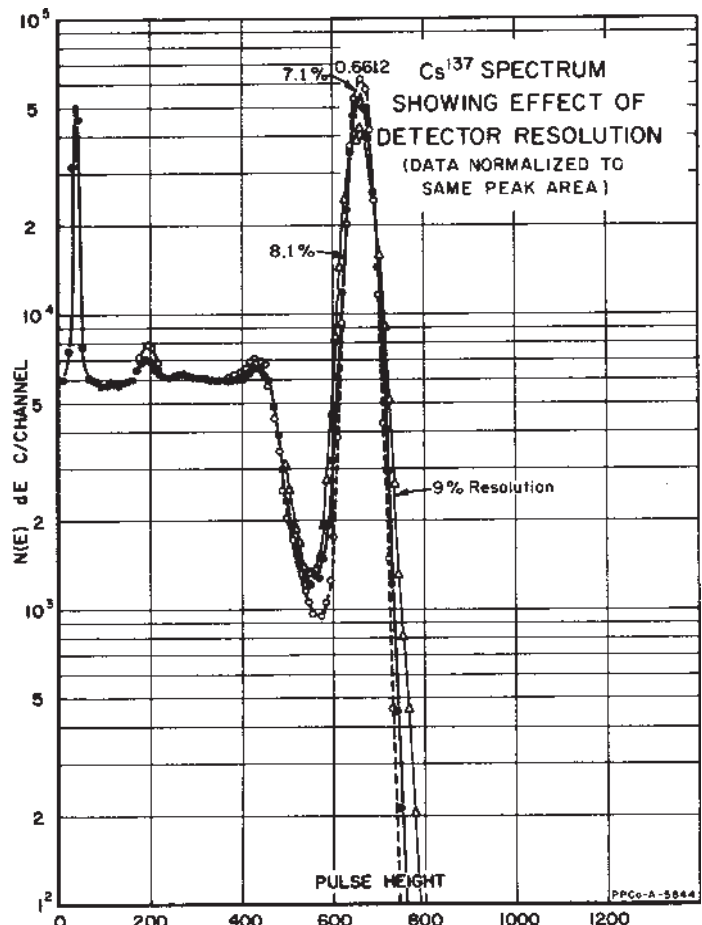


FIG. 5 - Effect of detector resolution on pulse-height spectrum.

In this manner essentially only those events which result in total energy loss in the central counter are recorded by the pulse,height analyzer. Improvement in the relative "photopeak" response (peak-to-total ratio) may also be obtained by using a well-type detector arrangement where the source is mounted in the interior of the detector. These latter detectors, however, have serious disadvantages when coincidence-sum effects are considered. These effects will also be discussed in a later section.

3. Detector Resolution

The energy resolution of a scintillation spectrometer is a measure of the ability to distinguish the presence of two gamma rays closely spaced in energy. Since the essential information is contained in the "photopeak," the practical measure of resolution is the width of the "photopeak" or "instrumental line width." The convention adopted is to define the resolution as the relative full width of the "photopeak" measured at half the maximum height of the peak. Thus, the resolution will be the full width at half maximum divided by the mean "photopeak" position on the pulse-height scale. As a matter of convenience, the resolution of a NaI scintillation detector is usually reported for the 0.662-MeV gamma ray emit-

⁸S. Raboy, C. C. Trail, and J. E. Monohan, Proceedings of the Total Absorption Gamma-ray Spectrometry Symposium, U. S. Atomic Energy Commission Report TID-7594, (1960).

ted by ^{137}Cs . For 3"x3" cylindrical detectors a resolution ranging from 7.5 to 8.5% for the Cs line can be readily achieved with commercially available detectors. Fig. 5 shows the effect of change in resolution on the shape of the pulse-amplitude distribution. Spectra of ^{137}Cs taken with three detectors having energy resolutions of 7.1, 8.1, and 9% are presented - all normalized in intensity to equal "photopeak area."

The photoline width is primarily a result of statistical fluctuations in each step following the initial event which produces ionization in the detector. Among these are the following:

- (1) Conversion of the kinetic energy of primary electrons to light.
- (2) Efficiency of light collection and transfer of photons to photocathode.
- (3) Efficiency of photocathode in the conversion of photons to photoelectrons.
- (4) Efficiency of electron optics in phototube for focusing of electrons on the first secondary-emitting dynode.

(5) Electron multiplication in the dynode structure.

All of these steps in the scintillation process will ultimately affect the statistical variance in the pulse amplitude appearing at the anode of the electron multiplier. An excellent treatment of this subject and the contribution each of these factors has been given by Breitenberger⁹. More recent discussions have been presented by Managan, Prescott, and Iredale.¹²

In addition to the statistical considerations basic to the scintillation process, there exist several instrumental variables which can also contribute to the observed width

⁹ E. Breitenberger, Prog. in Nuclear Physics, 4, 56 (1955).

¹⁰ W. W. Managan, IRE Trans. on Nuclear Science, Vol. NS-9, N 3 (1962).

¹¹ J. R. Prescott and P. S. Takar, IRE Trans. on Nuclear Scienc Vol. NS-9, No. 3 (1962)

¹² P. Iredale, Nucl. Instr. and Methods, 11, 340 (1961).

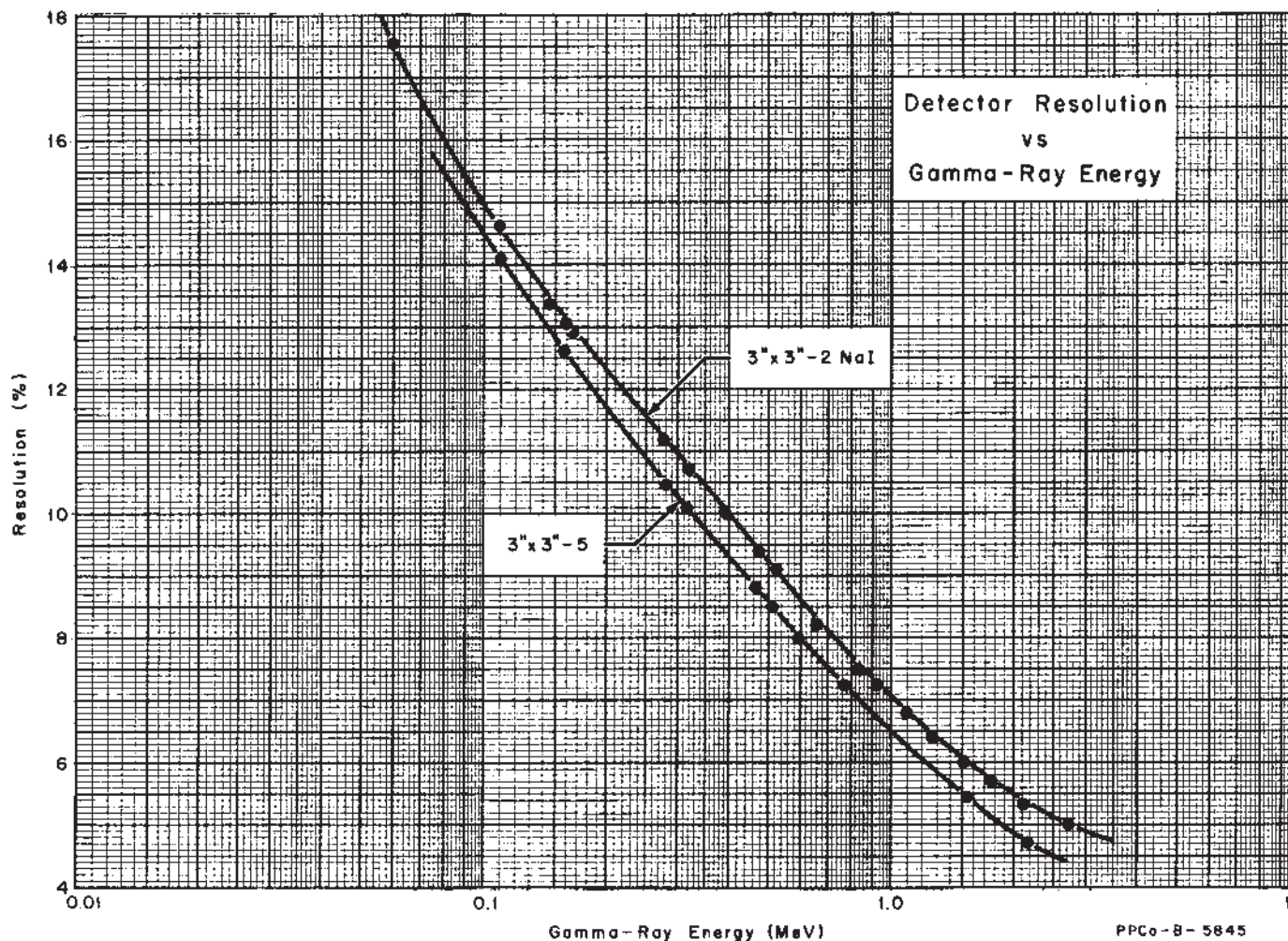


Fig. 6 - Plot of detector resolution (FWHM) as a function of gamma-ray energy for detectors used to measure catalogue spectra.

a “photopeak.” The finite width of a pulse-height channel in the pulse analyzer can contribute to the width of a “photopeak.” On a linear energy scale this effect is most noticeable in the first few channels of the spectrum where a “photopeak” may only be a few channels wide. An example is illustrated in **Fig. 52**. Peak width can also be effected by noise modulation when the amplitude of the noise spectrum at the input to the pulse-height analyzer is equal to or exceeds the width of one amplitude channel. Variation in the zero voltage reference in the analyzer, gain in the

electronic pulse amplifier or ramp slope in the analogue-to-digital converter of the analyzer during the measurement of a pulse-height spectrum will also result in peak broadening. Since these effects are difficult to separate and interpret, it is important that they be reduced to negligible proportions.

A plot of detector resolution for detectors used in the compilation of spectra for the catalogue is shown in **Fig. 6**. Resolution (FWHM) is plotted as a function of gamma, ray energy.

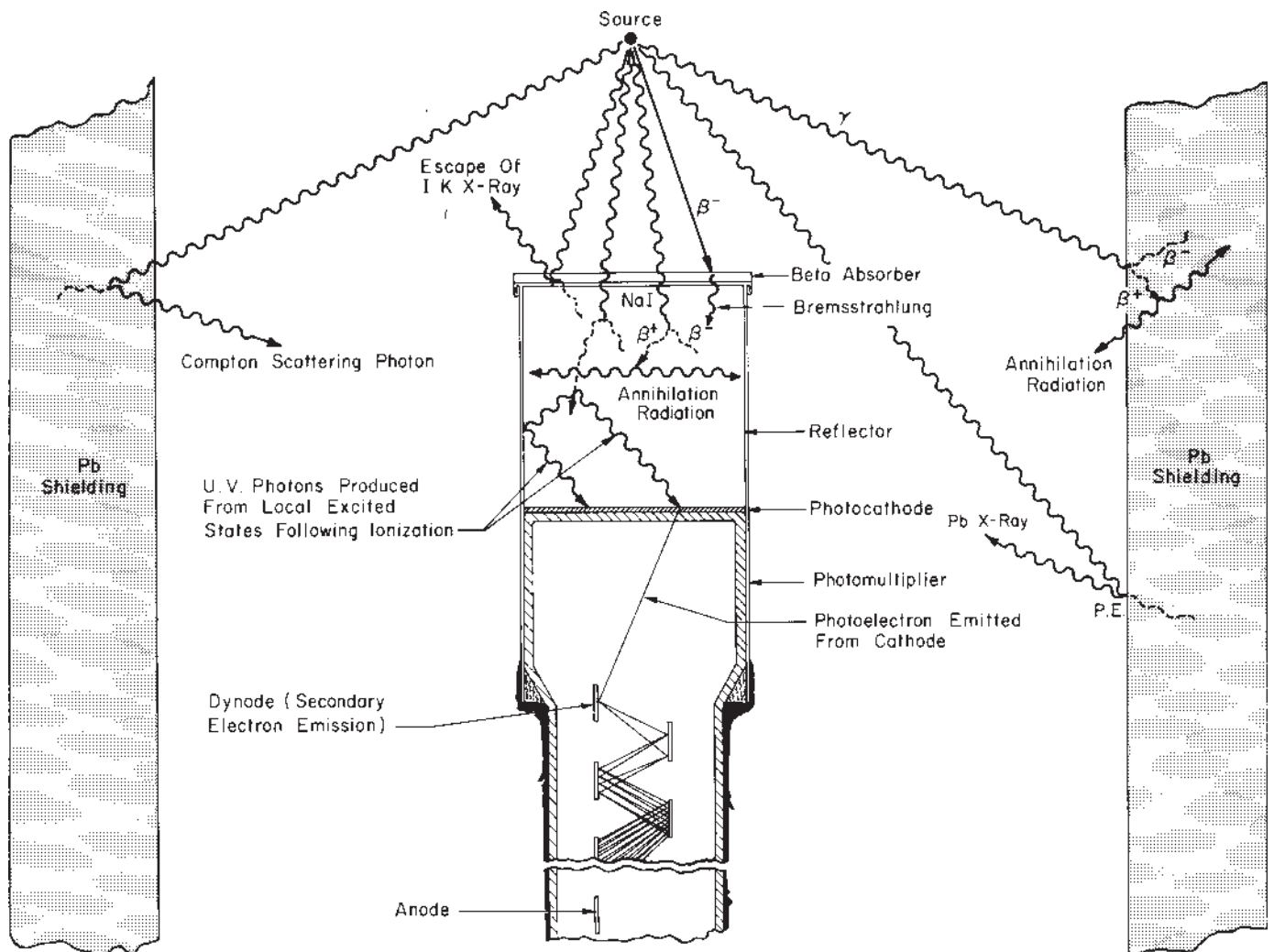


Fig. 7 - Illustration representing a NaI scintillation detector showing sequence of events producing output from electron multiplier and various processes which contribute to the response of a detector to a gamma-ray source.

IV. EFFECTS DUE TO DETECTOR ENVIRONMENT

If the radioactive source and the scintillation detector could be isolated from all surrounding material, the shape and magnitude of the observed pulse-amplitude spectrum would be dependent only upon the energy of the gamma ray, the physical properties of the source and detector, and the geometrical relationship between the two. Unfortunately this cannot be achieved in the laboratory. In practice, the shape of the observed pulse-amplitude distribution will be influenced by many factors related to the experimental environment. Since the response of a detector in a practical laboratory environment must be understood prior to any attempt to analyze a pulse-height distribution, let us examine in some detail the many variables which can influence the shape of spectra obtained under practical laboratory conditions.

Fig. 7 is a pictorial representation of a NaI detector in a lead shield. In this figure the different types of interactions which can contribute to an observed pulse-height spectrum are portrayed. Each type of interaction and its contribution to a pulse height spectrum will be discussed in the following paragraphs.

A. X-Ray Escape

Gamma rays in the energy region below 200 keV are detected almost entirely by the photoelectric process. As previously described, the ejection of a photoelectron from the K shell of an atom is followed by the emission of characteristic x-rays. If the interaction occurs near the surface of the detector, iodine K x-rays may escape without further interaction. When this occurs, the energy of the x-ray (28 keV) will be lost and an additional peak will appear in the spectrum at 28 keV less than the photopeak. The spectrum of a 0.068-MeV gamma ray emitted in the decay of Co⁶¹ is shown in **Fig. 8** as an illustration of this effect. The magnitude of this escape peak will vary as the photoelectric cross section and with source-detector geometry. The escape peak will not be present for energies less than the K-edge of Iodine (33.2 keV) and will decrease rapidly in relative intensity with increasing gamma-ray energy.

The probability for x-ray escape may be calculated as a function of energy and geometry or may be determined experimentally. Axel¹³, and McGowan¹⁴ have calculated escape peak intensities for various configurations. The results of an experimental determination of the probability for escape from a 3"x 3" NaI detector in the standard geometry (point source at 10 cm) is shown in **Fig. 9**. Experimental values, indicated by the open circles, are compared with results of calculations made by McGowan¹⁴ for a 1 1/2" diameter x 1" cylinder of NaI in a similar geometry.

B. Scattering from Surrounding Material

To reduce the level of background radiation it is usually necessary to operate a large NaI scintillator inside a shielded enclosure. This shield represents the major source of scattered radiation. Scattering also occurs from the source holder, the material

used to prepare the source, beta absorbers, and the packaging material surrounding the NaI crystal. The effect of scattering from this material on the shape of the spectrum will now be examined. Fig. 10 shows an experimental spectrum resulting from the detection of the 0.478-MeV gamma ray emitted in the decay of ⁷Be. This spectrum was taken under the same laboratory conditions used for the measurement of all spectra in the catalogue. The results of measurements made with and without the presence of a polystyrene beta absorber are shown to illustrate the effect of scattering from the absorber. The distribution of pulses above the photopeak which is labeled "random sum spectrum" will be dis-

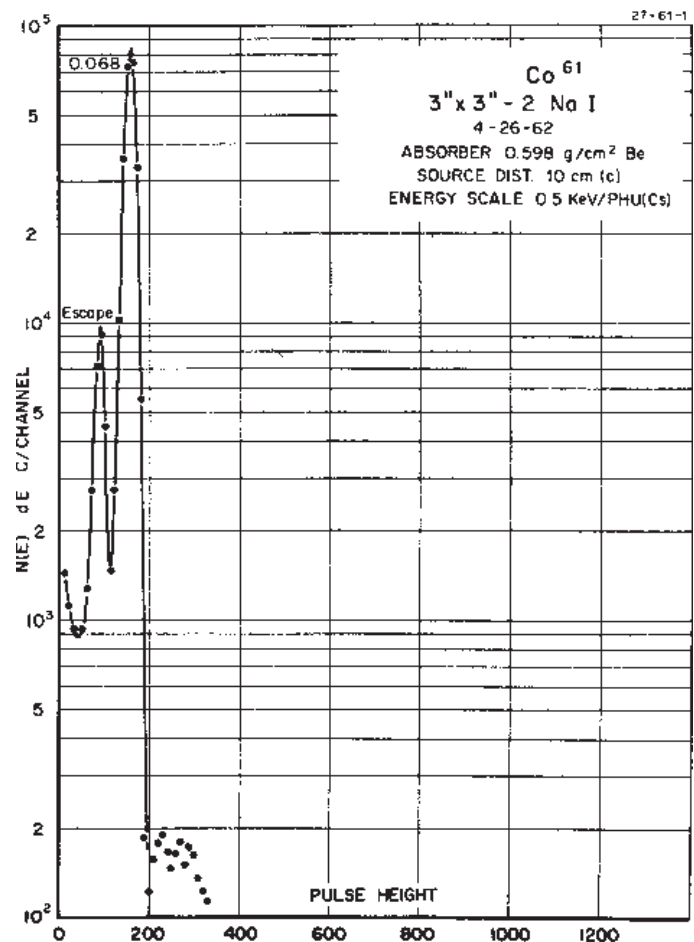


FIG. 8 - Pulse-height spectrum of 0.068-Mev gamma ray emitted in the decay of 3.3-hr ⁶¹Co illustrating iodine K x-ray escape.

cussed in a later section. If we examine the region of the pulse-height spectrum which results from Compton electrons we see a definite peak superimposed upon the otherwise flat energy distribution of electrons. This peak is termed the "backscatter peak" and arises from Compton scattering of gamma rays in the walls of the shield surrounding the detector. The shape and magnitude of this component of the spectrum is shown below.

¹³ P. Axel, AEC Report, BNL-271 (1953).

¹⁴ F. McGowan, *Phys. Rev.*, 93, 163 (1954).

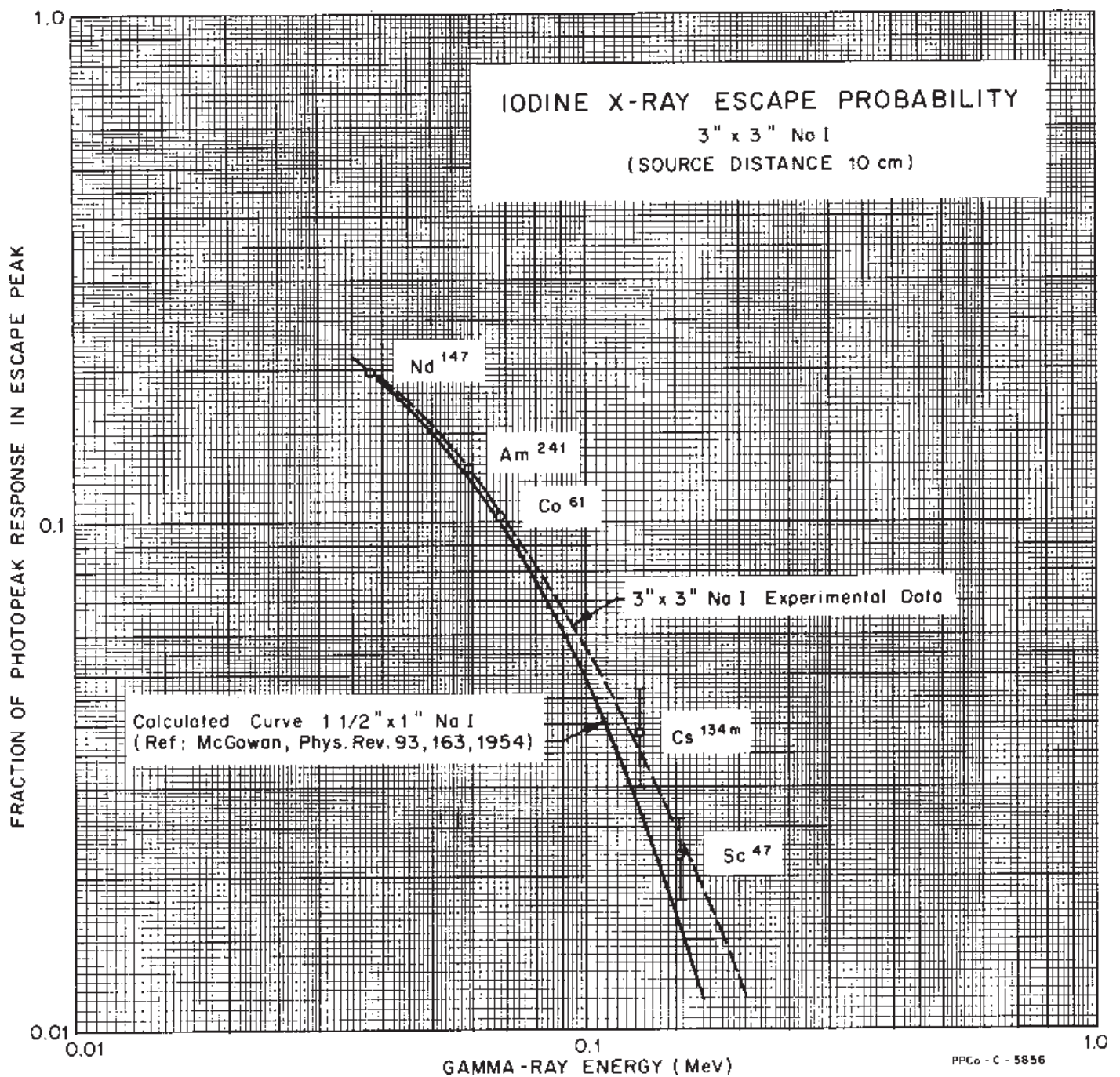


FIG. 9 - Probability for escape of the iodine K x ray following photoelectric interaction in a 3"x3" NaI detector. Data are plotted as the fraction of the total photoelectric response to a point source at 10 cm as a function of gamma-ray energy. Shown for comparison is the calculated escape fraction for a 1 1/2"x 1" NaI detector in a similar geometry.

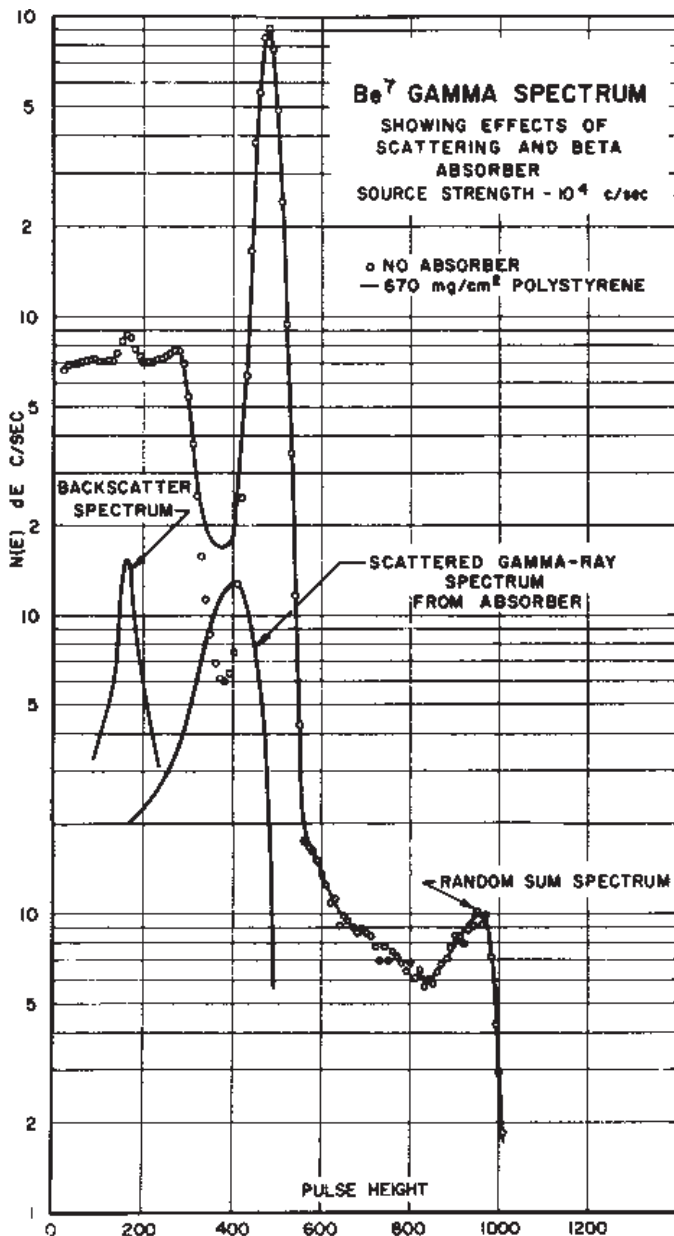


Fig. 10 - The pulse-height spectrum representing the response of a 3"x3" NaI detector to the 0.478-MeV gamma ray emitted in the decay of ^{7}Be . The contribution to the spectrum from photons scattered from the shield and beta absorber and the random sum spectrum are shown.

component of the spectrum is shown below the experimental spectrum. The character of the backscatter spectrum and the scattered component from the absorber will be explained below.

1. Backscatter Spectrum

To understand the shape of this spectrum let us consider the relationship between the energy of the scattered photon and the scattering angle as given by equation (1). A plot of this relationship is shown in **Fig. 11** for primary photon energies of 0.25, 0.51, 1.0 and 2.0 MeV. Examining this figure we see that

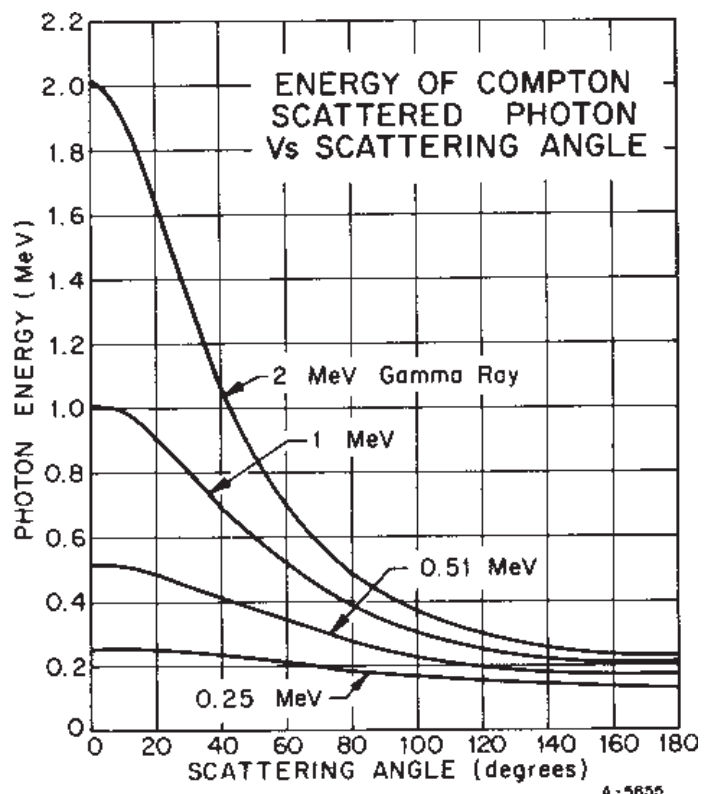


Fig. 11 -The energy of Compton scattered photons as a function of scattering angle for various primary gamma-ray energies.

for scattering angles greater than 120° , the energy of the scattered photon is relatively independent of angle and the energy of the primary photon. As a result, the spectrum of scattered gamma rays emerging from the walls of the shield used in the experiment shown in **Fig. 10**, is nearly monoenergetic.

To illustrate the effect of shield configuration on the shape and magnitude of the scattered component, let us examine the results of a series of measurements made with the different shield geometries shown in **Fig. 12**.

Three shields were constructed with 4" Pb walls having inside dimensions of 6"x 6"x 18", 12"x 12"x 24", and 32"x 32"x 32". Shield A (6"x 6") was duplicated with Fe to demonstrate the relative effect of the Z of the scattering material on the shape and magnitude of the scattered spectrum. **Fig. 13** indicates the response of a 3"x3" cylindrical NaI detector to the 0.835-MeV gamma ray emitted by a source of Mn^{54} in three different shield configurations. In the energy region of the scattered spectrum the top curve was obtained using the 6"x 6" Fe shield. The middle and lower curves show the response obtained using the 6"x 6" Pb shield and the 32"x 32" Pb shield. Comparing the two results for the small shield, identical except for the material of construction, we see a large difference in the magnitude of the scattered spectrum. This is due to the larger photo-electric cross section in Pb. A larger fraction of primary photons entering the lead walls are absorbed by the photo-electric process, either initially, or follow-

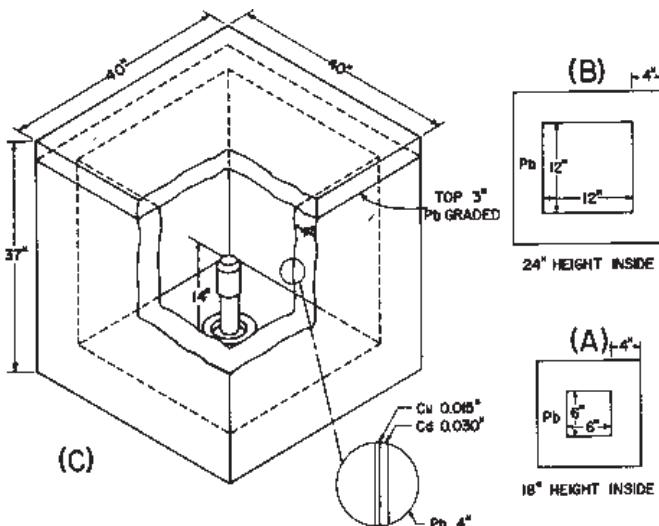


Fig. 12 - Detector shield configurations used to demonstrate effect of Compton scattering on response of detector to monoenergetic gamma radiation.

a single Compton scattering event. Comparison of the results obtained in the two Pb shields shows a large reduction in the magnitude of the scattered spectrum as the dimensions of the shield are increased.

It is of interest to compare the features of the scattered spectrum in all three cases. Scattering from the walls of the small shield gives rise to a rather broad peak with evidence of two major components. The high-energy component is attributed to 180° single scattering of photons and the second peak to processes involving two successive Compton events before the scattered photon strikes the detector. As the size of the shield is increased, the back-scattered spectrum assumes the shape of a fairly sharp line, indicating that the reduced solid angle subtended by the detector for scattering from a point on the surface of the shield wall has reduced the energy spread. The restriction of the scattered radiation to a very narrow energy region is in agreement with predictions based upon the energy/angle relationship given in **Fig. 11**. A consideration of these results would lead one to conclude that the detector shield should be as large as cost and space considerations will permit.

It should be noted that the relative magnitude of the scattered spectrum will depend upon the source-detector geometry. In all measurements described above, the source was mounted at 10 cm from the detector face. For most shield configurations the magnitude of the scattered spectrum will be relatively independent of source-detector distance, while the efficiency for the detection of gamma rays from the source will vary approximately as I/h^2 .

2. X-Ray Production in Shield

Analogous to the escape of iodine x-rays from the surface of the detector following a photoelectric event, a photo event occurring at the surface of the walls of the detector shield can result in the production of characteristic Pb x-rays. The probability of detecting these x-rays can be reduced by the use of critical absorption

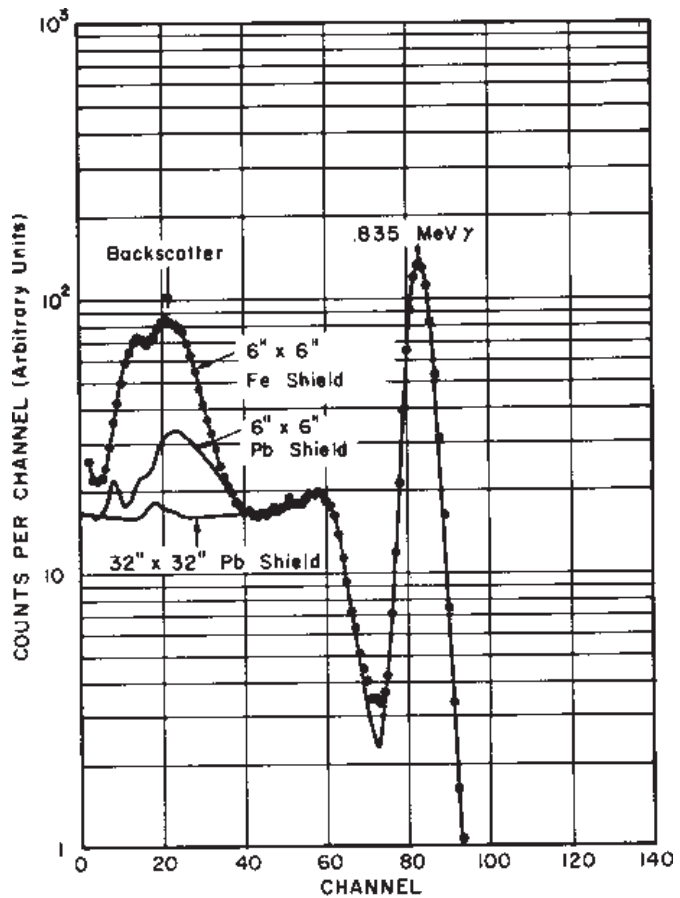


Fig. 13 - Effect of detector shield configuration on scattered component of pulse-height spectrum obtained from monoenergetic source.

techniques. To achieve this the shield is lined with one or more materials in decreasing order of Z.

Using the same shield configurations described above, a series of measurements were made to illustrate the use of "graded" shields. **Fig. 14** shows the results of these measurements. The spectrum obtained in the 6"x 6" Pb shield shows definite evidence of the Pb K x-ray at 0.072 MeV. The second curve (shown by the solid line in the x-ray energy region) indicates the response following the addition of a 0.030" Cd liner to the shield. The thin Cd sheet is very effective in reducing the intensity of the Pb x-ray. Finally, the lowest line indicates the response in a large shield lined with 0.030" Cd sheet and 0.015" Cu sheet in that order. The combination of reduced solid angle and the successive "grading" of the shield lining have reduced the fluorescent radiation to a negligible level.

C. Effect of Beta Absorber

Generally speaking, nature does not provide us with sources which emit only photons. The decay of most radioactive source includes the emission of charged particles (either positrons or electrons). Since NaI is an efficient detector of charged particles, it is nec

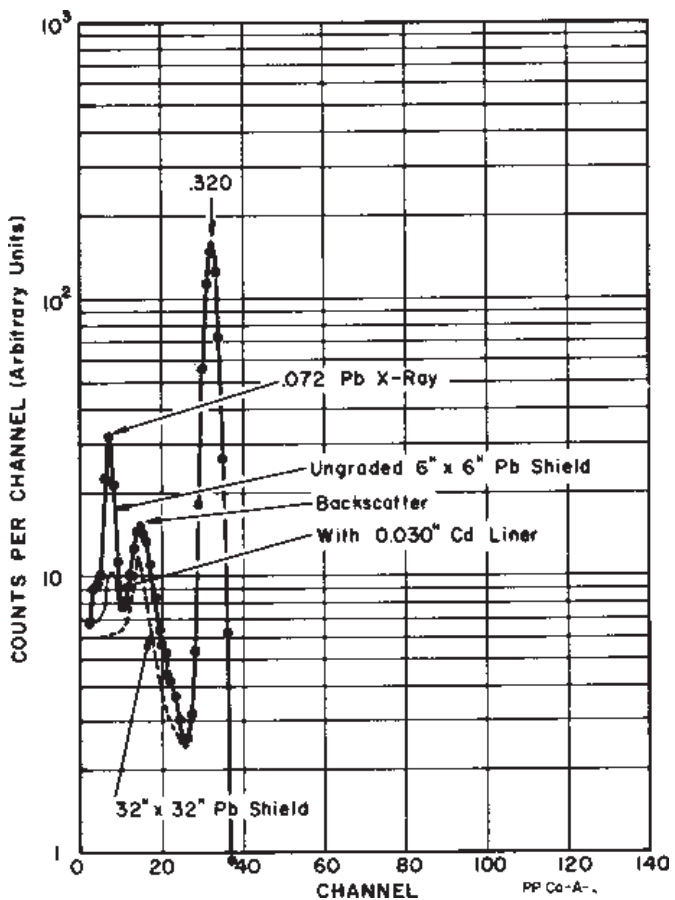


Fig. 14 - Illustration showing the effect of Pb x-rays produced by photoelectric interaction in the shield and the use of critical absorption techniques in "grading" shield to reduce this effect.

essary to prevent their entering the detector. The presence of these charged particles introduces several complications. **Fig. 15** shows a series of pulse spectra resulting from the measurement of radia, tions emitted from the decay of 3.6-hr ^{92}Y . This isotope, which decays by beta emission, emits very energetic beta particles (3.6 MeV) and a number of gamma rays. The upper curve results from a measurement made with no absorbing material between the source and detector. We see that the gamma-ray spectrum is almost completely obscured by the high energy betaray continuum. The second curve represents a measurement taken with a 1.18 g/cm^2 beryllium absorber interposed between the source and detector in the standard source-detector configuration illustrated in **Fig. 16**. The third curve was obtained by surrounding the sides of the cylindrical detector with a cap made of polystyrene (0.7 g/cm^2) as shown in **Fig. 17**. The difference observed with the polystyrene cap is the result of the absorption of beta particles scattered from the air and surrounding materials into the sides of the detector. In cases where high-energy beta radiation is present, care must be exercised to exclude all electrons from the detector if the pulse-amplitude spectrum is to represent only the response of the detector to gamma rays emitted by the source. This is particularly important for nuclides which have a high-intensity ground state beta transition.

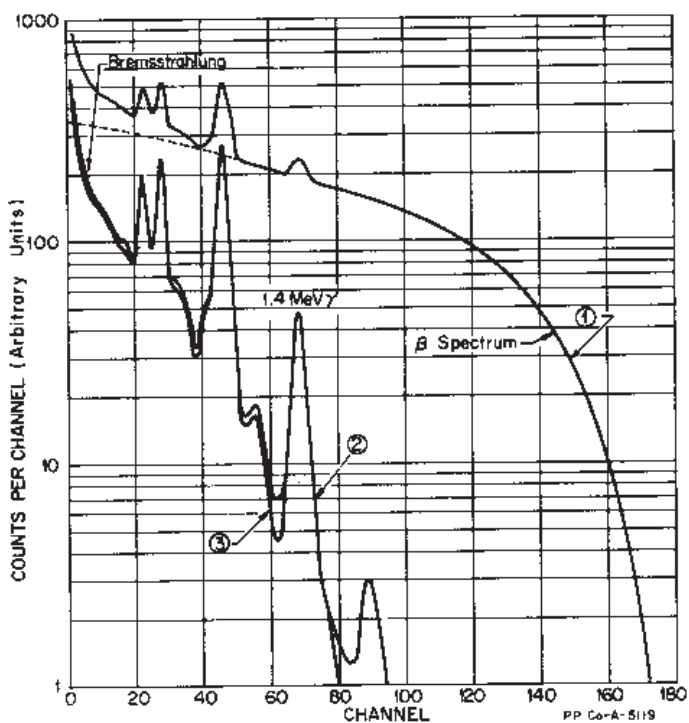


Fig. 15 - Effect of beta absorber on observed spectrum and use of absorber cap over detector to reduce rays scattered into side of detector.

Since absorbing material must be used to eliminate beta particles from the detector, one must be concerned with possible degradation of the spectrum from Compton scattering which occurs within the beta absorber. **Fig. 18** shows the effect on the ^{137}Cs pulse-height spectrum as increasing thicknesses of absorbing material are interposed between source and detector. In addition

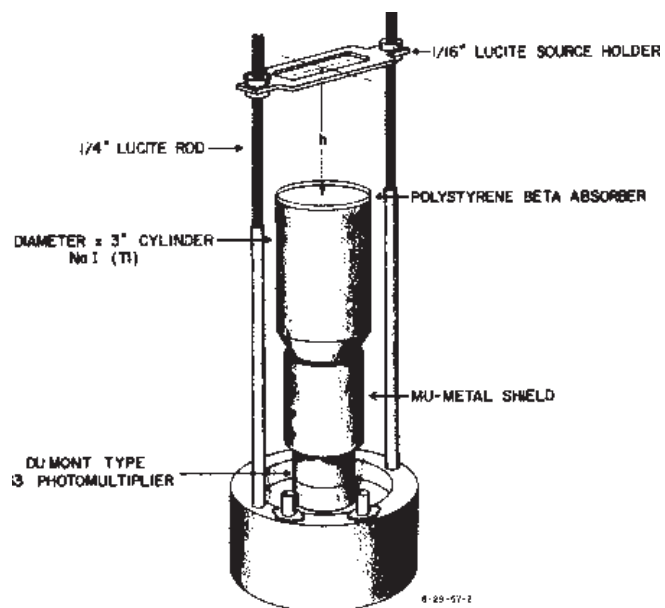


Fig. 16 - Standard laboratory source mounting geometry.

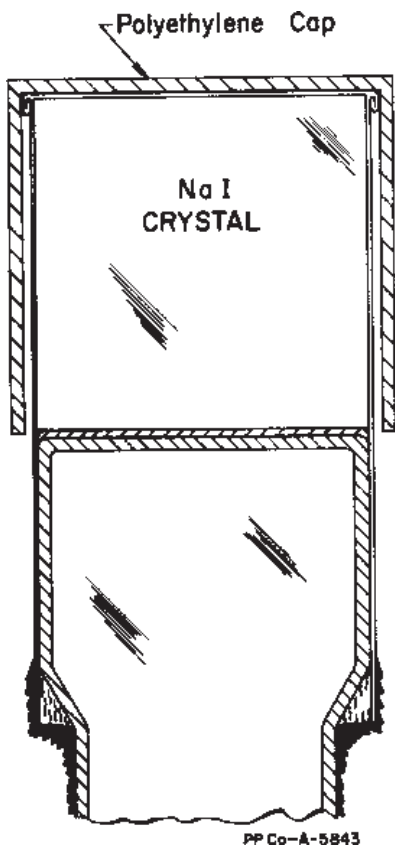


FIG. 17 - Illustration showing absorber cap over detector used to prevent scatter of electrons into side of detector.

to the attenuation of the entire spectrum, the shape of the spectrum is seen to change materially in the region just below the photopeak, with little change in the low-energy region of the Compton distribution. The observed degradation of spectrum shape is the result of detecting photons which have experienced Compton scattering in the forward direction. It should be noted that similar scattering effects can occur in the source if it has sufficient mass.

It is accepted practice to use beryllium as the absorbing material to minimize the production of bremsstrahlung. This subject will be discussed in Section VI.

D. Annihilation Radiation

In the measurement of sources emitting gamma rays whose energy exceeds the threshold for the pair production process, annihilation radiation will be observed in the pulse-height spectrum.

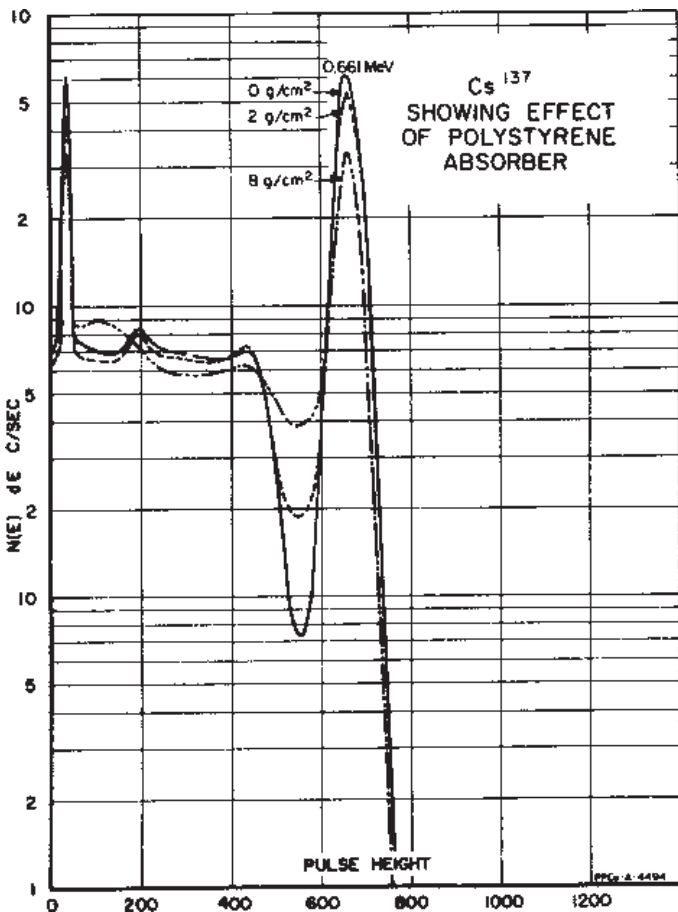


FIG. 18 - Effect of absorber thickness on monoenergetic response of detector.

This results from pair interaction in the walls of the detector shield and other material in the vicinity of the detector. Following the initial event, the annihilation of an electron-positron pair creates two (2) 0.511-MeV gamma rays which may interact with the detector. This type of event is illustrated in Fig. 7. It should be restated that annihilation radiation does not appear as a separate feature of the pulse-height distribution when high-energy photons experience a pair interaction within the volume of the detector. If one of the annihilation quanta is detected following the initial event, the energy loss is added to the kinetic energy of the electron-positron pair.

Since the cross section for pair production is highly dependent on the atomic number of the absorber, this source of spurious radiation can be reduced by removing all high-Z material from the immediate vicinity of the detector. Scatter shields and collimators, which are usually made of lead, are likely offenders.

V - SUMMATION EFFECTS

A. Coincidence Sum Spectrum

1. Coincident Gamma Rays

In the decay of most radioactive nuclides, beta emission is frequently followed by the emission of two or more gamma rays in cascade. In this case there is a finite probability that these gamma rays will be detected simultaneously. The light pulse produced in this instance will correspond to the sum of the energies deposited in the detector by the gamma rays. This results in a distribution of pulses extending in energy up to the sum of the energies of the coincident gamma rays - the "coincidence sum spectrum." The intensity of the coincidence sum spectrum for two coincident gamma rays is given by the simplified expression:

$$N_{c.s.s.} = N_0 \epsilon_1 \epsilon_2 \overline{W}(O^0) \quad (4)$$

where N_0 is the number of coincident pairs of gamma rays emitted by the source, ϵ_1 and ϵ_2 are the efficiencies for the detection of gamma rays 1 and 2, and $W(O^0)$ is a factor included to account

for the angular correlation of the two coincident gamma rays.¹⁵ A typical coincidence sum spectrum is illustrated in Fig. 19. This spectrum is characteristic of the radiation emitted by ^{94}Nb . In addition to the response of the detector to the two gamma rays individually, we also see the distribution of pulses resulting from coincidence summing. The most prominent feature of this spectrum is the so-called sum peak which results from total energy loss of both coincident gamma rays in the detector. The shape of the coincidence sum spectrum shown in the figure was calculated by convoluting the response of the detector to the two gamma rays. The method used to calculate coincidence sum spectra will be discussed in Section IX.

To demonstrate the effect of geometry on the magnitude of the coincidence sum spectrum, measurements with the source at 0.75 and 10.0 cm from the face of the detector are shown. The relative intensity of the sum spectrum is seen to be highly dependent upon source-detector geometry. As indicated in Eq. (4), the magnitude is proportional to the product of the detection efficiency for the

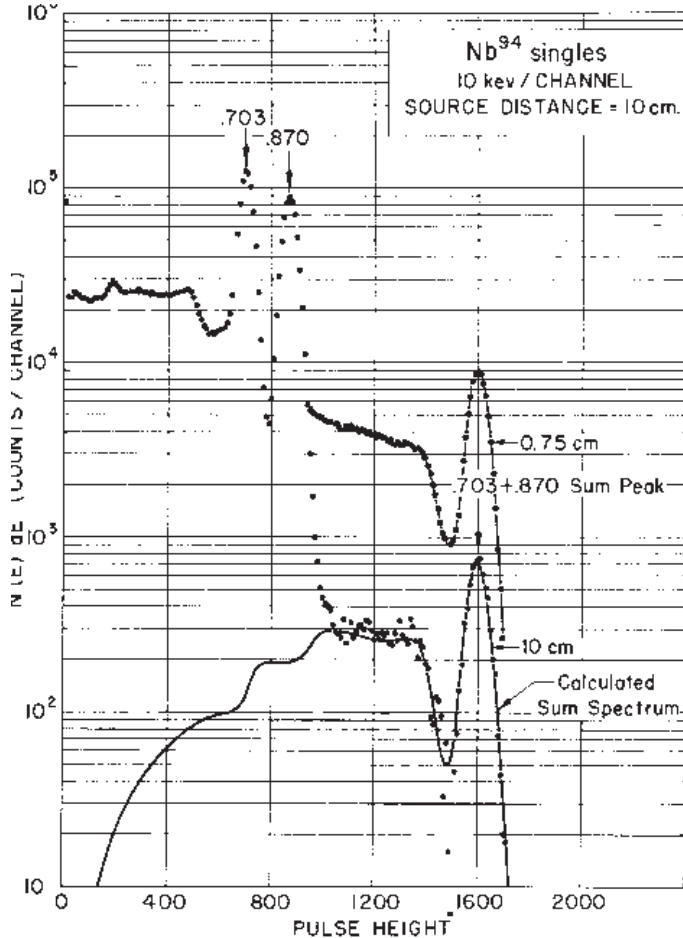


Fig. 19 - Spectrum of Nb^{94} showing coincidence sum spectrum and effect of source-detector geometry on intensity of sum spectrum.

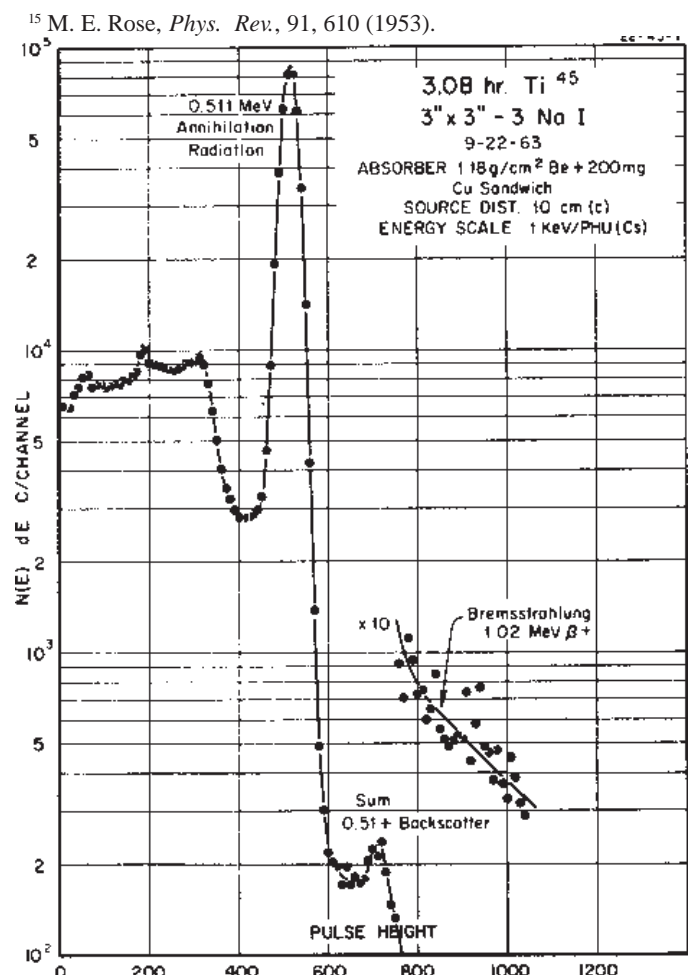


Fig. 20 - Pulse-height spectrum of 3.08-hr ^{45}Ti showing coincidence summing of annihilation radiation with 180°-scattered photons from the other annihilation quantum.

two gamma rays. From this it is evident that the analysis of complex spectra will be more complicated if the spectrum is measured under conditions of large solid angle. On the other hand, coincidence summing can be used to confirm coincidence relationships and offers a means of identifying nuclides whose spectra are characterized by prominent cascades. The coincidence sum effect was a major consideration in the adoption of a 10 cm source distance as the standard geometry for all spectra in the catalogue. At this reduced solid angle the sum spectrum can usually be neglected.

2. Annihilation Radiation

Sources which decay by positron emission represent a special case for coincidence summing. It is desirable to annihilate the positrons at the source in order to insure that the annihilation radiation will be detected in the same geometry as the other photons emitted by the source. This is achieved by surrounding the source with an absorber of sufficient thickness to annihilate the positrons. If one of the two annihilation quanta enters the detector, the other, which is emitted in the opposite direction, can be scattered from material surrounding the source. **Fig. 20** illustrates the resulting sum of these two events. In this spectrum we see a low intensity peak appearing at approximately 700 keV which is

due to the sum of pulses from the photopeak of the 0.511-MeV annihilation quantum and the backscattered radiation from the other member of the pair.

A discussion of the treatment of the coincidence sum effect in quantitative analysis of spectra appears in Section VII.

B. Random Sum Spectrum

If we re-examine the pulse-height spectrum of a mono-energetic source shown in **Fig. 10** (Section IV-B) in the region above the amplitude of the "photopeak," we see a continuous distribution of pulses extending to approximately twice the amplitude of the full-energy peak. This feature of the spectrum is due to accidental time-coincidence between events occurring in the detector. Since the processes of radioactive decay are completely random in time, and the resolving time of the electronic system finite, pulses from two events can overlap in time and the two events will sum in amplitude. The probability for accidental summing is given by:

$$I_{v.s.s} = N^2 2\tau \quad (5)$$

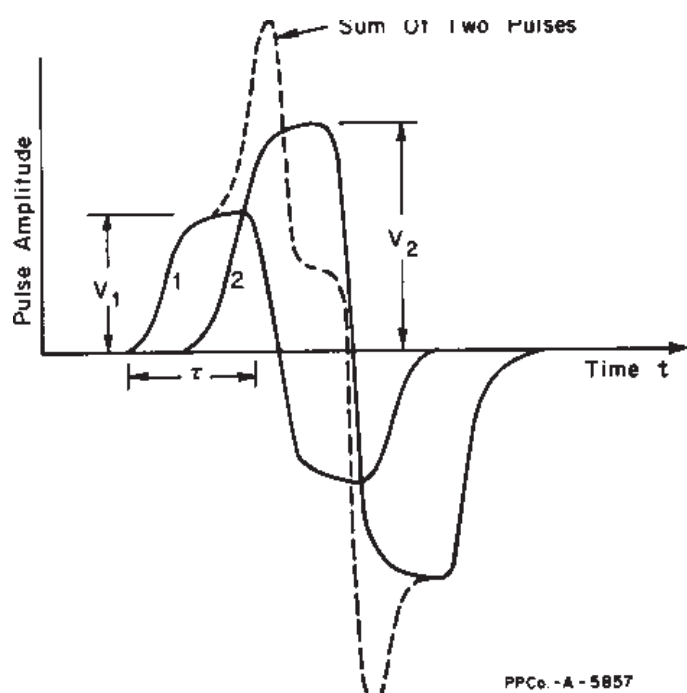


FIG. 21 - Illustration of the effect of superposition of two pulses within the sampling time of the analogue-to-digital converter. Variations in overlap will result in smearing of the random coincidence summation spectrum.

where N is the input pulse rate, τ is the resolving time of the electronic system, and I is the total number of pulses appearing in the summation spectrum. Pulses in this sum spectrum represent the detection of photons directly incident upon the detector and are considered as part of the energy response of the detector. Comparing the shapes of the random summation spectrum and the coincidence sum spectrum we see that the characteristic "sum peak" is not so pronounced. The degradation of the shape of the random sum spectrum is a result of variations in the time interval Δt between the leading edges of the two overlapping pulses. **Fig. 21** illustrates the superposition of two pulses which occur within the sampling time of the pulse-height analyzer. Two pulses, with amplitudes V_1 and V_2 , are shown partially superimposed in time. The sum of these two pulses is shown by the dashed line. Clearly, the shape of the resultant pulse will vary with the time interval between the two pulses and their respective amplitudes. The complex pulse which results can differ markedly from the normal pulse shape presented to the pulse height analyzer. Depending upon the method used in the analogue-to-digital converter to determine pulse amplitude, the recorded amplitude for such pulses can vary from $V_1 + V_2$ to the highest amplitude reached in the region of overlap. The result is the observed "smeared" pulse-height distribution.

As indicated in equation (5), the intensity of the random sum spectrum will vary as the square of the input counting rate. The variation in the intensity of the random sum spectrum with source intensity is indicated by the results of experimental measurements shown in **Fig. 22**.

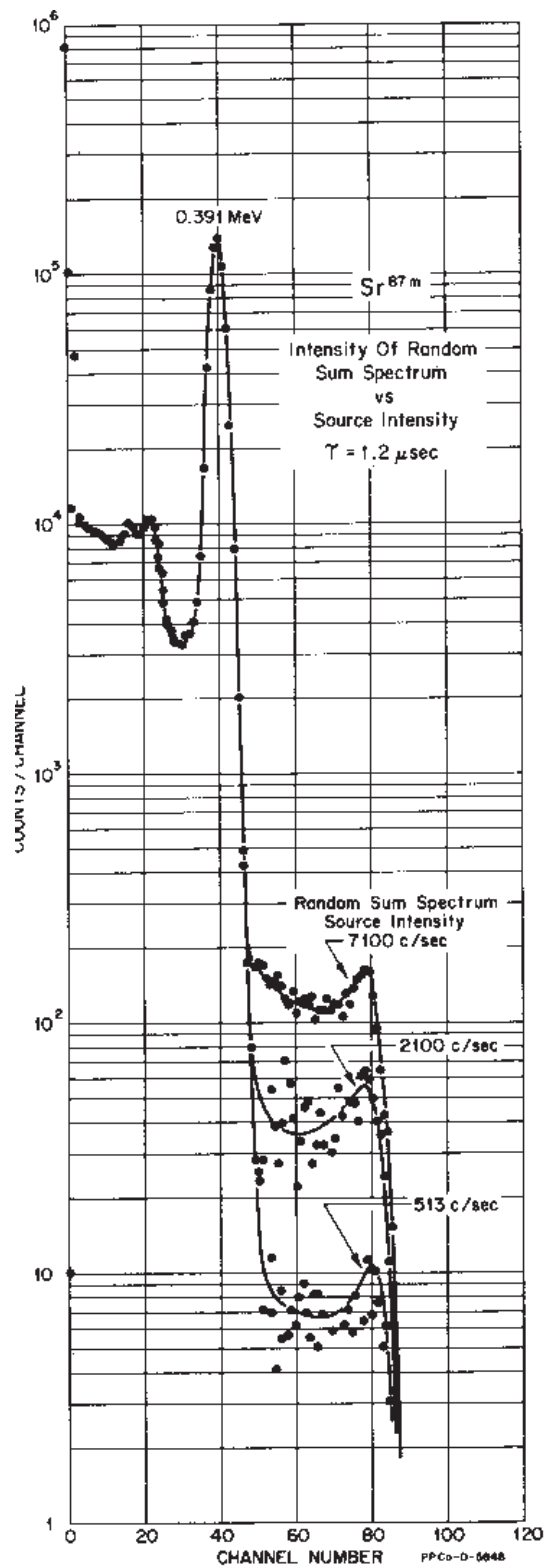


Fig. - 22 - Intensity of random sum spectrum vs count rate.

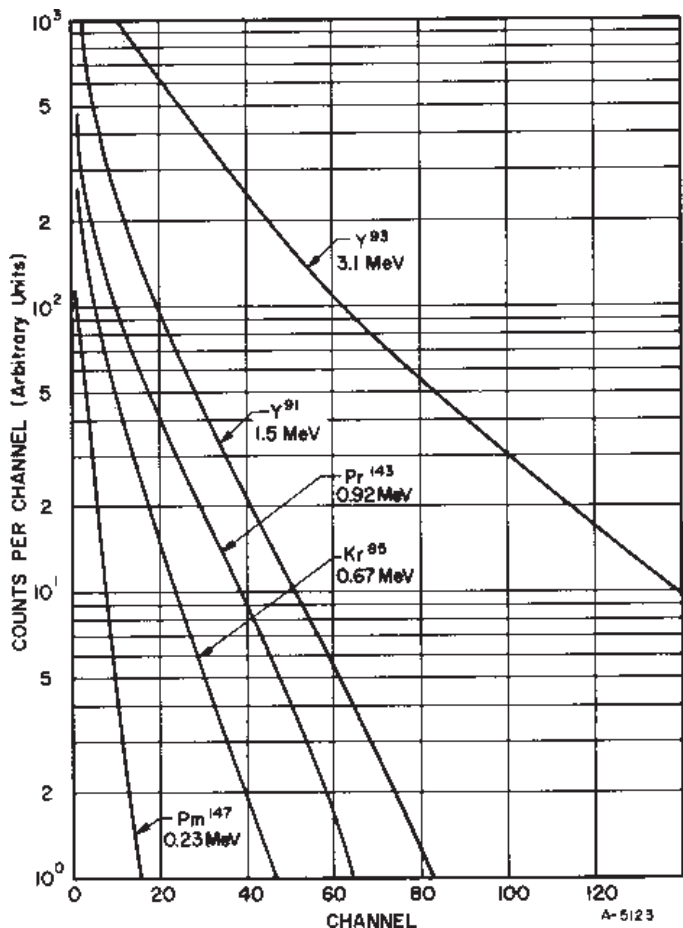


Fig. 23 - Typical bremsstrahlung spectra on a 3"x3" NaI detector. All spectra are normalized in intensity to 10^7 disintegrations.

VI. BREMSSTRAHLUNG

As electrons are stopped in an absorbing material, a certain fraction of their energy is radiated as bremsstrahlung. This process, which is the inverse of pair production, results from inelastic collision of electrons with nuclei. A continuous energy distribution of photons results which decreases rapidly in intensity with increasing energy up to the maximum electron energy. The probability for energy loss by radiative collision is proportional to electron energy and varies as the square of the atomic number, Z , of the absorbing material.

A set of typical bremsstrahlung spectra observed with a NaI spectrometer is shown in Fig. 23. A number of nuclides emitting essentially only one beta ray group were measured under the same experimental conditions. The disintegration rates of all sources were determined by 4π beta counting techniques to permit intensity normalization. The resulting bremsstrahlung spectra are normalized to 10^7 disintegrations of the source to provide an indication of the shape and intensity of bremsstrahlung distributions as

the energy of the beta-ray transition is increased. These data were obtained in the standard geometry using beryllium beta absorbers. As mentioned above, the choice of absorber is based upon the Z dependence for radiative collisions.

Although bremsstrahlung will be present in the spectra of all

VII. QUANTITATIVE ANALYSIS OF SCINTILLATION GAMMA-RAY SPECTRA

A. Detector Efficiency

The detection efficiency $T(E)$, the fraction of gamma rays emitted from the source which interact with the detector, can be calculated for known values of the absorption cross section $T(E)$ for NaI under a well defined source-detector geometry. Equations are derived for two cases: (A) a point source of radiation located on the extended axis of a right circular cylindrical detector and (B) a disk source whose center is on the extended axis of a right circular cylindrical detector with the plane of the disk parallel to the top surface of the detector. These are shown in Figs. 25 and 26. In these expressions t_0 is the thickness of the detector, r_0 is the radius of the detector, h is the perpendicular distance between the source and the top surface of the detector, and R is the radius of the disk source. Extensive calculations have been made by Vegors, Marsden, and Heath¹⁶ for point, disk, and line sources located on the central axis of the detector. These calculations are for 32 different detector sizes, for values of h from 0 to 100 cm, and for photon energies from 10 keV to 10 MeV. Curves and tables of calculated efficiencies for point, line, and disk sources for 3" diam. x 3" thick, 4" diam. x 4" thick, and 5" diam. x 5" thick cylindrical NaI detectors are given in Appendix II. The quantity $T(E)$, the absolute detection efficiency, obtained from these relationships, is the probability that a photon emitted from the source will interact in the detector with the loss of a finite amount of energy.

In a solid material such as NaI, which has a density of 2.67, the sensitive volume is very clearly defined. Since the amount of material which a secondary electron produced in the solid phosphor must traverse to leave a measurable amount of energy is negligible, edge effects are insignificant. Any error to be expected will be due to uncertainty in the value of τ used in the calculation. A plot of the percent error in detection efficiency versus percent error in absorption cross section for the detection of 0.32, 0.66, and 1.17 MeV gamma rays in a 1/4" thick x 3" diam. NaI phosphor is shown in Fig. 27. As one might expect, for small values of t , the detector thickness, the error will vary linearly with τ . Fig. 28 shows a similar plot for the 3" x 3" detector. In a large phosphor such as this, the error in detection efficiency due to an uncertainty in τ is reduced appreciably. Even at 1.11 MeV a 10% error in τ , which is considerably more than the expected uncertainty in the calculated values, will result in an error of only 5%. For lower energies the error will be considerably reduced.

beta emitters, the intensity is usually almost negligible. Exceptions are nuclides which have a very intense high-energy ground-state beta transition such as Y^{91} . The spectrum of this isotope is shown in Fig. 24. A number of pure bremsstrahlung spectra are included in the catalogue as an aid in the analysis of other spectra.

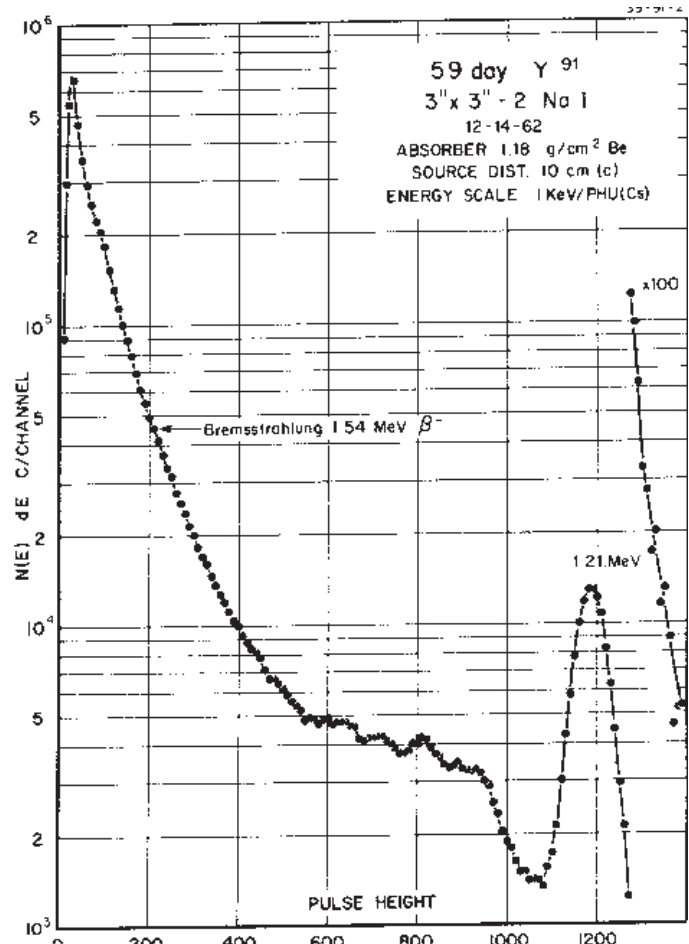


FIG. 24 - Pulse-height spectrum of radiations emitted by source of 58-day ^{91}Y showing contribution to spectrum from bremsstrahlung continuum.

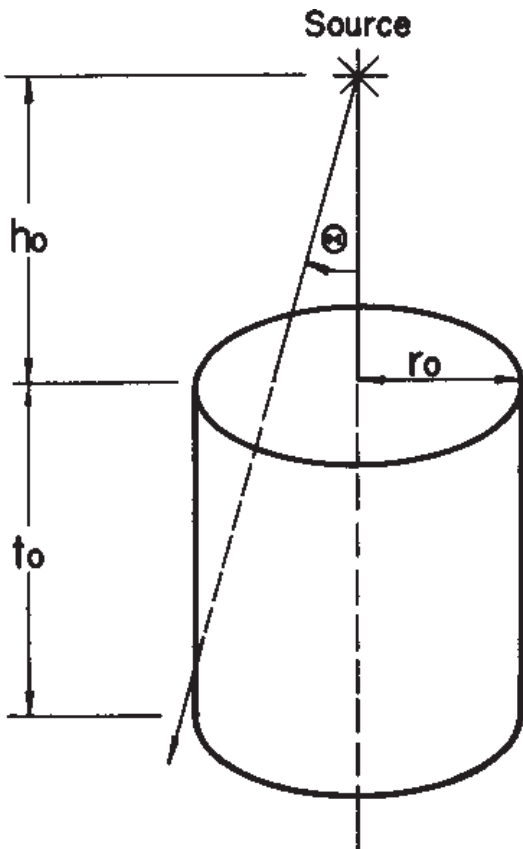
since the detector is almost opaque to gamma radiation of energy less than 300 keV.

The effect of varying the radius of a disk source on the detection efficiency for 0.661 MeV gamma rays is shown in Fig. 29.

B. Photopeak Efficiency

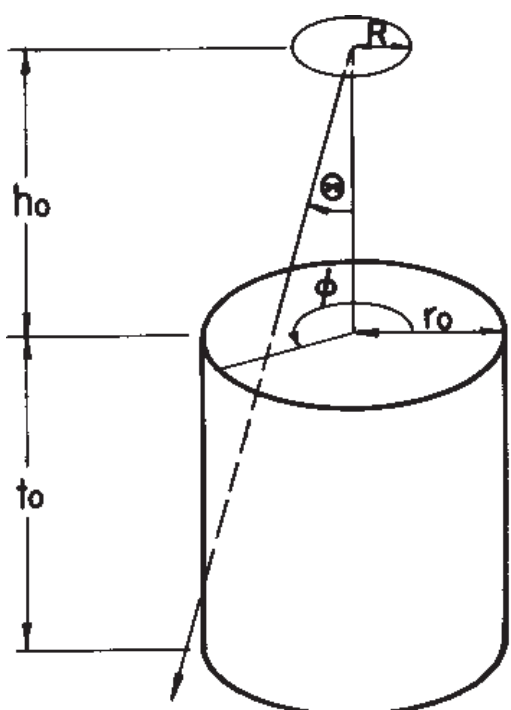
Consider a point source of radiation and a detector of specified size that is isolated from all material which might scatter into the detector gamma rays not originally emitted into the cone of solid angle subtended by the detector. The number of events in the observed pulse-height spectrum will then be related to the emission rate from the source by the expression given in

¹⁶S. H. Vegors, L. L. Marsden, and R. L. Heath, *Calculated Efficiencies of Cylindrical Radiation Detectors*, AEC Report IDO-16370 (1958).



POINT SOURCE

$$T(E) = \frac{1}{2} \left\{ \int_0^{\tan^{-1} \frac{r_0}{h_0+t_0}} \left[1 - e^{-\tau(E)} \frac{t_0}{\cos \theta} \right] \sin \theta d\theta + \int_{\tan^{-1} \frac{r_0}{h_0+t_0}}^{\tan^{-1} \frac{r_0}{h_0}} \left[1 - e^{-\tau(E)} \left(\frac{r_0}{\sin \theta} - \frac{h_0}{\cos \theta} \right) \right] \sin \theta d\theta \right\}$$



EXTENDED SOURCE

$$T(E) = \frac{1}{\pi R^2} \int_0^R x dx \int_{-\pi/2}^{\pi/2} d\phi \left\{ \int_0^{\tan^{-1} \frac{-x \sin \phi + \sqrt{x^2 \sin^2 \phi - (x^2 - r_0^2)}}{h_0 + t_0}} \left[1 - e^{-\tau(E)} \left(\frac{t_0}{\cos \theta} \right) \right] \sin \theta d\theta + \int_{\tan^{-1} \frac{-x \sin \phi + \sqrt{x^2 \sin^2 \phi - (x^2 - r_0^2)}}{h_0}}^{\tan^{-1} \frac{-x \sin \phi + \sqrt{x^2 \sin^2 \phi - (x^2 - r_0^2)}}{h_0 + t_0}} \left[1 - e^{-\tau(E)} \left(\frac{x \sin \phi + \sqrt{x^2 \sin^2 \phi - (x^2 - r_0^2)}}{\sin \theta} - \frac{h_0}{\cos \theta} \right) \right] \sin \theta d\theta \right\}$$

Fig. 26 - Expression for calculation of detector efficiency for disk source of radiation and cylindrical detector.

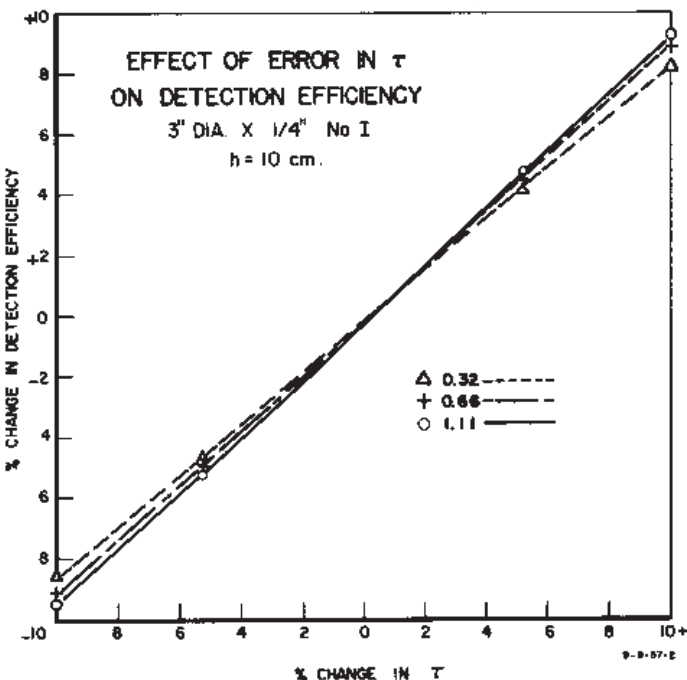


Fig. 27 Error in detection efficiency vs error in absorption coefficient for 3"x1/4" NaI detector ($h = 10$ cm).

the last section. From the preceding discussion of the contribution of scattered radiation to the detector response, it is evident that this relationship will hold only if this contribution can be removed. Since such radiation is of lower energy than the initial gamma ray energy, it is more convenient and precise to work in terms of the photopeak efficiency. This quantity, ϵ_p , is defined as the probability that a gamma ray of energy E , emitted from the source, will appear in the photopeak of the observed pulse-height spectrum. The value of this quantity is that most of the spurious contribution to the observed spectrum from scattering has virtually no effect on the photopeak. Thus the photopeak represents a more accurate measure of emission rate.

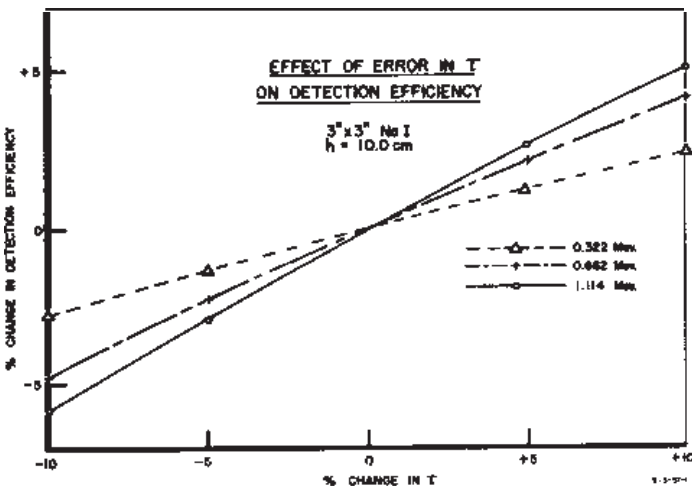


Fig. 28 - Error in detection efficiency vs error in absorption coefficient for 3"x3" NaI detector ($h = 10$ cm).

1. Peak-to-Total Ratio

It would be difficult to calculate ϵ_p directly because of the large number of multiple processes which occur in a scintillation detector. For this reason it is convenient to use the following expression:

$$\epsilon_p = T(E) P \quad (6)$$

where $T(E)$ is the calculated value for the absolute efficiency and the quantity P is defined as the fraction of the total number of events in the pulse-height spectrum which appear in the photopeak (the peak-to-total ratio). The peak-to-total ratio has been determined experimentally by careful measurement of selected sources under experimental conditions which reduce scattered radiation to negligible levels. An example is shown in **Fig. 30**. An alternative method is to determine the distintegration rate for sources using the $4\pi \beta-\gamma$ coincidence method¹⁷ and to calculate a value for the peak-to-total ratio from the integrated peak area in a spectrum obtained using the NaI detector. A plot of experimental values for the peak-to-total ratio, measured at this laboratory, for a 3" x 3" NaI detector as a function of energy is shown in **Fig. 31**. These experimental data are tabulated in Appendix III.

2. Absolute Emission Rate Determination

In this notation, the emission rate of a single gamma ray will be given by the following relationship:

$$N_o = \frac{N p}{T(E) P A} \quad (7)$$

where N_o is the number of gamma rays emitted from the source, N , (as shown in **Fig. 30**) is the area under the photopeak, $T(E)$ is the total absolute detection efficiency for the source-detector geometry used, P is the appropriate value for the peak-to-total ratio, and A is a correction factor for absorption of the gamma radiation by any beta absorber used in the measurement.

¹⁷P. J. Campion, National Academy of Sciences - National Research Council Publication No. 573, 24, (1958).

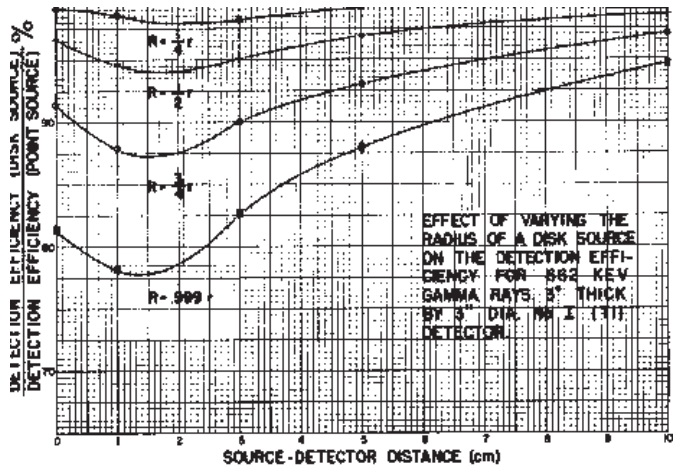


Fig. 29 - Detection efficiency for a 3"x3" detector (662 keV) as a function of source radius and distance from the detector.

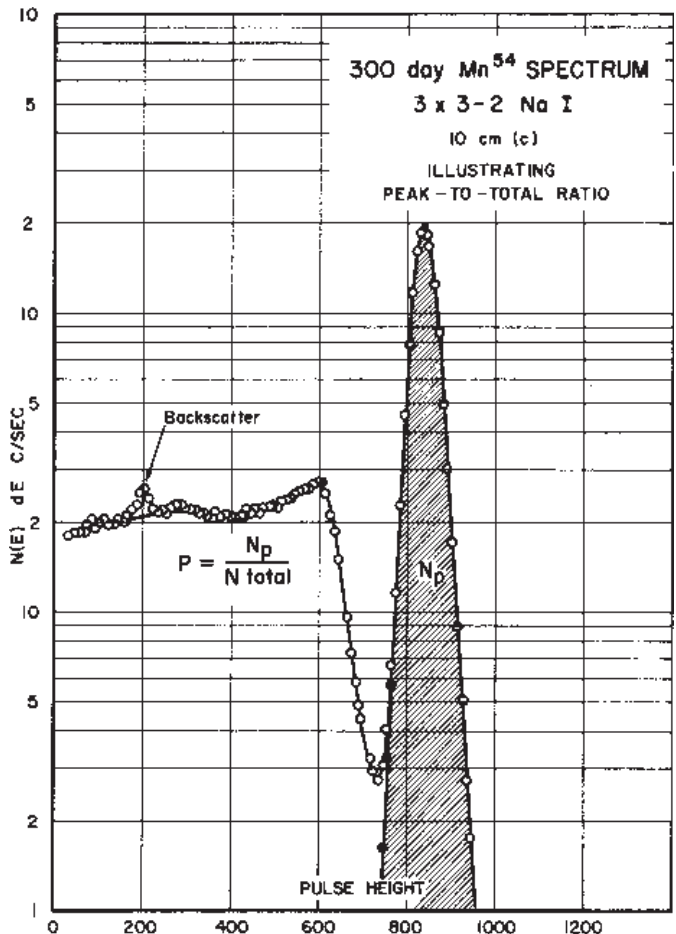


Fig. 30 - Illustration of Peak-to-total Ratio concept for NaI pulse-height spectrum.

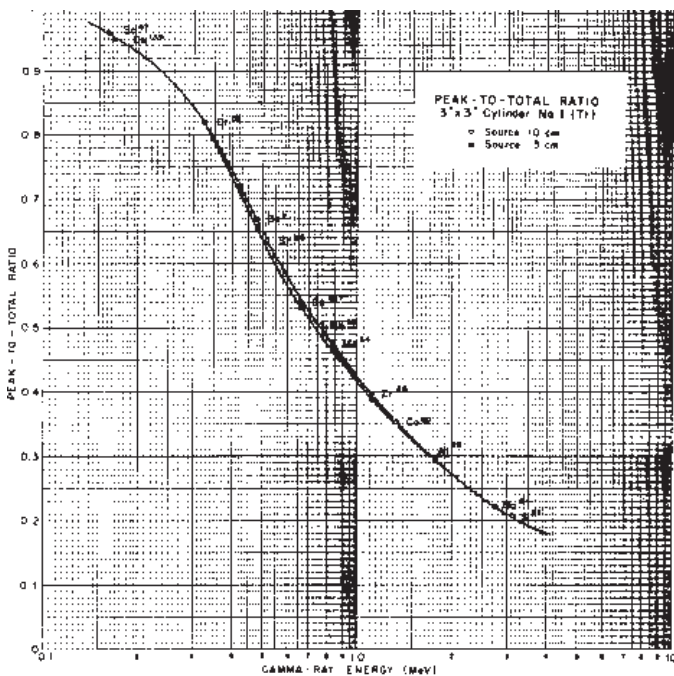


Fig. 31 - Peak-to-total ratio vs Energy for a 3"x3" NaI detector.

The absorption correction factor, A, for the standard set of beryllium absorbers used for all measurements is determined experimentally. It is necessary to determine the absorption correction for the particular geometry used rather than use values for the total absorption cross section of beryllium. Values of the total absorption cross section are generally reported for a highly collimated geometry. With the absorber placed directly on the top surface of the detector, the total absorption cross section does not represent the observed reduction in the intensity of the photopeak.

The results of an experimental determination of photopeak attenuation versus gamma-ray energy for a set of beryllium absorbers is shown in Fig. 32. These measurements were made with point sources in the standard geometry, with the absorbers positioned on the top surface of the detector. The absorption curve for a 1.18 g/cm^2 absorber, calculated from the total absorption cross section, is shown for comparison.

In the determination of the photopeak areas and the experimental measurement of the peak-to-total ratios, the region of the spectrum to be integrated must be well defined. Up to this point we have assumed that the photo peak could be satisfactorily described by a gaussian function

$$y(x) = y_0 e^{-(x-x_0)^2/b_0} \quad (8)$$

where y is the calculated count in channel x , x_0 is the pulse height at the center of the symmetrical distribution, y_0 is the number of counts per channel at x_0 , and the fullwidth at half-maximum of the peak is $w = 2\sqrt{\ln 2} \sqrt{b_0}$.

Fig. 33 shows the result of a fit to the photopeak of the ^{137}Cs gamma ray with a gaussian function. The solid circles indicate data points used in the fit. From this leastsquares fit to the data points, y_0 , X_0 , and b_0 , are determined. Examination of the figure shows considerable deviation from a gaussian shape on the wings of the peak. The residuals are plotted to show deviation. The low-energy tail is expected and is produced largely by multiple processes which do not result in full-energy loss. The residuals on the high-energy side of the peak are not expected and represent a problem in determining the peak area by leastsquares fitting techniques. The cause of this deviation from a gaussian shape is not completely understood and is observed to vary in magnitude for different detectors. For this reason it is thought to result from optical problems in the detector.

To account for this effect, an arbitrary functional form has been chosen to represent the photopeak response of the detector as a function of gamma-ray energy. It is given by:

$$y(x) = y_0 e^{-(X-X_0)^2/b_0} [1 + \alpha_1(x-x_0)^4 + \alpha_2(x-x_0)^{12}] \quad (9)$$

where the powers 4 and 12 were chosen to give the best fit and x_0 , y_0 , b_0 , α_0 , and α_2 are the parameters determined in the fit. These five parameters can be calculated in a non-linear leastsquares fitting program which has been written at this laboratory²⁹. Values for these parameters as a function of gamma-ray

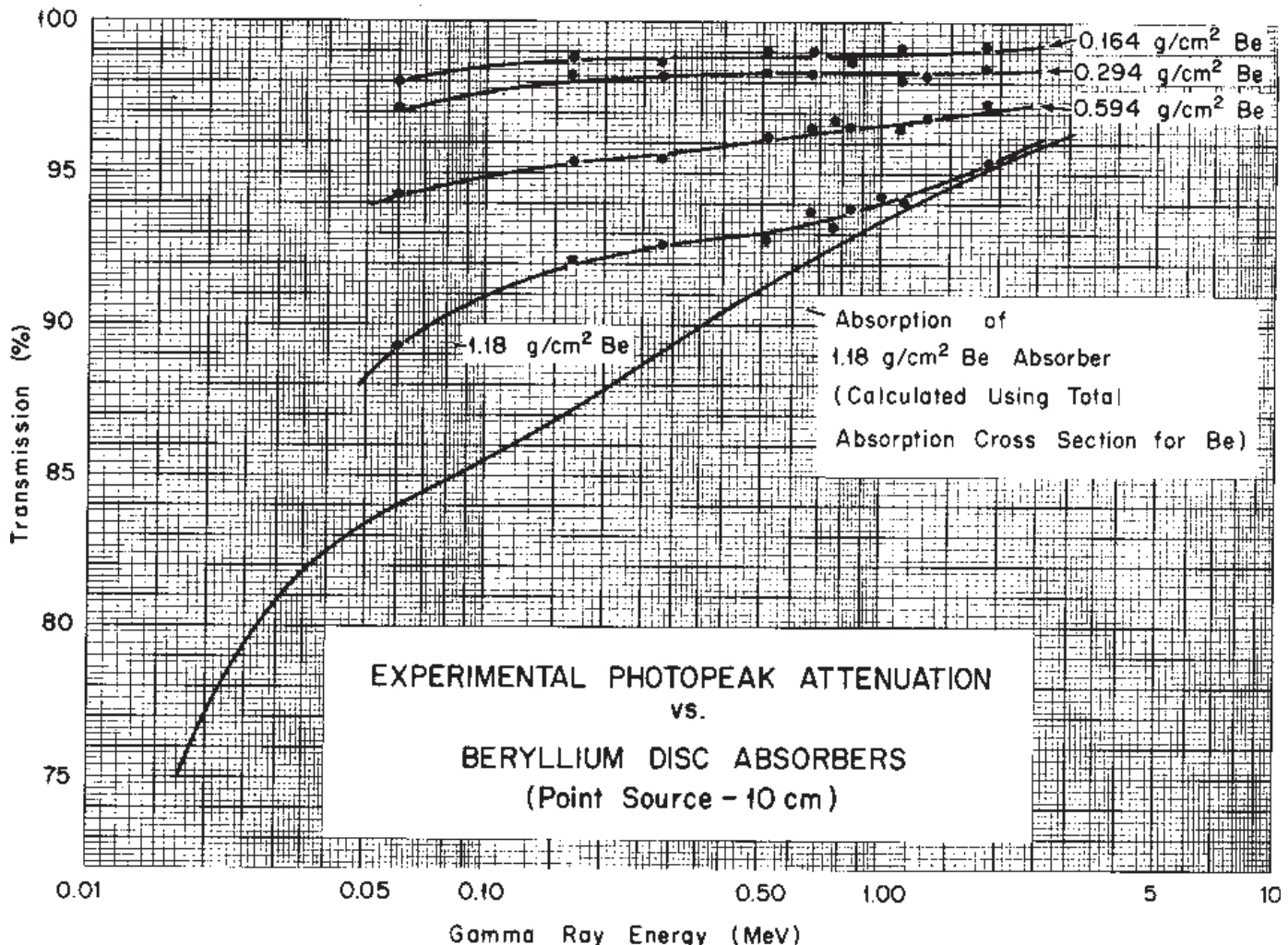


Fig. 32 - Results of experimental determination of photopeak attenuation for Be beta absorbers. These measurements were made for point sources of radiation at 10 cm distance from the detector. Absorbers positioned on top of cylindrical detector.

energy are determined by fitting photopeaks for a number of gamma-ray standards. A plot of α_1 and α_2 for the detector used to accumulate most of the spectra in the Catalogue (3"x 3" -2) are shown in Figs. 34, 35, and 36 for the 5 keV/channel and 10 keV/channel energy scales.

The photopeak area used is defined as the area obtained by fitting the experimental photopeak with the functional form described above. A simplified practical method for determining the photopeak area may be used which is based upon a symmetry requirement for the low-energy side of the peak. This method involves the construction of a set of parallel lines connecting data points on the high-energy side of the photopeak with corresponding points on the low-energy side. This will result in a family of parallel lines for points near the peak maximum. Once the slope of this set of parallel lines is established, points on the low energy side may be interpolated by extending the parallel lines down to include all points on the high-energy side of the peak. This procedure establishes the symmetry requirement and will produce results which agree very closely with those obtained from

the nonlinear least-squares fitting procedure.

For use with Eq. (7) it is convenient to combine the terms in the denominator. A plot of the product of these two quantities as a function of gamma-ray energy is shown in Fig. 37. The solid line represents the result of a least squares fit of a polynomial to experimental values of the product $\epsilon_p A$ for a number of monoenergetic gamma-ray sources. Note that the curve reaches a maximum at approximately 100 keV and then decreases in value. This is due to iodine x-ray escape from the surface of the detector which reduces the peak-to-total ratio. This is mentioned to stress that the peak-to-total ratio, as we define it, does not include the intensity of the escape peak.

To this point in the discussion we have considered only the case of a source which emits a single gamma ray. If more than one gamma ray is emitted and coincidence summing occurs then the problem is complicated. Although the effect of coincidence summing is somewhat difficult to analyze in every detail, the total

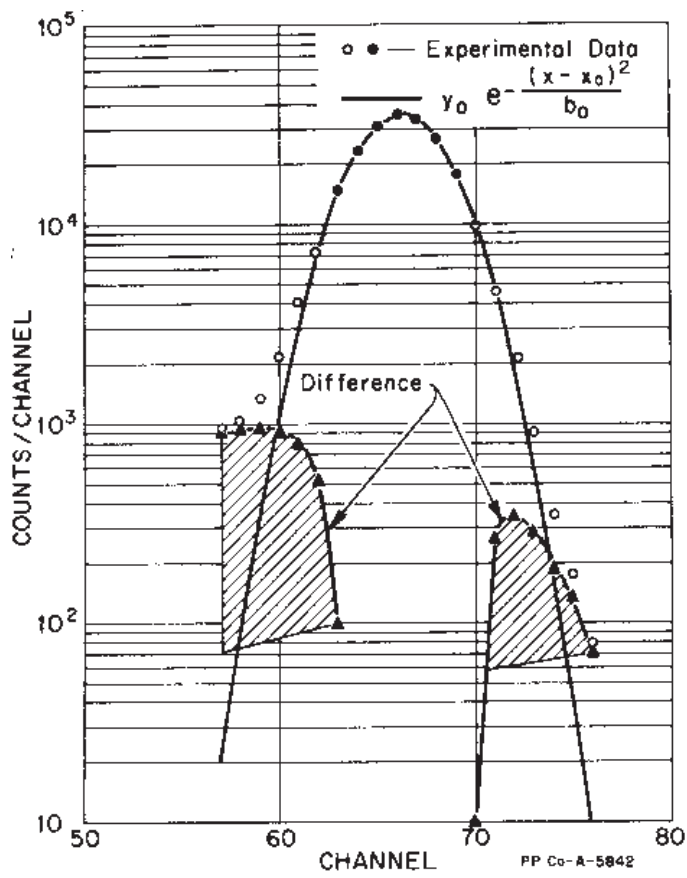
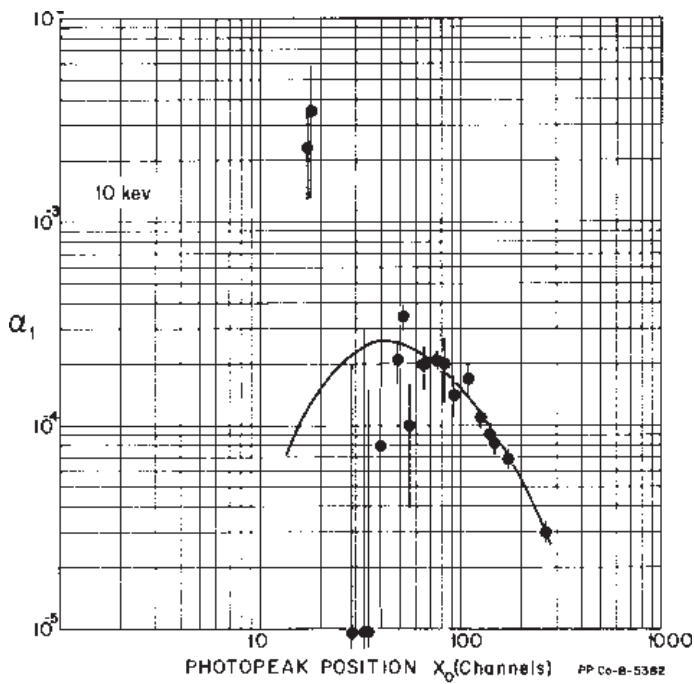


Fig. - 33 - Gaussian fit to experimental photopeak of Cs^{137} (0.662 MeV) showing deviation from functional



form.

Fig. 34 - Variation of the experimental parameter α_1 with gamma ray energy for the 10 keV/channel gain scale.

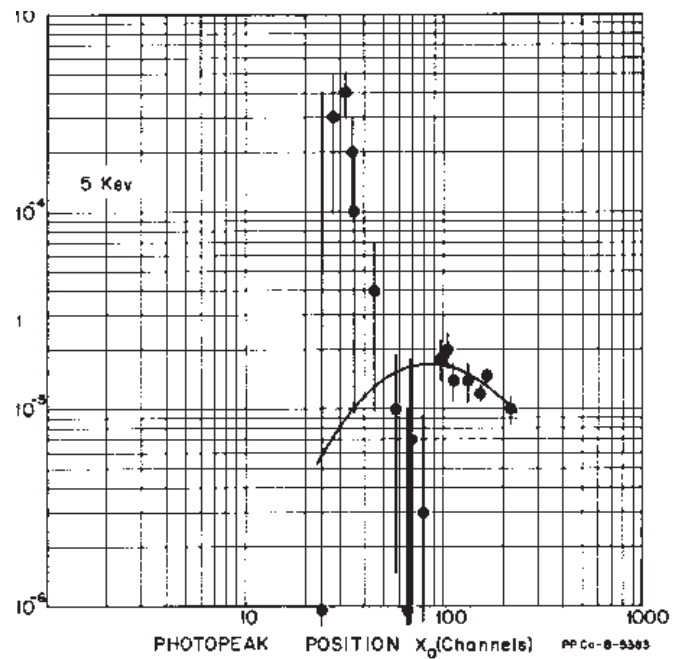


Fig. 35 - Variation of the experimental parameter α_1 with gamma ray energy for the 5 keV/channel gain scale.

area associated with the sum spectrum and the "sum spectrum" may be calculated from the known efficiencies and solid angle. Considering a simple scheme characterized by the emission of two cascade gamma rays (e.g., ^{60}Co) the emission rate of γ_1 will be given by equation:

$$N_1 = \frac{N_{p1} \overline{W}(0^\circ)}{A_{le1} P_1 [1 - \varepsilon_2 W(0^\circ) A_2]} \quad (10)$$

where N_{p1} is the area under the photopeak of γ_1 (with any contribution due to γ_2 or the sum spectrum subtracted), ε_1 and ε_2 are the total absolute efficiencies for γ_1 and γ_2 . P_1 is the peak-to-total ratio for γ_1 (experimental), A_1 and A_2 are the absorption corrections for the two gamma rays, and $W(0^\circ)$ is a factor to take into account the angular distribution function of the two gamma rays integrated over the face of the crystal, evaluated by the methods described by Rose.¹⁵ The third term in the denominator accounts for those pulses which would normally appear in the photopeak but, due to simultaneous detection of the other cascade gamma ray, appear in the coincidence sum spectrum. Another convenient expression is that for the area under the coincidence sum spectrum, or the probability that two coincident gamma rays will be detected simultaneously. This is given by equation (11)

$$N_{ss} = \frac{N_{p1} \varepsilon_2 A_2 \overline{W}(0^\circ)}{P_1 [1 - \varepsilon_2 A_2 \overline{W}(0^\circ)]} \quad (11)$$

VIII. EXPERIMENTAL MEASUREMENTS

A. Laboratory Scintillation Spectrometer

In this section the equipment, calibration procedures and experimental techniques used to obtain the data for the spectrum catalogue will be described. The experimental conditions adopted as standard for the catalogue spectra represent a reasonable compromise for the majority of routine applications for a scintillation spectrometer. This is with an understanding that the requirements for a specific measurement may require the modification of one or more parameters to achieve an optimum experiment.

1. The Detector

The 3" diameter x 3" thick cylindrical NaI detector was originally chosen as the standard reference detector for the spectrum catalogue. This choice was a compromise based upon the consideration of many factors. This size detector can be readily obtained as a package, integrally coupled to a photomultiplier, from commercial sources. These commercial units can now be obtained with an energy resolution for the 0.662-MeV gamma ray of ^{137}Cs of 7.5 to 8.0 %. The volume of a 3"x 3" detector is sufficient to give a reasonable photopeak efficiency in the energy region associated with radioactivity. To obtain appreciable improvement in the photofraction, one would have to consider increasing

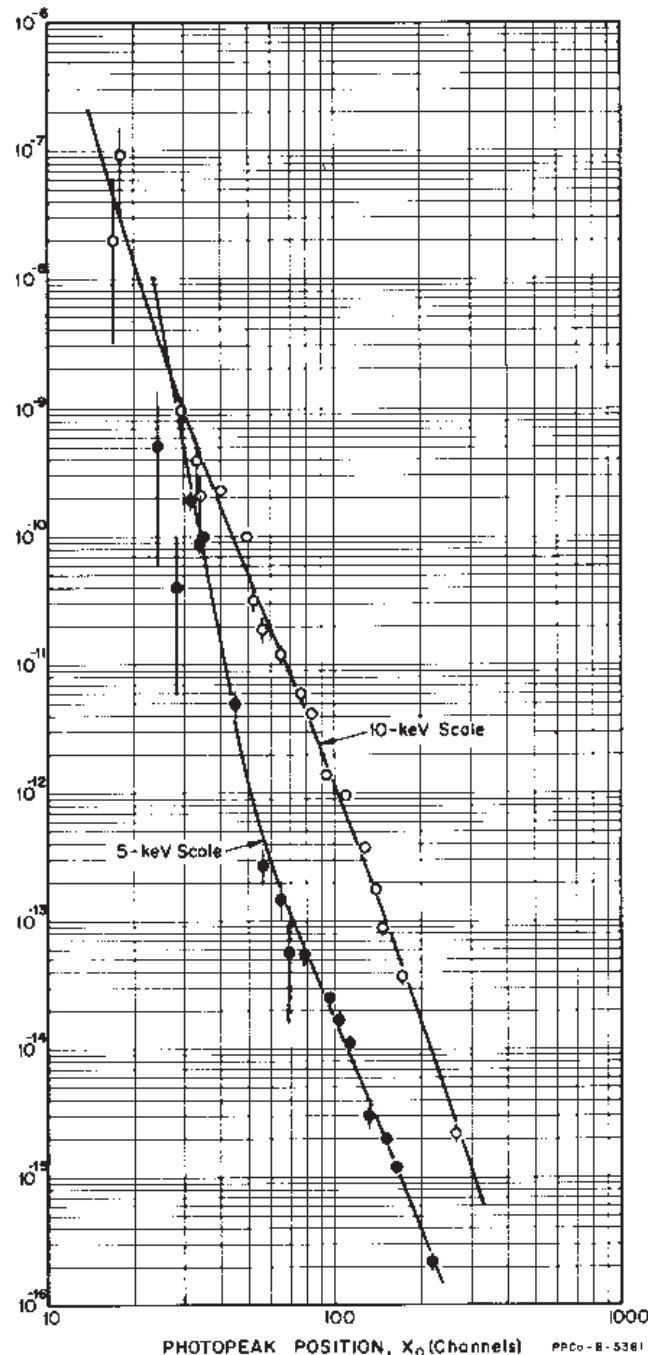


Fig. 36 - Variation of the experimental parameter a_2 with gamma-ray energy for both the 5 and 10 keV/channel gain scales.

the detector size to a 5" diameter x 5" cylinder or larger. These larger detectors are not only considerably more expensive, but usually exhibit poorer resolution. Although larger detectors are in use in this laboratory and much data has been obtained with 5"x 5" detectors, the 3"x 3" detector is still considered to be the best detector for most applications.

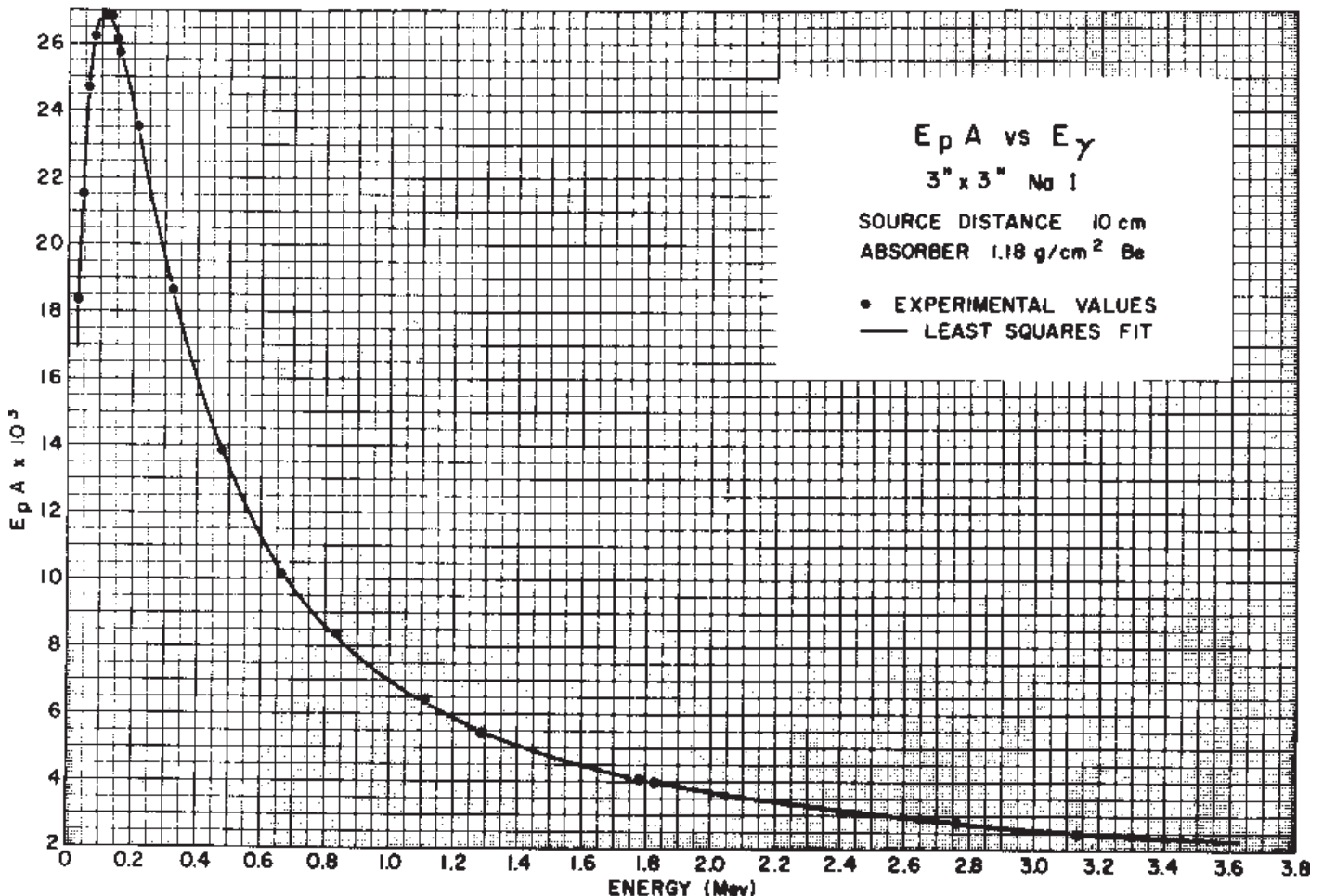


Fig. 37 - Least-squares polynomial fit to experimental values for $E_p A$ for 3" x 3" NaI Detector

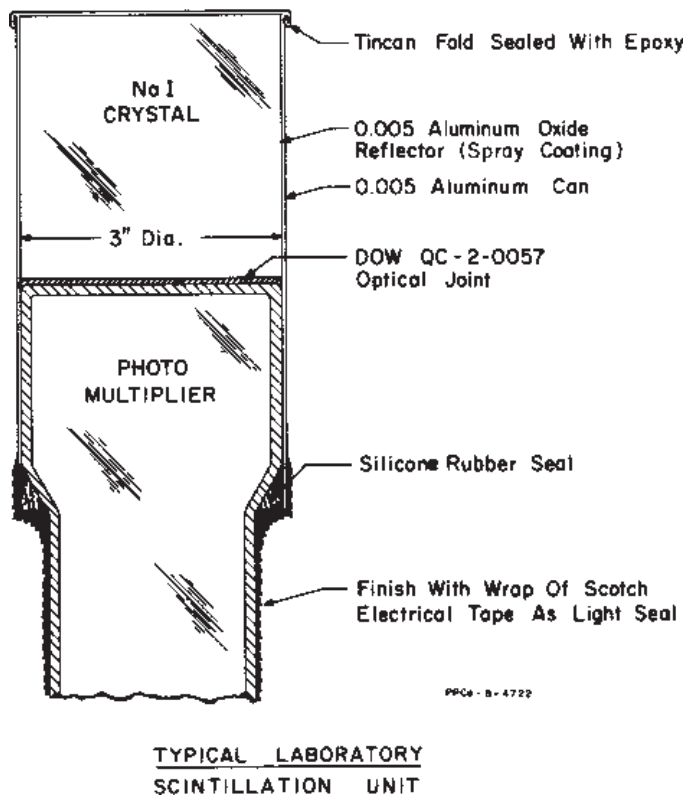
The detectors used to obtain all spectra included in the catalogue were fabricated in this laboratory using the packaging technique shown in Fig 38. The NaI crystal is contained in a thin-walled aluminum can (0.005" wall thickness) to reduce absorption of low energy photons and to prevent excessive Compton scattering from the packaging material. The optical reflector is a 0.005" thick sprayed coating of α -alumina. The crystal is mounted directly on the face of an RCA 8054 electron multiplier, optically coupled with silicon grease (Dow QC-2-0057), and the entire assembly evacuated. A mu-metal shield surrounds the dynode structure of the phototube to reduce the effect of stray magnetic fields. Energy resolution for detectors used varies from 7.0% to 8.1%. A drawing of a typical commercial detector package is shown in Fig. 39. The major difference between the two packaging techniques is in the quantity of packaging material used. For this reason quantitative application of a commercial detector would require the determination of the following parameters:

- (1) this distance from the top of the crystal to the top of the can to establish accurate source-detector geometry, and
- (2) the effective absorber thickness for the can and packaging material separating source and detector. This is particularly necessary if the detector is used for quantitative measurements of low-energy photons.

The distance from the top of the crystal to the outside of the package can be determined by radiographing the detector package with an x-ray machine or radioisotope camera. A typical radiograph of a commercial 3"x3" detector package is shown in Fig. 40. The typical separator between the surface of the detector and the outside surface of the can (4 - 8 mm) has recently been reduced by most manufacturers to approximately 3 mm. Some manufacturers will now supply this information with each detector package if requested.

The scintillation detector is mounted in a photomultiplier base which includes the source holder as shown by a photograph in Fig. 41. For a detailed description and drawings of this detector base and source holder, the reader is referred to a recent report which describes testing and calibration procedures for scintillation spectrometers.¹⁸

¹⁸ D. F. Crouch and R. L. Heath, *Routine Testing and Calibration Procedures for Multichannel Pulse Analyzers and Gamma-ray Spectrometers*, IDO-16923 (1963).



TYPICAL LABORATORY SCINTILLATION UNIT

Fig. 38 - Laboratory scintillation detector packaged in 0.005" Al can.

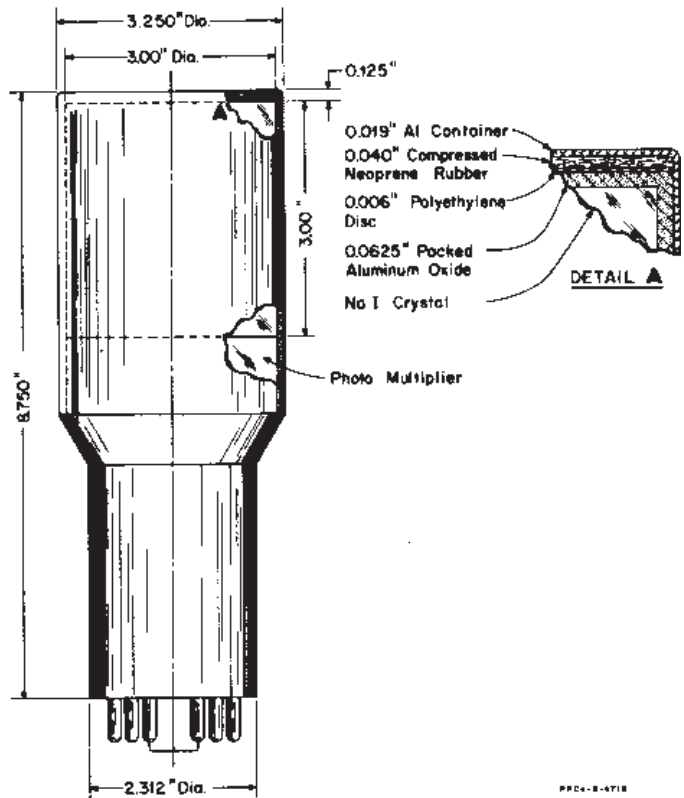


Fig. 39 - Typical commercial scintillation detector (3"x3") showing details of packaging technique. The increased mass of material used in the packaging of these detectors will produce some distortion of the spectrum due to scattering.

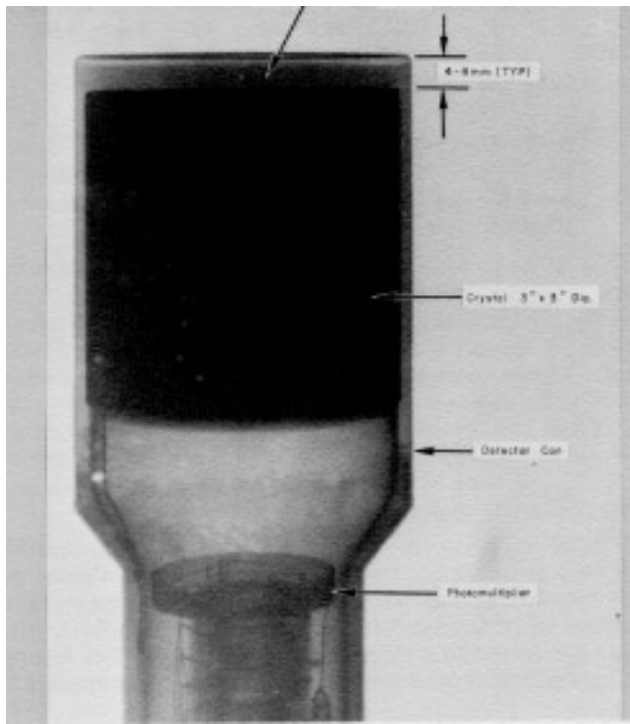


Fig. 40 - X-ray photograph of commercial 3"x3" NaI detector illustrating method used to locate position of crystal inside container.

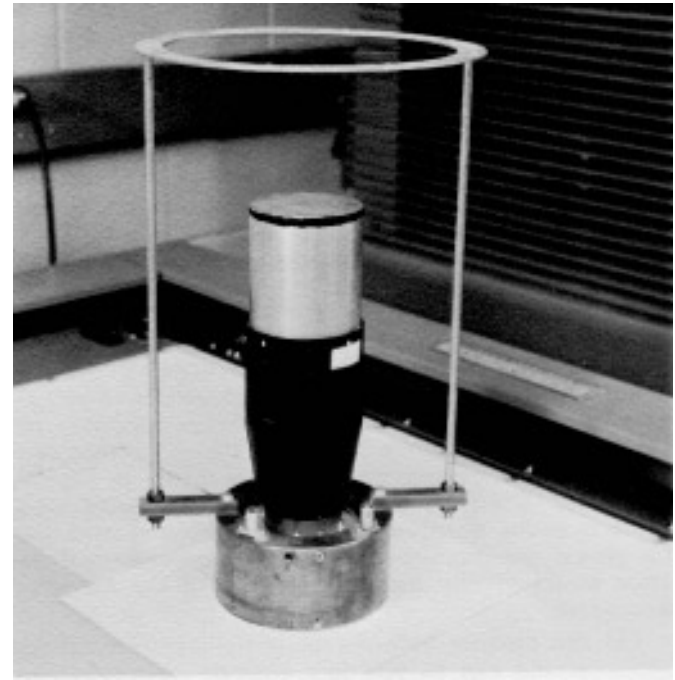


Fig. 41 - Photograph of standard laboratory detector showing source holder used to minimize scattering geometry.

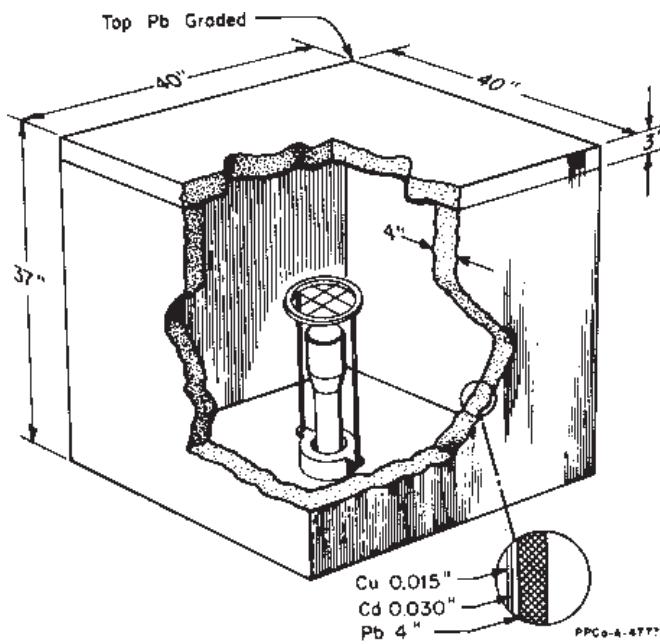


Fig. 42 - Standard laboratory detector shield used for experimental measurement of all spectra in the Spectrum Catalogue.

Unless otherwise stated, all spectra in the catalogue are measured in this geometry (point source at 10 cm).

2. Detector Shield

The standard detector shield enclosure used for the measurement of all spectra in the catalogue is shown in **Fig. 42**. This shield has inside dimensions of 32"x32"x 32". As indicated in the figure, the interior of the shield is lined with 0.030" Cd sheet and 0.015" Cu sheet in that order.

3. Electronics

The laboratory scintillation spectrometers used for all experimental measurements utilized the commercial components listed below:

- Photomultiplier Power Supply - Fluke Model 412A or Power Designs Model HV-1565.
- Linear Amplifier - An external vacuum tube amplifier (ORNL-type A-8) is used in the analyzer systems in preference to the amplifiers supplied as an integral part of the analyzer. This amplifier employs delay-line double-differentiation to produce a bi-polar output pulse similar to that shown in **Fig. 43**. The advantage of a double-differentiated amplifier is improved overload characteristics and negligible bias shift at high input counting rates.
- Multi-channel Pulse-height Analyzer - Nuclear Data Model 130-AT 512-channel analyzers were used for all measurements.

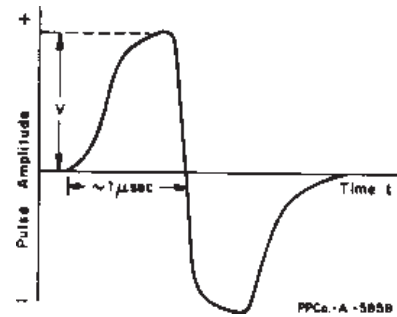


Fig. 43 - Output waveform from double-differentiated linear pulse amplifier.

- Digital Read-in and Readout Equipment - Tally Model 424 Paper Tape Reader and Tally Model 420 Paper Tape Punch.

A photograph of a typical analyzer system is shown in Fig 44. In addition to the equipment listed above, the system also includes a total count scaler for the determination of input counting rates and protective circuitry for monitoring over-voltage on the power bus²¹, and the output of the phototube Supply²¹.

For a detailed description of the testing and calibration procedures and performance specifications recommended for gamma-ray spectrometry, the reader should consult reference 18.

4. Source Preparation

To reduce the possibility of scattering, sources are prepared to approximate a weightless point source as nearly as possible. The two types of source mounting arrangements used are shown in **Fig. 45**. The source mounting card (Type A) is fabricated of paperboard and the source deposited between layers of cellulose tape ($\sim 10 \text{ mg/cm}^2$). The source mounting ring (Type B) is used for special sources where bremsstrahlung production or scattering must be reduced as much as possible (e. g., experimental determination of peak-to-total ratios).

¹⁹ Note: The listing of the products of manufacturers does not indicate a specific endorsement of a product, but only indicates that these products meet the rigid specifications established for this application.

²⁰ K. F. Smith, "Overvoltage Protector for High Voltage Power Supplies," *MTR-ETR Technical Branches Quarterly Report, 1st Quarter 1962*, IDO-16781 (1962).

²¹ K. F. Smith, "Line Surge Protector," *MTR-ETR Technic, Branches Quarterly Report, 4th Quarter 1961*, IDO-16760 (1962).

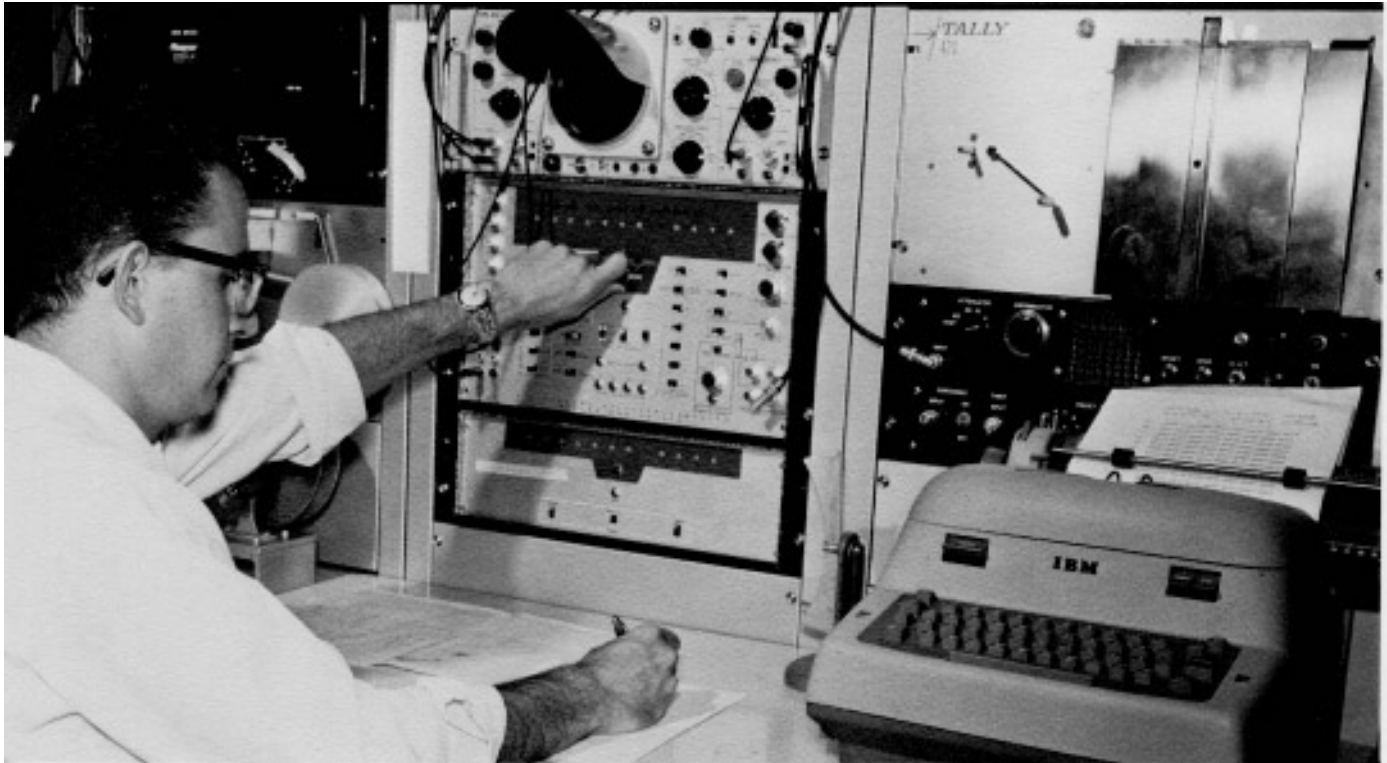


Fig. 44 - Photograph of one of the scintillation spectrometers used to obtain data for the Spectrum Catalogue.

To illustrate the importance of scattering from the source mount and source holder a series of measurements were conducted with sources of ^{141}Ce . Sources were prepared on the two types of source mounts described above and measurements made on each source on two 3"x3" detectors equipped with the two types of source holders shown in **Fig. 16** (source holder A) and **Fig. 41** (source holder B). The cardboard mounting is referred to as Type 1 and the thin film ring as Type 2. The results of these measurements, which appear in **Fig. 46**, show that most of the scattering from the source mount and holder assemblies appears as a contribution to the low-energy side of the photopeak. As the mass of scattering material in the immediate vicinity of the source is reduced, the contribution to the spectrum from scattering is likewise reduced. The purpose of these measurements was to illustrate the magnitude of this effect.

In the case of positron emitters, annihilation of positrons is localized to the position of the source by surrounding the source material with a Cu sandwich of sufficient thickness to stop most of the positrons. This is necessary to maintain the standard point source geometry for annihilation radiation. If the positrons are allowed to annihilate throughout the volume of the shield, the detection efficiency will be undefined. The use of the Cu sandwich will result in some deterioration in the quality of the spectrum as a result of Compton scattering.

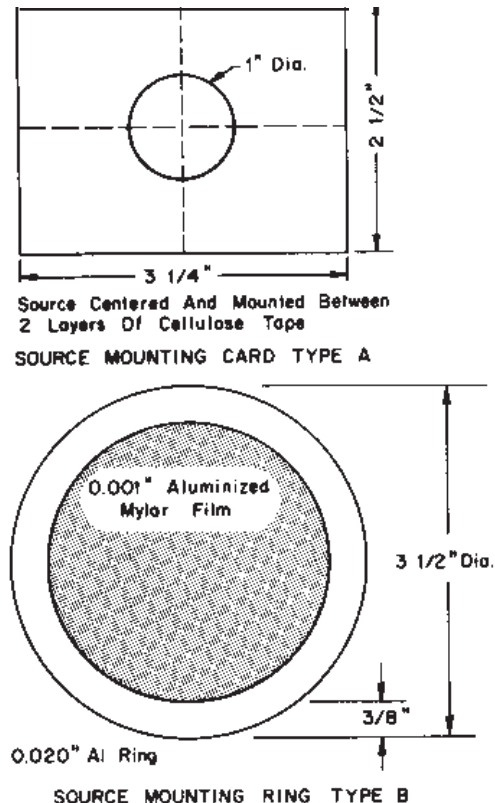


FIG. 45 - Examples of source mounting arrangements used.

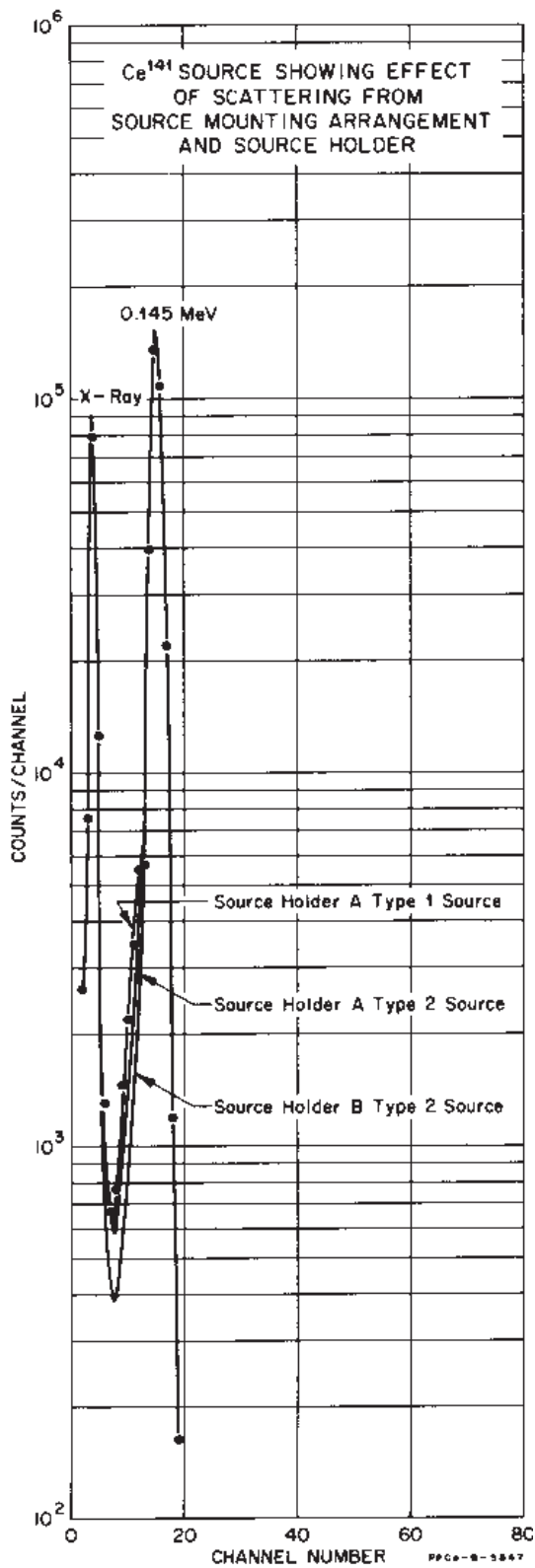


Fig. 46 Effect of scattering from source mount and source holder.

In the preparation of sources for catalogue spectra, considerable effort is expended to insure isotopic purity of the source. First, the possible methods for producing a given isotope are studied. Factors to be considered include: interference from other isotopes of the same element, half-life, possible elemental contamination of the material being irradiated, and production cross sections for the various nuclear reactions which may occur in the irradiation of a given material. In the production of sources by neutron capture, the choice of flux level and neutron spectrum is made after a consideration of competing processes [e.g. double neutron capture, (n,p) reactions, etc.]. In accelerator irradiations, the energy of the bombarding particle is important since several competing reactions are generally possible which are energy dependent. Operating parameters for the accelerator are chosen to enhance the relative production of the desired nuclide. The chemical form of the target material will depend upon the chemical procedures which are used in the purification of sample material following irradiation.

In many cases, high cross sections for some isotopes require the use of mass separated material to reduce interference when producing other isotopes which have relatively low cross sections.

The procedure usually followed in the production of sources is to make preliminary irradiations and then observe the energy spectrum of the irradiated sample as a function of time. In many cases obvious elemental contaminants can be removed by chemical separation. From half-life determinations and comparison of the observed energy spectrum with available nuclear data, all isotopes present in a given spectrum can usually be identified. If no interference from other isotopes is indicated, sources can be prepared in final form and the spectrum measured under the standard experimental conditions.

If chemical purification is necessary, solvent-extraction and ion-exchange methods are preferred since the mass of inert material in the source will usually be much less than with wet chemical procedures. In many cases carrier-free samples can be obtained with these techniques.

5. Data Preparation

For presentation in the catalogue, spectrometer data are prepared as point plot (semi-log) of the number of counts accumulated in each channel ($N(E)dE$) vs channel number. These graphs are prepared as templates to overlay the standard 8 1/2" x 11" or 11" x 17" K and E 3-cycle semi-log graph paper. The graphs were then printed on translucent paper to permit removal of spectra from the catalogue for comparison with experimental data plotted in a similar manner.

Experimental conditions used are listed with the experimental data for each spectrum. Included are the source-detector geometry, energy scale, and the beta absorber used in the measurement. A number of spectra have been analyzed to obtain an intensity normalization. For nuclides emitting a single gamma ray, the "photopeak" is fitted by least squares methods and the

total number of gamma rays emitted are obtained with the quantitative procedures discussed in Sections VII and IX. For nuclides emitting more than one gamma ray, the spectrum is analyzed to obtain the intensity of a prominent gamma ray. Appropriate corrections are made for geometry, photopeak efficiency, absorption, and coincidence summing effects. These results can be used to obtain decay rates when the decay scheme is well established.

B. Energy Calibration

1. Zero Convention for Pulse-height Scale

A well defined pulse-height scale is essential for reproducible precision energy measurements with a scintillation spectrometer. Perhaps the most important consideration in establishing a reproducible pulse-height scale is the convention adopted for setting the position of the zero position of the ADC (analogue-to-digital converter) in the analyzer. The convention adopted in this laboratory is to set electrical zero at - 0.5 channel.

Since a channel represents a band of pulses from V to $V + \Delta V$, the total number of pulses in a given channel i will be

$$N_i = \int_V^{V + \Delta V} n(V) dV \quad (12)$$

where V is the amplitude corresponding to the lower edge of the channel and ΔV is the channel width. If the channels are non-overlapping the average amplitude for a continuous function $n(V)$ will be approximately equal to the point at the center of the channel. This means that an observed channel count rate is considered as a measure of the count rate for pulses corresponding in amplitude to the center of the channel. If the first data channel is called channel 1, it will contain a range of pulse amplitudes from 0.5 to 1.5. Pulses with amplitude less than 0.5 will not be recorded. On this scale, zero pulse amplitude corresponds to -0.5 channel and channel 50 covers a range from 49.5 to 50.5 on an amplitude scale. The use of this scale makes the relative amplitude of two pulses independent of the zero reference. This scale is illustrated in Fig. 49. If the system is linear, there will be a one-to-one correspondence between channel number and pulse amplitude.

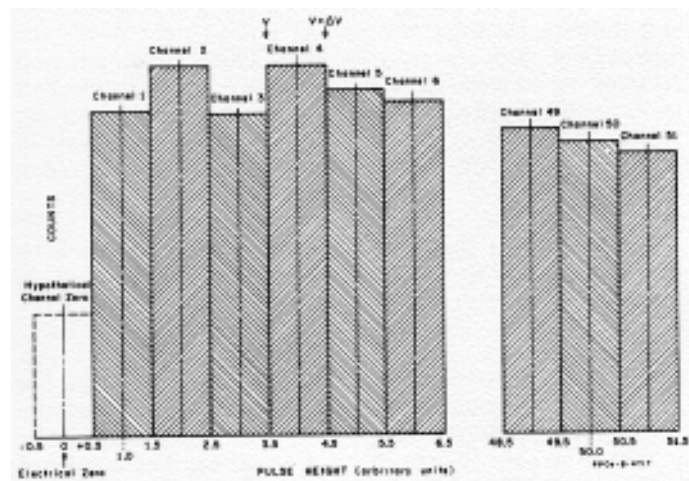


Fig. 49 - Histogram of pulse-height scale illustrating procedure for establishing zero position of pulse analyzer.

The method of zero alignment is achieved in the following manner: the voltage adjustment on a precision mercury-relay pulser is adjusted to obtain equal numbers of pulses in channels 199 and 200. This corresponds to the upper edge of channel 199. This adjustment is made with the decade potentiometer control on the pulser set at 199.5. The potentiometer control is then adjusted to 19.5. The zero control on the analyzer is then adjusted to obtain equal numbers of pulses in channels 19 and 20. This procedure is repeated until the slope and intercept of the pulse-height scale are determined. If the analyzer circuitry were absolutely linear the zero intercept would then be -0.5 channel. The upper edge of channel 19 was chosen because serious non-linearity exists in the bottom 10 channels of many analyzers. The linearity check described above can be used to evaluate the actual channel position to be expected for pulses of small amplitude.

2. Non-linear Energy Response of NaI

The nonlinear energy response of NaI to gamma radiation has been discussed in detail by several authors.^{22,23,24,25}

In any systematic treatment of data from NaI spectrometers it is essential that an absolute pulse-height vs energy scale be established. For a given experimental arrangement this scale depends on the light output from the detector as a function of E_{γ} (dL/dE), and the linearity of the electronic system. A determination was made of the pulse-height vs energy scale for the experimental arrangement employed to collect data for the catalogue.

A series of radioactive sources emitting gamma rays of precisely known energies were measured together with the ^{137}Cs gamma ray as a reference. The absolute pulse-height scale described above was used for these measurements. Least-squares fitting techniques were used to determine the photopeak posi-

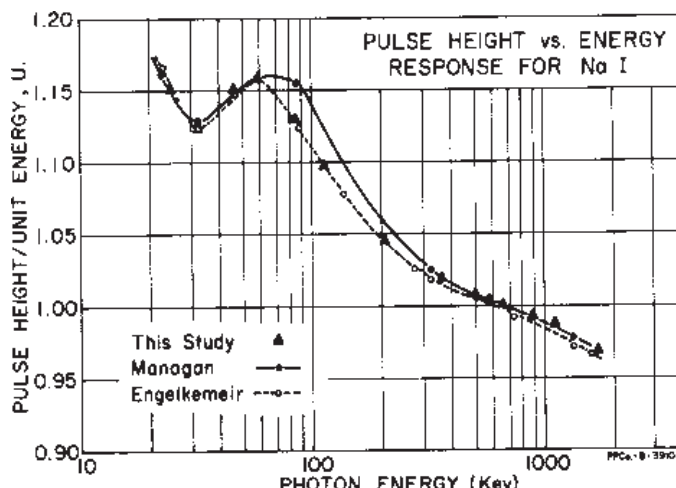


Fig. 50 - Pulse-height vs. gamma-ray energy response of 3"x3" NaI detector. To correspond with the energy scale adopted, all data are normalized to unit light output at 0.66162 MeV (^{137}Cs).

²²R. W. Pringle and S. Standhill, Phys. Rev., SC, 762, (1950).

²³D. Engelkemeir, Ret., Sci. Instr., 27, No. 8, 589, (1956).

²⁴P. Iredale, IAEA Report, AERE-R3440.

²⁵W. C. Kaiser, S. I. Baker, A. J. McKiv, and L. Shermin, IRE Trans. on Nuclear Science, Vol. NS-9, No. 3, (1962).

tions to an accuracy of 0.03 channels. The zero position and integral linearity of the electronic system were determined with a calibrated pulser. For the system used (A-8 amplifier and ND 130A analyzer), deviations from a straight line passing through the origin (channel zero) did not exceed 0.5 channels over a range of channel 5 to channel 250. The results of these measurements are tabulated in Table 11. **Fig. 50** shows a comparison of the experimental values obtained for L/E vs E_γ with those of Engelkemeir²³ and of Managan²⁶. Results for the detector used agree very closely with those of Engelkemeir. Similar measurements, using several commercial detectors, have indicated some variation in response below 100 keV. For this reason, the determination of the pulse-height vs energy response for a given detector must include a measurement of the nonlinear response for that detector.

For convenience, conversion tables between energy and pulse-height for the standard 10 keV/channel gain scale are presented in Appendix II.

TABLE I

Measured values of PH/E as a function of gamma-ray energy

	Gamma-Ray Energy	PH/E
²⁴¹ Am	0.05957	1.158
¹⁷⁷ Lu	0.11297	1.0943
¹⁷⁷ Lu	0.20836	1.0435
¹³¹ I	0.36447	1.019
⁷ Be	0.478	1.011
²⁰⁷ Bi	0.5695	1.006
¹³⁷ Cs	0.66162	1.000
⁸⁸ Y	0.8989	0.9893
²⁰⁷ Bi	1.0637	0.9854
⁶⁵ Zn	1.114	0.9828
⁸⁸ Y	1.837	0.9677
²⁴ Na	2.7535	0.958

²⁶ W. W. Managan in Applied Gamma-ray Spectrometry, Pergamon Press, New York, (1960). 33

3. Method of Energy-Pulse-height Calibration

The convention adopted for the pulse-height-energy scales used for all spectra in the catalogue (2.5, 5.0, 10, and 20 keV/channel) is that all pulse-height values are measured relative to that of the 0.66162-MeV gamma ray of ^{137}Cs . For this energy, there will be a one-to-one correspondence between energy and pulse-height (with the appropriate scale factor applied). This convention was adopted to correspond with the results of measurements of the non-linearity of NaI. Thus, the channel position for a peak of a given energy will be related to a gain scale in which the ^{137}Cs peak would appear at a multiple of channel 66.162 (10 keV scale). Energy calibration is made by measuring sources simultaneously with a source of ^{137}Cs and determining the channel position for each peak by least-squares fits to the data with a gaussian function, as discussed in Section VII. An example of this procedure is shown in Fig. 51. This figure shows the spectrum of Lu^{177} measured simultaneously with ^{137}Cs on the 5 keV/channel scale. The ^{137}Cs photopeak was fit with a gaussian. For

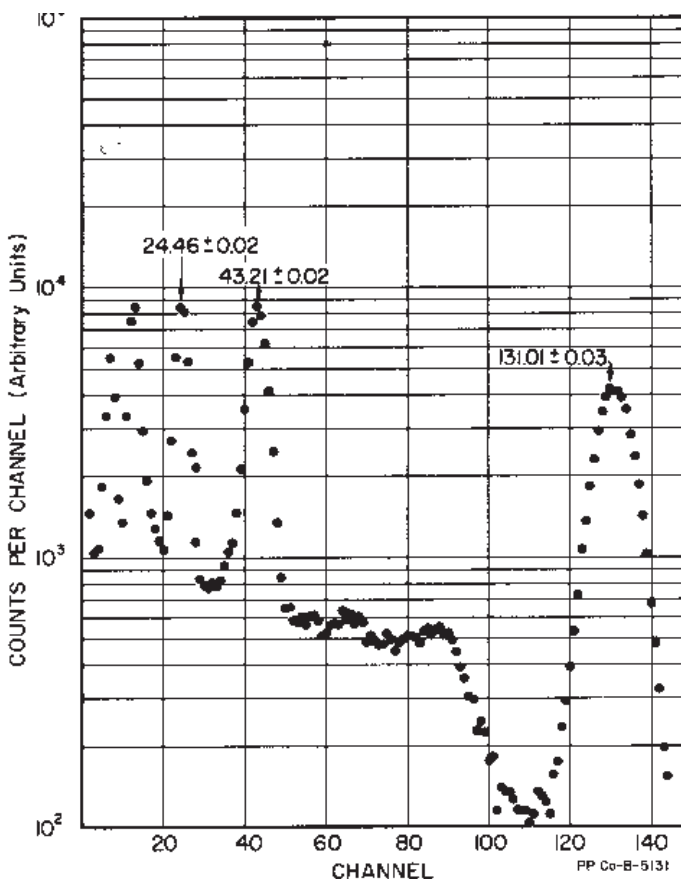


Fig. 51 - Example of energy calibration procedure using Cs^{137} gamma ray. Data were taken on a gain scale approximating 5 keV/channel. Peak channel positions indicated are result of least-squares fit of modified gaussian shape to each photo-line. Figure shows calibration of peaks due to 0.11297, and 0.20836-MeV gamma rays from Lu^{177} .

the two lower energy peaks, the contribution from the underlying Compton distribution was approximated by adding a straight line to the non-linear fit. The energy of the two low-energy lines is then determined from the peak positions by normalization of the Cs photopeak to channel 132.32 and applying the appropriate correction to account for the non-linear pulse-height vs energy response of the detector. A list of sources for energy calibration is given in Table II.

TABLE II

Energy Calibration Sources

Nuclide	E_{γ} (MeV)	Half-Life
^{241}Am	0.05957	458 yr
^{177}Lu	0.11297	6.8 d
^{177}Lu	0.20836	
^{131}I	0.36447	8.066 d
^{198}Au	0.41176	2.70 d
^7Be	0.478	53 d
Ann. Rad.	0.51094	
^{207}Bi	0.5695	28 yr
^{137}Cs	0.66162	30 yr
^{95}Nb	0.7657	35 d
^{88}Y	0.8989	105 d
^{207}Bi	1.0637	28 yr
^{65}Zn	1.114	244 d
^{22}Na	1.2736	2.58 yr
^{24}Na	1.3679	14.9 hr
^{88}Y	1.837	105 d
$^{207}\text{Tl}^2$ (ThC")	2.6142	1.91 yr
^{24}Na	2.7535	15 hr

4. Gain Shift Program

All spectra in the catalogue are normalized on the pulse-height vs energy scale as discussed above. This is accomplished by means of a computer program which allows one to shift either the gain or zero position of the pulse-height scale. Thus, a general linear transformation can be made between two pulse-height scales. This is accomplished by fitting the pulse-height spectrum as a series of polynomial least-squares fits to sets of three successive channel counts. The results of these successive fits around the original channel positions provides a means of interpolating values for the number of counts in a hypothetical

channel which lies somewhere between two channels on the original pulse-height scale. The program can either shift a spectrum by a ratio of two arbitrary gain scales or shift a given peak in a spectrum to a certain channel position. This second alternative is accomplished by incorporating a linear least-squares routine for locating the position of a photopeak by assuming a simple gaussian form.

The gain-shift program has been used in conjunction with the energy calibration procedures outlined in the previous section to shift all spectra in the catalogue to the standard pulse-height scales referred to ^{137}Cs . The general procedure adopted is to measure the energy of all prominent gamma rays with this procedure and then make a comparison of these results with literature values. If the precision of reported energies is well established, literature values are used and the spectrum is shifted to the appropriate position on the standard pulse-height scale. If this is not the case the energy values determined from the calibration with Cs^{137} are used.

Although the gain-shift routine is intended for use only with small gain shifts, it can be used to shift the gain of a spectrum by a large factor. **Fig. 52** shows two ^{137}Cs spectra, one measured at 5 keV/channel and the other at 10 keV/channel and then shifted by a factor of 2 in gain to correspond to the 5 keV scale. The agreement in shape between the two spectra is considered to be excellent, considering the large scale change. It is interesting to note the broadening of the x-ray peak of the shifted spectrum, due to the effect of finite channel width. For a detailed description of the gain-shift program the reader should consult reference 34.

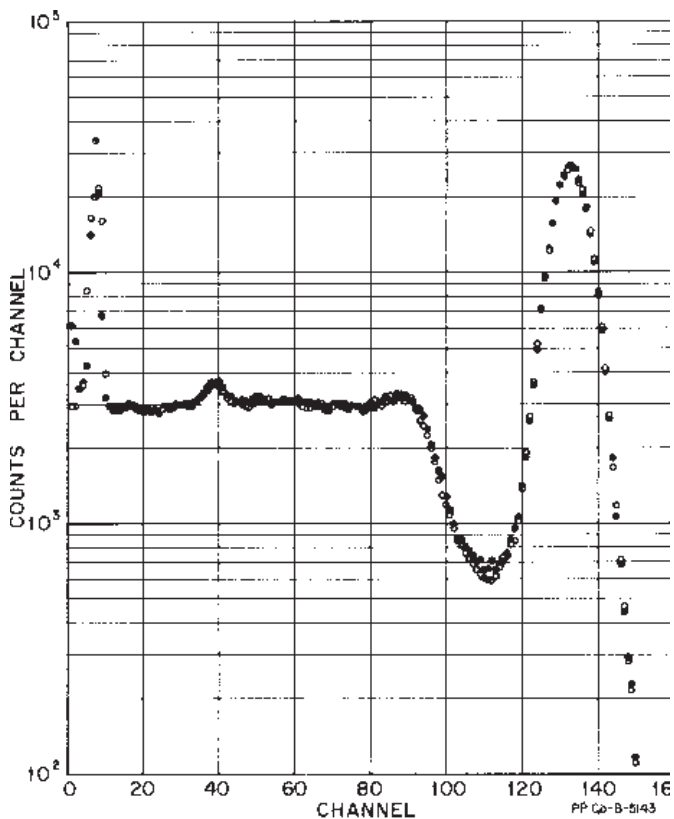


Fig. 52 - Illustration of results of gain shifting program. Closed circles represent ^{137}Cs spectrum on 5 keV/channel gain scale. Open circles show spectrum taken on 10 keV/channel gain scale shifted by a factor of two to match 5 keV spectrum.

IX. COMPUTER TECHNIQUES FOR DATA ANALYSIS

One of the most important areas of development in gamma-ray scintillation spectrometry during the past few years has been the perfection and use of computer programs for the analysis of complex pulse-height spectra. In this section a brief description of the techniques presently in use at this laboratory is presented. For a comprehensive survey of the present state of data processing as applied to the analysis of pulse-height spectra, the reader is referred to the proceedings of a conference c)n this subject held at Gatlinburg, Tennessee in 1962.²⁷

A. Computer Program for the Generation of the Detector Response to Monoenergetic Gamma Rays

The basic requirement for analysis of pulse-height spectra is a detailed knowledge of the pulse-height response to monoenergetic radiation. In the preceding sections the various factors influencing this response have been described in detail. To obtain correspondence between the true gamma-ray spectrum emitted by a source and the observed pulse-height distribution, two methods have been employed. One approach has been to attempt

to calculate the pulse-height distribution from a knowledge of the basic interactions occurring in the detector. This approach has been developed by the use of Monte Carlo computer programs such as that described by Zerby²⁸.

The other approach, which has been developed at this laboratory, is empirical in nature, and may be used to calculate response functions for any detector and experimental geometry. It is basically a systematic extension of the graphical interpolation scheme which has been used by nuclear spectroscopists for some time. First, a number of carefully measured spectra are obtained for single gamma rays as shown in **Fig. 53**. From these pulse-height distributions one may construct a three-dimensional surface for the response of a NaI scintillation detector to monoenergetic gamma rays. **Fig. 54** illustrates such a response function for a 3"x 3" NaI detector where the single gamma rays are normalized to the same emission rate and are arranged with gamma-ray energy as the third coordinate. A plane perpendicular to the energy axis through a given point will intersect this surface to form a curve which represents the detector response to a gamma-ray of that energy.

²⁷ Proceedings of a Conference on the Applications of Computers to Nuclear and Radiochemistry, NAS-NS Publication No. 3107 (1962).

²⁸ C. D. Zerby and H. S. Moran, Calculation of the Pulse-height Response of NaI Scintillation Counters, USAEC Report, ORNL-3165 (1962).

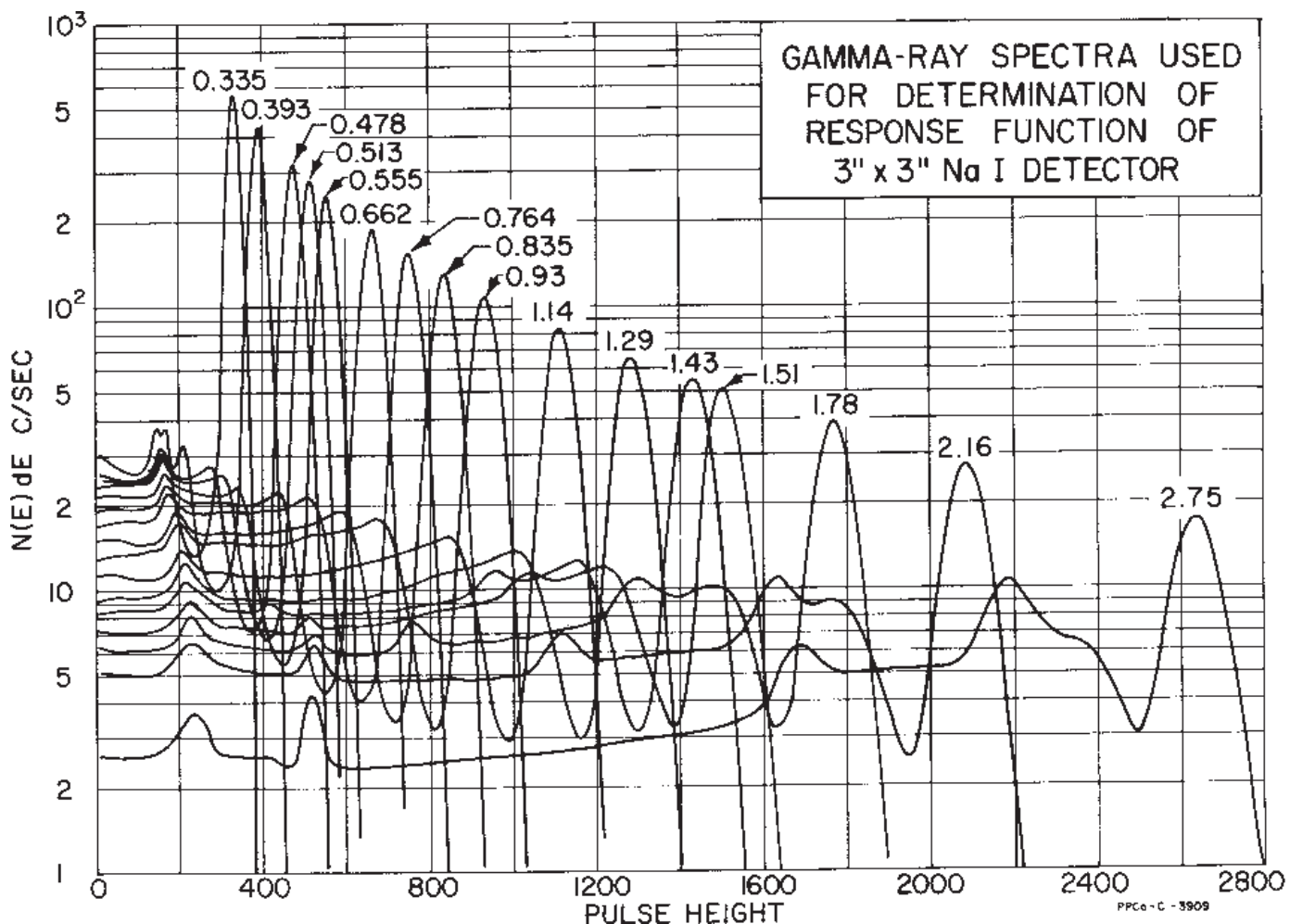


Fig. 53 -The response of a 3" x3" NaI detector to monoenergetic gamma rays from 0.335 to 2.75 MeV. All spectra are for a point source mounted 10 cm from the detector and have been normalized in intensity to 10^7 photons emitted from the source.

The generation of such a surface by means suitable for machine programming requires an analytical representation of the experimentally determined pulse-height spectra.

If the detailed structure of the pulse-height distributions obtained from monoenergetic gamma rays are examined, it is apparent that there are several features which vary in a uniform manner with gamma-ray energy. All features of the spectra can be interpreted from a knowledge of the three basic processes by which a photon interacts with the detector; i.e., photo-electric, Compton, and pair interactions. The most prominent feature, the photopeak, is essentially gaussian in shape with some assymetry on the low energy side due to multiple processes occurring in the detector and small-angle Compton scattering from absorbing materials frequently used to prevent detection of beta radiation emitted by the source. This peak, as described in Section VII, is represented by the "modified gaussian" expression:

$$y(x) = y_0 e^{-(x-x_0)^2/b^2} [1 + \alpha_1(x - x_0)^n + \alpha_2(x - x_0)^m] \quad (13)$$

where y , is the maximum amplitude of the peak, x_0 is the mid-point of the distribution on a pulse-height scale, and b_0 is related to the full width of the gaussian shape at half,maximum (resolution). The convention adopted is to fit the experimental photopeaks and to determine the parameters of the modified gaussian by least-squares techniques.²⁹ The deviation from a modified-Gaussian shape on the low-energy side is treated as though it belonged to the Compton distribution. From a knowledge of b_0 and the normalized area of the gaussian as a function of pulseheight (energy) it is possible to calculate the shape and magnitude of the photopeak for a gamma ray of any energy. It should be noted that the pulse-height vs. energy scale must include the effect of nonlinearity in the energy response of NaI. The remaining portion of the pulse-height distribution is due largely to the Compton process which produces a distribution

²⁹ R. G. Helmer, R. L. Heath, Marie Putnam, and D. H. Gipson, A Non-linear Least-Squares Program for the Determination of Parameters of Photopeaks by the Use of a Modified Gaussian Function, IDO-17015 (1964).

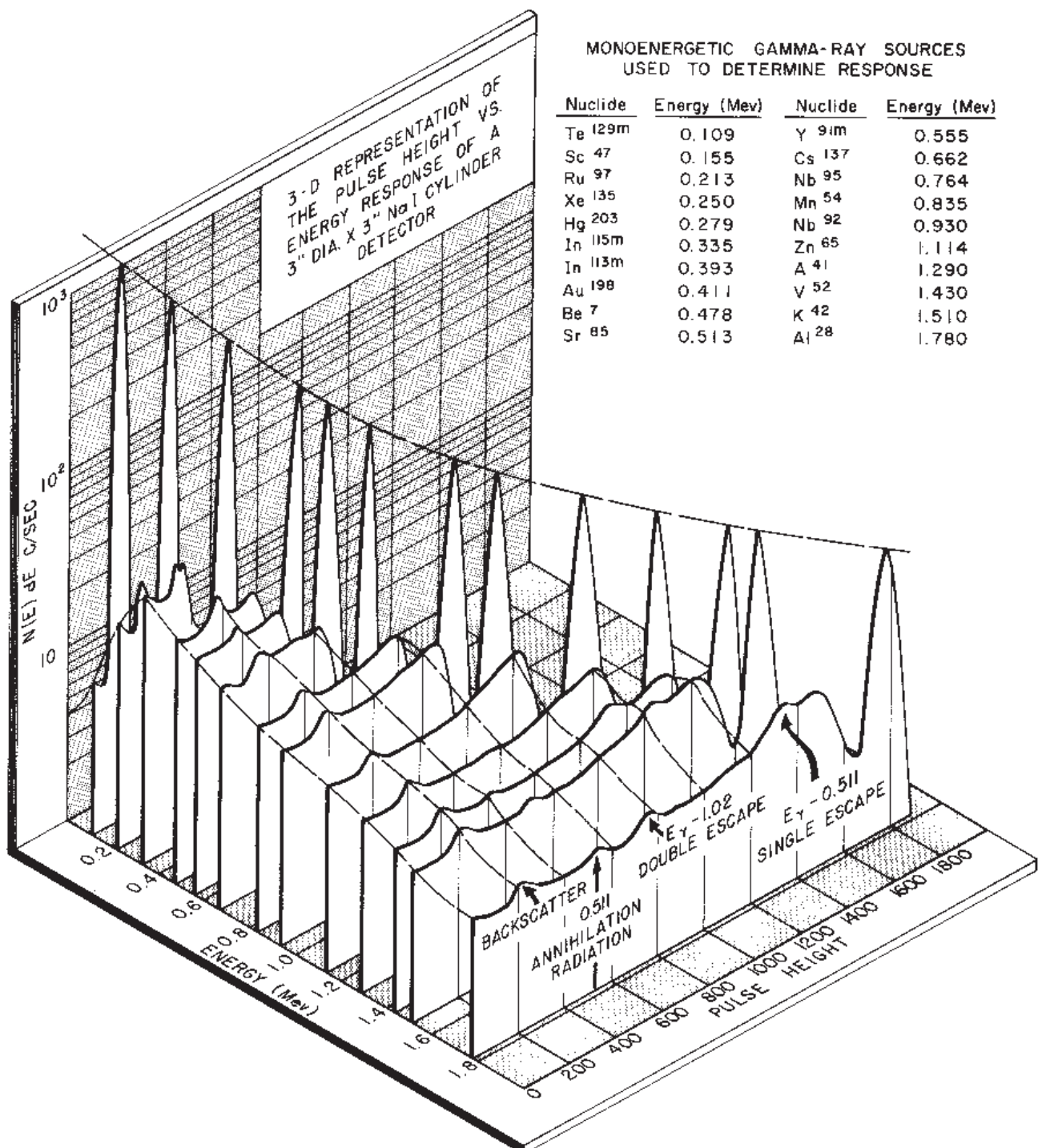


Fig. 54 - Three-dimensional model of the response of a 3"x3" NaI detector to monoenergetic gamma radiation.
This model illustrates the interpolation scheme used to obtain the energy response of a given detector.

of pulses from zero amplitude up to a sharp cutoff representing maximum energy transfer between the photon and a recoil electron. This point on the energy spectrum is termed the Compton edge (E_c) and is given by the following relationship:

$$E_c = E_y \frac{E_\gamma}{1 + \frac{2E_\gamma}{mc^2}} \quad (14)$$

Other prominent features of the spectrum are the backscatter peak which results mostly from photons comptonscattered at 180° by material surrounding the detector, the two peaks resulting from the escape of one or both of the annihilation photons from pair production, and the 0.511MeV peak from annihilation radiation. The portion of the spectrum below the full-energy peak is divided into 5 segments and each segment is fitted to a series of the form:

$$y = a + bx + \sum_{K=1}^{N_k} b_v \sin \frac{K\pi X}{L} \quad (15)$$

In order to insure a smooth fit at the segment end points, a region of overlap is included in the fitting procedure. The number of terms, N_k , in the expansion is chosen to give a certain amount of smoothing to the data points.

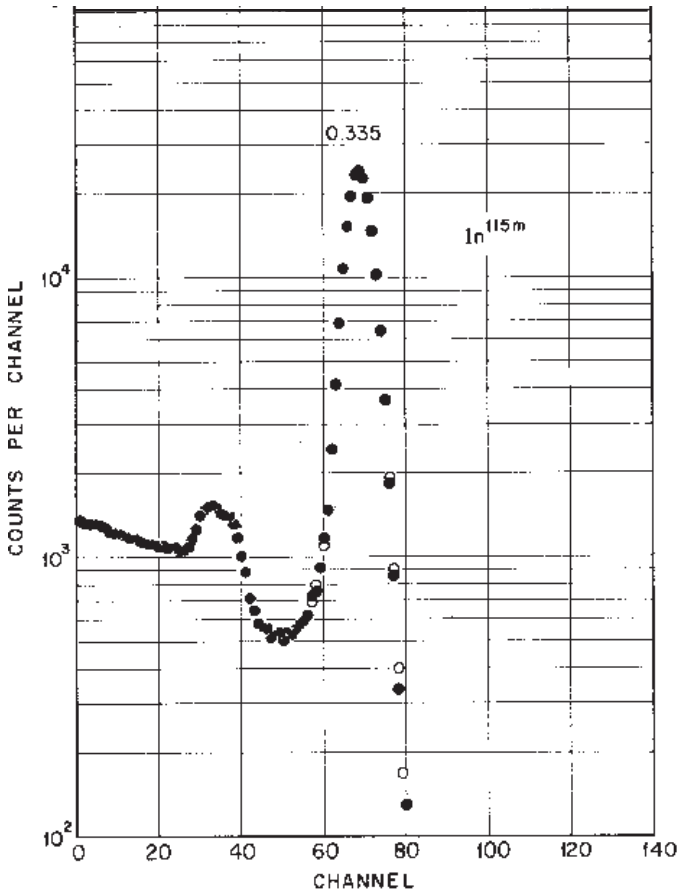


Fig. 55 - Comparison of computed detector response to experimental spectrum (0.335 MeV).

The next step is to determine the number of counts in a given channel as a function of gamma-ray energy. These points, which represent a section through the three-dimensional surface perpendicular to the pulse-height axis, are then fitted to a polynomial in gamma-ray energy. The number of terms in this polynomial is adjustable in order to give the most reasonable fit to the data points. Thus a set of polynomials in energy is obtained, one for each channel on the pulse-height scale. This process is repeated for each segment of the Compton distribution. To simplify this interpolation with a limited number of measured spectra, each group of segments is first stretched so that each segment has the same length for all gamma-ray energies. This preserves fine structure which varies with gamma-rays energy, i.e., backscatter and pair peaks. Since the number of segments required to describe the Compton distribution varies with E_γ , the program is divided into three sections. These sections treat the following ranges of gamma-ray energy: 0.020-0.300, 0.300-1.3, and 1.3-3 MeV.

To obtain the pulse-height distribution for a given gamma ray, channel count-rate values are computed from the set of polynomials representing $N(E)DE$ vs E for each channel. These values for each segment are combined with a photopeak calculated from the appropriate values of b_0 and A (area of the gaussian).

Figures 55 and 56 show a comparison between experimental pulse-height distributions for gamma rays of 0.335 and 1.114 MeV and the calculated shapes obtained from the shape generation program. Excellent agreement is indicated, with all details of the spectra reproduced. A detailed description of this program and its use has recently been prepared as an AEC report.³⁰.

B. Coincidence Sum Spectrum Program

An additional complication in the analysis of gamma-ray spectra occurs when the decay of a radioactive element gives rise to two or more coincident gamma rays. In this case the pulse spectrum

³⁰ R. L. Heath, R. G. Helmer, L. A. Schmittroth, and G. A. Cazier, *Generation of Detector Response Curves for Gamma-ray Scintillation Spectrometers*, IDO-17017 (1964).

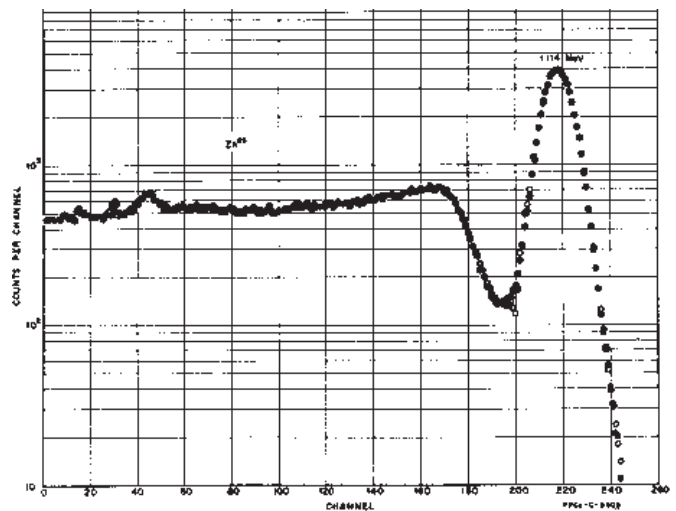


Fig. 56 - Comparison of computed detector response to experimental spectrum (1.114 MeV).

observed in a detector will also include a distribution of pulses known as the coincidencesum spectrum which results from the simultaneous detection of two coincident gamma rays. This spectrum will contain pulses of all sizes from the minimum detectable height to the sum of the maximum pulse heights obtainable from the individual gamma rays. The most prominent feature of this spectrum is the so-called sum peak which results from coincident detection of pulse from the photopeaks of the two coincident gamma rays.

In principle, it is possible to calculate both the shape and magnitude of this sum spectrum. Let us consider a two-gamma-ray cascade. Using the program previously described one may compute the detector response to the individual gamma rays for a given detector and experimental environment. If the computed pulse-height distributions for the two coincident gamma rays are normalized to one disintegration of the source, then the values of $N(E)DE$ represent the probability of detecting the corresponding gamma ray as a count in a given channel of the pulse-height spectrum. Pulse-height spectra for the two coincident gamma rays may be designated as $G_1(X)$ and $G_2(X)$.

The probability of detecting gamma 1 in channel a and gamma 2, from the same disintegration, in channel b is the product $G_1(a)G_2(b)$. This product is then the probability of producing a pulse in the sum spectrum in channel (a + b). The total contribution to any channel, c, of the sum spectrum is then the sum of contributions from all pairs of channels for which $a + b = c$. This may be expressed in the following manner:

$$S(c) = \sum_{n=1}^c G_1(n) \cdot G_2(c-n). \quad (16)$$

AFORTRAN program has been written which performs this summation for two, three, or four gamma-ray cascades, using as input data, calculated spectra from the previously described spectrum-generation program.

One further correction is necessary to obtain the correct intensity for the sum spectrum relative to the cascade gamma rays. Each pulse that appears in the sum spectrum represents a count missing from the pulse-height spectrum of each of the summing gamma rays.

As an example of the results of this program, **Fig. 19** shows the experimental spectrum of two coincident gamma rays together with the computed coincidence-sum spectrum. Both the shape and intensity are reproduced with considerable precision. With the addition of this program one now has the capability of computing the pulse-height distribution from gamma rays emitted by any radioactive nuclide. This requires only a knowledge of the decay scheme and may be applied in principle to any detector or experimental arrangement.

Fig. 57 shows a comparison between the experimental pulse-height spectrum of 41-day Pm¹⁴⁸ and the computed spectrum obtained using the programs described above. The computed spectrum was generated from data on the decay scheme of this nuclide obtained at this laboratory. This is a complicated case involving 17 gamma rays with many double and triple cascades. All features of both the singles and coincidence sum spectra are reproduced with high precision. The two spectra above leave been displaced on the vertical axis for comparison. With the ex-

ception of two low energy peaks, which were not included in the calculation, all points on the computed spectrum agree quite well with the experimental data.

C. Linear Least-Squares Program

For the analysis of discrete spectra which exhibit well defined photopeaks, the so-called least squares method of analysis represents an improvement over hand stripping techniques. This method can be programmed for computer use and has been proven to be very satisfactory for the analysis of many classes of data.^{31,32,33} It assumes that the pulse spectrum to be analyzed consists of a sum of i gamma rays of known energy, numbered 1-j-c, each represented as a pulse-height spectrum of i channels numbered a-i-n. It is further assumed that standard spectra, representing the response of the detector to gamma rays of these energies, are available for comparison. Then the count rate in channel i from the jth component will be S_{ij} and the total count rate in channel i from the composite is C_i . If the recorded standards are all normalized to a given disintegration rate from the source, then one must include a normalizing factor α_j , which is the ratio of the intensity of component j in the composite to the normalized standards. We may then write:

$$C_i = \sum_{j=1}^c \alpha_j S_{ij} + \delta_i \quad (17)$$

where δ represents the error in the count in channel i.

If we assume that the only error is the random fluctuation in the channel count, the principle of least-square may be applied. Then the sum of the squares of the residuals δ can be minimized over all channels, i.e.,

$$\text{minimize} \sum_{i=a}^n (C_i - \sum_{j=1}^c \alpha_j S_{ij})^2 w_i \quad (18)$$

where W_i is the weighting factor.

One then has a set of linear simultaneous equation which may be solved to obtain values for the α_j 's. This is most conveniently done by matrix techniques which can be readily programmed for machine solution. The advantage of this system is that the method is free from subjective error and it provides a method for estimating the quality of fit. The disadvantage is that it requires a knowledge of the number of components present in the spectrum to be analyzed and their energies. This requirement is not as restrictive as it might seem since the result of initial estimates may be observed and an iterative method applied. In general, results obtained with this method are more satisfactory than those obtained with graphical techniques. A recent version of this program has been written which includes the gain-shift program.³⁴ With this program it is possible to iterate with gain of the composite spectrum as a variable, thus removing one of the most troublesome problems in analyses of this type.

³¹ L. Salmon, Nucl. Instr. and Meth. 14, 193 (1961).

³² A. J. Ferguson, AECL-1398 (1961).

³³ R. L. Heath, "Recent Developments in Scintillation Spectrometry," Proceedings of the 8th Scintillation and Solid-State Counter Symposium, IRE Trans. on Nuclear Science, NS-9, No. 3, 294 (1962).

³⁴ R. G. Helmer, R. L. Heath, D. D. Metcalf, and C. A. Cazier, A Linear Least-Squares Fitting Program for the Analysis of Gamma-ray Spectra Including a Gain-shift Routine, IDO-17015 (1964).

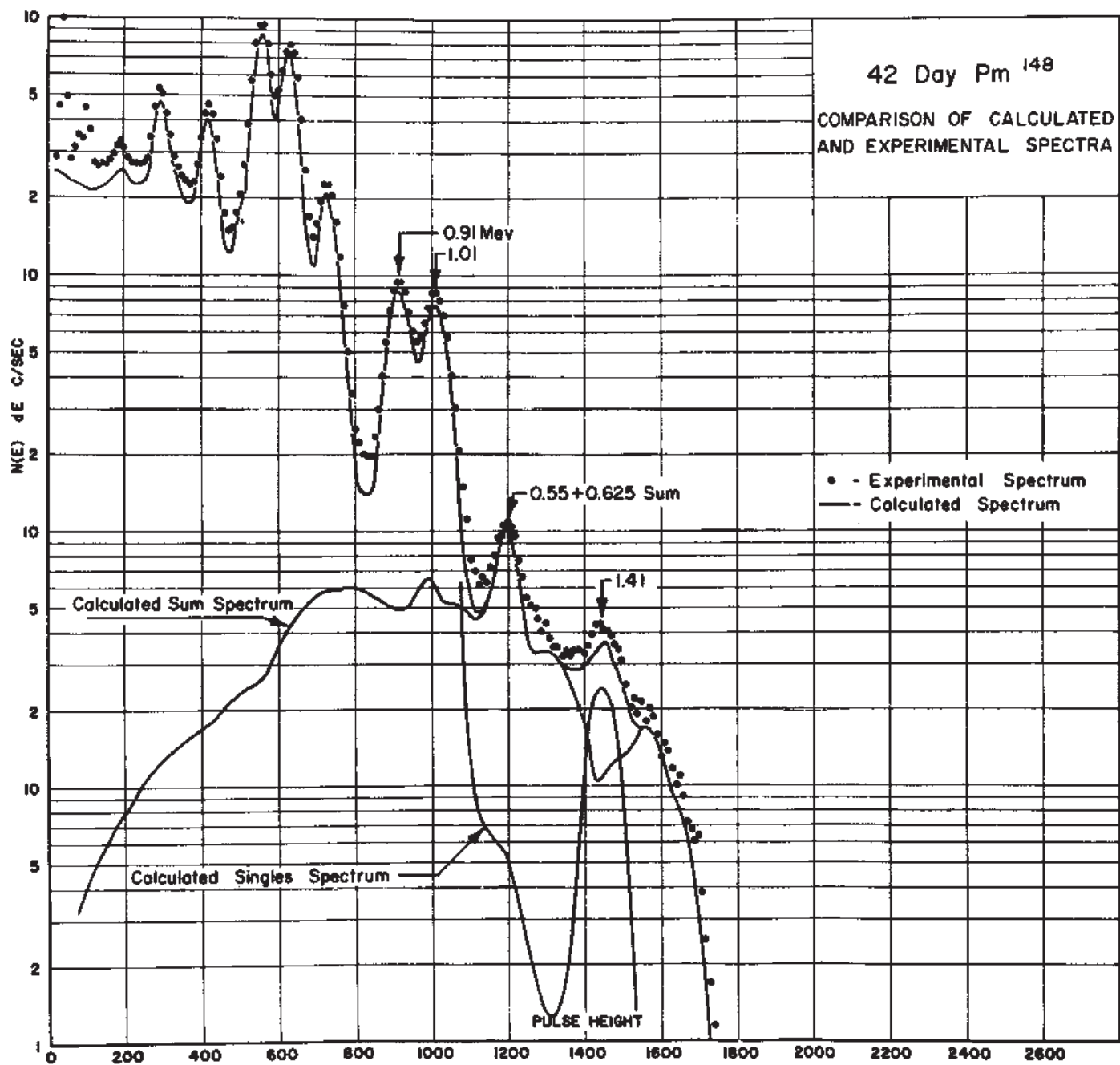


Fig 57 - Comparison of the experimental spectrum obtained from a source of 42-day ^{148}Pm on a 3"x3" detector with a spectrum calculated using the computer programs described for the generation of gamma-ray shapes, summation spectra, and a knowledge of the decay scheme of this nuclide.

.As an example of the application of the program, **Fig. 58** shows the results from the analysis of a complex spectrum containing five components and a total of ten gamma rays. In order to demonstrate the precision of the method the five standards were measured individually and then measured together to form the composite. The calculated values for the intensity of each component are tabulated on the figure and compared with intensities obtained from the five components measured separately. Deviations are less than 2% in all cases, even though the composite spectrum is quite complex. The residuals resulting from the least-squares analysis, in units of R/σ are shown plotted for each channel at the bottom of the figure. The maximum deviation for any point is seen to be less than 2σ .

As an example of the combined use of these programs, **Fig. 59** shows the results of a least-squares analysis of the ^{94}Nb spectrum. The procedure followed in this analysis was as follows:

(1) The energies of the two gamma rays were determined by a separate measurement of the Nb source taken simultaneously with a Cs¹³⁷ source. The positions of the Cs peak and the two Nb peaks were then determined with the non-linear least-squares program described in Section VII.

(2) With this information and the known pulse, height vs energy relationship for NaI, the energies of the Nb gamma rays were determined. The ^{94}Nb spectrum was then gain shifted to

place the peaks in the correct position on the standard 10 keV/channel gain scale.

(3) The shape generation program was used to determine the detector response of the detector for gamma rays of the energies determined above.

(4) With the generated shapes, the coincidence sum spectrum was calculated.

(5) With the two gamma-ray shapes and the computed sum spectrum as components for the fit, the experimental ^{94}Nb spectrum was analyzed with the linear least-squares program.

From an examination of the residuals, shown at the bottom of **Fig. 59**, it is concluded that the experimental spectrum is well represented by a linear combination of the three calculated components. Intensities obtained for the two gamma rays agreed to within 1%, in agreement with the published level scheme for this nuclide. This result is considered to be a good demonstration of the capabilities of the analysis techniques described above.

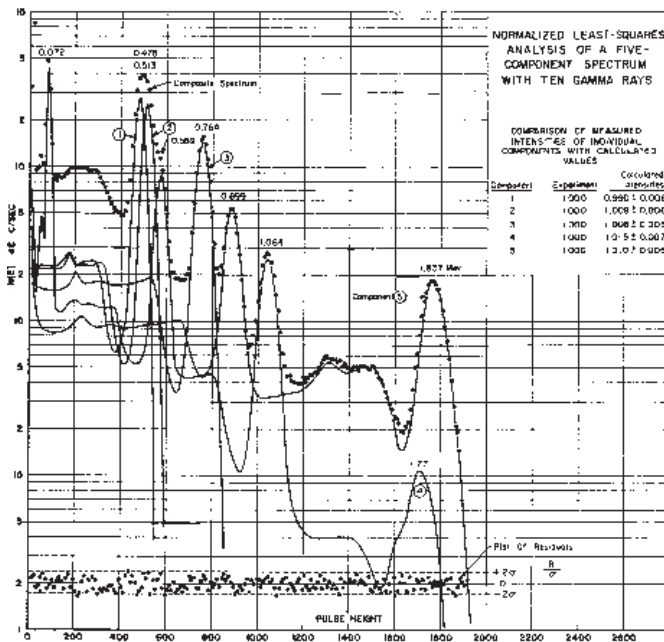


Fig. 58 - Example of least-squares analysis of a five-component pulse-height spectrum containing ten gamma rays. Residuals are shown for each channel.

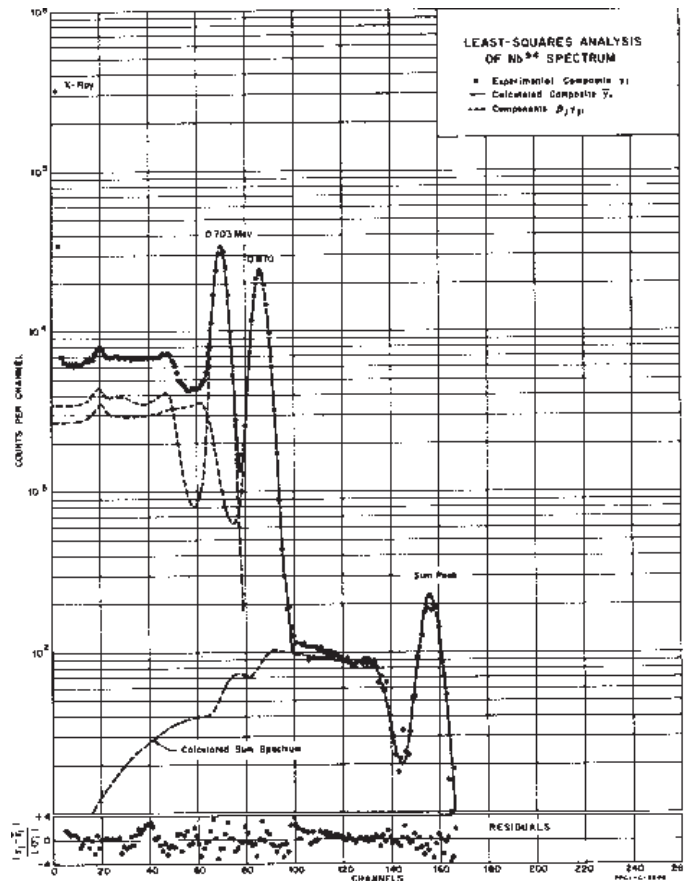
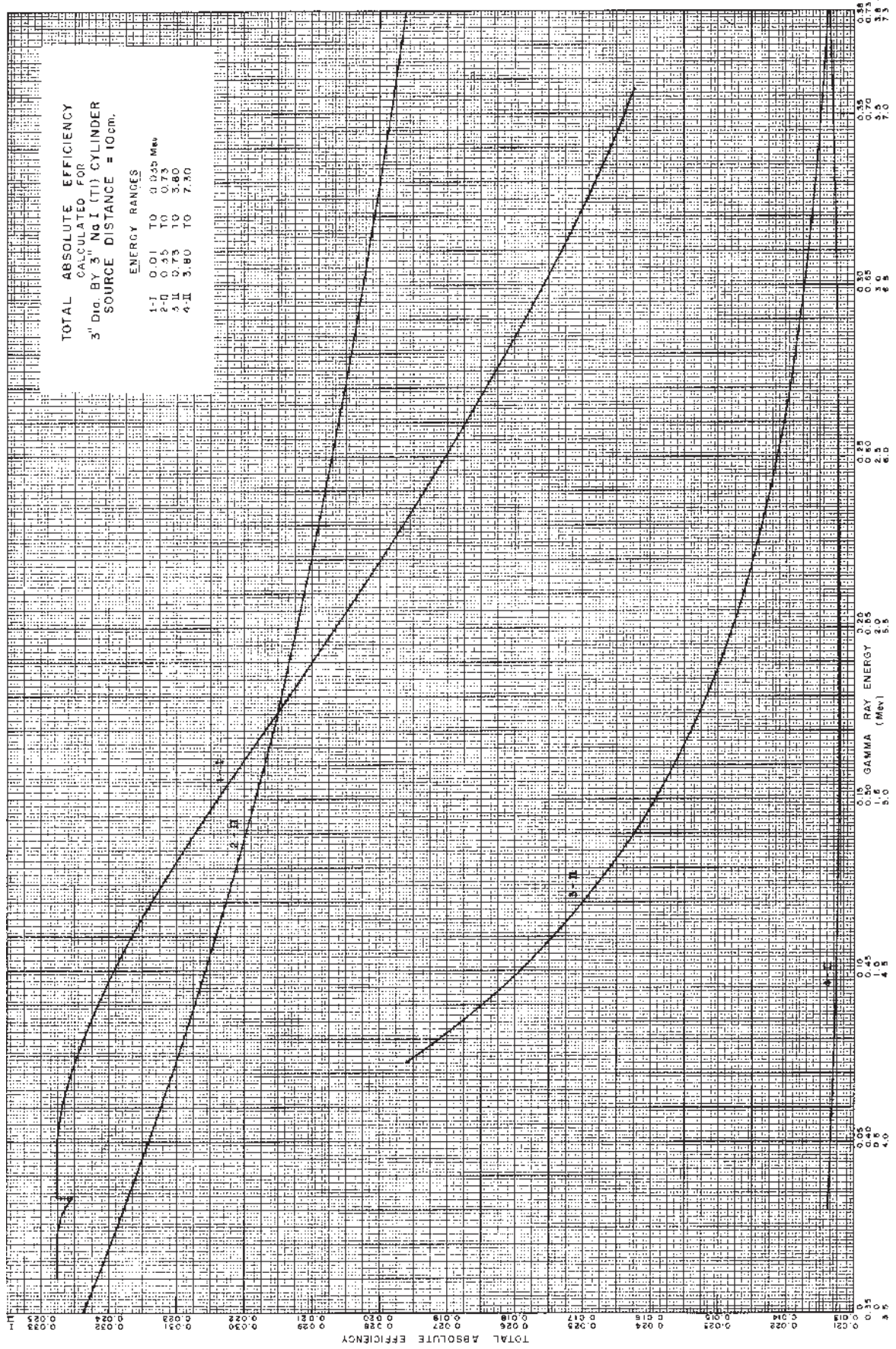


Fig. 59 - Results of least-squares analysis of ^{94}Nb spectrum. The Analysis used calculated shapes for the two gamma rays and the coincidence sum spectrum. The residuals are shown plotted at the bottom of the figure.

APPENDIX - II
INTRINSIC EFFICIENCIES FOR NaI DETECTORS



APPENDIX - III

PHOTOPEAK EFFICIENCY AND OTHER DATA FOR ANALYSIS OF GAMMA-RAY SPECTRA

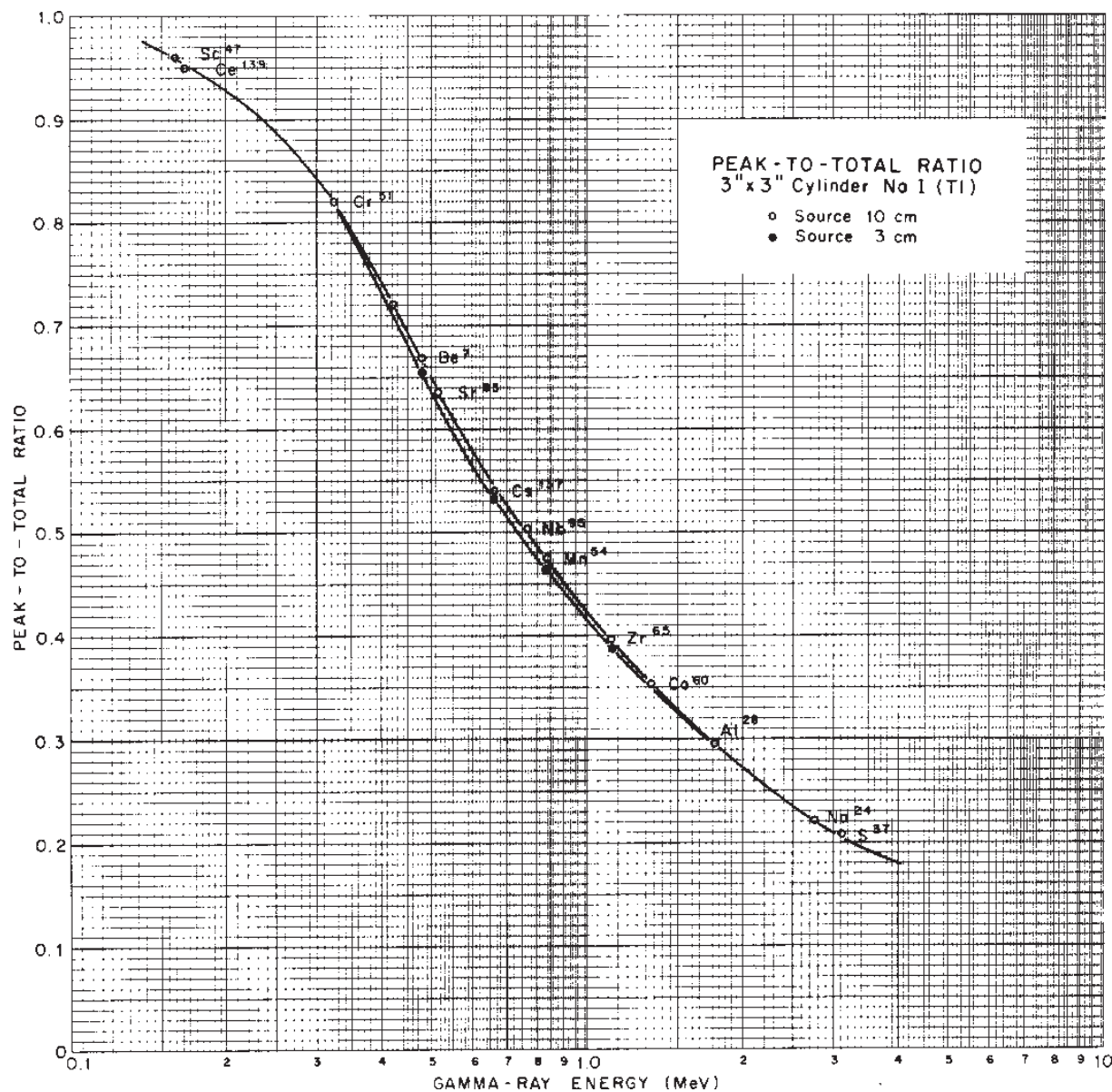
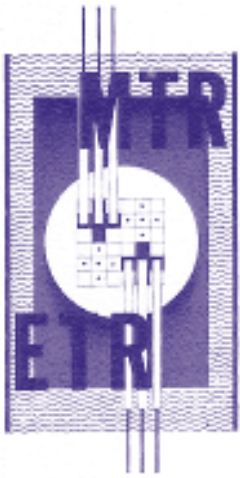


TABLE I
Experimental Peak-to-Total Ratios for 3''x 3'' NaI Detector

Isotope	E_γ (MeV)	Point Source		
		10 cm source distance		3 cm source distance
		integration	$4\pi\beta-\gamma$	integration
Sc ⁴⁷	0.155	0.960		0.962
Ce ¹³⁹	0.166	0.950		
Cr ⁵¹	0.323	0.820		0.813
Au ¹⁹⁸	0.4117		0.737	
Be ⁷	0.478	0.668		0.657
Cs ¹³⁷	0.6616	0.536		0.532
Nb ⁹⁵	0.766	0.500	0.504	
Mn ⁵⁴	0.835	0.474		0.464
Zn ⁶⁵	1.114	0.395		0.388
Co ⁶⁰	1.382		0.357	
Al ²⁸	1.78	0.290	0.295	
Y ⁸⁸	1.837	0.280		
Na ²⁴	2.753		0.225	
S ³⁷	3.13		0.207	



REVISED EDITION OF REPORT IDO-16880-2
AUGUST 1964
REISSUE DATE: JANUARY 1997

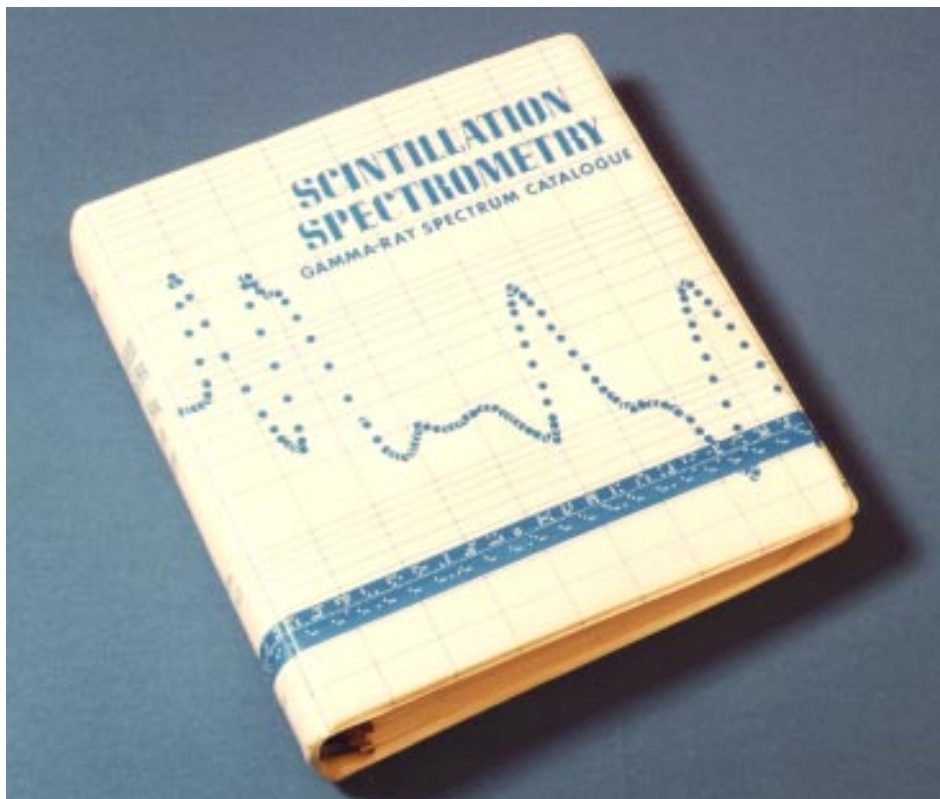
SCINTILLATION SPECTROMETRY

GAMMA-RAY SPECTRUM CATALOGUE

NEW VERSION OF 2ND EDITION
COMPILATION OF GAMMA-RAY SPECTRA
AND RELATED NUCLEAR DECAY DATA
VOLUME 2 OF 2

BY

R. L. HEATH



-RAY SPECTROMETRY CENTER

Idaho National Engineering & Environmental Laboratory

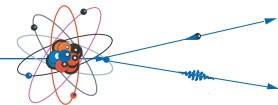


TABLE OF SPECTRA

Element	Isotope	Half-Life	Detector	Energy Scale	Plate Number	Method of Production
Beryllium	7	53 day	3"x3"-2	1 keV//PHU(Cs)	4-7-1	Li ⁷ (p,n)
Sodium	22	2.6 yr	3"x3"-2	1 keV//PHU(Cs)	11-22-2	Na ²³ (n,2n)
	24	1.5 h r	3"x3"-2	2 keV//PHU(Cs)	11-24-1	Na ²³ (n, γ)
	24	1.5 h r	3"x3"-2	1 keV//PHU(Cs)	11-24-2	Na ²³ (n, γ)
Magnesium	27	9.5 min	3"x3"-2	1 keV//PHU(Cs)	12-27-1	Mg26(n, γ)
	28	21.3 hr	3"x3"-2	2 keV//PHU(Cs)	12-28(13-28) -1	Mg26(2n, γ)
	with A1 ²⁸	2.3 min				
Aluminum	28	2.3 min	3"x3"-2	1 keV//PHU(Cs)	13-28-2	A1 ²⁷ (n, γ)
	29	6.6 min	3"x3"-2	1 keV//PHU(Cs)	13-29-1	Si ²⁹ (n,p)
Silicon	31	2.62 hr	3"x3"-2	1 keV//PHU(Cs)	14-31 -1	Si ³⁰ (n, γ)
Phosphorus	32	14.3 day	3"x3"-2	1 keV//PHU(Cs)	15-32-1	P ³¹ tn, γ)
Sulfur	37	5.1 min	3"x3"-2	2 keV//PHU(Cs)	16-37-2	S ³⁶ (n, γ)
Chlorine	34m	32.4 min	3"x3"-3	2 keV//PHU(Cs)	17-34m(17-34)-I	C1 ³⁵ (γ , n)
	with C1 ³⁴	1.6 sec	3"x3"-2	1 keV//PHU(Cs)	17-38-2	Cl ³⁷ (n, γ)
	38	38 min	3"x3"-2	1 keV//PHU(Cs)		
Argon	41	1.83 h r	3"x3"-2	1 keV//PHU(Cs)	18-41 -1	A ⁴⁰ (n, γ)
Potassium	38	7.7 min	3"x3"-3	1 keV//PHU(Cs)	19-38-1	K ³⁹ (γ ,n)
	38	7.7 min	3"x3"-3	2 keV//PHU(Cs)	19-38-2	K ³⁹ (γ ,n)
	40	1.27x 10 ⁹ yr	3"x3"-2	1 ke V//PHU(Cs)	19-40-1	nat.
	42	12.4 h r	3"x3"-2	1 keV//PHU(Cs)	19-42-2	K ⁴¹ (n, γ)
Calcium	47	4.5 day	3"x3"-2	1 keV//PHU(Cs)	20-47-1	Ti ⁵⁰ (n,a)
	49	8.7 min	3"x3"-2	2 keV//PHU(Cs)	20-49-1	Ca ⁴⁸ (n, γ)
Scandium	44m	2.4 day	3"x3"-2	1 keV//PHU(Cs)	21-44m (21 -44) -1	Sc ⁴⁵ (γ ,n)
	with Sc ⁴⁴	4 hr				
	44m	2.4 day	3"x3"-3	2 keV//PHU(Cs)	21-44m(21-44)-2	Sc ⁴⁵ (γ ,n)
with Sc ⁴⁴	44	4hr				
	46	85 day	3"x3"-2	1keV//PHU(Cs)	21-46-1	Sc ⁴⁵ (n, γ)
	47	3.4 day	3"x3"-2	1 keV//PHU(Cs)	21-47-1	Ti ⁴⁷ (n,p)
	47	3.4 day	3"x3"-2	0.5 keV//PHU(Cs)	21-47-2	Ti ⁴⁷ (n,p)
	48	1.4 h r	3"x3"-2	1 keV//PHU(Cs)	21-48-2	Ti ⁴⁸ (n,p)
Titanium	44	1.03 y r	3"x3"-2	1 keV PHU (Cs)	22-44(21 -44)-I	(p,2n)
	with Sc ⁴⁴	3.9 hr				
	45	3.08 hr	3"x3"-2	1 keV, PHU(Cs)	22-45-1	Ti ⁴⁶ (γ , n)
	51	5.8 min	3"x3"-2	1 ke V P H U (Cs)	22-51 -1	Ti ⁵⁰ (n,y)



Element	Isotope	Half-Life	Detector	Energy Scale	Plate Number	Method of Production
Vanadium	48	1.6 day	3"x3"-2	1 keV/I/ PHU(Cs)	23-48-1	Ti ⁴⁸ (p,n)
	52	3.77 min	3"x3"-2	1 keV/ PHU (Cs)	23-52-2	V ⁵¹ (n, γ)
Chromium	49	4.2 min	3"x3"-2	1 keV/ PHU(Cs)	24-49-1	Cr ⁵⁰ (γ , n)
	51	27.8 day	3"x3"-2	1keV/i PHU (Cs)	24-51 -1	Cr ⁵⁰ (n, γ)
	55	3.5 min	3"x3"-2	1 keV, PHU(Cs)	24-55 -1	Cr ⁵⁴ (n, γ)
Manganese	52	5.7 day	3"x3"-2	1 keV/PHU(Cs)	25-52-1	Cr ⁵² (p,n)
	54	314 day	3"x3"-2	1 keV/PHU(Cs)	25 -54-2	Cr ⁵⁴ (p,n)
	56	2.58 hr	3"x3"-2	1 keV/PHU@CS)	25 -56-2	Mn ⁵⁵ (n, γ)
Iron	53	9 min	3"x3"-2	1 keV,/PHU(Cs)	26-53-1	Fe ⁵⁴ (y,n)
	59	4.5 day	3"x3"-2	1 keV/PHU(Cs)	26-59-2	Fe ⁵⁸ (n, γ)
Cobalt	57	267 day	3"x3"-2	0.5 keV/ PHU(Cs)	27-57-1	Fe ⁵⁷ (p,n)
	57	267 day	3"x3"-2	0.25 keV 'PHU(Cs)	27-57-2	Fe ⁵⁷ (p,n)
	58	70 day	3" x 3"-2	1 keV/PHU(Cs)	27-58-1	Ni ⁵⁸ (n,p)
	60m	10.5 min	3" x 3"-2	1 keV/PHU(Cs)	27-60m-1	Co ⁵⁹ (n, γ)
	60	5.27 yr	3" x 3"-2	1 keV/PHU(Cs)	27-60-1	Co ⁵⁹ (n, γ)
	61	3.3 hr	3" x 3"-2	0.5 keV/PHU(Cs)	27-61 -1	N i ⁶¹ (n,p)
Nickel	57	36. h r	3" x 3"-2	1 keV/PHU(Cs)	28-57-1	N i ⁵⁸ (γ , n)
	65	2.65 h r	3" x 3"-2	1 keV/PHU(Cs)	28-65-2	Ni ⁶⁴ (n, γ)
Copper	61	3.3 h r	3" x 3"-3	1 keV/PHU(Cs)	29-61 -1	Cu ⁶³ (γ ,2n)
	62	9.9 min	3" x 3" -3	1 keV/PHU(Cs)	29-62-1	Cu ⁶³ (γ ,n)
	64	12.9 h r	3" x 3" -2	1 keV/PHU(Cs)	29-64-1	Cu ⁶³ (n, γ)
	66	5.1 min	3" x 3" -2	1 keV/PHU(Cs)	29-66-1	Cu ⁶⁵ (n, γ)
	67	6.1 hr	3" x 3" -2	1 keV/PHU(Cs)	29-67-1	Zn ⁶⁸ (γ ,p)
Zinc	63	3.8 min	3" x 3"-3	1 keV/PHU(Cs)	30-63-1	Zn ⁶⁴ (γ ,n)
	65	245 day	3" x 3" -2	1 keV/PHU (Cs)	30-65-2	Z n ⁶⁴ (n, γ)
	69m	1.4 h r	3" x 3"-2	1 keV/PHU(Cs)	30-69m(30-69)-1	Zn ⁶⁸ (n, γ)
	with Zn ⁶⁹	55 min				
	69m	14 hr	3" x 3" -2	0.5 keV/PHU(Cs)	30-69m(30-69)-2	Zn ⁶⁸ (n, γ)
	with Zn ⁶⁹	55 min				
Gallium	67	78 hr	3" x 3" -2	1 keV/ PHU(Cs)	31-67-1	Ga ⁶⁹ (γ ,2n)
	67	78 hr	3" x 3" -2	0.5 keV/PHU(Cs)	31-67-2	Ga ⁶⁹ (γ ,2n)
	68	68 min	3" x 3" -2	1 keV/PHU(Cs)	31-68-1	Ga ⁶⁹ (γ ,n)
	70	21 min	3" x 3t"-2	1 keV/"PHU(Cs)	31-70-1	Gal ⁶⁹ (n, γ)
	72	14.1 hr	3" x 3"-2	1 keV/PHU(Cs)	31-72-1	Ga ⁷¹ (n, γ)
Germanium	69	40 hr	3" x 3"-2	1 keV/PHU(Cs)	32-69-1	Ge ⁷⁰ (γ ,n)
	75	82 min	3"x 3'- 2	1 keV/PHU(Cs)	32-75-1	Ge ⁷⁴ (n,,y)
	75	8.2 min	3" x 3"-2	0.5 keV/PHU(Cs)	32-75-2	Ge ⁷⁴ (n,y)
	77m	54 sec	3" x 3"-2	0.5 keV/PHU(Cs)	32-77m - 1	Ge ⁷¹ (n, γ)
	77	1.1 hr	3"x 3"-2	1 keV/PHU(Cs)	32-77-1	Ge ⁷⁶ (n, γ)
						Index

Element	Isotope	Half-Life	Detector	Energy Scale	Plate Number	Method of Production
Arsenic	72	26 hr	3"x3"-2	1 keV/PHU(Cs)	33-72-1	Ge ⁷² (p,n)
	74	18 day	3"x3"-2	1 keV/PHU(Cs)	33-74-1	As ⁷⁵ (γ ,n)
	76	26.5 hr	3"x3"-2	1 keV/PHU(Cs)	33-76-2	As ⁷⁵ (n, γ)
	77	39 hr	3"x3"-2	1 keV/PHU(Cs)	33-77-2	Ge ⁷⁶ (n, γ , β)
Selenium	73	7.1 hr	3"x3"-2	1 keV/PHU(Cs)	34-73-1	Se ⁷⁴ (γ ,n)
	75	120 day	3"x3"-2	1 keV/PHU(Cs)	34-75-1	Se ⁷⁴ (n, γ)
	75	120 day	3"x3"-2	0.5 keV/PHU(Cs)	34-75-2	Se ⁷⁴ (n, γ)
	81 m	61 min	3" x 3"-2	1 keV/PHU(Cs)	34-81m(34-81)	Se ⁸⁰ (n,y)
with	Se ⁸¹	1.8 min				
Bromine	77	58 hr	3"x3"- 2	1 keV/PHU(Cs)	35-77-1	Br ⁷⁹ (γ ,2n)
	80	1.8 min	3"x3"- 2	1 keV/PHU(Cs)	35-80-1	Br ⁷⁹ (n, γ)
	82	36 hr	3"x3"- 2	1 keV/PHU(Cs)	35-82-1	Br ⁸¹ (n, γ)
Krypton	85m	4.4hr	3"x 3"- 2	1 keV/"PHU(Cs)	36-85m-1	Kr ⁸⁴ (n, γ)
	85	10.4 yr	3 "x 3"-2	1 keV/PHU(Cs)	36-85-1	Kr ⁸⁴ (n, γ)
Rubidium	84m	21 min	3"x 3"-3	1 keV/PHU(Cs)	37-84m-1	Rb ⁸⁵ (γ ,n)
	86	18.7 day	3" x 3"-2	1 keV/PHU(Cs)	37-86-1	Rb ⁸⁵ (n, γ)
	88	18 min	3" x 3"-2	1 keV/PHU(Cs)	37-88-1	Rb ⁸⁷ (n, γ)
	88	18 min	3"x3"-2	2 keV/PHU(Cs)	37-88-2	Rb ⁸⁷ (n, γ)
	89	15 min	3"x 3"-2	1 keV/PHU(Cs)	37-89-1	U ²³⁵ (n,f)
	89	15 min	3"x3"- 2	2 keV/PHU(Cs)	37-89-2	U ²³⁵ (n,f)
	90	2.9 min	3"x3"- 2	2 keV/PHU(Cs)	37-90-1	U ²³⁵ (n,f)
Strontium	85m	70 min	3"x3"- 2	0.5keV/PHU(Cs)	38-85m-1	Sr ⁸⁴ (n, γ)
	85	64day	3"x3"- 2	1 keV/PHU(Cs)	38-85-2	Rb ⁸⁵ (p,n)
Strontium	87m	2.8 hr	3" x 3"-2	1 keV/PHU(Cs)	38-87m-1	Sr ⁸⁶ (n, γ)
	87m	2.8 hr	3" x 3"-2	0.5 keV/PHU(Cs)	38-87m-2	Sr ⁸⁶ (n, γ)
	91	9.7 h r	3" x 3"-2	1 keV/PHU(Cs)	38-91-2	U ²³⁵ (n,f)
	92	2.7 h r	3" x 3"-2	1 keV/PHU(Cs)	38-92-1	U ²³⁵ (n,f)
Yttrium	86	1.5 h r	3" x 3"-2	1 keV/PHU(Cs)	39-86-1	Sr ⁸⁶ (p,n)
	88	1.05 day	3" x 3"-2	2 keV/PHU(Cs)	39-88-1	Sr ⁸⁸ (p,n)
	88	105 day	3" x 3"-2	1 keV//PHU(Cs)	39-88-2	Sr ⁸⁸ (p,n)
	90m	3.14 h r	3" x 3"-2	1 keV/PHU(Cs)	39-90m-1	Zr ⁹⁰ (n,p)
	91 m	50 min	3" x 3"-2	1 keV/PHU(Cs)	39-91m -2	U ²³⁵ (n,f)
	91	59 day	3" x 3"-2	1 keV/PHU(Cs)	39-91-2	U ²³⁵ (n,f)
	92	3.6 hr	3" x 3" - 2	1 keV/PHU(Cs)	39-92-1	U ²³⁵ (n,f)
	93	10.1 hr	3" x 3"-2	1 keV/PHU(Cs)	39-93-1	U ²³⁵ (n,f)
	94	1.7 min	3" x 3"-2	4 keV/PHU	39-94-1	U ²³⁵ (n,f)

Element	Isotope	Half-Life	Detector	Energy Scale	Plate Number	Method of Production
Zirconium	89m	4.4 min	3" x 3"-3	1 keV/PHU(Cs)	40-89m-1	Zr ⁹⁶ (γ,n)
	89	79 hr	3" x 3"- 3	1 keV/PHU(Cs)	40-89-1	Zr ⁹⁶ (γ,n)
	95	65 day	3" x 3" -2	1 keV/PHU(Cs)	40-95-2	U ²³⁵ (n,f)
	95	65 day	3" x 3"-2	1 keV/PHU(Cs)	40-95(41-95)-2	U ²³⁵ (n,f)
	with Nb ⁹⁵	35 day				
	97	1.7 hr	3" x 3" -2	1 keV/PHU(Cs)	40-97-2	Zr ⁹⁶ (n,γ)
	with NbUra 60	sec				
	97	1.7 hr	3" x 3"-2	1 keV/PHU(Cs)	40-97(41-97)-1	Zr ⁹⁶ (n,γ)
with NbI17	74	min				
Niobium	92	10 day	3" x 3"-2	1 keV/PHU(Cs)	41 -92-1	Nb ⁹³ (γ,n)
	94m	6.6 min	3" x 3"-2	1 keV/PHU(Cs)	41-94m-1	Nb ⁹³ (n,γ)
	94	2x 1 0 yr	3" x 3"-2	1 keV/PHU(Cs)	41-94-2	Nb ⁹³ (n,γ)
	95	35 day	3" x 3"-2	1 keV/PHU(Cs)	41 -95-2	U ²³⁵ (n,f)
	97m	60 sec	3" x 3"-2	1 keV/PHU(Cs)	41-97m-1	Zr ⁹⁶ (n,γ,β)
	97	74 min	3" x 3"-2	1 keV/PHU(Cs)	41-97-1	Zr'6(n,γ,β)
Molybdenum	91	16 min	3" x 3"-2	1 keV/PHU(Cs)	42-91-1	Mo ⁹² (γ,n)
	99	66 hr	3" x 3"-2	1 keV/PHU	42-99-1	Mo ⁹⁸ (n,γ)
with Tc ^{99m}	99	66 hr	3" x 3"-2	1 keV/PHU(Cs)	42-99(43-99m)-1	Mo ⁹⁸ (n,γ)
		6 hr				
	101	14.6 min	3" x 3"-2	1 keV/PHU(Cs)	42-101 -1	Mo ¹⁰⁰ (n,γ)
Technecium	95m	60 day	3" x 3"-2	1 keV/PHU(Cs)	43-95m(43-95)-1	Ru ⁹⁶ (γ,n,K)
with Tc ⁹⁵		20 hr				
	95	20 hr	3" x 3"-3	1 keV/PHU(Cs)	43 -95 -1	Ru ⁹⁶ (γ,n,K)
	96	4.3 day	3" x 3"-2	1 keV/PHU(Cs)	43-96-1	Mo ⁹⁶ (p,n)
	99	2.1 x10 ⁵ yr	3" x 3"-2	1 keV//PHU(Cs)	43 -99-1	U ²³⁵ (n,f)
	101	14 min	3" x 3"-2	1 keV//PHU(Cs)	43-1 01-1	Mo ¹⁰⁰ (n,γ,β)
Ruthenium	95	1.7 hr	3" x 3"- 3	1 keV,/PHU(Cs)	44-95-1	Ru ⁹⁶ (y,n)
	97	2.9 day	3 x 3"-2	1 keV//PHU(Cs)	44-97-1	Ru ⁹⁶ (n,y)
	103	40 day	3" x 3"-2	1 keV,/PHU(Cs)	44-103-1	Ru ¹⁰² (n,γ)
	105	4.45 hr	3" x 3"-2	1 keV,,/PHU(Cs)	44-105-1	Ru ¹⁰⁴ (n,γ)
with Rh ¹⁰⁶	106	1.0 yr	3" x 3"-2	1 keV//PHU(Cs)	44-106(45-1 06)-3	U ²³⁵ (n,f)
		30 sec				
Rhodium	101m	4.7 day	3" x 3"-2	1 keV/PHU(Cs)	45-101m-1	Rh ¹⁰³ (γ,2n)
with Ru ¹⁰⁴	104m	4.4 min	3" x 3"-2	0.5 keV/PHU	45-104m-1	R h ¹⁰³ (n,γ)
	Ru ¹⁰⁴	42 sec				
	105m	42sec	3" x 3"-2	0.5 keV/PHU	45-105m-1	Ru ¹⁰⁴ (n,γ,β)
Palladium	109	1 3.6 hr	3" x 3"-2	0.5 keV/PHU(Cs)	46-109-1	Pd ¹⁰⁸ (n,y)
Silver	105	40 day	3" x 3" - 2	1 keV/PHU(Cs)	47-105-1	Ag ¹⁰⁷ (γ,2n)
	106m	8.3 day	3" x 3"-2	1 keV/PHU(Cs)	47-106m-1	Ag ¹⁰⁷ (γ,n)
	106	24 min	3"x3"-3	1 keV/PHU(Cs)	47-106-1	Ag ¹⁰⁷ (γ,n)
	108m	> 5 yr	3"x3" -2	1 keV/PHU(Cs)	47-108m-1	Ag ¹⁰⁷ (n,γ)
	108	2.4 min	3"x3"-2	1 keV/PHU(Cs)	47-1 08-1	Ag ¹⁰⁷ (n,γ)



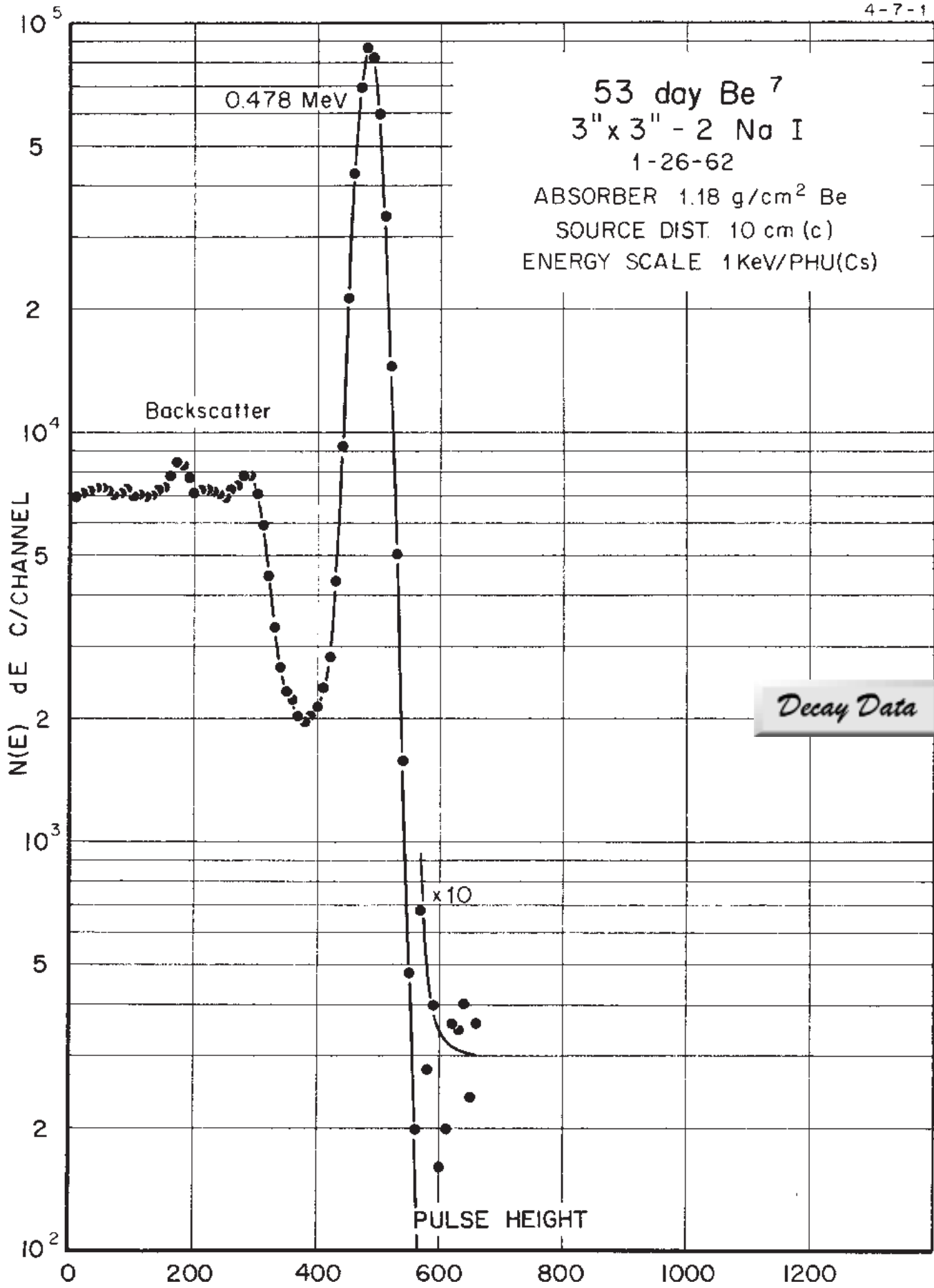
Element	Isotope	Half-Life	Detector	Energy Scale	Plate Number	Method of Production
Silver	110m	250 day	3"x3"-2	1 keV/PHU(Cs)	47-110m -2	Ag ¹⁰⁹ (n, γ)
	110	24 sec	3"X3"-2	1 keV/PHU(Cs)	47-11 0-1	Ag ¹⁰⁹ (n, γ)
	111	7.5 day	3"x3"-2	1 keV/PHU(Cs)	47-111 -1	Pd ¹¹⁰ (n, γ , β)
Cadmium	109	1.3yr	3" x 3"-2	0.5 keV/PHU(Cs)	48-1 09-1	Cd ¹⁰⁸ (n, γ)
	115m	43 day	3" x 3" - 3	1 keV/PHU(Cs)	48-115m-1	Cd ¹¹¹ (n, γ)
	115	2.3 day	3" x 3"-2	1 keV/PHU(Cs)	48-115(49-115m)-2	Cd ¹¹¹ (n, γ)
Indium	In ^{115m}	4.5 hr				
	111	2.8 day	3" x 3"-2	0.5 keV/PHU(Cs)	49-111 -1	In ¹¹³ (γ ,2n)
	112m	21 min	3" x 3"-3	1 keV/PHU(Cs)	49-11 2m(49-11 2)-l	In ¹¹³ (γ ,n)
Tin	In ¹¹²	14 min				
	113m	1.7 hr	3" x 3"-2	1 keV/PHU(Cs)	49-113m-1	Sn ¹¹² (n, γ , β)
	114m	49 day	3" x 3"-2	1 keV/PHU(Cs)	49-114m- 1	1n ¹¹³ (n, γ)
	115m	4.5 hr	3" x 3"-2	0.5 keV/PHU(Cs)	49-115m-2	Cd ¹¹¹ (n, γ , β)
	116m	54 min	3" x 3"-2	1 keV/PHU(Cs)	49-116m-1	In ¹¹⁵ (n, γ)
with	113	118 day	3" x 3"-2	1 keV/PHU(Cs)	50-113(49-113m)- l	Sn ¹¹² (n, γ)
	In ¹¹³	1.7 hr				
	125m	9.7 min	3" x 3"-2	1 keV/PHU(Cs)	50-125m-1	Sn ¹²⁴ (n, γ)
Antimony	125	9.4 day	3" x 3"-2	1 keV/PHU(Cs)	50-125-1	U ²³⁵ (n,f)
	120m	5.8 day	3" x 3"-2	1 keV/PHU(Cs)	51-120m-1	Sb ¹²¹ (γ ,n)
	120	1.6 min	3" x 3" -2	1 keV/PHU(Cs)	51 -120-1	Sb ¹²¹ (γ ,n)
	122m	3.4 min	3" x 3"-2	0.5 keV/PHU(Cs)	51-122m-1	Sb ¹²¹ (n, γ)
	122	2.8 day	3" x 3"-2	1 keV/PHU(Cs)	51-122-2	Sb ¹²¹ (n, γ)
	124	60 day	3" x 3"-2	1 keV/PHU(Cs)	51 -1 24-2	Sb ¹²³ (n, γ)
with	125	2.7 yr	3" x 3'-2	1 keV,/PHU(Cs)	51-125(52-125m)- l	U ²³⁵ (n,f)
	Te ^{125m}	58 day				
	125	2.7 yr	3" x 3"-2	1 keV/PHU(Cs)	51-125-2	U ²³⁵ (n,f)
Tellurium	129	4.2 hr	3" x 3"-2	2 keV/PHU	51-129-1	U ²³⁵ (n,f)
	125m	58 day	3" x 3"-2	0.5 keV/PHU(Cs)	52-125m-1	Te ¹²⁴ (n, γ)
	132	78 hr	3" x 3"-2	1 keV/PHU(Cs)	52-132-1	U ²³⁵ (n,f)
	132	78 hr	3" x 3"-2	1 keV/PHU(Cs)	52-132(53-132) -1	U ²³⁵ (n,f)
	I ¹³²	2.3 hr				
Iodine	124	4.5 day	3" x 3"-2	2 keV/PHU	53-124-1	Te124(p,n)
	126	13.2 day	3" x 3"-2	1 keV/PHU(Cs)	53-126-1	I ¹²⁷ (γ ,n)
	128	25 min	3" x 3"-2	1 keV/PHU(Cs)	53-128-1	I ¹²⁷ (n, γ)
	130	12.5 hr	3" x 3"-2	1 keV/"PHU(Cs)	53-130-1	Te ¹³⁰ (p,n)
	131	8 day	3" x 3"-2	1 keV/PHU(Cs)	53-131-2	U ²³⁵ (n,f)
	132	2.3 hr	3" x 3"-2	1 keV/PHU(Cs)	53-132-2	U ²³⁵ (n,f)
	133	20.8 hr	3" x 3"-2	1 keV/PHU(Cs)	53-133-2	U ²³⁵ (n,f)
	134	5.3 min	3" x 3"-2	1 keV/PHU(Cs)	53-134-1	U ²³⁵ (n,f)
	135	6.7 hr	3" x 3"-2	1 keV/PHU(Cs)	53-135-1	U ²³⁵ (n,f)

Element	Isotope	Half-Life	Detector	Energy Scale	Plate Number	Method of Production
Xenon	125	1.8 hr	3" x 3"-2	0.5 keV/PHU(Cs)	54-125-1	Xe ¹²⁴ (n, γ)
	133	5.3 day	3" x 3"-2	0.5 keV/PHU(Cs)	54-133-1	U ²³⁵ (n,f)
	135	9.2 h r	3" x 3"-2	1 keV/PHU(Cs)	54-135-1	U ²³⁵ (n,f)
Cesium	132	6.5 day	3"x 3" - 2	1 keV/PHU(Cs)	55 -132-1	Cs ¹³³ (γ ,n)
	134m	2.9 hr	3" x 3"-2	1 keV/PHU(Cs)	55-134m-1	Cs ¹³³ (n, γ)
	134m	2.9 hr	3" x 3"-2	0.5 keV/PHU(Cs)	55-134m-2	Cs ¹³³ (n, γ)
	134	2.1 y r	3" x 3"-2	1 keV/PHU(Cs)	55-134-1	Cs ¹³³ (n, γ)
Cesium	136	1.3 day	VxV-2	1 keV/PHU(Cs)	55 -136-1	U ²³⁵ (n,f)
	137	30 yr	VxV-2	1 keV/PHU(Cs)	55 -137-1	U ²³⁵ (n,f)
	138	32 min	Tlx3tf-2	1 keV/PHU(Cs)	55 -138 -1	U ²³⁵ (n,f)
	139	9.5 min	Tfx3r'-2	1 keV/PHU(Cs)	55 -139-1	U ²³⁵ (n,f)
Barium Ba ¹³⁰ (n, γ)	131	11.5 day	3px3ft-2	1 keV/PHU(Cs)		56-131 -1
with	133	7.5 yr	31fx3ol-2	1 keV/PHU(Cs)	56-133 -1	Ba ¹³² (n, γ)
	133	7.5yr	3ftx3lf -2	0.5 keV/PHU(Cs)	56-133 -2	Ba ¹³² (n γ)
	139	83 min	TfAlt-2	1 keV/PHU(Cs)	56-139 -1	Ba ¹³⁸ (n, γ)
	140	12.8 day	3" x3" -2	1 keV/PHU(Cs)	56-140-1	U ²³⁵ (n,f)
	140	1 2.8 day	3"x 3" - 2	1 keV /PHU(Cs)	56-140(57-140)-2	U ²³⁵ (n,f)
	La ¹⁴¹	40 hr				
Lanthanum	136	9.5 min	3" x 3"-3	1 keV//PHU(Cs)	57 -136-1	La ¹³⁹ (n,3n)
	140	40.2 hr	3"x 3 " -2	1 keV/PHU(Cs)	57 - 140- 1	La ¹³⁹ (n, γ)
	142	87 min	3" x 3"-2	4 keV/PHU(Cs)	57-142-2	U ²³⁵ (n,f)
Cerium	139	140 day	3"x 3" -2	1 keV/PHU(Cs)	58 -139-1	La ¹³⁹ (p,n)
	139	140 day	3" x 3" -2	0.5 keV/ PHU(Cs)	58 -139 -2	La ¹³⁹ (p,n)
	141	32.5 day	3" x 3." -2	1 keV/PHU(Cs)	58 -141 -1	Ce ¹⁴⁰ (n, γ)
	141	32.5 day	3" x 3" -2	0.5 keV/PHU(Cs)	58 -141 -2	Ce ¹⁴⁰ (n, γ)
	143	3.3 h r	3" x 3" -2	1 keV/PHU(Cs)	58-143 -1	Ce ¹⁴² (n, γ)
	143	3.3 h r	3" x 3" -2	0.5 keV/PHU(Cs)	58 -143 -2	Ce ¹⁴² (n, γ)
	144	284 day	3" x 3" '-2	1 keV/PHU(Cs)	58 -144(59-144)-1	U ²³⁵ (n,f)
	Pr ¹⁴⁴	17 min				
Praseodymium	139	4.5 hr	3" x 3" -3	1 keV/PHU(Cs)	59-139-1	P r ¹⁴¹ (γ ,2 n)
	142	19.2 hr	3 " x 3" - 2	1 keV/PHU(Cs)	59-142-1	Pr ¹⁴¹ (n, γ)
	143	13.7 day	3" x 3" -2	1 keV/PHU(Cs)	59-143-1	Ce ¹⁴² (n,, γ , β)
	145	5.9 h r	3" x 3"-2	1 keV/PHU(Cs)	59-145-1	U ²³⁵ (n,f)
Neodymium	141	2.4 h r	3" x 3"-3	1 keV/PHU(Cs)	60-141 1	Nd ¹⁴ 2(γ , n)
	147	11.1 day	3" x 3"- 2	1 keV/PHU(Cs)	60-1 47-1	Nd ¹⁴⁶ (n, γ)

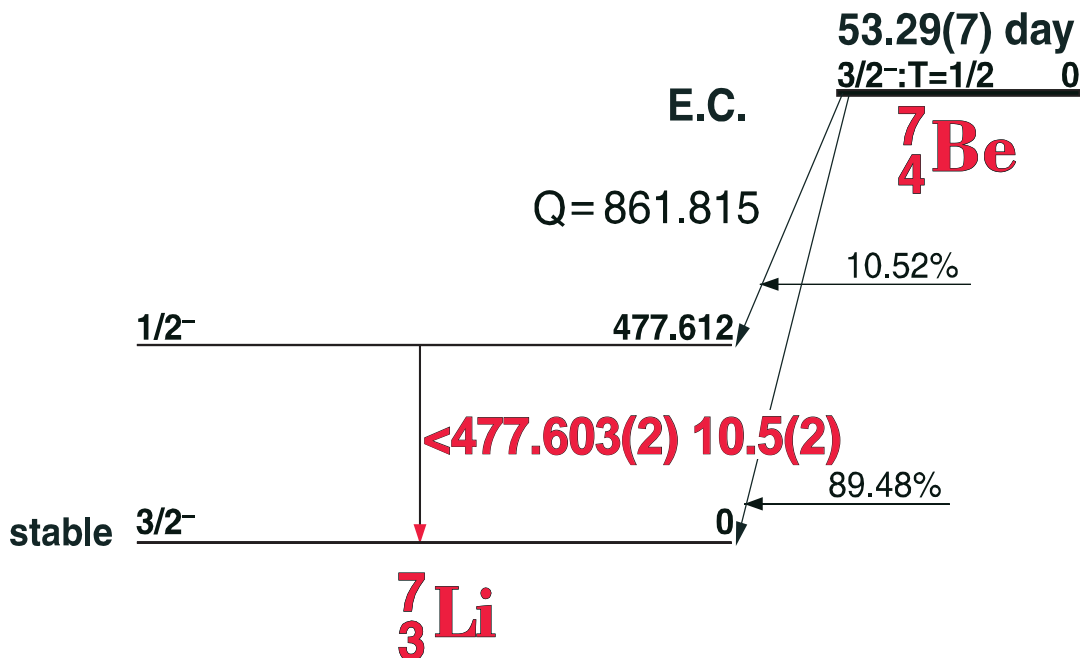
Element	Isotope	Half-Life	Detector	Energy Scale	Plate Number	Method of Production
Neodymium	147	11.1 day	3"x3"- 2	0.5 keV/PHU(Cs)	60-1 47-2	Nd ¹⁴⁶ (n, γ)
	149	1.9 hr	3" x 3" -2	0.5 keV/PHU(Cs)	60-1 49-1	Nd ¹⁴⁸ (n, γ)
	151	1.2 min	3"x3"- 2	1 keV./PHU(Cs)	60-1 51 -1	Nd ¹⁵⁰ (n, γ)
Promethium	147	2.5 yr	3" x 3" -2	1 keV/PHU(Cs)	61-147-1	Nd ¹⁴⁶ (n, γ , β)
	148m	41 day	3"x 3 " - 2	1 keV!PHU(Cs)	61-148m(61-148) -1	Sm ¹⁴⁸ (n,p)
	148	5.4 day	3"x3"-2	1 keV/PHU(Cs)	61-148 -1	Sm ¹⁴⁸ (n,p)
	151	28.4 hr	3" x 3" -2	1 keV/PHU(Cs)	61-151 -1	Nd ¹⁵⁰ (n,, γ , β)
Samarium	153	46.7 hr	3" x 3"-2	0.5 keV/PHU (Cs)	62-153 -1	Sm ¹⁵² (n, γ)
	155	25 min	3" x 3"-2	0.5 keV/PHU	62-155 -1	Sm ¹⁵⁴ (n, γ)
Europium	152m	9.3 h r	3" x 3"-2	1 keV/PHU(Cs)	63-152m-1	Eu ¹⁵¹ (n, γ)
	155	1.7 yr	3" x 3"-2	0.5 keV/PHU(Cs)	63-155 -1	U ²³⁵ (n,f)
	156	1.5 day	3" x 3"-2	1 keV/PHU(Cs)	63-156 -1	Sm ¹⁵¹ (n, γ , β ,n, γ)
	157	15 hr	3"x3"-2	1 keV/PHU(Cs)	63-157-1	U ²³⁵ (n,f)
Gadolinium	153	200 day	3"x3"-2	0.5 keV/PHU(Cs)	64-153 -1	Gd ¹⁵² (n, γ)
	159	18 hr	3" x 3"-2	1 keV/PHU(Cs)	64-159 -1	Gd ¹⁵⁸ (n,y)
	159	18 hr	3" x 3"-2	0.5 keV/PHU(Cs)	64-159-2	Gd ¹⁵⁸ (n,)
	161	3.7 min	3" x3"-2	1 keV /PHU	64-161 -1	Gd ¹⁶⁰ (n, γ)
Terbium	160	73 day	3" x 3"-2	1 keV/ PHU(Cs)	65-160-2	Tb ¹⁵⁹ (n, γ)
Dysprosium	165m	75 sec	3" x 3" -2	1 keV/ PHU (Cs)	66-165m-1	Dy ¹⁶⁴ (n, γ)
	165	2.3 hr	3" x 3"-2	1 keV/PHU(Cs)	66-165-1	Dy ¹⁶⁴ (n,y)
Holmium	164	37 min	3"x3f'-3	0.5 keV/PHU(Cs)	67-164-1	Ho ¹⁶⁵ (γ ,n)
	166m	1.03 yr	3" x 3"-2	1 keV/PHU(Cs)	67-166m-1	Ho ¹⁶⁰ (n, γ)
	166	27 hr	3" x 3"-2	1 keV/PHU(Cs)	67-1 66-1	Ho ¹⁶⁵ (n,y)
Erbium	171	7.5 hr	3" x 3"-2	0.5 keV/PHU(Cs)	68-171-1	Er ¹⁷⁰ (n, γ)
Thulium	168	85 day	3" x 3"-2	1 keV/PHU(Cs)	69-168-1	Tm ¹⁶⁹ (y,n)
	170	1 27 day	3" x 3"-2	0.5 keV/PHU(Cs)	69-170-1	Tm ¹⁶⁹ (n, γ)
	171	1 .9 yr	3" x 3"-2	0.5 keV/PHU(Cs)	69-171-1	Tm ¹⁶⁹ (n, γ ,n, γ)
Ytterbium	16Q	32 day	3 x 3"- 2	0.5 keV/PHU(Cs)	70-1 69-1	Yb ¹⁶⁸ (n,y)
	175	4.2 day	3" x 3"-2	0.5 keV/ PHU(Cs)	70-175-1	Yb ¹⁷⁴ (n, γ)
Lutetium	176m	3.7 hr	3" x 3"-2	0.5 keV/PHU(Cs)	71-176m-1	W ¹⁷⁵ (n,y)
	177	6.8 day	3"x 3"-2	0.5 keV/PHU(Cs)	71-177-1	Lu ¹⁷⁶ (n,y)
Hafnium	173	24 hr	3" x 3"-3	0.5 keV/PHU(Cs)	72-173-1	H f ¹⁷⁴ (n, γ)
	173	2 4 hr	3" x 3"-2	1 keV/PHU(Cs)	72-173-2	H f ¹⁷⁴ (n, γ)
	175	7.0 day	3" x 3"-2	I keV PHU(Cs)	72-175-1	Hf ¹⁷⁴ (n,y)
	175	70 day	3" x3"-2	0.5 keV/PHU(Cs)	72 -175-2	Hf ¹⁷⁴ (n,y)
	179m	1.9 sec	3" x 3"-2	I keV/PHU(Cs)	72-179m-1	Hf ¹⁷⁸ (n,y)
	180m	5.5 hr	3"x 3"-2	I keV/PHU(Cs)	72-180m-1	Hf ¹⁷⁹ (n, γ)
	181	43 day	3" x 3"-2	I keV/PHU(Cs)	72- 81-1	Hf ¹⁸¹ (n, γ)

Element	Isotope	Half-Life	Detector	Energy Scale	Plate Number	Method of Production
Tantalum	180m	8.1 hr	3" x 3"-5	0.5 keV/PHU(Cs)	73-180m-1	Ta $^{181}(\gamma, n)$
	182m	1.6 min	3" x 3"-2	0.5 keV/PHU	73-182m-1	Ta $^{181}(n,\gamma)$
	182	115 day	3" x 3"-2	1 keV/PHU(Cs)	73-1 82-1	Ta $^{181}(n,\gamma)$
	183	5.2 day	3" x 3"-2	1 keV/PHU(Cs)	73-1 83-1	Ta $^{181}(2n,\gamma)$
Wolfram (Tungsten)	187	24 hr	3" x 3"-2	1 keV/PHU(Cs)	74-1 87-1	W $^{186}(n,\gamma)$
Rhenium	188m	18.7 min	3" x 3"-2	0.5 keV/PHU(Cs)	75-188m -1	Re $^{187}(n,\gamma)$
	188	1.7 h r	3" x 3"-2	1 keV/PHU(Cs)	75- 188-1	Re $^{187}(n,\gamma)$
Osmium	185	94 day	3" x 3"-2	1 keV/PHU (Cs)	76-185-1	Os $^{184}(n,\gamma)$
	191	1.5 day	3" x 3"-2	0.5 keV/PHU(Cs)	76-191-1	Os $^{191}(n,\gamma)$
	193	32 hr	3" x 3"-2	1 keV/PHU(Cs)	76-193-1	Os $^{192}(n,\gamma)$
Iridium	192	74 day	3" x 3"-2	1 keV// PHU (Cs)	77-192-1	Ir $^{191}(n,\gamma)$
	194	1.9 hr	3" x 3"-2	1 keV, //PHU(Cs)	77-194-1	Ir $^{193}(n,\gamma)$
Platinum	195m	4.1 day	3" x 3"-2	0.5 keV// PHU(Cs)	78-195m-1	Pt $^{194}(n,\gamma)$
	197	2.0 h r	3" x 3"-2	0.5 keV/PHU(Cs)	78-197-1	Pt $^{196}(n,\gamma)$
	199	3.0 min	3" x 3"-2	1 keV/PHU(Cs)	78-199-1	Pt $^{198}(n,\gamma)$
Gold	196	6.1 day	3" x 3"-2	1 keV/PHU(Cs)	79-196-1	Au $^{197} (\gamma, n)$
	198	64.8 hr	3" x 3"-2	1 keV /PHUICs	79-198-1	Au $^{197}(n,\gamma)$
	199	3.2 day	3" x 3"-2	1 keV/PHU(Cs)	79-199-1	Pt $^{198}(n\gamma,fl)$
	199	3.2 day	3" x 3"-2	0,5 keV/PHU(Cs)	79-199-2	Pt $^{198}(n,\gamma,\beta)$
Mercury with Hg ¹⁹⁷	197m	2.4 hr	3" x 3"-2	0.5 keV/PHU(Cs)	80-197m(80-197)-l	Hg $^{196}(n,\gamma,\beta)$
	197	6.5 hr				
	197	6.5 hr	3" x 3"-2	0.5 keV/PHU(Cs)	80-97-1	Hg $^{196}(n,\gamma)$
	203	4.7 day	3" x 3"-2	1 keV/PHU(Cs)	80-203-1	Hg $^{202}(n\gamma)$
	203	4.7 day	3" x 3"-2	0.5 keV/PHU(Cs)	80-203-2	Hg $^{202}(n,\gamma)$
Thallium	202	1.2 day	3" x 3"-2	1 keV/"PHU(Cs)	81-202-1	Tl $^{203} (\gamma, n)$
	204	3.9 y r	3" x 3"-2	1 keV/PHU(Cs)	81-204-1	Tl $^{203}(n,\gamma)$
	208	3.1 min	3" x 3"-2	1 keV/PHU(Cs)	81-208-1	Th 228 decay
Lead	203	5.2 h r	3" x 3"-2	1 keV/PHU(Cs)	82-203-1	Pb $^{204}(\gamma,n)$
	204m	67 min	3" x 3"-2	1 keV/"PHU(Cs)	82-204m-1	Pb $^{204} (\gamma,\gamma)$
	207m	0.8 sec	3" x 3"-5	1 keV/PHU(Cs)	82-207m-1	Pb $^{201}(\gamma,n)$
	212	1 0.6 hr	3" x 3"-2	1 keV/PHU(Cs)	82-21 2-1	Th 228 decay
Bismuth	205	1 5 day	3" x 3"-2	1 keV/PHU(Cs)	83-205-2	Pb $^{206}(p,2n)$
	207	28 yr	3" x 3"-2	1 keV/PHU(Cs)	83-207-2	Pb $^{207}(p,n)$
	212	60 min	3" x 3"-2	1 keV/PHU(Cs)	83-21 2-1	Th 228 decay

Element	Isotope	Half-Life	Detector	Energy Scale	Plate Number	Method of Production
Radium with daughters	226	1620 yrs	3" x 3"-2	2 keV/PHU(Cs)	88-226-1	nat.
Thorium with daughters	228	1.91 yr	3" x 3"-2	1 keV/PHU(Cs)	90-228-1	Th decay
	228	1.91 yr	3" x 3"-2	2 keV/PHU(Cs)	90-228-2	Th decay
	with daughters					
	232	1.4×10^{11} yr	3" x 3"-2	1 keV/PHU(Cs)	90-232-1	nat.
	with daughters					
Protactinium	231	34,000 yr	3" x 3"-2	1 keV/PHU(Cs)	91-231-1	nat.
	233	27 day	3" x 3"-2	0.5 keV/PHU(Cs)	91-233-1	$\text{Th}^{231}(n,\gamma,\beta)$
	233	27 day	3" x 3"-2	1 keV/PHU(Cs)	91-233-2	$\text{Th}^{232}(n,\gamma,\beta)$
Uranium	235	1.1×10^{11} yr	3" x 3"-2	0.5 keV/PHU(Cs)	92-235-1	not.
	237	6.7 day	3" x 3"-2	0.5 keV/PHU(Cs)	92-237-1	Pu^{241} decay
	239	23.5 min	3" x 3"-2	0.5 keV//PHU(Cs)	92-239-1	$\text{U}^{238}(n,\gamma)$
Uranium ore			3" x 3"-2	2 keV/PHU	92-(ore)-1	nat.
Neptunium	239	2.35 day	3" x 3"-2	0.5 keV/PHU(Cs)	93-239-2	$\text{U}^{235}(n,\gamma,\beta)$



53.29 Day ${}^7\text{Be}$ Decay Scheme [C]



04-07-1

GAMMA-RAY ENERGIES AND INTENSITIES

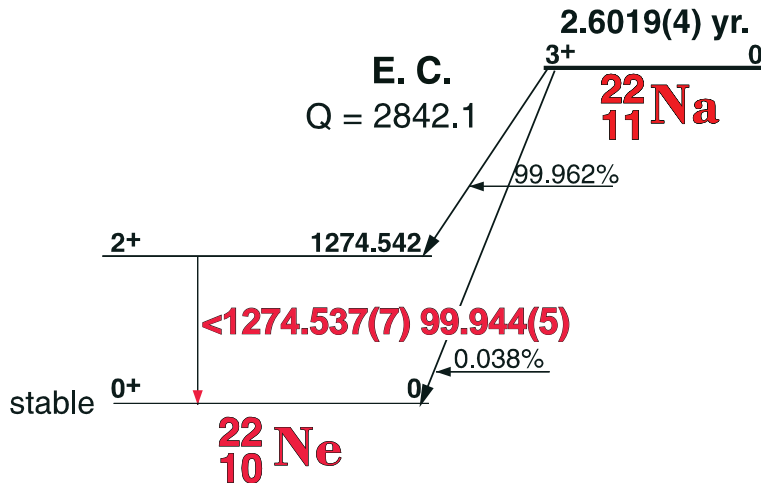
Nuclide ${}^7\text{Be}$ Half Life 53.29(7) day
 Detector 3" x 3" -2 NaI Method of Production: Li⁷(p,n)

E_γ (KeV)[S]	ΔE_γ	I_γ (rel)	$I_\gamma(\%)$ [E]	ΔI_γ	S
511.006		100	170	± 1.0	1
1274.537	± 0.008	62.2	99.94	± 0.01	1

2.6019 Yr. ^{22}Na [C]

^{22}Na Decay Scheme

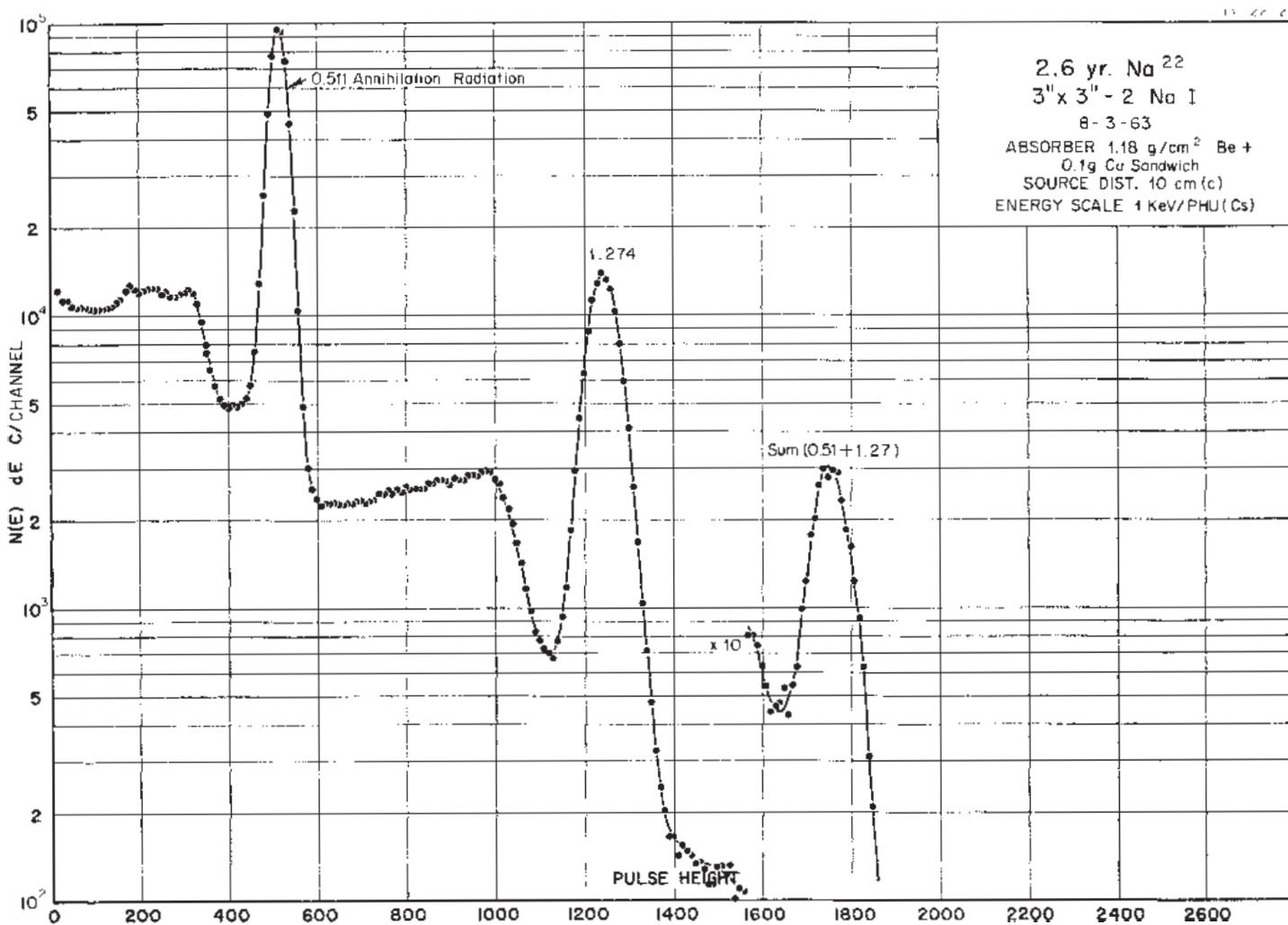
11-22-1



GAMMA-RAY ENERGIES AND INTENSITIES

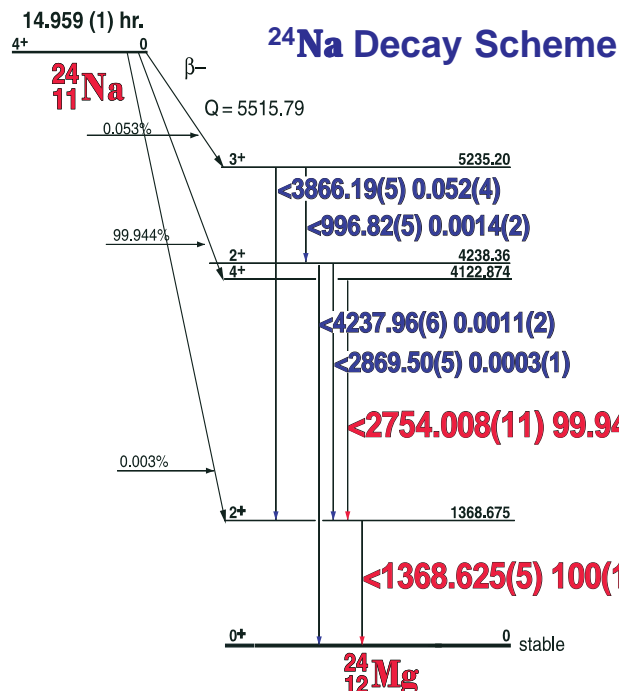
Nuclide ^{22}Na Half Life 2.6019(4) yr.
Detector 3" X 3" - 2 NaI Method of Production: Na^{23} ($n, 2n$)

E_{γ} (KeV)	ΔE_{γ}	$I_{\gamma}(\text{rel})$	$I_{\gamma}(\%)$	ΔI_{γ}	S
511.006		100	170	± 1.0	1
1274.537	± 0.008	62.2	99.94	± 0.01	1



14.965 Hr. ^{24}Na [C]

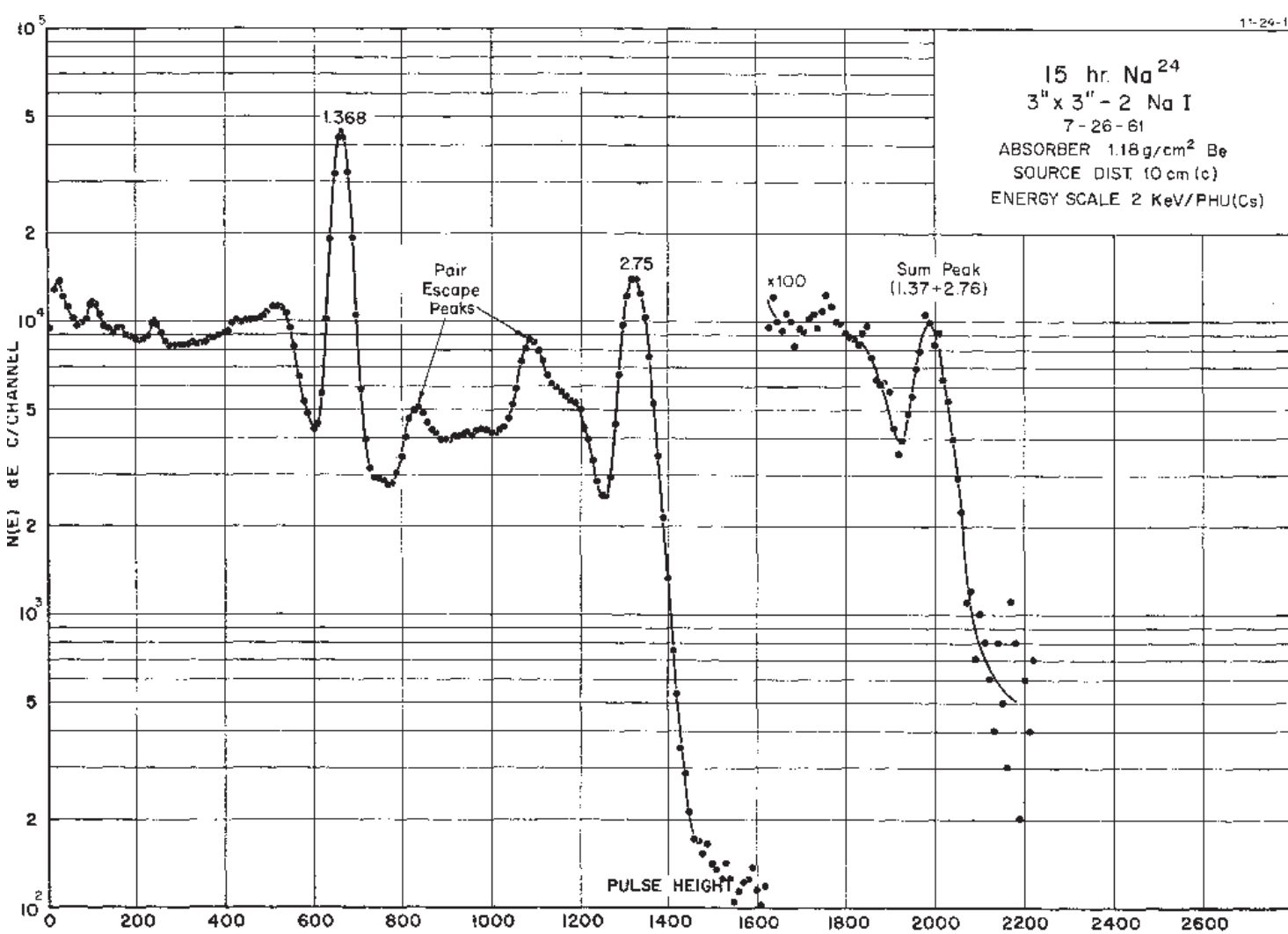
11-24-1



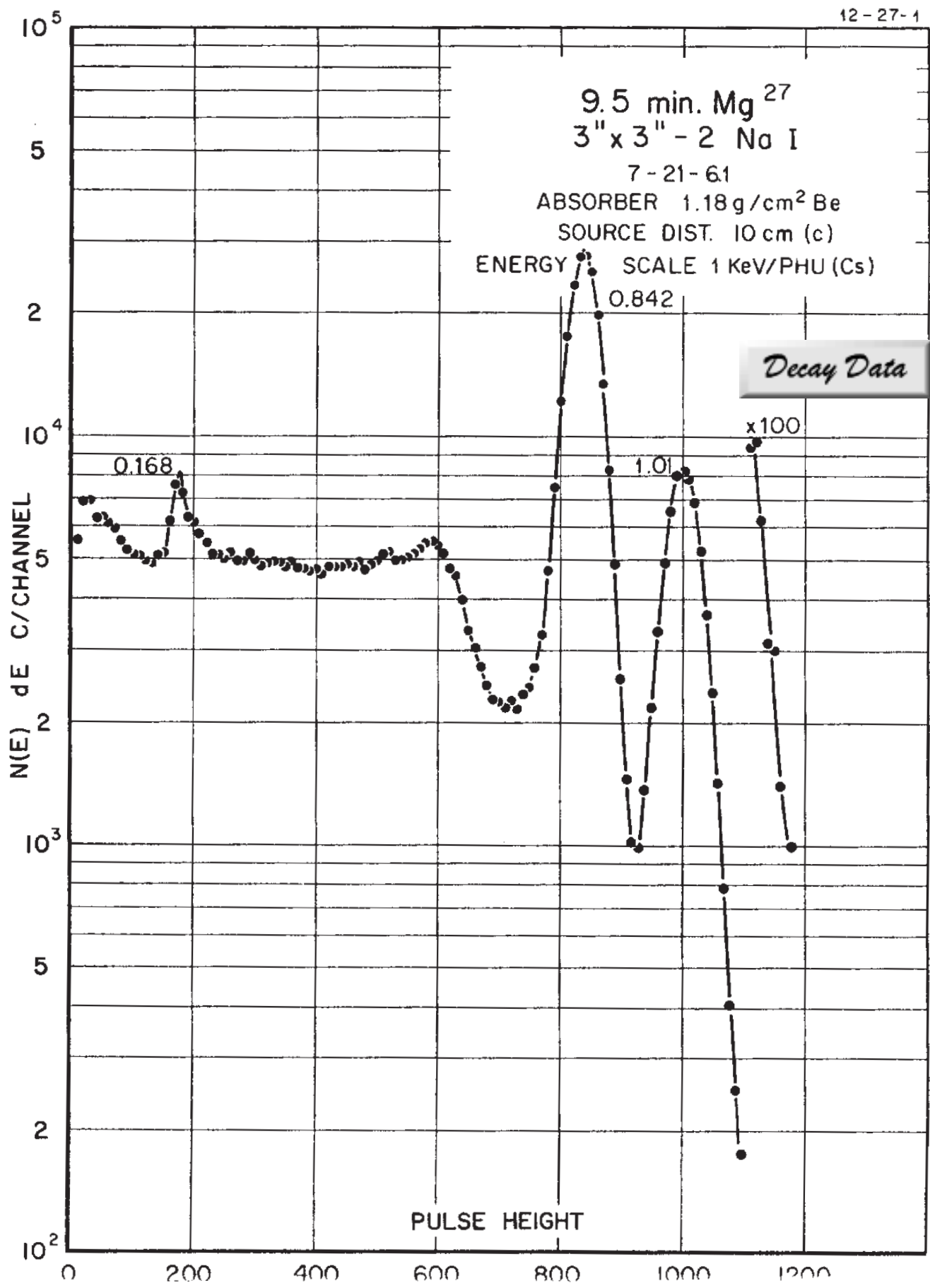
GAMMA-RAY ENERGIES AND INTENSITIES

Nuclide ^{24}Na
 Detector 3" X 3" NaI-2
 Half Life 14.96(1) hr.
 Method of Production: $\text{Na}^{23}(\text{n},\gamma)$

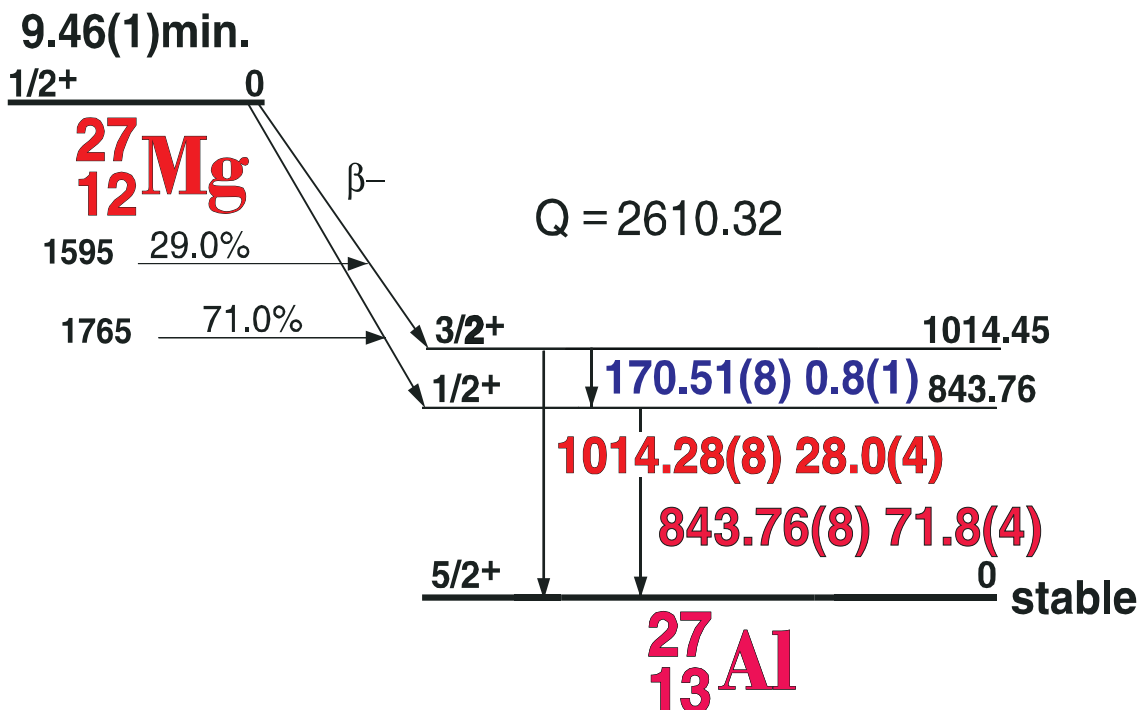
	E_γ (KeV)[S]	ΔE_γ	I_γ (rel)	I_γ (%) [E]	ΔI_γ	S
DE	346.42	± 0.2				4
Ann.	511.006					3
SE	857.43	± 0.2				4
	1368.626	± 0.005	100	99.99	± 0.01	1
DE	1732.17	± 0.13				1
SE	2243.00	± 0.18				2
	2754.007	± 0.01	98.6	99.87	± 0.02	1
DE	2844.1	± 0.2				4
SE	3355.1	± 0.3				4
	3867.5	± 0.3	0.07	0.056	± 0.01	2



12-27-1



9.46(1) min. ^{27}Mg Decay Scheme

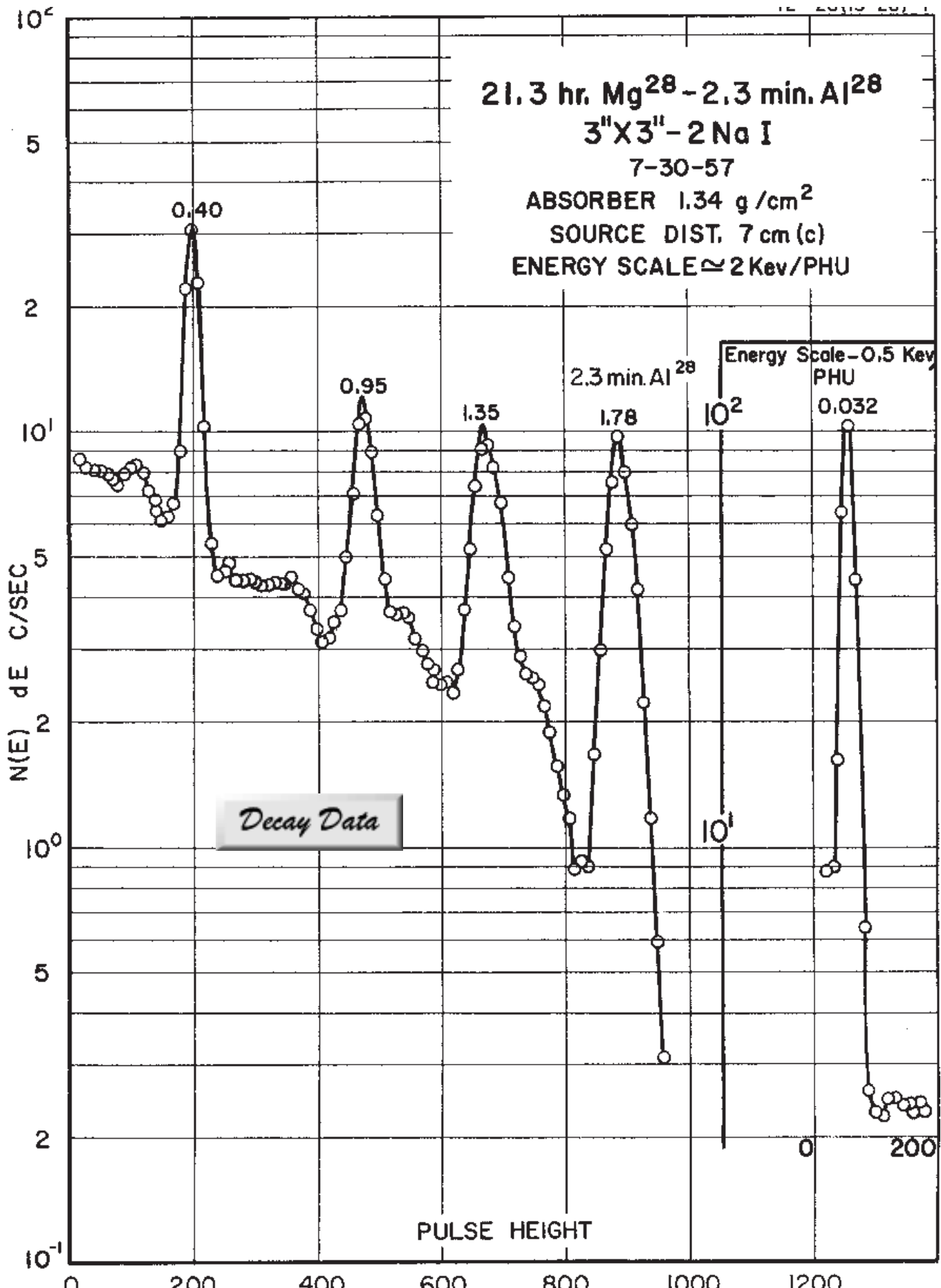


GAMMA-RAY ENERGIES AND INTENSITIES

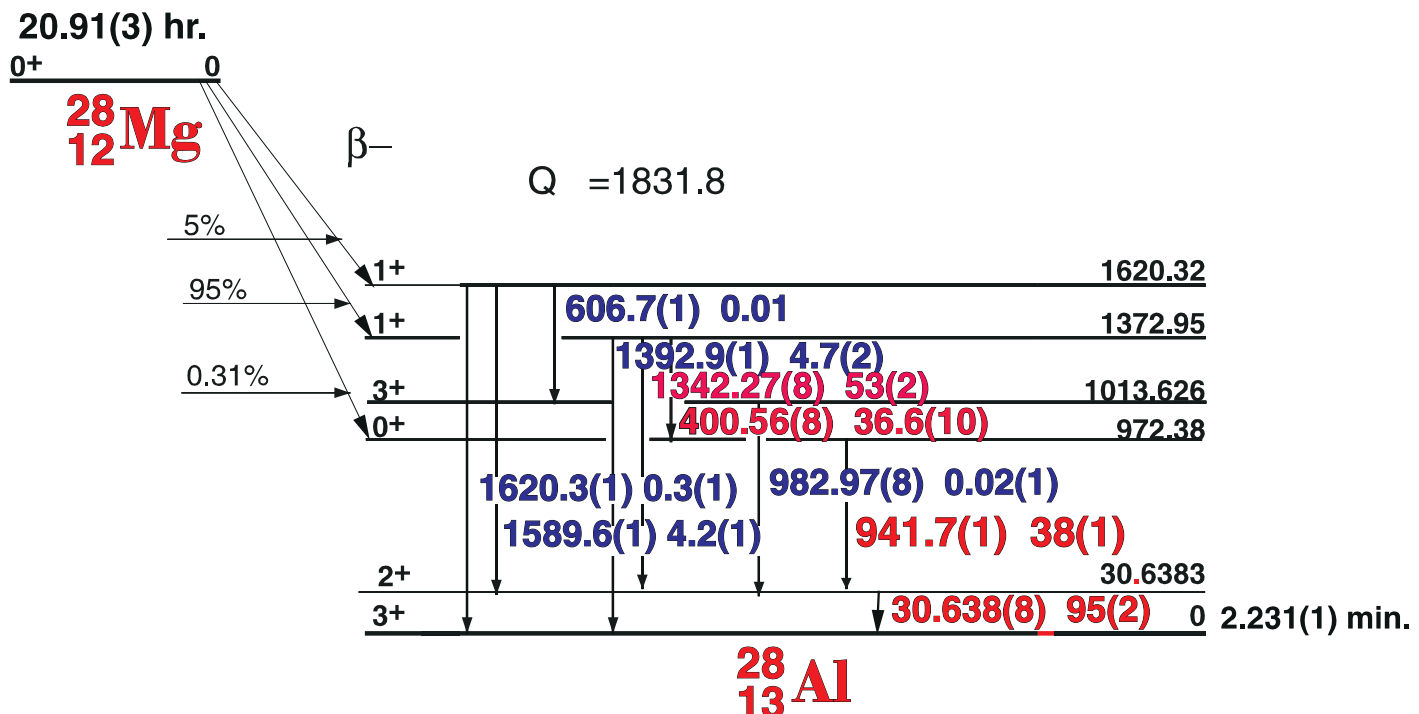
Nuclide ^{27}Mg
 Detector 3" x 3" -2 NaI

Half Life 9.46(1) min.
 Method of Production: $\text{Mg}^{26}(n,\gamma)$

E_γ (KeV)[S]	ΔE_γ	I_γ (rel)	$I_\gamma(\%)$ [E]	ΔI_γ	S
170.69	± 0.02	1.1	0.8	± 0.1	3
843.76	± 0.03	100	71.8	± 0.4	1
1014.44	± 0.04	39	28.0	± 0.4	1



20.91(3) hr. ^{28}Mg Decay Scheme



GAMMA-RAY ENERGIES AND INTENSITIES

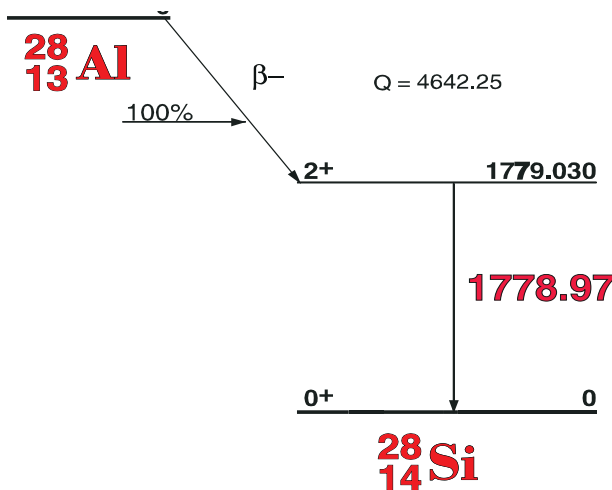
Nuclide ^{28}Mg
Detector 3" x 3" -2 NaI

Half Life 20.91(3) hr.
Method of Production: $\text{Mg}^{26}(2n, \gamma)$

E_γ (KeV)[S]	ΔE_γ	I_γ (rel)	I_γ (%) [E]	ΔI_γ	S
30.64	± 0.02		66	± 4	1
400.69	± 0.02		36.6	± 1.0	1
941.45	± 0.03		38.3	± 1.0	1
982.9	± 0.3		0.02	± 0.01	3
1342.25	± 0.05		52.6	± 1.6	1
1372.89	± 0.06		4.7	± 0.2	1
1620.0	± 0.2		0.3	± 0.1	4

2.241(1) min ^{28}Al Decay Scheme

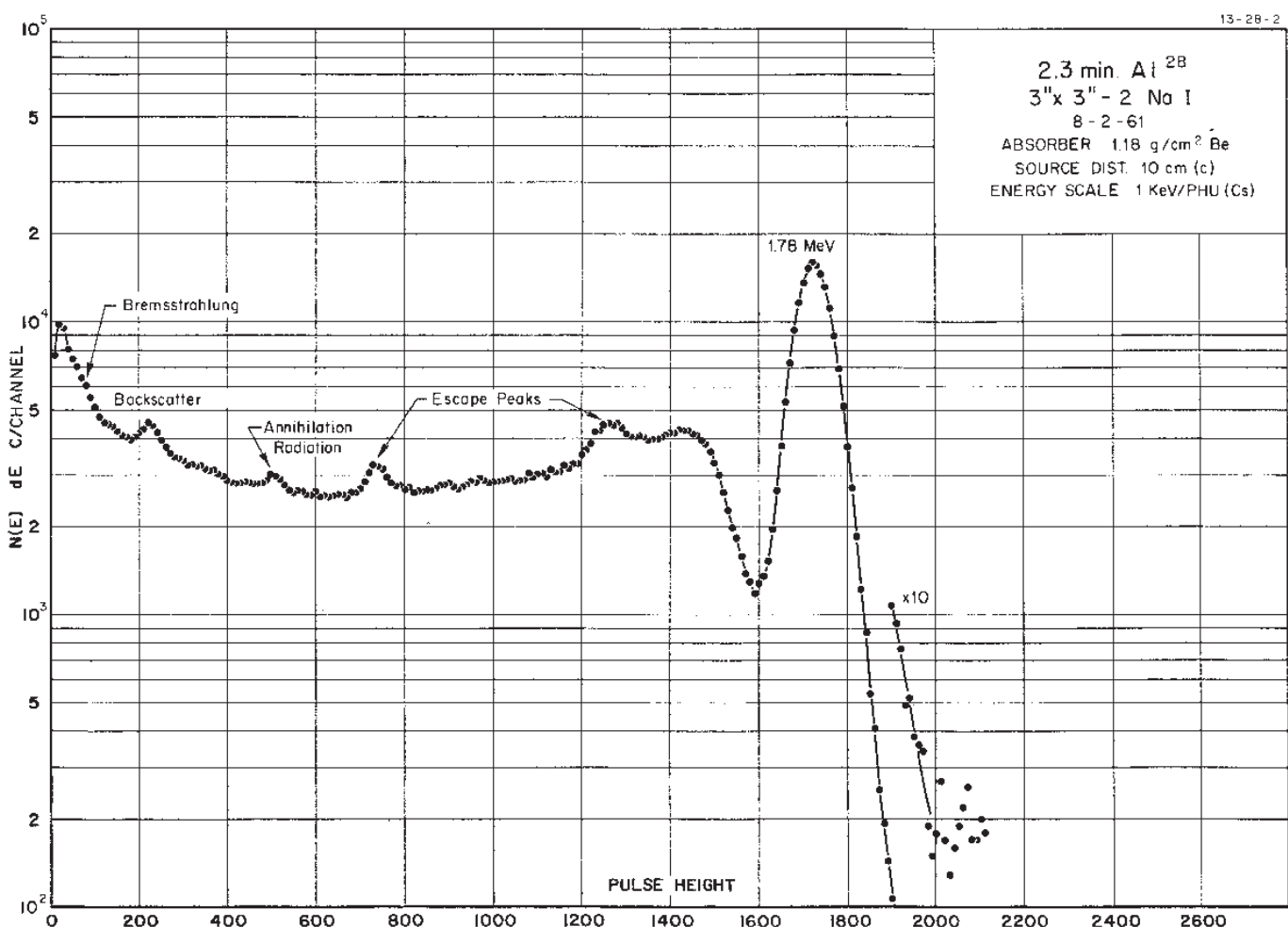
13-28-2



GAMMA-RAY ENERGIES AND INTENSITIES

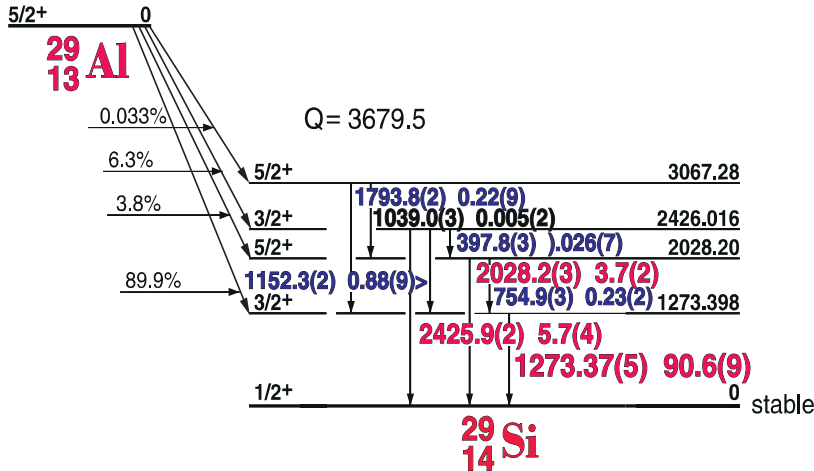
Nuclide ^{28}Al Half Life 2.241(1) min.
Detector 3" X 3" - 2 NaI Method of Production: $\text{Al}^{27}(n,\gamma)$

E_γ (KeV)	ΔE_γ	I_γ (rel)	I_γ (%)	ΔI_γ	S
1778.85	± 0.03	100	100	± 1	1



6.56(6) min. ^{29}Al Decay Scheme

6.56(6) min.



GAMMA-RAY ENERGIES AND INTENSITIES

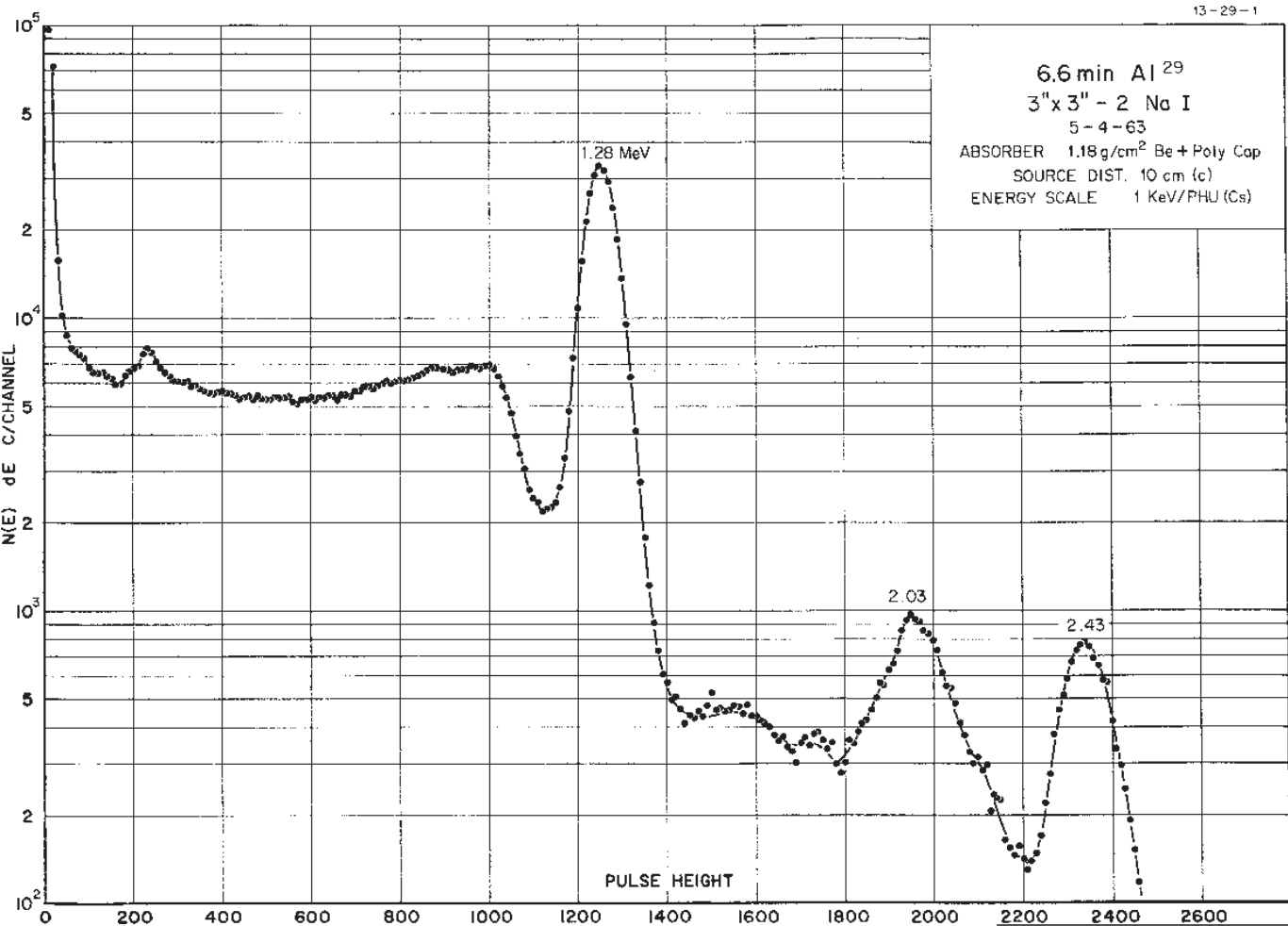
Nuclide ^{29}Al

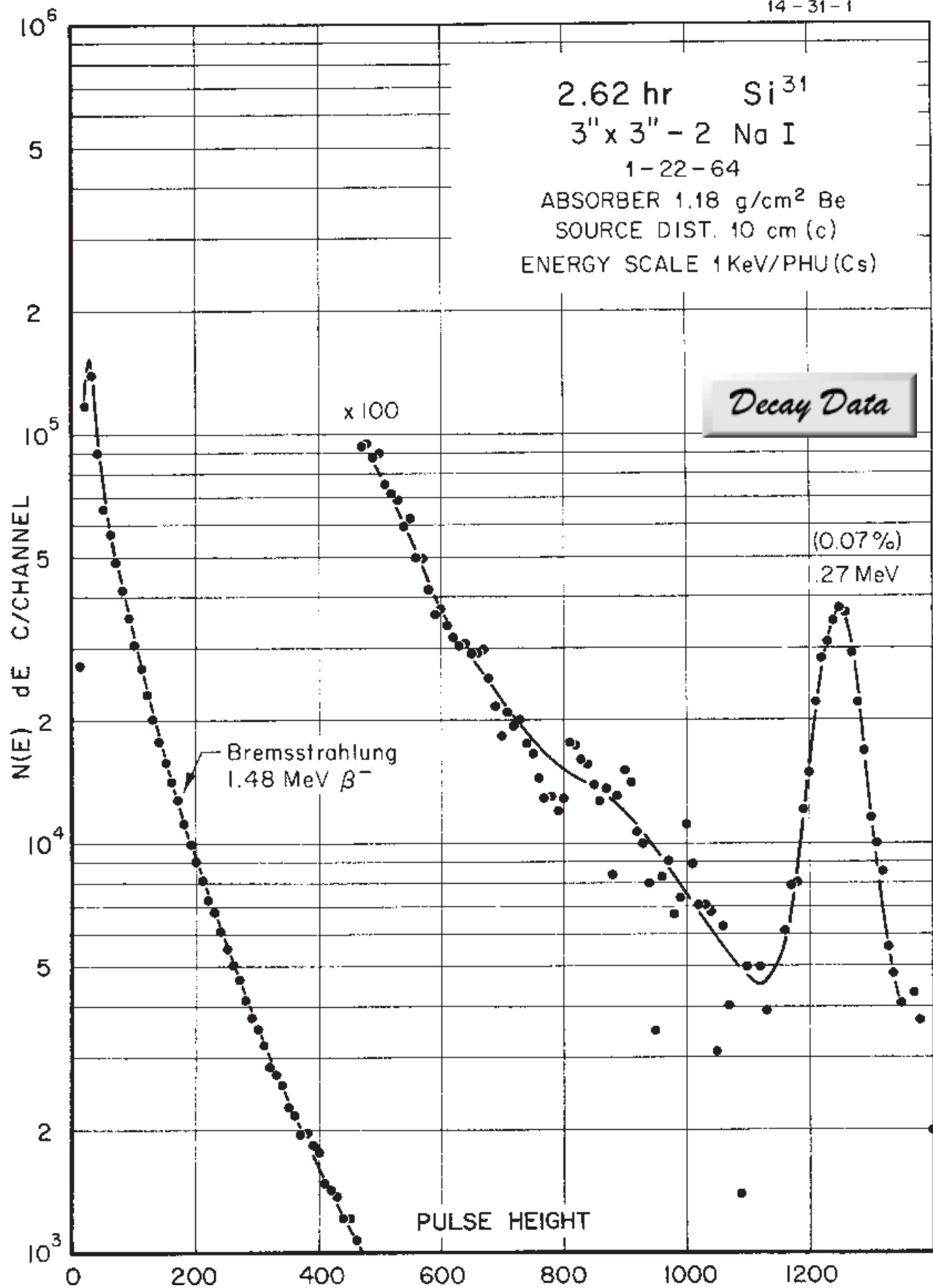
Detector 3" X 3" NaI-2

Half Life 6.56(6) min.

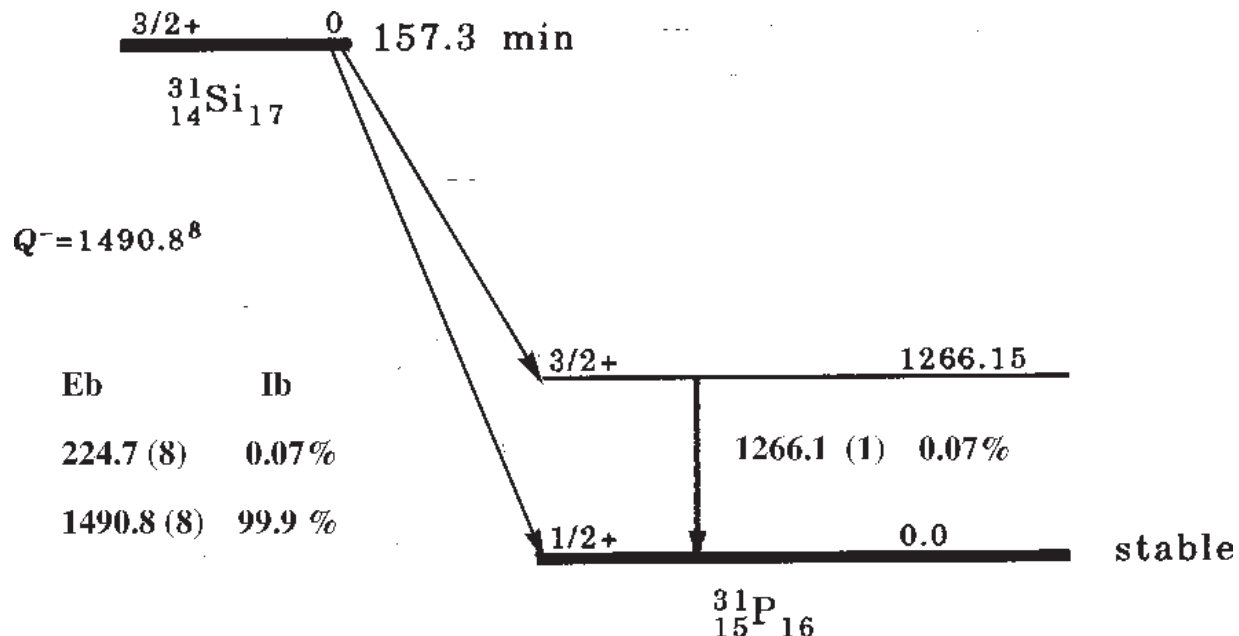
Method of Production: Si²⁹ (n,p)

E_{γ} (KeV)[S]	ΔE_{γ}	$I_{\gamma}(\text{rel})$	$I_{\gamma}(\%)[E]$	ΔI_{γ}	S
754.9	± 0.3		0.23	± 0.02	3
1152.3	± 0.2		0.88	± 0.09	3
1273.3	± 0.1		90.6	± 0.9	1
2028.2	± 0.3		3.7	± 0.2	2
2425.9	± 0.2		5.7	± 0.4	1





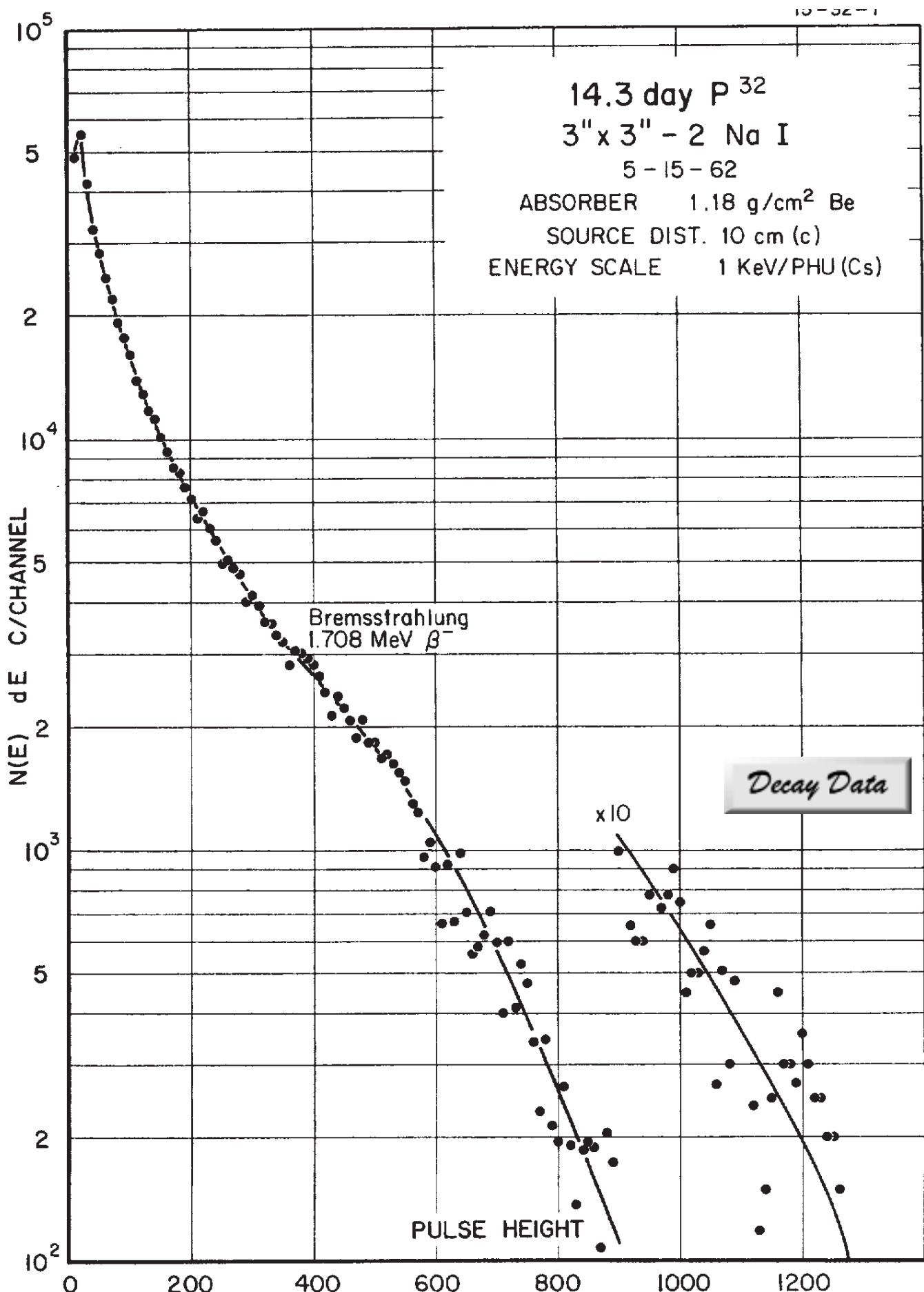
157.3(3) min ^{31}Si Decay Scheme



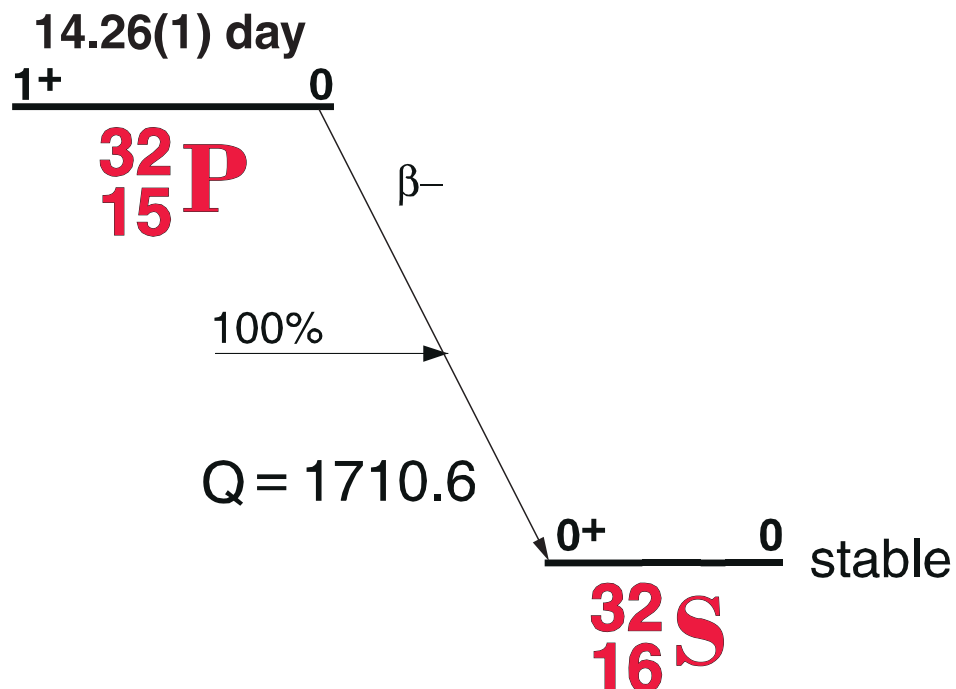
GAMMA-RAY ENERGIES AND INTENSITIES

Nuclide Detector	^{31}Si $3'' \times 3'' -2 \text{ NaI}$	Half Life 157.3(3) min. Method of Production: $\text{Si}^{30}(n,\gamma)$
---------------------	---	--

E_γ (KeV)[S]	ΔE_γ	I_γ (rel)	$I_\gamma(\%)$ [E]	ΔI_γ	S
1266.15	± 0.1	100	0.07		1



14.26(1) day ^{32}P Decay Scheme

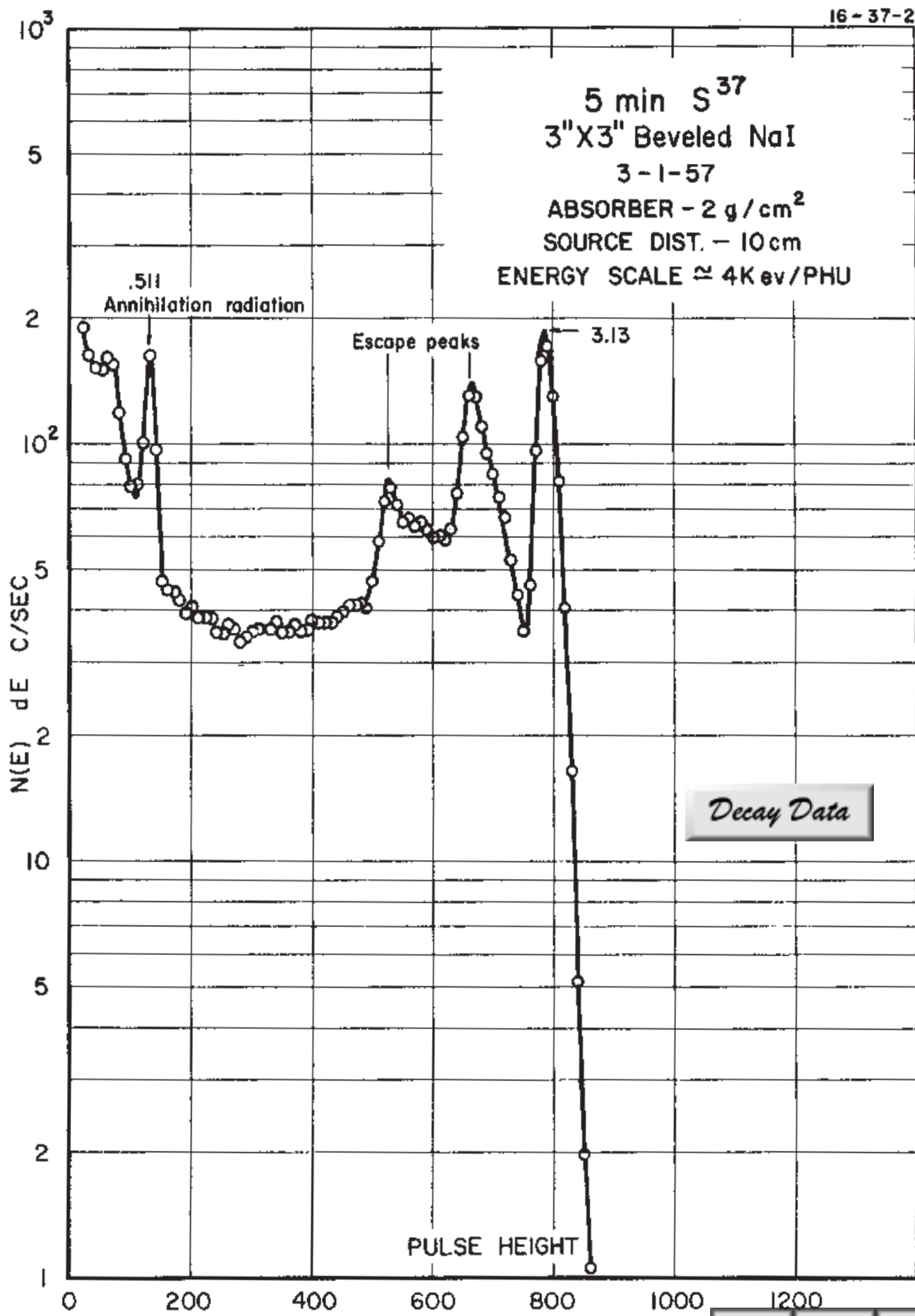


GAMMA-RAY ENERGIES AND INTENSITIES

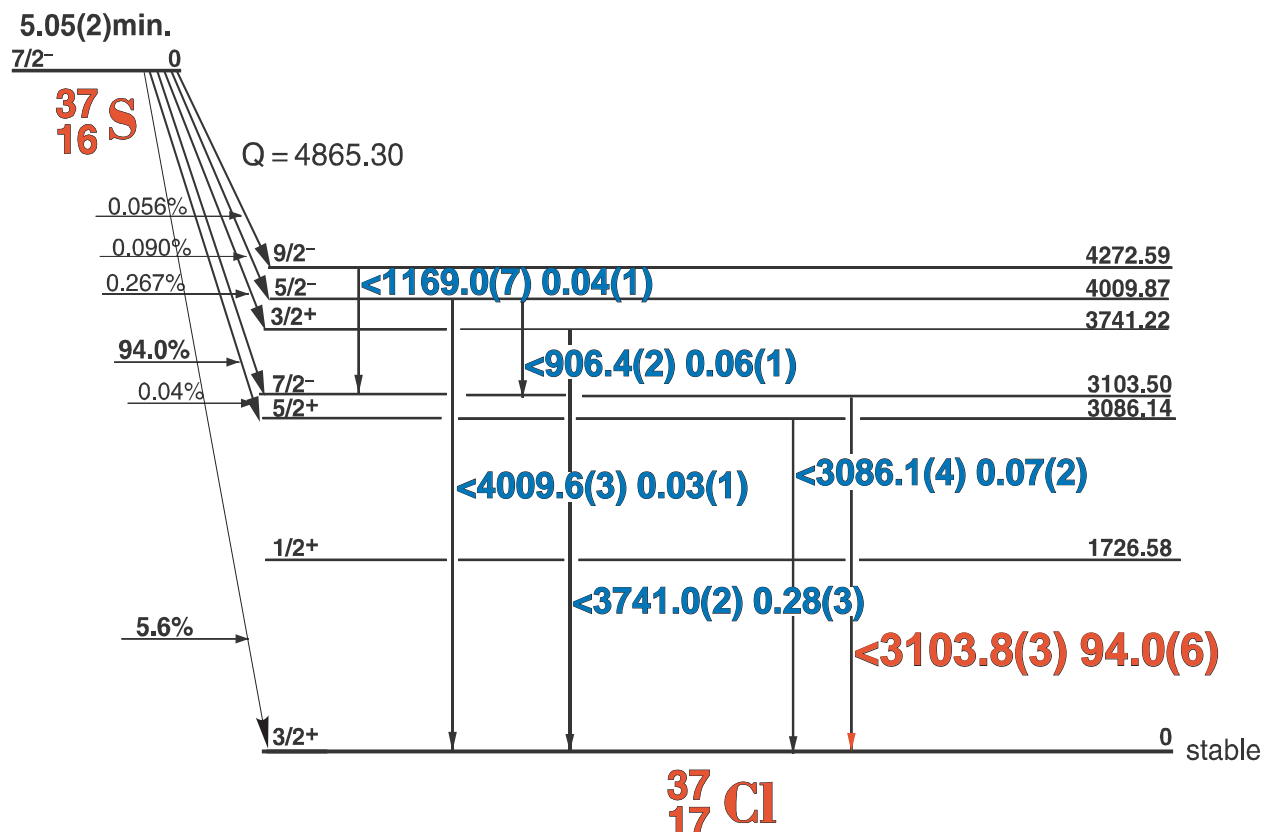
Nuclide ^{32}P
Detector 3" x 3" - 2Nal

Half Life 14.26(1) day
Method of Production: $\text{P}^{31}(n,\gamma)$

E_γ (KeV)[S]	ΔE_γ	I_γ (rel)	$I_\gamma(\%)$ [E]	ΔI_γ	S
1.708 bremsstrahlung		100	100		



5.05(2) min. ^{37}S Decay Scheme



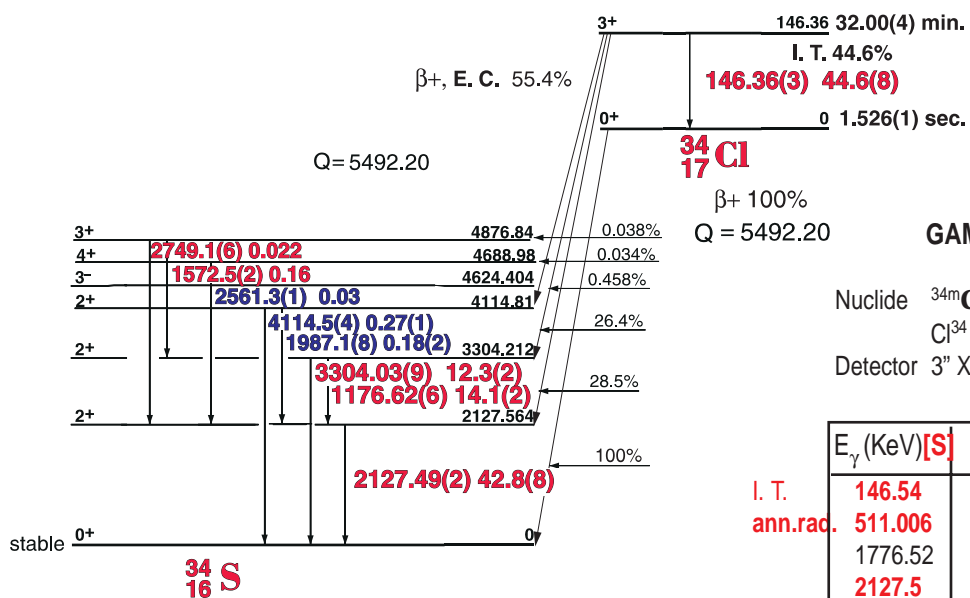
GAMMA-RAY ENERGIES AND INTENSITIES

Nuclide ^{37}S
Detector 3" x 3" - 2NaI

Half Life 5.05 Min.
Method of Production: $\text{S}^{36}(\text{n},\gamma)$

E_γ (KeV) [S]	ΔE_γ	I_γ (rel)	I_γ (%) [E]	ΔI_γ	S
3103.36	± 0.05	100	94	± 0.6	1
3741.02	$\pm 0.$	0.3	0.26		

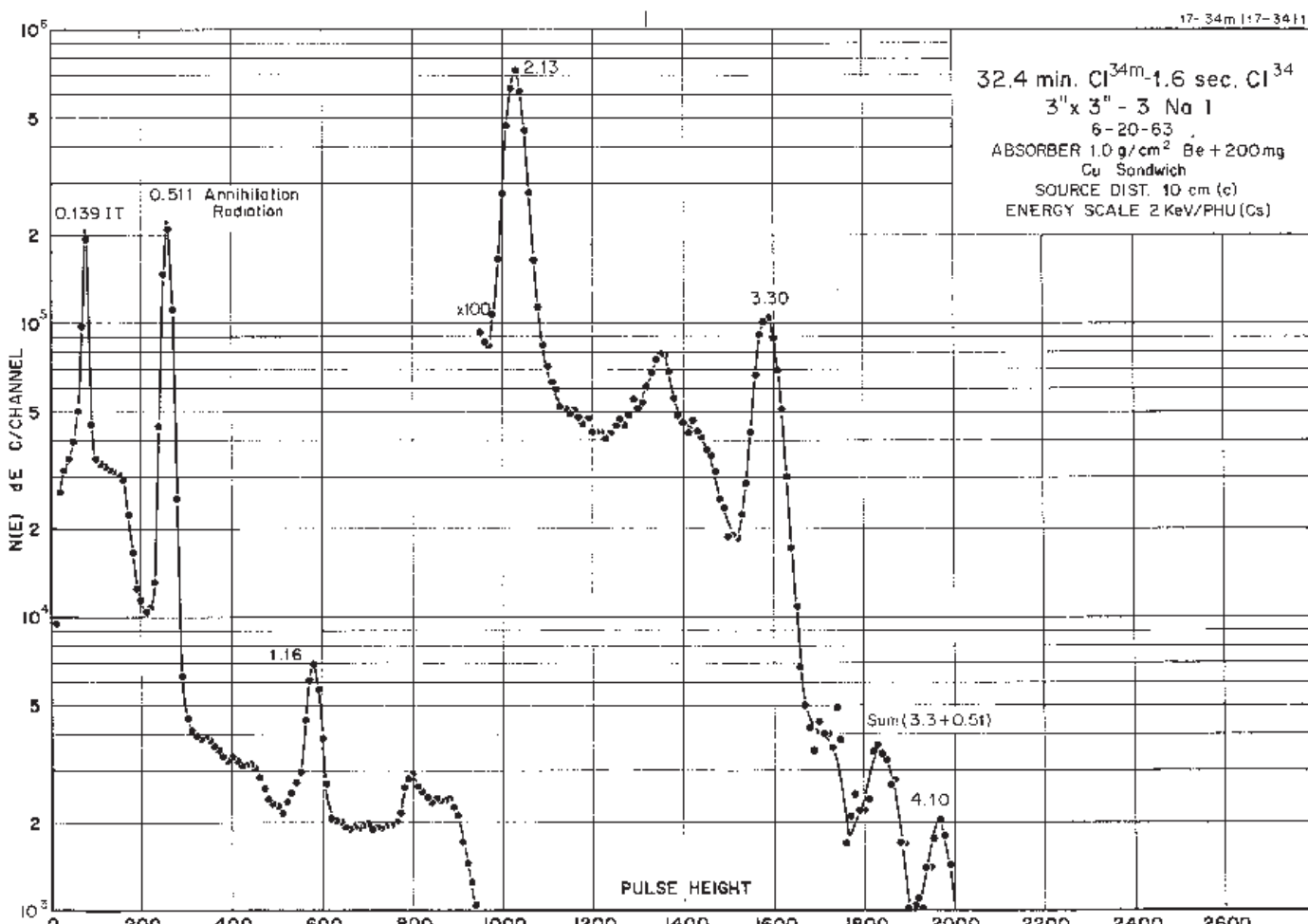
32.00 min. ^{34m}Cl - 1.6 sec. ^{34}Cl

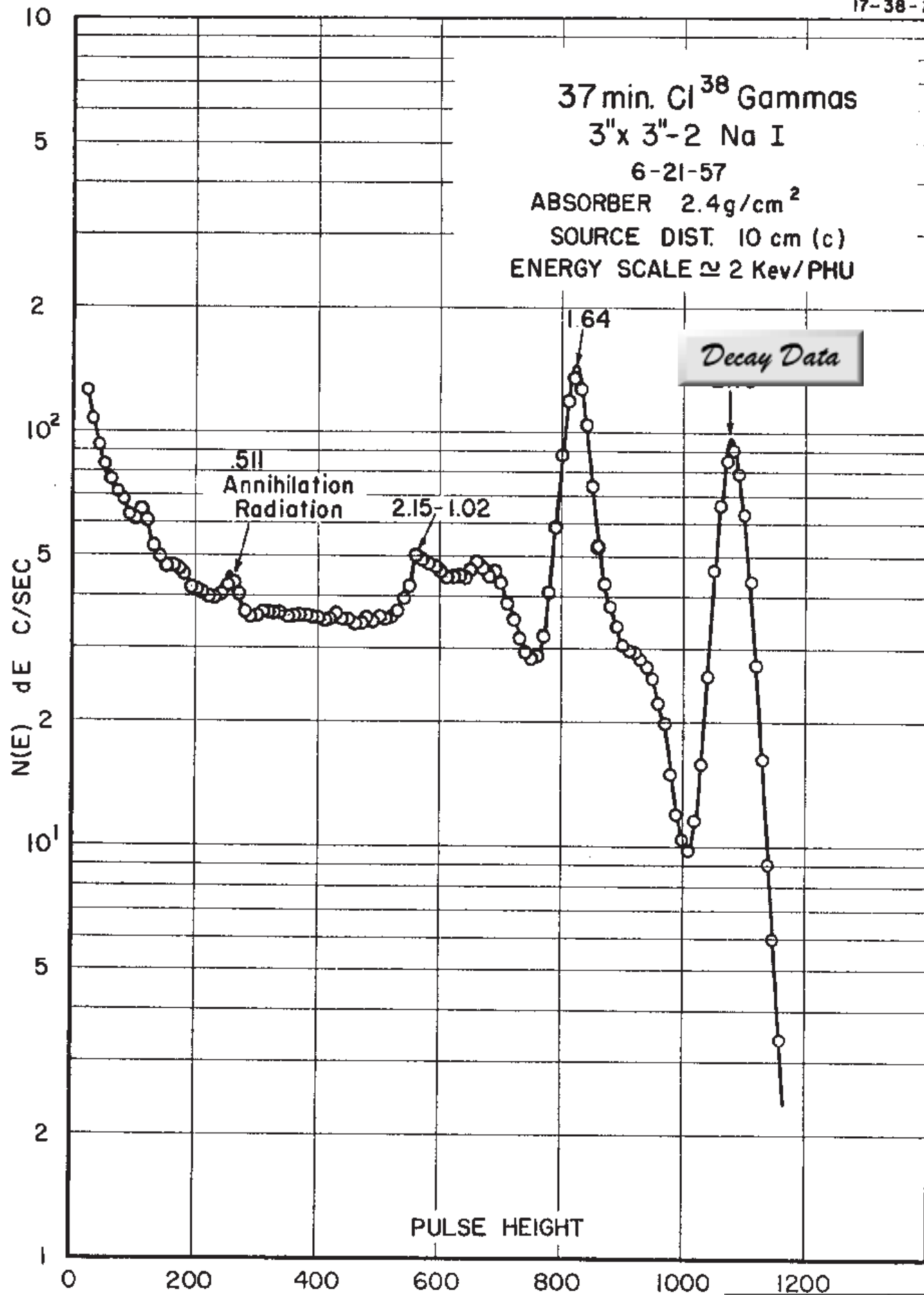


GAMMA-RAY ENERGIES AND INTENSITIES

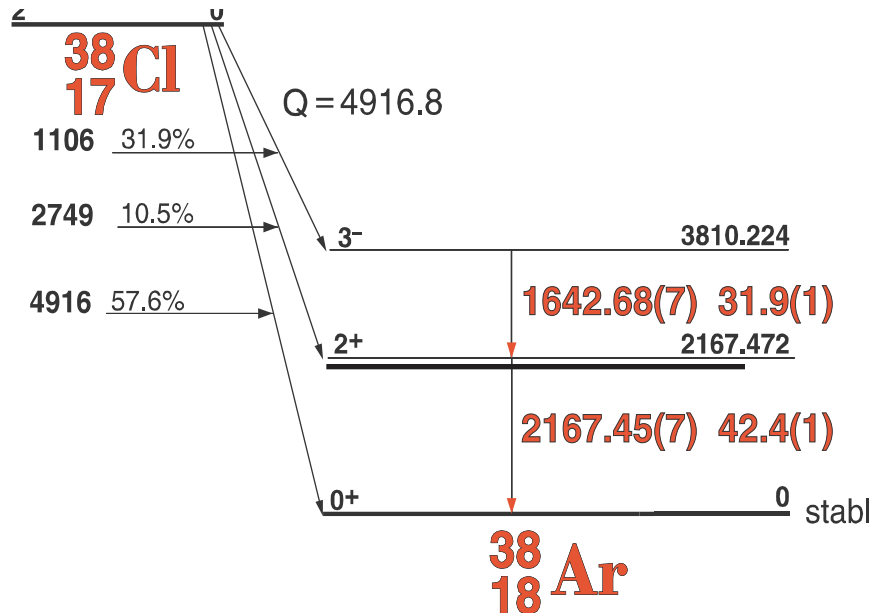
Nuclide ^{34m}Cl Half Life 32.00(4) min.
 Cl^{34} Half life 1.6 sec.
 Detector 3" X 3" - 2 NaI Method of Production: $\text{Cl}^{35}(\gamma, n)$

	$E_\gamma (\text{KeV}) [\text{S}]$	ΔE_γ	$I_\gamma (\text{rel})$	$I_\gamma (\%) [\text{E}]$	ΔI_γ	S
I. T.	146.54	± 0.03		40.6	± 0.8	1
ann.rad.	511.006					1
	1776.52	± 0.06		14.1	± 0.2	2
	2127.5	± 0.6		42.8	± 0.6	1
	3304.04	± 0.1		12.3	± 0.3	1





37.24 min. ^{38}Cl Decay Scheme



GAMMA-RAY ENERGIES AND INTENSITIES

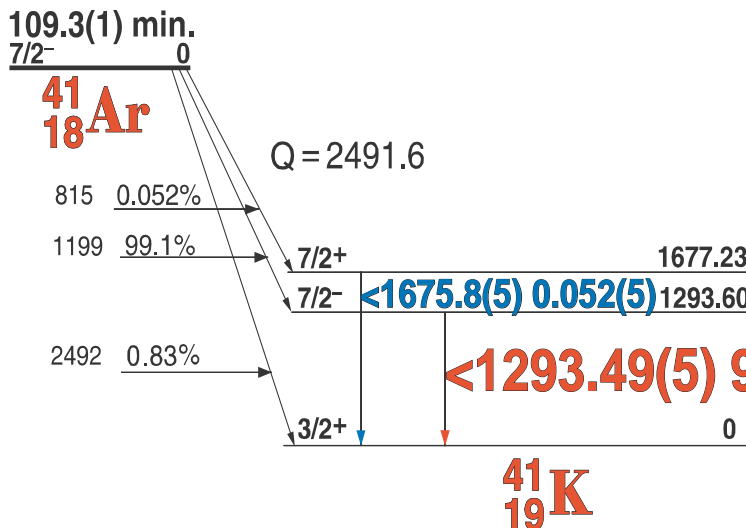
Nuclide ^{38}Cl
Detector 3" x 3" -2 NaI
Half Life 37.24(5) min.
Method of Production: $\text{Cl}^{37}(n,\gamma)$

E_γ (KeV) [S]	ΔE_γ	I_γ (rel)	$I_\gamma(\%)$ [E]	ΔI_γ	S
1642.71	± 0.04	76	31.9	± 1	1
2167.45	± 0.07	100	42.0	± 1.0	1

109.34 Min. ^{41}Ar

18-41-1

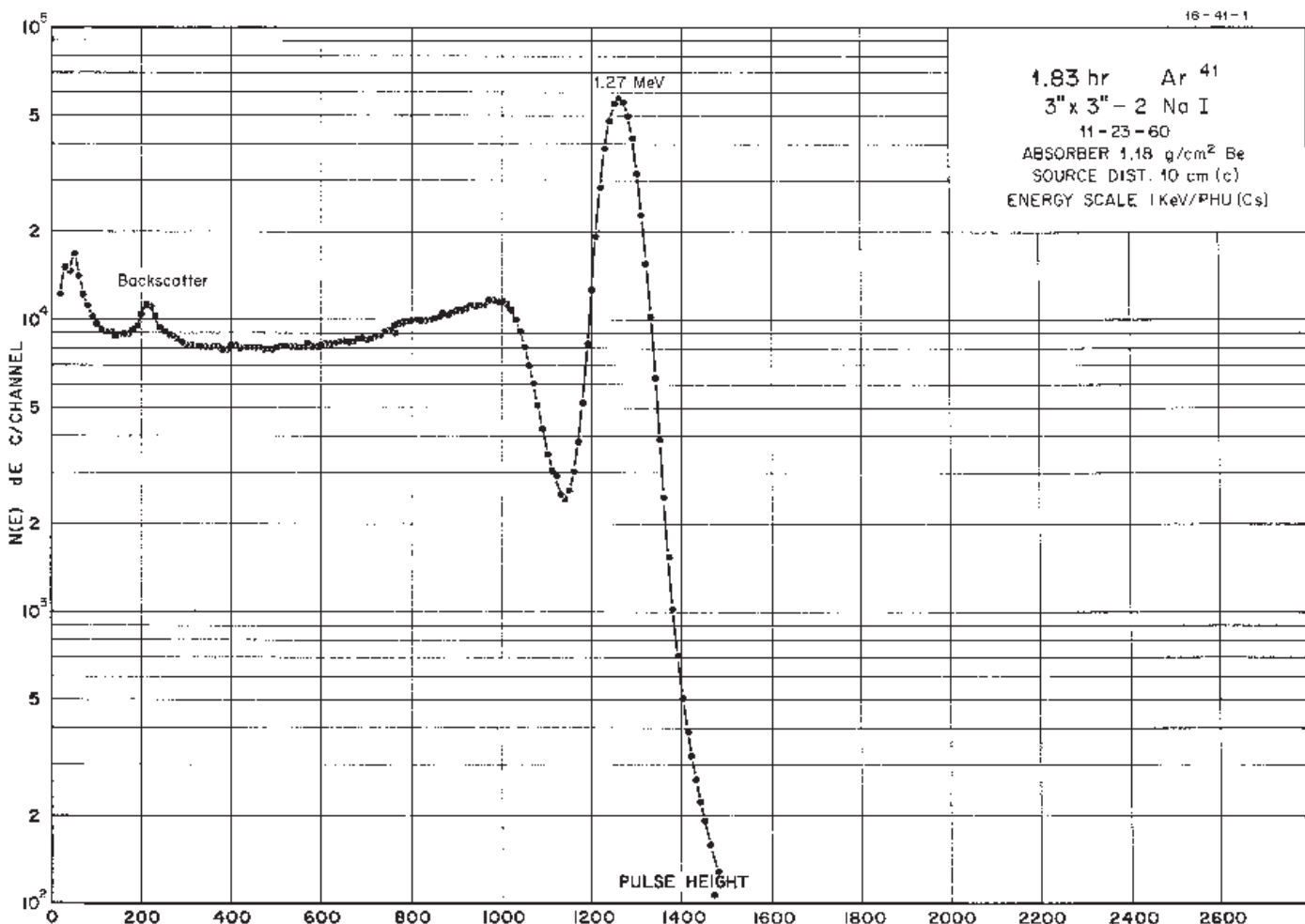
^{41}Ar Decay Scheme



GAMMA-RAY ENERGIES AND INTENSITIES

Nuclide ^{41}Ar Half Life 109.3(1) min.
Detector 3" X 3" - 2NaI Method of Production: Ar⁴⁰ (n,γ)

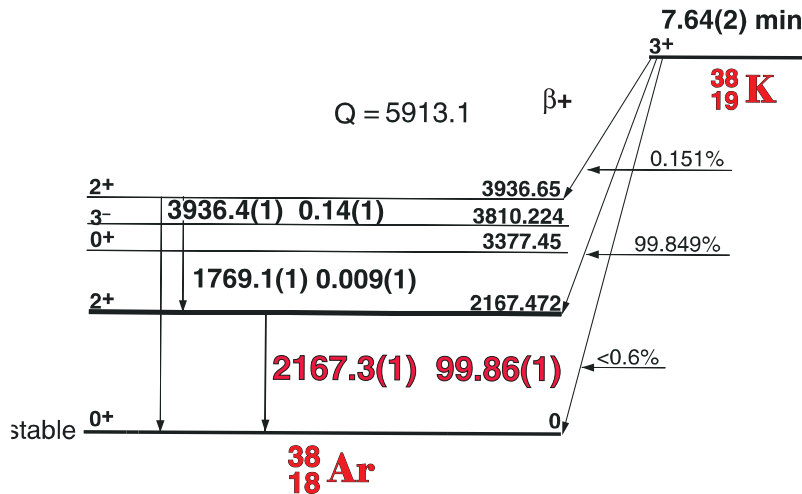
E_γ (KeV)[S]	ΔE_γ	I_γ (rel)	I_γ (%)[E]	ΔI_γ	S
1293.58	± 0.01	100	99.1	± 0.1	1



7.64 Min. ^{38}K

^{38}K Decay Scheme

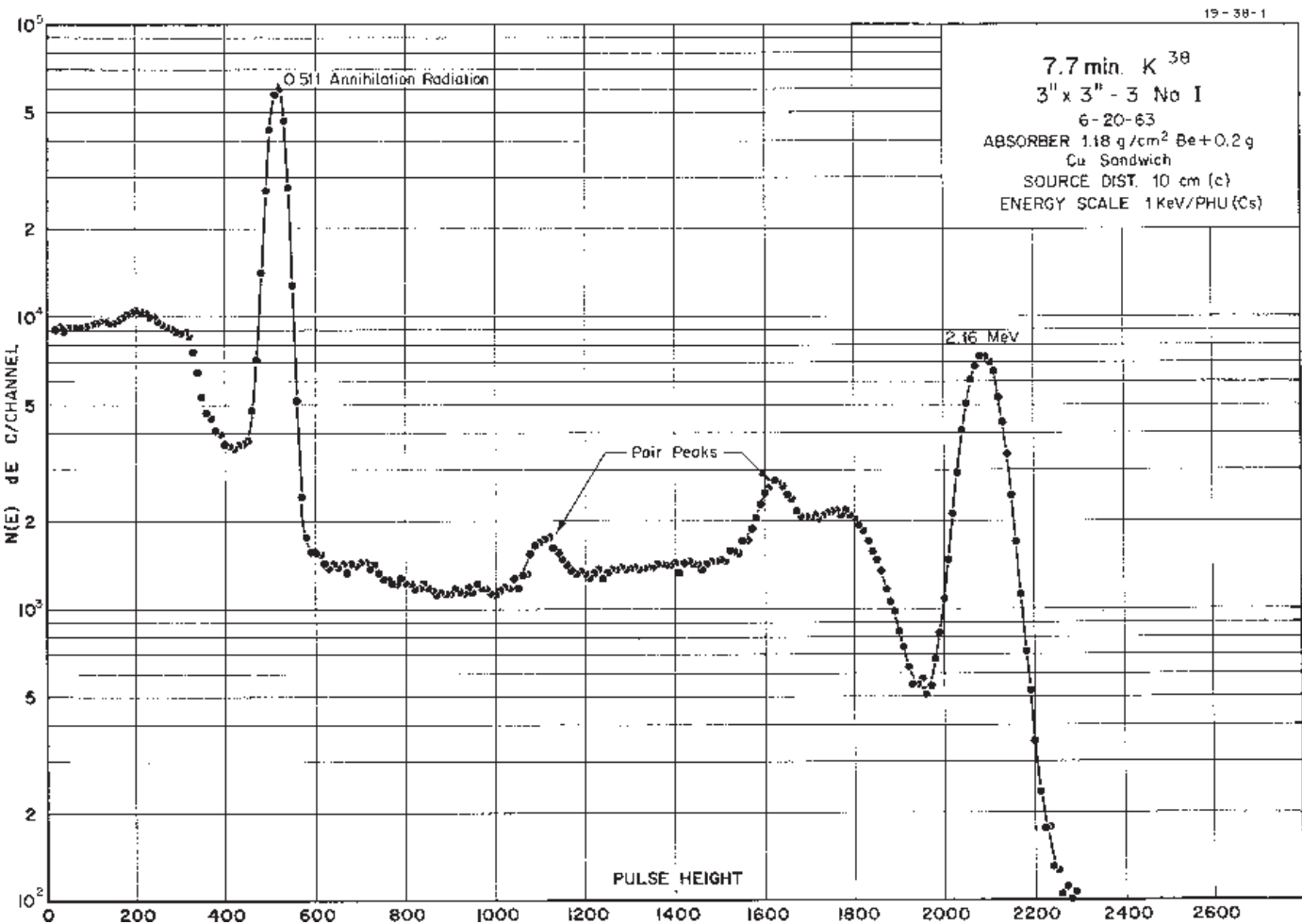
19-38-1



GAMMA-RAY ENERGIES AND INTENSITIES

Nuclide ^{38}K Half Life 7.64(2) min.
Detector 3" X 3" - 2 NaI Method of Production: $\text{K}^{39}(\gamma, n)$

E_γ (KeV) [S]	ΔE_γ	I_γ (rel)	I_γ (%) [E]	ΔI_γ	S
2167.40	± 0.01	100	99.86	± 0.01	1
1769.1	± 0.1		0.3		4

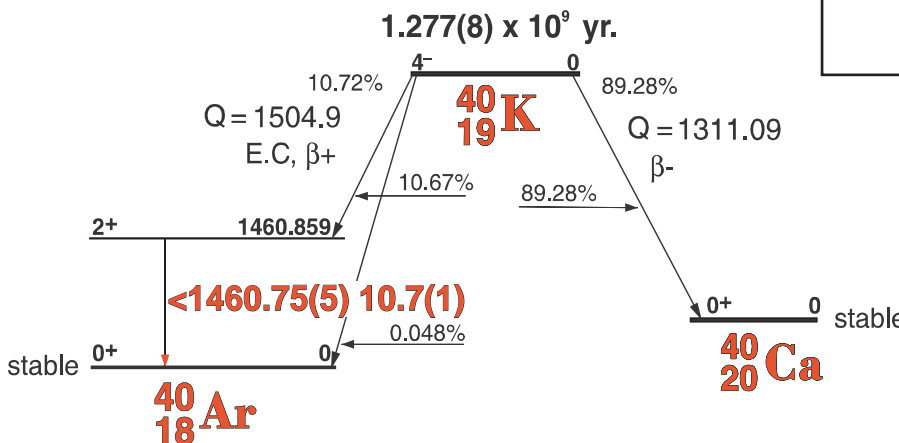


1.277×10^9 Yr. ^{40}K

19-40-2

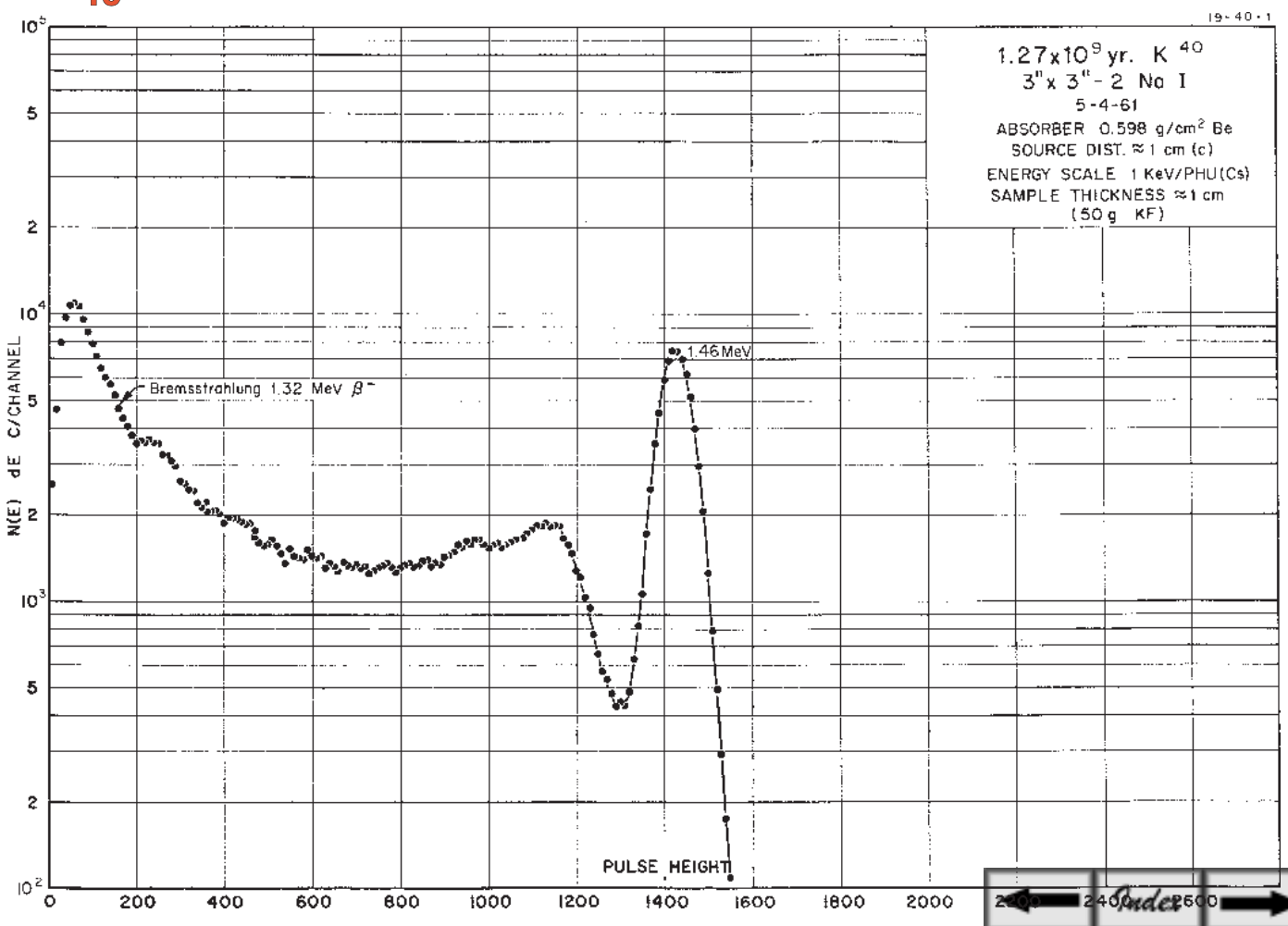
GAMMA-RAY ENERGIES AND INTENSITIES

^{40}K Decay Scheme



Nuclide ^{40}K
Detector 3" X 3" - 2 Nal
Half Life $1.277(8) \times 10^9$ Yr.
Method of Production:nat.

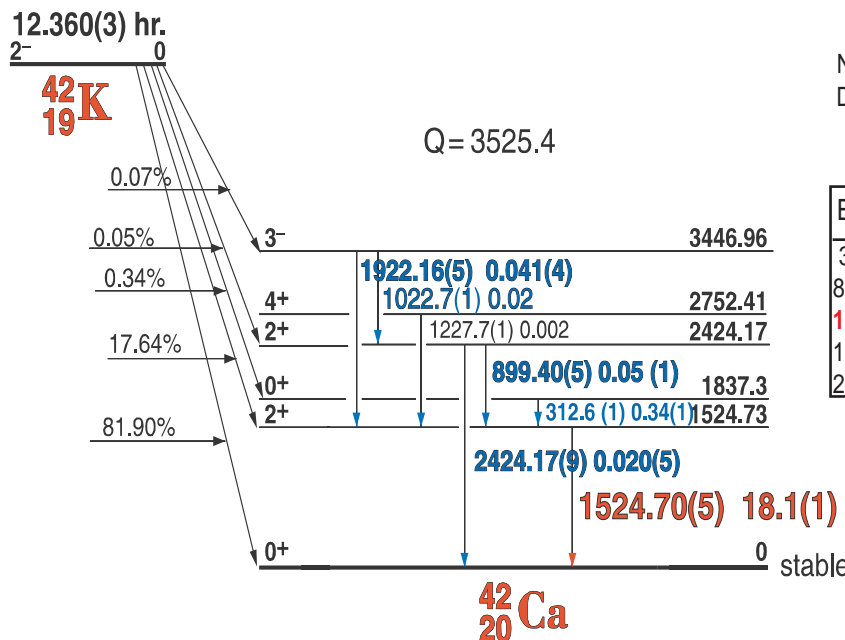
E_γ (KeV)[S]	ΔE_γ	I_γ (rel)	I_γ (%)[E]	ΔI_γ	S
bremsstrahlung (1.31 Mev β) 1460.83	± 0.02	100	10.6	± 0.1	1



12.36 Hr. ^{42}K

19-42-1

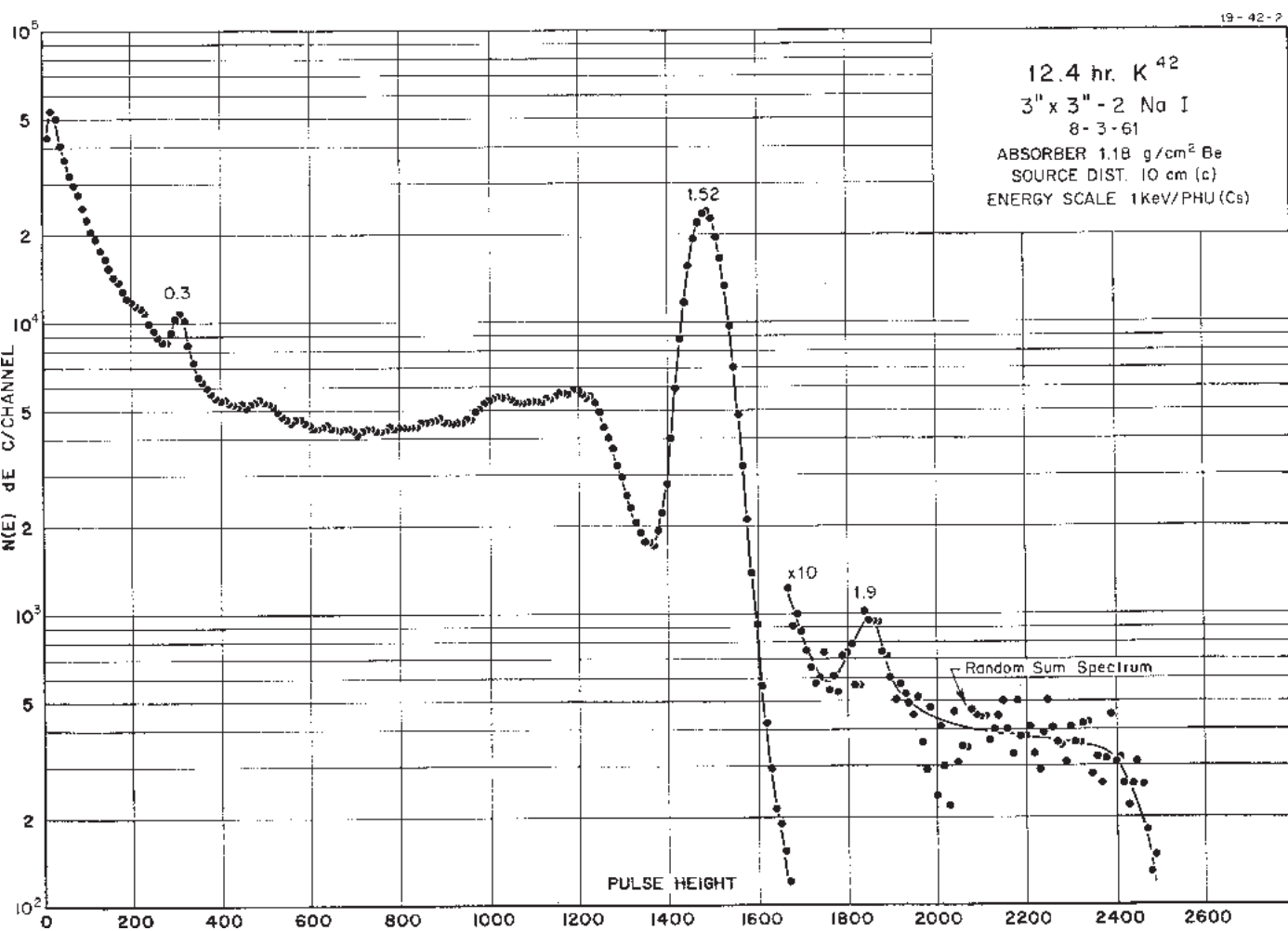
^{42}K Decay Scheme



GAMMA-RAY ENERGIES AND INTENSITIES

Nuclide ^{42}K Half Life 12.360(3) hr.
Detector 3" X 3" - 2 NaI Method of Production: K⁴¹(ny)

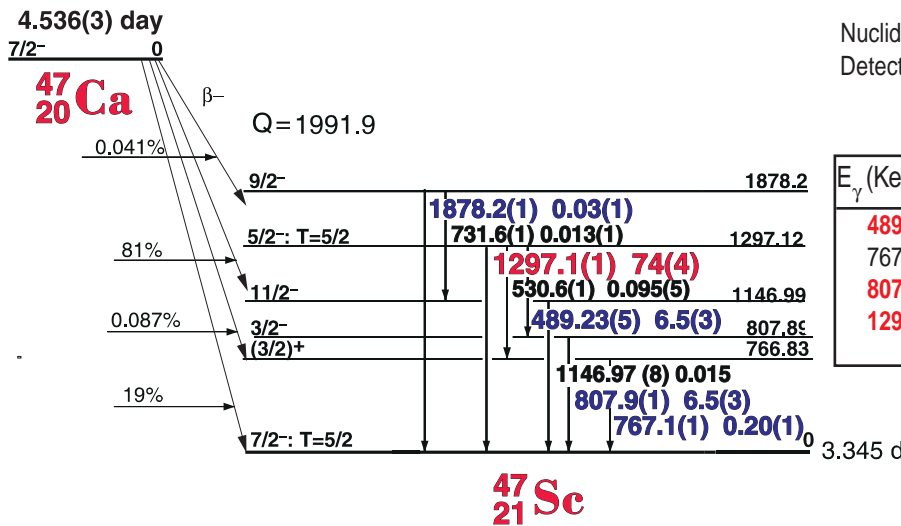
E_{γ} (KeV)[SI]	ΔE_{γ}	$I_{\gamma}(\text{rel})$	$I_{\gamma}(\%)[\text{E}]$	ΔI_{γ}	S
312.6	± 0.1	1.68	1.76	± 0.1	2
899.4	± 0.05	0.30	0.05	± 0.005	3
1524.7	± 0.05	100	18.1	± 0.1	1
1922.16	± 0.05	0.23	0.04	± 0.04	3
2424.17	± 0.09	0.12	0.02	± 0.002	3



4.536 Day ^{47}Ca

20-47-1

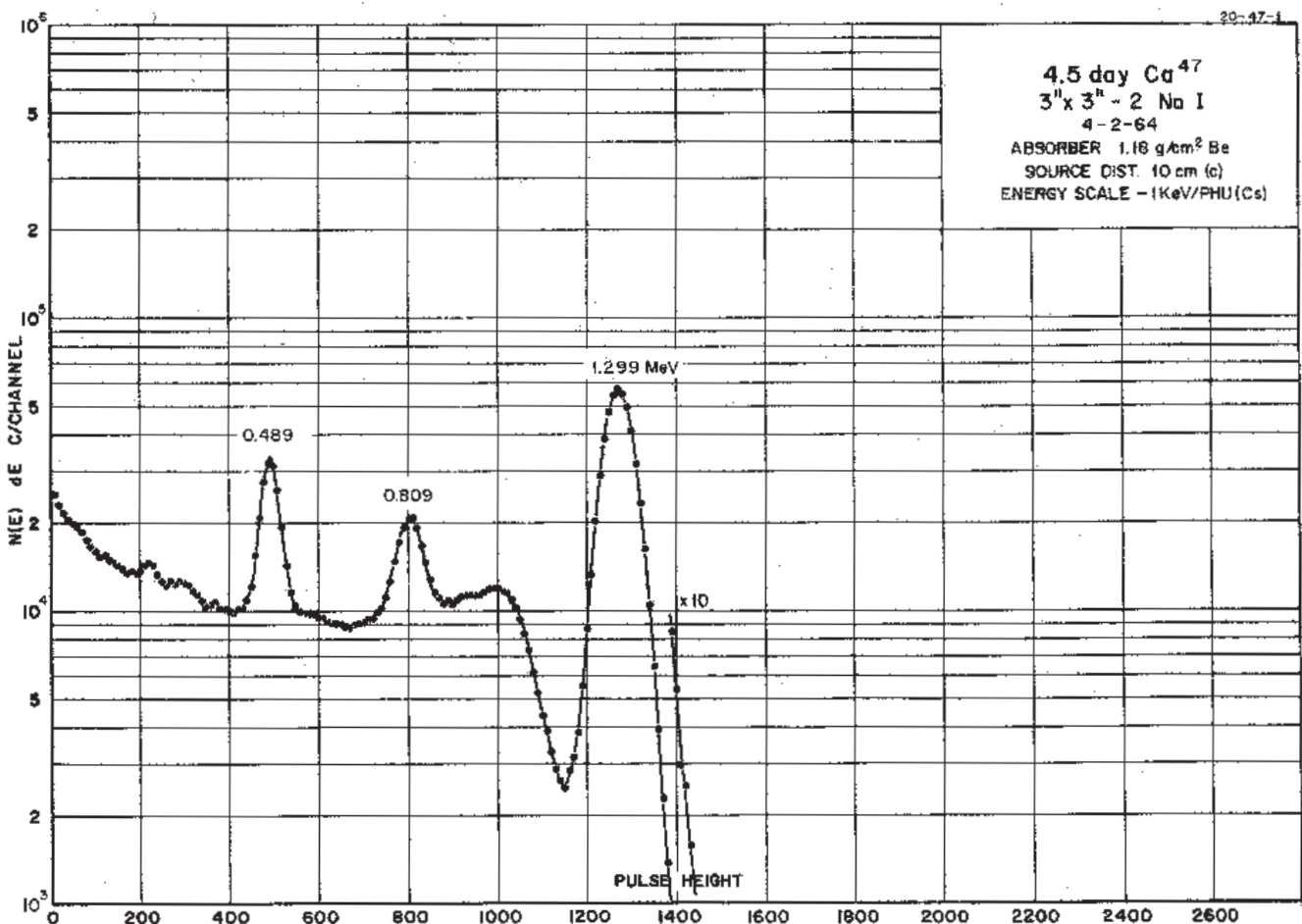
4.536(3) day ^{47}Ca Decay Scheme



GAMMA-RAY ENERGIES AND INTENSITIES

Nuclide ^{47}Ca Half Life 4.536(3) day
Detector 3" X 3" - 2 NaI Method of Production: Ti⁵⁰(n,α)

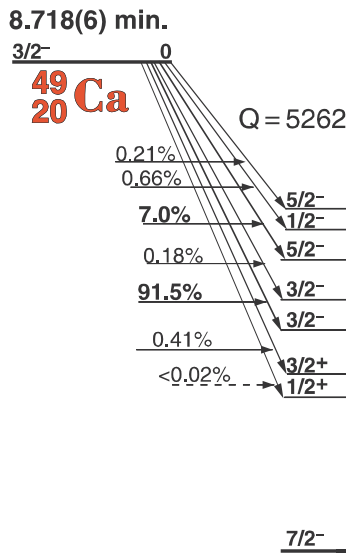
E_γ (KeV)[S]	ΔE_γ	I_γ (rel)	I_γ (%) [E]	ΔI_γ	S
489.23	± 0.1		6.2	± 0.3	1
767.1	± 0.3		0.27	± 0.02	3
807.9	± 0.1		6.2	± 0.6	1
1297.1	± 0.1		71	± 5	1



8.718 Min. ^{49}Ca

20-49-1

^{49}Ca Decay Scheme

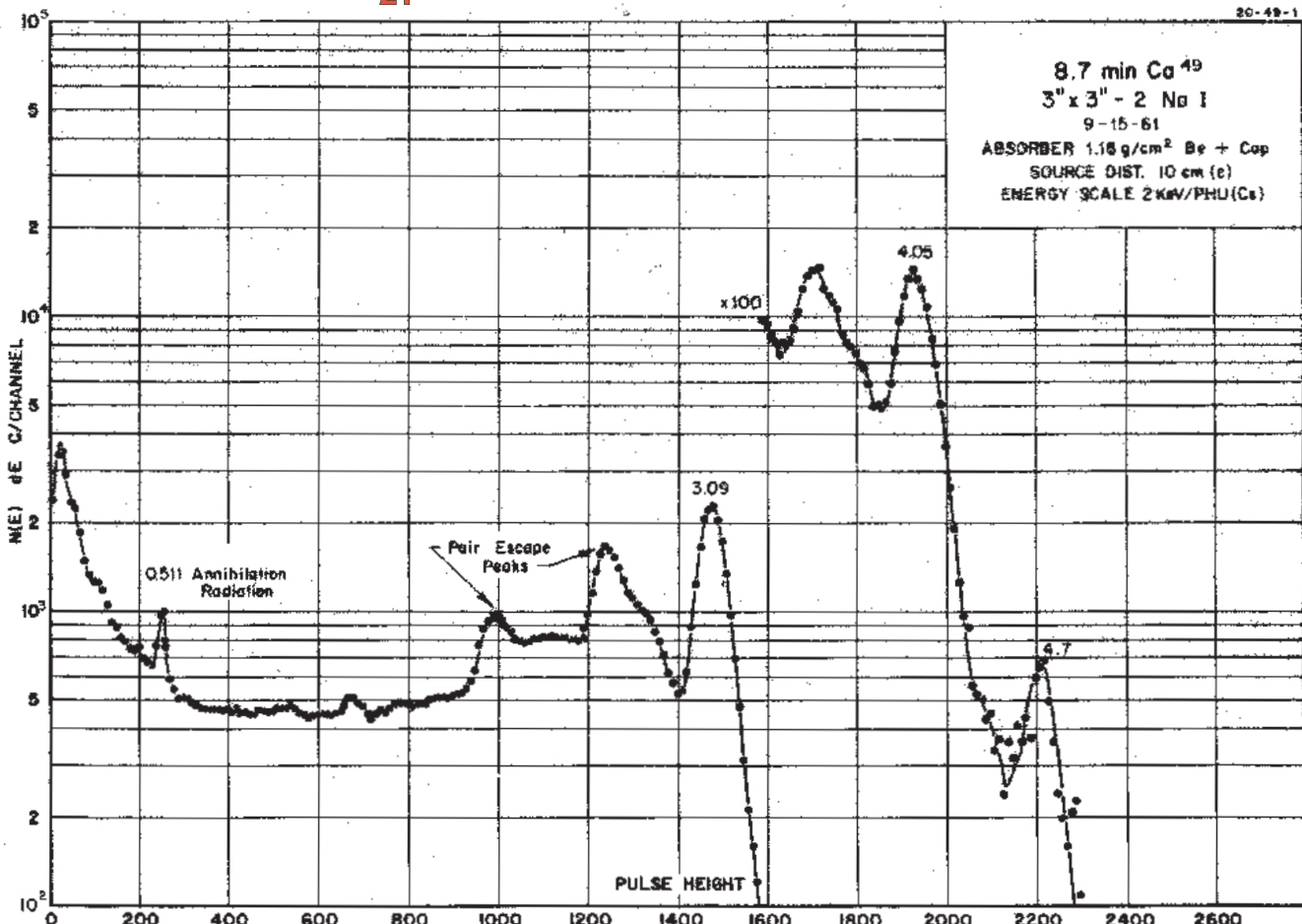


GAMMA-RAY ENERGIES AND INTENSITIES

Nuclide ^{49}Ca Half Life 8.718(6) min.
Detector 3" X 3" - 2 NaI Method of Production: Ca⁴⁸(n,γ)

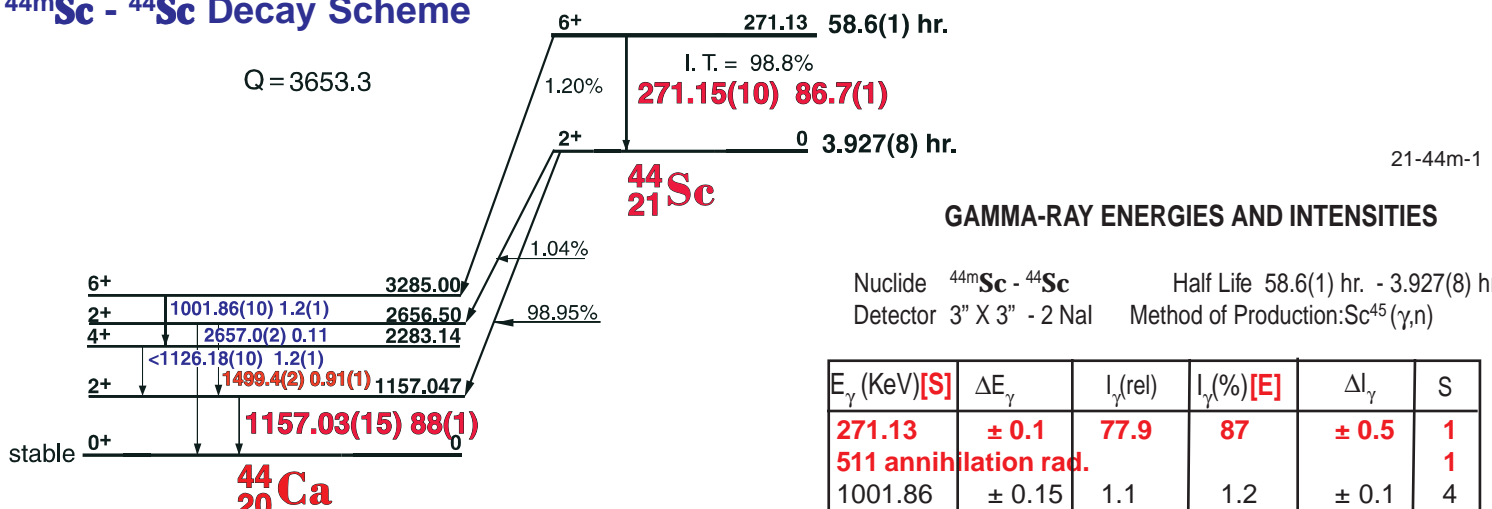
E_{γ} (KeV)[S]	ΔE_{γ}	$I_{\gamma}(\text{rel})$	$I_{\gamma}(\%)$ [E]	ΔI_{γ}	S
3084.3	± 0.2	100	92	± 1	1
4071.8	± 0.1	8.7	7	± 0.1	1
4738.2	± 0.5	0.4	0.3	± 0.1	3

^{49}Sc



58.6 Hr. ^{44m}Sc - 3.927 Hr. ^{44}Sc

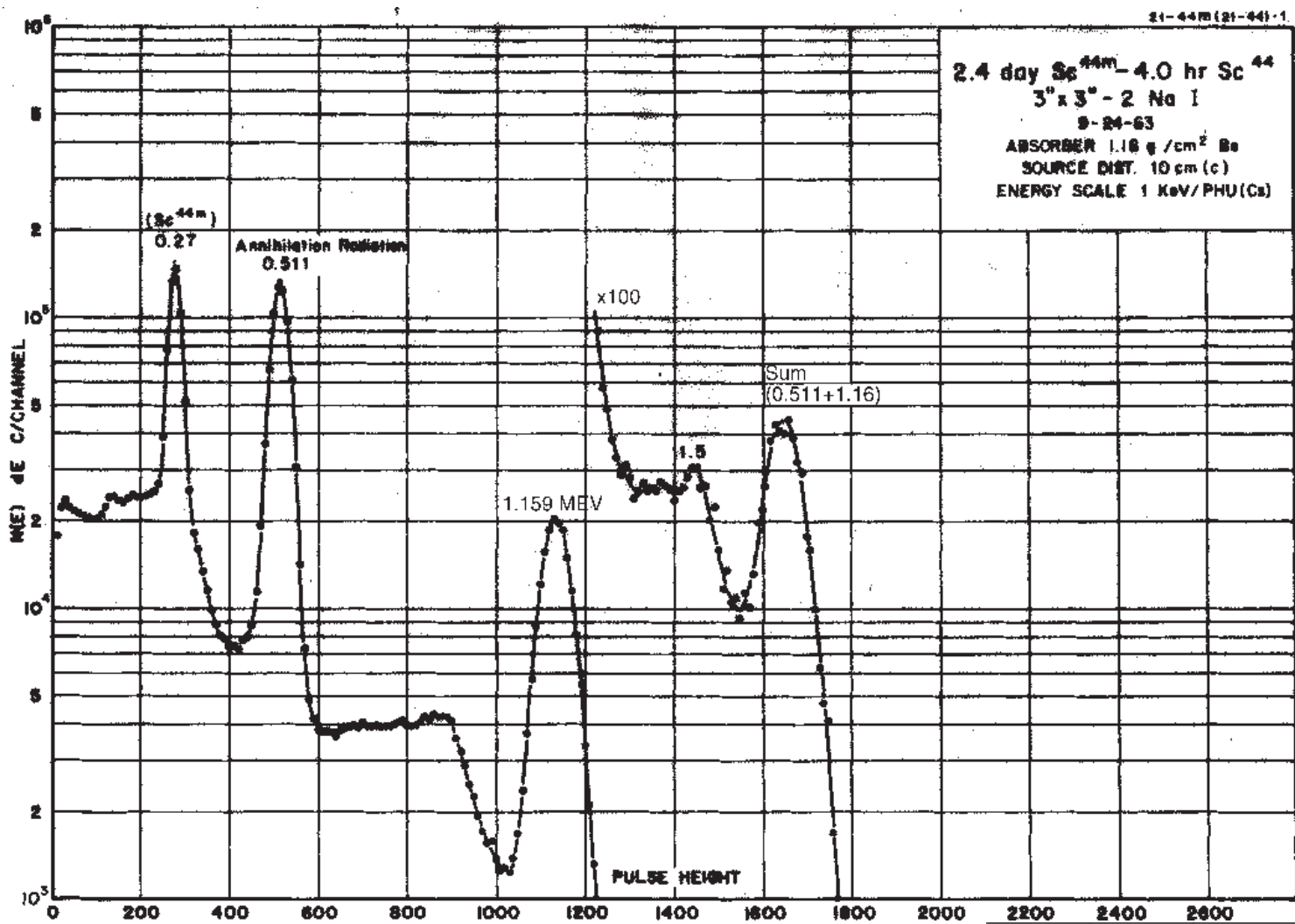
$^{44m}\text{Sc} - ^{44}\text{Sc}$ Decay Scheme

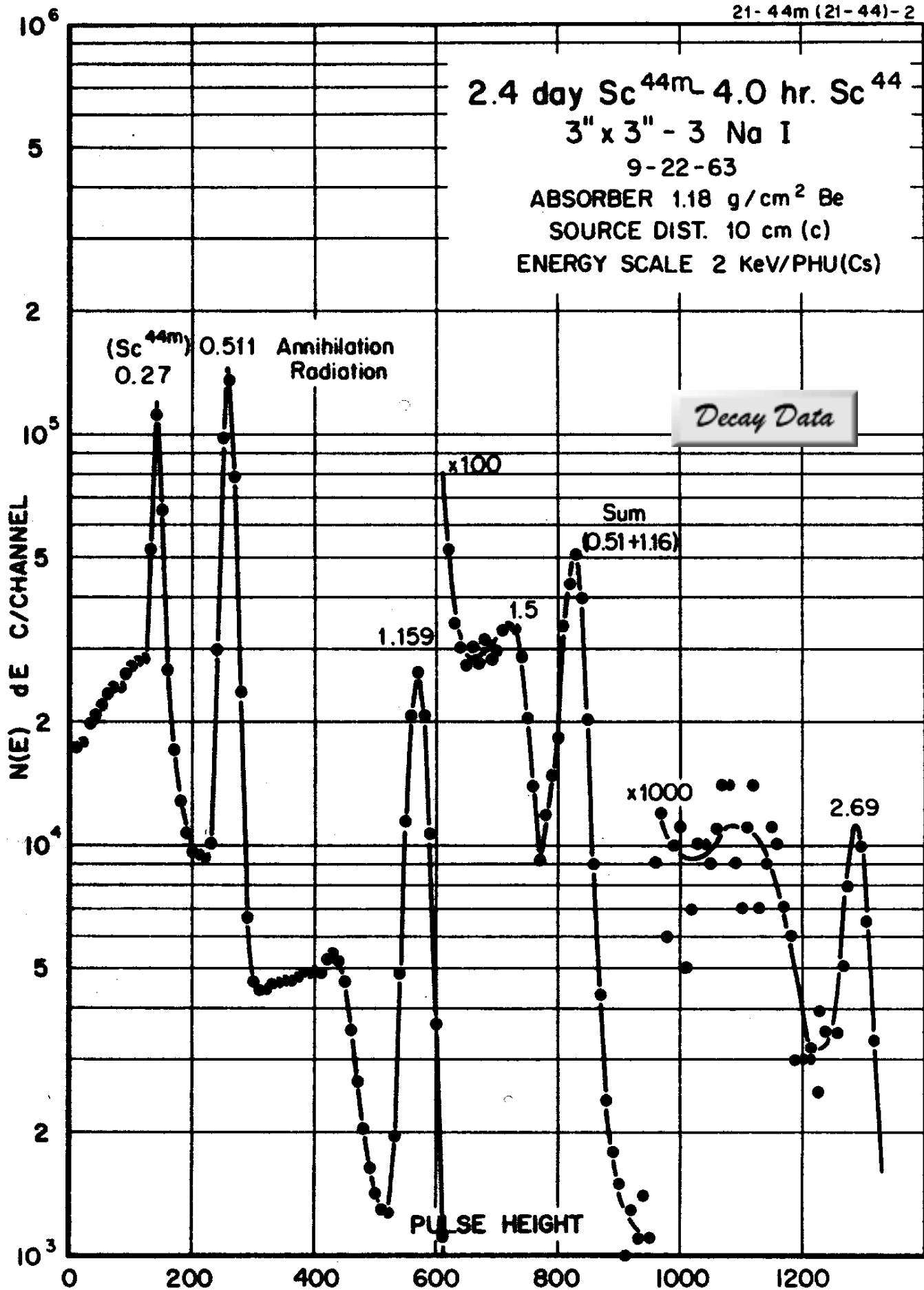


GAMMA-RAY ENERGIES AND INTENSITIES

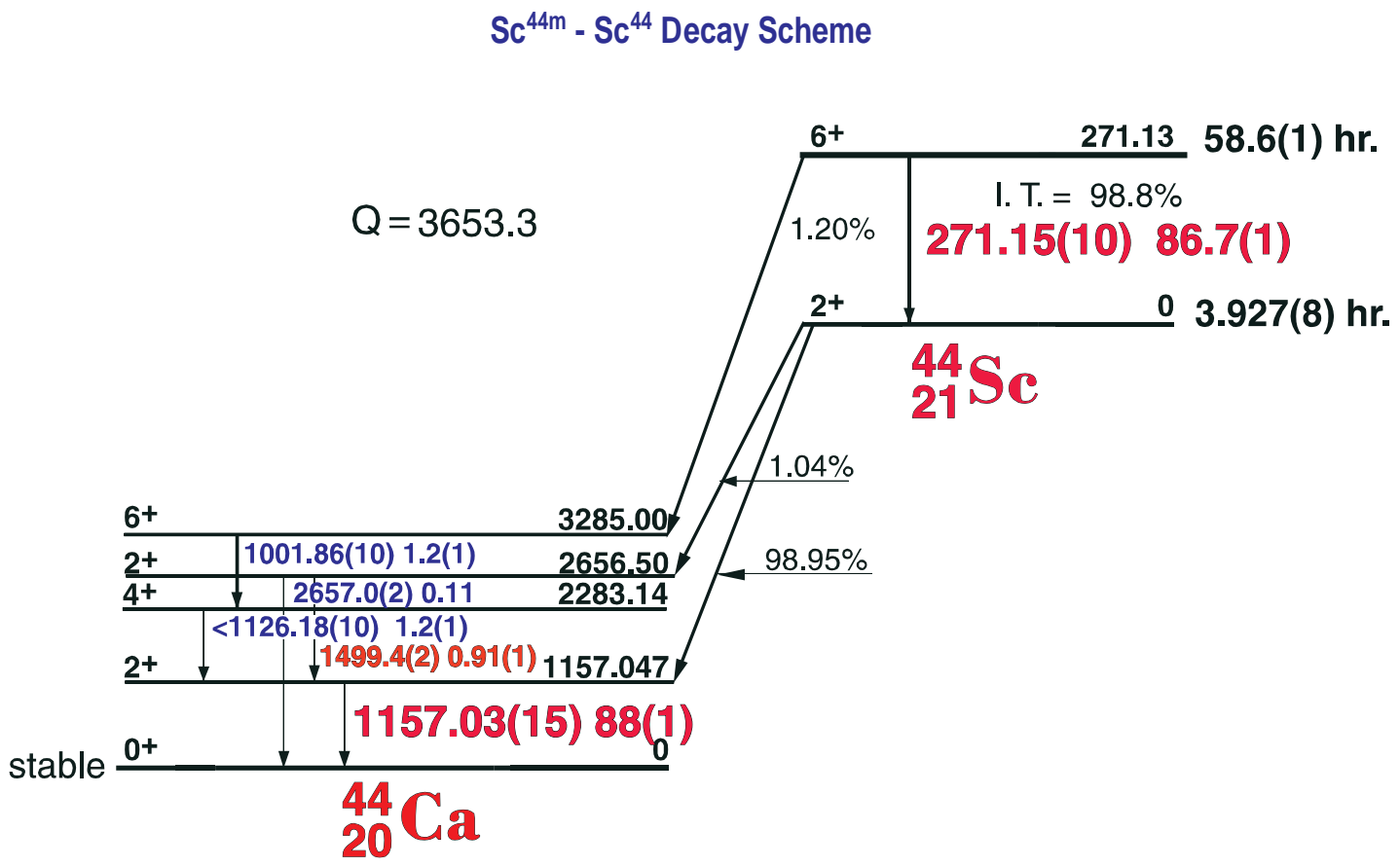
Nuclide $^{44m}\text{Sc} - ^{44}\text{Sc}$ Half Life 58.6(1) hr. - 3.927(8) hr.
Detector 3" X 3" - 2 NaI Method of Production: $\text{Sc}^{45}(\gamma, n)$

E_γ (KeV)[S]	ΔE_γ	I_γ (rel)	I_γ (%) [E]	ΔI_γ	S
271.13	± 0.1	77.9	87	± 0.5	1
511 annihilation rad.					1
1001.86	± 0.15	1.1	1.2	± 0.1	4
1126.18	± 0.15	1.1	1.2	± 0.1	3
1157.03	± 0.15	100	88	± 1.0	1
1499.43	± 0.2	0.9	0.91	± 0.05	1
2657.14	± 0.2	0.14	0.11	± 0.05	2





58.6 Hr. ^{44m}Sc - 3.927 Hr. ^{44}Sc



GAMMA-RAY ENERGIES AND INTENSITIES

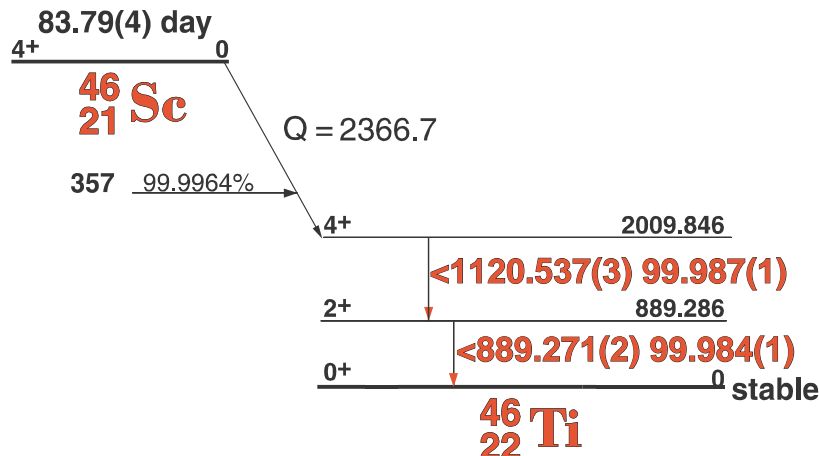
Nuclide $^{44m}\text{Sc} - ^{44}\text{Sc}$
 Detector 3" X 3" - 2 Nal

Half Life 58.6(1) hr. - 3.927(8) hr..
 Method of Production: $\text{Sc}^{45}(\gamma, n)$

E_{γ} (KeV)[S]	ΔE_{γ}	$I_{\gamma}(\text{rel})$	$I_{\gamma}(\%) [E]$	ΔI_{γ}	S
271.13	± 0.1	77.9	87	± 0.5	1
511 annihilation rad.					1
1001.86	± 0.15	1.1	1.2	± 0.1	4
1126.18	± 0.15	1.1	1.2	± 0.1	3
1157.03	± 0.15	100	88	± 1.0	1
1499.43	± 0.2	0.9	0.91	± 0.05	1
2657.14	± 0.2	0.14	0.11	± 0.05	2

85.81 Day Sc⁴⁶

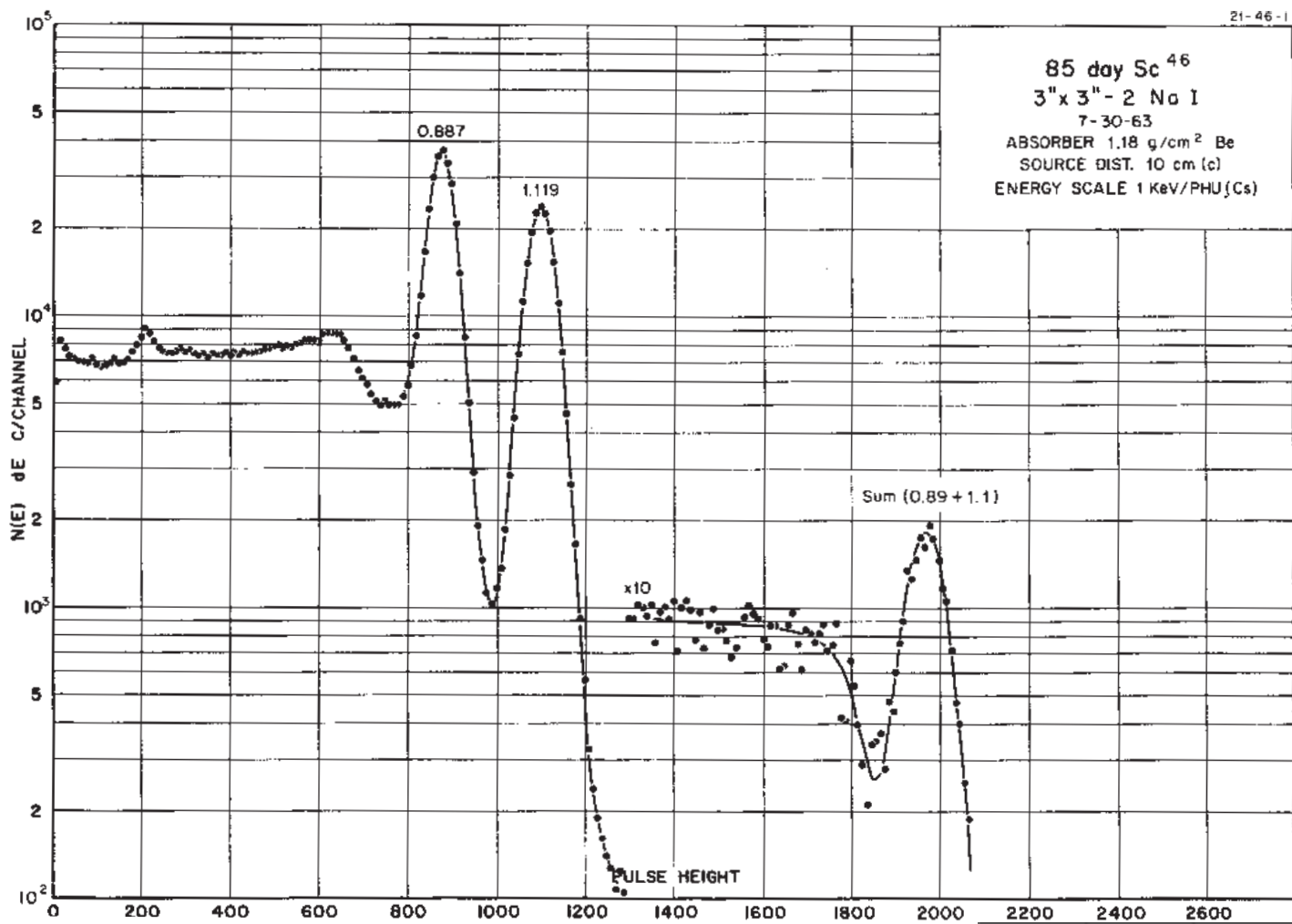
Sc⁴⁶ Decay Scheme

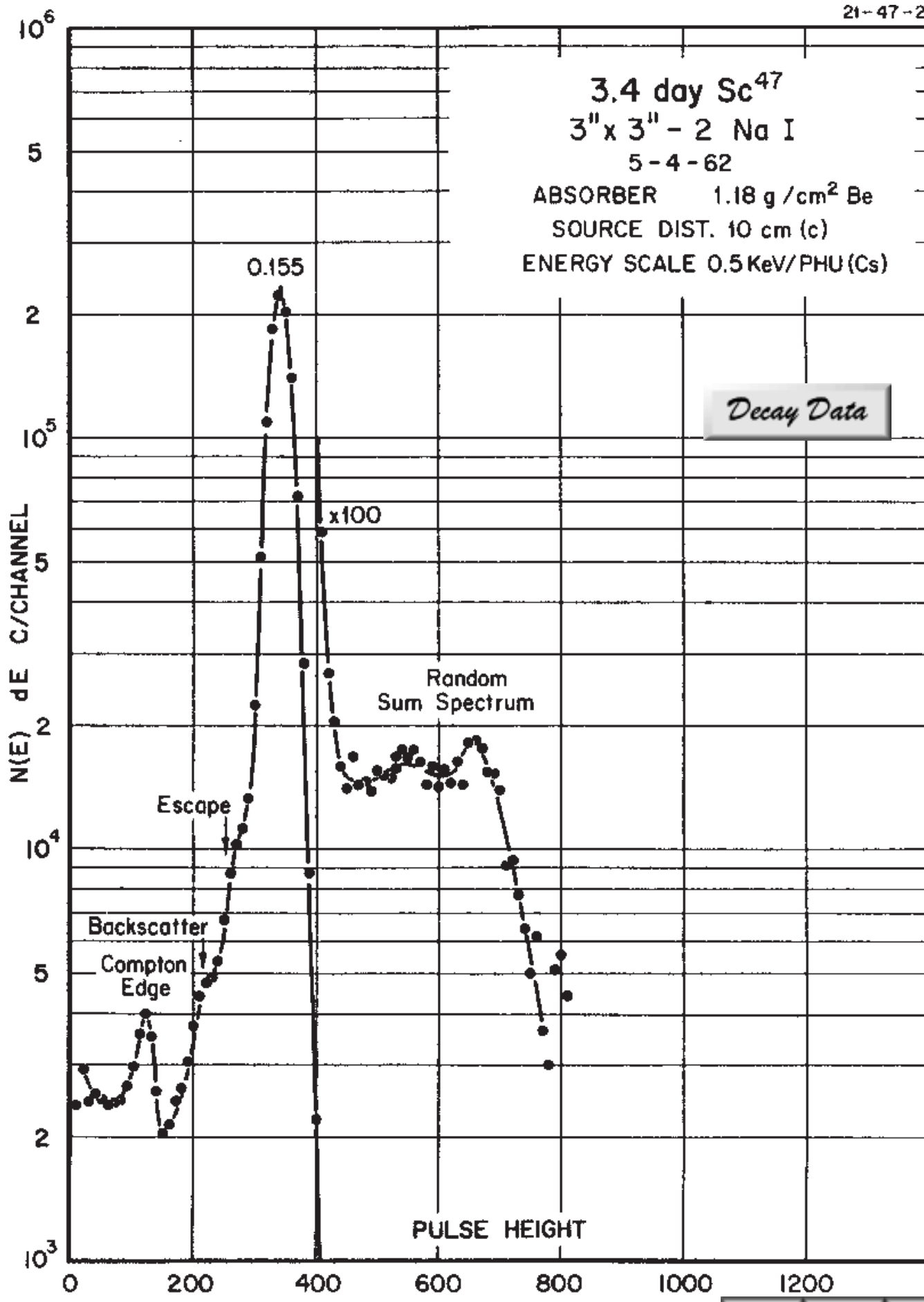


GAMMA-RAY ENERGIES AND INTENSITIES

Nuclide ^{46}Sc Half Life 83.79(4) day
Detector 3" X 3" - 2 NaI Method of Production: $\text{Sc}^{45}(\text{n},\gamma)$

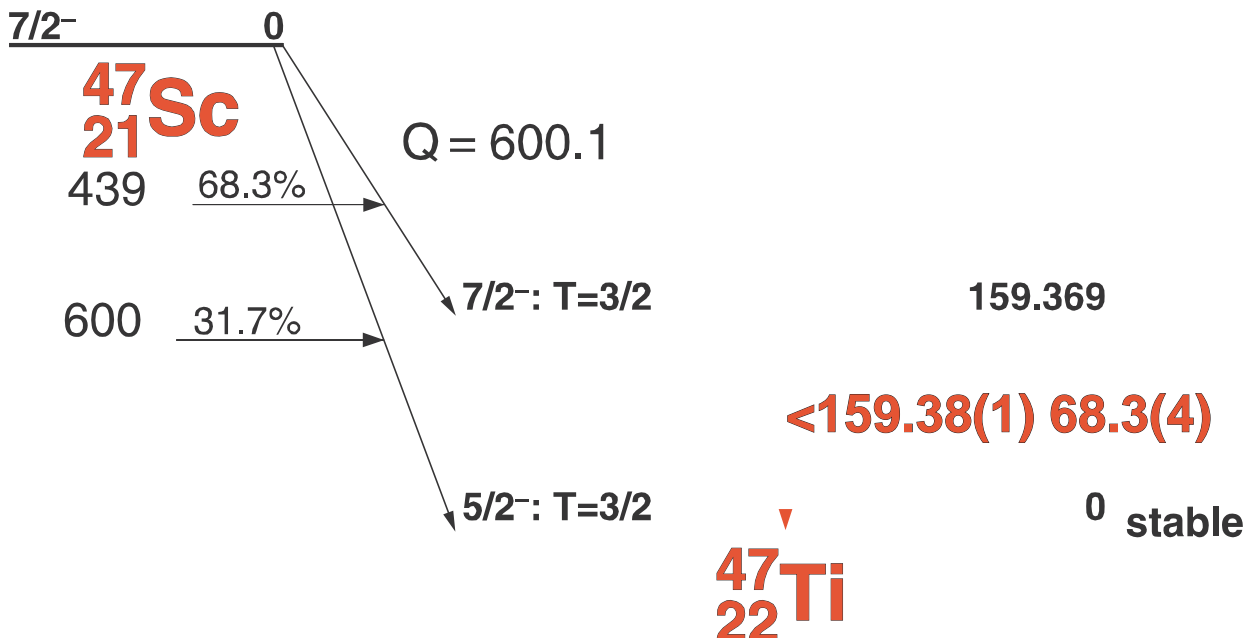
E_{γ} (KeV)[S]	ΔE_{γ}	$I_{\gamma}(\text{rel})$	$I_{\gamma}(\%)[\text{E}]$	ΔI_{γ}	S
889.268	± 0.04	100	99.987	± 0.004	1
1120.545	± 0.04	100	99.996	± 0.004	1
2010	± 0.1	weak	0.00001		5





3.3492 Day ^{47}Sc Decay Scheme

3.3492(6) day



GAMMA-RAY ENERGIES AND INTENSITIES

Nuclide
Detector

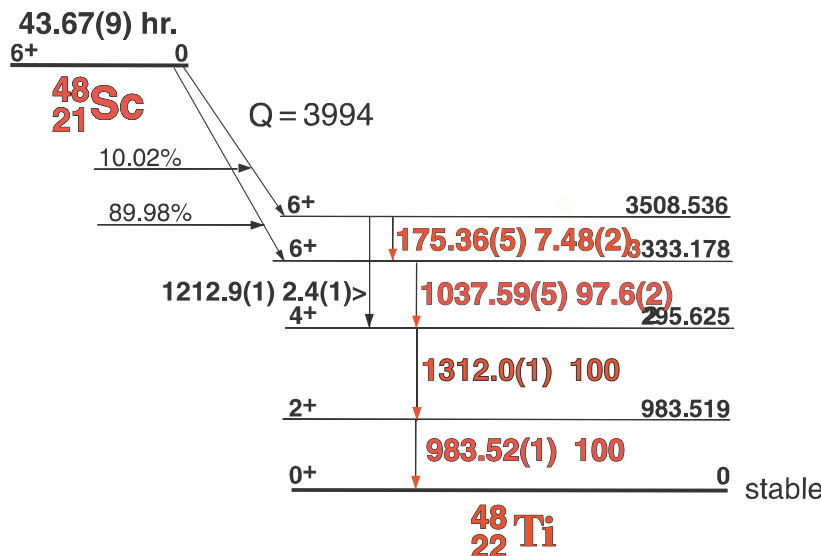
^{47}Sc
3" x 3" - 2NaI

Half Life 3.3492(6) day
Method of Production: $\text{Sc}^{46}(n,\gamma)$

E_γ (KeV)[S]	ΔE_γ	I_γ (rel)	$I_\gamma(\%)$ [E]	ΔI_γ	S
159.381	± 0.015	100	68.3	± 0.4	1

48.67 Hr. ^{48}Sc

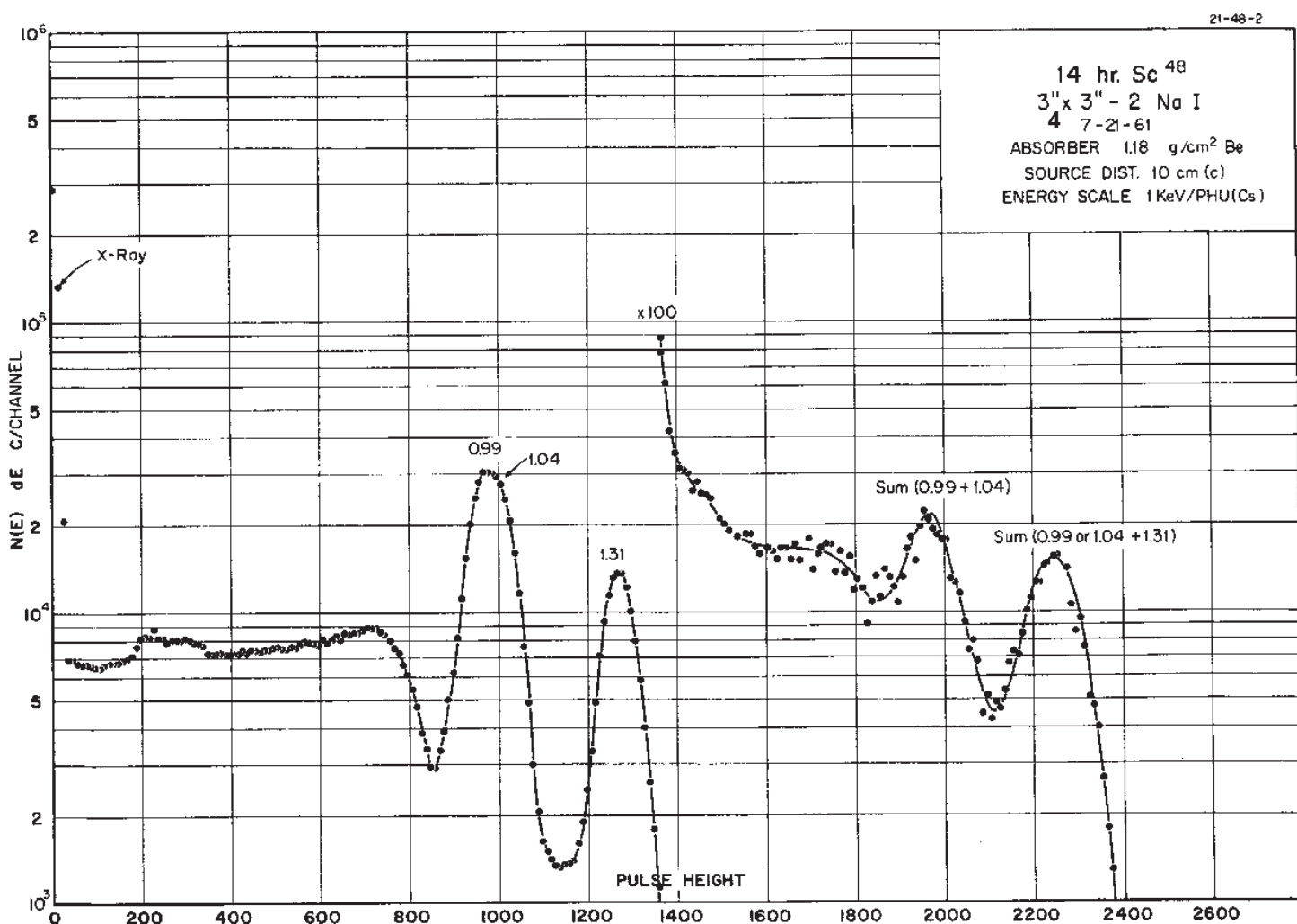
^{48}Sc Decay Scheme

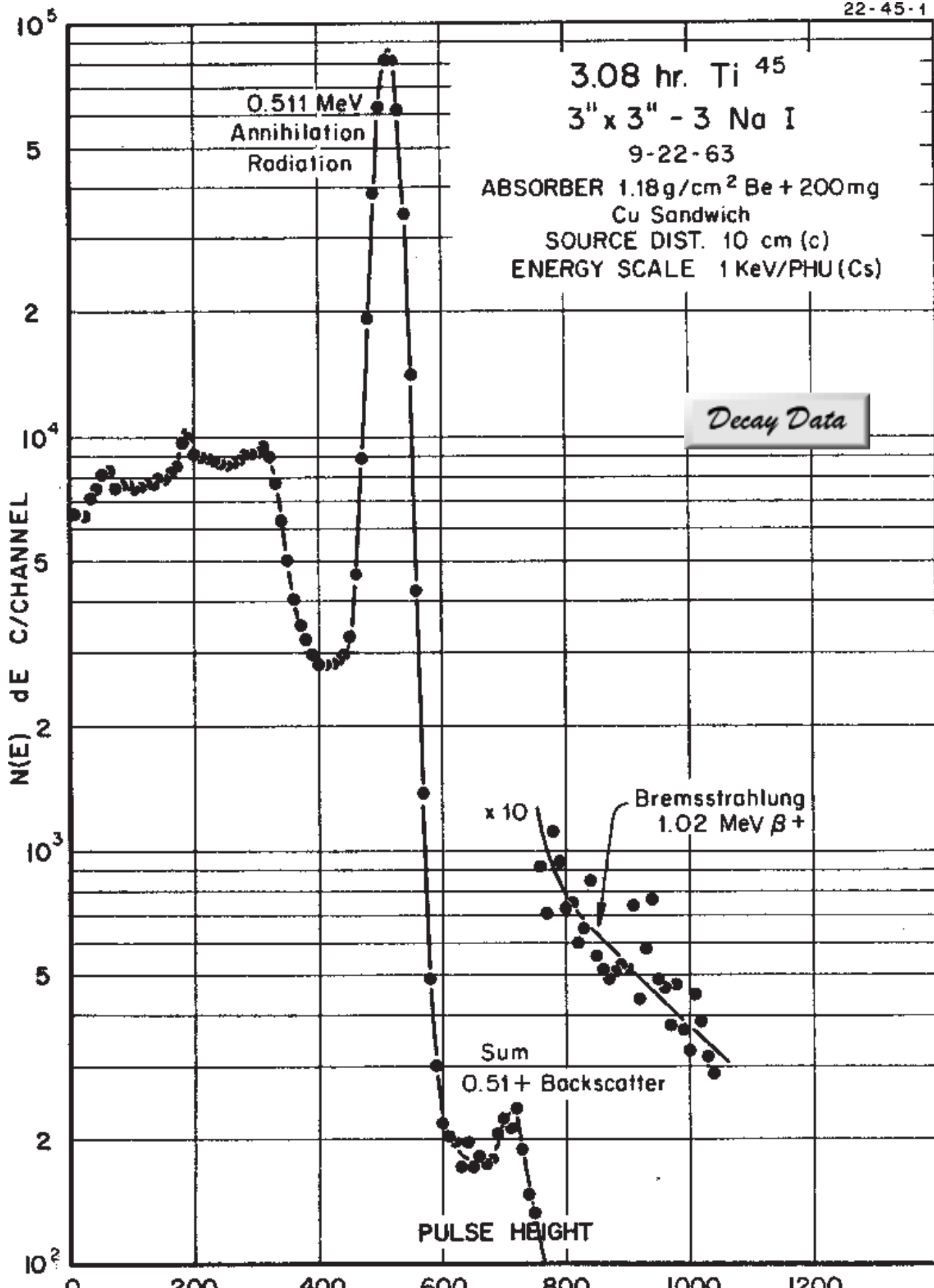


GAMMA-RAY ENERGIES AND INTENSITIES

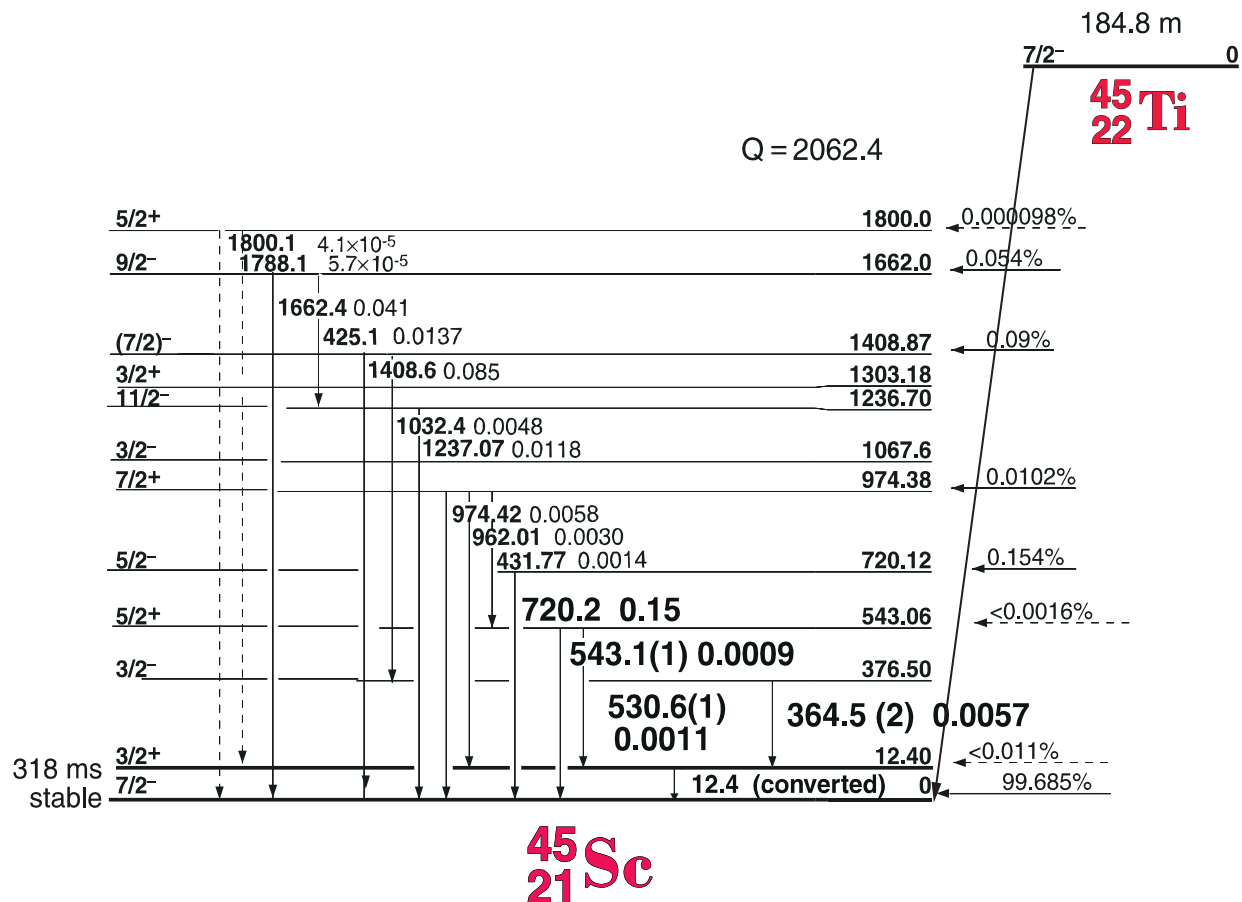
Nuclide ^{48}Sc Half Life 48.67 Hr..
Detector 3" X 3" - 2 NaI Method of Production: Ti⁴⁸ (n,p)

E_{γ} (KeV)[S]	ΔE_{γ}	$I_{\gamma}(\text{rel})$	$I_{\gamma}(\%)[E]$	ΔI_{γ}	S
175.361	± 0.005	7.69	7.47	± 0.1	1
983.526	± 0.01	99	100	± 0.3	1
1037.52	± 0.02	100	97.5	± 0.5	1
1312.1	± 0.1	98	100	± 0.5	1





184.8(5) min. ^{45}Ti Decay Scheme

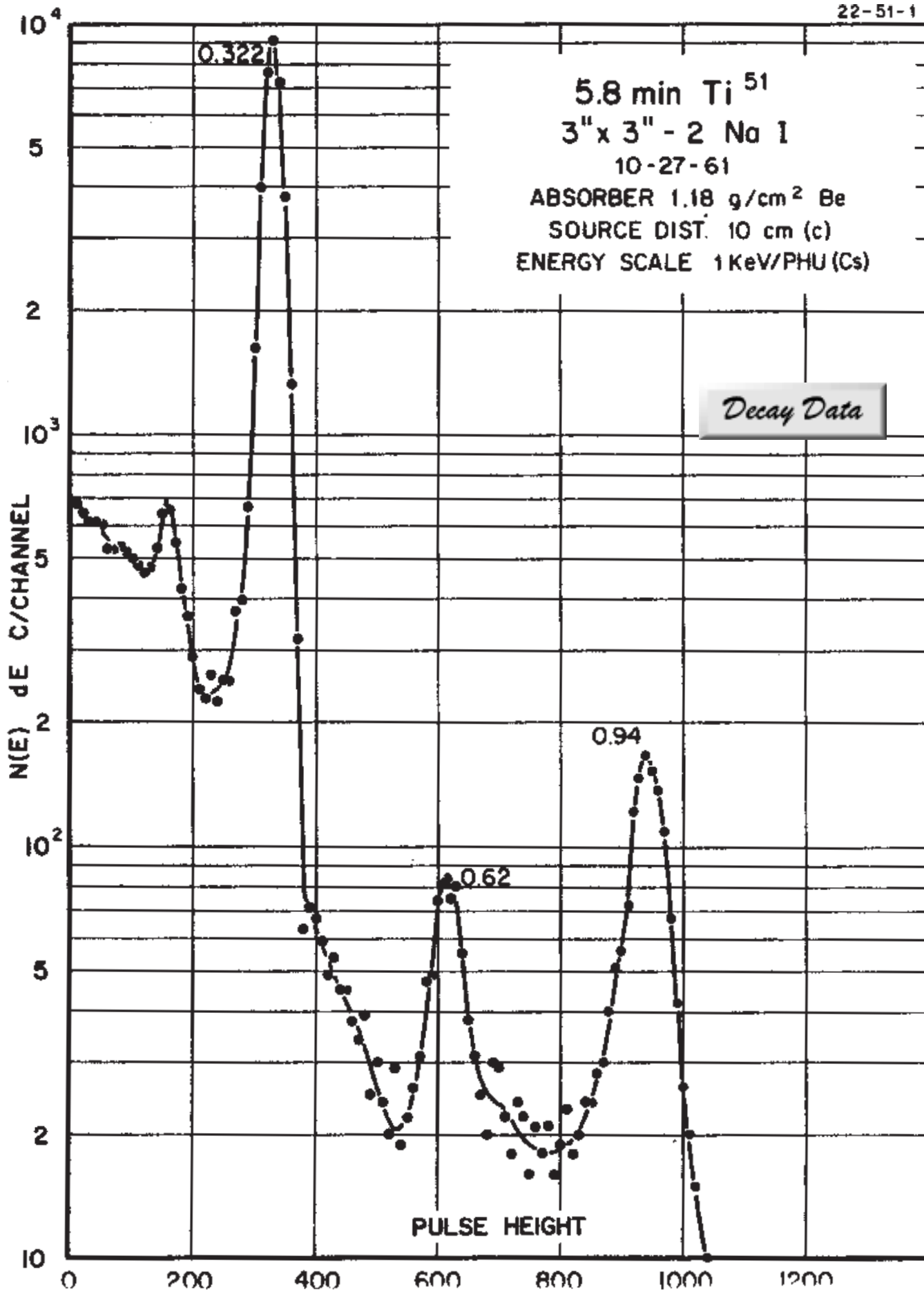


GAMMA-RAY ENERGIES AND INTENSITIES

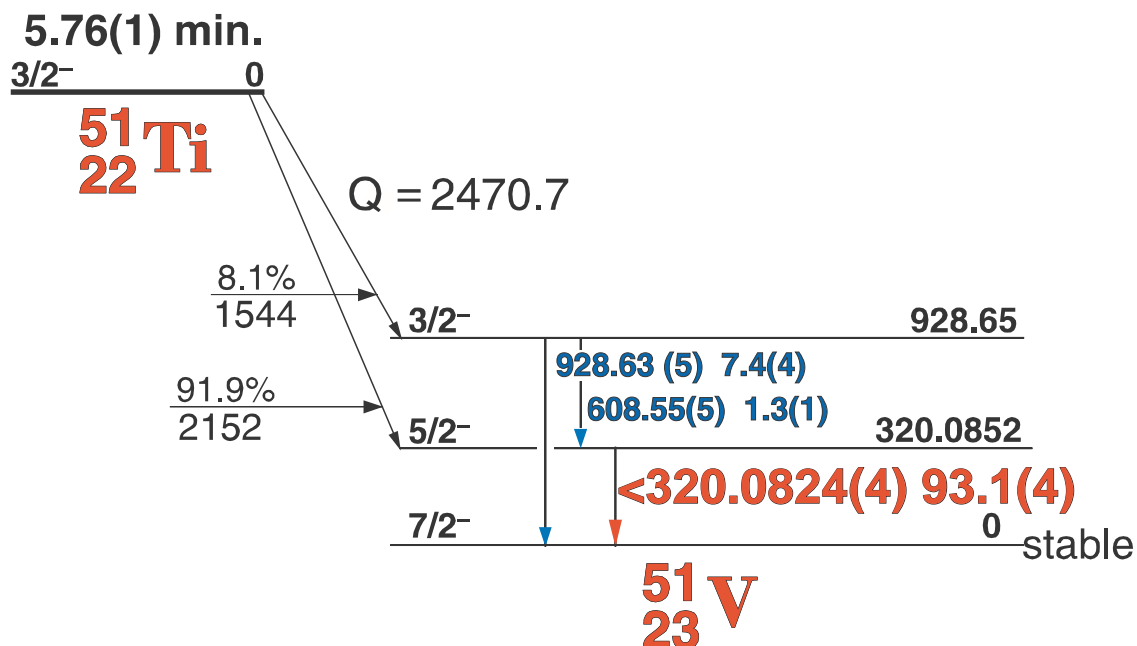
Nuclide ^{45}Ti Half Life 184.8(5) min.
Detector 3" x 3" - 2Nal Method of Production: $\text{Ti}^{46}(\gamma, n)$

E_γ (KeV)[S]	ΔE_γ	I_γ (rel)	I_γ (%) [E]	ΔI_γ	S
12.4 ann. rad. 511.006		100	0.00003 68.3	±	5 1
numerous gammas up to 1800 keV with intensities < 10 ⁻⁴					

22-51-1



5.76 Min. ^{51}Ti Decay Scheme



GAMMA-RAY ENERGIES AND INTENSITIES

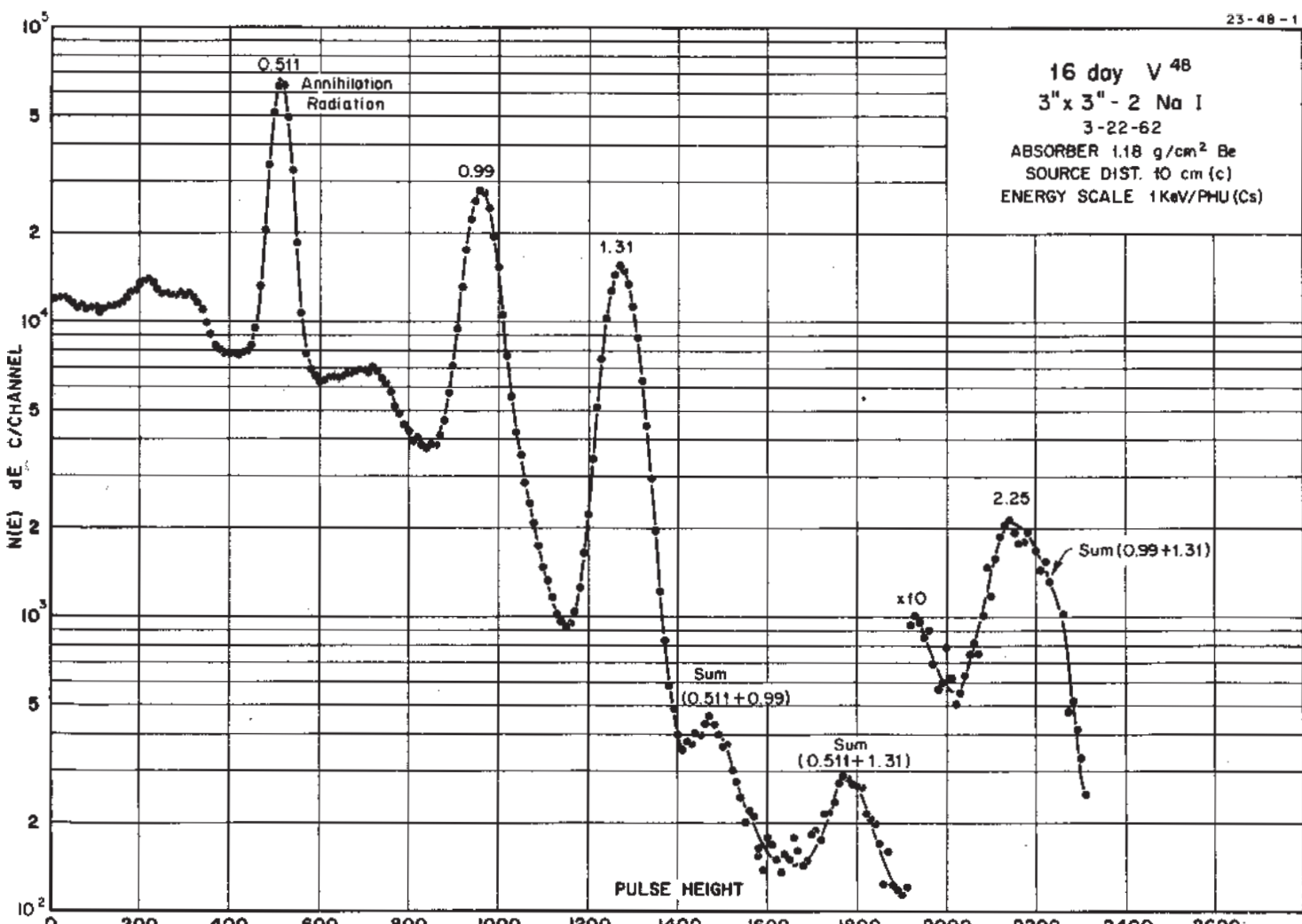
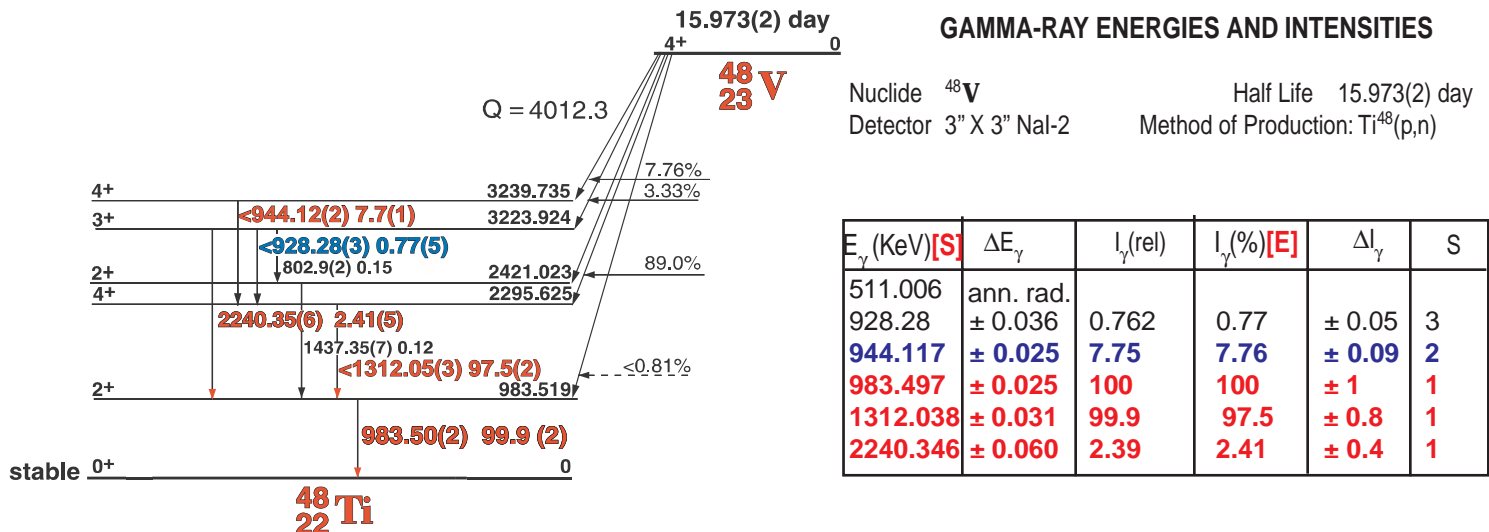
Nuclide ^{51}Ti Half Life 5.76 min.
Detector 3" x 3" - 2NaI Method of Production: $\text{Ti}^{50} (\text{n},\gamma)$

E_γ (KeV)[S]	ΔE_γ	I_γ (rel)	$I_\gamma(\%)$ [E]	ΔI_γ	S
320.018	± 0.008	100	93.1	± 0.04	1
608.55	± 0.05	1.27	1.17	± 0.1	3
928.63	± 0.05	7.41	6.95	± 0.1	2

15.973 Day ^{48}V

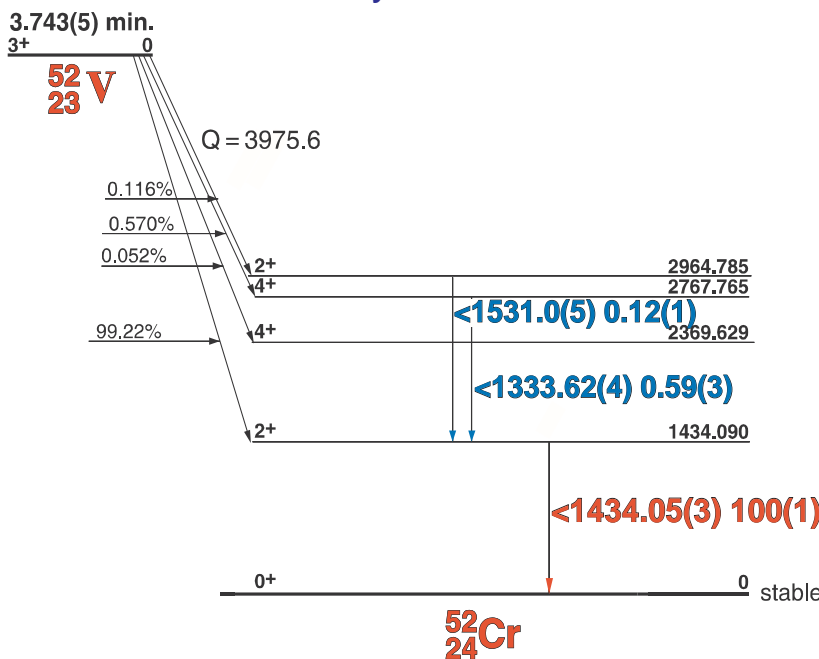
^{48}V Decay Scheme

23-48-1



3.743 Min. ^{52}V

^{52}V Decay Scheme



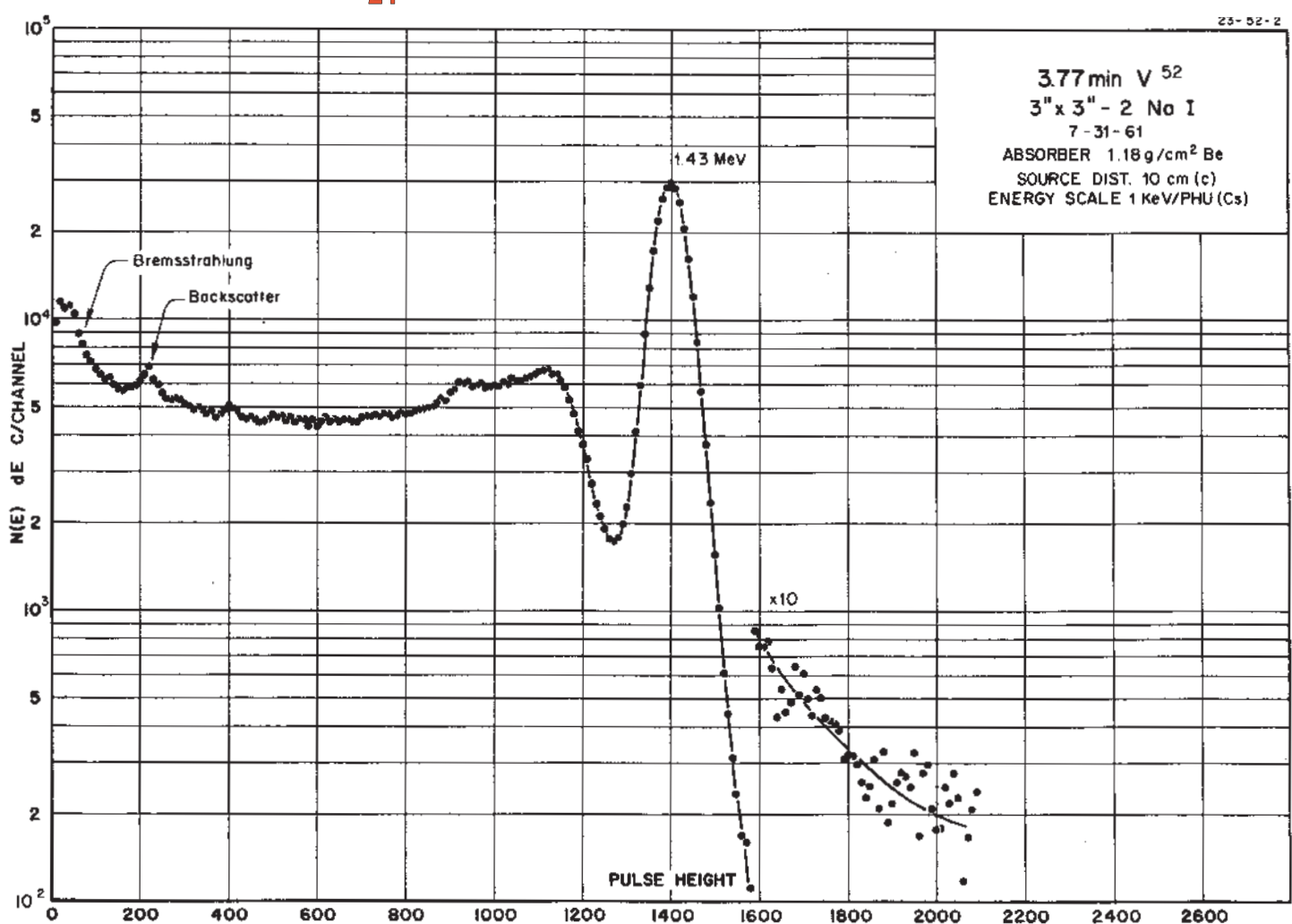
23-52-1

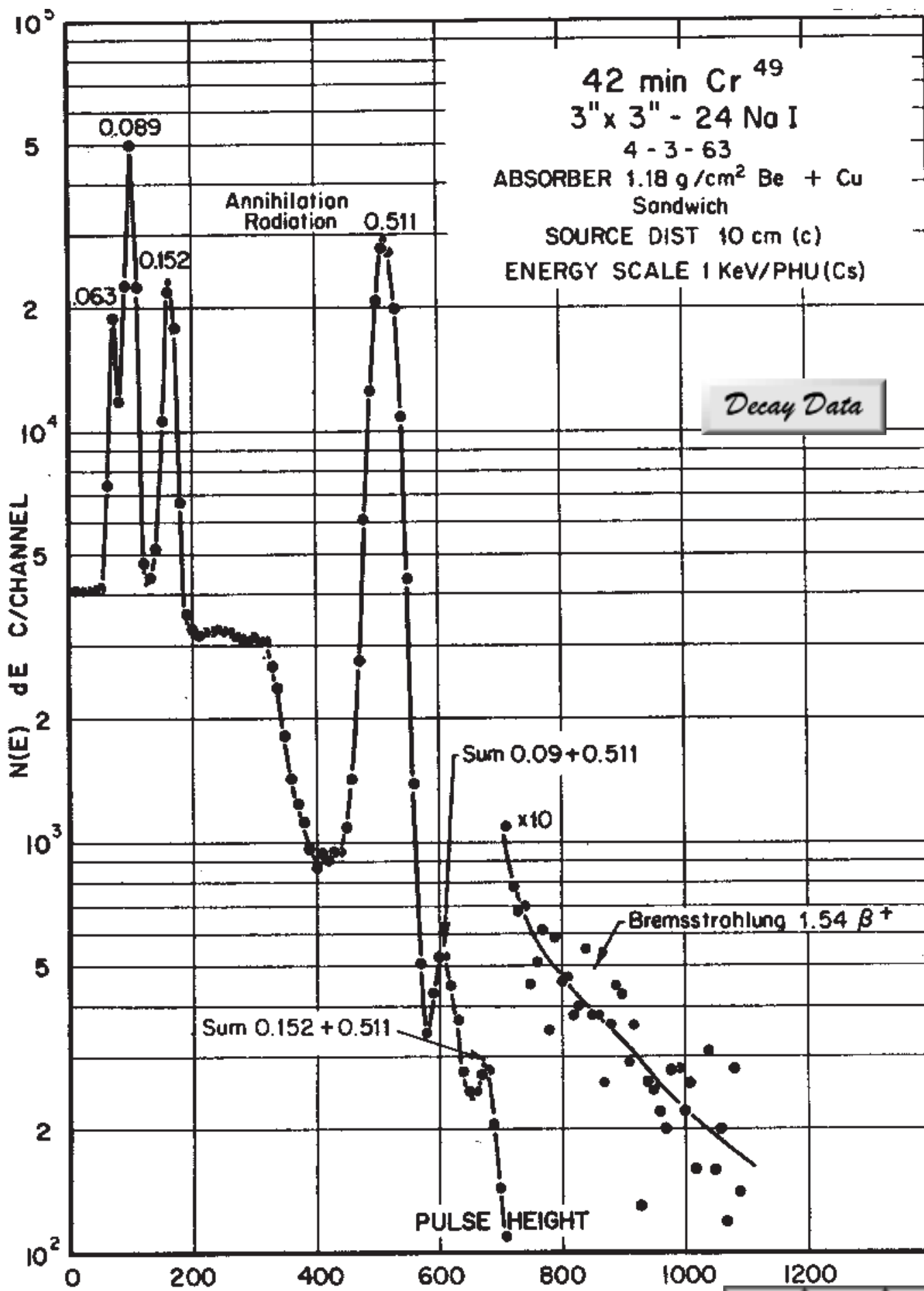
GAMMA-RAY ENERGIES AND INTENSITIES

Nuclide ^{52}V
Detector 3" X 3" NaI-2

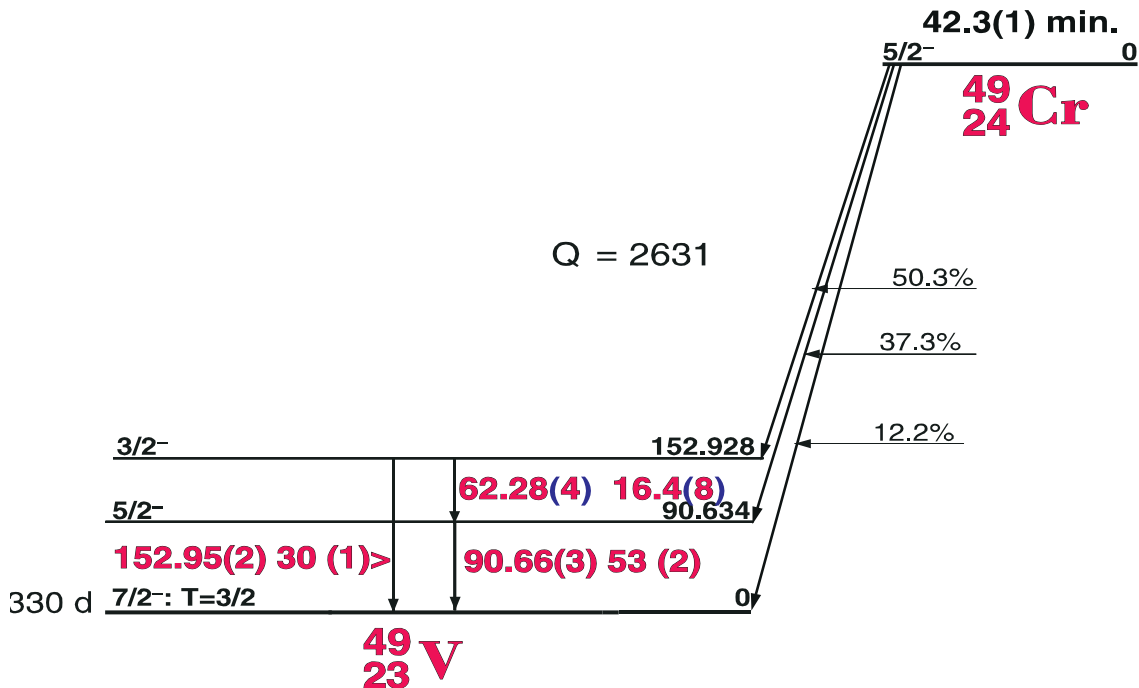
Half Life 3.743(5) min.
Method of Production: $\text{V}^{51}(n,\gamma)$

E_γ (KeV)[S]	ΔE_γ	I_γ (rel)	$I_\gamma(\%)$ [E]	ΔI_γ	S
647.45	± 0.1	0.02	0.024	± 0.002	4
935.52	± 0.05	0.06	0.061	± 0.003	4
947.05	± 0.05	0.02			4
1333.62	± 0.04	0.6	0.59	± 0.01	3
1434.047	± 0.03	100	100	± 1	1
1531.6	± 0.05	0.9	0.12	± 0.01	4





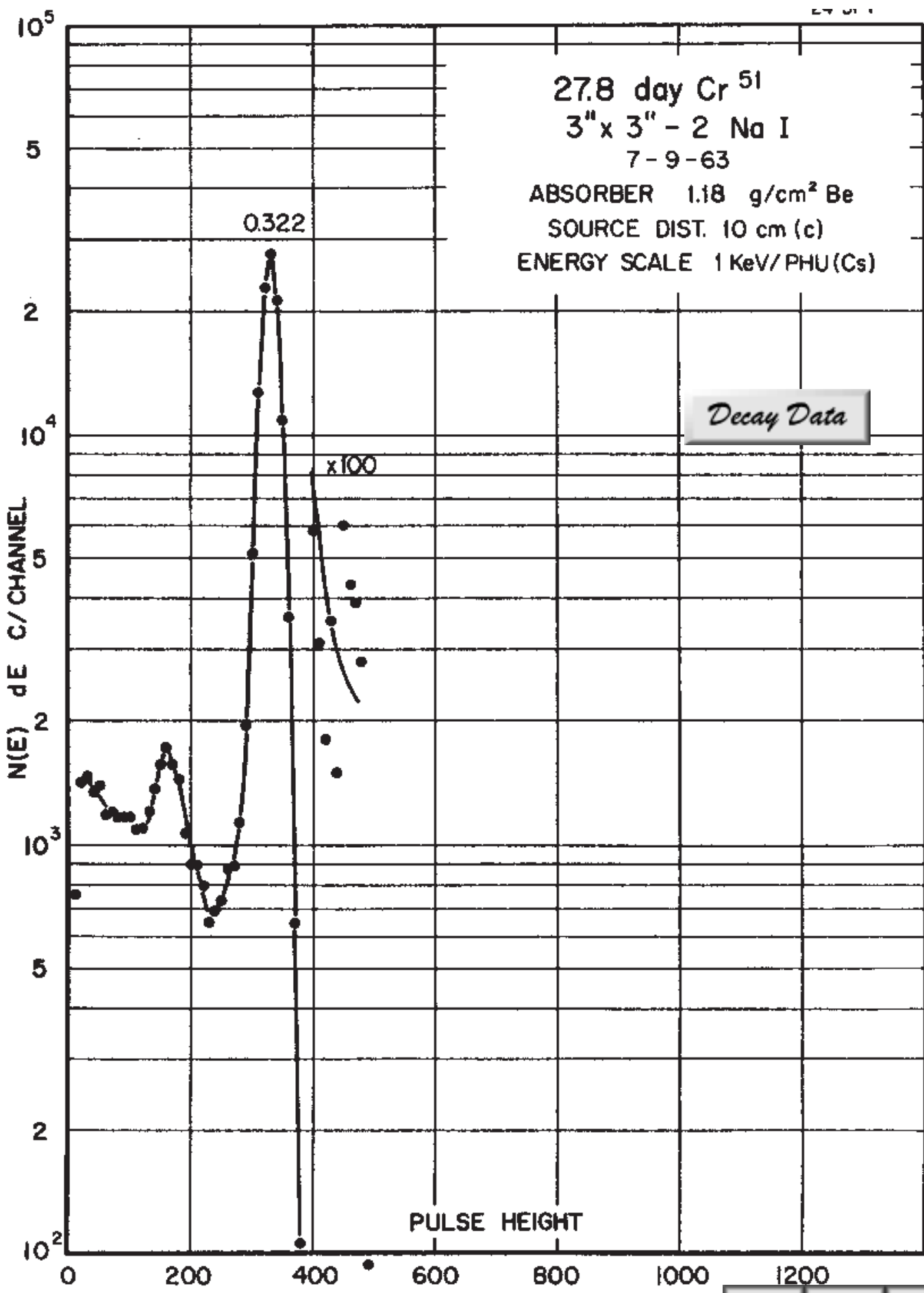
42.3 Min ^{49}Cr Decay Scheme



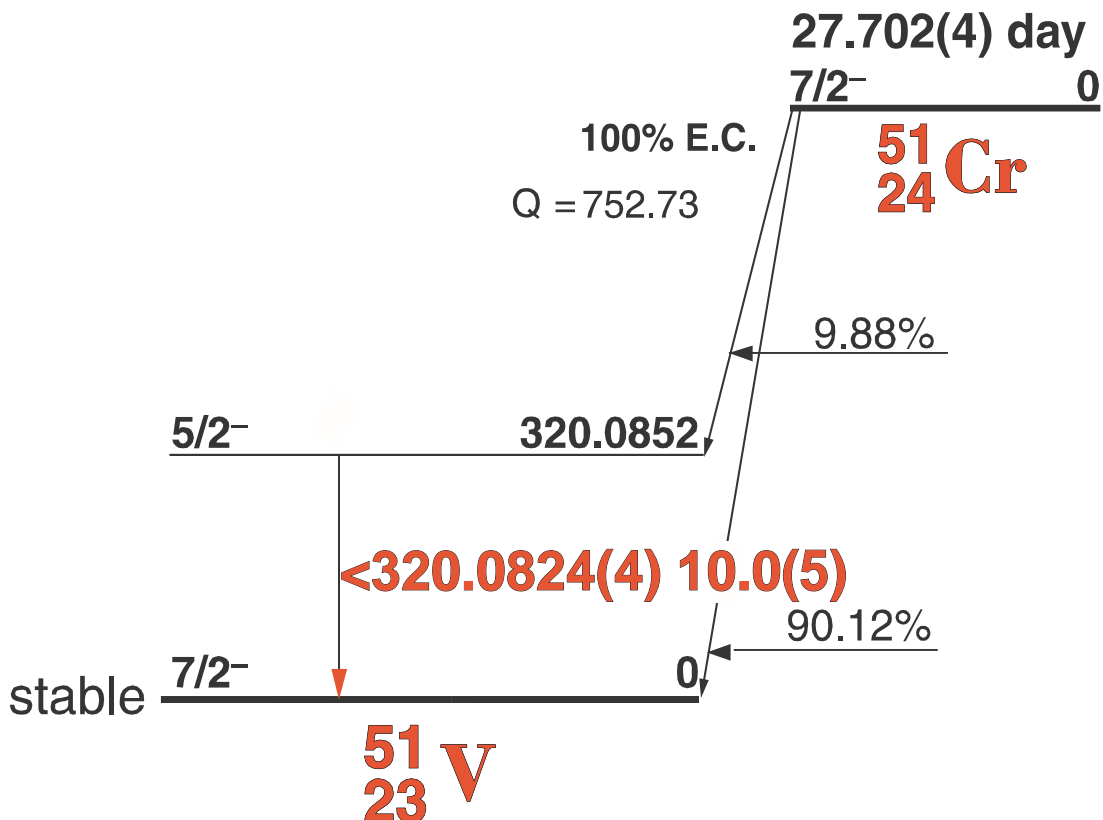
GAMMA-RAY ENERGIES AND INTENSITIES

Nuclide ^{49}Cr Half Life 42.3(1) min.
 Detector 3" x 3" - 2NaI Method of Production: $\text{Cr}^{50}(\gamma, n)$

E_γ (KeV)[S]	ΔE_γ	I_γ (rel)	$I_\gamma(\%)$ [E]	ΔI_γ	S
62.28	± 0.04	26.6	16.4	± 0.1	1
90.64	± 0.03	100	53.2	± 0.2	1
152.95	± 0.02	58.9	30.3	± 0.3	1
ann. rad. 511.006	\pm	100			1
1361.61	± 0.1		0.045	± 0.01	4
1514.1	± 0.1		0.03	± 0.01	4
1570.6	± 0.1		0.02	± 0.01	5



27.704 Day Cr 51 Decay Scheme



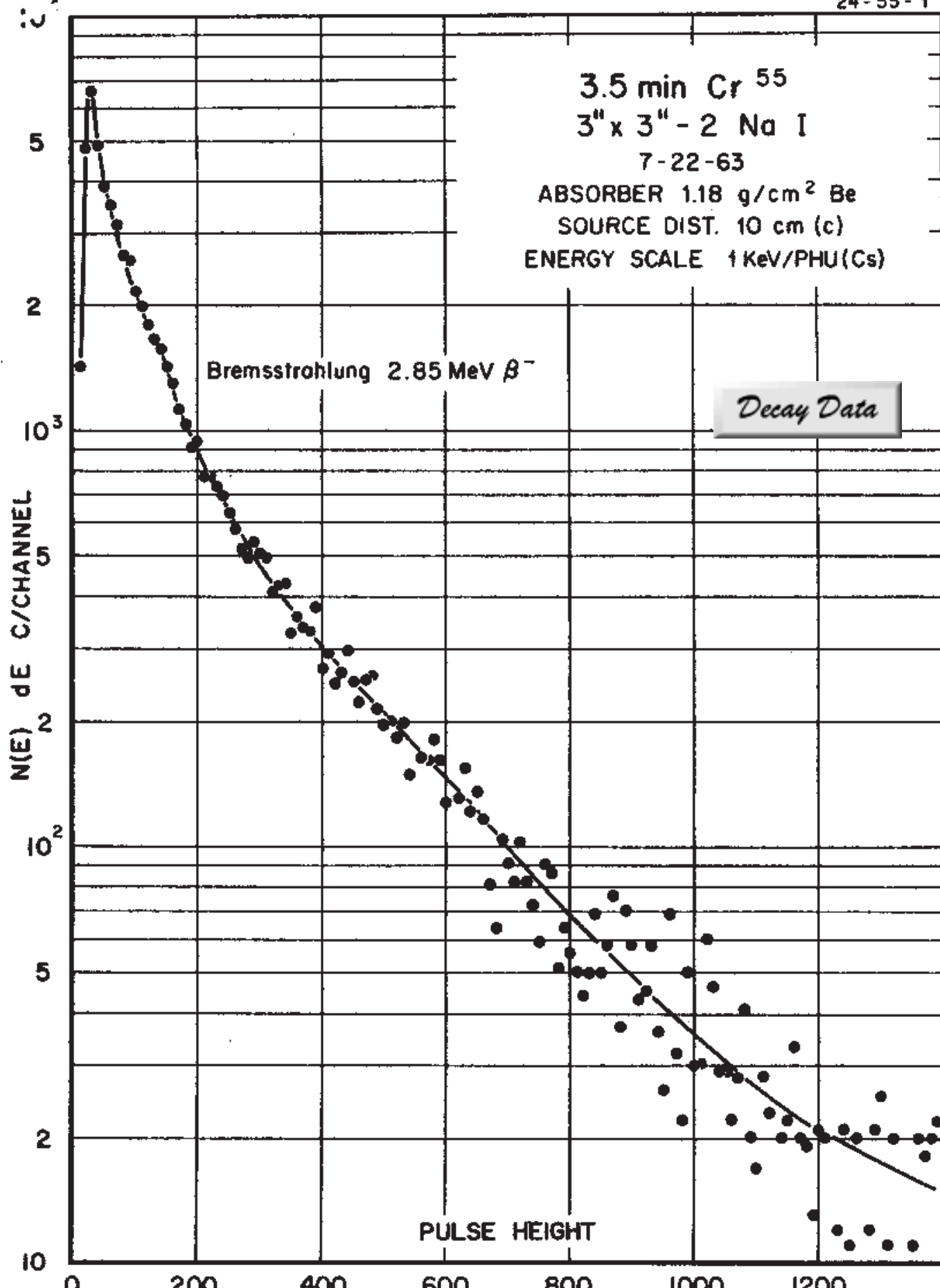
GAMMA-RAY ENERGIES AND INTENSITIES

Nuclide
Detector

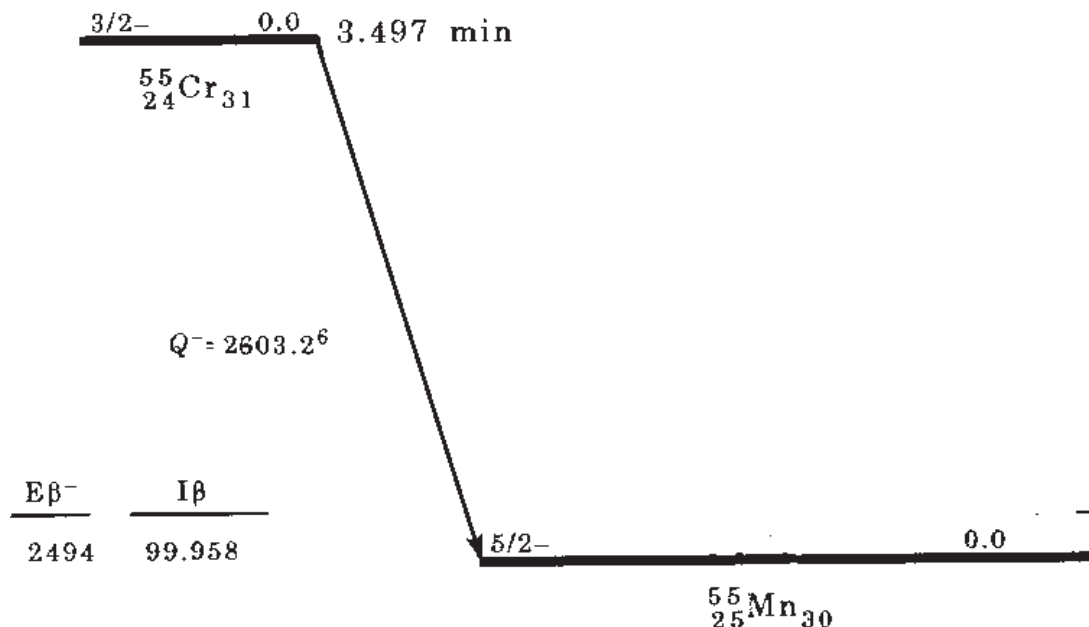
^{51}Cr
3" x 3" - 2Nal

Half Life 27.704(4) day
Method of Production: $\text{Cr}^{50}(n,\gamma)$

E_γ (KeV)[S]	ΔE_γ	I_γ (rel)	$I_\gamma(\%)$ [E]	ΔI_γ	S
320.078	± 0.008	100	10.1	± 0.2	1



3.497 Min ^{55}Cr Decay Scheme



GAMMA-RAY ENERGIES AND INTENSITIES

Nuclide
Detector

^{55}Cr
3" x 3" - 2NaI

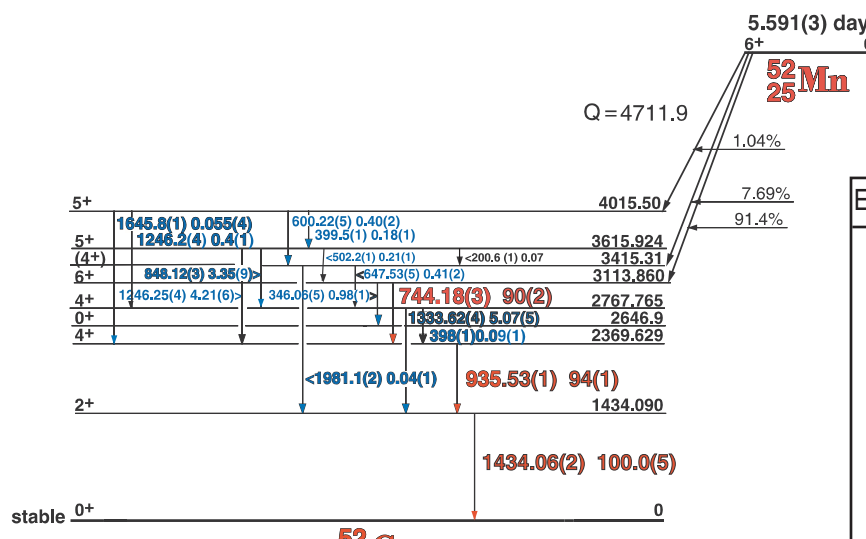
Half Life 3.497(3) min.
Method of Production: $\text{Cr}^{54}(n,\gamma)$

E_γ (KeV)[S]	ΔE_γ	I_γ (rel)	$I_\gamma(\%)$ [E]	ΔI_γ	S
bremstrahlung (2.603 β)					

5.591 Day ^{52}Mn

30-65-2

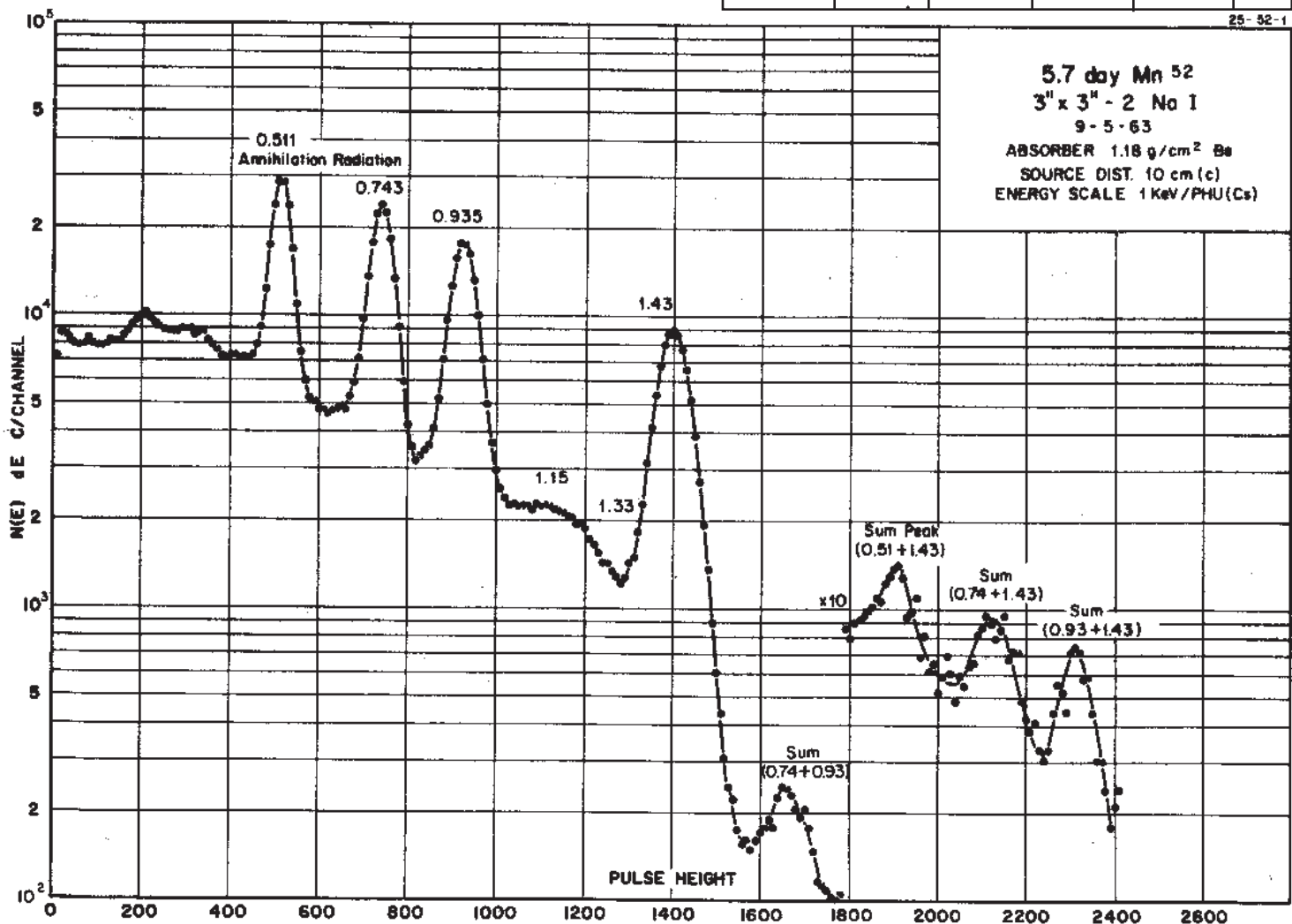
5.591(3) day ^{52}Mn Decay Scheme



GAMMA-RAY ENERGIES AND INTENSITIES

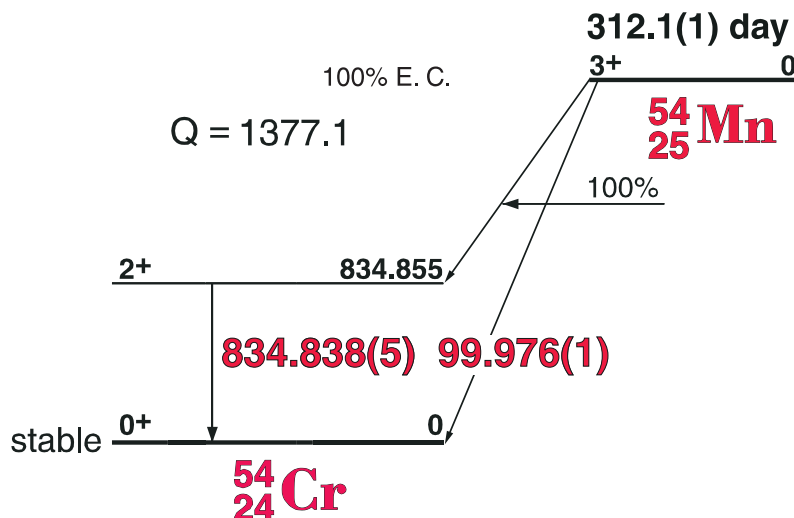
Nuclide Mn^{52}
Detector 3" X 3" NaI-2
Half Life 5.59 Day
Method of Production: $\text{Cr}^{52}(\text{p},\text{n})$

E_{γ} (KeV)[S]	ΔE_{γ}	$I_{\gamma}(\text{rel})$	$I_{\gamma}(\%)[\text{E}]$	ΔI_{γ}	S
346.062	± 0.050	1.2	0.980	± 0.01	4
399.2	± 0.4	0.36	0.189	± 0.007	4
502.17	± 0.10	0.14	0.21	± 0.02	4
600.22	± 0.05	0.53	0.39	± 0.01	4
647.531	± 0.05	0.40	0.40	± 0.02	4
744.179	± 0.03	88.2	90.0	± 0.8	1
848.175	± 0.03	3.4	3.32	± 0.03	3
935.504	± 0.030	95.0	94.5	± 0.9	1
1246.250	± 0.040	4.8	4.21	± 0.06	2
1333.624	± 0.040	5.3	5.07	± 0.05	1
1434.047	± 0.030	100	100	± 0.5	1
1645.82	± 0.15	0.06	0.05	± 0.01	3
1981.12	± 0.04	0.04	0.034	± 0.003	3



312.1 Day Mn⁵⁴

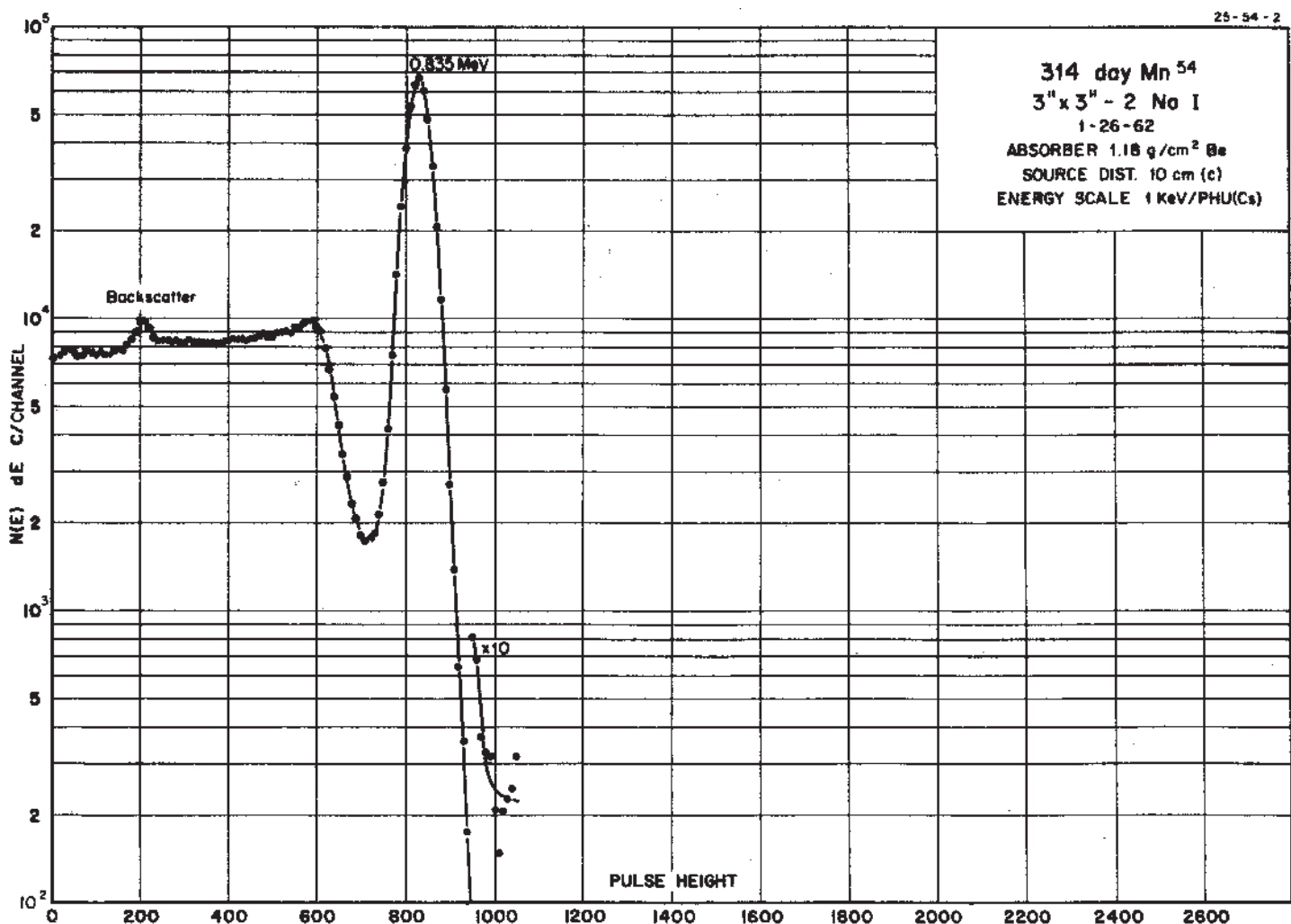
Mn⁵⁴ Decay Scheme



GAMMA-RAY ENERGIES AND INTENSITIES

Nuclide ^{54}Mn Half Life 312.1(2) day
 Detector 3" X 3" NaI-2 Method of Production: Cr⁵⁴(p,n)

E_{γ} (KeV)[S]	ΔE_{γ}	$I_{\gamma}(\text{rel})$	$I_{\gamma}(\%)$ [E]	ΔI_{γ}	S
834.838	± 0.003	100	100	2	1

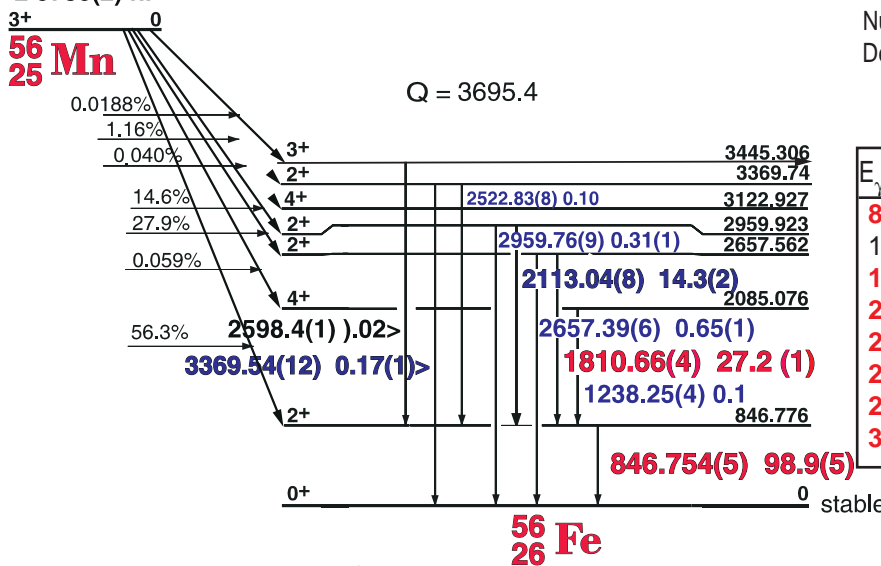


2.5785 Hr. ^{56}Mn

25-56-1

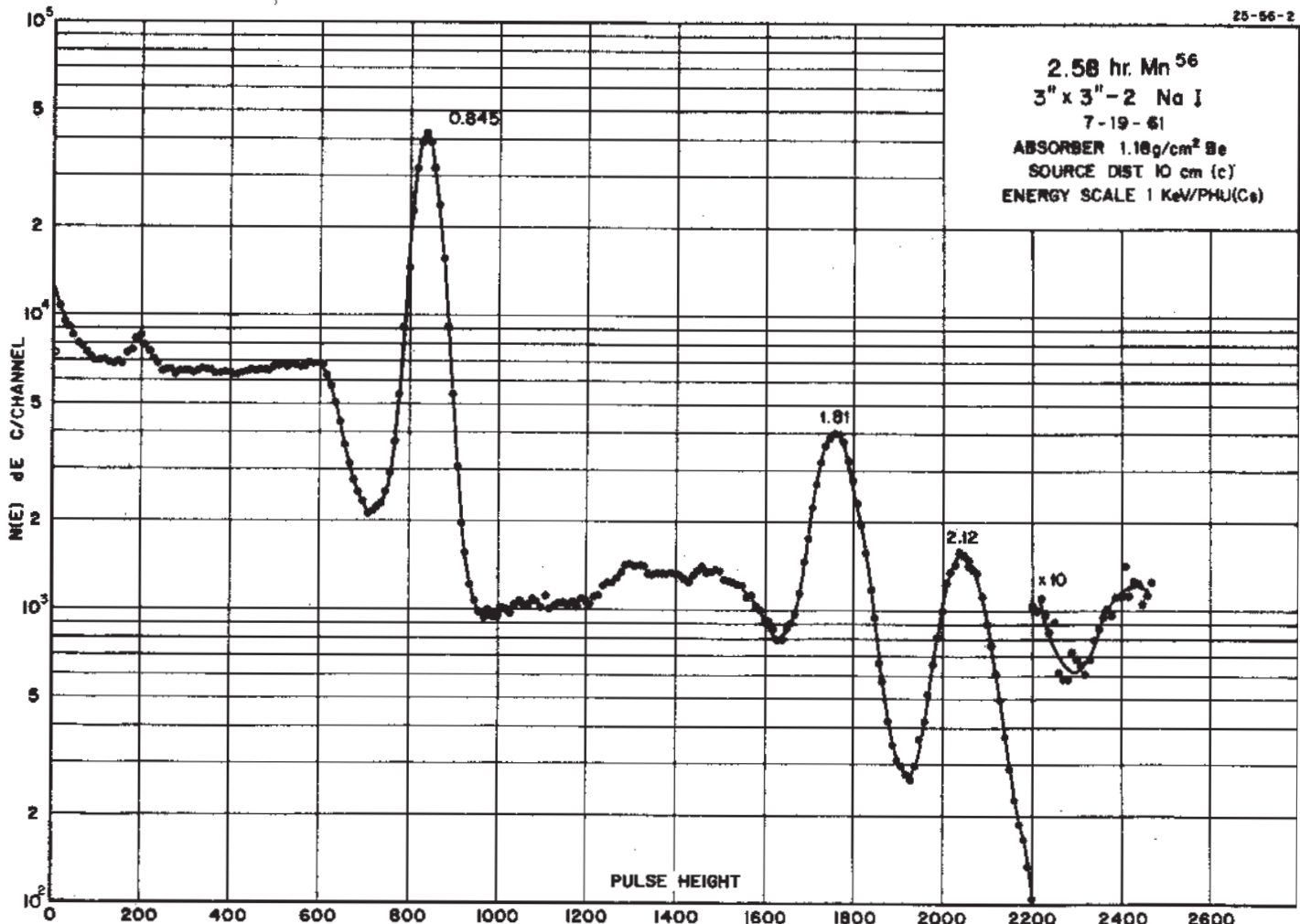
^{56}Mn Decay Scheme

2.5785(2) hr.



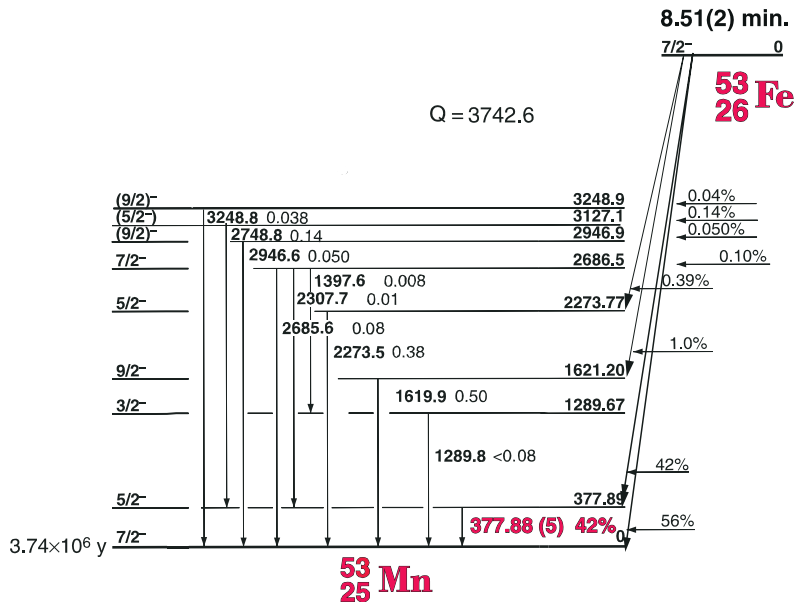
Nuclide ^{56}Mn Half Life 2.5785 Hr.
Detector 3" X 3" NaI-2 Method of Production: $\text{Mn}^{55}(n,\gamma)$

E_{γ} (KeV)[S]	ΔE_{γ}	$I_{\gamma}(\text{rel})$	$I_{\gamma}(\%) [E]$	ΔI_{γ}	S
846.754	± 0.005	100	93.9	± 1	1
1238.25	± 0.4	0.09	0.1	± 0.01	4
1810.665	± 0.039	28.7	27.2	± 0.3	1
2113.042	± 0.084	15.4	14.3	± 0.2	1
2522.83	± 0.08	1.15	1.0	± 0.05	1
2657.386	± 0.065	0.76	0.65	± 0.03	1
2959.76	± 0.09	0.33	0.31	± 0.01	1
3369.54	± 0.12	0.184	0.17	± 0.005	1



8.51(2) min. ^{53}Fe

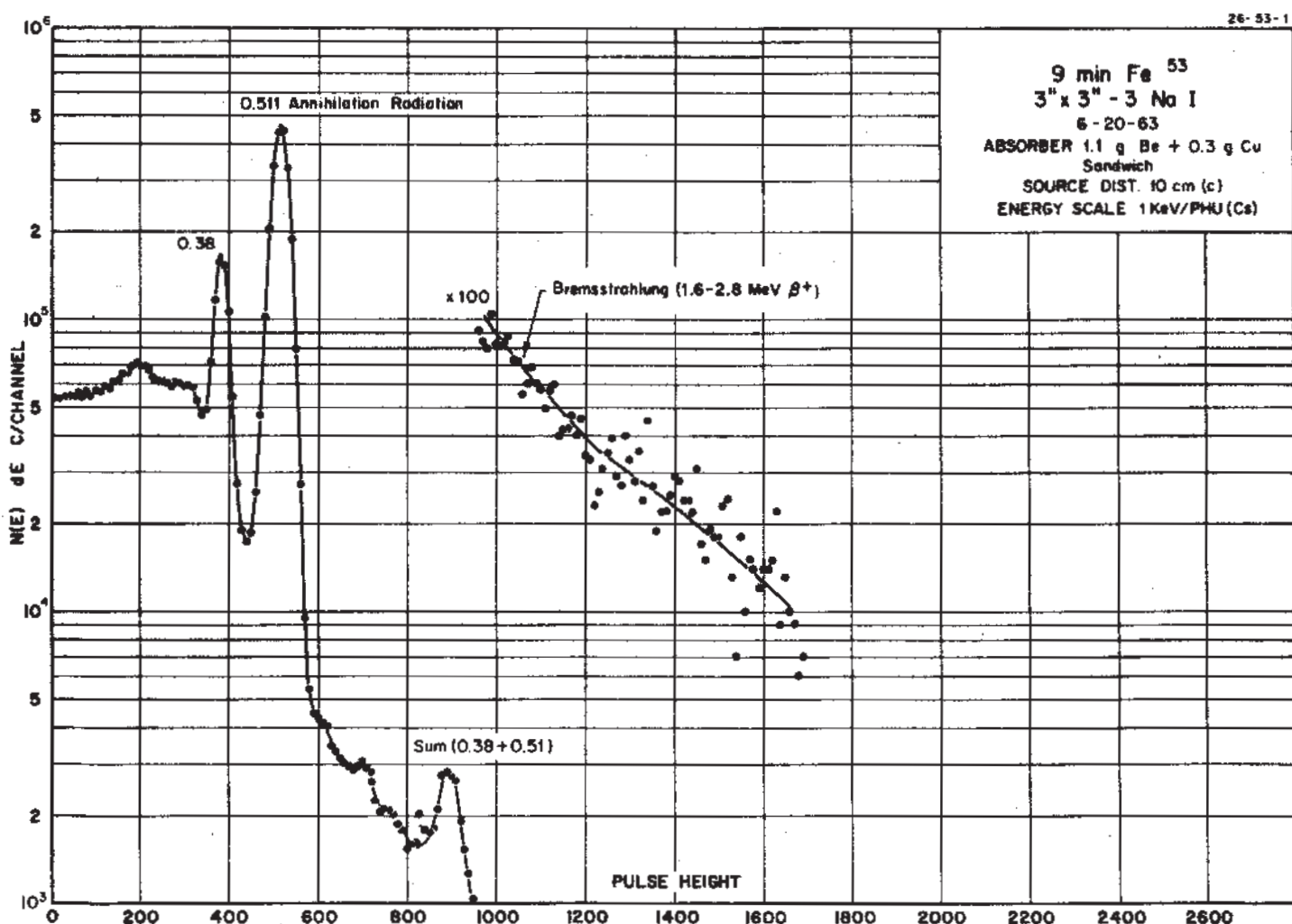
^{53}Fe Decay Scheme



GAMMA-RAY ENERGIES AND INTENSITIES

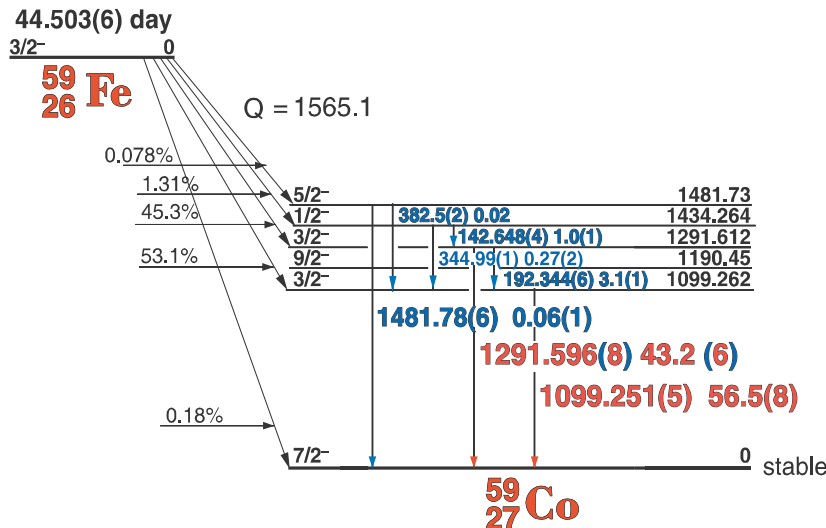
Nuclide ^{53}Fe Half Life 9 Min.
Detector 3" X 3" NaI-2 Method of Production: Fe⁵⁴(γ ,n)

E_{γ} (KeV)[S]	ΔE_{γ}	$I_{\gamma}(\text{rel})$	$I_{\gamma}(\%) [E]$	ΔI_{γ}	S
511.006 (ann. rad.)	100				1
377.88	± 0.05	100	42	± 2.0	1



44.503(6) day ^{59}Fe

^{59}Fe Decay Scheme

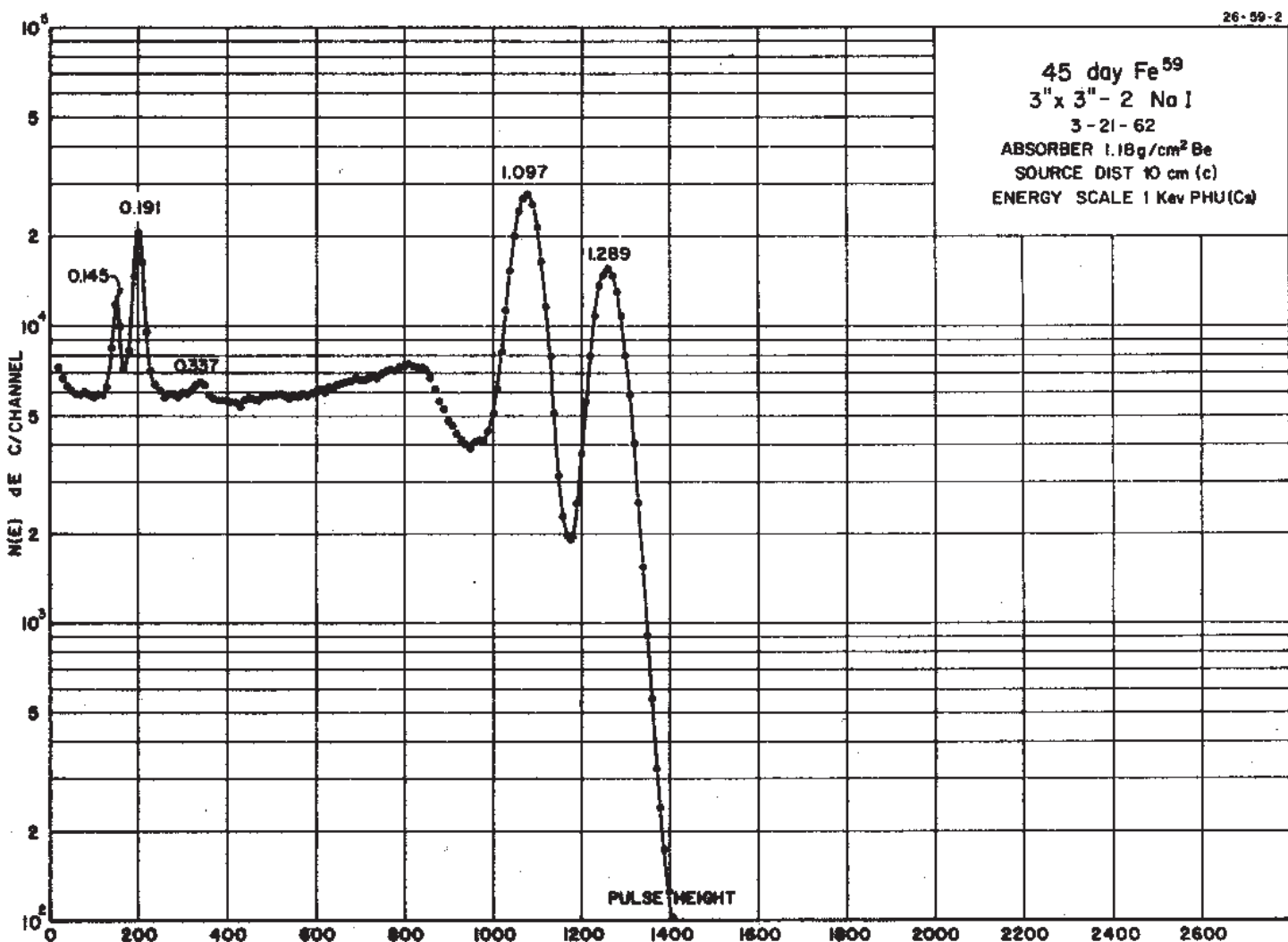


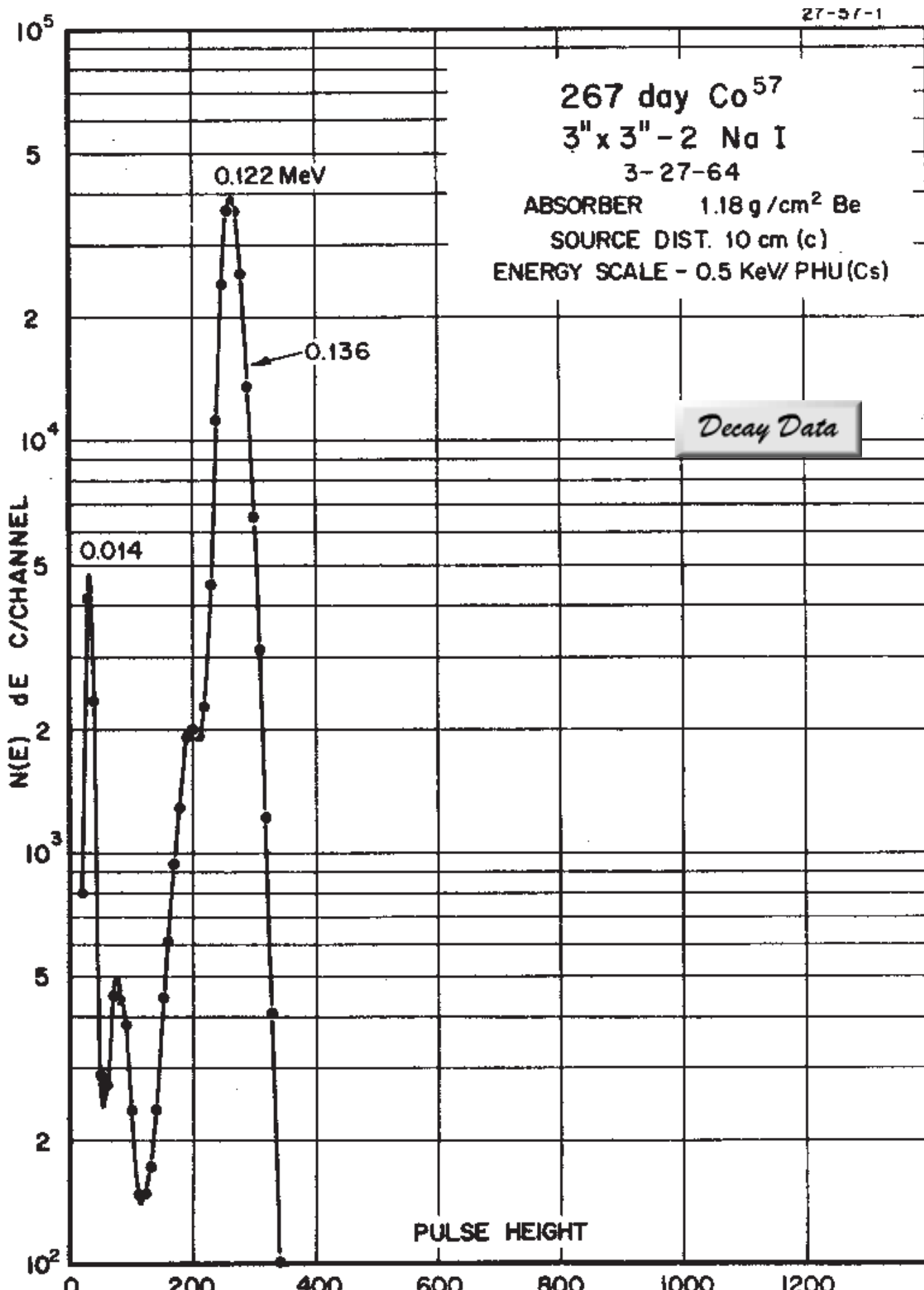
GAMMA-RAY ENERGIES AND INTENSITIES

Nuclide ^{59}Fe
Detector 3" X 3" NaI-2

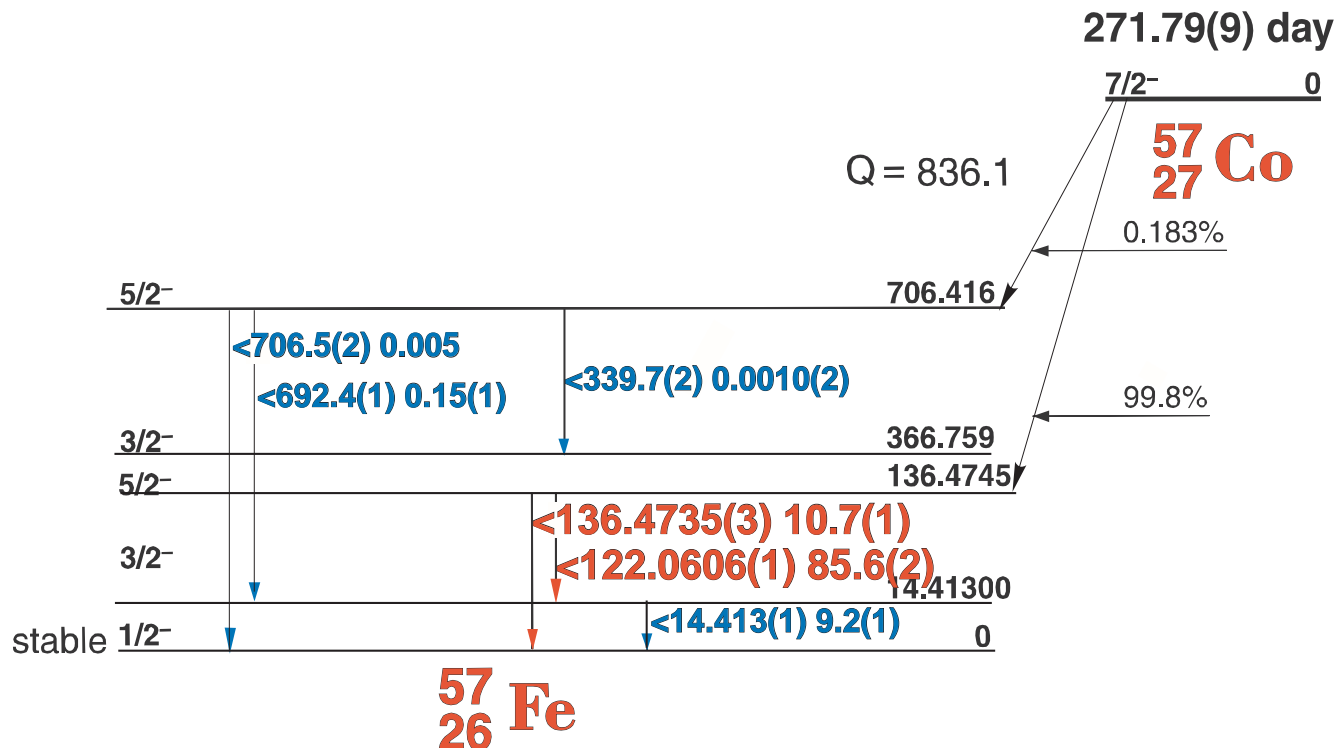
Half Life 45.0 day
Method of Production: $\text{Fe}^{58}(\text{n},\gamma)$

E_{γ} (KeV)[S]	ΔE_{γ}	$I_{\gamma}(\text{rel})$	$I_{\gamma}(\%)[\text{E}]$	ΔI_{γ}	S
142.648	± 0.004	1.54	1.02	± 0.04	2
192.344	± 0.006	4.7	1.02	± 0.04	1
334.992	± 0.010	0.47	0.271	± 0.005	3
382.56	± 0.2	0.05	0.018	± 0.002	4
1099.251	± 0.005	100	56.5	± 1.5	1
1291.596	± 0.008	77	43.2	± 1	1
1481.78	± 0.06	0.11	0.059	± 0.01	3





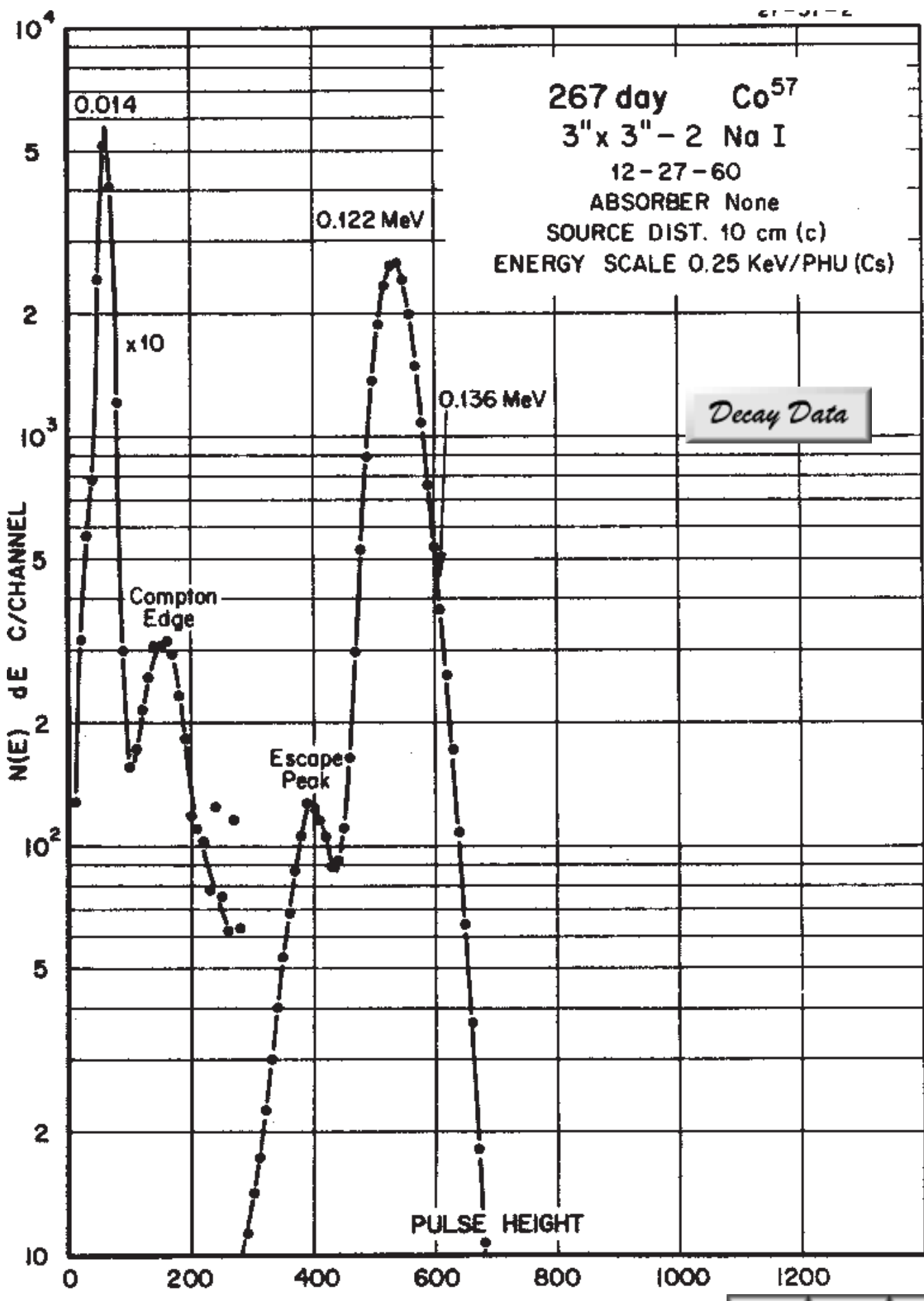
271.79(9) day ^{57}Co Decay Scheme



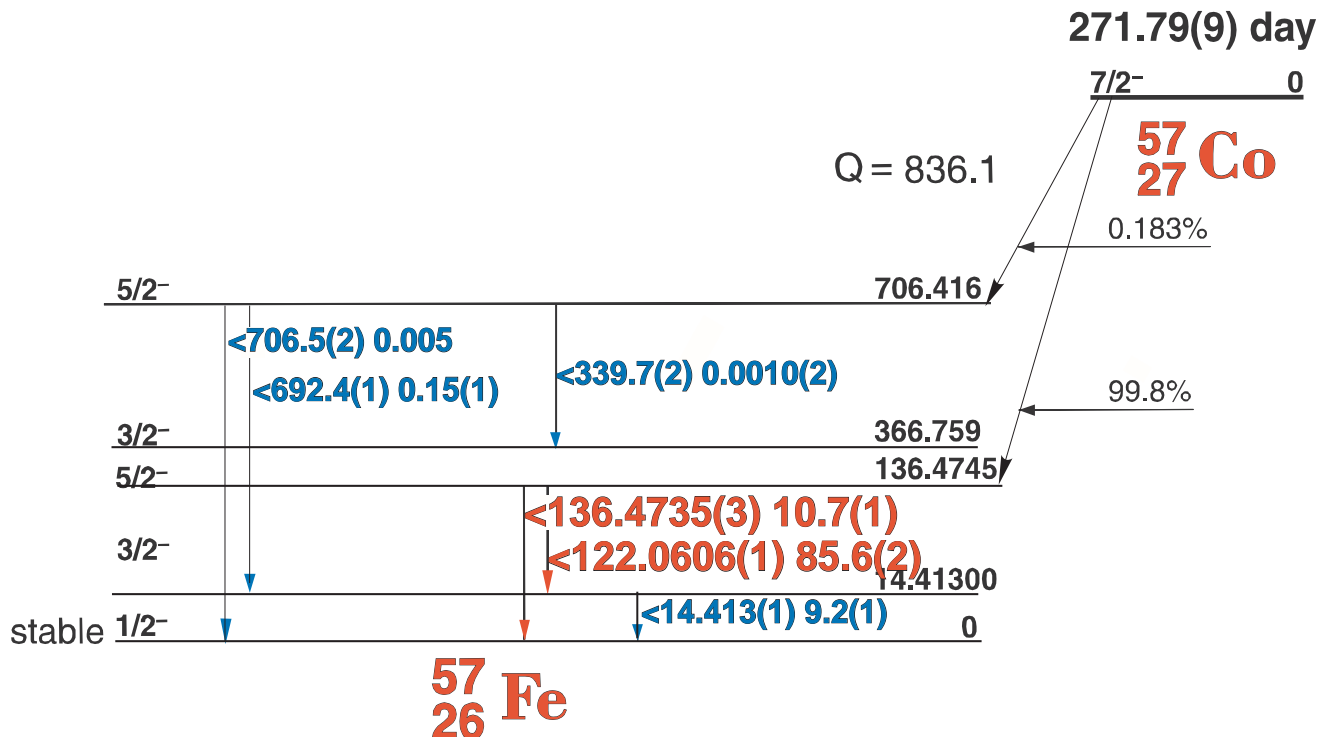
GAMMA-RAY ENERGIES AND INTENSITIES

Nuclide ^{57}Co Half Life 271.79(9) day
 Detector 3" x 3" - 2Nal Method of Production: $\text{Fe}^{57}(\text{p},\text{n})$

E_{γ} (KeV) [S]	ΔE_{γ}	I_{γ} (rel)	$I_{\gamma}(\%)$ [E]	ΔI_{γ}	S
14.4136	± 0.0003		6.18	± 0.1	
122.060	± 0.010	100	85.60	± 0.5	1
136.471	± 0.010	12.9	10.88	± 0.1	1
570.1	± 0.2	0.01	0.016	± 0.01	3
692.4	± 0.1	0.19	0.15	± 0.01	1



271.79(9) day ^{57}Co Decay Scheme



GAMMA-RAY ENERGIES AND INTENSITIES

Nuclide
Detector

^{57}Co

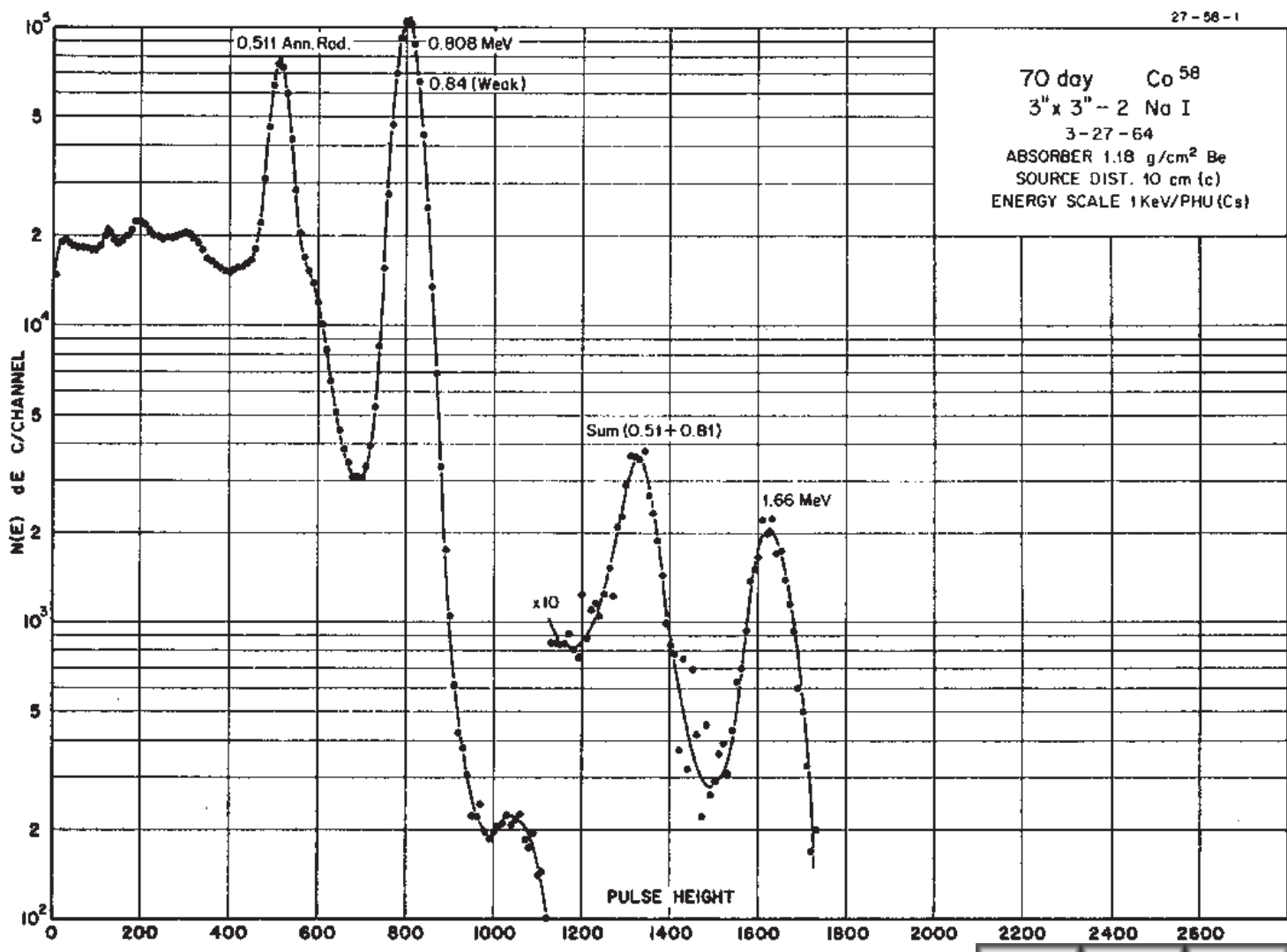
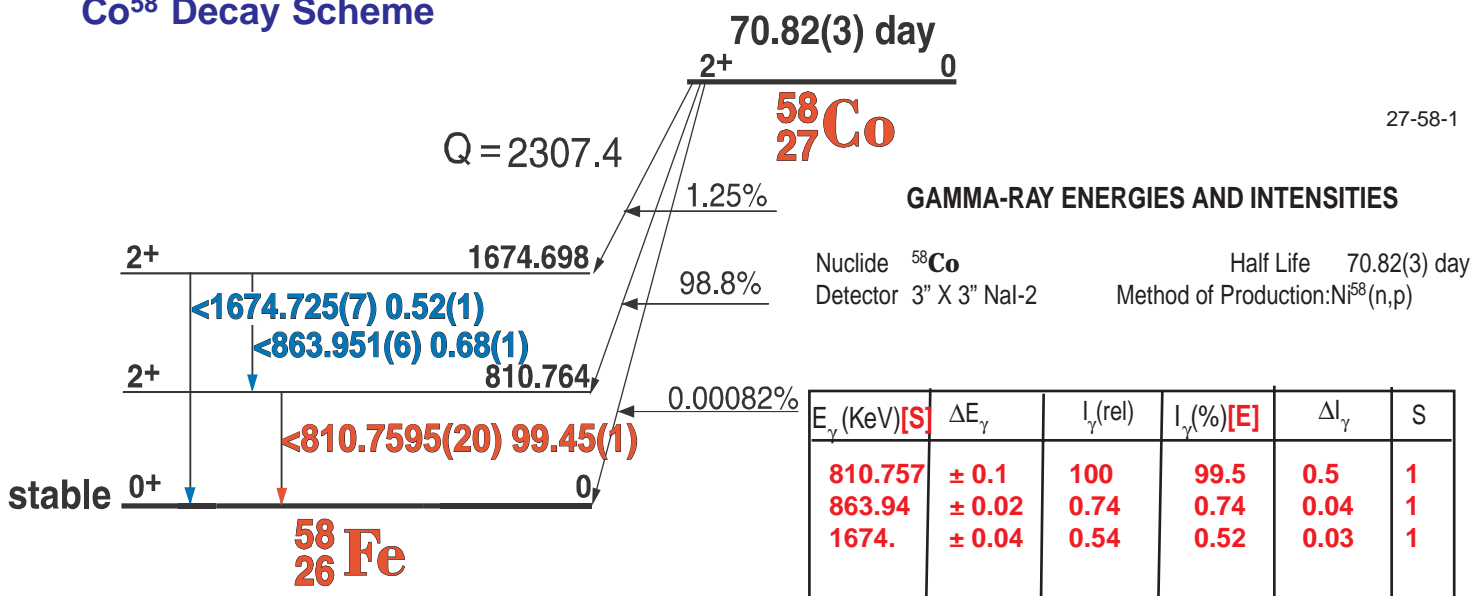
3" x 3" - 2Nal

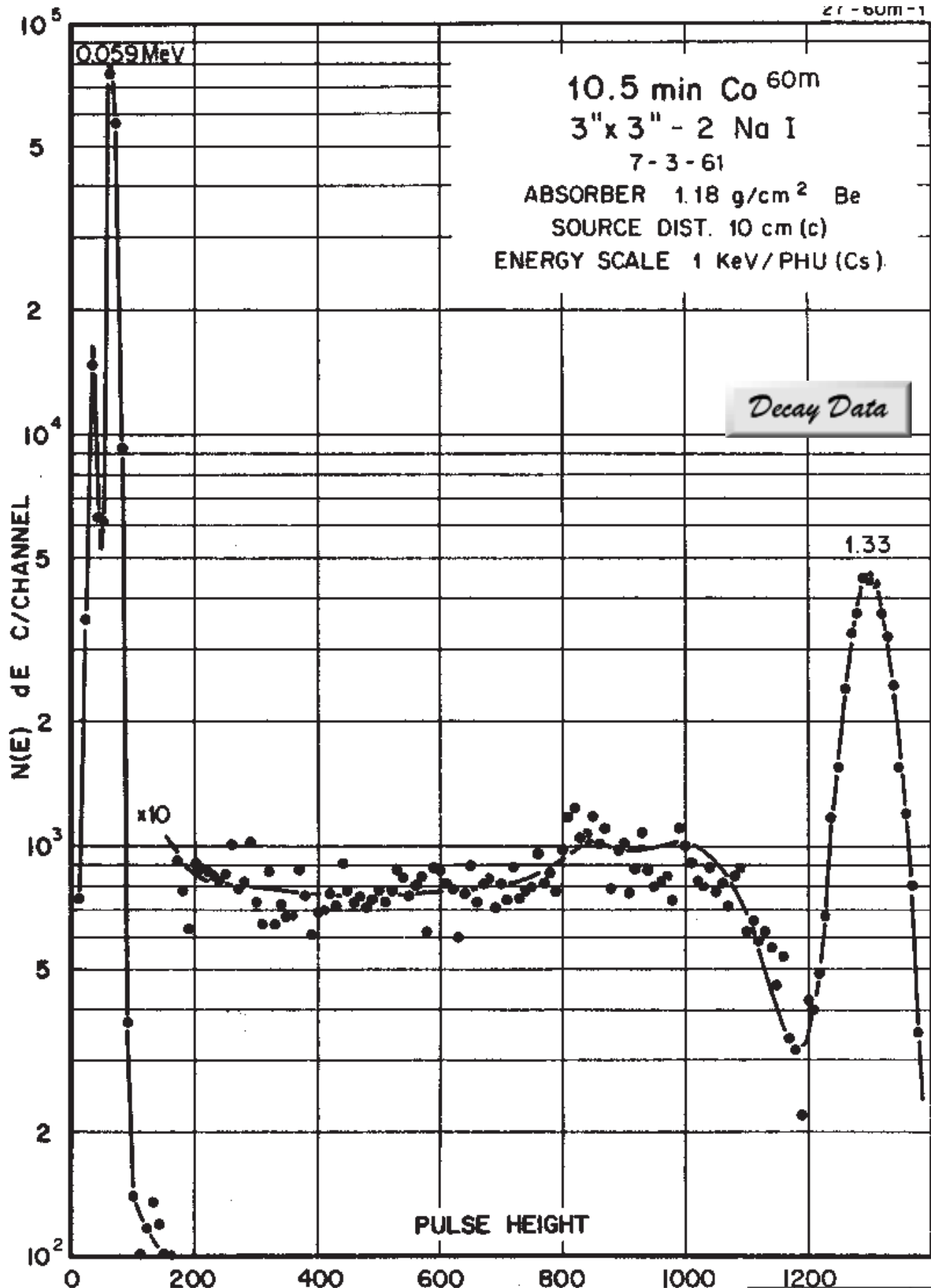
Half Life 271.79(9) day
Method of Production: $\text{Fe}^{57}(\text{p},\text{n})$

E_{γ} (KeV)[S]	ΔE_{γ}	I_{γ} (rel)	$I_{\gamma}(\%)$ [E]	ΔI_{γ}	S
14.4136	± 0.0003		6.18	± 0.1	
122.060	± 0.010	100	85.60	± 0.5	1
136.471	± 0.010	12.9	10.88	± 0.1	1
570.1	± 0.2	0.01	0.016	± 0.01	3
692.4	± 0.2	0.19	0.15	± 0.01	1

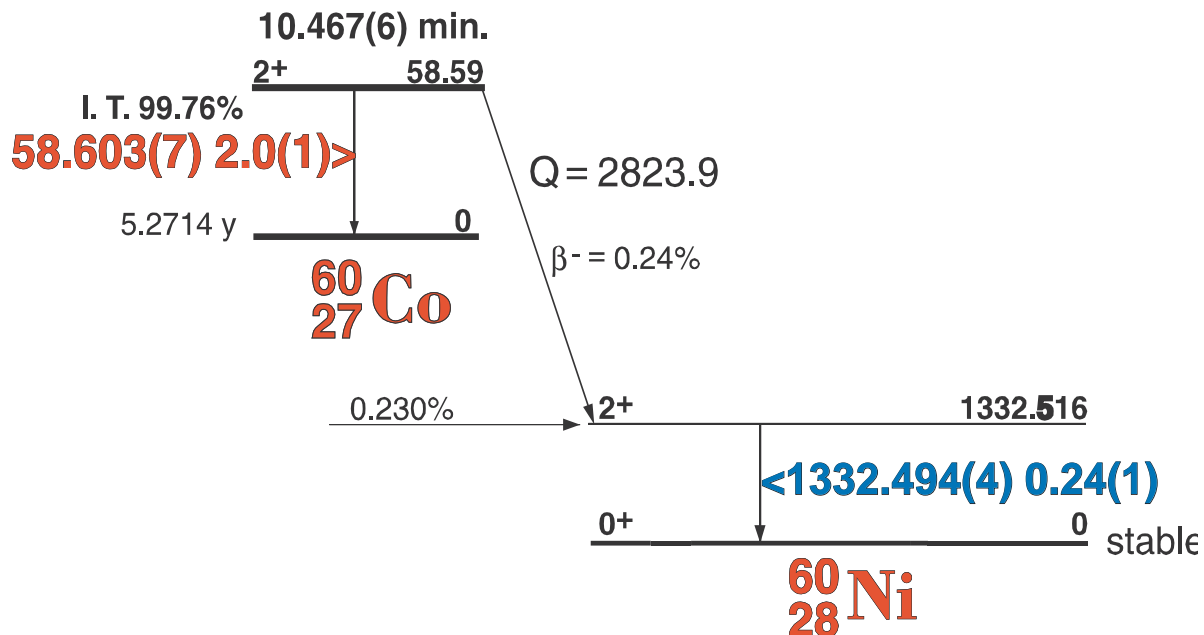
70.82(3) day ^{58}Co

Co^{58} Decay Scheme





10.46(7) Min ^{60m}Co Decay Scheme

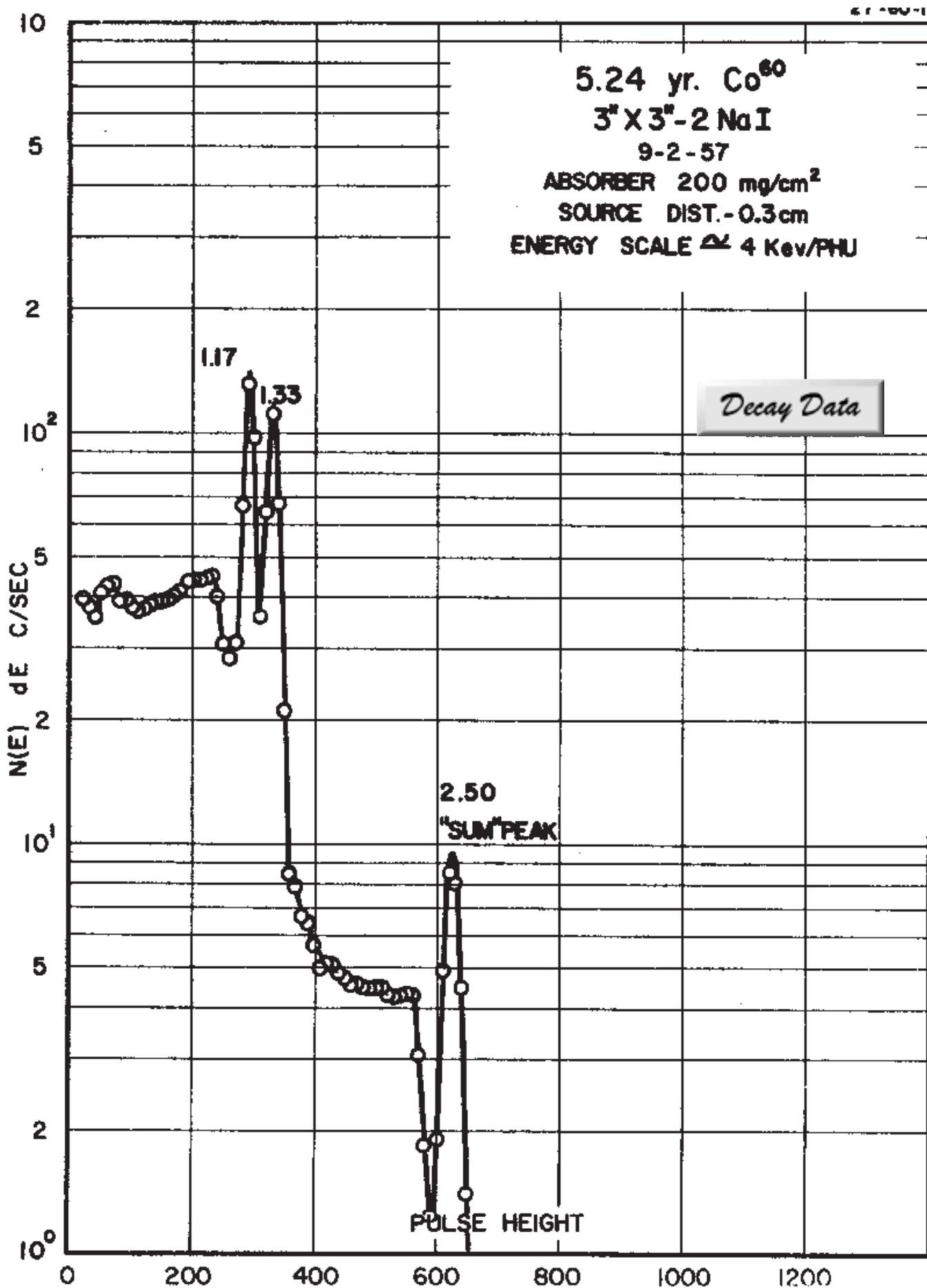


GAMMA-RAY ENERGIES AND INTENSITIES

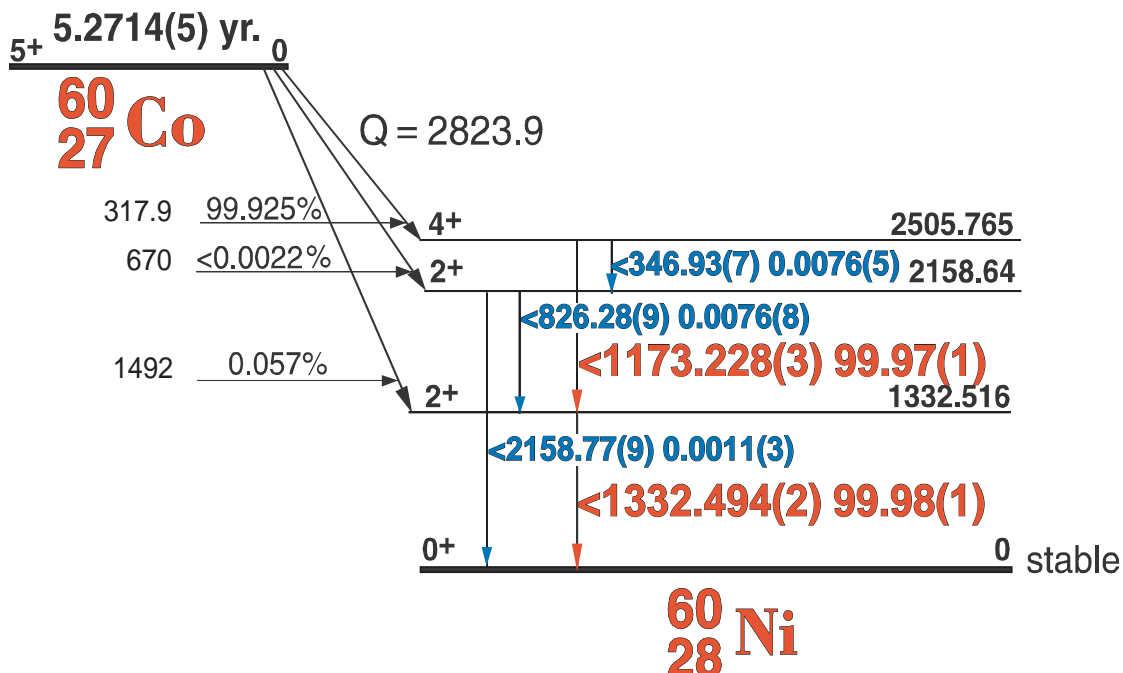
Nuclide ^{60m}Co
 Detector 3" x 3" - 2Nal

Half Life 10.467(6) min.
 Method of Production: $\text{Co}^{59}(n, \gamma)$

E_γ (KeV) [S]	ΔE_γ	I_γ (rel)	$I_\gamma(\%)$ [E]	ΔI_γ	S
Co K x-rays					
58.603	± 0.007	100	99.76	\pm	1
826.28	± 0.01		0.003		5
1332.501	± 0.005		2.4		1
2158.77	± 0.1		0.03		4



5.2714(5) yr. ^{60}Co Decay Scheme [C]



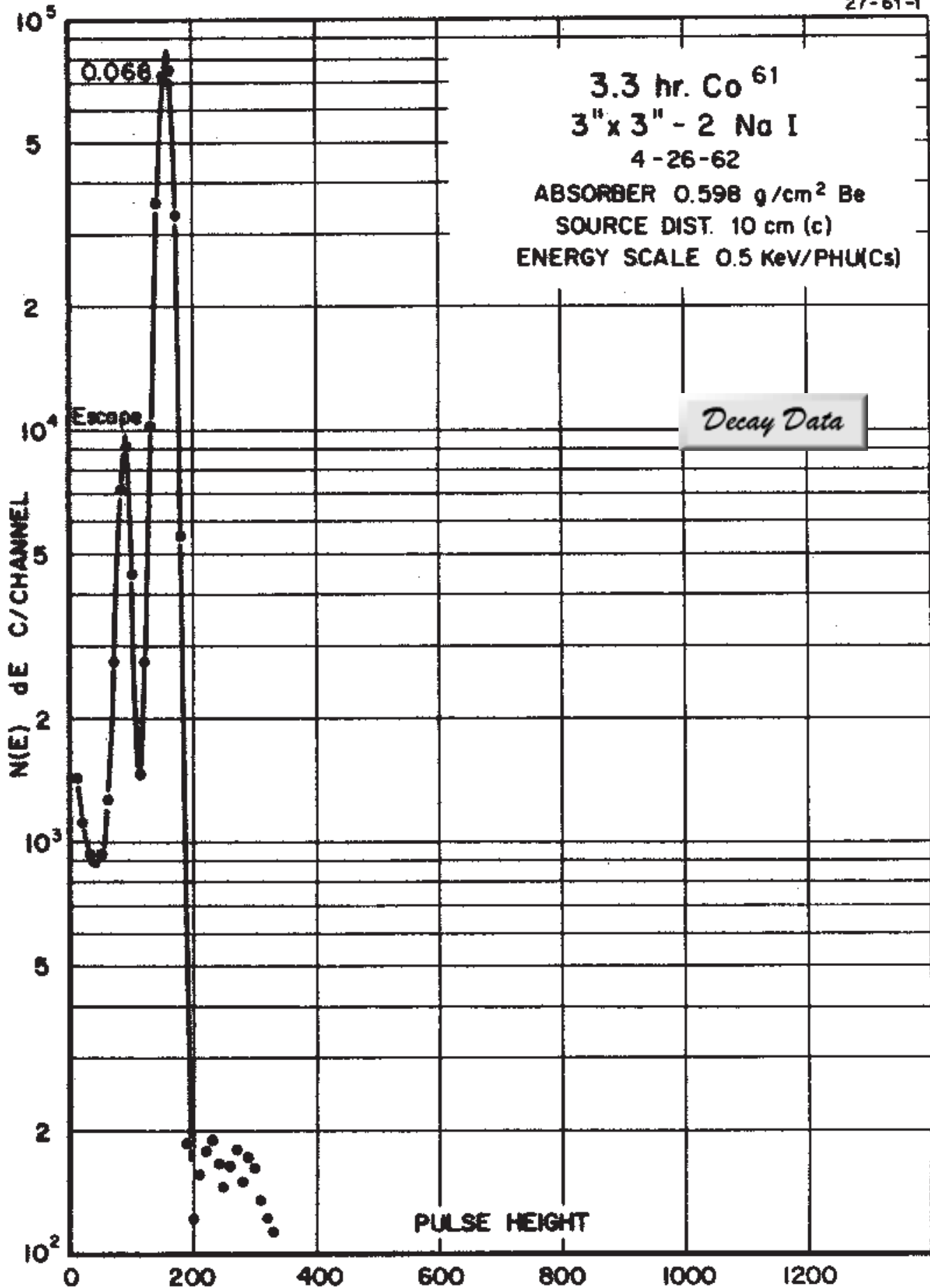
GAMMA-RAY ENERGIES AND INTENSITIES

Nuclide
Detector

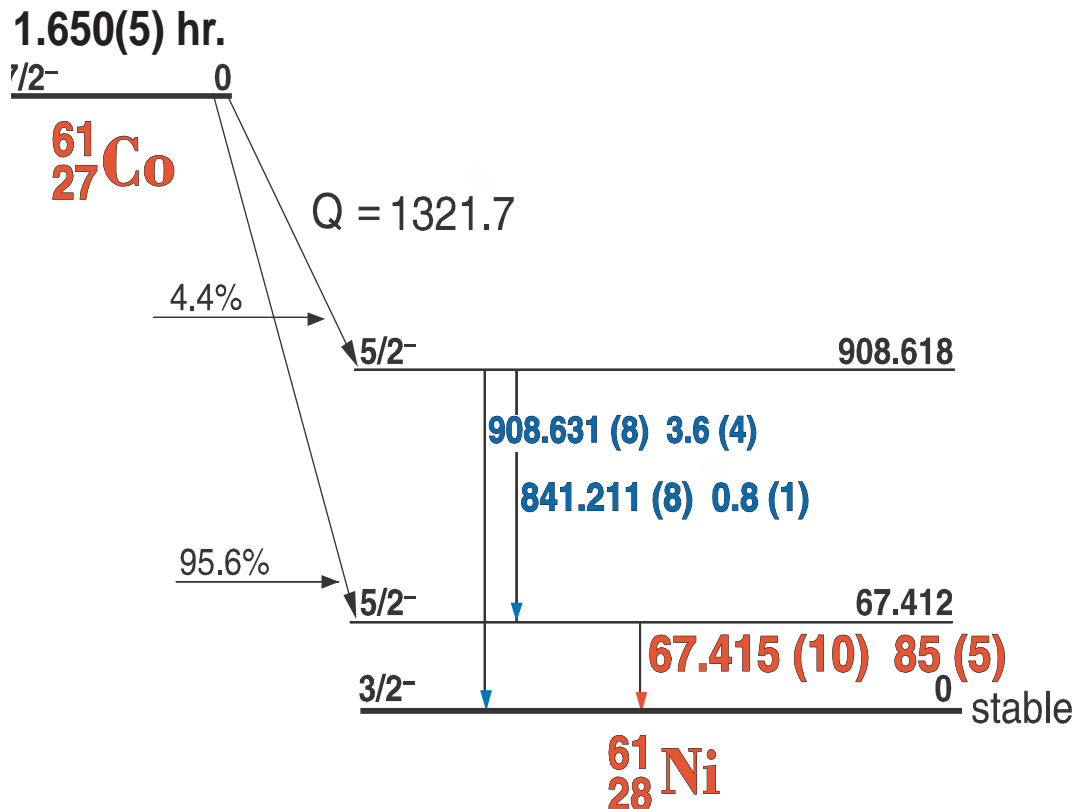
^{60}Co
 $3'' \times 3''$ - 2Nal

Half Life 5.2714(5) yr.
Method of Production: $\text{Co}^{59}(n,\gamma)$

E_γ (KeV)[S]	ΔE_γ	I_γ (rel)	$I_\gamma(\%)$ [E]	ΔI_γ	S
346.93	± 0.02	weak	0.0076	± 0.0007	4
1173.228 ± 0.003		100	99.9736	± 0.0007	1
1332.494 ± 0.002		100	99.9856	± 0.0004	1



1.650(5) hr. ^{61}Co Decay Scheme



GAMMA-RAY ENERGIES AND INTENSITIES

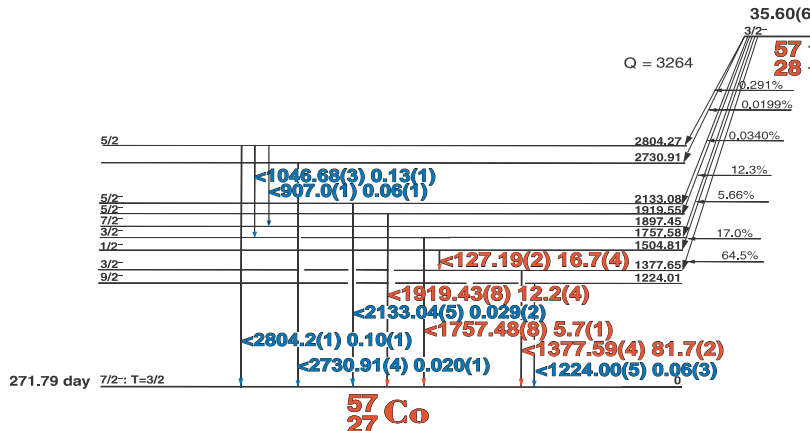
Nuclide ^{61}Co Half Life 1.650(5) hr.
Detector 3" x 3" - 2NaI Method of Production: Ni⁶¹(n,p)

E_{γ} (KeV)[S]	ΔE_{γ}	I_{γ} (rel)	$I_{\gamma}(\%)[E]$	ΔI_{γ}	S
67.415	± 0.010	100	85	± 2	1
841.7	± 0.1	weak	0.8	± 0.08	4
909.2	± 0.1	weak	3.2	± 0.03	4

36 Hr. Ni⁵⁷

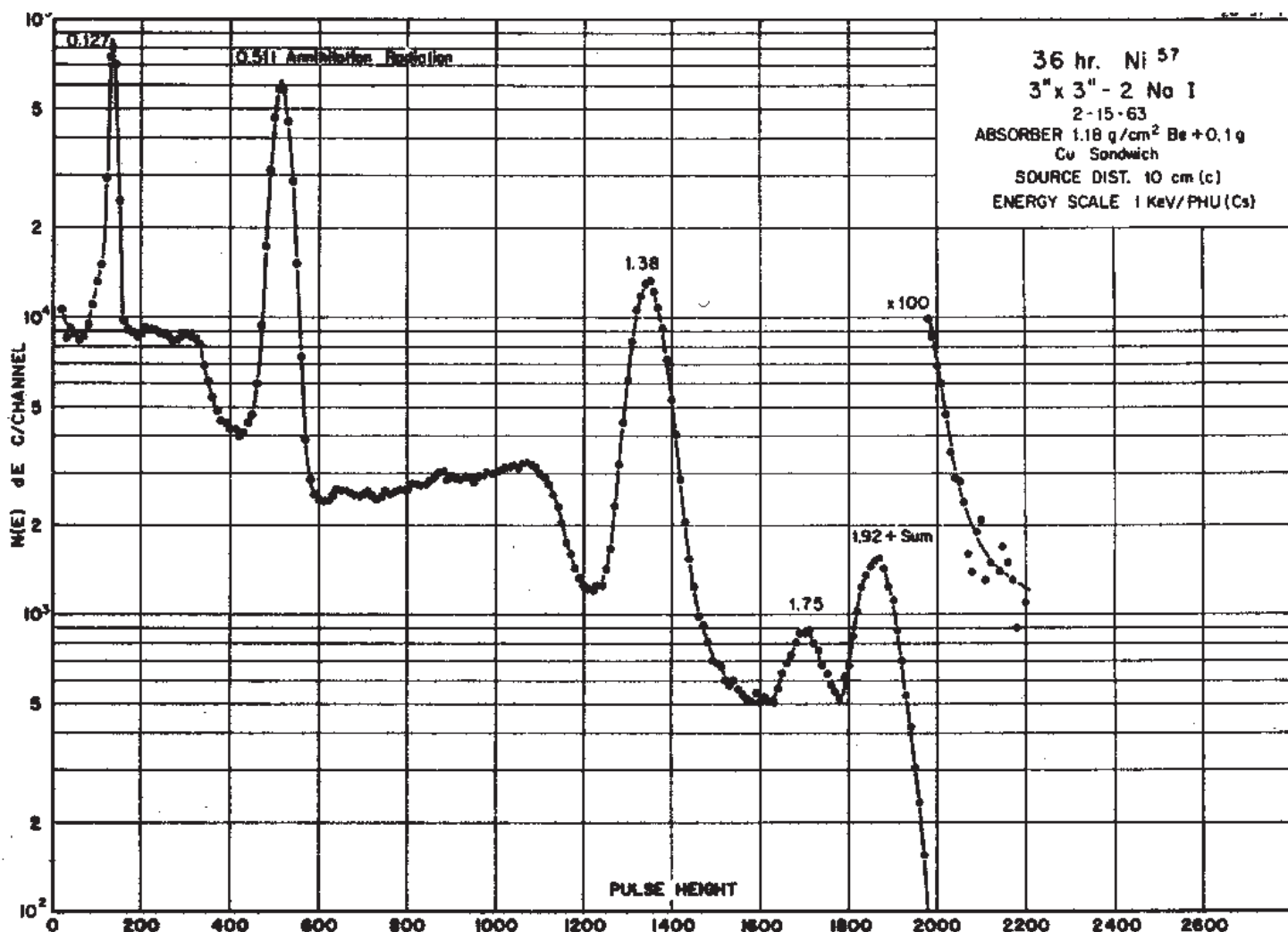
28-57-1

⁵⁷Ni Decay Scheme



GAMMA-RAY ENERGIES AND INTENSITIES

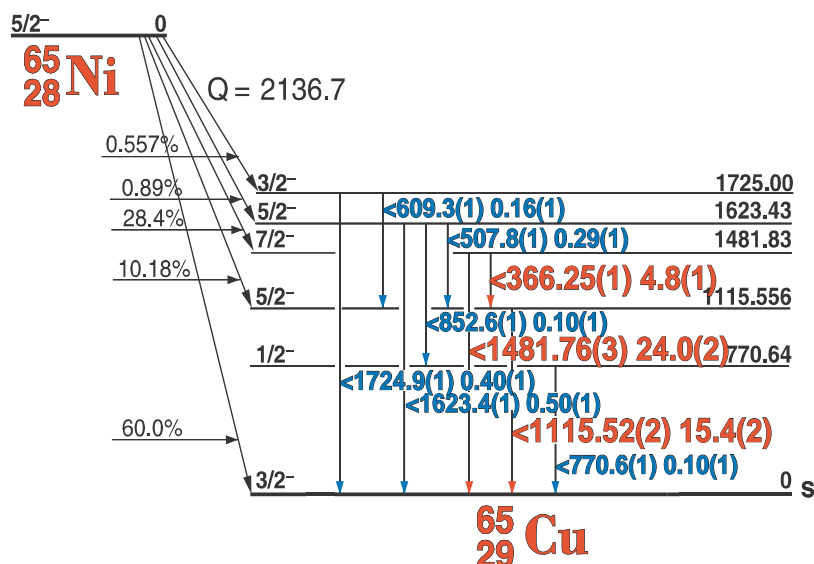
Nuclide	⁵⁷ Ni	Half Life	35.60(6) hr
Detector	3" X 3" NaI	Method of Production:	Ni ⁵⁸ (γ,n)
E _γ (KeV)[S]	ΔE _γ	I _γ (rel)	I _γ (%)[E]
127.192	± 0.025	16.6	14.7
511.006		10	
1377.59	± 0.04	100	81.7
1757.48	± 0.08	9.1	5.75
1919.43	± 0.08	18.9	12.3
numerous weak gammas (less than 0.01)			
		ΔI _γ	S



2.5173 Hr. ^{65}Ni

^{65}Ni Decay Scheme

28-65-2

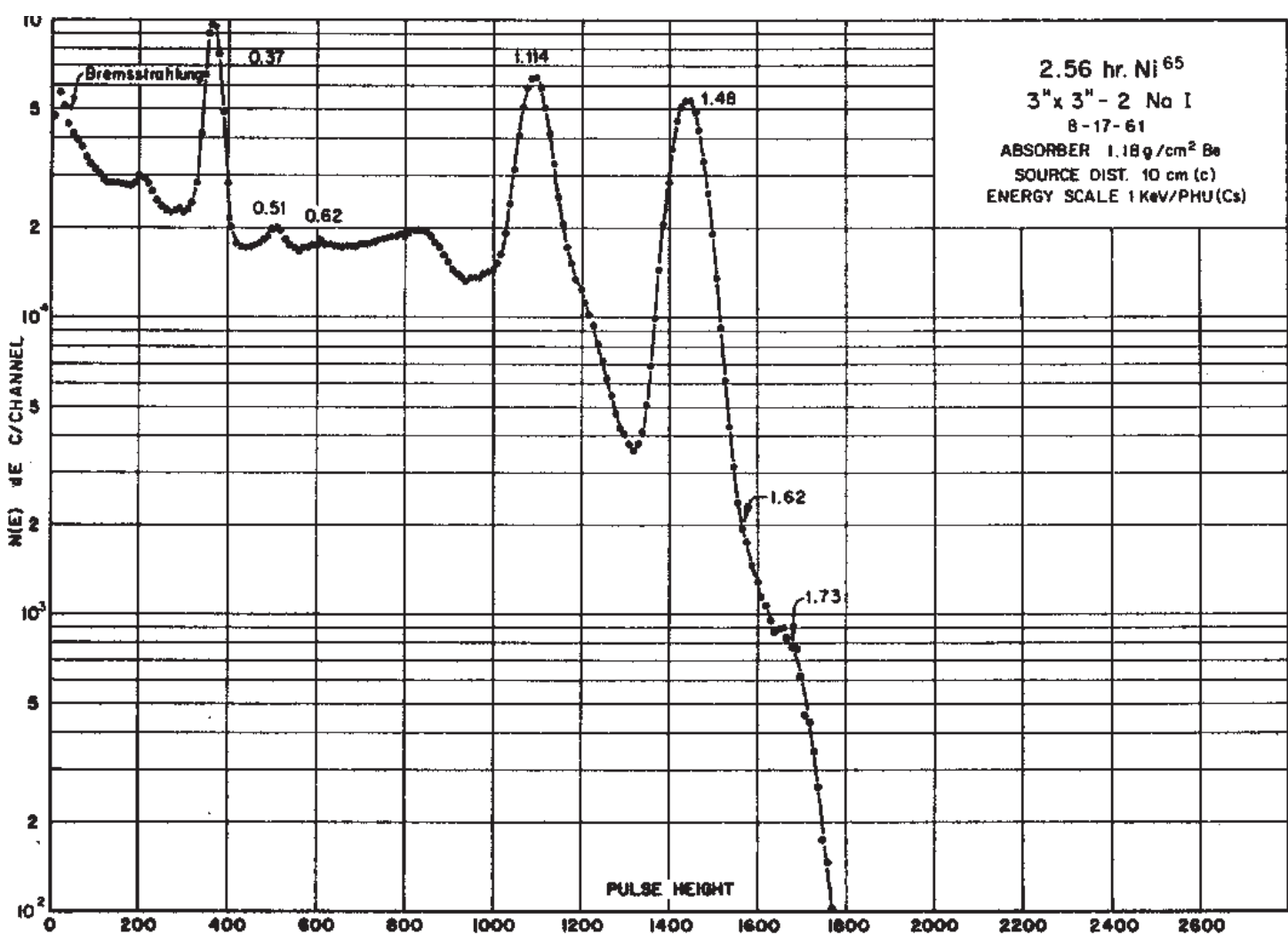


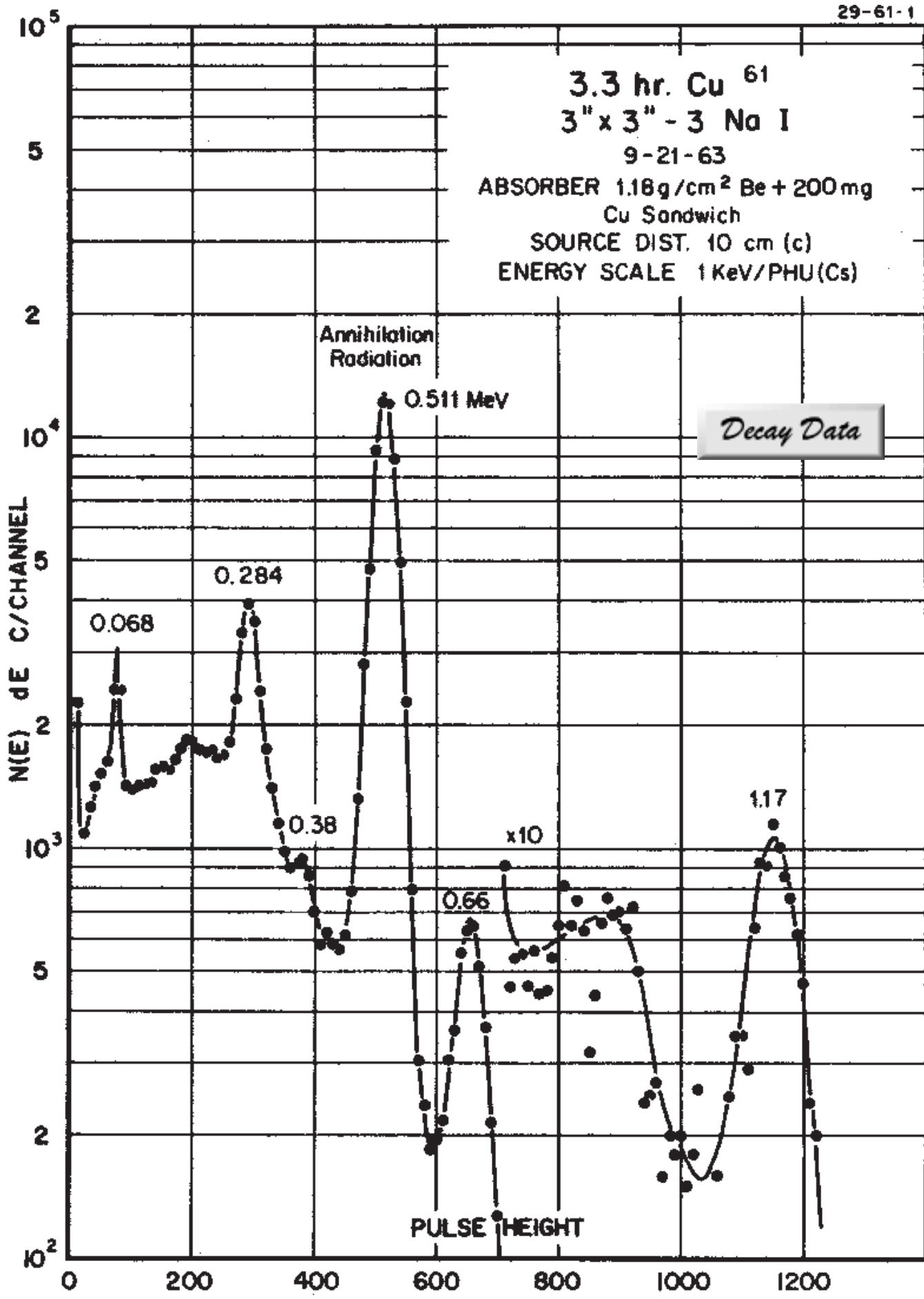
GAMMA-RAY ENERGIES AND INTENSITIES

Nuclide ^{65}Ni
Detector 3" X 3" NaI-2

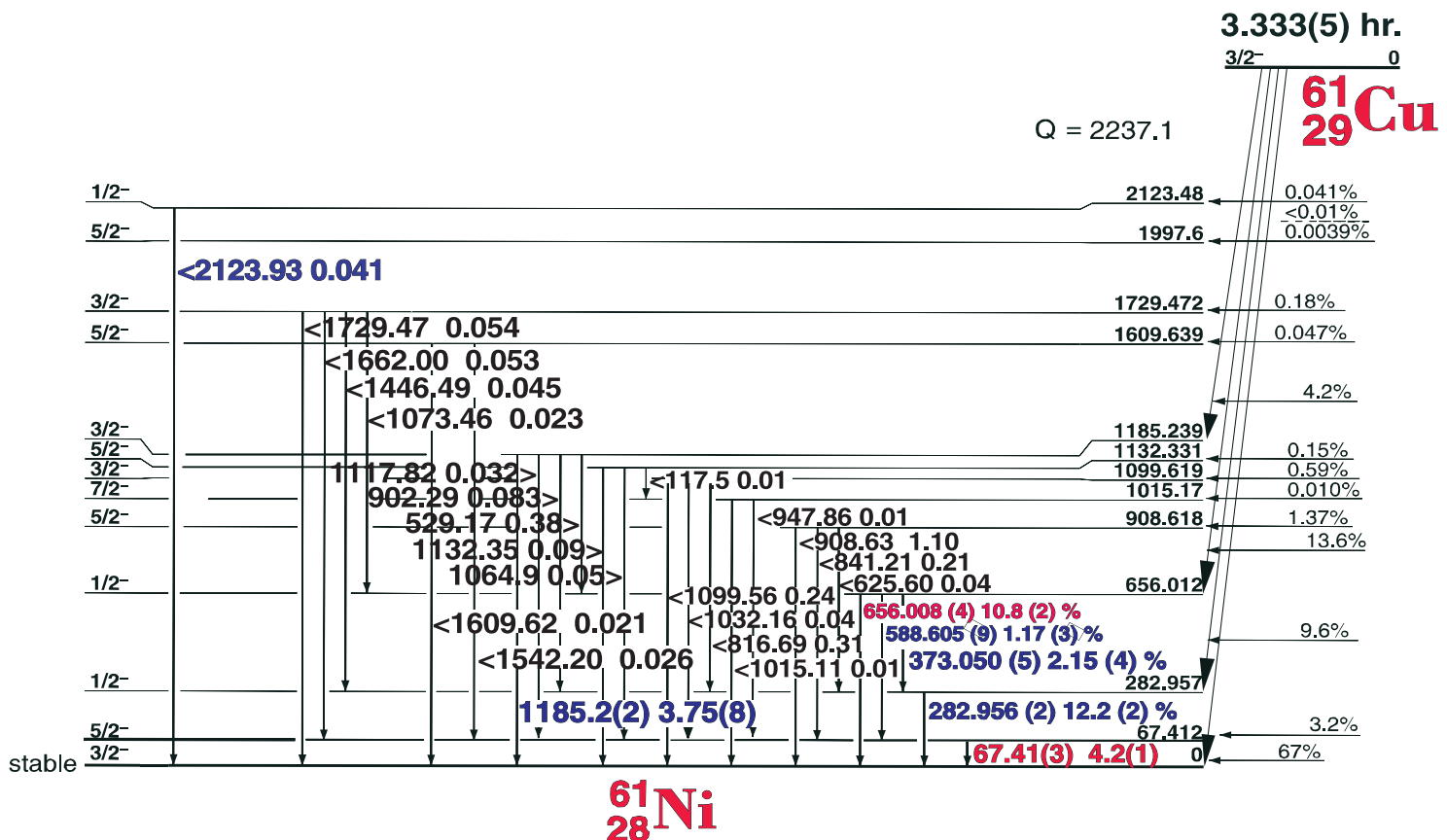
Half Life 2.5173(2) hr.
Method of Production: $\text{Ni}^{64}(n,\gamma)$

E_γ (KeV)[S]	ΔE_γ	I_γ (rel)	$I_\gamma(\%)$ [E]	ΔI_γ	S
366.27	± 0.1	0.02	4.81	± 0.1	1
507.8	± 0.1	1.2	0.293	± 0.02	3
609.3	± 0.1	0.68	0.155	± 0.02	4
770.6	± 0.2	0.52	0.10	± 0.02	4
852.6	± 0.2	0.38	0.1	± 0.02	4
1115.518	± 0.025	65	15.4	± 0.4	1
1481.765	± 0.028	100	23.6	± 0.8	1
1623.4	± 0.1	2.1	0.50	± 0.2	1
1724.9	± 0.1	1.6	0.40	± 0.2	1





3.333(5) hr. ^{61}Cu Decay Scheme



GAMMA-RAY ENERGIES AND INTENSITIES

Nuclide
Detector

^{61}Cu
3" x 3" - 2Nal

Half Life 3.333(5) hr.
Method of Production: Cu⁶³(γ ,2n)

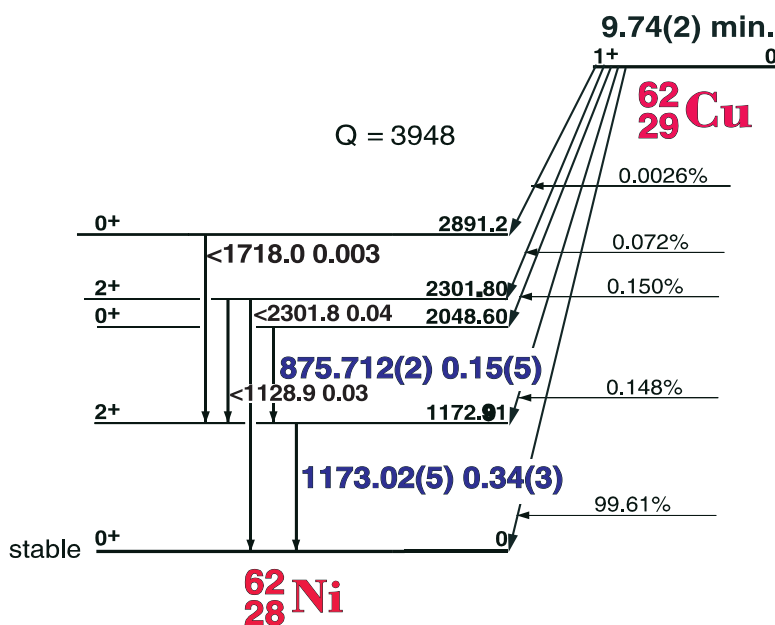
E_{γ} (keV)[S]	ΔE_{γ}	I_{γ} (rel)	$I_{\gamma}(\%)$ [E]	ΔI_{γ}	S
23.2	± 0.4				
44.8	± 0.5				
55.4	± 0.5				
67.412	± 0.003	6.2	4.2	± 0.1	2
282.956	± 0.002	9.2	12.2	± 0.2	1
373.050	± 0.005	2.35	2.15	± 0.4	3
405.2	± 0.2				4
511.006		100			1
529.169	± 0.022		0.376	± 0.01	4
588.605	± 0.009		1.17	± 0.03	4
656.008	± 0.004	7.0	10.8	± 0.2	1
1185.234	± 0.015	3.12	3.75	± 0.1	2

Ann.

9.74(2) min. ^{62}Cu

^{62}Cu Decay Scheme

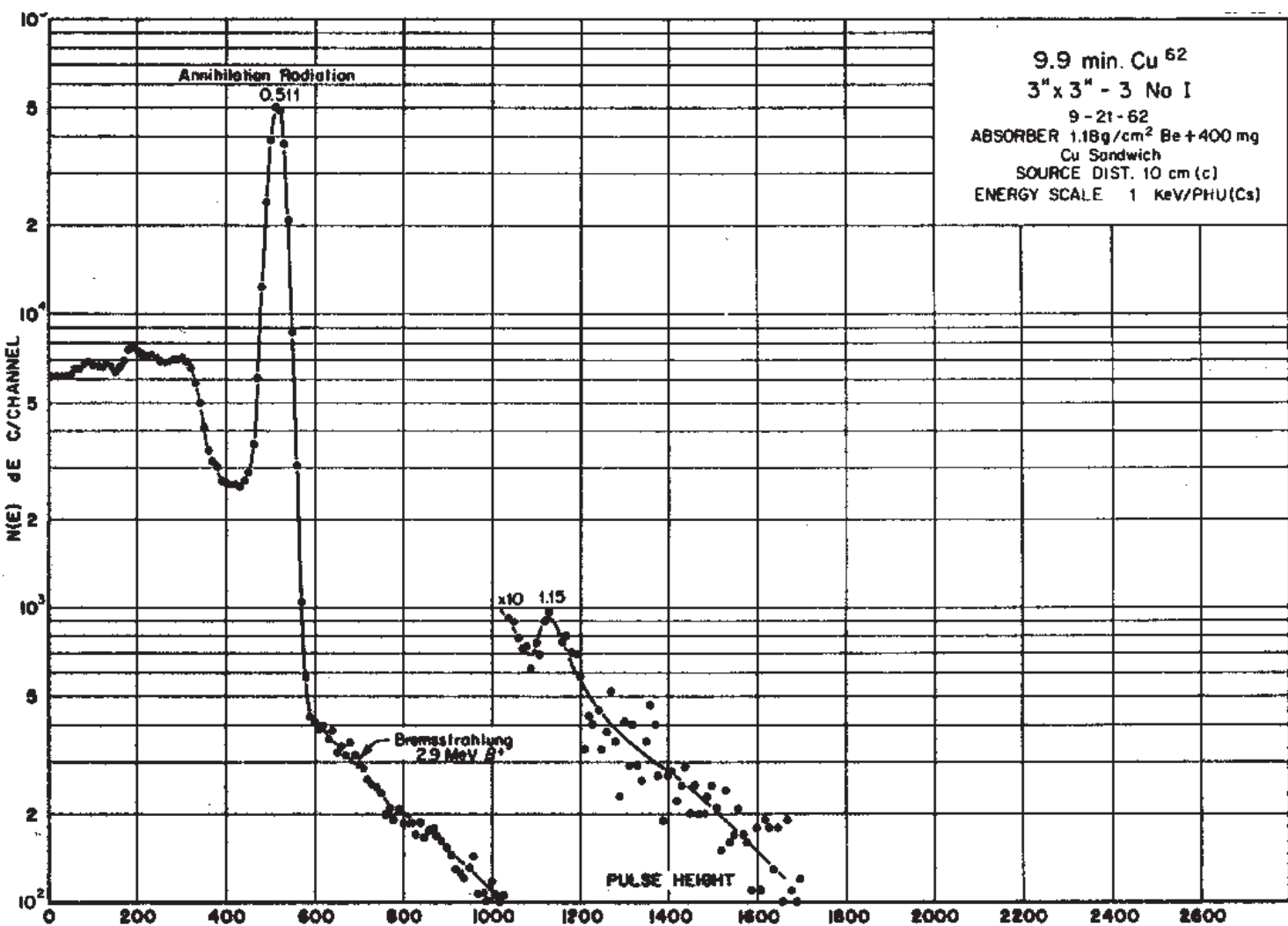
29-62-1

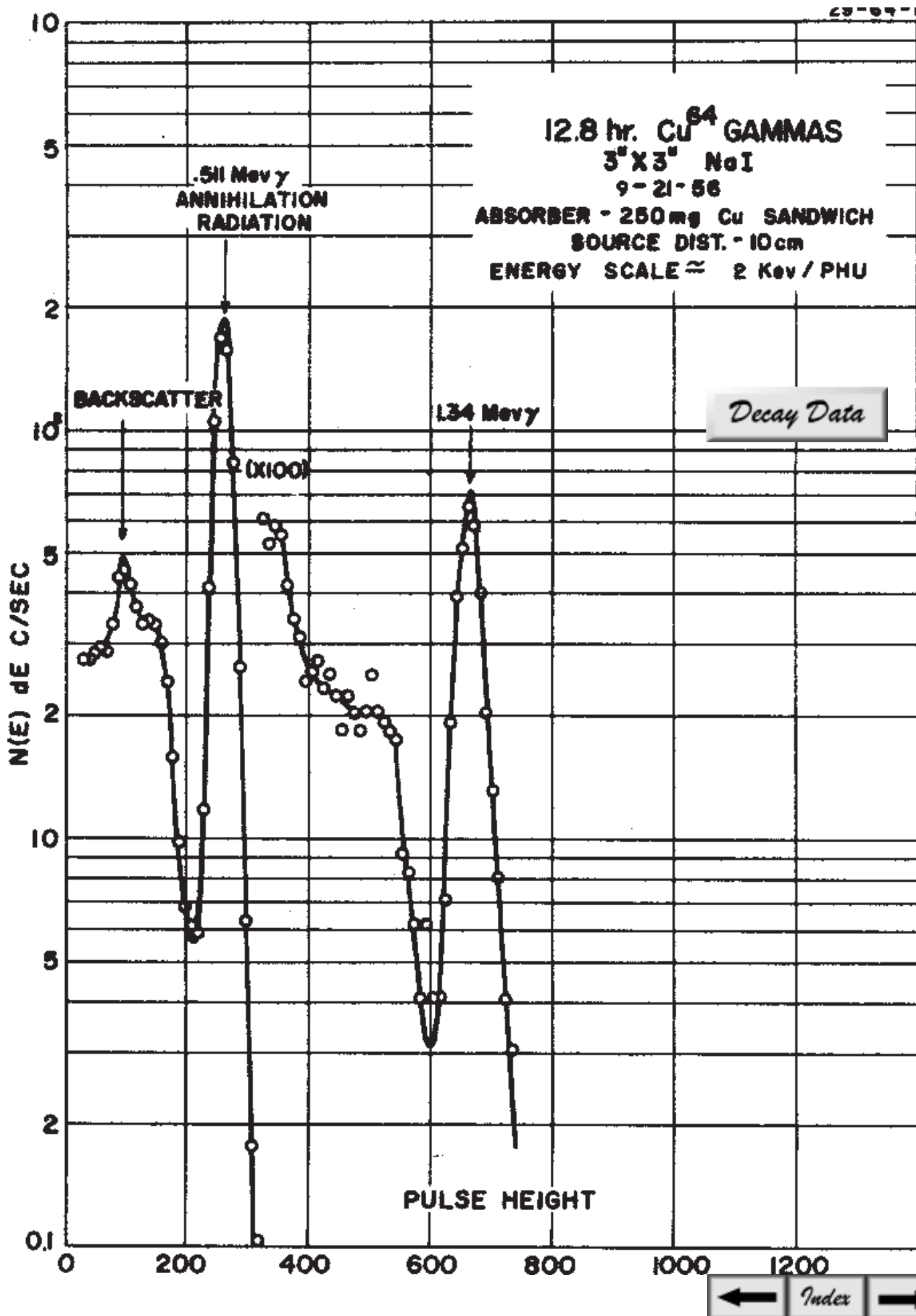


GAMMA-RAY ENERGIES AND INTENSITIES

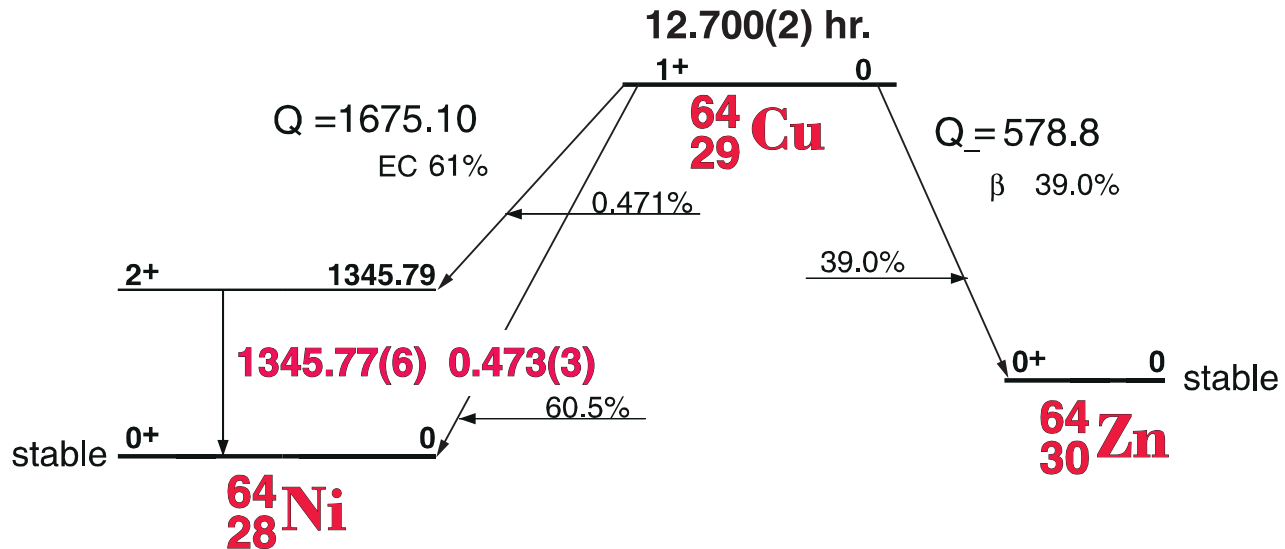
Nuclide ^{62}Cu Half Life 974(2) min
Detector 3" X 3" NaI-2 Method of Production: Cu⁶³(γ ,n)

E_{γ} (KeV)[S]	ΔE_{γ}	$I_{\gamma}(\text{rel})$	$I_{\gamma}(\%) [E]$	ΔI_{γ}	S
511.006	ann. rad.	100			1
875.71	± 0.2	weak	0.15	± 0.05	5
1173.02	± 0.1	weak	0.34	± 0.1	5





12.700(2) hr. ^{64}Cu Decay Scheme



GAMMA-RAY ENERGIES AND INTENSITIES

Nuclide
Detector

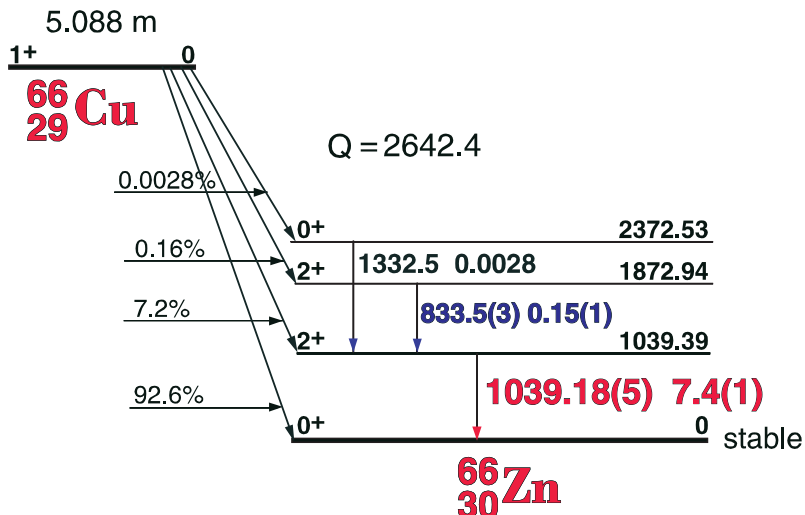
^{64}Cu
 $3'' \times 3'' - 2\text{NaI}$

Half Life 12.8 Hr.
Method of Production: $\text{Cu}^{63}(\text{n},\gamma)$

E_γ (KeV)[S]	ΔE_γ	I_γ (rel)	I_γ (%)[E]	ΔI_γ	S
ann. rad. 511.006		100			
1345.77	± 0.06	1.05	0.473	± 0.3	1

5.09(1) min. ^{66}Cu

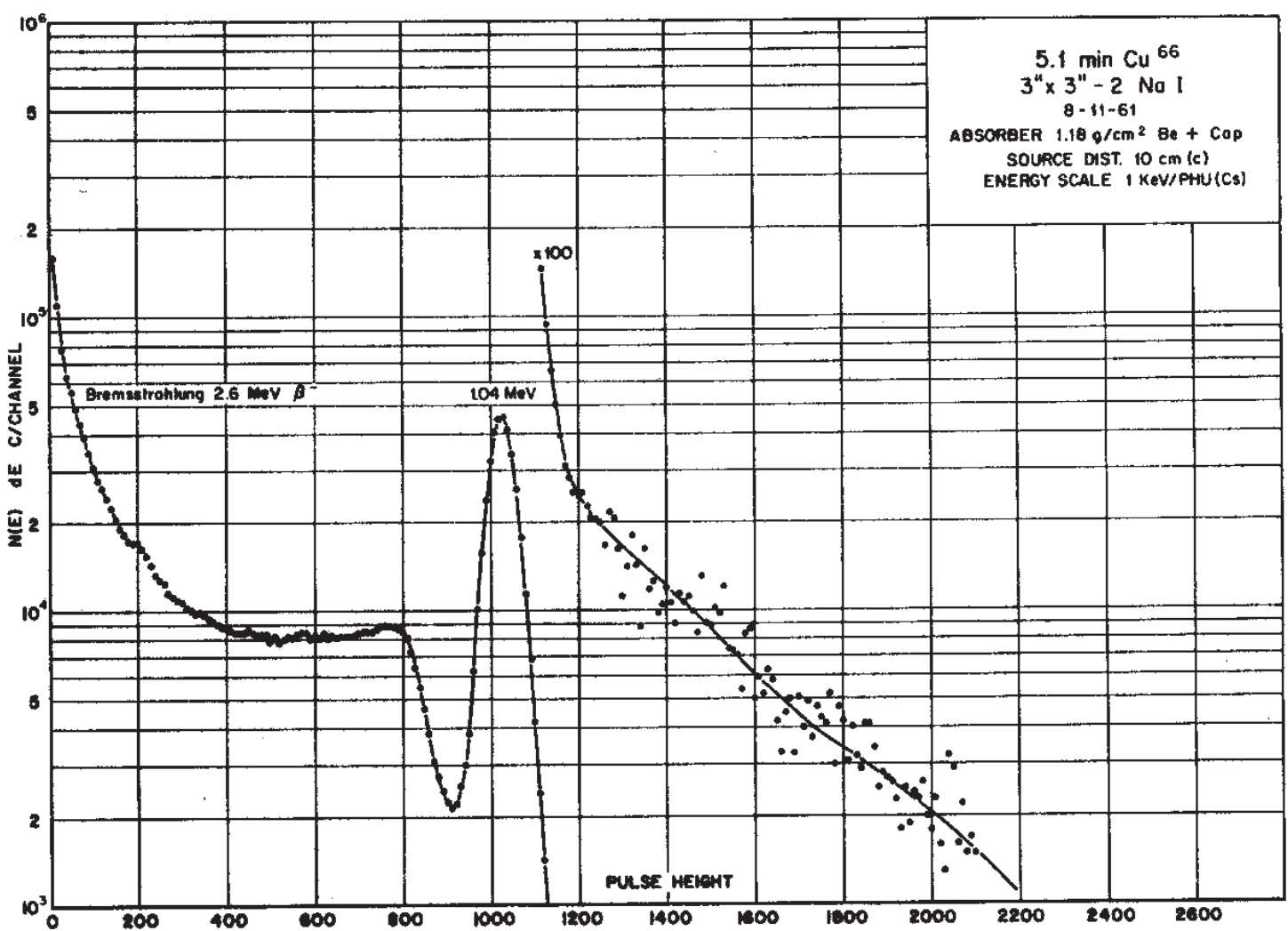
^{66}Cu Decay Scheme

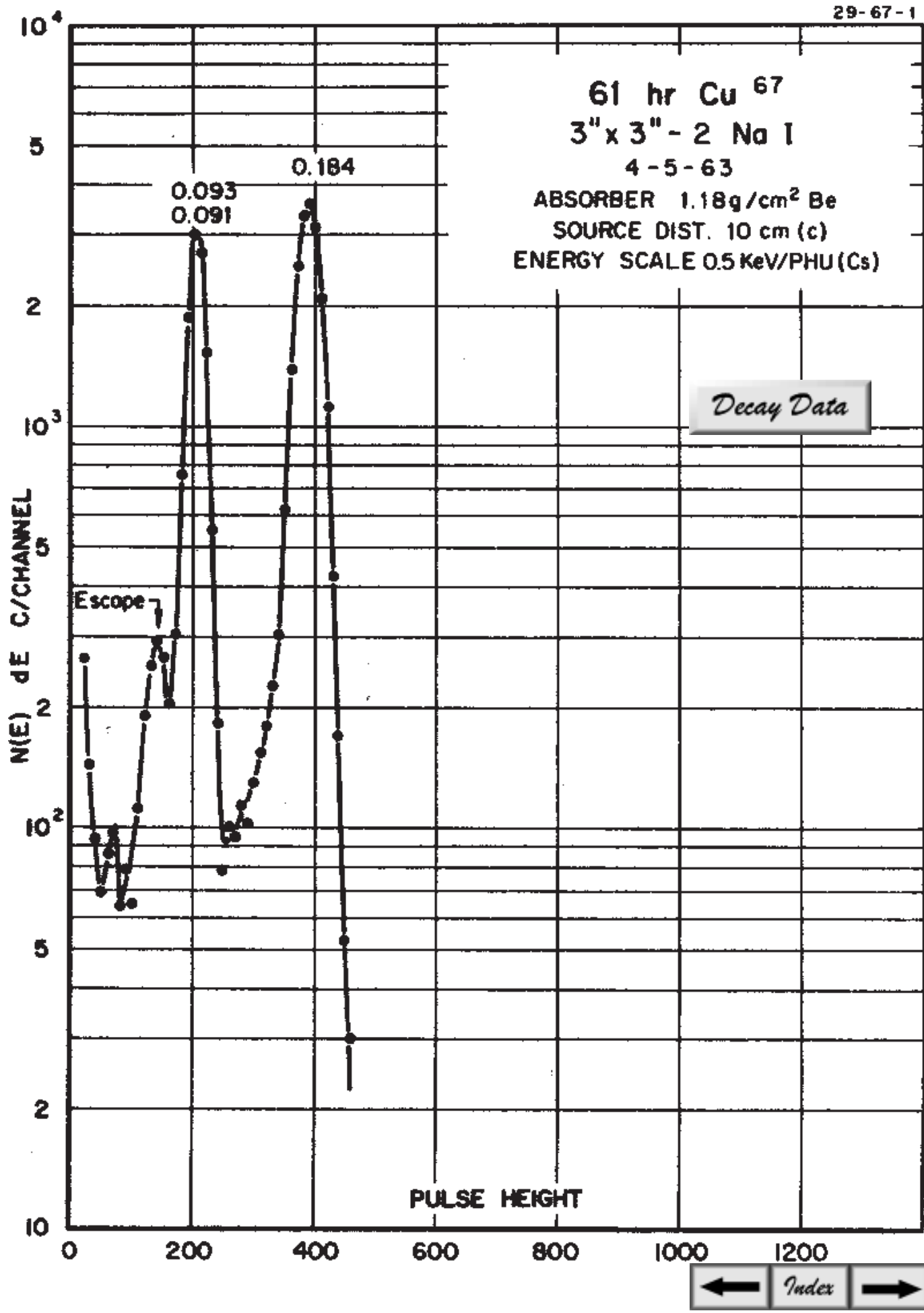


GAMMA-RAY ENERGIES AND INTENSITIES

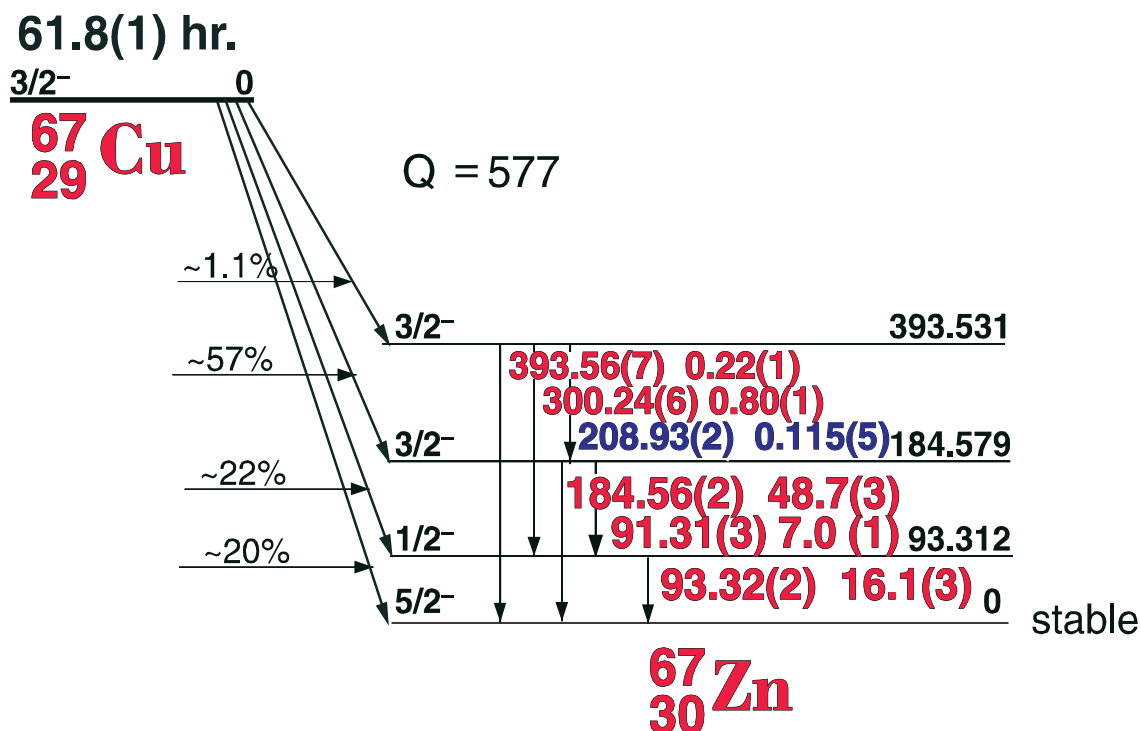
Nuclide ^{66}Cu Half Life 5.09(1) min.
Detector 3" X 3" NaI Method of Production: Cu⁶⁵(n,γ)

E_{γ} (KeV)[S]	ΔE_{γ}	$I_{\gamma}(\text{rel})$	$I_{\gamma}(\%)[E]$	ΔI_{γ}	S
511.006	ann. rad.				
833.5	± 0.3	3.8	0.15	± 0.1	4
1039.18	± 0.05	100	7.14	± 0.01	1
1332.5	± 0.1		0.003		4





61.8(1) hr. ^{67}Cu Decay Scheme

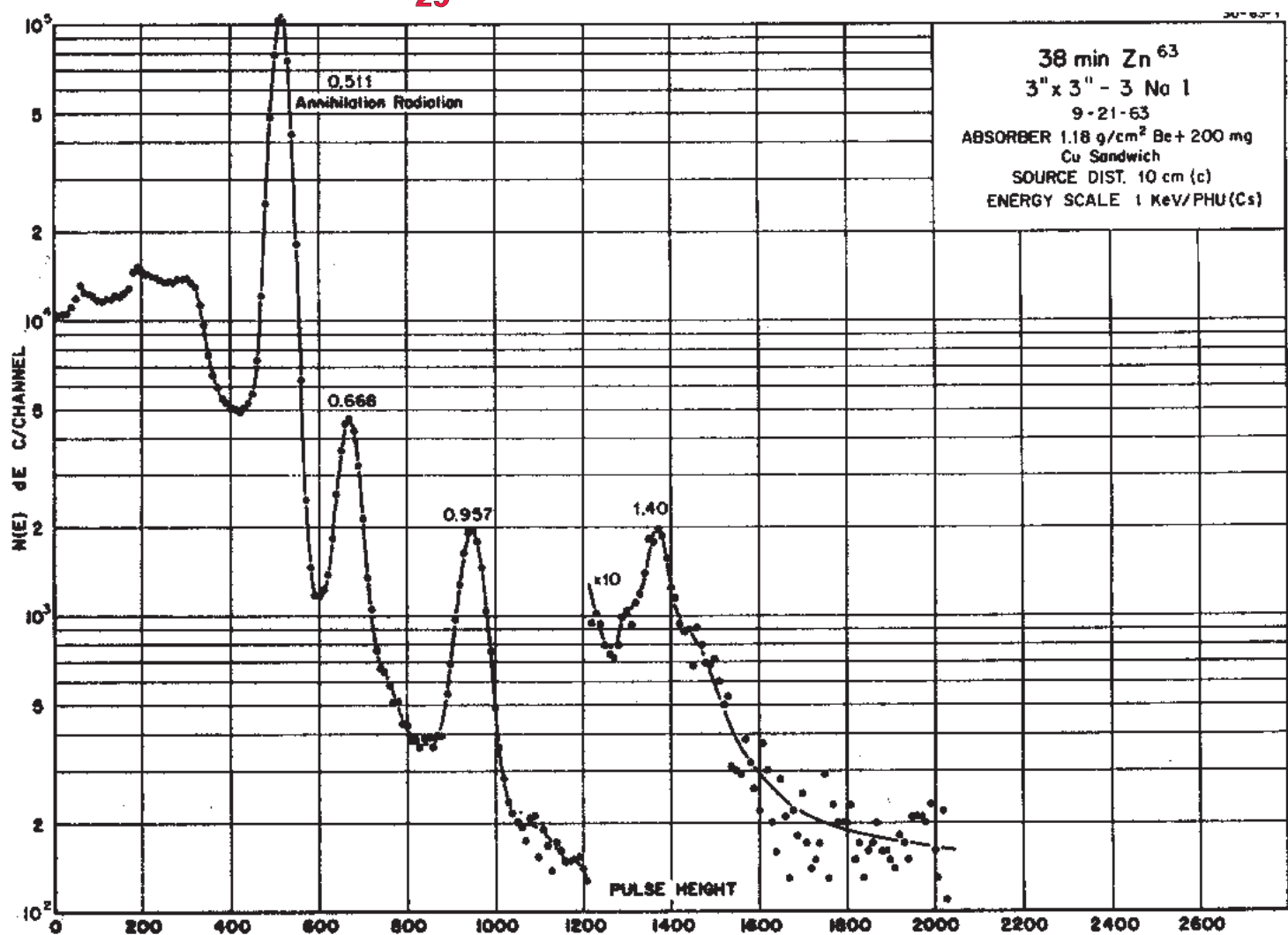
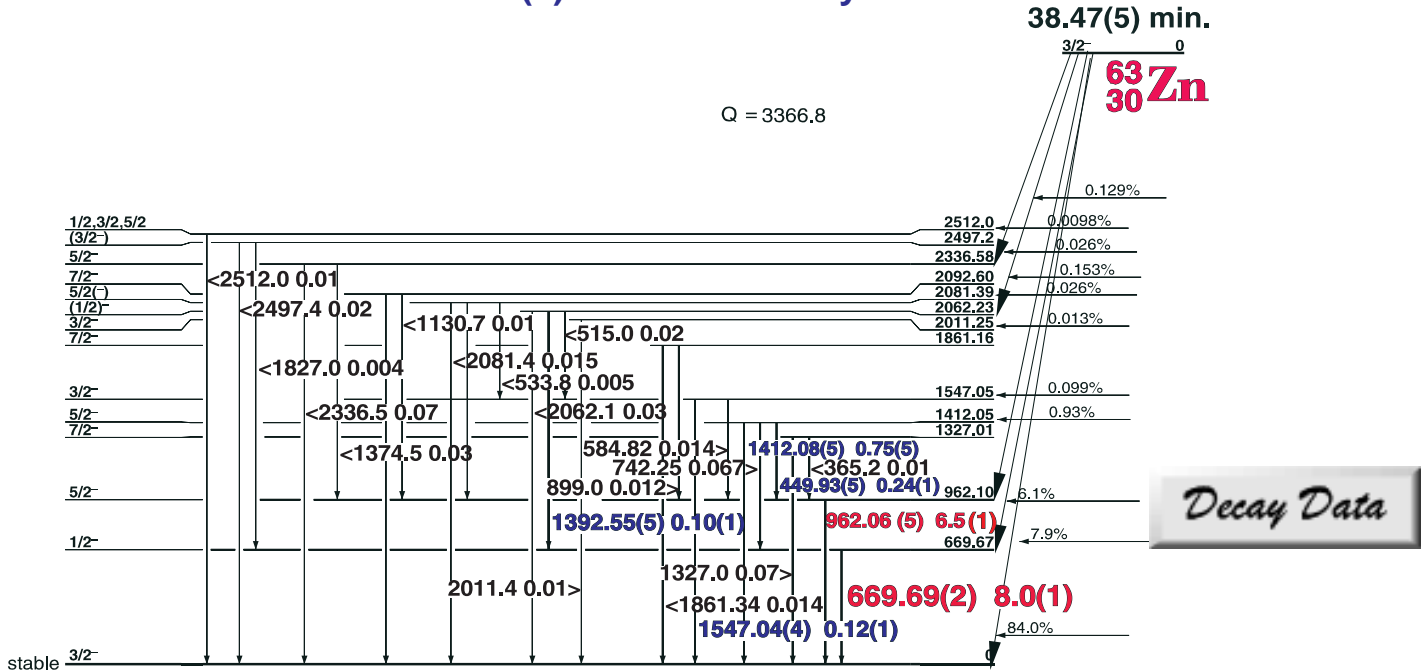


GAMMA-RAY ENERGIES AND INTENSITIES

Nuclide ^{67}Cu Half Life 61.9(1) hr.
Detector 3" x 3" - 2NaI Method of Production: $\text{Zn}^{68}(\gamma, p)$

E_γ (KeV)[S]	ΔE_γ	I_γ (rel)	$I_\gamma(\%)$ [E]	ΔI_γ	S
91.31	± 0.03	15.5	7.58		1
93.32	± 0.02	34.5	30.2		1
184.56	± 0.02	100	49.6		1
208.93	± 0.02	0.24	0.116		2
300.24	± 0.06	1.64	0.797		1
393.56	± 0.07	0.48	0.220		1

3.8 Min. Zn⁶³ 38.47(5) min. Zn⁶³ Decay Scheme



3.8 Min. ^{63}Zn

30-63-2

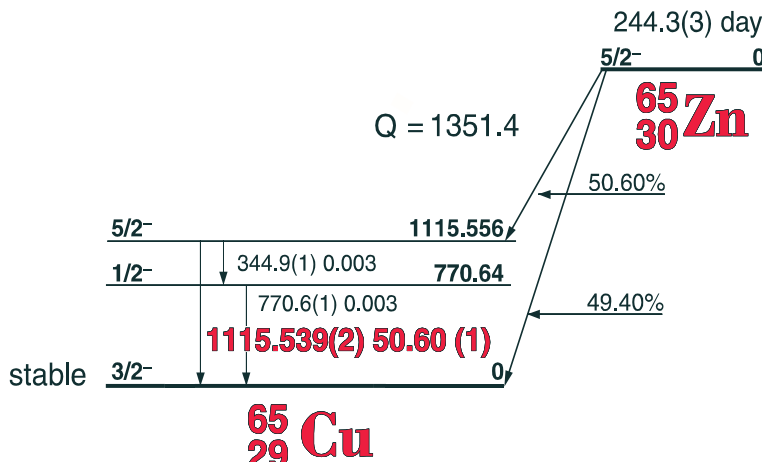
GAMMA-RAY ENERGIES AND INTENSITIES

Nuclide ^{63}Zn Half Life 3.8 Min.
Detector 3" X 3" NaI-2 Method of Production: $\text{Zn}^{64}(\gamma, n)$

Ann. Rad.	E_γ (KeV) [S]	ΔE_γ	I_γ (rel)	I_γ (%) [E]	ΔI_γ	S
	449.93	± 0.05		0.236	± 0.02	4
	511.006					2
	669.69	± 0.025	100	8.0	± 0.1	1
	962.06	± 0.05	75.0	6.5	± 0.1	1
	1392.55	± 0.05		0.097	± 0.01	4
	1412.08	± 0.05	10.0	0.75	± 0.05	2
	1547.04	± 0.04		0.122	± 0.01	4

244.3(3) Day ^{65}Zn [C]

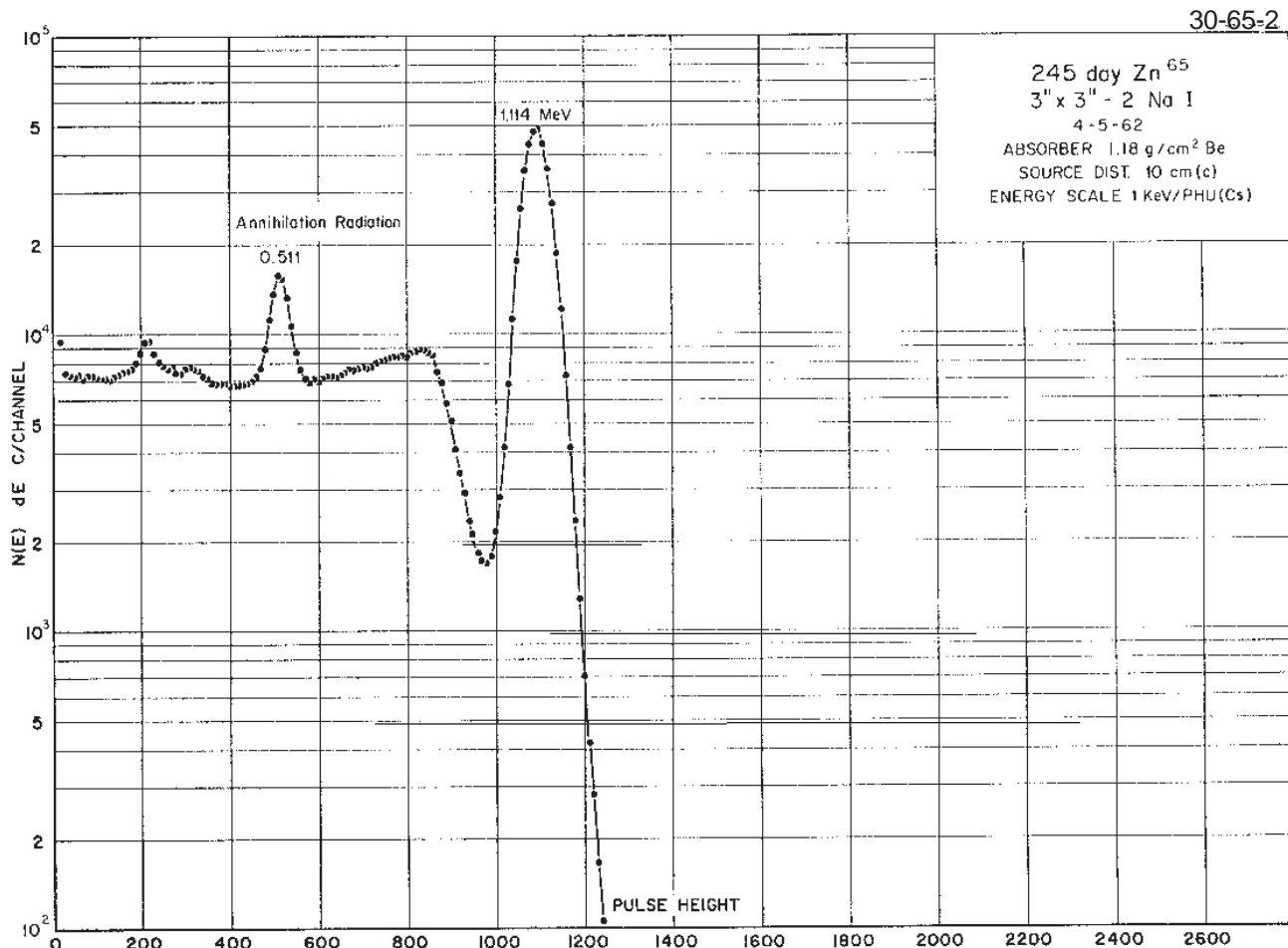
^{65}Zn Decay Scheme



GAMMA-RAY ENERGIES AND INTENSITIES

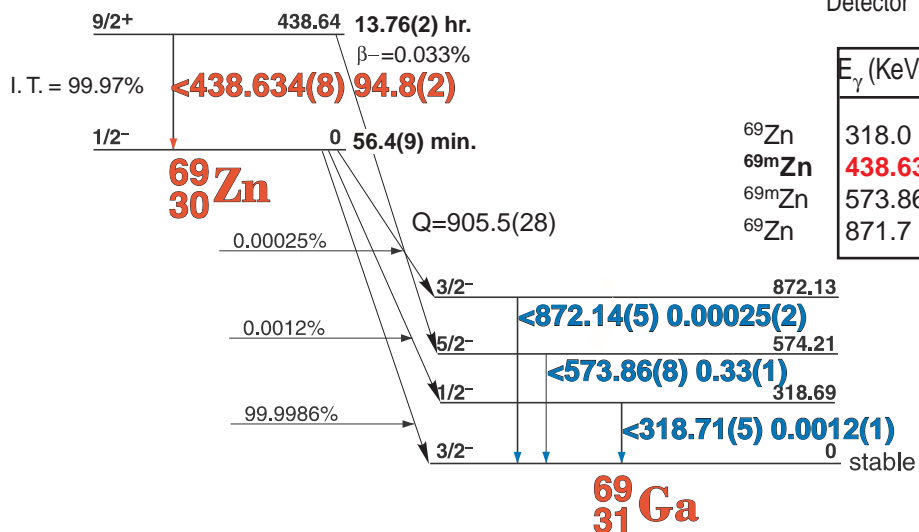
Nuclide ^{65}Zn Half Life 244.3(3) day
Detector 3" X 3" NaI-2 Method of Production: $\text{Zn}^{64}(n,\gamma)$

E_γ (KeV)[S]	ΔE_γ	I_γ (rel)	$I_\gamma(\%)$ [E]	ΔI_γ	S
344.95	± 0.1		0.033		4
511.006		10	170	± 1.0	2
770.6	± 0.1		0.033		4
1115.539 ± 0.002		100	50.60	± 0.01	1



13.76 hr ^{69m}Zn - 56.4 min. ^{69}Zn

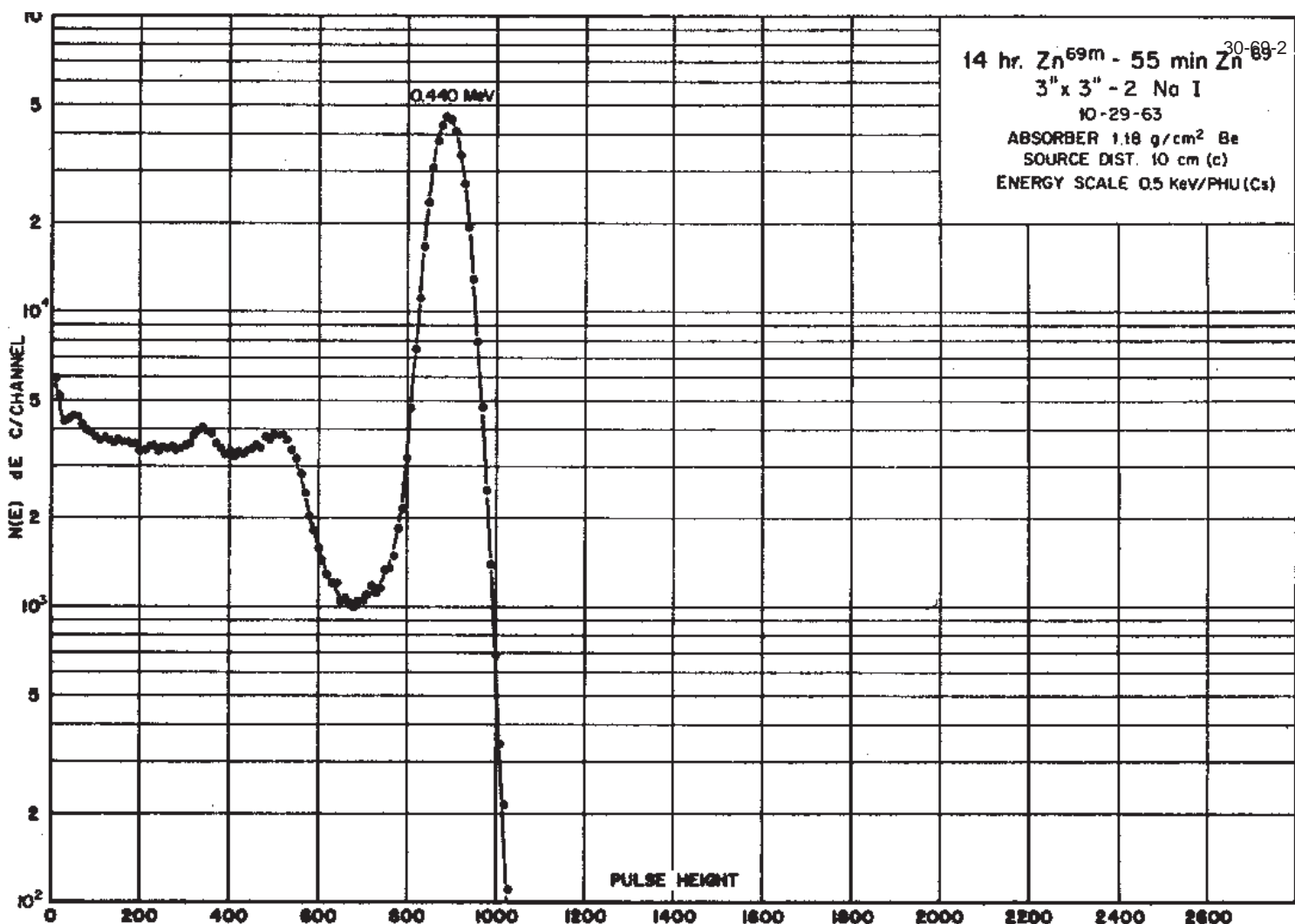
^{69m}Zn - ^{69}Zn Decay Scheme

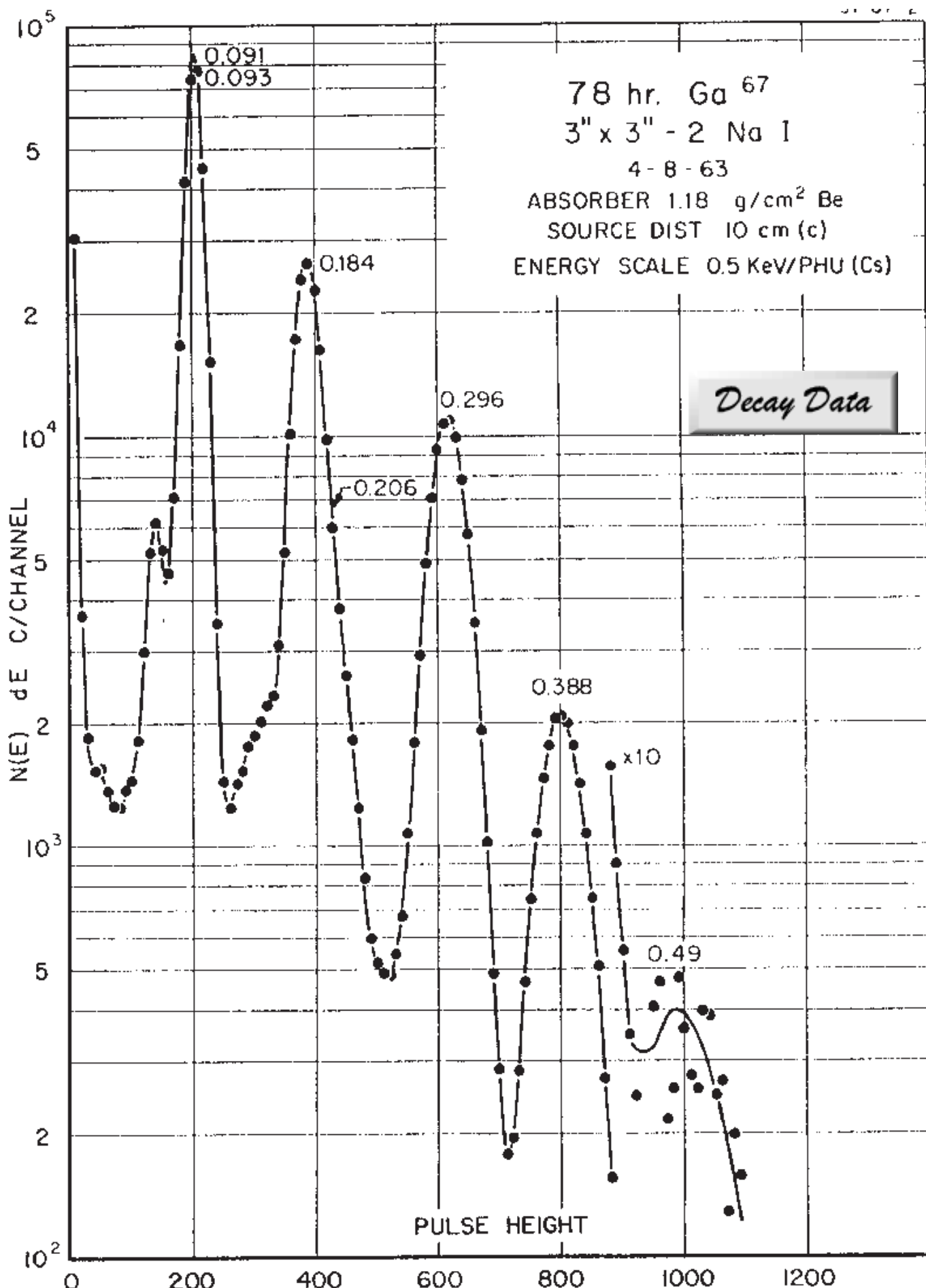


GAMMA-RAY ENERGIES AND INTENSITIES

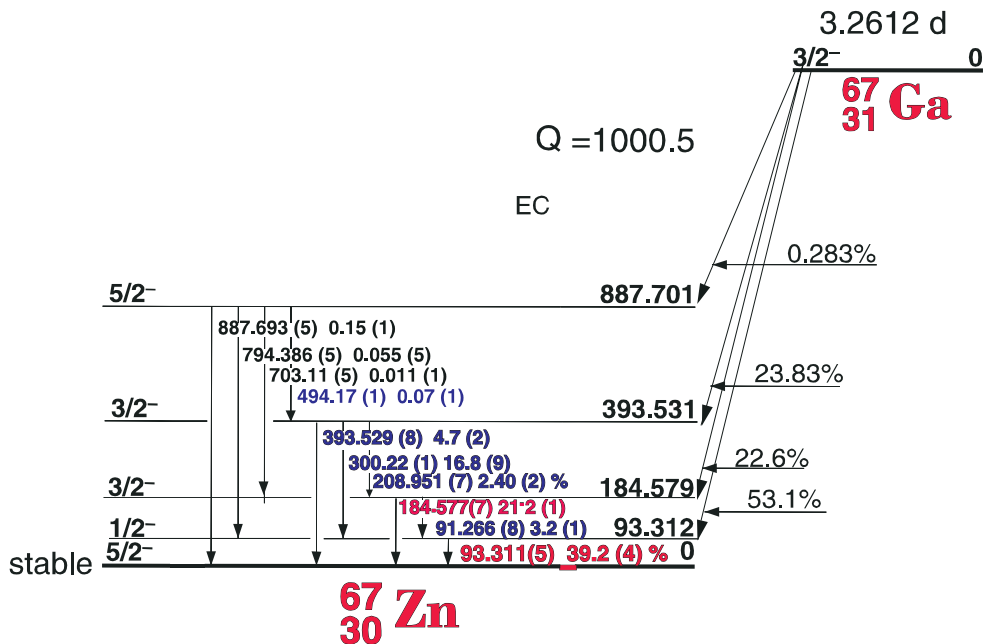
Nuclide $^{69m}\text{Zn} - ^{69}\text{Zn}$ Half Life 13.76(2) hr. (56.4(9) min.)
Detector 3" X 3" NaI Method of Production: $^{68}\text{Zn}(n,\gamma)$

E_{γ} (KeV)[S]	ΔE_{γ}	$I_{\gamma}(\text{rel})$	$I_{\gamma}(\%)[E]$	ΔI_{γ}	S
^{69}Zn 318.0	± 0.1	0.1	0.0012	\pm	4
^{69m}Zn 438.634	± 0.008	100	94.8	± 2	1
^{69m}Zn 573.86	± 0.08	0.09	0.033	± 0.01	4
^{69}Zn 871.7	± 0.2		0.0003		4





3.2612(6) day ^{67}Ga Decay Scheme



GAMMA-RAY ENERGIES AND INTENSITIES

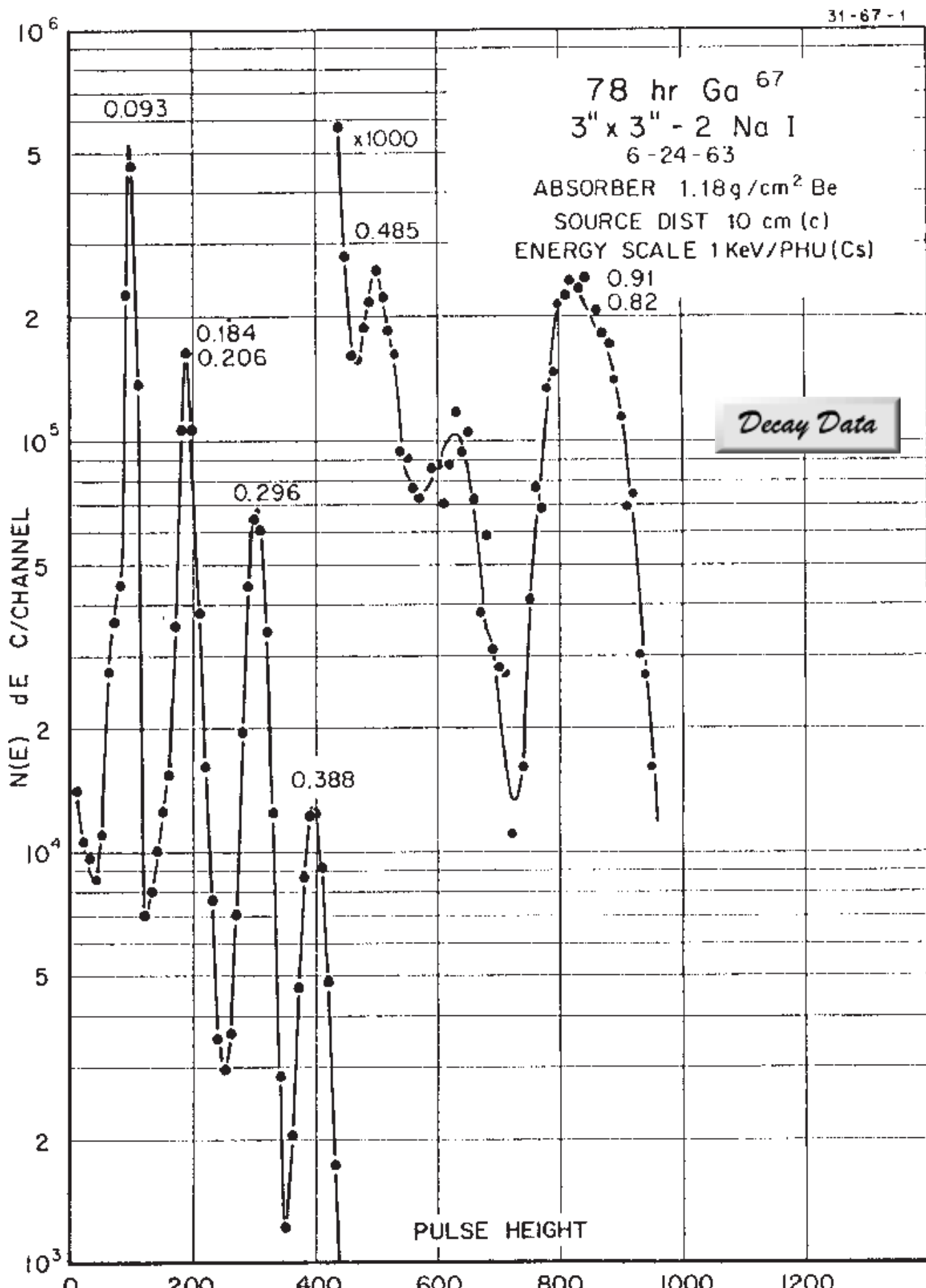
Nuclide
Detector

^{67}Ga
3" x 3" - 2NaI

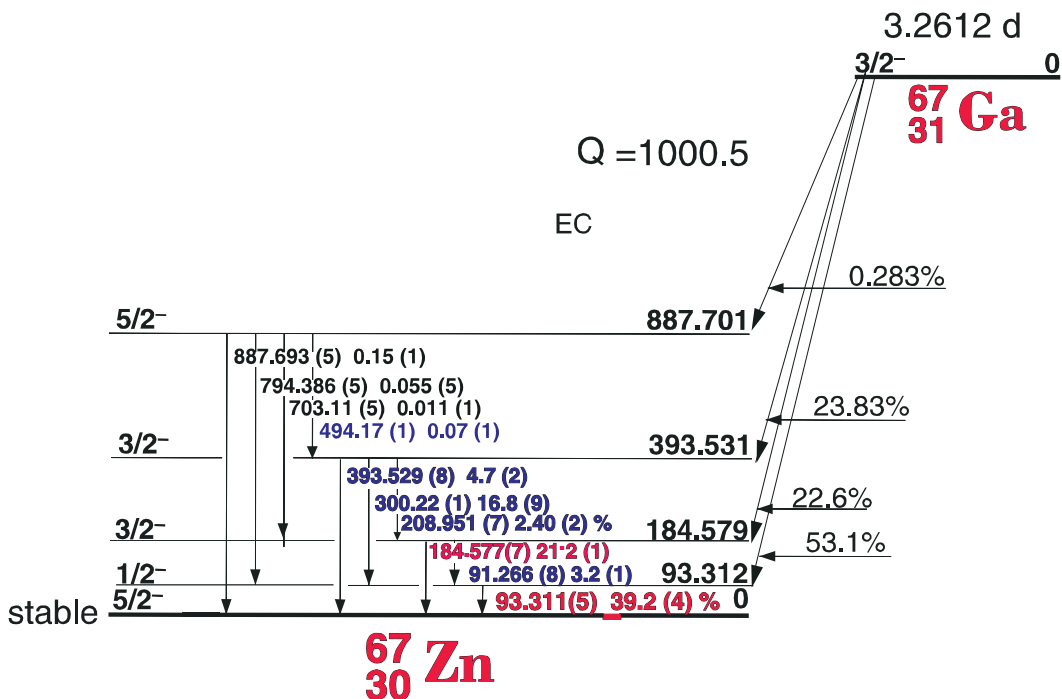
Half Life 3.2612(6) day
Method of Production: $\text{Zn}^{68}(\gamma, p)$

E_γ (KeV)[S]	ΔE_γ	I_γ (rel)	$I_\gamma(\%)$ [E]	ΔI_γ	S
91.266	± 0.008	13.0	3.2	± 0.1	2
93.311	± 0.005	100	39.2	± 0.4	1
184.577	± 0.007	624	21.2	± 0.1	1
208.951	± 0.007	7.1	2.40	± 0.02	1
300.22	± 0.01	50	18.8	± 1.0	1
393.529	± 0.008	14.0	4.7	± 0.2	1
494.17	± 0.01	3.7	0.07	± 0.01	4
511.006					4
794.886	± 0.005	0.15	0.005	± 0.005	5
887.693	± 0.005	0.43	0.15	± 0.01	5

ann.rad



3.2612(6) day ^{67}Ga Decay Scheme



GAMMA-RAY ENERGIES AND INTENSITIES

Nuclide
Detector

^{67}Ga
3" x 3" - 2NaI

Half Life 3.2612(6) day
Method of Production: $\text{Zn}^{68}(\gamma, p)$

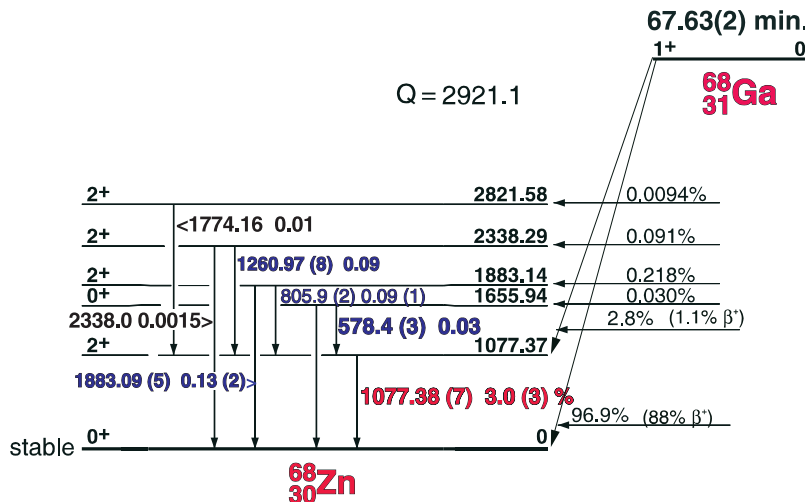
E_γ (KeV)[S]	ΔE_γ	I_γ (rel)	I_γ (%) [E]	ΔI_γ	S
91.266	± 0.008	13.0	3.2	± 0.1	2
93.311	± 0.005	100	39.2	± 0.4	1
184.577	± 0.007	624	21.2	± 0.1	1
208.951	± 0.007	7.1	2.40	± 0.02	1
300.22	± 0.01	50	18.8	± 1.0	1
393.529	± 0.008	14.0	4.7	± 0.2	1
494.17	± 0.01	3.7	0.07	± 0.01	4
511.006					4
794.886	± 0.005	0.15	0.005	± 0.005	5
887.693	± 0.005	0.43	0.15	± 0.01	5

ann.rad.

67.63(2) min. ^{68}Ga

^{68}Ga Decay Scheme

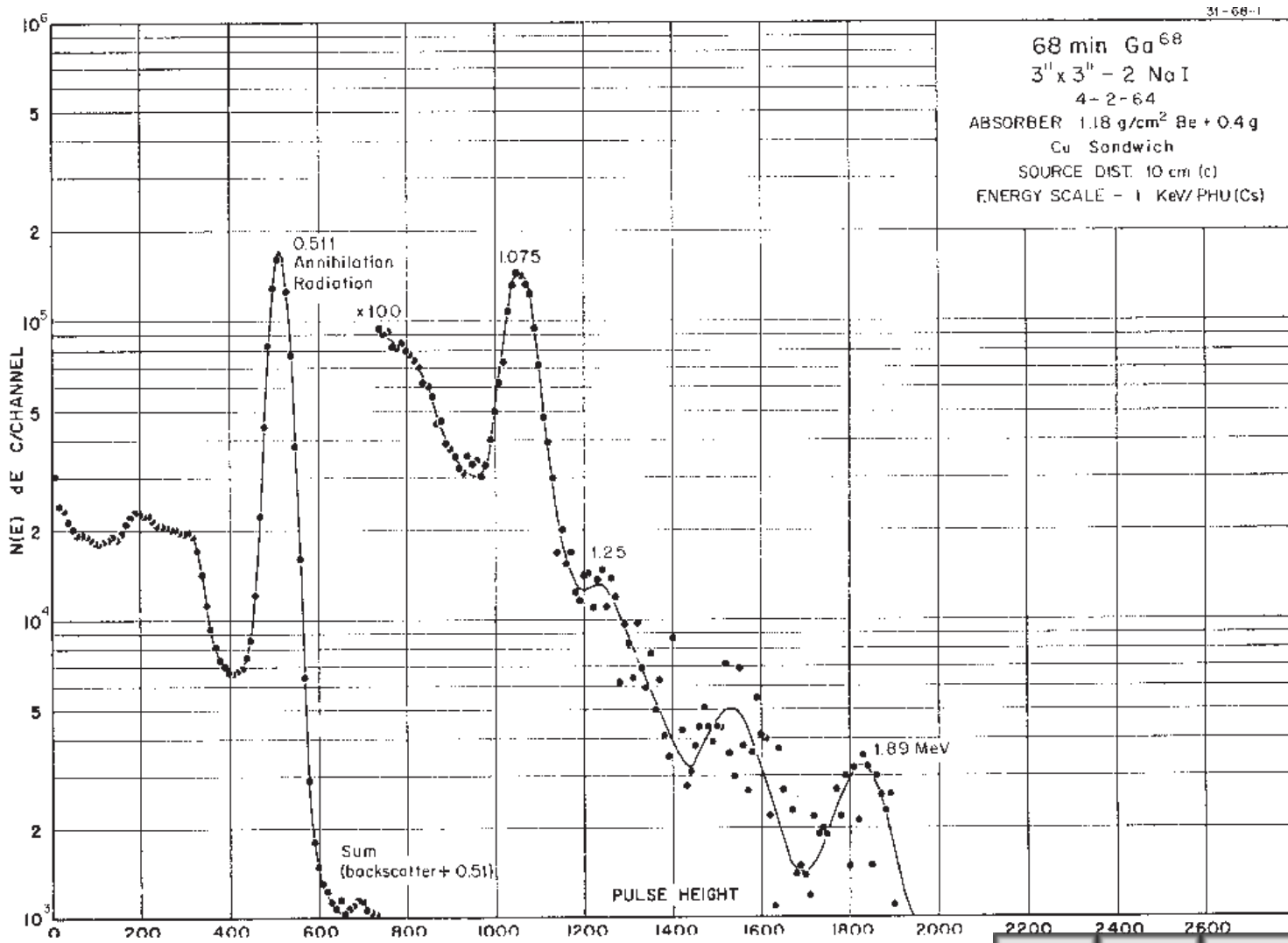
31-68-2



GAMMA-RAY ENERGIES AND INTENSITIES

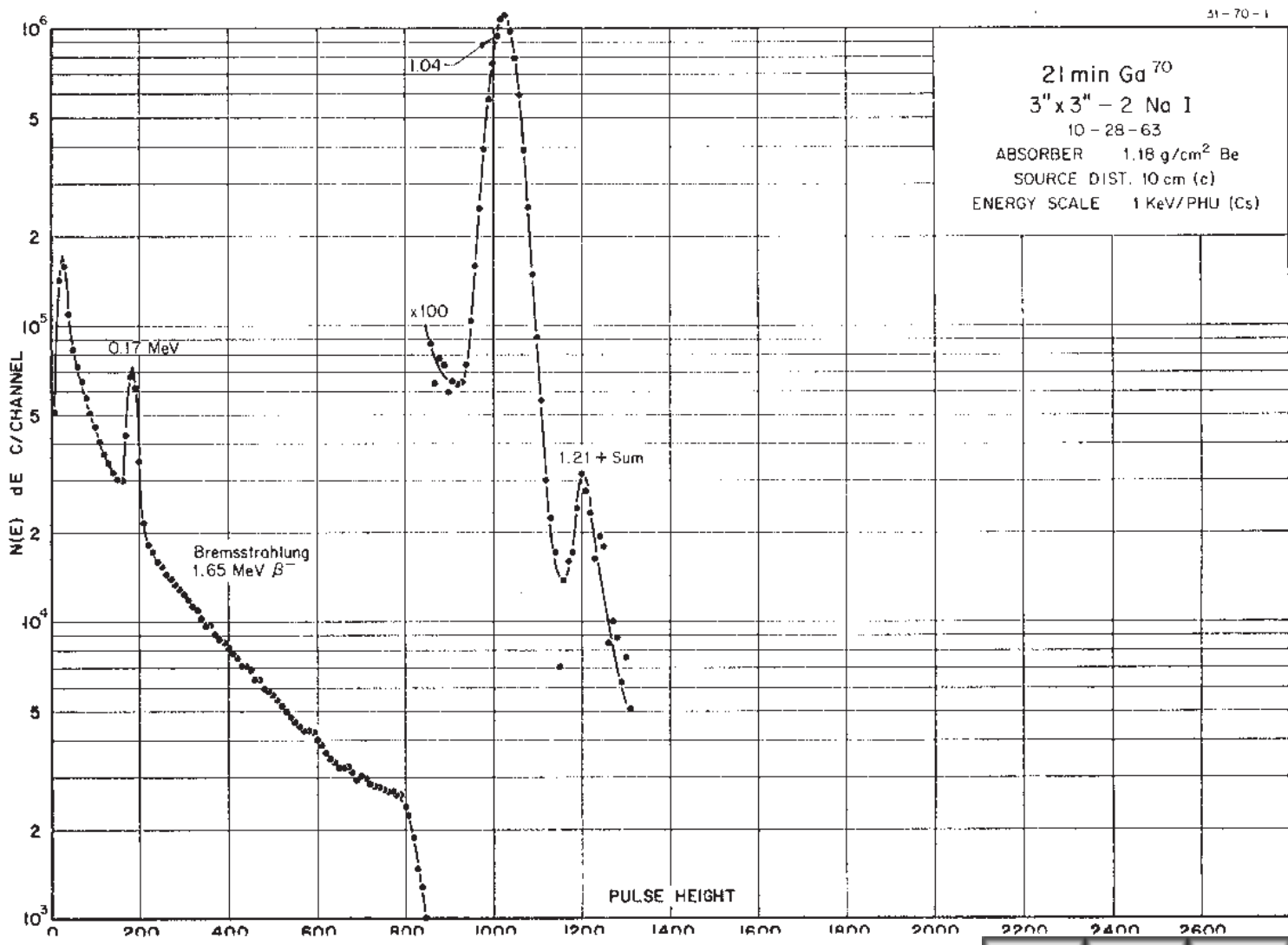
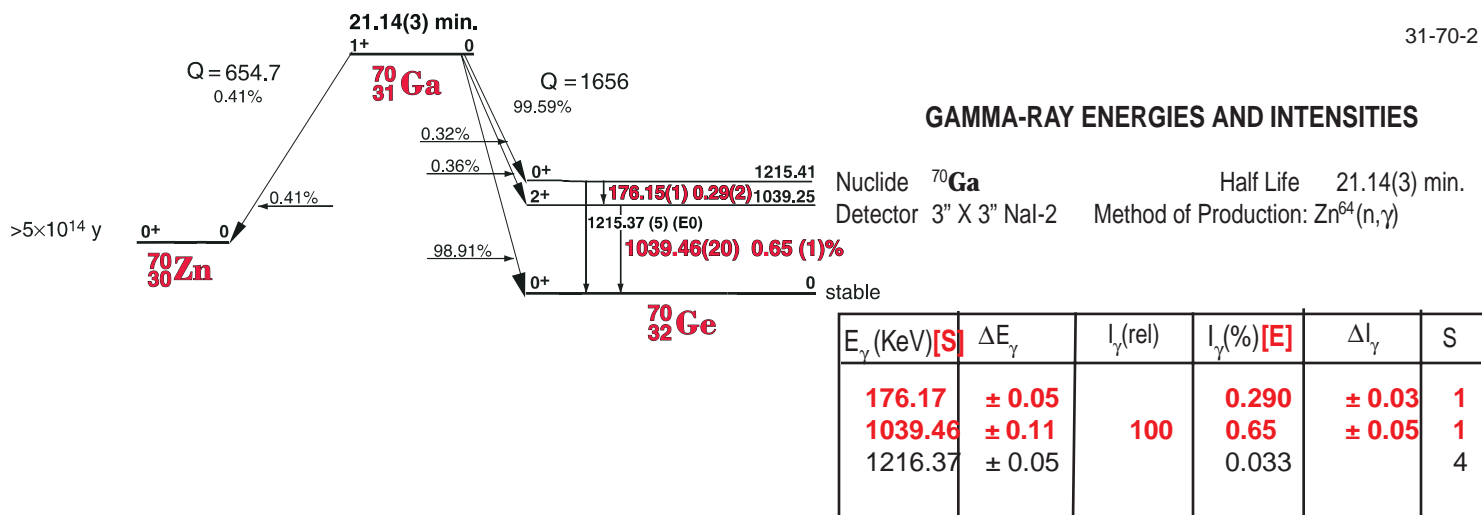
Nuclide ^{68}Ga Half Life 67.63(2) min.
 Detector 3" X 3" NaI-2 Method of Production: $\text{Zn}^{64}(n,\gamma)$

E_γ (KeV)[S]	ΔE_γ	I_γ (rel)	$I_\gamma(\%)$ [E]	ΔI_γ	S
511.006 (ann. rad.)					
578.4	± 0.3		0.03	± 0.005	4
805.9	± 0.2	3.2	0.09	± 0.01	4
1077.38	± 0.07	100	3.0	± 0.3	1
1260.97	± 0.08	2.7	0.09	± 0.009	3
1883.09	± 0.05	4.5	0.13	± 0.01	1

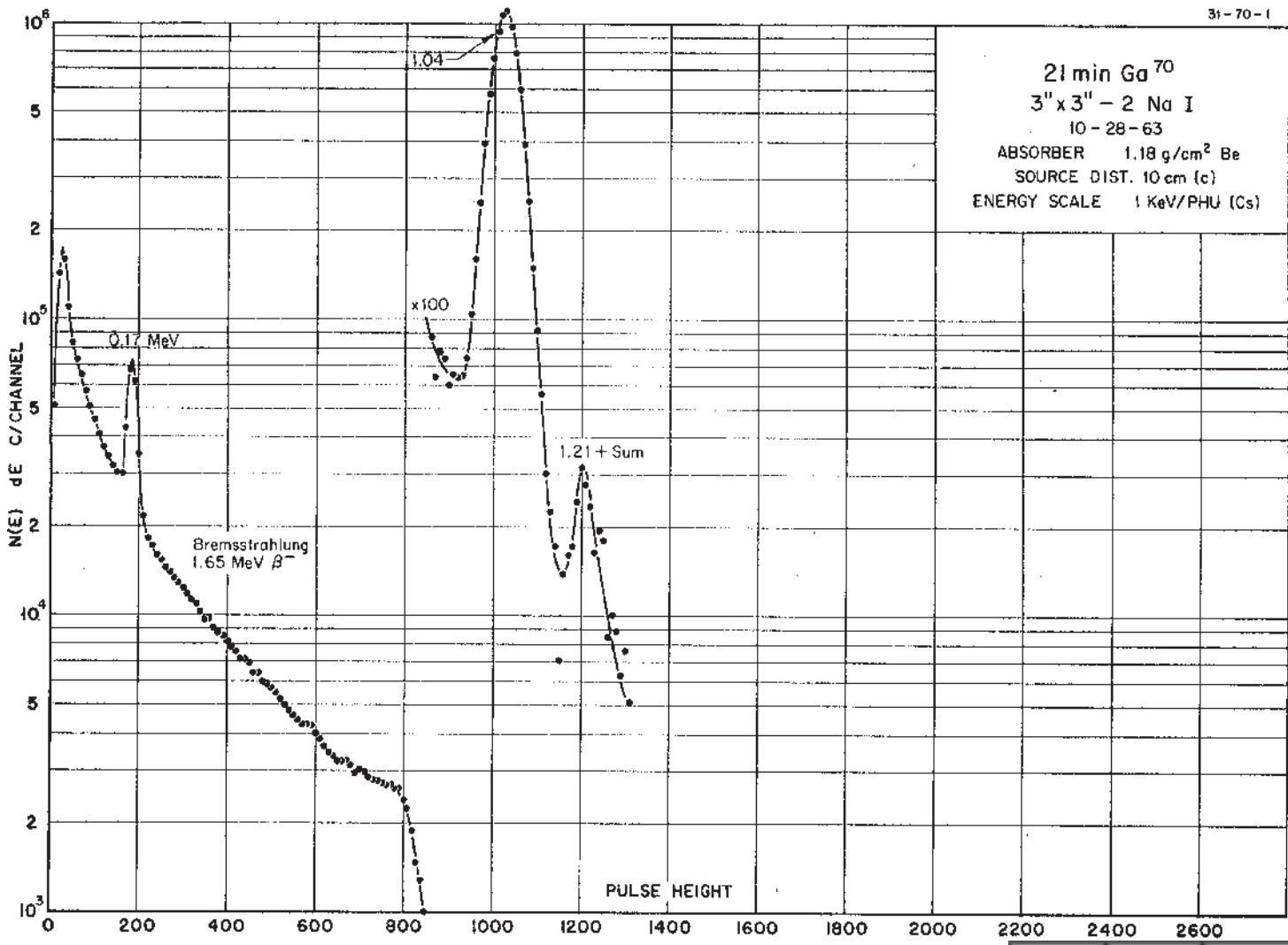
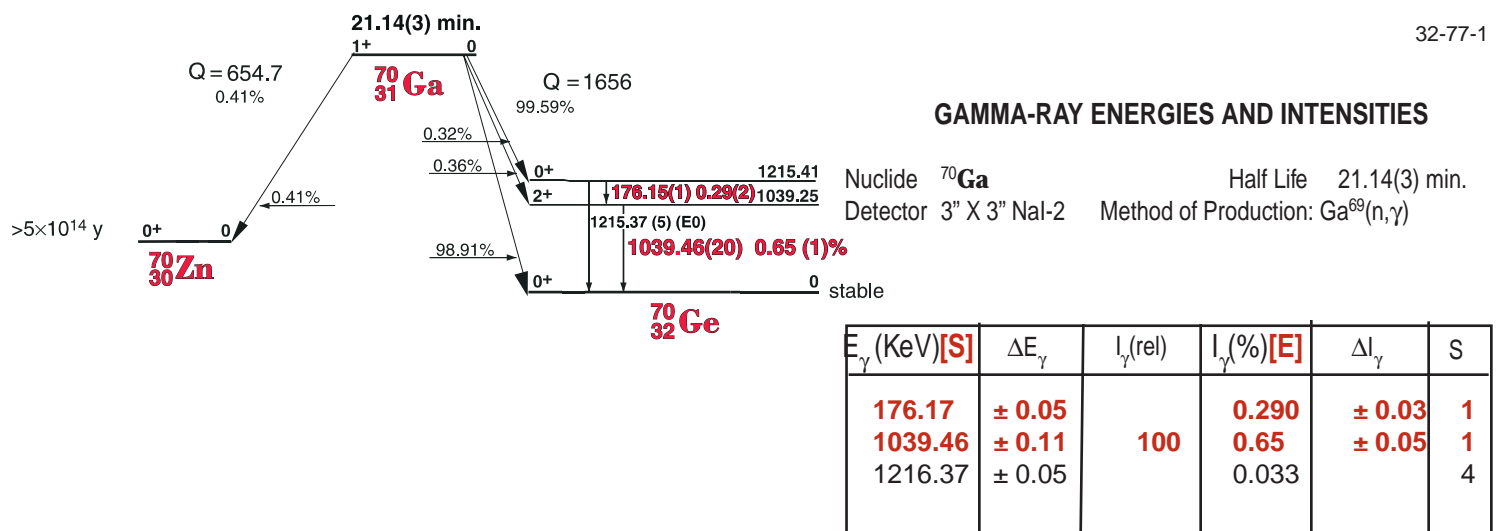


21.14(3) min. ${}^{70}\text{Ga}$

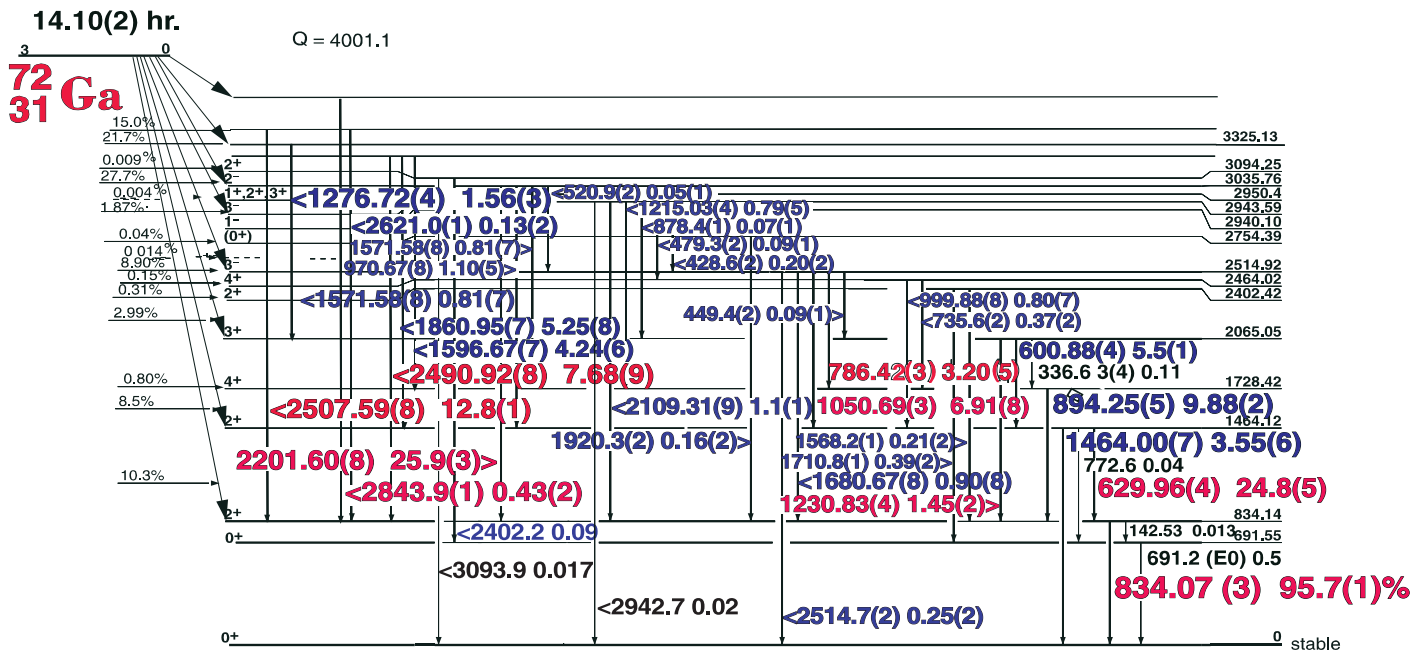
${}^{70}\text{Ga}$ Decay Scheme



21.14(3) Min. ^{70}Ga



14.10(2) hr. ^{72}Ga



14.10(2) hr. ^{72}Ga

32-77-1

GAMMA-RAY ENERGIES AND INTENSITIES

Nuclide ^{72}Ga
Detector 3" X 3" NaI-2

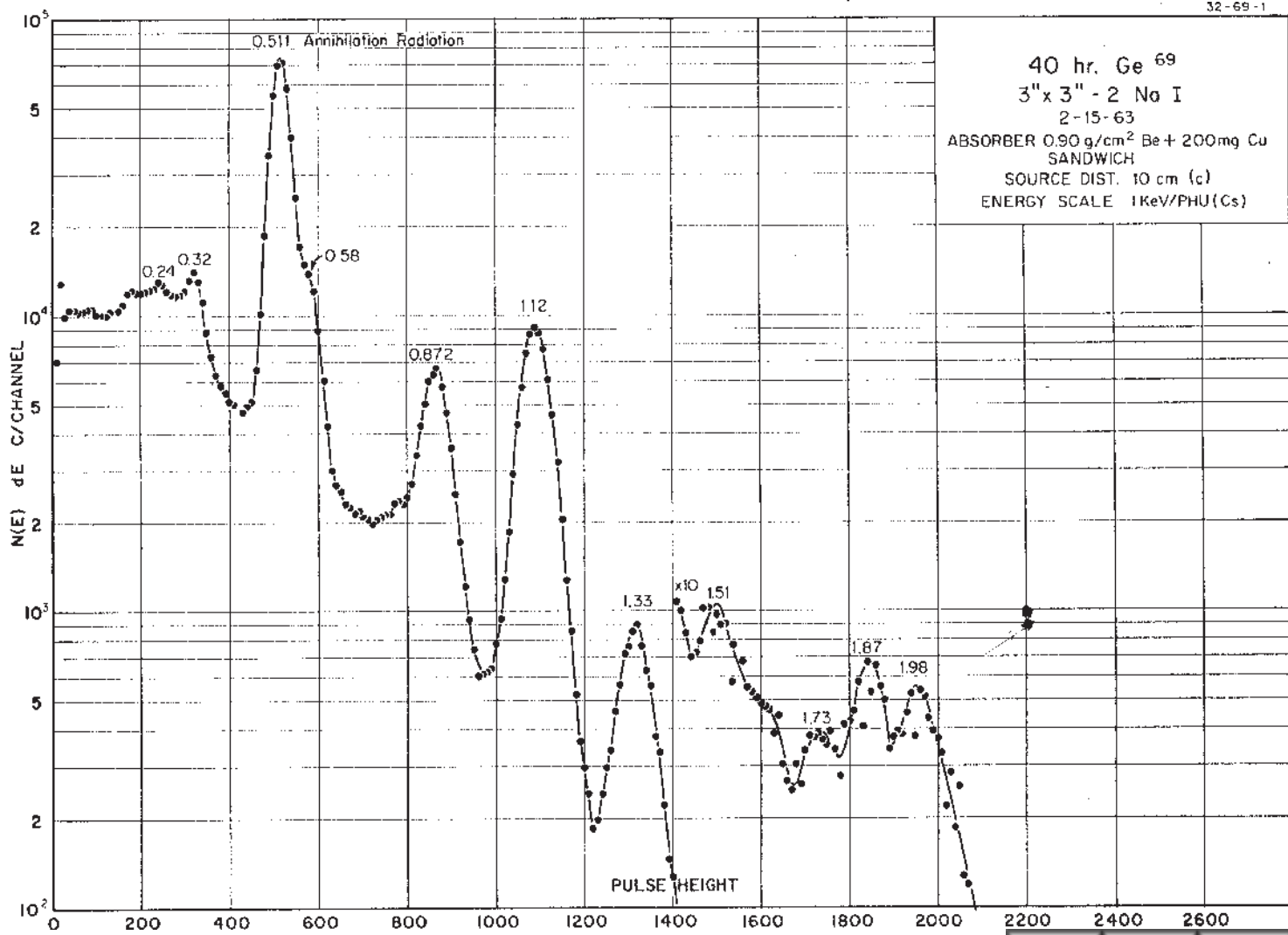
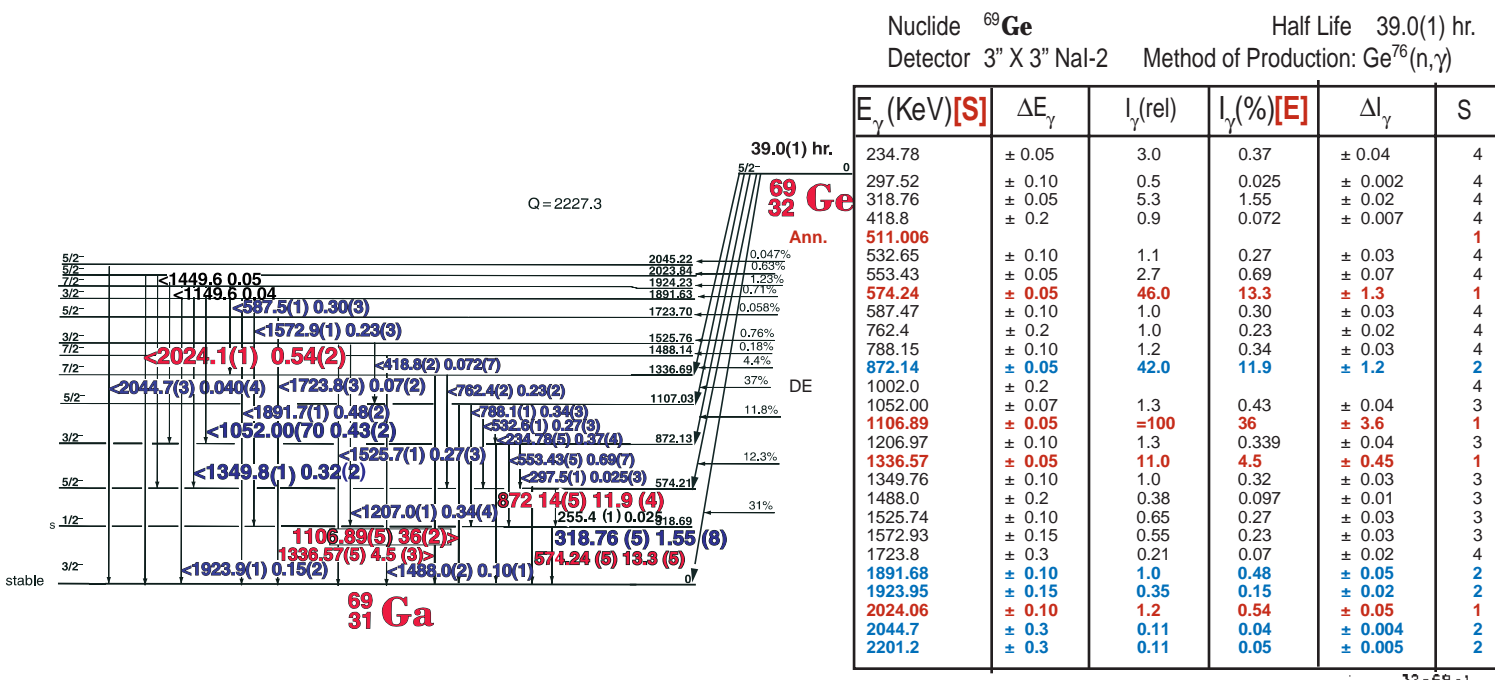
Half Life 14.10(2) hr.
Method of Production: Ga⁷¹(n,γ)

	E_{γ} (KeV) [S]	ΔE_{γ}	I_{γ} (rel)	$I_{\gamma}(\%)$ [E]	ΔI_{γ}	S		E_{γ} (KeV) [S]	ΔE_{γ}	I_{γ} (rel)	$I_{\gamma}(\%)$ [E]	ΔI_{γ}	S
D ann.	113.07	± 0.1	0.62	0.14	± 0.06	4	DE	1485.65	± 0.065	1.51		± 0.2	3
	289.2	± 0.15	0.27		± 0.03	4		1519.4	± 0.2	0.07	0.06	± 0.01	4
	336.63	± 0.04	0.14	0.11	± 0.03	4		1568.23	± 0.1	0.27	0.21	± 0.02	4
	381.5	± 0.2	0.03		± 0.01	4		1571.58	± 0.08	0.95	0.81	± 0.07	3
	428.6	± 0.15	0.23	0.20	± 0.01	4		1596.67	± 0.07	5.11	4.4	± 0.2	2
	449.4	± 0.2	0.10	0.094	± 0.005	4	SE	1667.31	± 0.09	0.08		± 0.015	3
	479.3	± 0.2	0.15	0.091	± 0.005	4		1680.67	± 0.08	1.07	0.90	± 0.08	3
	495.9	± 0.2	0.06		± 0.02	4		1690.47	± 0.08	2.04		± 0.18	3
	511.006		1.7			3		1710.80	± 0.1	0.54	0.39	± 0.02	4
	520.9	± 0.2	0.07	0.055	± 0.005	4	DE	1821.98	± 0.1	0.12		± 0.015	4
	587.6	± 0.2	0.11		± 0.03	4		1837.03	± 0.1	0.27	0.22	± 0.02	4
	600.88	± 0.04	5.75	5.5	± 0.1	3		1860.95	± 0.07	6.36	5.25	± 0.35	2
	629.92	± 0.030	27.3	24.8	± 0.5	1		1877.68	± 0.1	0.28		± 0.03	4
	735.60	± 0.2	0.5	0.37	± 0.02	4	SE	1920.38	± 0.1	0.18		± 0.02	4
	786.42	± 0.030	3.48	3.20	± 0.18	2		1979.81	± 0.1	1.04		± 0.1	4
	810.24	± 0.035	2.16	1.9	± 0.06	3		1991.32	± 0.2	0.36		± 0.05	4
	834.07	± 0.030	100	95.7	± 1.0	1		1996.56	± 0.1	1.71		± 0.15	3
	861.07	± 0.08	1.03	0.9	± 0.1	3		2028.83	± 0.15	0.30		± 0.06	4
	878.4	± 0.1	0.08	0.073	± 0.008	4	SE	2109.31	± 0.09	1.31	1.1	± 0.1	3
	894.24	± 0.030	10.75	9.88	± 0.02	1		2201.60	± 0.08	31.66	25.9	± 0.3	1
	924.28	± 0.10	0.18	0.15	± 0.02	4		2214.0	± 0.15	0.27		± 0.03	4
	939.36	± 0.08	0.384	0.34	± 0.03	4		2332.4	± 0.2	0.26		± 0.04	4
	970.67	± 0.08	1.20	1.10	± 0.05	3		2402.2	± 0.2	0.13	0.09	± 0.02	4
	999.88	± 0.08	0.89	0.80	± 0.07	3	SE	2490.92	± 0.08	9.02	7.68	± 0.09	1
	1031.92	± 0.09	0.08	0.07	± 0.02	4		2507.59	± 0.08	15.63	12.8	± 0.1	1
	1050.688	± 0.035	7.60	6.91	± 1.0	1		2514.70	± 0.12	0.41		± 0.04	3
	1163.17	± 0.1	0.07	0.06	± 0.008	4		2621.0	± 0.15	0.18	0.13	± 0.01	3
	1179.59	± 0.040	1.77		± 0.2	3		2632.5	± 0.2	0.04		± 0.01	4
	1215.03	± 0.04	0.90	0.79	± 0.05	3	SE	2785.96	± 0.2	0.05		± 0.015	4
	1230.83	± 0.04	1.60	1.45	± 0.08	3		2843.90	± 0.10	0.53	0.43	± 0.03	1
	1260.03	± 0.04	1.30	1.1	± 0.10	3		2940.1	± 0.25	0.02	0.02	0.005	4
	1276.72	± 0.04	1.74	1.56	± 0.1	3		2980.80	± 0.20	0.076	0.06	± 0.01	3
	1390.11	± 0.1	0.11	0.09	± 0.01	4		3034.0	± 1.0	0.04		± 0.01	4
	1464.00	± 0.06	4.08	3.55	± 0.06	2	D.E.	3094.0	± 1.0	0.035	0.017	± 0.002	4
	1468.99	± 0.08	0.82		± 0.1	3							

39.0(1) hr. ^{69}Ge

32-77-1

GAMMA-RAY ENERGIES AND INTENSITIES



32-75-1

32-75-1

82 min Ge⁷⁵

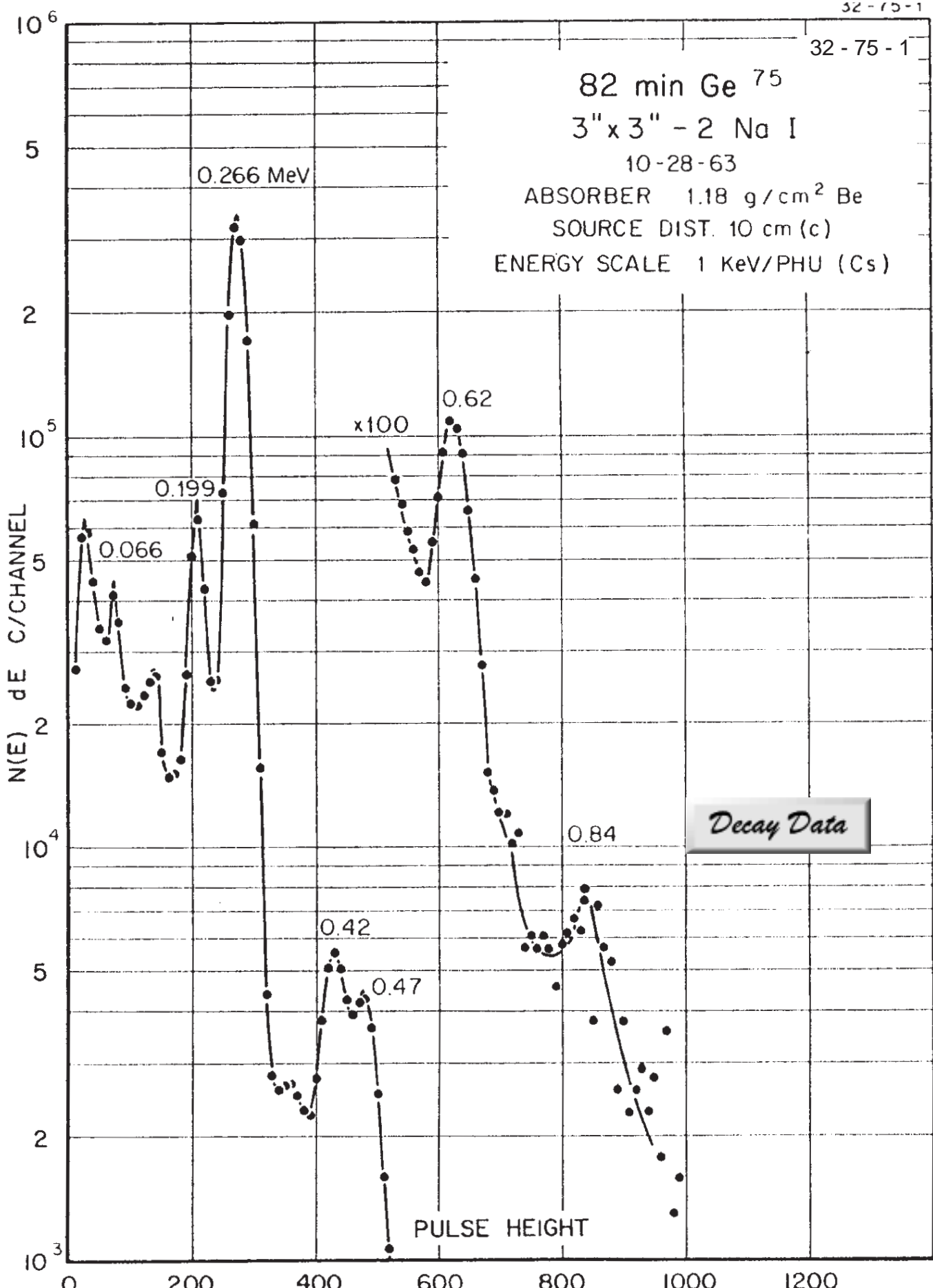
3" x 3" - 2 Na I

10-28-63

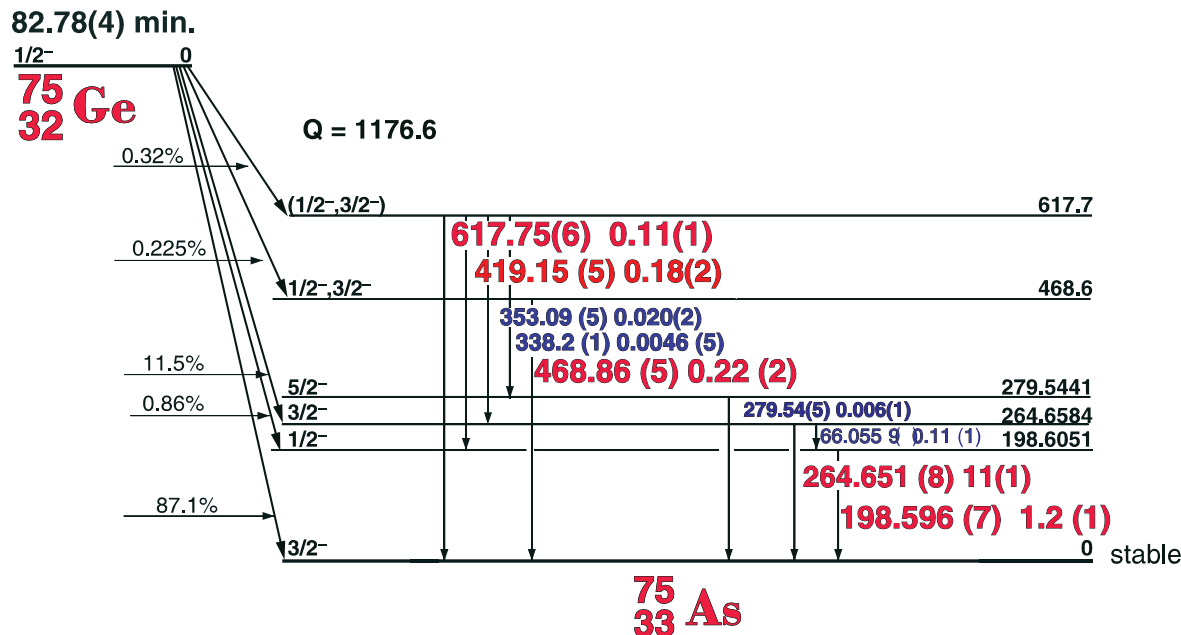
ABSORBER 1.18 g/cm² Be

SOURCE DIST. 10 cm (c)

ENERGY SCALE 1 KeV/PHU (Cs)



82.78(4) Min. ^{75}Ge Decay Scheme

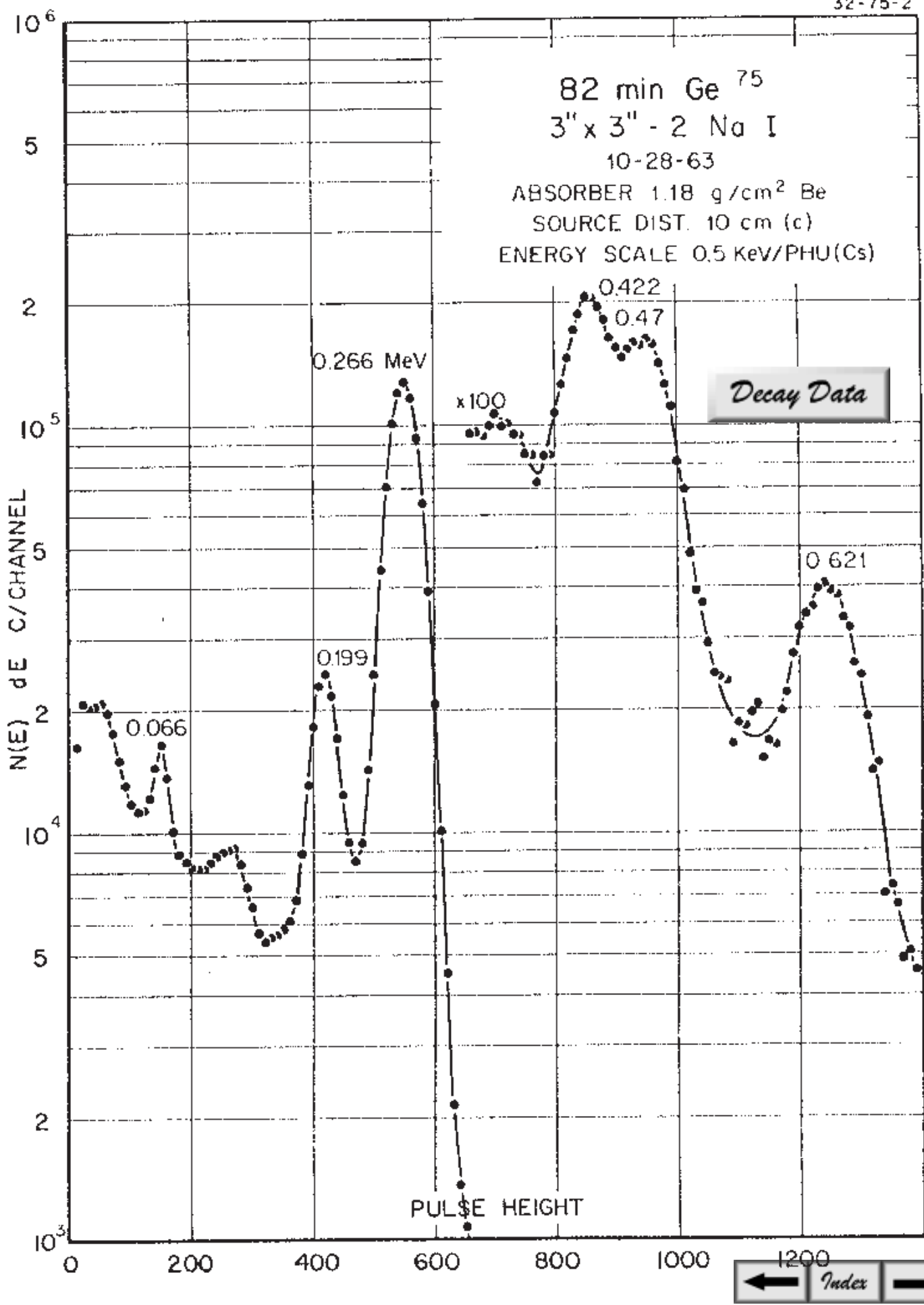


32-75-1

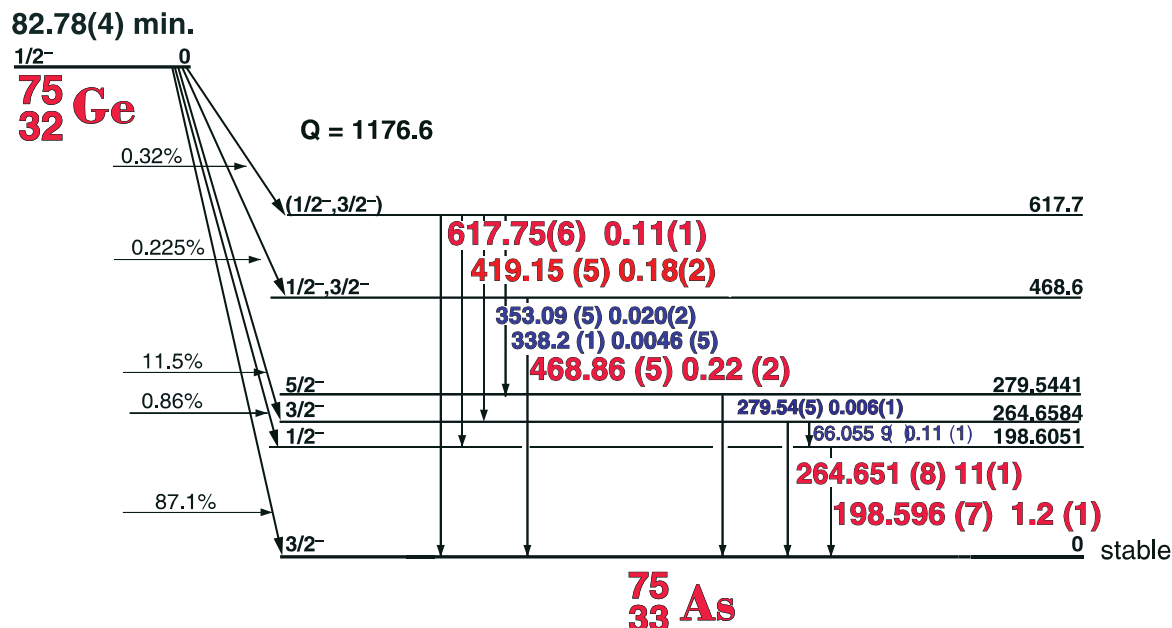
GAMMA-RAY ENERGIES AND INTENSITIES

Nuclide ^{75}Ge Half Life 82.78(4) min.
Detector 3" x 3" -2 Nal Method of Production: $\text{Ge}^{74}(\text{n},\gamma)$

E_γ (KeV)[S]	ΔE_γ	I_γ (rel)	$I_\gamma(\%)$ [E]	ΔI_γ	S
66.055	± 0.009	2.0	0.114	± 0.01	3
198.596	± 0.007	10.9	1.19	± 0.12	1
264.651	± 0.008	=100	11.4	± 0.12	1
279.50	± 0.09	0.14	0.006	± 0.001	4
338.2	± 0.1	0.14	0.005	± 0.001	4
353.09	± 0.05	0.30	0.021	± 0.002	3
419.15	± 0.05	2.4	0.185	± 0.02	1
468.86	± 0.05	2.3	0.223	± 0.02	1
617.75	± 0.06	0.84	0.114	± 0.01	1
846.79	± 0.08	0.29			2



82.78(4) Min ^{75}Ge Decay Scheme

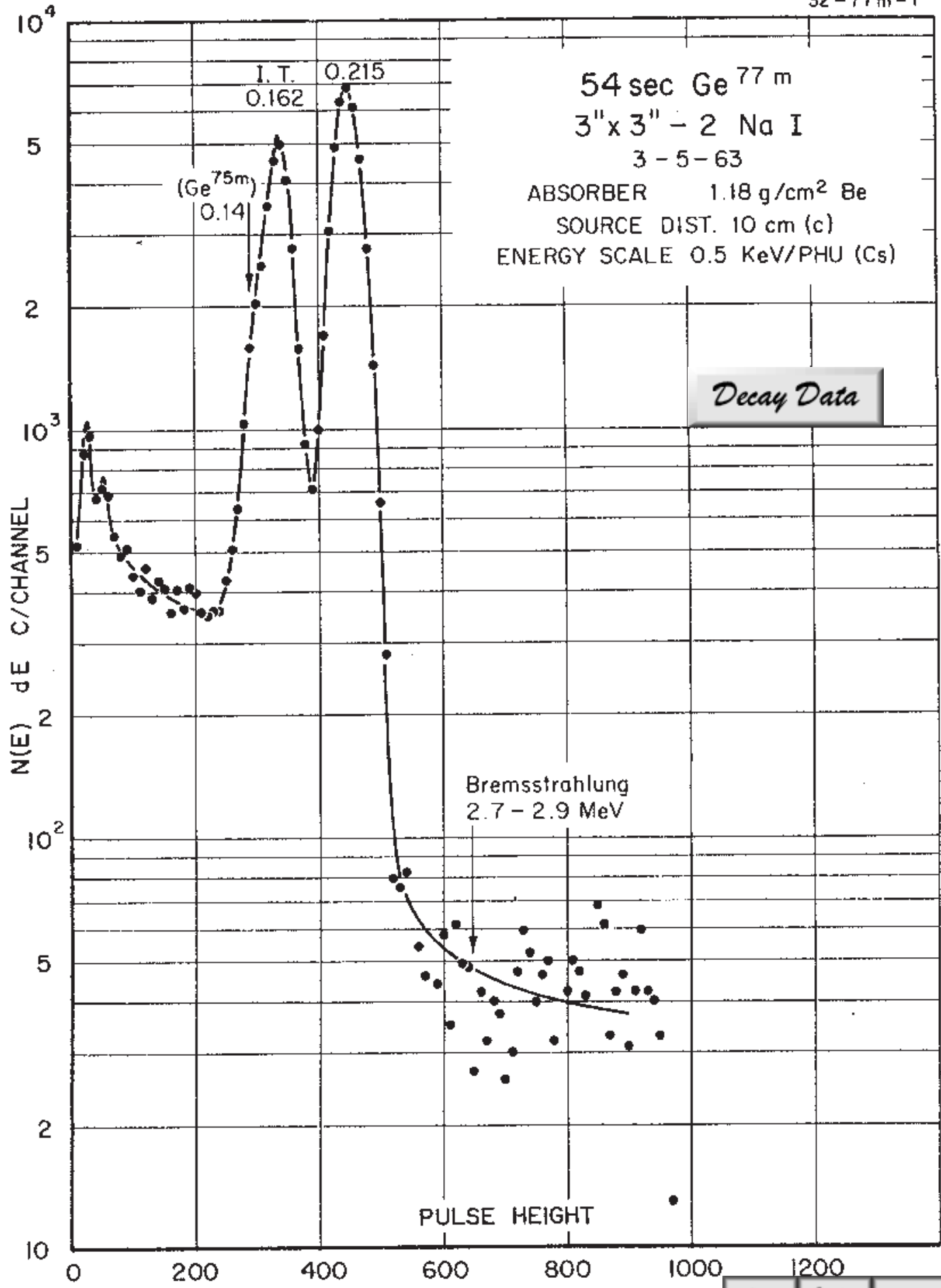


32-75-2

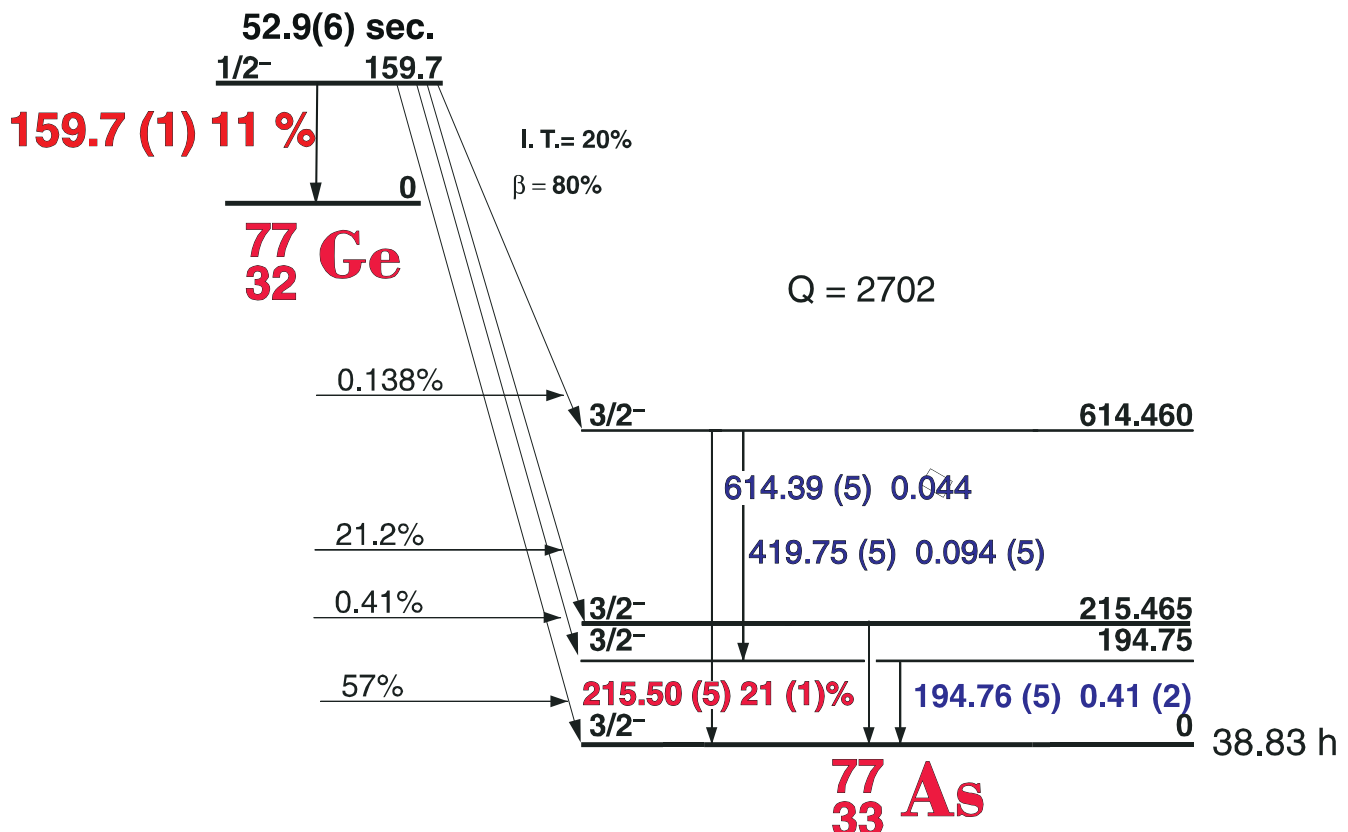
GAMMA-RAY ENERGIES AND INTENSITIES

Nuclide ^{75}Ge Half Life 82.78(4) min.
Detector 3" x 3" -2 Nal Method of Production: $\text{Ge}^{74}(n,\gamma)$

E_{γ} (KeV)[S]	ΔE_{γ}	I_{γ} (rel)	$I_{\gamma}(\%)[E]$	ΔI_{γ}	S
66.055	± 0.009	2.0	0.114	± 0.01	3
198.596	± 0.007	10.9	1.19	± 0.12	1
264.651	± 0.008	=100	11.4	± 0.12	1
279.50	± 0.09	0.14	0.006	± 0.001	4
338.2	± 0.1	0.14	0.005	± 0.001	4
353.09	± 0.05	0.30	0.021	± 0.002	3
419.15	± 0.05	2.4	0.185	± 0.02	1
468.86	± 0.05	2.3	0.223	± 0.02	1
617.75	± 0.06	0.84	0.114	± 0.01	1
846.79	± 0.08	0.29			2



52.9(6) sec. ^{77m}Ge



GAMMA-RAY ENERGIES AND INTENSITIES

Nuclide
Detector

^{77m}Ge
3" x 3" -2 NaI

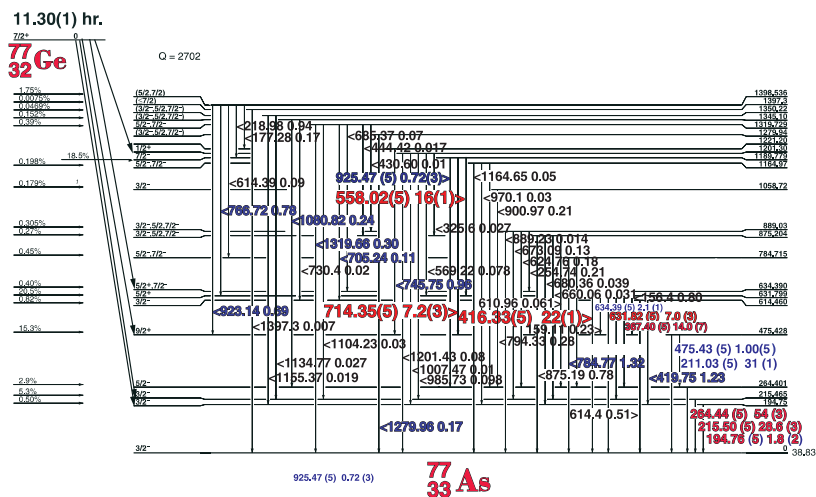
Half Life 52.9(6) sec
Method of Production: $\text{Ge}^{74}(n,\gamma)$

	E_γ (KeV)[S]	ΔE_γ	I_γ (rel)	$I_\gamma(\%)[E]$	ΔI_γ	S
I. T.	159.7	± 01	50	11.0	± 0.5	1
	194.76	± 0.05	0.4	0.41	± 0.02	2
	215.50	± 0.05	100	21.0	1.0	1
	419.75	± 0.05	0.05	0.094	± 0.005	1
	614.39	± 0.05	0.02	0.044	± 0.002	2

11.30(1) hr. ^{77}Ge

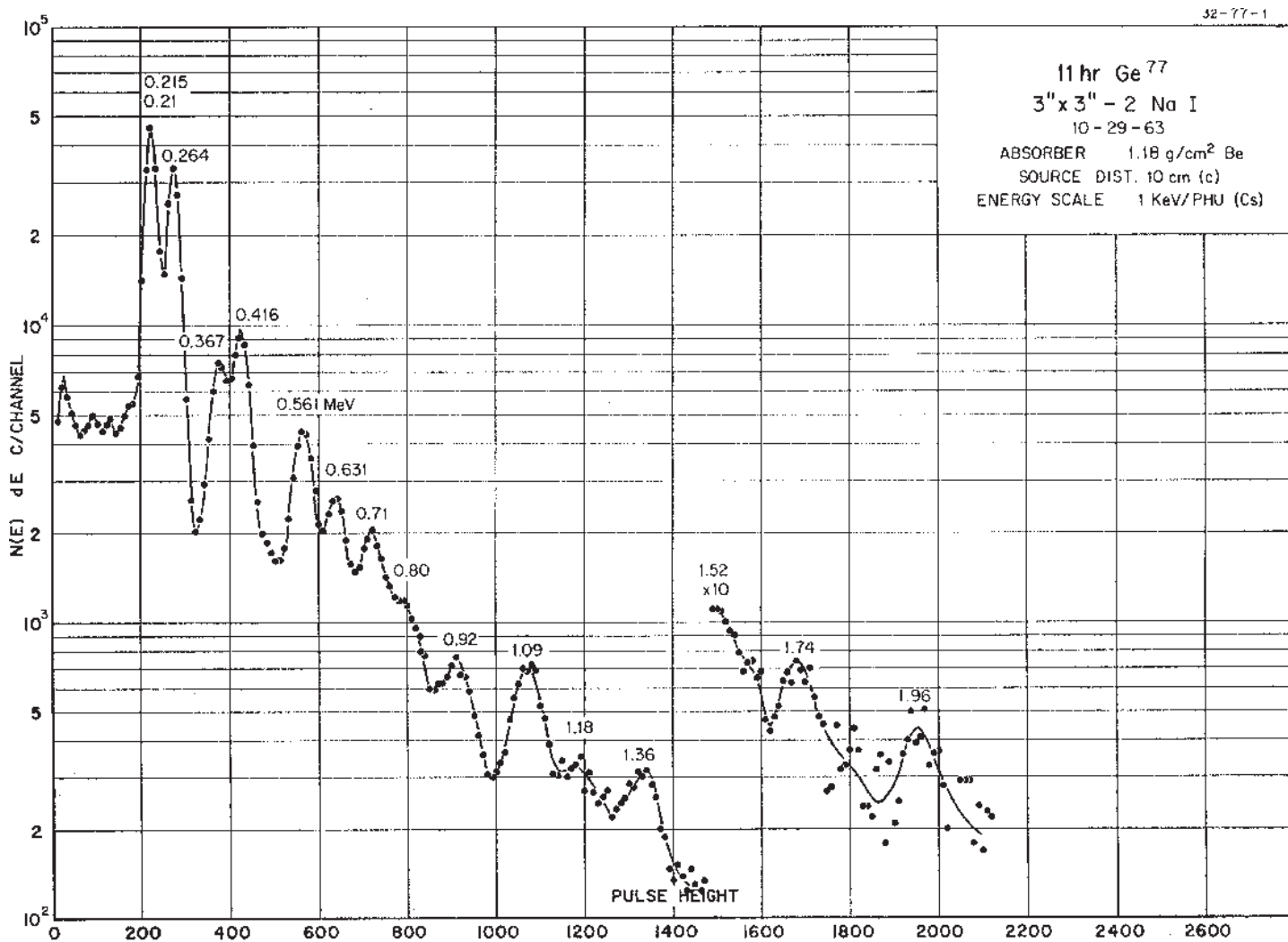
32-77-1

GAMMA-RAY ENERGIES AND INTENSITIES



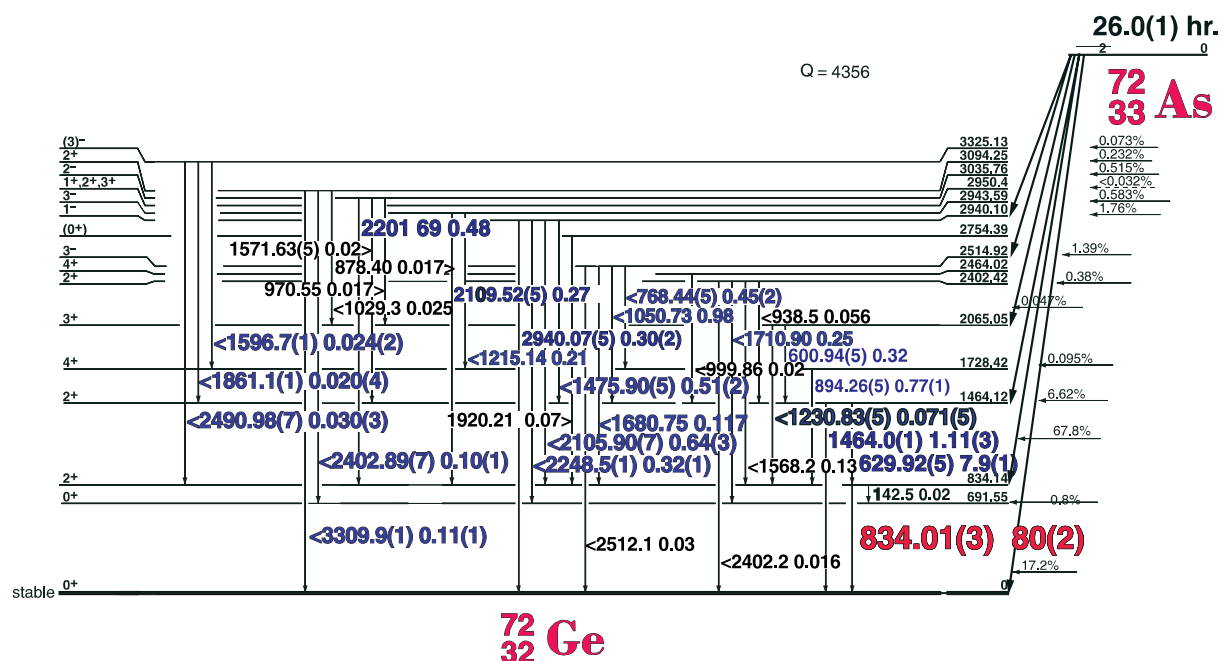
Nuclide Ge^{77}
 Detector 3" X 3" NaI-2
 Method of Production: $\text{Ge}^{76}(\text{n},\gamma)$

E_{γ} (KeV)[S]	ΔE_{γ}	$I_{\gamma}(\text{rel})$	$I_{\gamma}(\%) [E]$	ΔI_{γ}	S
159.7	± 0.1	50	11.0	± 0.5	1
194.76	± 0.05	0.4	0.41	± 0.02	2
215.50	± 0.05	100	21.0	1.0	1
264.44	± 0.05		54	± 0.03	1
419.75	± 0.05	0.05	0.094	± 0.005	1
475.43	± 0.05		1.00	± 0.05	2
558.02	± 0.05		18	± 1.0	1
614.39	± 0.05	0.02	0.044	± 0.002	2
714.35	± 0.05		7.2	± 0.03	1
834.39	± 0.05		2.1	± 0.1	1

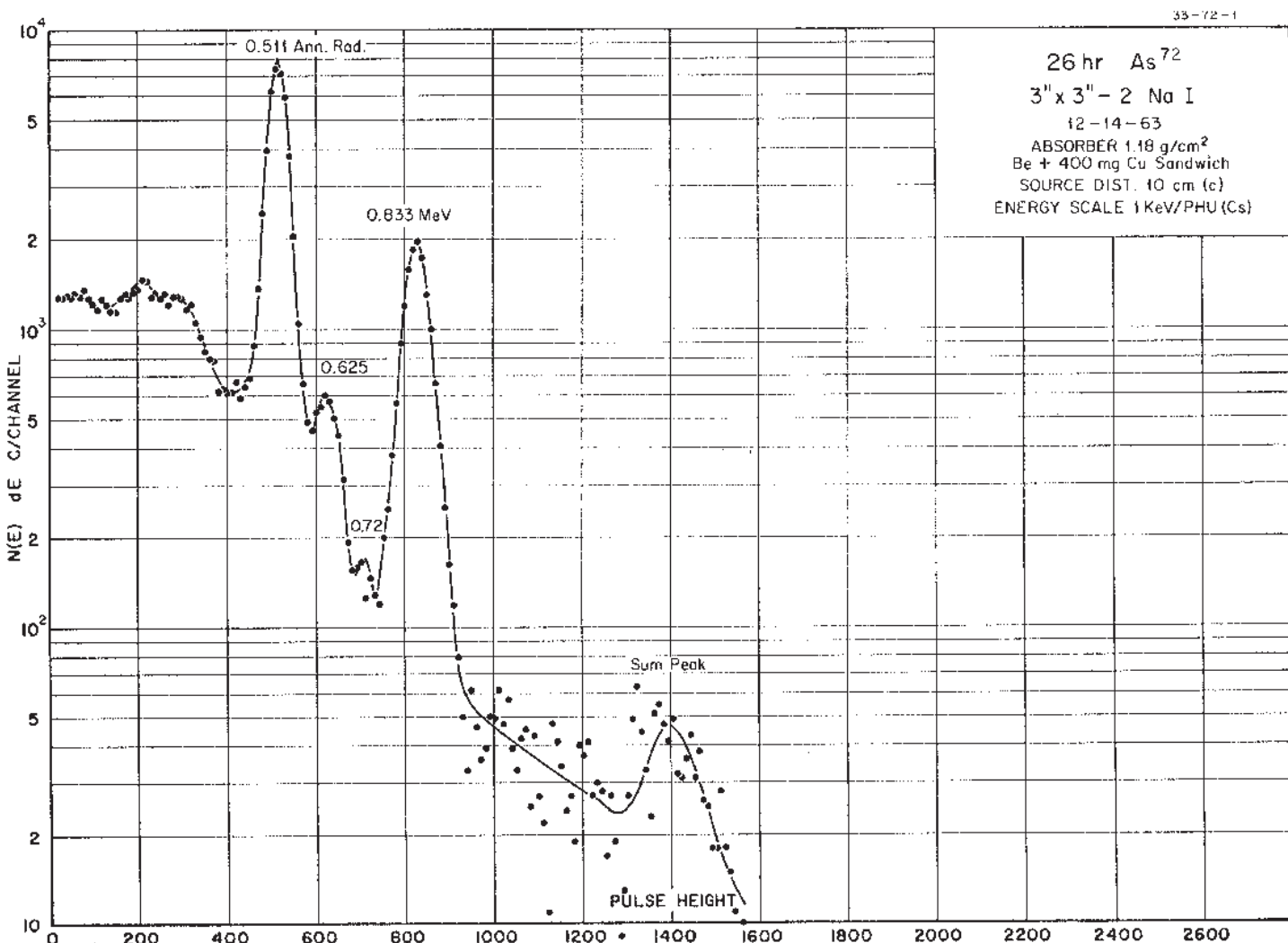


26.0(1) hr. ^{72}As

^{72}As Decay Scheme



^{72}Ge



26.0(1) hr. ^{72}As

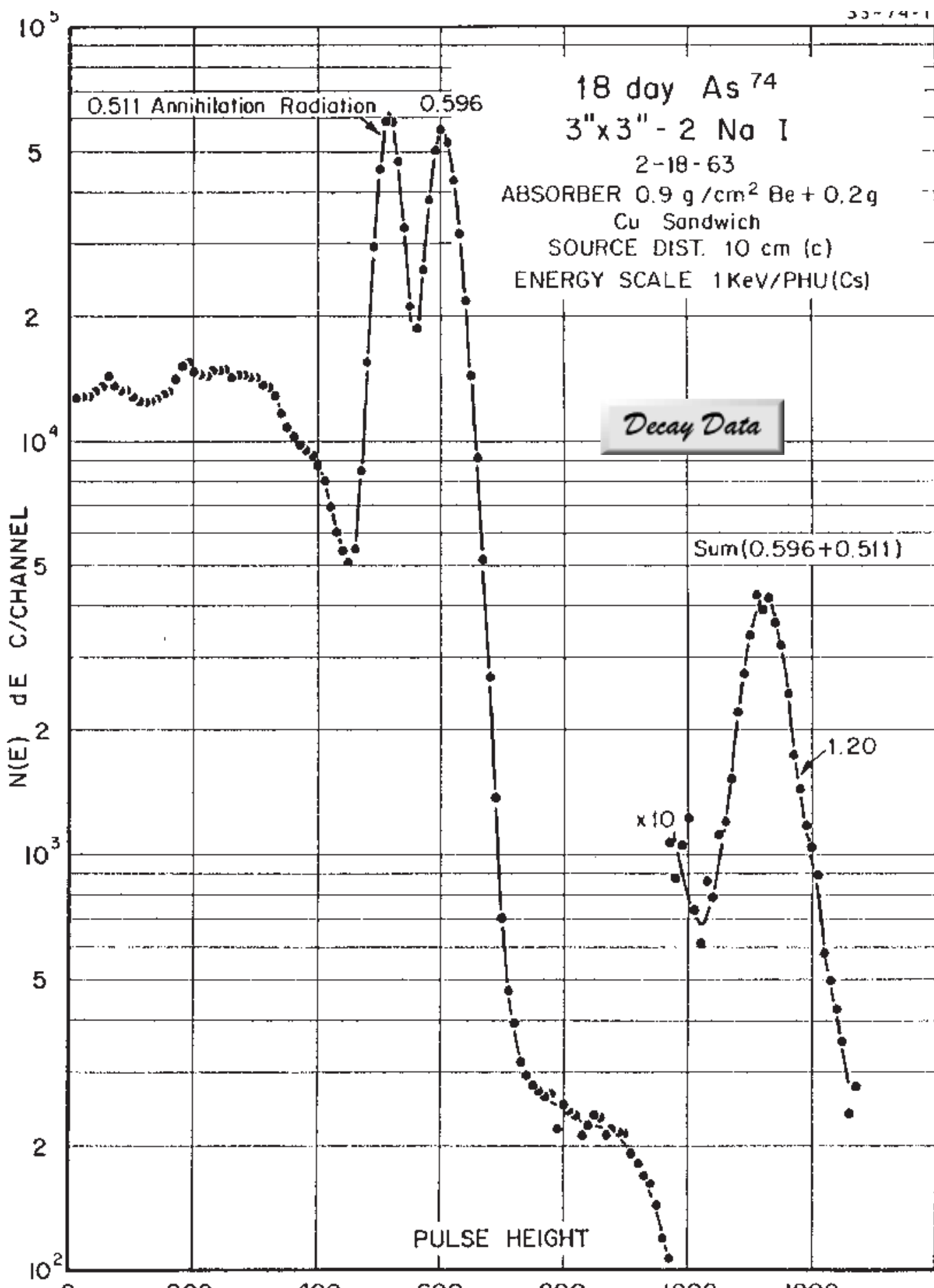
33-72-1

GAMMA-RAY ENERGIES AND INTENSITIES

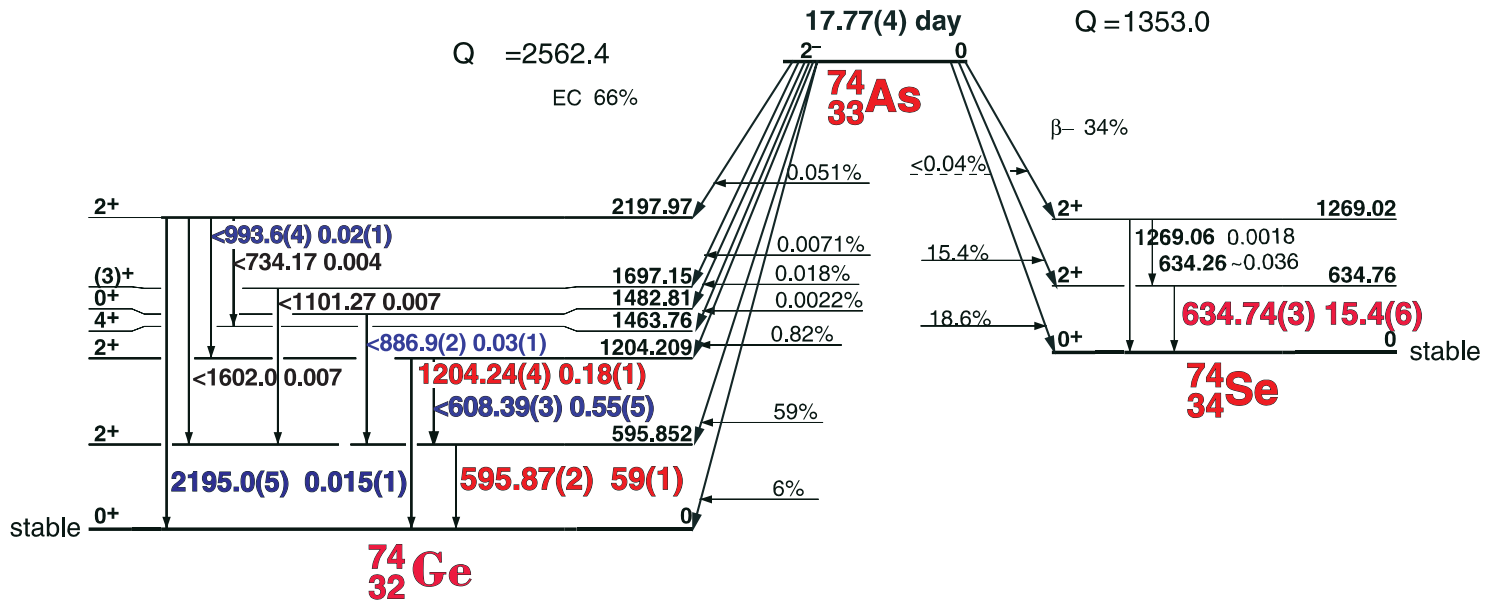
Nuclide ^{72}As
Detector 3" X 3" NaI-2

Half Life 26.0(1) hr.
Method of Production: $^{72}\text{Ge}(\text{p},\text{n})$

E_{γ} (KeV)[S]	ΔE_{γ}	I_{γ} (rel)	$I_{\gamma}(\%)$ [E]	ΔI_{γ}	S
600.94	± 0.05		0.32	± 0.1	2
629.92	± 0.05		7.9	± 0.1	1
834.01	± 0.03		80	± 2	1
894.26	± 0.05		0.77	± 0.01	2
1464.0	± 0.1		1.11	± 0.05	2
1710.90	± 0.05		0.25	± 0.01	1
2109.52	± 0.05		0.27	± 0.01	1
2201.69	± 0.09		0.48	± 0.02	1
2940.07	± 0.17		0.30	± 0.02	1



18 Day ^{74}As Decay Scheme



33-74-1

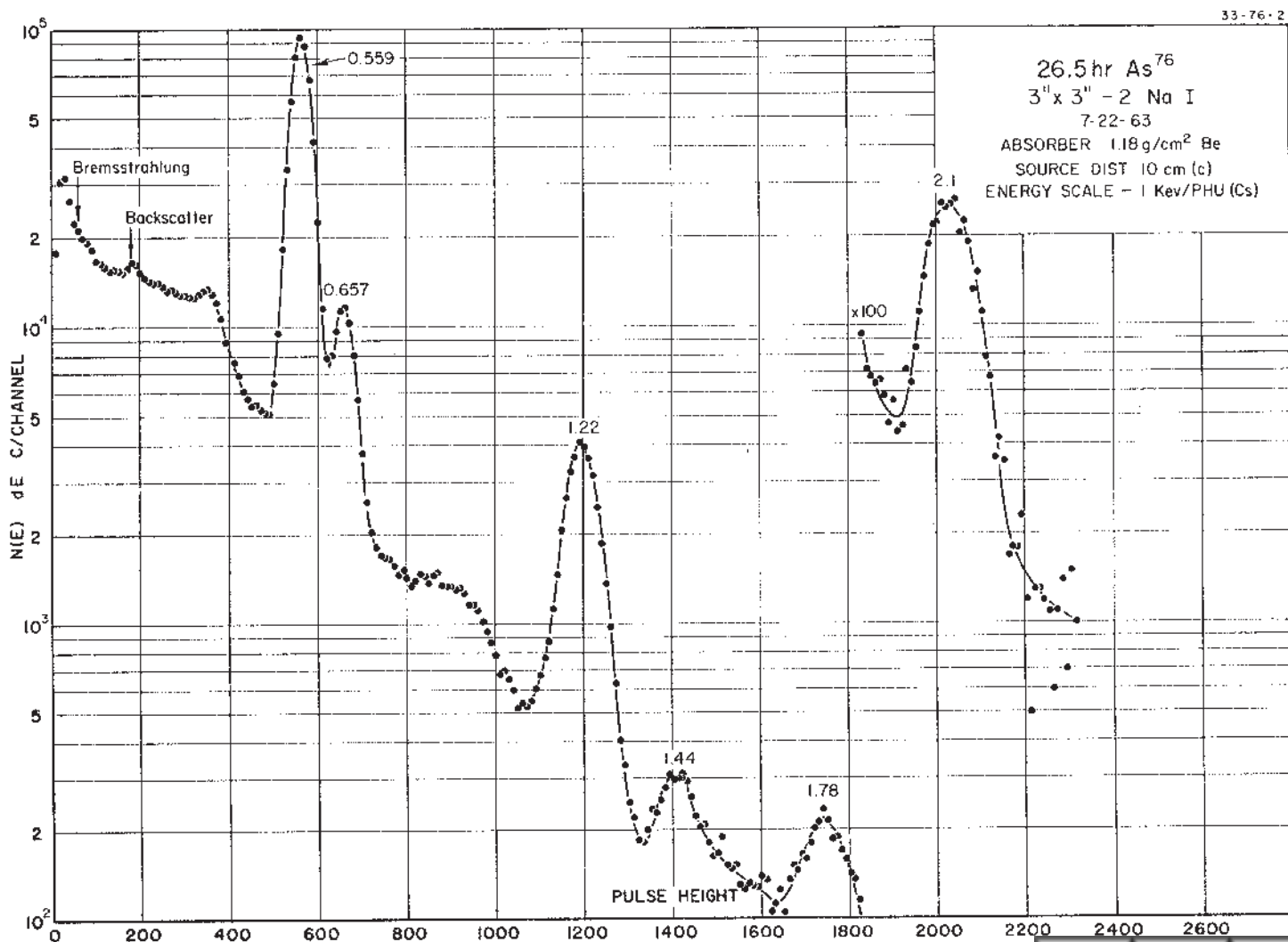
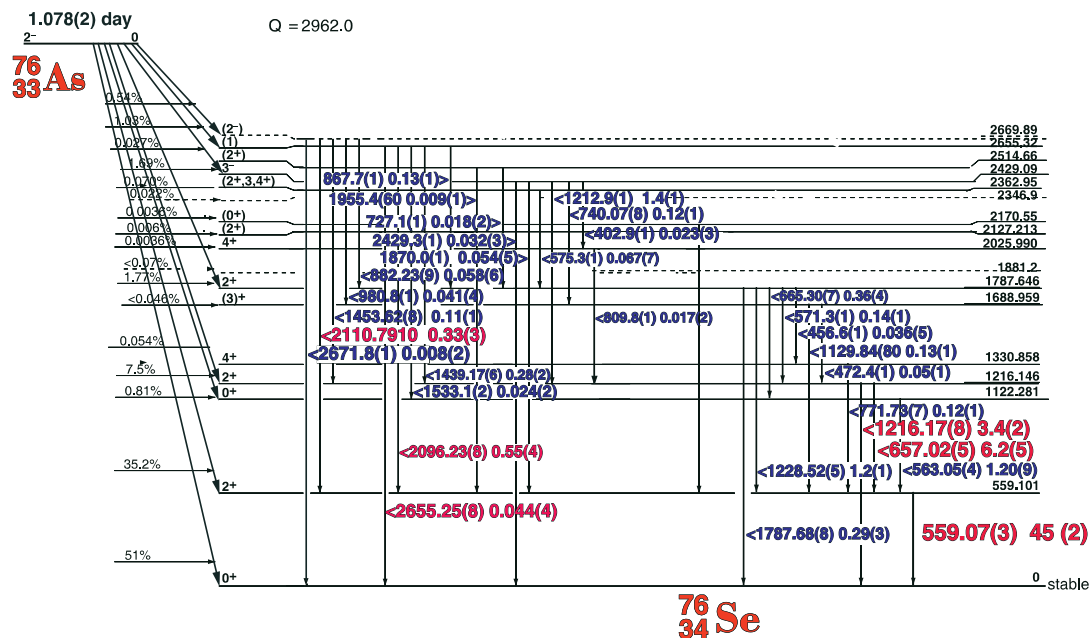
GAMMA-RAY ENERGIES AND INTENSITIES

Nuclide ^{74}As Half Life 17.77(2) day
Detector 3" x 3" -2 NaI Method of Production: $\text{As}^{75}(\gamma, n)$

E_γ (KeV)[S]	ΔE_γ	I_γ (rel)	I_γ (%) [E]	ΔI_γ	S
ann. rad.					
511.006					1
595.873	± 0.025	100	59.4	± 0.2	1
608.395	± 0.03	1.0	0.3	± 0.03	2
634.742	± 0.03	25.7	15.4	± 0.6	1
886.9	± 0.2	0.07	0.03	± 0.03	4
993.6	± 0.4	0.04	0.02	± 0.03	4
1204.24	± 0.04	0.48	0.3	± 0.03	1
2195.0	± 0.5	0.03	0.015	± 0.005	2

1.078(2) Day ^{76}As

^{76}As Decay Scheme



1.078(2) Day ⁷⁶As

33-76-2

GAMMA-RAY ENERGIES AND INTENSITIES

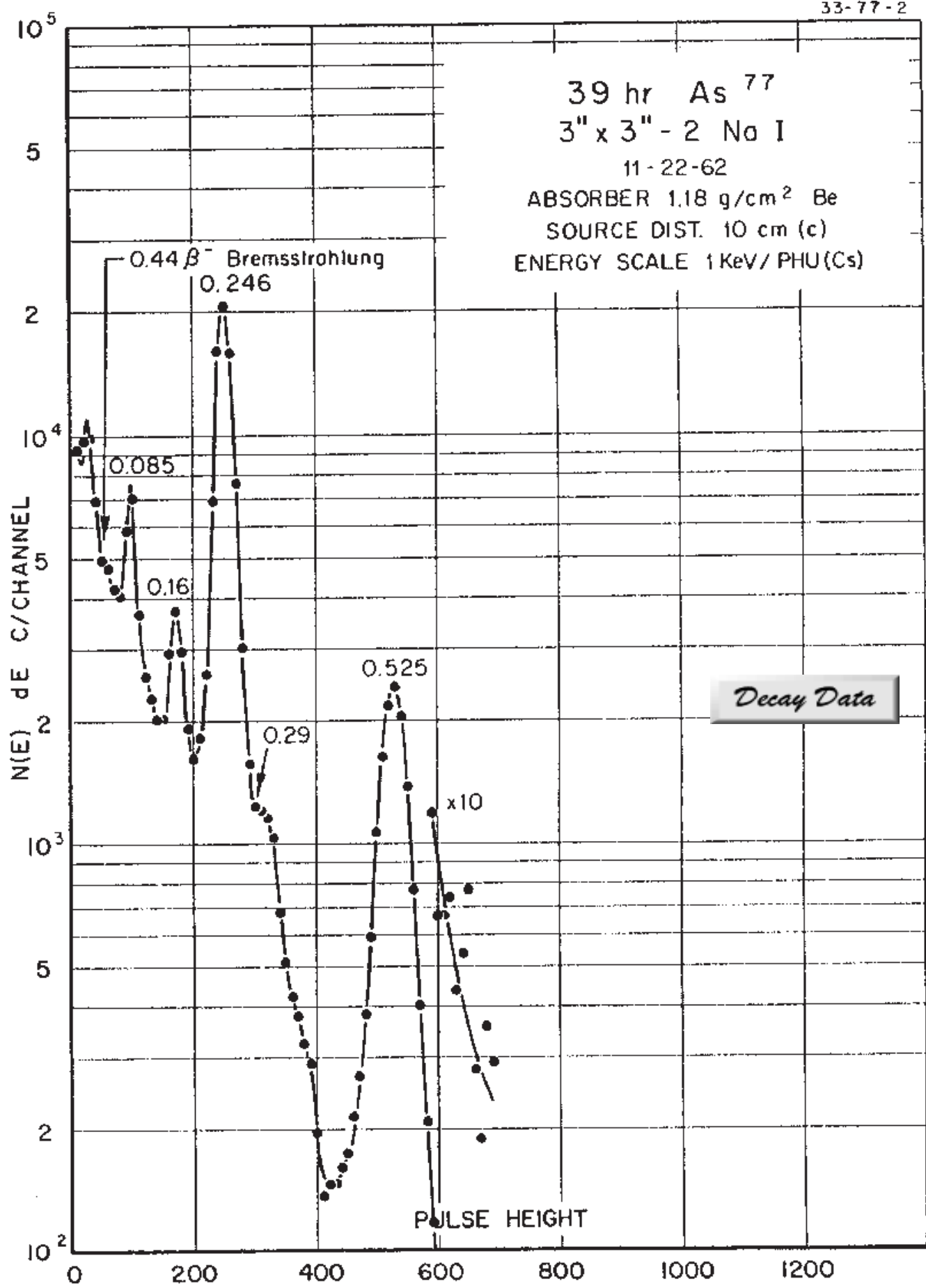
Nuclide ⁷⁶As

Detector 3" X 3" NaI-2

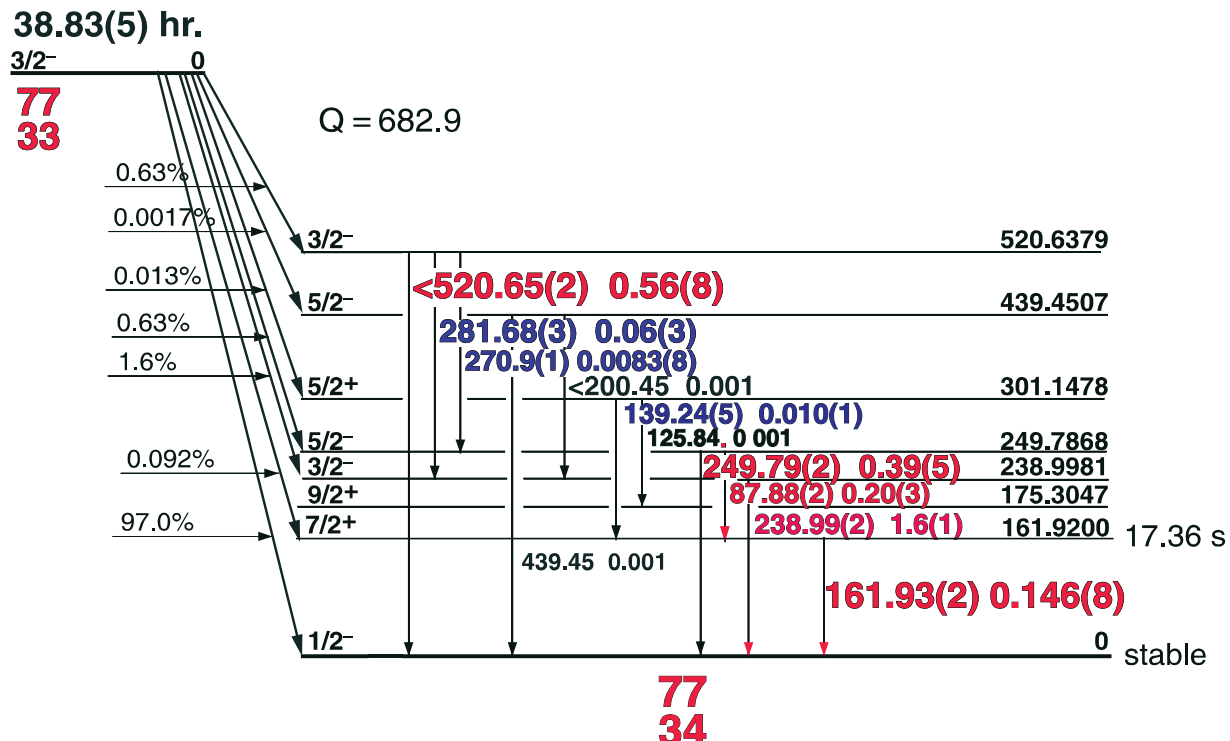
Half Life 1.078(2) Day

Method of Production: /as⁷⁵(n,γ)

E _γ (KeV)[S]	ΔE _γ	I _γ (rel)	I _γ (%)[E]	ΔI _γ	S
402.9	± 0.1	0.08		± 0.02	4
456.60	± 0.1	0.32		± 0.03	4
472.36	± 0.1	0.48		± 0.05	4
559.068	± 0.035	100	45.0	± 2.0	1
563.05	± 0.04	2.7	1.20	± 0.09	3
571.26	± 0.1	0.39	0.14	± 0.01	4
575.26	± 0.1	0.18	0.067	± 0.007	4
657.02	± 0.05	14.0	6.2	± 0.5	1
665.30	± 0.07	0.96	0.36	± 0.04	3
727.07	± 1.0	0.08	0.018	± 0.002	4
740.07	± 0.08	0.27	0.117	± 0.01	4
771.73	± 0.07	0.27	0.12	± 0.01	4
794.7	± 0.2	0.01	0.005	± (1)	4
809.8	± 0.1	0.03	0.017	± 0.002	4
867.7	± 0.1	0.28	0.13	± 0.01	4
882.23	± 0.09	0.14	0.058	± 0.006	4
980.8	± 1.0	0.09	0.041	± 0.004	4
1129.84	± 0.08	0.34	0.126	± 0.015	4
1212.9	± 0.1	3.4	1.44	± 0.11	2
1216.17	± 0.08	7.2	3.42	± 0.24	1
1228.52	± 0.05	2.6	1.22	± 0.11	2
1439.17	± 0.06	0.62	0.279	± 0.019	3
1453.62	± 0.08	0.29	0.108	± 0.011	4
1533.1	± 0.2	0.10	0.024	± 0.002	4
1787.68	+ 0.08	0.73	0.292	± 0.028	3
1870.0	± 0.1	0.28	0.054	+ 0.005	4
1955.4	± 0.6	0.04	0.009	± (1)	4
2096.23	± 0.08	1.3	0.55	± 0.04	1
2110.7	± 0.1	0.76	0.33	± 0.03	1
2429.35	± 0.1	0.10	0.032	± 0.003	2
2655.25	± 0.1	0.10	0.044	± 0.004	1
2671.8	± 0.15	0.02	0.008	± (2)	4



38.83(5) hr. ^{77}As Decay Scheme

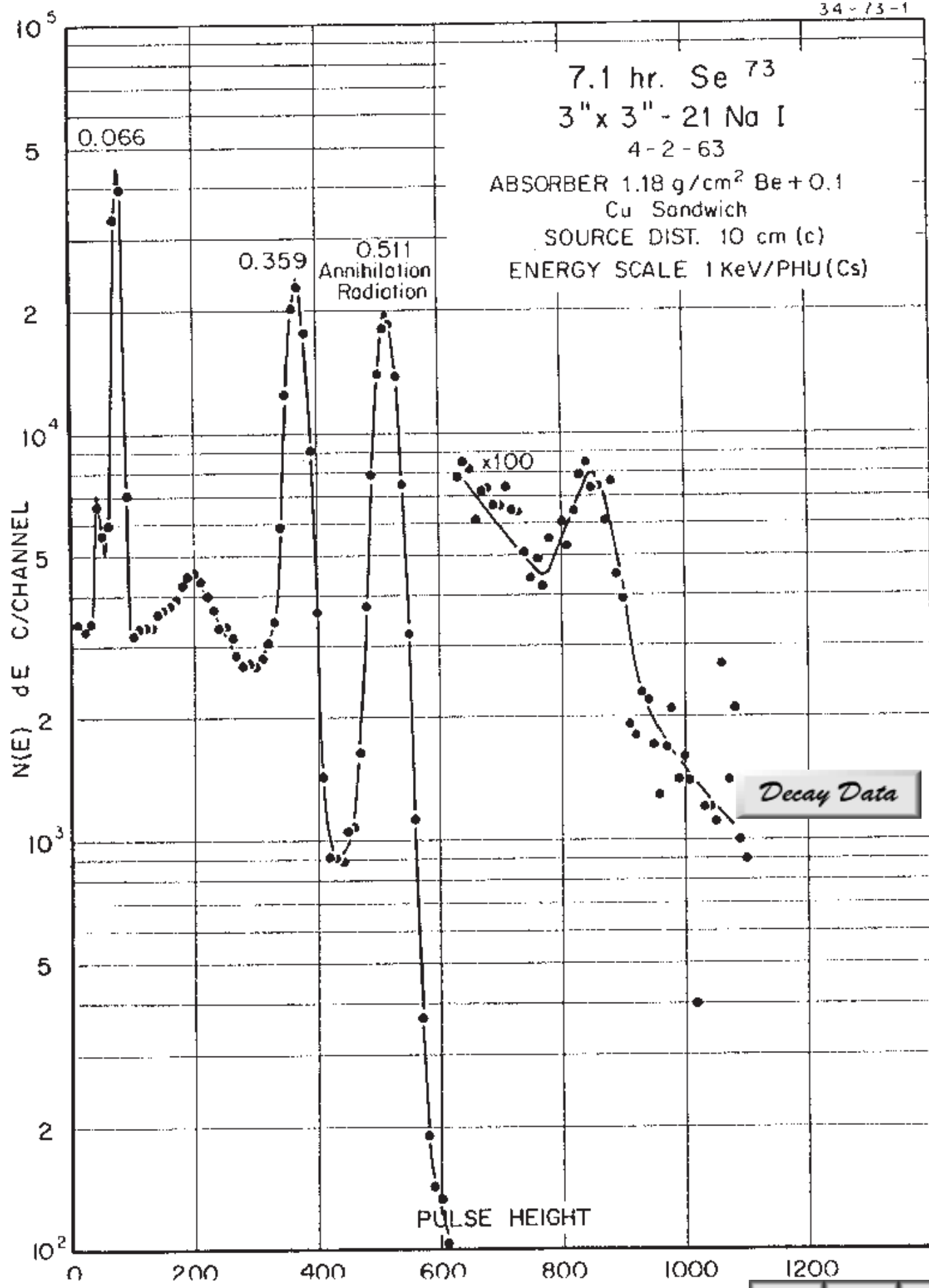


33-77-1

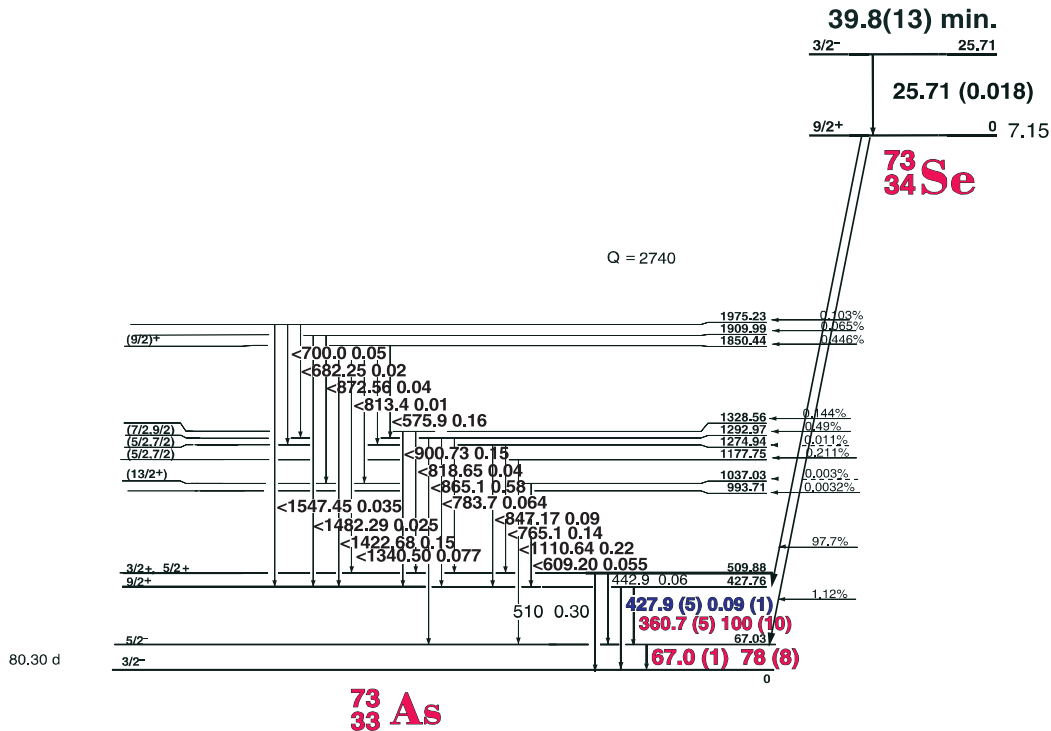
GAMMA-RAY ENERGIES AND INTENSITIES

Nuclide ^{77}As Half Life 38.83(5) Hr.
Detector 3" x 3" -2 NaI Method of Production: As⁷⁶(n, γ)

E_γ (KeV)[S]	ΔE_γ	I_γ (rel)	$I_\gamma(\%)$ [E]	ΔI_γ	S
87.876	± 0.02	13.0	0.20	± 0.03	1
139.24	± 0.05	1.0	0.010	± 0.002	3
161.933	± 0.02	8.1	0.146	± 0.02	1
238.999	± 0.02	100	1.59	± 0.2	1
249.790	± 0.02	27.0.	0.39	± 0.05	1
270.90	± 0.10	0.7	0.008	$\pm (1)$	3
281.684	± 0.03	3.9	0.06	± 0.01	1
520.652	± 0.02	39.0	0.56	± 0.08	1



7.15(8) hr. ^{73}Se Decay Scheme

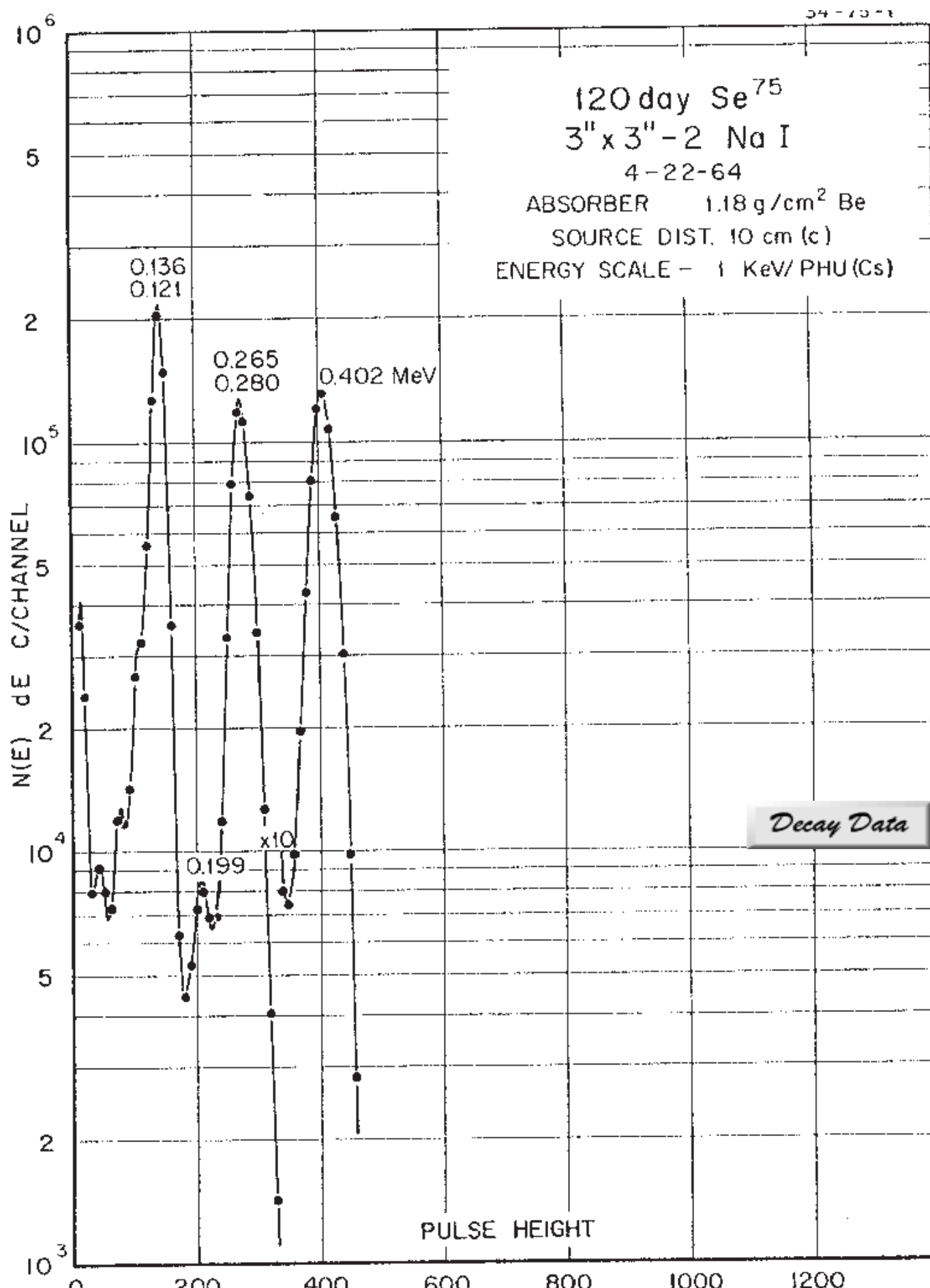


34-73-1

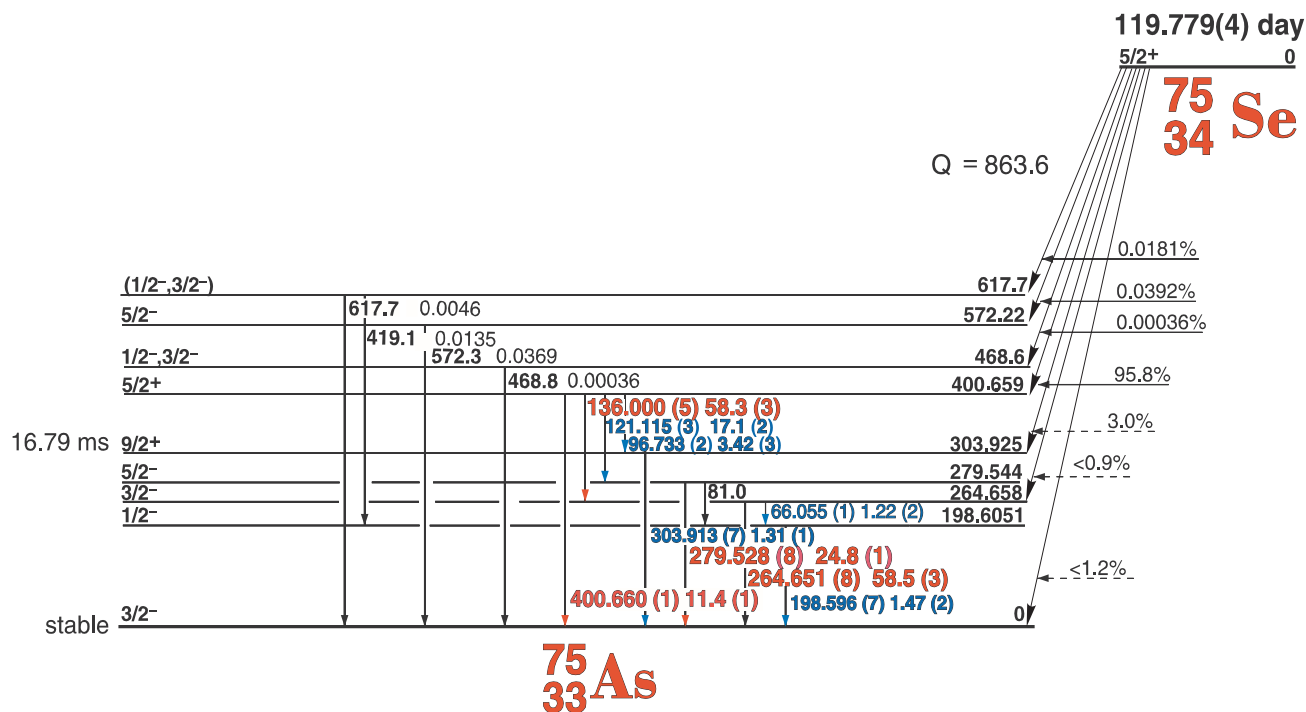
GAMMA-RAY ENERGIES AND INTENSITIES

Nuclide ^{73}Se Half Life 7.15(8) hr.
Detector 3" x 3" -2 NaI Method of Production: $\text{As}^{76}(n,\gamma)$

E_{γ} (KeV)[S]	ΔE_{γ}	I_{γ} (rel)	$I_{\gamma}(\%)$ [E]	ΔI_{γ}	S
67.0	± 0.1	100	78	± 8	1
360.7	± 0.5	50.7	100	± 5	1
427.9	± 0.5	1.1	0.09	± 0.009	3
ann. rad. 511.006					1



119.779 (4) day ^{75}Se Decay Scheme

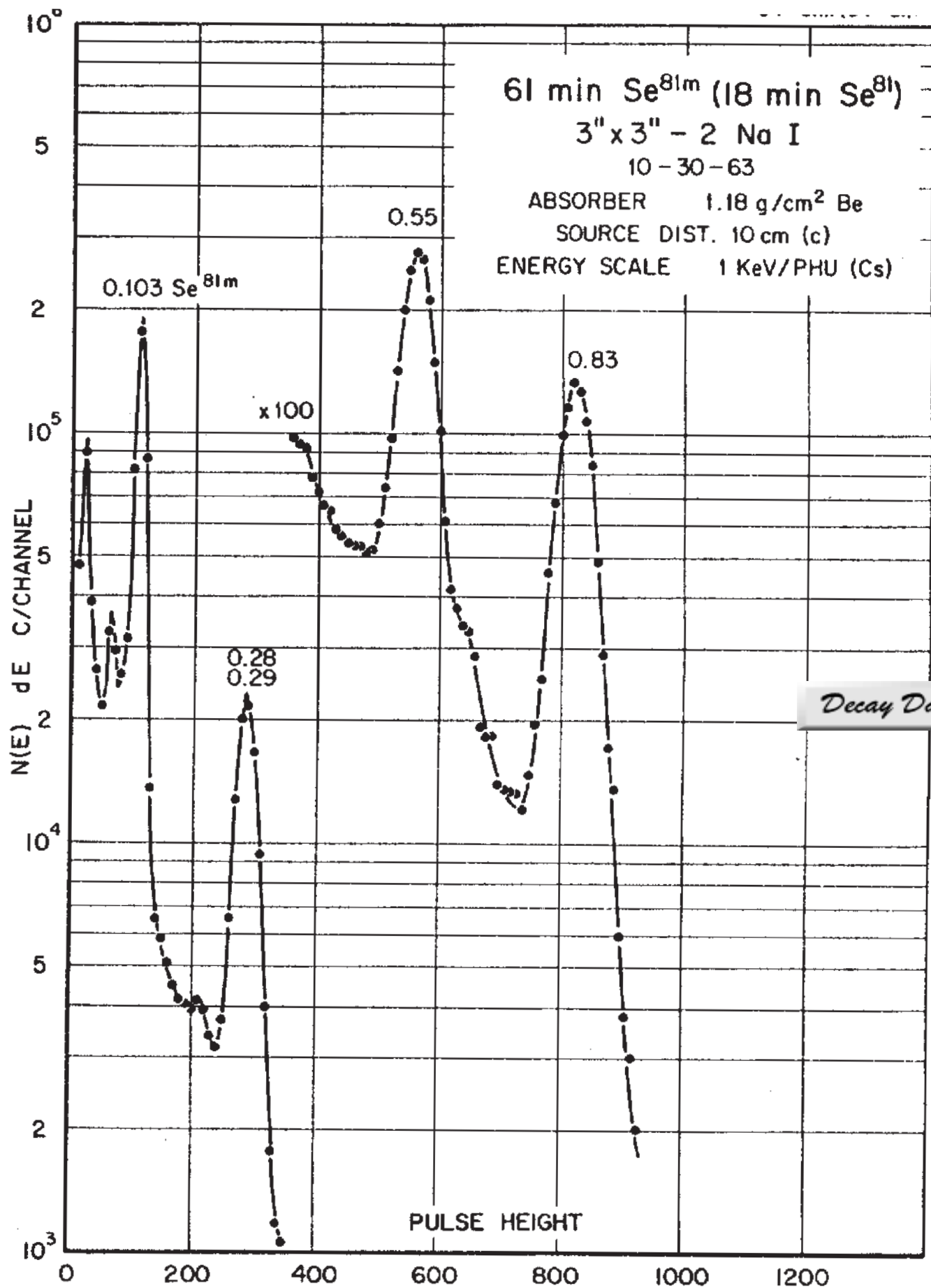


34-75-1

GAMMA-RAY ENERGIES AND INTENSITIES

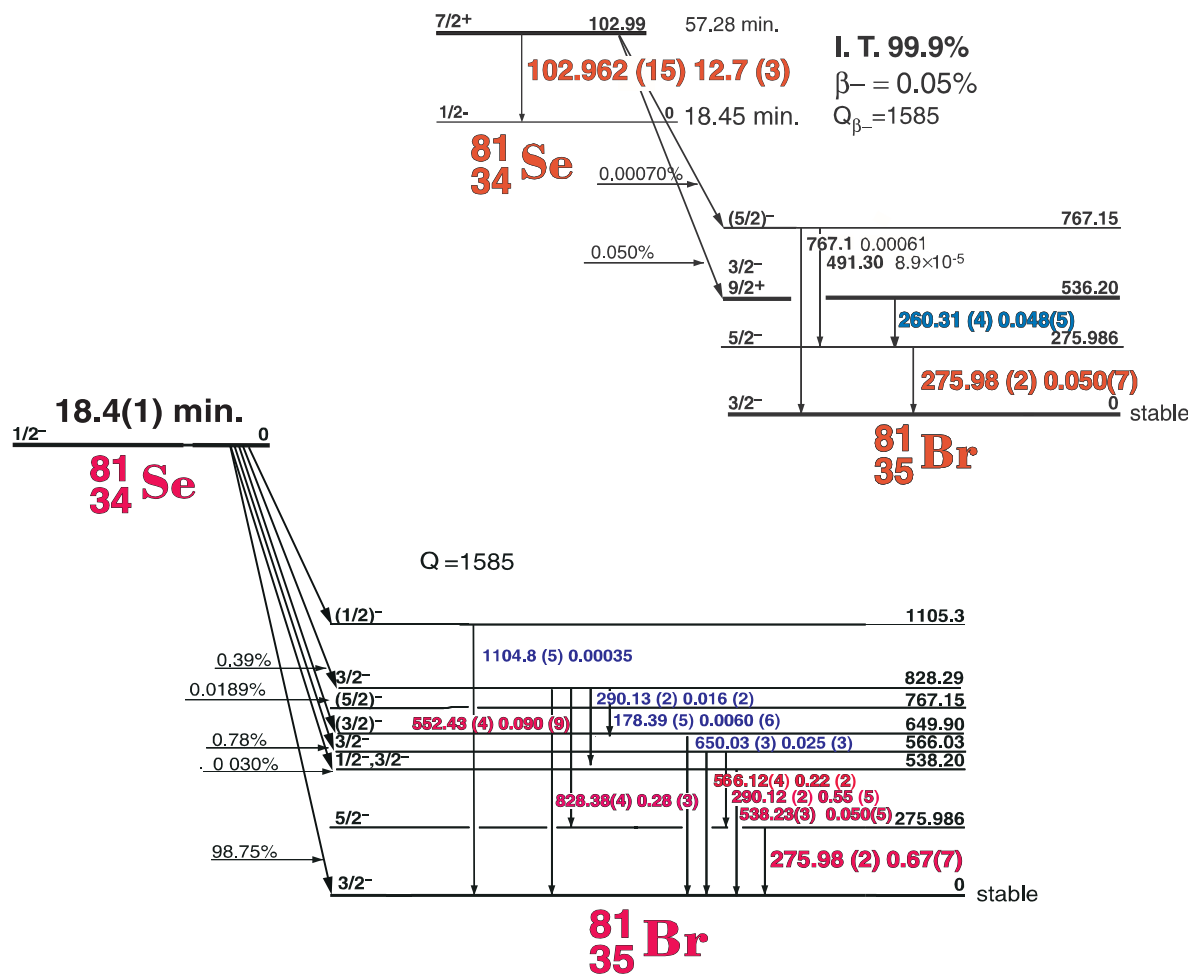
Nuclide **^{75}Se** Half Life 119.779(4) day
Detector 3" x 3" -2 NaI Method of Production: As⁷⁶(n,γ)

E_γ (KeV)[S]	ΔE_γ	I_γ (rel)	$I_\gamma(\%)$ [E]	ΔI_γ	S
66.055	± 0.001	1.9	1.22 ±	0.05	4
96.733	± 0.002	5.4	3.42 ±	0.03	3
121.115	± 0.003	27.4	17.1 ±	0.2	1
136.000	± 0.005	93.1	58.7 ±	0.3	1
198.596	± 0.007	2.44	1.47 ±	0.02	2
264.651	± 0.008	100	58.5 ±	0.3	1
279.528	± 0.008	42.88	24.8 ±	0.2	1
303.913	± 0.007	2.27	1.31 ±	0.01	1
400.646	± 0.009	19.95	11.4 ±	0.1	1
NA					
482.2	± 0.1	0.04	0.0004	± (1)	4
572.5	± 0.1	0.065	0.036	± 0.003	3



Decay Data

57.28 Min. Se^{81m} - 18.45 Min Se⁸¹ Decay Scheme



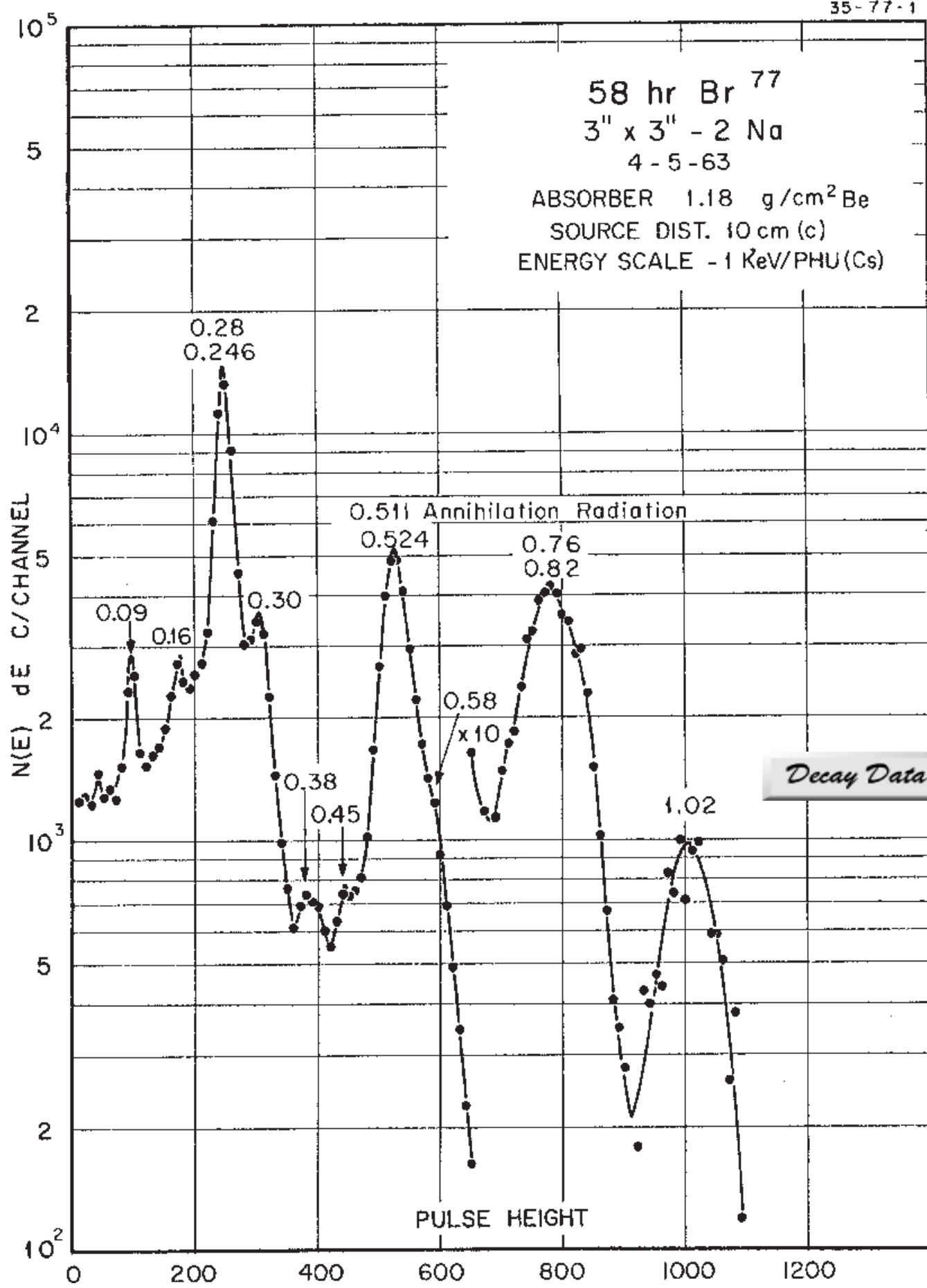
GAMMA-RAY ENERGIES AND INTENSITIES

34-81m (:34-81) -1-1

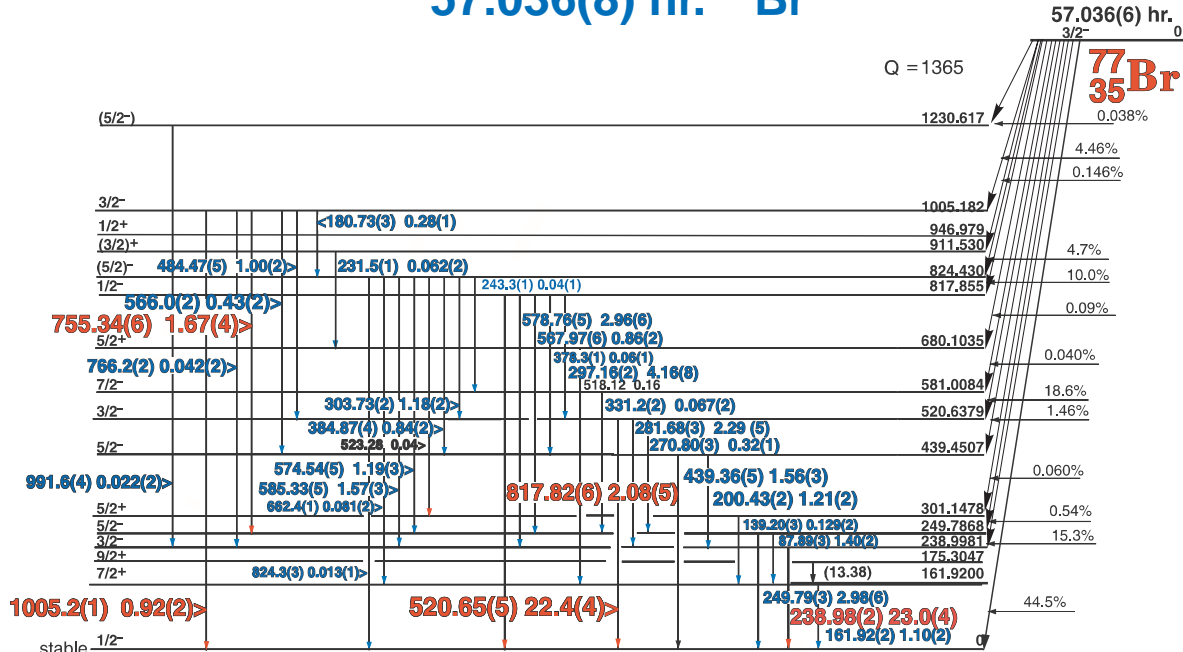
Nuclide Se^{81m} - Se⁸¹
Detector 3" x 3" -2 NaI

Half Life 57.25 Min. - 18.45 Min.
Method of Production: Se⁸⁰(n,γ)

	E_{γ} (KeV)[S]	ΔE_{γ}	I_{γ} (rel)	$I_{\gamma}(\%)$ [E]	ΔI_{γ}	S
^{81m} Se						
I.T.	102.962 260.310	± 0.015 ± 0.040	100 0.90	12.7 0.048	± 5.0 ± 0.005	1 2
⁸¹ Se	275.976	± 0.020	0.90	0.050	± 0.007	3
	178.393 275.976 290.126 538.226 552.434 566.121 650.030 789.1 828.385 1104.8	± 0.02 ± 0.020 ± 0.020 ± 0.03 ± 0.04 ± 0.04 ± 0.03 ± 0.2 ± 0.040 ± 0.5	1.1 100 82.0 8.0 14.8 35.0 4.3 0.33 46.0 0.04	0.0060 0.67 0.55 0.050 0.090 0.22 0.025 0.0020 0.28 0.00035	$\pm (6)$ ± 0.07 ± 0.05 ± 0.005 ± 0.009 ± 0.02 ± 0.003 $\pm (2)$ ± 0.03 $\pm (3)$	4 1 1 1 1 1 2 3 1 4



57.036(8) hr. ^{77}Br



$^{77}_{34}\text{Se}$

GAMMA-RAY ENERGIES AND INTENSITIES

35-77-1

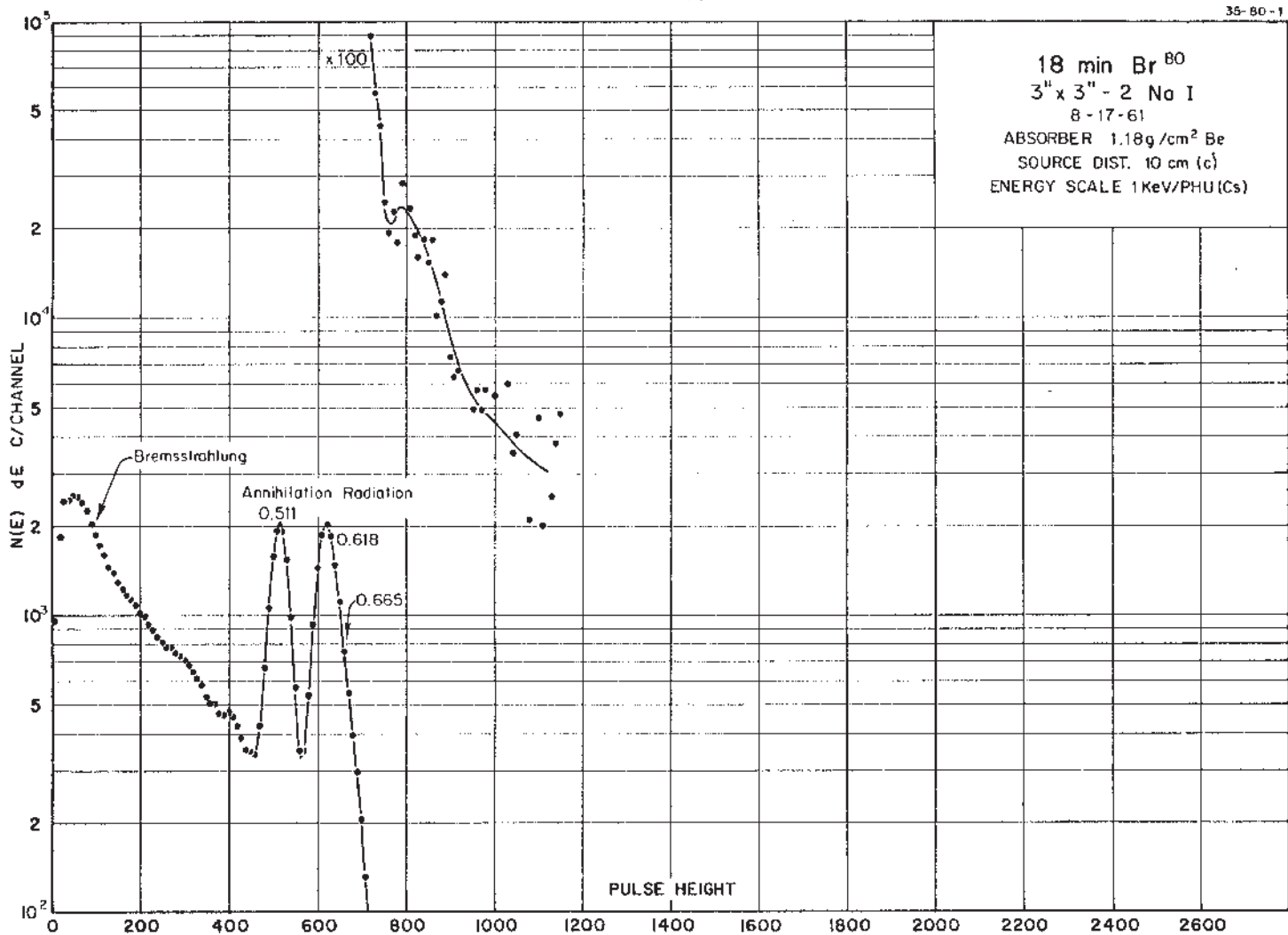
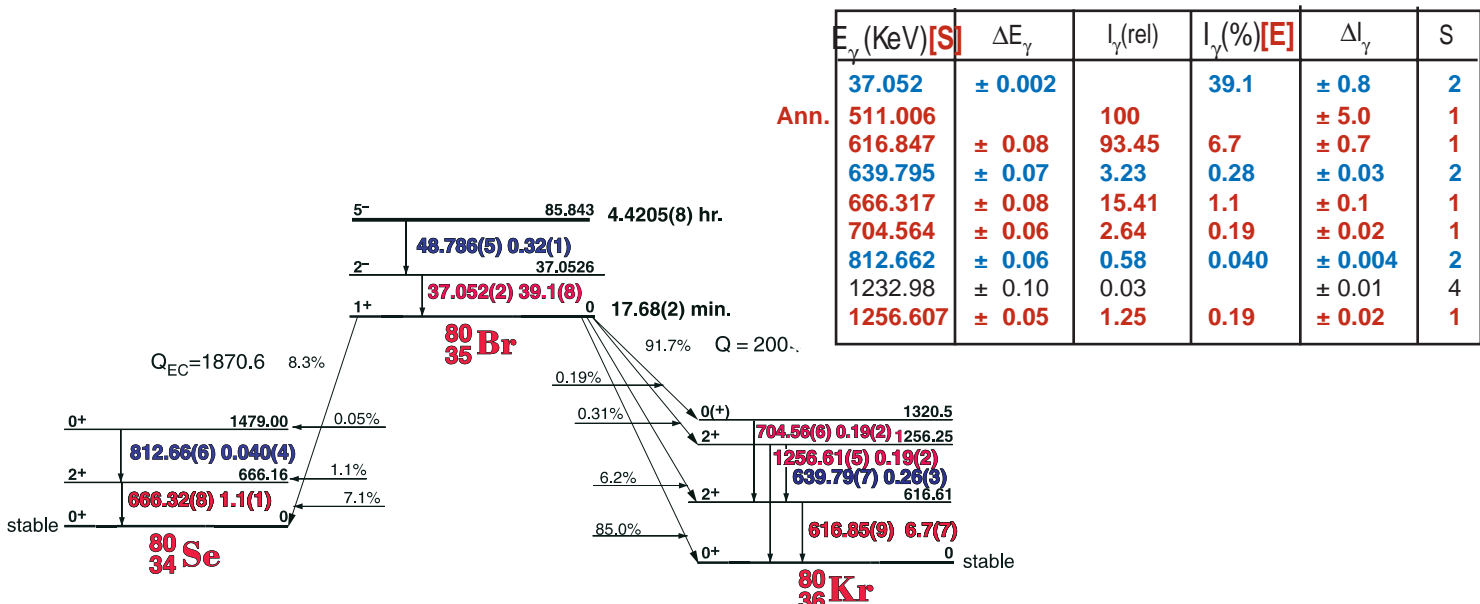
Nuclide ^{77}Br Half Life 57.036(8) hr.
Detector 3" x 3" -2 NaI Method of Production: $\text{Se}^{80}(n,\gamma)$

E_{γ} (KeV) [S]	ΔE_{γ}	I_{γ} (rel)	I_{γ} (%) [E]	ΔI_{γ}	S
87.89	± 0.03	4.7	1.40	± 0.02	2
139.20	± 0.03	0.49	0.129	± 0.002	4
161.92	± 0.02	4.2	1.10	± 0.02	2
180.73	± 0.03	0.96	0.28	± 0.01	3
187.28	± 0.04	0.33	0.08	± 0.01	4
200.43	± 0.02	4.5	1.21	± 0.02	2
231.48	± 0.10	0.15	0.062	± 0.02	4
238.98	± 0.08	7.0	23.0	± 0.4	1
243.35	± 0.10	0.30	0.04	± 0.01	4
249.79	± 0.03	11.0	2.98	± 0.06	2
270.80	± 0.03	1.2	0.32	± 0.01	4
281.68	± 0.03	8.6	2.29	± 0.05	3
297.16	± 0.02	16.0	4.16	± 0.08	2
303.73	± 0.02	4.7	1.18	± 0.02	3
331.2	± 0.2	0.21	0.067	± 0.002	4
378.32	± 0.15	0.31	0.06	± 0.01	4
384.87	± 0.04	3.4	0.84	± 0.02	3
439.36	± 0.05	7.0	1.56	± 0.03	2
484.47	± 0.05	4.2	1.00	± 0.02	2
520.65	± 0.05	100	22.4	± 0.4	1
566.0	± 0.2	2.3	0.43	± 0.02	4
567.97	± 0.06	5.0	0.86	± 0.02	2
574.54	± 0.05	3.3	0.19	± 0.03	2
578.76	± 0.05	12.0	2.96	± 0.06	2
585.33	± 0.05	6.9	1.57	± 0.03	2
655.8	± 0.2	0.17	0.04	± 0.008	4
662.42	± 0.10	0.49	0.081	± 0.002	3
755.34	± 0.06	6.9	1.67	± 0.04	1
766.2	± 0.2	0.19	0.042	± 0.002	4
817.82	± 0.06	9.8	2.08	± 0.05	1
824.3	± 0.3	0.57	0.013	± 0.001	3
842.8	± 0.3	0.19	0.05	± 0.007	3
991.6	± 0.4	0.06	0.022	± 0.002	3
1005.21	± 0.10	4.1	0.92	± 0.02	1

17.68 Min. ^{80}Br

GAMMA-RAY ENERGIES AND INTENSITIES

Nuclide ^{80}Br Half Life 17.68 Min
 Detector 3" X 3" NaI-2 Method of Production: Ge⁷⁶(n, γ)

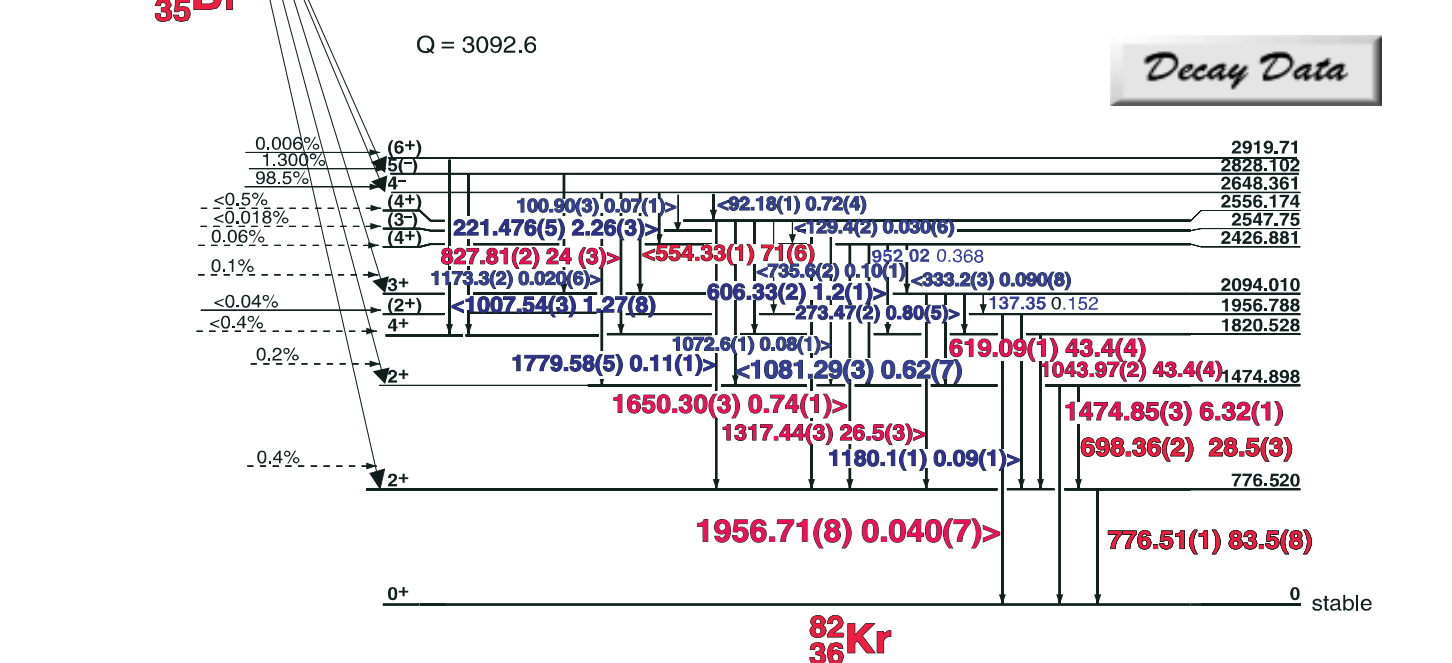


35.30 Hr. ^{82}Br

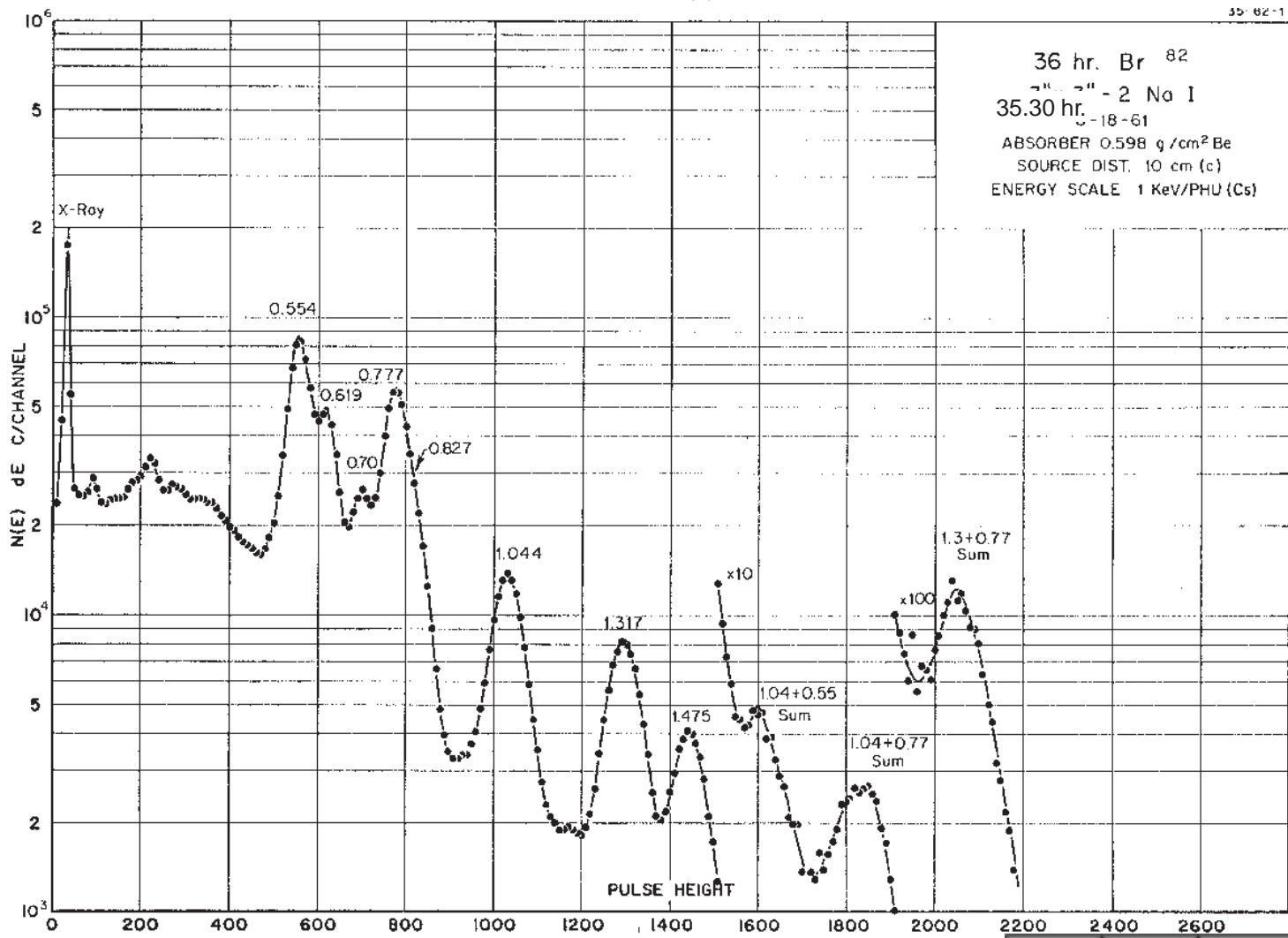
35.30(2) hr.

^{82}Br
35

Br⁸² Decay Scheme



^{82}Kr
36



35.30(2) Hr. ^{82}Br

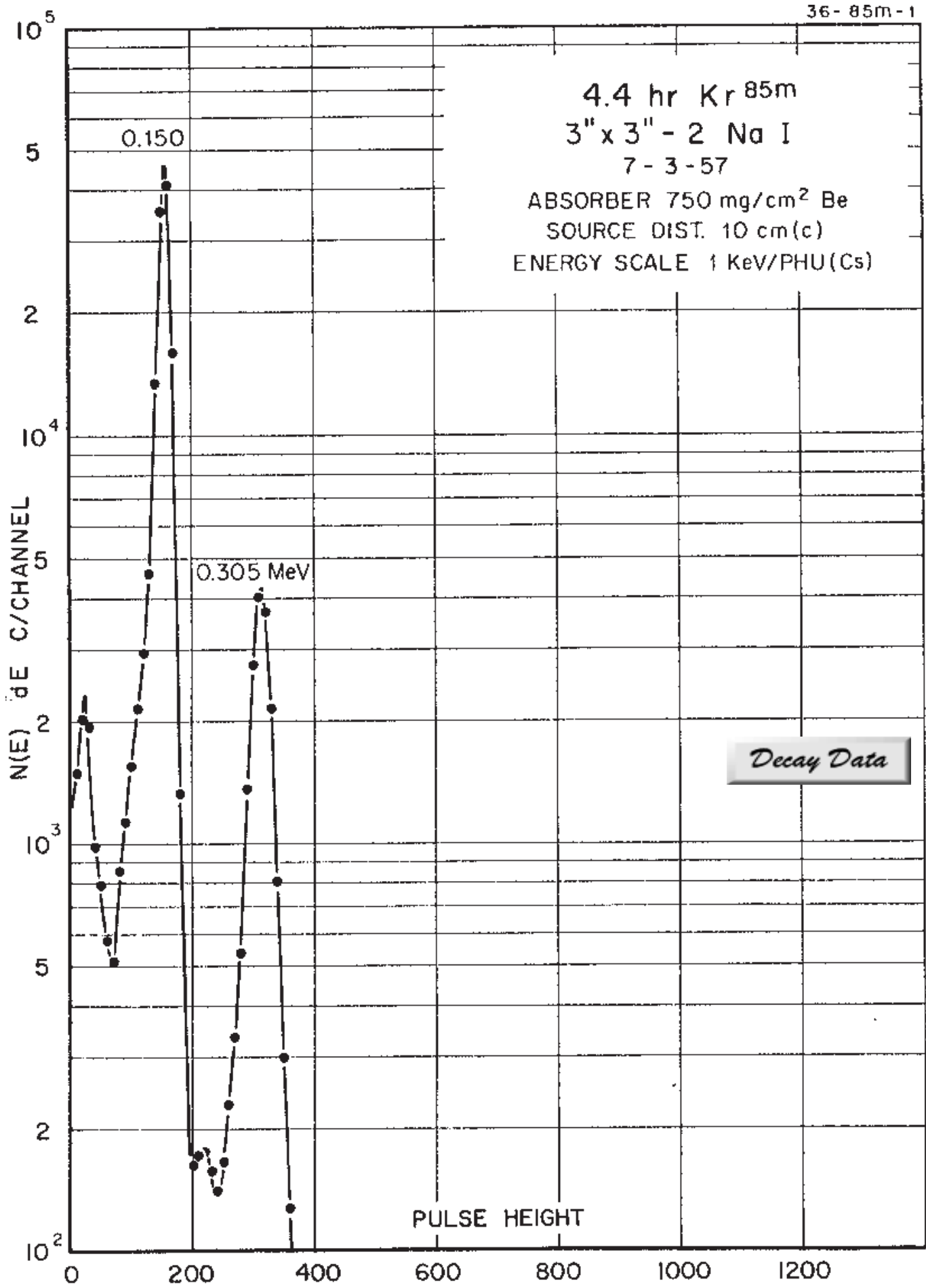
List of Gamma-ray Energies and Intensities

35-82-1

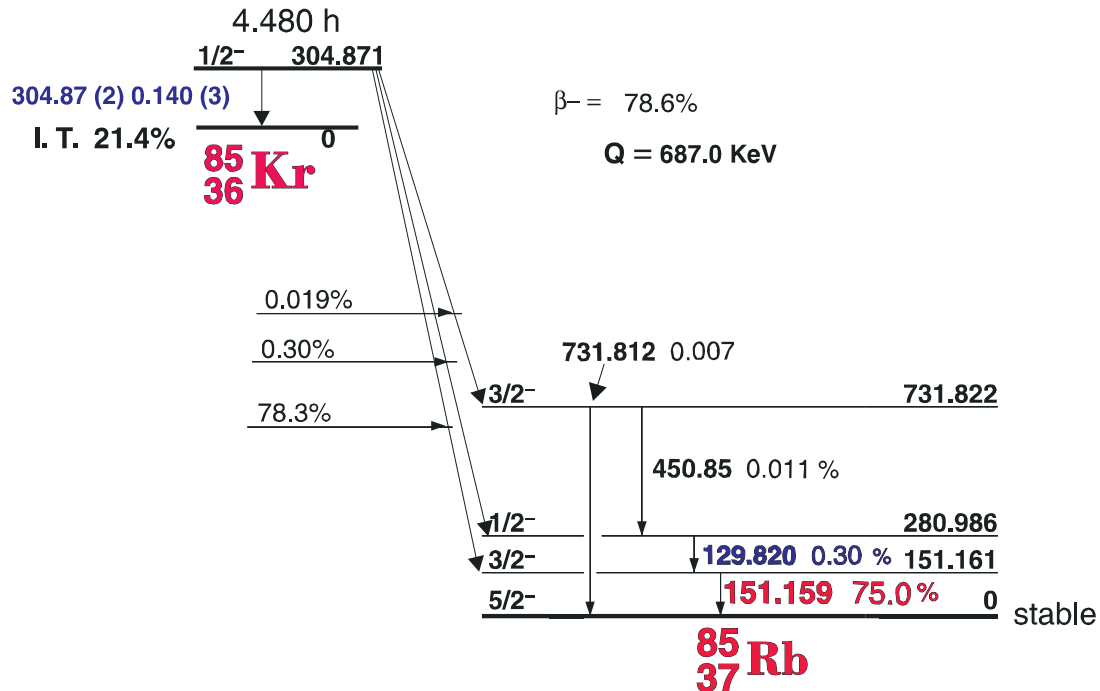
GAMMA-RAY ENERGIES AND INTENSITIES

Nuclide ^{82}Br
 Detector 3" X 3" Nal-2 Half Life 35.30(2) hr.
 Method of Production: $\text{Br}^{81}(\text{n},\gamma)$

E_{γ} (KeV)[S]	ΔE_{γ}	I_{γ} (rel)	$I_{\gamma}(\%)$ [E]	ΔI_{γ}	S
92.183	± 0.008	0.825	0.72	± 0.045	4
100.899	± 0.035	0.075	0.07	± 0.010	5
129.45	± 0.25	0.025	0.030	± 0.006	5
137.23	± 0.04	0.115	0.152	± 0.010	5
221.476	± 0.005	2.72	2.26	± 0.008	3
273.475	± 0.025	0.95	0.80	± 0.05	4
333.2	± 0.3	0.012	0.09	± 0.008	5
401.15	± 0.08	0.179		± 0.028	5
554.334	± 0.012	84.4	70.8	± 1.5	1
606.332	± 0.023	1.47	1.2	± 0.10	4
619.088	± 0.013	52.1	43.4	± 1.0	1
698.359	± 0.016	33.91	28.5	± 0.60	1
735.65	± 0.18	0.087	0.1	± 0.018	5
776.502	± 0.016	100	83.5	± 1.2	1
827.809	± 0.019	29.03	24.03	± 0.35	1
951.950	± 0.035	0.46	0.4	± 0.05	4
1007.542	± 0.034	1.57	1.27	± 0.08	3
1043.973	± 0.022	33.21	27.2	± 0.60	1
1072.63	± 0.12	0.079	0.079	± 0.012	5
1081.288	± 0.030	0.78	0.618	± 0.07	4
1173.30	± 0.25	0.131	0.02	± 0.006	5
1180.13	± 0.10	0.183	0.086	± 0.01	5
1317.440	± 0.028	32.6	26.48	± 0.8	1
1474.853	± 0.031	19.7	6.32	± 0.4	1
1650.296	± 0.034	0.90	0.74	± 0.01	1
1779.58	± 0.05	0.140	0.114	± 0.010	2
1956.711	± 0.081	0.054	0.04	± 0.007	2



4.480(8) hr. ^{85m}Kr Decay Scheme



36-85m-1

GAMMA-RAY ENERGIES AND INTENSITIES

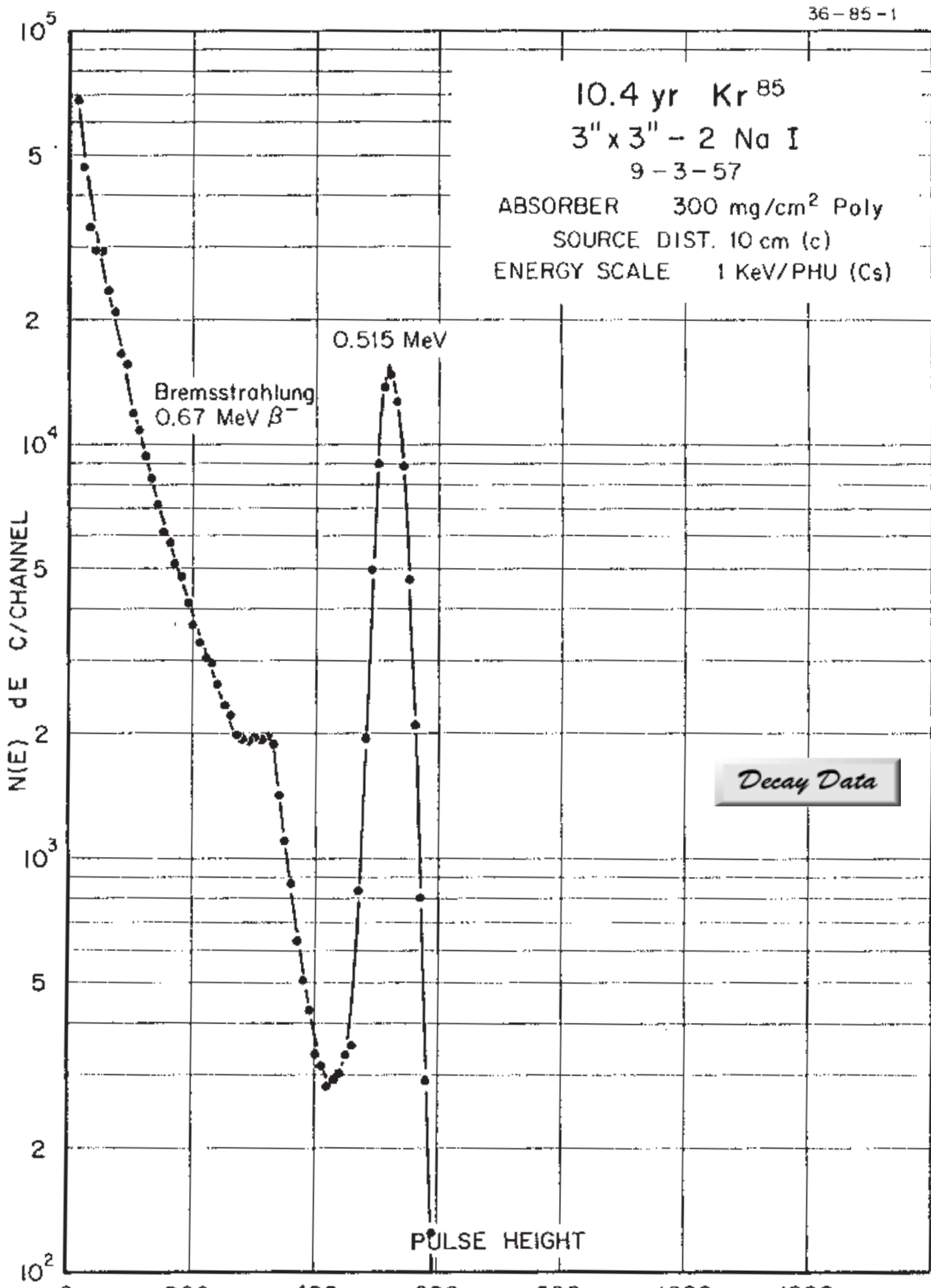
Nuclide
Detector

^{85m}Kr
3" x 3" -2 Nal

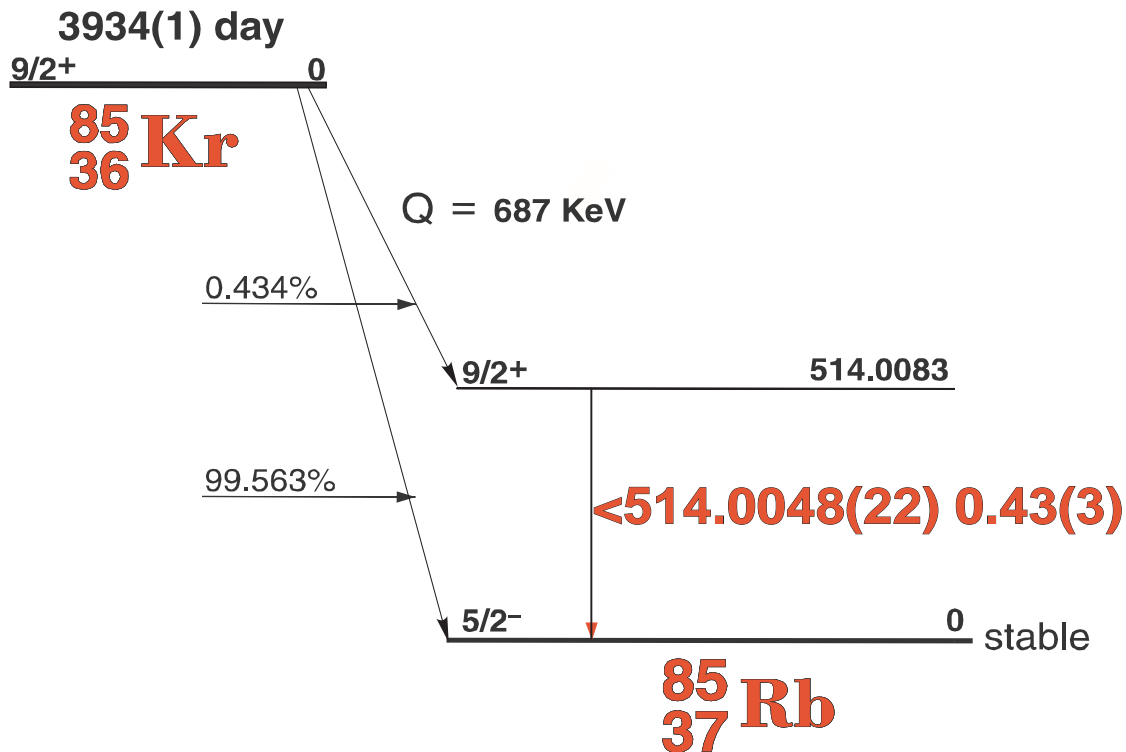
Half Life 4.480(8) hr
Method of Production: $\text{Kr}^{84}(n,\gamma)$

^{85m}Kr I. T.

E_γ (KeV)[S]	ΔE_γ	I_γ (rel)	$I_\gamma(\%)[E]$	ΔI_γ	S
129.820	± 0.02		0.3		2
151.159	± 0.02		75	± 1.0	1
304.87	± 0.05		15		1
450.85	± 0.05		0.01	± 0.01	4
731.812	± 0.02		0.007		4



10.76(1) Yr. ^{85}Kr Decay Scheme [C]

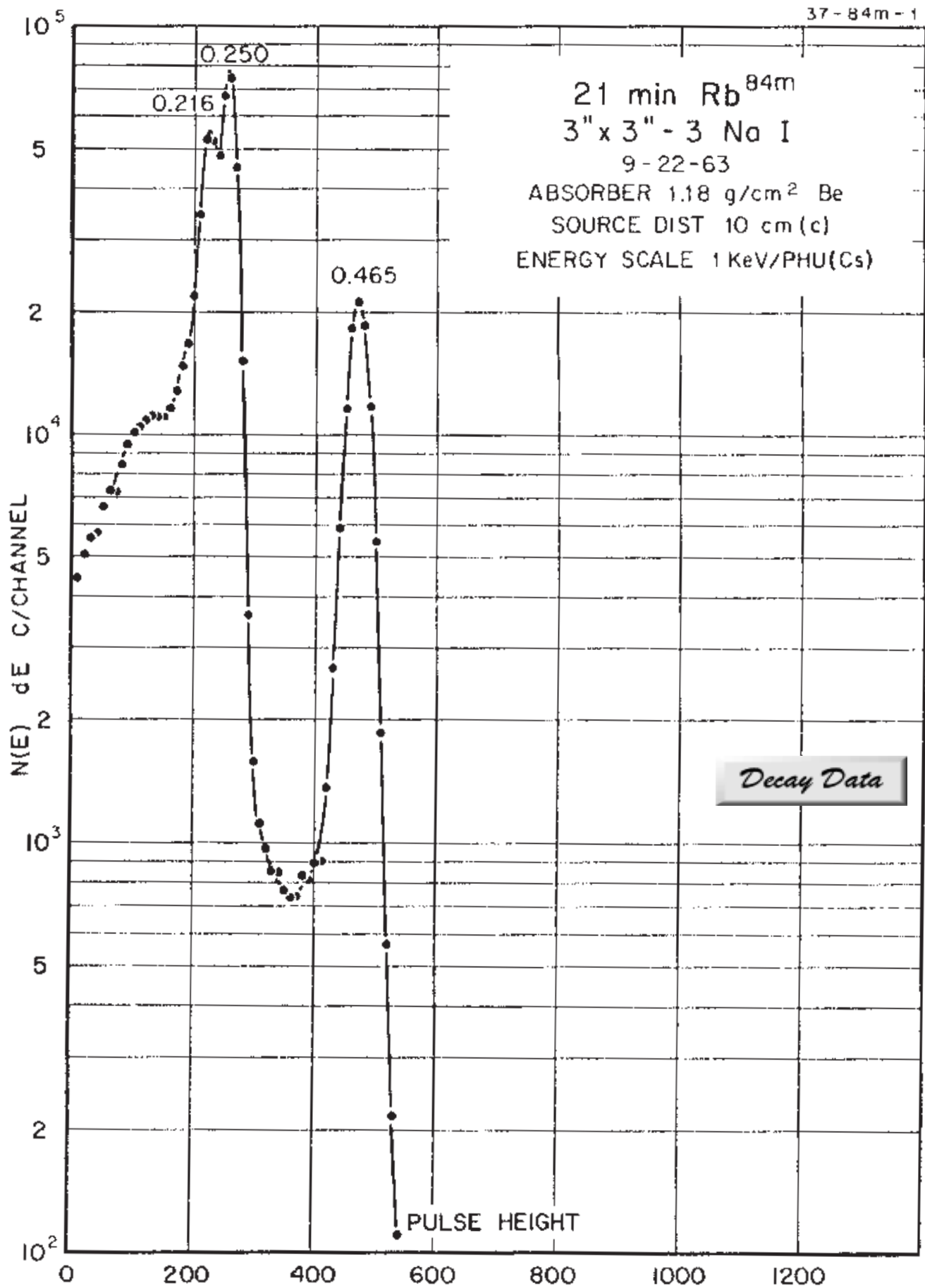


36-85-1

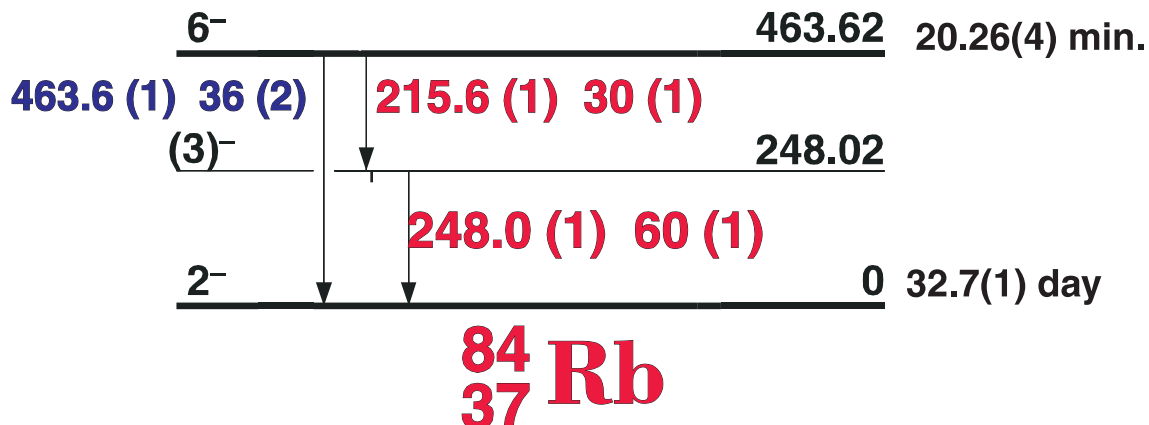
GAMMA-RAY ENERGIES AND INTENSITIES

Nuclide ^{85}Kr Half Life 10.76(1) yr.
Detector 3" x 3" -2 Nal Method of Production: $\text{Kr}^{85}(n,\gamma)$

E_γ (KeV)[S]	ΔE_γ	I_γ (rel)	$I_\gamma(\%)$ [E]	ΔI_γ	S
514.0048	± 0.0022	100	0.43	± 0.03	1



20.26(4) min. ^{84m}Rb Decay Scheme

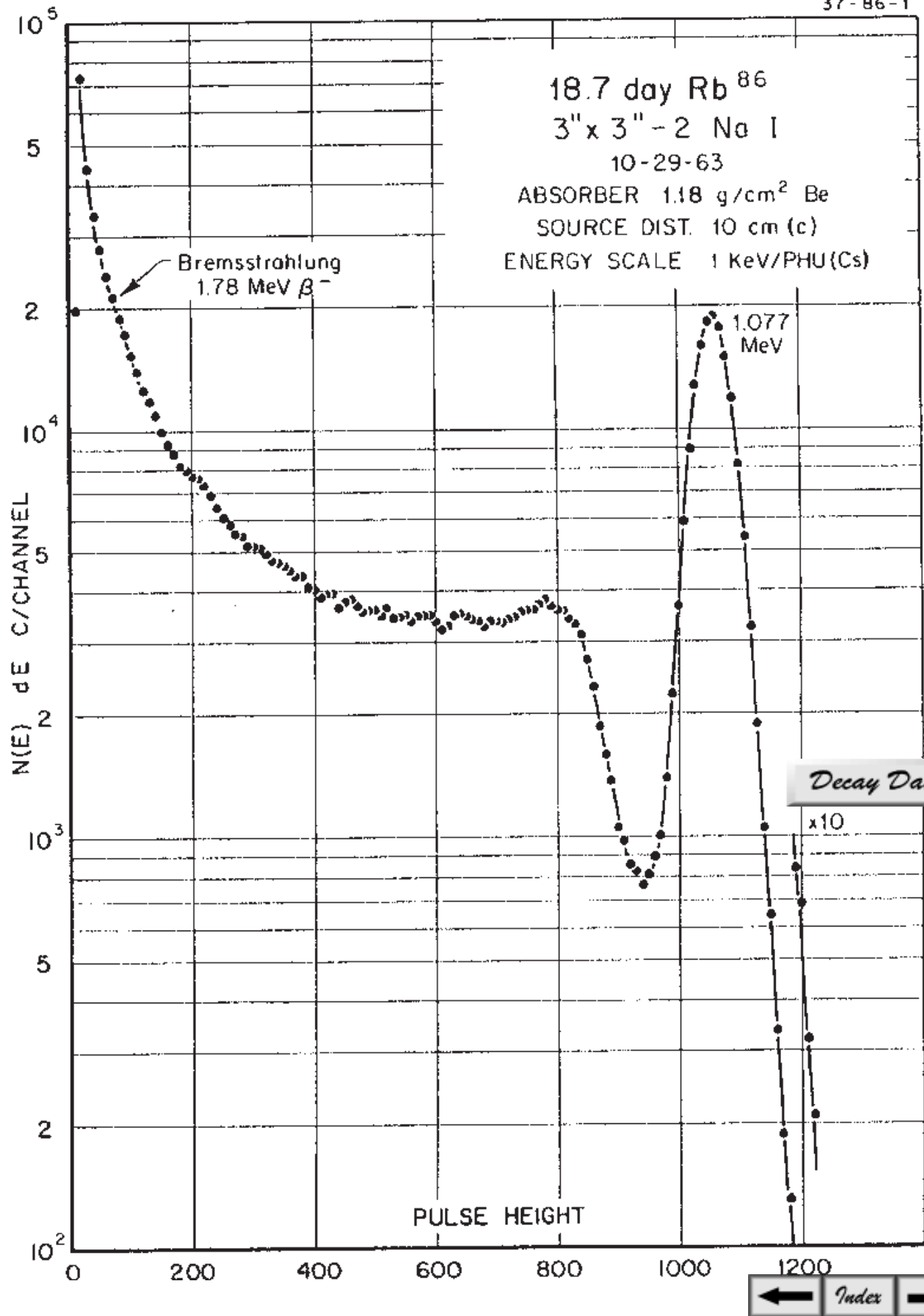


37-84-1

GAMMA-RAY ENERGIES AND INTENSITIES

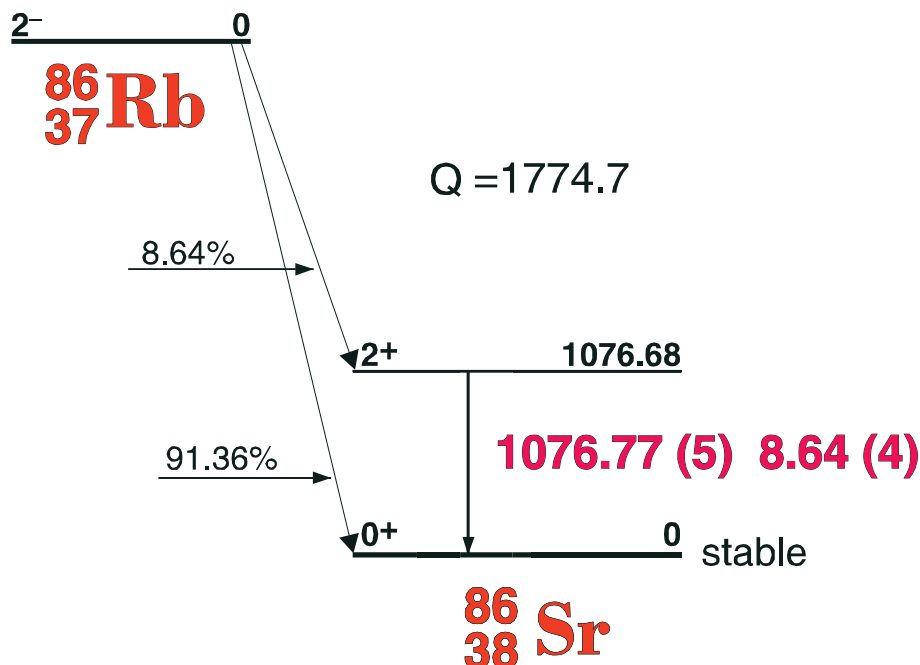
Nuclide ^{84m}Rb Half Life 20.26(4) min.
Detector 3" x 3" -2 NaI Method of Production: $\text{Rb}^{85}(\gamma, n)$

E_γ (KeV)[S]	ΔE_γ	I_γ (rel)	$I_\gamma(\%)$ [E]	ΔI_γ	S
215.61	± 0.05	49	30	± 1	1
248.02	± 0.05	100	60	± 1	1
463.62	± 0.05	60	36	± 2	1



18.63(2) day ^{86}Rb Decay Scheme

18.63(2) day



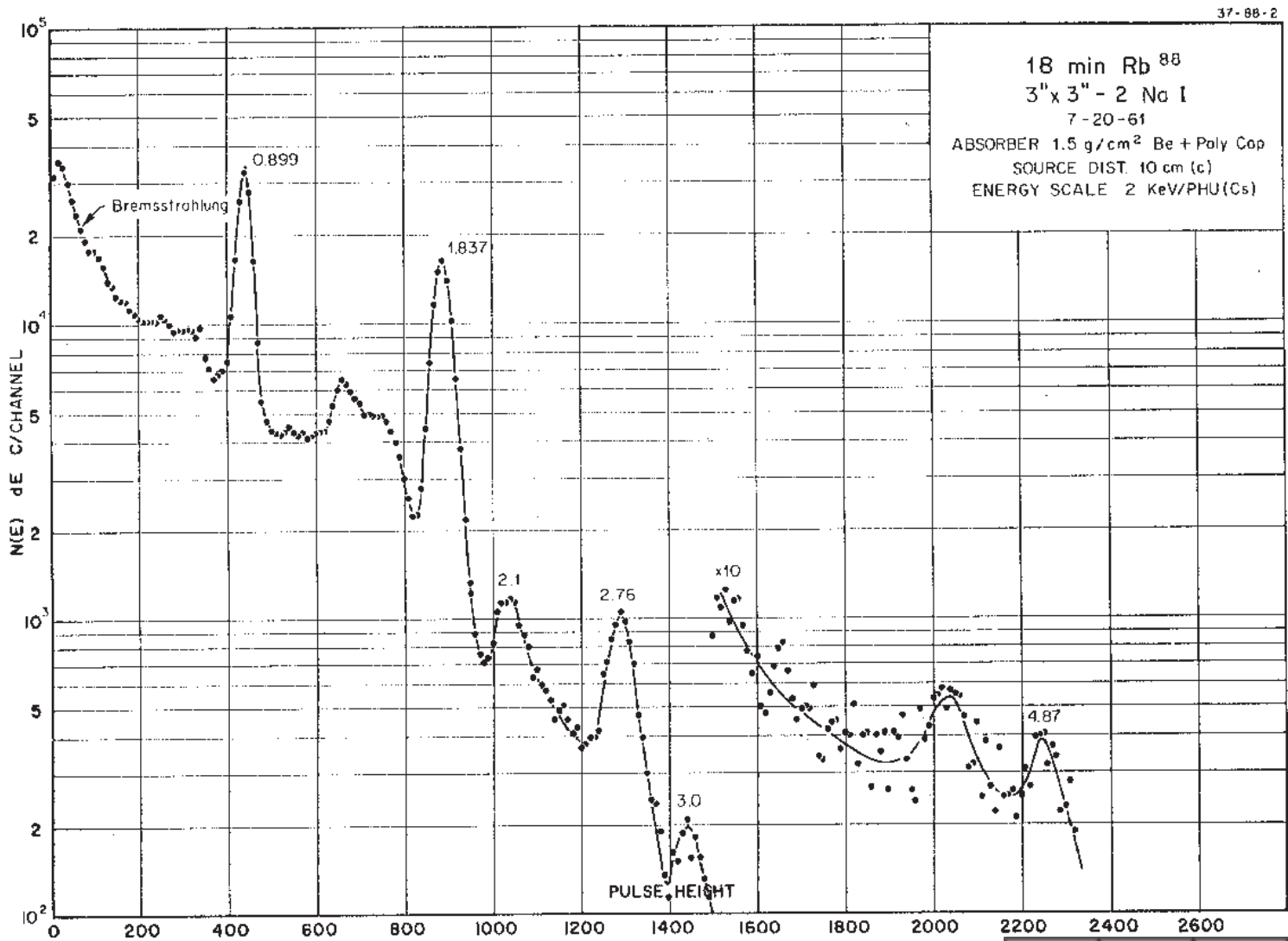
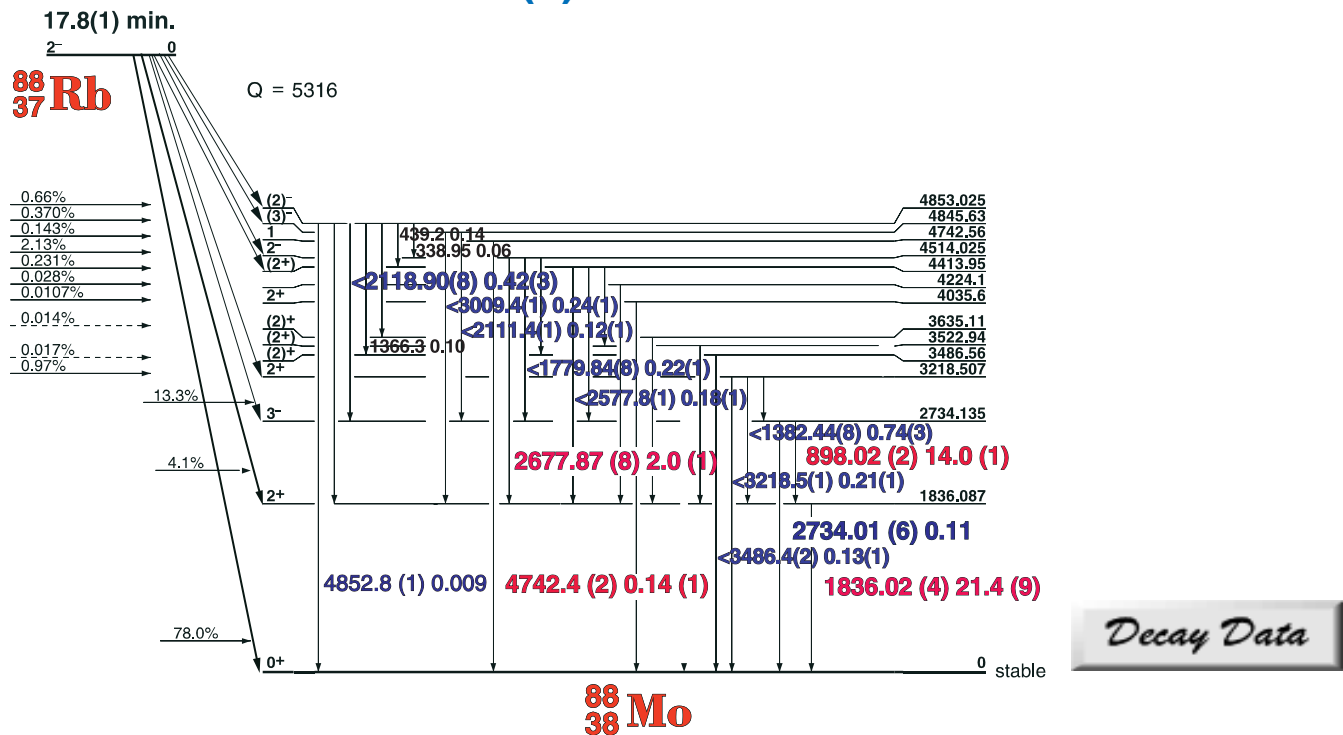
37-86-1

GAMMA-RAY ENERGIES AND INTENSITIES

Nuclide Detector	^{86}Rb 3" x 3" -2 Nal	Half Life 18.63(2) day Method of Production: $\text{Rb}^{85}(\text{n},\gamma)$
---------------------	------------------------------------	---

E_γ (KeV)[S]	ΔE_γ	I_γ (rel)	I_γ (%)[E]	ΔI_γ	S
1076.77	± 0.05	100	8.64	± 0.08	1

17.8(1) Min. ^{88}Rb



17.8(1) min. ^{88}Rb

List of Gamma-ray Energies and Intensities

37-88-1

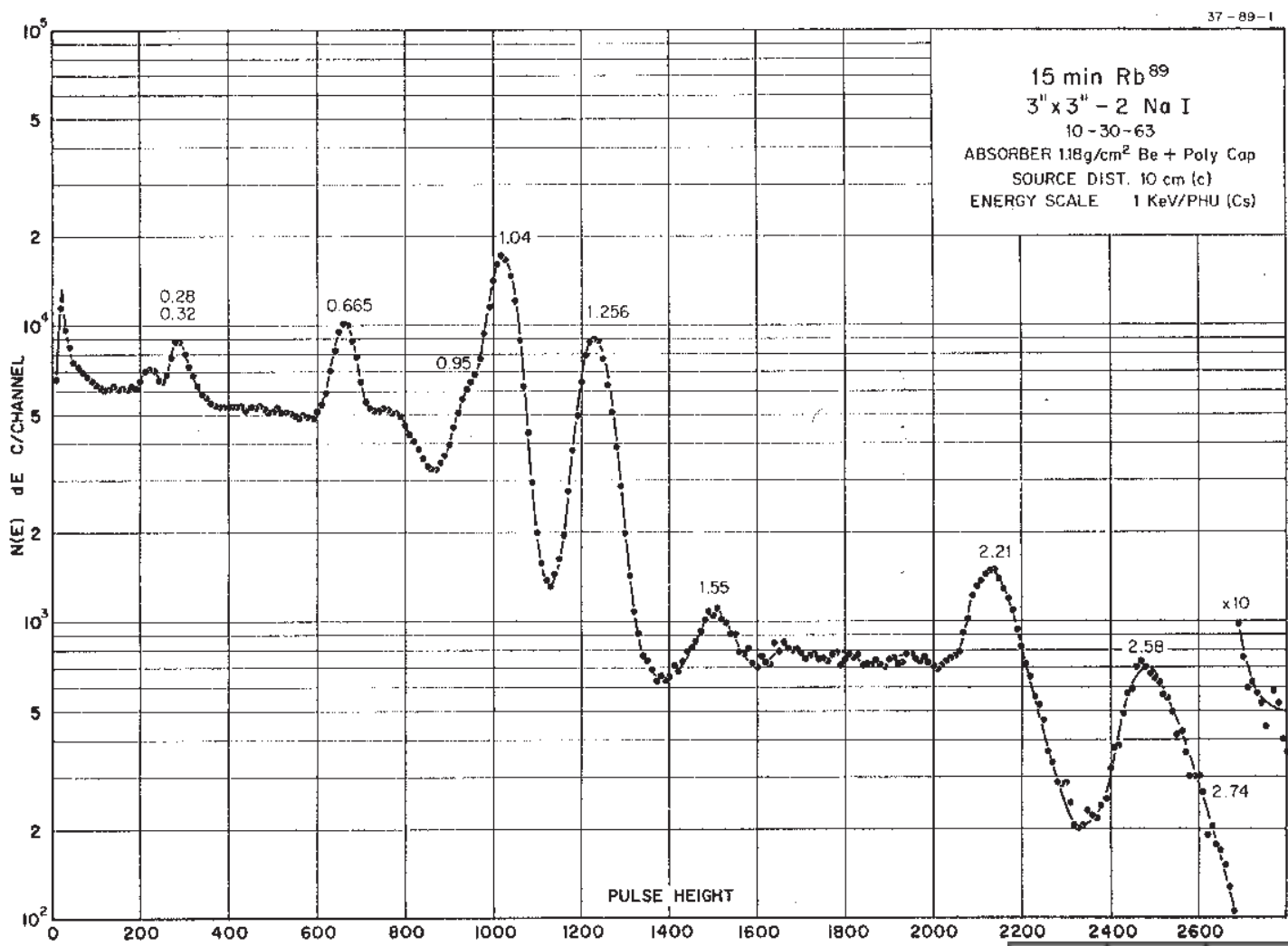
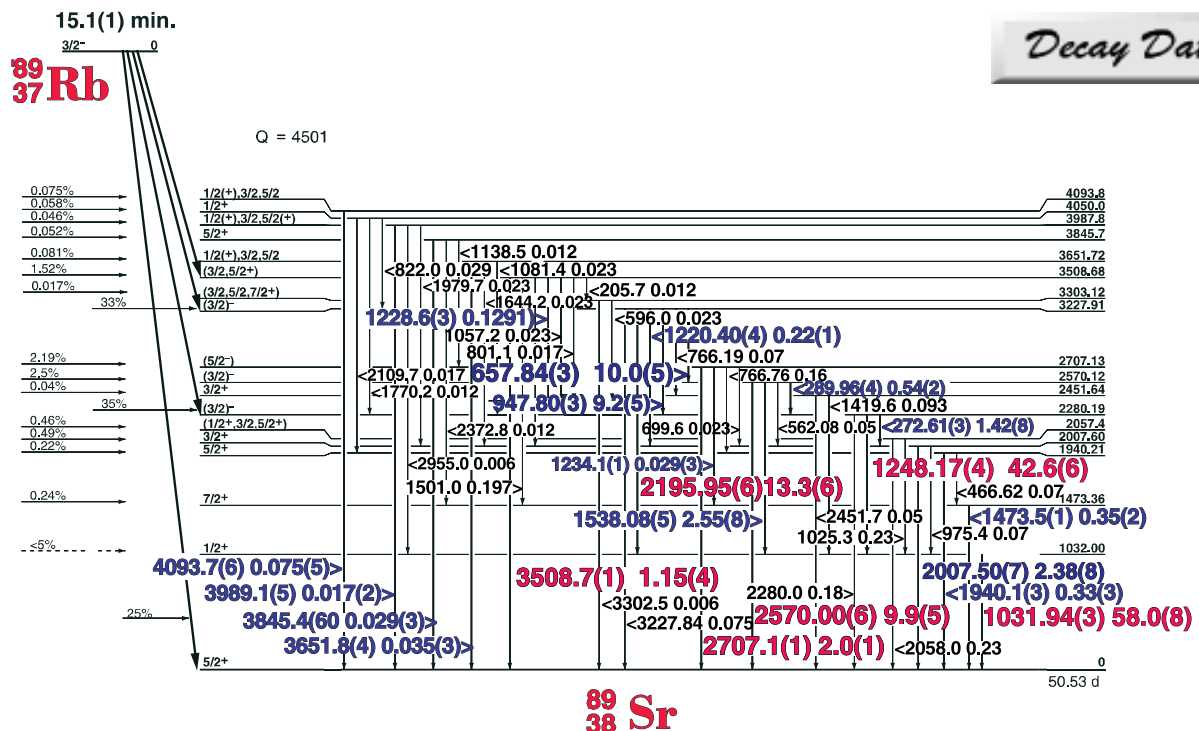
GAMMA-RAY ENERGIES AND INTENSITIES

Nuclide ^{88}Rb
Detector 3" X 3" NaI-2

Half Life 17.8(1) min.
Method of Production: Rb⁸⁷(n,γ)

	E_{γ} (KeV)[S]	ΔE_{γ}	I_{γ} (rel)	$I_{\gamma}(\%)[E]$	ΔI_{γ}	S
	338.5	± 1.0	0.25	0.06	± 0.02	4
	484.5	± 0.2	0.16	0.028	± 0.01	4
Ann.	511.006					3
DE	814.16	± 0.04				3
	898.021	± 0.019	61.4	14.0	± 0.02	1
DE	1097.8	± 0.4				4
SE	1325.03	± 0.08				4
	1366.72	± 0.25	0.39	0.11	± 0.02	4
	1382.44	± 0.08	3.2	0.70	± 0.03	3
DE	1656.15	± 0.15				4
	1779.84	± 0.08	1.03	0.21	± 0.01	4
	1836.017	± 0.04	100	21.4	± 1.2	1
DE	1987.61	± 0.15				4
	2111.43	± 0.15	0.60	0.12	± 0.04	4
SE	2118.90	± 0.08	2.07	0.42	± 0.12	3
SE	2166.80	± 0.08				3
SE	2196.86	± 0.15				4
	2390.7	± 0.5	0.15	0.03	± 0.01	4
DE	2464.44	± 0.2				4
SE	2498.0	± 0.4				4
	2577.78	± 0.1	0.98		± 0.06	4
SE	2677.87	± 0.10	9.4	2.0	± 0.4	1
	2707.71	± 0.25				4
SE	2734.015	± 0.060	0.47	0.11	± 0.02	3
SE	2975.2	± 0.3				4
	3009.45	± 0.14	1.25	0.244	± 0.01	2
	3218.50	± 0.08	1.08	0.21	± 0.06	2
	3486.40	± 0.15	0.65	0.13	± 0.03	2
DE	3720.73	± 0.15				1
SE	4231.33	± 0.30				2
SE	4341.9	± 0.8				4
	4742.40	± 0.15	0.78	0.14	0.03	1
	4852.81	± 0.15	0.054	0.009	0.003	3

15.1(1) Min. ^{89}Rb



15.1(1) Min. ^{89}Rb

List of Gamma-ray Energies and Intensities

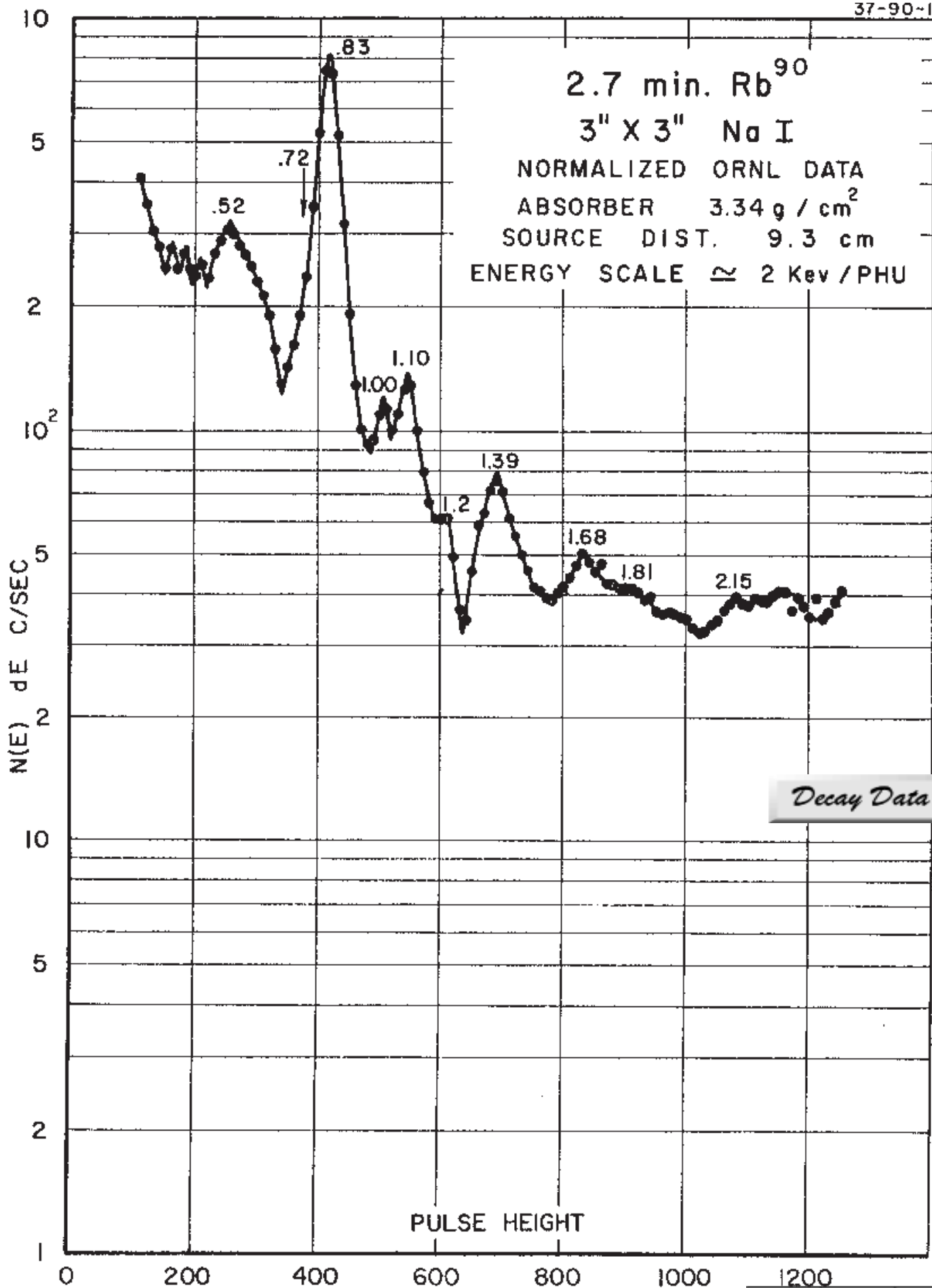
37-89-1

GAMMA-RAY ENERGIES AND INTENSITIES

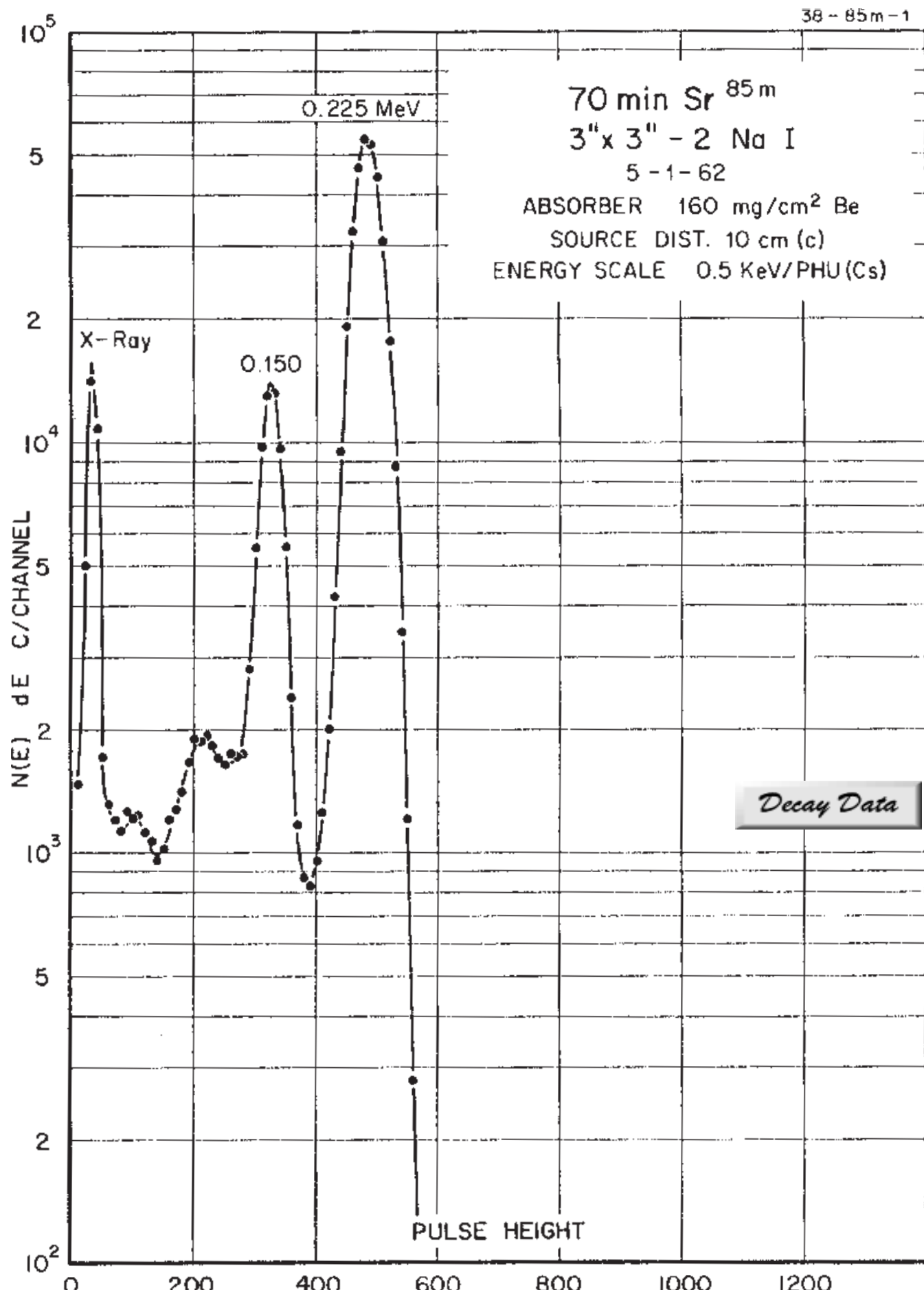
Nuclide ^{89}Rb
Detector 3" X 3" NaI-2

Half Life 15.1(1) min.
Method of Production: U $^{235}(\text{n},\text{f})$

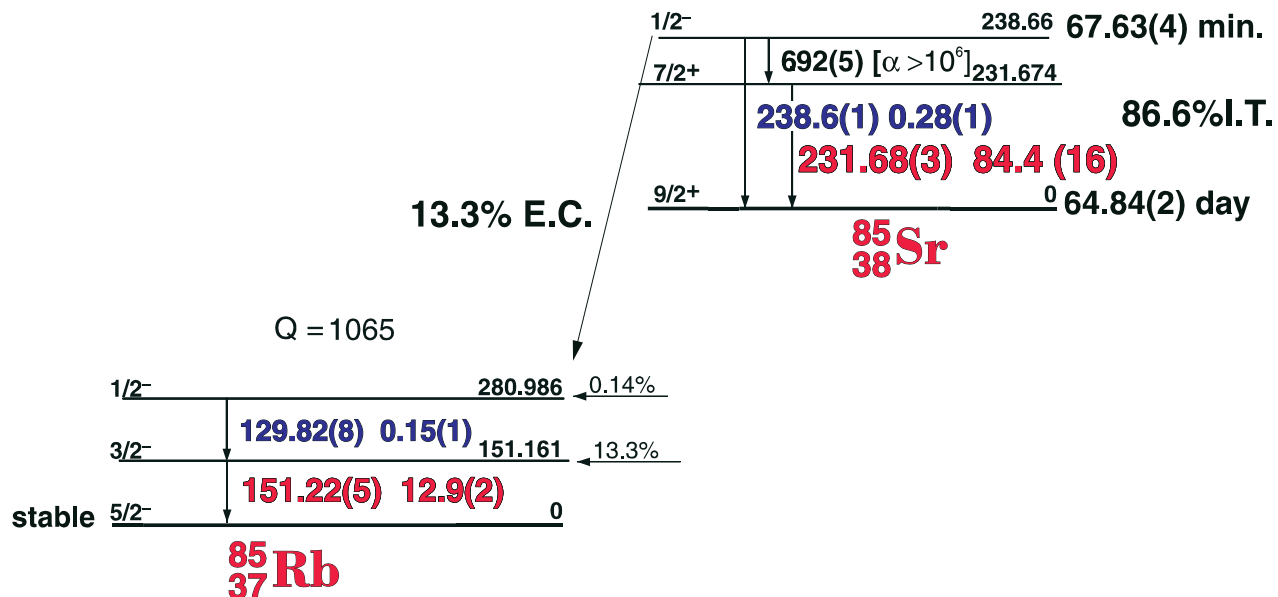
	E_{γ} (KeV)[S]	ΔE_{γ}	I_{γ} (rel)	$I_{\gamma}(\%)[E]$	ΔI_{γ}	S
DE	272.606	± 0.030	2.4	1.42	± 0.02	3
	289.957	± 0.040	0.96	0.54	± 0.02	3
	657.845	± 0.030	16.8	10	± 0.6	2
	947.800	± 0.030	15.9	9.2	± 0.5	2
	1031.940	± 0.030	100	58	± 3.0	1
	1173.0					3
	1220.403	± 0.040	0.38	0.22	± 0.02	4
	1228.6	± 0.3	0.21	0.12	± 0.01	4
	1234.1	± 0.1	0.06	0.03	± 0.002	4
	1248.17	± 0.045	71.2	43	± 2.0	1
DE	1473.58	± 0.15	0.60	0.35	± 0.02	4
	1501.04	± 0.20	0.42	0.20	± 0.01	5
NA	1538.083	± 0.050	4.2	2.6	± 0.1	2
	1548.0					3
DE	1684.0					3
NA	1940.08	± 0.30	0.56		± 0.07	4
	2007.496	± 0.070	4.1	2.4	± 0.1	2
DE	2195.957	± 0.060	23.7	13.3	± 0.6	1
	2486.0					3
SE	2570.054	± 0.060	16.1	9.9	± 0.5	1
	2707.07	± 0.10	3.43	2.0	± 0.1	1
SE	2997.0					2
	3508.9	± 0.1	1.8	1.2	± 0.06	1
	3651.8	± 0.4	0.06	0.04	± 0.01	3
	3845.4	± 0.6	0.05	0.03	± 0.01	3
	3989.1	± 0.5	0.03	0.02	± 0.001	4
	4093.7	± 0.6	0.13	0.08	± 0.004	3



258(4) sec. ^{90m}Rb - 158(5) sec. ^{90}Rb Decay Scheme



67.63(4) min. ^{85m}Sr Decay Scheme

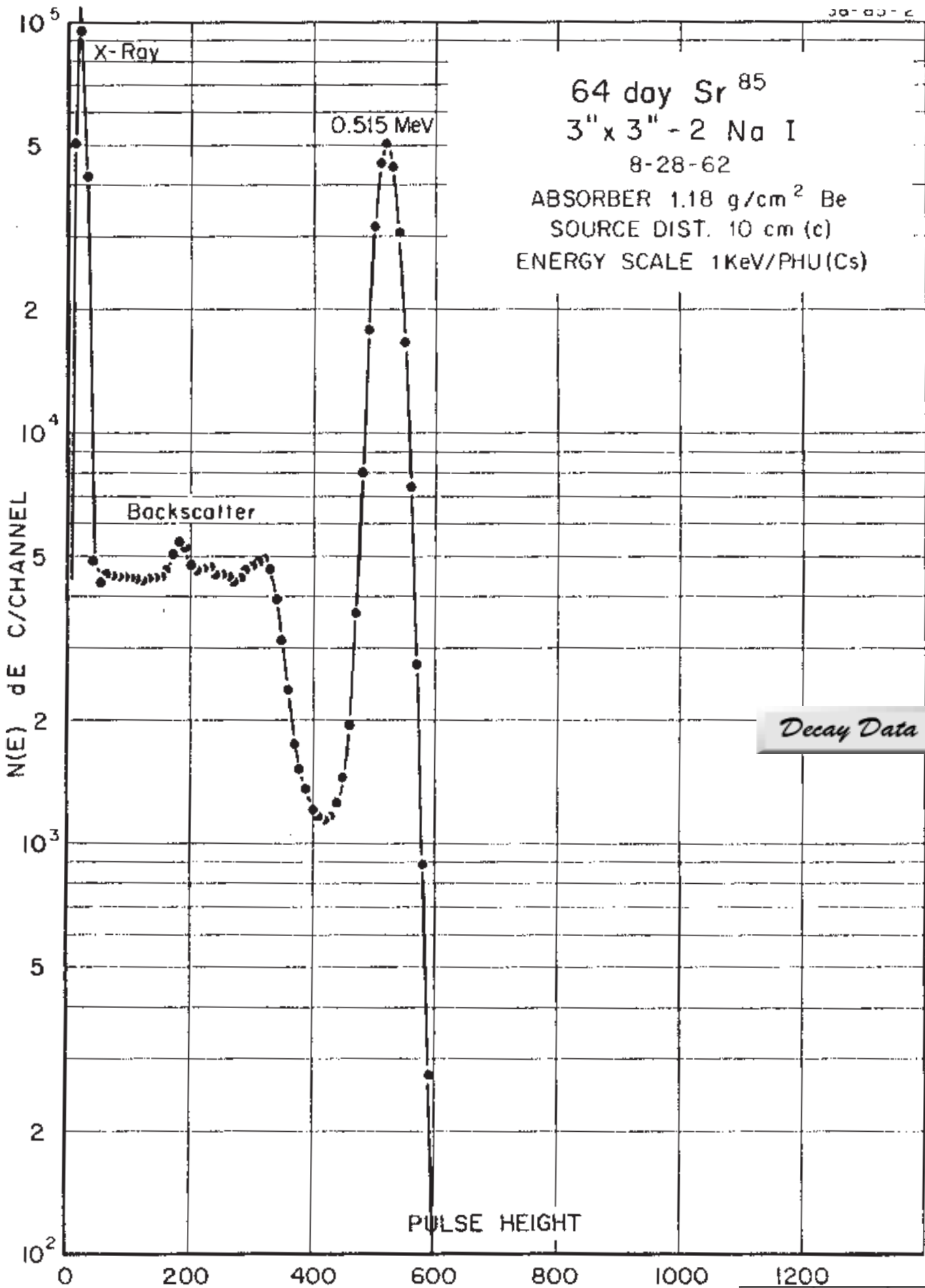


38-85m-1

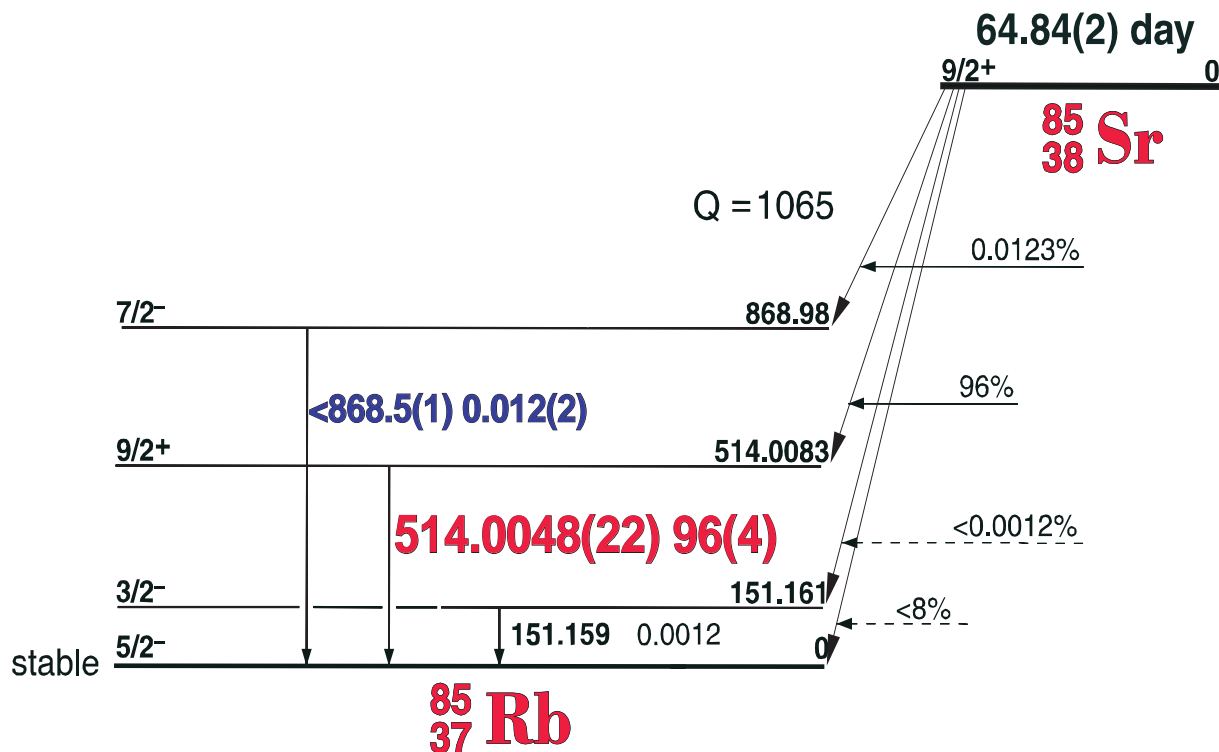
GAMMA-RAY ENERGIES AND INTENSITIES

Nuclide ^{85m}Sr Half Life 67.63(4) min.
Detector 3" x 3" -2 NaI Method of Production: $\text{Sr}^{84}(n,\gamma)$

E_γ (KeV)[S]	ΔE_γ	I_γ (rel)	$I_\gamma(\%)$ [E]	ΔI_γ	S
151.22	± 0.05	8.6	12.9	± 0.1	1
231.684	± 0.030	100	86.6	± 0.1	1
238.65	± 0.015	0.5	0.5	± 0.05	3
450.85	± 0.05		0.01		
731.81	± 0.05		0.015		



64.84(2) day ^{85}Sr Decay Scheme [C]

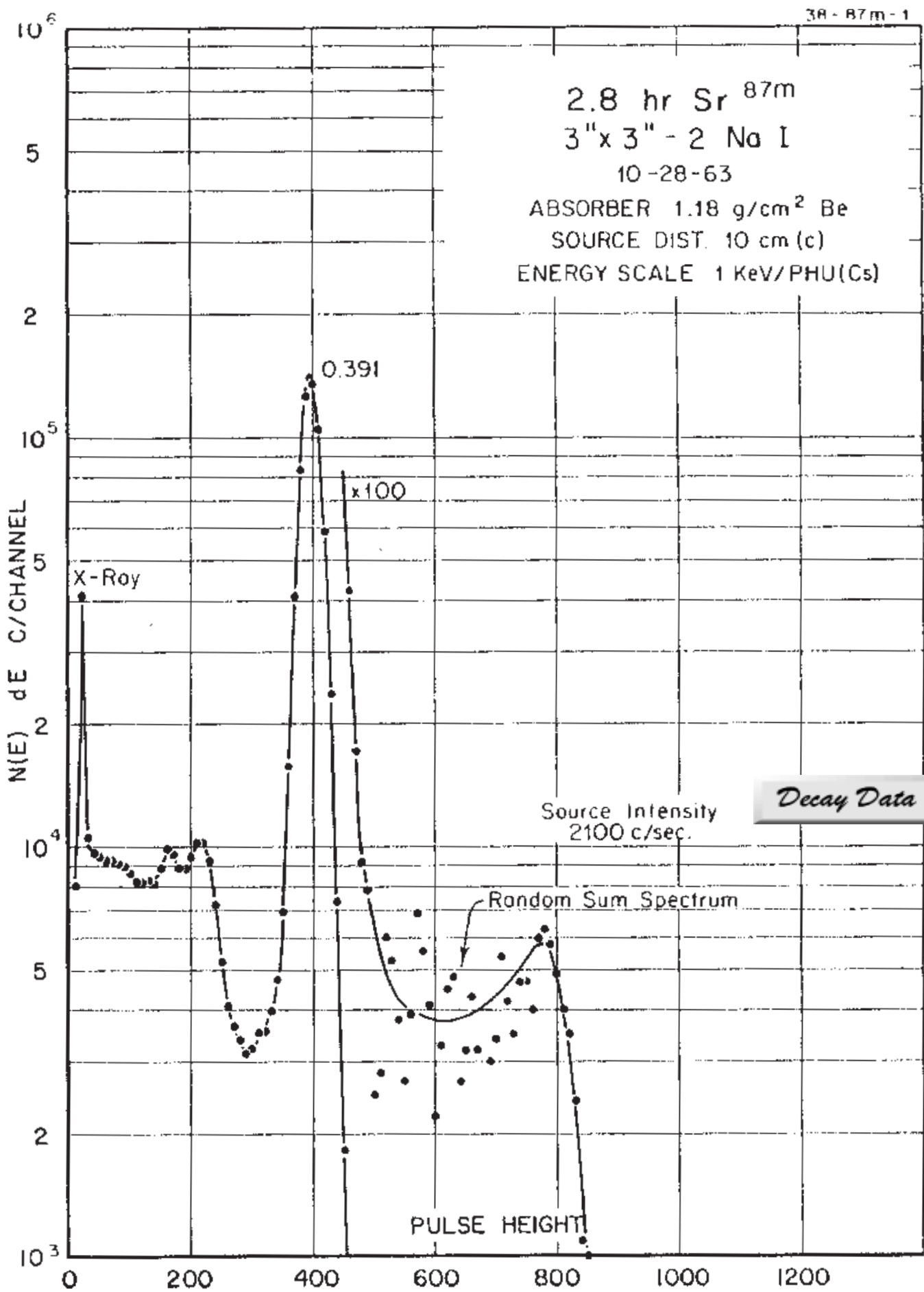


38-85-1

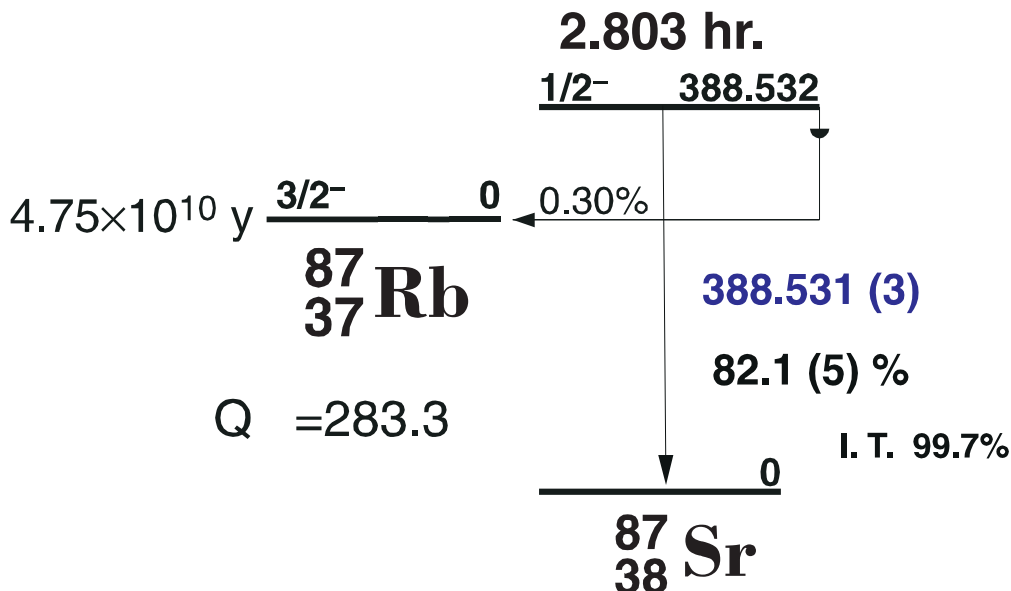
GAMMA-RAY ENERGIES AND INTENSITIES

Nuclide ^{85}Sr Half Life 64.84(2) day
Detector 3" x 3" -2 Nal Method of Production: Rb⁸⁵ (p,n)

E_γ (KeV)[S]	ΔE_γ	I_γ (rel)	$I_\gamma(\%)$ [E]	ΔI_γ	S
514.0048	± 0.0022	100	96	± 0.05	1



2.827(1) hr. ^{87m}Sr Decay Scheme



38-87m-1

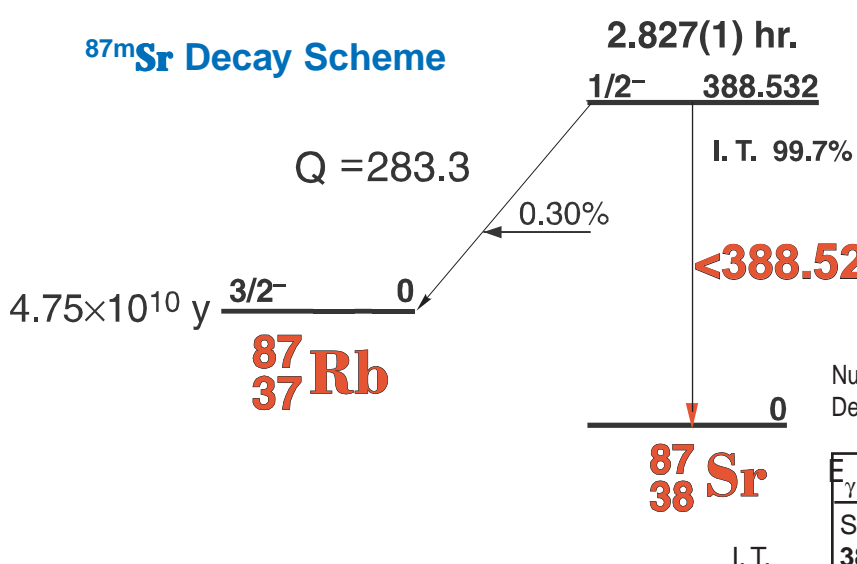
GAMMA-RAY ENERGIES AND INTENSITIES

Nuclide	^{87m}Sr	Half Life 2.827(1) hr. Method of Production: $\text{Sr}^{86}(n,\gamma)$
Detector	3" x 3" -2 Nal	

	E_γ (KeV)[S]	ΔE_γ	I_γ (rel)	$I_\gamma(\%)$ [E]	ΔI_γ	S
I. T.	Sr K x-rays from internal conversion 388.531	± 0.003	100	82.1	± 0.5	1

2.803 Hr. ^{87m}Sr

^{87m}Sr Decay Scheme



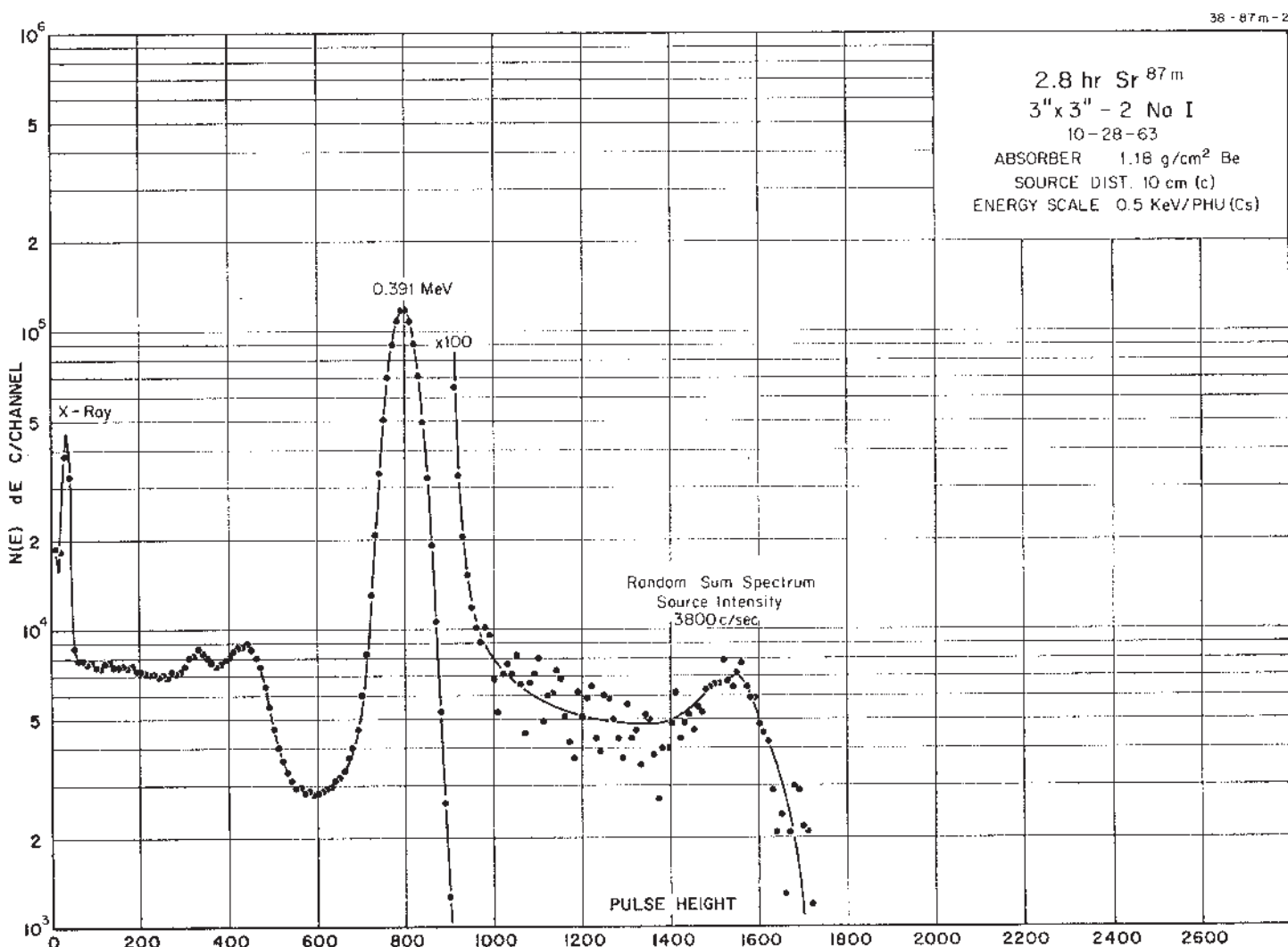
<388.52(2) 82.1(5)

GAMMA-RAY ENERGIES AND INTENSITIES

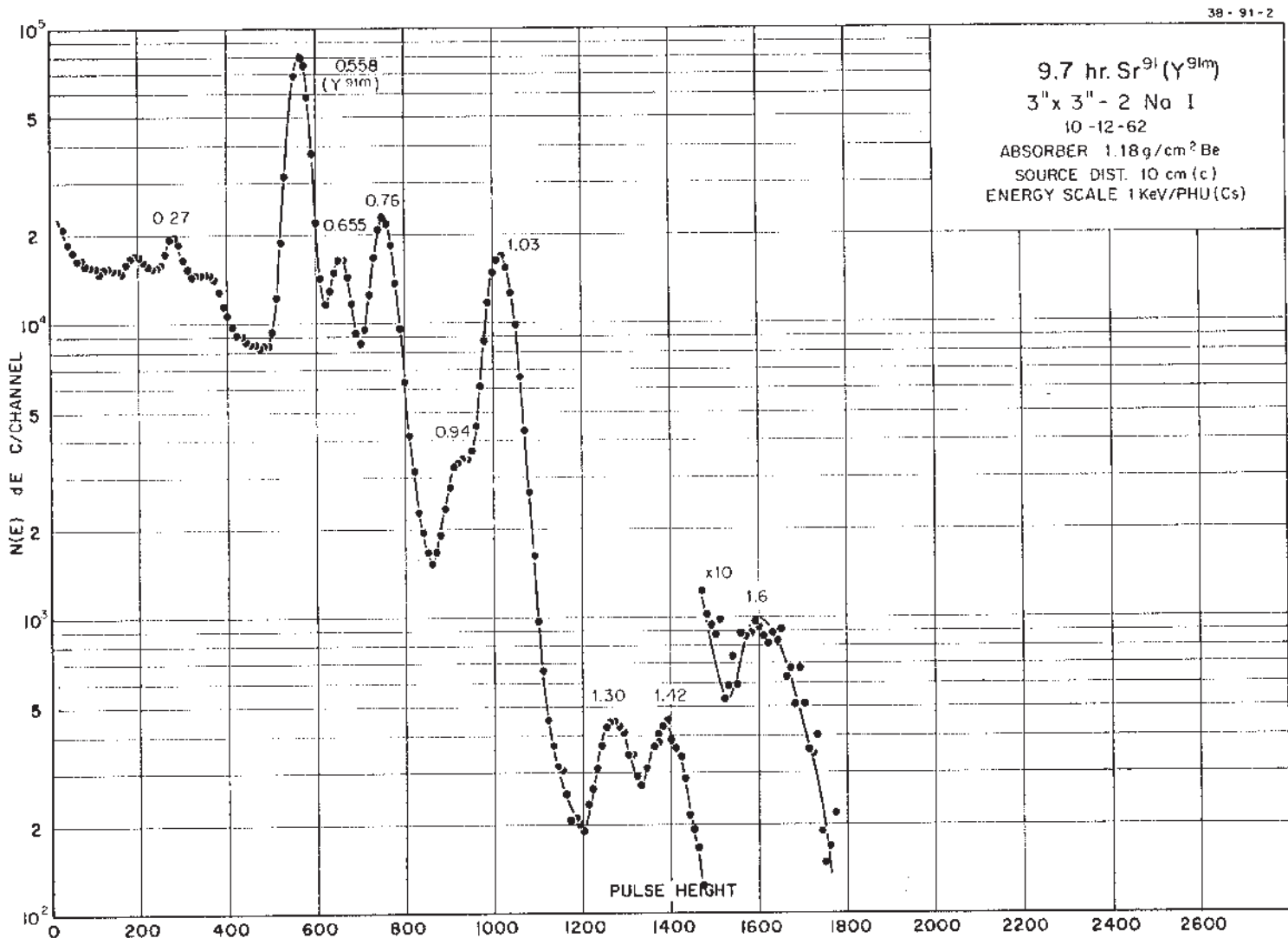
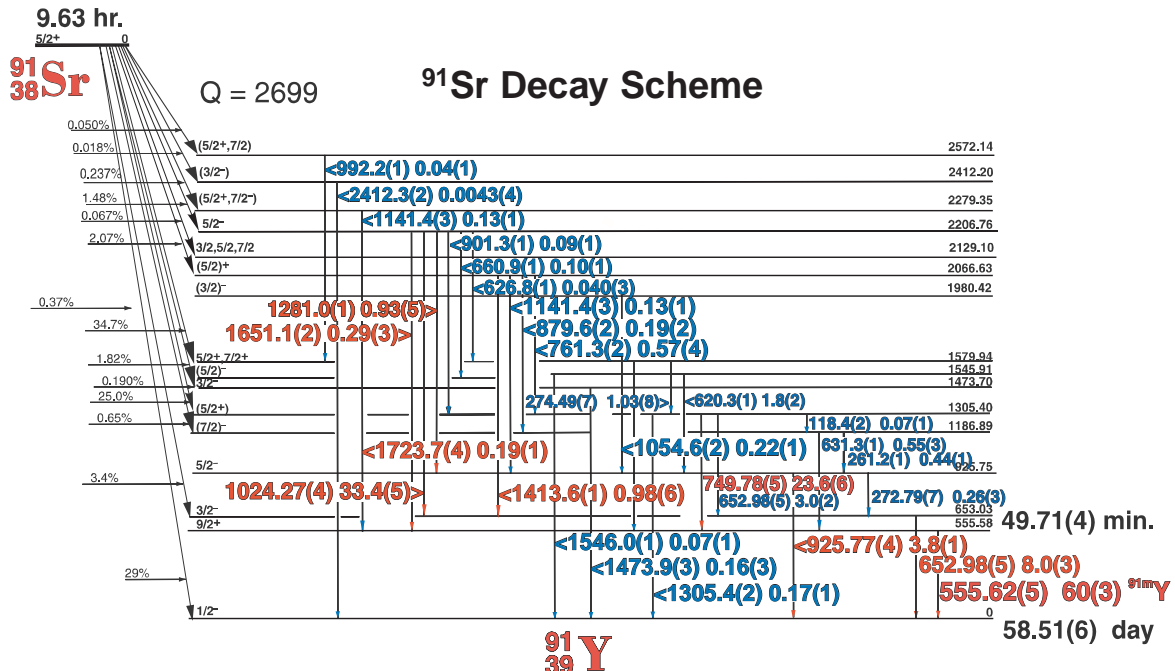
Nuclide ^{87m}Sr
Detector 3" X 3" NaI-2

Half Life 2.827(1) hr.
Method of Production: $\text{Sr}^{86}(n,\gamma)$

E_γ (KeV)[S]	ΔE_γ	$I_\gamma(\text{rel})$	$I_\gamma(\%)[E]$	ΔI_γ	S
Sr x-rays from internal conversion 388.532	± 0.003	100	82.1	± 0.5	1



9.63(5) hr. ^{91}Sr



Decay Data

◀ Index ▶

9.63(5) hr. ^{91}Sr

38-91-1

GAMMA-RAY ENERGIES AND INTENSITIES

Nuclide ^{91}Sr
Detector 3" X 3" NaI-2

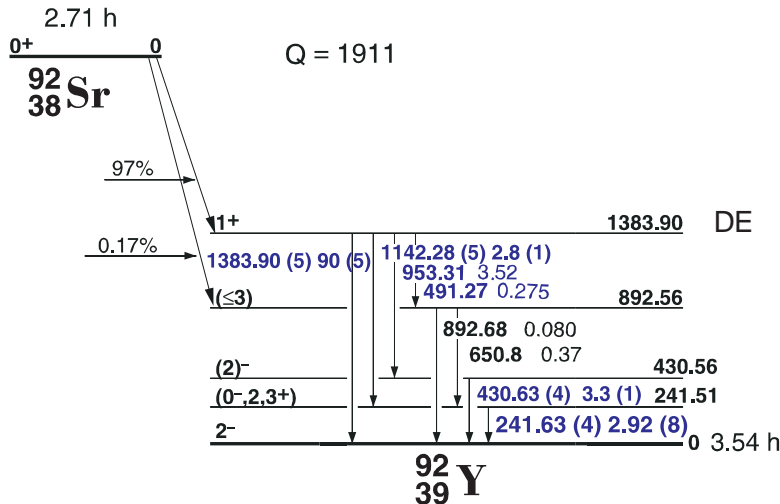
Half Life 9.63(5) hr
Method of Production: U $^{235}(\text{n},\text{f})$

E_{γ} (KeV)[S]	ΔE_{γ}	I_{γ} (rel)	$I_{\gamma}(\%)$ [E]	ΔI_{γ}	S	
118.4	± 0.2	0.35	0.07	± 0.01	4	
261.21	± 0.1	1.60	0.44	± 0.01	4	
272.79	± 0.07	0.7	0.26	± 0.05	4	
274.49	± 0.07	3.4	1.03	± 0.03	3	
γ^{91m}	555.620	± 0.05			1	
	620.26	± 0.10	5.6	1.8	± 0.03	3
	631.34	± 0.15	2.1	0.55	± 0.05	4
	652.977	± 0.050	34.0	11.0	± 2.0	1
	749.779	± 0.05	72.0	23.6	± 0.2	1
	761.35	± 0.2	1.9	0.60	± 0.01	3
	879.6	± 0.2	0.74	0.19	± 0.005	4
	925.771	± 0.040	11.8	3.84	± 0.01	1
	1024.271	± 0.04	=100	33.4	± 0.5	1
	1054.63	± 0.3	0.75	0.22	± 0.10	3
	1141.4	± 0.4	0.6	0.12	± 0.01	4
	1281.00	± 0.15	2.8	1.0	± 0.05	1
	1305.4	± 0.2	0.24	0.02	± 0.002	4
	1413.57	± 0.15	3.1	0.98	± 0.02	1
	1473.9	± 0.4	0.5	0.16	± 0.01	2
	1546.02	± 0.15	0.23	0.06	± 0.005	3
	1651.15	± 0.2	0.74	0.29	± 0.005	1
	1723.9	± 0.5	0.24	0.17	± 0.002	1

2.71(1) hr. ^{92}Sr

38-92-1

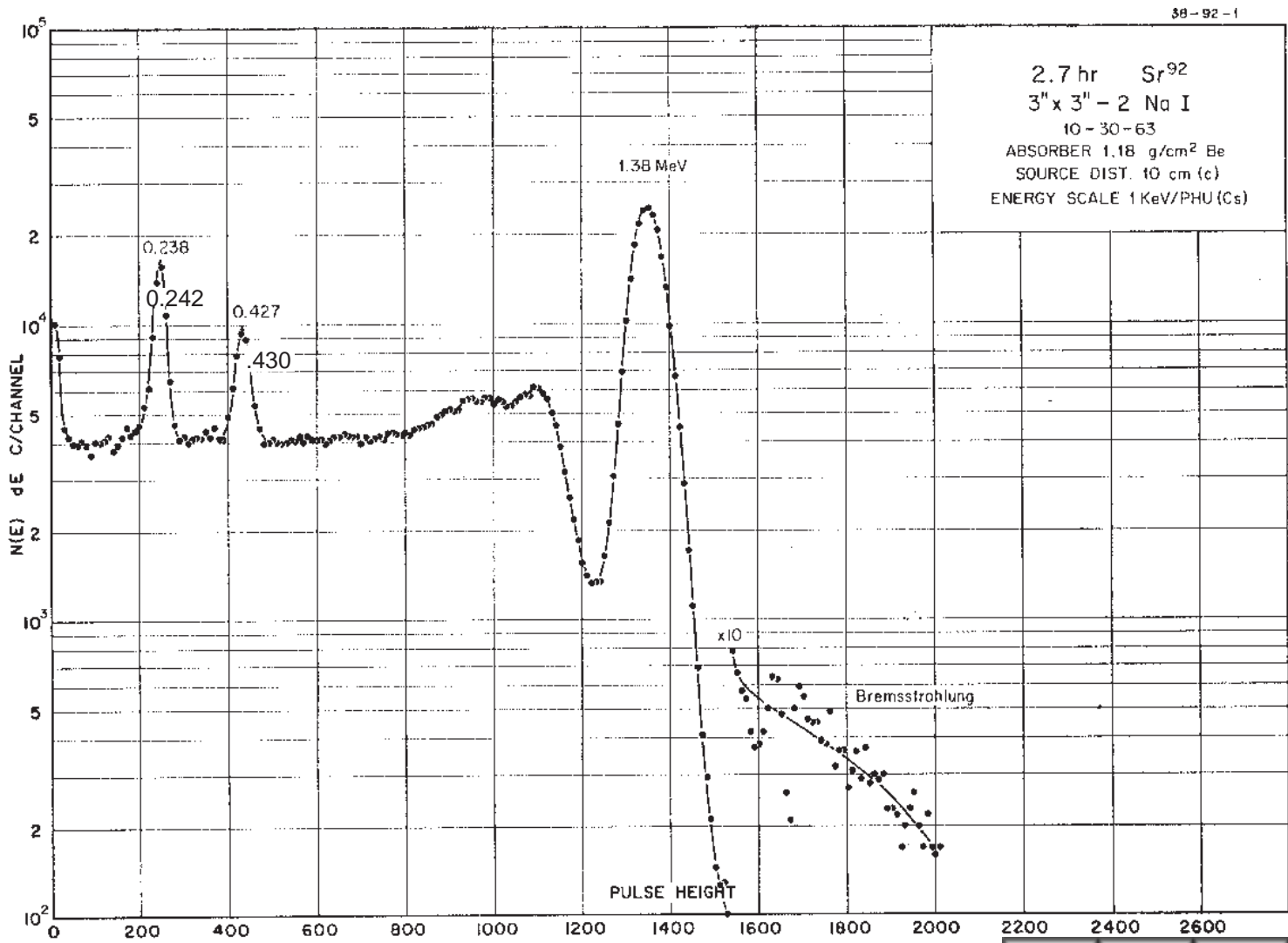
^{92}Sr Decay Scheme



GAMMA-RAY ENERGIES AND INTENSITIES

Nuclide ^{92}Sr
Detector 3" X 3" NaI-2
Method of Production: U²³⁵(n,f)

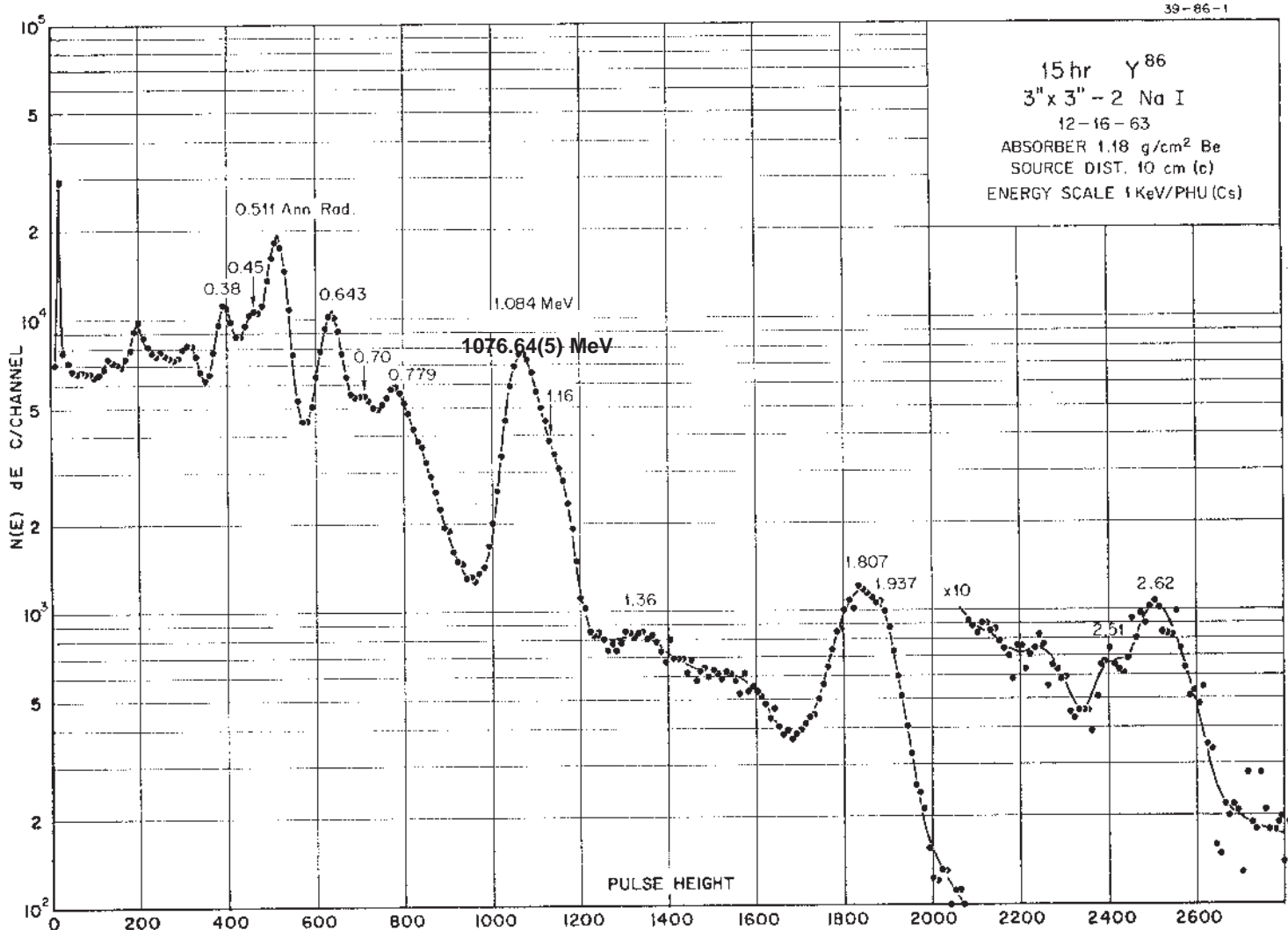
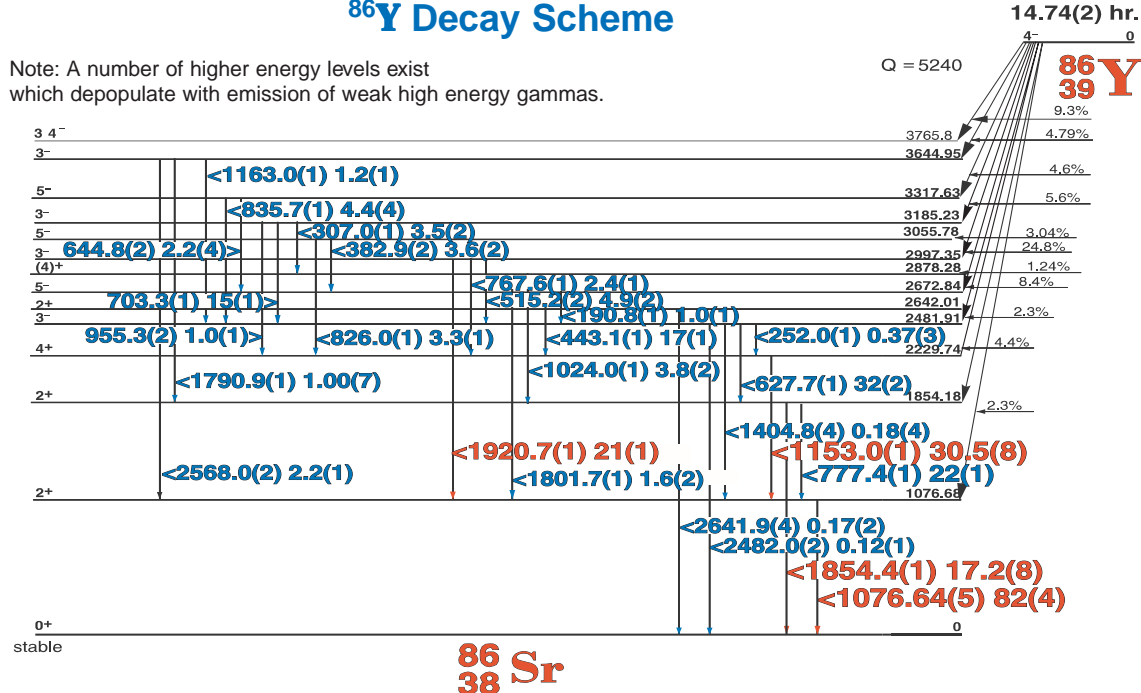
E_{γ} (KeV) [S]	ΔE_{γ}	$I_{\gamma} (\text{rel})$	$I_{\gamma} (\%) [E]$	ΔI_{γ}	S
241.628	± 0.040	3.9	2.92	± 0.3	3
351.8	± 0.1	0.09		± 0.02	4
361.0					4
430.632	± 0.040	4.6	3.28	± 0.4	3
491.6	± 0.1	0.48	0.275	± 0.10	4
650.8					4
953.318	± 0.050	4.2	3.52	± 0.3	3
1142.279	± 0.050	3.2	2.79	± 0.3	3
1383.898	± 0.050	=100	90	± 5.0	1



14.74(2) hr. ^{86}Y

^{86}Y Decay Scheme

Note: A number of higher energy levels exist which depopulate with emission of weak high energy gammas.



14.74(2) hr. ^{86}Y

GAMMA-RAY ENERGIES AND INTENSITIES

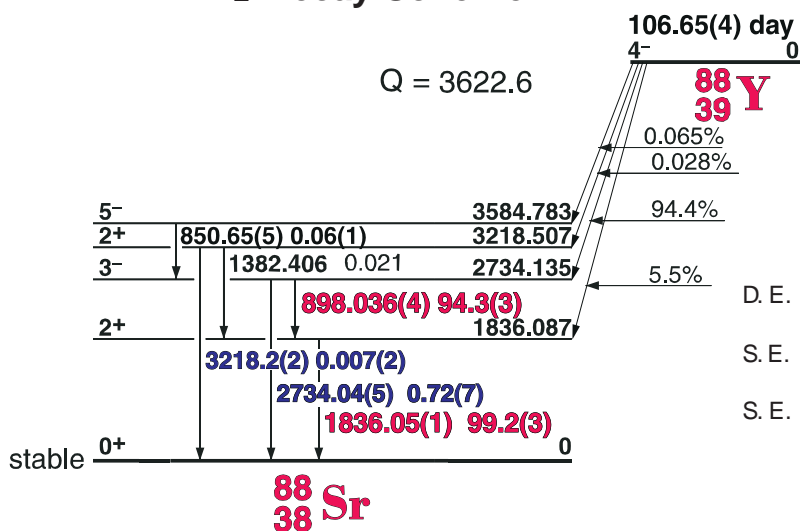
Nuclide ^{86}Y Half Life 14.74(2) hr.
Detector 3" X 3" NaI-2 Method of Production: Br⁸¹(n, γ)

E_{γ} (KeV)[S]	ΔE_{γ}	$I_{\gamma}(\text{rel})$	$I_{\gamma}(\%)[E]$	ΔI_{γ}	S
383.02	± 0.05		3.63	± 0.3	2
443.14	± 0.05		16.9	± 0.9	2
ann. rad. 511.006					1
644.8	± 0.06		2.2	± 0.1	3
627.72	± 0.05		32.6	± 0.9	1
703.34	± 0.06		15.4	± 0.9	2
777.35	± 0.05		22.4	± 1.0	1
1076.64	± 0.05	100	82	± 4	1
1153.01	± 0.05		30.5	± 1.5	1
1854.38	± 0.07		17.2	± 1.0	1
1920.72	± 0.07		21	± 1	1
2567.97	± 0.1		2.25	± 0.1	1

106.65(4) day Y^{88}

39-88-2

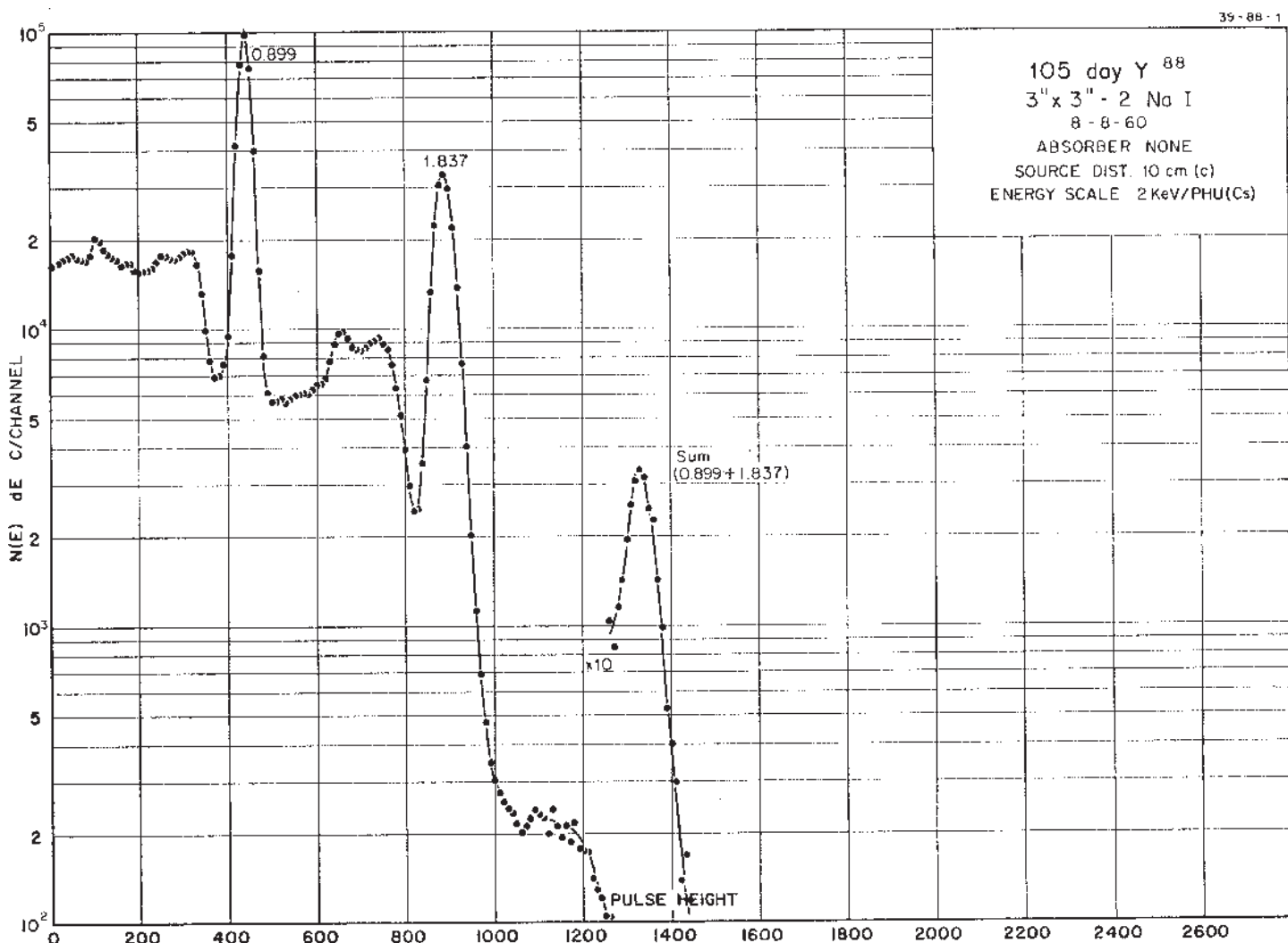
^{88}Y Decay Scheme

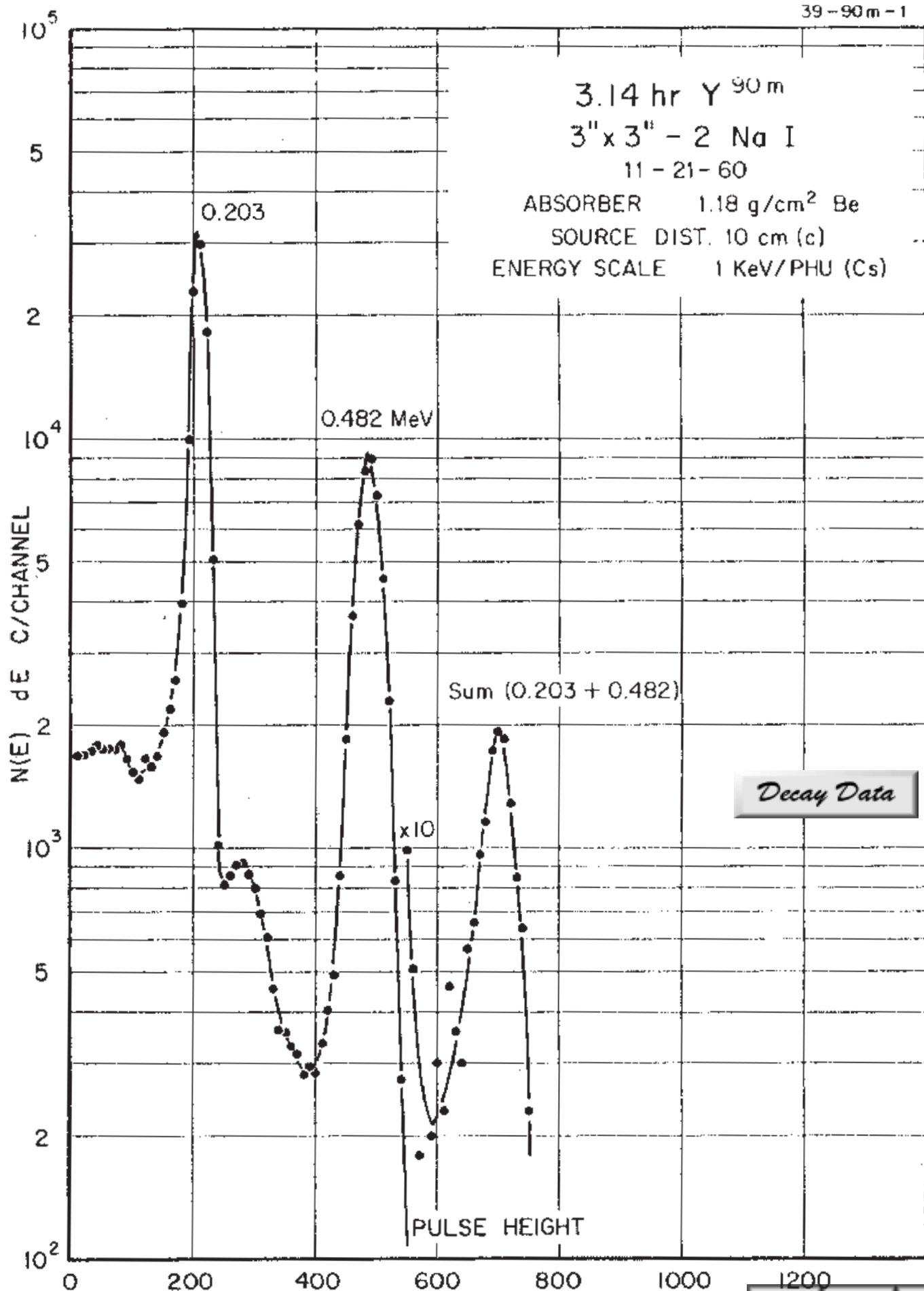


GAMMA-RAY ENERGIES AND INTENSITIES

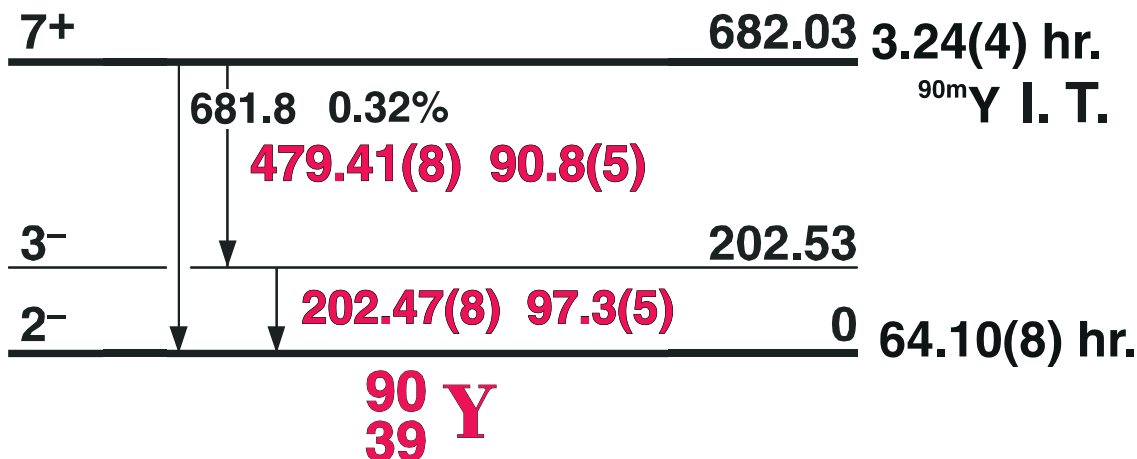
Nuclide ^{88}Y
 Detector 3" X 3" NaI-2
 Method of Production: $\text{Sr}^{88}(\text{p},\text{n})$

E_{γ} (KeV)	[S]	ΔE_{γ}	$I_{\gamma}(\text{rel})$	$I_{\gamma}(\%)$ [E]	ΔI_{γ}	S
511.006	(ann. rad.)					
814.185	± 0.08	2.66				4
898.042	± 0.003	92.12	94.2	± 0.5	1	
1325.12	± 0.08	2.69				3
1836.063	± 0.012	100	99.2	± 0.5	1	
1911.84	± 0.1	0.54	0.7	± 0.1	2	4
2734.04	± 0.05	0.007	0.007	± 0.002		
3218.2	± 0.2					4





3.244(5) hr. ^{90m}Y Decay Scheme

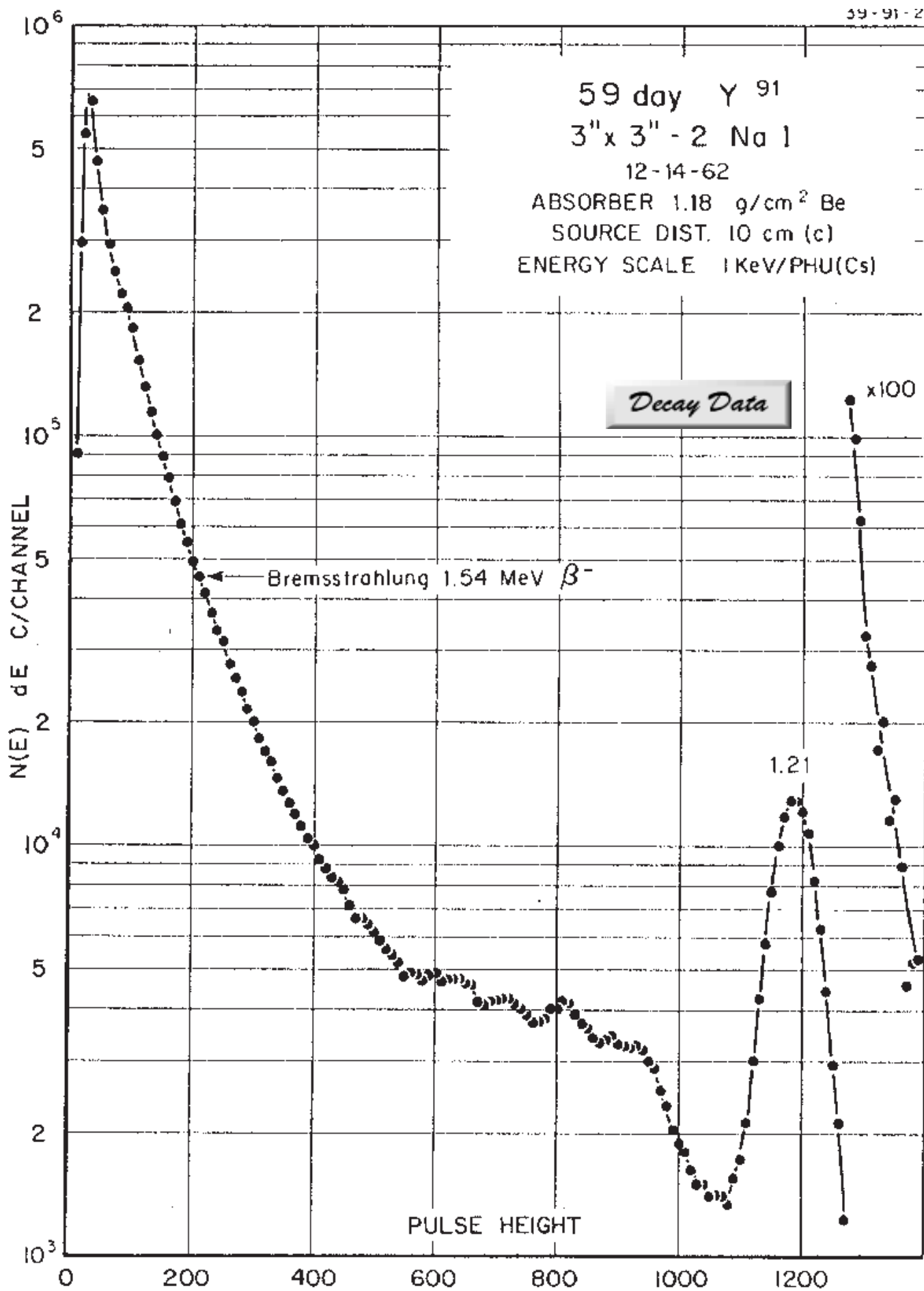


39-90m-1

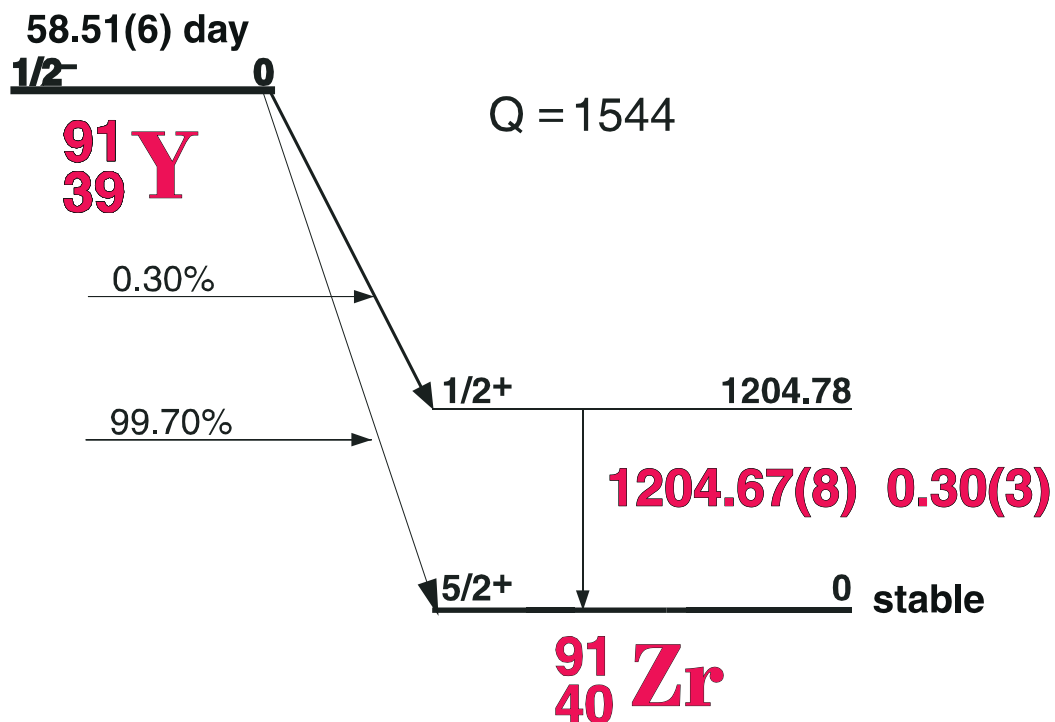
GAMMA-RAY ENERGIES AND INTENSITIES

Nuclide ^{90m}Y Half Life 3.244(5) hr.
Detector 3" x 3" -2 Nal Method of Production: Zr⁹⁰(n,p)

E_{γ} (KeV)[S]	ΔE_{γ}	I_{γ} (rel)	$I_{\gamma}(\%) [E]$	ΔI_{γ}	S
202.53	± 0.05	100	97.3	± 1.0	1
479.51	± 0.02	90	90.8	± 1.0	1



58.51(6) day ^{91}Y Decay Scheme



39-91-1

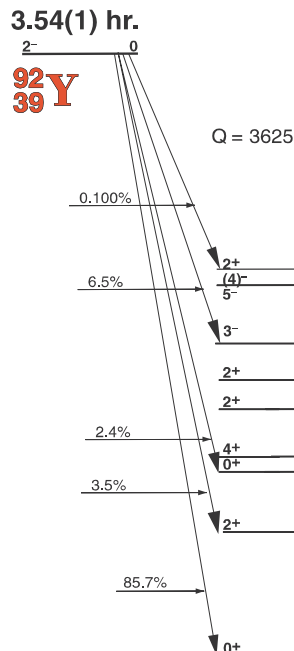
GAMMA-RAY ENERGIES AND INTENSITIES

Nuclide ^{91}Y
Detector 3" x 3" -2 Nal

Half Life 58.51(6) day
Method of Production: $\text{U}^{235}(\text{n},\text{f})$

E_γ (KeV)[S]	ΔE_γ	I_γ (rel)	I_γ (%)[E]	ΔI_γ	S
1204.67	± 0.08	100	0.30	± 0.02	1

3.54(1) hr. Y^{92}

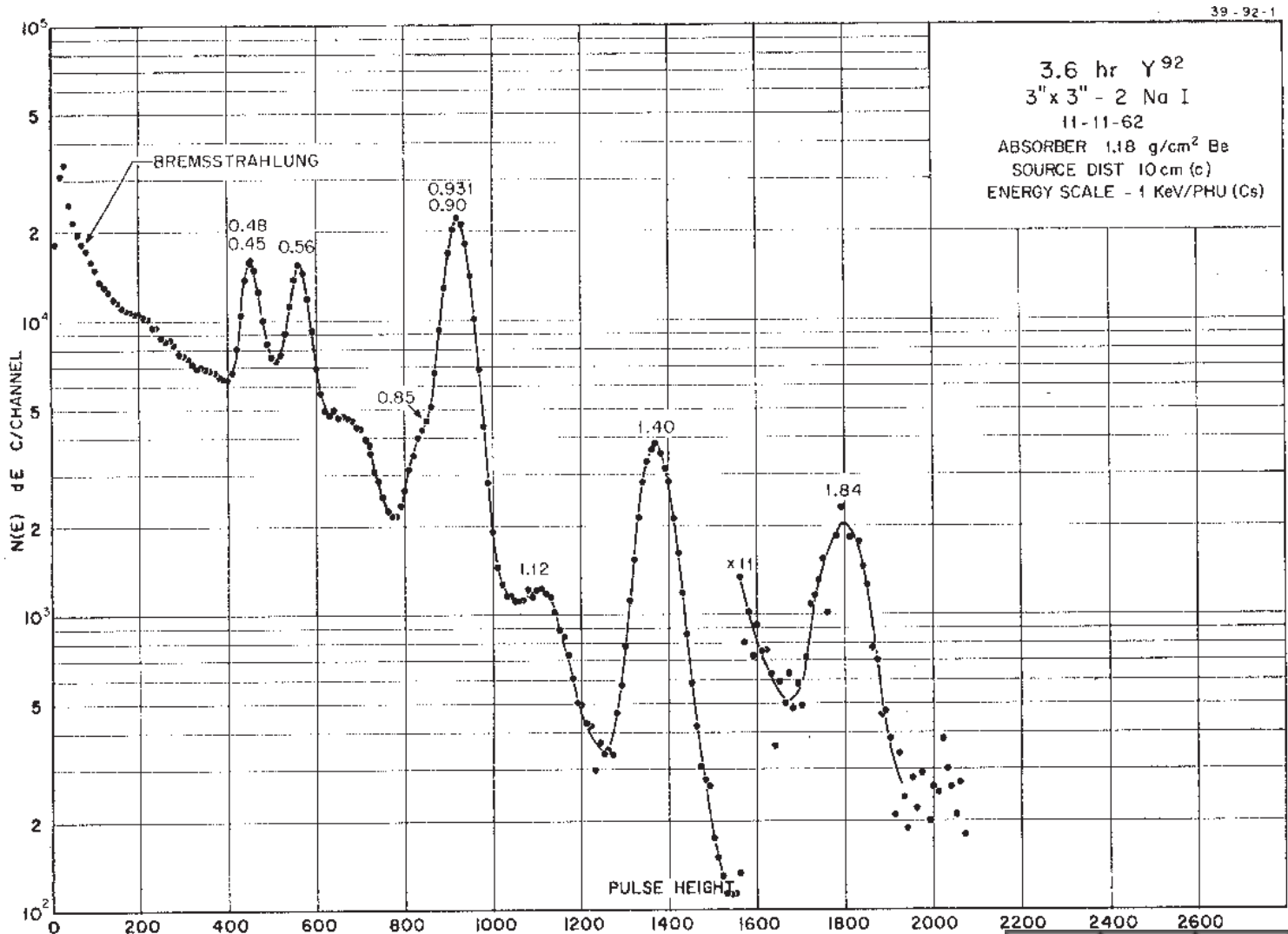


Y^{92} Decay Scheme

Decay Data

<2819.8 0.004	2819.73
<1885.0 0.028	2485.98
<972.32 0.07	2339.77
<2339.9 0.014>	2066.66
1405.17(5) 4.8(2)>	1847.33
	1132.3(1) 0.24(1)
	1847.4(3) 0.36(3)
	912.8(2) 0.63(5)
	1495.47
	1382.83
	560.99(5) 2.40(5)
	448.22(5) 2.34(5)
	934.49
	934.53(5) 13.9(5)
	0 stable

92Zr



3.54(1) Hr. ^{92}Y

GAMMA-RAY ENERGIES AND INTENSITIES

Nuclide ^{92}Y Half Life 3.54(1) hr.
Detector 3" X 3" NaI-2 Method of Production: $\text{U}^{235}(\text{n},\text{f})$

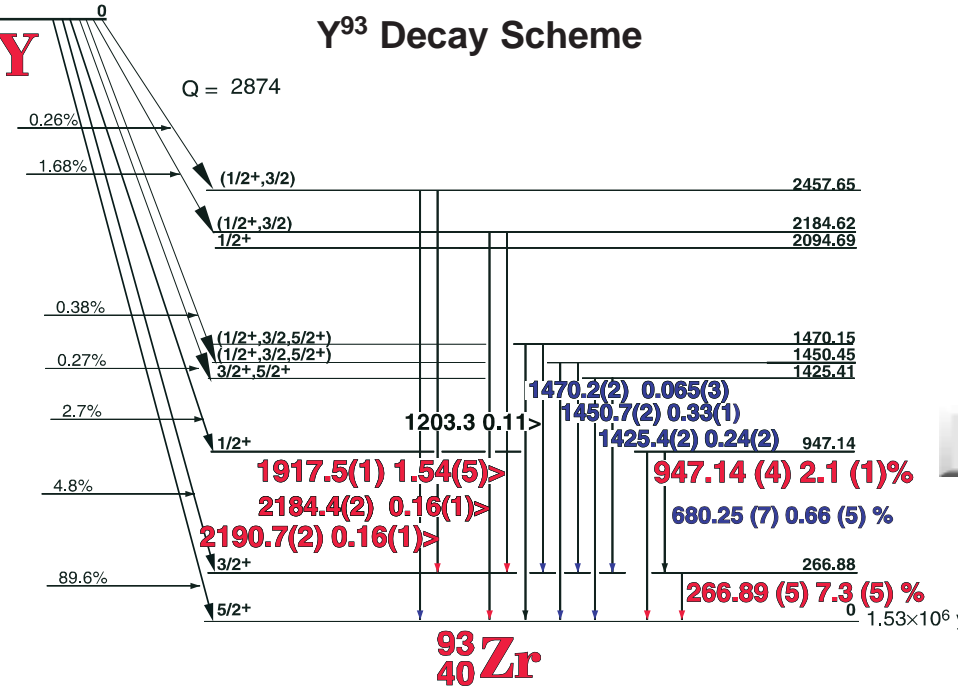
E_{γ} (KeV)[S]	ΔE_{γ}	I_{γ} (rel)	$I_{\gamma}(\%)[E]$	ΔI_{γ}	S
448.218	± 0.050	20.0	2.34	± 0.5	2
492.39	± 0.1	4.3	0.49	± 0.02	3
560.990	± 0.050	26.9	2.40	± 0.6	1
844.26	± 0.07	9.3	1.25	± 0.4	2
912.78	± 0.2	5.5	0.83	± 0.04	3
934.528	± 0.05	=100	13.9	± 0.5	1
1132.4	± 0.3	1.9	0.24	± 0.01	4
1293.5	± 0.4	0.8		± 0.3	4
1405.170	± 0.050	34.2	4.8	± 0.2	1
1847.4	± 0.3	2.9	0.38	± 0.01	3

10.18 Hr. ^{93}Y

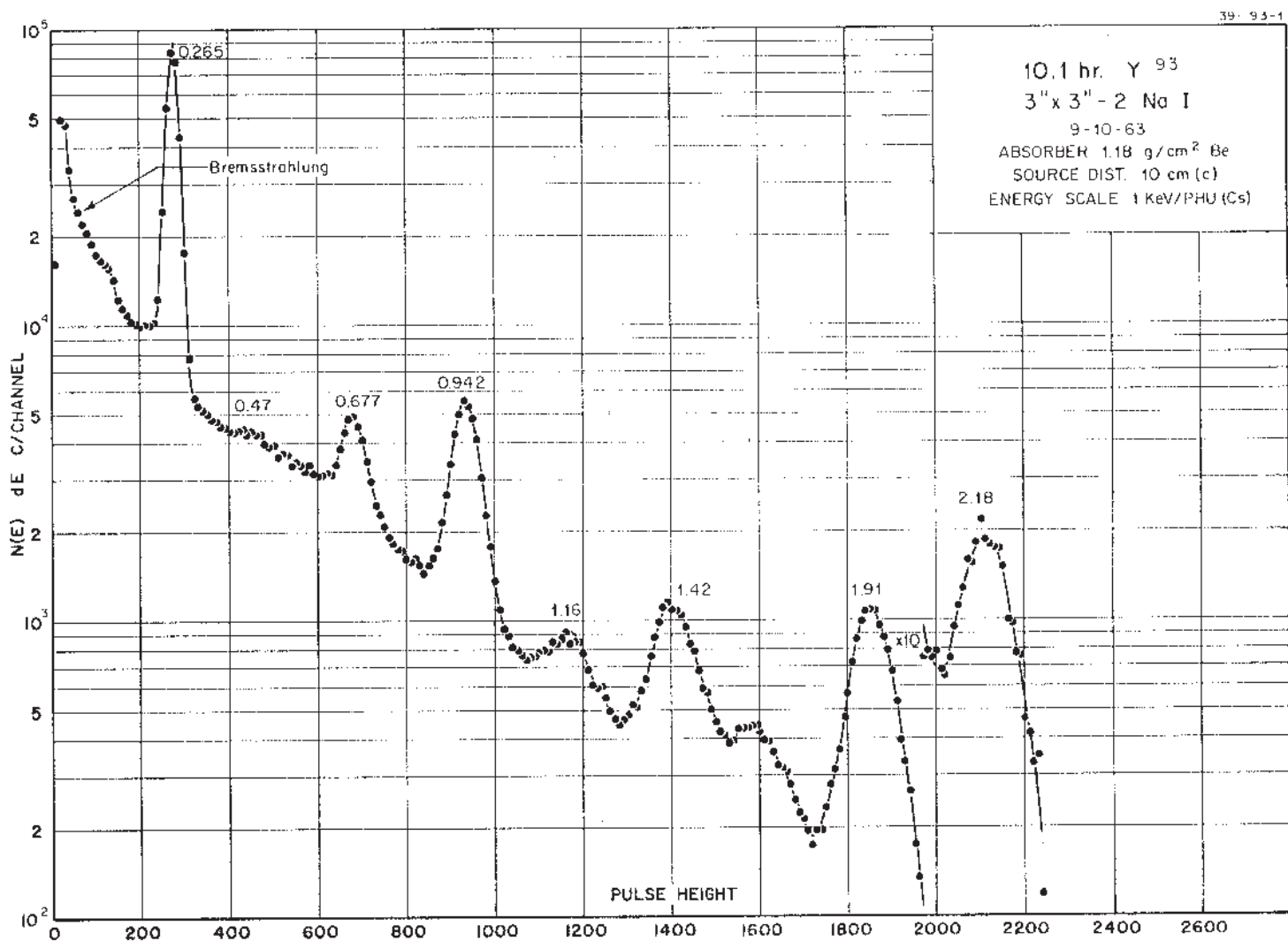
10.18(8) hr.

^{93}Y
39

γ^{93} Decay Scheme



^{93}Zr
40



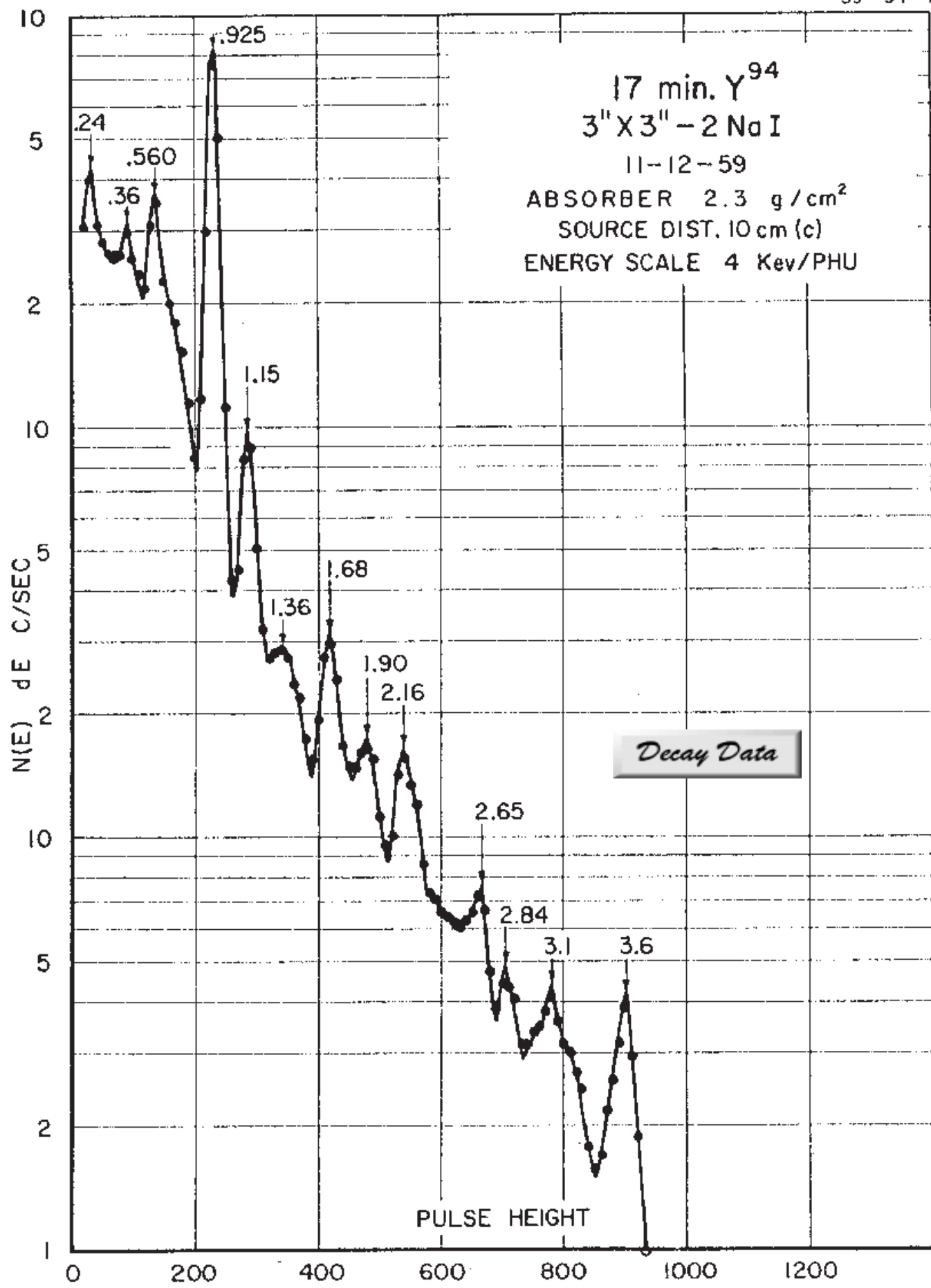
10.18(8) hr. ^{93}Y

39-93-1

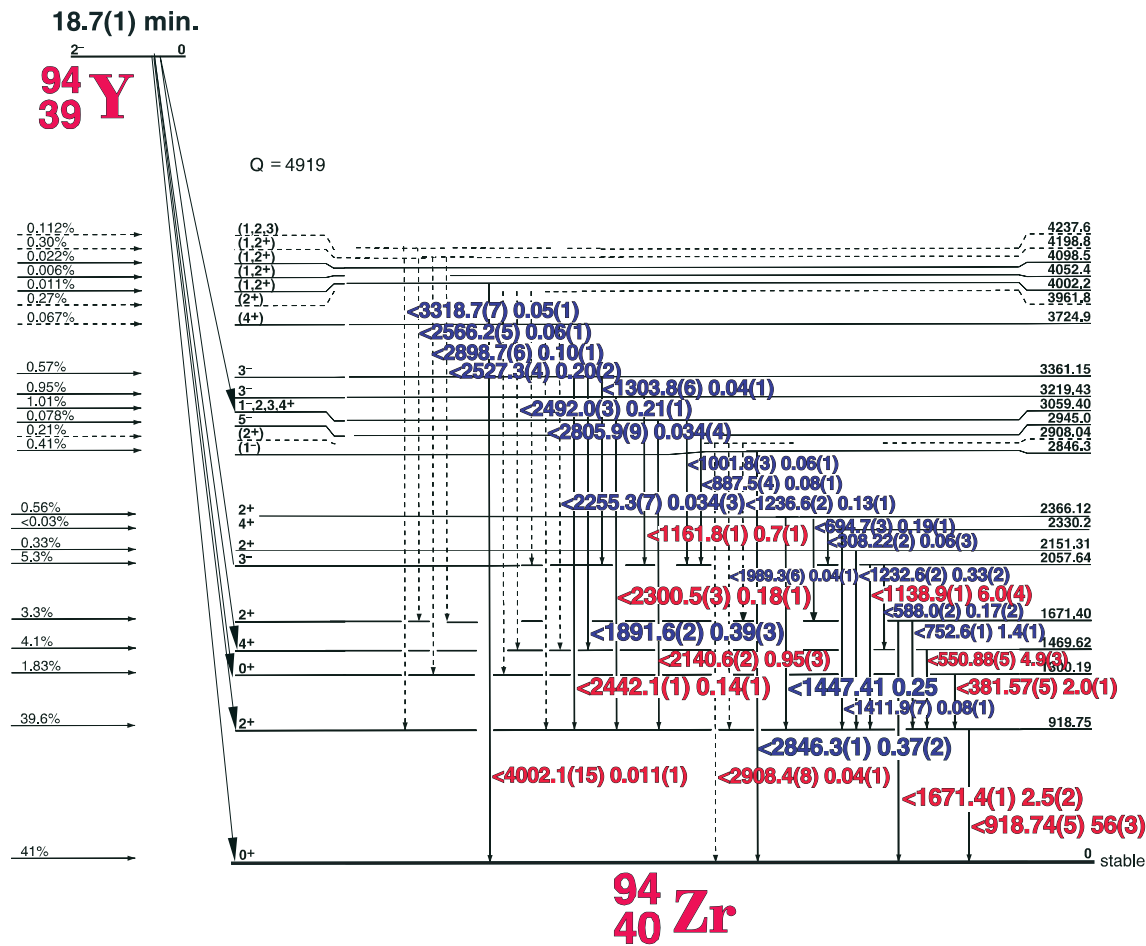
GAMMA-RAY ENERGIES AND INTENSITIES

Nuclide ^{93}Y Half Life 10.18(8) hr.
Detector 3" X 3" NaI-2 Method of Production: U²³⁵(n,f)

E_{γ} (KeV)[S]	ΔE_{γ}	I_{γ} (rel)	$I_{\gamma}(\%)$ [E]	ΔI_{γ}	S
266.886	± 0.050	100	7.3	± 0.5	1
680.25	± 0.07	9.5	0.56	± 0.03	3
947.137	± 0.040	27.1	2.1	± 0.1	1
1183.9	± 0.2	0.98	0.048	± 0.01	4
1425.4	± 0.2	3.3	0.244	± 0.01	3
1450.7	± 0.2	4.6	0.327	± 0.02	2
1470.2	± 0.3	1.3	0.07	± 0.01	3
1917.51	± 0.10	21.0	1.54	± 0.08	1
2184.40	± 0.15	2.3	0.157	± 0.02	2
2190.7	± 0.2	2.5	0.16	± 0.01	2



18.7(1) min. ^{94}Y Decay Scheme



39-94-1

GAMMA-RAY ENERGIES AND INTENSITIES

Nuclide Detector

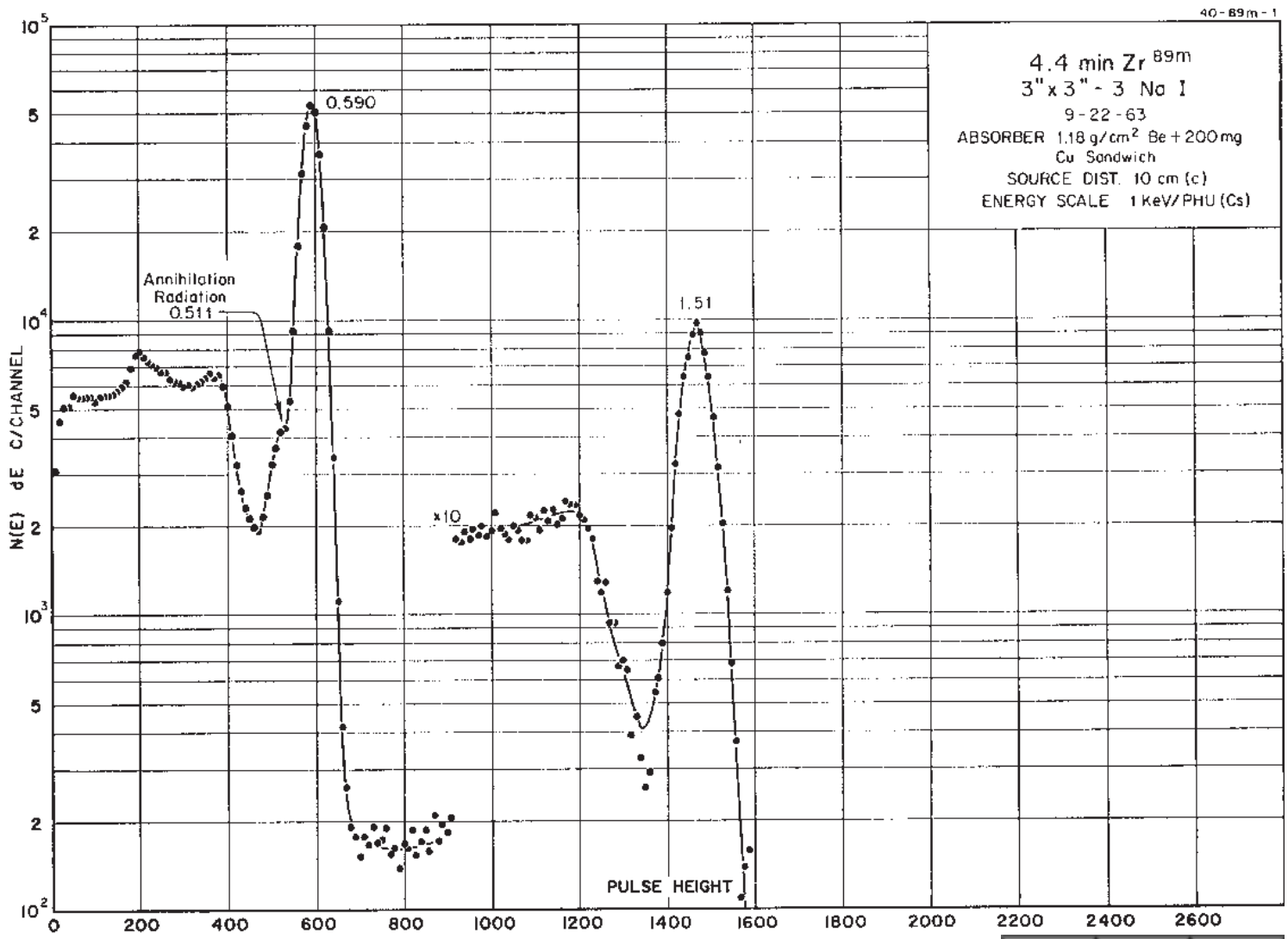
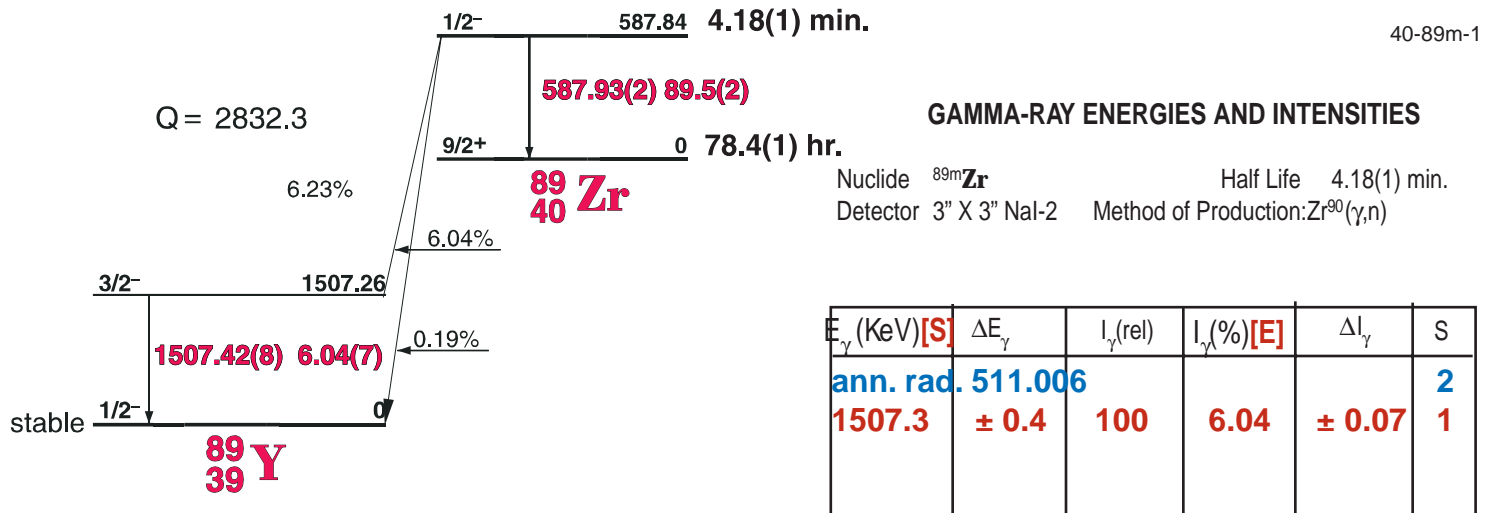
94Y
3" x 3" -2 NaI

Half Life 18.7(1) min.
Method of Production: U²³⁵(n,f)

E_{γ} (KeV)[S]	ΔE_{γ}	$I_{\gamma}(\text{rel})$	$I_{\gamma}(\%)[E]$	ΔI_{γ}	S
381.6	± 0.2	0.63	3.6	± 0.3	2
550.88	± 0.10	8.8	4.9	± 0.2	1
752.60	± 0.1	2.5	1.4	± 0.07	2
918.74	± 0.05	100	56	± 1.0	1
1138.9	± 0.1	13.7	10.7	± 0.7	1
1161.8	± 0.1	1.24	0.69	± 0.03	2
1671.4	± 0.1	4.4	2.46	± 0.12	1
2140.6	± 0.2	1.7	0.95	± 0.05	1
2300.5	± 0.3	0.32	0.18	± 0.01	2
2492.0	± 0.3	0.38	0.21	± 0.01	2
2527.3	± 0.3	0.36	0.20	± 0.01	2
3264.4	± 0.7	0.11	0.07	± 0.01	2
3318.7	± 0.7	0.09	0.05	± 0.01	2

4.18(1) min. ^{89m}Zr

^{89m}Zr Decay Scheme



78.4(1) hr. ^{89}Zr

⁸⁹Zr Decay Scheme

$Q = 2832.3$ $\beta_+ = 22.8\%$

State	Energy (MeV)	Decay Path	Branching Ratio (%)
$9/2^+$	2622.04		
$11/2^+$	2566.24		
$(7/2)^+$	2529.87		
1657.5 (3) 0.11 (1)%			
$5/2^-$			
1713.2 (1) 0.76 (1) %			
$9/2^+$			
1621.3 (3) 0.072 (5) %			
$5/2^-$			
1744.5 (2) 0.13 %			
$9/2^+$			
$909.10(30)$ 99.9%			
stable $1/2^-$			
	0		

89 Y

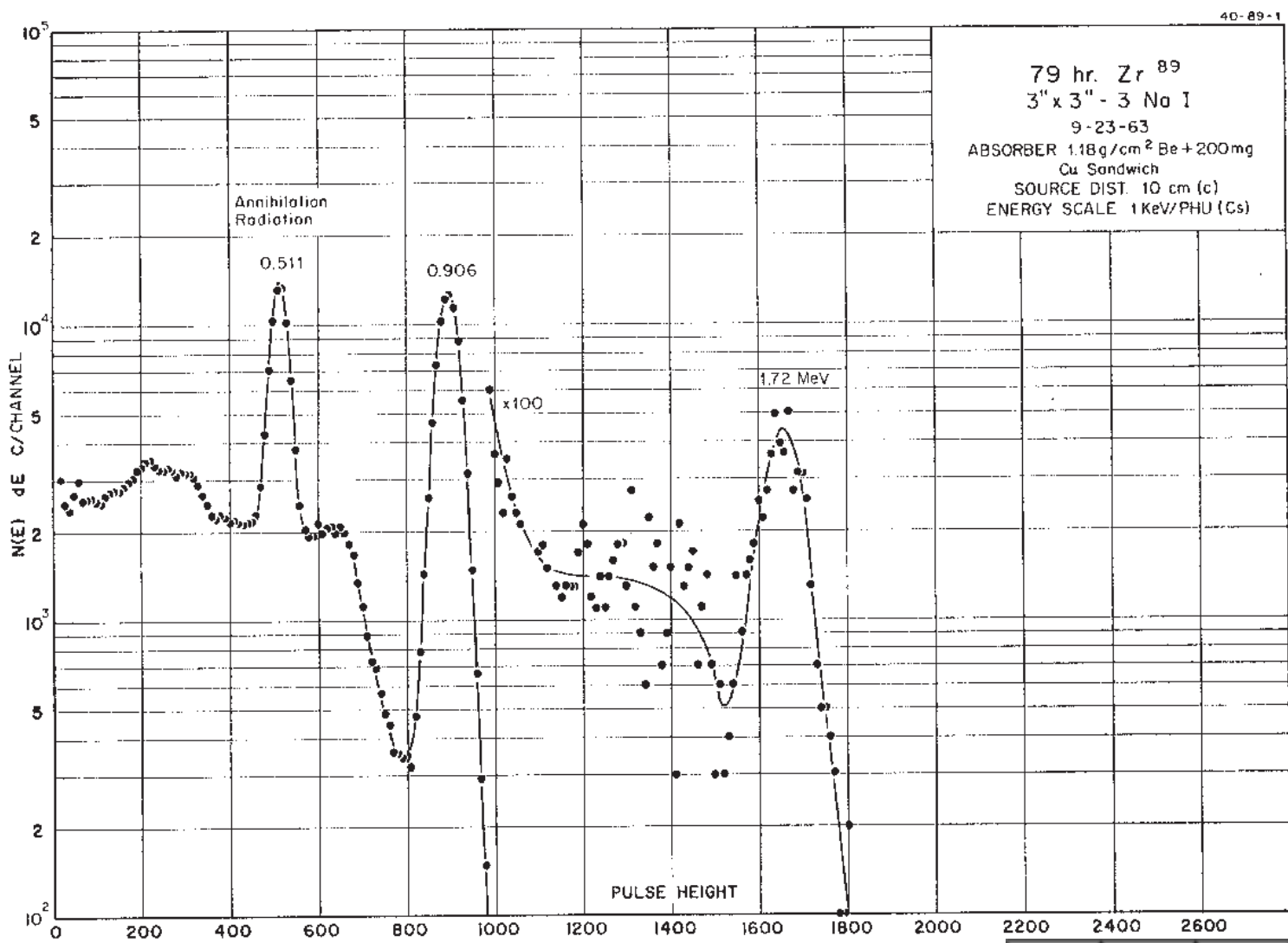
78.4(1) hr.

40-89-1

GAMMA-RAY ENERGIES AND INTENSITIES

Nuclide ^{89}Zr Half Life 78.4(1) hr.
 Detector 3" X 3" NaI-2 Method of Production: $\text{Zr}^{90}(\gamma, n)$

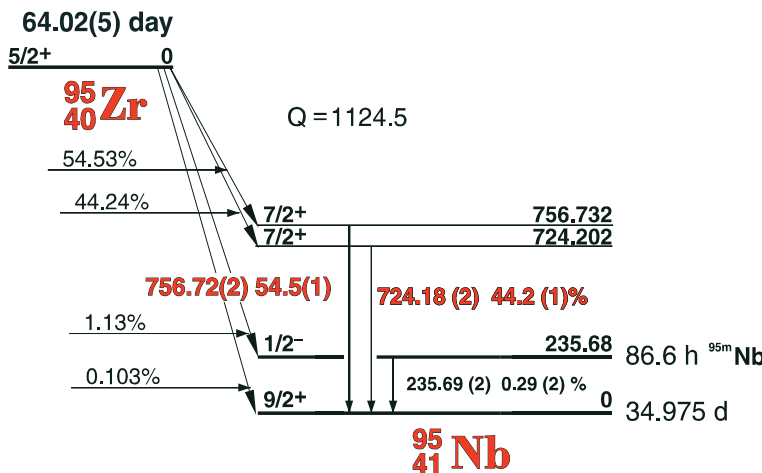
E_γ (KeV) [S]	ΔE_γ	I_γ (rel)	I_γ (%) [E]	ΔI_γ	S
ad.	511.006				
909.10	± 0.30	100	99.9	± 1.0	1
1621.3	± 0.3	0.07	0.072	± 0.05	3
1657.5	± 0.5	0.10	0.11	± 0.01	2
1713.2	± 0.1	0.75	0.76	± 0.01	2
1744.5	± 0.2	0.13	0.13	± 0.01	3



64.02(5) day ^{95}Zr

^{95}Zr Decay Scheme

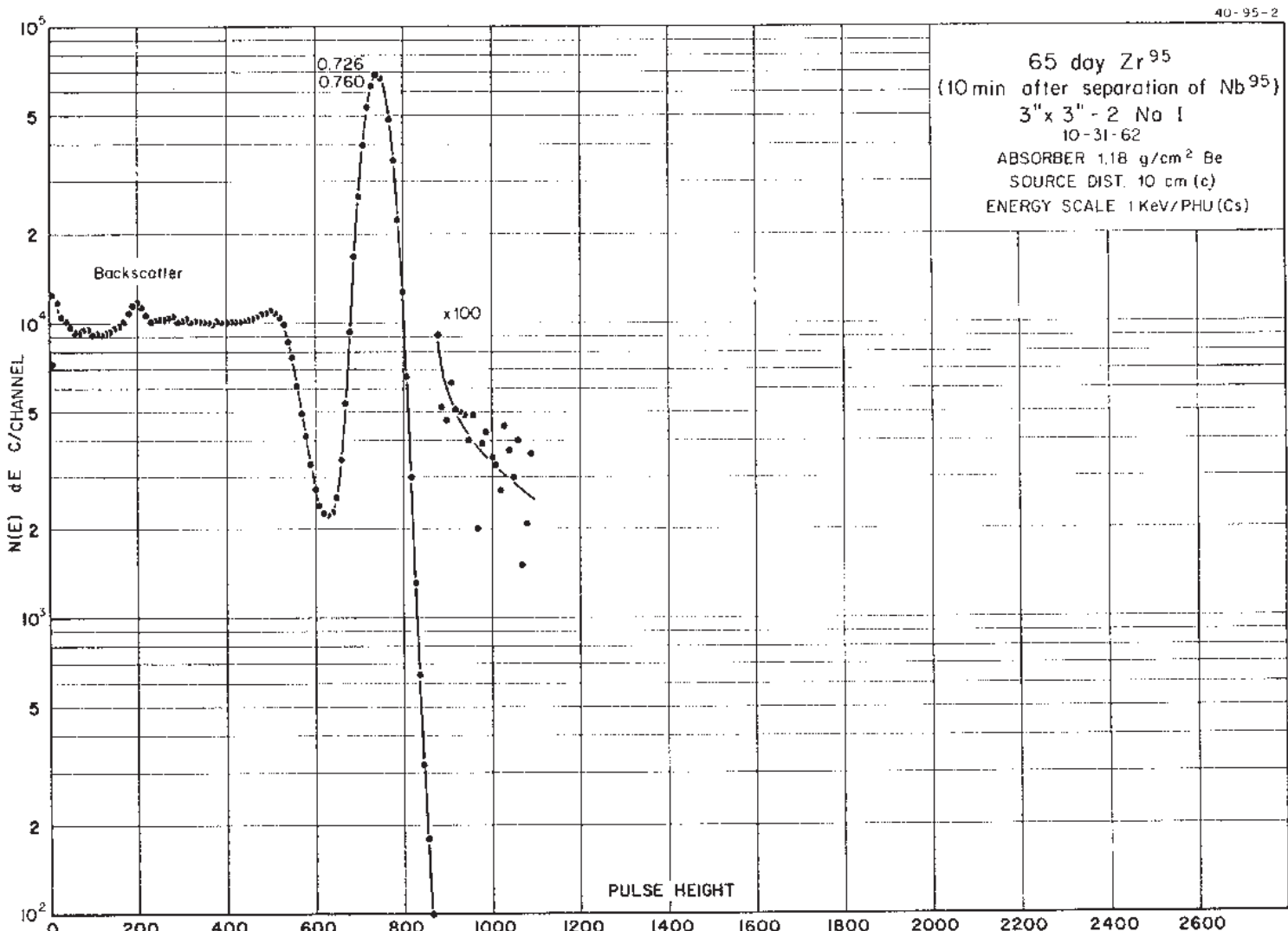
40-95-2

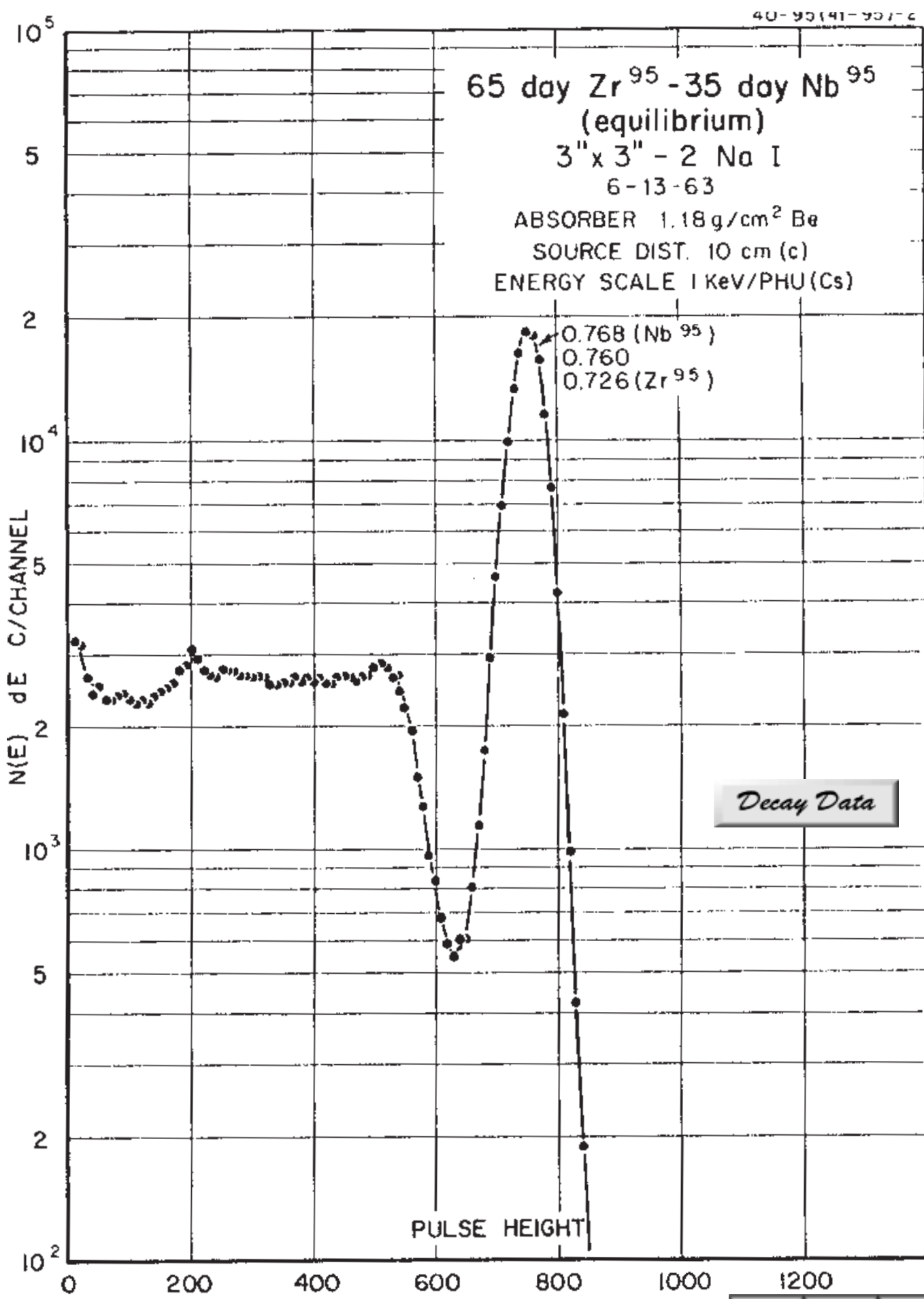


GAMMA-RAY ENERGIES AND INTENSITIES

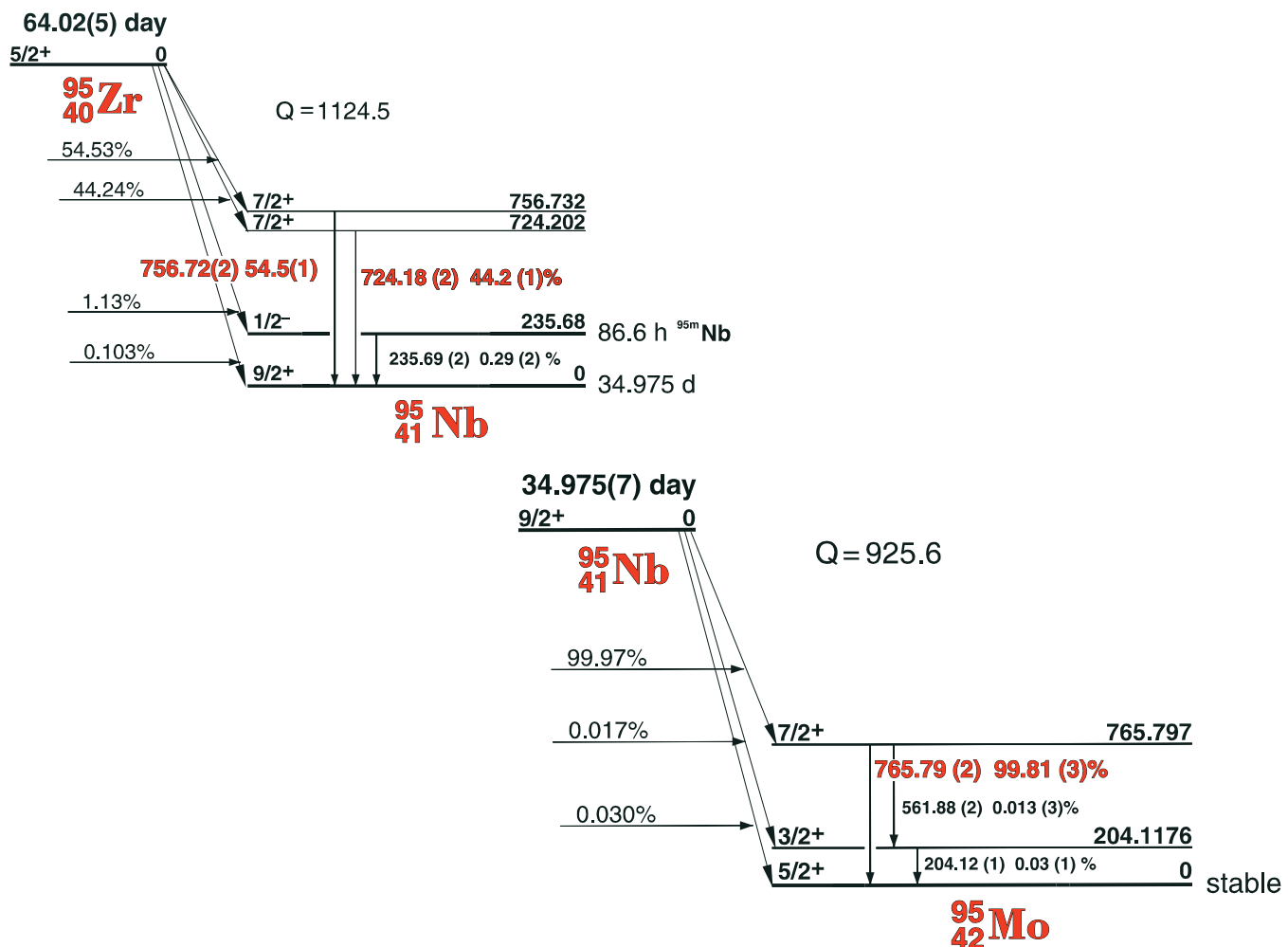
Nuclide ^{95}Zr Half Life 64.02(50) day
Detector 3" X 3" NaI-2 Method of Production: U²³⁵(n,,f)

E_{γ} (KeV) [S]	ΔE_{γ}	$I_{\gamma}(\text{rel})$	$I_{\gamma}(\%) [E]$	ΔI_{γ}	S
235.69	± 0.02		0.29	± 0.02	4
724.18	± 0.02	80.6	44.2	± 0.1	1
756.72	± 0.02	100	54.5	± 0.1	1





64.02(5) Day ^{95}Zr - 34.975(7) Day ^{95}Nb Decay Scheme



40-95(41-95)-1

GAMMA-RAY ENERGIES AND INTENSITIES

Nuclide $^{95}\text{Zr} - ^{95}\text{Nb}$ Half Life (64.02(5) Day - 34.975(7) day)
 Detector 3" x 3" -2 NaI Method of Production: U²³⁵(n,,f)

	E_{γ} (KeV)[S]	ΔE_{γ}	I_{γ} (rel)	$I_{\gamma}(\%)[E]$	ΔI_{γ}	S
Nb^{95m}	235.69	± 0.02	0.16	0.29	± 0.02	4
	724.18	± 0.02	20.52	44.2	± 0.1	1
	756.72	± 0.02	25.29	54.5	± 0.1	1
	765.786	± 0.02	100	99.5	± 0.5	1

16.90(5) Hr. ^{97}Zr

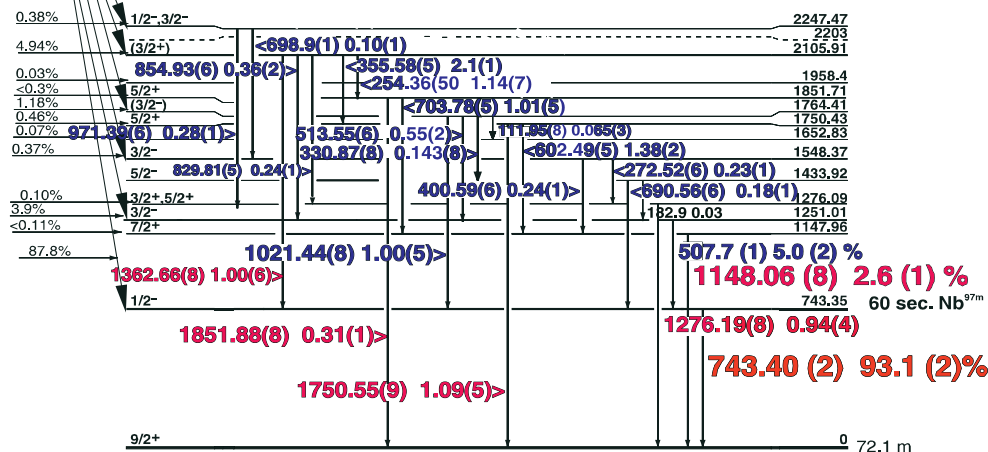
^{97}Zr Decay Scheme

16.90(5) hr.

^{97}Zr
40

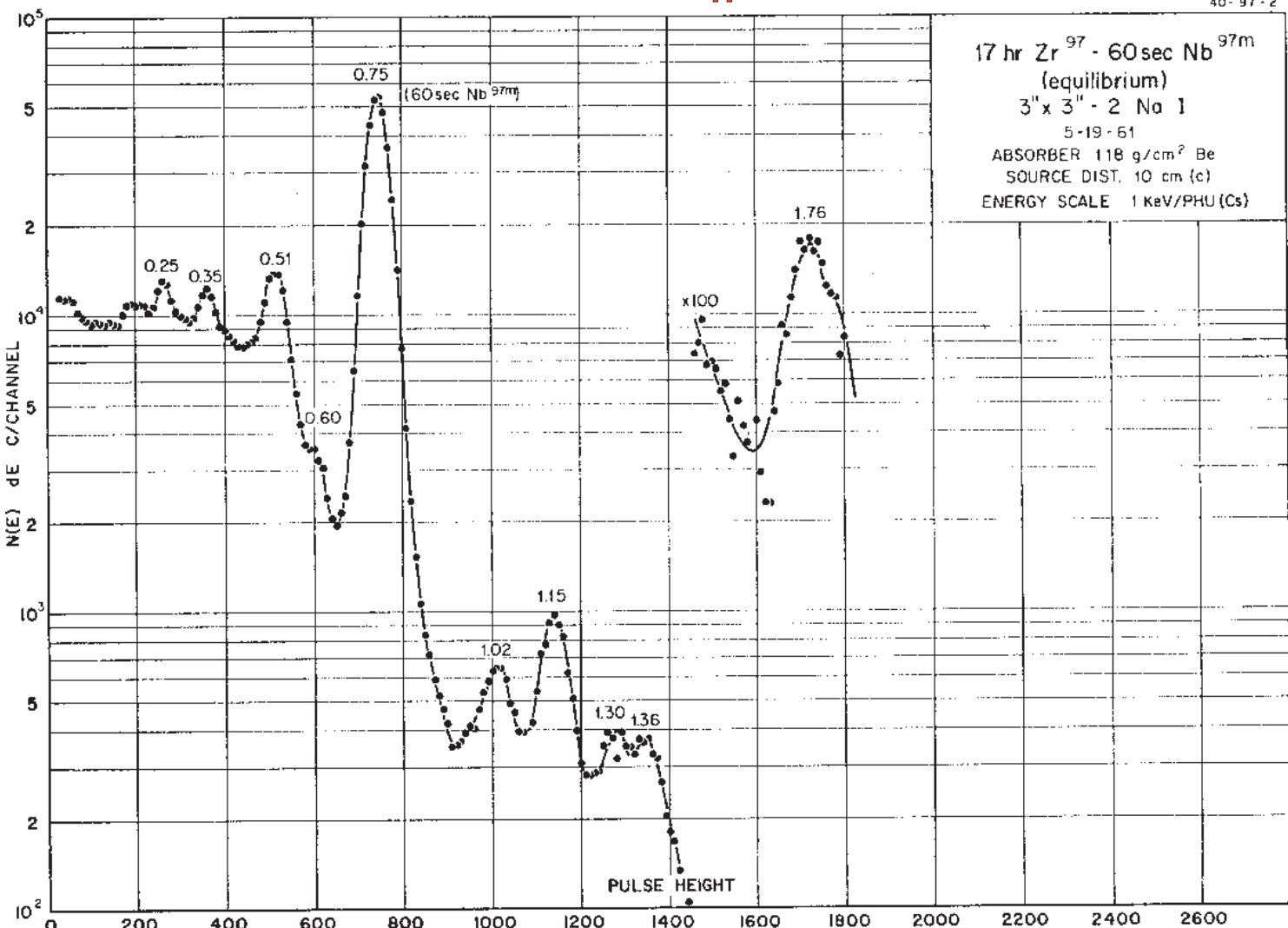
$Q = 2658.1$

Decay Data



^{97}Nb
41

40 - 97 - 2



16.90(5) Hr. ^{97}Zr

40-97-2

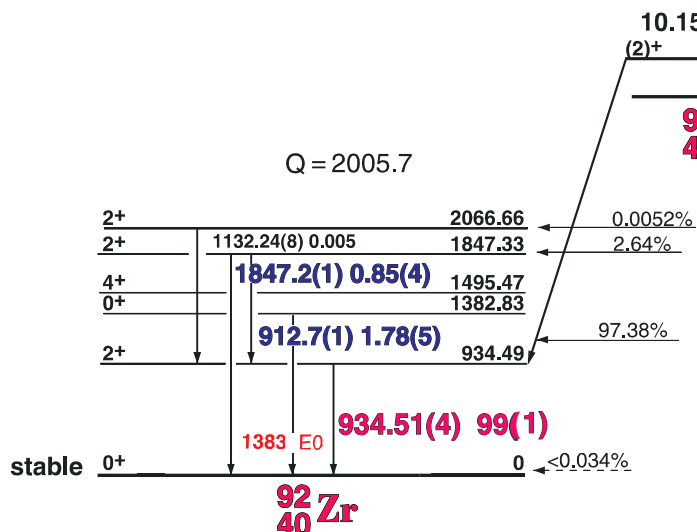
GAMMA-RAY ENERGIES AND INTENSITIES

Nuclide $^{97}\text{Zr} - ^{97m}\text{Nb}$ Half Life 16.90(5) hr.
 Detector 3" X 3" NaI-2 Method of Production: $\text{Zr}^{96}(\text{n},\gamma)$

	E_{γ} (KeV)[S]	ΔE_{γ}	I_{γ} (rel)	$I_{\gamma}(\%)$ [E]	ΔI_{γ}	S
Nb ^{97m}	111.95	± 0.08	0.115	0.07	± 0.01	2
	182.9	± 0.5	0.072	0.03	± 0.01	4
	218.90	± 0.1	0.292	0.17	± 0.02	4
	254.3	± 0.2	1.42	1.20	± 0.1	3
	272.52	± 0.2	0.32	0.25	± 0.03	4
	330.53	± 0.1	0.25	0.15	± 0.02	4
	355.5	± 0.1	2.39	2.2	± 0.15	3
	400.58	± 0.06	0.247	0.25	± 0.02	4
	507.79	± 0.08	5.35	5.3	± 0.25	3
	513.55	± 0.06	0.60	0.57	± 0.05	4
	602.49	± 0.05	1.75	1.38	± 0.10	4
	658.17	± 0.03	108.8	98	± 5.0	1
	690.56	± 0.06	0.29	0.18	± 0.025	4
	698.9	± 0.1	0.07	0.094	± 0.015	4
DE	703.78	± 0.05	1.10	0.94	± 0.06	3
	743.40	± 0.035	100	93	± 5.0	1
	756.68	± 0.08	0.29		± 0.08	4
	804.55	± 0.05	0.72	0.62	± 0.08	3
	829.809	± 0.050	0.30		± 0.02	4
Nb ⁹⁷	854.935	± 0.06	0.38	0.35	± 0.025	3
	971.39	± 0.06	0.32	0.27	± 0.02	3
	1021.44	± 0.08	1.36	0.93	± 0.18	2
	1024.47	± 0.08	0.11	1.1	± 0.1	2
	1110.3	± 0.3	0.10	0.09	± 0.03	4
Nb ⁹⁷	1116.74	± 0.1	w			4
	1148.06	± 0.08	2.59	2.61	± 0.12	1
	1268.47	± 0.08	0.14	0.15	± 0.02	4
	1276.19	± 0.08	0.90	0.93	± 0.05	1
	1362.66	± 0.08	1.14	0.95	± 0.06	1
	1750.55	± 0.09	1.13	0.96	± 0.09	1
	1851.8	± 0.08	0.32	0.30	± 0.03	1

10.15(2) Day ^{92m}Nb

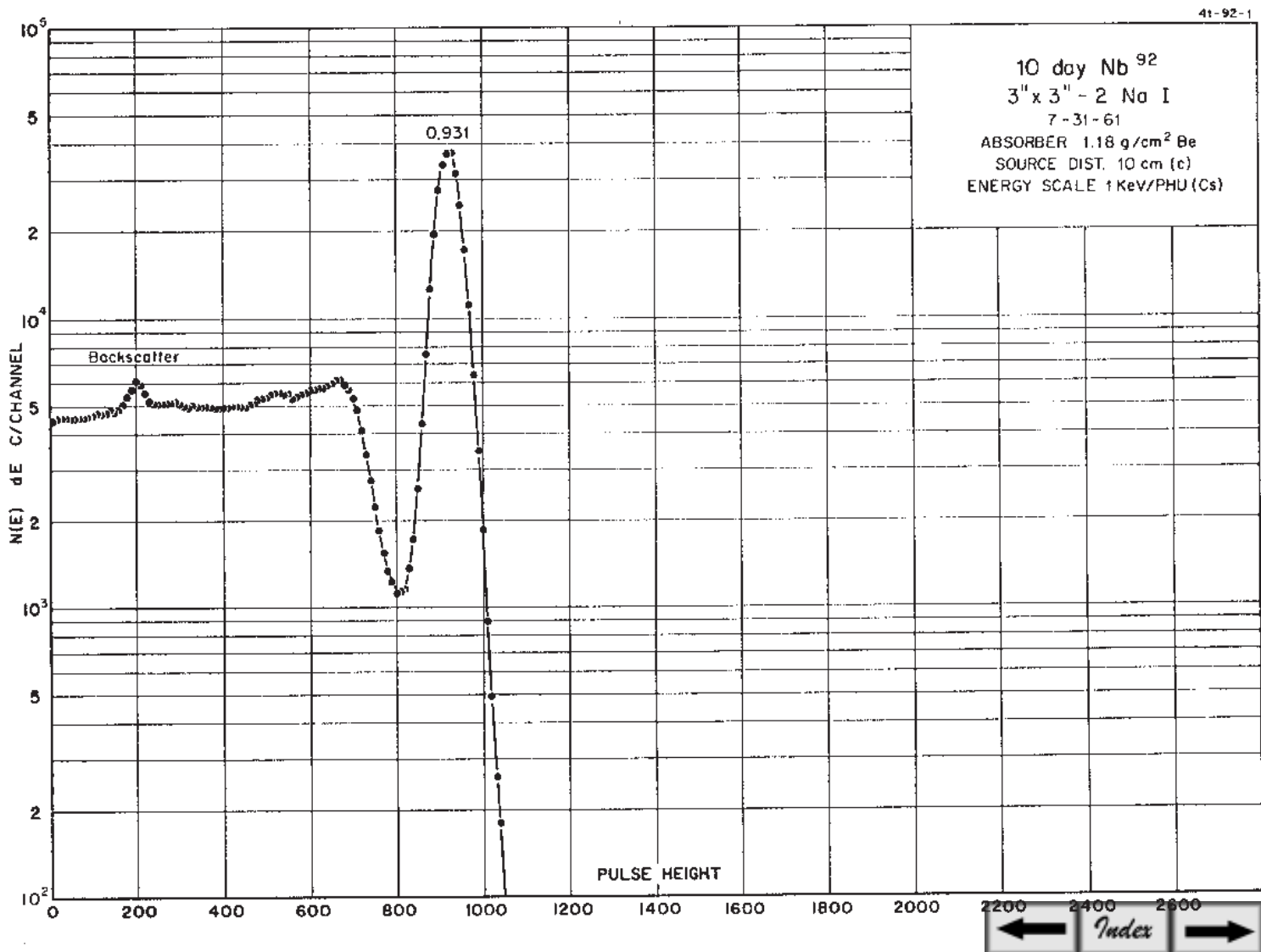
^{92m}Nb Decay Scheme

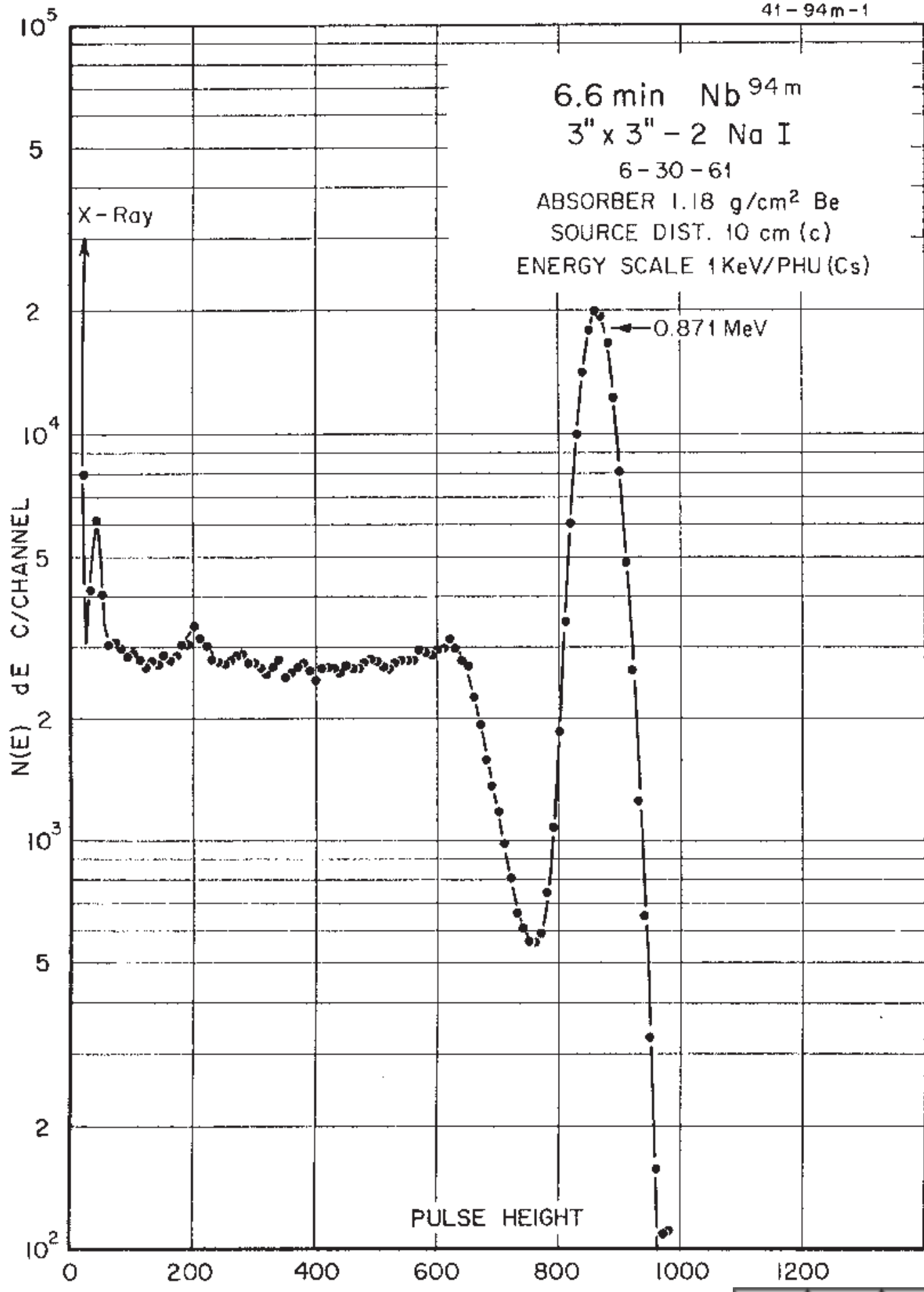


GAMMA-RAY ENERGIES AND INTENSITIES

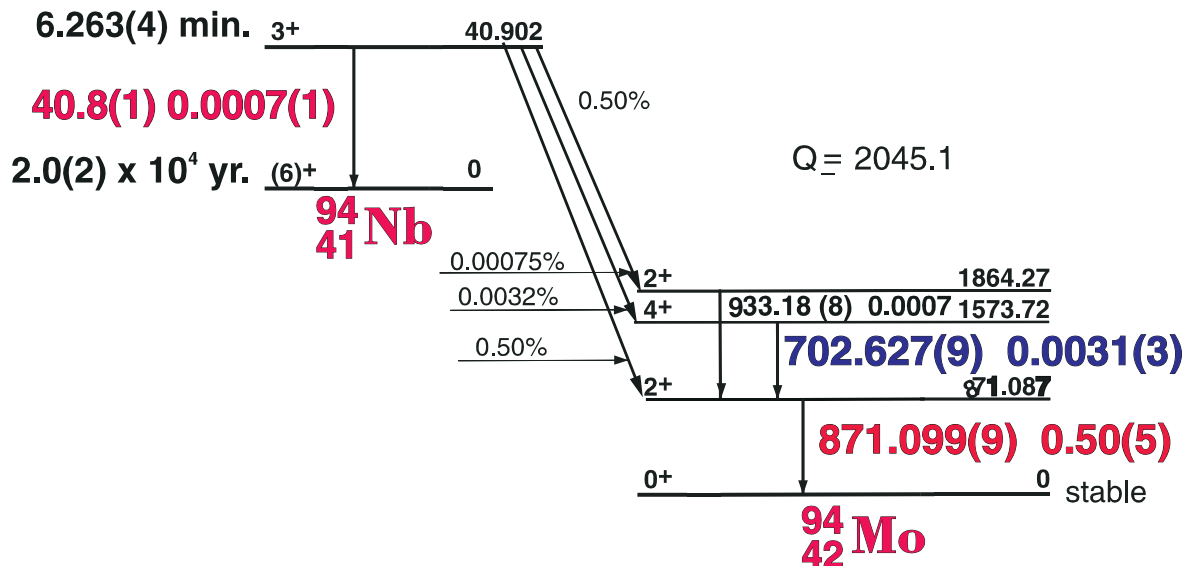
Nuclide ^{92}Nb Half Life 10.15 Day
 Detector 3" X 3" NaI-2 Method of Production: $\text{Nb}^{93}(\gamma, n)$

E_γ (KeV) [S]	ΔE_γ	I_γ (rel)	I_γ (%) [E]	ΔI_γ	S
912.71	± 0.10	2.0	1.78	± 0.05	3
934.51	± 0.04	100	99	± 1	1
1132.24	± 0.05	0.005	0.005	$\pm (5)$	5
1847.2	± 0.1	1.0	0.85	± 0.04	2





6.263(4) min. ^{94m}Nb Decay Scheme



41-94m-1

GAMMA-RAY ENERGIES AND INTENSITIES

Nuclide
Detector

^{94m}Nb

3" x 3" -2 Nal

Half Life 6.263(4) min.

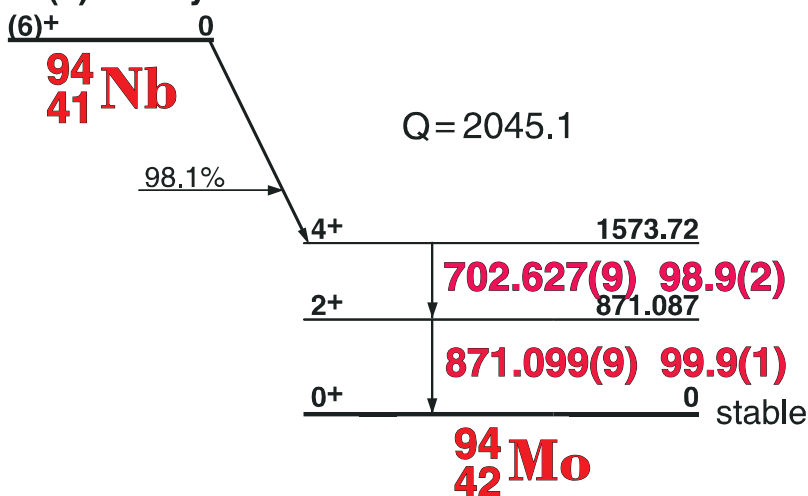
Method of Production: Nb⁹³(n,γ)

E_γ (KeV)[S]	ΔE_γ	I_γ (rel)	$I_\gamma(\%)$ [E]	ΔI_γ	S
40.8	± 0.1	0.8	0.0007	$\pm (1)$	1
702.627	± 0.009	0.70	0.0031	$\pm (3)$	4
871.099	± 0.009	100	0.50	± 0.05	1
933.18	± 0.08		0.0007	$\pm 0.(1)$	5

$2.0(2) \times 10^4$ Yr. ^{94}Nb

^{94}Nb Decay Scheme

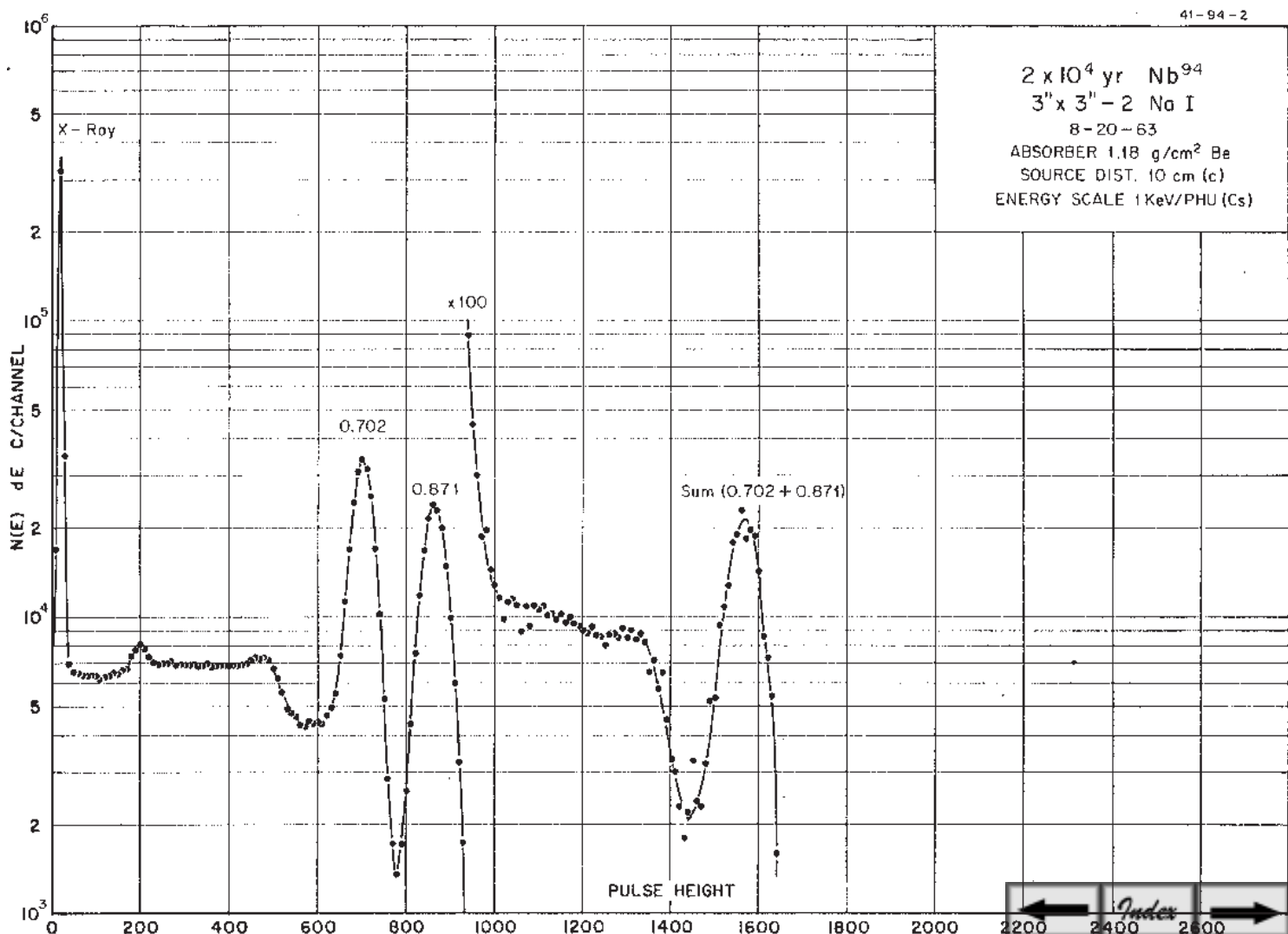
$2.0(2) \times 10^4$ yr.

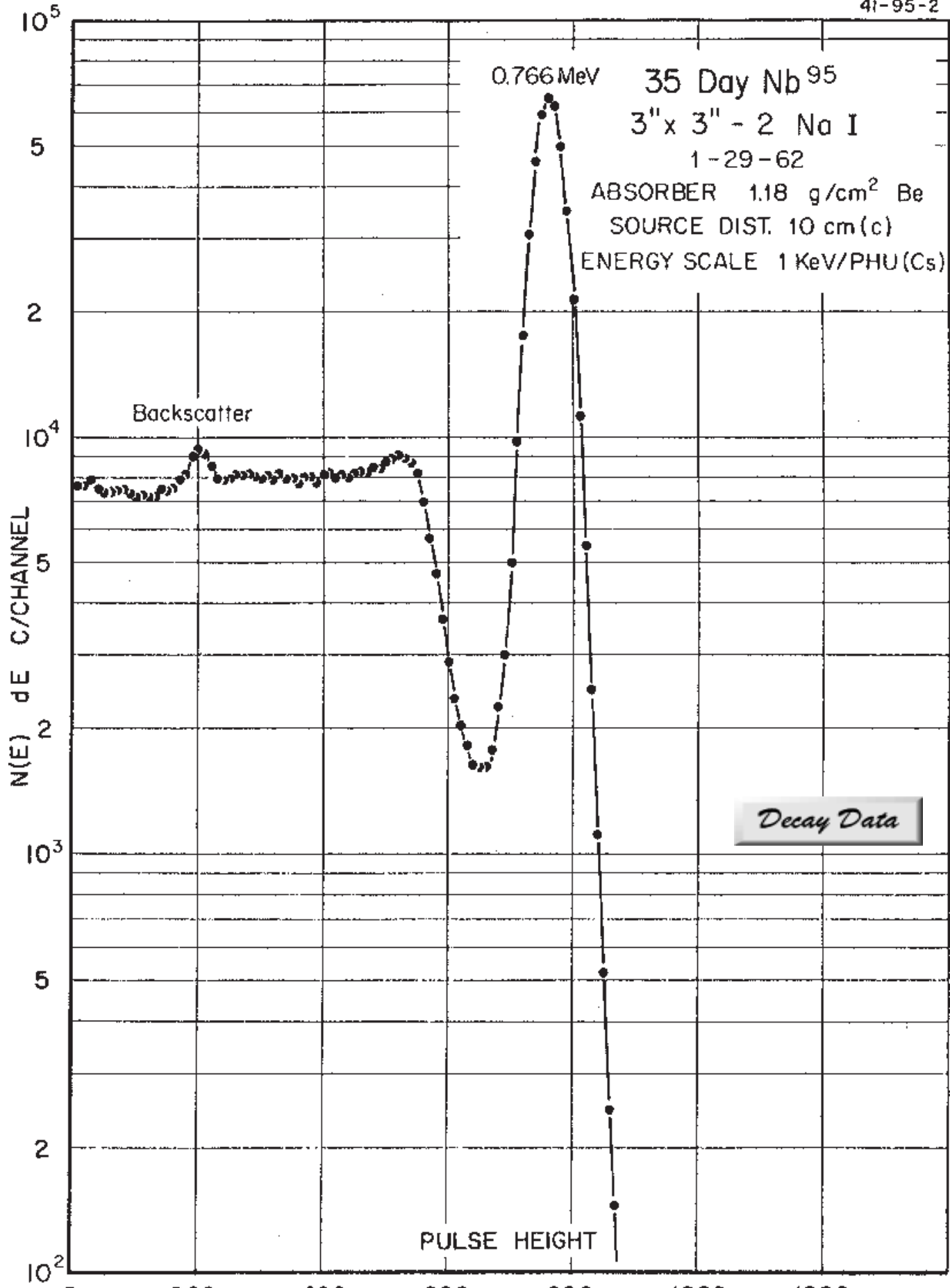


GAMMA-RAY ENERGIES AND INTENSITIES

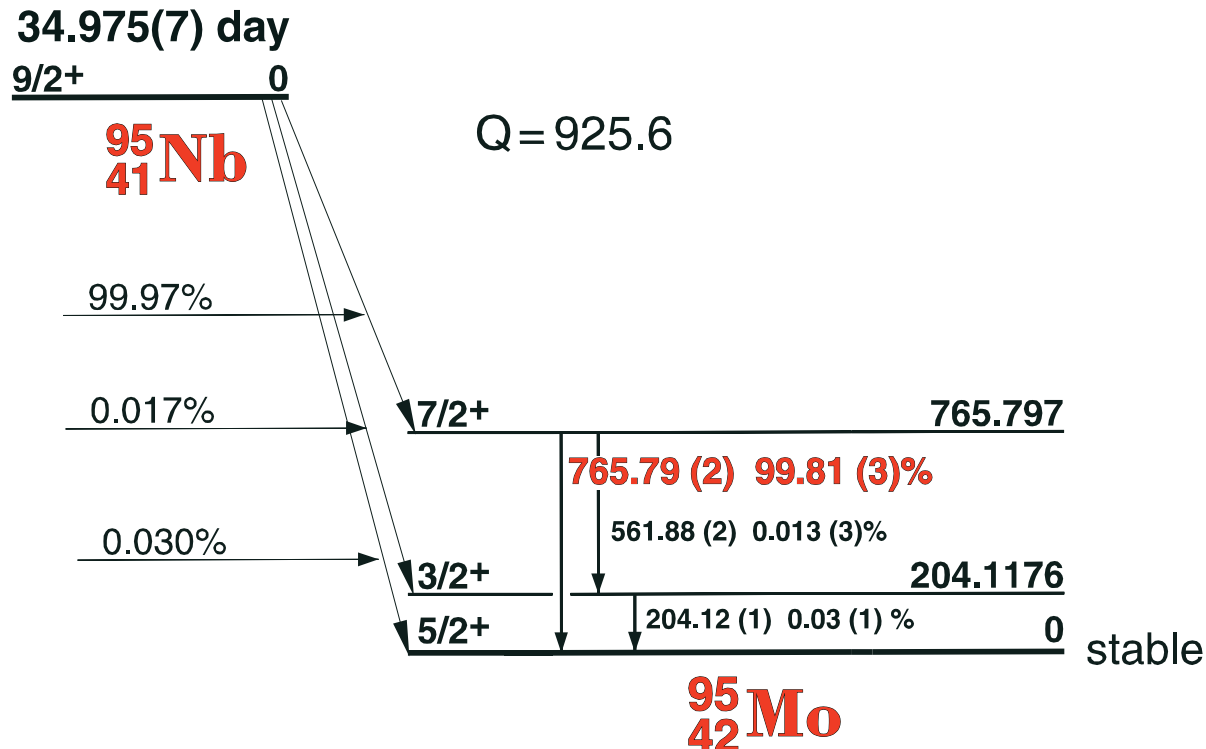
Nuclide ^{94}Nb Half Life $2.0(2) \times 10^4$ Yr.
Detector 3" X 3" NaI-2 Method of Production:Nb⁹³(n, γ)

E_γ (KeV)[S]	ΔE_γ	I_γ (rel)	I_γ (%) [E]	ΔI_γ	S
Mo x-rays					
702.627	± 0.009	100	98.9	± 0.2	1
871.099	± 0.009	100	99.9	± 0.1	1





34.975(7) day ^{95}Nb Decay Scheme

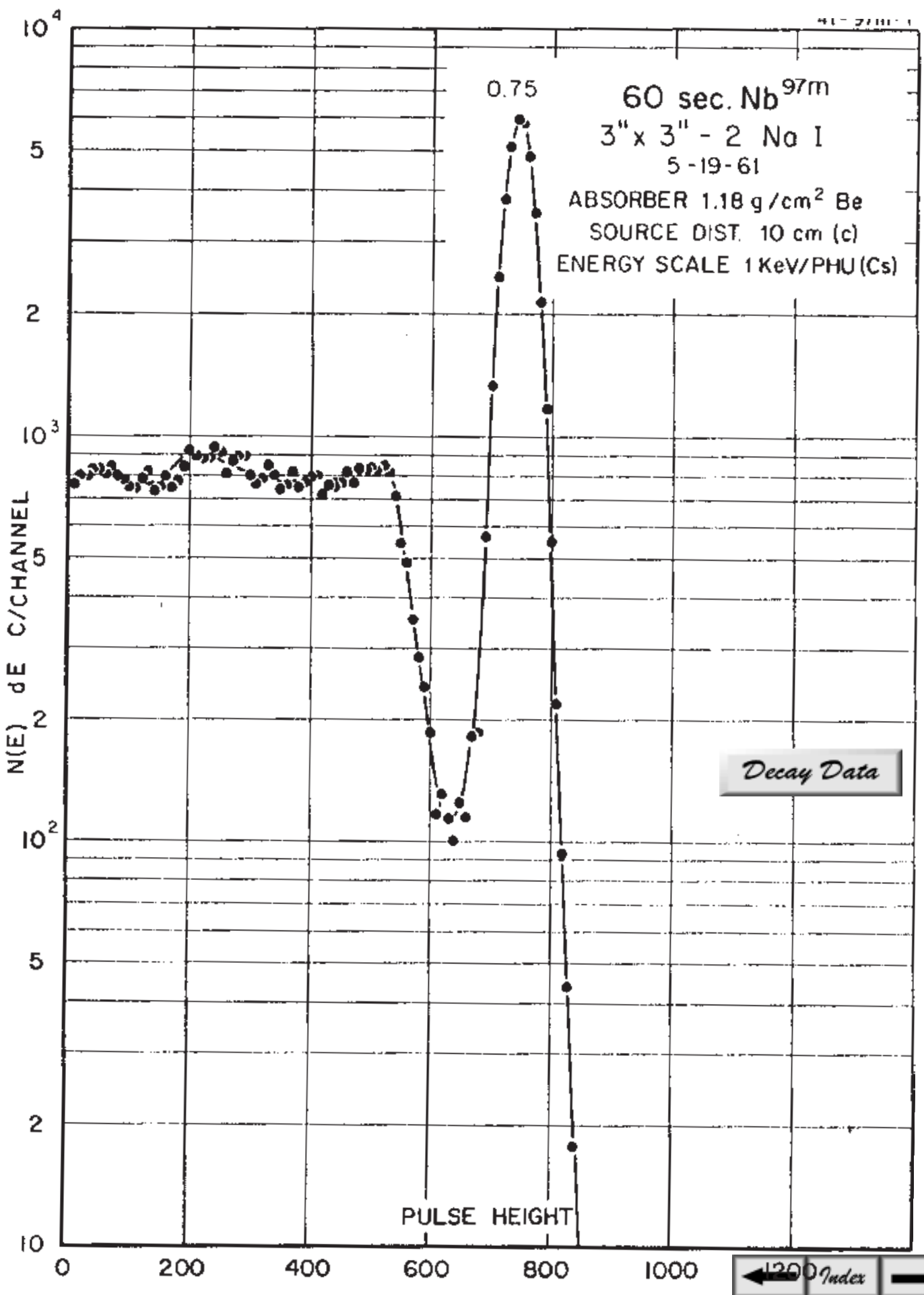


41-95-1

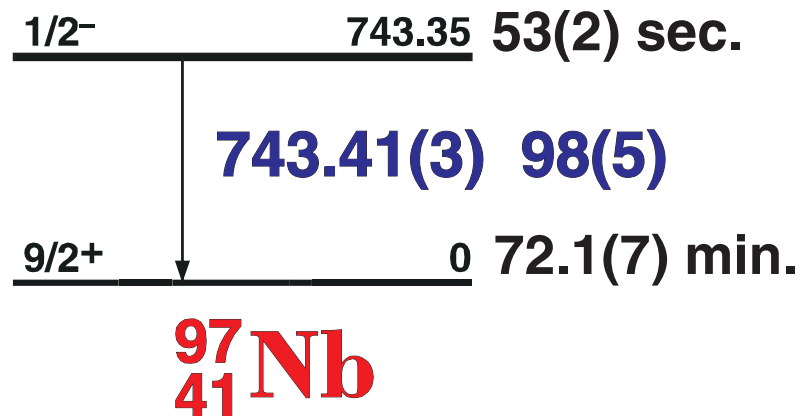
GAMMA-RAY ENERGIES AND INTENSITIES

Nuclide ^{95}Nb Half Life 34.975(7) day
Detector 3" x 3" -2 NaI Method of Production: $^{94}\text{Zr}(n,\gamma,\beta)$

E_{γ} (KeV)[S]	ΔE_{γ}	$I_{\gamma}(\text{rel})$	$I_{\gamma}(\%)[\text{E}]$	ΔI_{γ}	S
204.12	± 0.01		0.03	± 0.01	5
561.88	± 0.02		0.013	± 0.001	5
756.786	± 0.019	100	99.81	± 0.03	1



53(2) sec. ^{97m}Nb Decay Scheme



41-97m-1

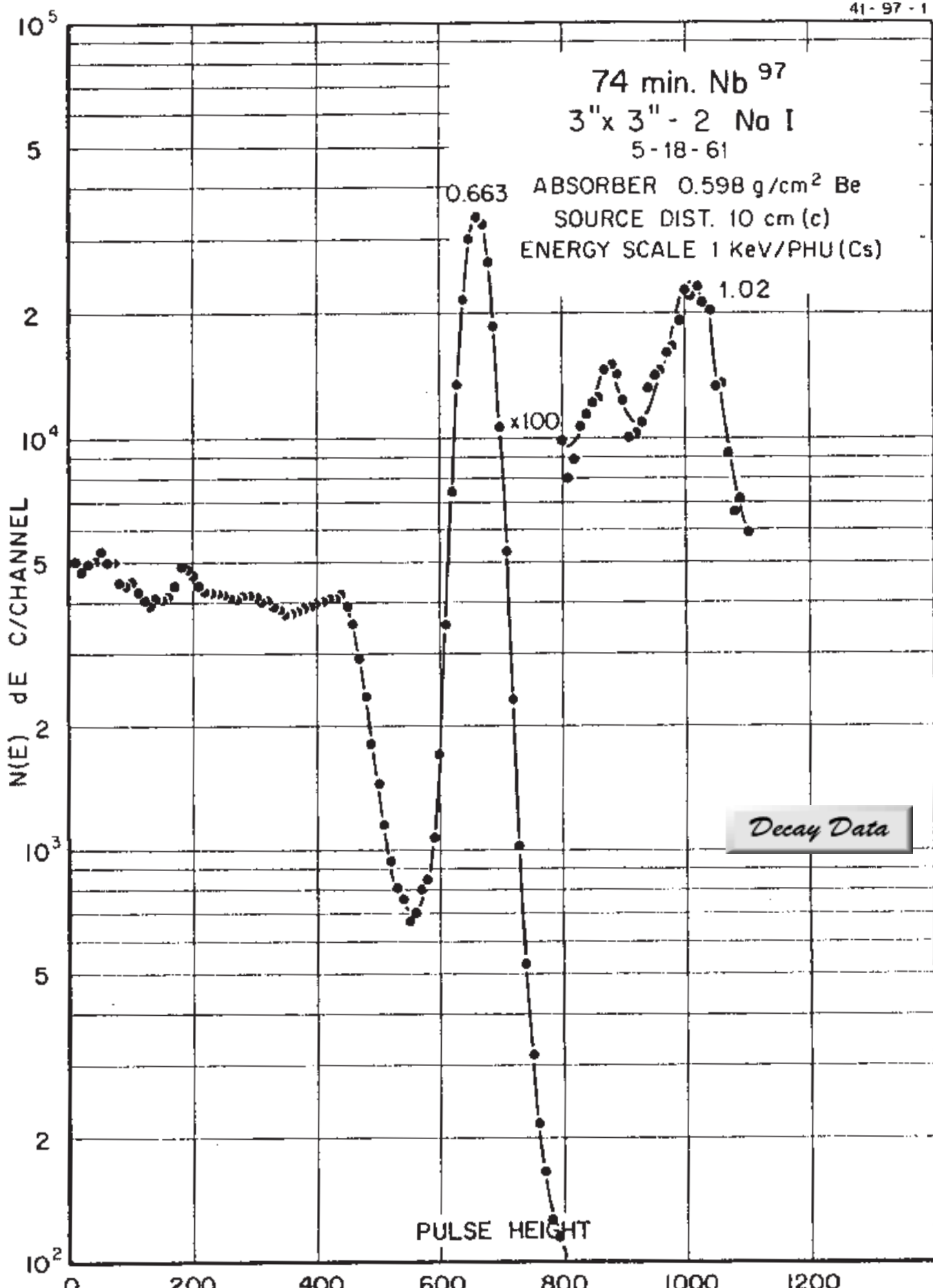
GAMMA-RAY ENERGIES AND INTENSITIES

Nuclide
Detector

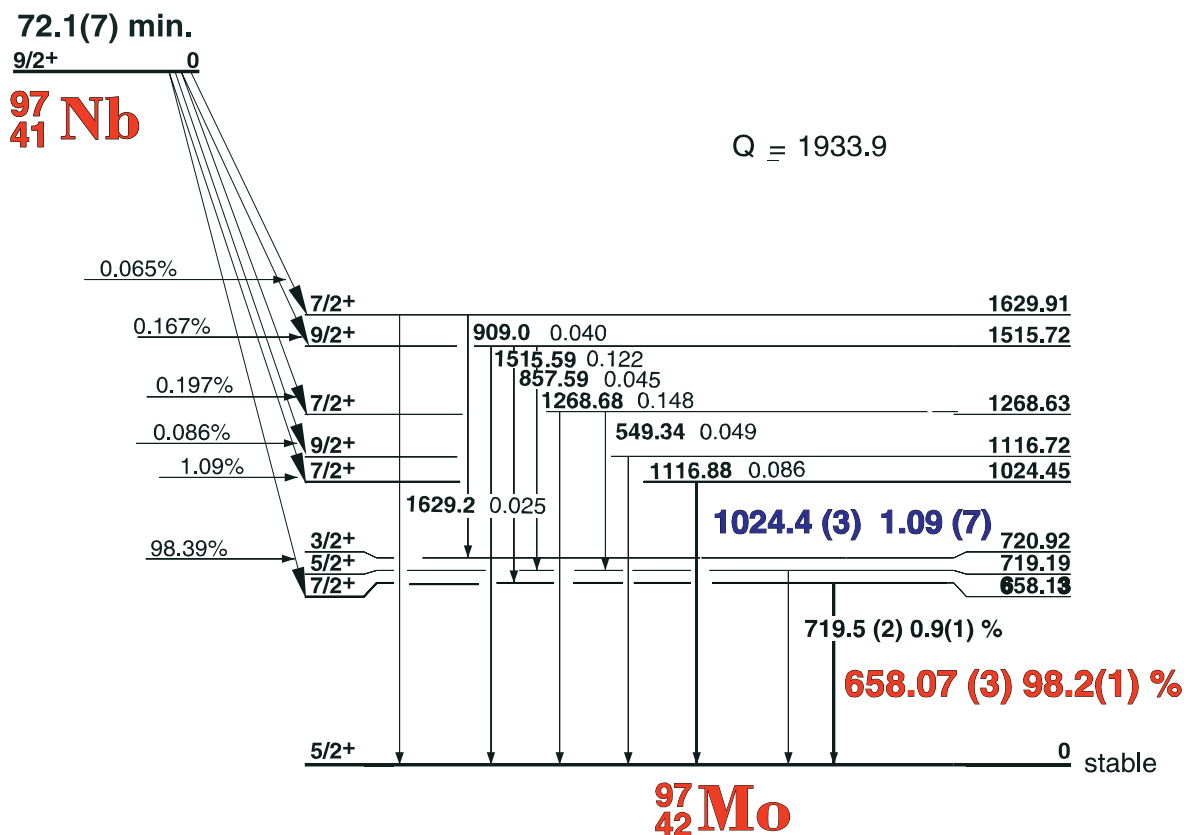
^{97m}Nb
3" x 3" -2 Nal

Half Life 53(2) sec.
Method of Production: $\text{Zr}^{96}(n,\gamma,\beta)$

E_γ (KeV)[S]	ΔE_γ	I_γ (rel)	$I_\gamma(\%)$ [E]	ΔI_γ	S
743.40	± 0.035	100	98	± 5.0	1



72.1(7) min. ^{97}Nb Decay Scheme



41-97-1

GAMMA-RAY ENERGIES AND INTENSITIES

Nuclide
Detector

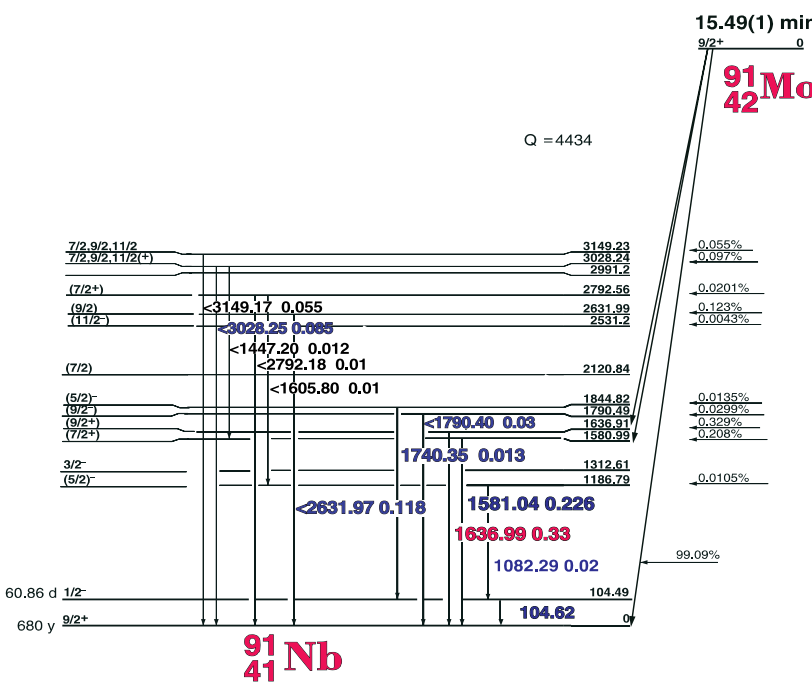
^{97}Nb
3" x 3" -2 NaI

Half Life 72.1(7) min.
Method of Production: $\text{Zr}^{96}(\text{n},\gamma,\beta)$

E_{γ} (KeV)[S]	ΔE_{γ}	I_{γ} (rel)	$I_{\gamma}(\%)$ [E]	ΔI_{γ}	S
658.174	± 0.05	100	98.2	± 0.1	1
719.6	± 0.1	0.12	0.9	± 0.1	4
1024.47	± 0.08	1.12	1.09	± 0.07	2
1116.6	± 0.2	0.10	0.065	± 0.01	4
1268.47	± 0.1	0.15	0.15	± 0.1	3
1515.45	± 0.15	0.12	0.122	± 0.01	3

15.49(1) min. ^{91}Mo

^{91}Mo Decay Scheme



GAMMA-RAY ENERGIES AND INTENSITIES

Nuclide ^{91}Mo

Detector 3" X 3" NaI-2

Half Life 15.49(1) min.

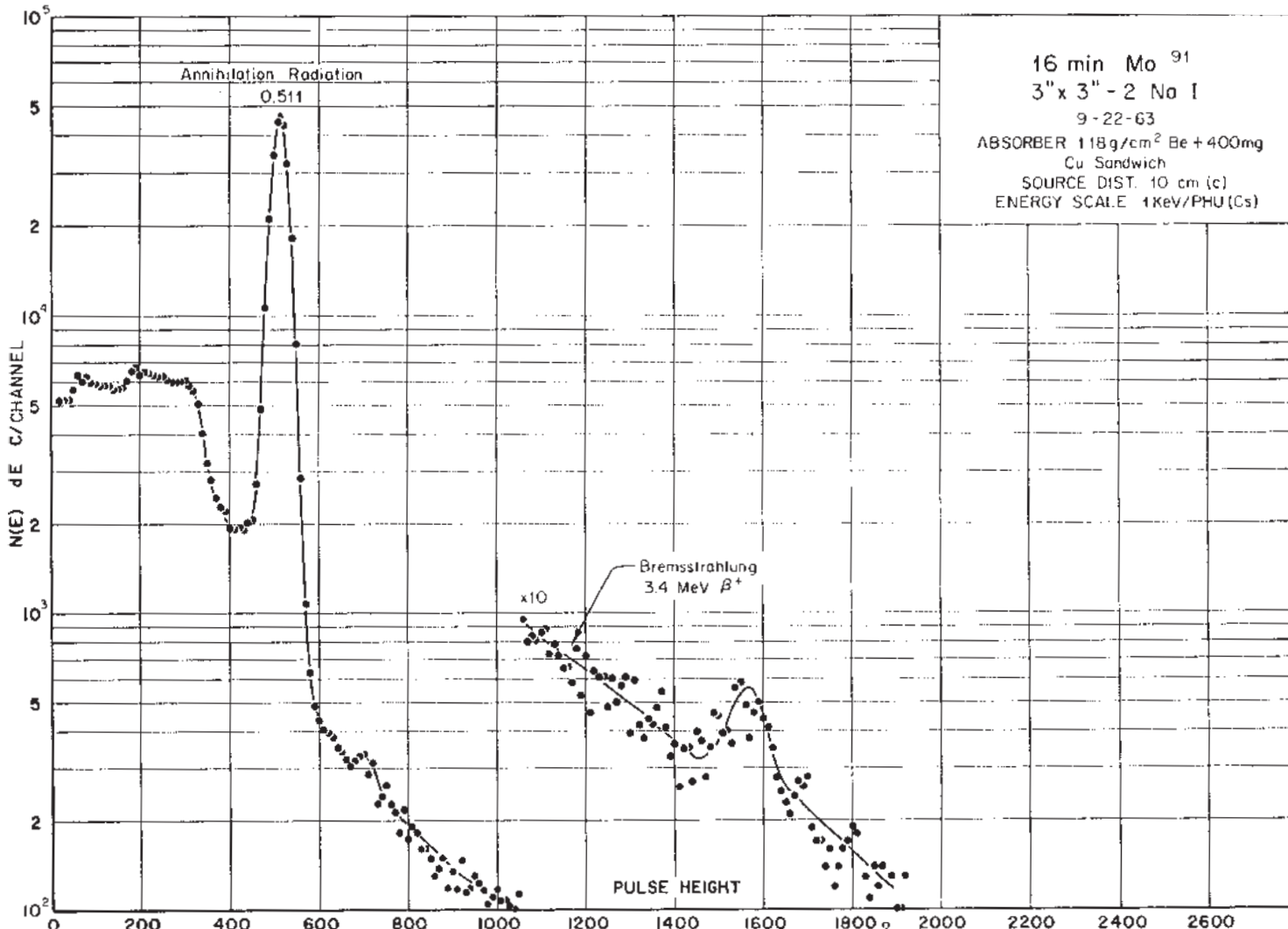
Method of Production: Mo⁹²(γ ,n)

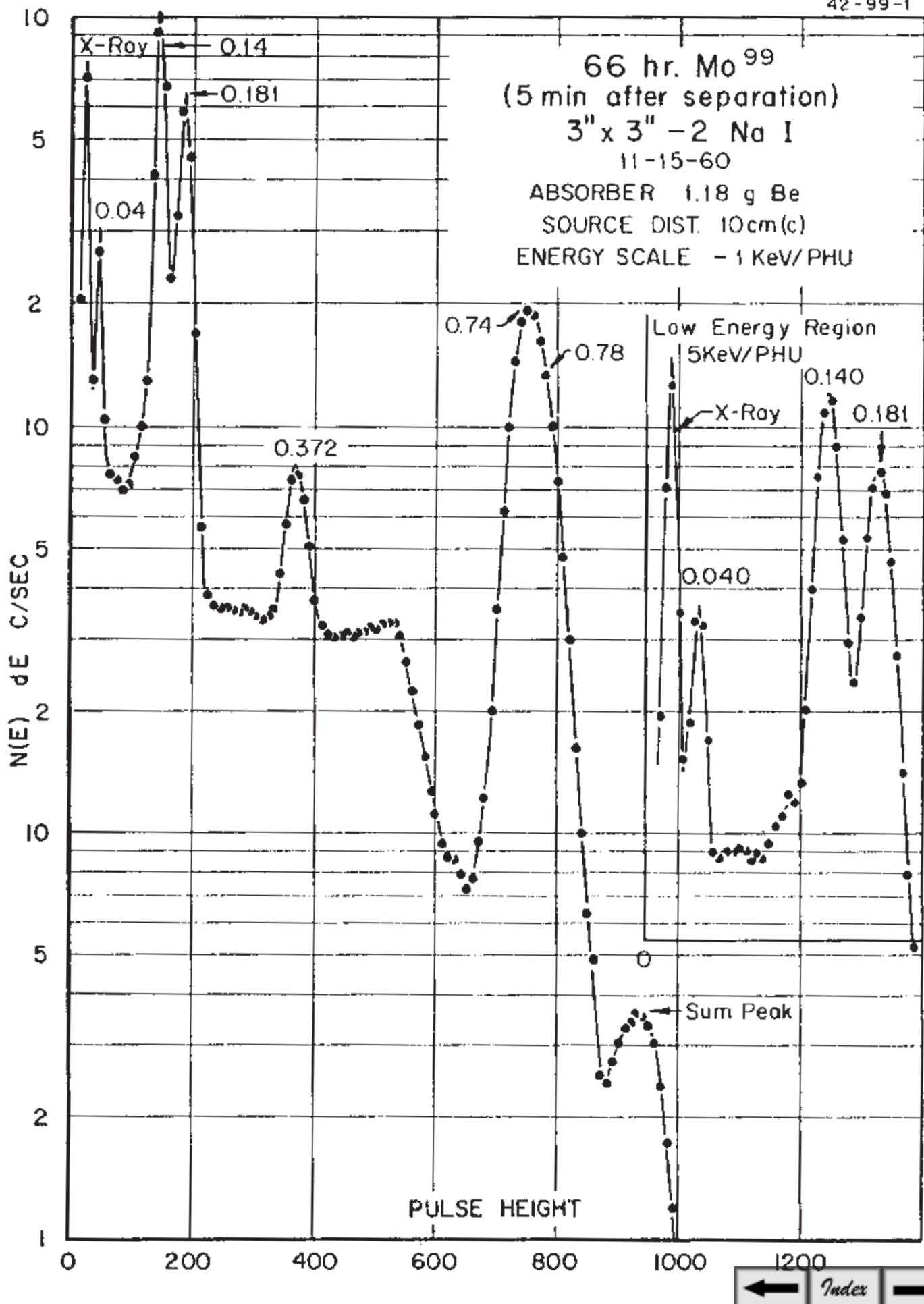
E_{γ} (KeV)[S]	ΔE_{γ}	$I_{\gamma}(\text{rel})$	$I_{\gamma}(\%)$ [E]	ΔI_{γ}	S

60.86 d 1/2⁻

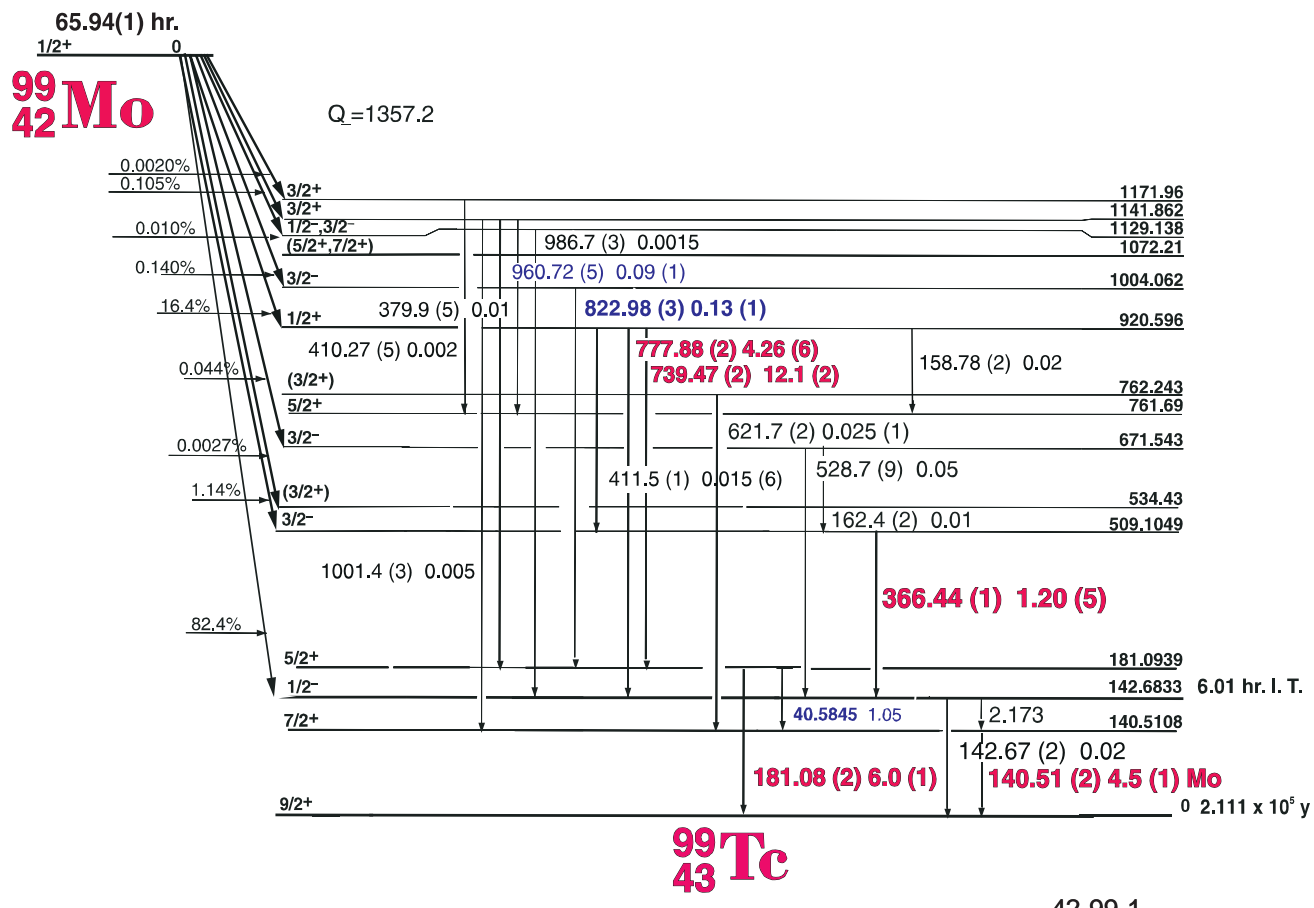
680 y 9/2⁺

^{91}Nb 41





65.94(1) hr. ^{99}Mo Decay Scheme

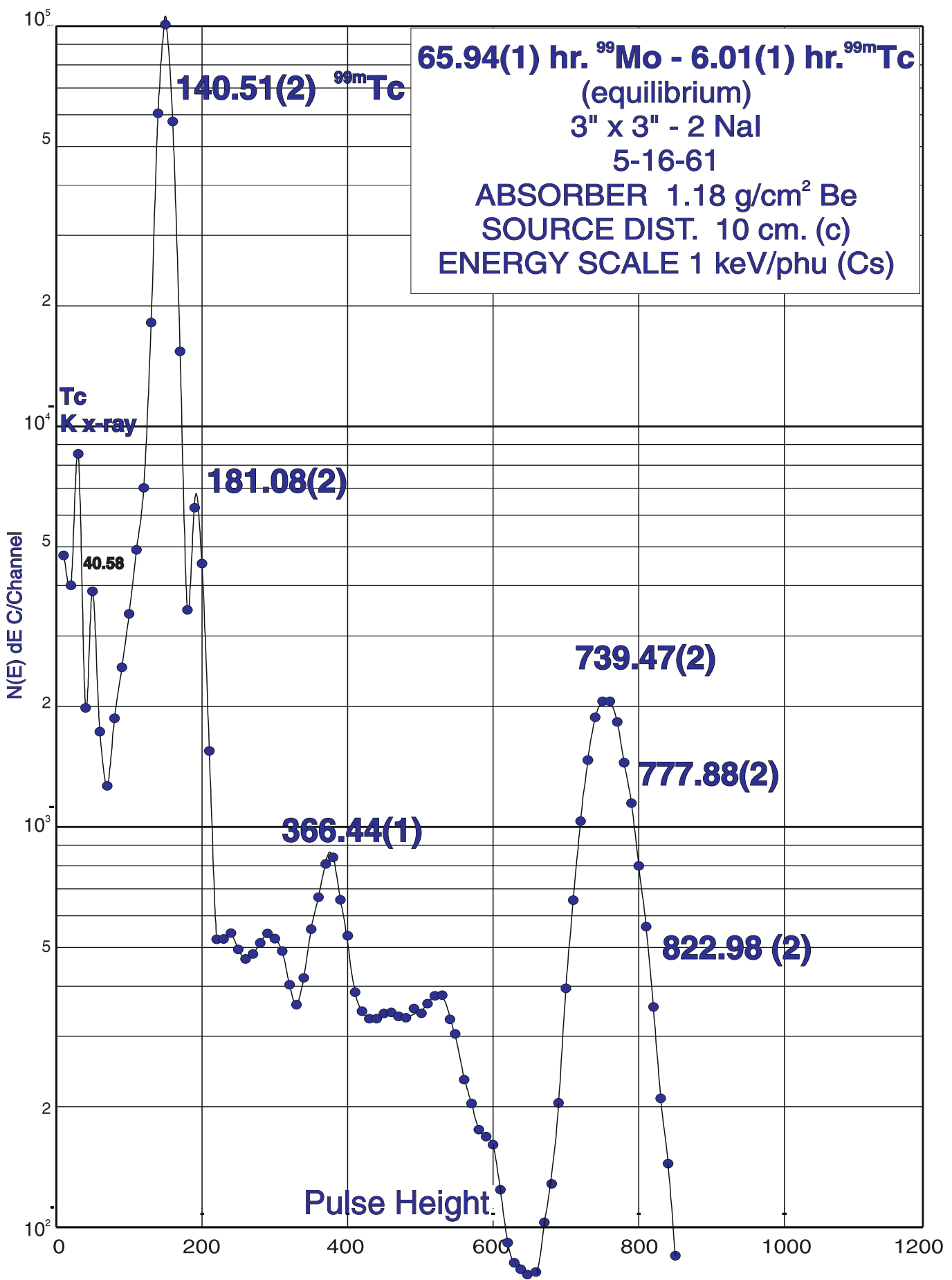


42-99-1

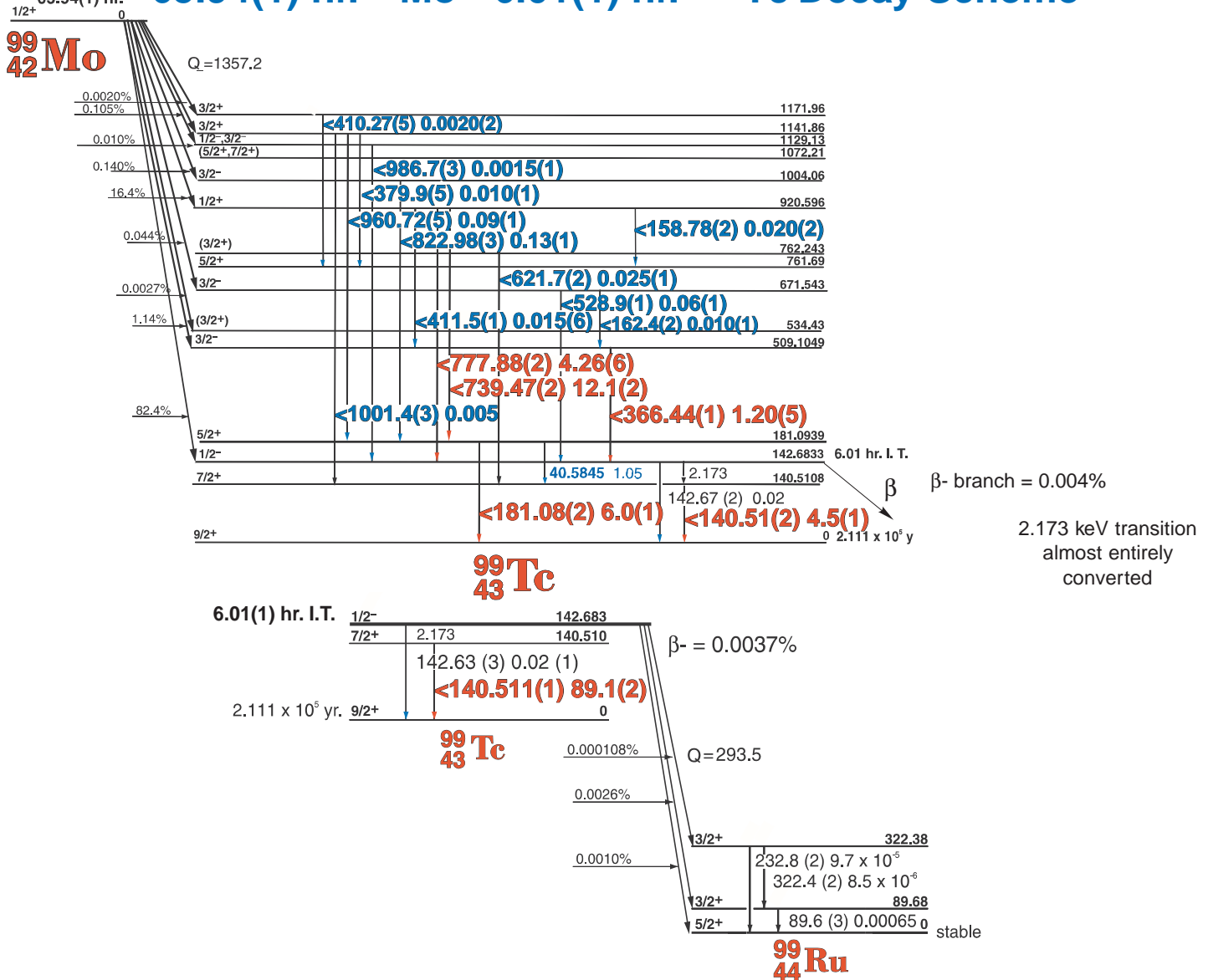
GAMMA-RAY ENERGIES AND INTENSITIES

Nuclide ^{99}Mo Half Life 65.94(1) hr. (Tc 6.01(1) min.)
 Detector 3" x 3" -2 NaI Method of Production: $^{98}\text{Mo}(n,\gamma)$

	E_{γ} (KeV)[S]	ΔE_{γ}	$I_{\gamma}(\text{rel})$	$I_{\gamma}(\%)[E]$	ΔI_{γ}	S
$^{99\text{m}}\text{Tc}$	40.576	± 0.02	0.63	0.95	± 0.09	4
	140.509	± 0.02	100	4.5 (82)	± 0.05	1
	181.085	± 0.016	6.8	6.0	± 0.1	1
	366.44	± 0.015	1.37	1.20	± 0.05	1
	379.9	± 0.5	0.01	0.01	± 0.005	4
	411.5	± 0.1	0.05	0.015	± 0.005	4
	528.9	± 0.1	0.05	0.06	± 0.01	4
	621.9	± 0.15	0.026	0.04	± 0.01	4
	739.469	± 0.025	13.7	12.1	± 0.9	1
	777.878	± 0.025	4.9	4.26	± 0.3	1
	822.98	± 0.03	0.15	0.13	± 0.01	2
	859.2	± 0.5	0.002	0.007	± 0.003	4
	960.7	± 0.02	0.11	0.09	± 0.01	2
	986.7	± 0.3	0.002	0.0015	± 0.0005	4
	1001.4	± 0.3	0.004	0.0055	± 0.0005	4



65.94(1) hr. ^{99}Mo - 6.01(1) hr. $^{99\text{m}}\text{Tc}$ Decay Scheme



GAMMA-RAY ENERGIES AND INTENSITIES

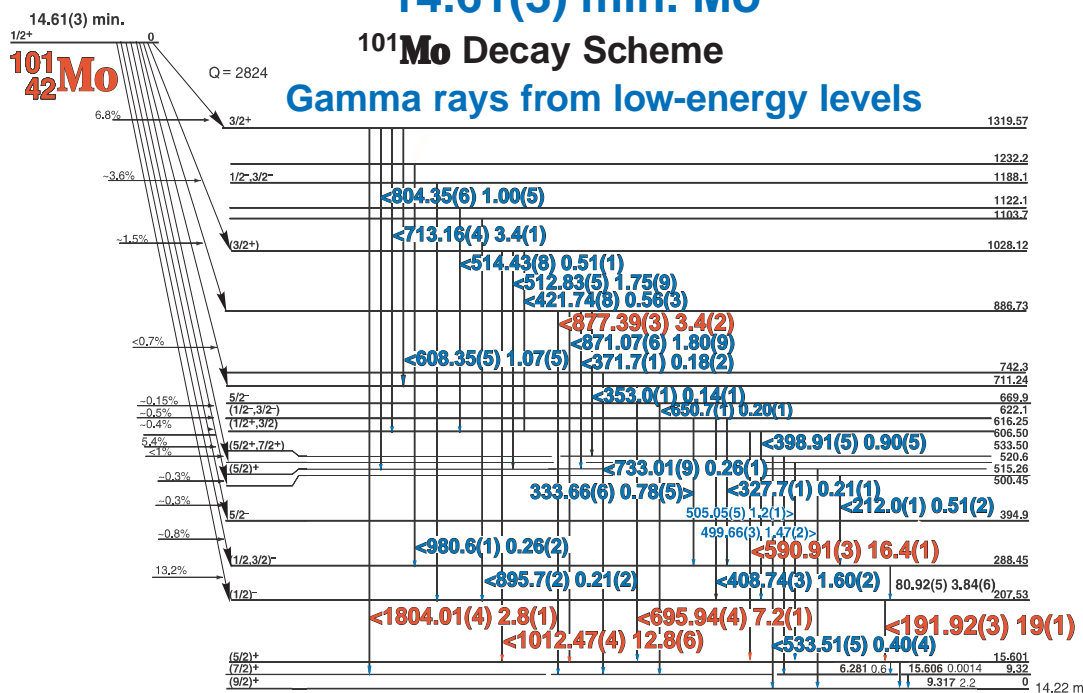
42-99(43-99m)-1

Nuclide Detector	$^{99}\text{Mo} - {}^{99\text{m}}\text{Tc}$		Half Life 65.94(1) hr. (Tc 6.01(1) hr.)			
	3" x 3" -2 NaI		Method of Production: Mo ⁹⁸ (n,γ)			
	E_γ (KeV)[S]	ΔE_γ	I _γ (rel)	I _γ (%) [E]	ΔI_γ	S
${}^{99\text{m}}\text{Tc}$	40.576	± 0.02	0.63	0.95	± 0.09	4
	140.509	± 0.02	100	4.5 (82)	± 0.05	1
	181.085	± 0.016	6.8	6.0	± 0.1	1
	366.44	± 0.015	1.37	1.20	± 0.05	1
	379.9	± 0.5	0.01	0.01	± 0.005	4
	411.5	± 0.1	0.05	0.015	± 0.005	4
	528.9	± 0.1	0.05	0.06	± 0.01	4
	621.9	± 0.15	0.026	0.04	± 0.01	4
	739.469	± 0.025	13.7	12.1	± 0.9	1
	777.878	± 0.025	4.9	4.26	± 0.3	1
	822.98	± 0.03	0.15	0.13	± 0.01	2
	859.2	± 0.5	0.002	0.007	± 0.003	4
	960.7	± 0.02	0.11	0.09	± 0.01	2
	986.7	± 0.3	0.002	0.0015	± 0.0005	4
	1001.4	± 0.3	0.004	0.0055	± 0.0005	4

14.61(3) min. Mo¹⁰¹

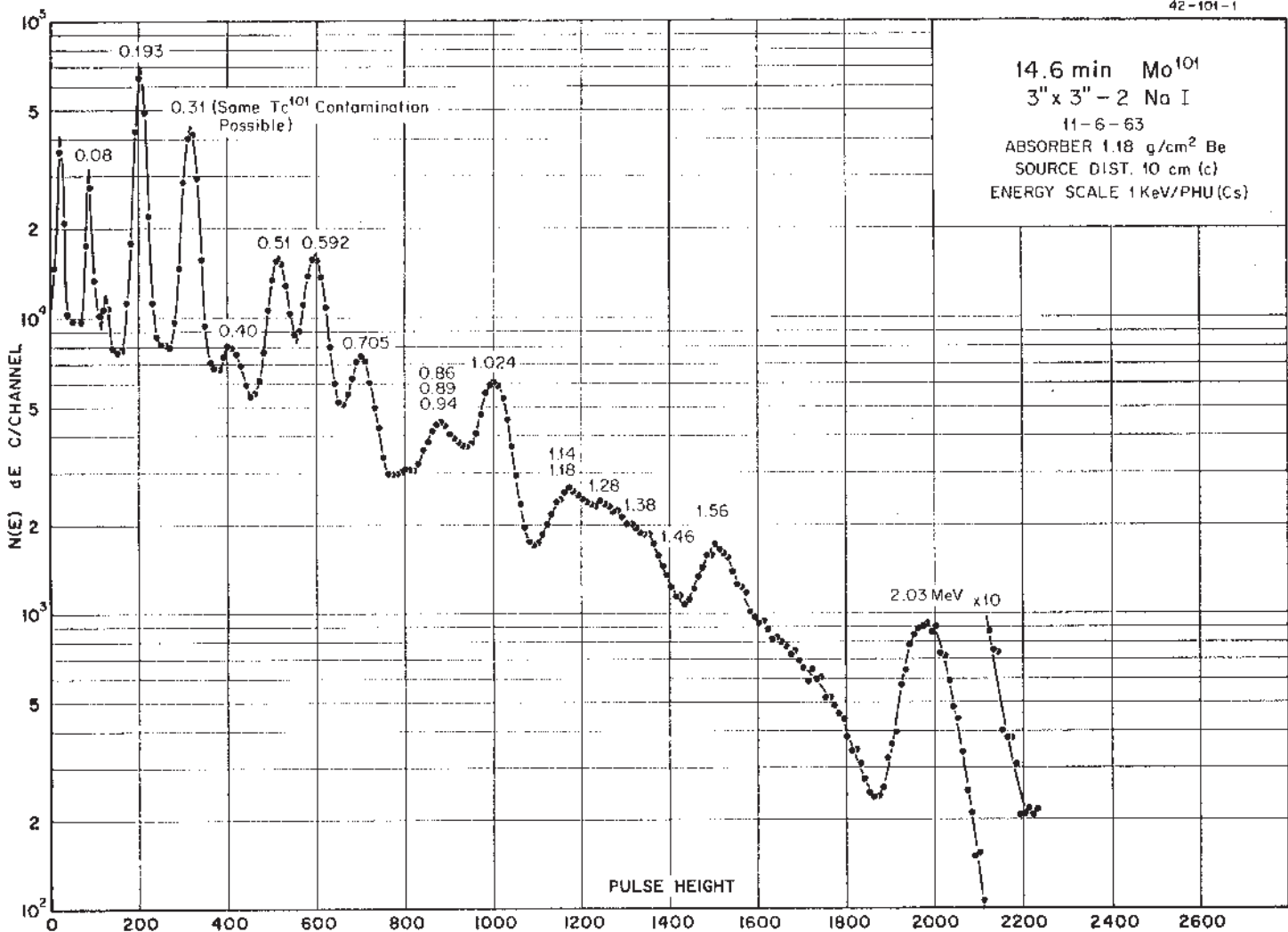
¹⁰¹Mo Decay Scheme

Gamma rays from low-energy levels

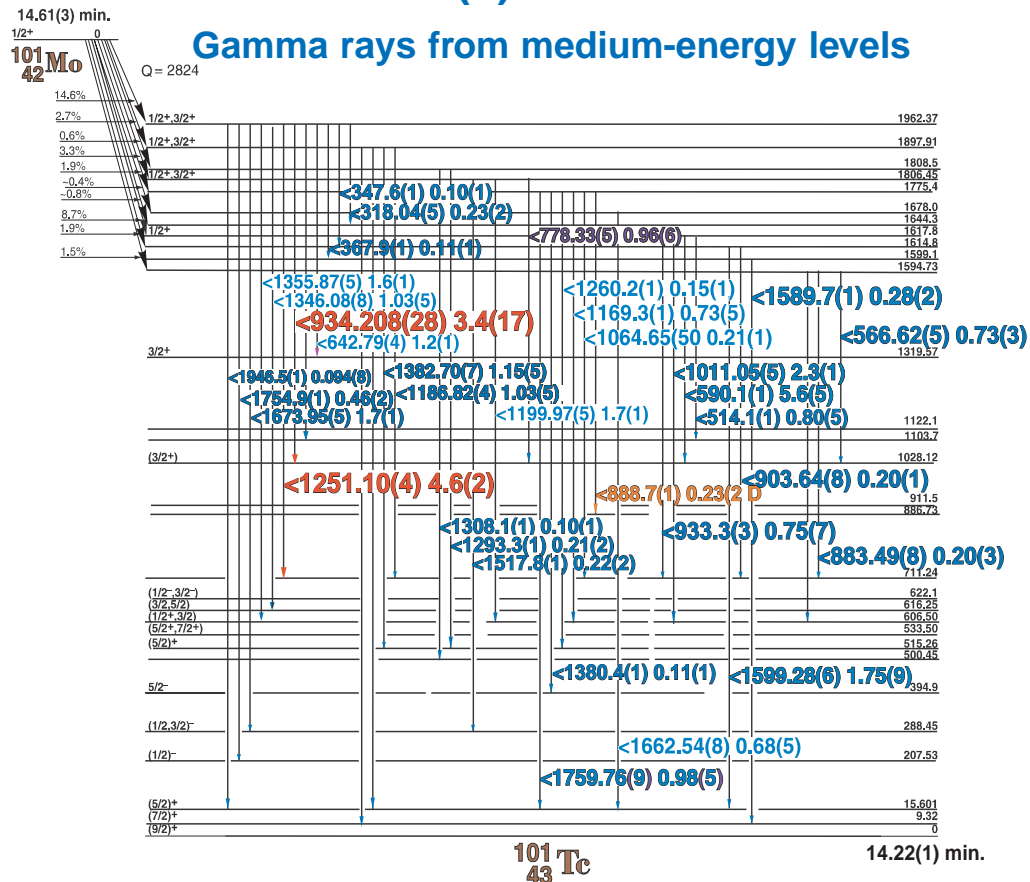


¹⁰¹Tc 43

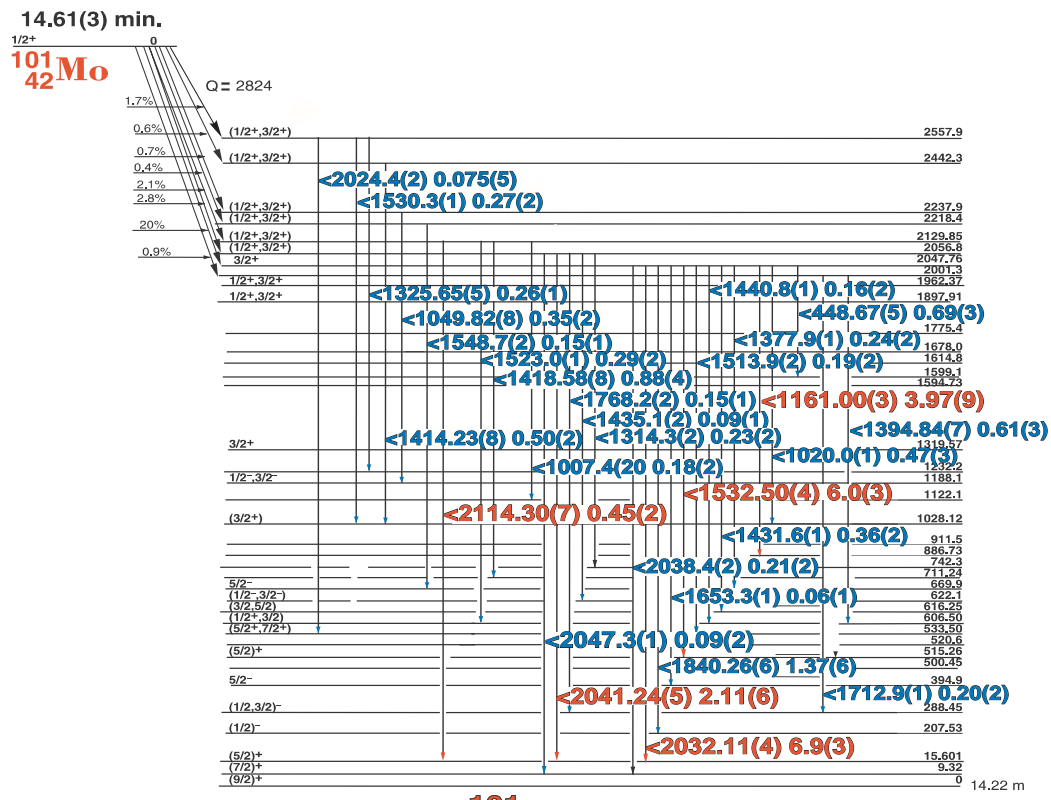
42 - 101 - 1



14.61(3) min. Mo¹⁰¹



Gamma rays from high-energy levels



101 Tc



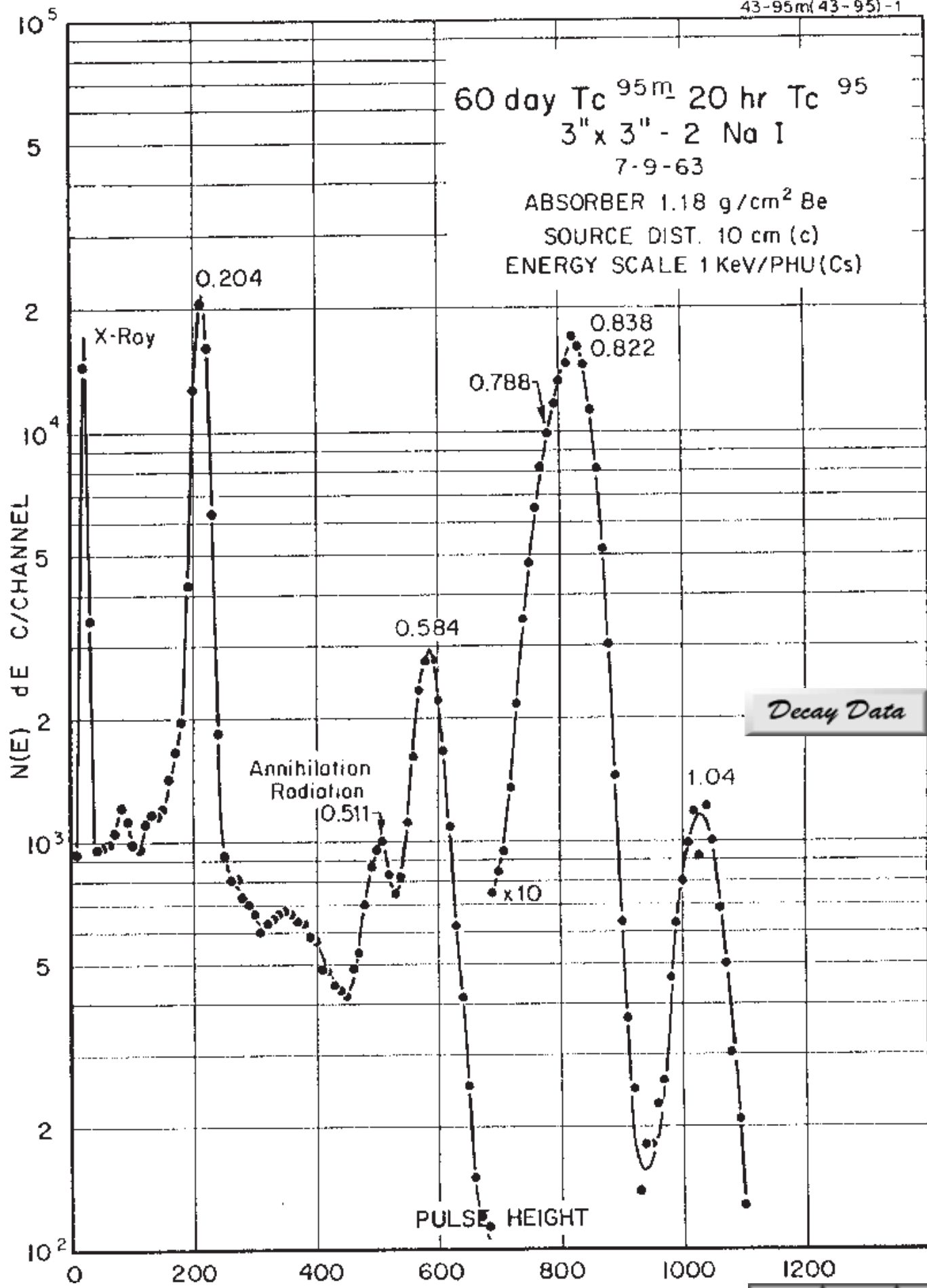
14.61(3) min. Mo¹⁰¹

GAMMA-RAY ENERGIES AND INTENSITIES

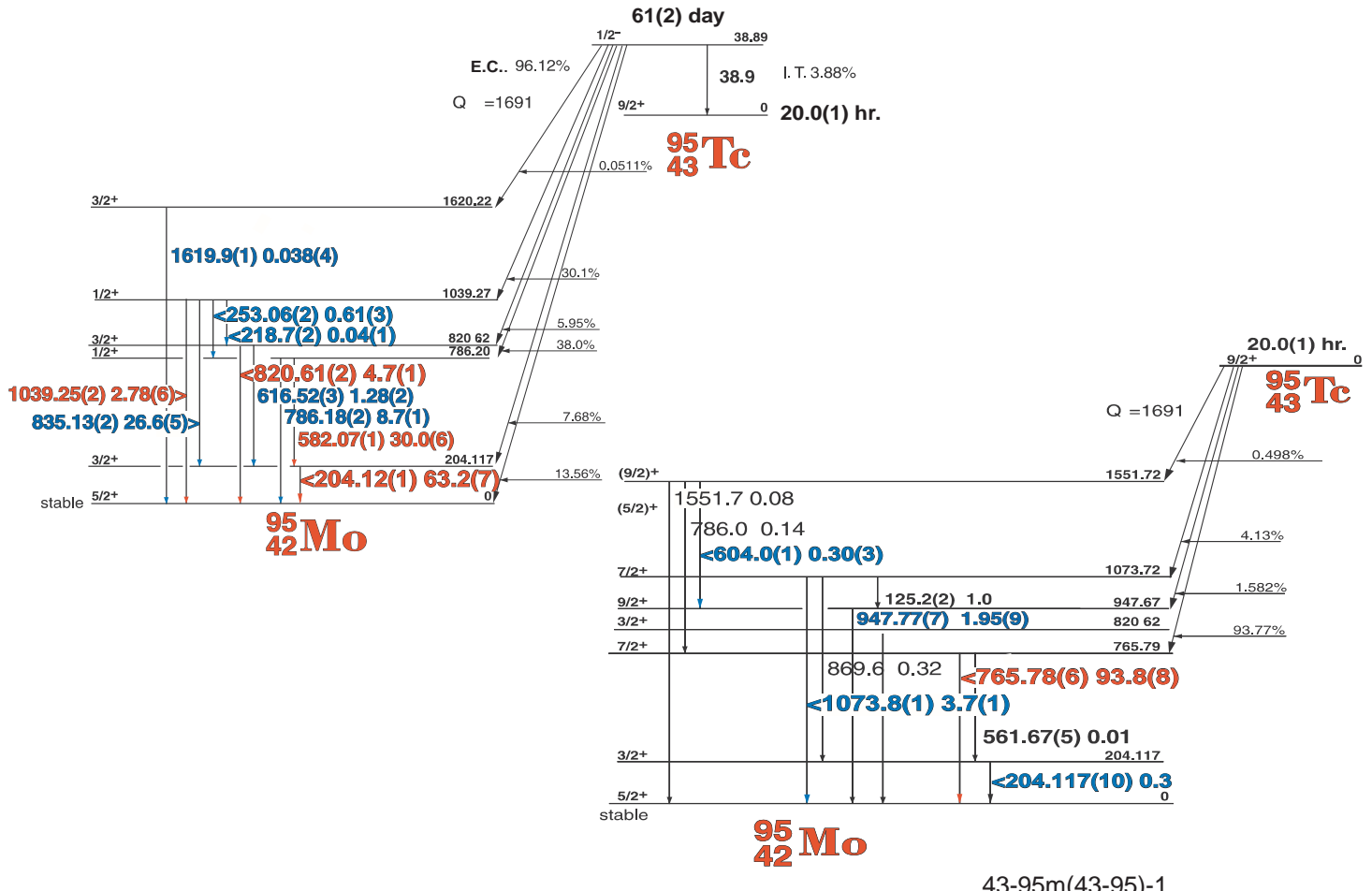
Nuclide ⁹¹Mo
Detector 3" X 3" NaI-2 Half Life 14.61(3) min.
Method of Production: Mo¹⁰⁰(n,γ)

	E _γ (KeV)[S]	ΔE _γ	I _γ (rel)	I _γ (%)[E]	ΔI _γ	S
¹⁰¹ Tc	127.23	± 0.05	9.01		+ 0.5	3
	191.923	± 0.028	81.9	19	± 1.0	1
	195.95	± 0.06	11.52		+ 0.6	3
	212.00	± 0.04	2.20	0.51	± 0.05	4
¹⁰¹ Tc	306.819	± 0.025	353		± 10.0	1
	311.33	± 0.1	0.77		± 0.07	4
	318.04	± 0.05	1.03	0.20	± 0.10	4
	327.67	± 0.1	1.31	0.22	± 0.01	4
	333.66	± 0.06	3.36	0.78	± 0.04	3
	347.61	± 0.1	0.77		± 0.10	4
	353.0	± 0.1	0.84	0.13	± 0.01	4
	370.12	± 0.15	1.0	0.20	± 0.01	4
	371.87	± 0.15	0.8	0.13	± 0.01	4
	398.91	± 0.05	4.13		± 0.3	3
	408.736	± 0.03	7.45	1.60	± 0.50	3
	421.74	± 0.08	3.01	0.56	± 0.03	3
	432.61	± 0.15	0.46		± 0.1	4
	448.67	± 0.05	3.46	0.69	± 0.03	3
	468.99	± 0.15	0.76		± 0.15	4
	482.52	± 0.12	0.73		± 0.15	4
	499.66	± 0.03	7.21	1.47	± 0.08	3
	505.938	± 0.030	57.1	11.8	± 0.6	1
	512.83	± 0.05	7.28	1.75	± 0.09	3
	515.43	± 0.08	3.99	0.51	± 0.03	3
¹⁰¹ Tc	531.52	± 0.08	4.63		± 0.35	3
¹⁰¹ Tc	533.62	± 0.1	2.1	0.40	± 0.04	3
	545.050	± 0.035	24.5		± 1.5	1
	566.625	± 0.05	4.06	0.73	± 0.03	3
	590.908	± 0.030	100	16.4	± 0.8	1
¹⁰¹ Tc	608.35	± 0.05	5.09	1.07	± 0.05	3
	626.96	± 0.1	1.2		± 0.2	4
	642.79	± 0.04	6.65	1.24	± 0.06	3
	660.66	± 0.1	1.10	0.20	± 0.02	4
	695.938	0.040	34.7	7.2	± 0.3	1
	702.1	0.08	1.66	0.38	± 0.02	4
¹⁰¹ Tc	713.159	0.045	16.82	3.4	± 0.15	2
¹⁰¹ Tc	715.70	0.15	2.70		± 0.25	3
¹⁰¹ Tc	720.20	0.2	1.10		± 0.1	4
	728.28	± 0.2	0.53		± 0.08	4
	733.01	± 0.09	1.66	0.26	± 0.01	4
	774.21	± 0.07	2.19		± 0.25	4
	778.334	± 0.05	4.63	0.96	± 0.05	3
	790.1	± 0.2	0.63		± 0.1	4
	804.35	± 0.06	4.98	1.00	± 0.05	3
	815.32	± 0.09	1.33	0.18	± 0.01	4
	842.85	± 0.2	0.88		± 0.1	4
	853.17	± 0.1	1.20		± 0.15	4
	871.070	± 0.06	8.94	1.80	± 0.09	3
	877.39	± 0.035	17.04	3.4	± 0.17	1

	E _γ (KeV)[S]	ΔE _γ	I _γ (rel)	I _γ (%)[E]	ΔI _γ	S	
	883.49	± 0.08	3.14		0.70	± 0.03	3
	888.00	± 0.15	2.40		0.46	± 0.02	4
	895.73	± 0.25	1.38		0.21	± 0.01	4
	903.640	± 0.12	1.32		0.20	± 0.01	4
	934.208	± 0.028	21.84	3.4	± 0.17	1	
	944.14	± 0.15	0.67		0.15	± 0.01	4
	980.58	± 0.10	1.73		0.27	± 0.02	4
	988.25	± 0.2	1.09			± 0.15	4
	1012.475	± 0.038	76.63	12.8	± 0.7	1	
	1019.27	± 0.05	4.98		0.67	± 0.05	3
	1049.82	± 0.08	1.90		0.35	± 0.02	3
	1064.65	± 0.12	1.60		0.25	± 0.02	4
	1161.005	± 0.035	22.0	3.97	± 0.2	1	
	1169.39	± 0.12	4.24		0.63	± 0.05	4
	1186.826	± 0.045	5.09		0.93	± 0.1	3
	1199.966	± 0.05	9.50		1.75	± 0.08	2
	1251.10	± 0.040	25.77	4.6	± 0.2	1	
	1260.17	± 0.15	0.83			± 0	4
	1304.01	± 0.04	15.1		2.78	± 0.14	2
	1308.13	± 0.20	0.49				4
	1325.65	± 0.15	2.05		0.26	± 0.01	3
	1336.33	± 0.15	0.77		0.36	± 0.02	4
¹⁰¹ Tc	1339.43	± 0.10	1.10				4
	1346.08	± 0.08	5.69		0.95	± 0.1	3
	1355.87	± 0.05	9.93		1.67	± 0.08	2
	1378.08	± 0.15	1.22		0.24	± 0.02	4
	1382.70	± 0.07	6.47		1.15	± 0.08	2
	1394.84	± 0.07	3.64		0.61	± 0.04	3
	1414.23	± 0.08	3.00		0.50	± 0.04	3
	1418.58	± 0.08	4.70		0.88	± 0.07	3
	1429.16	± 0.15	0.95				4
	1431.59	± 0.12	1.8		0.32	± 0.03	3
	1440.82	± 0.18	1.09				4
	1532.501	± 0.038	32.91	6.0	± 0.5	1	
	1589.73	± 0.12	1.57		0.28	± 0.01	3
	1599.28	± 0.055	9.47		1.7	± 0.2	2
	1662.538	± 0.08	3.78		0.68	± 0.04	3
	1673.948	± 0.05	8.83	1.6	± 0.02	2	
	1713.06	± 0.15	1.0		0.2	± 0.02	4
	1754.94	± 0.10	2.0		0.40	± 0.04	3
	1759.76	± 0.09	5.54		0.98	± 0.06	3
	1840.258	± 0.06	7.45	1.37	± 0.1	2	
	2032.113	± 0.045	36.94	6.5	± 0.5	1	
	2041.24	± 0.050	11.94	2.1	± 0.15	1	
	2047.28	± 0.15	0.39		0.08	± 0.01	4
	2088.78	± 0.06	4.13				1
	2114.30	± 0.075	3.07		0.47	± 0.04	1
	2223.24	± 0.15	0.87				3



61(2) day Tc^{95m} - 20.0(1) hr. Tc⁹⁵ Decay Scheme



43-95m(43-95)-1

GAMMA-RAY ENERGIES AND INTENSITIES

Nuclide Tc^{95m}-Tc⁹⁵
Detector 3" x 3" -2 NaI

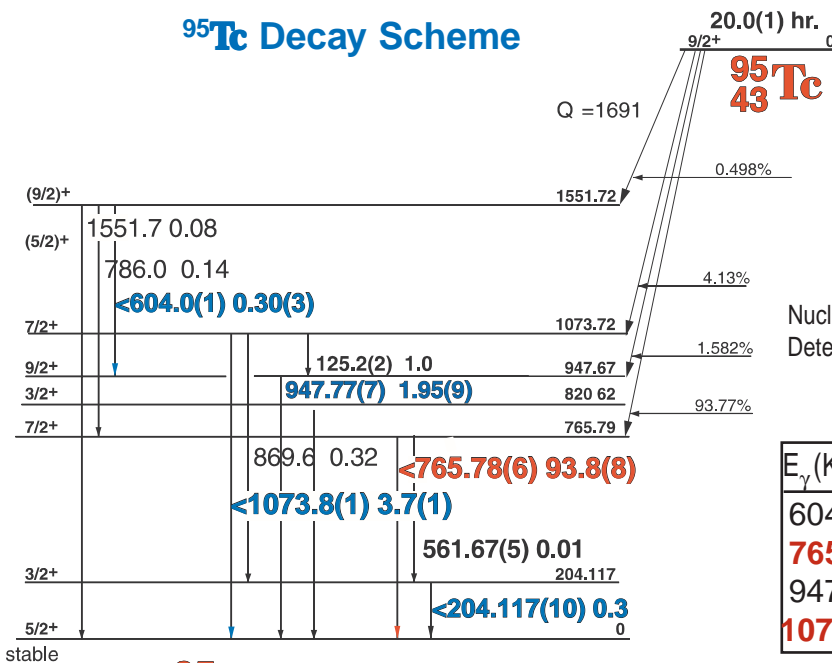
Half Life 61 Day (20.0 Hr.)
Method of Production: Ru⁹⁶(γ,n,K)

E _γ (KeV)[S]	ΔE _γ	I _γ (rel)	I _γ (%)[E]	ΔI _γ	S
95mTc	204.117	± 0.010	100	63.2	± 0.7 1
	218.7	± 0.2	0.06	0.04	± 0.01 4
	253.064	± 0.020	0.95	0.61	± 0.3 3
	582.068	± 0.013	49.6	30.0	± 0.6 1
	616.516	± 0.030	2.23	1.28	± 0.02 2
	765.786	± 0.019	5.7	3.6	± 0.3 1
	786.184	± 0.017	14.5	8.7	± 0.1 1
	820.608	± 0.019	7.9	4.7	± 0.1 1
	835.132	± 0.018	44.9	26.6	± 0.5 1

E _γ (KeV)[S]	ΔE _γ	I _γ (rel)	I _γ (%)[E]	ΔI _γ	S
95Tc	604.0	± 0.1	0.30	0.03	5
	765.786	± 0.019	100	93.8	± 0.8 1
	947.77	± 0.07	2.10	1.05	± 0.09 4
	1073.80	± 0.12	3.9	3.7	± 0.1 3

20.0(1) Hr. ^{95}Tc

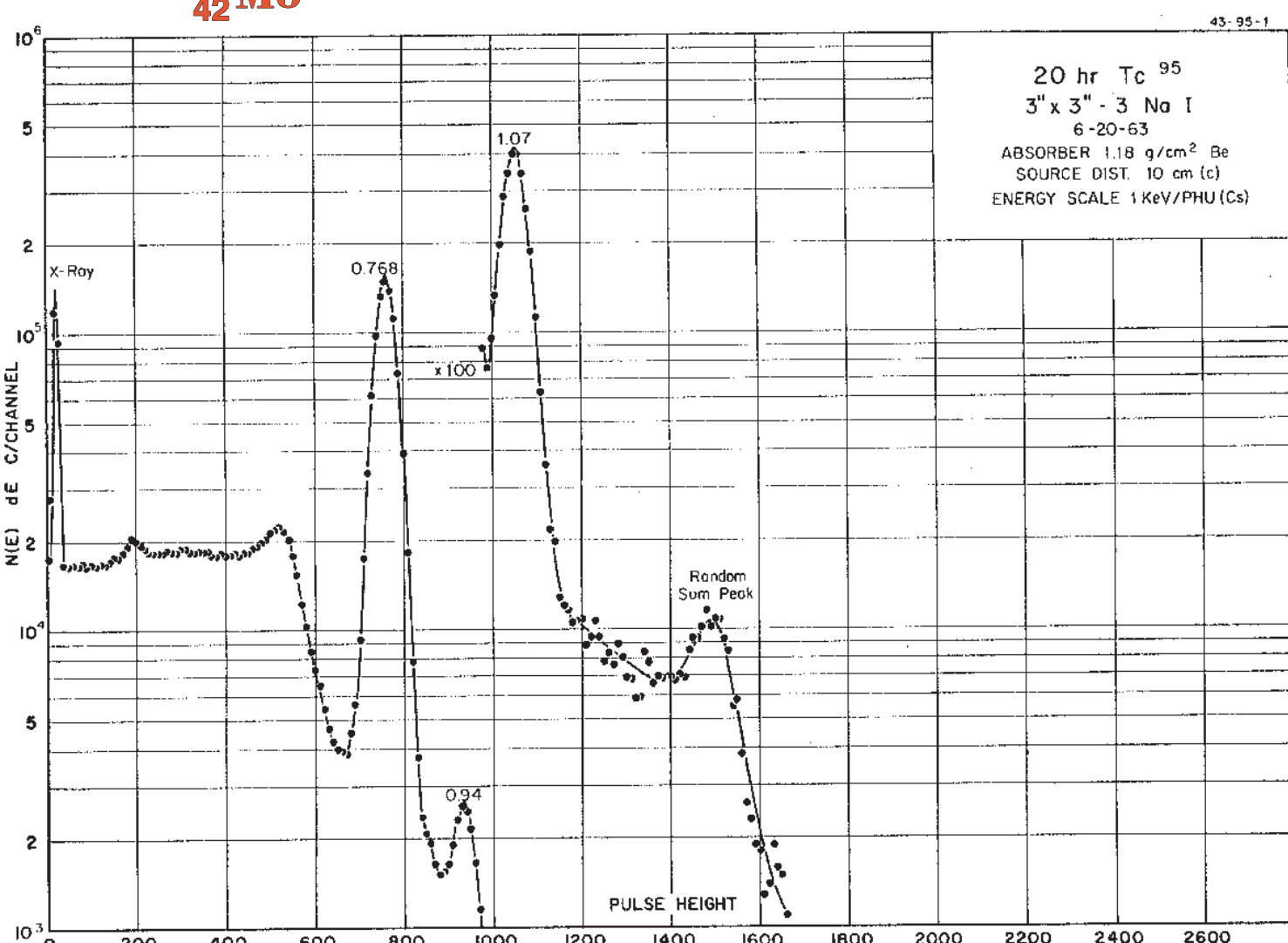
^{95}Tc Decay Scheme

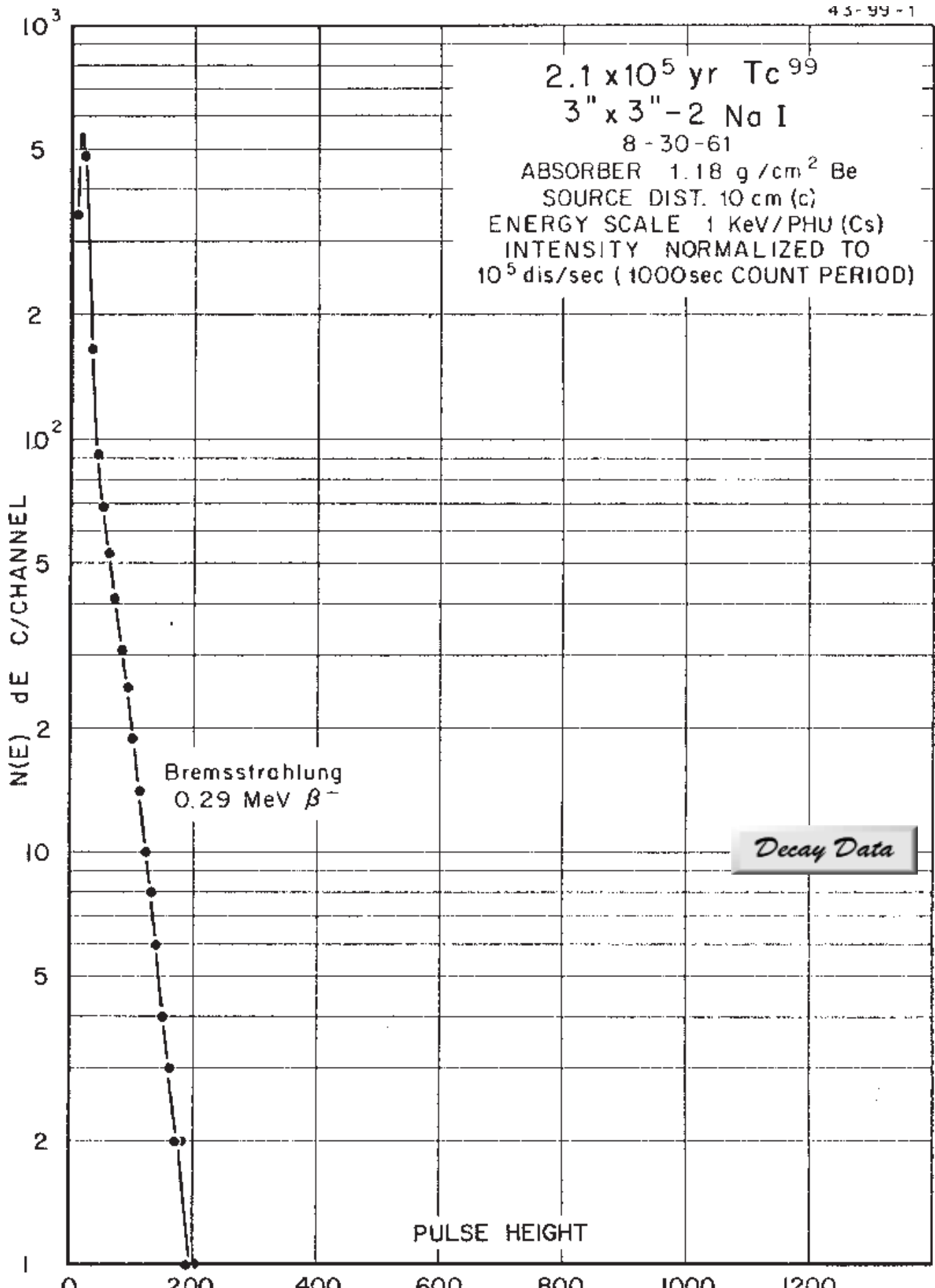


GAMMA-RAY ENERGIES AND INTENSITIES

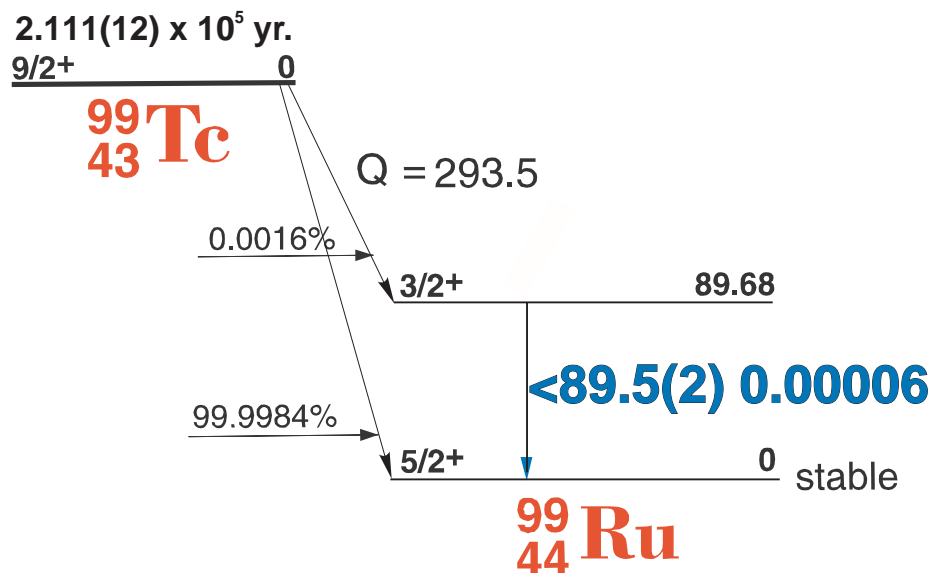
Nuclide Tc^{95} Half Life 20.0(1) hr.
Detector 3" X 3" NaI-2 Method of Production: Ru⁹⁶(γ ,n,K)

E_γ (KeV) [S]	ΔE_γ	I_γ (rel)	I_γ (%) [E]	ΔI_γ	S
604.0	± 0.1		0.30	± 0.03	5
765.786 ± 0.019		100	93.8	± 0.8	1
947.77	± 0.07	2.10	1.95	± 0.09	4
1073.80 ± 0.12		3.9	3.7	± 0.1	1





2.11(1) 1×10^5 yr. ^{99}Tc Decay Scheme

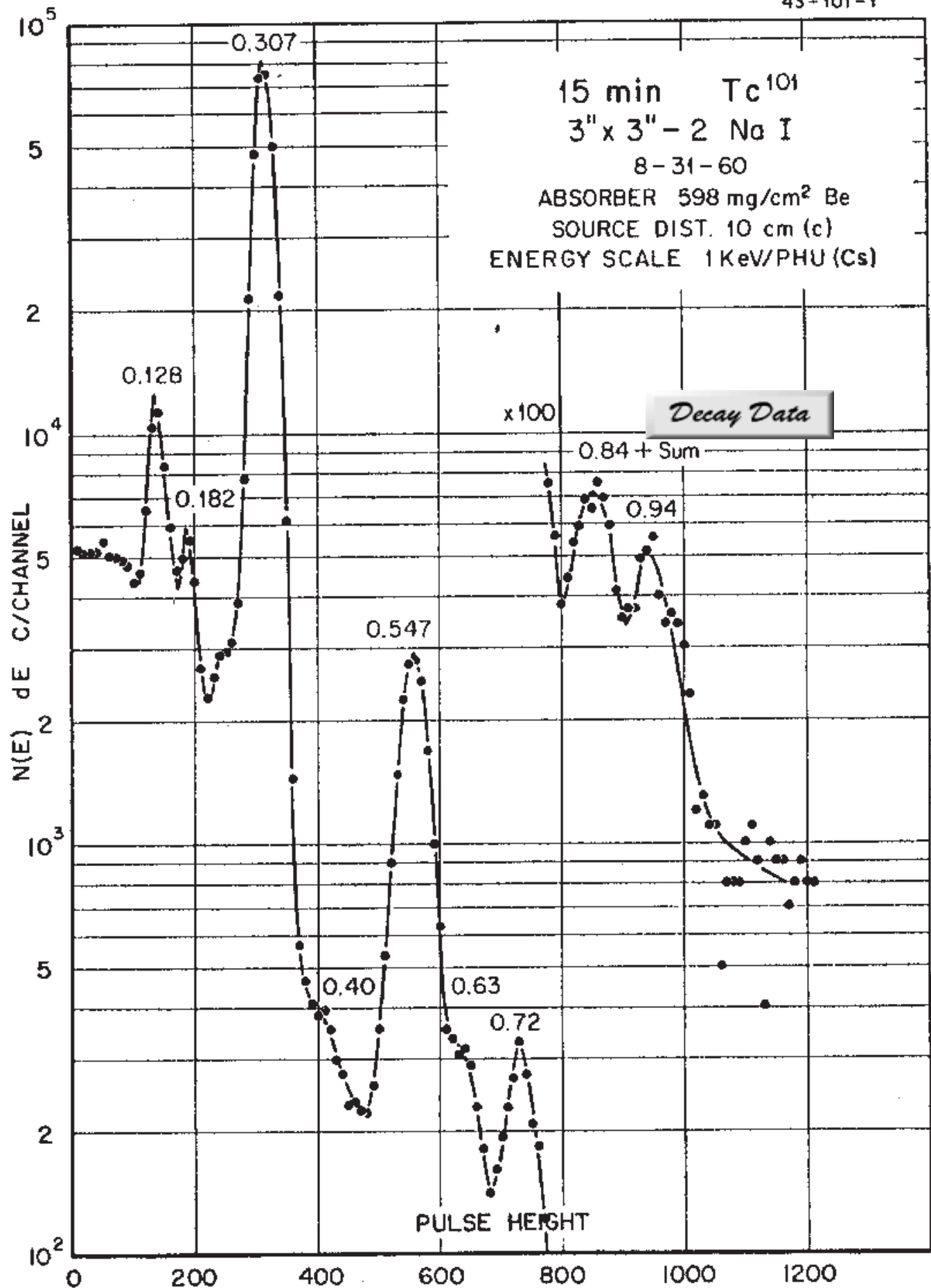


43-99-1

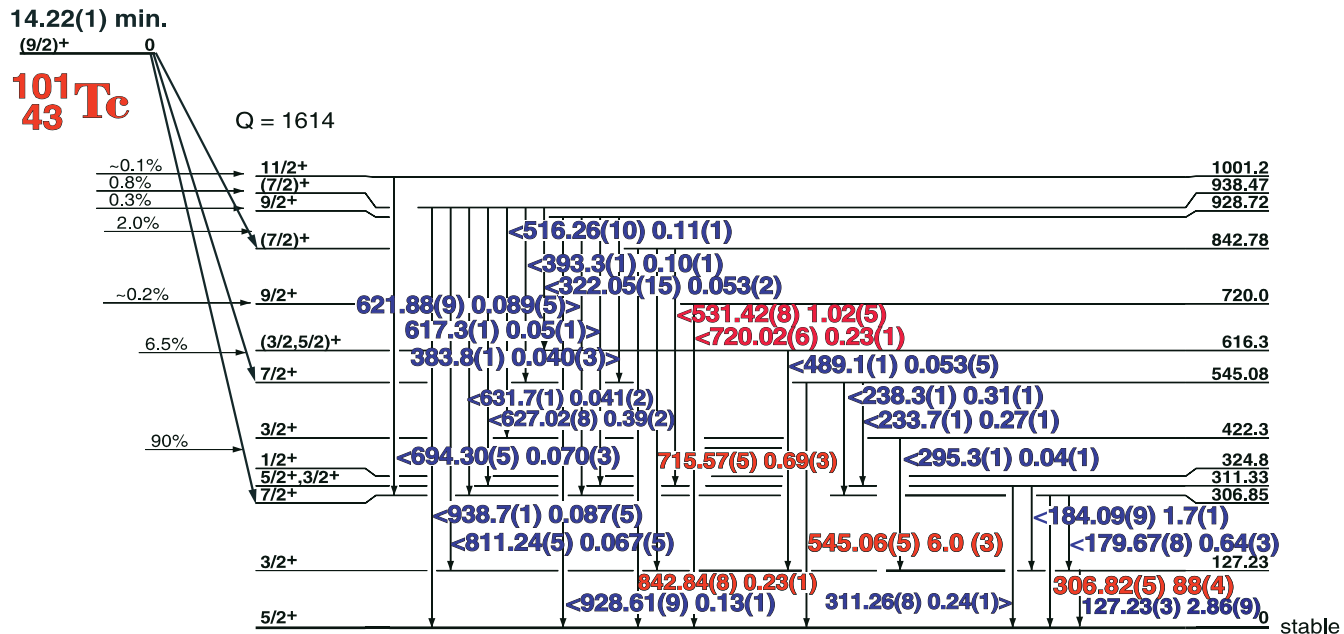
GAMMA-RAY ENERGIES AND INTENSITIES

Nuclide ^{99}Tc Half Life $2.11(1) \times 10^5$ Yr.
Detector 3" x 3" -2 Nal Method of Production: Mo⁹⁸(n,γ)

E_γ (KeV)[S]	ΔE_γ	I_γ (rel)	$I_\gamma(\%)$ [E]	ΔI_γ	S
89.5	± 0.2		0.00006		1



14.22(1) min. ^{101}Tc Decay Scheme



^{101}Ru

GAMMA-RAY ENERGIES AND INTENSITIES

43-101-1

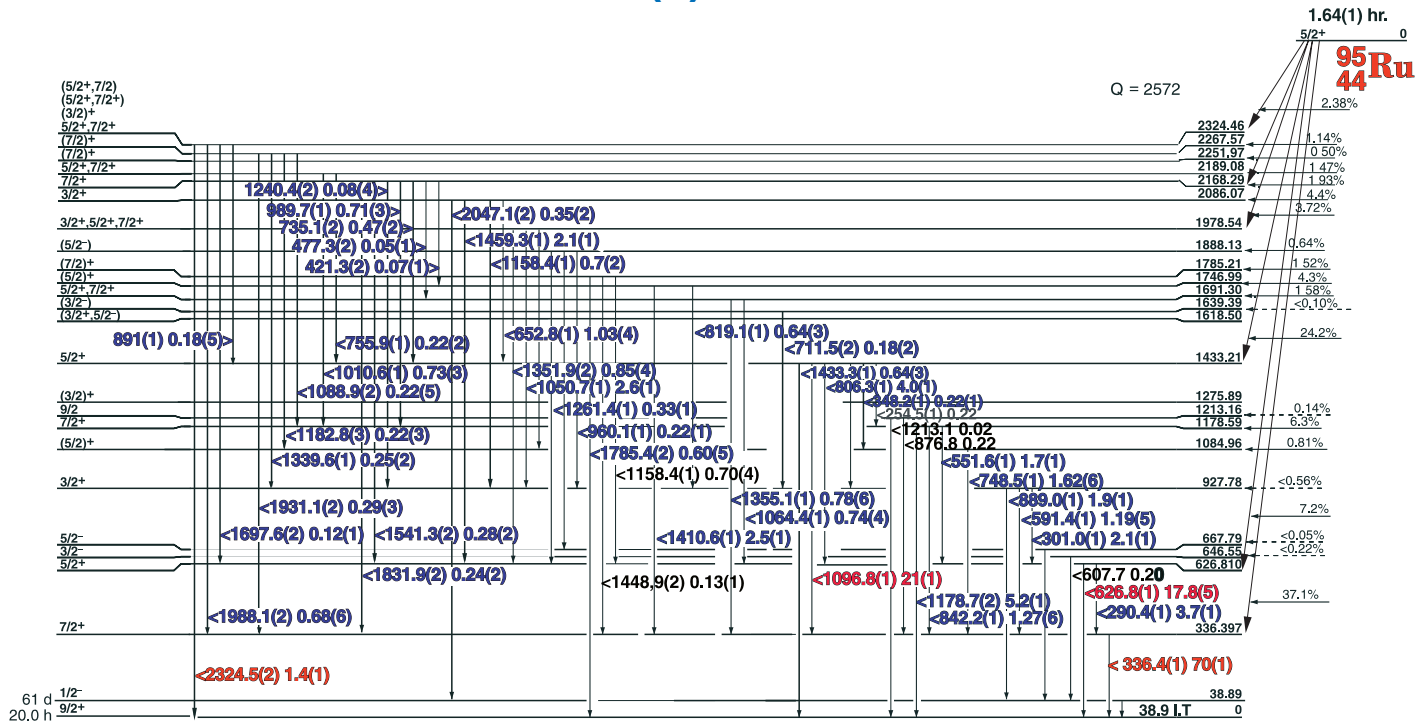
Nuclide ^{101}Tc
 Detector 3" x 3" -2 NaI

Half Life 14.22(1) min.

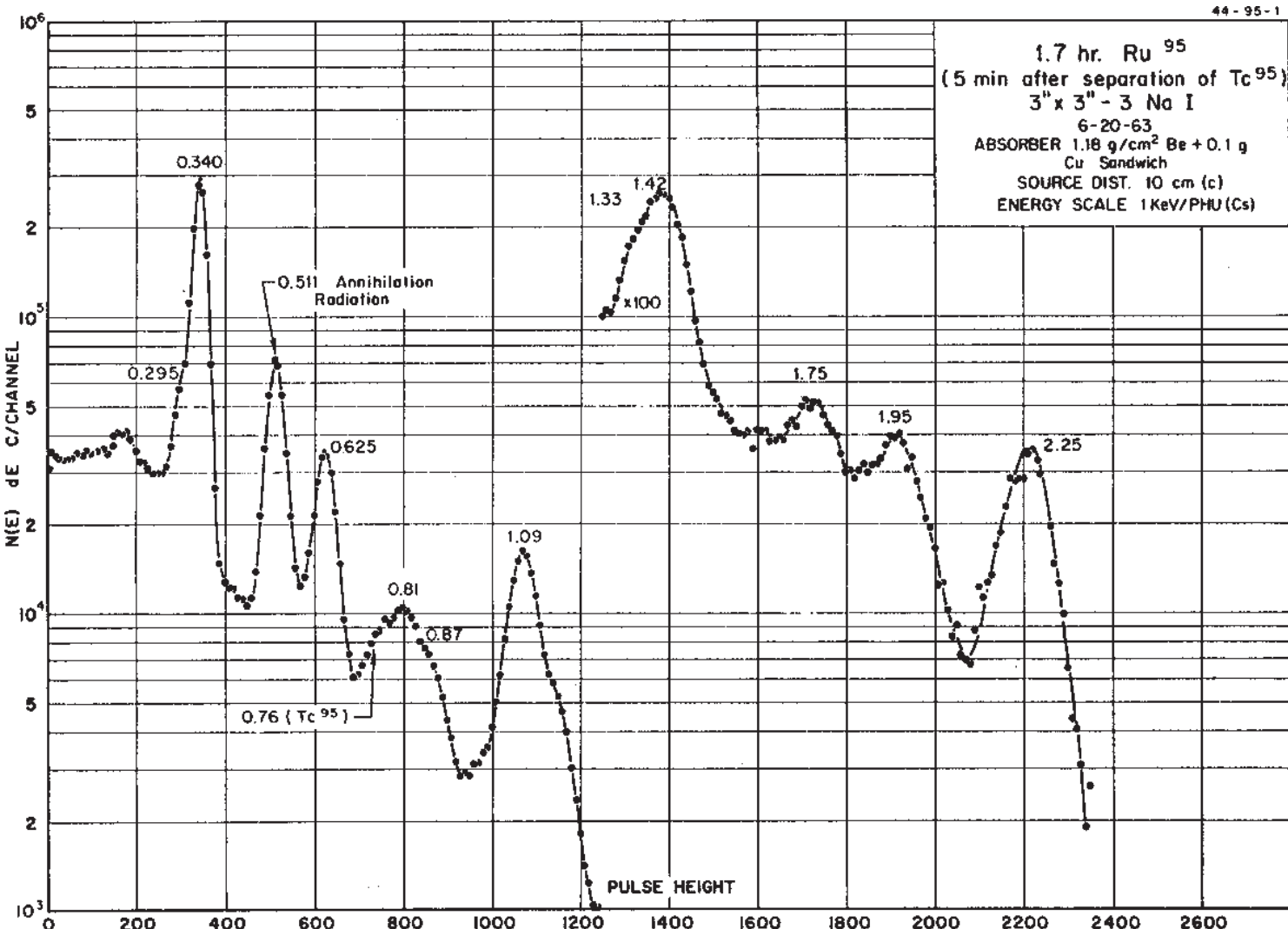
Method of Production: $^{100}\text{Mo}(n, \gamma, \beta)$

E_{γ} (KeV) [S]	ΔE_{γ}	I_{γ} (rel)	$I_{\gamma}(\%)$ [E]	ΔI_{γ}	S
127.23	± 0.03	3.2	2.86	± 0.09	3
179.673	± 0.08	1.2	0.64	± 0.03	4
184.09	± 0.09	2.2	1.7	± 0.1	3
233.73	± 0.10	0.41	0.27	± 0.01	4
238.32	± 0.10	0.55	0.31	± 0.01	4
295.3	± 0.15	0.05	0.04	± 0.01	4
306.829	± 0.05	100	88	± 4.0	1
311.26	± 0.08	0.27	0.24	± 0.01	4
322.05	± 0.15	0.06	0.053	± 0.002	4
351.89	± 0.10	0.09		± 0.02	4
383.83	± 0.10	0.08	0.040	± 0.003	4
393.34	± 0.10	0.11	0.10	± 0.01	4
489.1	± 0.15	0.06	0.053	± 0.005	4
516.26	± 0.10	0.15	0.11	± 0.01	3
531.42	± 0.08	1.16	1.02	± 0.05	1
545.061	± 0.050	6.92	6.0	± 0.3	1
583.1	± 0.15	0.09		± 0.03	3
609.3	± 0.15	0.11		± 0.04	3
617.34	± 0.10	0.11	0.05	± 0.01	3
621.88	± 0.09	0.12	0.089	± 0.005	3
627.020	± 0.08	0.54	0.39	± 0.02	1
631.70	± 0.15	0.06	0.041	± 0.002	3
694.3	± 0.15	0.08	0.070	± 0.003	3
715.568	± 0.05	0.834	0.69	± 0.03	1
718.023	± 0.06	0.31	0.29	± 0.03	1
727.5	± 0.15	0.04		± 0.01	3
811.24	± 0.10	0.08	0.067	± 0.005	3
842.84	± 0.08	0.29	0.29	± 0.01	1
911.57	± 0.12	0.10		± 0.03	3
928.61	± 0.09	0.13	0.13	± 0.01	2
938.68	± 0.10	0.10	0.087	± 0.005	3
963.9	± 0.15	0.05		± 0.02	4
968.8	± 0.15	0.07		± 0.025	4

1.64(1) hr. ^{95}Ru



^{95}Tc



Decay Data

← Index →

1.64(1) hr. ^{95}Ru

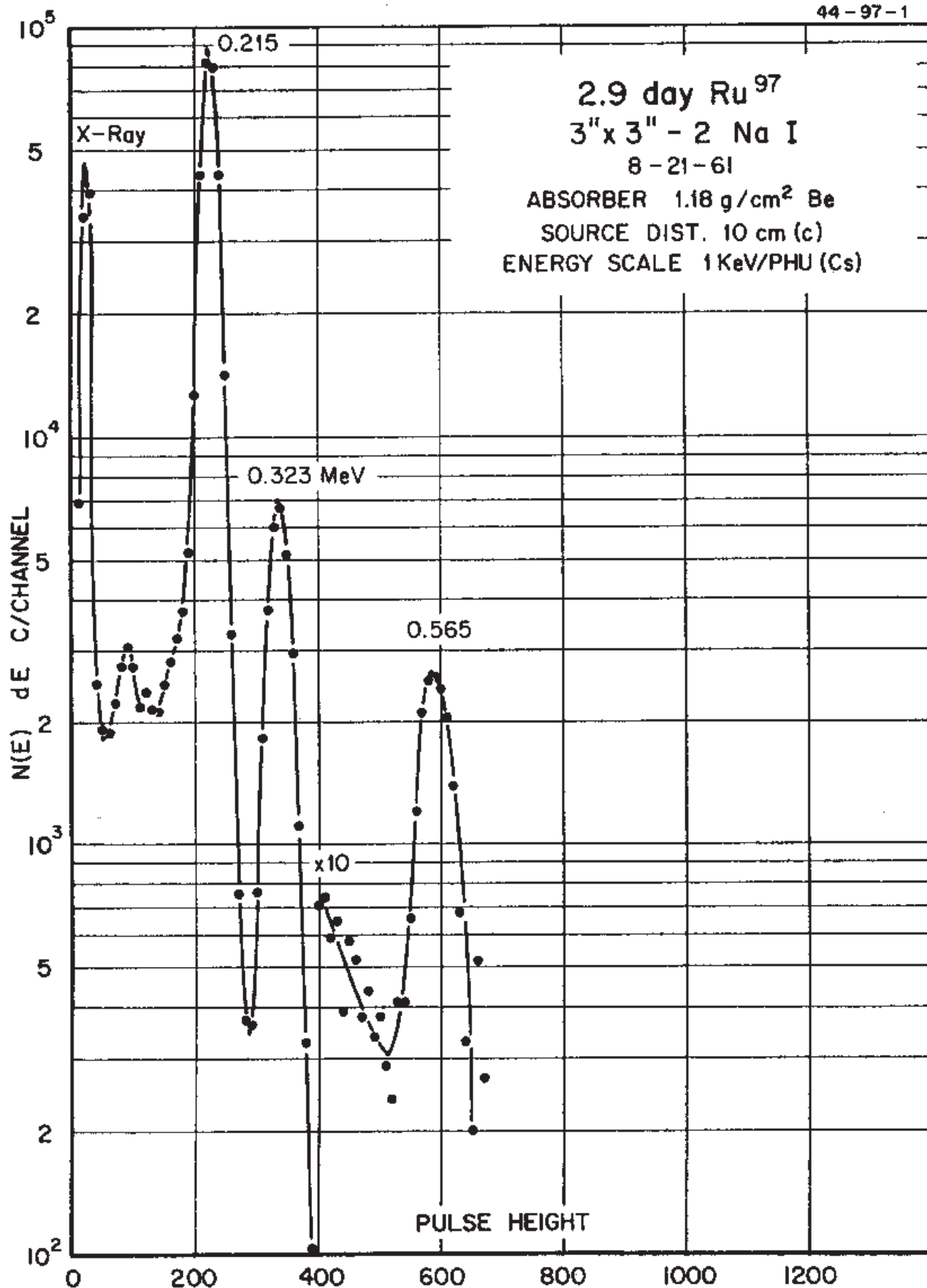
GAMMA-RAY ENERGIES AND INTENSITIES

Nuclide ^{95}Ru Half Life 1.64(10 hr.
Detector 3" X 3" NaI-2 Method of Production: $^{96}\text{Ru}(\gamma,\text{n})$

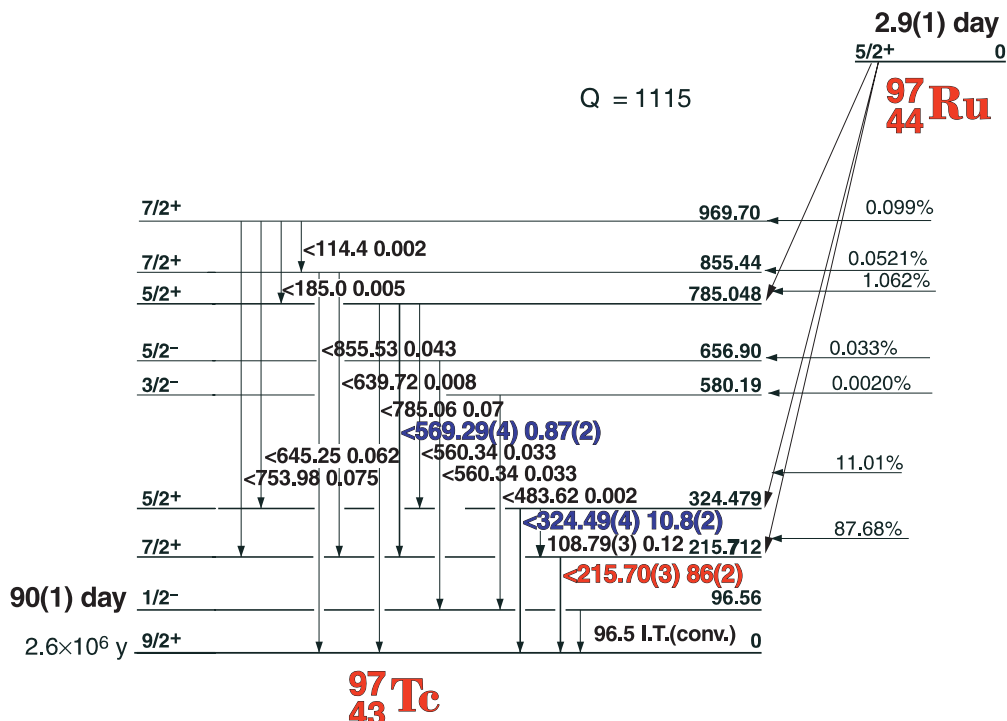
E_{γ} (KeV)[S]	ΔE_{γ}	I_{γ} (rel)	$I_{\gamma}(\%)[E]$	ΔI_{γ}	S
290.38	± 0.05		3.70	± 0.1	2
336.40	± 0.05		70.2	± 2.0	1
511 ann.	rad.				1
626.83	± 0.05		17.8	± 1.0	1
806.28	± 0.05		4.05	± 0.2	2
1096.80	± 0.05		21	± 1.0	1
1410.63	± 0.06		2.49	± 0.1	2
2252.0	± 0.1		0.36	± 0.02	1

2.9(1) day ^{97}Ru

44-97-1



2.9(1) day ^{97}Ru



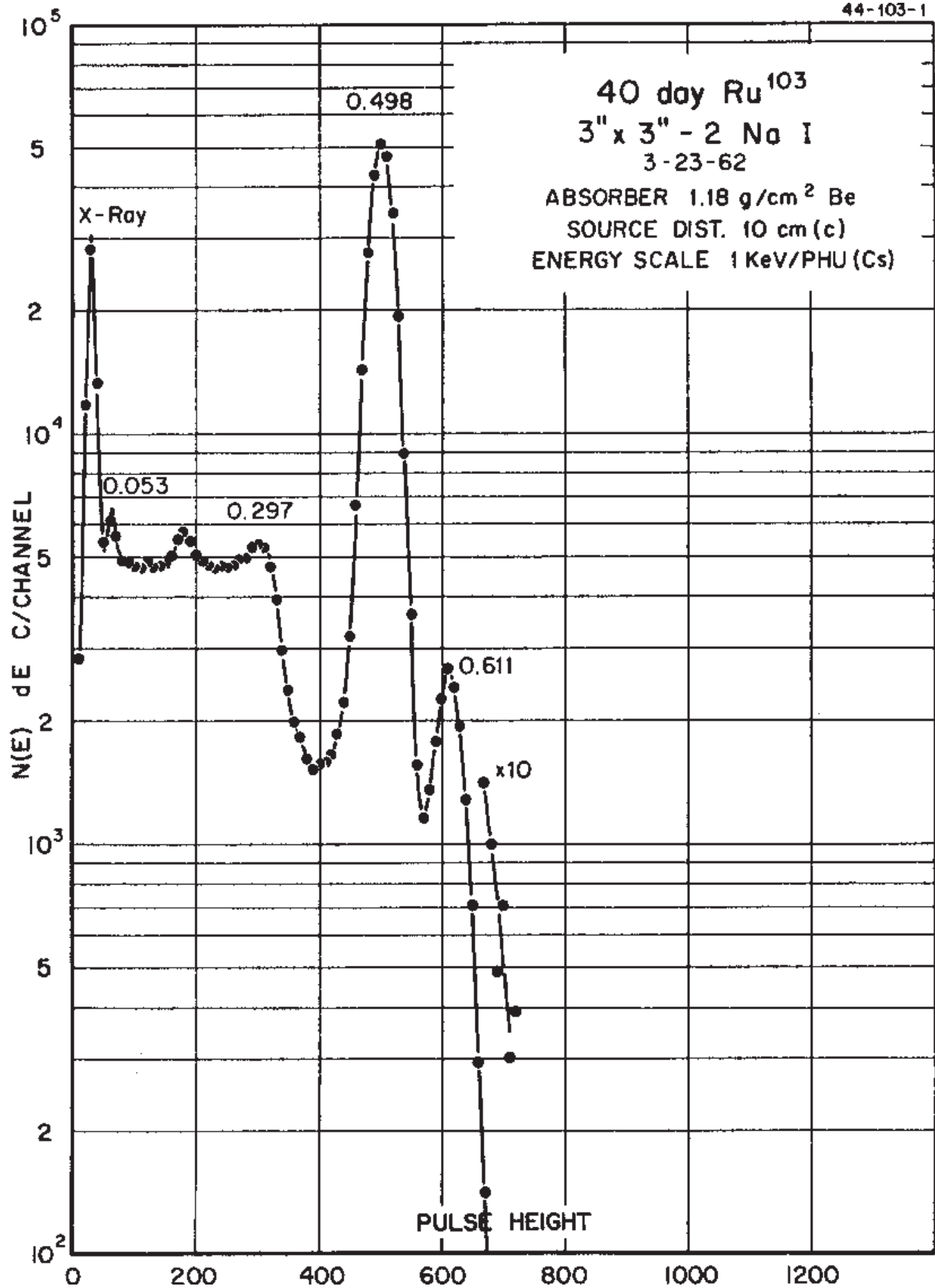
GAMMA-RAY ENERGIES AND INTENSITIES

Nuclide ^{97}Ru Half Life $2.9(1)$ day
 Detector 3" X 3" NaI-2 Method of Production: $^{96}\text{Ru}(n,\gamma)$

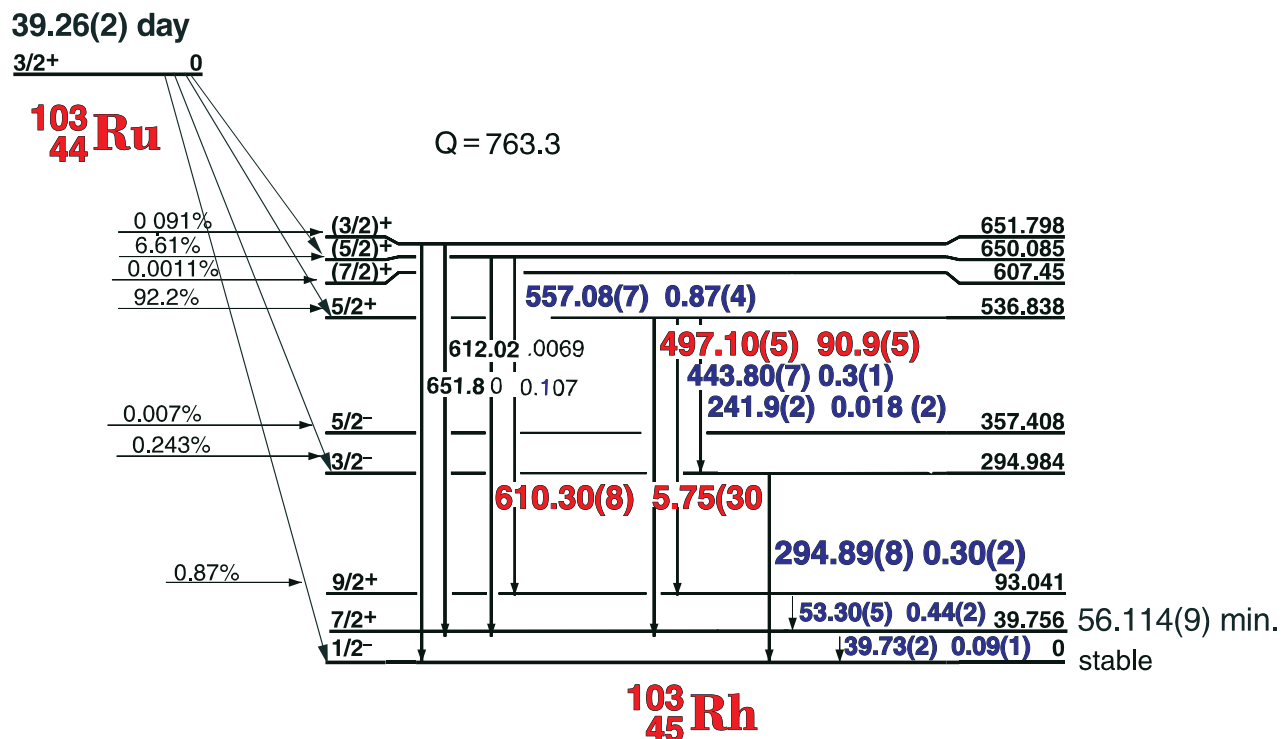
E_γ (KeV) [S]	ΔE_γ	I_γ (rel)	$I_\gamma(\%)$ [E]	ΔI_γ	S
96.5	I. T. (conv.)				4
108.79	± 0.03		0.12	± 0.01	4
114.4			0.002		4
185.0	± 0.1	0.005			4
215.70	± 0.03		85	± 2.0	1
324.49	± 0.04		10.8	± 0.2	2
483.62	± 0.07	0.002			4
569.29	± 0.04		0.87	± 0.2	1
639.72	± 0.07	0.008			4
645.25	± 0.05	0.062		± 0.03	4
753.98	± 0.05	0.075		± 0.004	4
855.53	± 0.05	0.043		± 0.003	4

44-103-1

40 day Ru¹⁰³
 3" x 3" - 2 No I
 3-23-62
 ABSORBER 1.18 g/cm² Be
 SOURCE DIST. 10 cm (c)
 ENERGY SCALE 1 KeV/PHU (Cs)



39.26(2) day ^{103}Ru Decay Scheme

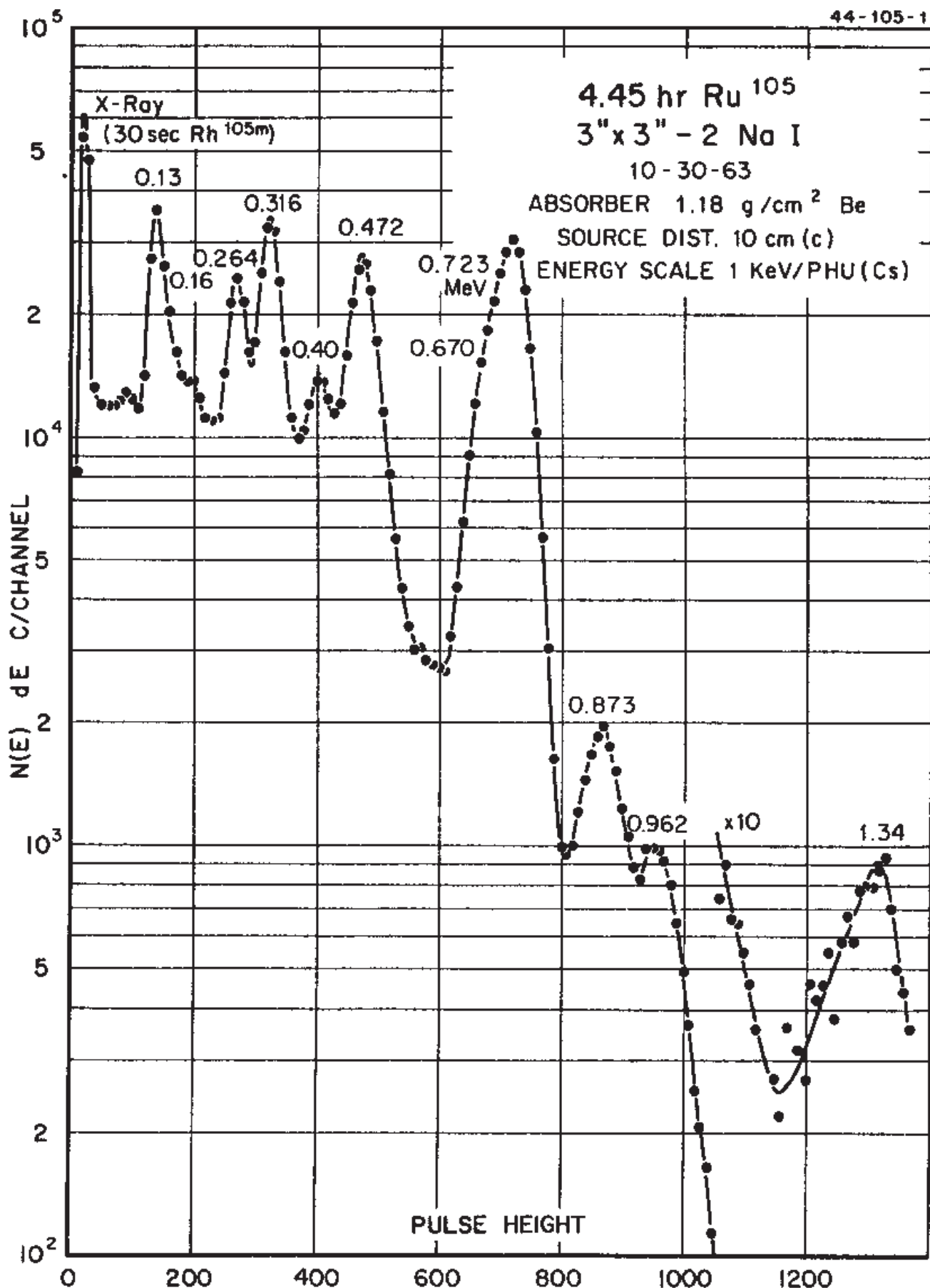


44-103-1

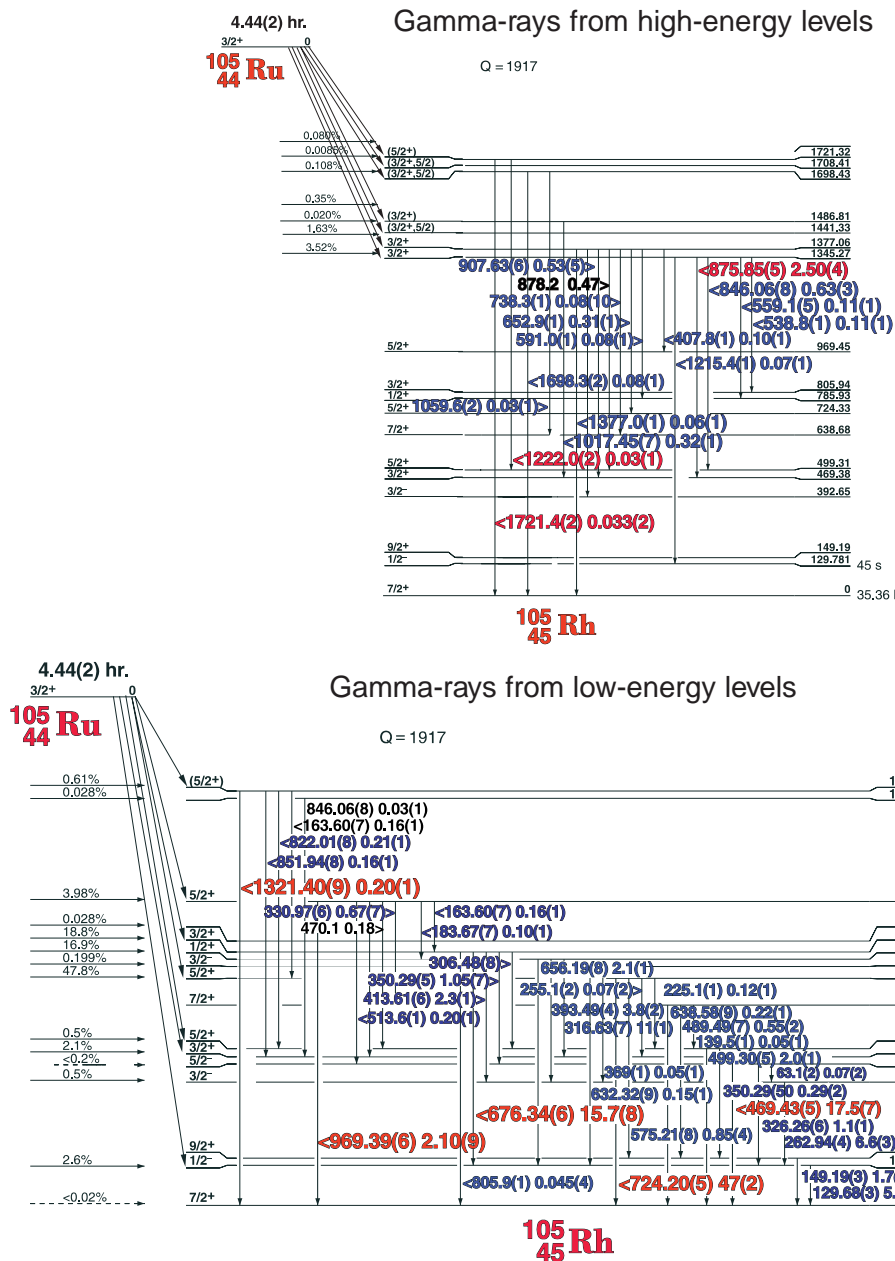
GAMMA-RAY ENERGIES AND INTENSITIES

Nuclide **^{103}Ru** Half Life 39.26(2) day
Detector 3" x 3" -2 NaI Method of Production: $^{102}\text{Ru}(n,\gamma)$

E_{γ} (KeV)[S]	ΔE_{γ}	$I_{\gamma}(\text{rel})$	$I_{\gamma}(\%)$ [E]	ΔI_{γ}	S
39.73	± 0.02	0.060	0.09	± 0.01	4
53.30	± 0.05	0.41	0.44	± 0.02	4
113.2	± 0.1	V.W.			4
241.9	± 0.2	V.W.	0.018	± 0.002	4
294.89	± 0.08	0.31	0.30	± 0.02	3
443.80	± 0.07	0.40	0.3	± 0.03	3
497.10	± 0.05	100	90.9	± 0.5	1
557.08	± 0.07	0.87	0.87	± 0.04	4
610.30	± 0.08	7.4	5.75	± 0.03	1



4.44(2) hr. ^{105}Ru Decay Scheme



44-105-1

GAMMA-RAY ENERGIES AND INTENSITIES

Nuclide ^{75}Ge Half Life 82.78(4) min.
Detector 3" x 3" -2 NaI Method of Production: $\text{Ge}^{74}(n,\gamma)$

E_{γ} (KeV)[S]	ΔE_{γ}	I_{γ} (rel)	$I_{\gamma}(\%)$ [E]	ΔI_{γ}	S
63.15	± 0.10		0.07	± 0.02	4
87.64	± 0.20	0.010		± 0.005	4
103.42	± 0.07	0.13		± 0.01	4
129.68	± 0.03	11.1	5.7	± 0.2	2
139.50	± 0.10	0.030	0.05	± 0.01	4
149.19	± 0.03	3.4	1.7	± 0.1	3
163.60	± 0.07	0.37	0.16	± 0.01	4
183.67	± 0.07	0.25	0.20	± 0.01	4
225.15	± 0.10	0.41	0.12	± 0.01	4
255.14	± 0.20	0.17	0.12	± 0.01	4

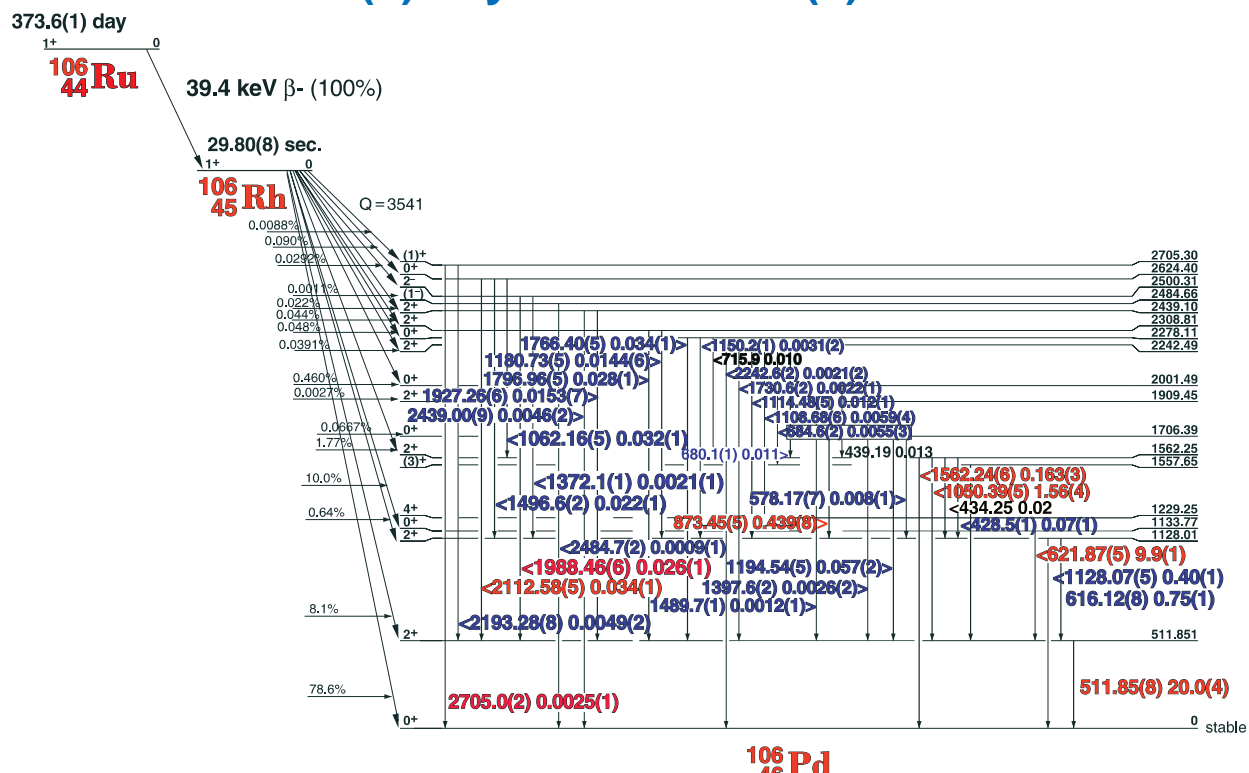
Decay Data

GAMMA-RAY ENERGIES AND INTENSITIES

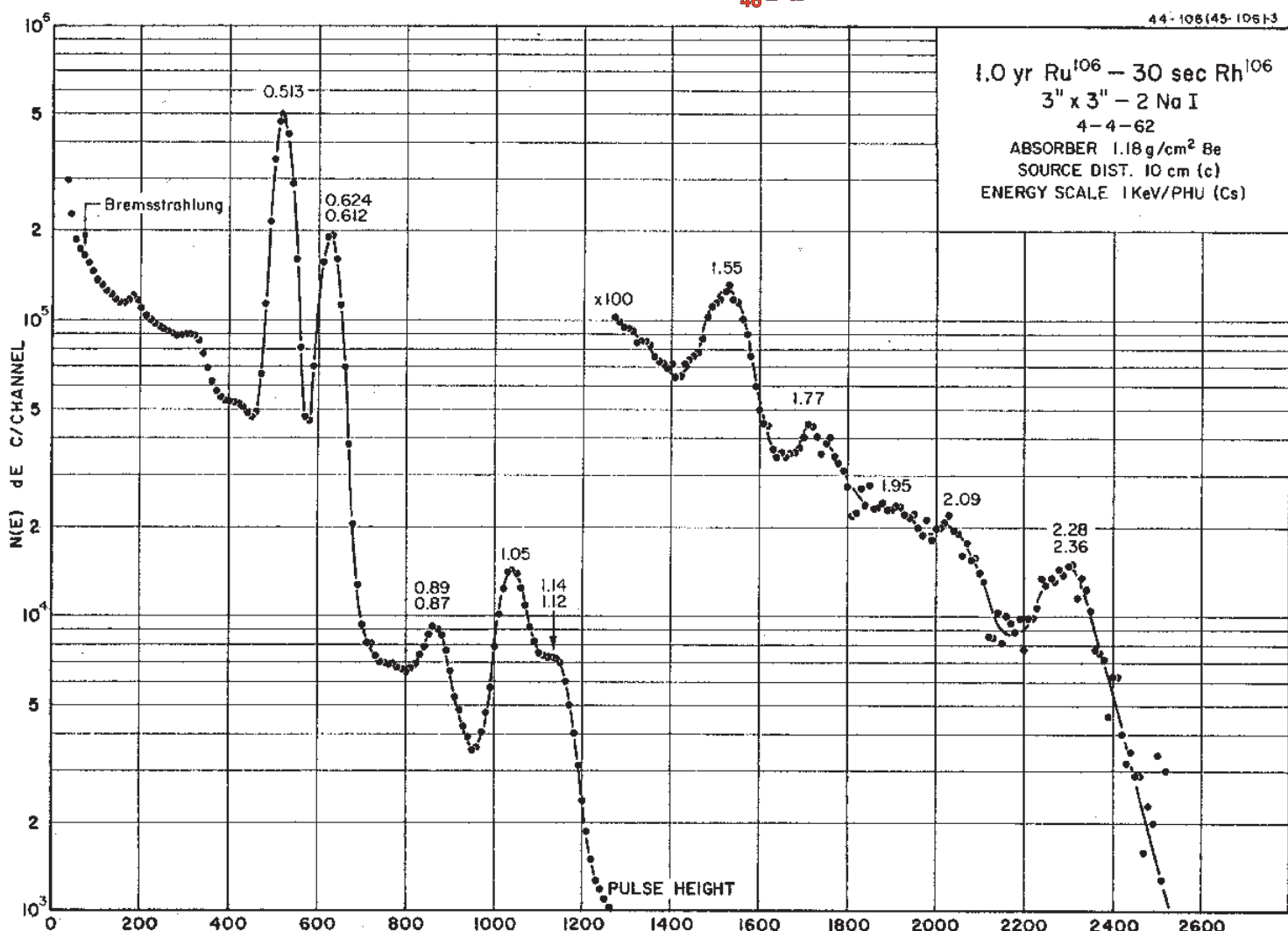
Nuclide **¹⁰⁵Ru** Half Life 4.44(2) hr.
 Detector 3" x 3" -2 NaI Method of Production: ¹⁰⁴Ru(n,γ)

	E _γ (KeV)[S]	ΔE _γ	I _γ (rel)	I _γ (%)[E]	ΔI _γ	S
¹⁰⁵ Rh	262.94	± 0.04	14.4	8.6	± 0.3	2
	306.48	± 0.05				
¹⁰⁵ Rh	316.63	± 0.07	25.0	11	± 1.0	2
	319.27	± 0.07				
	326.26	± 0.06	2.7	1.1	± 0.1	3
	330.97	± 0.06	1.6	0.67	± 0.7	4
	350.29	± 0.05	2.9	1.05	± 0.07	3
	369.0	± 1.0	w	0.05	± 0.01	4
	393.49	± 0.04	8.1	3.8	± 0.2	3
	407.76	± 0.10	0.37	0.10	± 0.01	4
	413.61	± 0.05	4.8	2.3	± 0.1	3
	469.43	± 0.05	37.0	17.5	± 0.7	1
	489.49	± 0.07	1.3	0.55	± 0.02	4
	499.30	± 0.05	5.1	2.0	± 0.1	3
	513.59	± 0.10	0.60	0.30	± 0.01	4
	538.81	± 0.10	1.5	0.61	± 0.01	4
	559.0	± 0.5	0.63	0.25	± 0.01	4
	575.21	± 0.08	2.40	1.1	± 0.1	3
	591.0	± 0.1	0.54	0.20	± 0.01	4
	620.8	± 0.2	0.20		± 0.03	4
	632.32	± 0.09	0.43	0.15	± 0.03	4
	638.58	± 0.09	0.60	0.30	± 0.02	4
	652.9	± 0.1	0.7	0.31	± 0.01	4
	656.19	± 0.08	4.9	2.1	± 0.1	2
	676.34	± 0.06	33.1	15.7	± 0.8	1
	724.20	± 0.05	100	47	± 2.0	1
	738.29	± 0.10	0.28	0.09	± 0.01	4
	785.77	± 0.08	0.46		± 0.03	3
	805.94	± 0.10	0.16	0.65	± 0.06	4
	822.01	± 0.08	0.51	0.21	± 0.01	3
	846.06	± 0.08	1.9	0.8	± 0.1	2
	851.94	± 0.08	0.39	0.16	± 0.01	3
	875.85	± 0.05	6.4	2.50	± 0.09	1
	907.63	± 0.06	1.17	0.53	± 0.05	1
	953.0	± 0.5	0.08	0.04	± 0.01	4
	969.39	± 0.06	4.6	2.10	± 0.09	1
	1017.45	± 0.07	0.70	0.32	± 0.02	2
	1059.65	± 0.20	0.06	0.03	± 0.01	4
	1215.37	± 0.10	0.15	0.07	± 0.01	3
	1221.99	± 0.20	0.06	0.03	± 0.01	3
	1321.40	± 0.09	0.45	0.20	± 0.01	1
	1376.99	± 0.15	0.12	0.06	± 0.01	2
	1698.3	± 0.2	0.17	0.08	± 0.01	1
	1721.4	± 0.2	0.07	0.033	± 0.01	1

373.6(1) day ^{106}Ru - 29.80(8) sec. ^{106}Rh



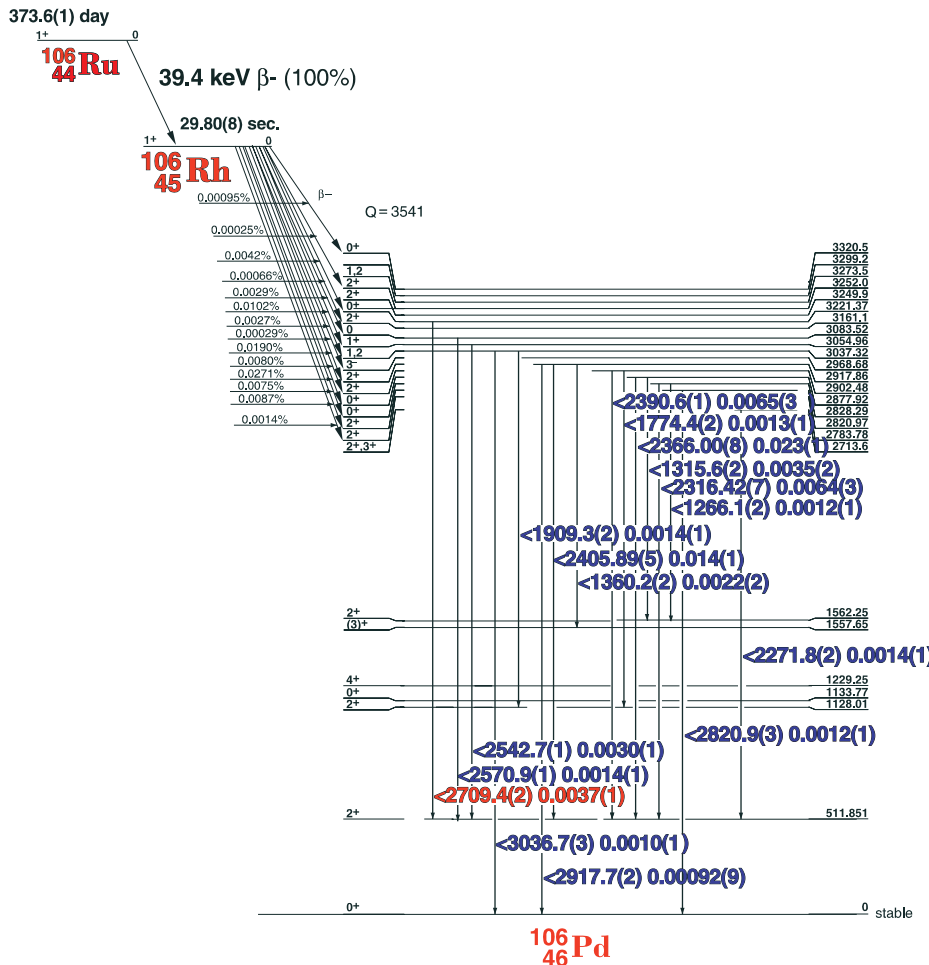
$^{106}_{46}\text{Pd}$



Decay Data

← Index →

373.6(1) day ^{106}Ru - 29.80(8) sec. ^{106}Rh Decay Scheme



GAMMA-RAY ENERGIES AND INTENSITIES

Nuclide $^{106}\text{Ru} - ^{106}\text{Rh}$ Half Life 373.6(1) day - 29.80(8) sec.
 Detector 3" x 3" -2 NaI Method of Production: $^{235}\text{U}(\text{n},\text{f})$

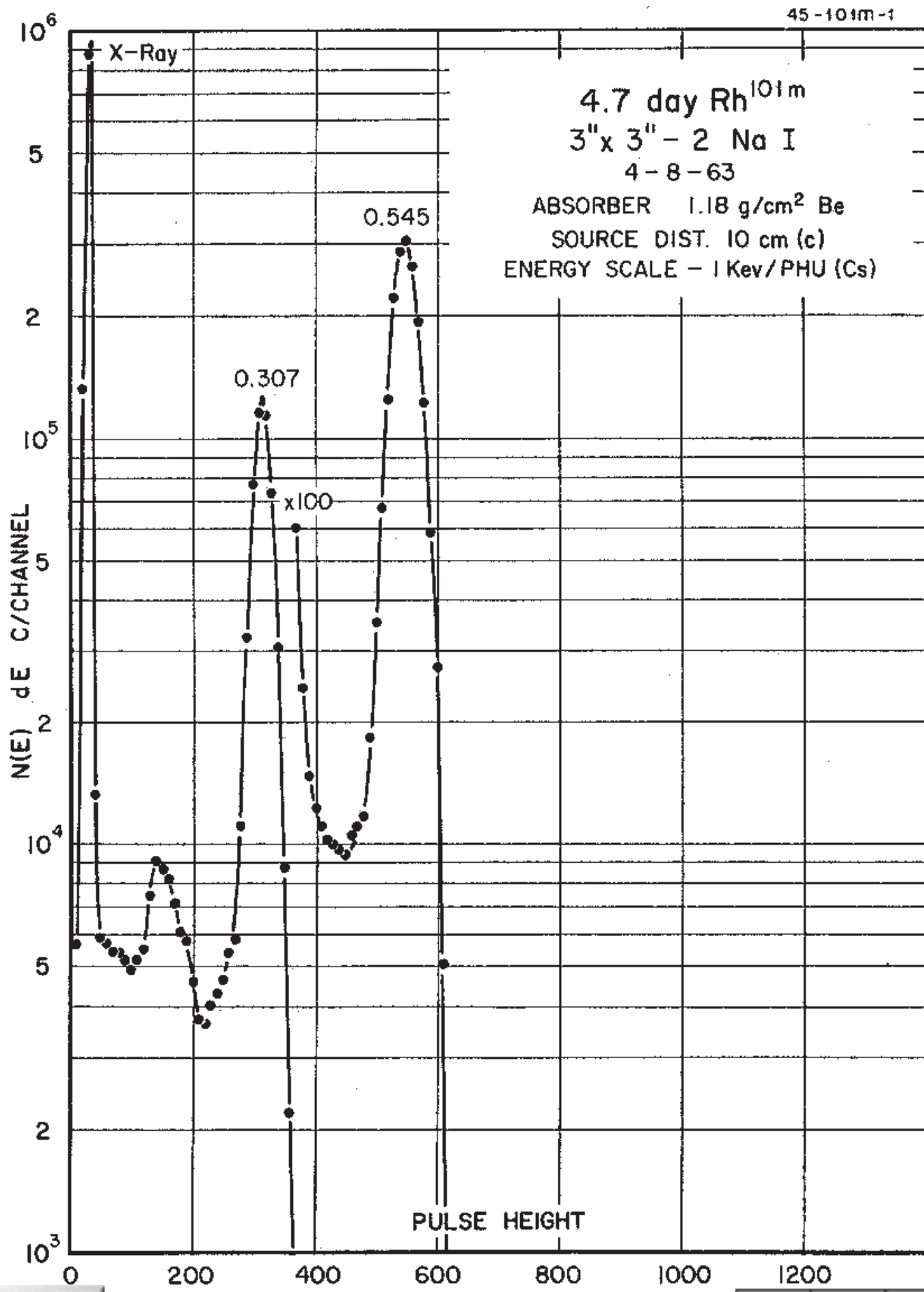
	E_{γ} (KeV)[S]	ΔE_{γ}	I_{γ} (rel)	$I_{\gamma}(\%)$ [E]	ΔI_{γ}	S
NA	428.5	± 0.2	1.38	0.07	± 0.01	4
	434.25	± 0.04	1.7	0.020	± 0.002	4
	437.80	± 0.25	1.8			4
	439.0	± 0.7	1.1	0.013	± 0.001	4
	462.6	± 0.7	0.49		± 0.15	4
	511.85	± 0.08	100	20.0	± 0.4	1
	578.17	± 0.07	0.054	0.008	± 0.001	4
NA	604.7	± 0.3	0.016			4
	616.12	± 0.08	4.1	0.75	± 0.01	3
	621.87	± 0.05	48.8	9.9	± 0.1	1
NA	635.71	± 0.09	0.030			4
	680.09	± 0.15	0.075	0.011	± 0.001	3
NA	684.58	± 0.20	0.041	0.0055	$\pm (3)$	4
	702.53	± 0.25	0.025			4
NA	716.0	± 0.10	0.089	0.010	± 0.001	4
	795.75	± 0.12	0.026			4
	873.45	± 0.05	2.20	0.439	± 0.008	1
	1050.39	± 0.05	7.6	1.56	± 0.04	1
	1062.16	± 0.05	0.161	0.032	± 0.001	3
	1108.68	± 0.06	0.029	0.0059	$\pm (4)$	3
	1114.48	± 0.05	0.057	0.012	± 0.001	3

373.6(1) day ^{106}Ru - 29.80(8) sec. ^{106}Rh

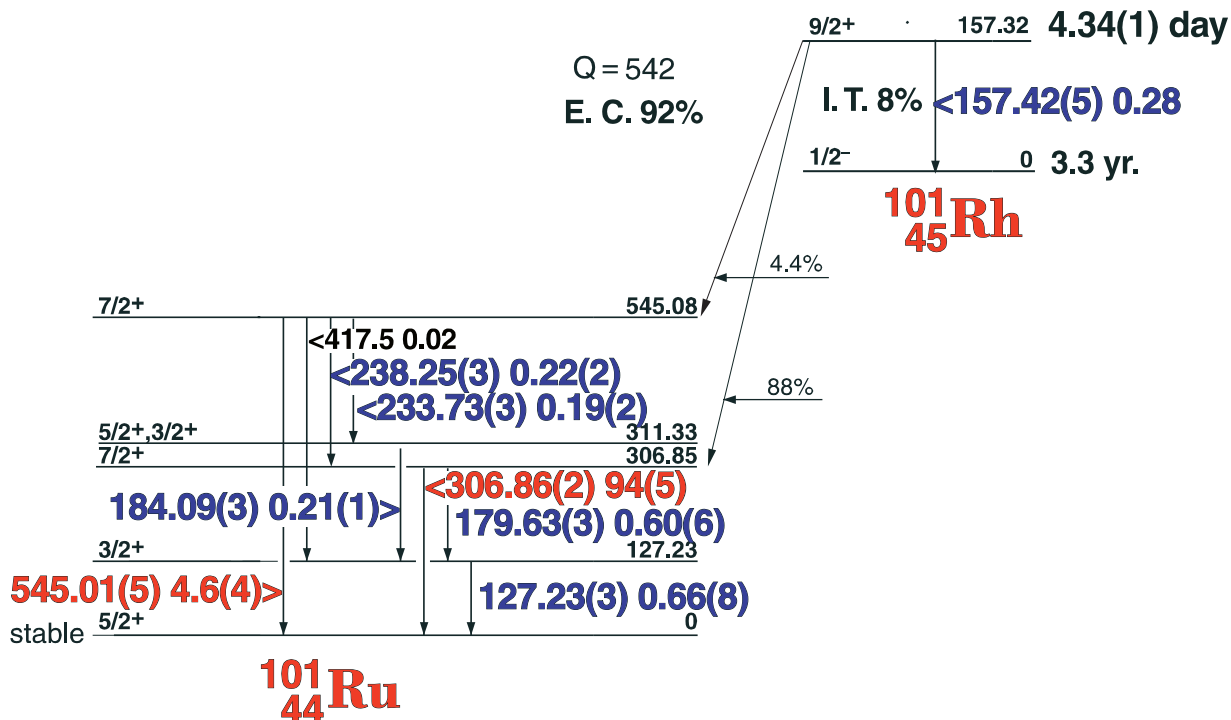
GAMMA-RAY ENERGIES AND INTENSITIES

Nuclide ^{106}Ru - ^{106}Rh Half Life 373.6(1) day - 29.80(8) sec.
 Detector 3" x 3" -2 NaI Method of Production: $^{235}\text{U}(\text{n},\text{f})$

E_{γ} (KeV)[S]	ΔE_{γ}	I_{γ} (rel)	$I_{\gamma}(\%)$ [E]	ΔI_{γ}	S
1128.07	± 0.05	1.98	0.40	± 0.01	1
1150.20	± 0.10	0.018	0.0031	$\pm (2)$	4
1180.73	± 0.05	0.073	0.0144	$\pm (6)$	3
1194.54	± 0.05	0.28	0.057	± 0.002	2
1266.11	± 0.20	0.008	0.0012	$\pm (1)$	4
1315.60	± 0.20	0.018	0.0035	$\pm (2)$	4
1360.15	± 0.25	0.013	0.0022	$\pm (2)$	4
1372.01	± 0.18	0.017	0.0021	$\pm (1)$	4
1397.82	± 0.20	0.018	0.0026	$\pm (2)$	4
1489.71	± 0.12	0.015	0.0012	$\pm (1)$	4
1496.72	± 0.25	0.14	0.022	± 0.001	2
1562.24	± 0.06	0.80	0.163	± 0.003	1
NA					
1572.55	± 0.20	0.016			4
1601.34	± 0.25	0.016			4
1730.66	± 0.18	0.013	0.0022	$\pm (1)$	4
1766.40	± 0.05	0.142	0.034	± 0.001	2
1774.36	± 0.25	0.007	0.0013	$\pm (1)$	4
1796.96	± 0.05	0.126	0.028	± 0.001	2
1853.9	± 0.20	0.017	0.0012	$\pm (1)$	4
1909.28	± 0.25	0.008	0.0014	$\pm (1)$	4
1927.26	± 0.06	0.075	0.0153	$\pm (7)$	2
1988.46	± 0.06	0.126	0.026	± 0.001	1
2112.58	± 0.05	0.17	0.034	± 0.001	1
2193.28	± 0.08	0.028	0.0049	$\pm (2)$	2
2242.60	± 0.15	0.012	0.0021	$\pm (2)$	3
2271.82	± 0.25	0.008	0.0014	$\pm (1)$	4
2308.95	± 0.07	0.030	0.0056	$\pm (6)$	2
2316.42	± 0.07	0.031	0.0064	$\pm (3)$	2
2365.99	± 0.08	0.110	0.023	± 0.001	1
2390.56	± 0.12	0.031	0.0065	$\pm (3)$	2
2405.89	± 0.05	0.069	0.014	± 0.001	1
2438.99	± 0.09	0.023	0.0046	$\pm (2)$	2
2484.72	± 0.20	0.004	0.0009	$\pm (1)$	3
2542.70	± 0.10	0.015	0.0030	$\pm (1)$	2
2570.85	± 0.10	0.008	0.0014	$\pm (1)$	2
2651.30	± 0.20	0.004	0.0006	$\pm (1)$	3
2705.00	± 0.20	0.014	0.0025	$\pm (1)$	1
2709.4	± 0.2	0.020	0.0037	$\pm (1)$	1
2808.7	± 0.3	M03	0.0007	$\pm (1)$	3
2820.9	± 0.3	0.006	0.0012	$\pm (1)$	2
2917.7	± 0.2	0.005	0.0010	$\pm (1)$	2
3036.61	± 0.25	0.005	0.0010	$\pm (1)$	2



4.34(1) day ^{101m}Rh

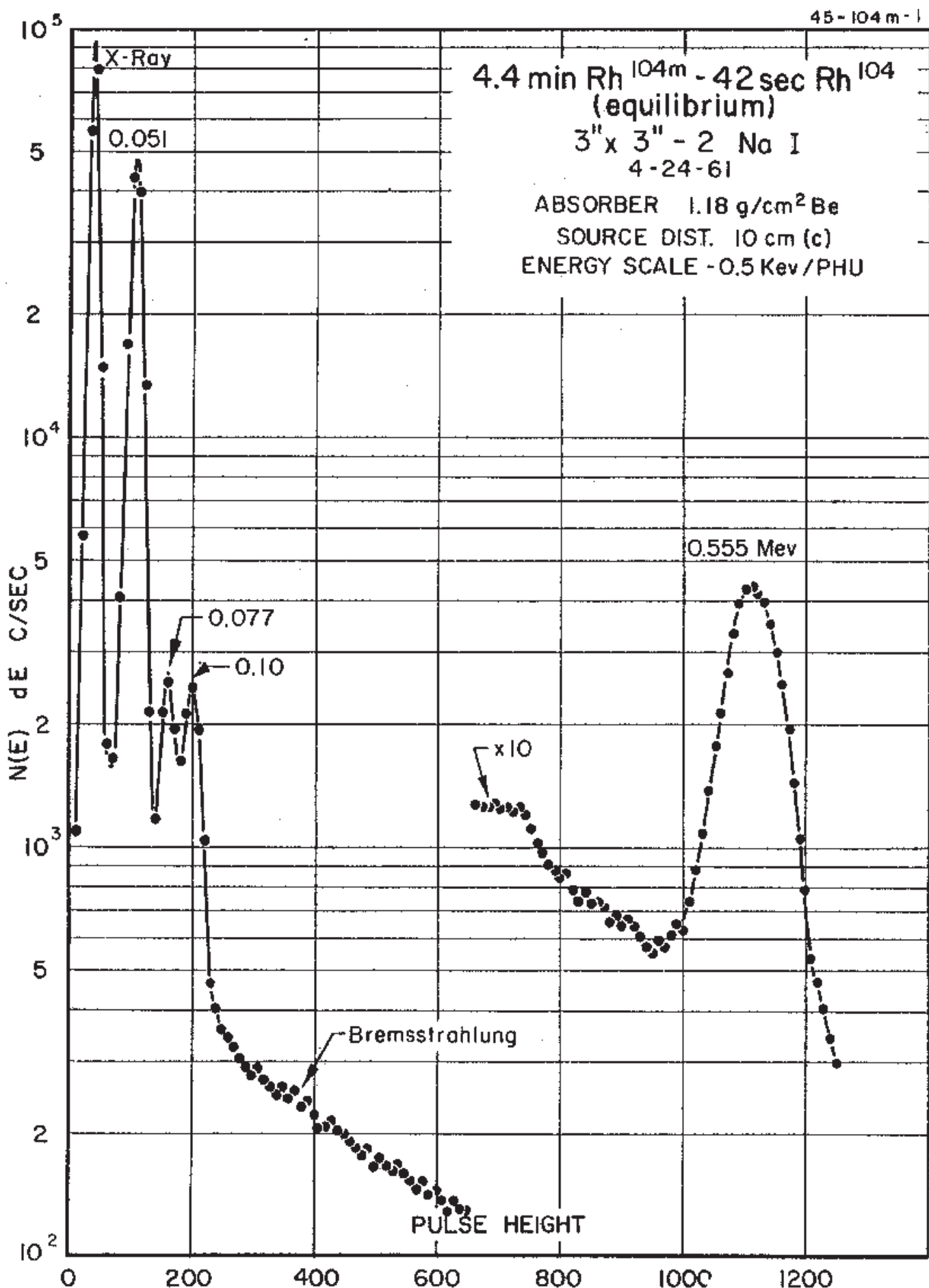


45-101m-1

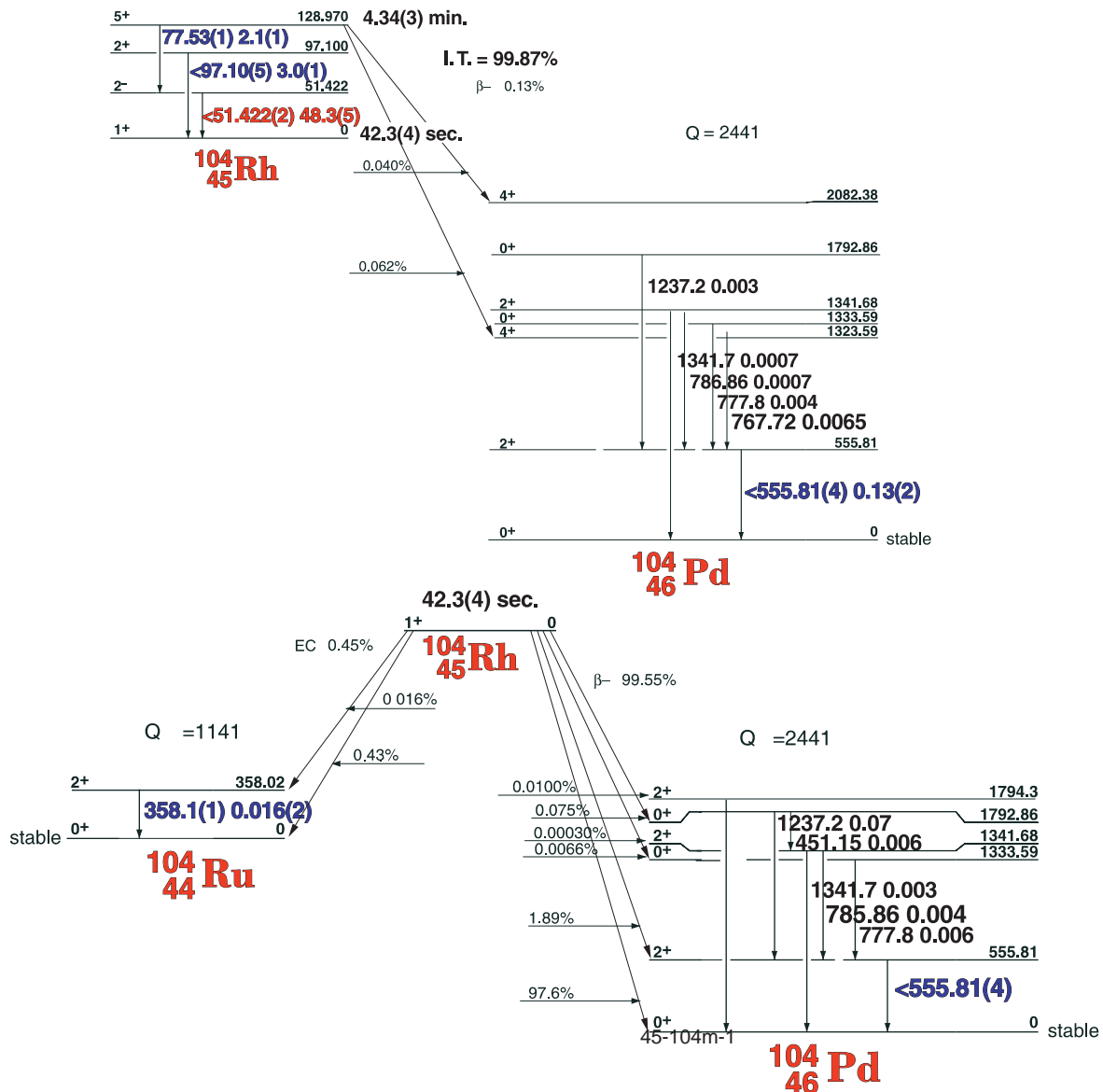
GAMMA-RAY ENERGIES AND INTENSITIES

Nuclide ^{101m}Rh Half Life 4.34(1) day
Detector 3" X 3" NaI-2 Method of Production: $^{103}\text{Rh}(\gamma, 2n)$

	E_γ (KeV)[S]	ΔE_γ	I_γ (rel)	I_γ (%) [E]	ΔI_γ	S
I. T.	127.23	± 0.03	0.74	0.88	± 0.08	2
	157.42	± 0.05	0.31	0.28	± 0.02	4
	179.63	± 0.03	0.67	0.60	± 0.06	3
	184.09	± 0.03	0.24	0.21	± 0.01	4
	233.73	± 0.03	0.20	0.19	± 0.02	4
	238.25	± 0.03	0.24	0.22	± 0.02	4
	306.86	± 0.02	100	94	± 5.0	1
Ann.	511.006					2
	545.01	± 0.15	5.3	4.6	± 0.4	1



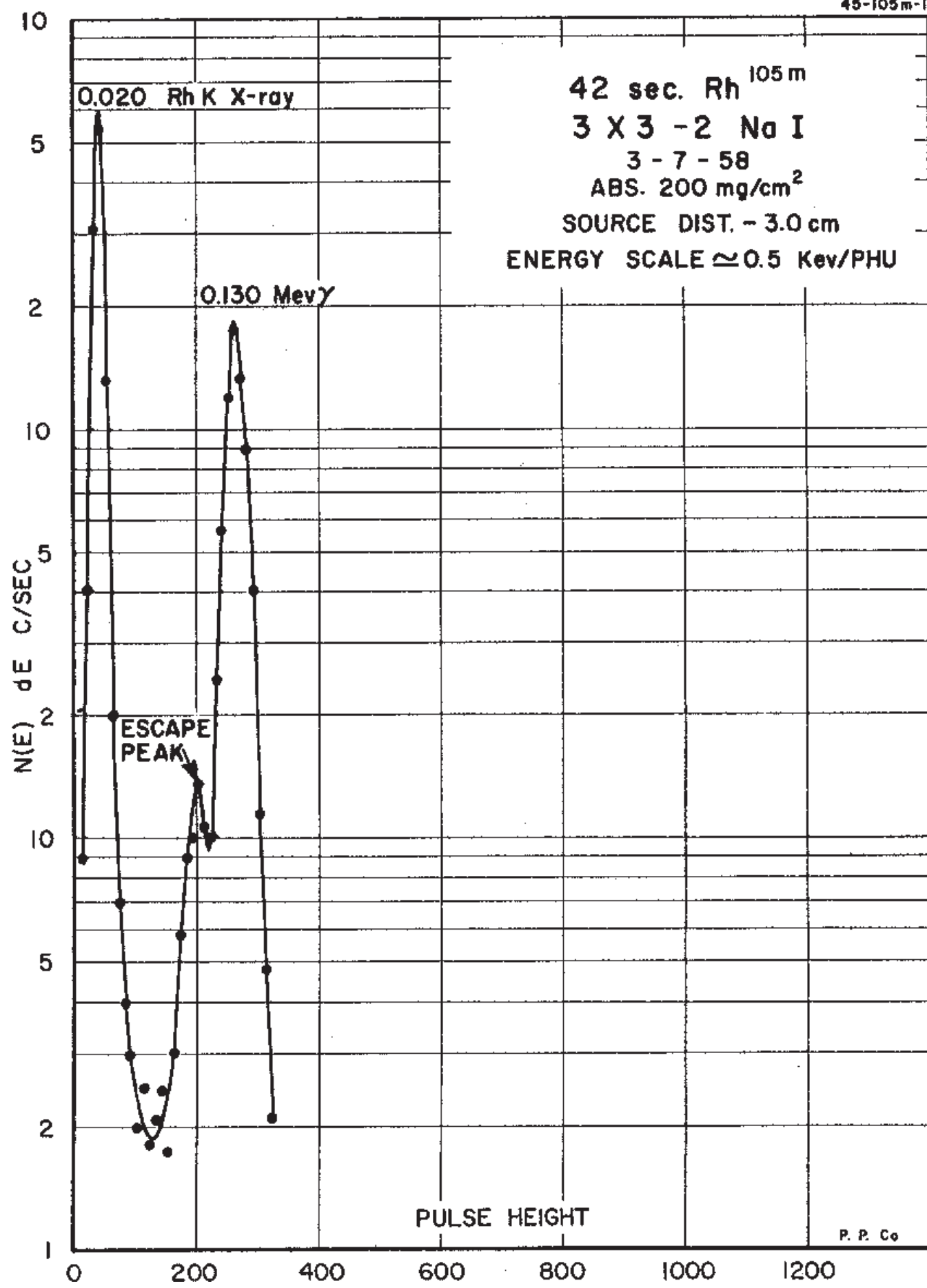
4.34(3) min. ^{104m}Rh - 42.3(4) sec. ^{104}Rh



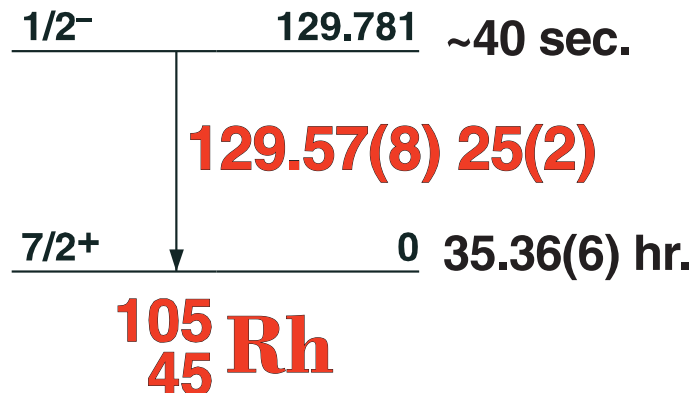
GAMMA-RAY ENERGIES AND INTENSITIES

Nuclide ^{104m}Rh
Detector 3" X 3" NaI-2
Half Life 4.34(3) min - 42.3(4) sec.
Method of Production: $^{103}\text{Rh}(n,\gamma)$

E_γ (KeV)[S]	ΔE_γ	I_γ (rel)	I_γ (%) [E]	ΔI_γ	S
^{104m}Ru					
51.422	± 0.002		48.2	± 0.5	1
77.53	± 0.01		2.1	± 0.1	1
97.10	± 0.05		3.0	± 0.1	1
555.81	± 0.04		0.13	± 0.02	2
^{104}Ru					
358.1	± 0.1		0.016	± 0.002	3
555.81	± 0.04		2.0	± 0.3	2



40 sec. ^{105m}Rh Decay Scheme



45-105m-1

GAMMA-RAY ENERGIES AND INTENSITIES

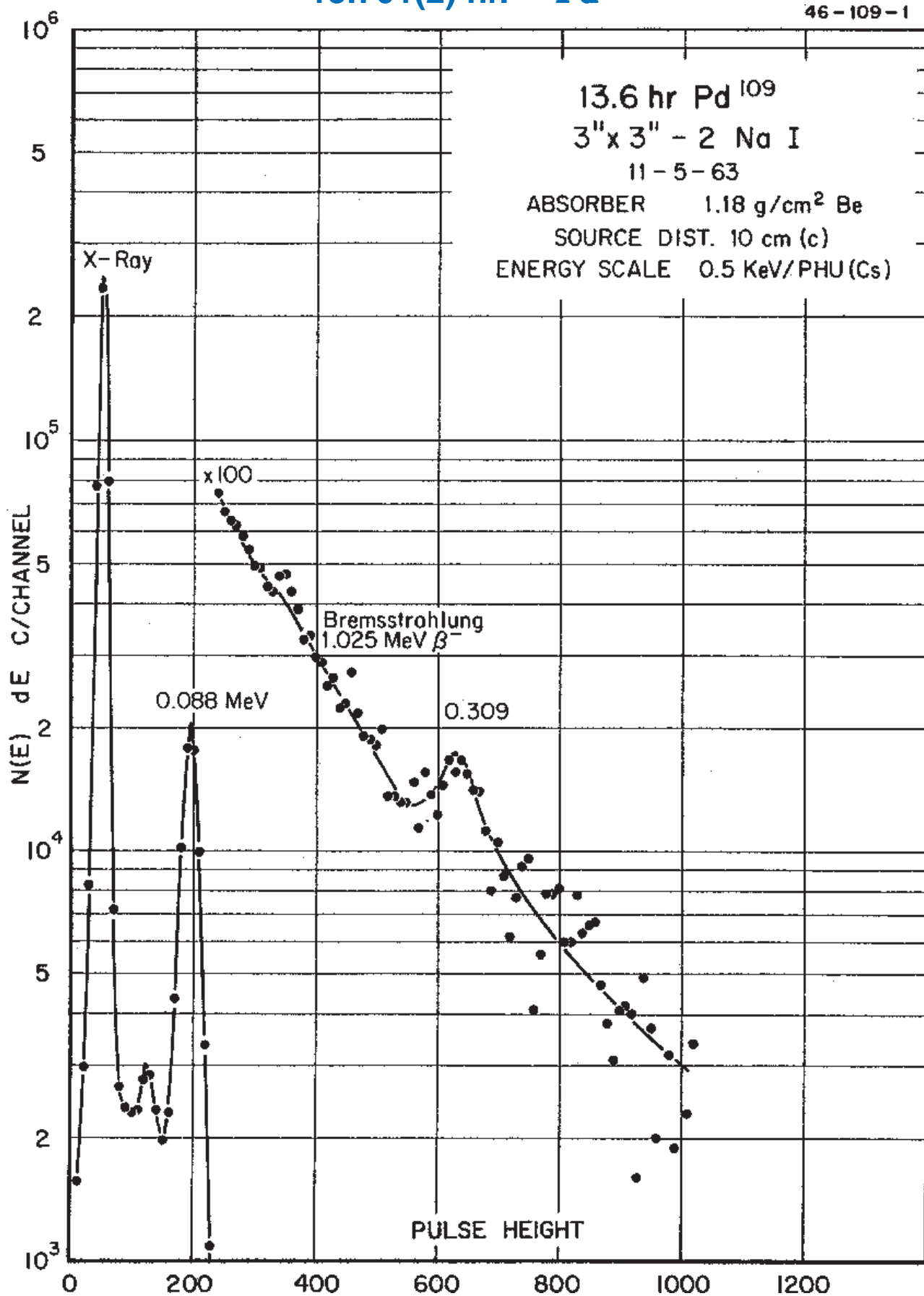
Nuclide ^{105m}Rh
Detector 3" x 3" -2 NaI

Half Life ~40 sec.
Method of Production: $^{104}\text{Ru}(n,\gamma,\beta,)$

E_{γ} (KeV)[S]	ΔE_{γ}	$I_{\gamma}(\text{rel})$	$I_{\gamma}(\%)[E]$	ΔI_{γ}	S
129.57	± 0.08	100	25	± 2.0	1

13.701(2) hr. ^{109}Pd

46-109-1



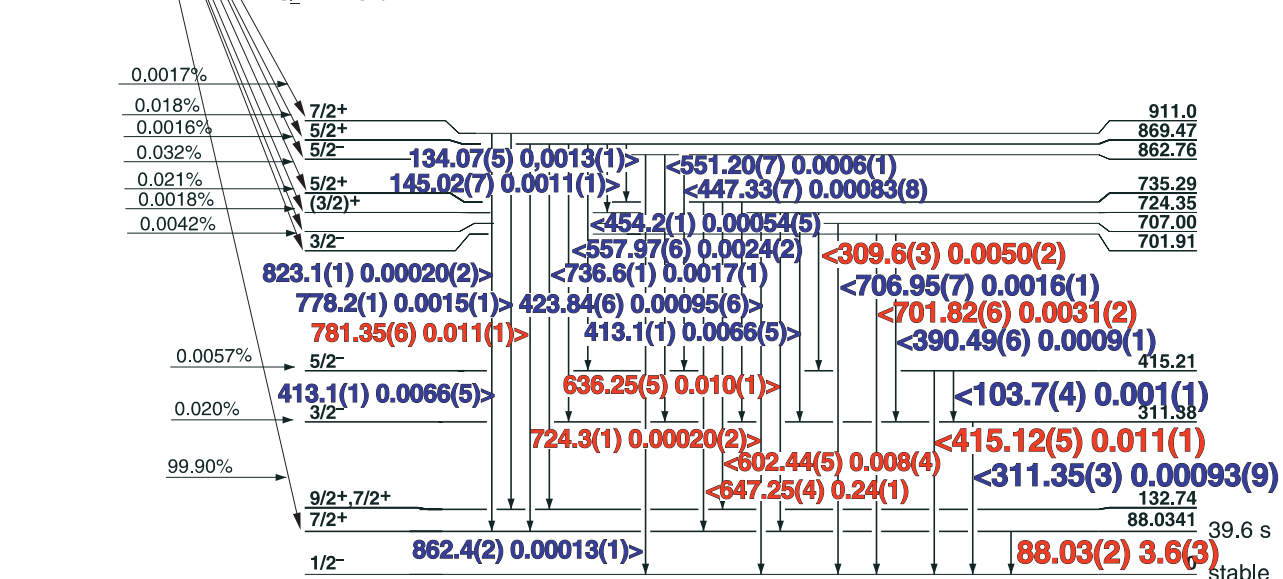
13.701(2) hr. ^{109}Pd

13.701(2) hr.

5/2⁺

^{109}Pd

$Q_\gamma = 1115.9$



^{109}Ag

GAMMA-RAY ENERGIES AND INTENSITIES

Nuclide ^{76}As
Detector 3" X 3" NaI-2

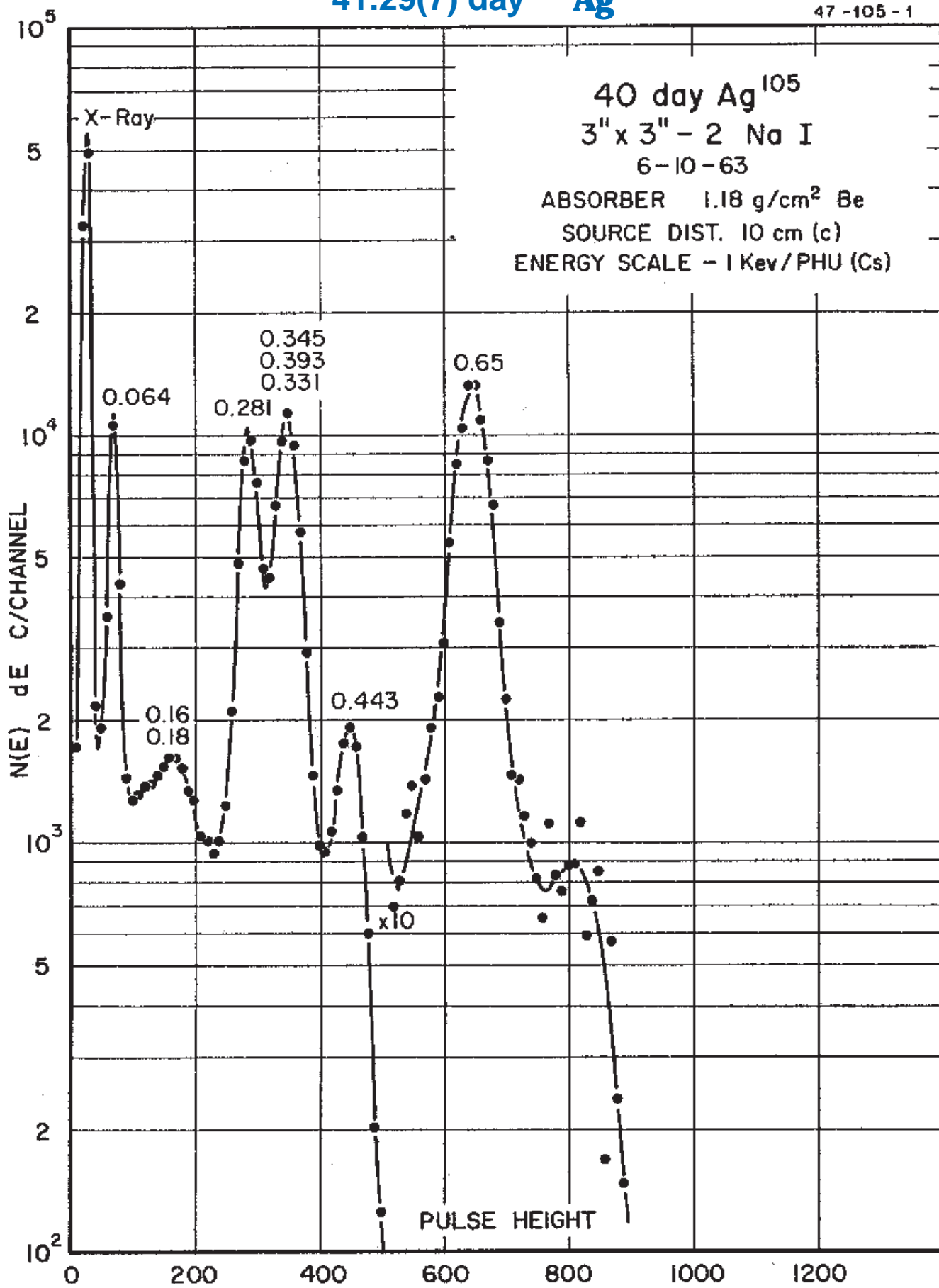
Half Life 1.078(2) Day
Method of Production: /as $^{75}(\text{n},\gamma)$

E_γ (KeV)[S]	ΔE_γ	I_γ (rel)	I_γ (%) [E]	ΔI_γ	S
88.035	± 0.020	100	3.6	± 0.3	1
103.7	± 0.4	0.094	0.0010	± 0.0001	4
134.067	± 0.050	0.071	0.0013	± 0.0001	4
145.020	± 0.070	0.045	0.00011	$\pm (1)$	4
309.6	± 0.3	0.19	0.0050	± 0.0002	3
311.346	± 0.030	0.86	0.00003	$\pm (9)$	1
390.486	± 0.060	0.026	0.0009	± 0.0001	3
413.10	± 0.15	0.23	0.0088	± 0.0005	2
415.125	± 0.05	0.29	0.011	± 0.001	1
423.843	± 0.06	0.027	0.00095	± 0.00006	3
447.331	± 0.07	0.028	0.00083	± 0.00008	3
454.21	± 0.10	0.016	0.00054	± 0.00005	4
551.20	± 0.07	0.017	0.0006	± 0.0001	4
557.974	± 0.06	0.064	0.0024	± 0.0002	3
602.439	± 0.05	0.22	0.008	± 0.0004	1
636.25	± 0.05	0.27	0.010	± 0.001	1
647.25	± 0.04	0.65	0.24	± 0.01	1
701.82	± 0.060	0.082	0.0031	± 0.0002	1
706.95	± 0.070	0.041	0.0016	± 0.0001	2
724.31	± 0.15	0.005	0.00020	± 0.00002	3
736.56	± 0.10	0.056	0.0017	± 0.0001	2
778.18	± 0.10	0.023	0.0015	± 0.0001	2
781.353	± 0.060	0.30	0.011	± 0.001	1
823.1	± 0.2	0.005	0.00020	± 0.00002	3
862.4	± 0.2	0.005	0.00013	± 0.00001	3

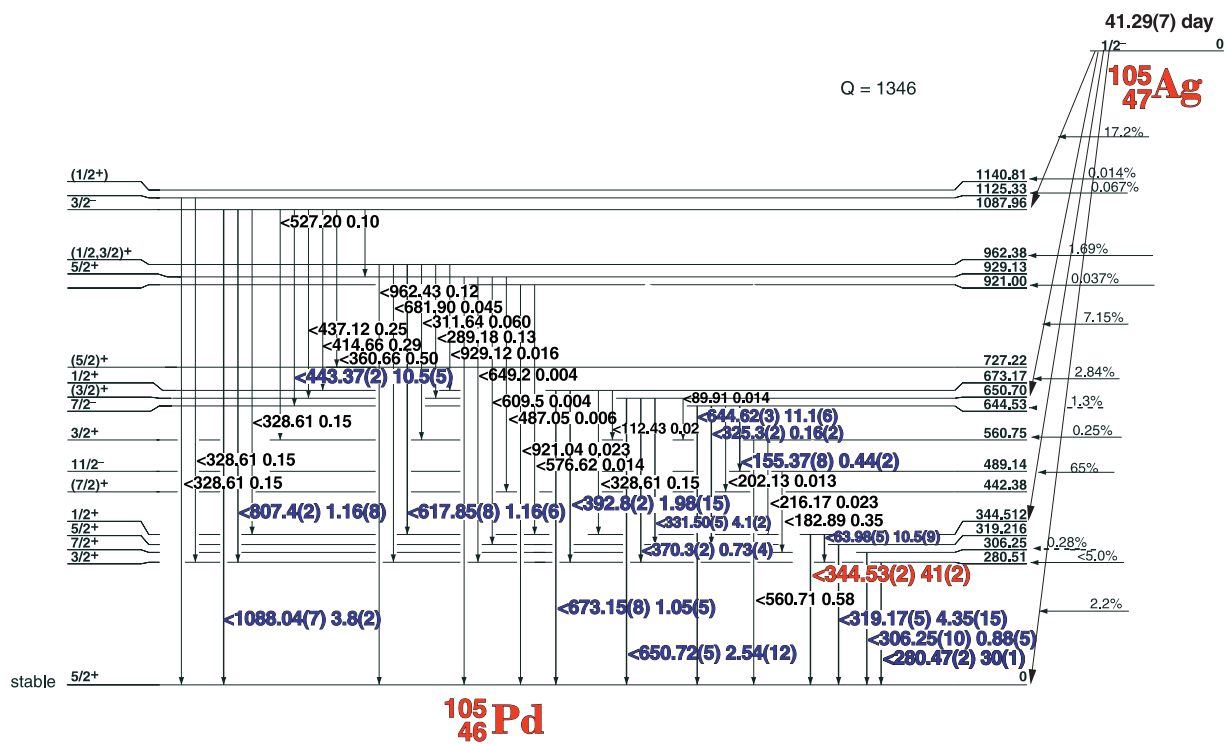
46-109-1

41.29(7) day ^{105}Ag

47 - 105 - 1



41.29(7) day ^{105}Ag Decay Scheme



GAMMA-RAY ENERGIES AND INTENSITIES

47-105-1

Nuclide ^{105}Ag
Detector 3" x 3" -2 NaI

Half Life 41.29(7) day
Method of Production: $^{107}\text{Ag}(\gamma,2n)$

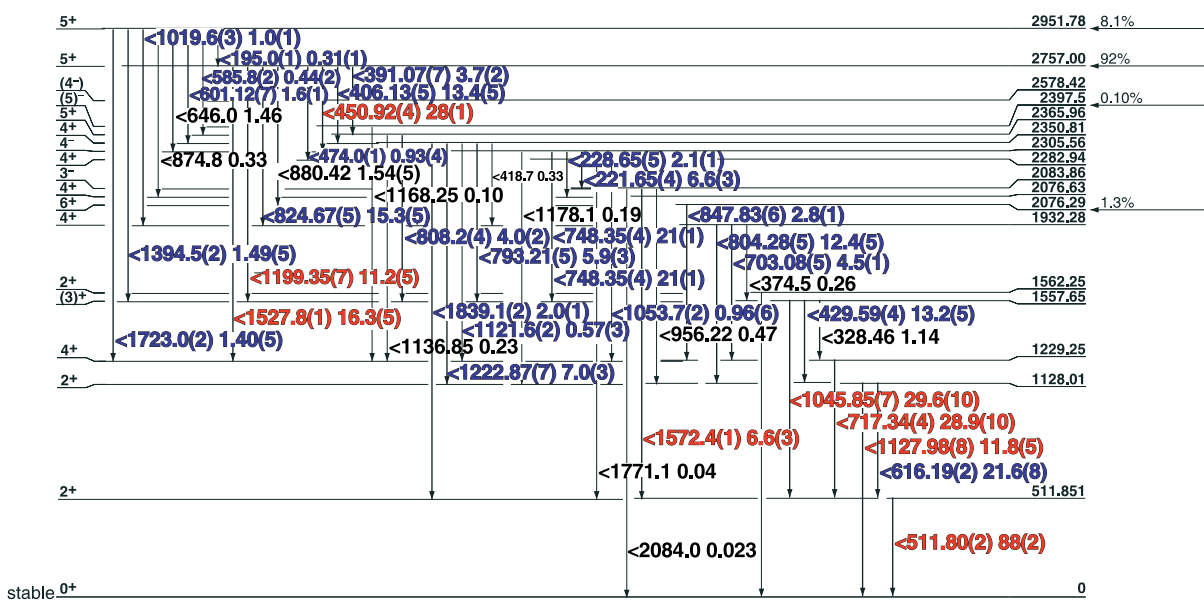
E_{γ} (KeV)[S]	ΔE_{γ}	I_{γ} (rel)	$I_{\gamma}(\%)$ [E]	ΔI_{γ}	S
63.98 \pm 0.05			10.5 \pm 0.9		2
155.37	\pm 0.10	1.0	0.44	\pm 0.02	4
182.75	\pm 0.10	1.1	0.35	\pm 0.02	4
280.47 \pm 0.02	70.0		30 \pm 1.0		2
306.25	\pm 0.10	2.5	0.88	\pm 0.05	4
319.17	\pm 0.05	10.0	4.35	\pm 0.15	3
325.6	\pm 0.3	0.7	0.16	\pm 0.02	4
331.50	\pm 0.05	10.0	4.1	\pm 0.2	4
344.53 \pm 0.02	100		41 \pm 2.0		1
360.70	\pm 0.10	1.3	0.50	\pm 0.03	4
370.27	\pm 0.10	2.2	0.73	\pm 0.04	4
392.8	\pm 0.2	3.6	1.98	\pm 0.15	4
414.9	\pm 0.2	0.7	0.29	\pm 0.02	4
443.37	\pm 0.025	25.0	10.5	\pm 0.5	3
644.62 \pm 0.030	26.0		11.1 \pm 0.6		2
650.72	\pm 0.050	6.2	2.54	\pm 0.12	4
673.15	\pm 0.08	2.8	1.05	\pm 0.05	4
807.0	\pm 0.5	w	1.16	\pm 0.08	4
1088.04	\pm 0.07	8.4	3.8	\pm 0.2	3

8.28(2) day ^{106m}Ag

Q = 2965

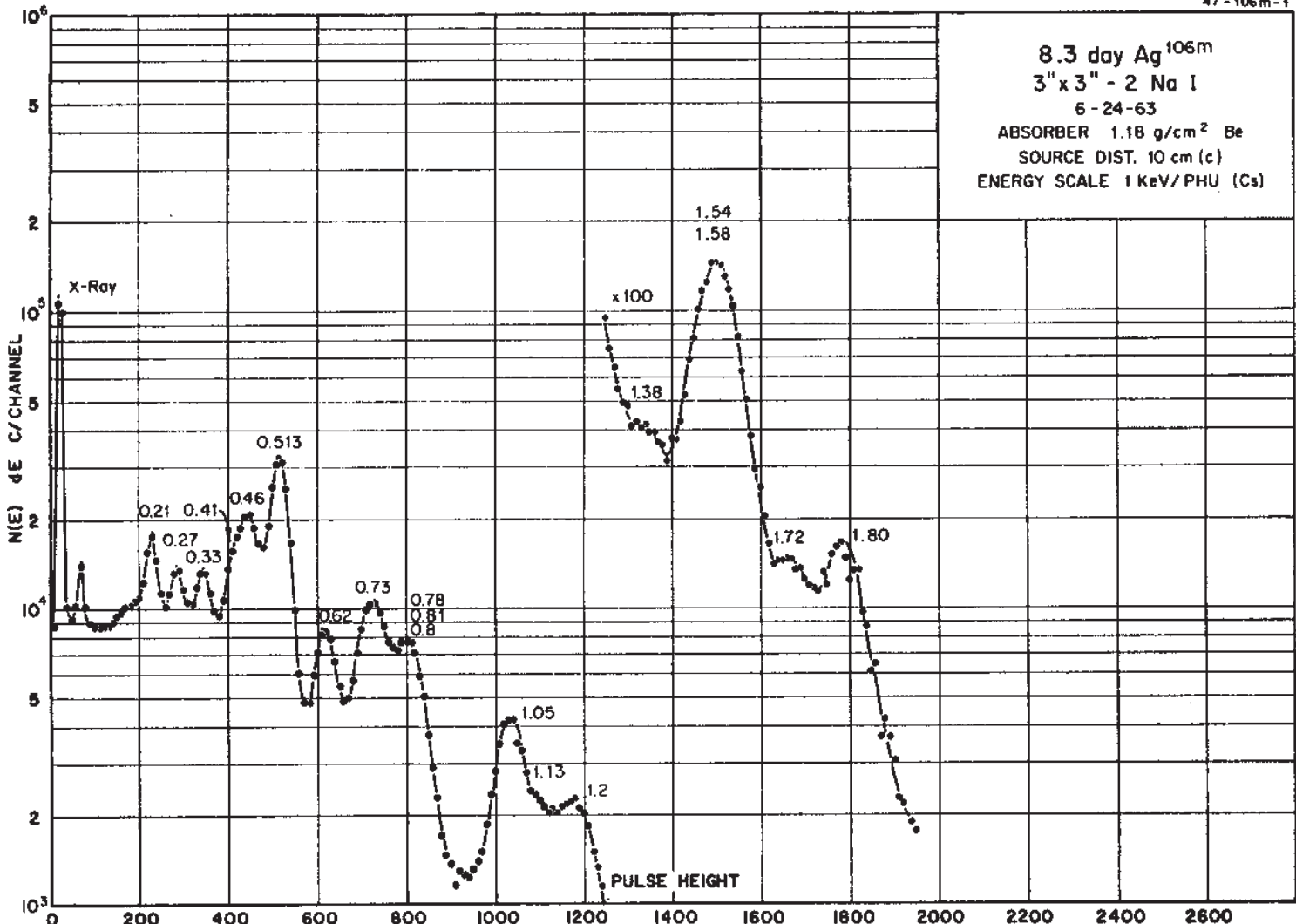
8.28 d
6+ 89.66
0

$^{106}_{47}\text{Ag}$



$^{106}_{46}\text{Pd}$

47 - ^{106m}Ag



Decay Data

← Index →

8.28(2) day ^{106m}Ag

GAMMA-RAY ENERGIES AND INTENSITIES

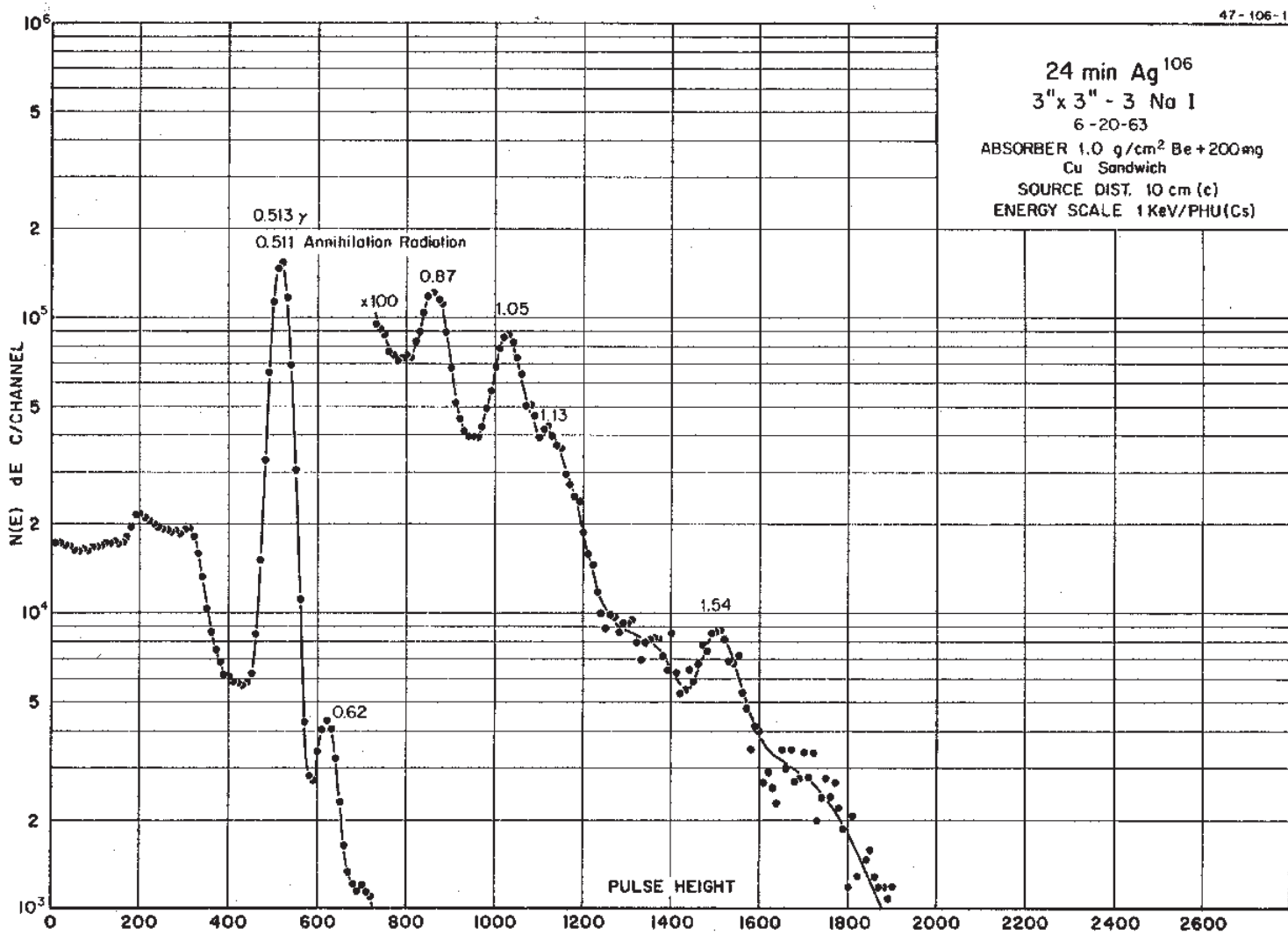
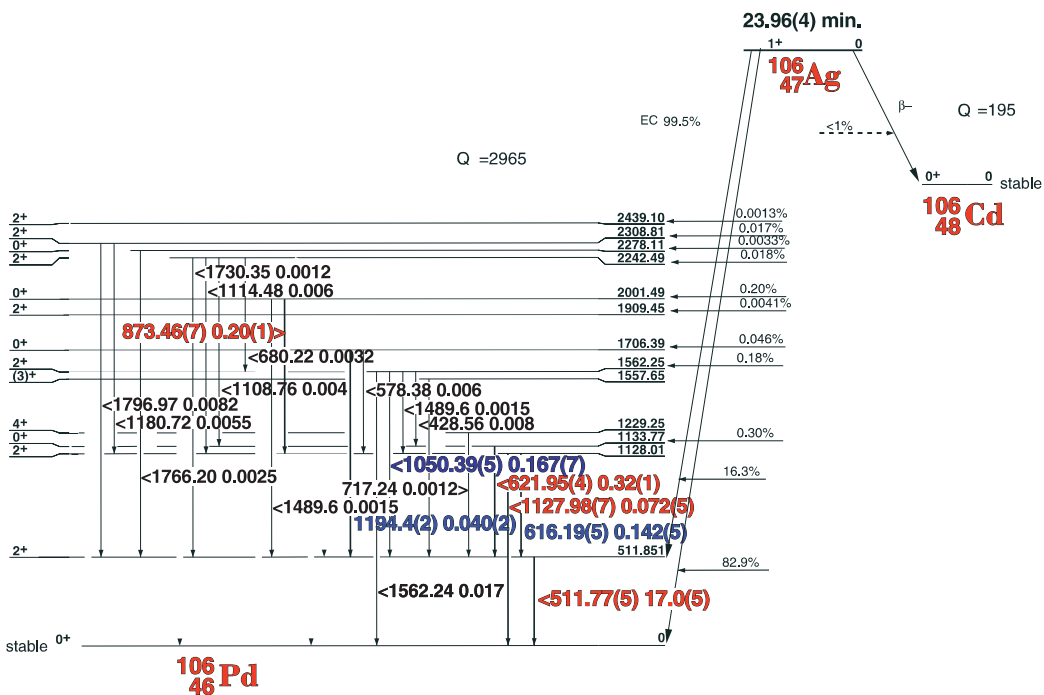
Nuclide
Detector

^{106m}Ag
3" x 3" -2 NaI

Half Life 8.28(2) day.
Method of Production: $^{107}\text{Ag}(\gamma, n)$

E_{γ} (KeV)[S]	ΔE_{γ}	I_{γ} (rel)	$I_{\gamma}(\%)[E]$	ΔI_{γ}	S
195.0	± 0.3	0.8	0.31	± 0.01	4
221.65	± 0.035	7.8	6.6	± 0.3	3
228.65	± 0.05	2.7	2.1	± 0.1	4
391.07	± 0.07	4.8	3.7	± 0.2	3
406.13	± 0.05	16.0	13.4	± 0.5	2
418.5	± 0.3	0.4	0.33	± 0.03	4
429.59	± 0.045	15.0	13.2	± 0.5	2
450.92	± 0.035	32.0	28.0	± 1.0	1
473.99	± 0.10	1.0	0.93	± 0.04	4
511.80	± 0.025	100	88	± 2.0	1
585.8	± 0.2	1.0	0.44	± 0.02	4
601.12	± 0.07	2.0	1.6	± 0.1	4
616.19	± 0.05	26.0	21.6	± 0.8	2
680.20	± 0.09	2.5	1.54	± 0.07	4
703.08	± 0.05	5.4	4.5	± 0.1	3
717.34	± 0.045	33.0	28.9	± 1.0	1
748.35	± 0.04	24.0	21	± 1.0	1
793.21	± 0.05	7.0	5.9	± 0.3	3
804.28	± 0.05	13.0	12.4	± 0.5	3
808.2	± 0.2	5.0	4.0	± 0.2	4
824.67	± 0.05	17.0	15.3	± 0.5	2
847.83	± 0.06	5.2	2.8	± 0.1	3
1019.6	± 0.3	1.2	1.0	± 0.1	4
1045.85	± 0.07	32.0	29.6	± 1.0	1
1053.7	± 0.2	1.4	0.96	± 0.08	4
1121.6	± 0.3	0.75	0.57	± 0.03	4
1127.98	± 0.08	13.0	11.8	± 0.5	1
1199.35	± 0.07	12.0	11.2	± 0.5	1
1222.87	± 0.07	7.4	7.0	± 0.3	2
1394.5	± 0.2	1.9	1.49	± 0.05	3
1527.78	± 0.10	17.0	6.6	± 0.3	1
1565.8	± 0.2	0.7	0.48	± 0.3	4
1572.49	± 0.15	7.3	6.6	± 0.3	1
1723.0	± 0.2	1.5	1.40	± 0.05	2
1839.1	± 0.2	2.3	2.0	± 0.1	2
2084.0	± 0.1		0.023	± 0.006	

23.96(4) min. ^{106}Ag



23.96(4) min. ^{106}Ag

47-106-1

GAMMA-RAY ENERGIES AND INTENSITIES

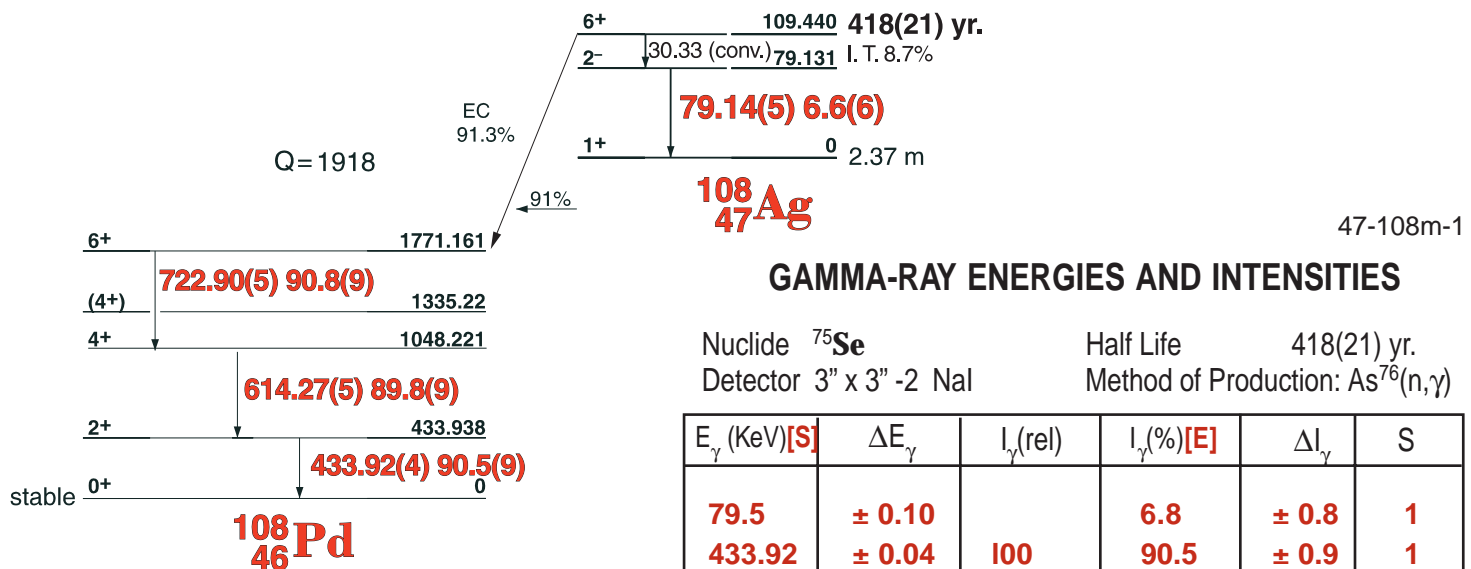
Nuclide
Detector

^{106}Ag
3" x 3" -2 Nal

Half Life 23.96(4) min.
Method of Production: $^{107}\text{Ag}(\gamma, n)$

	E_γ (KeV)[S]	ΔE_γ	I_γ (rel)	$I_\gamma(\%)$ [E]	ΔI_γ	S
Ann.	511.006					
	511.80	± 0.02		17.0	± 0.5	1
	616.19	± 0.05	47.0	0.142	± 0.005	2
	621.95	± 0.04	100	0.32	± 0.01	1
	873.46	± 0.07	61.0	0.20	± 0.01	1
	1050.31	± 0.10	47.0	0.167	± 0.007	1
	1127.98	± 0.07	23.0	0.072	± 0.005	1
	1194.4	± 0.2	11.0	0.040	± 0.002	2

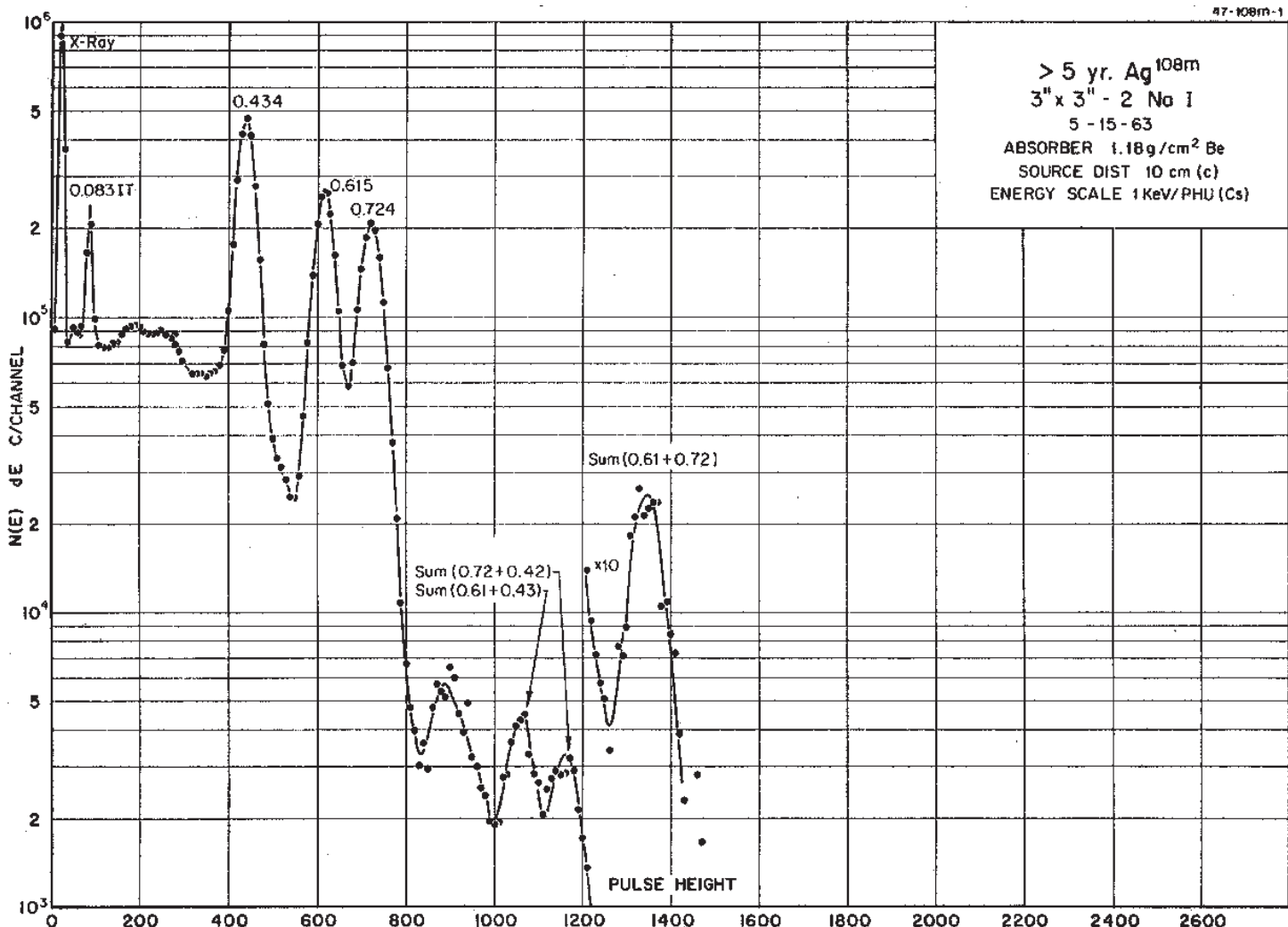
418(21) yr. ^{108m}Ag



GAMMA-RAY ENERGIES AND INTENSITIES

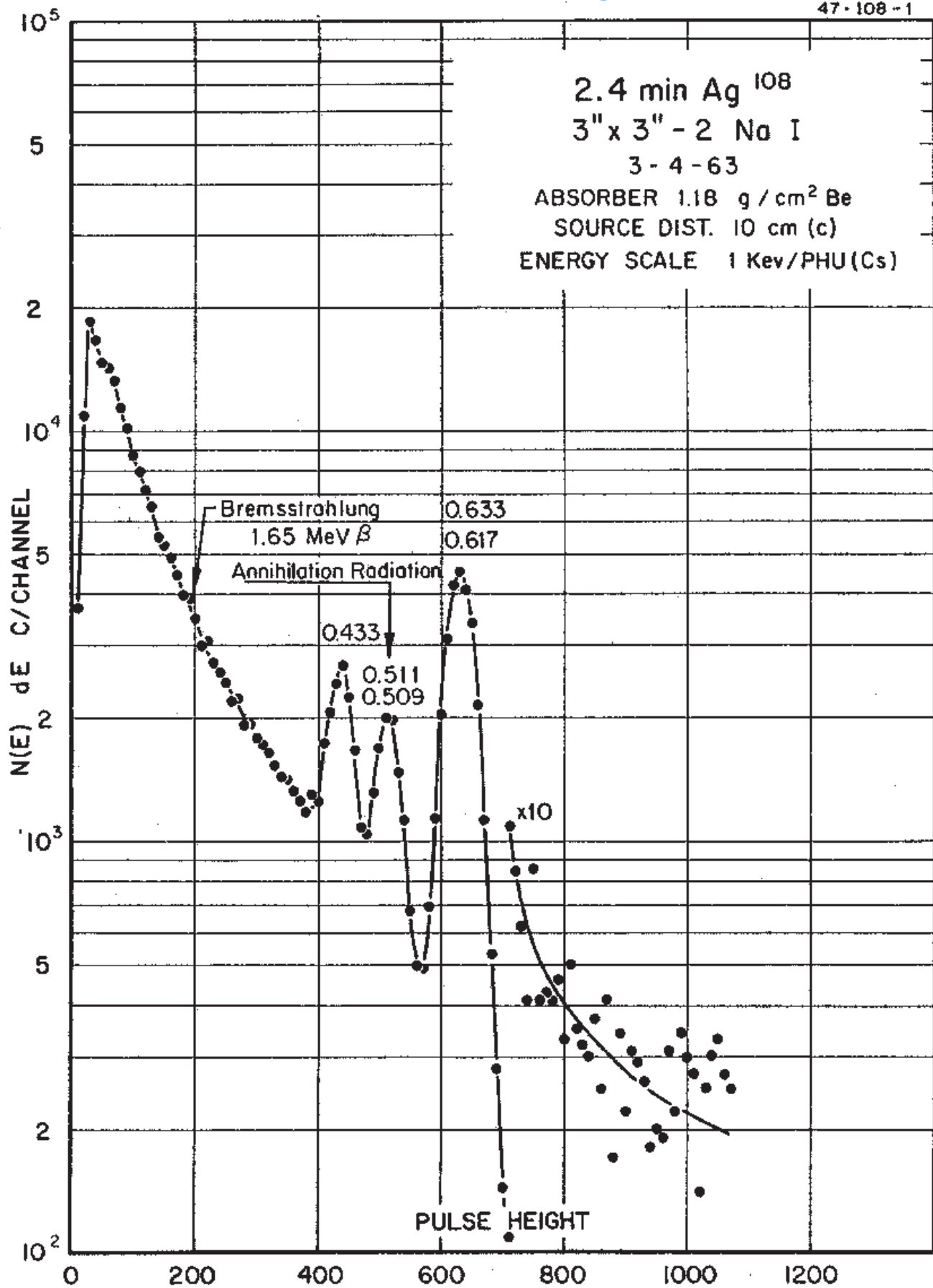
Nuclide ^{75}Se
Detector 3" x 3" - 2 NaI
Half Life 418(21) yr.
Method of Production: As⁷⁶(n,γ)

E_{γ} (KeV)[S]	ΔE_{γ}	$I_{\gamma}(\text{rel})$	$I_{\gamma}(\%)[E]$	ΔI_{γ}	S
79.5	± 0.10		6.8	± 0.8	1
433.92	± 0.04	100	90.5	± 0.9	1
614.27	± 0.05	100	89.8	± 0.9	1
722.90	± 0.05	100	90.8	± 0.9	1

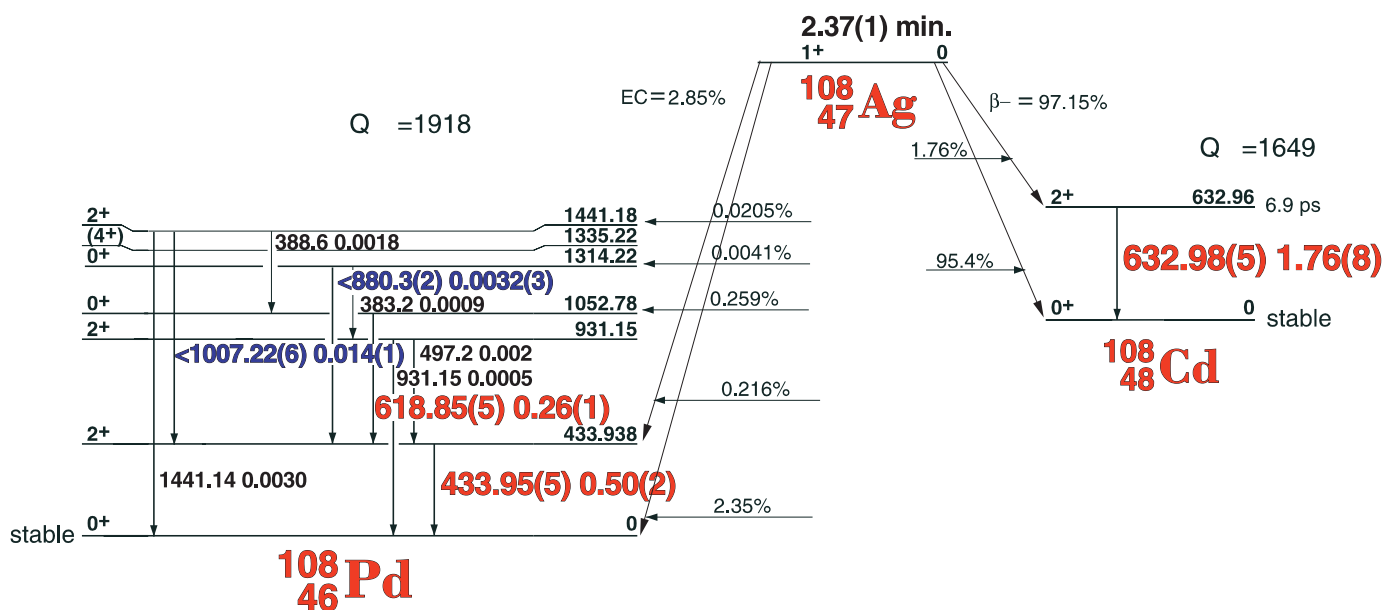


2.37(1) min. ^{108}Ag

47 - 108 - 1



2.37(1) Min. ^{108}Ag Decay Scheme



47-108-1

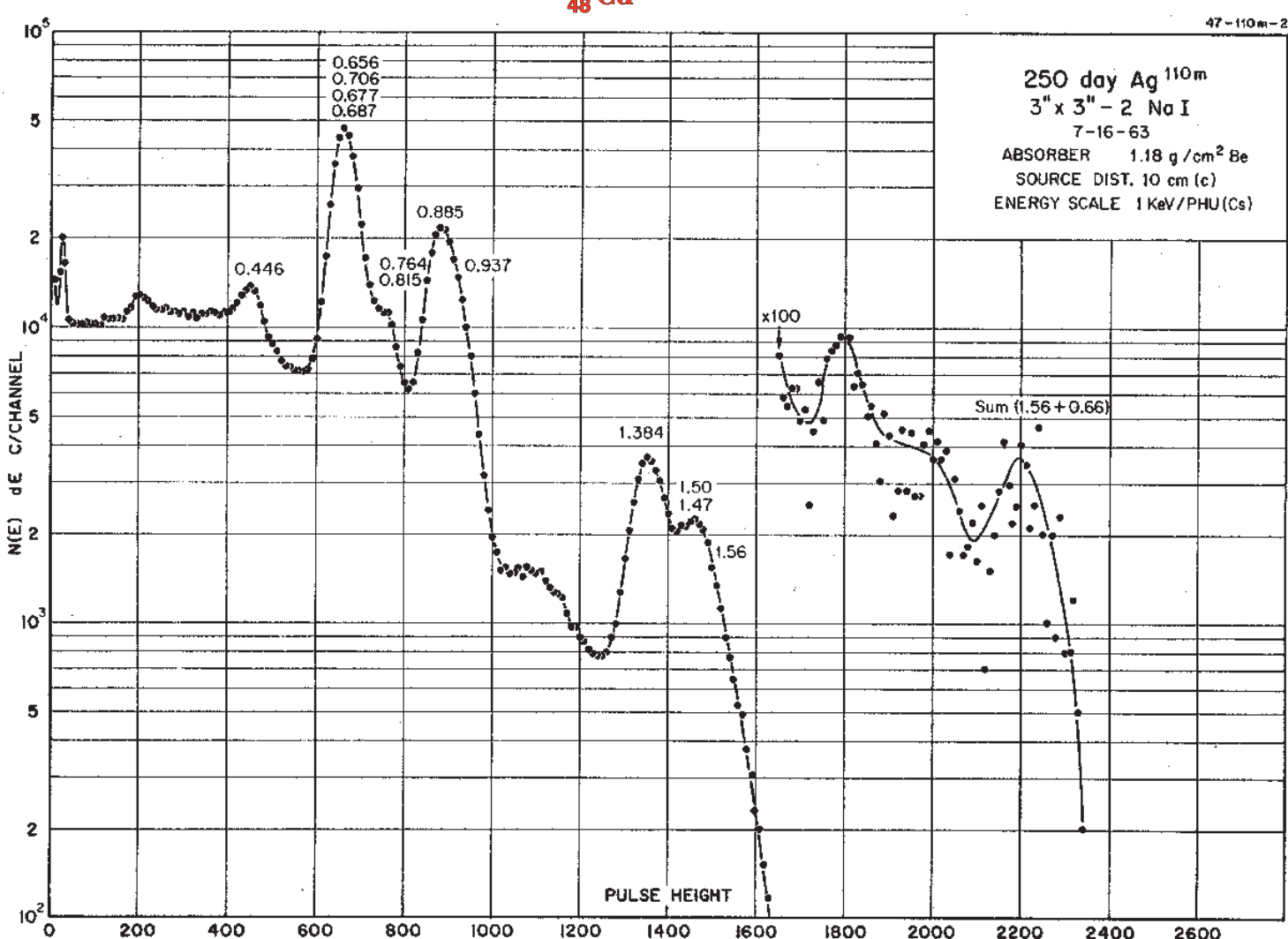
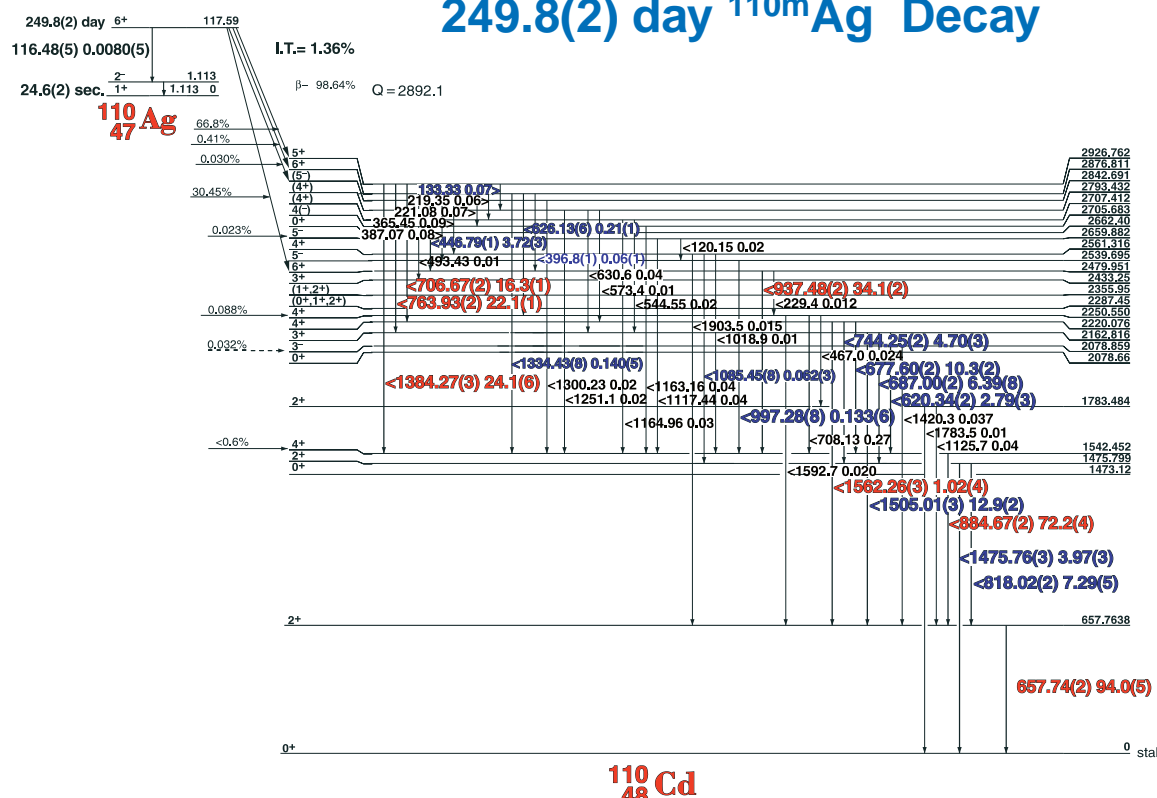
GAMMA-RAY ENERGIES AND INTENSITIES

Nuclide ^{108}Ag
Detector 3" x 3" -2 NaI

Half Life 2.37(1) min.
Method of Production: $^{107}\text{Ag}(n,\gamma)$

E_γ (KeV)[S]	ΔE_γ	I_γ (rel)	$I_\gamma(\%)$ [E]	ΔI_γ	S
433.95	± 0.05	28.3	0.50	± 0.02	1
618.85	± 0.05	52.5	0.26	± 0.01	1
632.98	± 0.05	100	1.76	± 0.08	1
880.26	± 0.1	0.17	0.0032	$\pm (3)$	3
1007.22	± 0.06	0.81	0.014	$+ 0.001$	2

249.8(2) day ^{110m}Ag Decay



249.8(2) day ^{110m}Ag

47-110m-1

GAMMA-RAY ENERGIES AND INTENSITIES

Nuclide
Detector

^{110m}Ag
3" x 3" -2 Nal

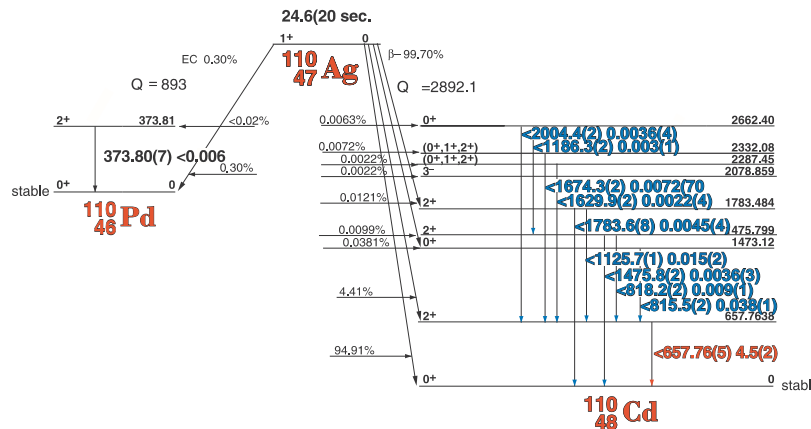
Half Life 249.8(20 day
Method of Production: $^{109}\text{Ag}(n,\gamma)$

E_{γ} (KeV)[S]	ΔE_{γ}	I_{γ} (rel)	$I_{\gamma}(\%)[E]$	ΔI_{γ}	S
133.29	± 0.10	0.08	0.08	± 0.008	4
220.3	± 0.5	0.27		± 0.10	4
220.7	± 0.4	0.12		± 0.01	4
266.85	± 0.08	0.07		± 0.007	4
362.22	± 0.09	0.07		± 0.007	4
365.4	± 0.1	0.11	0.09	± 0.015	4
387.0	± 0.1	0.06	0.08	± 0.01	4
396.8	± 0.1	0.06	0.06	± 0.01	4
446.791	± 0.010	3.81	3.72	± 0.03	3
620.342	± 0.016	2.93	2.79	± 0.03	3
626.13	± 0.06	0.225	0.21	± 0.01	4
657.744	± 0.017	100	94.0	± 0.5	1
677.601	± 0.018	11.26	10.3	± 0.2	2
687.00	± 0.019	7.33	6.39	± 0.08	2
706.669	± 0.020	17.57	16.3	± 0.1	1
744.254	± 0.020	5.18	4.70	± 0.26	2
763.928	± 0.019	23.99	22.1	± 0.1	1
818.018	± 0.022	7.94	7.29	± 0.05	1
884.667	± 0.018	77.87	72.2	± 0.4	1
937.483	± 0.020	37.40	34.1	± 0.2	1
997.28	± 0.08	0.122	0.133	± 0.008	4
1085.45	± 0.08	0.067	0.062	± 0.003	4
1334.43	± 0.08	0.21	0.140	± 0.005	4
1384.267	± 0.029	26.79	24.1	± 0.6	1
1421.40	± 0.08	0.074	0.05	± 0.01	4
1475.757	± 0.034	4.37	3.97	± 0.05	1
1505.006	± 0.032	14.32	12.9	± 0.2	1
1562.264	± 0.034	1.33	1.02	± 0.04	1

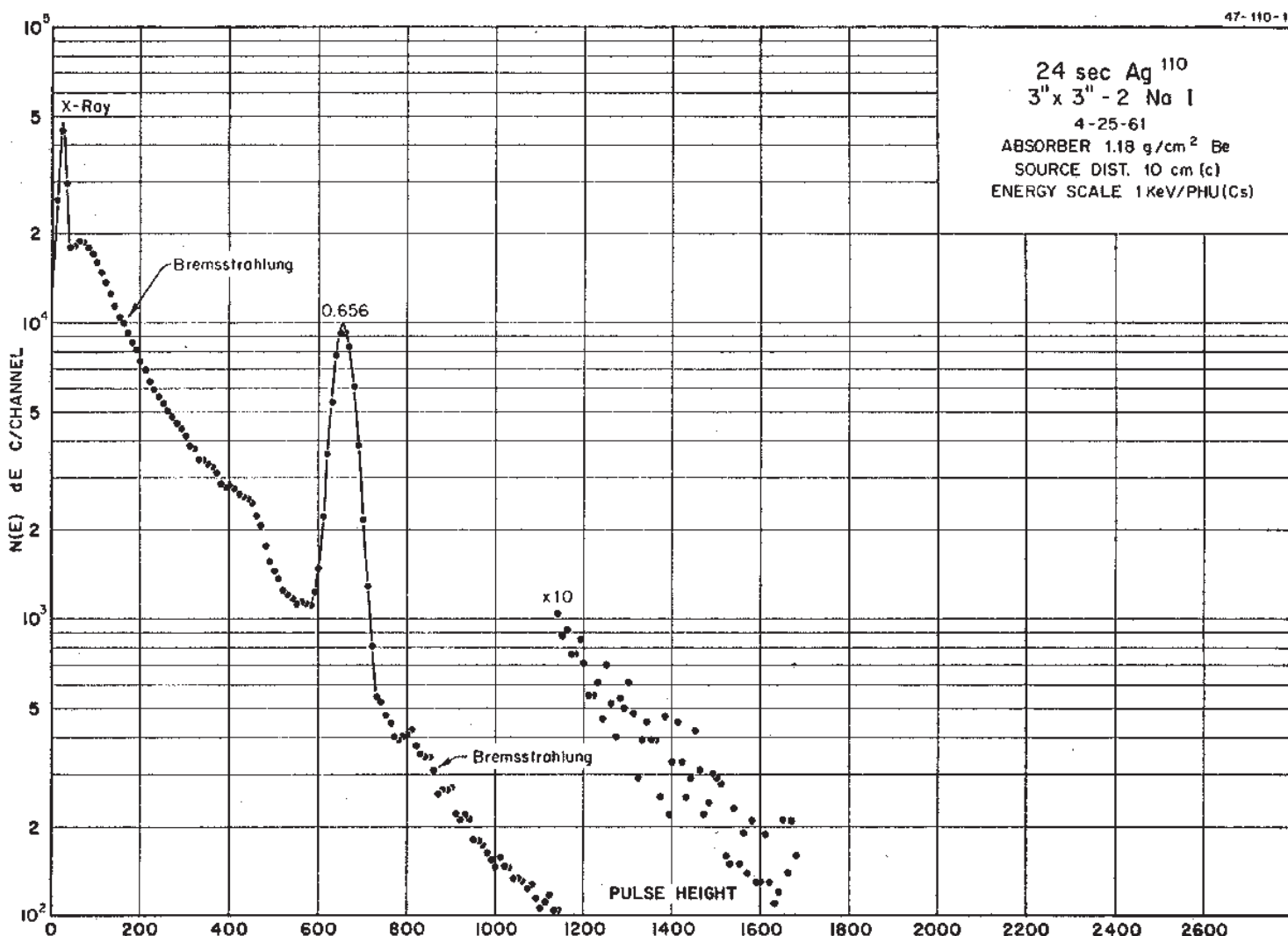
24.6(2) sec. ^{110}Ag

GAMMA-RAY ENERGIES AND INTENSITIES

Nuclide ^{110}Ag Half Life 24.6(2) sec.
 Detector 3" X 3" NaI-2 Method of Production: $^{109}\text{Ag}(n,\gamma)$

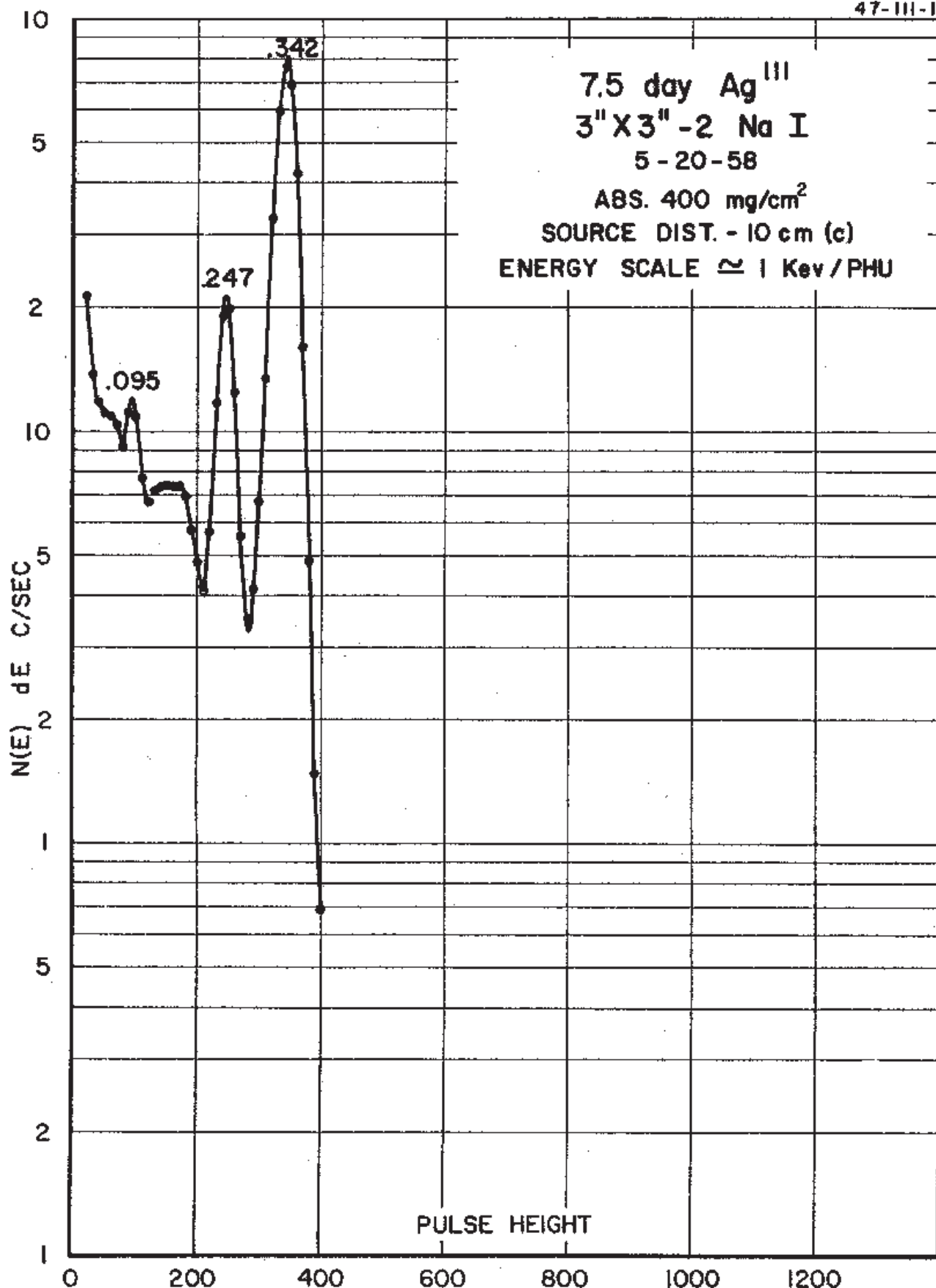


E_γ (KeV)[S]	ΔE_γ	I_γ (rel)	I_γ (%)[E]	ΔI_γ	S
657.79	± 0.05		0.26	± 0.01	1
815.35	± 0.05		0.038	± 0.005	4
1125.7	± 0.1		0.015	± 0.002	3
1674.3	± 0.1		0.007	± 0.001	4

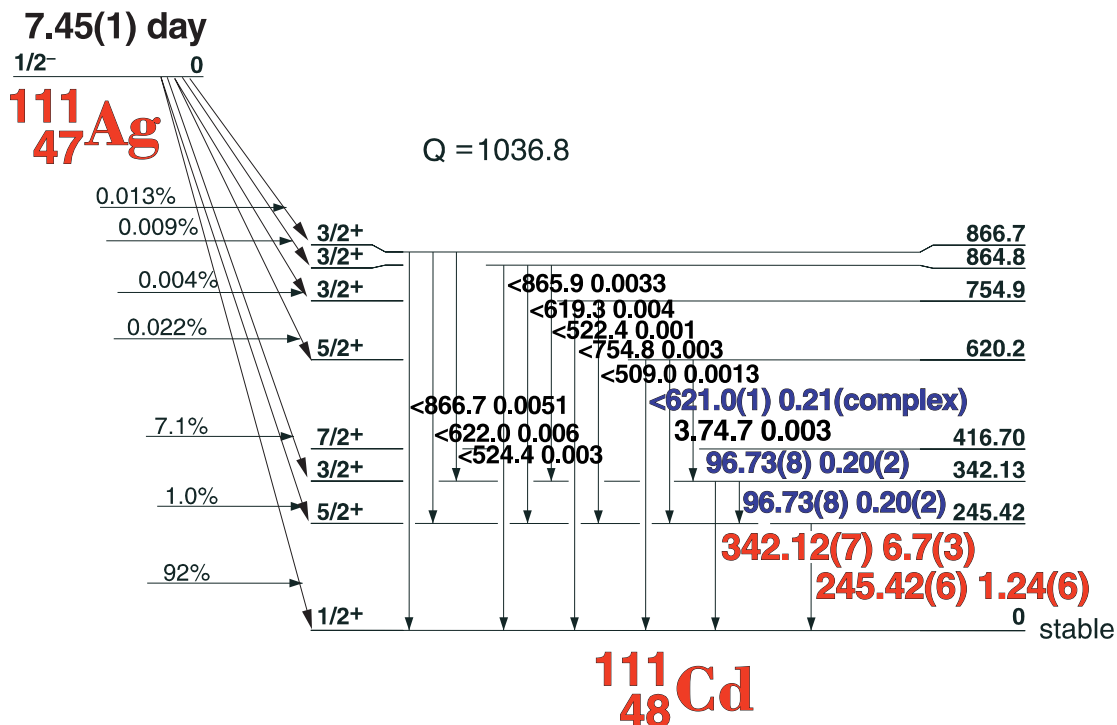


7.45(1) day ^{111}Ag

47-III-1



7.45(1) day ^{111}Ag Decay Scheme



47-111-1

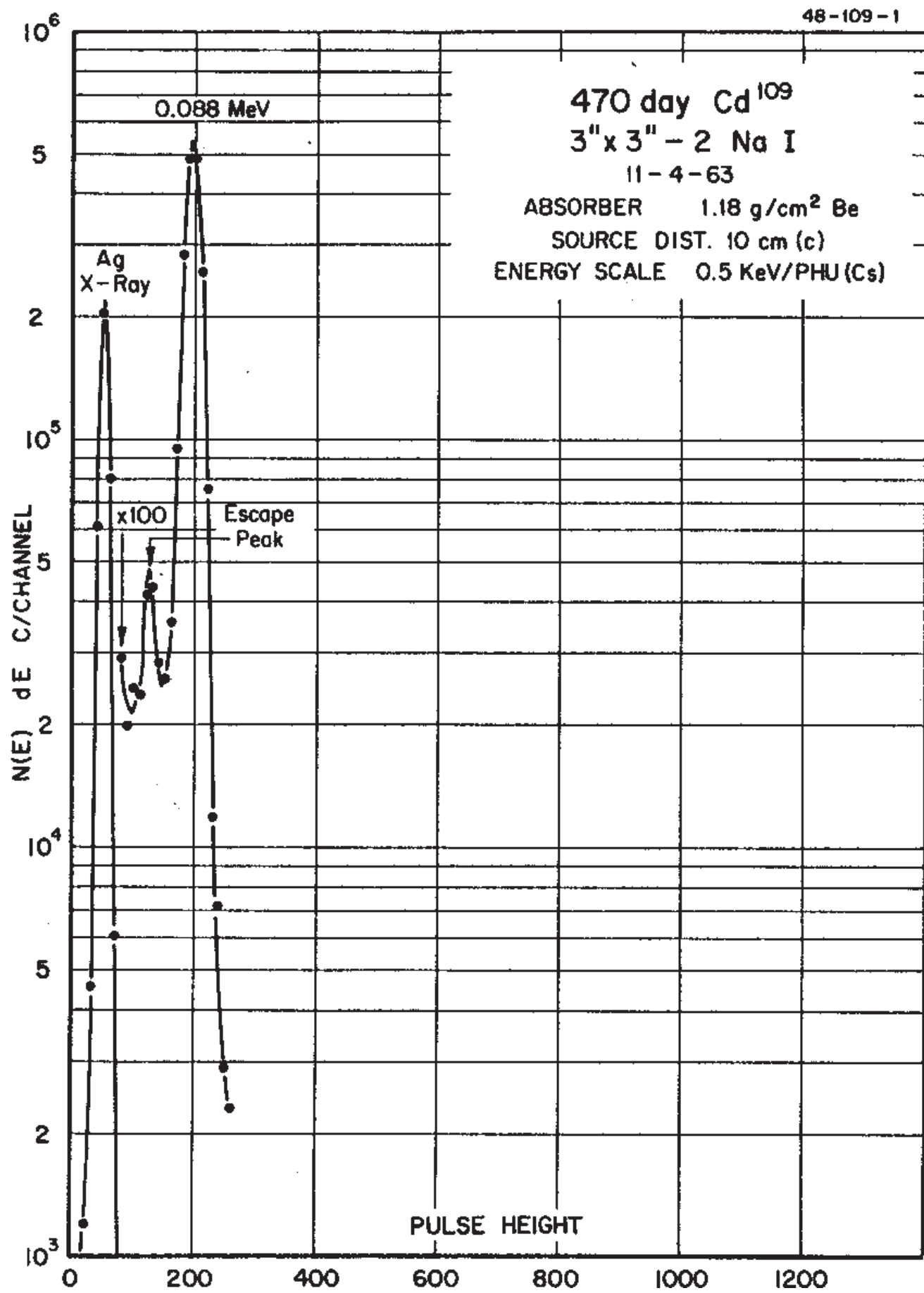
GAMMA-RAY ENERGIES AND INTENSITIES

Nuclide ^{111}Ag
Detector 3" X 3" NaI-2

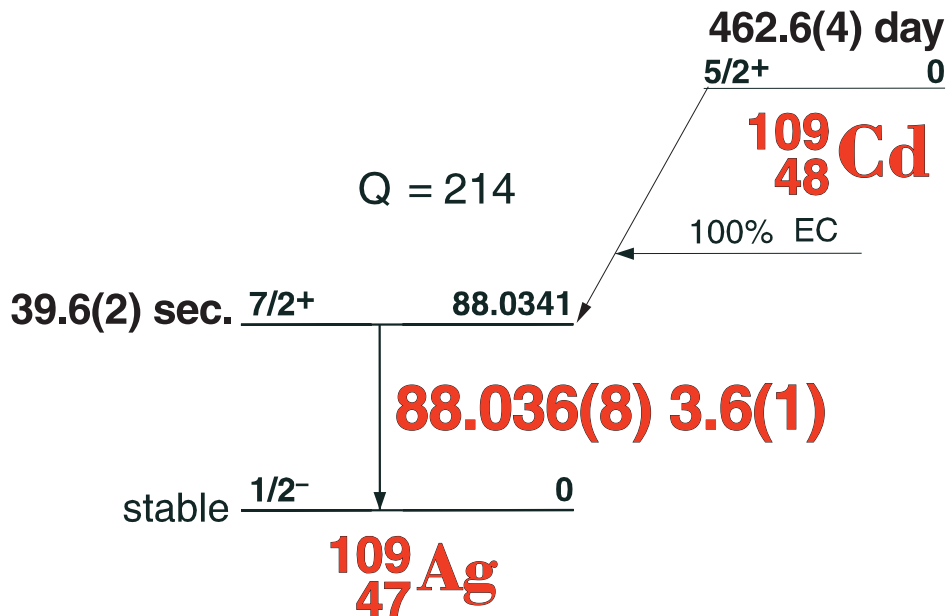
Half Life 7.45(12) day
Method of Production: $^{110}\text{Pd}(n,\gamma,\beta)$

E_{γ} (KeV)[S]	ΔE_{γ}	$I_{\gamma}(\text{rel})$	$I_{\gamma}(\%)[E]$	ΔI_{γ}	S
96.73	± 0.08	1.6	0.29	± 0.02	3
245.422	± 0.06	16.9	1.24	± 0.06	1
342.118	± 0.07	100	6.7	± 0.3	1
621.0	± 0.1	0.35	0.21	± 0.02	4
866.0	± 1.0	w			4

462.6(4) day ^{109}Cd



462.6(4) day ^{109}Cd Decay Scheme



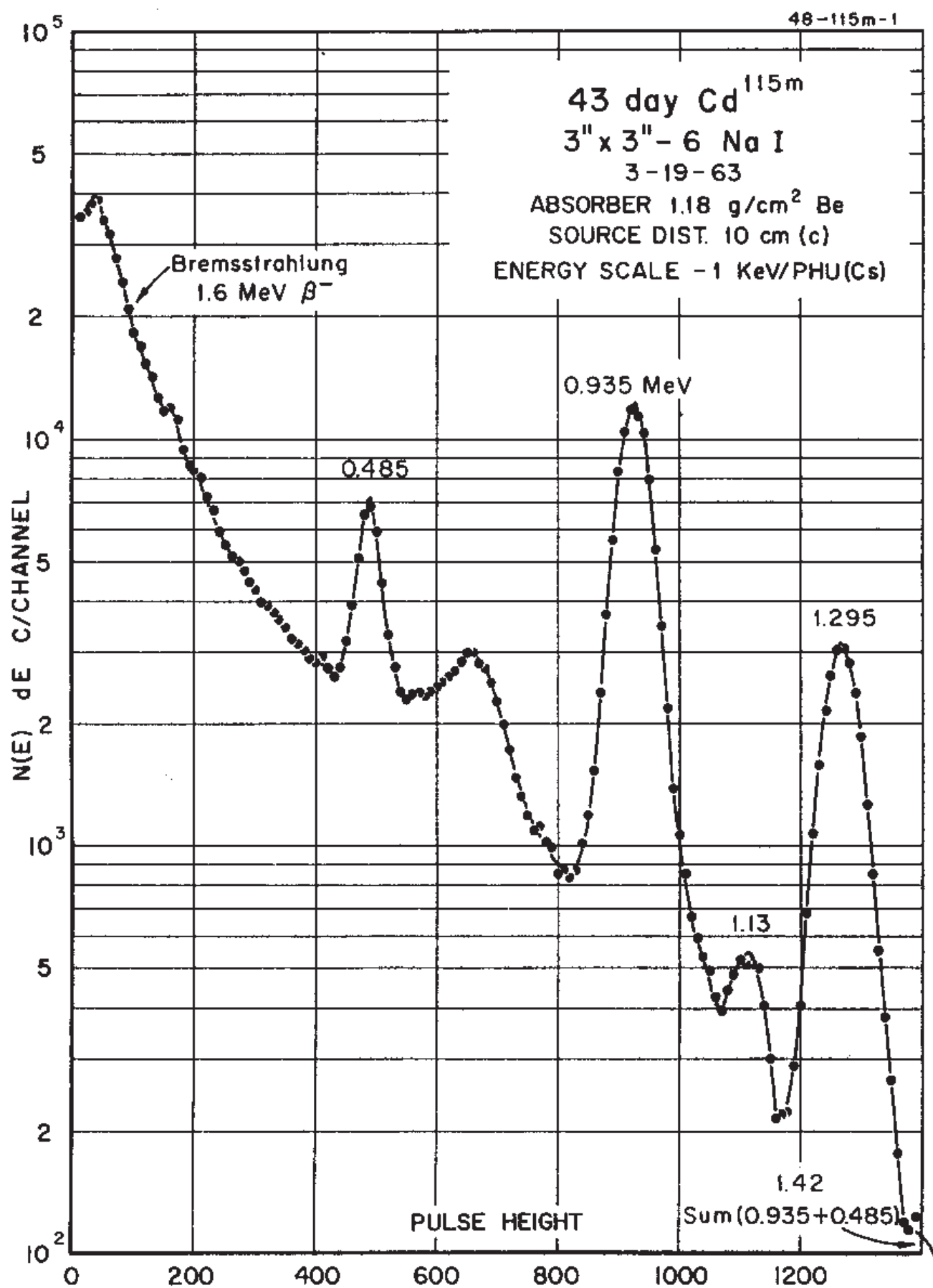
GAMMA-RAY ENERGIES AND INTENSITIES

48-109-1

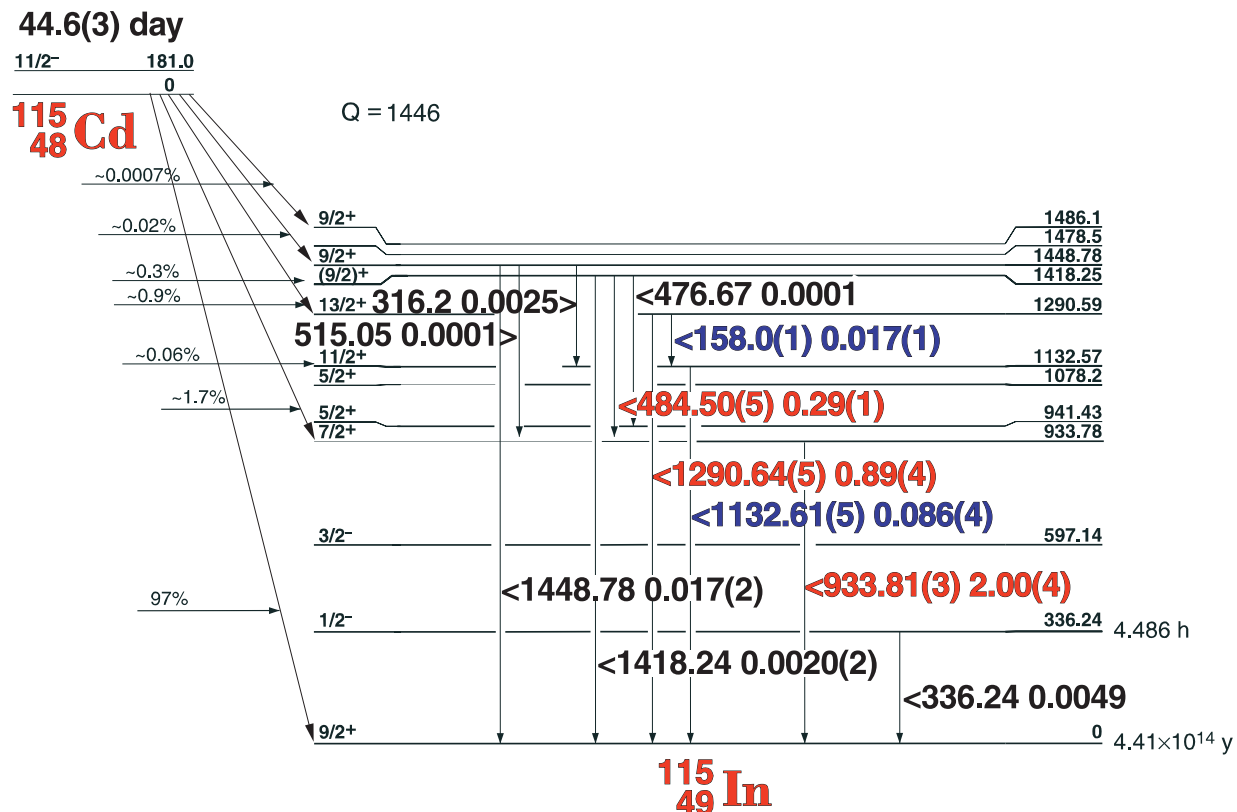
Nuclide ^{109}Cd Half Life 462.6(4) day
 Detector 3" x 3" -2 Nal Method of Production: $^{108}\text{Cd}(n,\gamma)$

	E_γ (KeV)[S]	ΔE_γ	I_γ (rel)	$I_\gamma(\%)$ [E]	ΔI_γ	S
X	Ag K x-ray! 88.036	± 0.008	100	3.6	± 0.1	1 1

44.6(3) day ^{115m}Cd



44.6(3) day ^{115m}Cd Decay Scheme



48-115m-1

GAMMA-RAY ENERGIES AND INTENSITIES

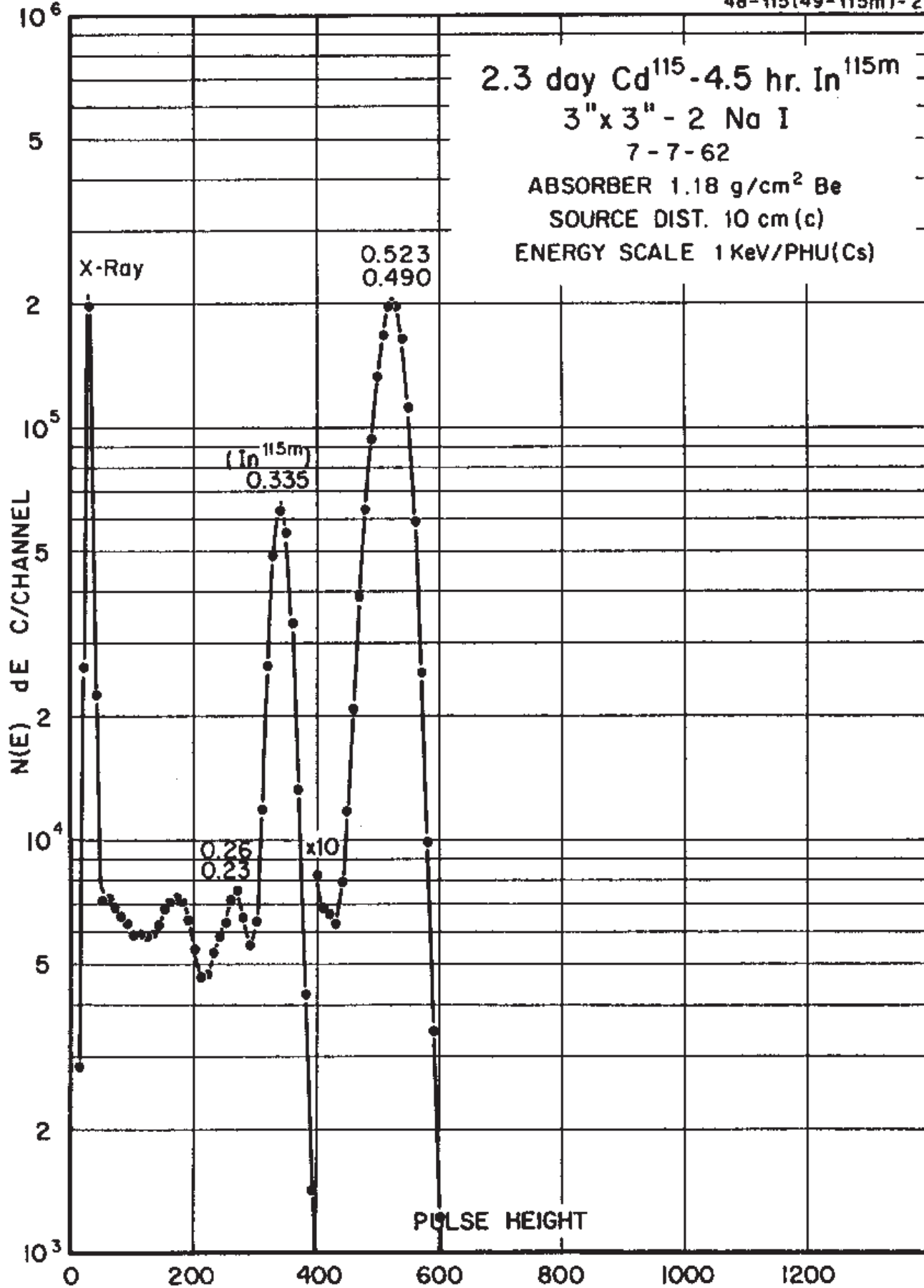
Nuclide **^{85}Kr**
Detector 3" x 3" -2 NaI

Half Life 44.6(3) day
Method of Production: $^{114}\text{Cd}(\text{n},\gamma)$

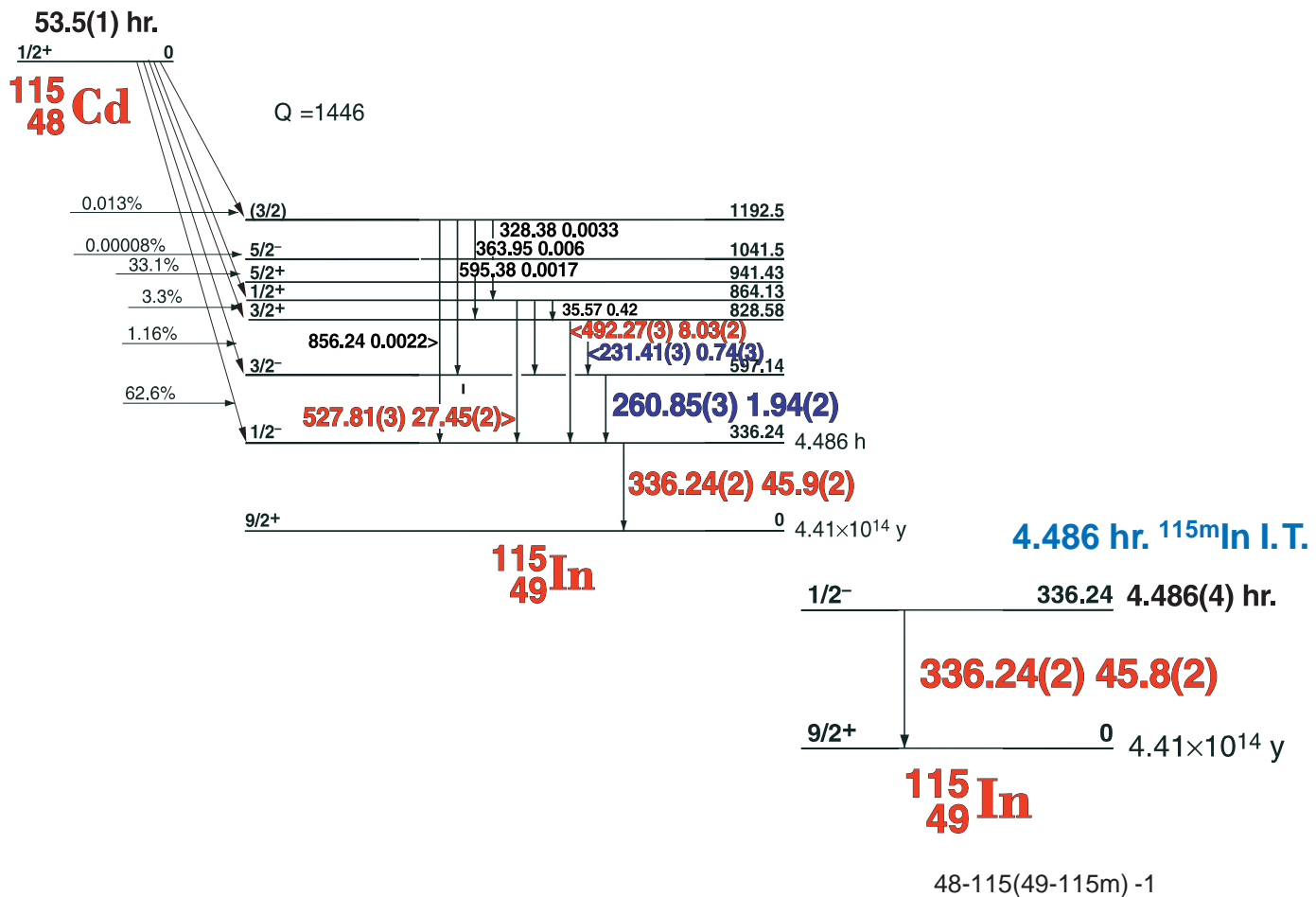
E_{γ} (KeV)[S]	ΔE_{γ}	$I_{\gamma}(\text{rel})$	$I_{\gamma}(\%)[E]$	ΔI_{γ}	S
158.0	± 0.1	1.44	0.017	$\pm (1)$	4
484.50	± 0.05	16.4	0.29	± 0.01	1
933.808	± 0.035	100	2.00	± 0.04	1
1132.608	± 0.050	4.79	0.086	$+ (4)$	3
1290.637	± 0.050	42.9	0.89	± 0.04	1

53.5(1) hr. ^{115}Cd - 4.486(4) $^{115\text{m}}\text{In}$

48-115(49-115m)-2



53.5(1) hr. ^{115}Cd - 4.486(4) hr. $^{115\text{m}}\text{In}$ Decay Schemes

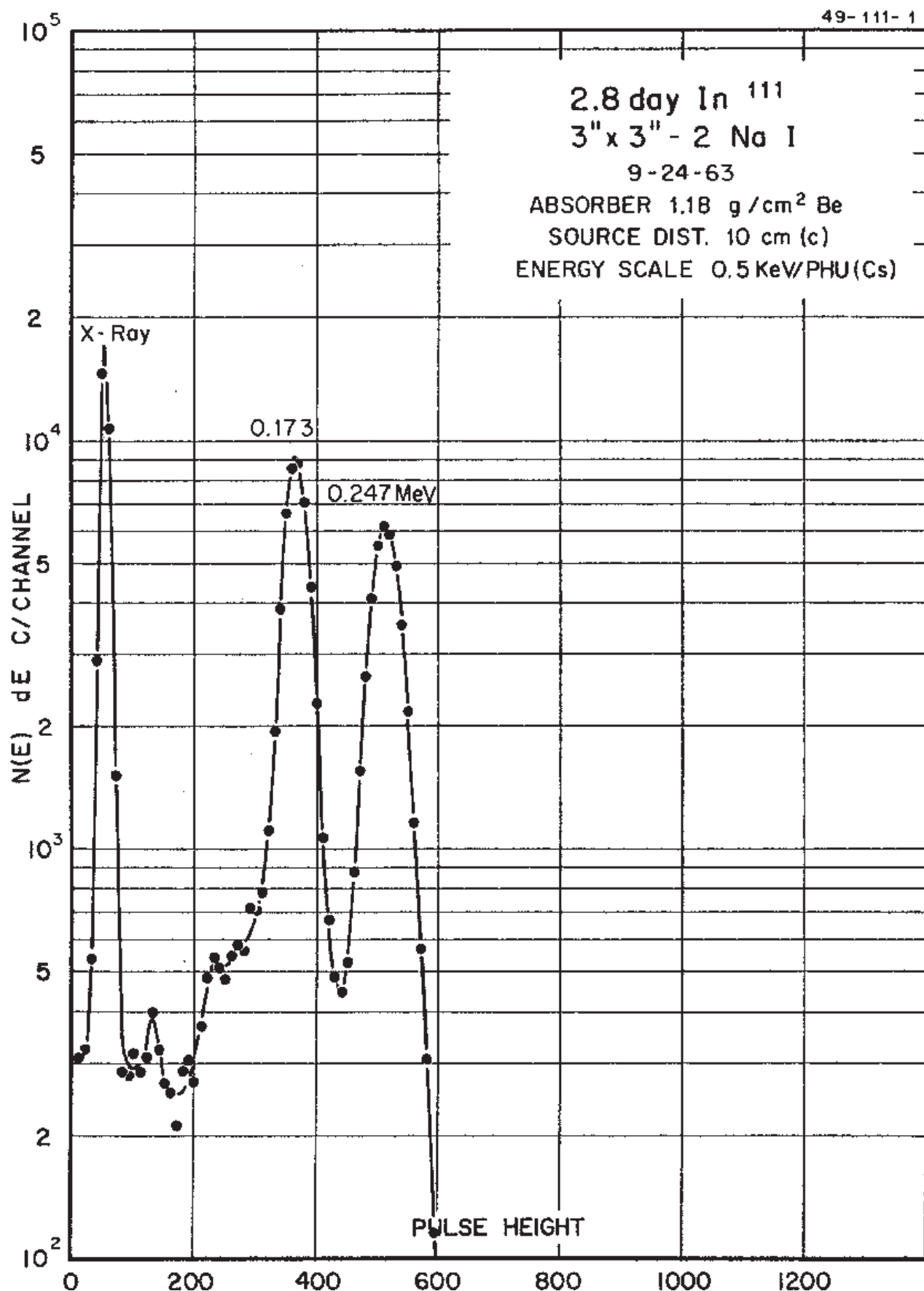


GAMMA-RAY ENERGIES AND INTENSITIES

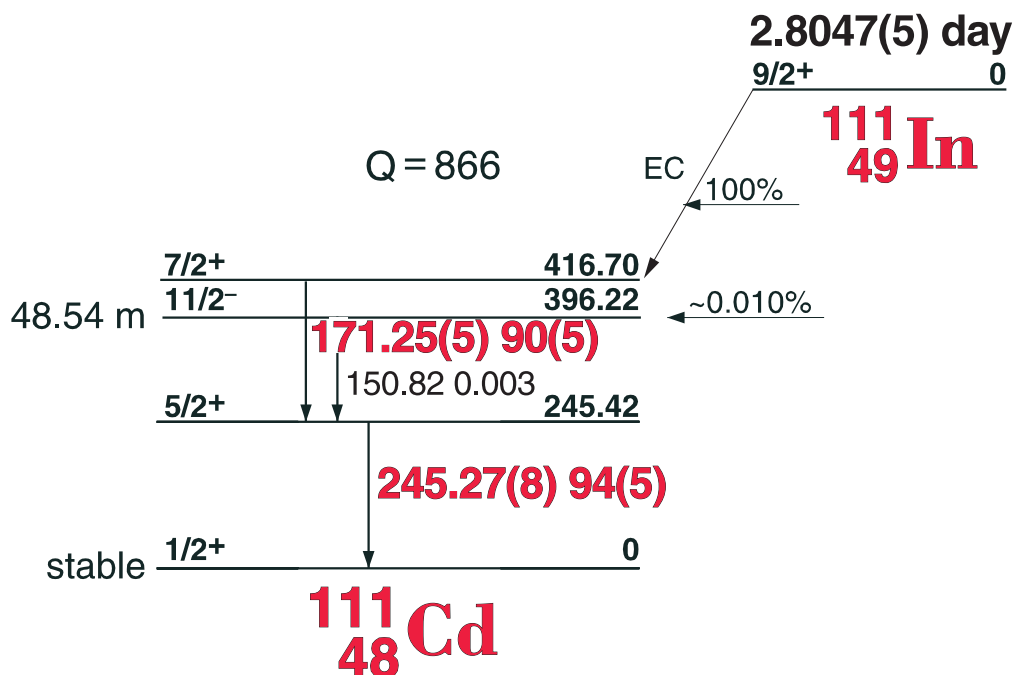
Nuclide **$^{115}\text{Cd} - ^{115\text{m}}\text{In}$** Half Life 53.5(1) hr. - 4.486(4) hr.
Detector 3" x 3" -2 Nal Method of Production: $^{114}\text{Cd}(n,\gamma)$

E_{γ} (KeV)[S]	ΔE_{γ}	$I_{\gamma}(\text{rel})$	$I_{\gamma}(\%)[E]$	ΔI_{γ}	S
231.41	± 0.03	1.40	0.74	± 0.03	3
260.85	± 0.06	3.86	1.94	± 0.02	2
266.90	± 0.08	0.18		± 0.01	4
336.241	± 0.025	100	45.9	± 0.2	1
492.274	± 0.035	16.98	8.09	± 0.02	1
497.08	± 0.1	0.09		± 0.01	4
527.807	± 0.035	58.01	27.45	± 0.02	1

2.8047(5) day ^{111}In



2.8047(5) day ^{111}In Decay Scheme



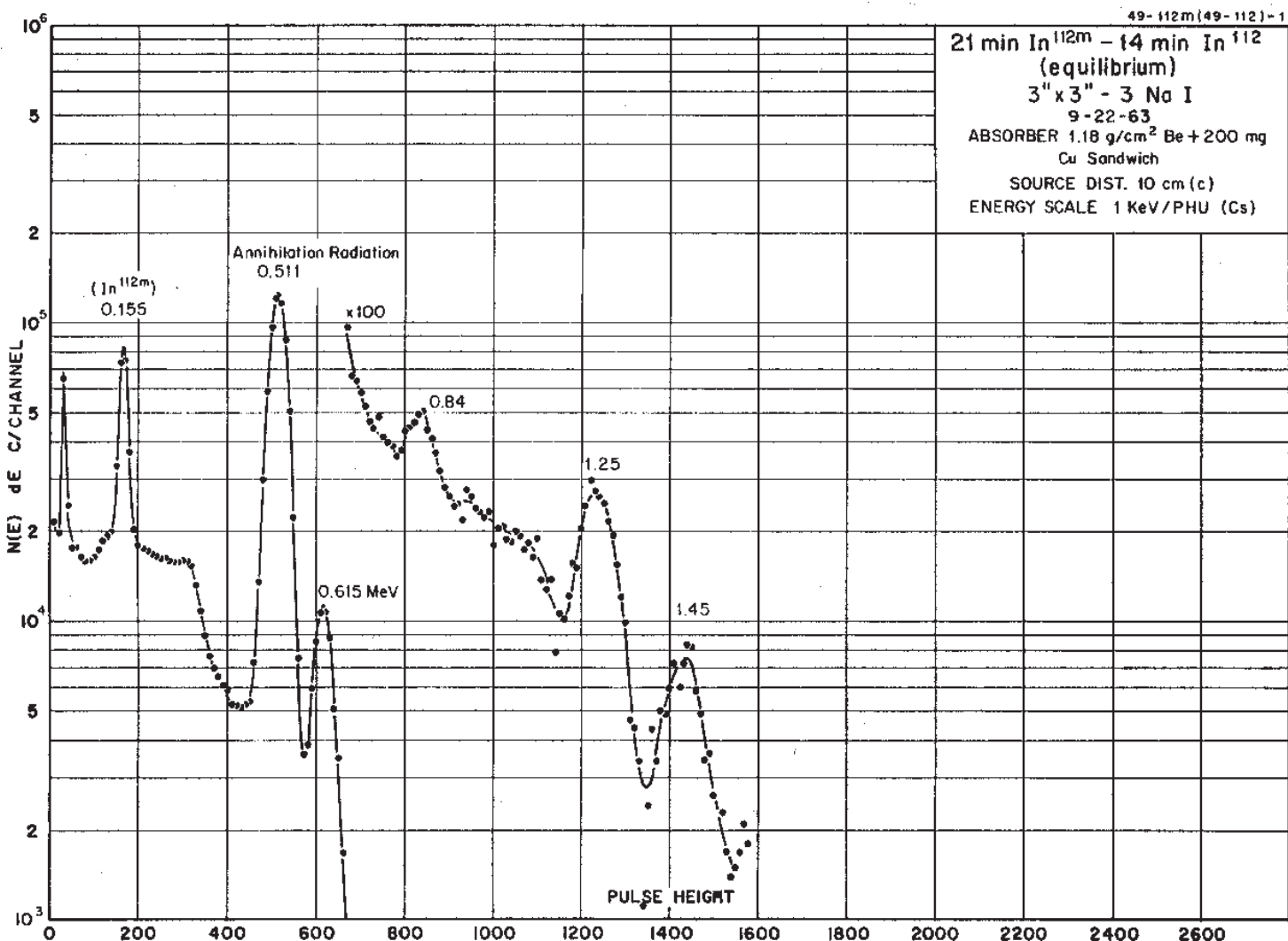
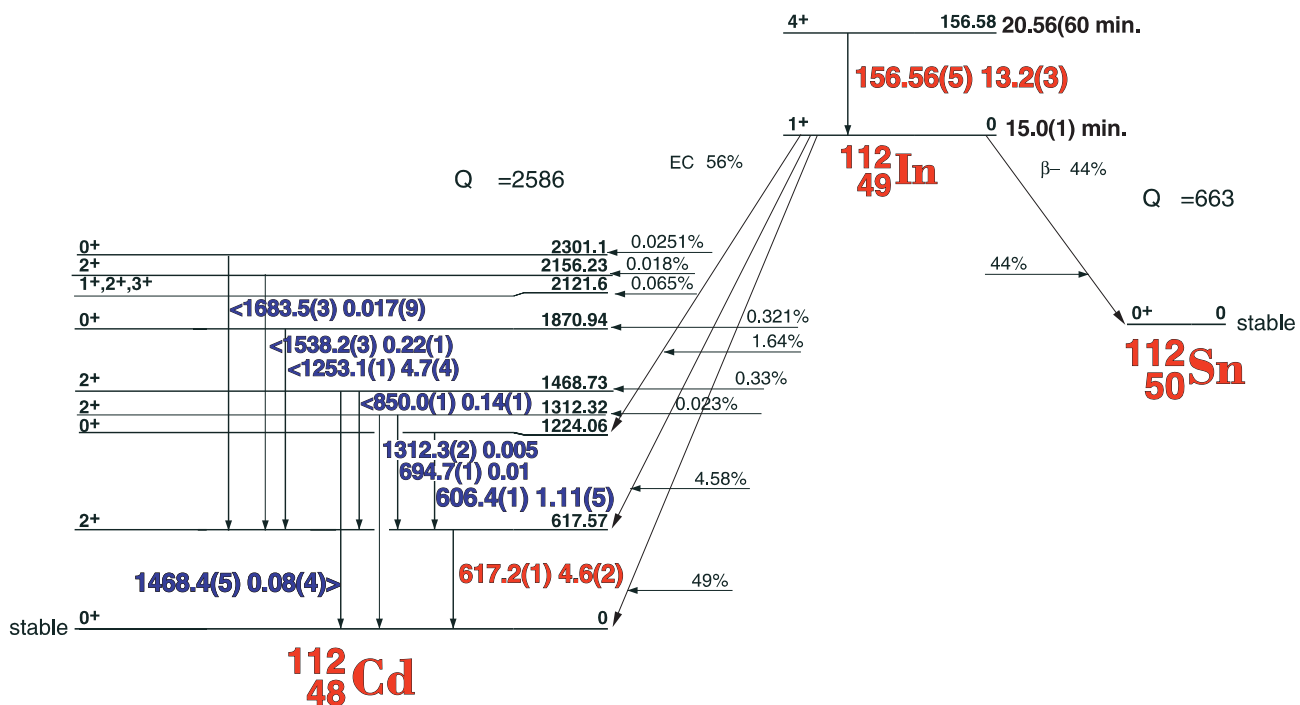
49-111-1

GAMMA-RAY ENERGIES AND INTENSITIES

Nuclide **^{111}In** Half Life **2.8047(50) day**
 Detector **3" x 3" -2 Nal** Method of Production: $^{113}\text{In}(\gamma, 2n)$

E_γ (KeV)[S]	ΔE_γ	I_γ (rel)	$I_\gamma(\%)$ [E]	ΔI_γ	S
171.20	± 0.05	100	90	± 5.0	1
245.27	± 0.08	93.0	94	± 5.0	1

20.56(6) min. ^{112m}In - 15.0(1) min ^{112}In



Decay Data

← Index →

20.56(6) min. ^{112m}In - 15.0(1) min ^{112}In

List of Gamma-ray Energies and Intensities

49-112m(49-112) -1

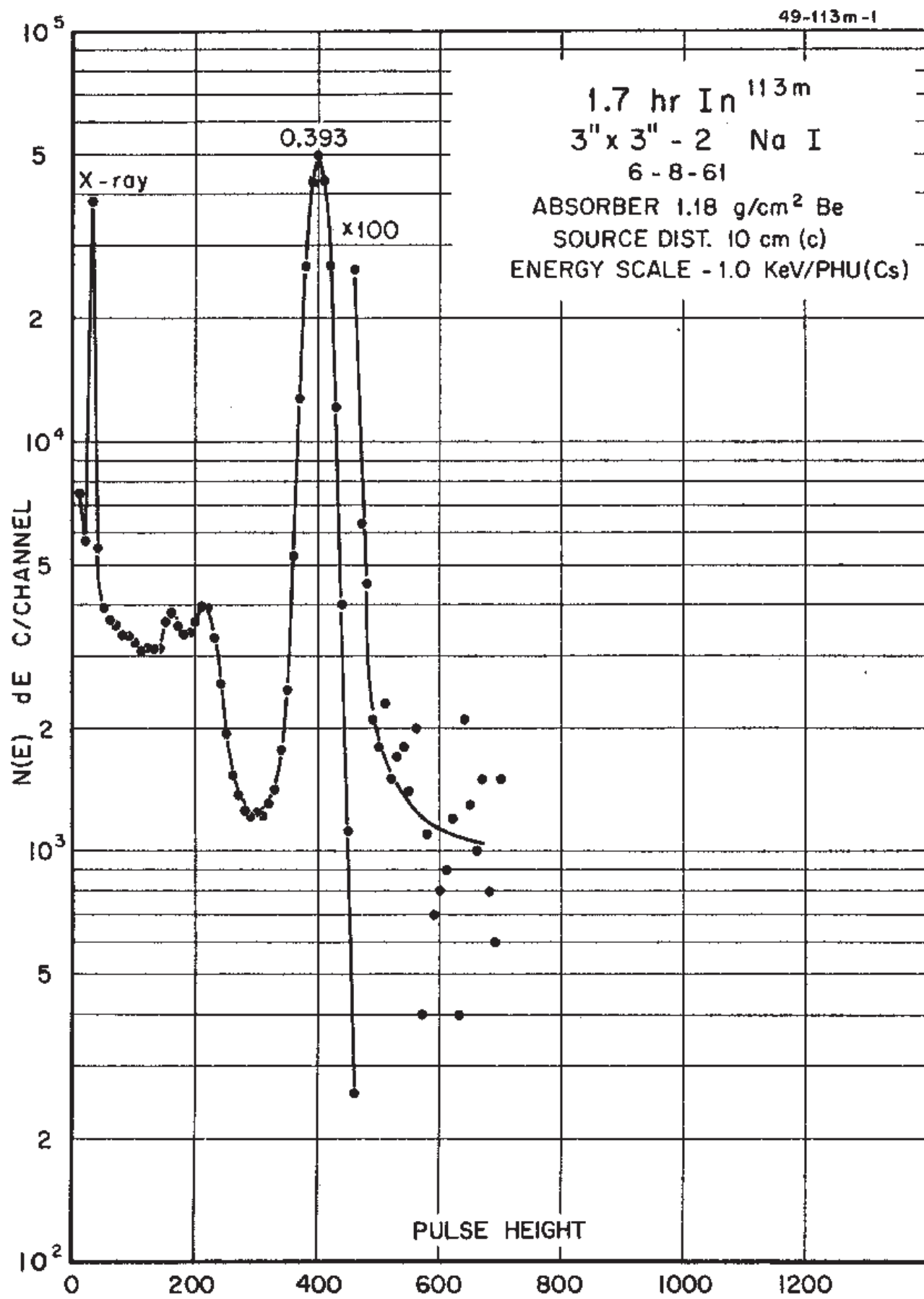
GAMMA-RAY ENERGIES AND INTENSITIES

Nuclide $^{112m}\text{In} - ^{112}\text{In}$
Detector 3" X 3" NaI-2

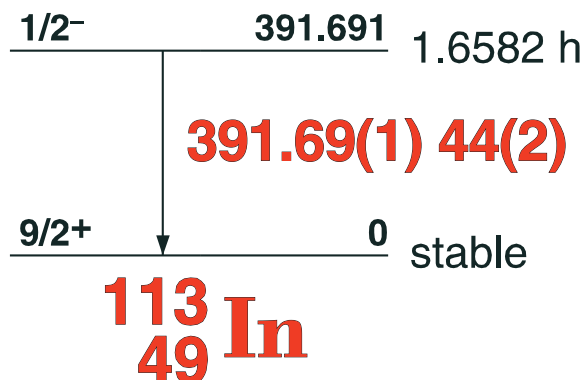
Half Life 20.56(6) min - 15.0(1) min.
Method of Production: $^{113}\text{In}(\gamma, n)$

	E_{γ} (KeV)[S]	ΔE_{γ}	$I_{\gamma}(\text{rel})$	$I_{\gamma}(\%)[E]$	ΔI_{γ}	S
$^{112m}\text{In IT}$	156.56	± 0.05	100	13.2	± 0.3	1
^{112}In	In K x-ray					
	606.4	± 0.1		1.11	± 0.05	3
	617.2	± 0.1		4.6	± 0.2	2
	694.7	± 0.1		0.01	± 0.004	4
	850.0	± 0.1		0.14	± 0.02	3
	1253.1	± 0.1		4.7	± 0.4	2
	1312.3	± 0.2		0.005	± 0.001	2
	1468.4	± 0.5		0.08	± 0.04	3
	1538.2	± 0.3		0.22	± 0.01	2
	1683.5	± 0.3		0.017	± 0.009	3

1.6582(6) hr. ^{113m}In



1.6582(6) hr. ^{113m}In



49-113m-1

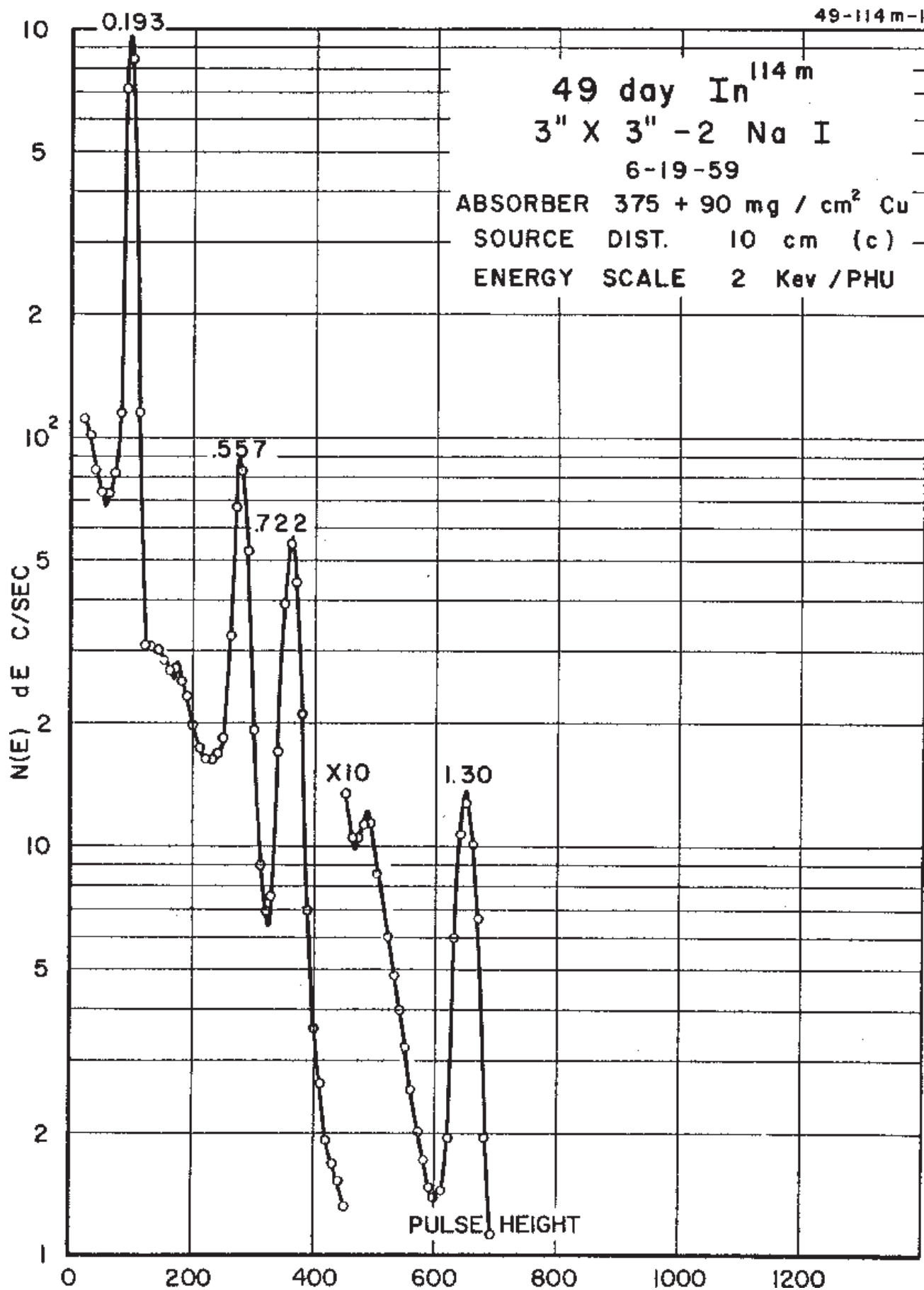
GAMMA-RAY ENERGIES AND INTENSITIES

Nuclide ^{113m}In
Detector 3" X 3" NaI-2

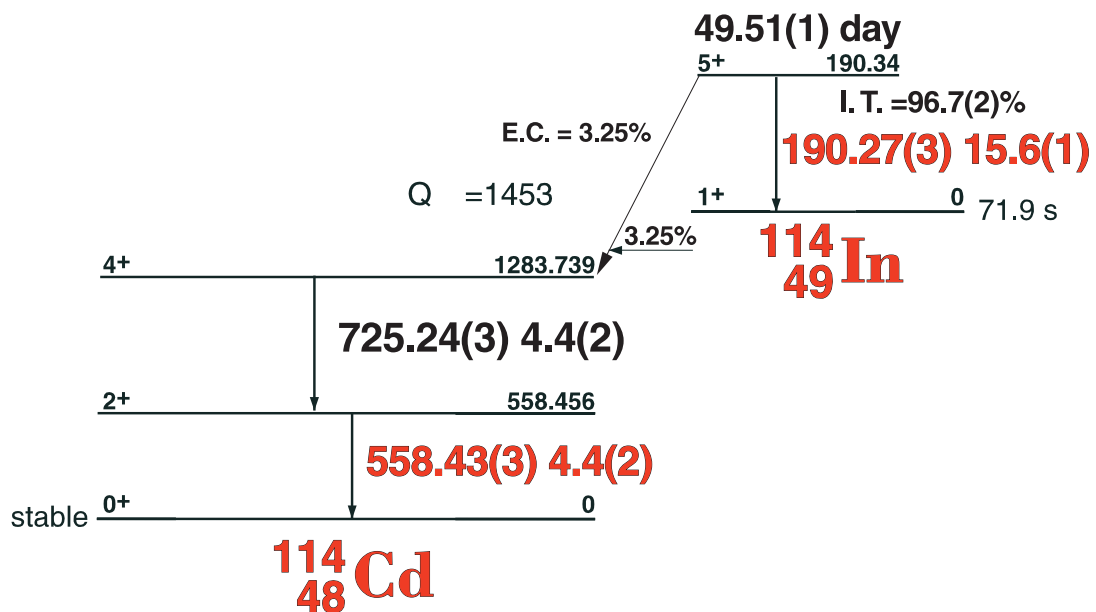
Half Life 1.6582(6) hr.
Method of Production: $^{112}\text{Sn}(n,\gamma,\beta)$

E_{γ} (KeV)[S]	ΔE_{γ}	$I_{\gamma}(\text{rel})$	$I_{\gamma}(\%)[E]$	ΔI_{γ}	S
391.69	± 0.01	100	44	± 2.0	1

49.51(1) day ^{114m}In



49.51(1) day ^{114m}In



49-114m-1

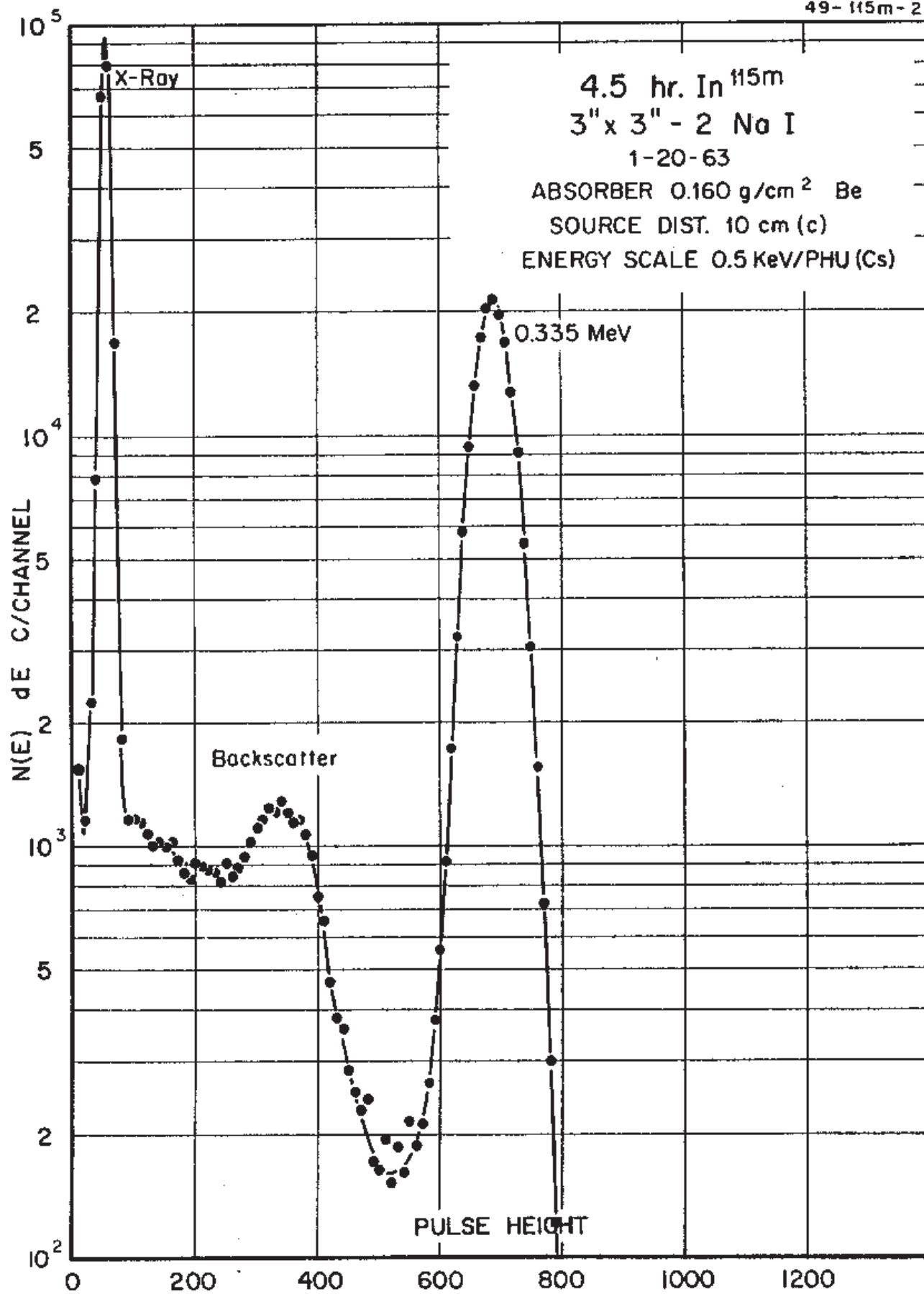
GAMMA-RAY ENERGIES AND INTENSITIES

Nuclide ^{114m}In
Detector 3" x 3" -2 NaI
Half Life 49.51(10 day)
Method of Production: $^{113}\text{In}(n,\gamma)$

	E_{γ} (KeV)[S]	ΔE_{γ}	$I_{\gamma}(\text{rel})$	$I_{\gamma}(\%)[\text{E}]$	ΔI_{γ}	S
^{114m}In	190.274	± 0.030	100	15.8	± 0.1	1
	558.430	± 0.030	28.5	4.4	± 0.2	1
	725.238	± 0.030	28.1	4.4	± 0.2	1

49.51(1) day ^{115m}In

49- 115m - 2



4.486(4) hr. ^{115m}In



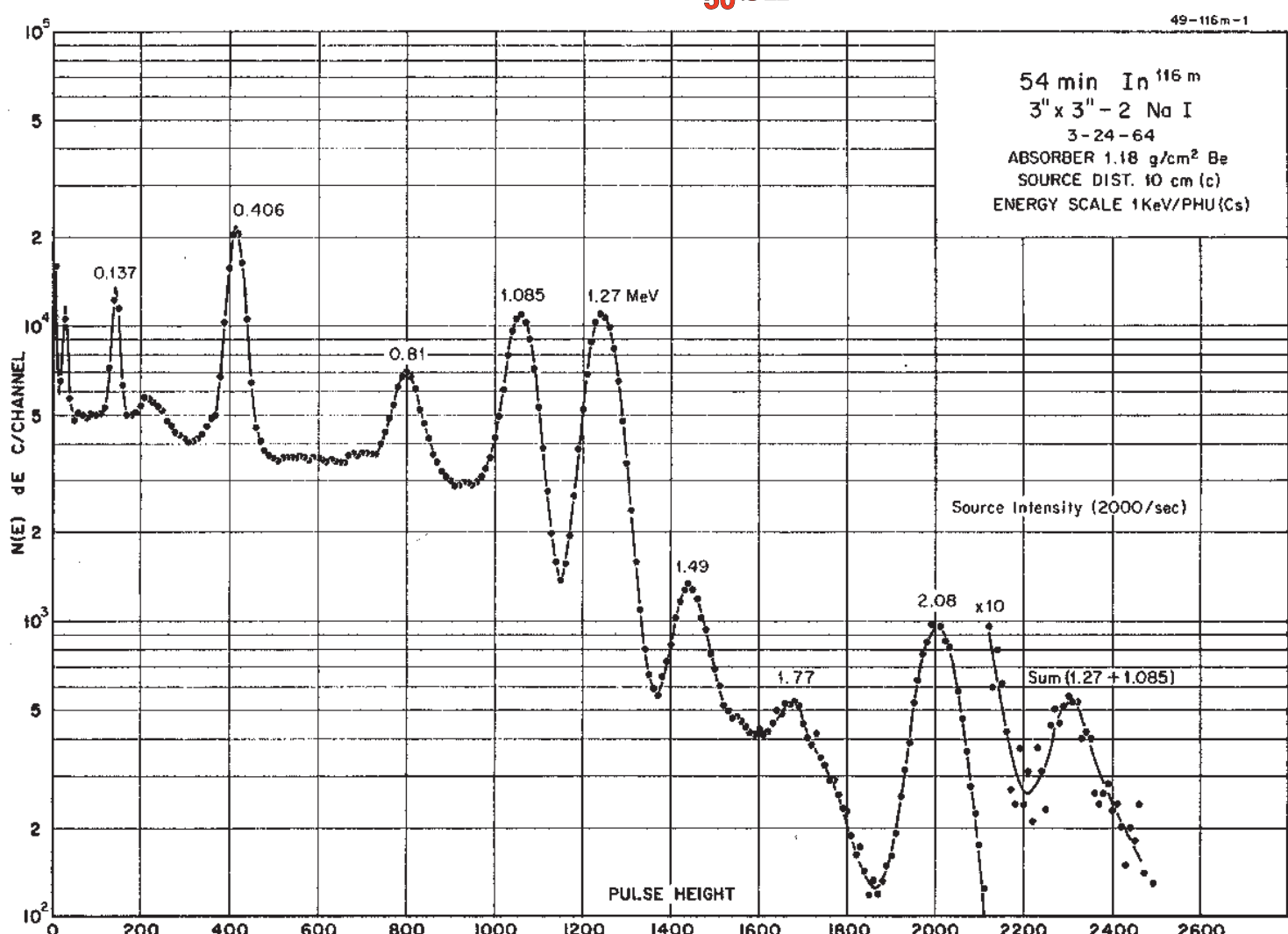
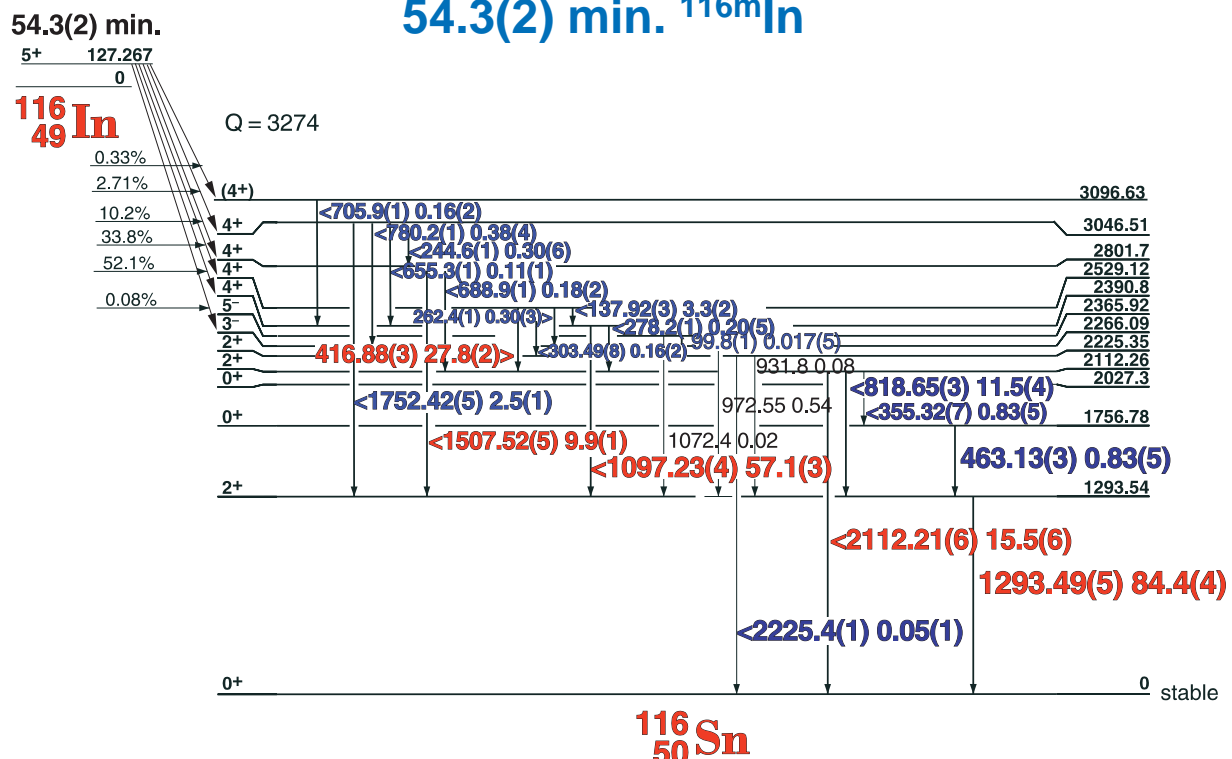
49-115m-1

GAMMA-RAY ENERGIES AND INTENSITIES

Nuclide ^{115m}In Half Life 4.486(4) hr.
 Detector 3" x 3" -2 NaI Method of Production: $^{114}\text{Cd}(n,\gamma,\beta)$

E_γ (KeV)[S]	ΔE_γ	I_γ (rel)	$I_\gamma(\%)$ [E]	ΔI_γ	S
336.24	± 0.02	100	45.8	± 0.2	1

54.3(2) min. ^{116m}In



Decay Data



54.3(2) min. ^{116m}In

49-116m-1

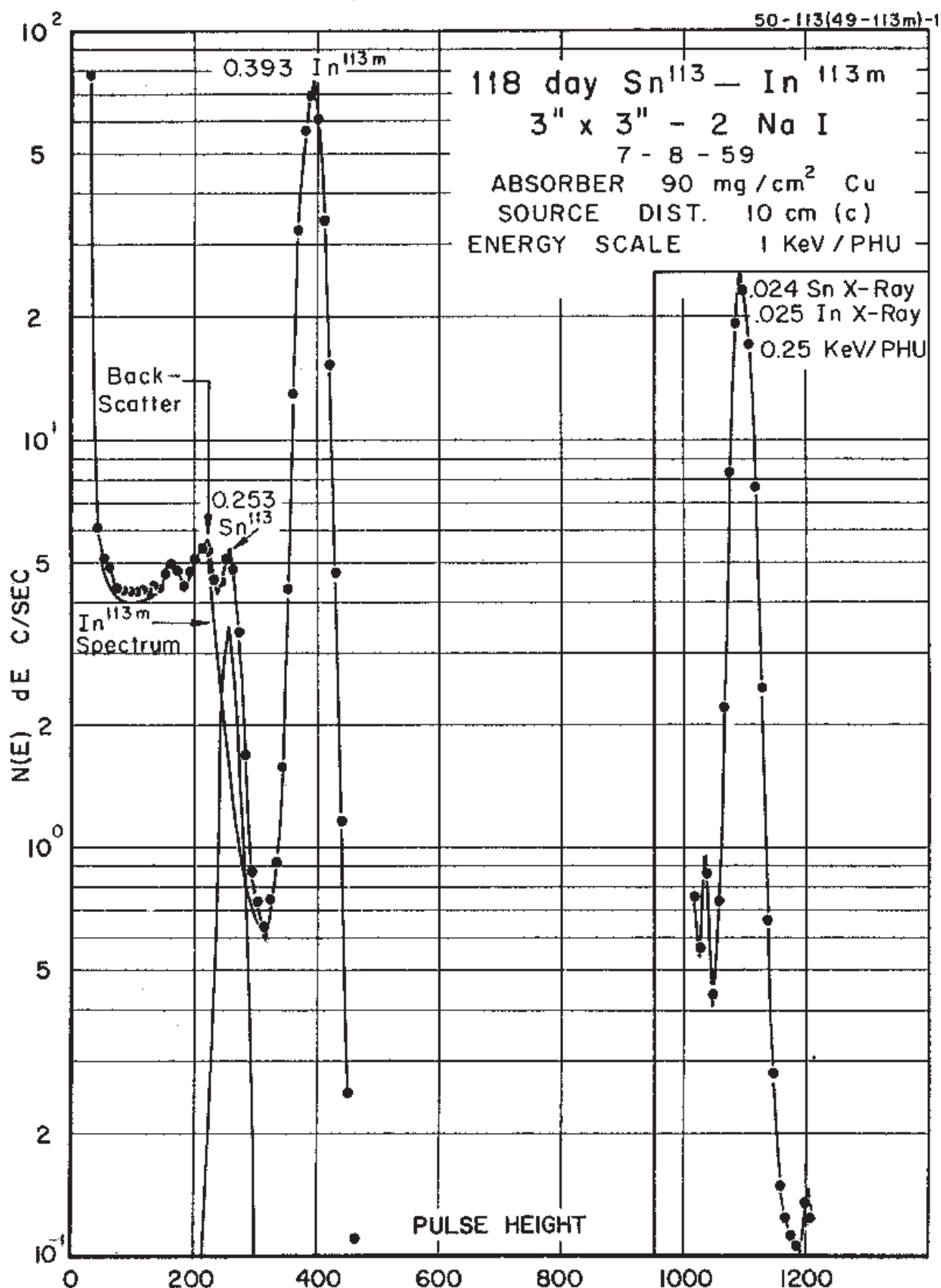
GAMMA-RAY ENERGIES AND INTENSITIES

Nuclide ^{116m}In
 Detector 3" x 3" -2 NaI

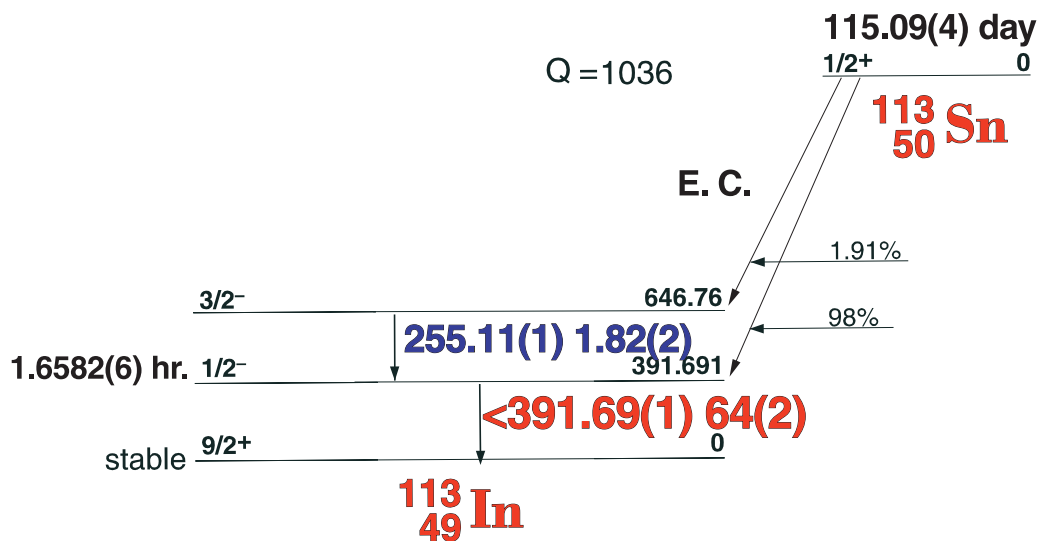
Half Life 54.3(2) min.
 Method of Production: $^{115}\text{In}(\text{n},\gamma)$

E_{γ} (KeV)[S]	ΔE_{γ}	I_{γ} (rel)	$I_{\gamma}(\%)[E]$	ΔI_{γ}	S
99.8	± 0.017		0.017	± 0.005	5
137.916	± 0.030	3.50	3.3	± 0.2	2
244.59	± 0.10	0.38	0.30	± 0.06	4
262.40	± 0.1	0.34	0.12	± 0.01	4
278.20	± 0.1	0.25	0.20	± 0.05	4
303.49	± 0.08	0.22	0.16	± 0.02	4
355.32	± 0.07	0.84	0.83	± 0.05	3
416.88	± 0.03	29.37	27.8	± 0.2	1
463.13	± 0.04	0.83	0.83	± 0.05	3
655.30	± 0.1	0.14	0.11	± 0.01	4
688.94	± 0.1	0.26	0.18	± 0.02	4
705.93	± 0.1	0.20	0.17	± 0.01	4
780.2	± 0.1	0.38	0.04	± 0.02	4
818.65	± 0.03	13.72	11.5	± 0.4	2
SE 972.51	± 0.05	0.63		± 0.06	4
DE 1090.29	± 0.06	2.0		± 0.2	4
	1097.23	± 0.04	67.91	57.1	1
	1293.49	± 0.05	100	84.4	1
	1507.52	± 0.05	11.86	9.9	1
SE 1601.12	± 0.06	1.07		± 0.1	3
	1752.42	± 0.05	2.89	2.5	2
	2112.21	± 0.06	18.58	15.5	1
2225.41	± 0.10	0.06	0.05	± 0.01	3

115.09(40 day ^{113}Sn - 1.6582(6) hr. ^{113m}In



115.09(4) day ^{113}Sn - 1.6582(6) hr. $^{113\text{m}}\text{In}$



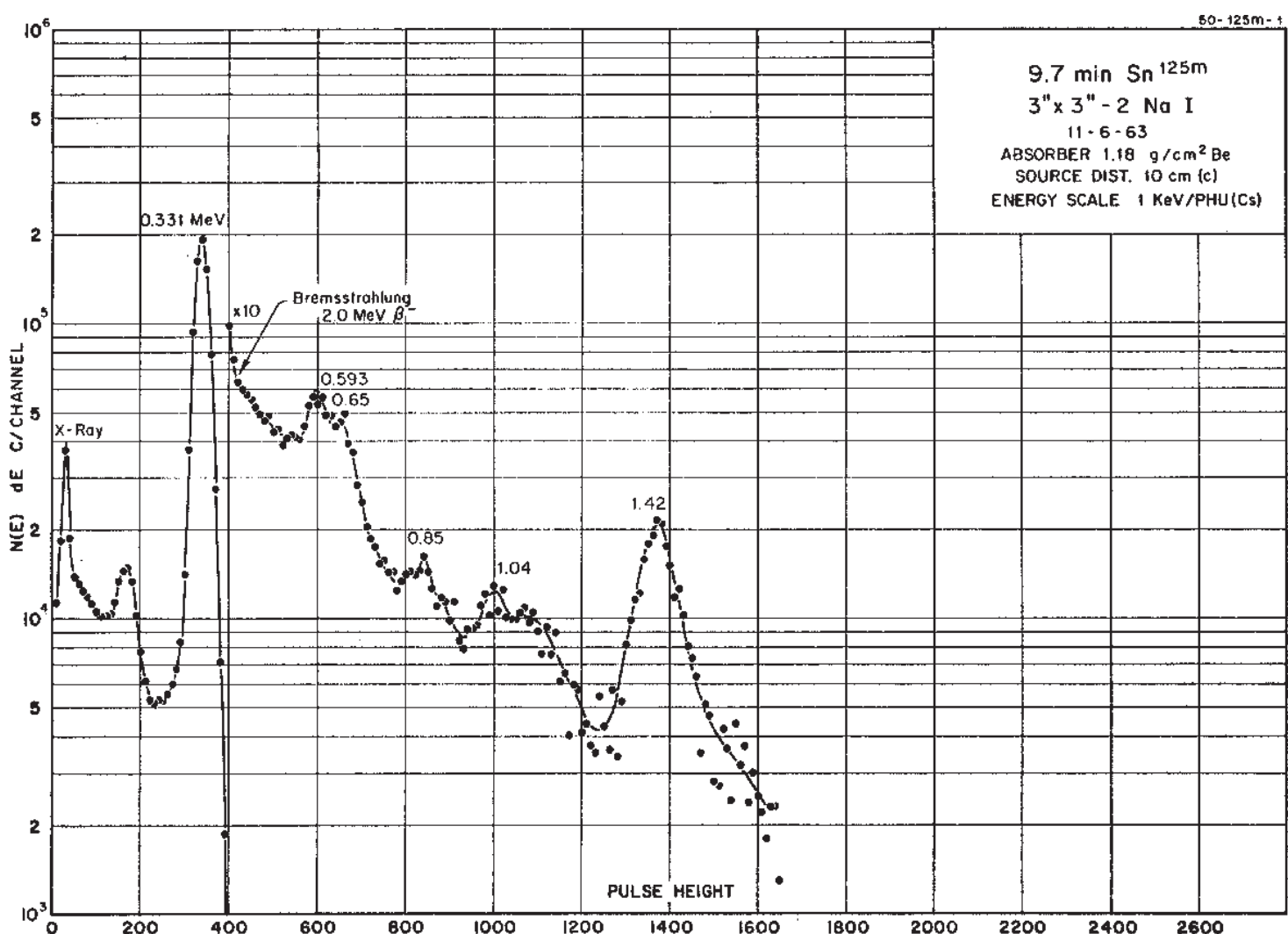
50-113(49-113m)-1

GAMMA-RAY ENERGIES AND INTENSITIES

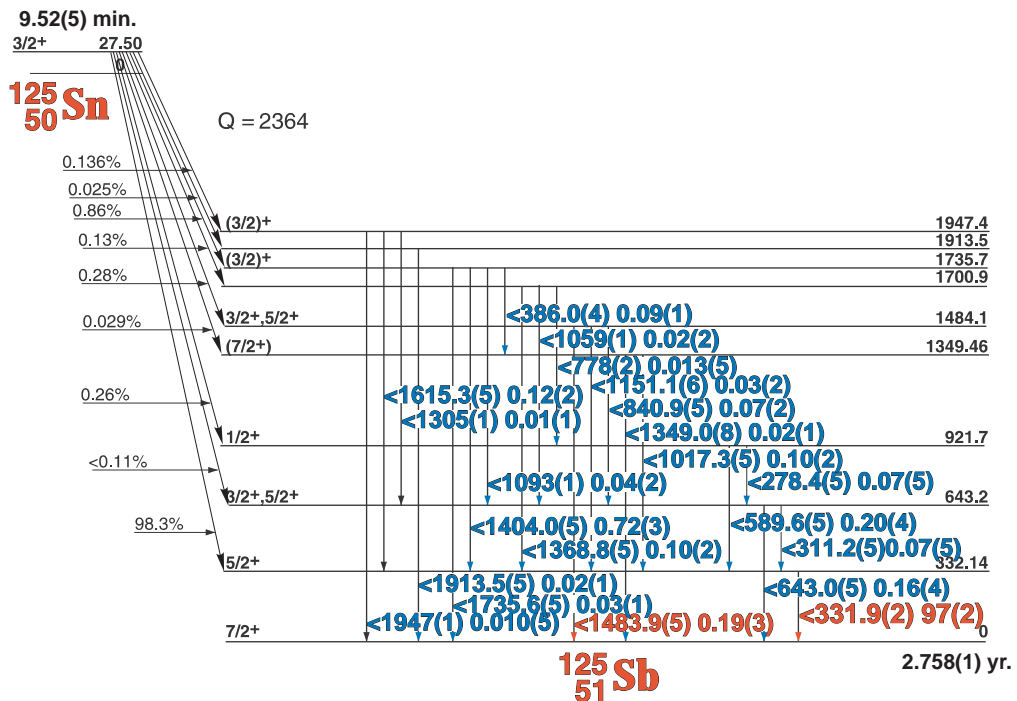
Nuclide $^{87\text{m}}\text{Sr}$ Half Life 115.09(4) 1.6582(6) hr.
 Detector 3" x 3" -2 Nal Method of Production: $\text{S}^{112}\text{Sn}(n,\gamma)$

E_γ (KeV)[S]	ΔE_γ	I_γ (rel)	$I_\gamma(\%)$ [E]	ΔI_γ	S
255.115	± 0.015	3.44	1.82	± 0.02	3
$^{113\text{m}}\text{In}$ 391.688	± 0.010	100	64	± 2.0	1

9.52(5) min. ^{125m}Sn



9.52(5) min. ^{125m}Sn

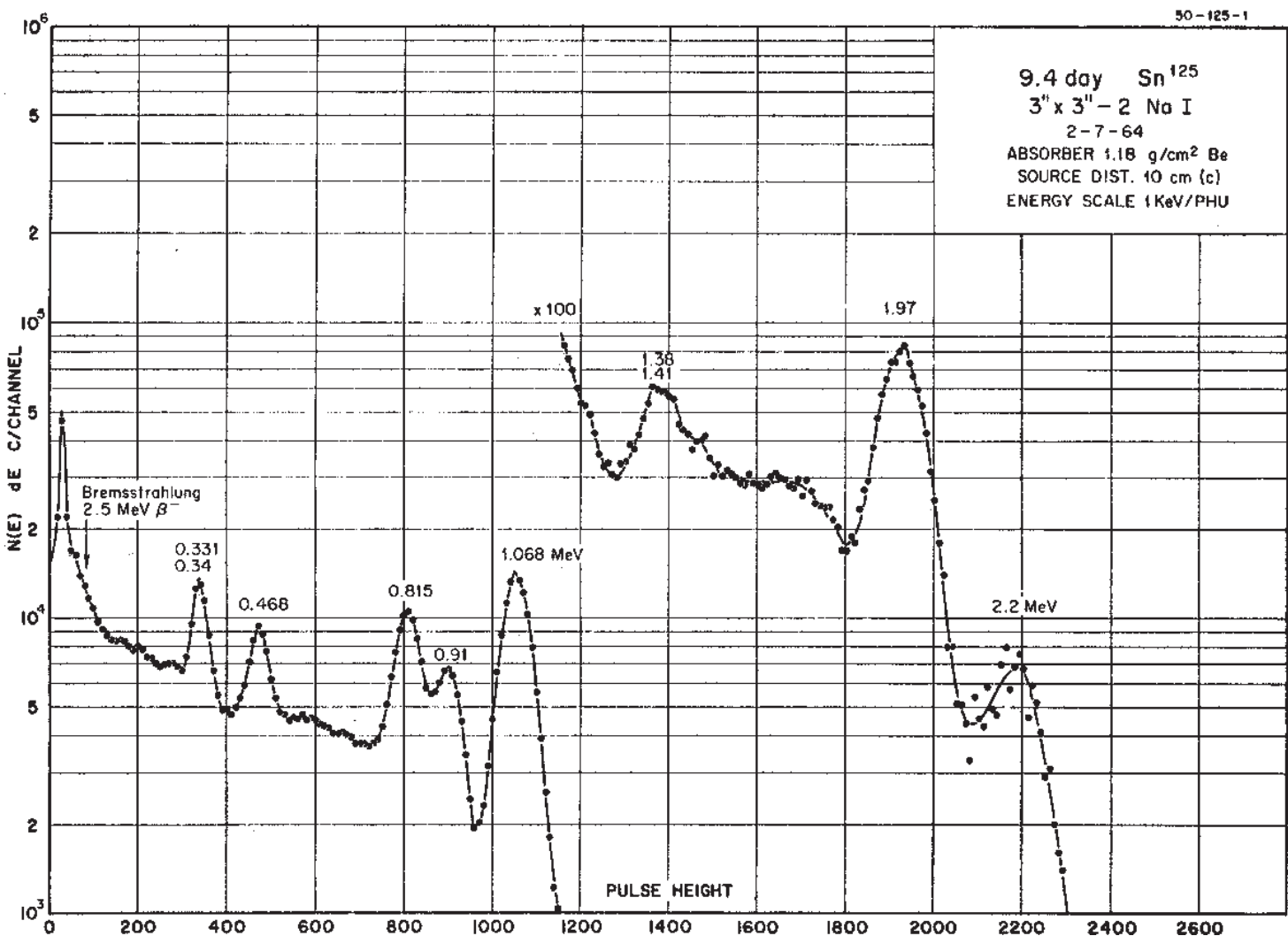
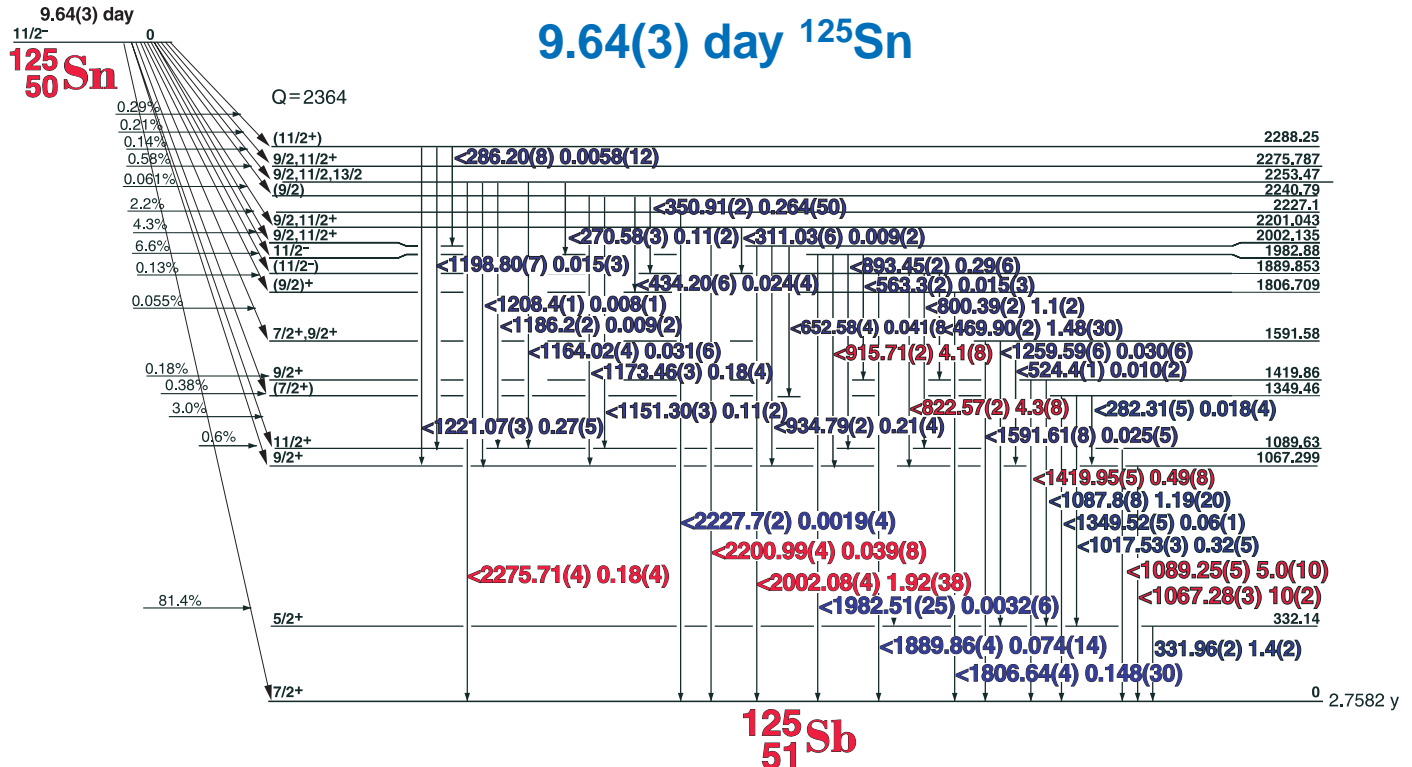


50-113(49-113m)-1

GAMMA-RAY ENERGIES AND INTENSITIES

Nuclide ^{125m}Sn Half Life 9.52(5) min.hr.
 Detector 3" x 3" -2 NaI Method of Production: $^{124}\text{Sn}(n,\gamma)$

E_{γ} (KeV)[S]	ΔE_{γ}	$I_{\gamma}(\text{rel})$	$I_{\gamma}(\%)[E]$	ΔI_{γ}	S
278.4	± 0.5		0.07	± 0.05	4
311.2	± 0.5		0.07	± 0.05	4
331.9	± 0.2		97	± 2.0	1
386.0	± 0.4		0.09	± 0.01	4
589.6	± 0.5		0.20	± 0.04	3
643.0	± 0.5		0.16	± 0.04	3
778	± 2.0		0.013	± 0.005	4
840.9	± 0.023		0.07	± 0.02	4
1017.3	± 0.5		0.10	± 0.02	3
1059	± 1.0		0.02	± 0.02	4
1093	± 1.0		0.04	± 0.02	4
1151.1	± 0.6		0.03	± 0.02	4
1305	± 1.0		0.01	± 0.01	4
1349.0	± 0.8		0.02	± 0.01	4
1368.8	± 0.5		0.10	± 0.2	3
1404.0	± 0.5		0.72	± 0.03	1
1483.9	± 0.5		0.19	± 0.03	3
1615.3	± 0.5		0.12	± 0.02	3
1735.6	± 0.5		0.03	± 0.01	4
1913.5	± 0.5		0.02	± 0.01	4
1947	± 1.0		0.010	± 0.005	4



9.64(3) day ^{125}Sn

50-113(49-113m)-1

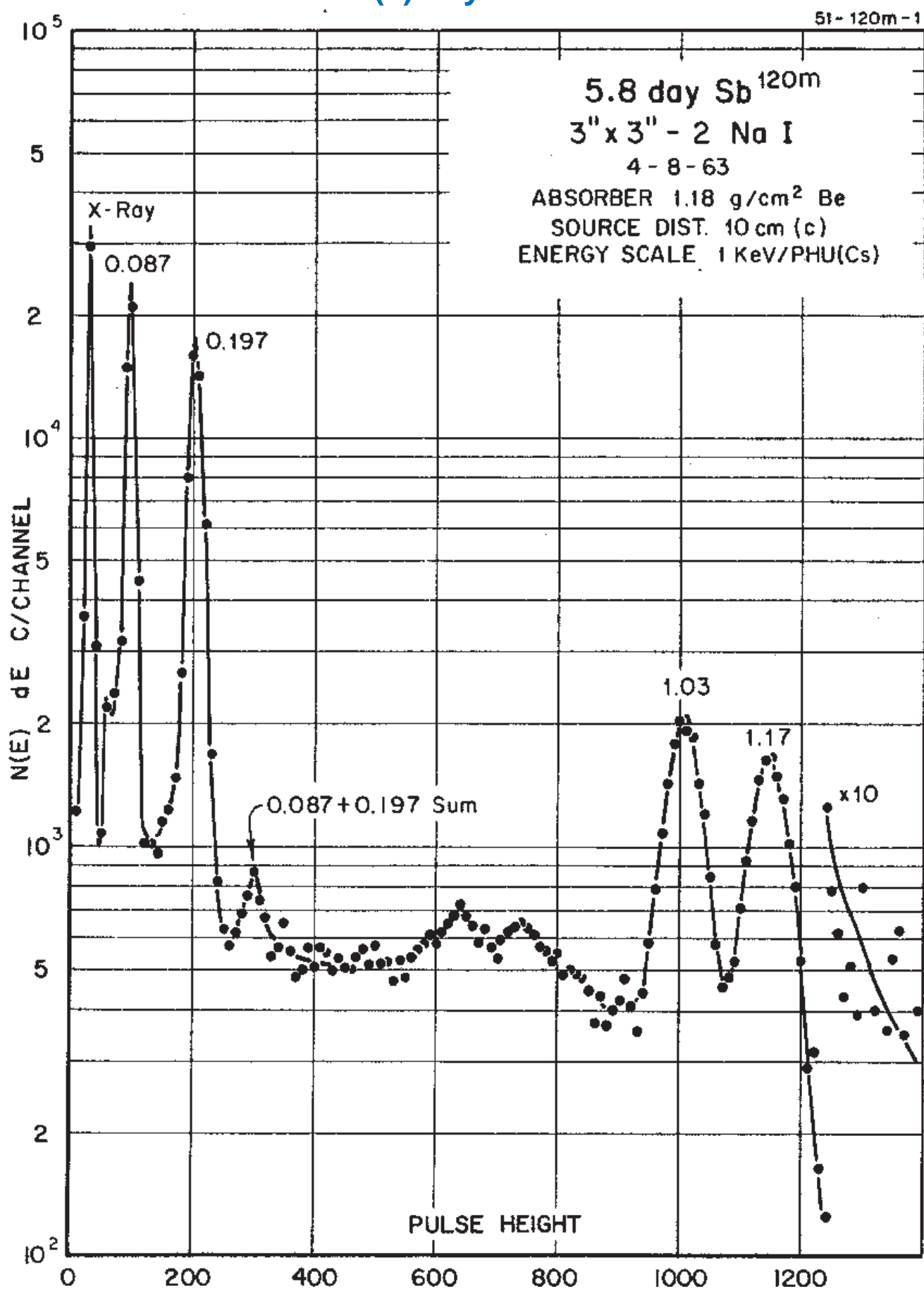
GAMMA-RAY ENERGIES AND INTENSITIES

Nuclide $^{87\text{m}}\text{Sr}$
 Detector 3" x 3" -2 Nal

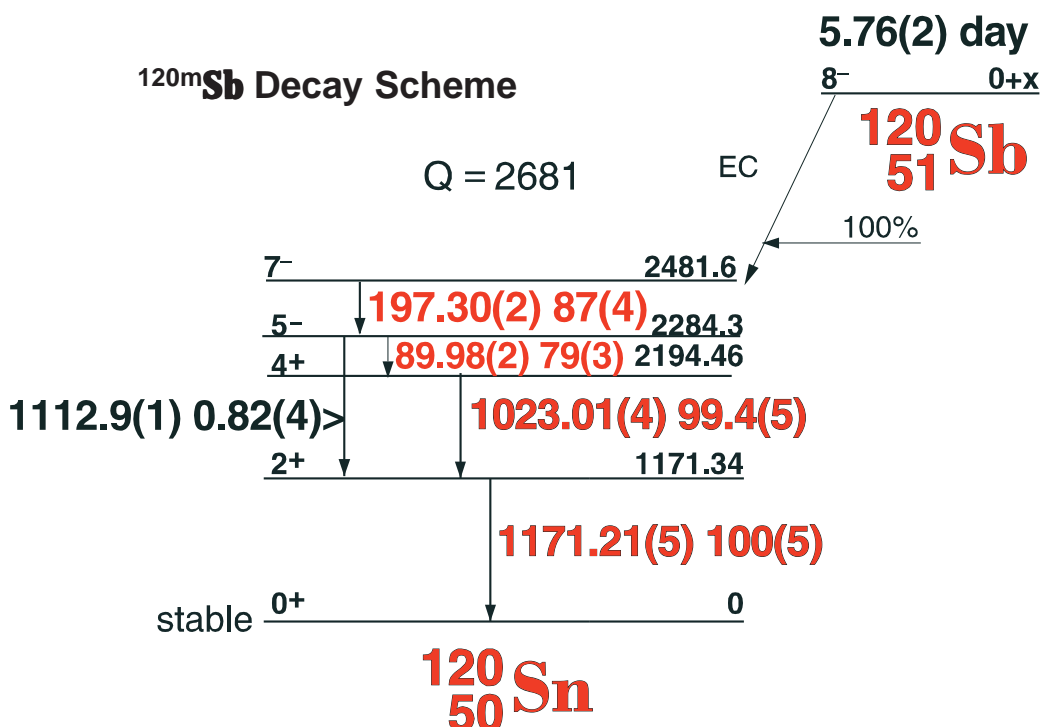
Half Life 115.09(4) 1.6582(6) hr.
 Method of Production: $\text{S}^{112}(\text{n},\gamma)$

	E_{γ} (KeV)[S]	ΔE_{γ}	I_{γ} (rel)	$I_{\gamma}(\%)$ [E]	ΔI_{γ}	S		E_{γ} (KeV)[S]	ΔE_{γ}	I_{γ} (rel)	$I_{\gamma}(\%)$ [E]	ΔI_{γ}	S
SE	234.52	± 0.08	0.34		± 0.05	4		1259.59	± 0.06	0.259	0.030	± 0.006	3
	257.85	± 0.25	0.136	0.014	± 0.002	4		1349.52	± 0.05	0.63	0.06	± 0.01	3
	270.582	± 0.030	0.99	0.11	± 0.02	4		1419.95	± 0.05	5.31	0.49	± 0.08	1
	282.31	± 0.05	0.150	0.018	± 0.012	4		1491.0					3
	286.20	± 0.08	0.057	0.0058	± 0.001	4		1591.61	± 0.08	0.169	0.025	± 0.005	4
	311.03	± 0.06	0.095	0.009	± 0.001	4		1806.64	± 0.04	1.73	0.148	± 0.03	2
	331.964	± 0.020	13.9	1.4	± 0.2	2		1889.865	± 0.04	1.00	0.074	± 0.01	2
	350.91	± 0.023	2.73	0.264	± 0.05	3		1982.51	± 0.25	0.081	0.0032	$\pm 0.(6)$	4
	434.20	± 0.06	0.303	0.024	± 0.004	4		2002.082	± 0.038	22.1	1.92	± 0.38	1
	469.899	± 0.020	15.2	1.48	± 0.3	1		2200.99	± 0.04	0.46	0.039	± 0.008	1
	524.37	± 0.12	0.10	0.010	± 0.018	4		2227.68	± 0.20	0.015	0.0019	$\pm 0.(4)$	4
	563.27	± 0.25	0.07	0.015	± 0.003	4		2275.71	± 0.04	2.10	0.18	± 0.04	1
	652.585	± 0.038	0.44	0.041	± 0.008	4							
	800.386	± 0.024	11.4	1.1	± 0.2	3							
	822.568	± 0.024	45.0	4.3	± 0.8	1							
	893.454	± 0.025	3.42	0.29	± 0.06	3							
	915.714	± 0.024	43.1	4.1	± 0.8	1							
	921.598	± 0.038	1.25		± 0.08	4							
DE	934.790	± 0.025	2.54	0.21	± 0.04	3							
	980.24	± 0.032				3							
	1017.528	± 0.030	3.36	0.32	± 0.05	3							
	1067.284	± 0.030	100	10	± 2.0	1							
	1089.25	± 0.05	59.8	5.0	± 1.0	1							
	1151.296	± 0.030	1.22	0.11	± 0.02	3							
	1164.025	± 0.040	0.32	0.031	± 0.006	4							
	1173.461	± 0.035	1.71	0.18	± 0.04	3							
	1186.17	± 0.18	0.078	0.009	± 0.002	4							
	1198.80	± 0.07	0.220	0.015	± 0.003	4							
DE	1208.37	± 0.15	0.104	0.008	± 0.001	4							
	1221.075	± 0.035	2.66	0.27	± 0.05	2							
	1253.82	± 0.06				3							

5.76(2) day ^{120m}Sb



5.76(2) day ^{120m}Sb



51-120m-1

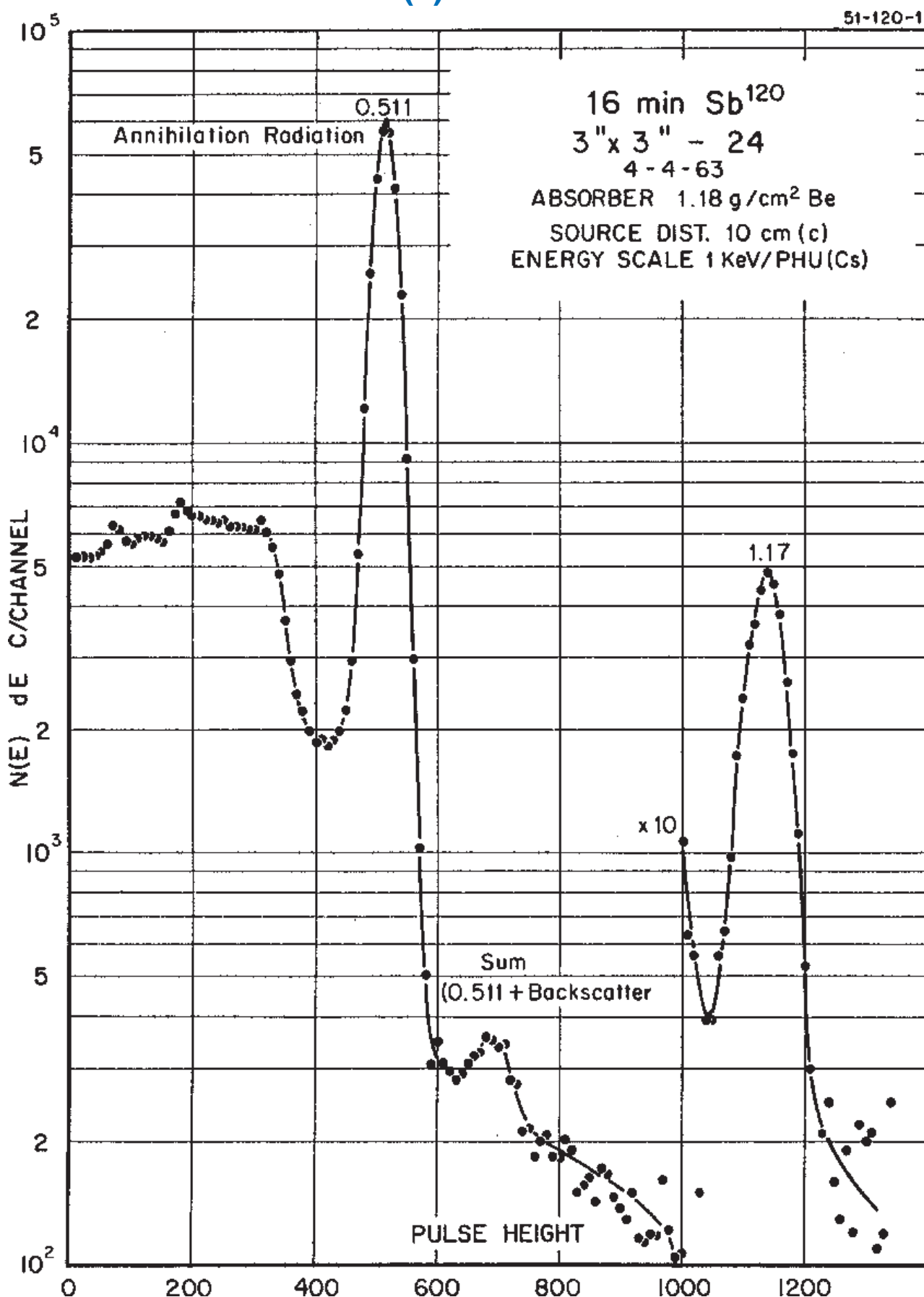
GAMMA-RAY ENERGIES AND INTENSITIES

Nuclide ^{120m}Sb Half Life 5.76(2) day
 Detector 3" X 3" NaI-2 Method of Production: $^{121}\text{Sb}(\gamma, n)$

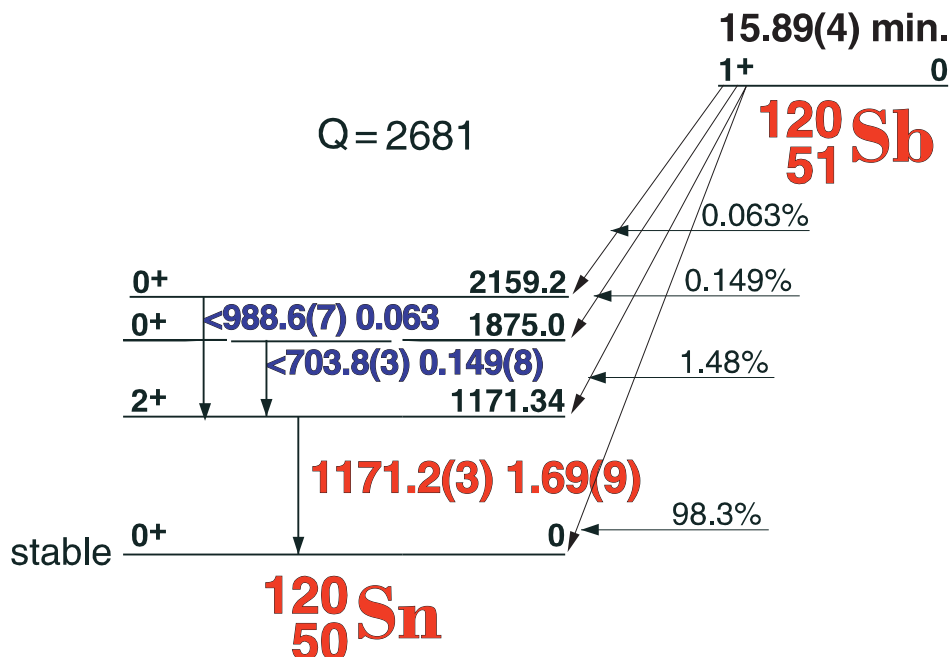
E_γ (KeV)[S]	ΔE_γ	I_γ (rel)	$I_\gamma(\%)$ [E]	ΔI_γ	S
89.98	± 0.02		79	± 3.0	1
197.30	± 0.02		87	± 4.0	1
1023.01	± 0.04		99.4	± 0.5	1
1112.9	± 0.1	0.82	± 0.04	3	
1171.21	± 0.05		100	± 5.0	1

15.89(4) min. ^{120}Sb

51-120-1



15.89(4) min. ^{120}Sb



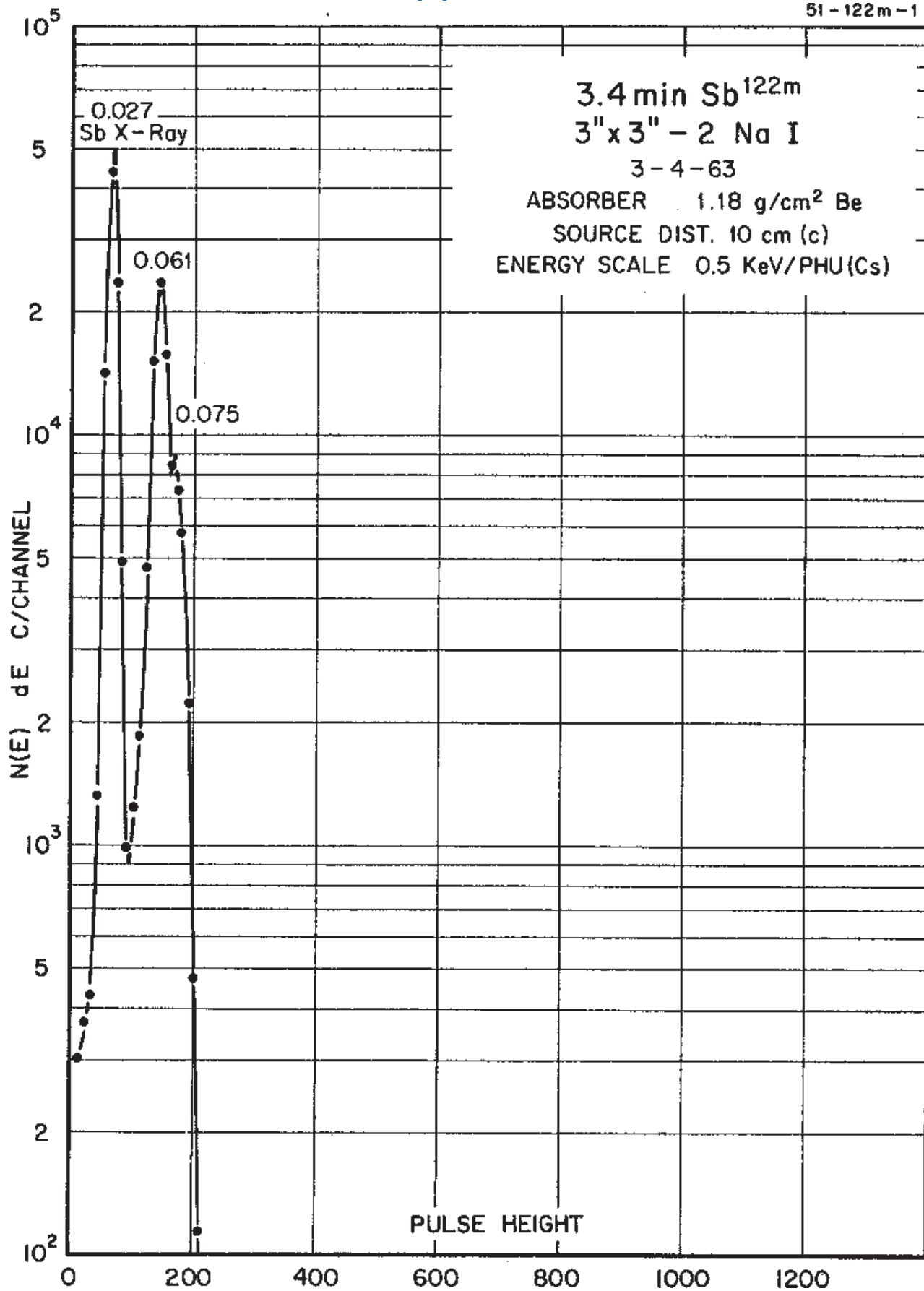
51-120-1

GAMMA-RAY ENERGIES AND INTENSITIES

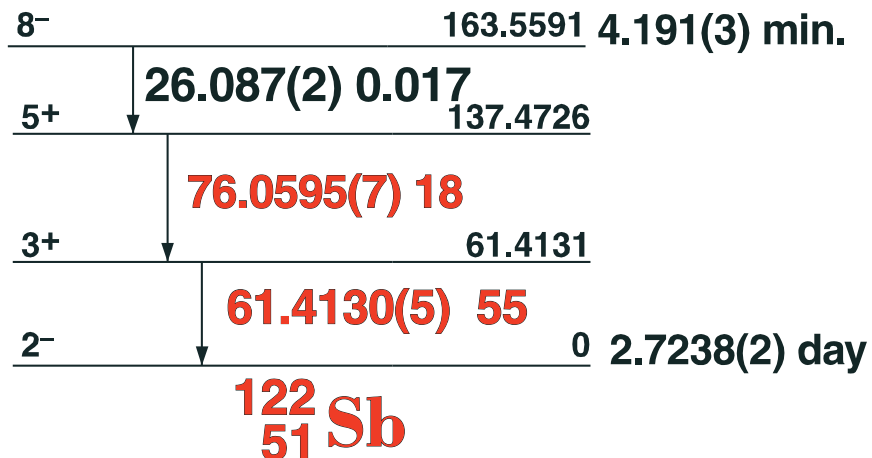
Nuclide	^{120}Sb	Half Life	15.89(4) min.		
Detector	3" X 3" NaI-2	Method of Production:	$^{121}\text{Sb}(\gamma, n)$		
E_γ (KeV)[S]	ΔE_γ	I_γ (rel)	I_γ (%)[E]	ΔI_γ	S
ann.rad 511.006					1
703.8	± 0.3		0.149	± 0.008	3
988.6	± 0.7		0.063	± 0.03	3
1171.2	± 0.3		1.69	± 0.09	1

4.191(3) min. ^{122m}Sb

SI - 122m - 1



4.191(3) min. ^{122m}Sb

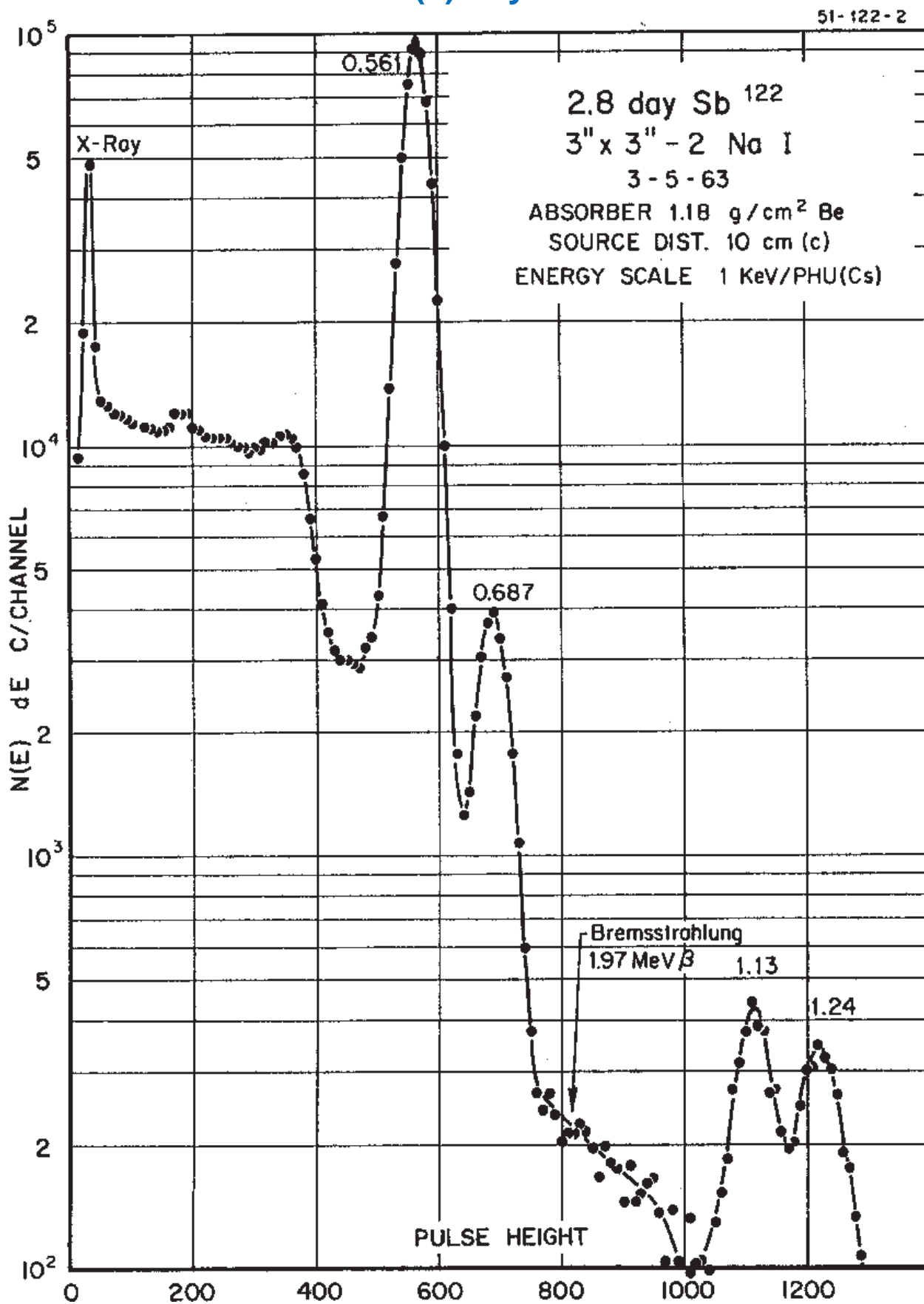


GAMMA-RAY ENERGIES AND INTENSITIES

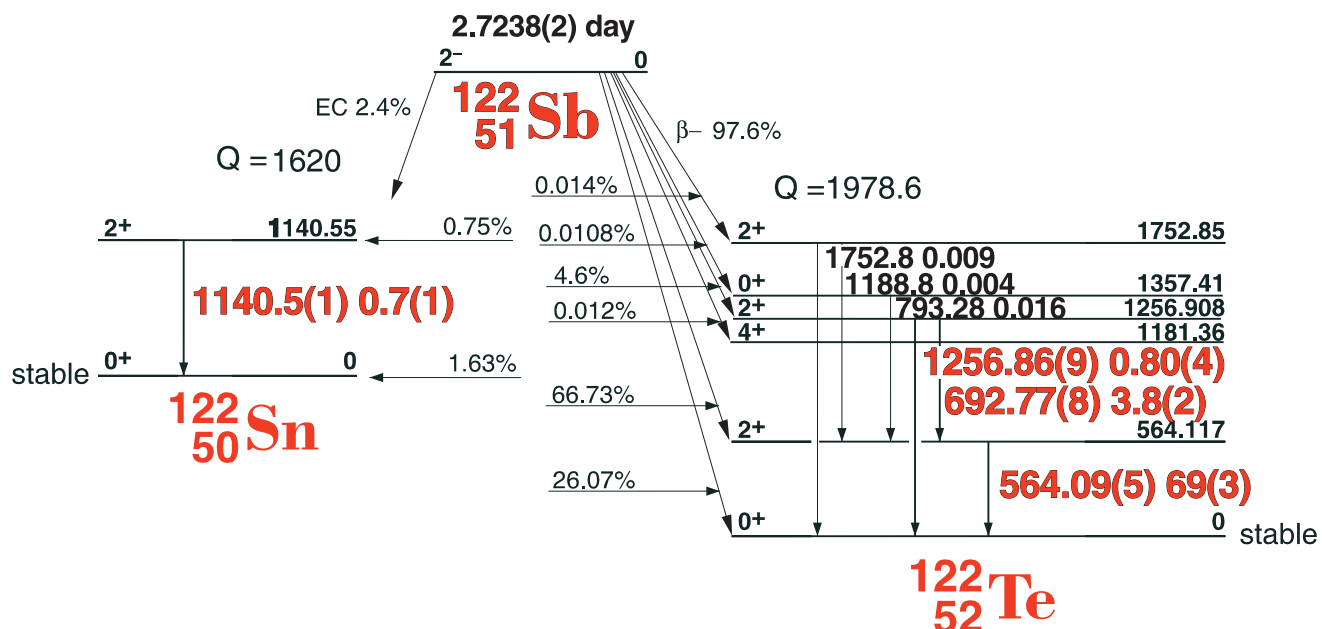
Nuclide ^{122m}Sb Half Life 4.191(3) min.
 Detector 3" X 3" NaI-2 Method of Production: $^{121}\text{Sb}(n,\gamma)$

E_γ (KeV)[S]	ΔE_γ	I_γ (rel)	$I_\gamma(\%)$ [E]	ΔI_γ	S
Sb x-ray					
26.087	± 0.002		0.017	\pm	4
61.4130	± 0.0005		55	\pm	1
76.0595	± 0.0007		13.6	\pm	2

2.7238(2) day ^{122}Sb



2.7238(2) day ^{122}Sb



51-122-2

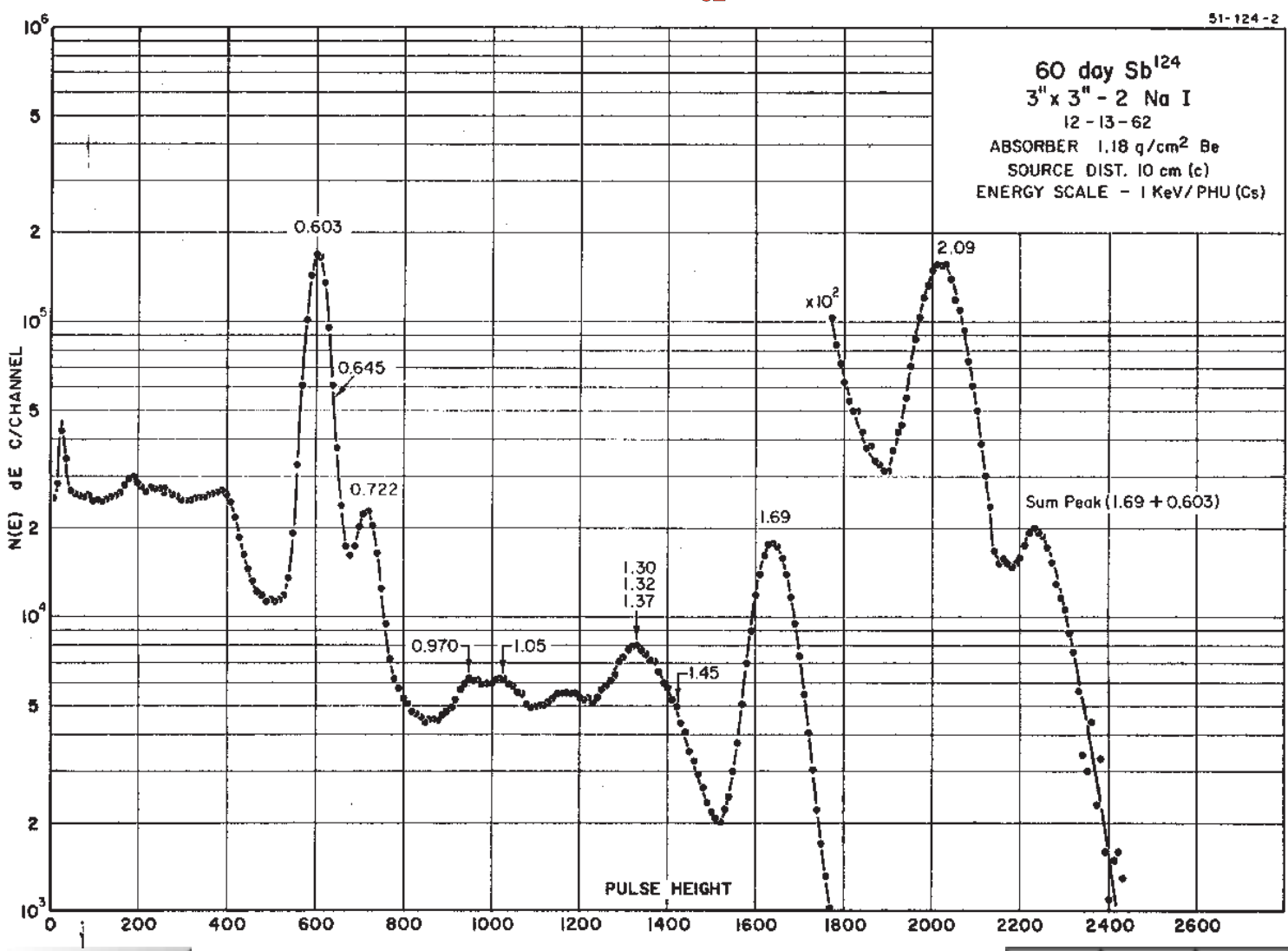
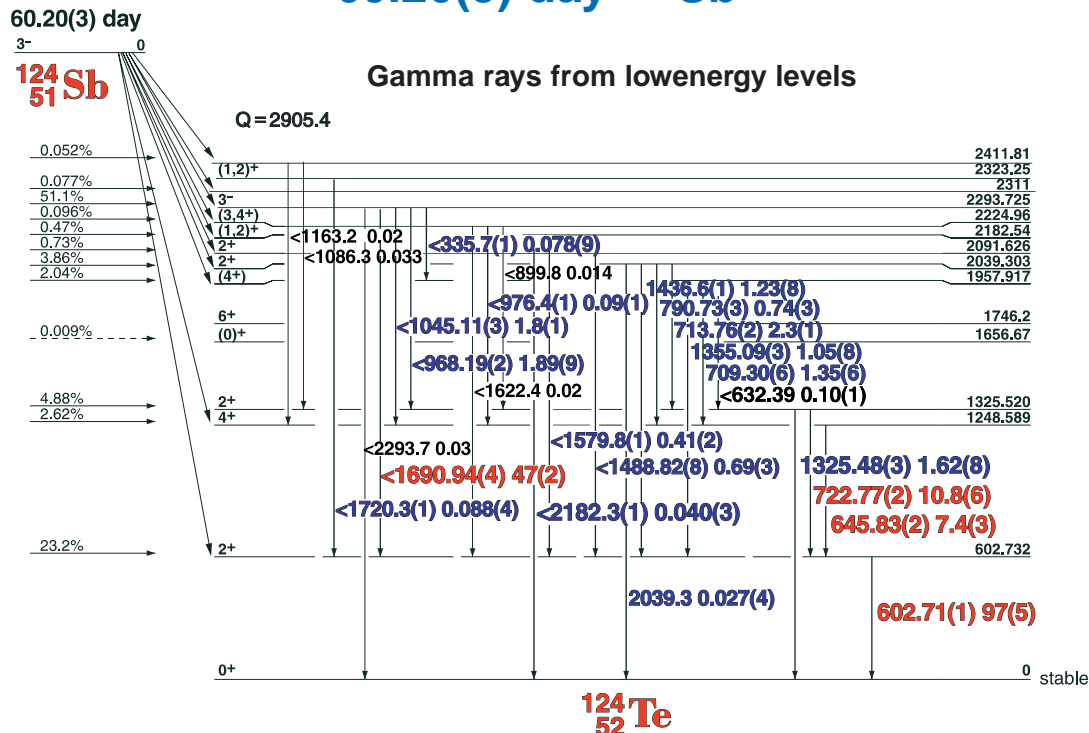
GAMMA-RAY ENERGIES AND INTENSITIES

Nuclide ^{122}Sb
Detector 3" x 3" -2 NaI

Half Life 2.7238(2) day
Method of Production: $^{121}\text{Sb}(n,\gamma)$

E_γ (KeV)[S]	ΔE_γ	I_γ (rel)	$I_\gamma(\%)$ [E]	ΔI_γ	S
564.09	± 0.05	100	69	± 3.0	1
692.77	± 0.08	5.6	3.8	± 0.2	1
1140.5	$+ 0.10$	1.2	0.7	± 0.1	1
1256.86	± 0.09	1.0	0.80	± 0.04	1

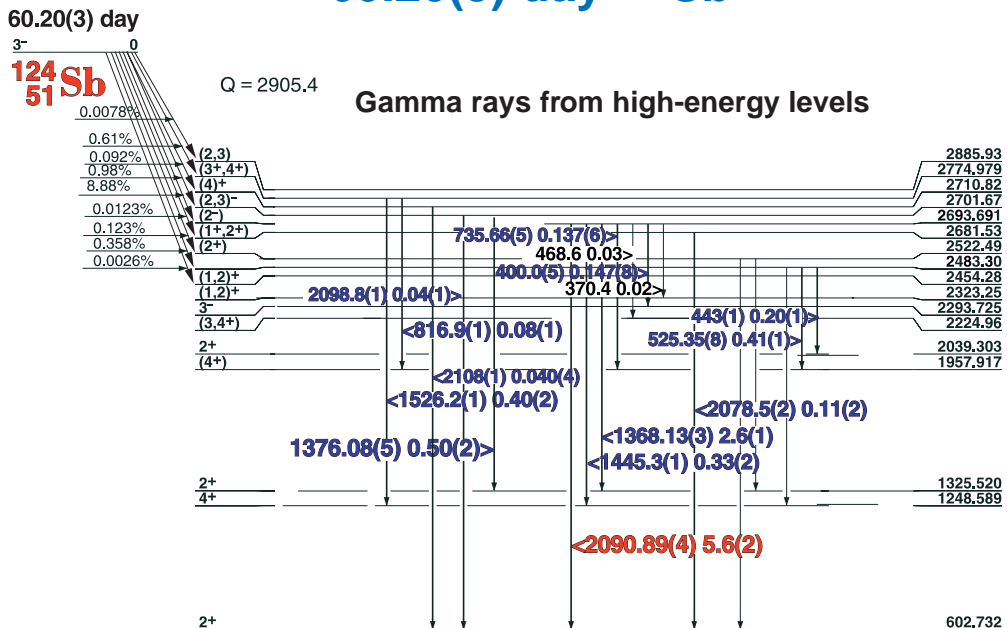
60.20(3) day ^{124}Sb



Decay Data

← Index →

60.20(3) day ^{124}Sb



GAMMA-RAY ENERGIES AND INTENSITIES

Nuclide ^{124}Sb
Detector 3" x 3" -2 NaI

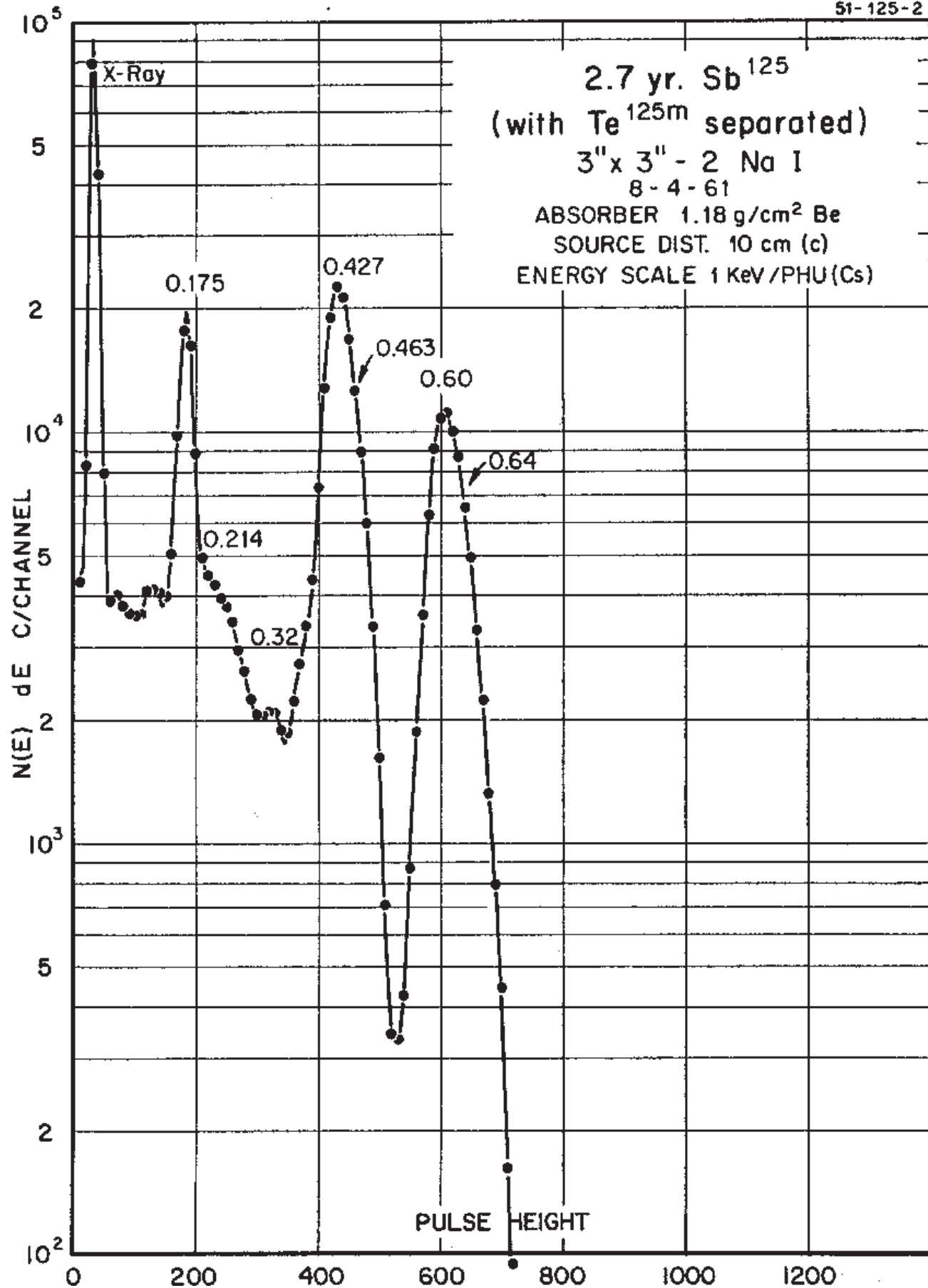
Half Life 60.20(3) day
Method of Production: $^{123}\text{Sb}(n,\gamma)$

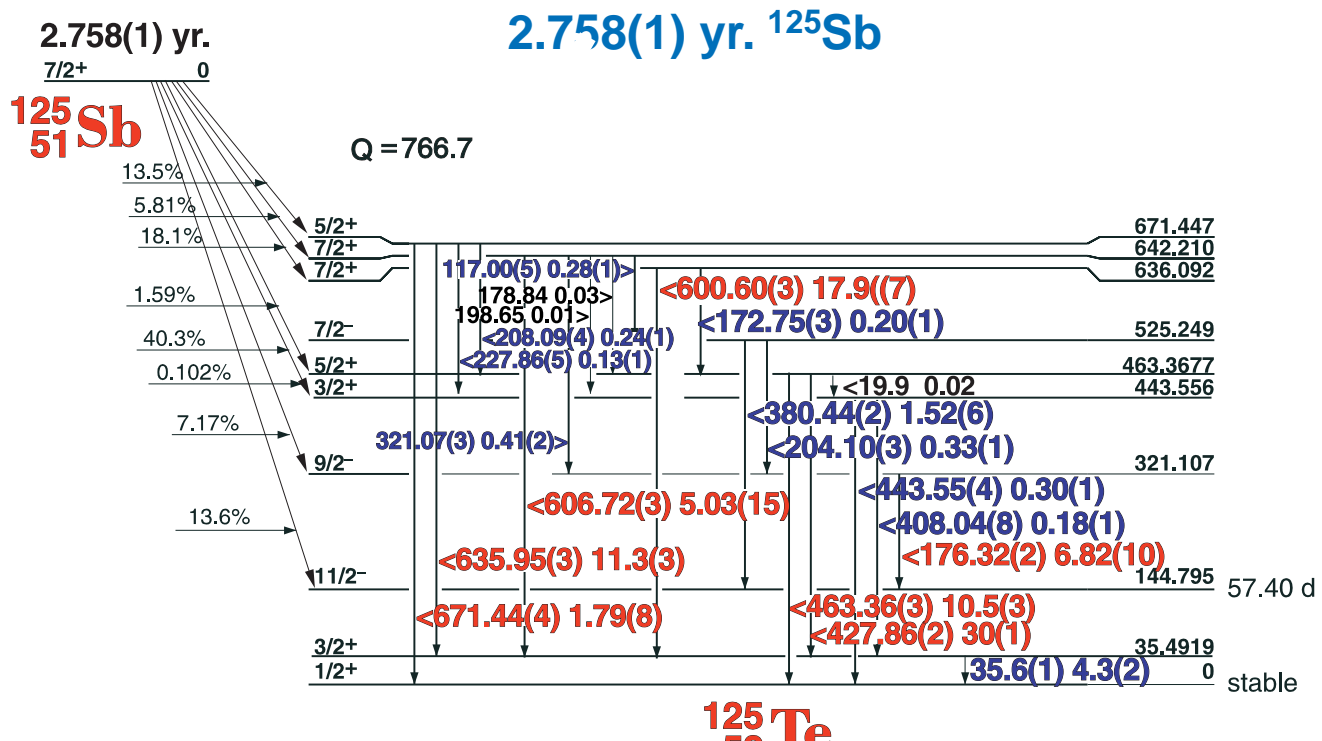
	E_γ (KeV)[S]	ΔE_γ	I_γ (rel)	I_γ (%)[E]	ΔI_γ	S
DE	158.96	± 0.10	0.177		± 0.01	4
	335.7	± 0.1	0.078	0.078	± 0.005	4
	400.0	± 1.0	0.099	0.147	± 0.008	4
	419.0	± 1.0	0.32	0.078	± 0.005	4
	443.0	± 1.0	0.5	0.45	± 0.02	4
	525.35	± 0.08	0.41	0.41	± 0.01	4
	602.715	± 0.013	100	97	± 3.0	1
	645.835	± 0.017	7.53	7.4	± 0.3	1
	669.1	± 0.1	0.82		± 0.10	2
	709.30	± 0.06	1.35	1.35	± 0.06	2
	713.761	± 0.018	2.31	2.3	± 0.1	2
	722.767	± 0.018	10.89	10.8	± 0.6	1
	735.66	± 0.05	0.14	0.137	± 0.006	4
	790.73	± 0.03	0.77	0.74	± 0.03	3
	816.9	± 0.1	0.11	0.08	± 0.01	4
	968.188	± 0.022	1.95	1.89	± 0.09	3
	976.4	± 0.1	0.09	0.088	± 0.004	4
DE	1045.106	± 0.028	1.94	1.8	± 0.1	3
	1069.0	± 0.06	0.33		± 0.03	4
SE	1179.85	± 0.05	0.84		± 0.10	4
	1325.478	± 0.027	1.66	1.62	± 0.08	3

	E_γ (KeV)[S]	ΔE_γ	I_γ (rel)	I_γ (%)[E]	ΔI_γ	S
SE	1355.092	± 0.031	1.09	1.05	± 0.08	4
	1368.130	± 0.029	2.61	2.6	± 0.1	3
	1376.08	± 0.05	0.50	0.50	± 0.02	4
	1436.6	± 0.1	1.26	1.23	± 0.08	3
	1445.3	± 0.1	0.31	0.33	± 0.02	4
	1488.82	± 0.08	0.91	0.69	± 0.03	4
	1526.2	± 0.1	0.53	0.40	± 0.02	4
	1579.8	± 0.1	0.59	0.41	± 0.02	3
	1690.942	± 0.036	49.15	47	± 2.0	1
	1720.3	± 0.1	0.10	0.088	± 0.004	4
	2039.3	± 0.1	0.07	0.027	± 0.004	3
	2078.5	± 0.2		0.11	± 0.02	4
	2090.889	± 0.044	5.70	5.6	± 0.2	1
	2098.7	± 0.1	0.05	0.04	± 0.007	4
	2108	± 1.0	0.05	0.040	± 0.004	4
	2182.3	± 0.1	0.05	0.04	± 0.01	3

2.758(1) yr. ^{125}Sb

51-125-2





51-125-1

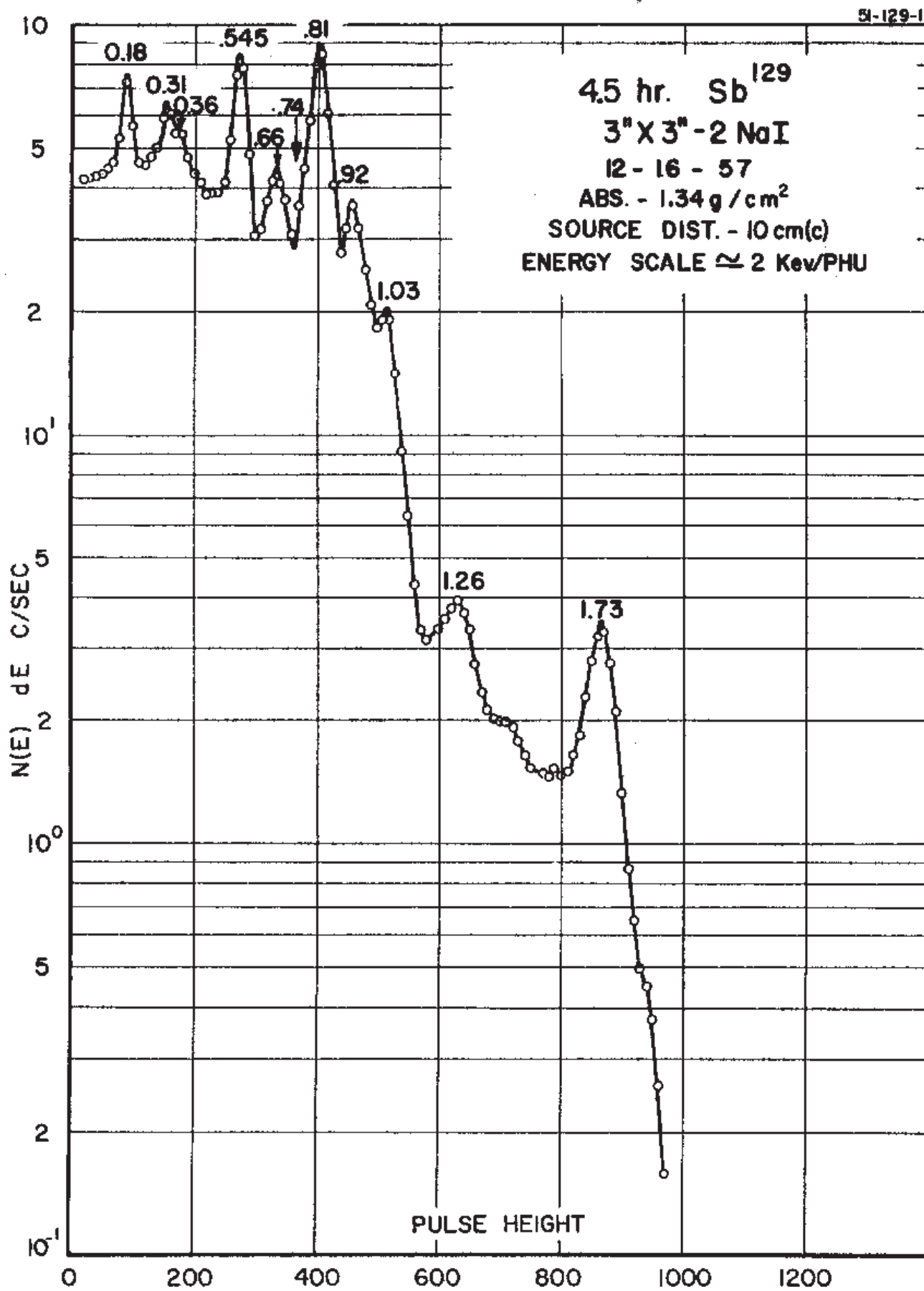
GAMMA-RAY ENERGIES AND INTENSITIES

Nuclide ^{125}Sb
Detector 3" x 3" -2 NaI

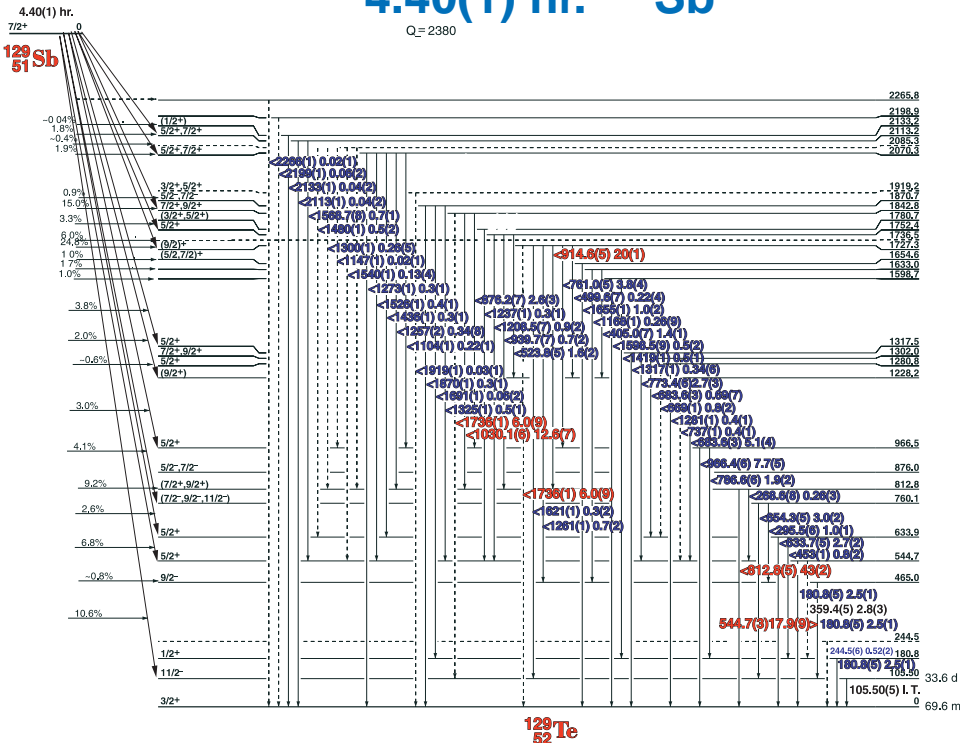
Half Life 58.51(6) day
Method of Production:

E_{γ} (KeV)[S]	ΔE_{γ}	I_{γ} (rel)	$I_{\gamma}(\%)$ [E]	ΔI_{γ}	S
19.9	± 0.05		0.02		5
35.62	± 0.10	w	4.3	± 0.2	4
109.38	± 0.05	0.27		± 0.03	4
117.00	± 0.05	0.73	0.28	± 0.01	3
172.750	± 0.030	0.94	0.20	± 0.01	4
176.320	± 0.020	21.5	5.82	± 0.10	1
198.65	± 0.05		0.01		4
204.104	± 0.030	1.14	0.33	± 0.01	3
208.093	± 0.040	0.91	0.24	± 0.01	4
227.86	± 0.05	0.54	0.13	± 0.01	4
321.071	± 0.030	1.45	0.41	± 0.02	3
380.442	± 0.020	5.12	1.52	± 0.06	2
408.04	± 0.08	0.63	0.18	± 0.01	4
427.864	± 0.020	100	30	± 1.0	1
443.552	± 0.040	1.20	0.30	± 0.01	3
463.359	± 0.030	35.4	10.5	± 0.3	1
600.601	± 0.030	59.5	17.9	± 0.7	1
606.716	± 0.030	17.0	5.03	± 0.15	1
635.954	± 0.030	38.1	11.3	± 0.3	1
671.443	± 0.040	6.26	1.79	± 0.08	1

4.40(1) hr. ^{129}Sb



4.40(1) hr. ^{129}Sb



GAMMA-RAY ENERGIES AND INTENSITIES

51-129-1

Nuclide ^{129}Sb
Detector 3" X 3" NaI-2

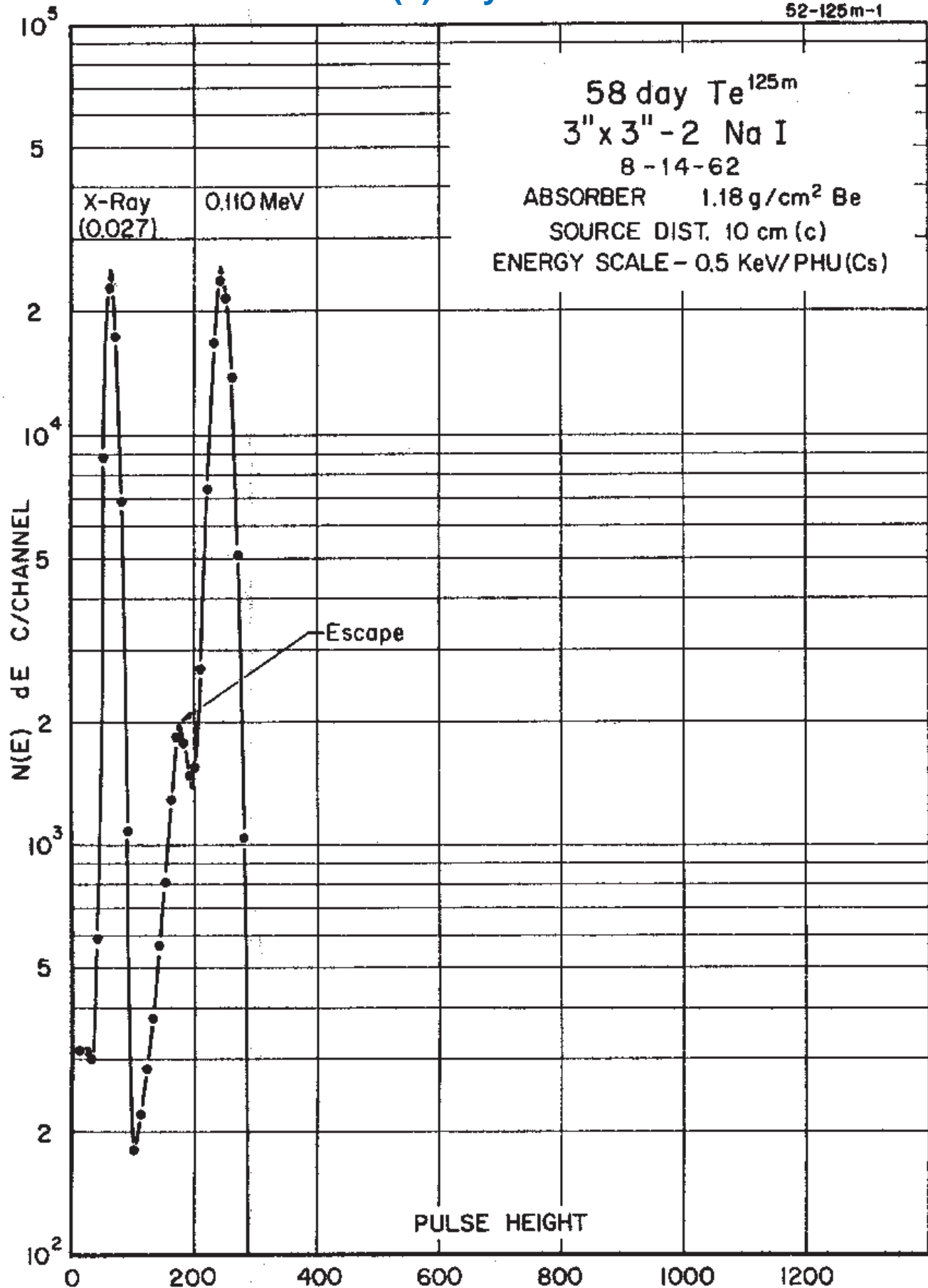
Half Life 4.40(1) hr.
Method of Production: $^{235}\text{U}(\text{n},\text{f})$

E_{γ} (KeV)[S]	ΔE_{γ}	I_{γ} (rel)	$I_{\gamma} (\%) [E]$	ΔI_{γ}	S
96.1	± 0.7		0.17	± 0.05	
116.2	± 0.7		0.17	± 0.05	
146.6	± 0.7		0.21	± 0.05	
180.8	± 0.5		2.54	± 0.15	
232.1	± 1.0		0.301	± 0.11	
244.5	± 0.6		0.52	± 0.9	
268.6	± 0.8		0.26	± 0.5	
295.5	± 0.6		1.03	± 0.9	
313.5	± 1.0		0.84	± 0.9	
359.4	± 0.5		2.8	± 0.3	
363.0	± 1.0		0.430	10	
405.0	± 0.7		1.38	14	
453.5	± 1.0		0.77	22	
499.6	± 0.7		0.21	9	
523.8	± 0.5		1.59	14	
544.7	± 0.3		17.9	± 1.0	1
633.7	± 0.5		2.75	23	
654.3	5		3.01	23	
669.8	10		0.82	18	
683.6	3		5.1	4	
683.6	3		0.69	22	
737.1	10		0.39	9	
761.0	5		3.8	3	
773.4	6		2.75	23	
786.6	6		1.89	18	
812.8	5		43.0	± 1.0	1
876.2	7		2.58	23	
914.6	5		20.0	± 1.2	1
939.7	7		0.73	18.	
966.4	6		7.7	5	
995.4	11		0.13	9	
1030.1	6		12.6	± 0.9	1
1083.8	7		0.52	18	
1104.3	10		0.21	9	

E_{γ} (KeV)[S]	ΔE_{γ}	I_{γ} (rel)	$I_{\gamma} (\%) [E]$	ΔI_{γ}	S
1125.4	± 1.0			0.107	± 0.022
1139.2	± 1.0			0.17	± 0.05
1161.8	± 1.0			0.107	± 0.022
1167.8	± 1.0			0.26	± 0.09
1208.5	± 0.7			0.90	± 0.13
1223.3	10			0.17	5
1237.4	15			0.26	9
1257.0	18			0.34	18
1261.3	10			0.73	18
1273.0	15			0.26	13
1280.8	10			0.56	13
1300.0	12			0.26	9
1317.2	10			0.34	9
1325.9	10			0.52	9
1418.6	11			0.52	± 0.9
1436.1	12			0.30	13
1479.7	10			0.47	22
1525.9	10			0.43	13
1540.0	15			0.13	5
1568.7	± 0.8			0.69	9
1598.5	9			0.52	13
1621.1	12			0.26	13
1654.6	10			0.99	22
1724.1	20			0.26	13
1736.5	± 1.0		6.0	± 0.8	1
1736.5	± 1.0		6.0	± 0.8	1
1841.8	10			0.21	9
1869.9	11			0.30	9
2069.6	15			0.56	13
2071.6	10			0.43	± 0.7

57.4(1) day ^{125m}Te

52-125 m-1



57.4(1) day ^{125m}Te



52-125m-1

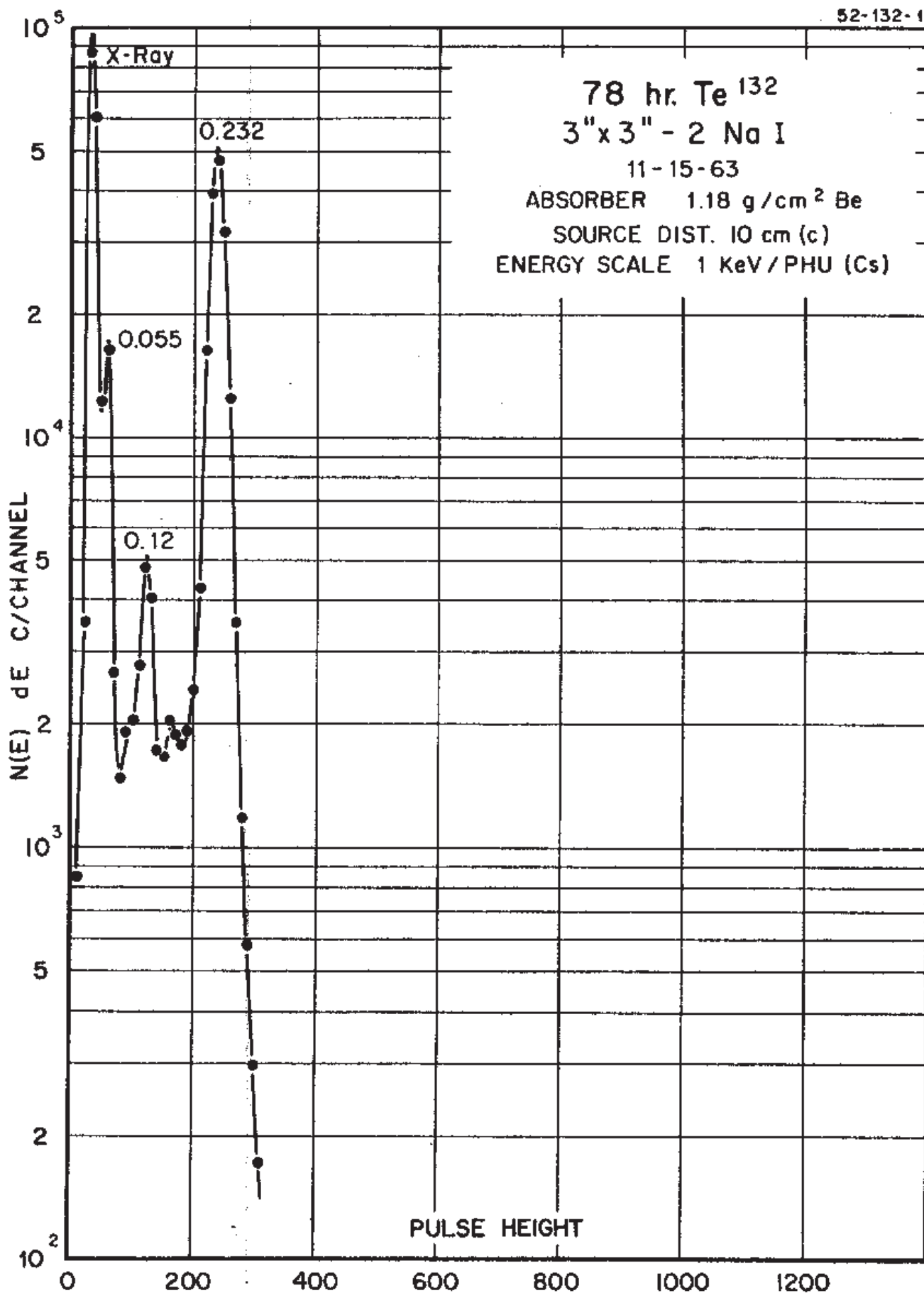
GAMMA-RAY ENERGIES AND INTENSITIES

Nuclide ^{125m}Te Half Life 57.4(1) day
 Detector 3" X 3" NaI-2 Method of Production: $^{124}\text{Te}(n,\gamma)$

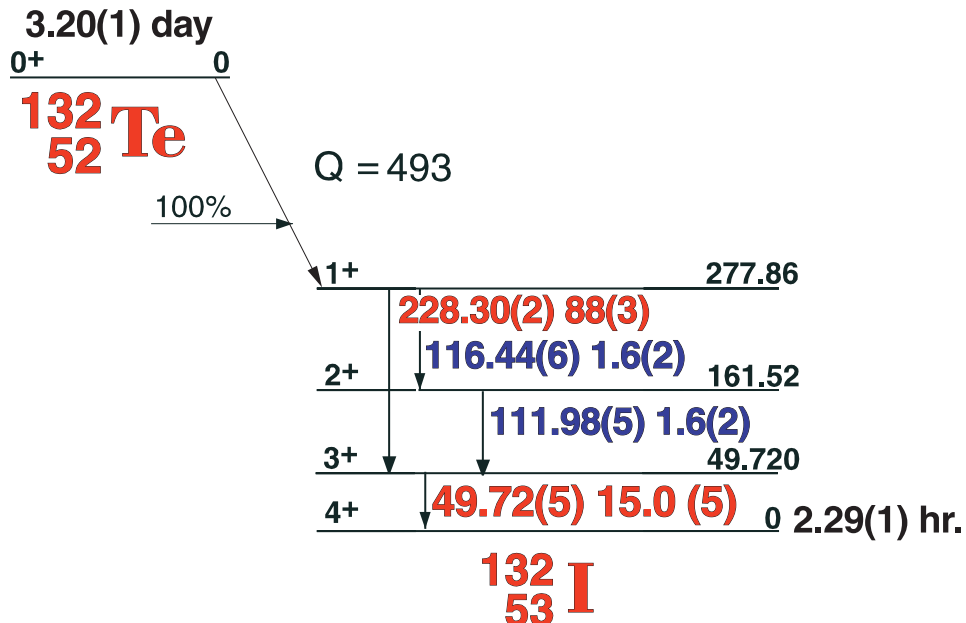
E_{γ} (KeV)[S]	ΔE_{γ}	$I_{\gamma}(\text{rel})$	$I_{\gamma}(\%)[E]$	ΔI_{γ}	S
Te x-ray					
35.50	± 0.01		6.7	± 0.2	1
109.28	± 0.01		0.27	± 0.01	2

3.20(1) day ^{132}Te

52-132-1



3.20(1) day ^{132}Te



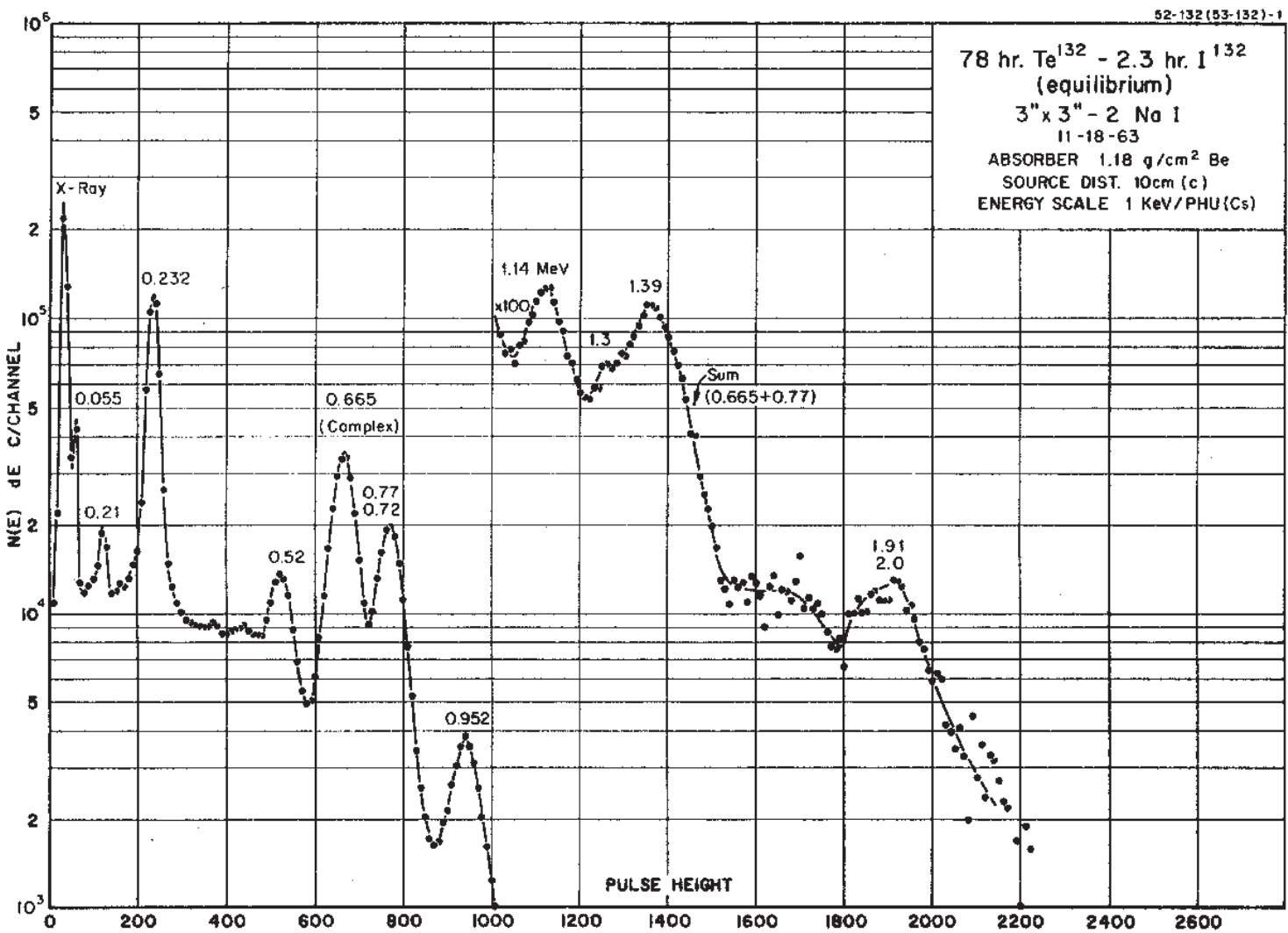
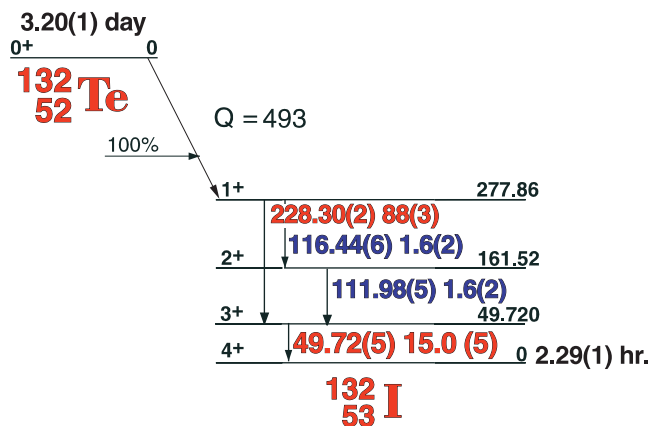
52-132-1

GAMMA-RAY ENERGIES AND INTENSITIES

Nuclide ^{132}Te Half Life 3.20(1) day
 Detector 3" x 3" -2 NaI Method of Production: $^{235}\text{U}(n,f)$

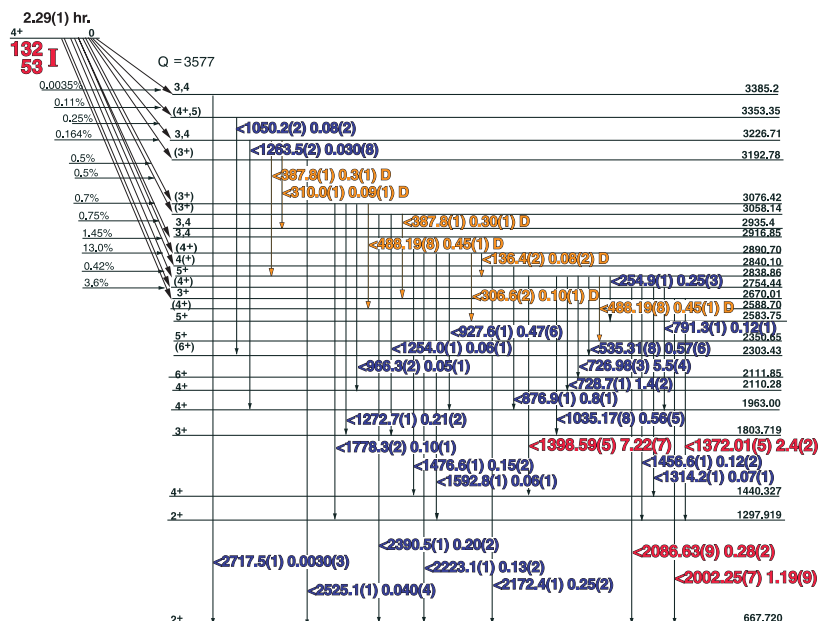
E_γ (KeV)[S]	ΔE_γ	I_γ (rel)	$I_\gamma(\%)$ [E]	ΔI_γ	S
49.725	± 0.05	18.1	15.0	± 0.5	1
111.984	± 0.05	1.61	1.6	± 0.2	3
116.440	± 0.06	1.60	1.6	± 0.2	3
228.302	± 0.025	100	88	± 2.0	1

3.20(1) day ^{132}Te - 2.29(1) hr. ^{132}I

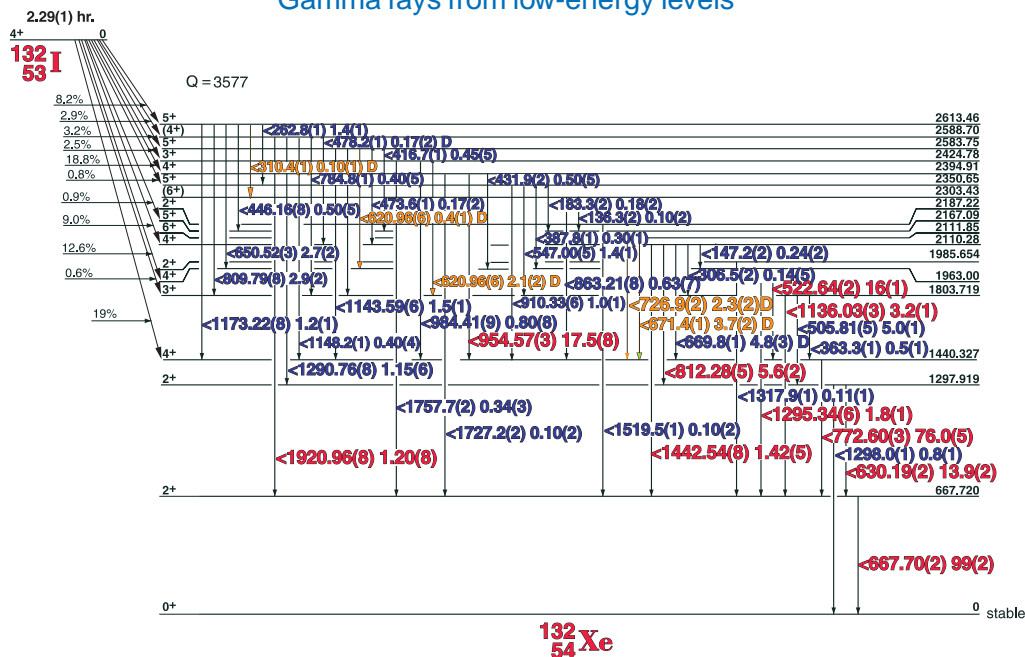


3.20(1) day ^{132}Te - 2.29(1) hr. ^{132}I

Gamma rays from high-energy levels



Gamma rays from low-energy levels



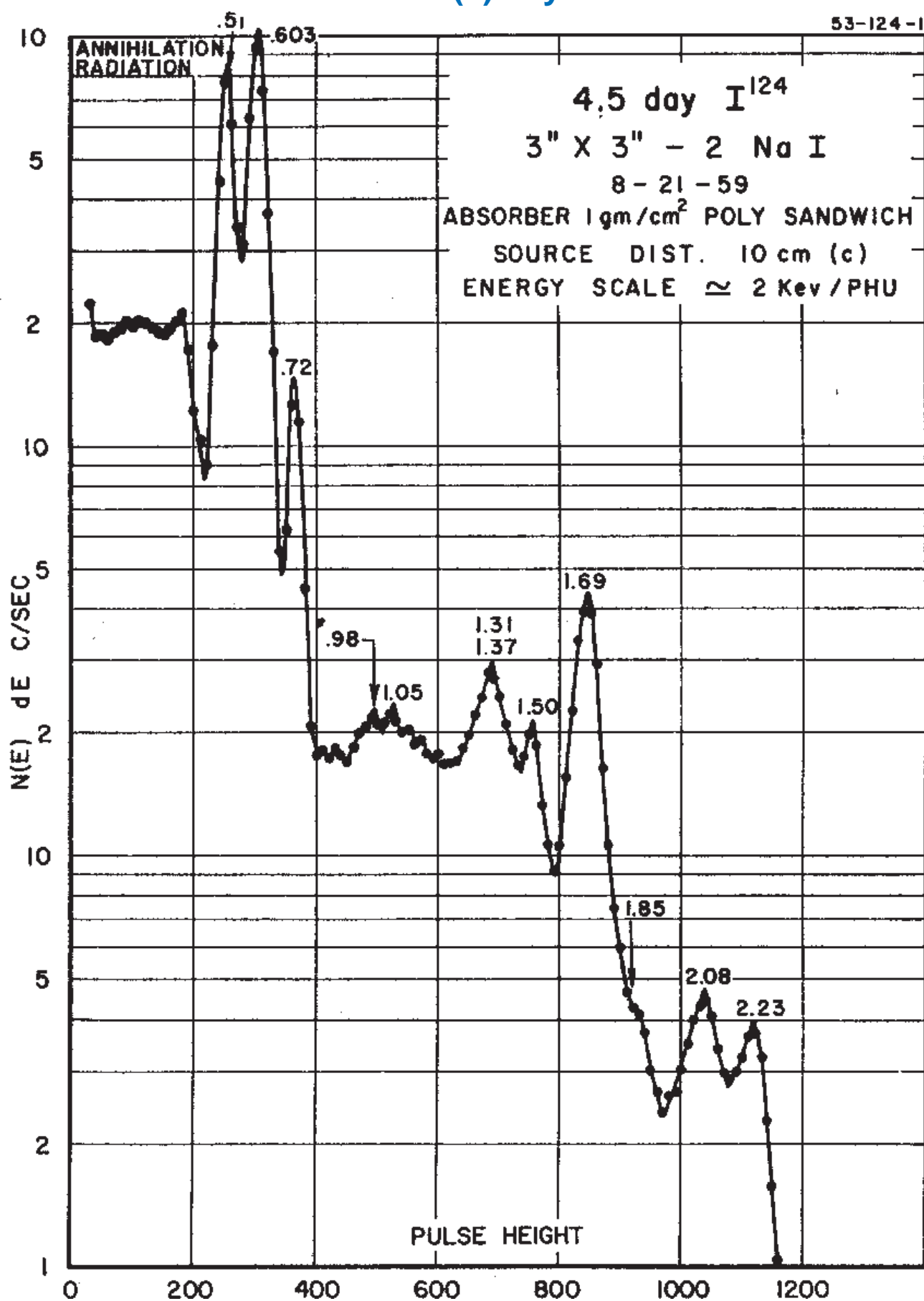
3.20(1) day ^{132}Te - 2.29(1) hr. ^{132}I

GAMMA-RAY ENERGIES AND INTENSITIES

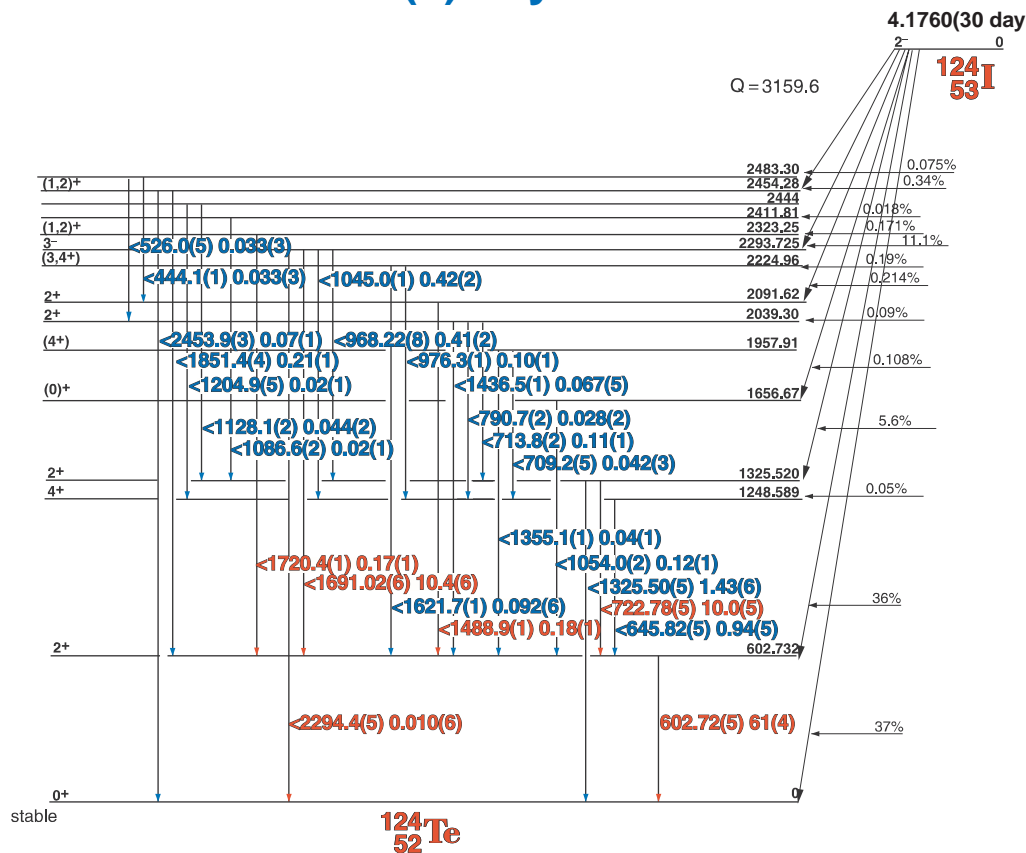
Nuclide $^{132}\text{Te} - ^{132}\text{I}$ Half Life 3.20(1) day - 2.29(1) hr.
 Detector 3" X 3" NaI-2 Method of Production: Zr⁹⁰(γ, n)

	E_{γ} (KeV)[S]	ΔE_{γ}	I_{γ} (rel)	$I_{\gamma}(\%)[E]$	ΔI_{γ}	S	E_{γ} (KeV)[S]	ΔE_{γ}	I_{γ} (rel)	$I_{\gamma}(\%)[E]$	ΔI_{γ}	S
D	136.3	± 0.2	0.10	0.10	± 0.01	4	984.41	± 0.09	0.80	0.80	± 0.08	3
	147.2	± 0.1	0.24	0.24	± 0.02	4	1035.17	± 0.08	0.57	0.52	± 0.05	3
	183.30	± 0.2	0.18	0.18	± 0.02	4	1050.22	± 0.15	0.10	0.08	± 0.02	4
	254.86	± 0.15	0.25	0.25	± 0.02	4	1087.10	± 0.10	0.09	0.08	± 0.01	4
D	262.84	± 0.10	1.47	1.4	± 0.12	3	1136.026 ± 0.040	3.23	3.2	± 0.1	1	
D	306.7	± 0.1	0.14	0.14	± 0.02	4	1143.59	± 0.06	1.57	1.5	± 0.1	2
D	310.0	± 0.1	0.10	0.09	± 0.01	4	1148.30	± 0.10	0.40	0.40	± 0.04	4
D	310.4	± 0.1	0.10	0.10	± 0.01	4	1173.22	± 0.08	1.29	1.2	± 0.10	3
	387.75	± 0.10	0.20	0.30	± 0.03	4	1254.0	± 0.2	0.05	0.06	± 0.01	4
	416.65	± 0.1	0.46	0.45	± 0.05	4	1263.5	± 0.2	0.03	0.030	± 0.008	4
	431.96	± 0.08	0.50	0.50	± 0.05	4	1272.68	± 0.10	0.21	0.21	± 0.02	3
	446.16	± 0.08	0.53	0.50	± 0.05	4	1290.76	± 0.08	1.21	1.15	± 0.06	2
	473.52	± 0.10	0.17	0.17	± 0.02	4	1295.34	± 0.06	1.85	1.8	± 0.10	1
	488.16	± 0.08	0.92	0.45	± 0.01	4	1298.09	± 0.10	0.71	0.70	± 0.06	2
	505.810	± 0.05	4.97	5.0	± 0.10	3	1314.24	± 0.15	0.08	0.06	± 0.01	4
	522.640	± 0.025	16.18	16	± 0.90	1	1317.76	± 0.10	0.11	0.11	± 0.01	3
D	535.31	± 0.08	0.58	0.52	± 0.05	4	1372.01	± 0.05	2.52	2.4	± 0.20	1
D	547.00	± 0.08	1.38	1.4	± 0.11	3	1398.59	± 0.05	7.42	7.22	± 0.07	1
D	620.963	± 0.06	2.15	2.0	± 0.2	3	SE 1410.0					
	630.194	± 0.030	13.90	13.9	± 0.2	1	sum 1440.11	± 0.10	0.41		± 0.04	3
	650.516	± 0.035	2.74	2.7	± 0.25	2	1442.537	± 0.08	1.44	1.42	± 0.05	1
	667.683	± 0.030	100	99	± 2.0	1	1456.6	± 0.15	0.12	0.12	± 0.02	3
	669.8	± 0.1		4.8	± 0.3	2	1476.64	± 0.10	0.15	0.15	± 0.02	3
	671.4	± 0.10	9.47	3.7	$\pm .4$	2	SE 1491.0					
	726.95	± 0.035	5.65	5.5	± 0.45	1	1519.5	± 0.10	0.10	0.10	± 0.02	3
	728.72	± 0.10	1.39	1.4	± 0.2	3	1592.8	± 0.15	0.07	0.06	± 0.01	4
	772.605	± 0.030	76.99	76.0	± 0.5	1	1727.15	± 0.15	0.11	0.10	± 0.02	4
	780.19	± 0.08	1.28	1.2	± 0.2	3	1757.7	± 0.2	0.35	0.34	± 0.03	3
	784.85	± 0.10	0.42	0.40	± 0.05	4	1778.3	± 0.2	0.10	0.10	± 0.01	4
	791.27	± 0.10	0.13	0.11	± 0.04	4	1920.96	± 0.08	1.24	1.20	± 0.08	1
	809.79	± 0.08	3.03	2.9	± 0.2	2	2002.25	± 0.07	1.22	1.19	± 0.09	1
	812.277	± 0.05	5.74	5.6	± 0.2	1	2086.63	± 0.09	0.28	0.28	± 0.02	1
	863.21	± 0.08	0.63	0.61	± 0.06	3	2172.38	± 0.10	0.25	0.25	± 0.02	2
	875.86	± 0.1	0.80	0.8	± 0.1	3	2223.10	± 0.10	0.126	0.13	± 0.02	2
	876.9	± 0.1	0.60	0.8	± 0.1	3	2249.4	± 0.2	0.04	0.034	± 0.002	3
	910.33	± 0.06	1.04	1.0	± 0.08	3	2390.5	± 0.1	0.20	0.20	± 0.02	3
	927.67	± 0.08	0.47	0.47	± 0.06	3	2525.1	± 0.04	0.04	0.040	± 0.004	3
	954.575	± 0.030	17.60	17.5	± 0.8	1	2717.0	± 1.0	0.003	0.0035	± 0.001	3
	966.36	± 0.10	0.06	0.05	± 0.01	4						

4.1760(3) day I^{124}



4.1760(3) day ^{124}I



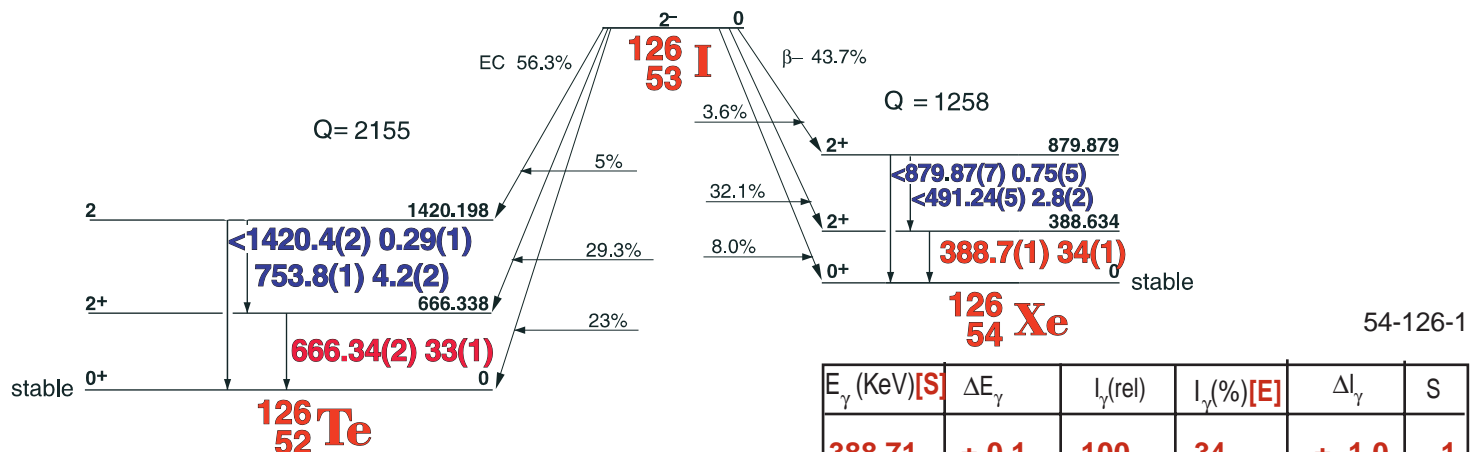
GAMMA-RAY ENERGIES AND INTENSITIES

Nuclide ^{124}I Half Life 4.1760(3) day
Detector 3" X 3" NaI-2 Method of Production: $^{124}\text{Te}(\text{p},\text{n})$

E_γ (KeV)[S]	ΔE_γ	I_γ (rel)	$I_\gamma(\%)$ [E]	ΔI_γ	S
444.1	± 0.1		0.033	± 0.0003	4
526.0	± 0.5		0.033	± 0.0003	4
602.72	± 0.05		61	± 4.0	1
645.82	± 0.05		0.94	± 0.05	3
709.2	± 0.5		0.042	± 0.003	4
713.8	± 0.2		0.11	± 0.01	3
722.78	± 0.05		10.0	± 0.5	2
790.7	± 0.2		0.028	± 0.002	4
968.22	± 0.08		0.41	± 0.02	3
976.3	± 0.1		0.10	± 0.01	4
1045.0	± 0.10		0.42	± 0.02	3
1054.0	± 0.2		0.42	± 0.02	3
1086.6	± 0.2		0.02	± 0.01	3
1128.1	± 0.2		0.044	± 0.002	4
1204.9	± 0.5		0.02	± 0.01	4
1325.50	± 0.05		1.43	± 0.06	2
1355.1	± 0.1		0.04	± 0.01	4
1436.5	± 0.1		0.067	± 0.005	4
1488.9	± 0.1		0.18	± 0.01	3
1621.7	± 0.1		0.092	± 0.006	4
1691.02	± 0.06		10.4	± 0.6	1
1720.4	± 0.1		0.17	± 0.01	3
1851.4	± 0.4		0.21	± 0.01	3
2294.4	± 0.5		0.010	± 0.06	4
2453.9	± 0.3		0.07	± 0.01	4

13.11(5) day ^{126}I

13.11(5) day

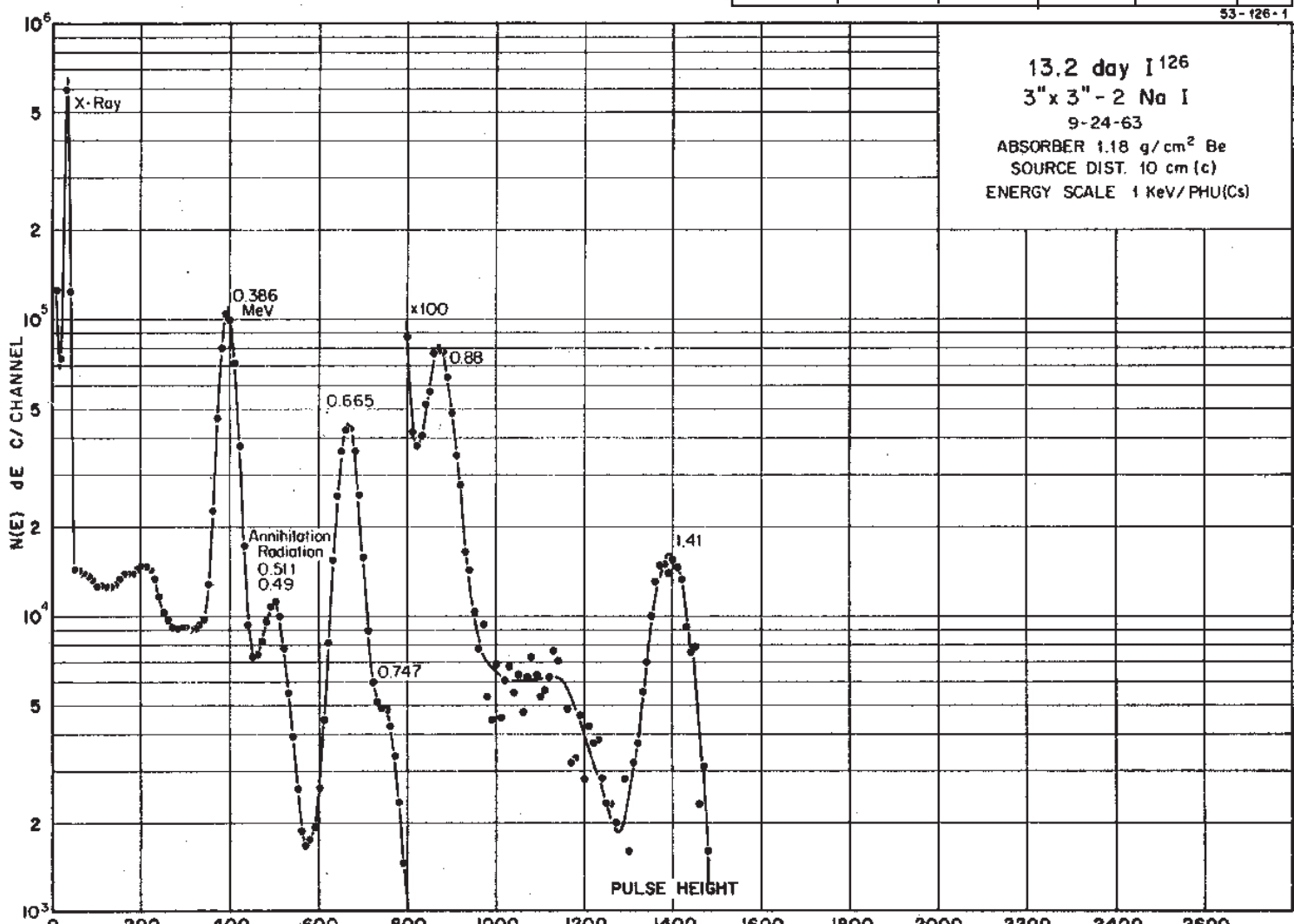


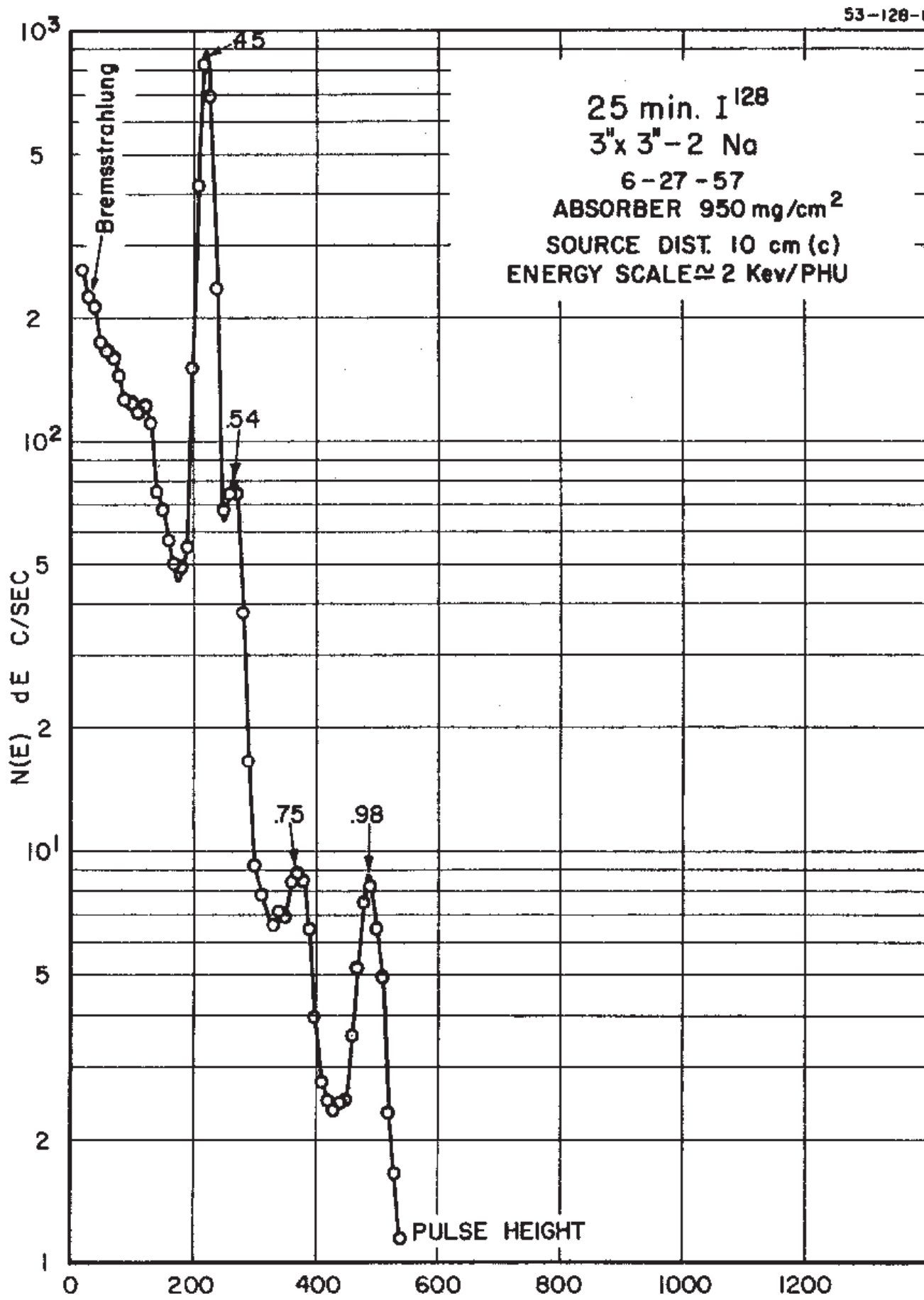
GAMMA-RAY ENERGIES AND INTENSITIES

Nuclide ^{126}I
Detector $3'' \times 3''$ -2 NaI

Half Life (64.02(5) Day
Method of Production: $^{127}\text{I}(\gamma, n)$

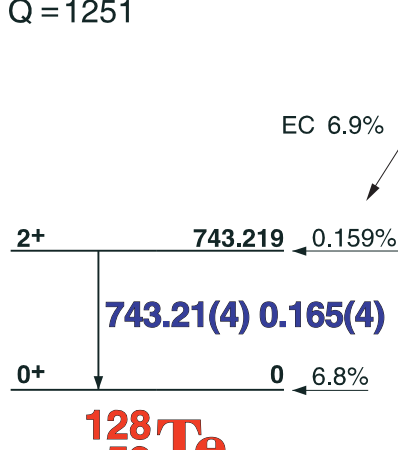
E_γ (KeV)[S]	ΔE_γ	I_γ (rel)	I_γ (%)[E]	ΔI_γ	S
388.71	± 0.1	100	34	± 1.0	1
491.24	± 0.05	9.5	2.8	± 0.2	2
511.006		5.8		± 1.0	2
666.34	± 0.02	94.0	33	± 1.0	1
753.80	± 0.1	11.6	4.2	± 0.2	2
879.87	± 0.07	2.5	0.75	± 0.05	3
1420.40	± 0.2	0.85	0.29	± 0.01	2



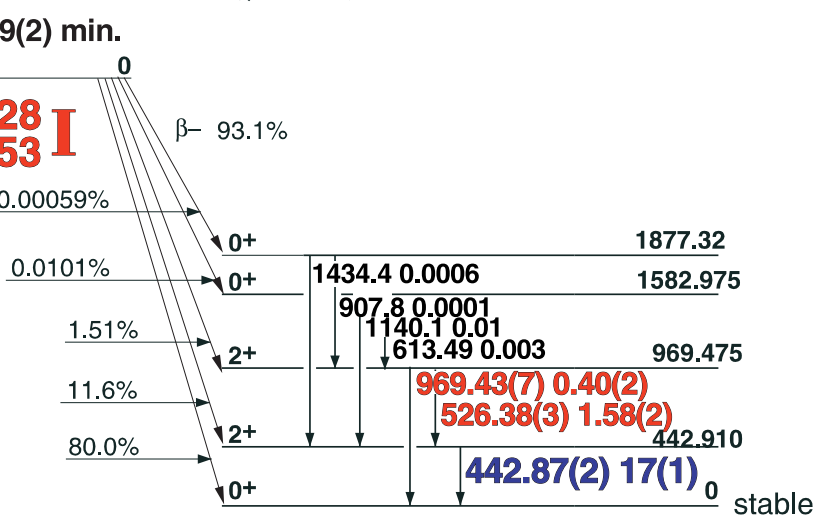


24.99(2) min. ^{128}I

$Q = 1251$



$Q = 2118$



54-128-1

GAMMA-RAY ENERGIES AND INTENSITIES

Nuclide ^{128}I

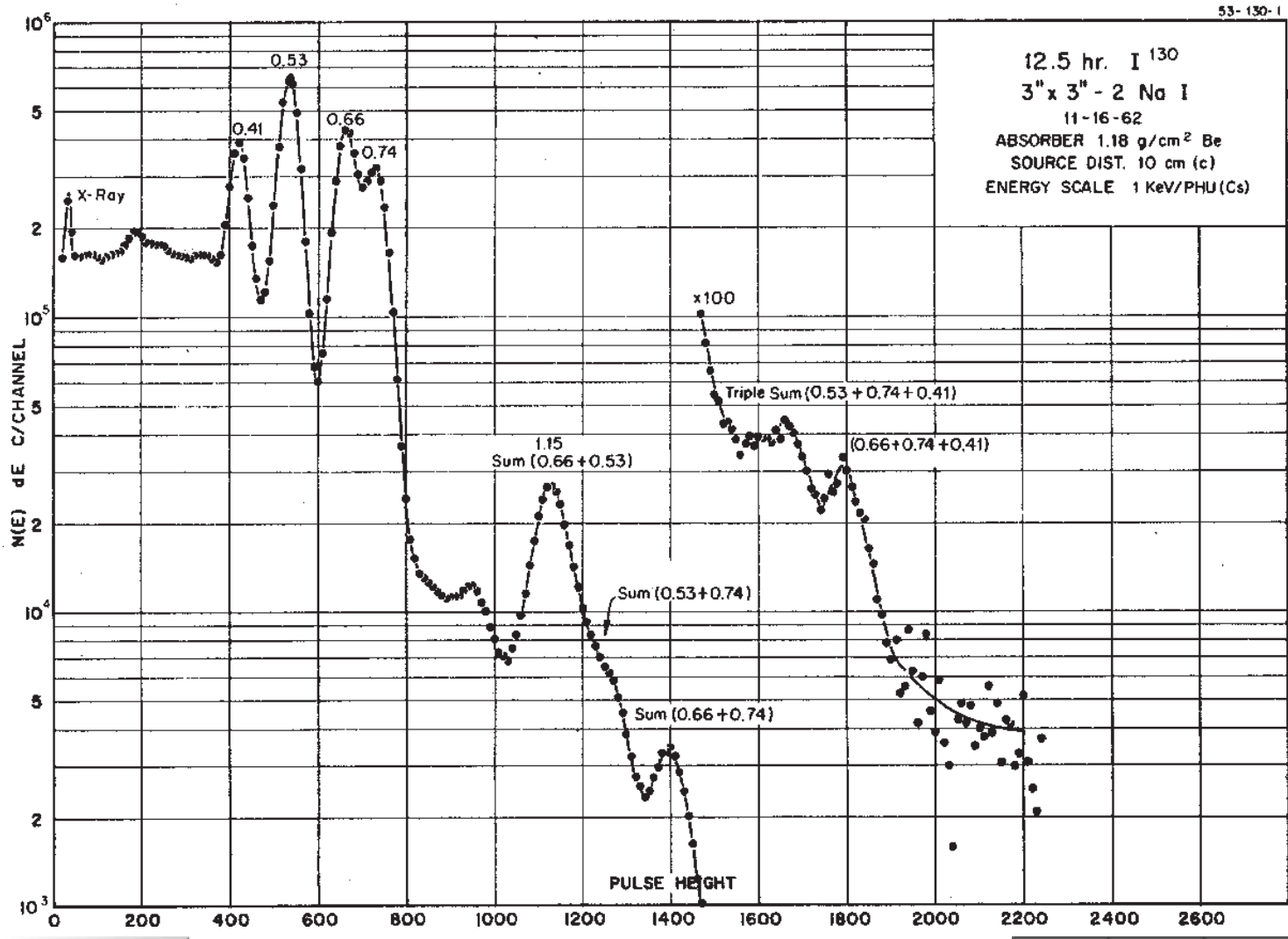
Detector 3" x 3" -2 NaI

Half Life 24.99(2) min.

Method of Production: $^{127}\text{I}(\text{n},\gamma)$

E_γ (KeV)[S]	ΔE_γ	I_γ (rel)	I_γ (%)[E]	ΔI_γ	S
Xe x-rays					3
442.87	± 0.02	100	17	± 1.0	1
526.38	± 0.03	9.89	1.58	± 0.02	1
743.21	± 0.04	1.03	0.165	$\pm (4)$	2
969.43	± 0.07	2.74	0.40	± 0.02	1

12.36(3) hr. I^{130}



12.36(3) hr. ^{130}I

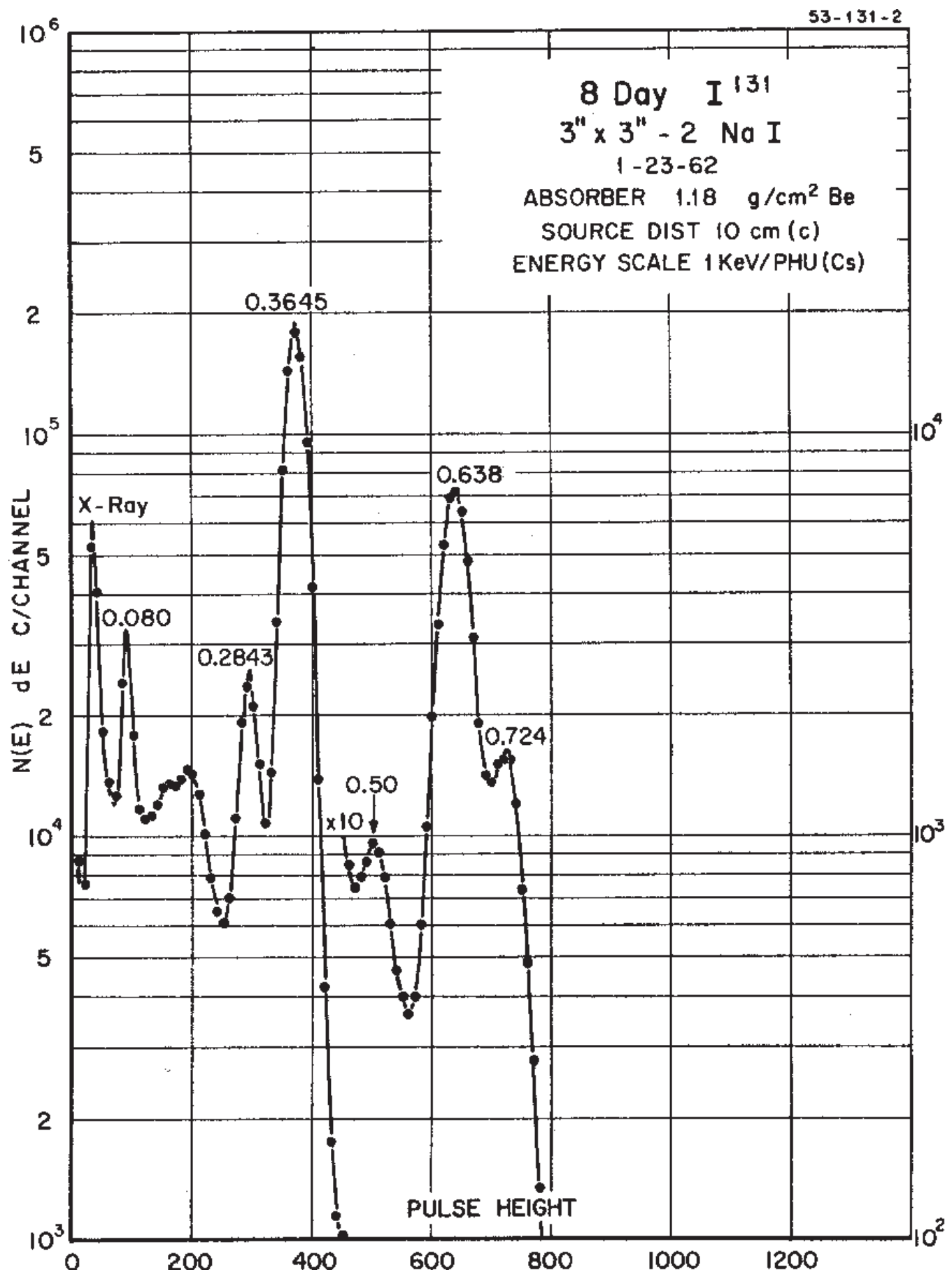
54-130-1

GAMMA-RAY ENERGIES AND INTENSITIES

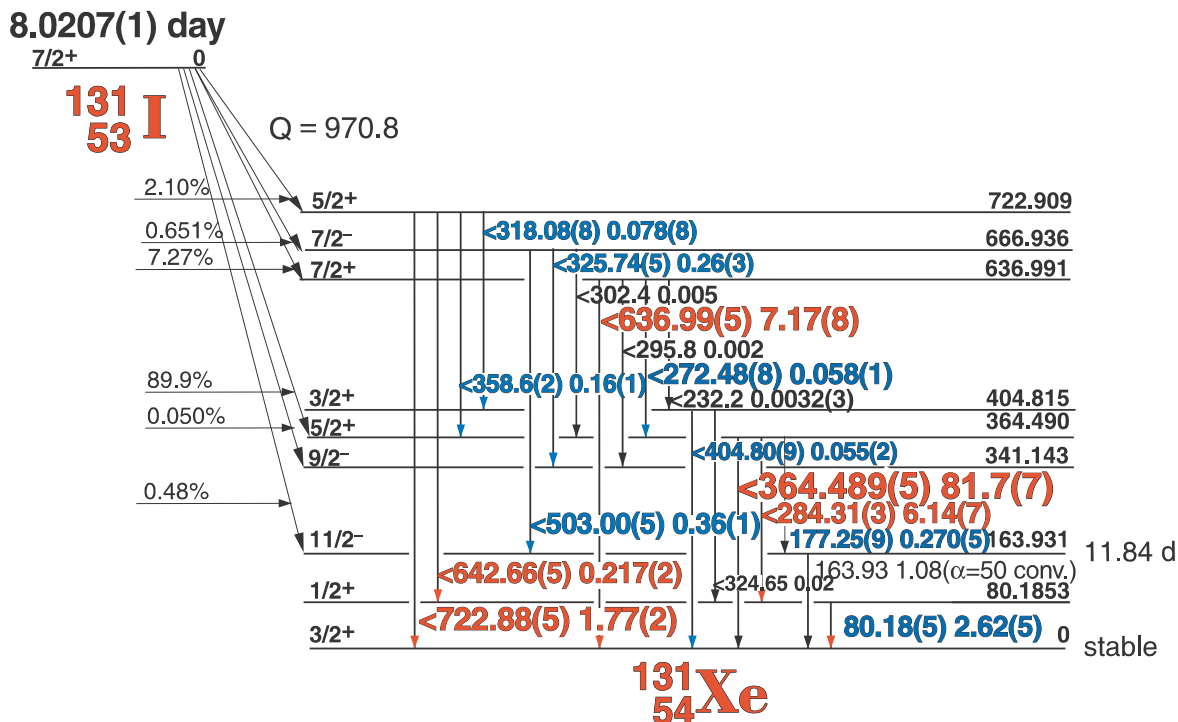
Nuclide ^{130}I
Detector 3" x 3" -2 Nal

Half Life 12.36(3) hr.
Method of Production: $^{130}\text{Te}(\text{p},\text{n})$

E_{γ} (KeV) [S]	ΔE_{γ}	I_{γ} (rel)	$I_{\gamma}(\%)$ [E]	ΔI_{γ}	S



8.0207(1) day ^{131}I



54-131-1

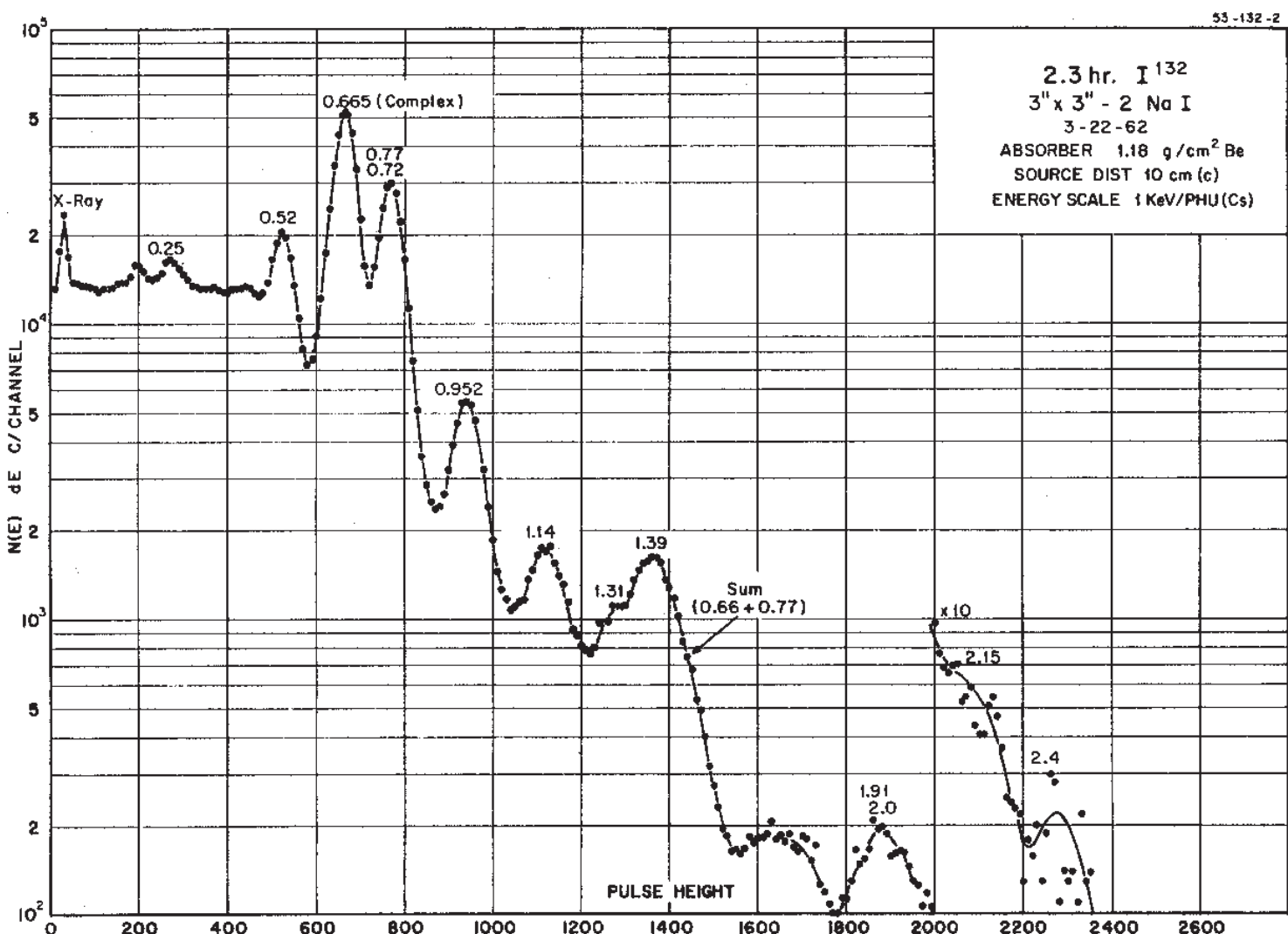
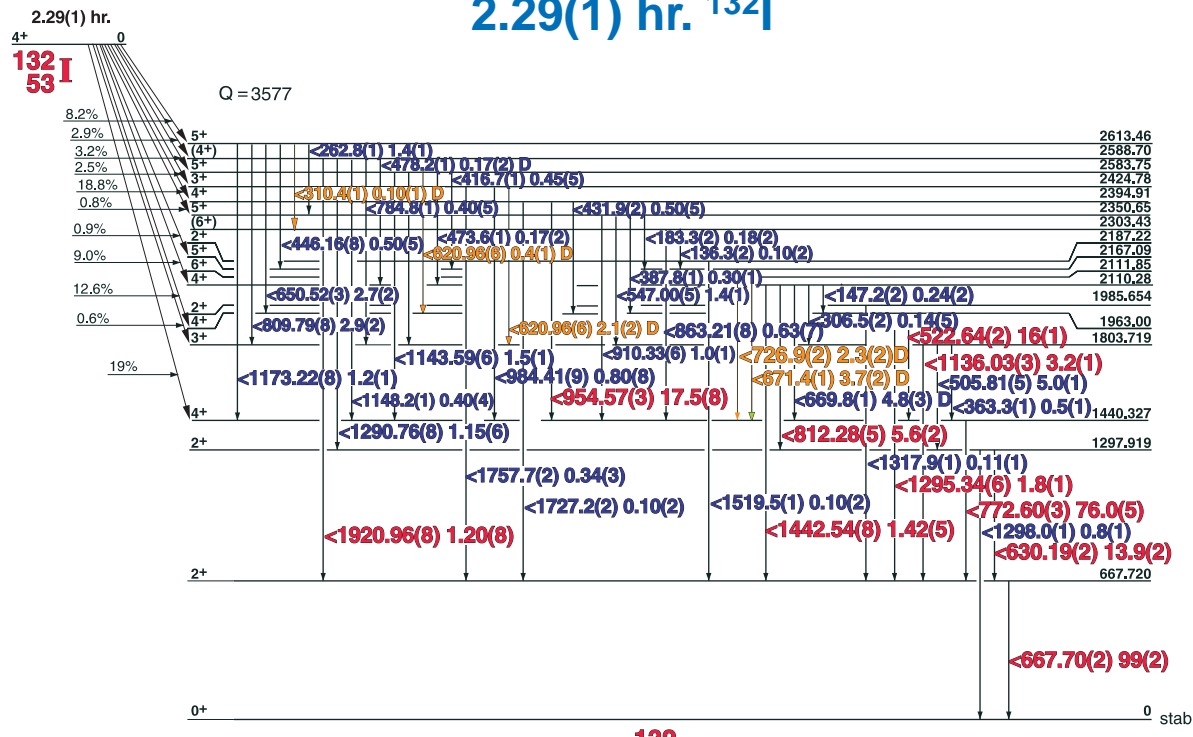
GAMMA-RAY ENERGIES AND INTENSITIES

Nuclide ^{131}I
Detector 3" x 3" -2 NaI

Half Life 8.0207(1) day
Method of Production: $^{235}\text{U}(\text{n},\text{f})$

E_{γ} (KeV)[S]	ΔE_{γ}	I_{γ} (rel)	$I_{\gamma}(\%)$ [E]	ΔI_{γ}	S
80.18	± 0.05	2.8	2.52	± 0.5	2
177.25	± 0.09	0.36	0.270	$\pm (5)$	4
272.48	± 0.08	0.11	0.058	$\pm (1)$	4
284.31	± 0.03	7.6	6.14	± 0.07	1
318.08	± 0.08	0.10	0.078	± 0.08	4
325.74	± 0.05	0.34	0.26	± 0.03	4
358.64	± 0.2	<0.01	0.016	$\pm (2)$	5
364.460	± 0.028	100	81.7	± 0.7	1
404.79	± 0.09	0.07	0.055	$\pm (2)$	4
503.00	± 0.05	0.46	0.35	± 0.01	2
636.99	± 0.05	9.1	7.17	± 0.08	1
642.66	± 0.05	0.28	0.217	$\pm (2)$	1
722.88	± 0.05	2.3	1.77	± 0.02	1

2.29(1) hr. ^{132}I

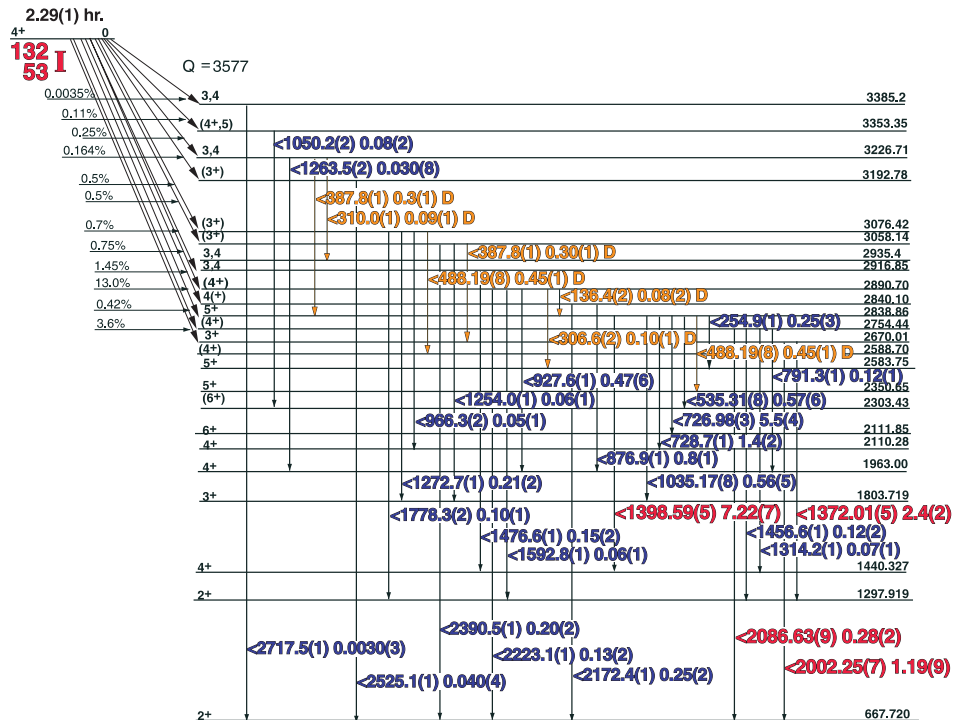


Decay Data

[Index](#)

2.29(1) hr. ^{132}I Decay Scheme

Gamma rays from high-energy levels



2.29(1) hr. ^{132}I

GAMMA-RAY ENERGIES AND INTENSITIES

Nuclide ^{132}I
Detector 3" X 3" NaI-2

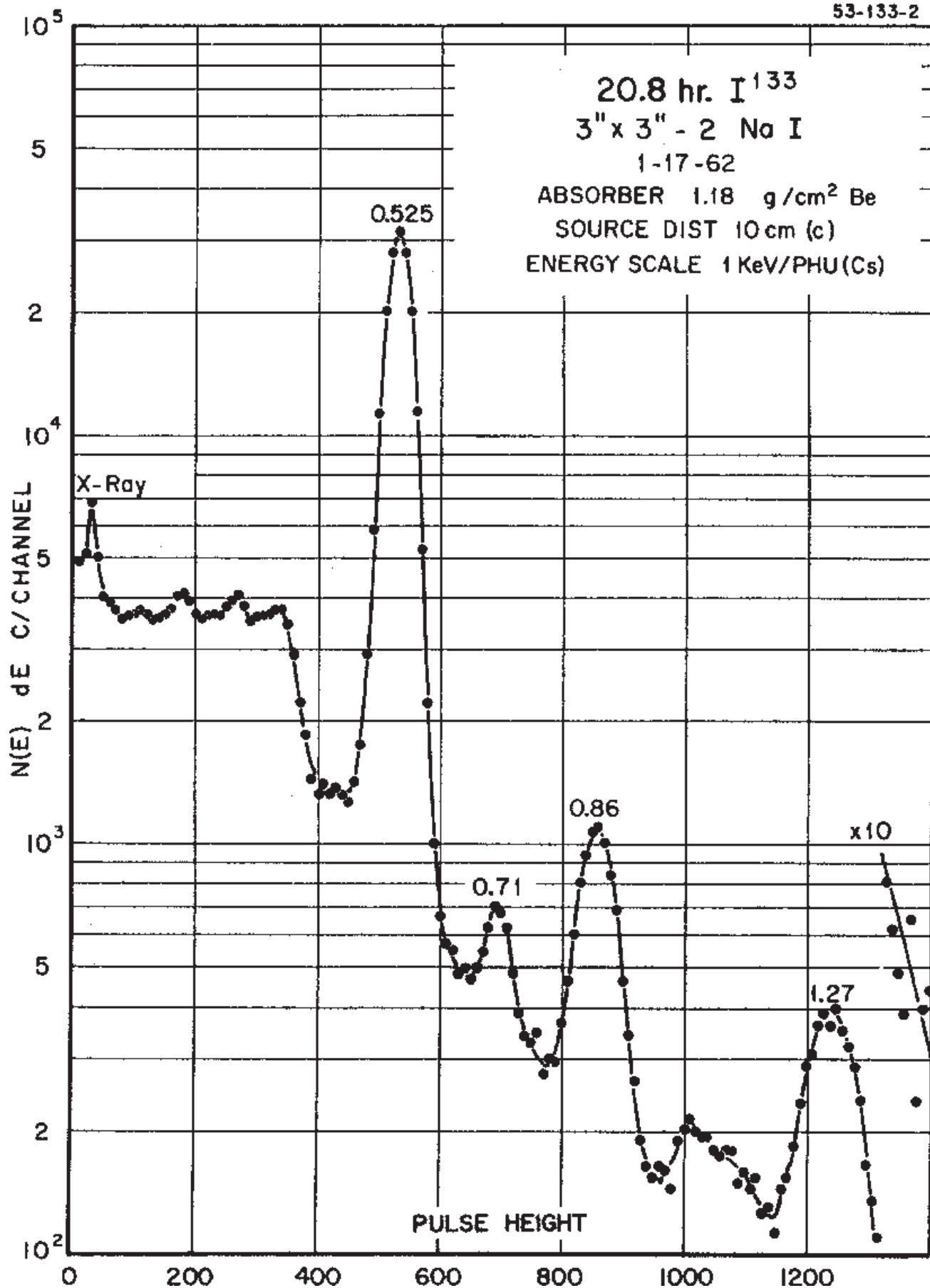
Half Life 2.29(1) hr.
Method of Production: $^{235}\text{U}(\text{n},\text{f})$

	E_{γ} (KeV)[S]	ΔE_{γ}	I_{γ} (rel)	$I_{\gamma}(\%)[E]$	ΔI_{γ}	S
D	136.3	± 0.2	0.10	0.10	± 0.01	4
	147.2	± 0.1	0.24	0.24	± 0.02	4
	183.30	± 0.2	0.18	0.18	± 0.02	4
	254.86	± 0.15	0.25	0.25	± 0.02	4
	262.84	± 0.10	1.47	1.4	± 0.12	3
D	306.7	± 0.1	0.14	0.14	± 0.02	4
D	310.0	± 0.1	0.10	0.09	± 0.01	4
D	310.4	± 0.1	0.10	0.10	± 0.01	4
	387.75	± 0.10	0.20	0.30	± 0.03	4
	416.65	± 0.1	0.46	0.45	± 0.05	4
	431.96	± 0.08	0.50	0.50	± 0.05	4
	446.16	± 0.08	0.53	0.50	± 0.05	4
	473.52	± 0.10	0.17	0.17	± 0.02	4
	488.16	± 0.08	0.92	0.45	± 0.01	4
	505.810	± 0.05	4.97	5.0	± 0.10	3
	522.640	± 0.025	16.18	16	± 0.90	1
	535.31	± 0.08	0.58	0.52	± 0.05	4
	547.00	± 0.08	1.38	1.4	± 0.11	3
D	620.963	± 0.06	2.15	2.0	± 0.2	3
	630.194	± 0.030	13.90	13.9	± 0.2	1
	650.516	± 0.035	2.74	2.7	± 0.25	2
	667.683	± 0.030	100	99	± 2.0	1
	669.8	± 0.1		4.8	± 0.3	2
	671.4	± 0.10	9.47	3.7	$\pm .4$	2
	726.95	± 0.035	5.65	5.5	± 0.45	1
	728.72	± 0.10	1.39	1.4	± 0.2	3
	772.605	± 0.030	76.99	76.0	± 0.5	1
	780.19	± 0.08	1.28	1.2	± 0.2	3
	784.85	± 0.10	0.42	0.40	± 0.05	4
	791.27	± 0.10	0.13	0.11	± 0.04	4
	809.79	± 0.08	3.03	2.9	± 0.2	2
	812.277	± 0.05	5.74	5.6	± 0.2	1
	863.21	± 0.08	0.63	0.61	± 0.06	3
	875.86	± 0.1	0.80	0.8	± 0.1	3
	876.9	± 0.1	0.60	0.8	± 0.1	3
	910.33	± 0.06	1.04	1.0	± 0.08	3
	927.67	± 0.08	0.47	0.47	± 0.06	3
	954.575	± 0.030	17.60	17.5	± 0.8	1
	966.36	± 0.10	0.06	0.05	± 0.01	4

	E_{γ} (KeV)[S]	ΔE_{γ}	I_{γ} (rel)	$I_{\gamma}(\%)[E]$	ΔI_{γ}	S
	984.41	± 0.09	0.80	0.80	± 0.08	3
	1035.17	± 0.08	0.57	0.52	± 0.05	3
	1050.22	± 0.15	0.10	0.08	± 0.02	4
	1087.10	± 0.10	0.09	0.08	± 0.01	4
	1136.026	± 0.040	3.23	3.2	± 0.1	1
	1143.59	± 0.06	1.57	1.5	± 0.1	2
	1148.30	± 0.10	0.40	0.40	± 0.04	4
	1173.22	± 0.08	1.29	1.2	± 0.10	3
	1254.0	± 0.2	0.05	0.06	± 0.01	4
	1263.5	± 0.2	0.03	0.030	± 0.008	4
	1272.68	± 0.10	0.21	0.21	± 0.02	3
	1290.76	± 0.08	1.21	1.15	± 0.06	2
	1295.34	± 0.06	1.85	1.8	± 0.10	1
	1298.09	± 0.10	0.71	0.70	± 0.06	2
	1314.24	± 0.15	0.08	0.06	± 0.01	4
	1317.76	± 0.10	0.11	0.11	± 0.01	3
	1372.01	± 0.05	2.52	2.4	± 0.20	1
	1398.59	± 0.05	7.42	7.22	± 0.07	1
	SE 1410.0					
	sum1440.11		0.41		± 0.04	3
	1442.537	± 0.08	1.44	1.42	± 0.05	1
	1456.6	± 0.15	0.12	0.12	± 0.02	3
	1476.64	± 0.10	0.15	0.15	± 0.02	3
	SE 1491.0					
	1519.5	± 0.10	0.10	0.10	± 0.02	3
	1592.8	± 0.15	0.07	0.06	± 0.01	4
	1727.15	± 0.15	0.11	0.10	± 0.02	4
	1757.7	± 0.2	0.35	0.34	± 0.03	3
	1778.3	± 0.2	0.10	0.10	± 0.01	4
	1920.96	± 0.08	1.24	1.20	± 0.08	1
	2002.25	± 0.07	1.22	1.19	± 0.09	1
	2086.63	± 0.09	0.28	0.28	± 0.02	1
	2172.38	± 0.10	0.25	0.25	± 0.02	2
	2223.10	± 0.10	0.126	0.13	± 0.02	2
	2249.4	± 0.2	0.04	0.034	± 0.002	3
	2390.5	± 0.1	0.20	0.20	± 0.02	3
	2525.1	± 0.04	0.04	0.040	± 0.004	3
	2717.0	± 1.0	0.003	0.0035	± 0.001	3

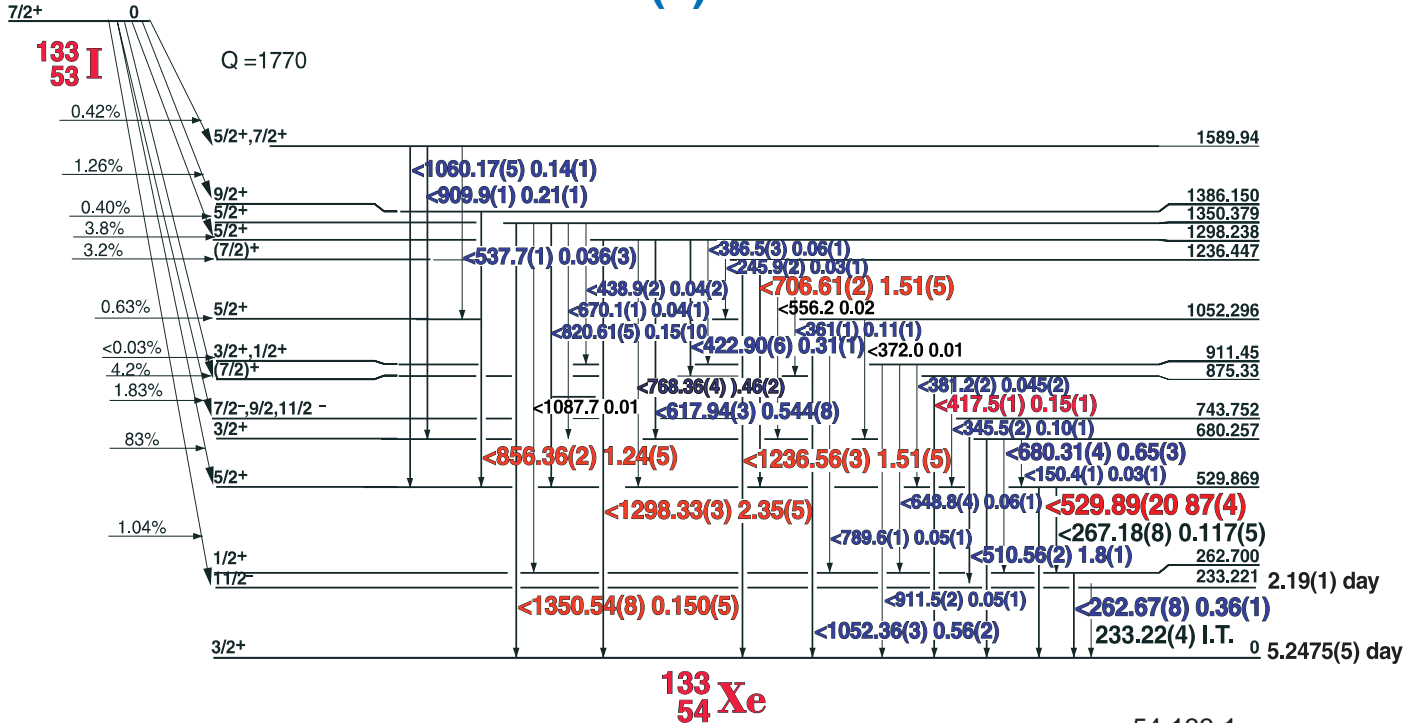
20.8(1) hr. I^{133}

53-133-2



20.8(1) hr.

7/2+

20.8(1) hr. ^{133}I  **^{133}Xe**

54-133-1

GAMMA-RAY ENERGIES AND INTENSITIESNuclide
Detector ^{133}I
3" x 3" -2 NaI

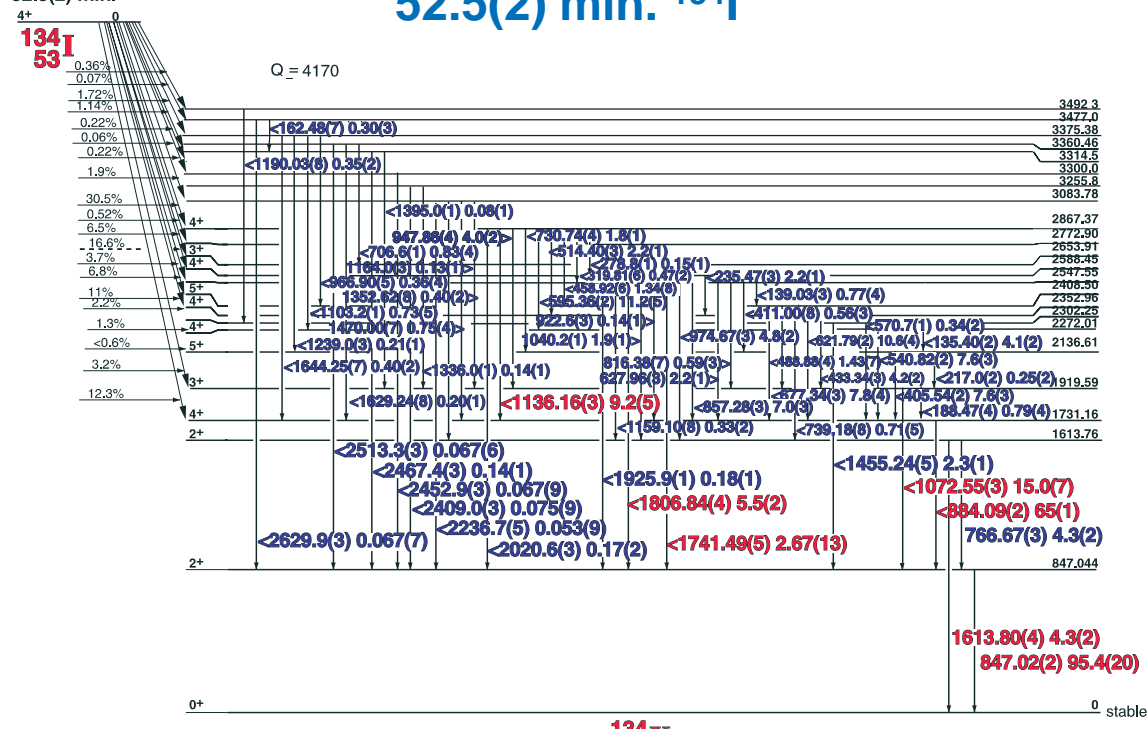
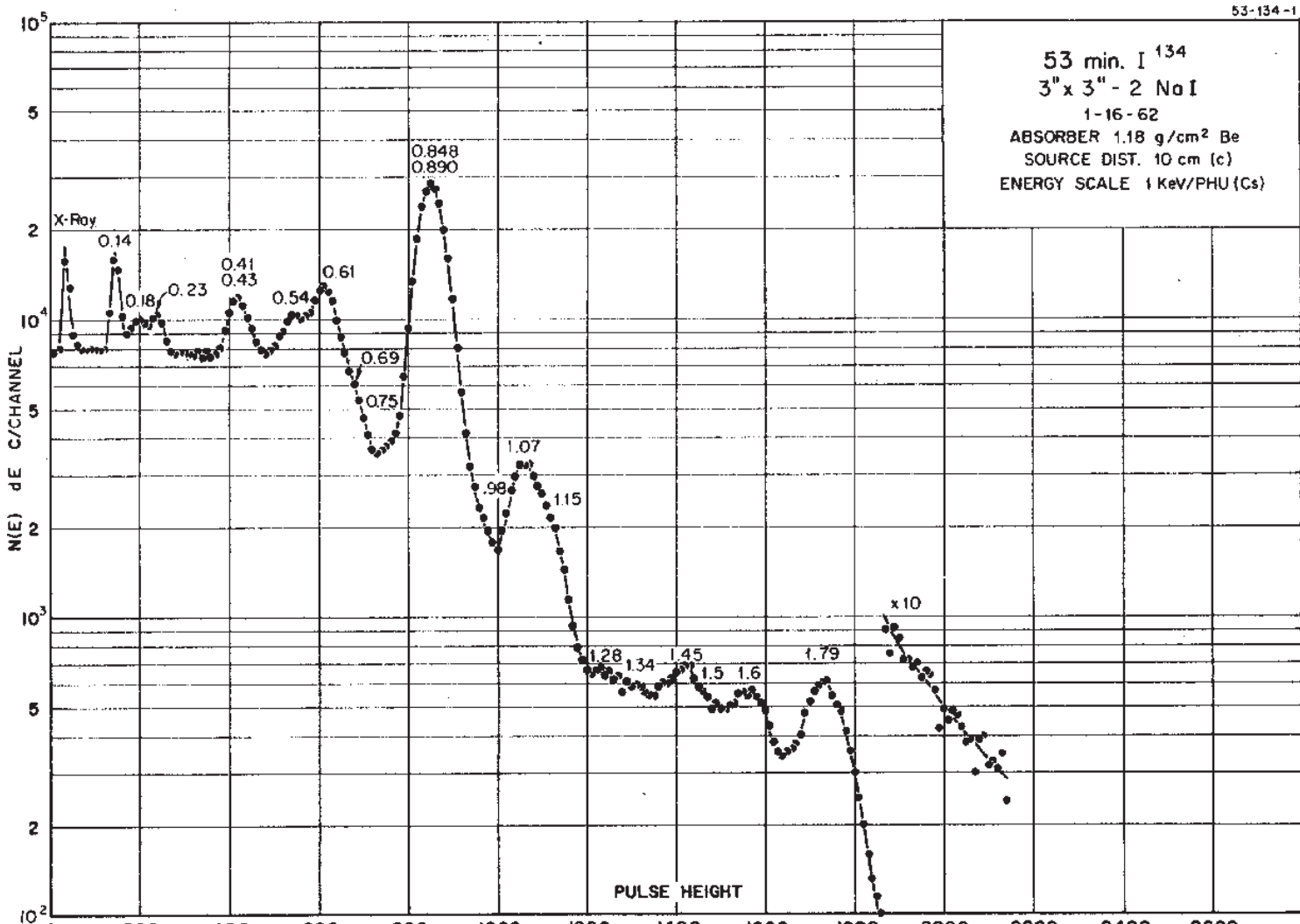
Half Life 20.8(1) hr.

Method of Production: $^{235}\text{U}(\text{n},\text{f})$ ^{133}Xe

E_{γ} (KeV)[S]	ΔE_{γ}	I_{γ} (rel)	$I_{\gamma}(\%)$ [E]	ΔI_{γ}	S
80.99					1
150.0	± 0.5	0.018	0.03	± 0.01	4
233.18	± 0.2	0.13	0.10	± 0.01	4
245.92	± 0.2	0.099	0.03	± 0.015	4
262.67	± 0.08	0.46	0.36	± 0.01	4
267.18	± 0.08	0.16	0.117	± 0.005	4
345.7	± 0.5	0.49	0.10	± 0.01	4
361.0	± 0.3	0.27	0.11	± 0.01	4
381.23	± 0.25	0.062	0.045	± 0.002	5
386.5	± 0.3	0.079	0.06	± 0.010	5
417.50	± 0.2	0.17	0.15	± 0.02	4
422.90	± 0.06	0.36	0.31	± 0.01	3
438.92	± 0.20	0.046	0.04	± 0.02	4
503.0	± 0.5	0.025		± 0.005	5
510.565 ± 0.020	2.09	1.8	± 0.15	2	
529.889 ± 0.018	100	87	± 4.0	1	
537.7	± 0.1	0.036	0.31	± 0.01	4
617.94	± 0.03	0.65		± 0.06	3
642.6	± 0.5	0.0257		± 0.005	4
648.8	± 0.5	0.055		± 0.005	4
667.5	± 0.6				
670.0	± 1.0	0.14	0.04	± 0.01	4

E_{γ} (KeV)[S]	ΔE_{γ}	I_{γ} (rel)	$I_{\gamma}(\%)$ [E]	ΔI_{γ}	S
680.31	± 0.04	0.80	0.65	± 0.03	2
706.606	± 0.025	1.71	1.61	± 0.06	1
768.36	± 0.04	0.56	0.46	± 0.02	2
789.50	± 0.10	0.046	0.05	± 0.01	4
820.61	± 0.05	0.19	0.15	± 0.01	3
846.4	± 1.0	0.012		± 0.007	4
856.361	± 0.025	1.41	1.24	± 0.05	1
875.370	± 0.025	5.10	4.51	± 0.20	1
909.92	± 0.10	0.27	0.21	± 0.01	3
911.5	± 0.2	0.263	0.06	± 0.01	3
1052.365	± 0.030	0.65	0.56	± 0.02	2
1060.17	± 0.05	0.18	0.14	± 0.01	3
1236.565	± 0.035	1.8	1.51	± 0.05	1
1298.329	± 0.030	2.71	2.35	± 0.14	1
1350.54	± 0.08	0.167	0.150	± 0.05	1

52.5(2) min.

52.5(2) min. ^{134}I  **^{134}Xe** 

52.5(2) min. ^{134}I

54-134-1

GAMMA-RAY ENERGIES AND INTENSITIES

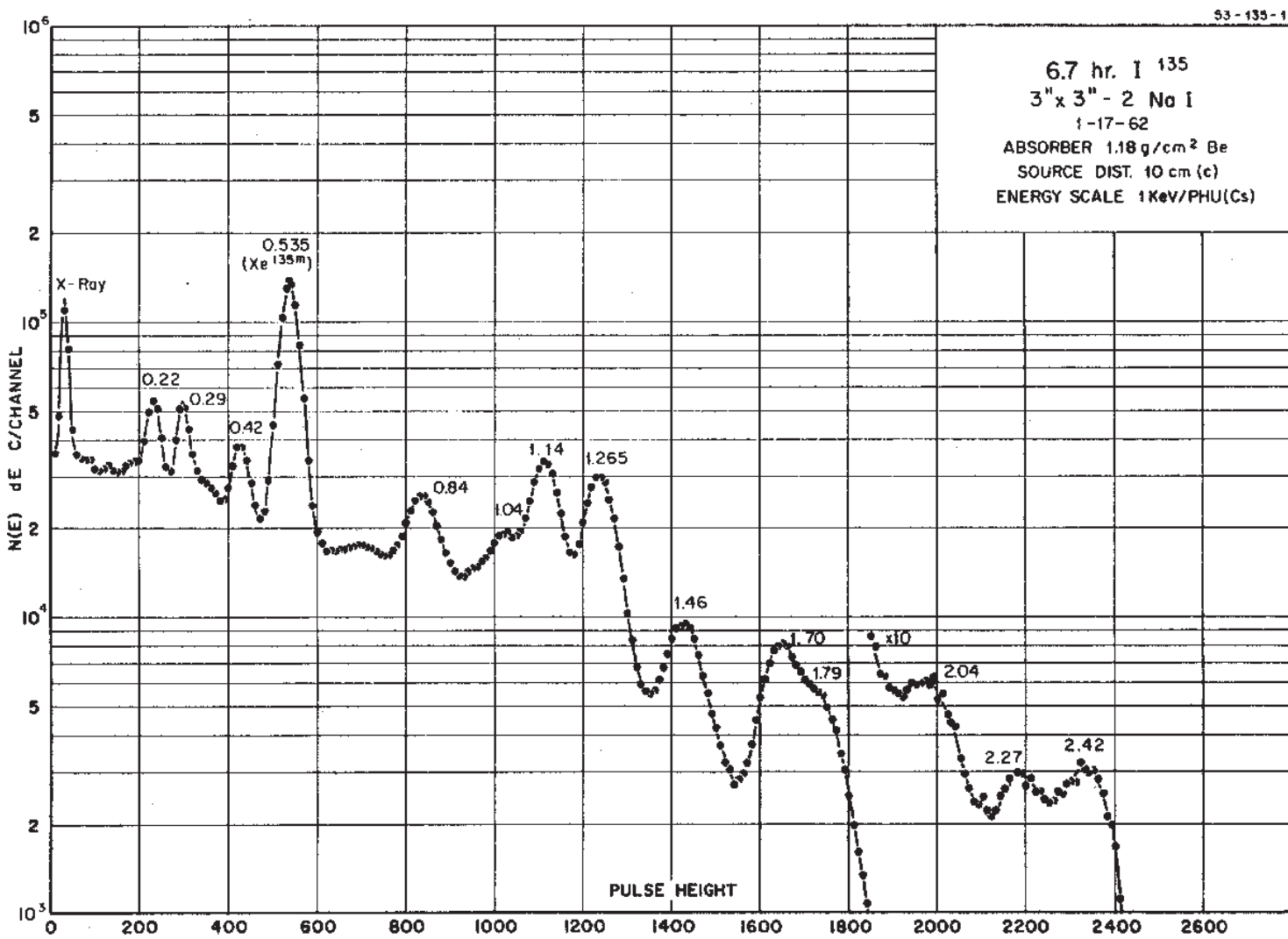
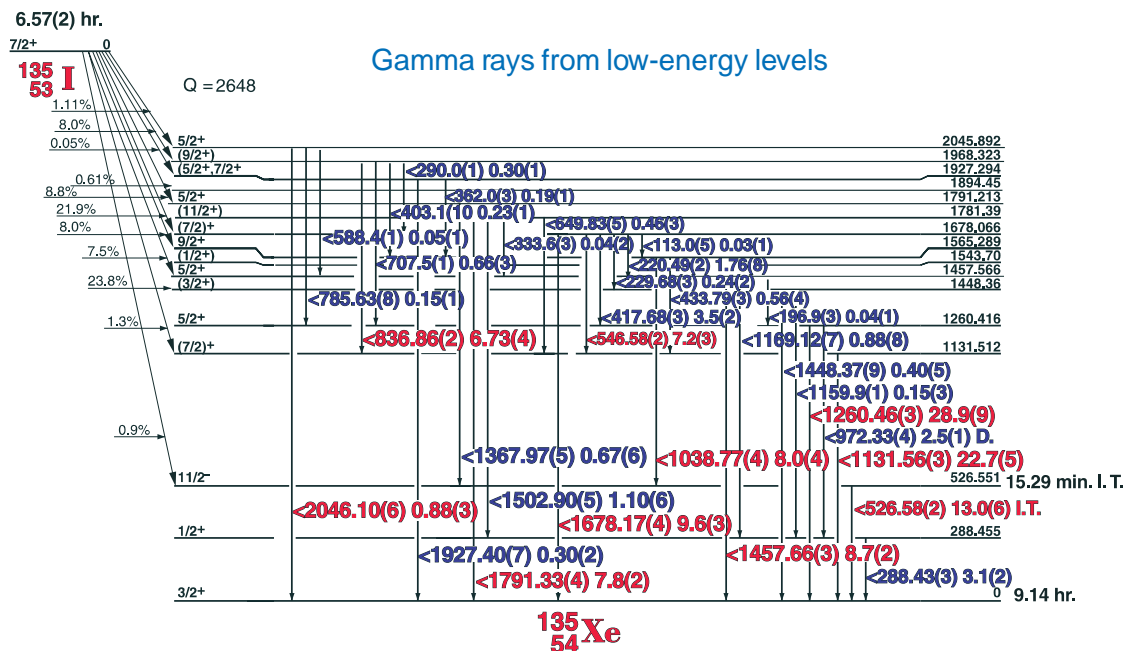
Nuclide ^{134}I
 Detector 3" x 3" -2 Nal

Half Life 52.5(2) min.
 Method of Production: $^{235}\text{U}(\text{n},\text{f})$

E_{γ} (KeV)[S]	ΔE_{γ}	$I_{\gamma}(\text{rel})$	$I_{\gamma}(\%)[E]$	ΔI_{γ}	S
135.399	± 0.022	3.94	4.1	± 0.2	3
139.030	± 0.030	0.72	0.77	± 0.04	4
151.98	± 0.15	0.11		± 0.012	4
162.48	± 0.07	0.27	0.30	± 0.03	4
188.47	± 0.04	0.73	0.79	± 0.04	3
217.0	± 0.2	0.26	0.23	± 0.02	4
235.471	± 0.026	2.08	2.2	± 0.1	3
262.6	± 0.3	0.44		± 0.02	4
278.80	± 0.15	0.13	0.15	± 0.01	4
319.81	± 0.06	0.54	0.47	± 0.02	4
351.08	± 0.10	0.52		± 0.06	4
405.541	± 0.020	7.7	7.6	± 0.3	2
411.00	± 0.08	0.64	0.56	± 0.03	4
433.345	± 0.030	4.39	4.2	± 0.2	3
458.92	± 0.06	1.36	1.34	± 0.08	3
465.50	± 0.10	0.38		\pm	
488.88	± 0.04	1.48	1.43	± 0.07	3
514.400	± 0.030	2.45	2.2	± 0.1	3
540.825	± 0.025	8.2	7.63	± 0.3	2
565.52	± 0.04	0.92		± 0.06	4
595.362	± 0.020	11.9	11.2	± 0.5	2
621.790	± 0.025	11.1	10.6	± 0.4	2
627.960	± 0.030	2.48	2.2	± 0.1	3
677.338	± 0.030	8.9	7.8	± 0.4	3
706.65	± 0.10	0.87	0.83	± 0.04	4
730.74	± 0.04	2.00	1.8	± 0.1	3
739.18	± 0.08	0.80	0.71	± 0.05	4
766.675	± 0.035	4.30	4.3	± 0.2	3
784.9	± 0.3	0.28		± 0.05	4
816.38	± 0.07	0.55	0.59	± 0.03	4
847.025	± 0.025	100	95.4	± 2.0	1
857.285	± 0.030	7.3	7.0	± 0.3	2
884.090	± 0.025	68.4	65	± 1.0	1
922.6	± 0.3	0.15	0.14	± 0.02	4
947.86	± 0.04	4.23	4.0	± 0.20	2
966.90	± 0.05	0.37	0.36	± 0.04	4
974.670	± 0.035	4.88	4.8	± 0.2	2
1040.25	± 0.10	2.01	1.9	± 0.1	3
1072.55	± 0.030	16.0	15.0	± 0.7	1
1103.18	± 0.12	0.76	0.73	± 0.05	3
1136.16	± 0.035	10.2	9.2	± 0.51	

E_{γ} (KeV)[S]	ΔE_{γ}	$I_{\gamma}(\text{rel})$	$I_{\gamma}(\%)[E]$	ΔI_{γ}	S
1159.10	± 0.08	0.32	0.33	± 0.02	3
1164.0	± 0.3	0.14	0.13	± 0.01	4
1190.03	± 0.08	0.37	0.35	± 0.02	3
1239.0	± 0.3	0.22	0.21	± 0.01	4
1336.0	± 0.2	0.15	0.14	± 0.01	4
1352.62	± 0.08	0.47	0.40	± 0.02	3
1395.0	± 1.0	0.08	0.08	± 0.01	4
1455.24	± 0.05	2.40	2.3	± 0.1	2
1470.00	± 0.07	0.81	0.75	± 0.04	3
1505.5	± 0.4	0.12		± 0.04	4
1541.51	± 0.07	0.53		± 0.04	3
1613.800	± 0.043	4.57	4.3	± 0.2	1
1629.24	± 0.08	0.27	0.20	± 0.01	3
1644.25	± 0.07	0.43	0.40	± 0.02	3
1655.19	± 0.10	0.24		± 0.03	3
1741.49	± 0.05	2.8	2.67	± 0.15	1
1806.84	± 0.040	5.95	5.5	± 0.30	1
1868.5	± 0.2	0.07		± 0.02	3
1893.2	± 0.3	0.06		± 0.01	4
1925.88	± 0.10	0.19	0.18	± 0.01	3
1947.3	± 0.3	0.10		± 0.02	3
2020.6	± 0.3	0.18	0.17	± 0.02	3
2159.9	± 0.3	0.22		± 0.03	2
2236.7	± 0.5	0.056	0.053	± 0.009	3
2262.5	± 0.3	0.10		± 0.02	3
2312.4	± 0.2	0.25		± 0.03	2
2409.0	± 0.3	0.079	0.075	± 0.009	3
2452.9	± 0.3	0.067	0.067	± 0.009	3
2467.4	± 0.3	0.16	0.14	± 0.01	2
2513.3	± 0.3	0.073	0.067	± 0.006	3
2629.9	± 0.3	0.070	0.067	± 0.008	3
2699.5	± 0.5	0.034		± 0.008	3
2840.0	± 4.0	0.02		± 0.01	4

6.57(2) hr. ^{135}I

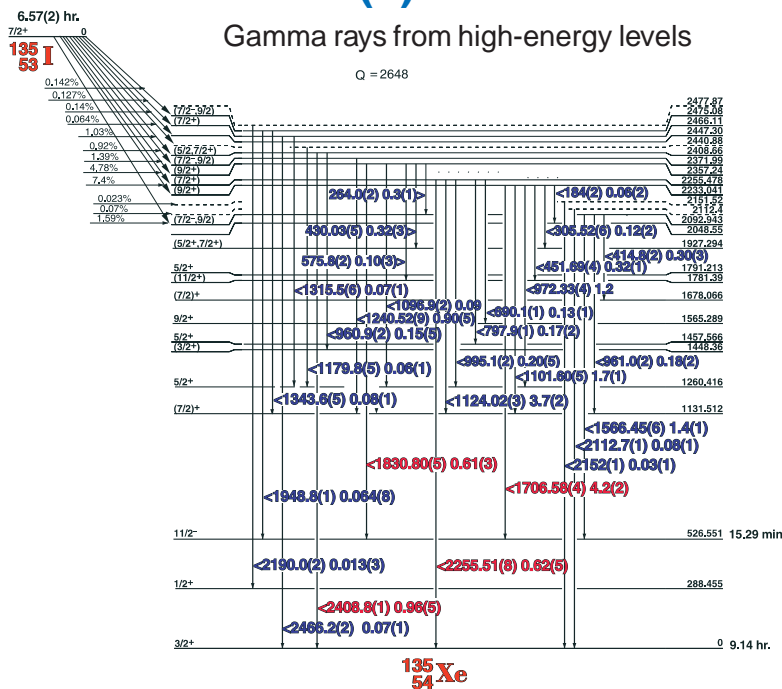


Decay Data

← Index →

6.57(2) hr. ^{135}I

Gamma rays from high-energy levels



54-135-1

GAMMA-RAY ENERGIES AND INTENSITIES

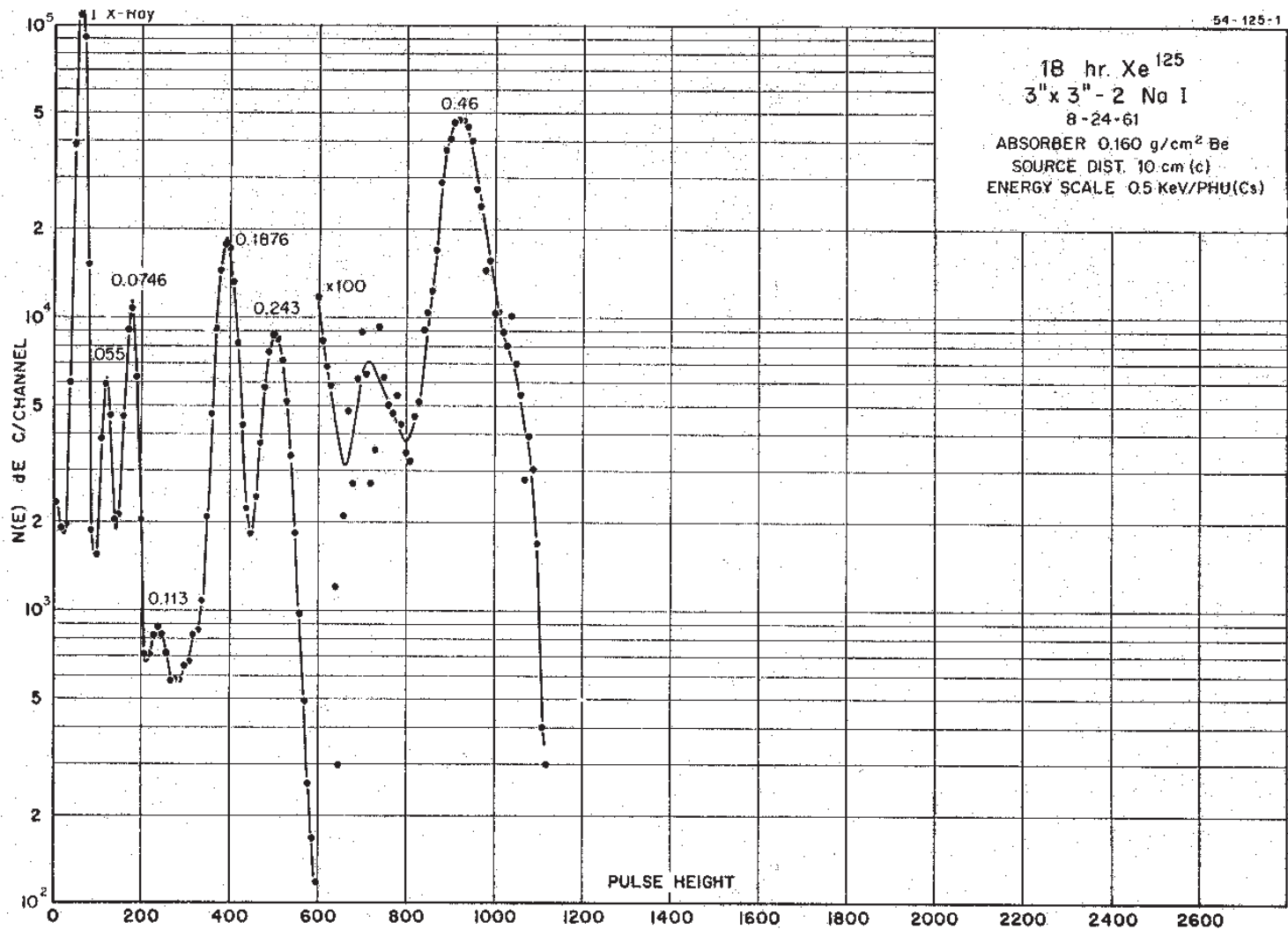
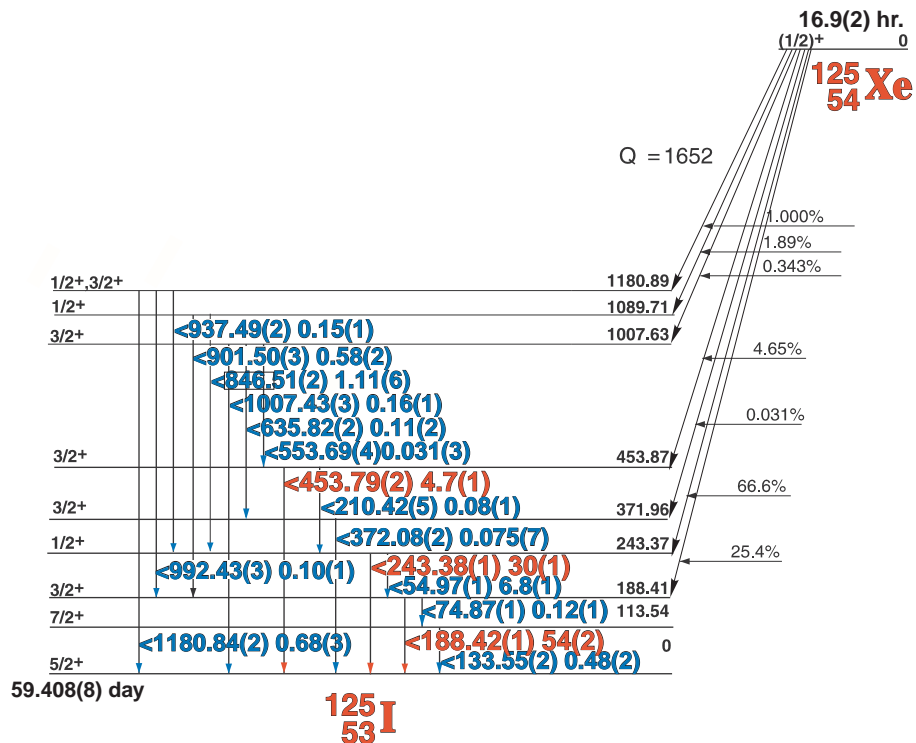
Nuclide ^{135}I
Detector 3" x 3" -2 NaI

Half Life 6.57(2) hr.
Method of Production: $^{235}\text{U}(\text{n},\text{f})$

	E_{γ} (KeV)[S]	ΔE_{γ}	$I_{\gamma}(\text{rel})$	$I_{\gamma}(\%)[E]$	ΔI_{γ}	S
D	113.0	± 0.6	0.097	0.03	± 0.01	4
	158.18	± 0.05	0.83		± 0.07	4
	184.0	$+ 2.0$	0.19	0.06	± 0.02	4
	196.85	± 0.30	0.16	0.04	± 0.01	4
	220.490	± 0.020	6.4	1.76	± 0.03	3
	229.680	$+ 0.026$	0.74	0.24	± 0.02	4
	264.03	$+ 0.25$	1.1	0.31	± 0.03	4
	288.43	± 0.03	11.7	3.1	± 0.2	3
	289.8	± 0.5		0.30	± 0.06	4
	305.52	± 0.06	0.47	0.12	± 0.02	4
	333.6	± 0.3	0.163	0.04	± 0.01	4
	362.0	± 0.3	0.43	0.19	± 0.01	4
	403.10	± 0.08	1.05	0.23	± 0.01	4
	414.8	± 0.3	1.1	0.30	± 0.03	4
	417.685	± 0.028	12.5	3.5	± 0.2	2
	430.026	± 0.053	1.10	0.32	± 0.03	4
	433.789	± 0.035	1.81	0.56	± 0.04	4
	451.691	± 0.038	1.03	0.32	± 0.02	4
135m	Xe 526.581	± 0.018	45.0	13.0	± 0.6	1
	546.579	± 0.020	24.8	7.2	± 0.3	1
	575.8	± 0.2	0.31	0.10	± 0.01	4
	588.37	± 0.14	0.09	0.05	± 0.01	4
	649.83	± 0.05	1.56	0.46	± 0.03	4
	690.10	± 0.15	0.58	0.13	± 0.01	4
	707.53	± 0.12	2.8	0.66	± 0.07	3
	785.63	± 0.08	0.48	0.15	± 0.01	4
	797.88	± 0.15	0.53	0.17	± 0.02	4
	813.0	± 0.8	0.23		± 0.04	4
	836.865	± 0.022	22.5	6.73	± 0.33	1
D	960.98	± 0.20	0.63	0.16	± 0.02	4
	972.33	± 0.04	7.6	2.4	± 0.12	3
	995.09	± 0.20	0.76	0.24	± 0.02	4

	E_{γ} (KeV)[S]	ΔE_{γ}	$I_{\gamma}(\text{rel})$	$I_{\gamma}(\%)[E]$	ΔI_{γ}	S
	1038.77	± 0.04	28.2	8.2	± 0.41	1
	1096.9	± 2.0	0.2	0.09	± 0.01	4
	1101.60	± 0.05	5.6	1.7	± 0.09	3
	1124.020	± 0.030	12.7	3.8	± 0.19	2
	1131.561	± 0.028	76.4	22.7	± 0.5	1
	1159.95	± 0.15	0.53	0.15	± 0.03	4
	1169.12	± 0.07	3.22	0.88	± 0.08	3
	1179.8	± 0.6	0.19	0.06	± 0.01	4
	1240.52	± 0.09	3.00	0.90	± 0.05	3
	1260.462	± 0.030	100	28.9	± 0.9	1
	1315.5	± 0.5	0.40	0.07	± 0.01	4
	1343.6	± 0.5	0.31	0.09	± 0.01	4
	1367.97	± 0.05	2.30	0.69	± 0.06	3
	1448.37	± 0.09	1.5	0.45	± 0.05	4
	1457.660	± 0.035	30.4	8.7	± 0.2	1
	1502.90	± 0.05	3.9	1.10	± 0.06	2
	1566.45	± 0.06	4.9	1.4	± 0.08	2
	1678.175	± 0.038	34.1	9.6	± 0.3	1
	1706.580	± 0.045	14.5	4.2	± 0.21	1
	1791.326	± 0.038	28.1	7.8	± 0.2	1
	1830.80	± 0.05	2.11	0.62	± 0.04	1
	1927.40	± 0.07	1.12	0.30	± 0.02	2
	1948.80	± 0.12	0.278	0.064	± 0.008	3
	1968.2	± 1.5	VW			4
	2046.10	± 0.06	3.13	0.88	± 0.03	1
	2112.68	± 0.14	0.27	0.08	± 0.01	3
	2152.1	± 1.5	0.11	0.03	± 0.008	4
	2190.0	VW		0.013	± 0.001	4
	2255.51	± 0.08	2.16	0.63	± 0.05	1
	2408.77	± 0.12	3.22	0.96	± 0.05	1
	2466.25	± 0.25	0.24	0.07	± 0.01	2

16.9(2) hr. ^{125}Xe



16.9(2) hr. ^{125}Xe

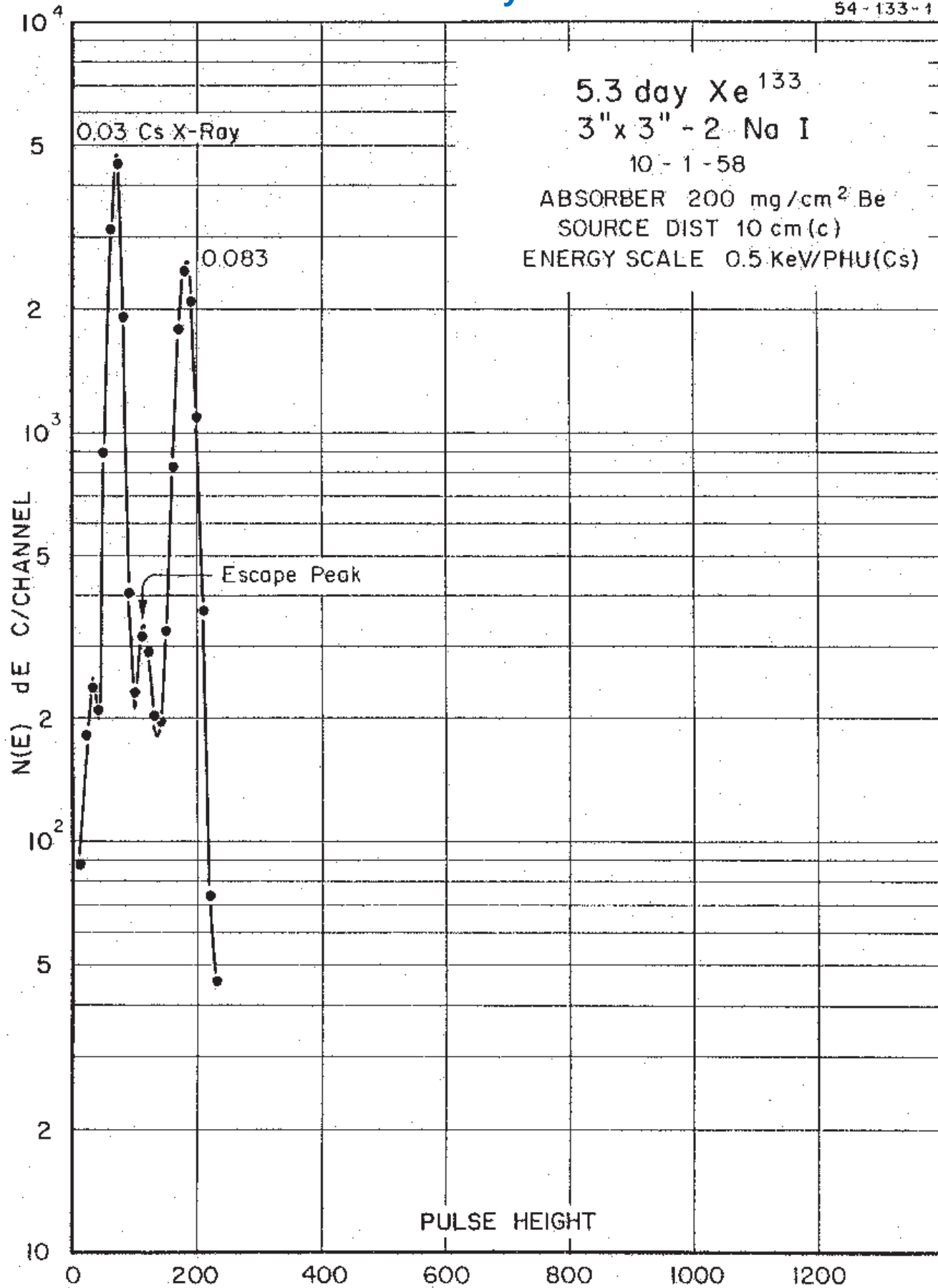
GAMMA-RAY ENERGIES AND INTENSITIES

Nuclide ^{125}Xe Half Life 16.9(2) hr.
Detector 3" X 3" NaI-2 Method of Production: $^{124}\text{Xe}(n,\gamma)$

E_γ (KeV)[S]	ΔE_γ	I_γ (rel)	$I_\gamma(\%)$ [E]	ΔI_γ	S
53.15	± 0.05	3.0	2.2	± 0.1	3
79.60	± 0.05	5.6	2.6	± 0.1	3
80.998	± 0.008	52.0	34.0	± 0.3	1
160.605	± 0.015	1.12	0.64	± 0.01	3
223.246	± 0.030	0.85	0.45	± 0.02	3
276.397	± 0.012	11.69	7.16	± 0.07	1
302.851	± 0.015	29.78	18.3	± 0.1	1
356.005	± 0.017	100	62.0	± 0.8	1
383.851	± 0.020	14.43	8.9	± 0.1	1

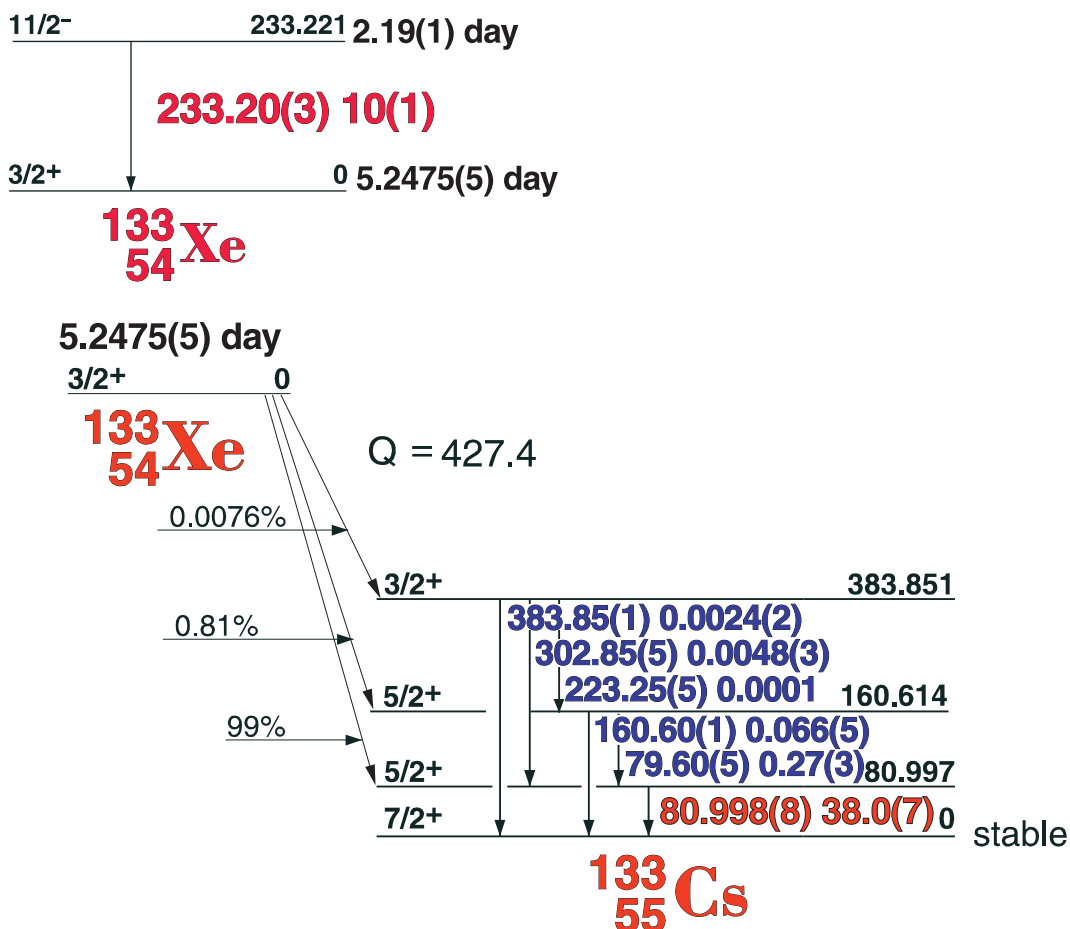
5.2475 day ^{133}Xe

54 - 133 - 1



5.2475(5) day ^{133}Xe

^{133}Xe Decay Scheme



GAMMA-RAY ENERGIES AND INTENSITIES

Nuclide ^{133}Xe Half Life 5.2475(5) day
 Detector 3" X 3" NaI-2 Method of Production: $^{235}\text{U}(\text{n},\text{f})$

E_γ (KeV) [S]	ΔE_γ	I_γ (rel)	I_γ (%) [E]	ΔI_γ	S
79.60	+ 0.05	0.8	0.27	± 0.03	4
80.998	± 0.008	100	38.0	± 0.7	1
160.605	± 0.015	0.09	0.088	± 0.005	3
223.25	± 0.05	<0.01	0.0001		5
302.851	± 0.05	0.02	0.0048	± 0.0003	3
383.851	± 0.07	0.01	0.0024	± 0.0002	4
^{133}mXe	233.185 ± 0.04		10	± 1.0	1

9.14 hr. ^{135}Xe

54-135-1

5.3 day- Xe^{133} 9.2 hrs.

Xe^{135} GAMMAS

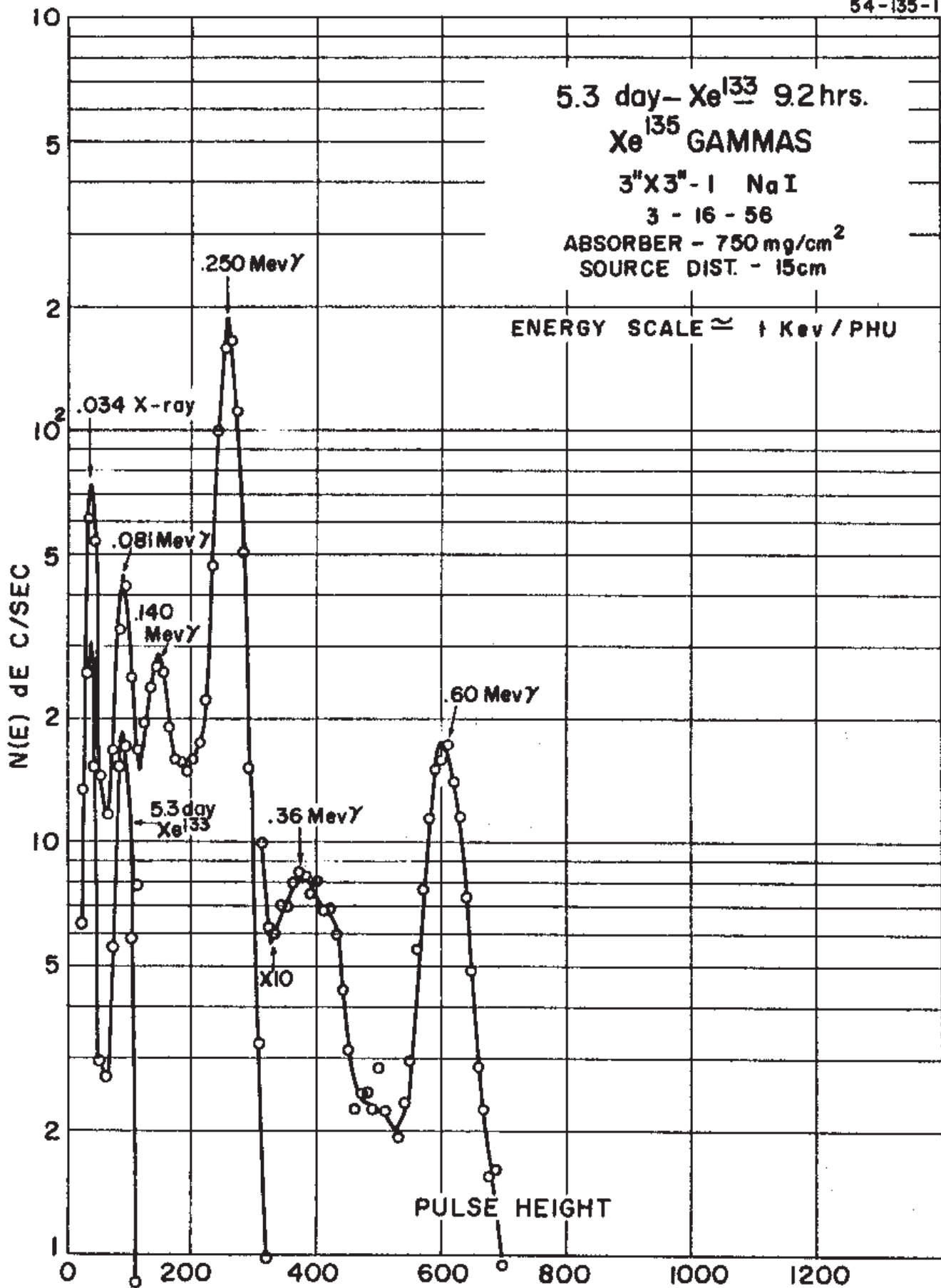
3" X 3" - 1 NaI

3 - 16 - 56

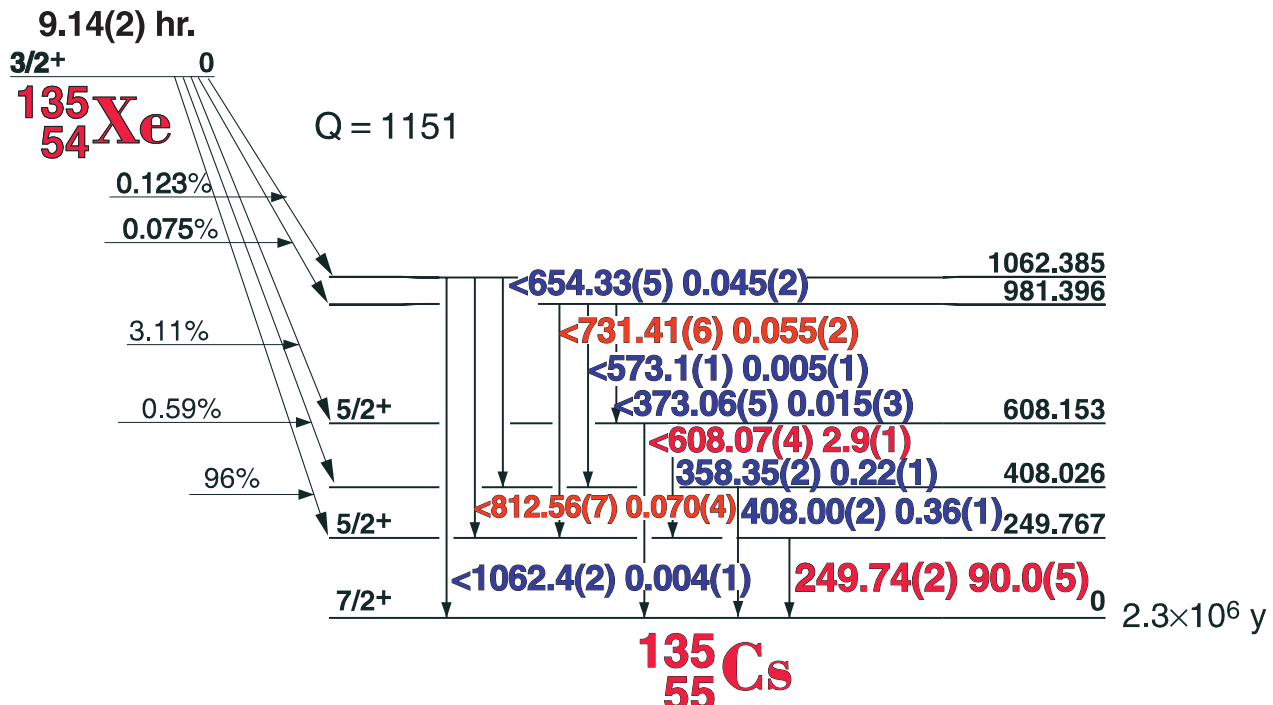
ABSORBER - 750 mg/cm²

SOURCE DIST. - 15cm

ENERGY SCALE \approx \pm Kev / PHU



9.14(2) hr. ^{135}Xe Decay Scheme

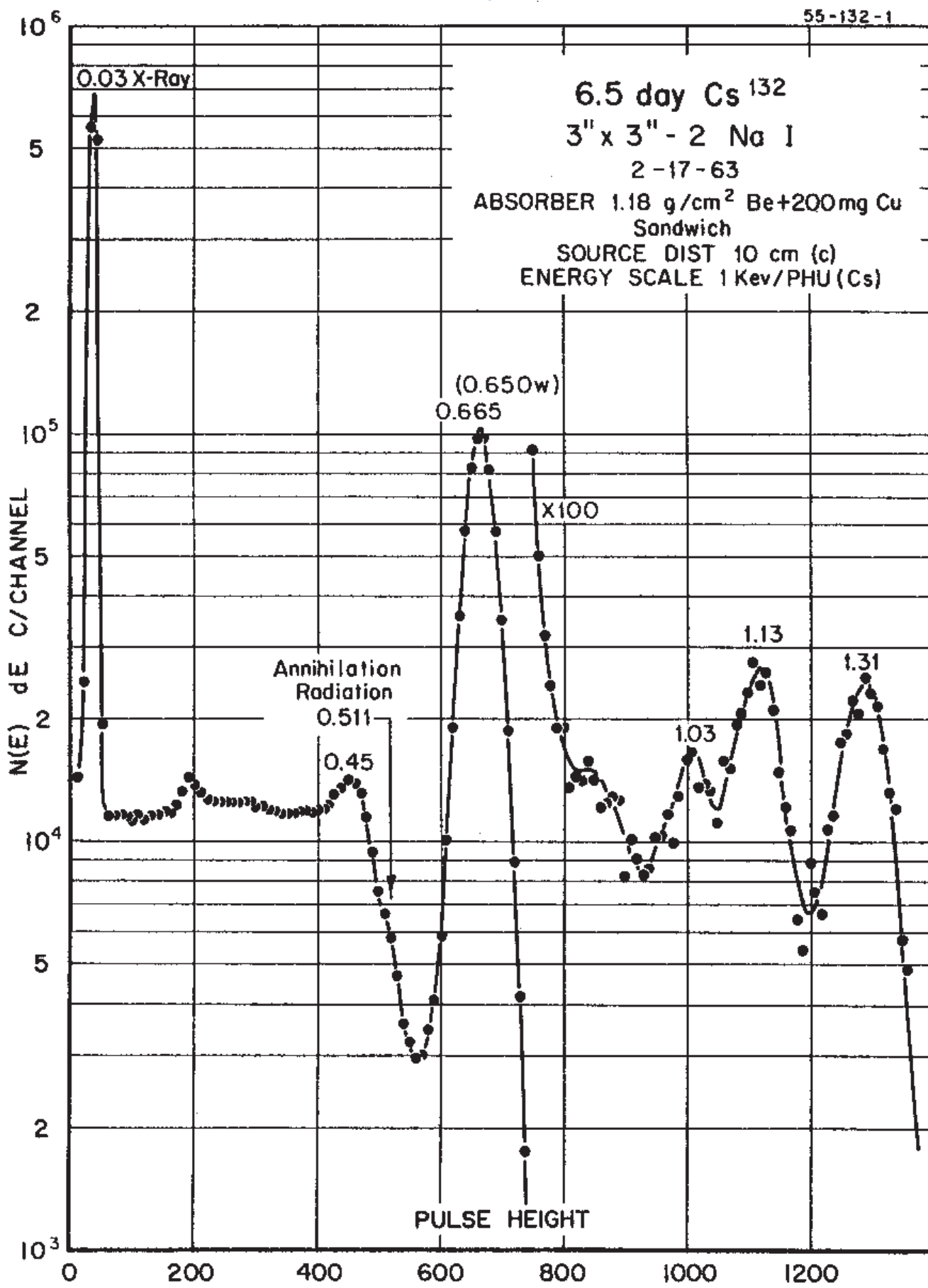


GAMMA-RAY ENERGIES AND INTENSITIES

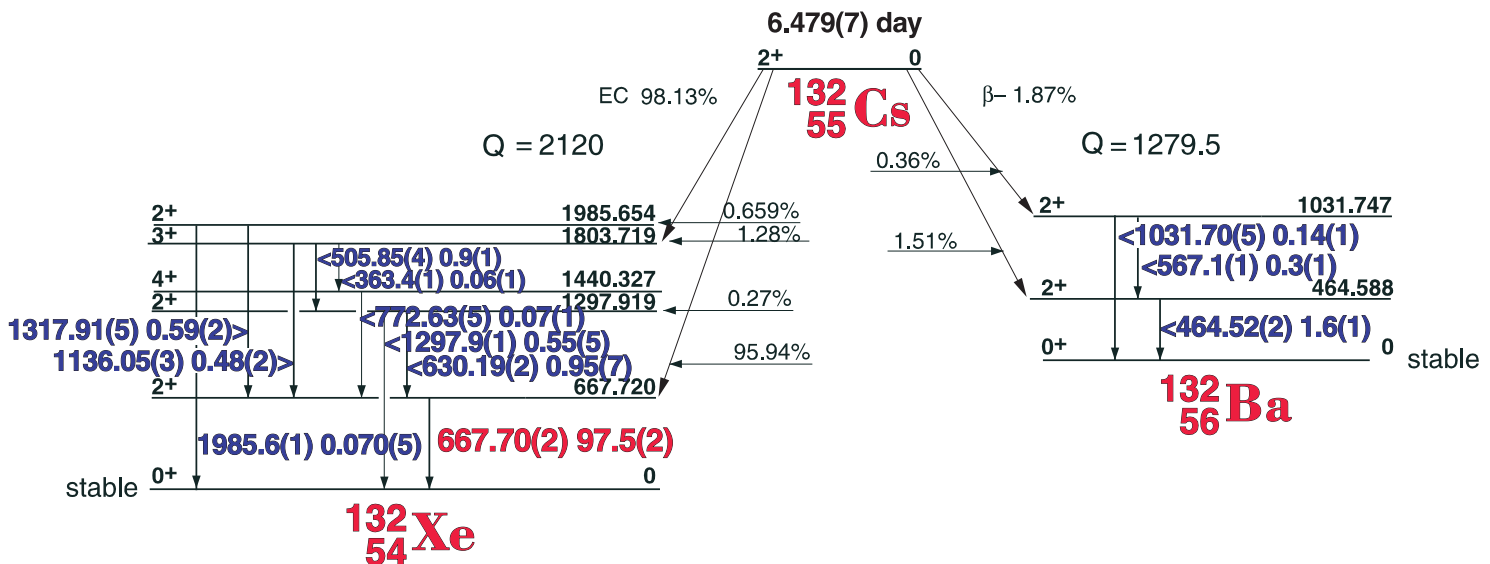
Nuclide ^{135}Xe
Detector 3" X 3" NaI-2
Half Life 9.14(2) hr.
Method of Production: $^{235}\text{U}(\text{n},\text{f})$

E_γ (KeV)[S]	ΔE_γ	I_γ (rel)	I_γ (%)[E]	ΔI_γ	S
158.23	± 0.08	0.28		± 0.003	4
249.738	± 0.015	100	90.0	± 0.5	1
358.35	± 0.02	0.26	0.22	± 0.01	2
373.06	± 0.05	0.016	0.015	± 0.003	4
408.00	± 0.02	0.39	0.36	± 0.01	2
573.1	± 0.1	0.003	0.005	± 0.001	4
608.07	± 0.04	3.33	2.9	± 0.1	1
654.33	± 0.06	0.061	0.045	± 0.002	2
731.41	± 0.06	0.067	0.055	± 0.002	2
812.56	± 0.07	0.086	0.070	± 0.004	2
981.2	± 0.2	0.003		± 0.001	4
1062.4	± 0.2	0.003	0.004	± 0.001	4

6.479 day ^{132}Cs



6.479(2) day ^{132}Cs Decay Scheme



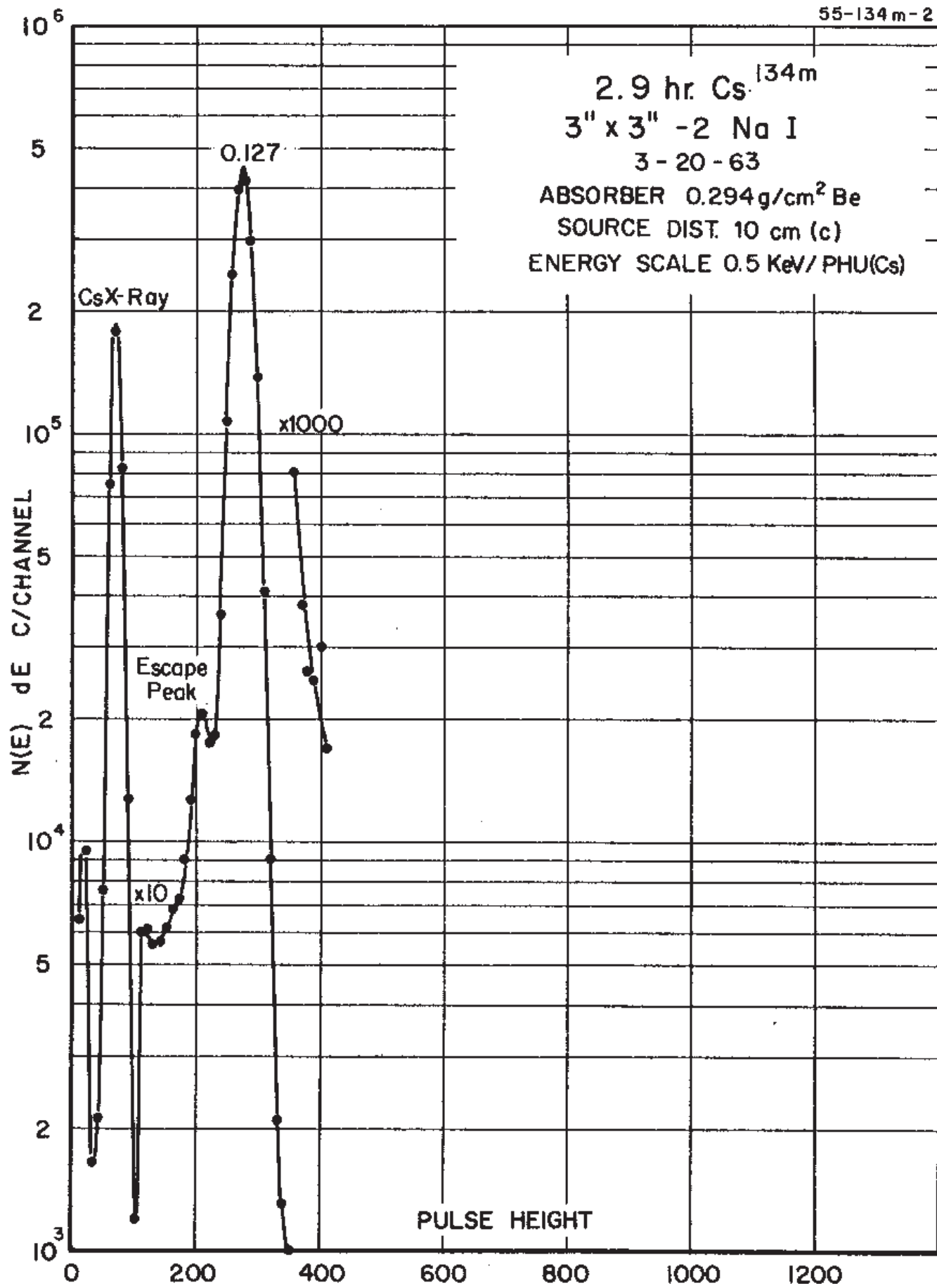
GAMMA-RAY ENERGIES AND INTENSITIES

Nuclide ^{132}Cs
 Detector 3" X 3" NaI-2 Half Life 6.479(7) day
 Method of Production: $^{133}\text{Cs}(\gamma, n)$

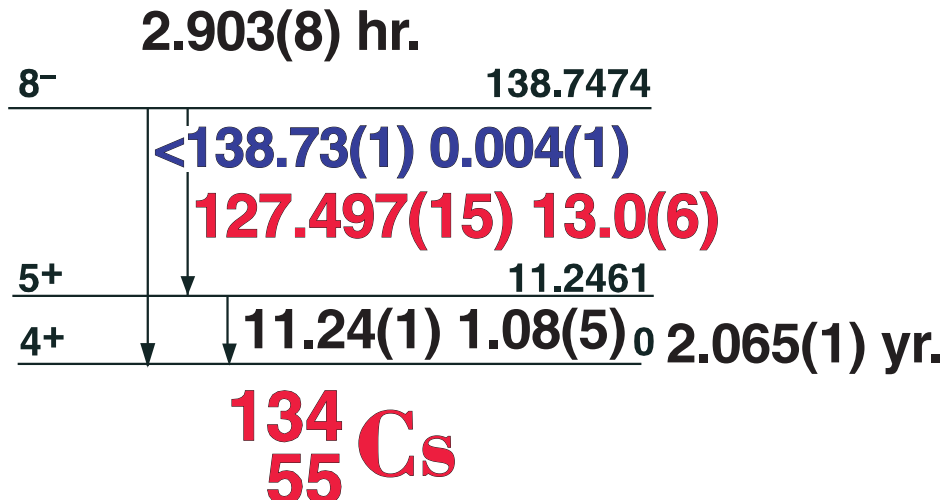
E_γ (KeV)[S]	ΔE_γ	I_γ (rel)	I_γ (%)[E]	ΔI_γ	S
363.45	± 0.10	0.06	0.05	± 0.01	4
464.52	± 0.02	1.6	1.5	± 0.1	4
505.85	± 0.04	1.0	0.9	± 0.1	4
511.006					
567.08	± 0.10	0.40	0.35	± 0.06	4
630.19	± 0.02	1.0	0.95	± 0.07	2
667.699	± 0.020	100	97.5	± 0.2	1
772.63	± 0.05	0.10	0.07	± 0.01	3
795.8	± 0.1	0.12	0.12	± 0.02	3
1031.70	± 0.05	0.14	0.14	± 0.01	2
1136.05	± 0.03	0.48	0.48	± 0.02	1
1297.86	± 0.15	0.065	0.55	± 0.05	2
1317.91	± 0.05	0.56	0.59	± 0.02	1
1985.59	± 0.15	0.070	0.070	± 0.005	1

2.903 hr. ^{134m}Cs

55-134 m-2



2.903(8) hr. ^{134m}Cs Decay Scheme



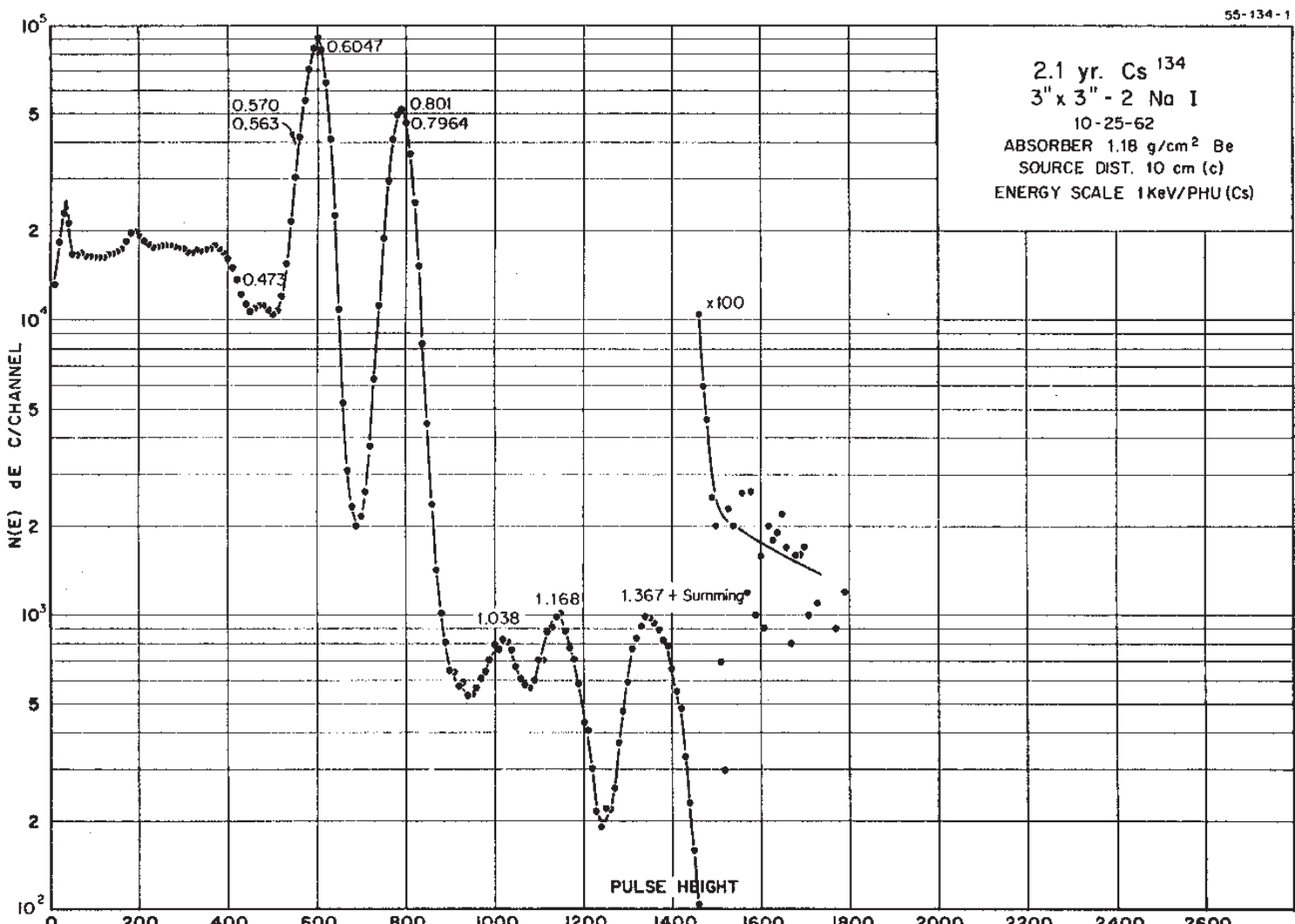
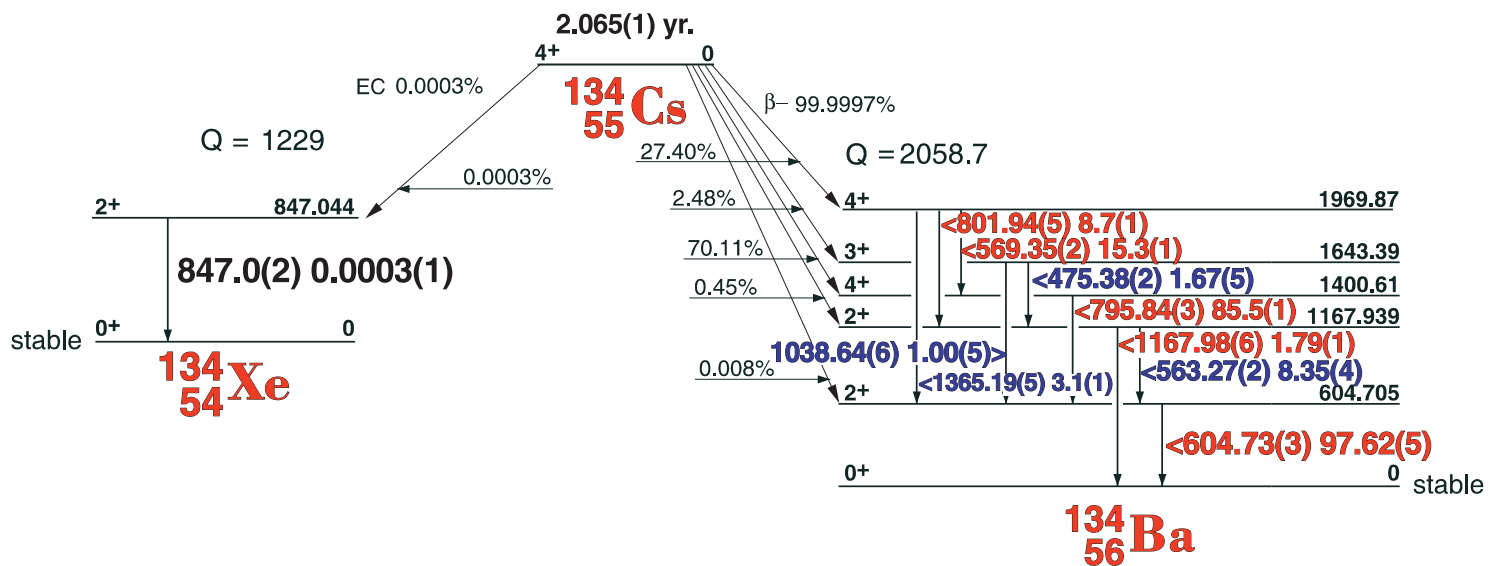
GAMMA-RAY ENERGIES AND INTENSITIES

Nuclide ^{134m}Cs
Detector 3" x 3" -2 NaI

Half Life 2.903(8) hr.
Method of Production: $^{133}\text{Cs}(n,\gamma)$

E_{γ} (KeV)[S]	ΔE_{γ}	I_{γ} (rel)	$I_{\gamma}(\%)[E]$	ΔI_{γ}	S
11.24	± 0.01		1.08	± 0.05	5
Cs k x-rays					
127.497	± 0.015	100	13.0	± 0.6	1
138.73	± 0.01		0.004	± 0.001	5

2.865(1) yr. ^{134}Cs Decay Scheme



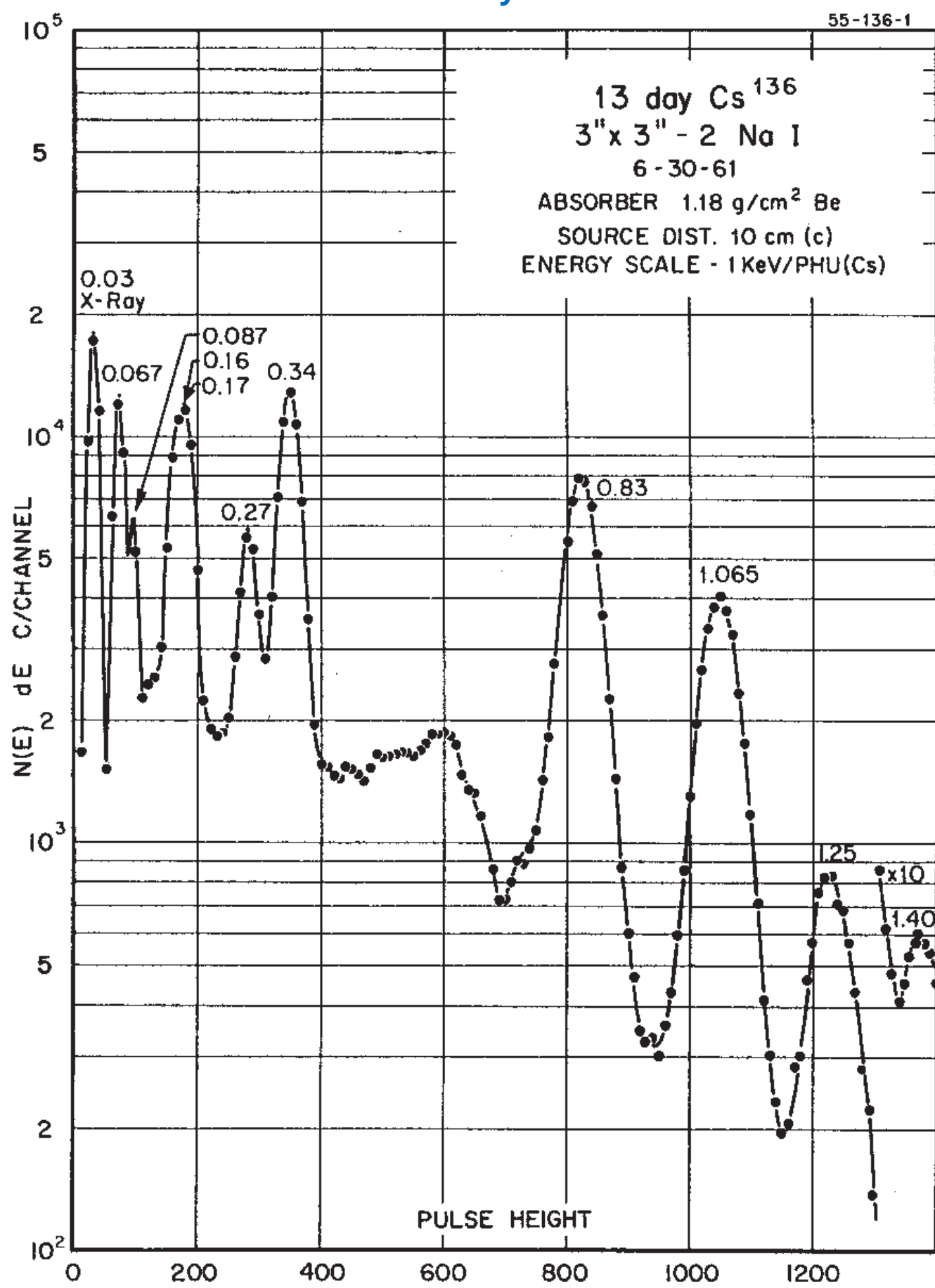
2.865(1) yr. ^{134}Cs Decay Scheme

GAMMA-RAY ENERGIES AND INTENSITIES

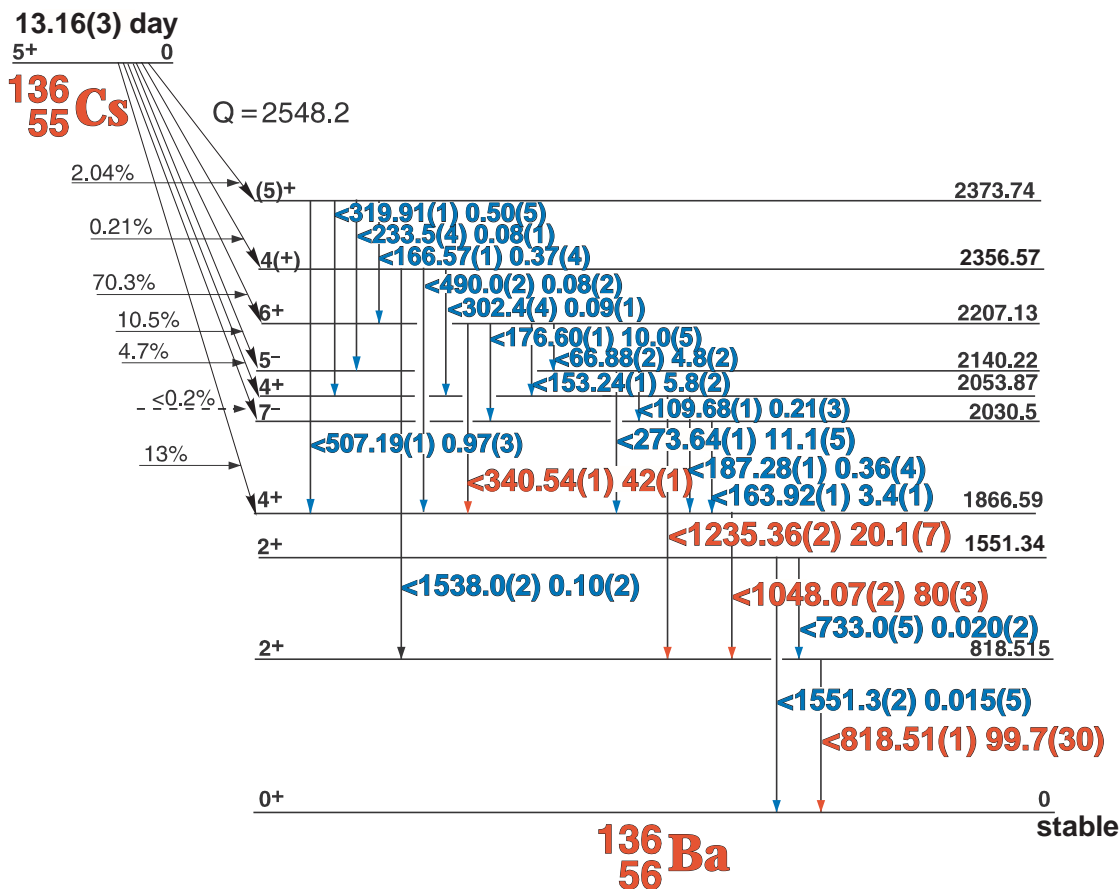
Nuclide ^{134}Cs Half Life 2.865(1) yr.
Detector 3" x 3" -2 NaI Method of Production: $^{133}\text{Cs}(n,\gamma)$

E_{γ} (KeV)[S]	ΔE_{γ}	$I_{\gamma}(\text{rel})$	$I_{\gamma}(\%)[E]$	ΔI_{γ}	S
475.38	± 0.02	1.86	1.57	± 0.05	3
563.27	± 0.02	8.0	8.35	± 0.04	2
569.35	± 0.02	15.3	15.3	± 0.1	1
604.73	± 0.03	100	97.62	± 0.05	1
795.84	± 0.03	87.0	85.5	± 0.1	1
801.94	± 0.05	8.8	8.7	± 0.1	1
847.0	± 0.2		0.0003	$\pm (1)$	5
1038.64	± 0.06	1.05	1.00	± 0.05	1
1167.98	± 0.06	1.96	1.79	± 0.01	1
1365.19	± 0.05	3.26	3.1	± 0.1	1

13.16 day ^{136}Cs



13.16(3) day ^{136}Cs Decay Scheme

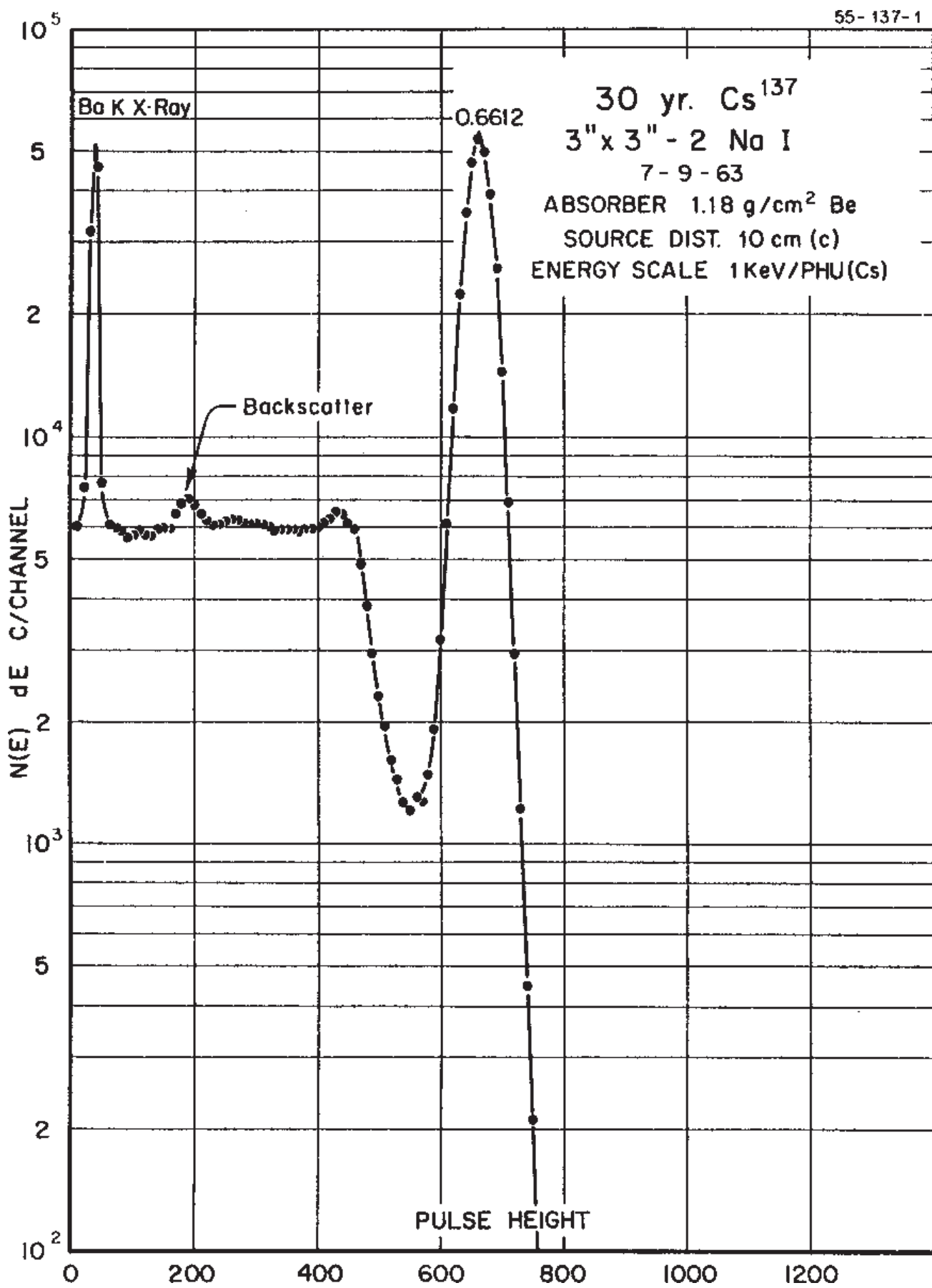


GAMMA-RAY ENERGIES AND INTENSITIES

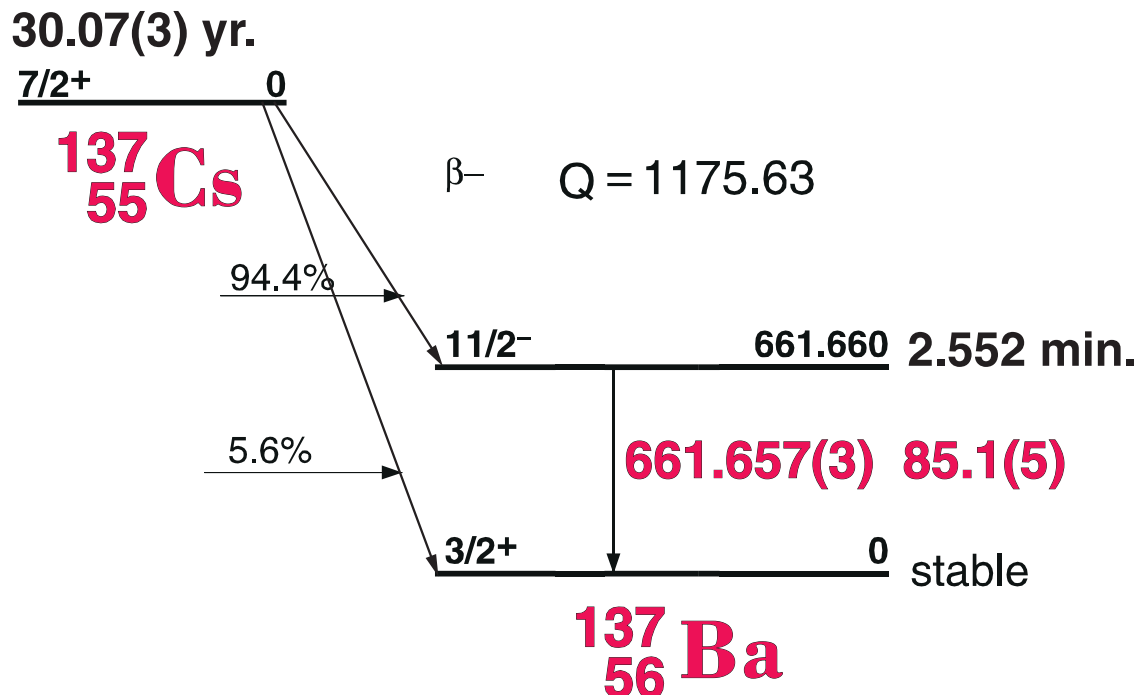
Nuclide ^{136}Cs Half Life 13.16(3) day
Detector 3" x 3" -2 NaI Method of Production: $^{235}\text{U}(\text{n},\text{f})$

E_{γ} (KeV)[S]	ΔE_{γ}	I_{γ} (rel)	$I_{\gamma}(\%)[E]$	ΔI_{γ}	S
66.88	± 0.02		4.8	± 0.2	1
109.68	± 0.01	0.21	± 0.03	4	
153.24	± 0.01		5.8	± 0.2	2
163.92	± 0.01	3.4	± 0.1	3	
176.60	± 0.01		10.0	± 0.5	1
187.28	± 0.01	0.36	± 0.04	3	
233.5	± 0.4	0.08	± 0.01	4	
273.64	± 0.01		11.1	± 0.5	1
302.4	± 0.4	0.09	± 0.01	4	
319.91	± 0.01	0.50	± 0.05	3	
340.54	± 0.01		42	± 1.0	1
490.0	± 0.2	0.08	± 0.02	4	
507.19	± 0.01	0.97	± 0.03	3	
733.0	± 0.5	0.020	± 0.002	4	
818.51	± 0.01		99.7	± 3.0	1
1048.07	± 0.02		80	± 3.0	1
1235.36	± 0.02		20.1	± 0.7	1
1538.0	± 0.2	0.10	± 0.02	3	
1551.3	± 0.2	0.015	± 0.005	4	

30.07 yr. ^{137}Cs [C]



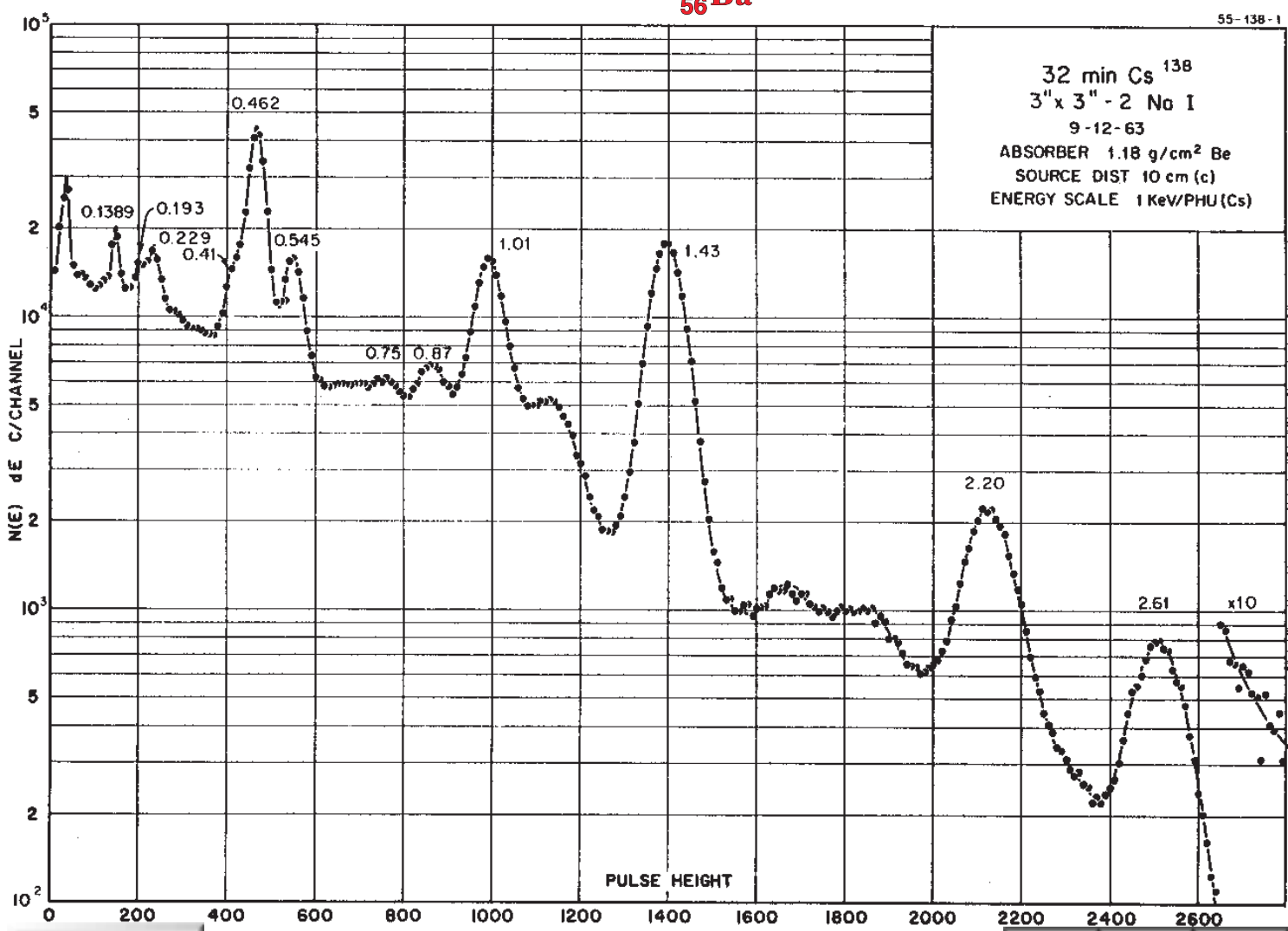
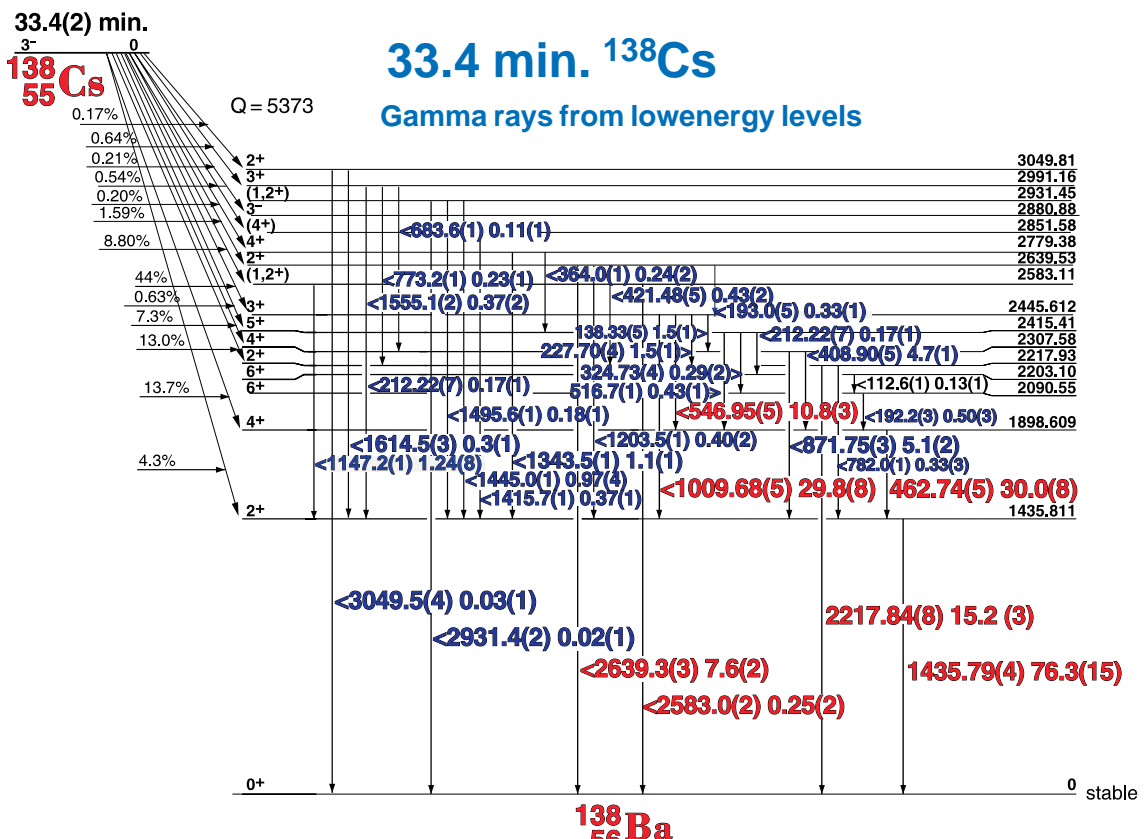
30.07(3) yr. ^{137}Cs Decay Scheme [C]



GAMMA-RAY ENERGIES AND INTENSITIES

Nuclide ^{137}Cs Half Life 4.34(1) day
 Detector 3" X 3" NaI-2 Method of Production: $^{103}\text{Rh}(\gamma,2n)$

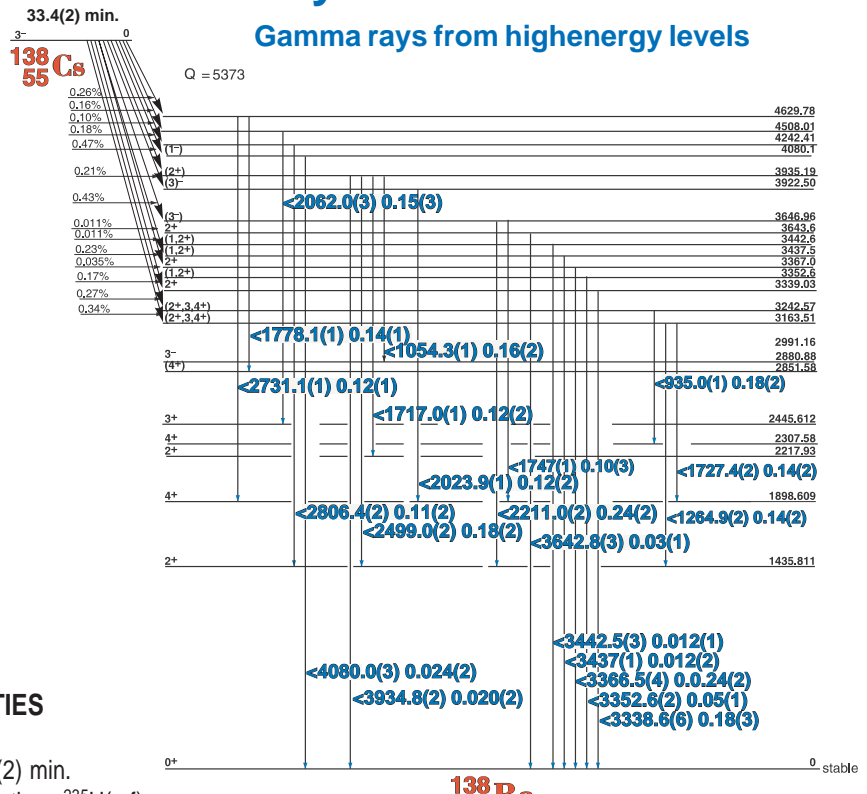
	E_γ (KeV)[C]	ΔE_γ	I_γ (rel)	$I_\gamma(\%)$ [E]	ΔI_γ	S
Ba K _{α} X	31.8			5.4		
Ba K _{β} X	37.3			1.3		
	661.657 ± 0.003	100		85.1	± 0.5	1



Decay Data

[Index](#)

33.4(2) min. ^{138}Cs Decay Scheme



GAMMA-RAY ENERGIES AND INTENSITIES

Nuclide ^{138}Cs

Detector 3" X 3" NaI-2

Half Life 33.4(2) min.

Method of Production: $^{235}\text{U}(\text{n},\text{f})$

Ann

SE

DE

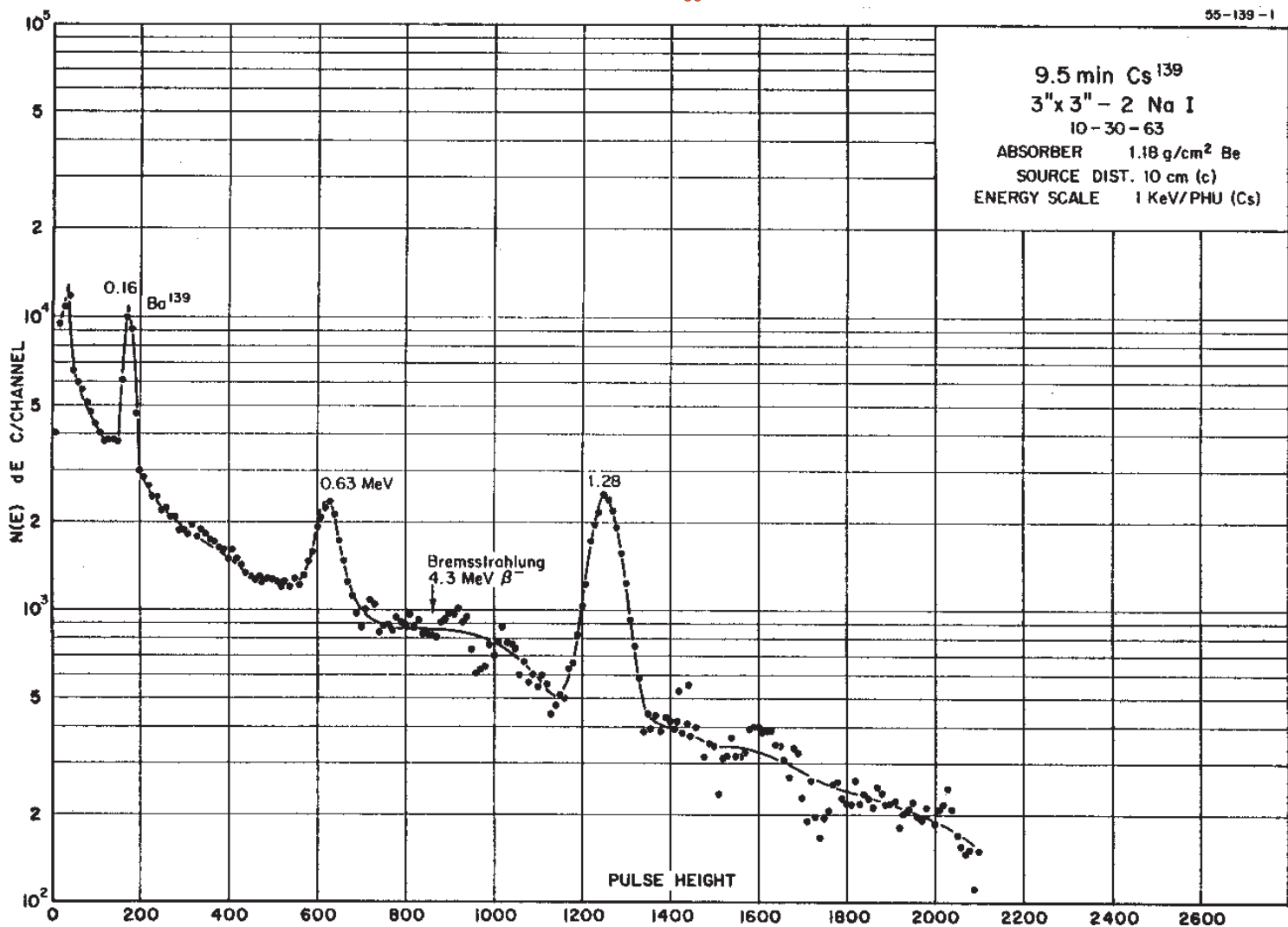
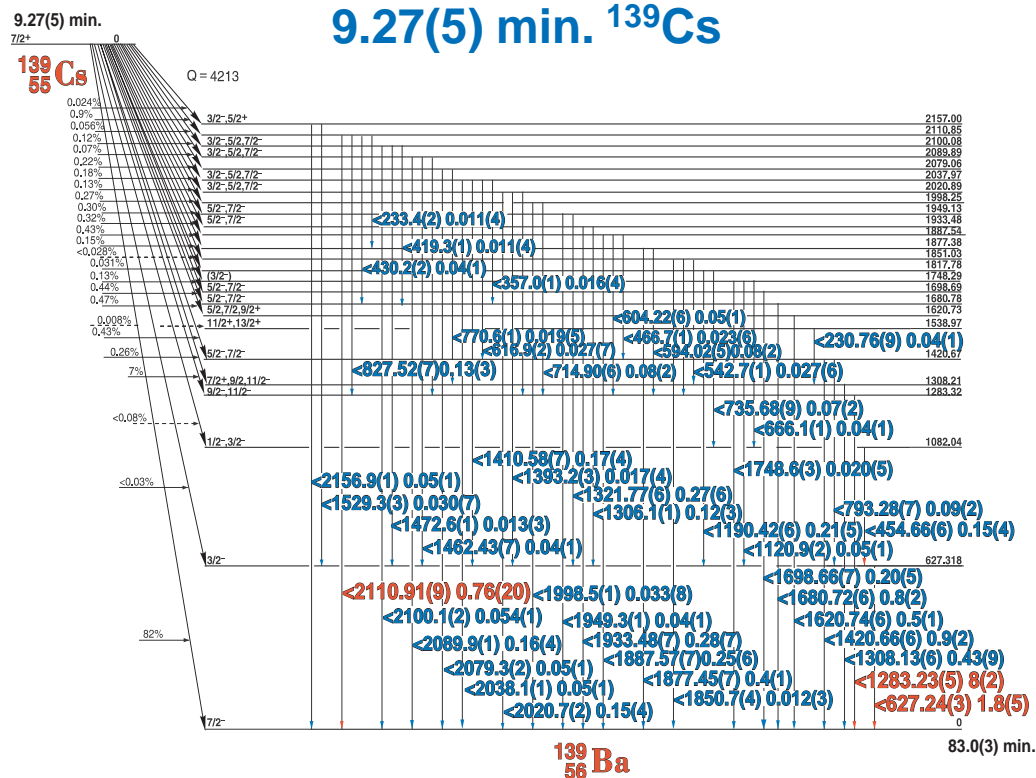
DE

SE

E_{γ} (KeV)[S]	ΔE_{γ}	I_{γ} (rel)	$I_{\gamma}(\%)[E]$	ΔI_{γ}	S
138.33	± 0.05	1.70	1.5	± 0.10	4
193.0	± 0.2	1.10	0.33	± 0.01	4
212.22	± 0.07	0.21	0.17	± 0.01	4
227.70	± 0.04	1.80	1.5	± 0.1	3
324.73	± 0.04	0.54	0.29	± 0.02	4
364.15	± 0.15	0.85	0.24	± 0.02	4
408.90	± 0.03	5.90	4.7	± 0.1	2
421.48	± 0.07	0.60	0.43	± 0.02	4
462.74 ± 0.028	37.4	30.0	± 0.8	1	
511.00		0.46		± 0.05	4
516.7	± 0.1	0.74	0.43	± 0.01	4
546.950 ± 0.05	13.2	10.8	± 0.3	1	
773.17	± 0.12	0.35	0.23	± 0.01	4
782.0	± 0.11	0.46	0.33	± 0.03	4
871.70	± 0.03	6.60	5.1	± 0.2	2
880.26	± 0.1	0.50		± 0.05	3
935.0	± 0.1	0.25	0.18	± 0.02	4
1009.64 ± 0.03	38.5	29.8	± 0.8	1	
1054.3	± 0.1		0.16	± 0.02	4
1147.10	± 0.08	1.62	1.24	± 0.10	3
1195.6	± 0.1	0.5		± 0.1	3
1203.5	± 0.1	0.5	0.40	± 0.02	3
1264.9	± 0.2	1.50	0.14	± 0.02	3
1343.42	± 0.08	1.73	1.1	± 0.1	3
1415.76	± 0.15	0.59	0.37	± 0.01	4
1435.79 ± 0.040	100	76.3	± 0.5	1	
1445.0	± 0.1	1.54	0.97	± 0.04	3
1495.6	± 0.1	0.25	0.18	± 0.01	4
1555.07	± 0.15	0.60		± 0.07	4
1614.5	± 0.3	0.85	0.3	± 0.1	3
1617.62	± 0.08	0.70		± 0.07	3
1706.74	± 0.08	1.47		± 0.12	3

E_{γ} (KeV)[S]	ΔE_{γ}	I_{γ} (rel)	$I_{\gamma}(\%)[E]$	ΔI_{γ}	S
1717.0	± 0.10	0.18	0.12	± 0.02	4
1727.4	± 0.2	0.22	0.14	± 0.02	4
1747	± 1.0	0.18	0.10	± 0.03	4
1778.1	± 0.1	0.20	0.14	± 0.01	4
2023.9	± 0.1	0.43	0.12	± 0.02	3
2062.0	± 0.2	0.56	0.15	± 0.03	3
2128.19	± 0.08	1.36		± 0.20	3
2217.74	± 0.08	20.4	15.2	± 0.3	1
2344.40	± 0.15	0.11		± 0.04	4
2499.0	± 0.4	0.46	0.18	± 0.02	3
2583.0	± 0.2	0.34	0.25	± 0.02	4
2639.09	± 0.12	9.95	7.6	± 0.2	1
2731.1	± 0.15	0.20	0.12	± 0.01	3
2806.4	± 0.15	0.12	0.11	± 0.02	4
2827.67	± 0.15	0.06		± 0.02	4
2855.20	± 0.15	0.12		± 0.02	3
2913.9	± 0.15	0.06		± 0.02	4
2931.36	± 0.20	0.03	0.020	± 0.004	4
3049.5	± 0.4	0.05	0.03	± 0.01	4
3338.6	± 0.5	0.25	0.18	± 0.03	3
3352.6	± 0.2	0.09	0.05	± 0.01	4
3366.5	± 0.4	0.35	0.24	± 0.02	3
3437.0	± 0.8	0.02	0.012	± 0.002	4
3442.5	± 0.3	0.015	0.012	± 0.001	3
3642.8	± 0.25	0.05	0.03	± 0.01	3
3652.0	± 0.3	0.025	0.010	± 0.003	4
3934.8	± 0.2	0.025	0.020	± 0.002	3
4080.0	± 0.25	0.030	0.024	± 0.002	2
4278.8	± 0.4	0.009		± 0.003	4

9.27(5) min. ^{139}Cs



9.27(5) min. ^{139}Cs Decay Scheme

GAMMA-RAY ENERGIES AND INTENSITIES

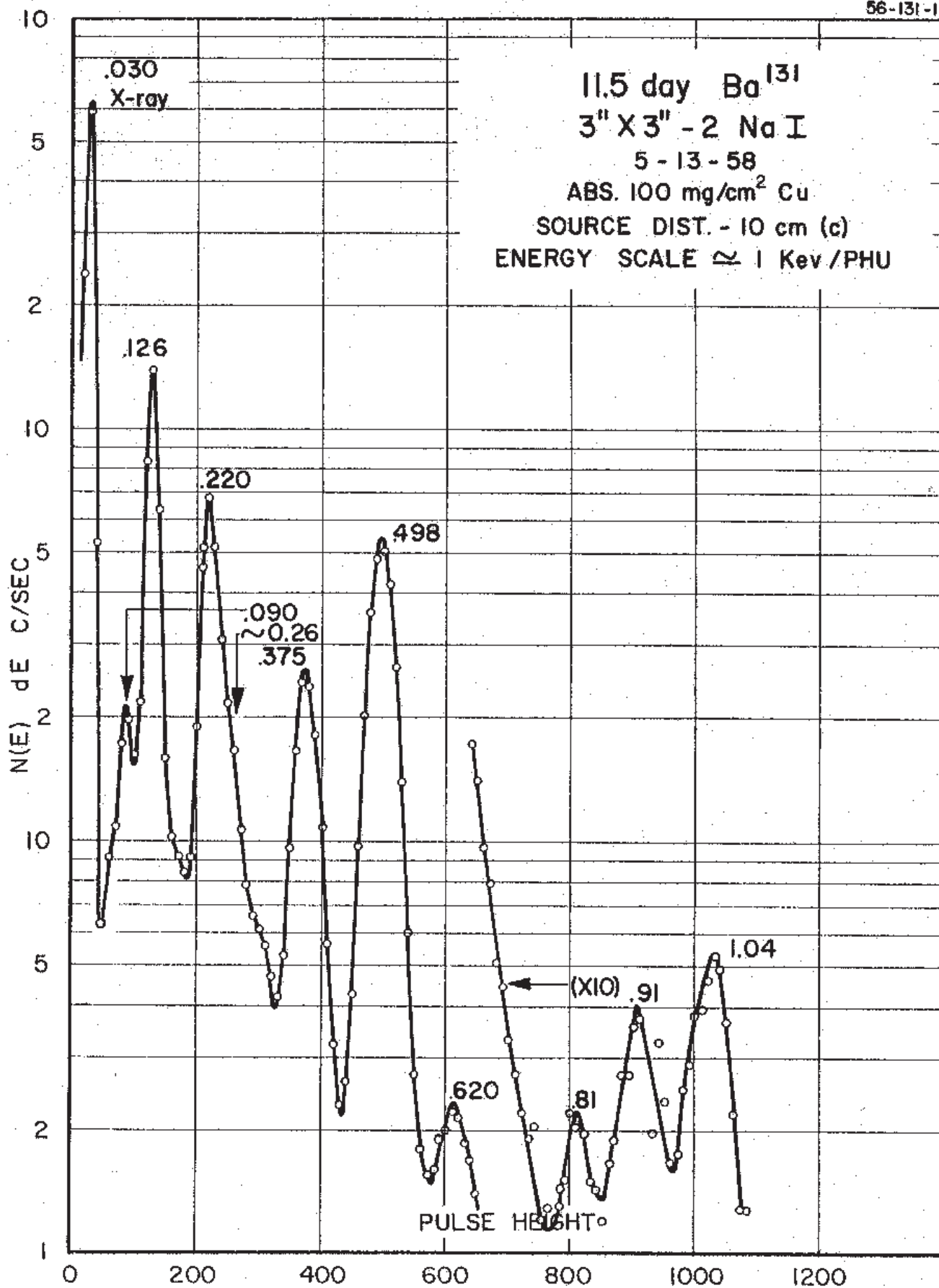
Nuclide ^{139}Cs
Detector 3" x 3" -2 NaI

Half Life: 9.27(5) min.
Method of Production: $^{235}\text{U}(\text{n},\text{f})$

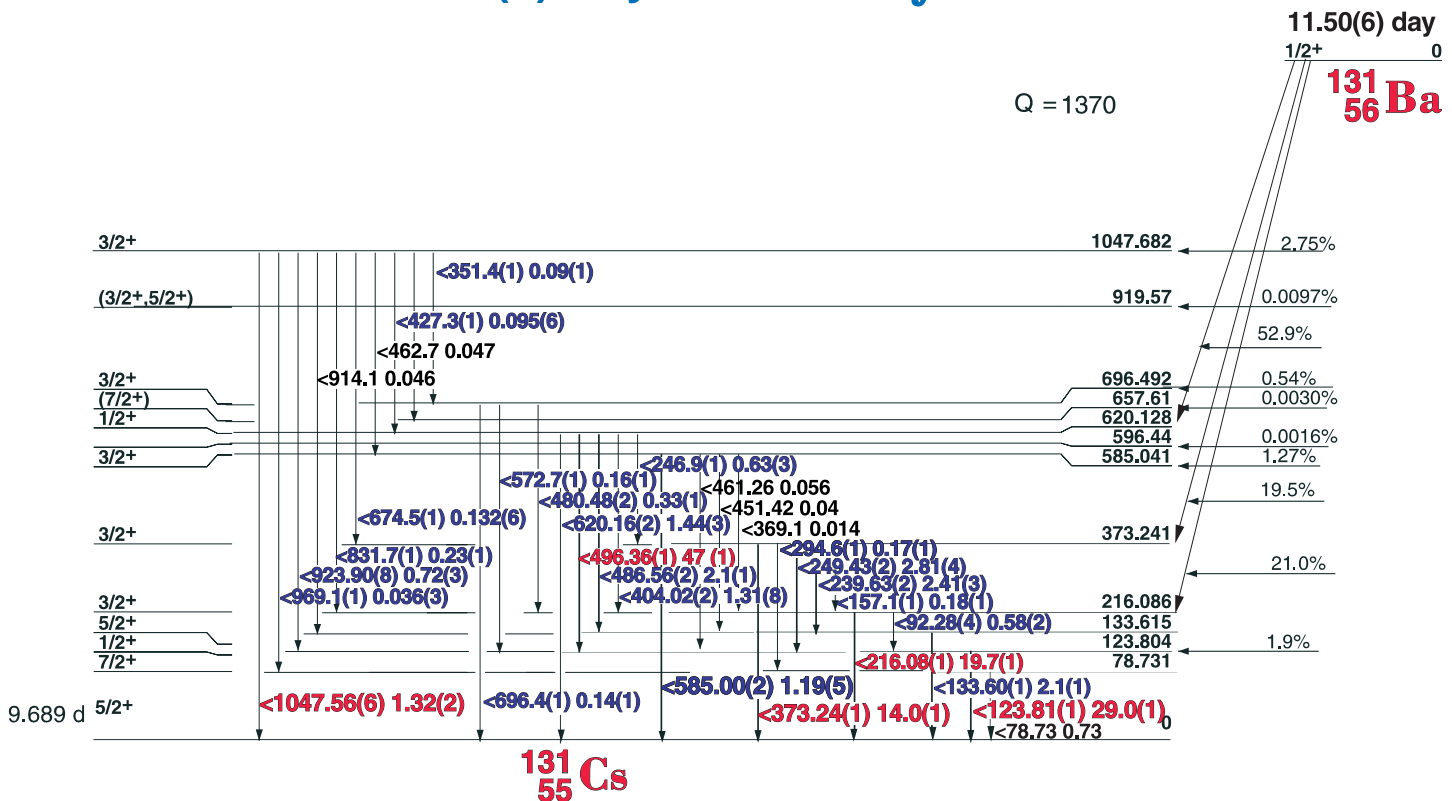
E_{γ} (KeV)[S]	ΔE_{γ}	I_{γ} (rel)	$I_{\gamma}(\%)[E]$	ΔI_{γ}	S
230.76	± 0.09		0.04	± 0.01	4
233.4	± 0.2		0.011	± 0.004	4
357.0	± 0.1		0.016	± 0.004	4
419.3	± 0.1		0.011	± 0.004	4
430.2	± 0.2		0.04	± 0.01	3
454.66	± 0.06		0.15	± 0.04	3
466.7	± 0.1		0.023	± 0.006	3
542.7	± 0.1		0.027	± 0.006	4
594.02	± 0.05		0.08	± 0.02	4
604.22	± 0.06		0.05	± 0.01	4
616.9	± 0.2		0.027	± 0.007	3
627.24	± 0.03		1.8	± 0.5	1
666.1	± 0.1		0.04	± 0.01	4
714.90	± 0.06		0.08	± 0.02	4
735.68	± 0.09		0.07	± 0.02	4
770.6	± 0.1		0.019	± 0.005	4
793.28	± 0.07		0.09	± 0.02	3
827.52	± 0.07		0.13	± 0.03	3
1120.9	± 0.2		0.05	± 0.01	3
1190.42	± 0.06		0.21	± 0.05	3
1283.23	± 0.05		8.0	± 2	1
1306.1	± 0.1		0.12	± 0.03	3
1308.13	± 0.06		0.43	± 0.09	3
1321.77	± 0.06		0.27	± 0.06	3
1393.2	± 0.3		0.017	± 0.004	4
1410.58	± 0.07		0.17	± 0.04	3
1420.66	± 0.06		0.9	± 0.2	2
1462.43	± 0.06		0.04	± 0.01	4
1472.6	± 0.1		0.013	± 0.003	4
1529.3	± 0.3		0.030	± 0.007	4
1620.74	± 0.06		0.5	± 0.1	3
1680.72	± 0.06		0.8	± 0.2	3
1698.66	± 0.07		0.20	± 0.05	3
1748.6	± 0.3		0.020	± 0.005	4
1850.7	± 0.4		0.012	± 0.003	4
1877.45	± 0.07		0.4	± 0.1	2
1887.57	± 0.07		0.25	± 0.06	3
1933.48	± 0.07		0.28	± 0.07	3
1949.3	± 0.1		0.04	± 0.01	4
1998.5	± 0.1		0.033	± 0.008	4
2020.7	± 0.2		0.15	± 0.04	3
2038.1	± 0.1		0.05	± 0.01	4
2079.3	± 0.2		0.05	± 0.01	4
2089.9	± 0.1		0.16	± 0.04	3
2100.1	± 0.2		0.054	± 0.01	4
2110.91	± 0.09		0.76	± 0.20	1
2156.9	± 0.1		0.05	± 0.01	4
2173.98	± 0.07		0.23	± 0.06	2

11.50(6) day ^{131}Ba

56-131-1



11.50(6) day ^{131}Ba Decay Scheme



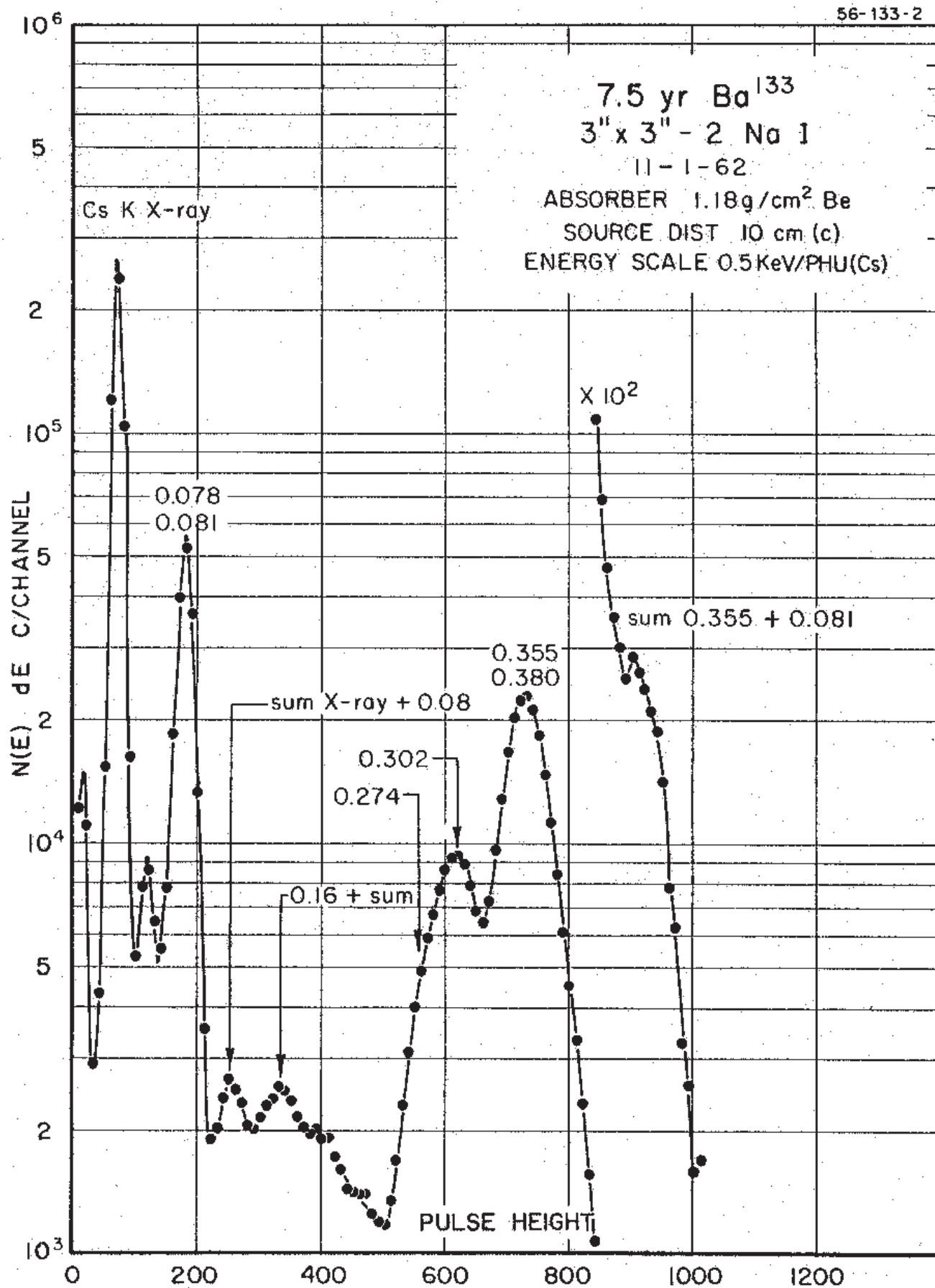
GAMMA-RAY ENERGIES AND INTENSITIES

Nuclide ^{131}Ba **Half Life** 1.078(2) Day
Detector 3" X 3" NaI-2 **Method of Production:** /as $^{75}(\text{n},\gamma)$

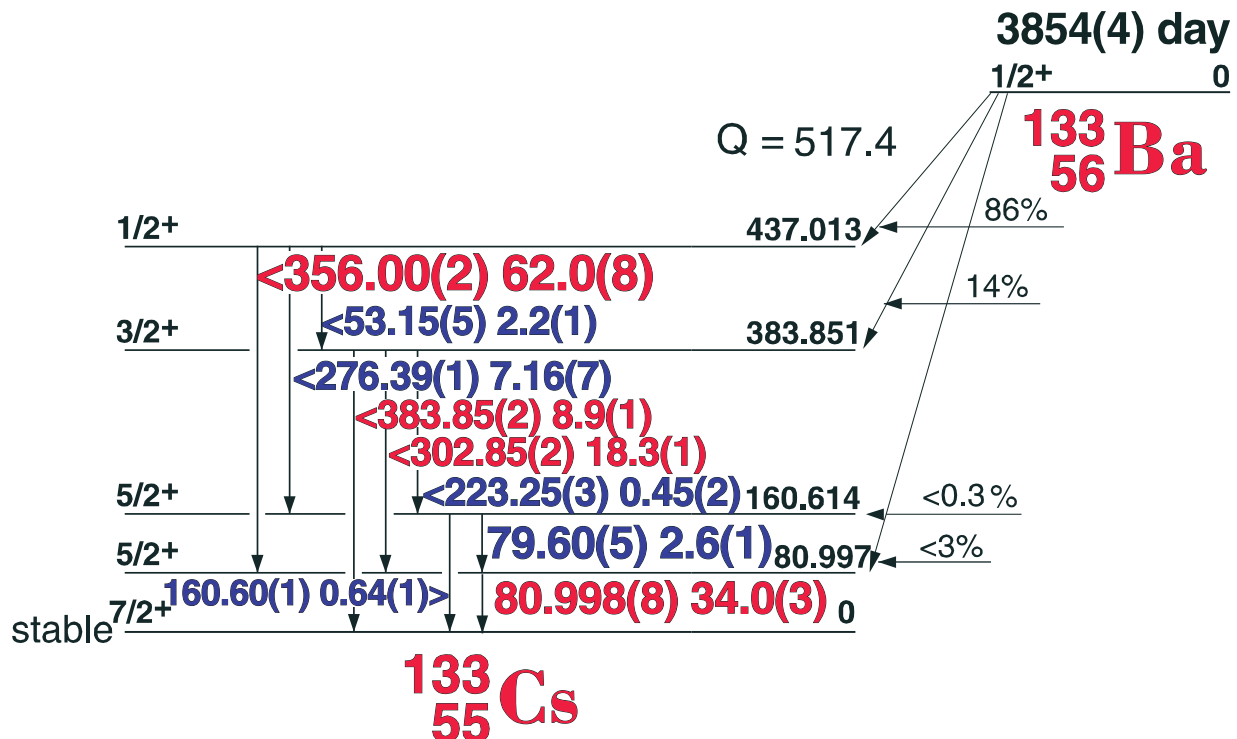
E_{γ} (KeV)[S]	ΔE_{γ}	I_{γ} (rel)	$I_{\gamma}(\%)$ [E]	ΔI_{γ}	S
Cs x-rays					4
92.3	± 0.1	2.0	0.58	± 0.02	4
123.806	± 0.008	62.1	29.0	± 0.1	1
133.601	± 0.012	4.86	2.1	± 0.1	3
157.1	± 0.1	0.47	0.18	± 0.01	4
216.083	± 0.01	41.66	10.7	± 0.1	1
239.63	± 0.025	5.76	2.41	± 0.03	3
246.93	± 0.1	66	0.63	± 0.03	4
249.430	± 0.025	6.22	2.81	± 0.04	3
294.57	± 0.1	0.62	0.17	± 0.01	4
351.40	± 0.1	1.0	0.09	± 0.01	4
373.244	± 0.010	31.3	14.0	± 0.1	1
404.02	± 0.02	3.07	1.3	± 0.2	2
427.34	± 0.10	0.64	0.095	± 0.006	4
462.7	± 0.1		0.047	± 0.004	5
480.485	± 0.02	0.82	0.33	± 0.01	3
486.56	± 0.025	4.34	2.1	± 0.1	2
496.365	± 0.015	100	47.0	± 0.6	1
572.77	± 0.1	0.32	0.16	± 0.01	4
585.00	± 0.02	2.75	1.19	± 0.05	2
609.41	± 0.05	0.68		± 0.07	4
620.157	± 0.025	4.06	1.44	± 0.03	1

E_{γ} (KeV) [S]	ΔE_{γ}	I_{γ} (rel)	$I_{\gamma}(\%)$ [E]	ΔI_{γ}	S
674.51	± 0.1	0.39	0.132	± 0.006	4
696.4	± 0.1	0.44	0.14	± 0.01	4
831.7	± 0.1	0.45	0.23	± 0.01	3
911.7	± 0.2	0.5		± 0.2	4
923.9	± 0.08	1.59	0.72	± 0.03	3
969.1	± 0.1	0.12	0.036	± 0.003	4
1047.56	± 0.06	2.89	1.32	± 0.02	1

3854(4) day ^{133}Ba [C]



3854(4) day ^{133}Ba Decay Scheme



GAMMA-RAY ENERGIES AND INTENSITIES

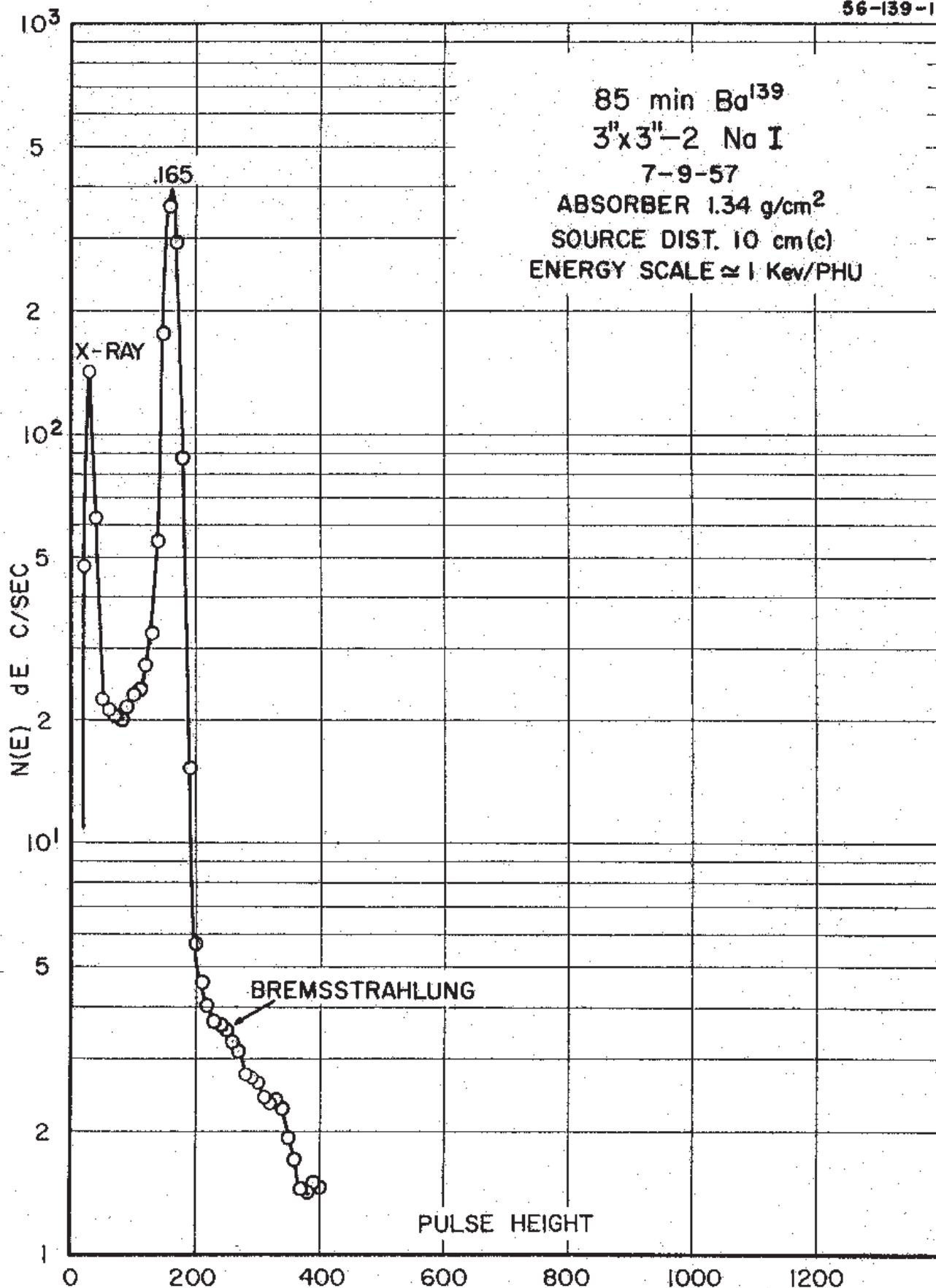
Nuclide ^{133}Ba
Detector 3" x 3" -2 Nal

Half Life 3854(4) day
Method of Production: $^{132}\text{Ba}(n,\gamma)$

E_{γ} (KeV)[C]	ΔE_{γ}	$I_{\gamma}(\text{rel})$	$I_{\gamma}(\%)[E]$	ΔI_{γ}	S
53.15	± 0.05	3.0	2.2	± 0.1	3
79.60	± 0.05	5.6	2.6	± 0.1	3
80.998	± 0.008	52.0	34.0	± 0.3	1
160.605	± 0.015	1.12	0.64	$+ 0.01$	3
223.246	± 0.030	0.85	0.45	± 0.02	3
276.397	± 0.012	11.69	7.16	± 0.07	1
302.851	± 0.015	29.78	18.3	± 0.1	1
356.005	± 0.017	100	62.0	± 0.8	1
383.851	± 0.020	14.43	8.9	± 0.1	1

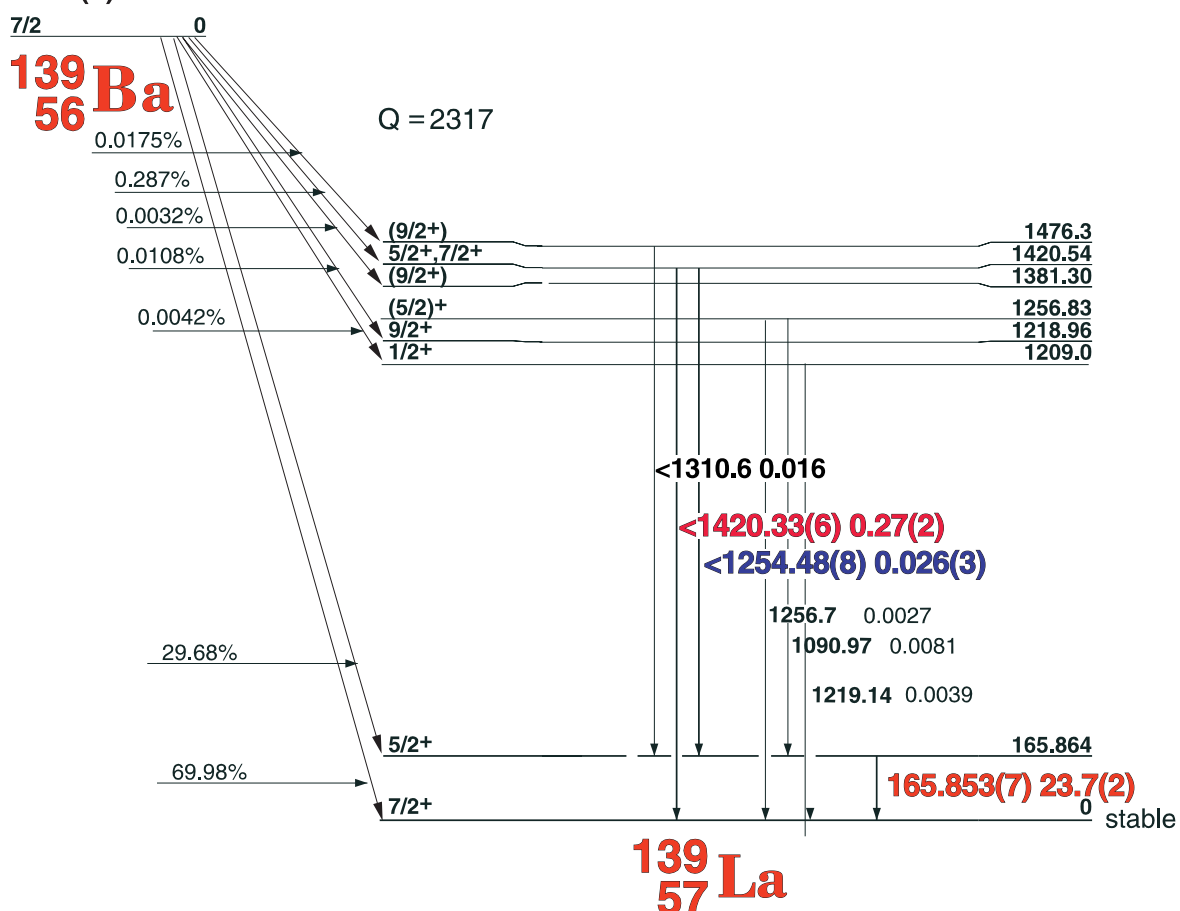
83.1 min. ^{139}Ba

56-139-1



83.1(6) min. ^{139}Ba Decay Scheme

83.1(3) min.



GAMMA-RAY ENERGIES AND INTENSITIES

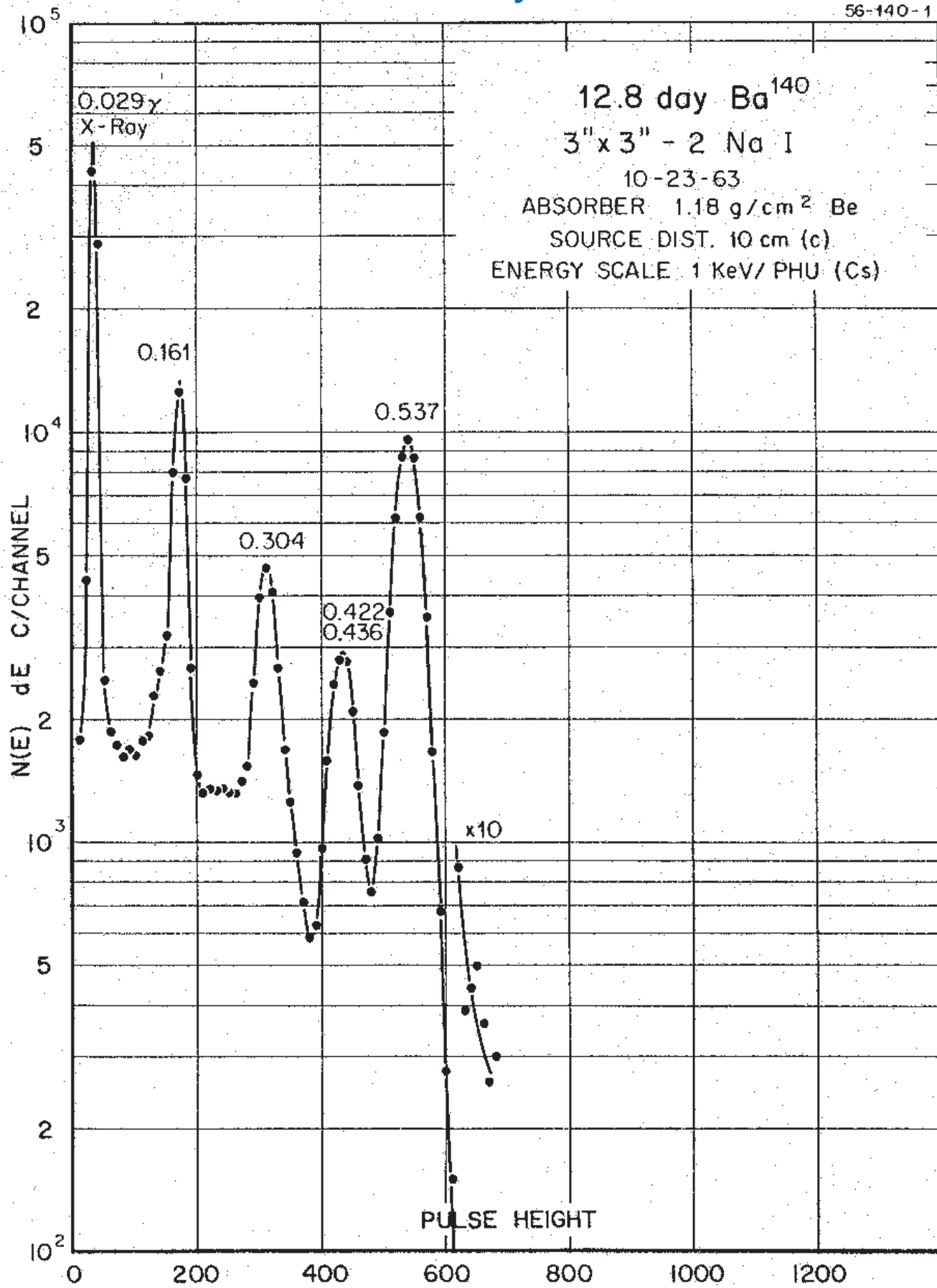
Nuclide ^{139}Ba
Detector 3" x 3" -2 NaI

Half Life 83.1 (6) min.
Method of Production: $^{138}\text{Ba}(n,\gamma)$

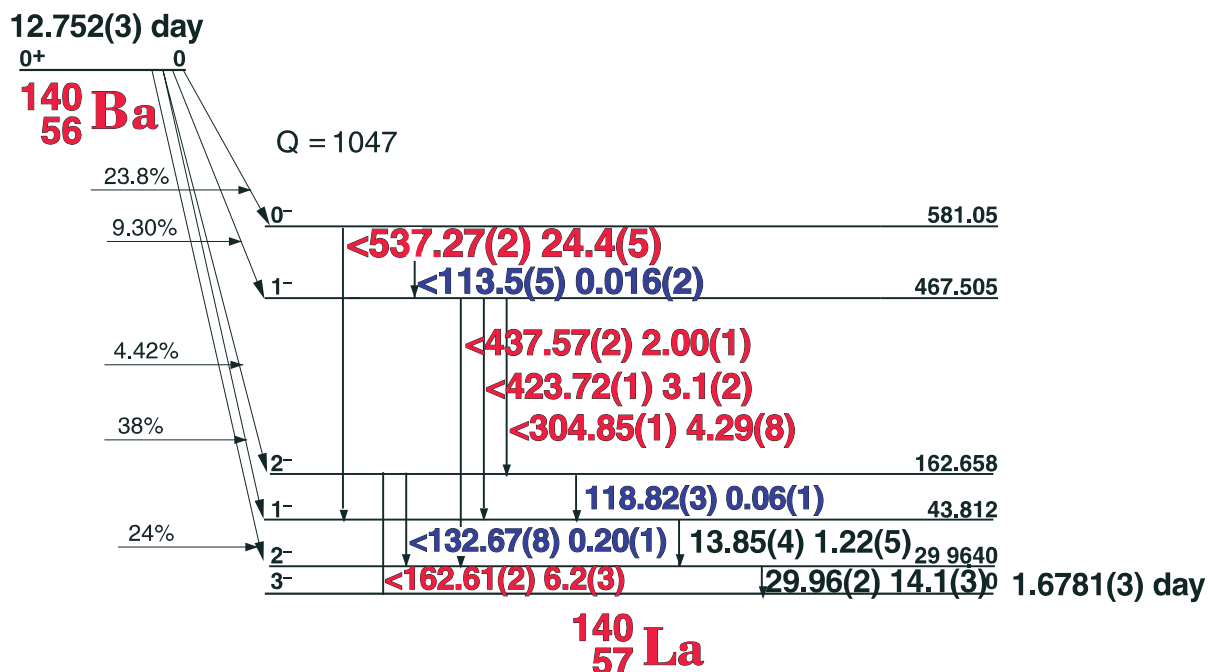
E_{γ} (KeV)[S]	ΔE_{γ}	I_{γ} (rel)	$I_{\gamma}(\%)[E]$	ΔI_{γ}	S
165.853	± 0.007	100	23.7	± 0.2	1
1254.48	± 0.08	0.14	0.026	± 0.003	2
1420.33	± 0.06	1.12	0.27	± 0.02	1

12.752 day ^{140}Ba

56-140-1



12.752(3) day ^{140}Ba

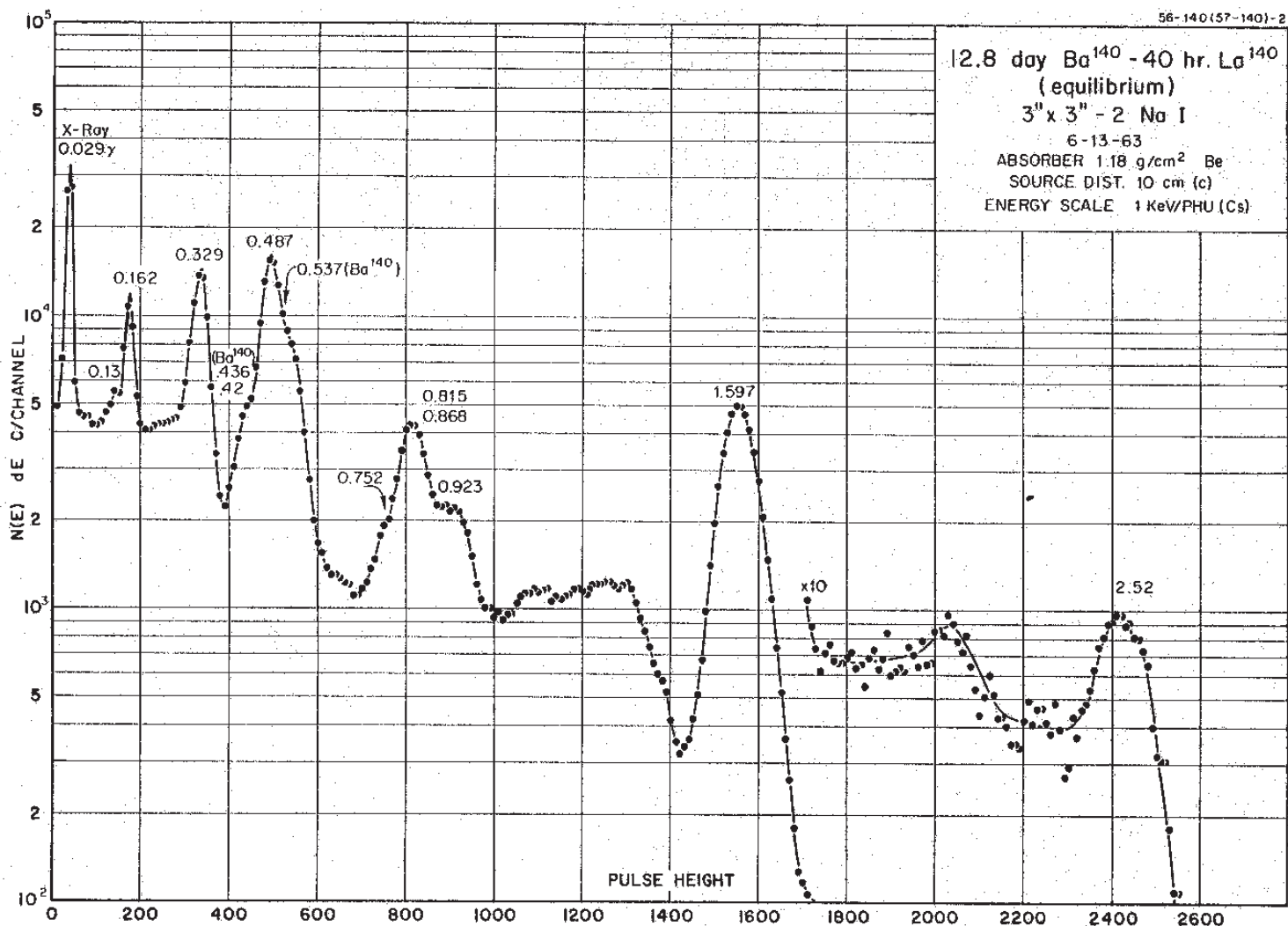
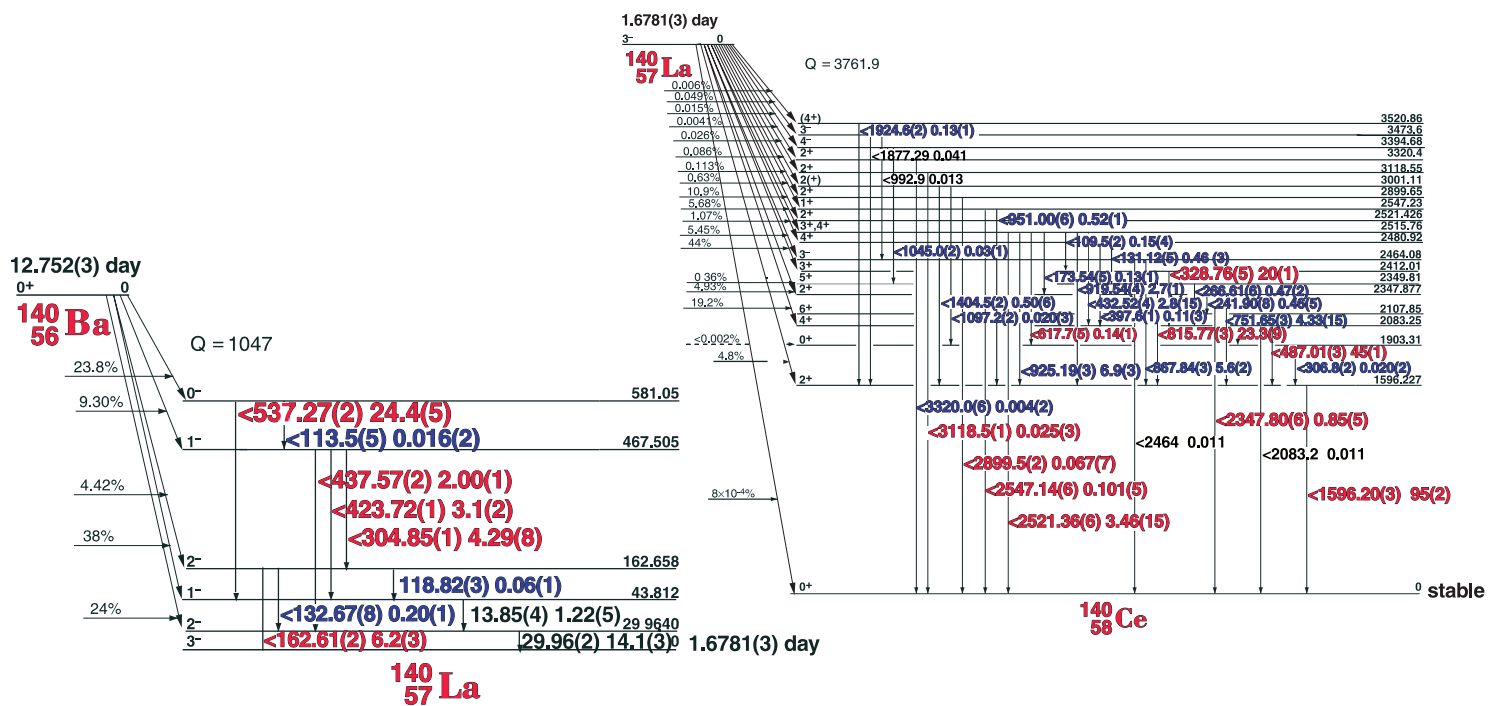


GAMMA-RAY ENERGIES AND INTENSITIES

Nuclide ^{140}Ba
 Detector 3" x 3" -2 NaI
 Half Life 12.752(6) day
 Method of Production: $^{235}\text{U}(\text{n},\text{f})$

E_γ (KeV)[S]	ΔE_γ	I_γ (rel)	I_γ (%)[E]	ΔI_γ	S
29.96	± 0.02		14.1	± 0.3	5
113.5	± 0.5		0.016	± 0.002	5
118.82	± 0.10	0.32	0.08	± 0.01	4
132.67	± 0.08	0.90	0.20	± 0.01	3
162.609	± 0.020	28.4	6.2	± 0.3	1
304.850	± 0.010	18.8	4.29	± 0.08	1
423.722	± 0.012	12.99	3.1	± 0.2	1
437.575	± 0.02	8.10	2.00	± 0.01	1
537.274	± 0.020	100	24.4	± 0.5	1

12.752(3) day ^{140}Ba - 1.6781(3) day ^{140}La



Decay Data

[Index](#)

12.752(3) day ^{140}Ba - 1.6781(3) day ^{140}La

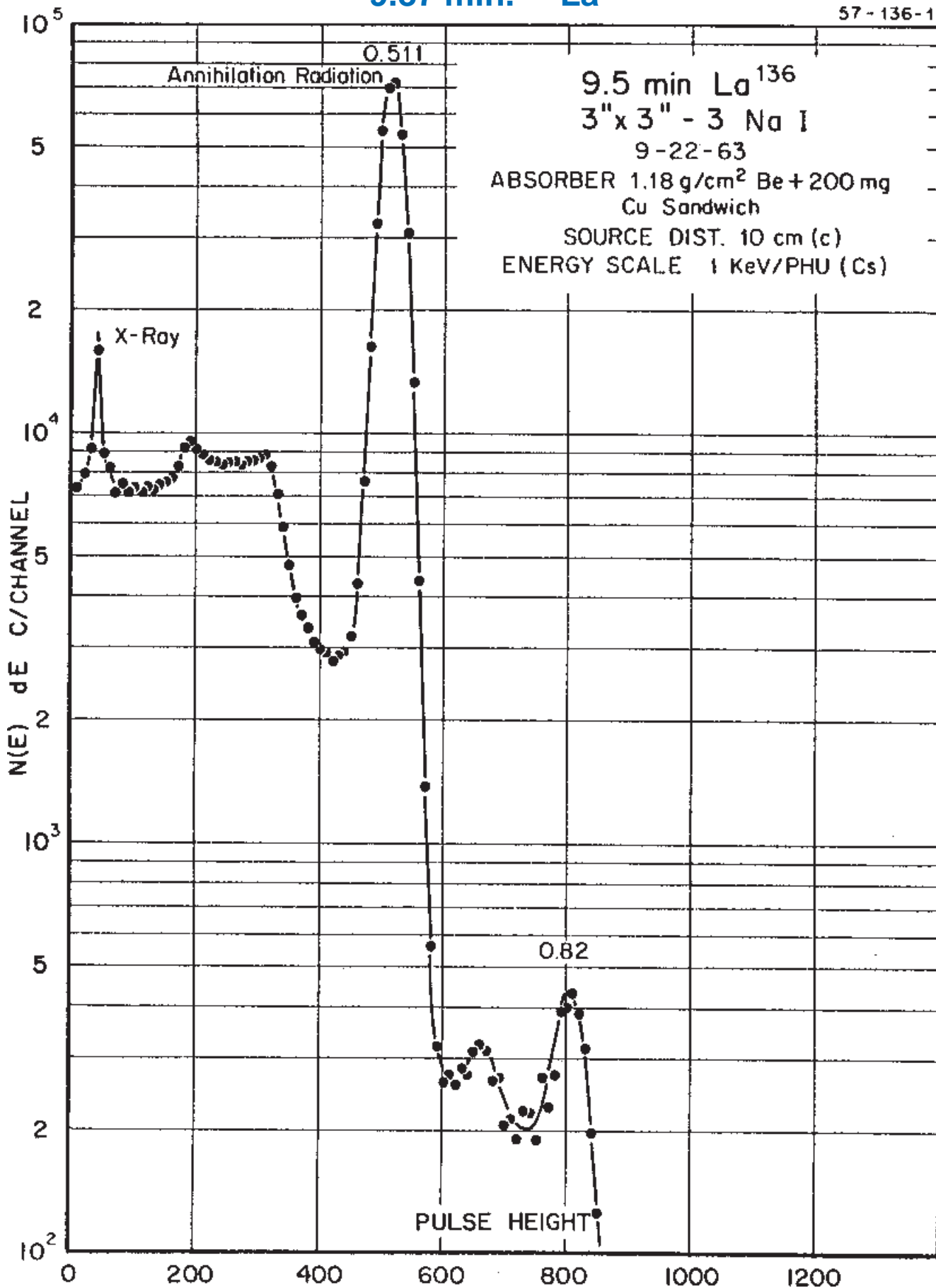
GAMMA-RAY ENERGIES AND INTENSITIES

Nuclide $^{140}\text{Ba} - ^{140}\text{La}$
 Detector 3" x 3" -2 Nal
 Half Life 12.752(30 day - 1.6781(3) day
 Method of Production: $^{235}\text{U}(\text{n},\text{f})$

	$E_{\gamma}(\text{KeV})[\text{S}]$	ΔE_{γ}	$I_{\gamma}(\text{rel})$	$I_{\gamma}(\%)[\text{E}]$	ΔI_{γ}	S
^{140}Ba	109.47 \pm 0.020	0.17	0.15	\pm 0.04	4	
	131.15	\pm 0.020	0.42	0.46	\pm 0.03	4
	162.53	\pm 0.03	5.28	5.0	\pm 0.15	2
	173.5	\pm 0.2	0.6	0.13	\pm 0.01	4
	241.90	\pm 0.08	0.51	0.46	\pm 0.03	4
	266.61	\pm 0.06	0.50	0.47	\pm 0.02	4
	304.89	\pm 0.05	4.1	3.9	\pm 0.2	3
	328.76	\pm 0.05	19.6	20	\pm 1.0	1
	397.8	\pm 0.1	0.12	0.11	\pm 0.02	4
	423.72	\pm 0.02	2.78	2.64	\pm 0.10	3
^{140}Ba	432.52	\pm 0.02	2.94	2.8	\pm 0.10	3
	437.58	\pm 0.03	1.75	1.7	\pm 0.10	3
	487.009	\pm 0.030	44.7	45	\pm 1.0	1
	Ann.	511.006	0.2		\pm 0.05	4
^{140}Ba	537.29	\pm 0.03	21.50	20.5	\pm 1.0	1
DE	574.3	\pm 0.1				3
	751.655	\pm 0.035	4.5	4.33	\pm 0.1	2
	815.775	\pm 0.030	24.2	23.3	\pm 1.5	1
	867.842	\pm 0.035	5.7	5.6	\pm 0.2	2
	919.54	\pm 0.04	2.89	2.7	\pm 0.10	3
	925.188	\pm 0.035	7.2	6.9	\pm 0.3	1
	951.00	\pm 0.06	0.56	0.52	\pm 0.01	4
	1085.2	\pm 0.1				3
	1499.5	\pm 0.1				3
	1596.17	\pm 0.06	100	95	\pm 2.0	1
SE	1836.7	\pm 0.1				4
	1877.3	\pm 0.2	0.05	0.04	\pm 0.01	4
	1924.2	\pm 0.3	0.023	0.13	\pm 0.01	4
	2347.80	\pm 0.06	0.89	0.85	\pm 0.05	1
	2521.32	\pm 0.06	3.59	3.46	\pm 0.10	1
	2547.14	\pm 0.06	0.110	0.101	\pm 0.006	2
	2899.5	\pm 0.2	0.073	0.067	\pm 0.007	1
	3118.52	\pm 0.15	0.028	0.025	\pm 0.003	1
	3320.0	\pm 0.6	0.005	0.004	\pm 0.001	3

9.87 min. ^{136}La

57 - 136 - 1



9.87(3) min. ^{136}La

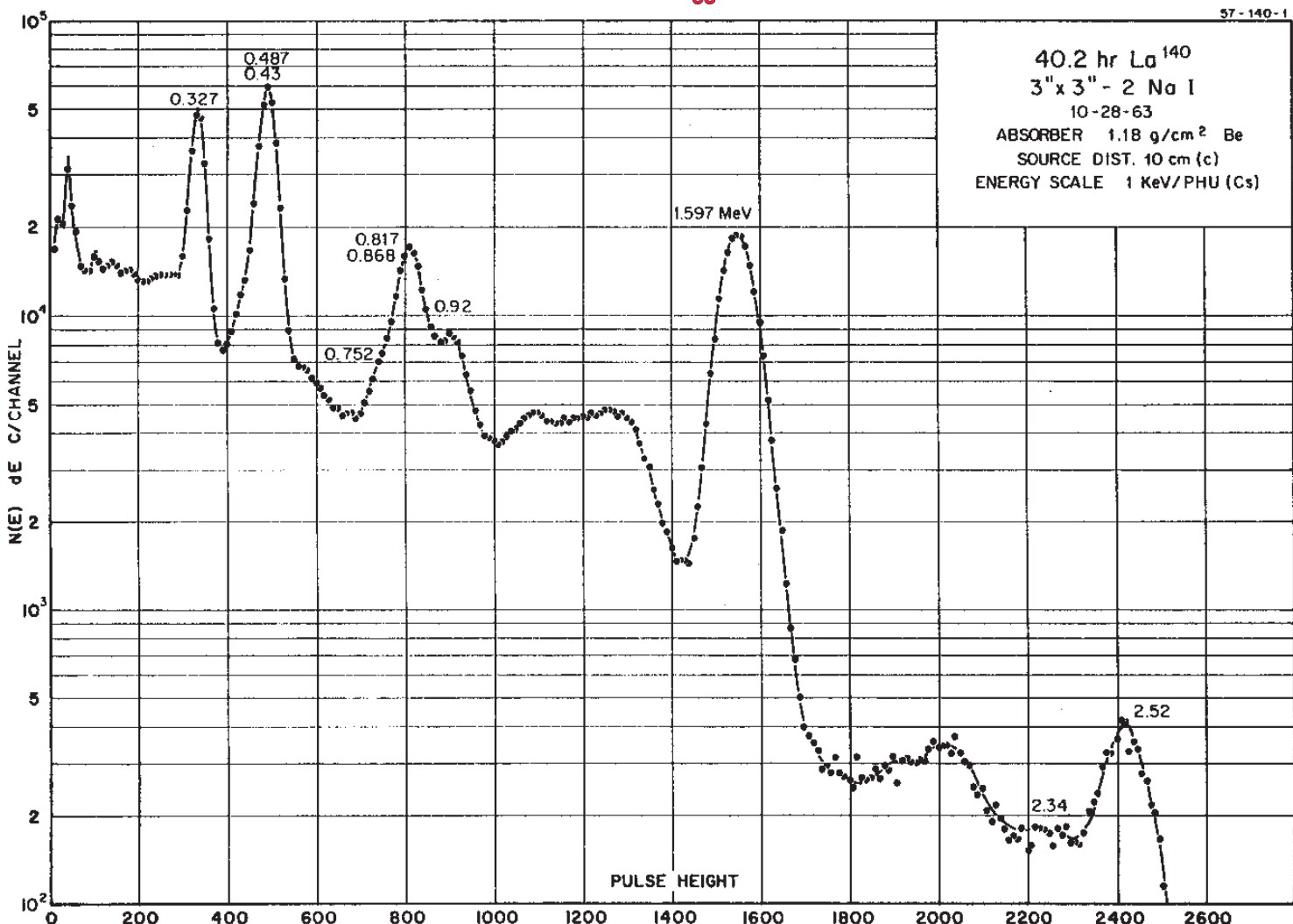
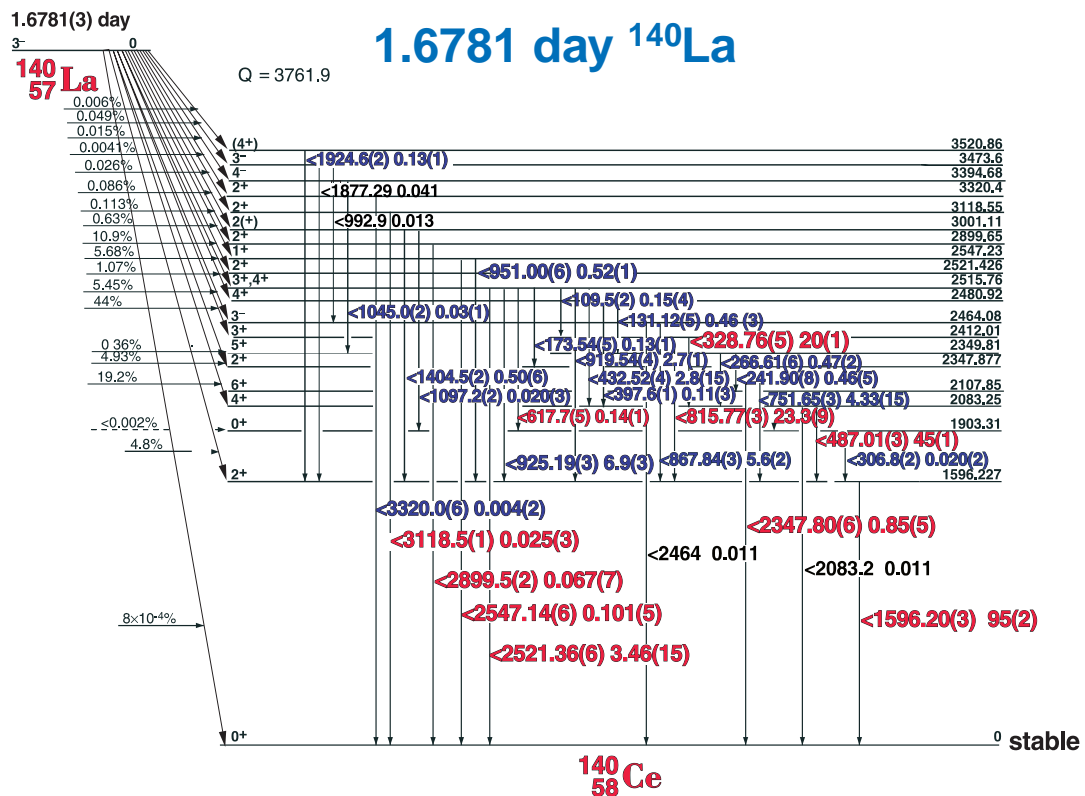
GAMMA-RAY ENERGIES AND INTENSITIES

Nuclide
Detector

^{136}La
3" x 3" -2 Nal

Half Life 9.87(3) min.
Method of Production: $^{139}\text{La}(\gamma, 3n)$

E_{γ} (KeV)[S]	ΔE_{γ}	I_{γ} (rel)	$I_{\gamma}(\%)$ [E]	ΔI_{γ}	S



Decay Data

← Index →

1.6781(3) day ^{140}La

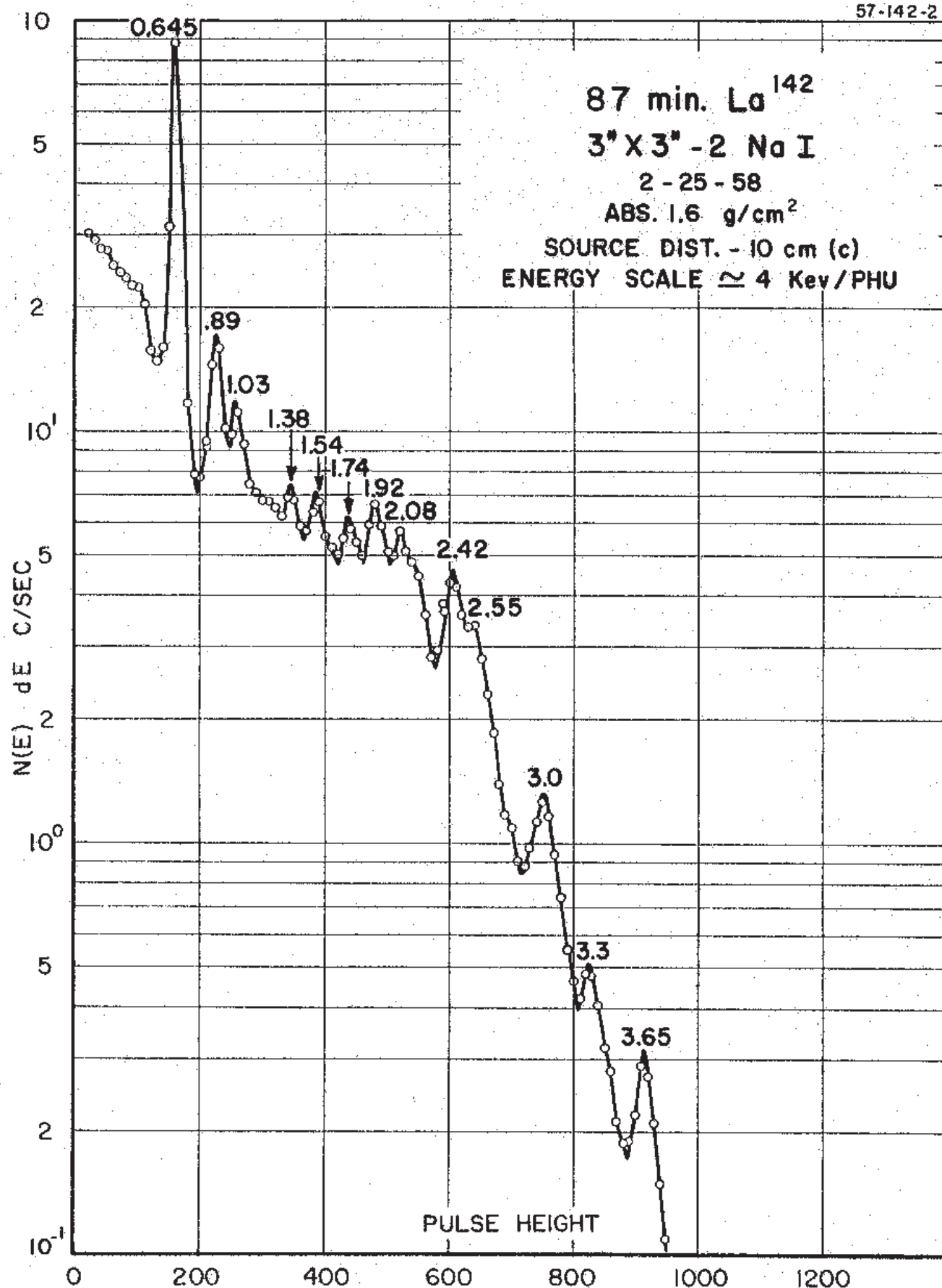
GAMMA-RAY ENERGIES AND INTENSITIES

Nuclide ^{140}La Half Life 1.6781(3) day
 Detector 3" X 3" NaI-2 Method of Production: $^{139}\text{La}(n,\gamma)$

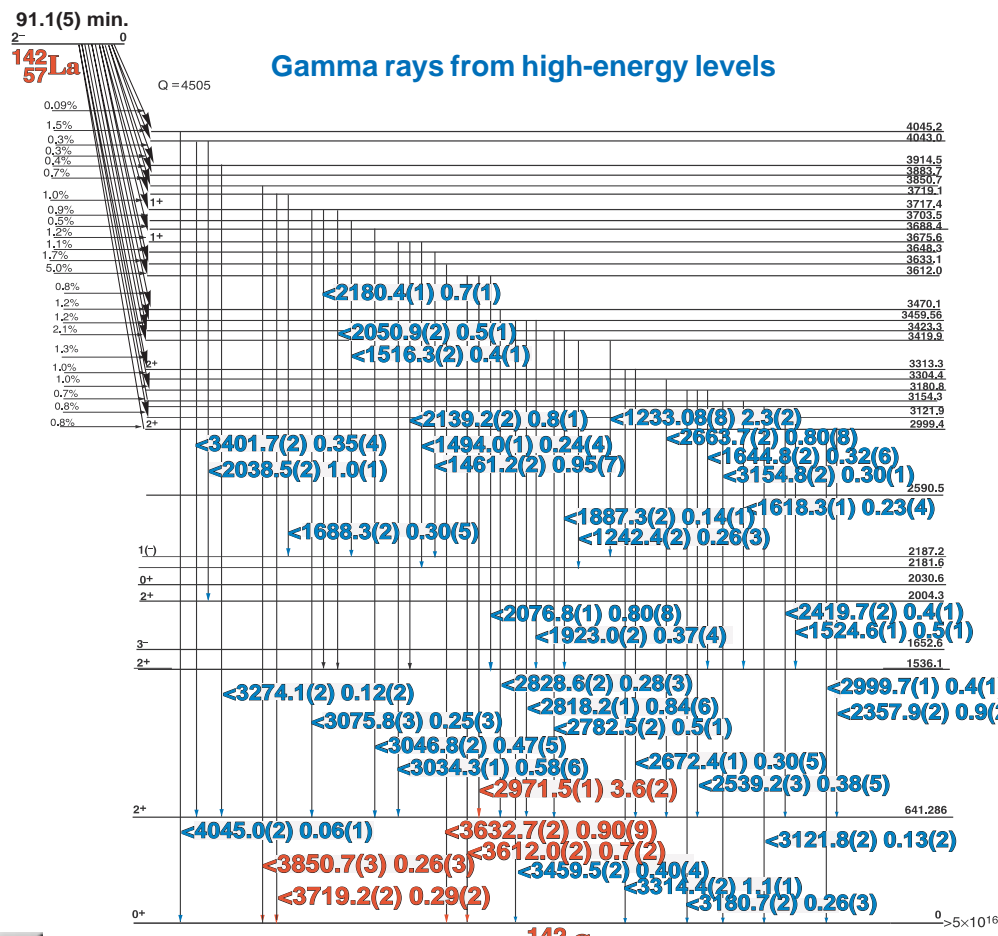
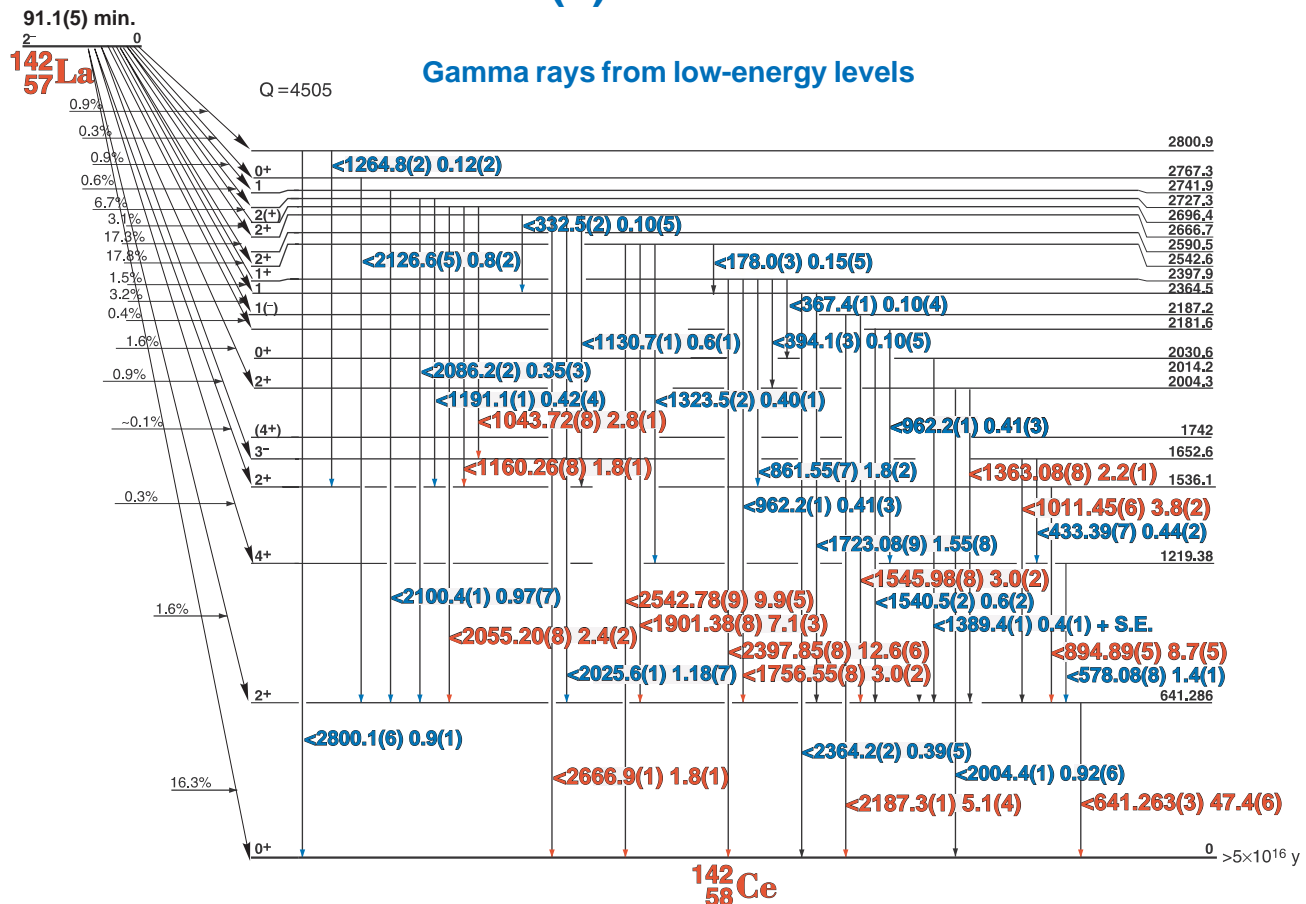
E_{γ} (KeV)[S]	ΔE_{γ}	I_{γ} (rel)	$I_{\gamma}(\%)[E]$	ΔI_{γ}	
109.47	± 0.20	0.17	0.15	± 0.04	4
131.15	± 0.20	0.42	0.46	± 0.03	4
173.50	± 0.20	0.6	0.13	± 0.01	4
241.90	± 0.08	0.51	0.46	± 0.02	4
266.61	± 0.06	0.50	0.47	± 0.02	4
306.5	± 0.4	v.w.	0.020	± 0.002	4
328.76	± 0.05	19.6	20	± 1.0	1
397.66	± 0.10	0.12	0.11	± 0.03	4
432.52	± 0.04	2.94	2.8	± 0.10	2
487.009	± 0.030	44.7	45	± 1.0	1
617.7	± 0.3	v.w.	0.14	± 0.01	4
751.655	± 0.035	4.5	4.33	± 0.15	2
815.775	± 0.030	24.2	23.3	± 0.7	1
867.842	± 0.035	5.7	5.6	± 0.2	2
919.54	± 0.04	2.89	2.7	± 0.10	3
925.188	± 0.035	7.2	6.9	± 0.3	1
951.00	± 0.06	0.56	0.52	± 0.02	4
1045.2	± 0.3	0.04	0.03	± 0.01	4
1097.2	± 0.3	0.020	0.020	± 0.003	4
1404.5	± 0.2	0.50	0.50	± 0.04	4
1596.17	± 0.06	100	95	± 2.0	1
1924.6	± 0.3	0.08	0.13	± 0.01	4
2347.80	± 0.06	0.89	0.85	± 0.05	1
2521.32	± 0.06	3.59	3.46	± 0.15	1
2547.14	± 0.06	0.110	0.101	± 0.005	2
2899.5	± 0.2	0.073	0.067	± 0.007	1
3118.52	± 0.15	0.028	0.025	± 0.003	1
3320.0	± 0.6	0.005	0.004	± 0.001	3

91.1 min. ^{142}La

57-142-2



91.1(5) min. ^{142}La



Decay Data

← Index →

91.1(5) min. ^{142}La

GAMMA-RAY ENERGIES AND INTENSITIES

Nuclide ^{142}La

Detector 3" X 3" NaI-2

Half Life 91.1(30 min.

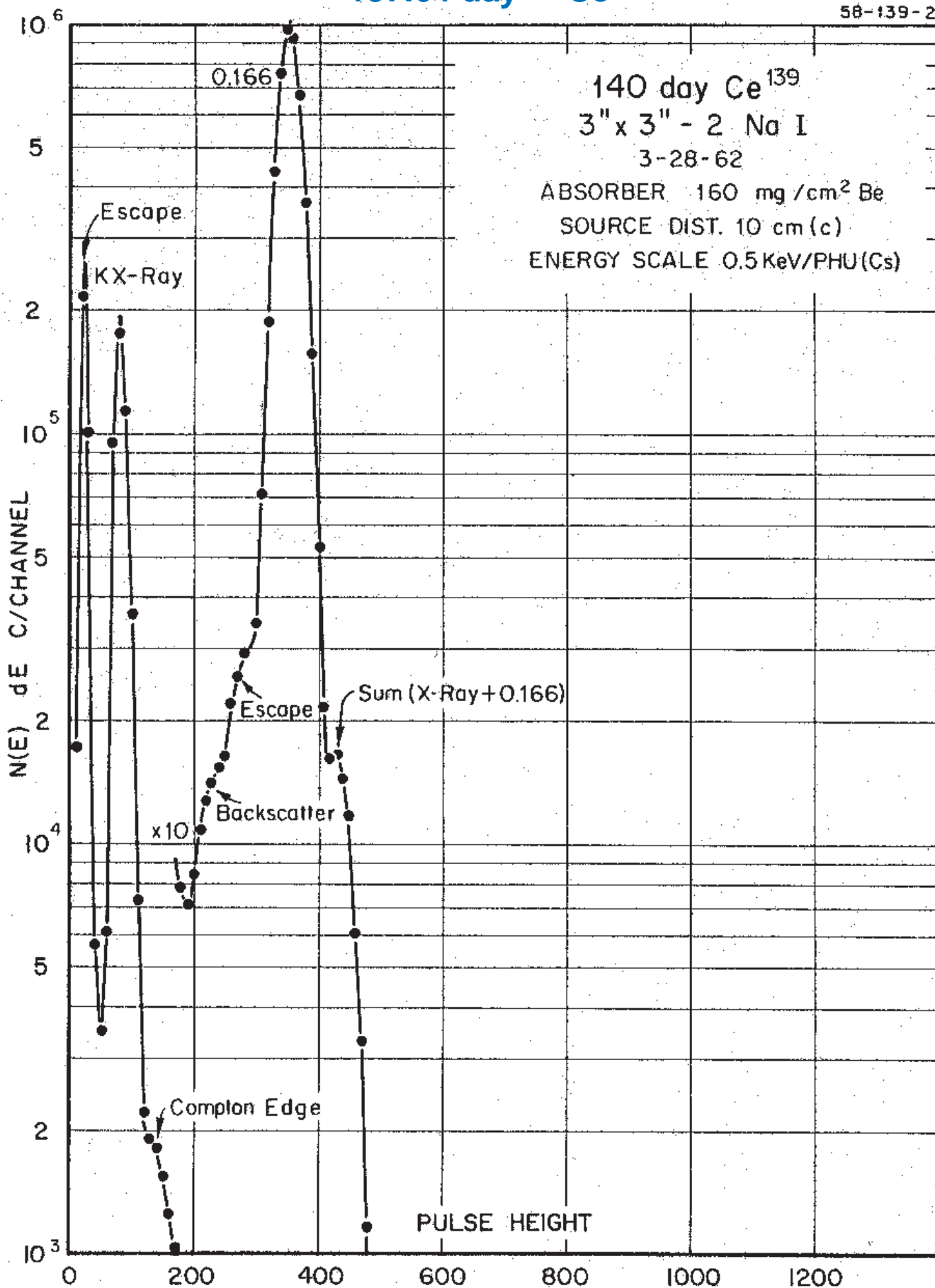
Method of Production: $^{235}\text{U}(\text{n},\text{f})$

	E_{γ} (KeV)[S]	ΔE_{γ}	I_{γ} (rel)	$I_{\gamma}(\%)[E]$	ΔI_{γ}	S
	145.1	± 0.2	0.26	± 0.04		4
	178.0	± 0.2	0.25	0.15	± 0.03	4
	332.55	± 0.1	0.22	0.10	± 0.05	4
	367.39	± 0.1	0.20	0.10	± 0.03	4
	394.24	± 0.1	0.15	0.10	± 0.05	4
	420.72	± 0.10	0.48	0.25	± 0.05	4
Ann.	433.39	± 0.07	0.93	0.45	± 0.02	1
	511.006					4
	531.80	± 0.2	0.60	0.30	± 0.04	4
	578.08	± 0.08	2.83	1.4	± 0.25	3
	619.45	± 0.08	0.39	0.20	± 0.03	3
	641.263	± 0.035	100	47.4	± 0.6	1
DE	793.5	± 0.1	0.32	0.16	± 0.02	4
	861.55	± 0.07	3.86	1.8	± 0.2	2
	879.22	± 0.1	1.06		± 0.10	3
	894.89	± 0.05	17.97	8.7	± 0.5	1
	962.25	± 0.15	0.83	0.41	± 0.03	4
	1008.30	± 0.08	1.85	0.90	± 0.08	3
	1011.45	± 0.06	7.77	3.8	± 0.2	1
	1043.72	± 0.08	5.88	2.85	± 0.1	1
	1061.2	± 0.15	0.42	0.20	± 0.02	4
	1130.70	± 0.10	1.30	0.6	± 0.1	3
	1144.9	± 0.2	0.45	0.21	± 0.02	4
DE	1160.26	± 0.08	3.76	1.8	± 0.1	1
	1165.2	± 0.2	0.62		± 0.08	3
	1191.1	± 0.15	0.90	0.44	± 0.04	4
	1233.08	± 0.08	4.65	2.3	± 0.2	1
	1242.4	± 0.2	0.54	0.26	± 0.03	4
	1264.8	± 0.25	0.26	0.12	± 0.01	4
	1288.5	± 0.3	0.26	0.12	± 0.02	4
	1323.5	± 0.2	0.85	0.40	± 0.01	3
	1354.52	± 0.08	3.44	1.66	± 0.2	2
DE	1363.08	± 0.08	4.60	2.2	± 0.1	1
SE	1375.98	± 0.1	2.39		± 0.23	2
	1389.4	± 0.1	1.76	0.4	± 0.04	3
	1395.66	± 0.15	0.60	0.29	± 0.04	4
	1445.4	± 0.2	0.28	0.14	± 0.02	4
	1461.2	± 0.2	0.95	0.45	± 0.03	4
DE	1493.97	± 0.15	0.48	0.23	± 0.02	3
	1520.67	± 0.10	2.50		± 0.20	2
	1540.6	± 0.15	1.44	0.6	± 0.15	3
	1545.98	± 0.08	6.07	3.0	± 0.1	1
	1618.30	± 0.15	0.46	0.23	± 0.04	4
	1644.8	± 0.2	0.77	0.32	± 0.06	4
	1688.30	± 0.15	0.59	0.28	± 0.03	4
	1723.08	± 0.09	3.29	1.55	± 0.08	2
	1756.55	± 0.08	6.42	3.0	± 0.20	1
E	1886.8	± 0.1	3.2	1.5	± 0.28	
	1901.38	± 0.08	14.7	7.1	± 0.3	1
E	1923.0	± 0.2	0.75	0.37	± 0.04	4
	1949.3	± 0.15	1.74		± 0.15	
	1960.13	± 0.2	0.82	0.40	± 0.04	4
	2004.39	± 0.10	1.90	0.92	± 0.06	3
	2025.6	± 0.10	2.43	1.18	± 0.07	2
SE	2031.8	± 0.3	2.4		± 0.1	4
	2038.4	± 0.10	1.98	1.0	± 0.1	3
	2055.20	± 0.08	5.25	2.4	± 0.2	1
	2076.87	± 0.10	1.55	0.80	± 0.08	3

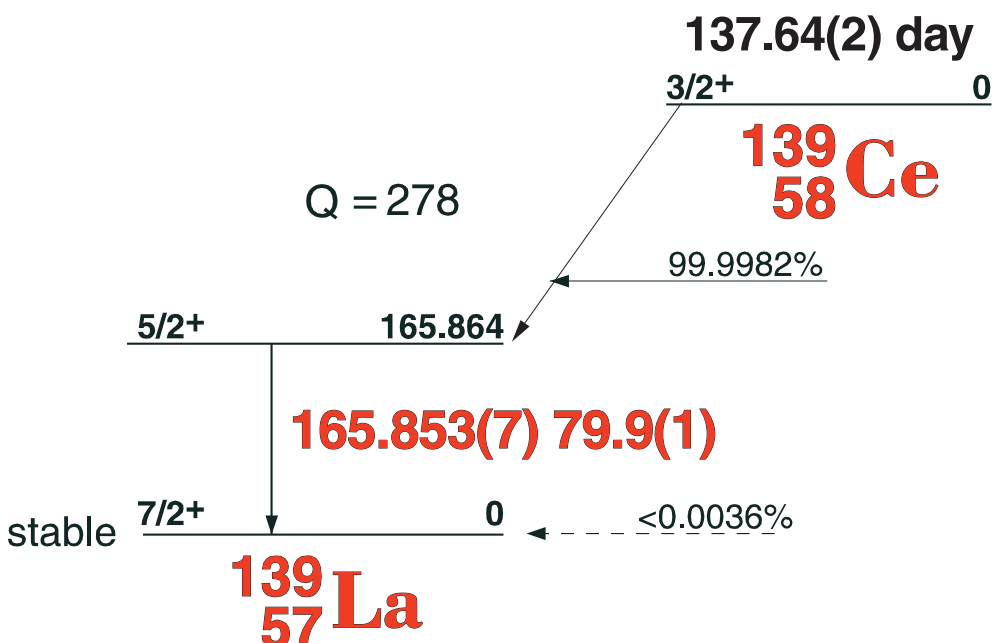
	E_{γ} (KeV)[S]	ΔE_{γ}	I_{γ} (rel)	$I_{\gamma}(\%)[E]$	ΔI_{γ}	S
	2086.22	± 0.15	0.74	0.35	± 0.02	4
	2100.4	± 0.10	2.00	0.97	± 0.07	2
	2126.8	± 0.2	1.84	0.8	± 0.15	3
	2139.2	± 0.2	1.63	0.8	± 0.1	3
	2180.4	± 0.15	1.54	0.70	± 0.07	3
	2187.31	± 0.10	10.4	5.1	± 0.4	1
DE	2291.5	± 0.2	1.67		± 0.2	3
	2304.3	± 0.2	1.92	0.94	± 0.09	3
	2357.9	± 0.2	1.90	0.9	± 0.2	3
	2364.2	± 0.25	0.78	0.39	± 0.05	4
	2397.853	± 0.12	24.80	12.6	± 0.6	1
	2419.7	± 0.2	0.94	0.4	± 0.10	4
SE	2460.51	± 0.15	1.44		± 0.15	3
	2501.4	± 0.2	0.73		± 0.09	4
	2542.78	± 0.09	20.3	9.9	± 0.5	1
	2598.4	± 0.2	0.40	0.20	± 0.04	4
	2663.7	± 0.2	1.6	0.80	± 0.08	2
	2666.98	± 0.15	3.72	1.8	± 0.1	2
	2672.4	± 0.15	0.61	0.30	± 0.05	3
	2696.7	± 0.3	0.35	0.15	± 0.03	4
	2782.5	± 0.2	1.03	0.5	± 0.1	3
	2801.7	± 0.15	1.91	0.9	± 0.1	3
	2818.2	± 0.15	1.69	0.84	± 0.06	3
	2828.6	± 0.2	0.9		± 0.10	4
	2971.55	± 0.10	7.23	3.6	± 0.1	1
	2999.73	± 0.15	0.89	0.4	± 0.1	3
	3007.16	± 0.2	0.35	0.16	± 0.05	3
	3012.75	± 0.12	1.20	0.55	± 0.08	3
	3034.3	± 0.15	1.14	0.58	± 0.06	3
	3046.6	± 0.2	0.94	0.47	± 0.05	4
	3061.8	± 0.2	0.55	0.25	± 0.04	4
	3075.8	± 0.25	0.49	0.25	± 0.03	4
	3101.0	± 0.25	0.6		± 0.08	4
	3121.8	± 0.25	0.7	0.13	± 0.02	4
	3154.8	± 0.2	0.6	0.30	± 0.01	4
	3180.75	± 0.2	0.52	0.26	± 0.03	4
	3242.5	± 0.2	0.37	0.18	± 0.02	4
	3274.1	± 0.25	0.24	0.12	± 0.02	4
	3314.40	± 0.2	2.35	1.1	± 0.1	2
	3333.5	± 0.2	0.09	0.05	± 0.02	4
	3339.58	± 0.25	0.27		± 0.06	4
	3401.5	± 0.25	0.62	0.30	± 0.04	3
	3459.5	± 0.20	0.82	0.40	± 0.04	3
	3612.0	± 0.20	1.26	0.7	± 0.1	1
	3632.72	± 0.20	1.72	0.90	± 0.09	1
	3719.2	± 0.25	0.55	0.29	± 0.02	1
	3746.2	± 0.3	0.09	0.05	± 0.01	3
	3850.75	± 0.3	0.41	0.26	± 0.03	1
	3974.9	± 0.25	0.07	0.04	± 0.01	3
	4045.0	± 0.3	0.09	0.05	± 0.01	3
	4190.5	± 0.3	0.035	0.04	± 0.01	4

137.64 day ^{139}Ce

56-139-2



137.64(2) day ^{139}Ce



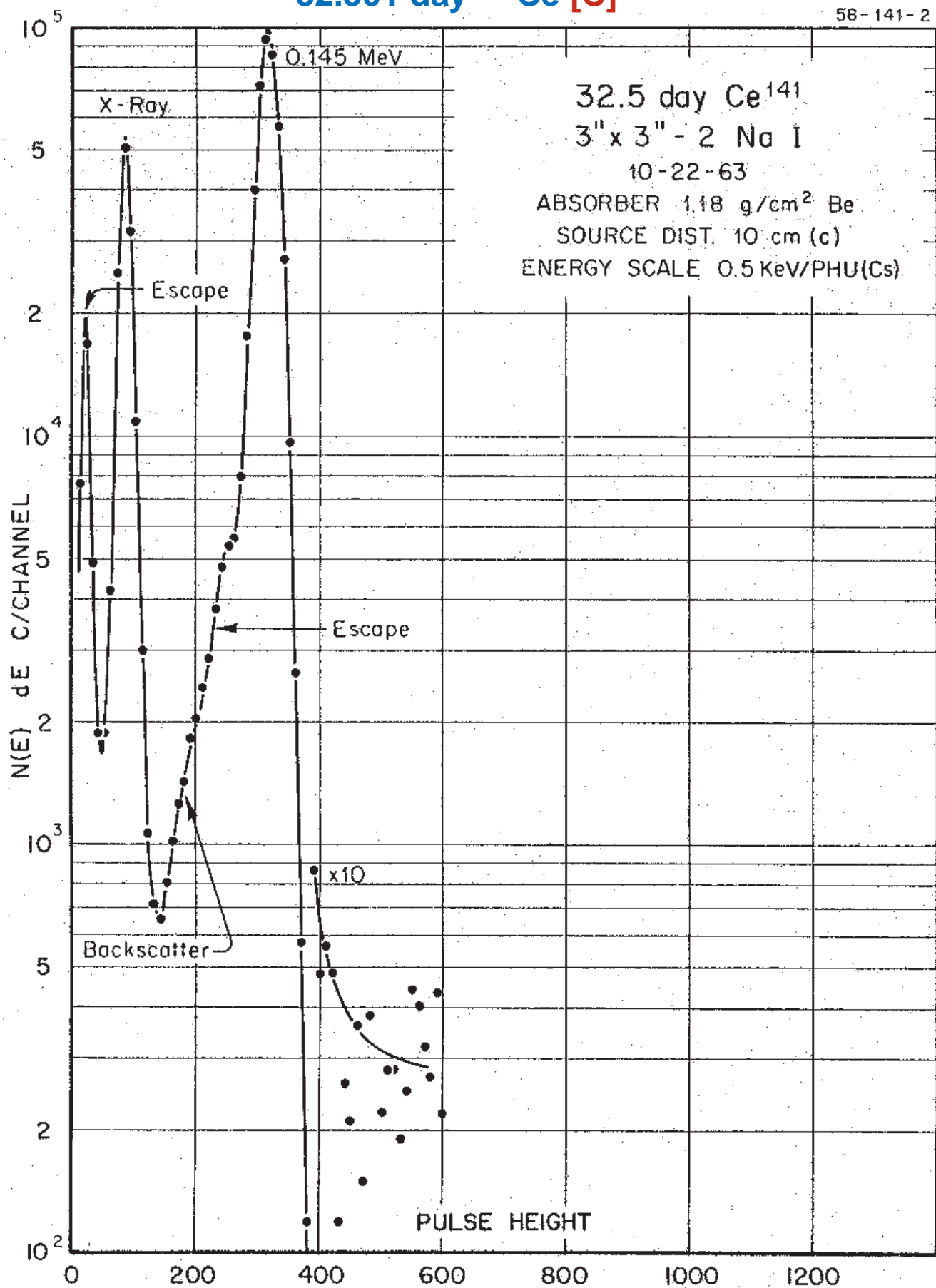
GAMMA-RAY ENERGIES AND INTENSITIES

Nuclide **^{139}cE** Half Life **137.64(2) day**
 Detector **3" x 3" -2 NaI** Method of Production: $^{139}\text{La}(\text{p},\text{n})$

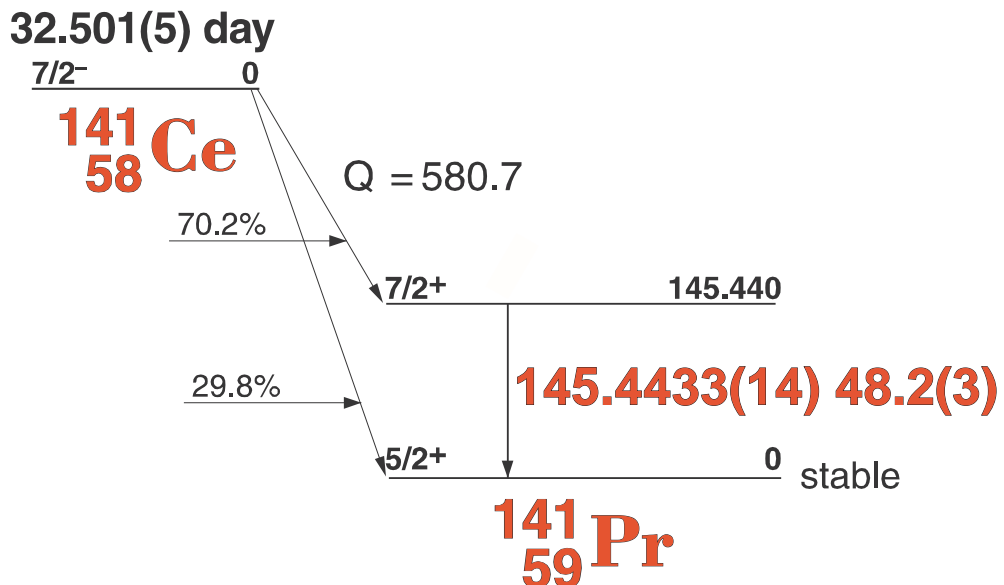
E_{γ} (KeV)[S]	ΔE_{γ}	I_{γ} (rel)	$I_{\gamma}(\%)[E]$	ΔI_{γ}	S
165.863	± 0.007	100	79.9	± 0.1	1

32.501 day ^{141}Ce [C]

58-141-2



32.501(5) day ^{141}Ce [C]



GAMMA-RAY ENERGIES AND INTENSITIES

Nuclide ^{141}Ce
Detector 3" x 3" -2 NaI

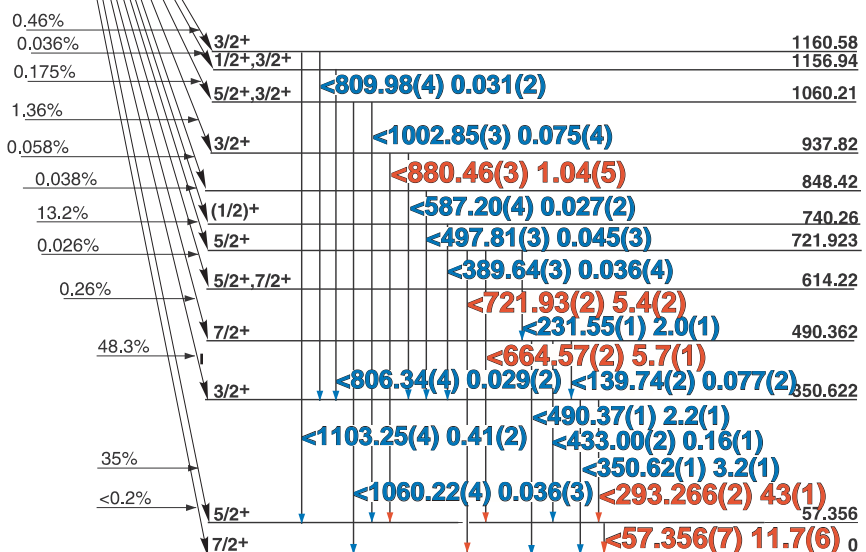
Half Life 32.501(5) day
Method of Production: $^{140}\text{Ce}(n,\gamma)$

E_{γ} (KeV)[C]	ΔE_{γ}	I_{γ} (rel)	$I_{\gamma}(\%)[E]$	ΔI_{γ}	S
145.4433	± 0.0014	100	48.2	± 0.3	1

33.039(6) hr.
 ^{143}Ce
58

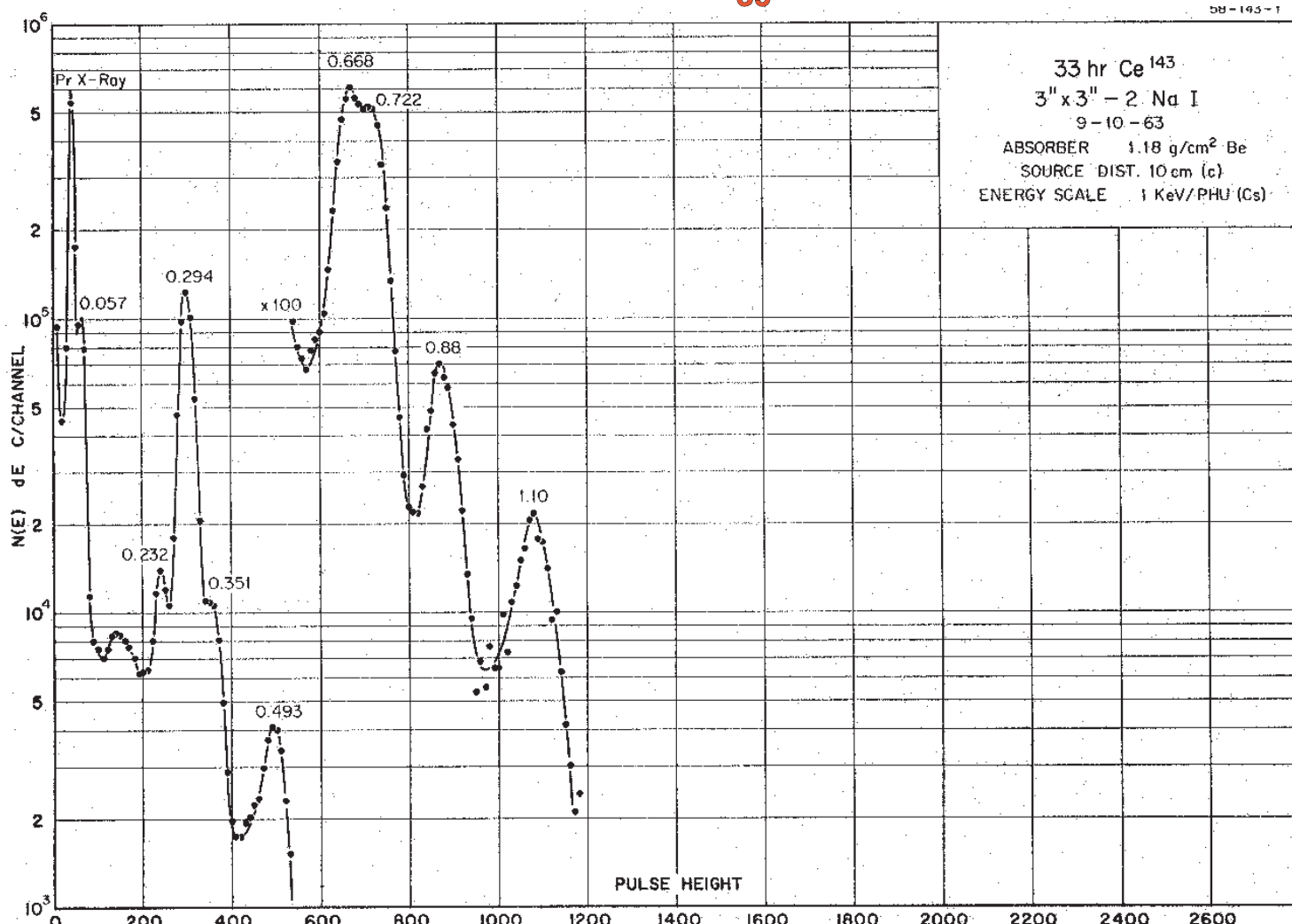
33.039(6) hr. ^{143}Ce

$Q = 1461.6$



143 Pr
59

13.57(2) day



33.039(6) hr. ^{143}Ce

GAMMA-RAY ENERGIES AND INTENSITIES

Nuclide ^{143}Ce
 Detector 3" x 3" -2 NaI

Half Life 33.039(6) hr.
 Method of Production: $^{142}\text{Ce}(n,\gamma)$

E_{γ} (KeV)[E]	ΔE_{γ}	I_{γ} (rel)	$I_{\gamma}(\%)$	ΔI_{γ}	S
Pr x-rays					
57.356	± 0.007		11.7	± 0.6	1
139.74	± 0.02		0.077	± 0.002	4
231.55	± 0.01		2.0	± 0.1	3
293.266	± 0.002		43.0	± 1.0	1
350.56	± 0.01		3.2	± 0.1	2
389.64	± 0.03		0.036	± 0.004	4
433.00	± 0.02		0.16	± 0.01	3
490.37	± 0.01		2.2	± 0.1	3
497.81	± 0.03		0.045	± 0.003	4
587.20	± 0.04		0.027	± 0.002	4
664.57	± 0.02		5.7	± 0.1	1
721.93	± 0.02		5.4	± 0.2	1
806.34	± 0.04		0.34	± 0.04	3
809.98	± 0.04		0.031	± 0.002	4
1002.85	± 0.03		0.075	± 0.004	4
1060.22	± 0.04		0.036	± 0.003	4
1103.25	± 0.04		0.41	± 0.02	2

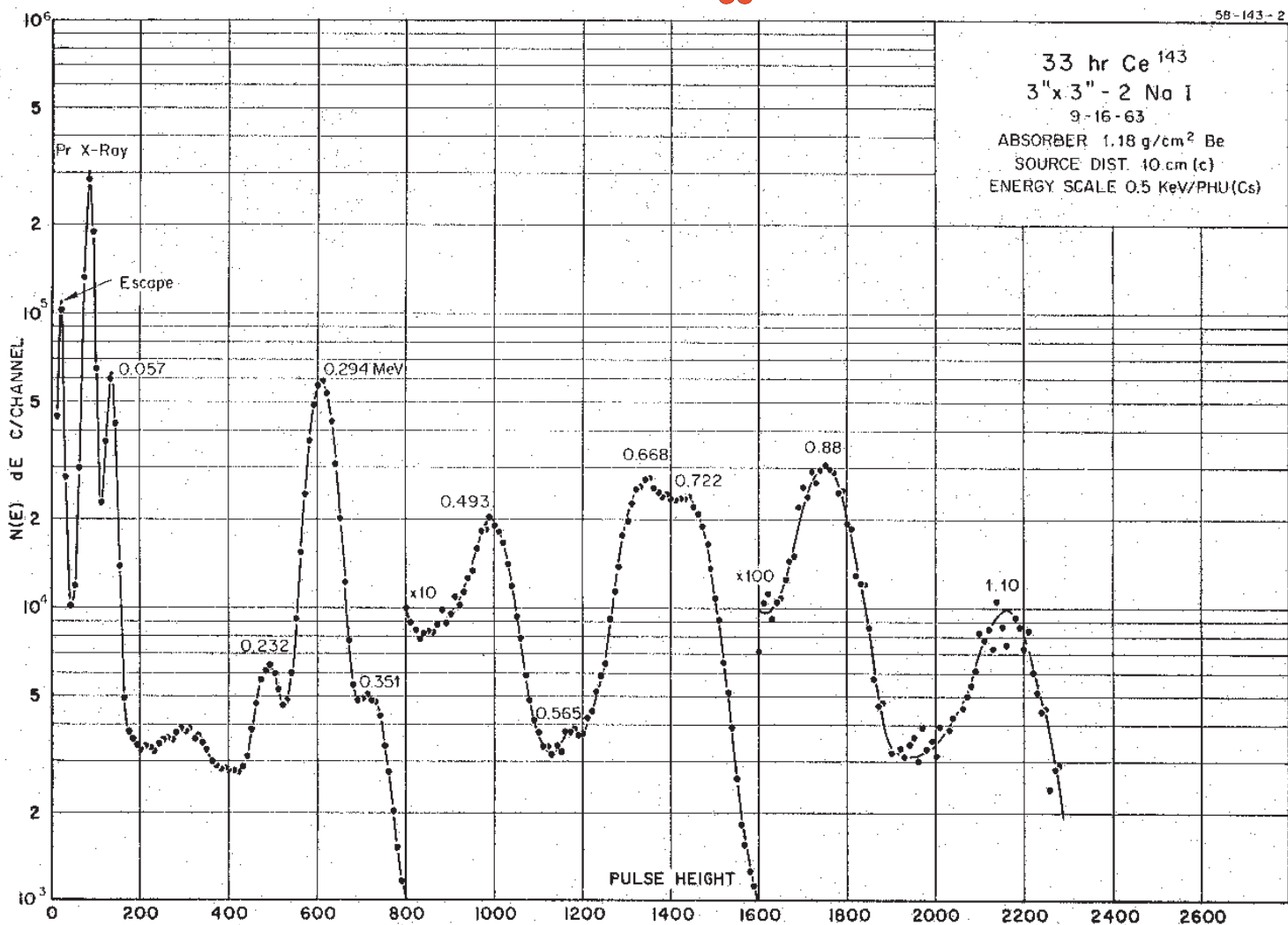


0.46%	3/2+	1160.58
0.036%	1/2+, 3/2+	1156.94
0.175%	5/2+, 3/2+	1060.21
1.36%	3/2+	
0.058%		<809.98(4) 0.031(2)
0.038%		<1002.85(3) 0.075(4)
13.2%	(1/2)+	<880.46(3) 1.04(5)
0.026%	5/2+	<587.20(4) 0.027(2)
0.26%	5/2+, 7/2+	<497.81(3) 0.045(3)
48.3%	7/2+	<389.64(3) 0.036(4)
35%	3/2+	<721.93(2) 5.4(2)
<0.2%	5/2+	<231.55(1) 2.0(1)
	7/2+	<664.57(2) 5.7(1)
		<806.34(4) 0.029(2) <139.74(2) 0.077(2)
		<1103.25(4) 0.41(2) <433.00(2) 0.16(1)
		<1060.22(4) 0.036(3) <350.62(1) 3.2(1)
		<293.266(2) 43(1)
		<57.356(7) 11.7(6)

143 Pr

13.57(2) day

58-143-2



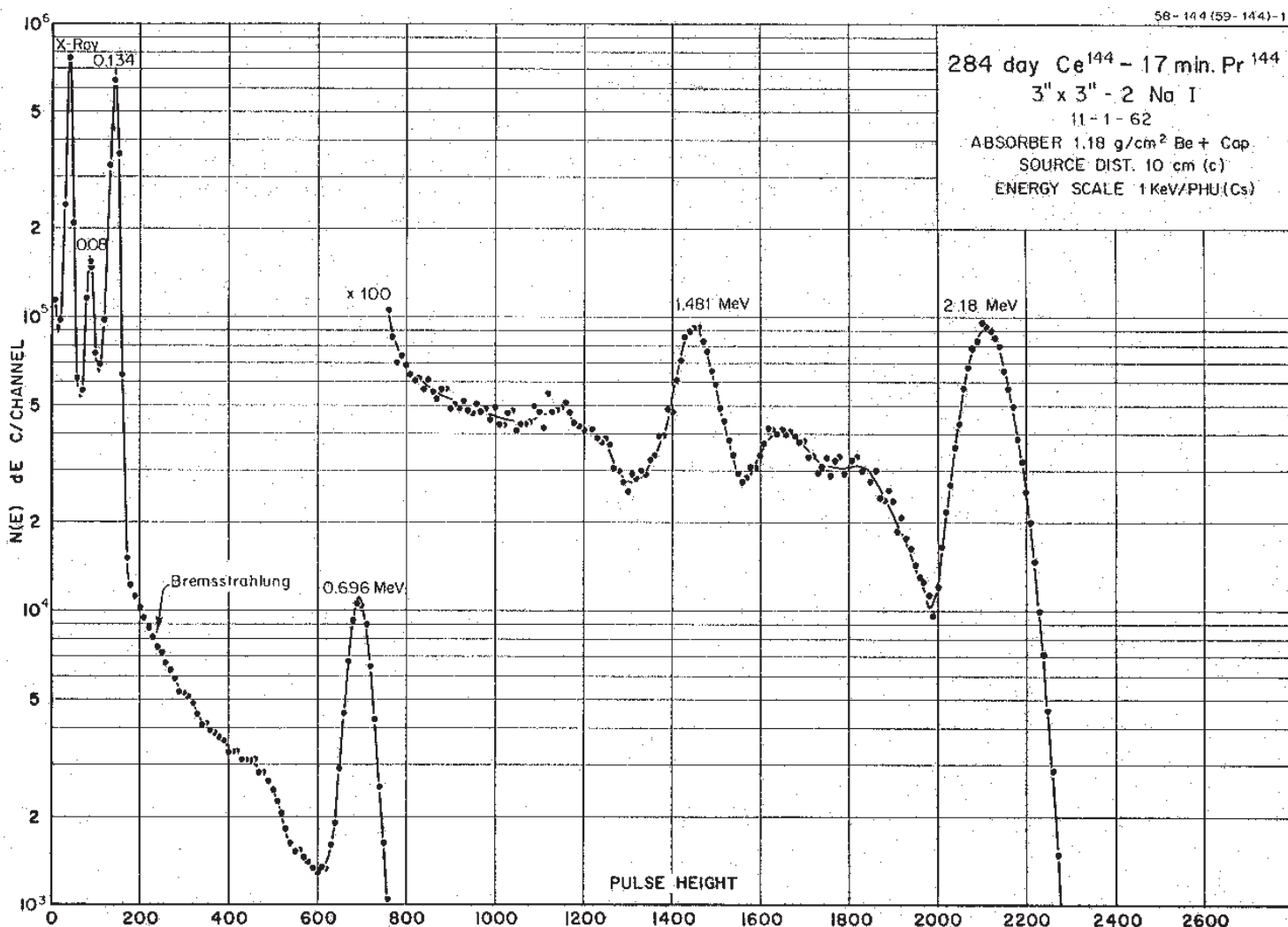
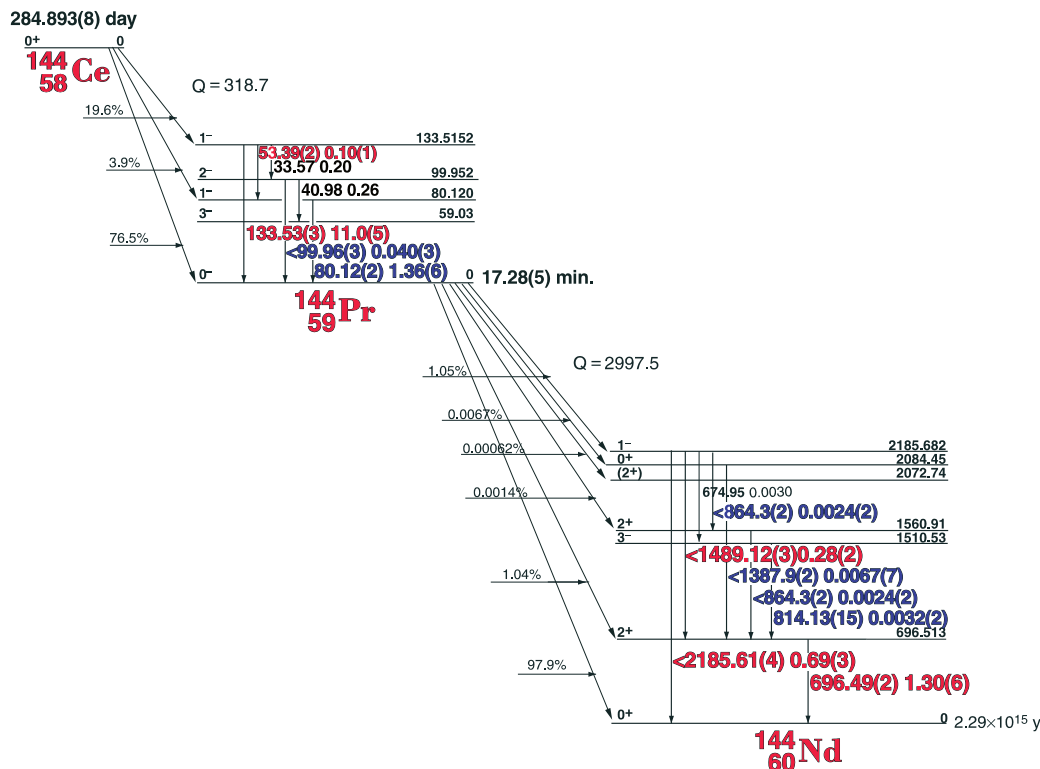
33.039(6) hr. ^{143}Ce

GAMMA-RAY ENERGIES AND INTENSITIES

Nuclide ^{143}Ce Half Life 33.039(6) hr.
 Detector 3" x 3" -2 Nal Method of Production: $^{142}\text{Ce}(n,\gamma)$

E_{γ} (KeV) [E]	ΔE_{γ}	$I_{\gamma}(\text{rel})$	$I_{\gamma}(\%)$	ΔI_{γ}	S
Pr x-rays					
57.356	± 0.007		11.7	± 0.6	4
139.74	± 0.02		0.077	± 0.002	4
231.55	± 0.01		2.0	± 0.1	3
293.266	± 0.002		43.0	± 1.0	1
350.56	± 0.01		3.2	± 0.1	2
389.64	± 0.03		0.036	± 0.004	4
433.00	± 0.02		0.16	± 0.01	3
490.37	± 0.01		2.2	± 0.1	3
497.81	± 0.03		0.045	± 0.003	4
587.20	± 0.04		0.027	± 0.002	4
664.57	± 0.02		5.7	± 0.1	1
721.93	± 0.02		5.4	± 0.2	1
806.34	± 0.04		0.34	± 0.04	3
809.98	± 0.04		0.031	± 0.002	4
1002.85	± 0.03		0.075	± 0.004	4
1060.22	± 0.04		0.036	± 0.003	4
1103.25	± 0.04		0.41	± 0.02	2

284.893 day ^{144}Ce - 17.28 min. ^{144}Pr [C]



Decay Data

← Index →

284.893(8) day ^{144}Ce - 17.28(5) min. ^{144}Pr [C]

List of Gamma-ray Energies and Intensities

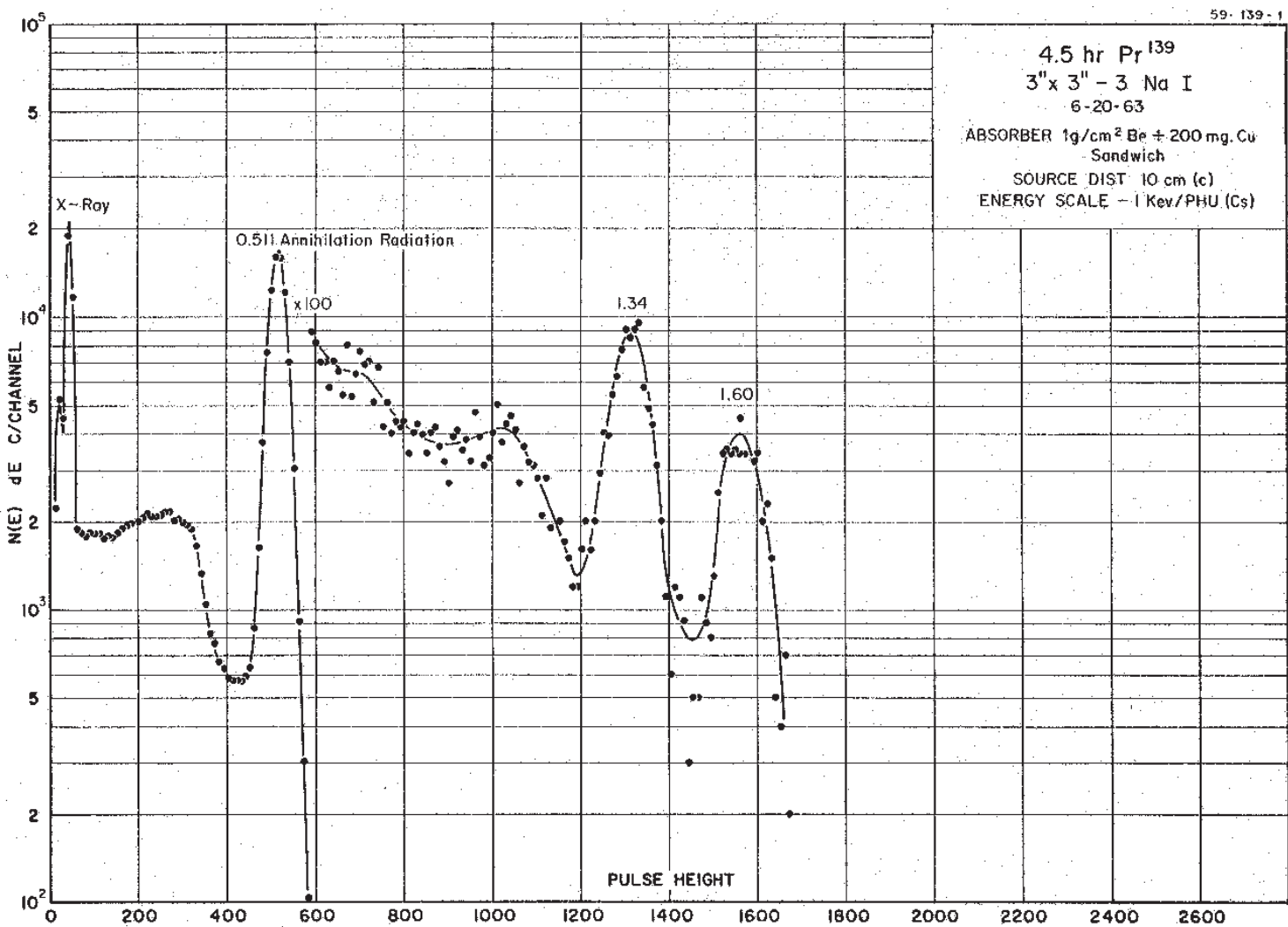
GAMMA-RAY ENERGIES AND INTENSITIES

Nuclide ^{144}Ce - ^{144}Pr
Detector 3" X 3" NaI-2

Half Life 284/893(8) day - 17.28(5) min.
Method of Production: $^{235}\text{U}(\text{n},\text{f})$ chem.

	E_{γ} (KeV)[C]	ΔE_{γ}	$I_{\gamma}(\text{rel})$	$I_{\gamma}(\%)$ [E]	ΔI_{γ}	S
^{144}Ce	53.34	± 0.02	6.64	0.10	± 0.01	3
^{144}Ce	80.12	± 0.025	108.3	1.36	± 0.06	2
^{144}Ce	99.96	± 0.035	2.67	0.040	± 0.003	3
^{144}Ce	133.53	± 0.03	80.0	11.0	± 0.3	1
^{144}Pr	624.84	± 0.20	0.07		± 0.04	4
	696.492	± 0.019	100	1.30	± 0.06	1
	814.13	± 0.15	0.18	0.0032	$\pm 0.(2)$	4
	864.28	± 0.18	0.21	0.0024	$\pm 0.(2)$	4
DE	1163.73	± 0.05	3.56		± 0.25	2
	1387.92	± 0.18	0.57	0.0087	$\pm 0.(7)$	3
	1489.124	± 0.032	21.	0.28	± 0.02	1
SE	1674.59	± 0.080	3.53		± 0.25	2
	2185.608	± 0.046	57.0	0.69	± 0.03	1

4.41 hr. ^{139}Pr



Decay Data

◀ Index ▶

19.12 hr. ^{142}Pr

GAMMA-RAY ENERGIES AND INTENSITIES

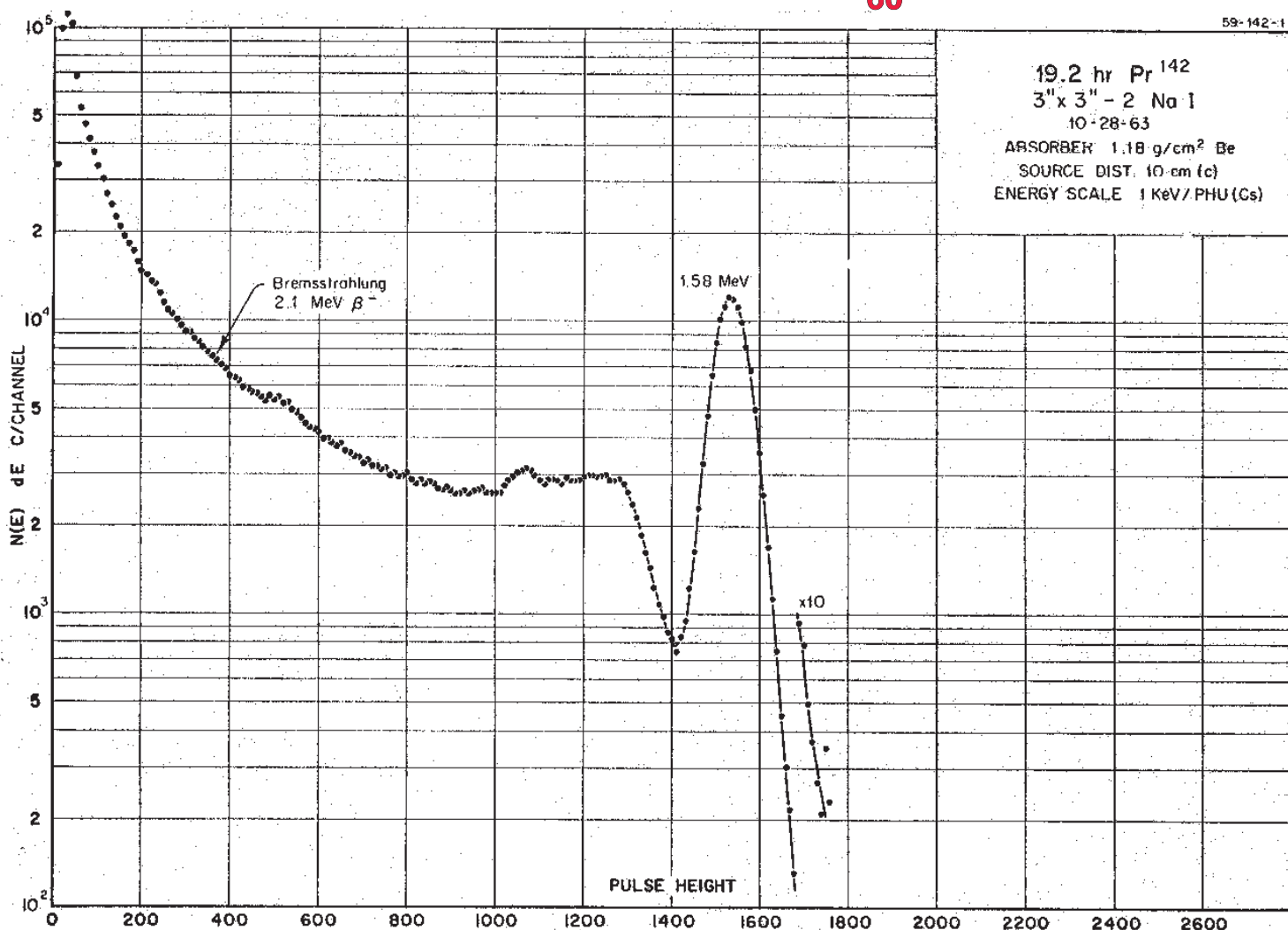
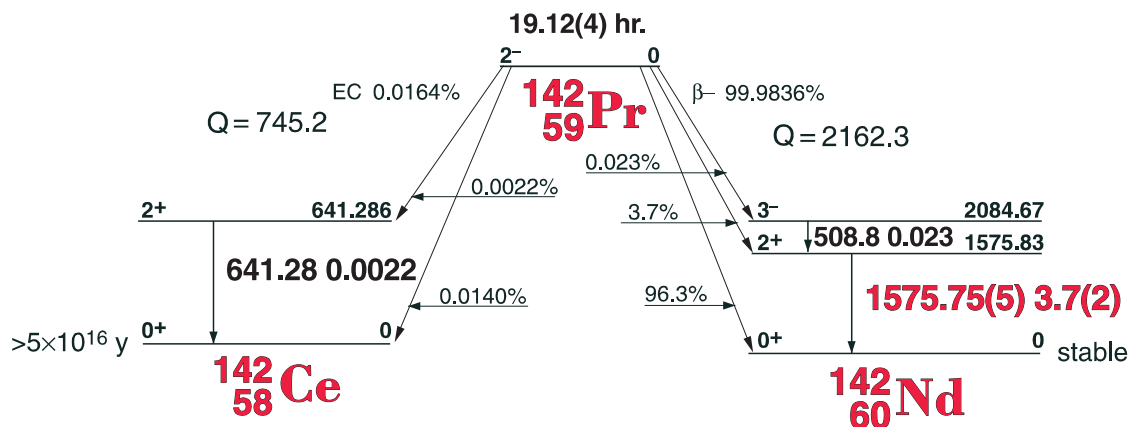
Nuclide ^{142}Pr

Half Life 19.12(4) hr.

Detector 3" x 3" -2 NaI

Method of Production: $^{141}\text{Pr}(\text{n},\gamma)$

Detector	χ^2/ν	Method of Production			PR(%)	
	E $_{\gamma}$ (KeV)[S]	ΔE_{γ}	I $_{\gamma}$ (rel)	I $_{\gamma}$ (%)[E]	ΔI_{γ}	S
Ann.	641.28	± 0.08		0.0022	$\pm 0.(2)$	5
	511.006					1
	1575.75	± 0.05	100	3.7	± 0.2	1



5.98 hr. ^{143}Pr

5-9-143-1

13.7 day Pr^{143}

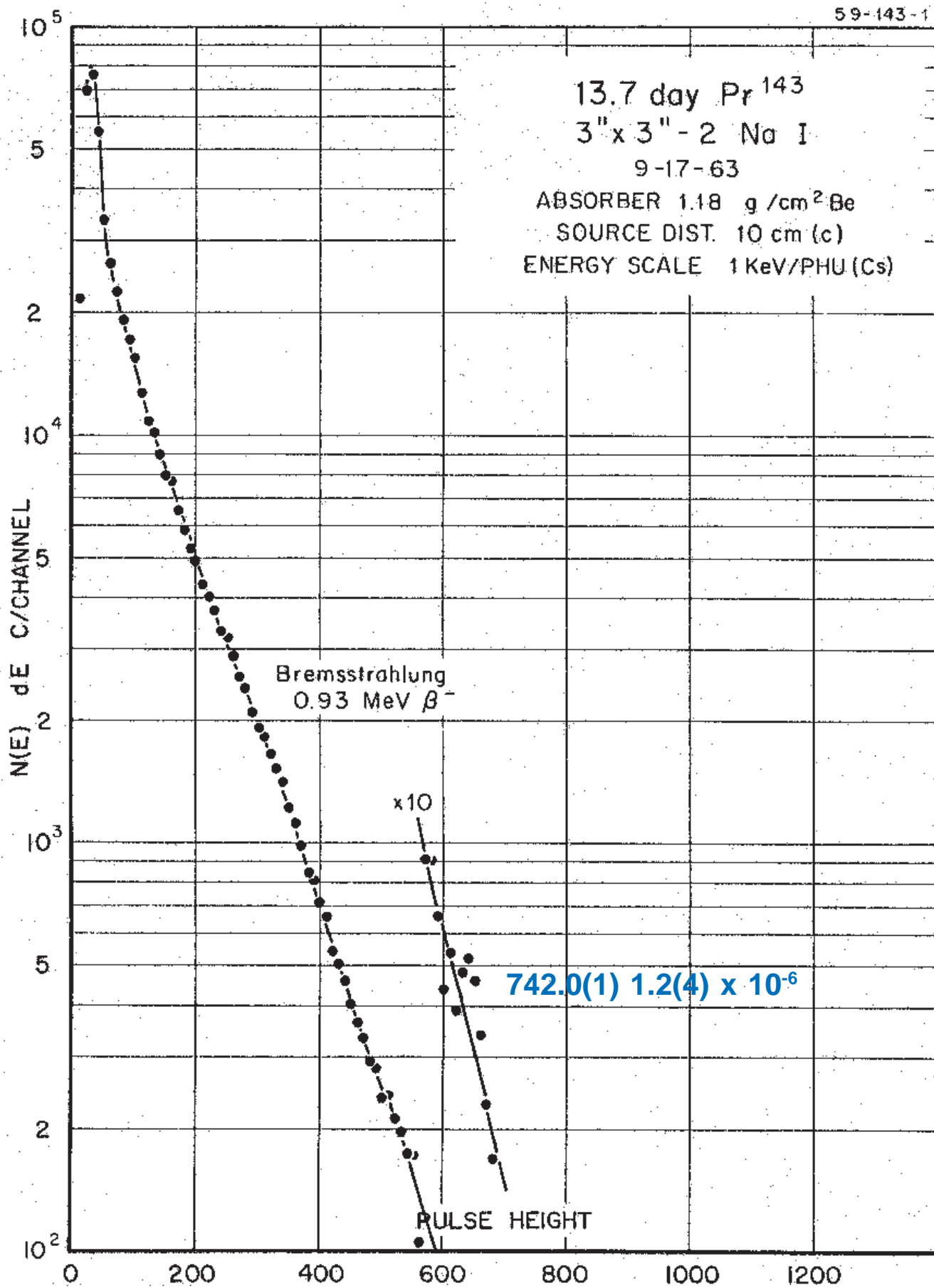
$3'' \times 3'' - 2 \text{ No I}$

9-17-63

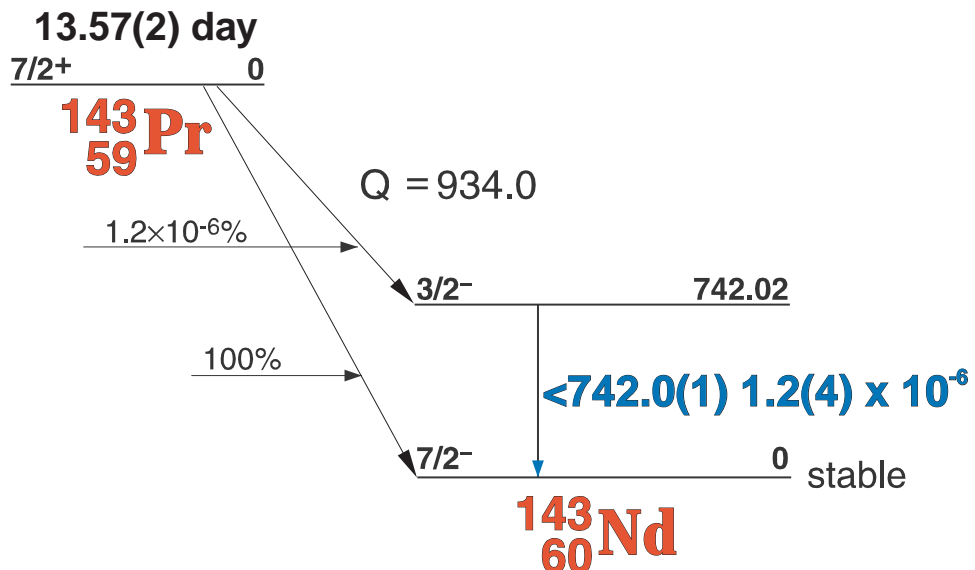
ABSORBER $1.18 \text{ g/cm}^2 \text{Be}$

SOURCE DIST. 10 cm (c)

ENERGY SCALE 1 KeV/PHU (Cs)



13.57(2) day ^{143}Pr



GAMMA-RAY ENERGIES AND INTENSITIES

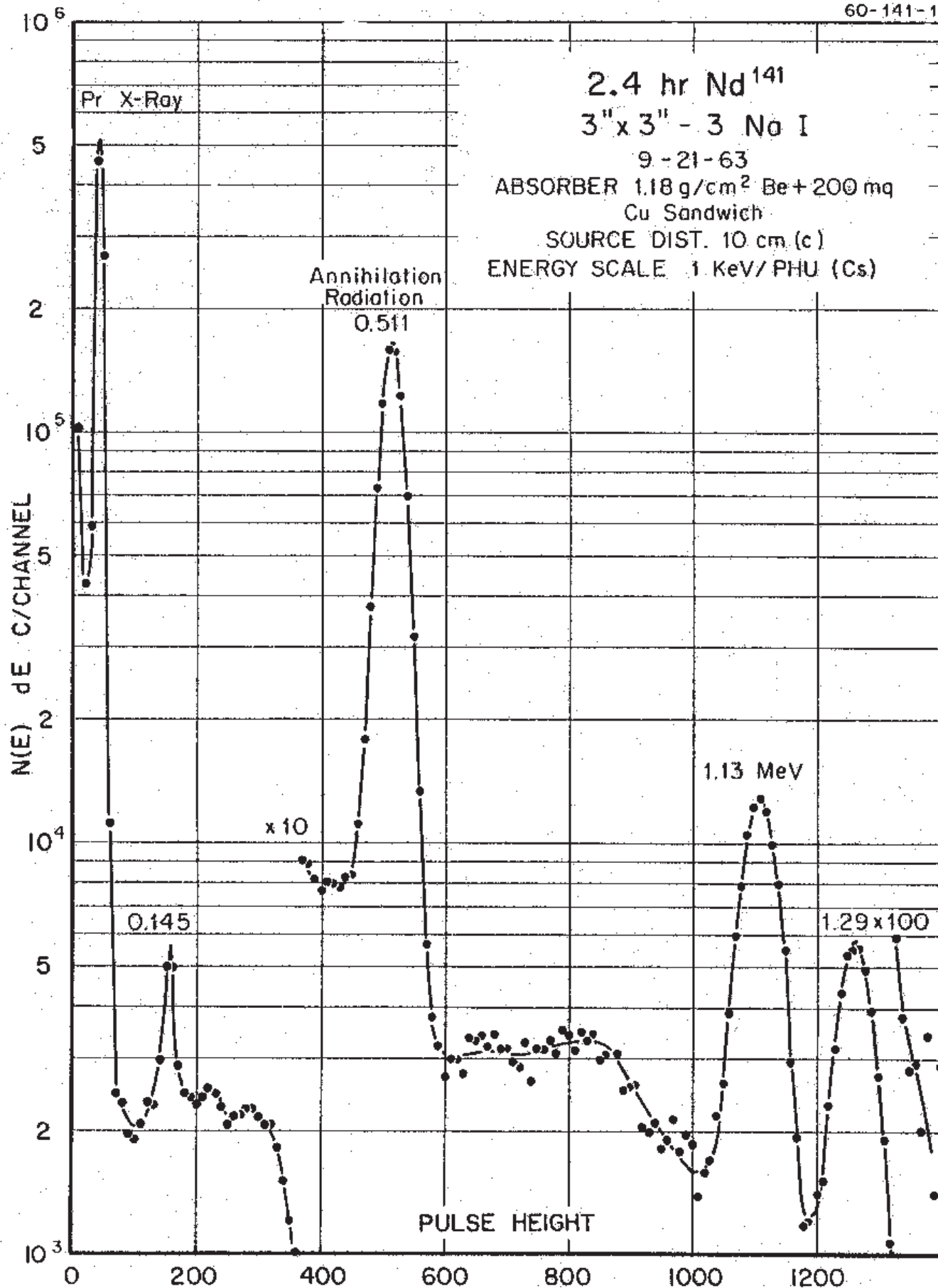
Nuclide ^{143}Pr
Detector 3" X 3" NaI-2

Half Life 13.57(2) day
Method of Production: $^{142}\text{Ce}(n,\gamma,\beta)$

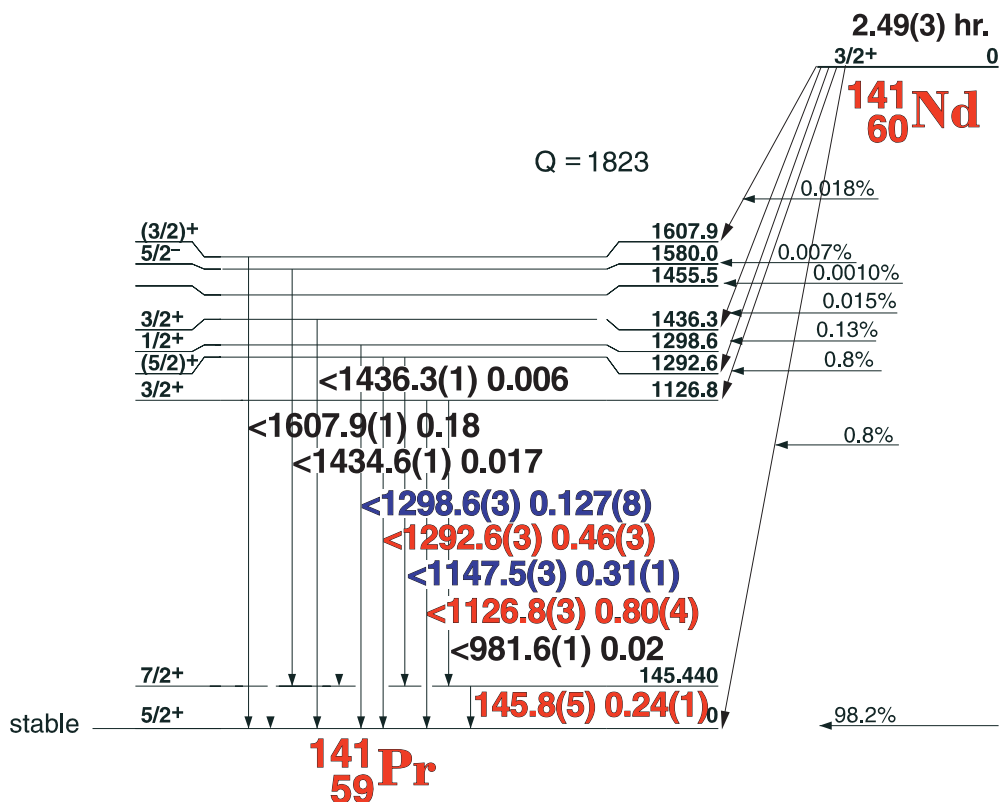
E_γ (KeV)[S]	ΔE_γ	I_γ (rel)	$I_\gamma(\%)$ [E]	ΔI_γ	S
Yb K x-rays 742.0	± 0.1		1.2×10^{-6}	$\pm 0.(4)$	2

2.49 hr. ^{141}Nd

60-141-1



2.49(3) hr. ^{141}Nd Decay Scheme



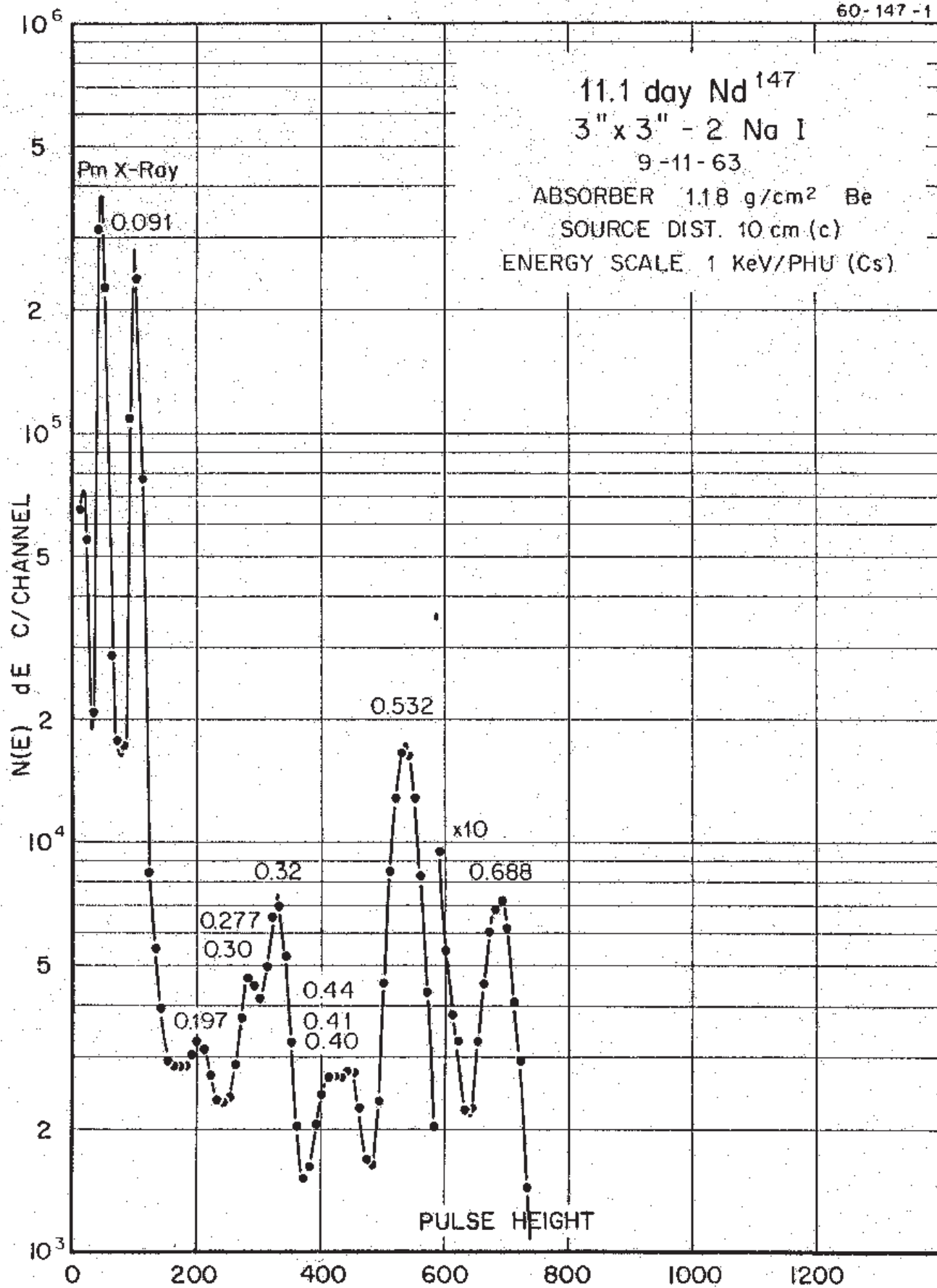
GAMMA-RAY ENERGIES AND INTENSITIES

Nuclide ^{141}Nd Half Life 2.49(3) hr.
 Detector 3" x 3" -2 NaI Method of Production: $^{142}\text{Nd}(\gamma, n)$

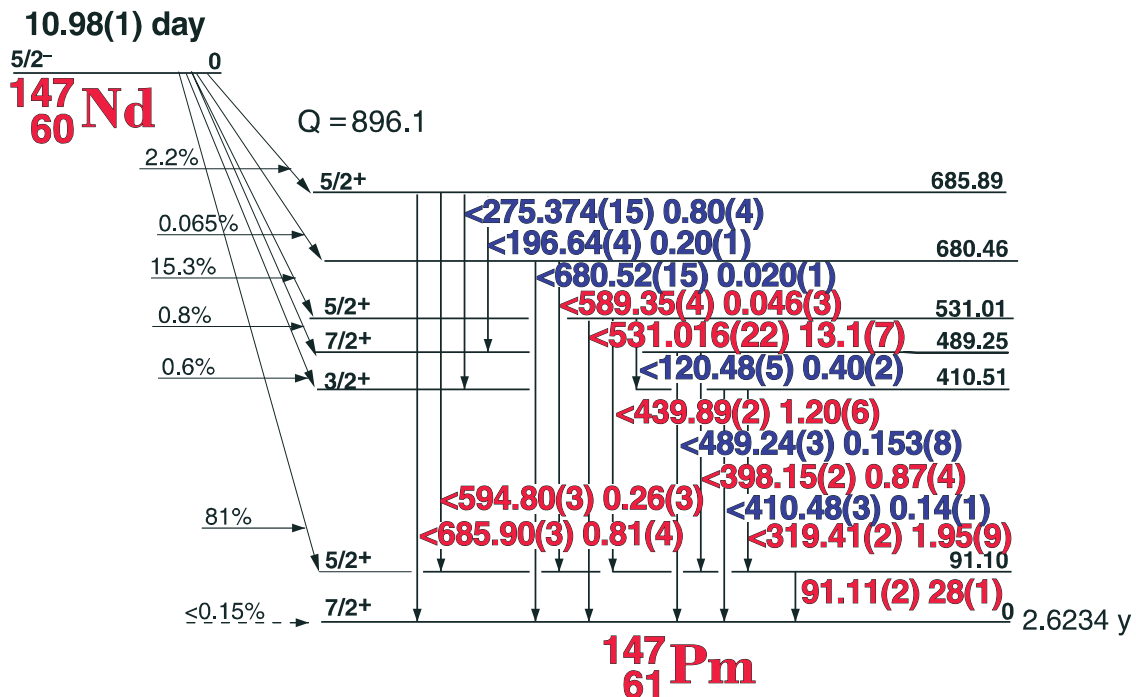
E_{γ} (KeV)[S]	ΔE_{γ}	I_{γ} (rel)	$I_{\gamma}(\%)[E]$	ΔI_{γ}	S
145.8	± 0.5		0.24	± 0.01	1
1126.8	± 0.3		0.80	± 0.04	1
1147.5	± 0.3		0.31	± 0.01	2
1292.6	± 0.3		0.46	± 0.03	1
1298.6	± 0.3		0.127	± 0.008	2
1434.6	± 0.1		0.017	± 0.002	5
1436.3	± 0.1		0.006	$\pm 0.(1)$	5
1607.9	± 0.1		0.18	± 0.02	4

10.98 day ^{147}Nd

60-147-1



10.98(1) day ^{147}Nd Decay Scheme



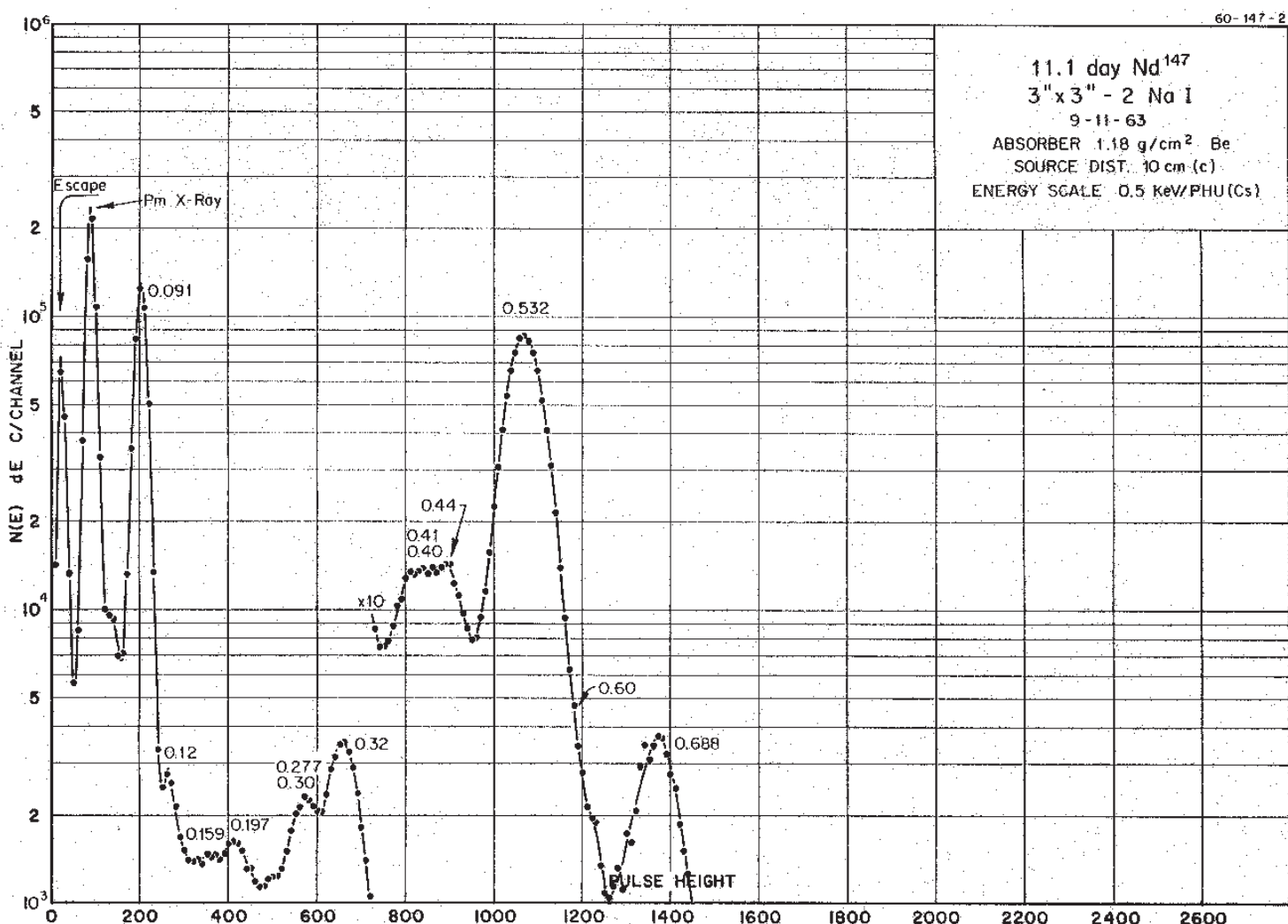
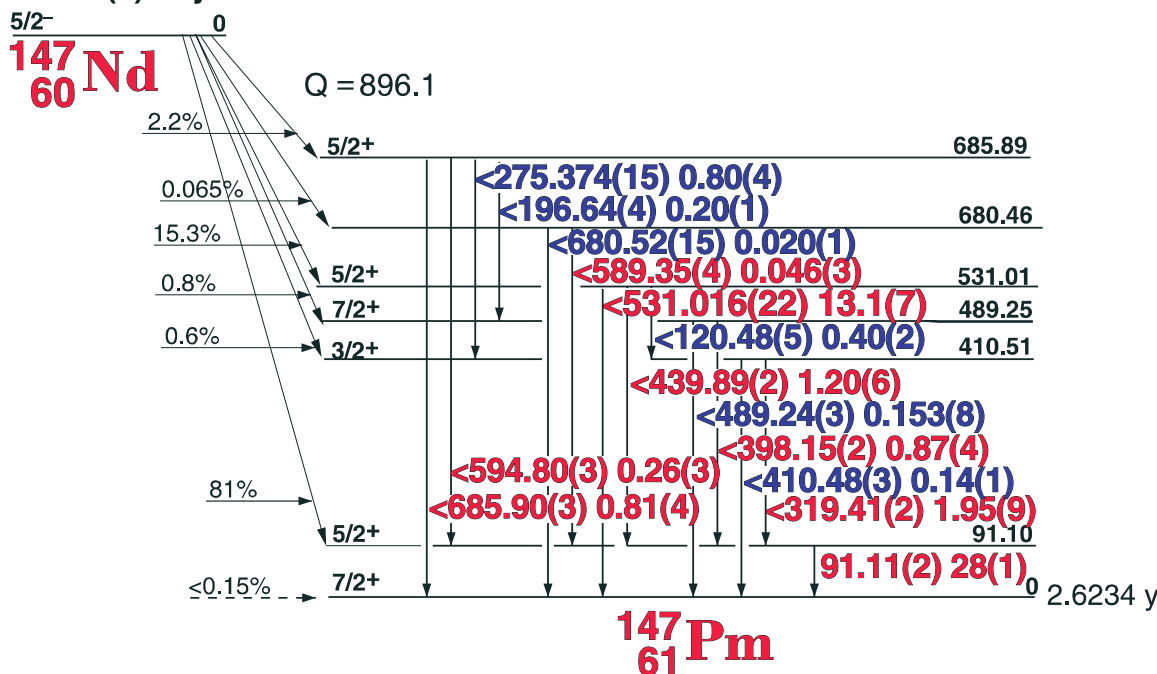
GAMMA-RAY ENERGIES AND INTENSITIES

Nuclide ^{147}Nd Half Life 10.98(1) day
 Detector 3" x 3" -2 NaI Method of Production: $^{146}\text{Nd}(n,\gamma)$

E_{γ} (KeV)[S]	ΔE_{γ}	I_{γ} (rel)	$I_{\gamma}(\%)$ [E]	ΔI_{γ}	S
91.106	± 0.020	100	28	± 1.0	1
120.48	± 0.05	1.42	0.40	± 0.02	2
196.64	t 0.04	0.73	0.20	± 0.01	3
275.374	± 0.015	2.87	0.80	± 0.04	2
319.411	± 0.018	7.0	1.95	± 0.09	1
398.155	± 0.020	3.12	0.87	± 0.04	1
410.48	± 0.03	0.50	0.14	± 0.01	3
439.895	± 0.022	4.3	1.20	± 0.05	1
489.240	± 0.028	0.55	0.153	± 0.008	3
531.016	± 0.022	46.9	13.1	± 0.6	1
589.35	± 0.04	0.164	0.046	± 0.003	2
594.803	± 0.03	0.95	0.26	± 0.03	1
680.52	± 0.15	0.070	0.020	± 0.01	4
685.902	± 0.035	2.91	0.81	± 0.04	1

10.98(1) day ^{147}Nd Decay Scheme

10.98(1) day



Decay Data

← Index →

10.98(1) day ^{147}Nd Decay Scheme

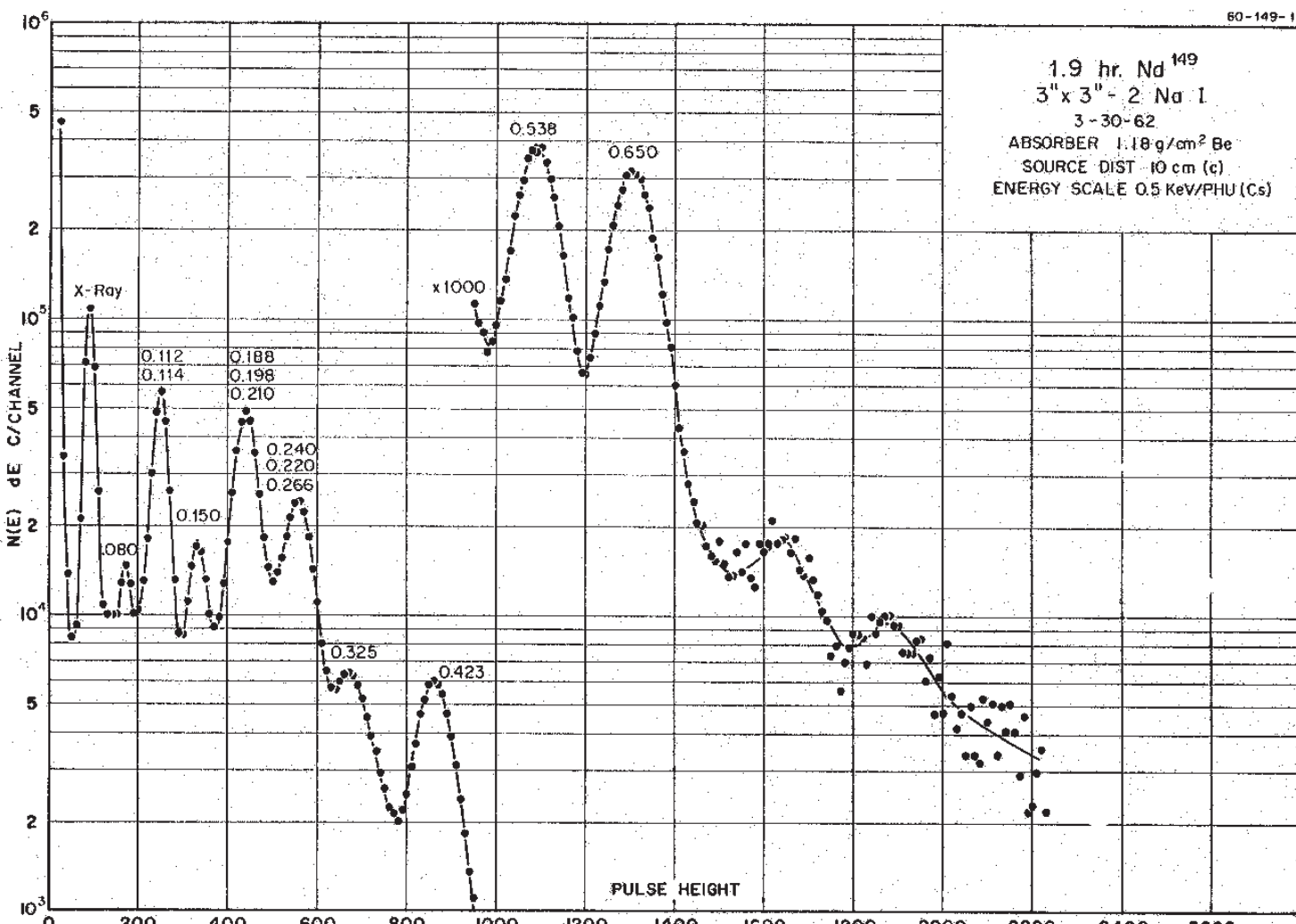
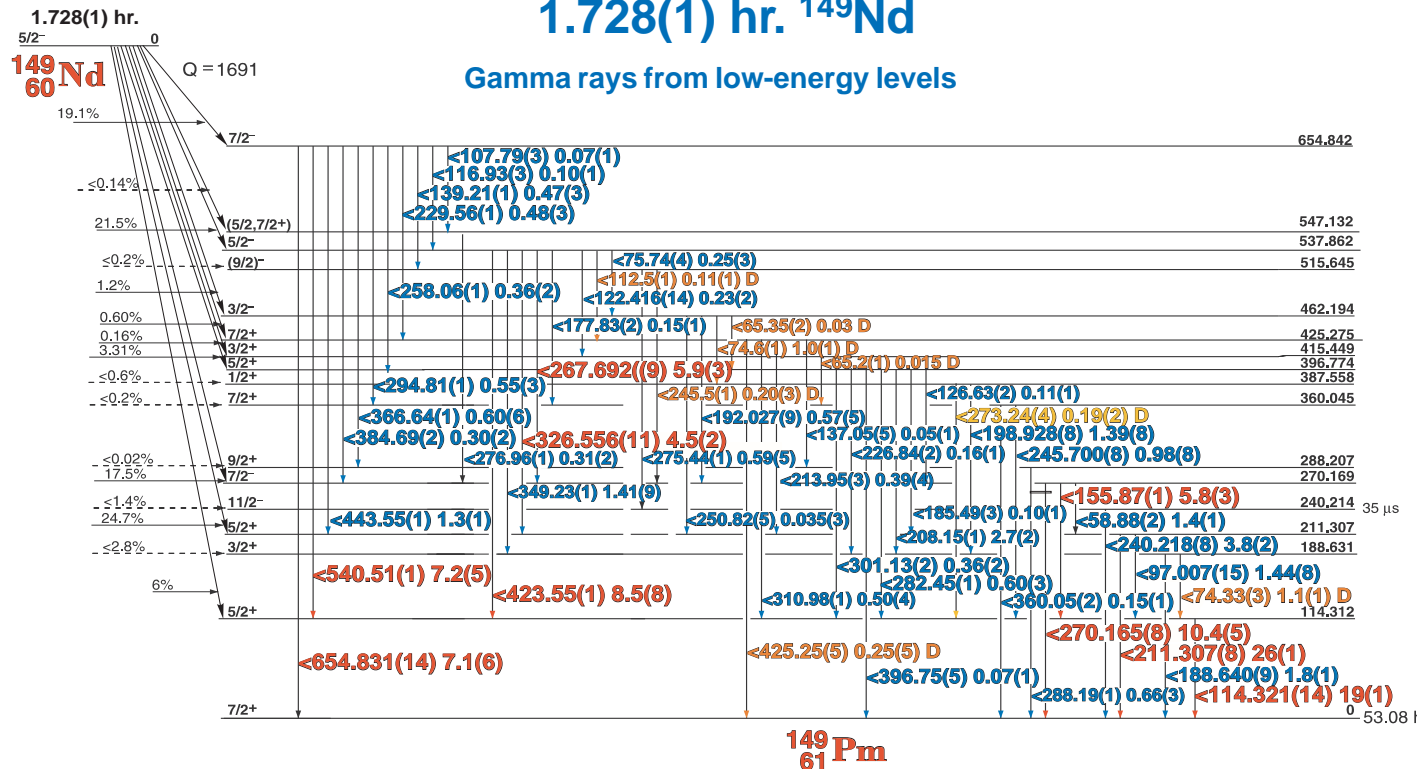
GAMMA-RAY ENERGIES AND INTENSITIES

Nuclide ^{147}Nd Half Life 10.98(1) day
 Detector 3" x 3" -2 Nal Method of Production: $^{146}\text{Nd}(\text{n},\gamma)$

E_{γ} (KeV)[S]	ΔE_{γ}	I_{γ} (rel)	$I_{\gamma}(\%)[E]$	ΔI_{γ}	S
91.106	± 0.020	100	28	± 1.0	1
120.48	± 0.05	1.42	0.40	± 0.02	2
196.64	t 0.04	0.73	0.20	± 0.01	3
275.374	± 0.015	2.87	0.80	± 0.04	2
319.411	± 0.018	7.0	1.95	± 0.09	1
398.155	± 0.020	3.12	0.87	± 0.04	1
410.48	± 0.03	0.50	0.14	± 0.01	3
439.895	± 0.022	4.3	1.20	± 0.05	1
489.240	± 0.028	0.55	0.153	± 0.008	3
531.016	± 0.022	46.9	13.1	± 0.6	1
589.35	± 0.04	0.164	0.046	± 0.003	2
594.803	± 0.03	0.95	0.26	± 0.03	1
680.52	± 0.15	0.070	0.020	± 0.01	4
685.902	± 0.035	2.91	0.81	± 0.04	1

1.728(1) hr. ^{149}Nd

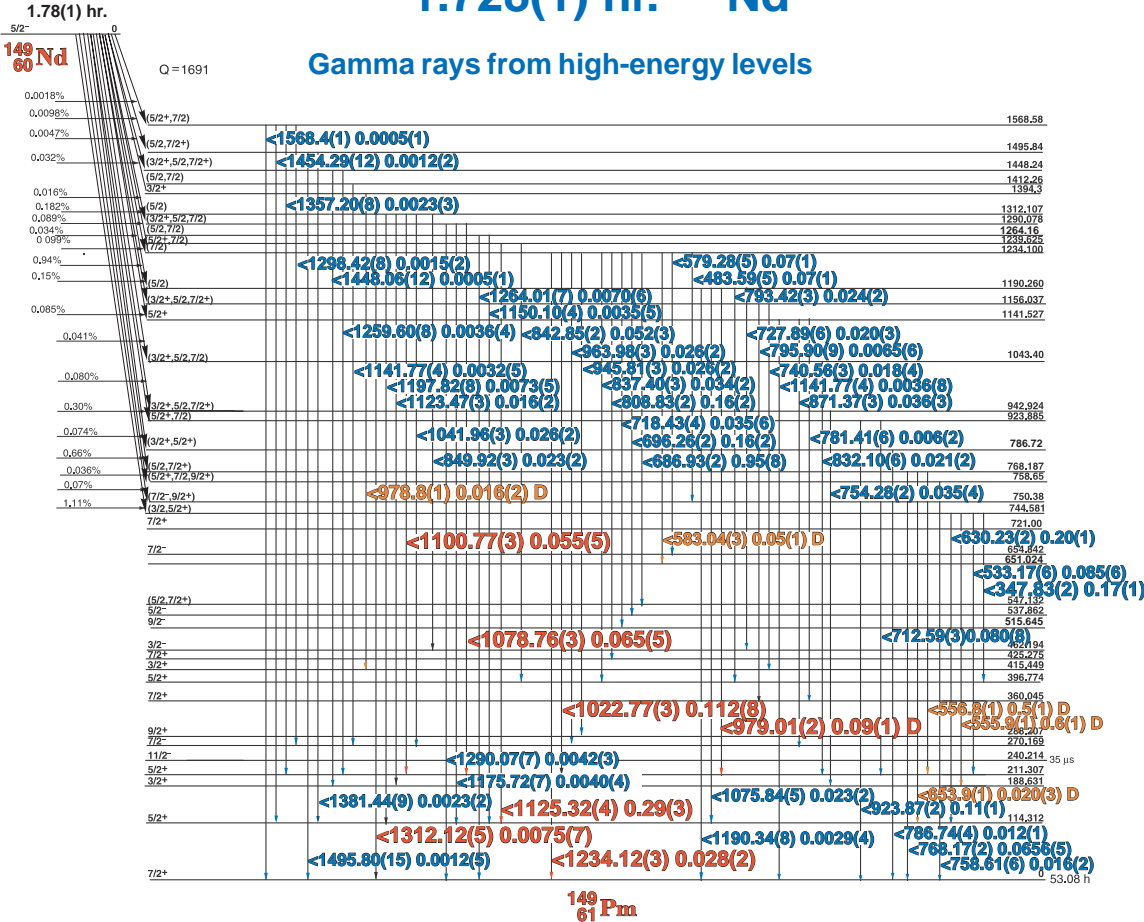
Gamma rays from low-energy levels



Decay Data

← Index →

1.728(1) hr. ^{149}Nd



GAMMA-RAY ENERGIES AND INTENSITIES

Nuclide ^{149}Nd Half Life 1.728(1) hr.
Detector 3" x 3" -2 NaI Method of Production: $^{148}\text{Nd}(n,\gamma)$

E_{γ} (KeV)[S]	ΔE_{γ}	I_{γ} (rel)	$I_{\gamma}(\%)$ [E]	ΔI_{γ}	S
Pr x-rays					
30.00	± 0.031	64.0	0.017	± 0.003	1
58.883	± 0.020	5.55	1.4	± 0.1	3
65.356	± 0.024	0.175	0.03	± 0.03	4
D74.328	± 0.030	4.9	1.1	± 0.1	2
D74.8	± 0.1	4.5	1.0	± 0.1	2
75.74	± 0.04	9.4	0.25	± 0.03	3
97.007	± 0.015	5.55	1.44	± 0.08	3
107.793	± 0.030	0.23	0.07	± 0.01	4
112.5	± 0.1	0.44	0.11	± 0.01	4
114.321	± 0.014	68.75	19	± 1.0	1
116.93	± 0.030	3.0	0.10	± 0.01	4
122.416	± 0.014	0.85	0.23	± 0.02	4
126.630	± 0.019	0.42	0.11	± 0.01	4
137.05	± 0.05	0.17	0.05	± 0.01	4
139.21	± 0.014	1.75	0.47	± 0.03	3
155.876	± 0.010	22.2	5.8	± 0.3	1
177.831	± 0.019	0.60	0.15	± 0.01	4
185.496	± 0.030	0.34	0.10	± 0.01	4
188.640	± 0.009	7.26	1.8	± 0.1	2
192.027	± 0.009	2.18	0.57	± 0.05	3
198.928	± 0.009	5.34	1.39	± 0.08	3

1.728(1) hr. ^{149}Nd

GAMMA-RAY ENERGIES AND INTENSITIES

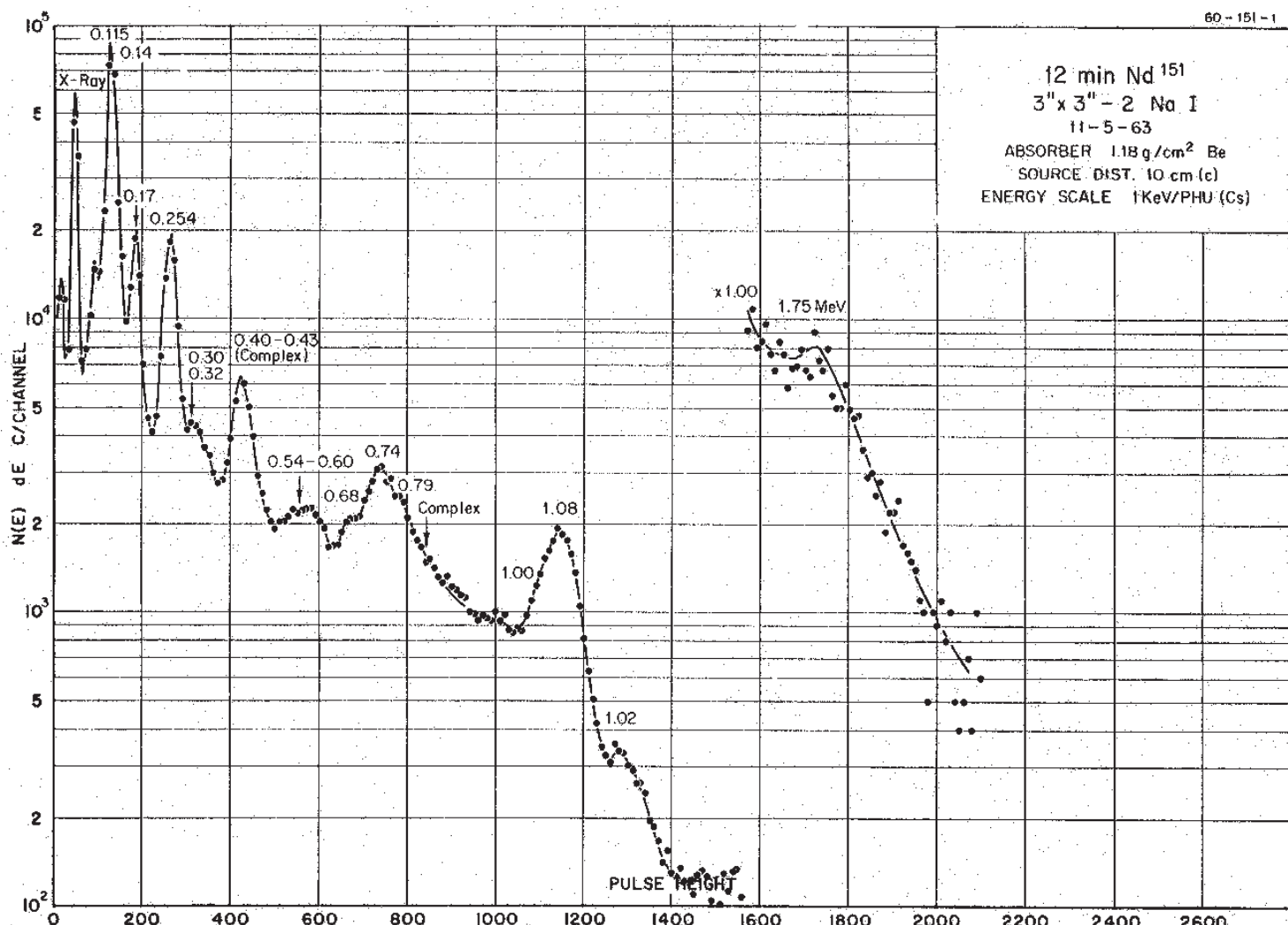
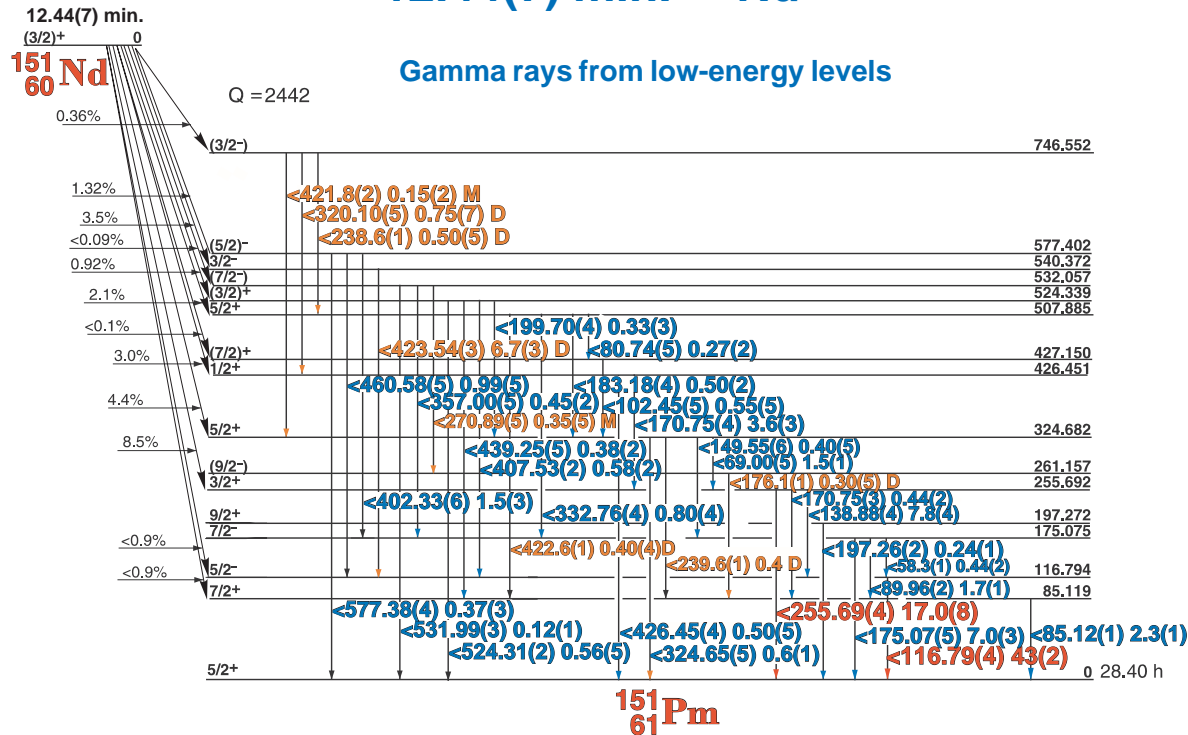
Nuclide ^{149}Nd
Detector 3" x 3" -2 NaI

Half Life 1.728(1) hr.
Method of Production: $^{148}\text{Nd}n,\gamma$

E_{γ} (KeV)[S]	ΔE_{γ}	$I_{\gamma}(\text{rel})$	$I_{\gamma}(\%)[E]$	ΔI_{γ}	S
208.148	± 0.010	10.67	2.7	± 0.2	2
211.307	± 0.008	100	26	± 1.0	1
213.946	± 0.017	1.5	0.39	± 0.04	3
226.846	± 0.021	0.60	0.16	± 0.01	4
229.562	± 0.010	1.83	0.48	± 0.03	3
240.218	± 0.008	14.5	3.8	± 0.2	1
245.699	± 0.008	3.80	0.96	± 0.08	3
250.822	± 0.049	0.14	0.035	± 0.003	4
254.204	± 0.032	0.32	0.08	± 0.01	4
258.064	± 0.014	1.40	0/36	± 0.03	3
267.692	± 0.009	22.2	0.59	± 0.03	1
270.165	± 0.008	39.3	10.4	± 0.5	1
D273.240	± 0.038	0.85	0.19	± 0.02	4
275.445	± 0.013	2.18	0.59	± 0.05	3
276.960	± 0.019	1.19	0.31	± 0.02	4
282.455	± 0.011	2.26	0.60	± 0.03	3
288.192	± 0.012	2.48	0.66	± 0.03	3
294.807	± 0.012	2.13	0.55	± 0.03	3
301.133	± 0.016	1.40	0.36	± 0.02	3
310.982	± 0.014	1.9	0.50	± 0.04	3
326.556	± 0.011	17.1	4.5	± 0.2	1
347.833	± 0.023	0.68	0.17	± 0.01	4
349.233	± 0.010	5.42	1.41	± 0.09	3
360.055	± 0.020	0.60	0.15	± 0.01	4
366.637	± 0.015	2.43	0.80	± 0.08	3
384.691	± 0.018	1.23	0.30	± 0.02	4
423.554	± 0.010	34.6	8.5	± 0.7	1
443.550	± 0.012	5.51	1.3	± 0.1	2
533.169	± 0.069	0.32	0.085	± 0.006	4
540.510	± 0.010	28.2	7.2	± 0.5	1
D555.9	± 0.1	2.2	0.6	± 0.1	1
D556.8	± 0.09	2.1	0.5	± 0.1	1
583.040	± 0.030	0.307	0.05	± 0.01	3
630.238	± 0.021	0.81	0.20	± 0.01	3
635.482	± 0.025	0.41		± 0.04	3
654.831	± 0.014	26.9	7.1	± 0.6	1
686.933	± 0.025	0.38	0.95	± 0.08	3
696.266	± 0.025	0.63	0.16	± 0.02	2
712.595	± 0.030	0.31	0.080	± 0.008	3
718.430	± 0.040	0.11	0.035	± 0.006	4
727.895	± 0.065	0.08	0.020	± 0.003	4
740.564	± 0.037	0.07	0.018	± 0.004	4

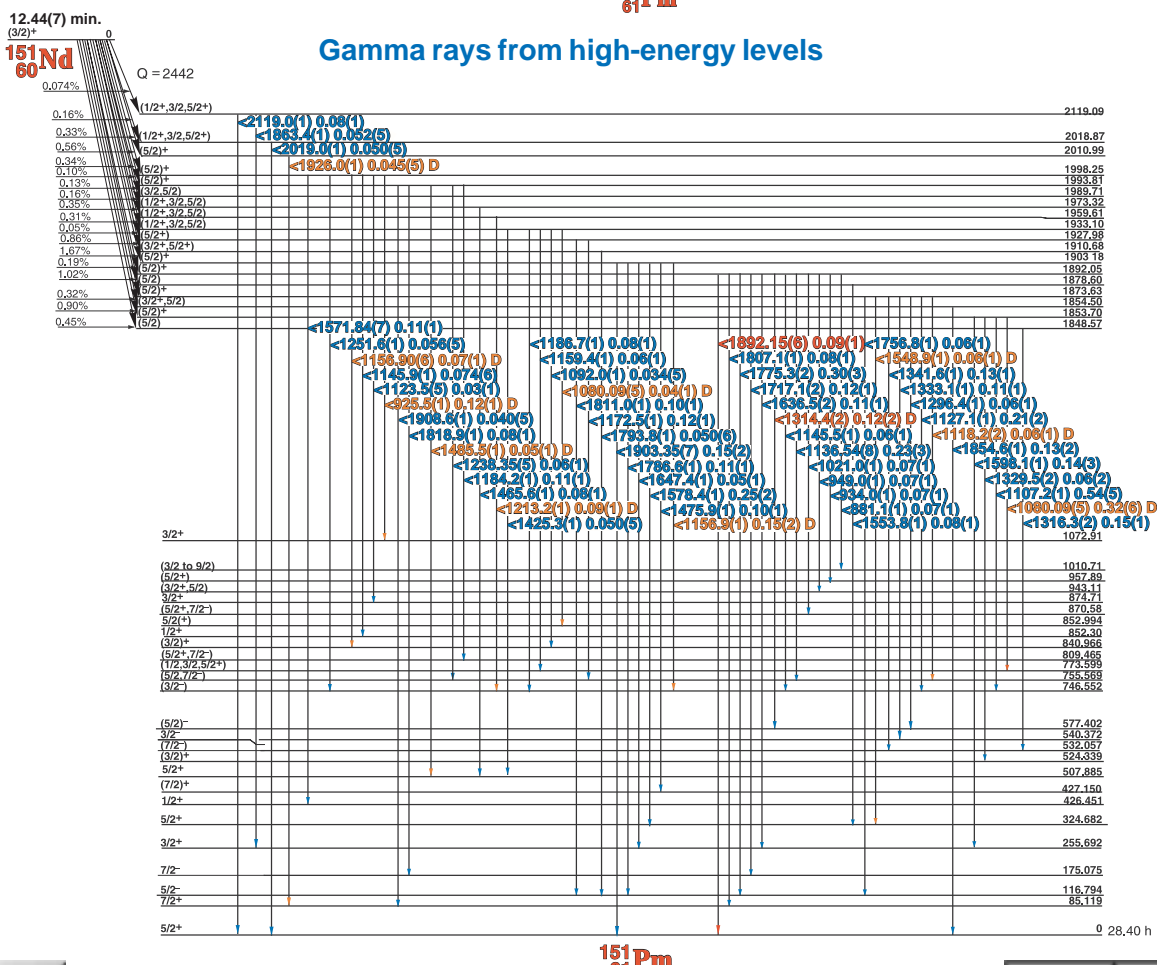
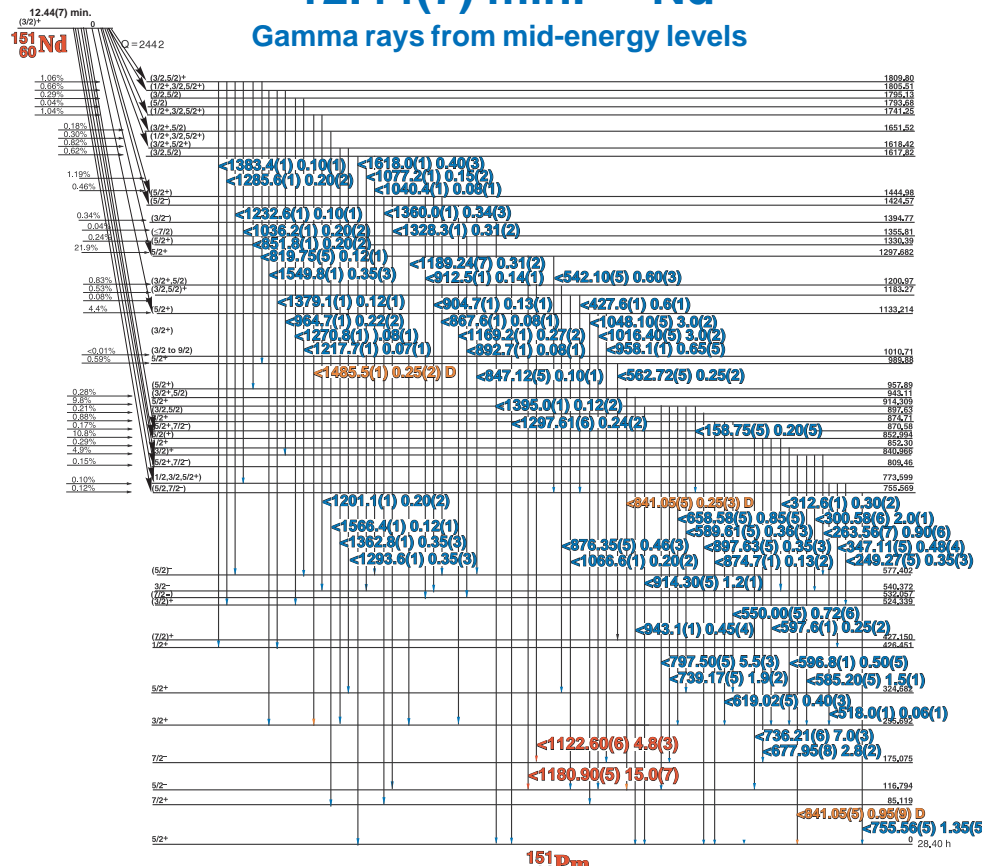
E_{γ} (KeV)[S]	ΔE_{γ}	$I_{\gamma}(\text{rel})$	$I_{\gamma}(\%)[E]$	ΔI_{γ}	S
754.284	± 0.023	0.128	0.035	± 0.004	3
758.606	± 0.104	0.06	0.016	± 0.002	4
768.170	± 0.022	0.25	0.066	± 0.001	3
781.412	± 0.068	0.026	0.006	± 0.002	4
786.737	± 0.043	0.046	0.012	± 0.001	4
793.424	± 0.034	0.093	0.024	± 0.002	4
795.907	± 0.099	0.025	0.0065	± 0.0006	4
808.834	± 0.022	0.623	0.10	± 0.008	2
832.106	± 0.064	0.081	0.021	± 0.002	4
837.408	± 0.033	0.130	0.034	± 0.002	4
842.85	± 0.024	0.20	0.052	± 0.003	3
849.92	± 0.027	0.09	0.023	± 0.002	4
871.37	± 0.03	0.14	0.036	± 0.003	4
923.876	± 0.025	0.42	0.11	± 0.01	2
945.81	± 0.035	0.089	0.026	± 0.002	3
963.984	± 0.035	0.077	0.026	± 0.002	3
979.016	± 0.04	0.41	0.09	± 0.008	1
1022.775	± 0.027	0.44	0.112	± 0.008	1
1041.96	± 0.035	0.098	0.026	± 0.002	3
1075.842	± 0.05	0.09	0.023	± 0.002	3
1078.76	± 0.03	0.25	0.065	± 0.005	1
1100.77	± 0.03	0.22	0.055	± 0.004	1
1123.47	± 0.035	0.06	0.016	± 0.002	3
1125.32	± 0.04	0.11	0.29	± 0.025	1
1141.77	± 0.04	0.014	0.0036	± 0.0008	3
1150.10	± 0.04	0.012	0.0035	± 0.0003	3
1172.08	± 0.12	0.018	0.0045	± 0.0004	3
1175.72	± 0.07	0.019	0.0040	± 0.0004	3
1190.34	± 0.08	0.012	0.0029	± 0.0004	3
1197.82	± 0.08	0.028	0.0073	± 0.0005	3
1234.118	± 0.045	1.07	0.028	± 0.002	1
1259.60	± 0.086	0.014	0.0036	± 0.0004	3
1264.01	± 0.07	0.026	0.0070	± 0.0006	2
1290.07	± 0.07	0.016	0.0042	± 0.0003	3
1298.42	± 0.08	0.0064	0.0015	± 0.0002	3
1312.113	± 0.070	0.029	0.0075	± 0.0007	1
1357.18	± 0.14	0.009	0.0023	± 0.0002	2
1381.44	± 0.09	0.0089	0.0023	± 0.0002	2
1448.06	± 0.2	0.0017	0.0005	± 0.0001	3
1454.28	± 0.14	0.0046	0.0012	± 0.0002	2
1495.80	± 0.16	0.003	0.0012	± 0.0005	3
1568.34	± 0.22	0.002	0.0005	± 0.0001	3

12.44(7) min. ^{151}Nd



12.44(7) min. ^{151}Nd

Gamma rays from mid-energy levels



12.44(7) min. ^{151}Nd

GAMMA-RAY ENERGIES AND INTENSITIES

Nuclide ^{151}Nd
Detector 3" x 3" -2 NaI

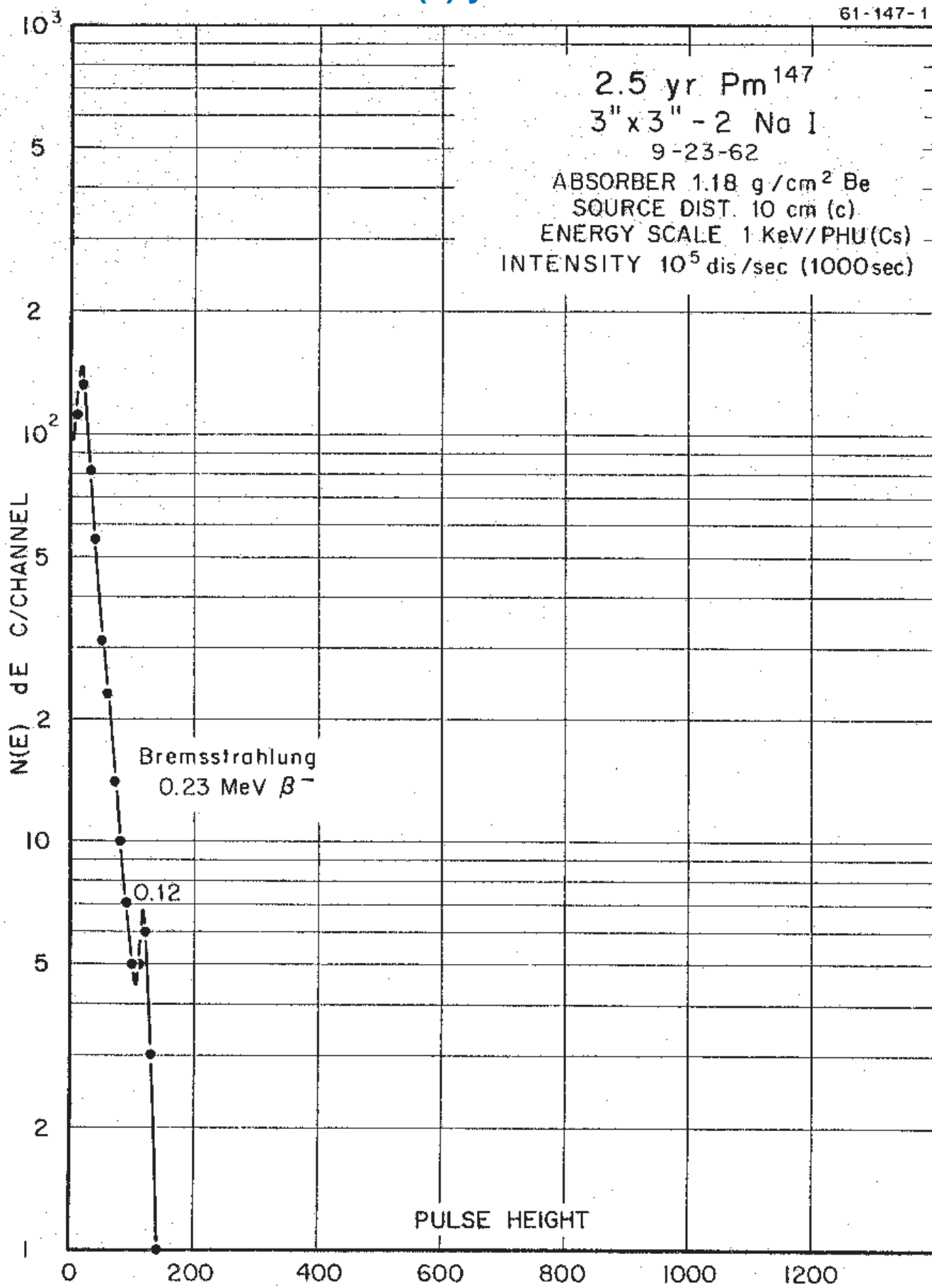
Half Life 12.44(7) min.
Method of Production: $^{150}\text{Nd}(n,\gamma)$

E_{γ} (KeV)[S]	ΔE_{γ}	$I_{\gamma}(\text{rel})$	$I_{\gamma}(\%)[E]$	ΔI_{γ}	S
58.3	± 0.10	1.07	0.44	± 0.02	4
69.00	± 0.05	3.89	1.5	± 0.1	3
80.74	± 0.05		0.27	± 0.02	4
81.85	± 0.49	1.50		± 0.14	4
85.12	± 0.02	6.07	2.3	± 0.1	3
89.96	± 0.05	4.91	1.7	± 0.1	3
102.45	± 0.05		0.55	± 0.05	4
116.79	± 0.04	100	43	± 2.0	1
138.88	± 0.04	19.4	7.8	± 0.4	2
149.55	± 0.06	1.0	0.40	± 0.059	4
158.75	± 0.05	1.53	0.20	± 0.05	4
D170.75	± 0.03	10.4	3.6	± 0.3	3
175.07	± 0.05	18.8	7.0	± 0.3	2
176.1	± 0.1		0.30	± 0.05	4
183.18	± 0.04	1.1	0.50	± 0.02	4
197.26	± 0.02	0.83	0.24	± 0.01	4
199.70	± 0.04	0.92	0.33	± 0.03	4
208.0	± 0.1	0.95	0.050	± 0.005	4
D238.6	± 0.1		0.50	± 0.05	4
D239.6	± 0.1	2.54	0.4	± 0.1	4
249.27	± 0.05	0.49	0.35	± 0.03	4
255.69	± 0.04	40.8	17.0	± 0.8	1
263.56	± 0.07	2.05	0.90	± 0.06	4
300.58	± 0.08	4.85	2.0	± 0.1	3
312.6	± 0.1	0.77	0.30	± 0.02	4
320.10	± 0.05	1.9	0.75	± 0.07	4
324.65	± 0.05	1.47	0.6	± 0.1	4
332.76	± 0.04	1.9	0.80	± 0.04	4
347.11	± 0.05	1.2	0.48	± 0.04	4
357.00	± 0.05	1.2	0.45	± 0.02	4
402.33	± 0.06	4.32	1.5	± 0.30	3
407.53	± 0.02	1.4	0.58	± 0.02	4
D422.8	± 0.1		0.40	± 0.04	4
423.54	± 0.03	16.3	6.7	± 0.3	2
426.45	± 0.04	1.5	0.50	± 0.05	4
439.25	± 0.05	1.1	0.38	± 0.02	4
460.58	± 0.05	2.3	0.99	± 0.05	4
524.31	± 0.02	1.3	0.56	± 0.05	4
531.99	± 0.03	0.49	0.12	± 0.01	4
542.10	± 0.05	1.4	0.60	± 0.03	4
550.00	± 0.05	2.15	0.72	± 0.06	4
562.72	± 0.05	0.64	0.25	± 0.02	4
577.38	± 0.05	0.80	0.37	± 0.03	4
585.20	± 0.05	3.35	1.5	± 0.10	4
589.61	± 0.05	0.92	0.36	± 0.03	4
596.8	± 0.1	1.80	0.50	± 0.05	4
597.6	± 0.1		0.25	± 0.02	4
619.02	± 0.05	1.1	0.40	± 0.03	4
658.58	± 0.05	2.0	0.85	± 0.05	4
670.39	± 0.06	0.67	0.40	± 0.04	4
677.95	± 0.08	6.81	2.8	± 0.20	3
736.21	± 0.06	18.2	7.0	± 0.3	3
739.17	± 0.05	5.25	1.9	± 0.2	4
755.56	± 0.06	3.31	1.35	± 0.07	4
797.50	± 0.06	14.3	5.5	± 0.3	2
819.75	± 0.05		0.12	± 0.01	4
D841.05	± 0.05	2.94	0.95	± 0.09	4
847.12	± 0.05		0.10	± 0.01	4
D853.00	± 0.05	1.29	0.35	± 0.03	4
874.7	± 0.1		0.13	± 0.02	4
867.6	± 0.1		0.08	± 0.01	4
876.35	± 0.05	1.47	0.46	± 0.03	4
892.7	± 0.1		0.08	± 0.01	4
897.63	± 0.05		0.35	± 0.03	4

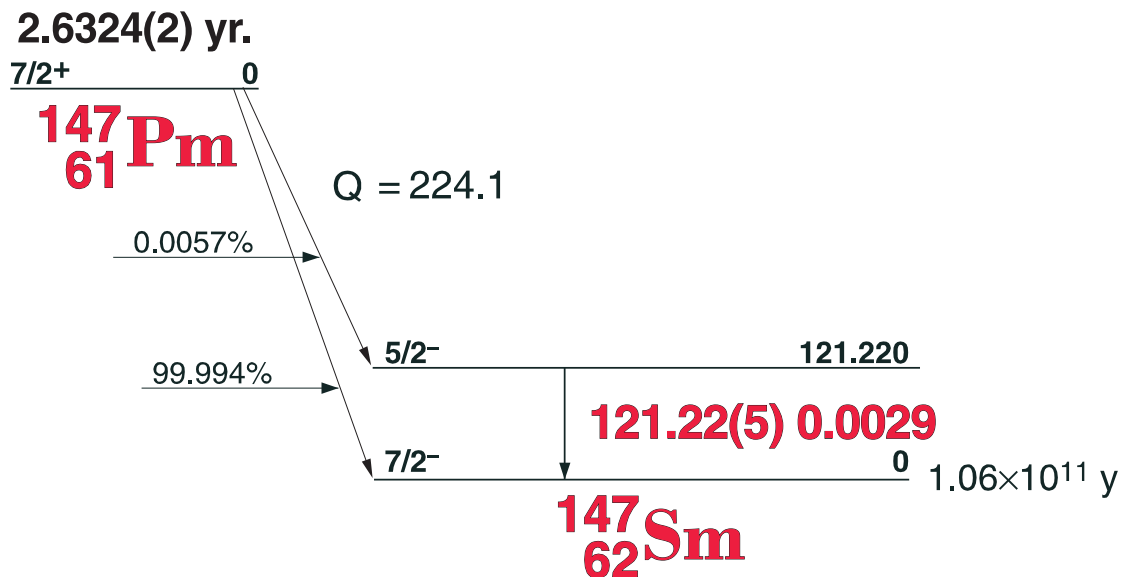
E_{γ} (KeV)[S]	ΔE_{γ}	$I_{\gamma}(\text{rel})$	$I_{\gamma}(\%)[E]$	ΔI_{γ}	S
904.7	± 0.1		0.13	± 0.01	4
914.30	± 0.05	3.71	1.2	± 0.1	4
925.5	± 0.1	0.49	0.12	± 0.01	4
943.11	± 0.09	1.14	0.45	± 0.04	4
958.10	± 0.08	1.41	0.65	± 0.05	4
964.7	± 0.1		0.22	± 0.02	4
1016.40	± 0.05	8.60	3.0	± 0.2	3
1066.6	± 0.1		0.20	± 0.02	4
1048.10	± 0.05	2.06	3.0	± 0.17	4
1080.09	± 0.05	0.92	0.32	± 0.06	4
1107.20	± 0.11	1.35	0.54	± 0.05	4
1122.60	± 0.05	13.69	4.8	± 0.3	1
1123.5	± 0.1		0.03	± 0.01	4
1136.58	± 0.08	0.61	0.020	± 0.002	4
1156.90	± 0.06	0.64	0.07	± 0.01	4
1169.2	± 0.1	0.75	0.27	± 0.02	4
1180.90	± 0.06	45.0	15.0	± 0.7	1
1201.1	± 0.1	0.61	0.20	± 0.02	4
1213.2	± 0.1	0.28	0.09	± 0.01	4
1217.7	± 0.1	0.14	0.07	± 0.01	4
1232.6	± 0.1	0.34	0.10	± 0.01	4
1238.35	± 0.05	0.55	0.06	± 0.01	4
1270.8	± 0.1	0.58	0.08	± 0.01	4
1285.6	± 0.1	0.80	0.20	± 0.02	4
1293.6	± 0.1		0.35	± 0.03	4
1297.61	± 0.06		0.24	± 0.02	4
1314.4	± 0.1	0.95	0.12	± 0.02	4
1328.3	± 0.1	0.95	0.31	± 0.02	4
1360.0	± 0.1	0.46	0.34	± 0.03	3
1362.8	± 0.1	0.95	0.35	± 0.03	4
1379.1	± 0.1		0.12	± 0.01	4
1383.4	± 0.1		0.10	± 0.01	4
1395.0	± 0.1	0.34	0.12	± 0.01	4
1465.6	± 0.1	0.24	0.08	± 0.01	4
1475.9	± 0.1	0.34	0.11	± 0.01	4
1485.5	± 0.1	0.86	0.25	± 0.02	3
1549.9	± 0.1	1.10	0.35	± 0.02	3
1571.84	± 0.07		0.11	± 0.01	4
1578.4	± 0.1	0.64	0.25	± 0.02	4
1598.0	± 0.1	0.37	0.14	± 0.03	4
1618.0	± 0.1	1.26	0.40	± 0.03	3
1636.5	± 0.2	0.31	0.11	± 0.01	4
1647.4	± 0.1	0.16	0.05	± 0.01	4
1717.1	± 0.2	0.28	0.12	± 0.01	3
1731.9	± 0.1	0.15	0.06	± 0.01	3
1775.30	± 0.08	0.77	0.30	± 0.03	2
1793.8	± 0.1		0.05	± 0.01	4
1807.1	± 0.1	0.21	0.08	± 0.01	4
1811.0	± 0.1	0.21	0.10	± 0.01	4
1818.9	± 0.1	0.20	0.08	± 0.01	3
1863.4	± 0.1	0.13	0.052	± 0.05	3
1892.15	± 0.06	0.05	0.09	± 0.01	1
1903.35	± 0.07		0.15	± 0.02	3
1908.6	± 0.1	0.11	0.040	± 0.005	4
1926.0	± 0.1	0.13	0.045	± 0.005	3
1932.83	± 0.3	0.074	0.02	± 0.02	4
2019.0	± 0.1	0.11	0.050	± 0.005	2
2106.8	± 0.2	0.02	0.010	± 0.002	2
2119.0	± 0.1	0.08	0.01	± 0.01	2
2254.92	± 0.2	0.02	0.04	± 0.005	2

2.6234(2) yr. ^{147}Pm

61-147-1



2.6234(2) yr. ^{147}Pm Decay Scheme

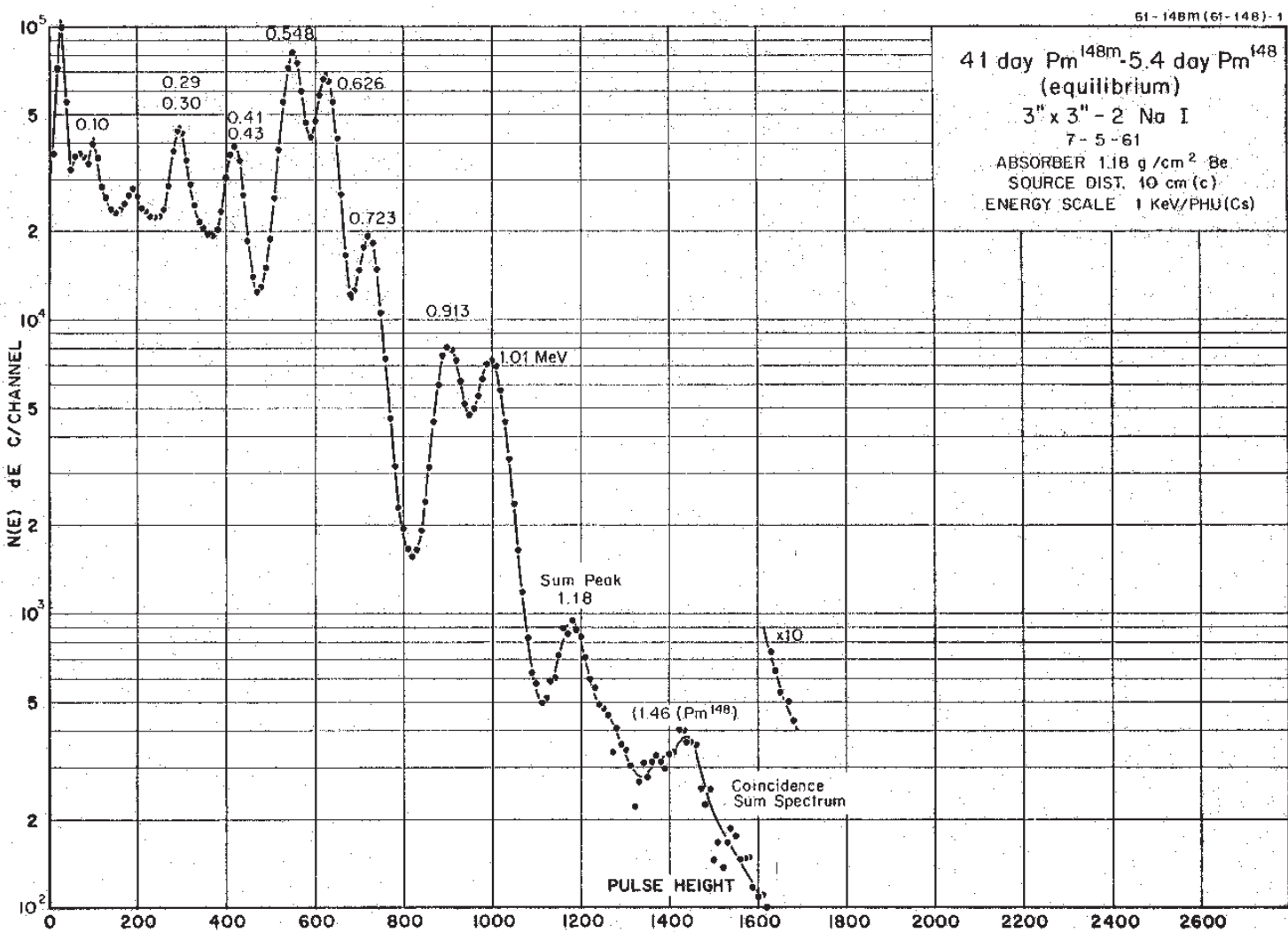


GAMMA-RAY ENERGIES AND INTENSITIES

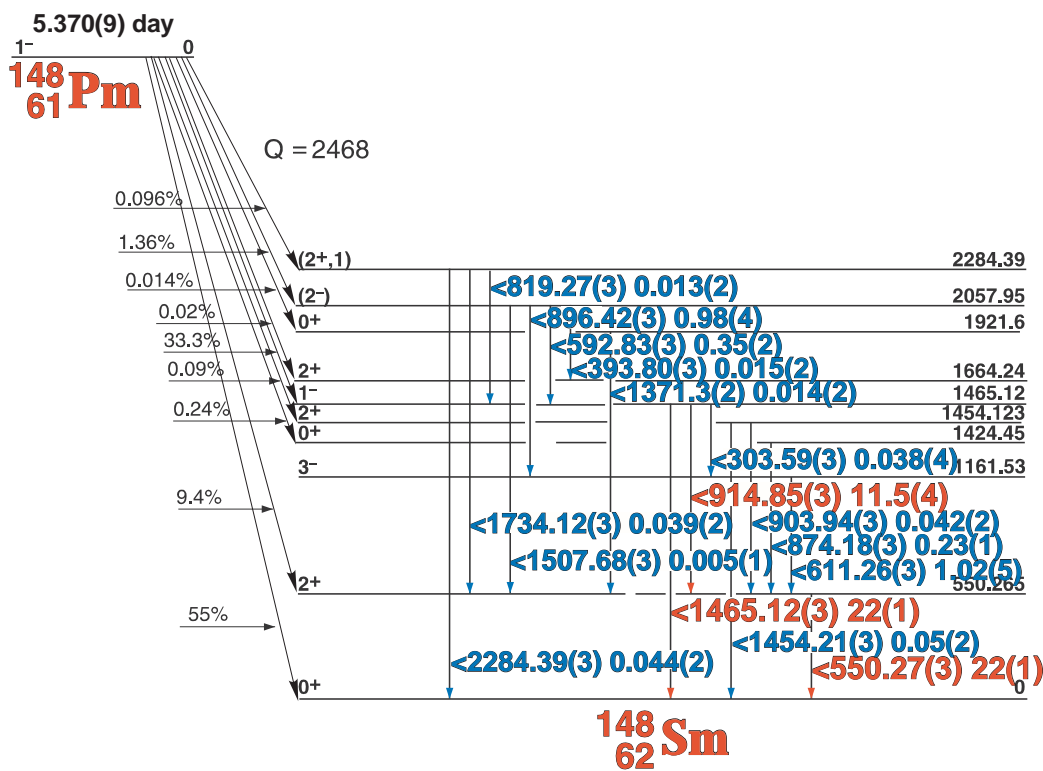
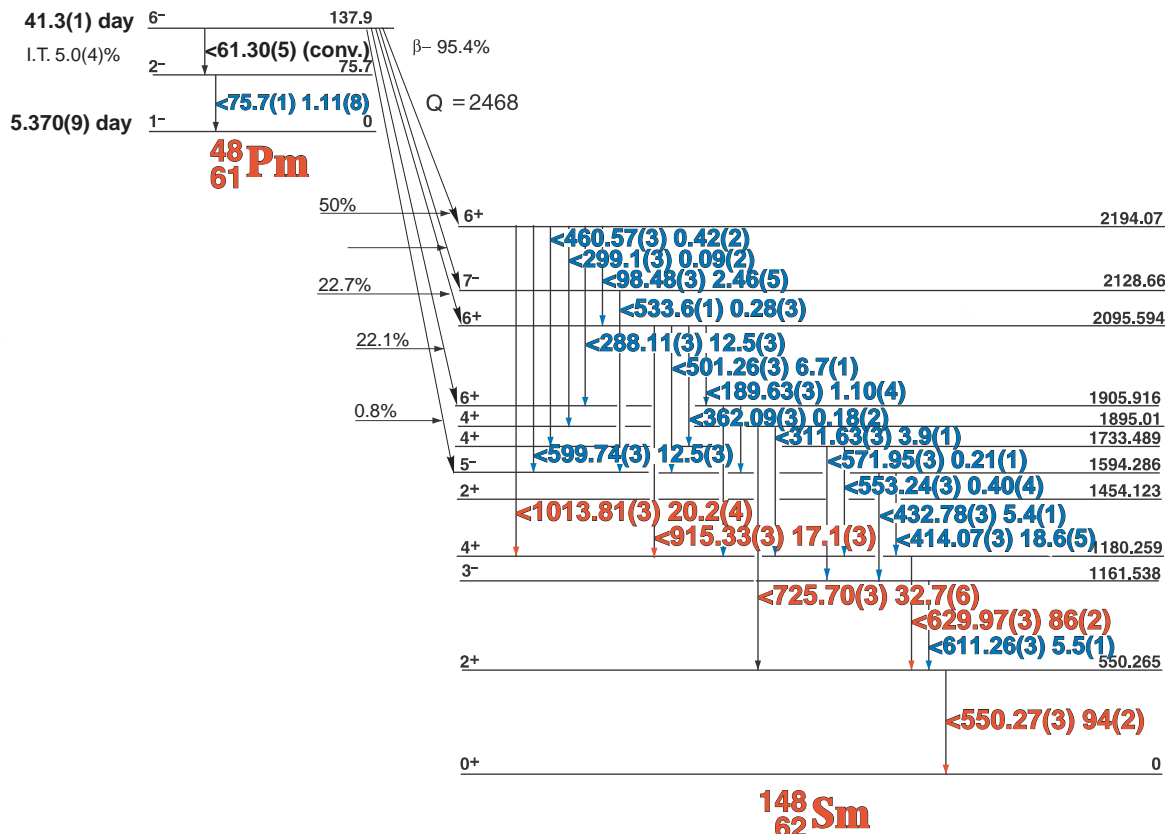
Nuclide ^{147}Pm Half Life 2.6234(2) yr.
Detector 3" X 3" NaI-2 Method of Production: $^{146}\text{Nd}(n,\gamma,\beta)$

E_γ (KeV)[S]	ΔE_γ	I_γ (rel)	$I_\gamma(\%)$ [E]	ΔI_γ	S
Sm k x-rays					
121.22	± 0.05	100	0.0029	$\pm 0.(2)$	1

41.3(1) day ^{148m}Pm - 5.370(9) day ^{148}Pm



41.3(1) day ^{148}Pm - 5.370(9) day ^{148}Pm



41.3(1) day ^{148m}Pm - 5.370(9) day ^{148}Pm

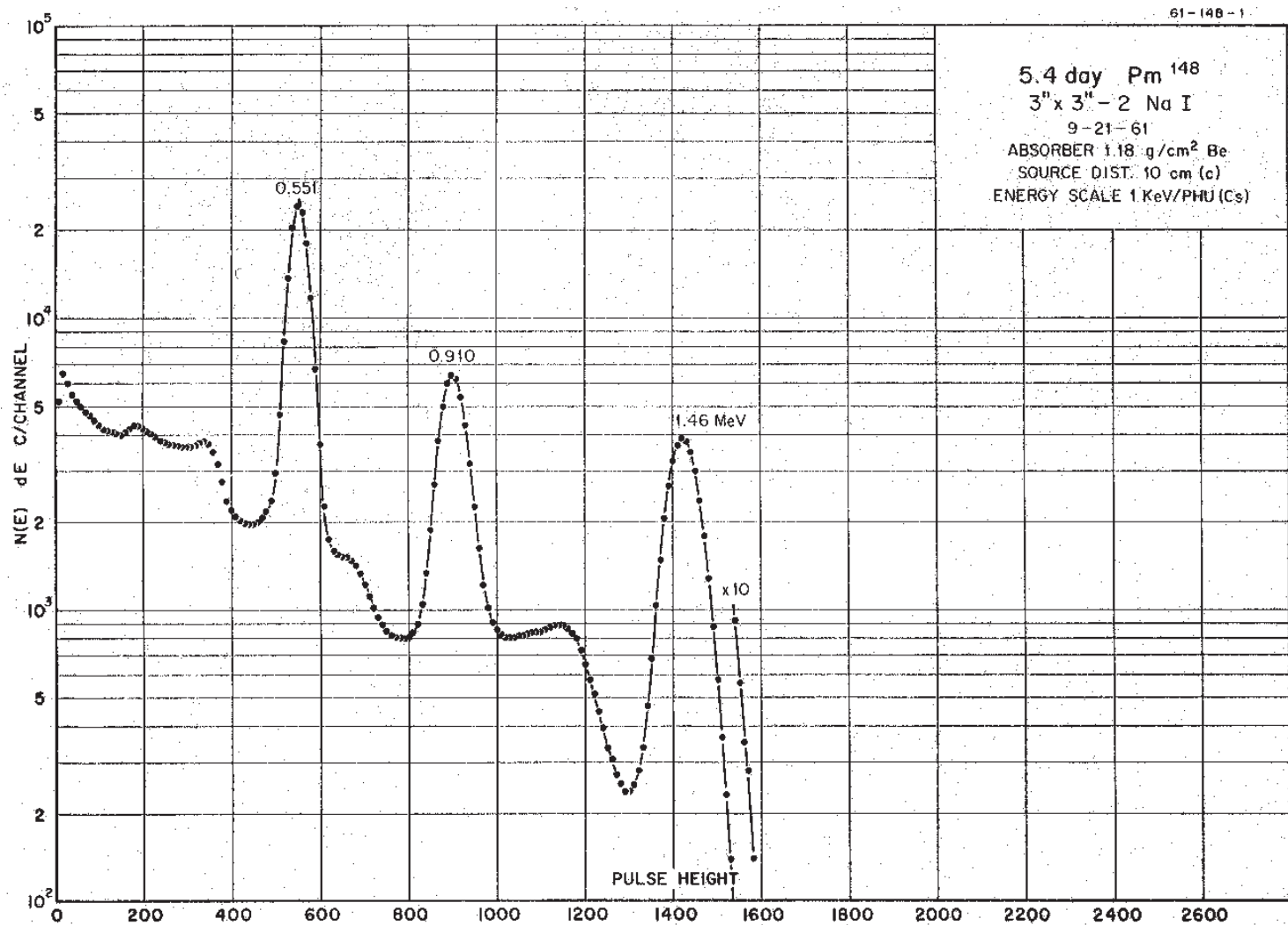
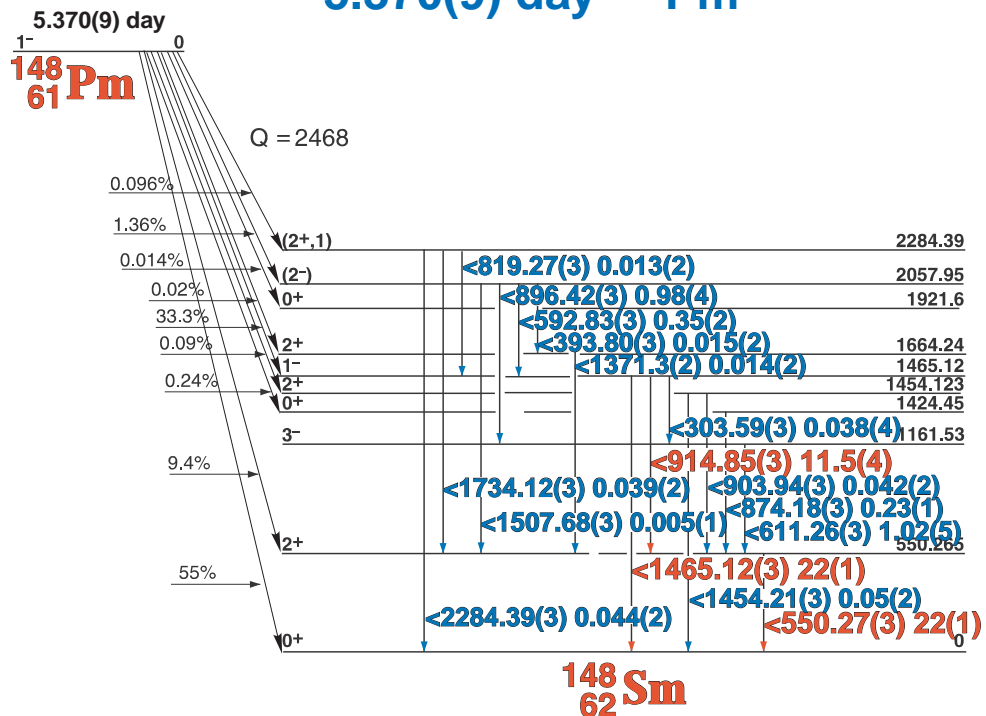
GAMMA-RAY ENERGIES AND INTENSITIES

Nuclide ^{148m}Pm - ^{148}Pm
 Detector 3" X 3" NaI-2

Half Life: 41.3(10) day - 5.370(9) day
 Method of Production: $^{148}\text{Sm}(\text{n},\text{p})$

E_{γ} (KeV)[S]	ΔE_{γ}	I_{γ} (rel)	$I_{\gamma}(\%)$ [E]	ΔI_{γ}	S
41.3 day ^{148m}Pm					
62.2		I.T.(conv.)			
75.7	± 0.1	I.T.	1.11	± 0.08	4
98.48	± 0.03		2.46	± 0.05	3
189.63	± 0.03		1.10	± 0.04	4
288.11	± 0.03		12.5	± 0.3	3
299.1	± 0.3		0.09	± 0.01	4
311.63	± 0.03		3.9	± 0.1	3
362.09	± 0.03		0.18	± 0.02	4
414.07	± 0.03		18.6	± 0.5	2
432.78	± 0.03		5.4	± 0.1	2
460.57	± 0.03		0.42	± 0.02	4
501.26	± 0.03		6.7	± 0.1	1
533.6	± 0.1		0.28	± 0.03	3
553.24	± 0.03		0.40	± 0.04	4
571.95	± 0.03		0.21	± 0.01	4
599.74	± 0.03		12.5	± 0.3	1
611.26	± 0.03		5.5	± 0.1	2
629.97	± 0.03		86	± 2.0	1
725.70	± 0.03		32.7	± 0.6	1
915.33	± 0.03		17.1	± 0.3	1
1013.81	± 0.03		20.2	± 0.4	1
5.37 day ^{148}Pm					
303.59	± 0.03		0.038	± 0.004	4
393.80	$+ 0.03$		0.015	± 0.002	4
550.27	± 0.03		22	± 1.0	1
592.83	± 0.03		0.35	± 0.02	4
611.26	± 0.03		1.02	± 0.05	4
819.27	± 0.03		0.014	± 0.002	4
874.18	± 0.03		0.23	± 0.01	4
896.42	± 0.03		0.98	± 0.04	4
903.94	± 0.03		0.042	± 0.004	4
914.85	± 0.03		11.5	± 0.4	1
1454.21	± 0.03		0.05	± 0.02	4
1465.12	± 0.03		22	± 1.0	1
1507.68	± 0.03		0.005	± 0.001	4
1734.12	± 0.03		0.039	± 0.002	4
2284.39	± 0.03		0.044	± 0.002	4

5.370(9) day ^{148}Pm



5.370(9) day ^{148}Pm Decay Data

GAMMA-RAY ENERGIES AND INTENSITIES

Nuclide ^{148}Pm
Detector 3" X 3" NaI-2

Half Life: 5.370(9) day
Method of Production: $^{148}\text{Sm}(\text{n},\text{p})$

E_{γ} (KeV)[S]	ΔE_{γ}	$I_{\gamma}(\text{rel})$	$I_{\gamma}(\%)[\text{E}]$	ΔI_{γ}	S
303.59	± 0.03		0.038	± 0.004	4
393.80	$+ 0.03$		0.015	± 0.002	4
550.27	± 0.03		22	± 1.0	1
592.83	± 0.03		0.35	± 0.02	4
611.26	± 0.03		1.02	± 0.05	4
819.27	± 0.03		0.014	± 0.002	4
874.18	± 0.03		0.23	± 0.01	4
896.42	± 0.03		0.98	± 0.04	4
903.94	± 0.03		0.042	± 0.004	4
914.85	± 0.03		11.5	± 0.4	1
1454.21	± 0.03		0.05	± 0.02	4
1465.12	± 0.03		22	± 1.0	1
1507.68	± 0.03		0.005	± 0.001	4
1734.12	± 0.03		0.039	± 0.002	4
2284.39	± 0.03		0.044	± 0.002	4

28.40(4) hr. ^{151}Pm

61-151-1

28 hr. Pm^{151}

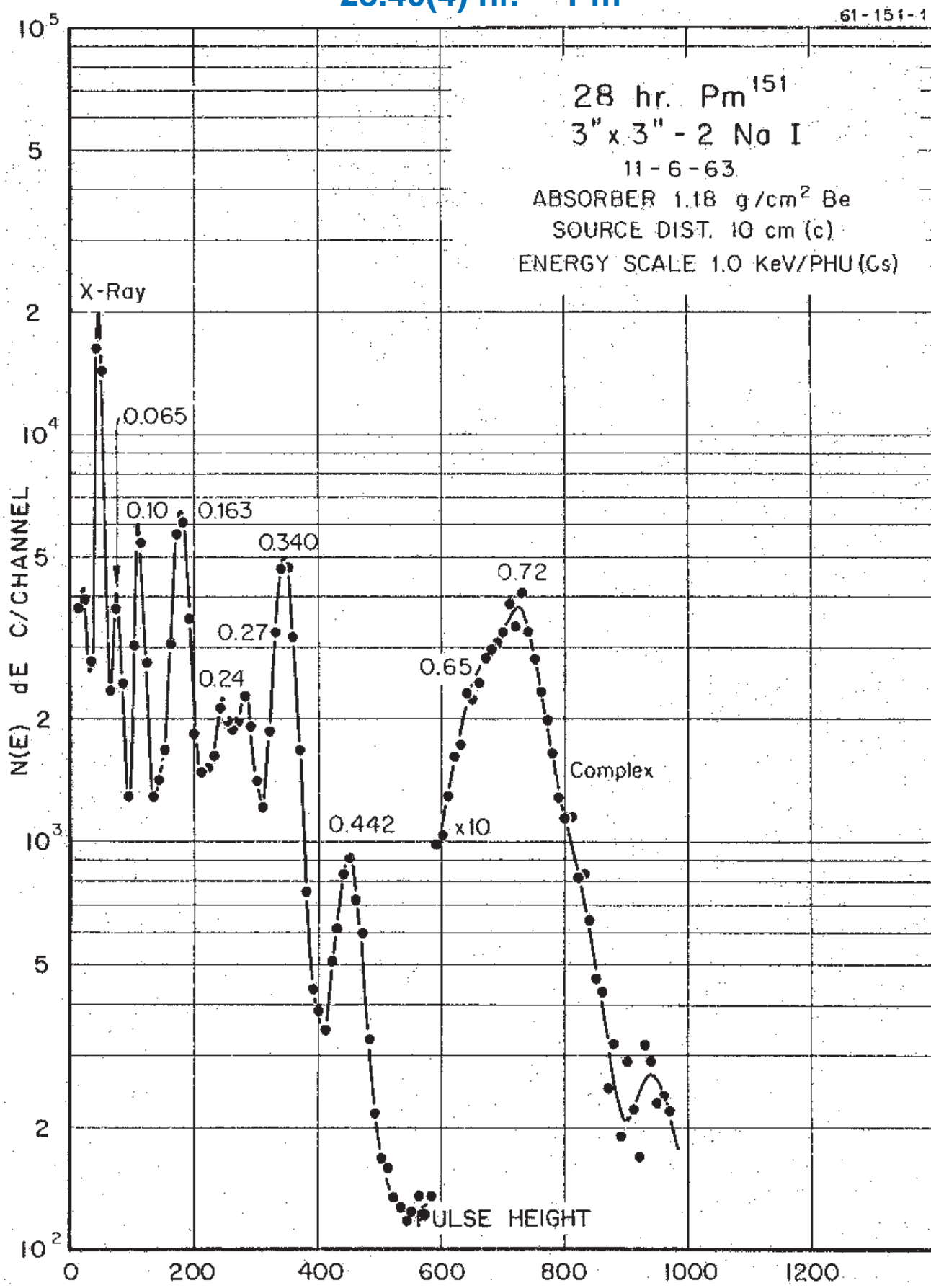
3" x 3" - 2 No I

11-6-63

ABSORBER 1.18 g/cm² Be

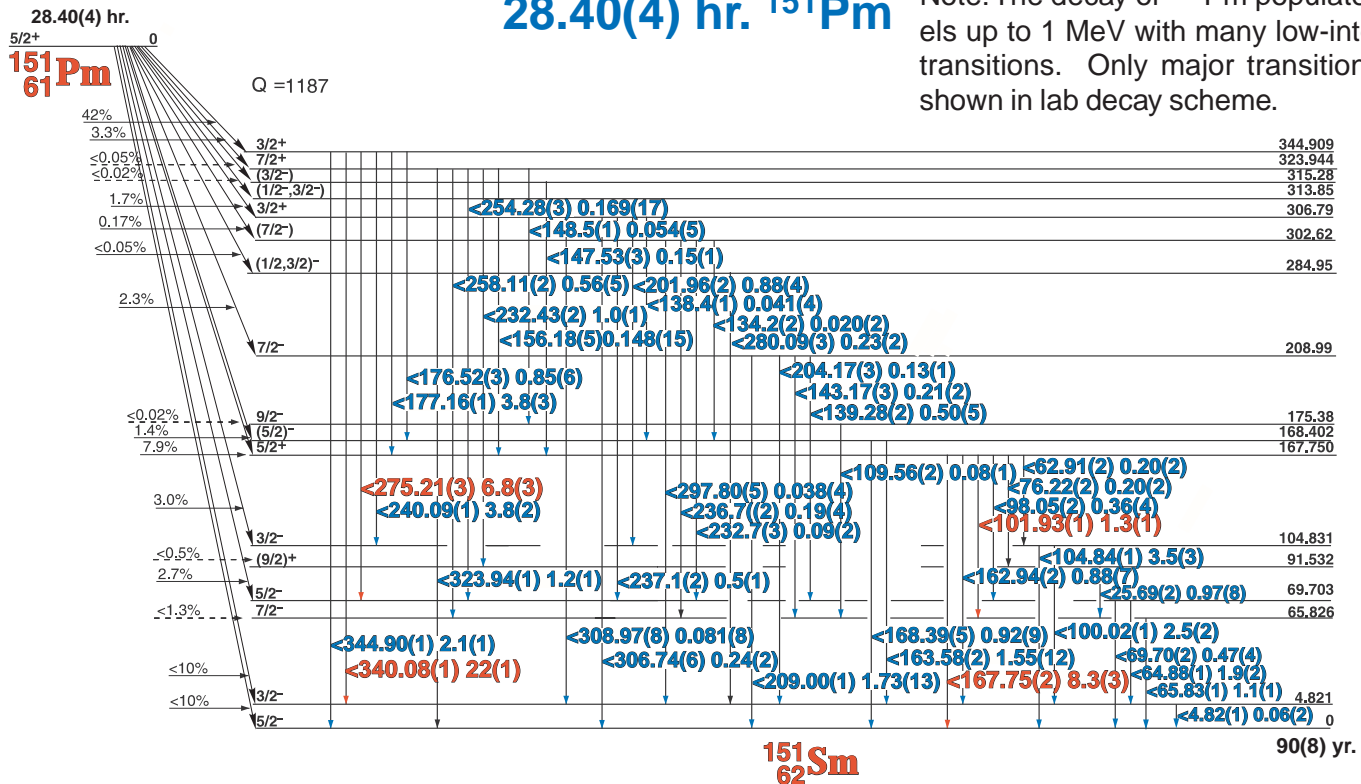
SOURCE DIST. 10 cm (c)

ENERGY SCALE 1.0 KeV/PHU (Cs)



28.40(4) hr. ^{151}Pm

Note: The decay of ^{151}Pm populates levels up to 1 MeV with many low-intensity transitions. Only major transitions are shown in lab decay scheme.



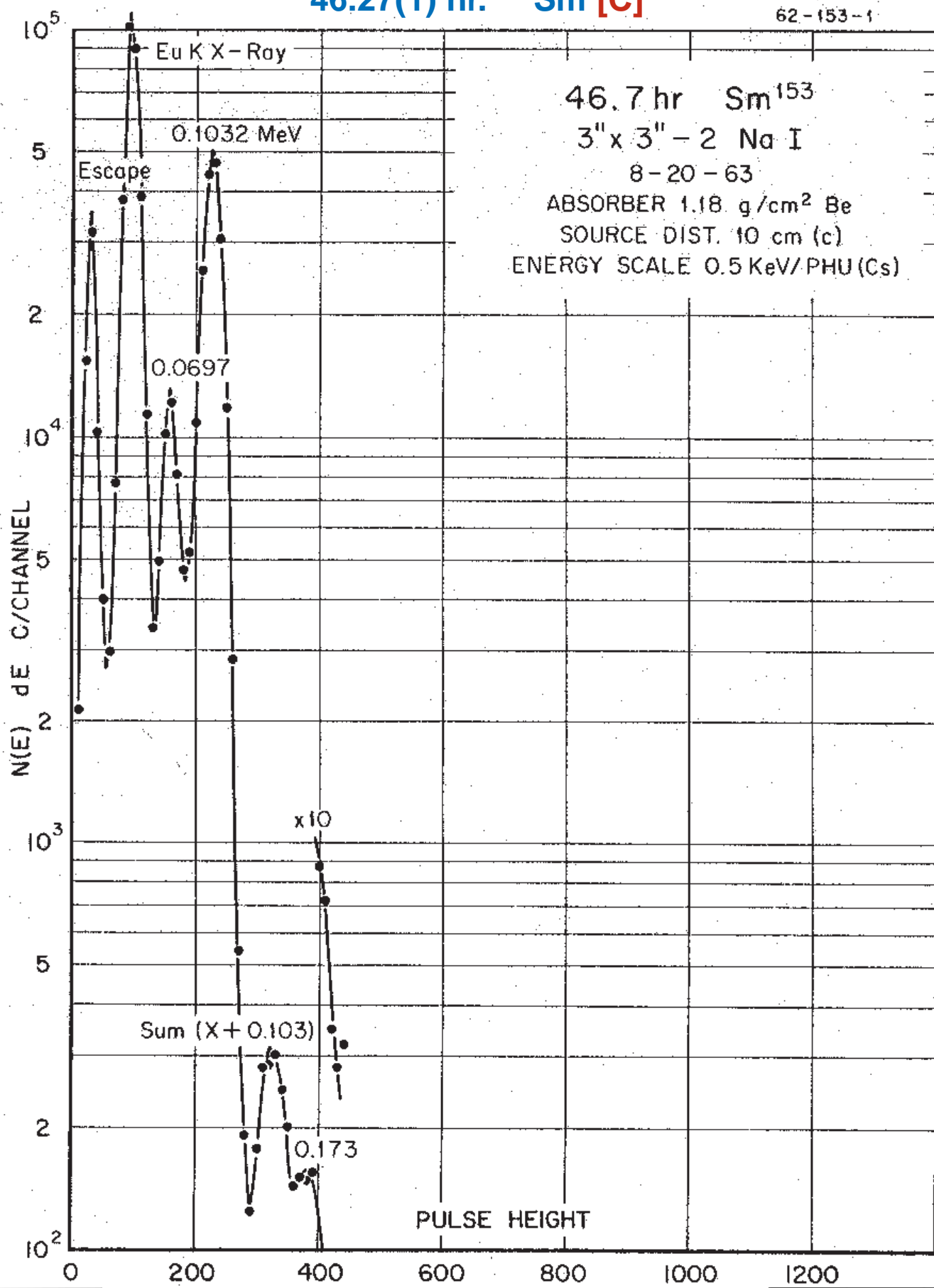
GAMMA-RAY ENERGIES AND INTENSITIES

Nuclide ^{151}Pm Half Life 28.40(4) hr.
Detector 3" X 3" NaI-2 Method of Production: $^{150}\text{Nd}(n,\gamma,\beta)$

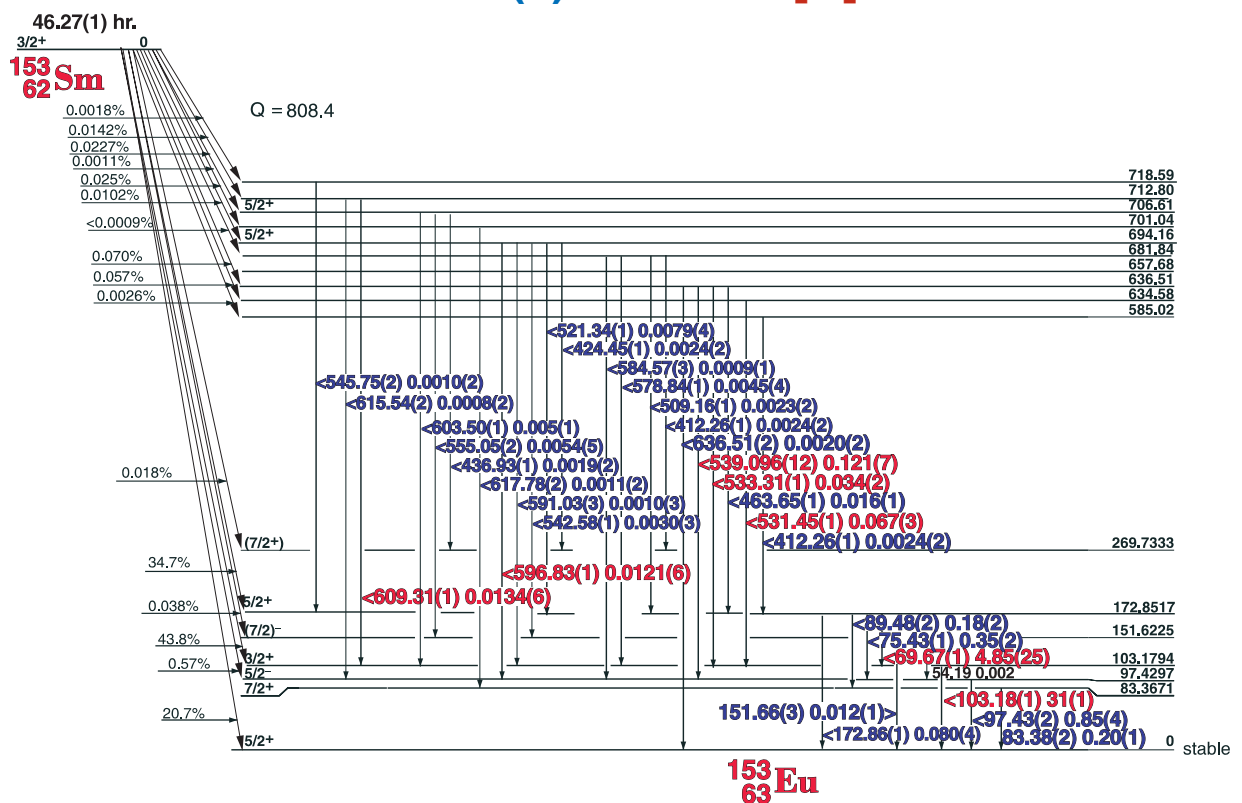
E_{γ} (KeV) [E]	ΔE_{γ}	I_{γ} (rel)	$I_{\gamma}(\%)$ [E]	ΔI_{γ}	S
25.69	± 0.02		0.97	± 0.08	4
64.88	± 0.01		1.9	± 0.2	3
65.83	± 0.01		1.1	± 0.1	3
69.70	± 0.02		0.47	± 0.04	4
76.22	± 0.02		0.20	± 0.02	4
98.05	± 0.02		0.36	± 0.04	3
100.02	± 0.01		2.5	± 0.2	2
101.93	± 0.01		1.3	± 0.1	3
104.84	± 0.01		3.5	± 0.3	1
139.28	± 0.02		0.50	± 0.05	3
143.17	± 0.03		0.21	± 0.02	4
147.53	± 0.03		0.15	± 0.01	4
156.18	± 0.05		0.15	± 0.01	4
162.94	± 0.02		0.88	± 0.07	3
163.58	± 0.02		1.5	± 0.1	2
167.75	± 0.02		8.3	± 0.3	1
168.39	± 0.05		0.92	± 0.09	3
176.52	± 0.03		0.85	± 0.06	3
177.16	± 0.01		3.8	± 0.3	1
204.17	± 0.03		0.13	± 0.01	3
209.00	± 0.01		1.7	± 0.1	2
232.43	± 0.02		1.0	± 0.2	3
237.1	± 0.2		0.5	± 0.1	4
240.09	± 0.01		3.8	± 0.2	1
258.11	± 0.02		0.56	± 0.05	3
275.21	± 0.03		6.8	± 0.3	1
323.94	± 0.01		1.2	± 0.1	3
340.08	± 0.01		22	± 1.0	1
344.90	± 0.01		2.1	± 0.1	3

46.27(1) hr. ^{153}Sm [C]

62-153-1



46.27(1) hr. ^{153}Sm [C]



GAMMA-RAY ENERGIES AND INTENSITIES

Nuclide ^{153}Sm
Detector 3" x 3" -2 NaI

Half Life 46.27(1) hr.
Method of Production: $^{152}\text{Sm}(n,\gamma)$

E_{γ} (KeV)[C]	ΔE_{γ}	$I_{\gamma}(\text{rel})$	$I_{\gamma}(\%)[E]$	ΔI_{γ}	S
69.6730 ± 0.0001	16.2	4.85	± 0.25	1	
75.4221 ± 0.0002	1.1	0.35	± 0.02	4	
83.3672 ± 0.0002	0.63	0.20	± 0.01	4	
89.4859 ± 0.0002	0.32	0.18	± 0.02	4	
97.4310 ± 0.0002	2.33	0.85	± 0.04	3	
103.1801 ± 0.0002	100	31	± 1.0	1	
151.66 ± 0.03	0.03	0.010	± 0.001	3	
172.8531 ± 0.0002	0.28	0.080	± 0.004	3	
412.260 ± 0.014	0.008	0.0024	± 0.0002	3	
424.450 ± 0.015	0.007	0.0020	± 0.0002	3	
436.929 ± 0.015	0.008	0.0020	± 0.0002	3	
463.655 ± 0.012	0.053	0.016	± 0.001	2	
482.16 ± 0.08	0.004	0.001	± 0.0005	4	
509.164 ± 0.015	0.010	0.0028	± 0.0002	3	
521.345 ± 0.012	0.028	0.008	± 0.0015	3	
531.454 ± 0.012	0.238	0.067	± 0.003	1	
533.307 ± 0.012	0.119	0.034	± 0.002	1	
539.096 ± 0.012	0.086	0.025	± 0.002	1	
542.577 ± 0.015	0.014	0.0030	± 0.0003	3	
545.75 ± 0.025	0.003	0.0010	± 0.0002	4	
555.055 ± 0.015	0.020	0.0054	$\pm 0.(5)$	2	
578.839 ± 0.015	0.018	0.0045	± 0.0004	3	
583.4 ± 0.1	0.003	0.0008	± 0.0001	4	
584.573 ± 0.03	0.004	0.0009	$\pm 0.(1)$	4	

E_{γ} (KeV)[C]	ΔE_{γ}	$I_{\gamma}(\text{rel})$	$I_{\gamma}(\%)[E]$	ΔI_{γ}	S
587.557	± 0.025	0.002	0.0005	± 0.0001	4
591.03	± 0.03	0.005	0.001	± 0.0002	3
596.829 ± 0.015	0.045	0.0121	± 0.0006	1	
598.64	± 0.10	0.005	0.0001	± 0.00002	4
603.502 ± 0.015	0.019	0.005	± 0.001	2	
609.310 ± 0.015	0.051	0.134	± 0.006	1	
610.55	± 0.08	0.009	0.002	± 0.0002	4
615.54	± 0.06	0.003	0.0008	$\pm 0.(1)$	3
617.786	± 0.025	0.003	0.0011	± 0.0001	3
634.57	± 0.08	0.002	0.0005	± 0.0001	4
636.512	± 0.019	0.007	0.0020	± 0.0002	3
657.282	± 0.042	0.001	0.0002	± 0.0001	4
685.76	± 0.06	0.004	0.001	± 0.0006	3
713.754	± 0.07	0.001	0.0002	± 0.0001	4

22.3(2) min. ^{155}Sm

62-155-1

25 Min. Sm^{155}

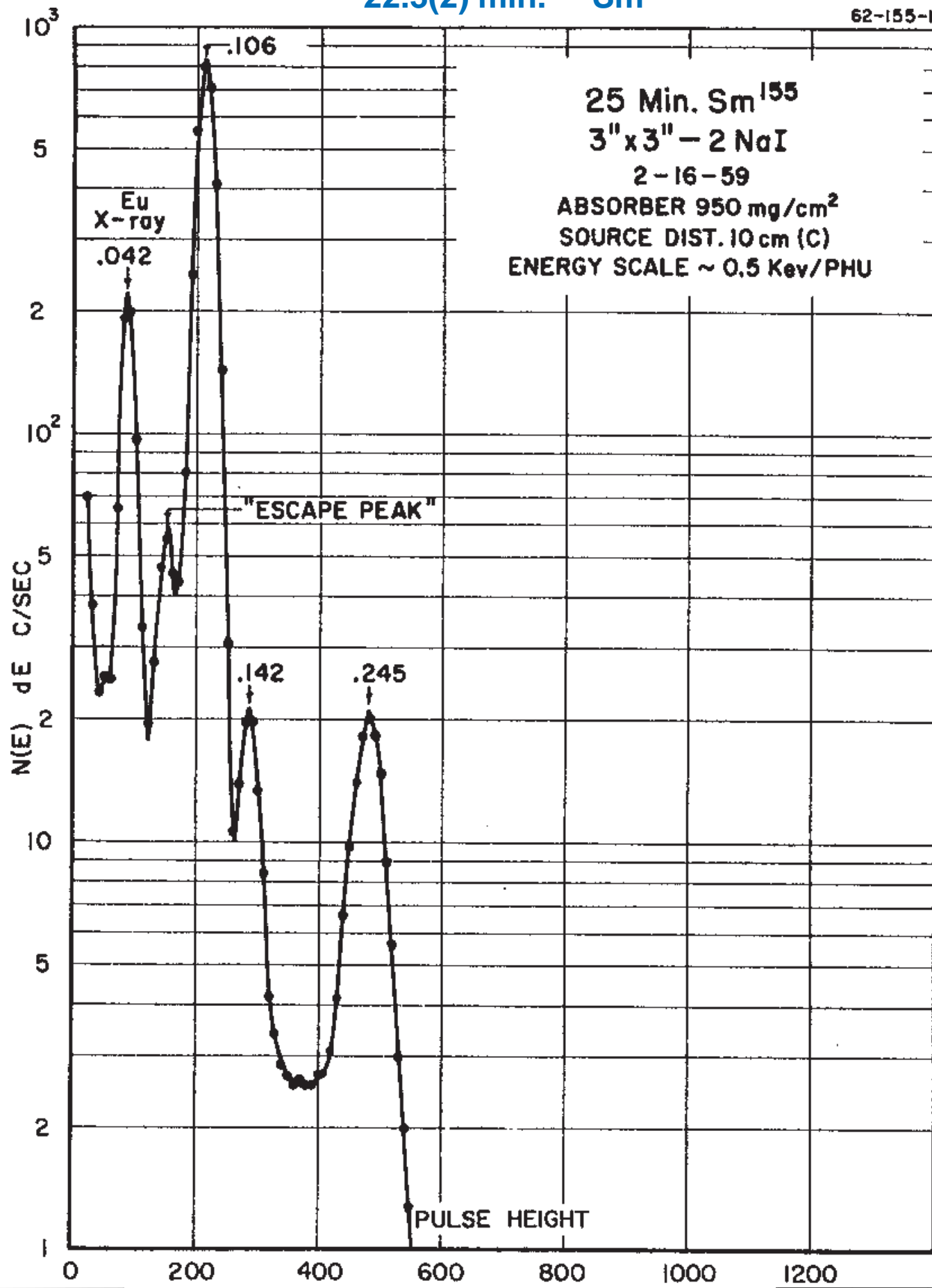
3" x 3" - 2 NaI

2-16-59

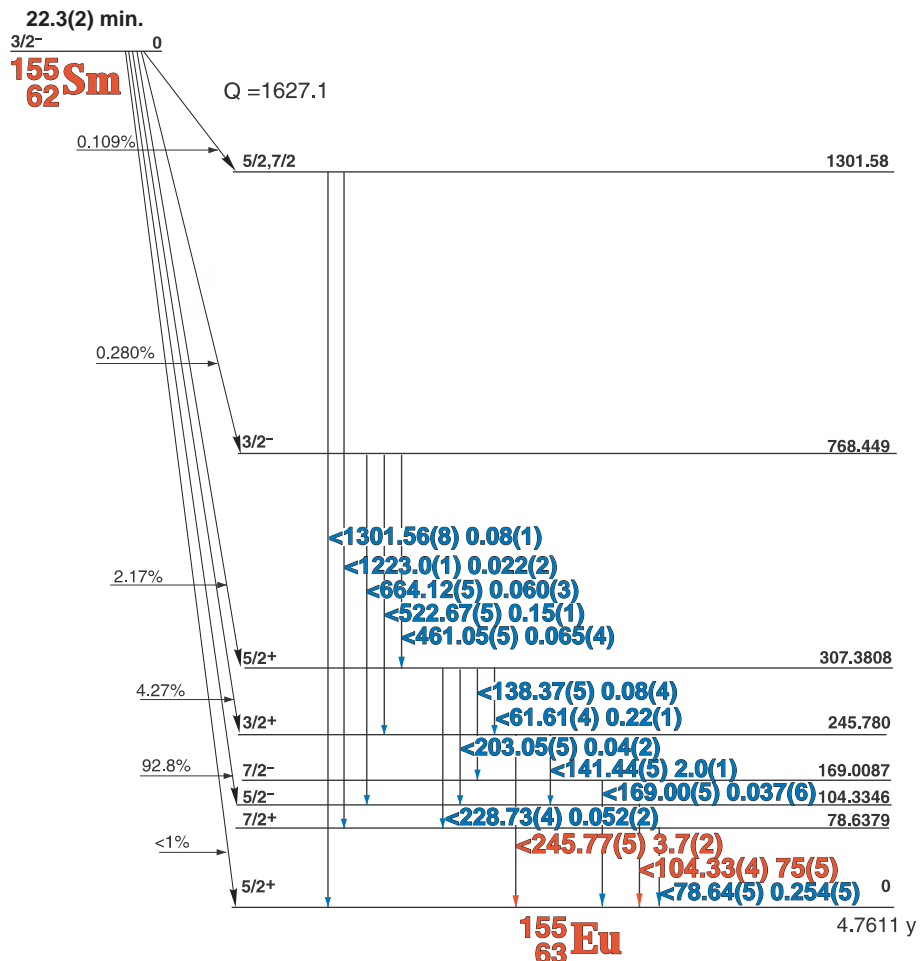
ABSORBER 950 mg/cm²

SOURCE DIST. 10 cm (C)

ENERGY SCALE ~ 0.5 Kev/PHU



22.3(2) min. ^{155}Sm



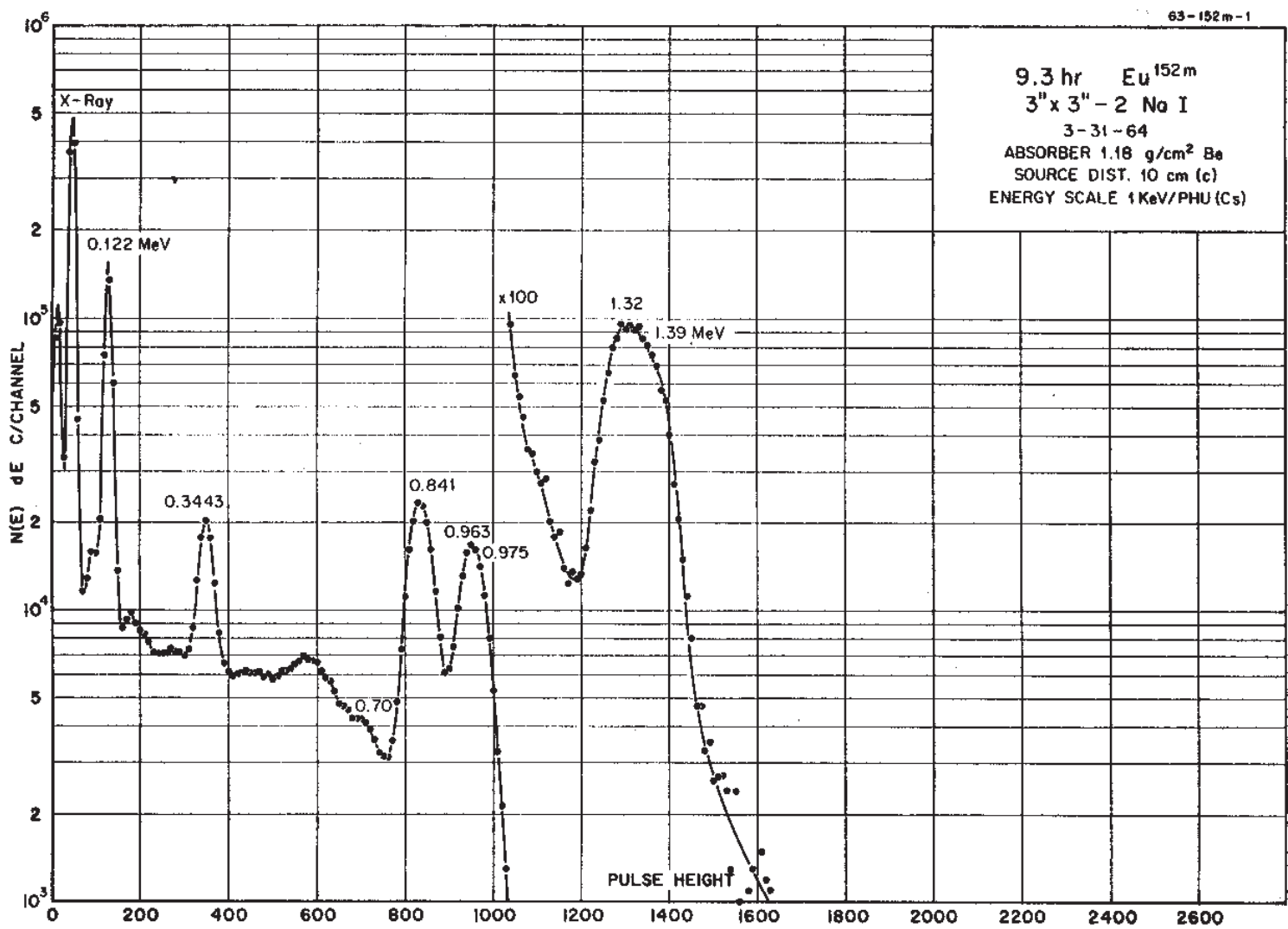
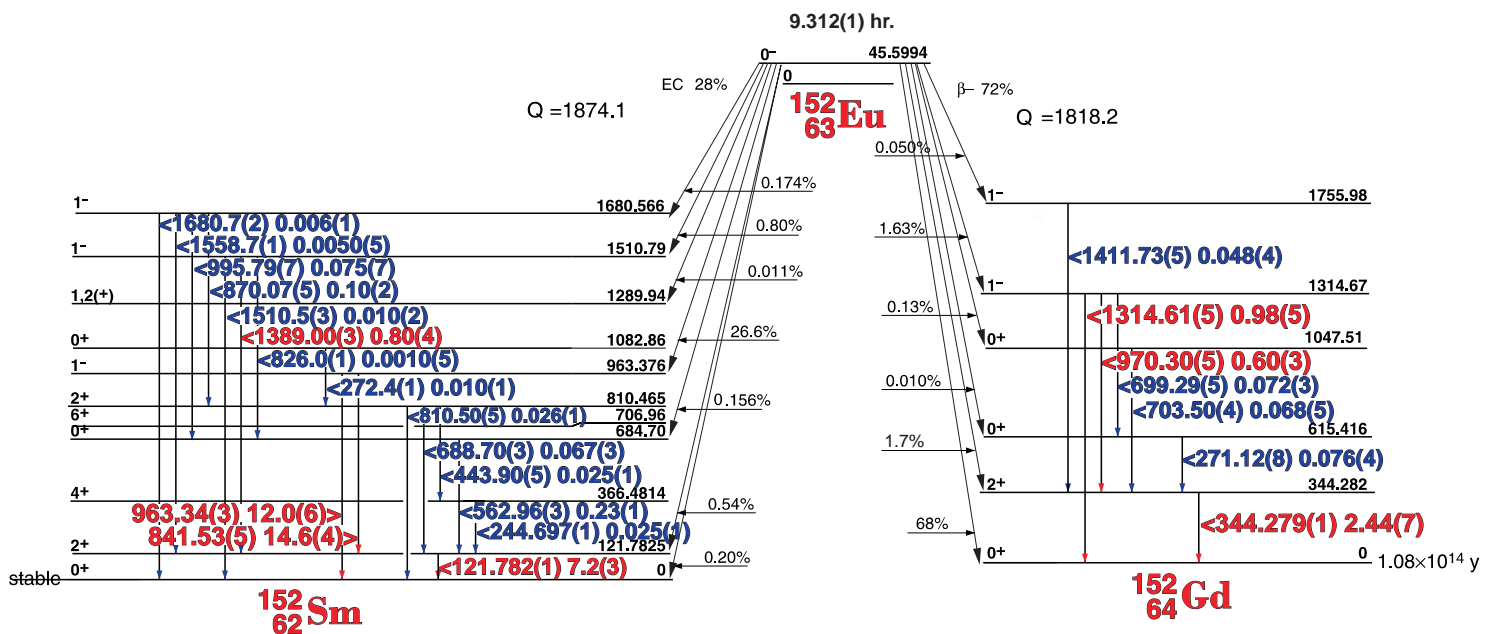
GAMMA-RAY ENERGIES AND INTENSITIES

Nuclide ^{155}Sm
Detector 3" X 3" NaI-2

Half Life 22.3(2) min.
Method of Production: $^{154}\text{Sm}(n,\gamma)$

E_{γ} (KeV)[E]	ΔE_{γ}	I_{γ} (rel)	$I_{\gamma}(\%)$ [E]	ΔI_{γ}	S
78.64	± 0.05		0.254	± 0.005	3
104.33	± 0.04		75	± 2.0	1
141.44	± 0.05		0.20	± 0.02	3
169.00	± 0.05		0.037	± 0.005	4
203.05	± 0.05		0.040	± 0.002	4
228.73	± 0.04		0.052	± 0.002	4
245.77	± 0.05		3.7	± 0.2	1
522.57	± 0.05		0.15	± 0.01	3
664.12	± 0.05		0.06	± 0.03	3
1301.56	± 0.08		0.08	± 0.01	3

9.312 hr. ^{152}mEu



9.312 hr. ^{152m}Eu

GAMMA-RAY ENERGIES AND INTENSITIES

Nuclide ^{152m}Eu
 Detector 3" x 3" -2 NaI

Half Life 9.312(1) hr.

Method of Production: $^{151}\text{Eu}(n,\gamma)$

E_{γ} (KeV)[S]	ΔE_{γ}	$I_{\gamma}(\text{rel})$	$I_{\gamma}(\%)[E]$	ΔI_{γ}	S
121.783	± 0.009	50.66	7.2	± 0.3	1
244.697	± 0.001	0.37	0.025	± 0.001	4
272.4	± 0.08	0.669	0.010	± 0.001	4
344.267	± 0.008	17.36	2.44	± 0.07	1
443.90	± 0.05	0.21	0.025	± 0.001	4
562.96	± 0.03	1.55	0.23	± 0.01	3
688.70	± 0.03	0.62	0.067	± 0.003	4
699.29	± 0.05	0.84	0.072	± 0.003	4
703.50	± 0.04	0.73	0.068	± 0.005	4
810.51	± 0.05	0.34	0.026	± 0.001	4
826.0	± 0.12	0.23	0.0010	$\pm 0.(5)$	4
841.535	± 0.015	100	14.6	± 0.4	1
870.07	± 0.05	0.80	0.10	± 0.02	3
911.33	± 0.2	0.21		± 0.05	4
963.337	± 0.025	82.4	12.0	± 0.6	1
970.30	± 0.04	4.60	0.60	± 0.03	1
995.79	± 0.07	0.51	0.075	± 0.007	3
1314.61	± 0.05	6.67	0.98	± 0.05	1
1389.000	± 0.028	5.74	0.80	± 0.04	1
1411.735	± 0.05	0.35	0.048	± 0.004	2
1510.5	± 0.2	0.075	0.010	± 0.002	3
1558.7	± 0.1	0.060	0.0050	$\pm 0.(5)$	3
1680.7	± 0.20	0.04	0.006	± 0.001	3
1756.56	± 0.10		0.001		

4.761 yr. ^{155}Eu

63-155-1

1.7 yr Eu^{155}

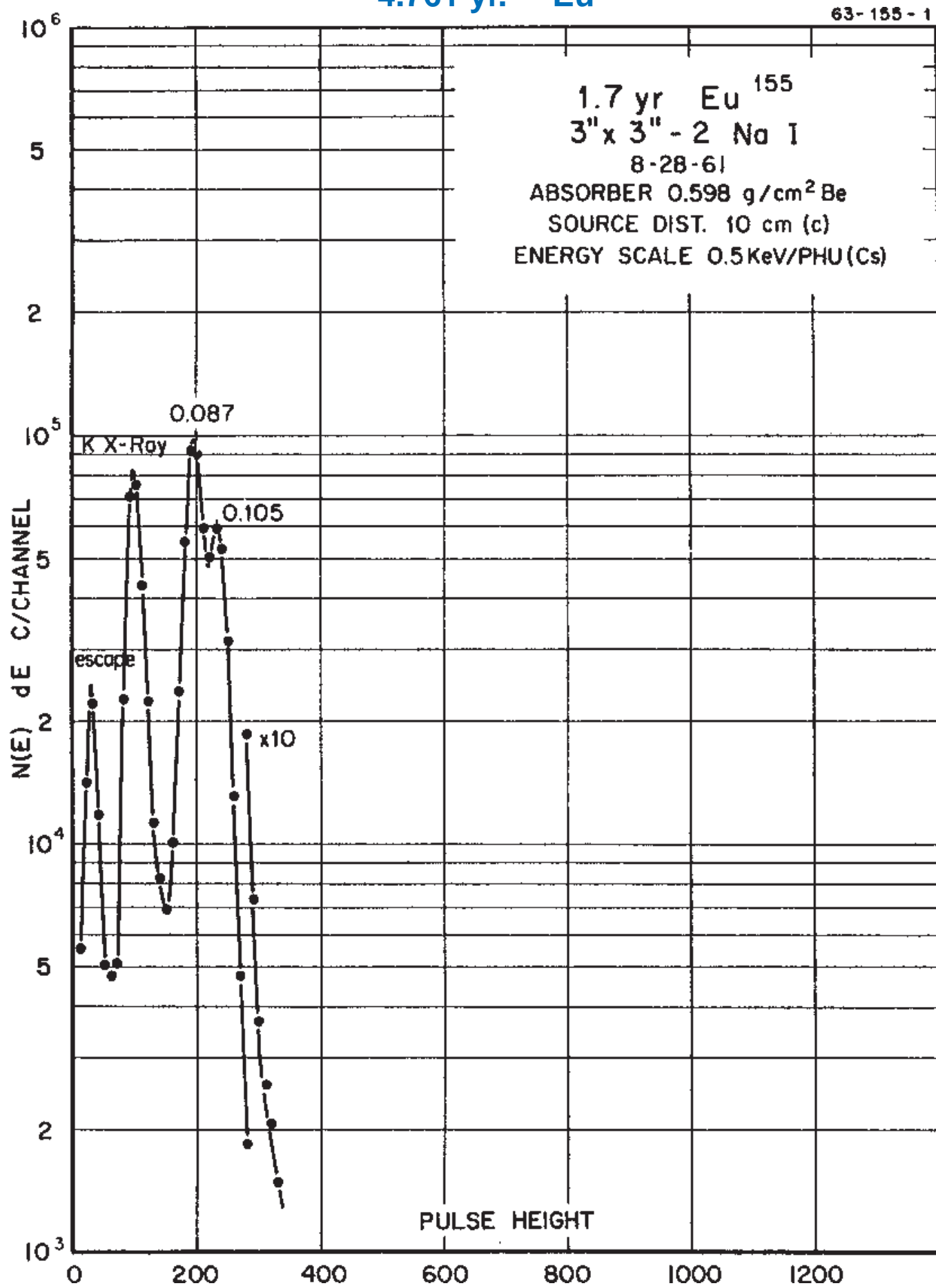
3" x 3" - 2 Na I

8-28-61

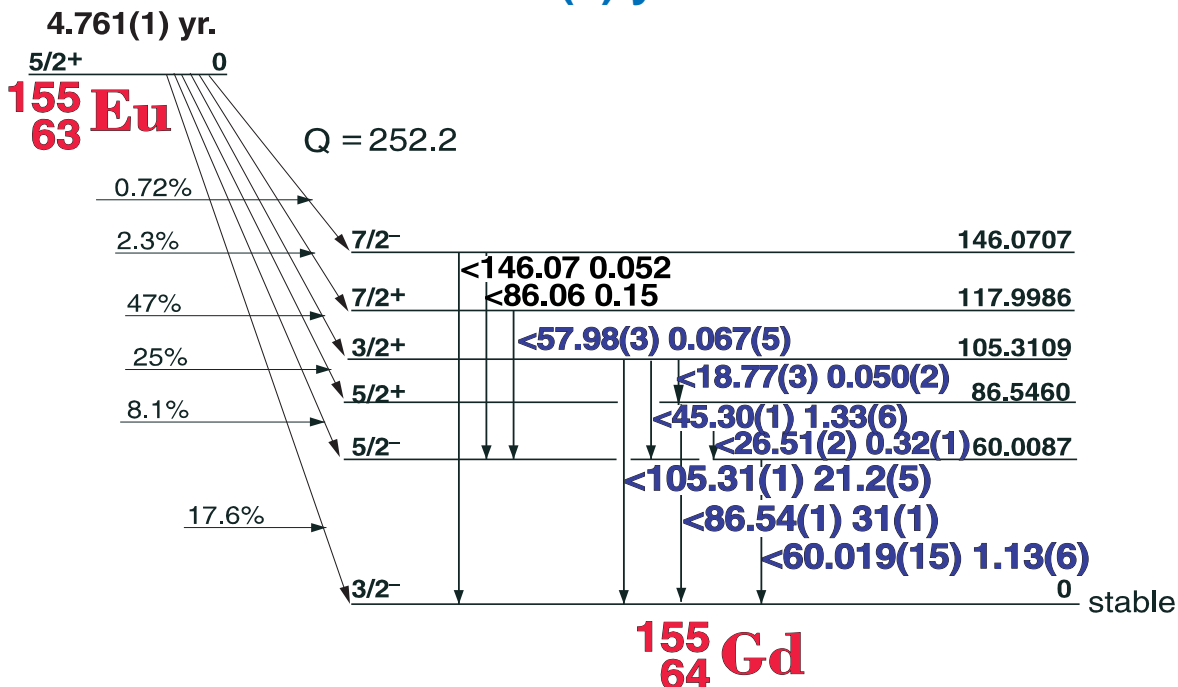
ABSORBER 0.598 g/cm² Be

SOURCE DIST. 10 cm (c)

ENERGY SCALE 0.5KeV/PHU(Cs)



4.761(1) yr. ^{155}Eu



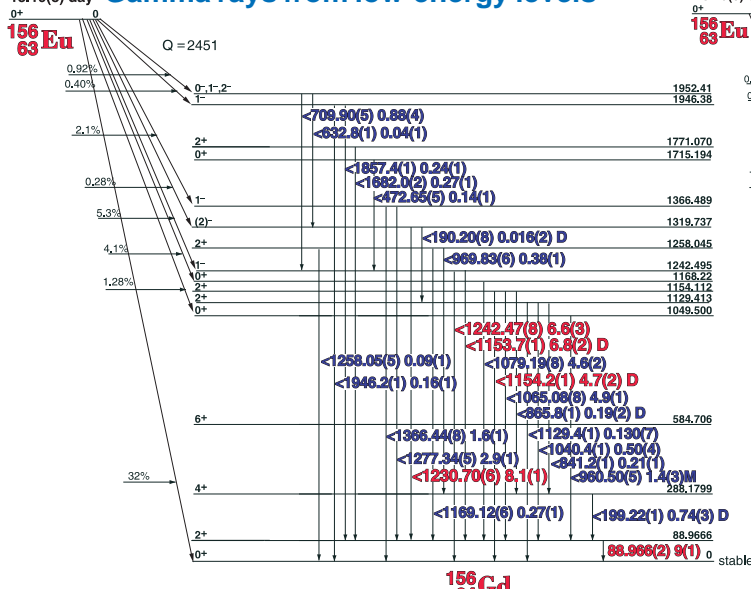
GAMMA-RAY ENERGIES AND INTENSITIES

Nuclide ^{155}Eu Half Life 4.761(10 YR.
Detector 3" X 3" NaI-2 Method of Production: $^{235}\text{U}(n,f)$

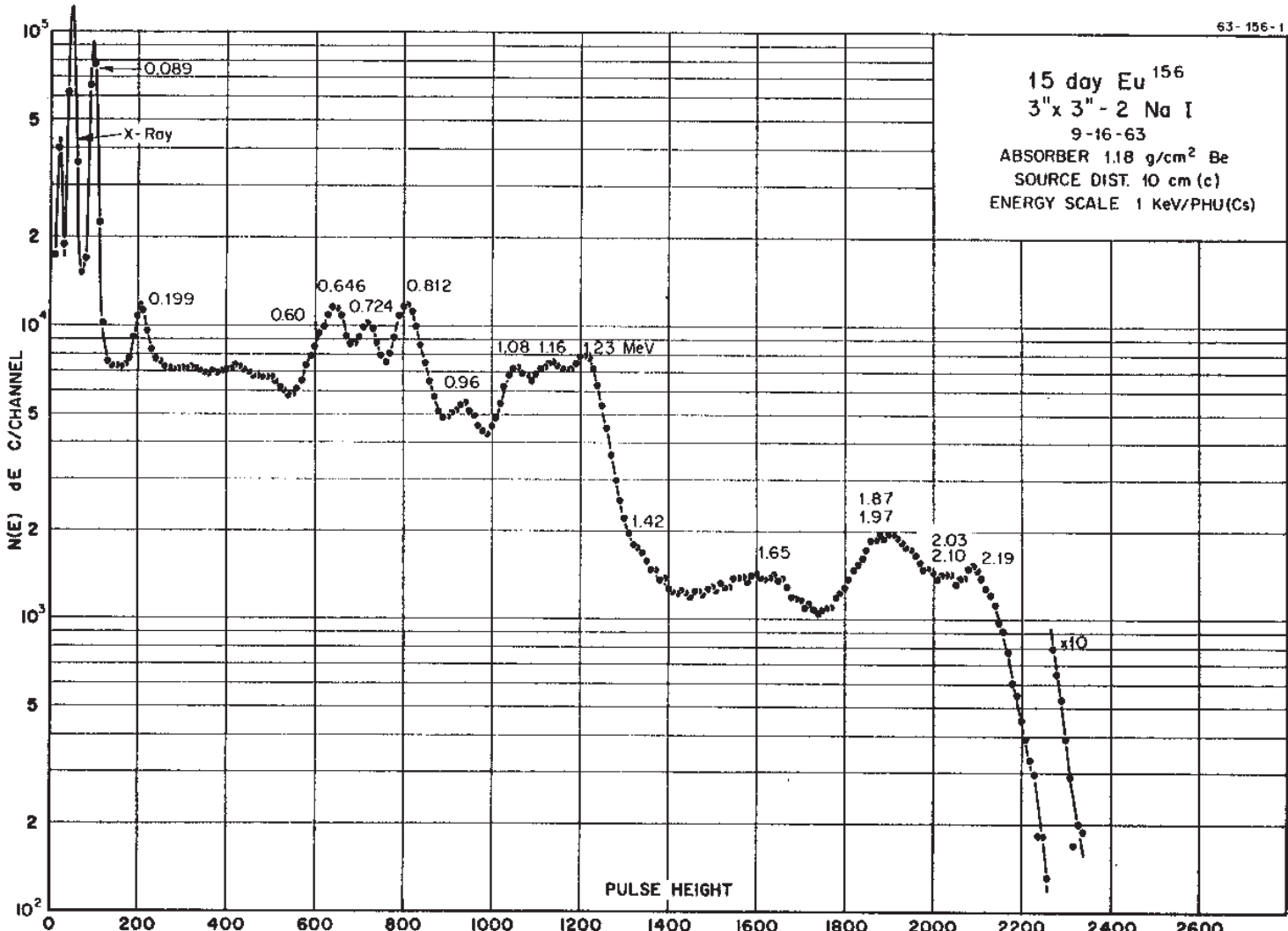
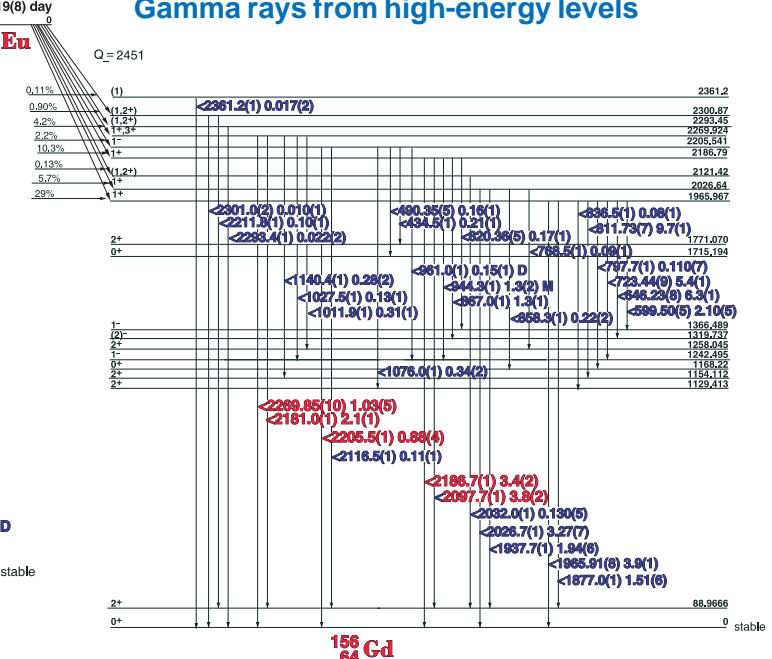
E_γ (KeV)	ΔE_γ	I_γ (rel)	I_γ (%)	ΔI_γ	S
Gd L x-ray					
18.776	± 0.035	0.16	0.05	± 0.002	4
26.513	± 0.021	1.00	0.32	± 0.01	4
Gd K x-ray					
45.299	± 0.013	4.1	1.33	± 0.06	3
57.983	± 0.030		0.067	± 0.006	4
60.019	± 0.015	3.9	1.13	± 0.06	4
86.539	± 0.015	100	31	± 1.0	2
105.315	± 0.015	68.3	21.1	± 0.5	2

15.19(8) day ^{156}Eu

15.19(8) day Gamma rays from low-energy levels



15.19(8) day Gamma rays from high-energy levels



15.19(8) day ^{156}Eu

GAMMA-RAY ENERGIES AND INTENSITIES

Nuclide ^{156}Eu
Detector 3" X 3" NaI-2

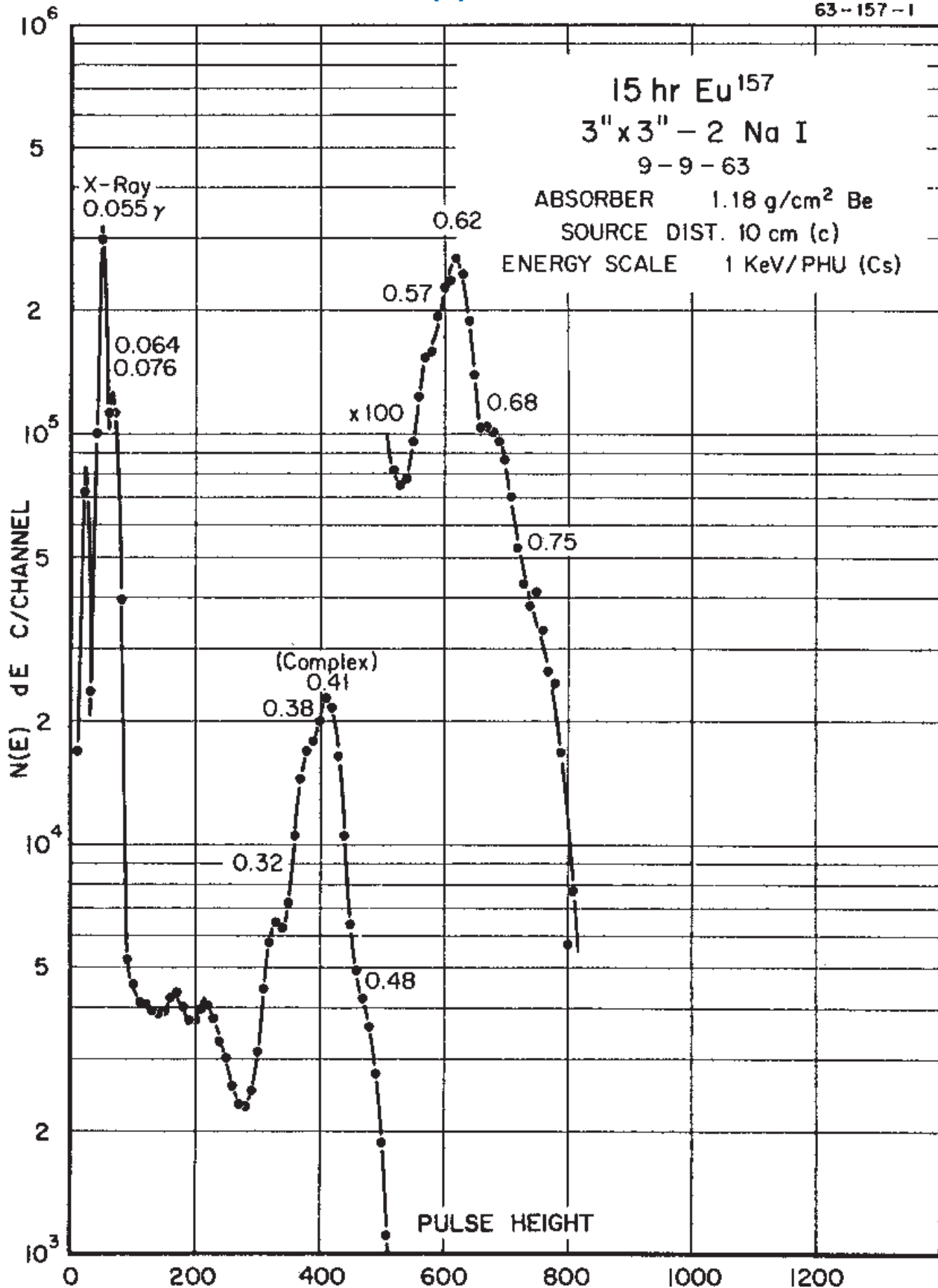
Half Life 15.19(8) day
Method of Production: $^{154}\text{Sm}(n,\gamma,\beta,n,\gamma)$

E_{γ} (KeV)[S]	ΔE_{γ}	$I_{\gamma}(\text{rel})$	$I_{\gamma}(\%)[E]$	ΔI_{γ}	S
88.966	± 0.002	100	9	± 1.0	1
190.20	± 0.08	1.1	0.080	± 0.04	4
199.22	± 0.01	1.3	0.74	± 0.04	3
434.5	± 0.1	0.51	0.21	± 0.01	4
472.65	± 0.05	0.38	0.14	± 0.01	4
490.35	± 0.05	0.38	0.16	± 0.01	4
599.50	± 0.05	4.67	2.10	± 0.05	3
646.23	± 0.08	14.0	6.3	± 0.1	2
709.90	± 0.05	2.0	0.88	± 0.04	4
723.44	± 0.09	12.0	5.4	± 0.1	2
768.5	± 0.1	0.2	0.09	± 0.01	4
797.73	± 0.07	0.2	0.011	± 0.007	4
811.73	± 0.07	21.5	9.7	± 0.1	2
820.36	± 0.07	0.35	0.17	± 0.01	4
836.5	± 0.1	0.24	0.08	± 0.01	4
841.2	± 0.1	0.49	0.21	± 0.01	4
858.3	± 0.1	0.60	0.22	± 0.02	4
867.0	± 0.10	3.34	1.3	± 0.1	4
944.3	± 0.1	5.32	1.3	± 0.2	3
960.50	± 0.05	3.54	1.4	± 0.3	3
969.83	± 0.06	0.84	0.38	± 0.01	4
1011.9	± 0.1	1.20	0.31	± 0.01	4
1027.5	± 0.12	0.84	0.13	± 0.01	4
1040.4	± 0.1	1.19	0.50	± 0.04	4
1065.08	± 0.08	11.80	4.9	± 1.0	2
1076.0	± 0.10	5.32	0.34	± 0.02	3
1079.19	± 0.08	10.40	4.6	± 0.2	2
1129.4	± 0.12	0.38	0.130	± 0.007	4
1140.4	± 0.1	0.68	0.28	± 0.02	4
1153.72	± 0.08	16.0	6.8	± 0.2	1
1154.2	± 0.1	12.0	4.7	± 0.1	2
1158.88	± 0.10	6.2		± 1.5	3
1164.81	± 0.12	3.5	0.07	± 0.01	3
1169.12	± 0.06	0.69	0.27	± 0.01	4
1230.70	± 0.06	19.30	8.1	± 0.1	1
1242.47	± 0.08	15.8	6.6	± 0.3	2

E_{γ} (KeV)[S]	ΔE_{γ}	$I_{\gamma}(\text{rel})$	$I_{\gamma}(\%)[E]$	ΔI_{γ}	S
1247.99	± 0.15	0.47		± 0.08	3
1258.1	± 0.1	0.20		± 0.01	4
1277.34	± 0.05	7.10		± 0.1	3
1366.44	± 0.08	4.0		± 0.1	3
1455.02	± 0.15	0.31		± 0.08	4
1587.1	± 0.2	0.45		± 0.10	4
1675.9	± 0.3	0.38		± 0.09	4
1682.0	± 0.15	0.93		± 0.01	4
1857.4	± 0.15	0.71		± 0.01	4
1877.0	± 0.10	3.30		± 0.06	3
1937.7	± 0.1	4.45		± 0.06	3
1946.2	± 0.1	0.27		± 0.01	4
1965.91	± 0.10	9.78	3.9	± 0.1	2
2026.7	± 0.10	8.44	3.27	± 0.07	2
2032.0	± 0.1	0.98		± 0.005	4
2097.7	± 0.1	11.78	3.8	± 0.2	1
2110.64	± 0.2	0.35		± 0.09	4
2116.5	± 0.15	0.38		± 0.01	4
2181.05	± 0.10	9.11	2.1	± 0.1	1
2186.7	± 0.10	13.55	3.4	± 0.2	1
2205.5	± 0.10	3.78	0.88	± 0.04	1
2211.85	± 0.12	0.44		± 0.01	3
2269.85	± 0.10	5.33	1.03	± 0.05	1
2293.4	± 0.1			± 0.002	4
2301.0	± 0.2			± 0.001	4
2361.2	± 0.1			± 0.002	4

15.18(3) hr. ^{157}Eu

63-157-1



15.18(3) hr. ^{157}Eu

GAMMA-RAY ENERGIES AND INTENSITIES

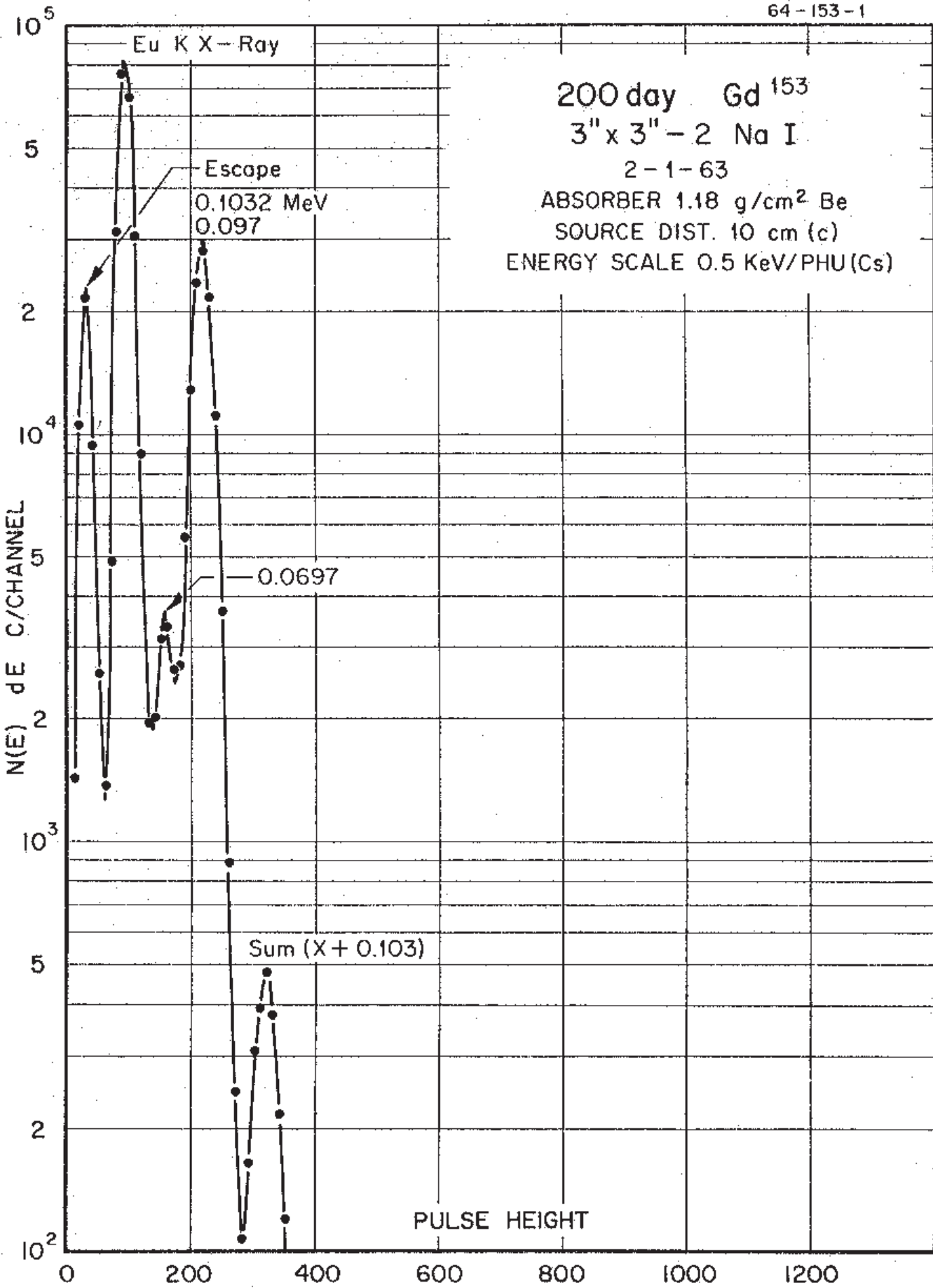
Nuclide ^{157}Eu
Detector 3" x 3" -2 NaI

Half Life 15.18(3) hr.
Method of Production: $^{235}\text{U}(\text{n},\text{f})$

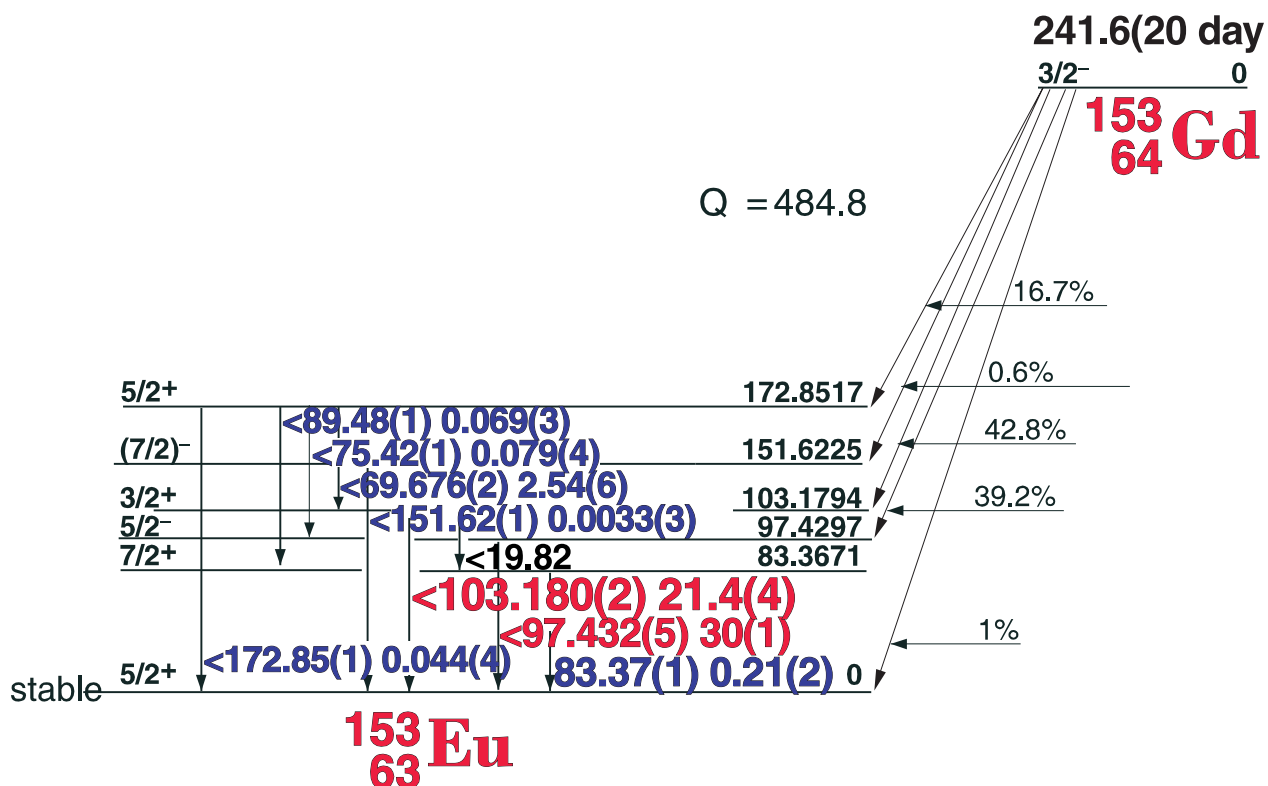
E_γ (KeV)[S]	ΔE_γ	I_γ (rel)	I_γ (%)[E]	ΔI_γ	

241.6(2) day day ^{153}Gd [C]

64 - 153 - 1



241.6(2) day day ^{153}Gd [C]



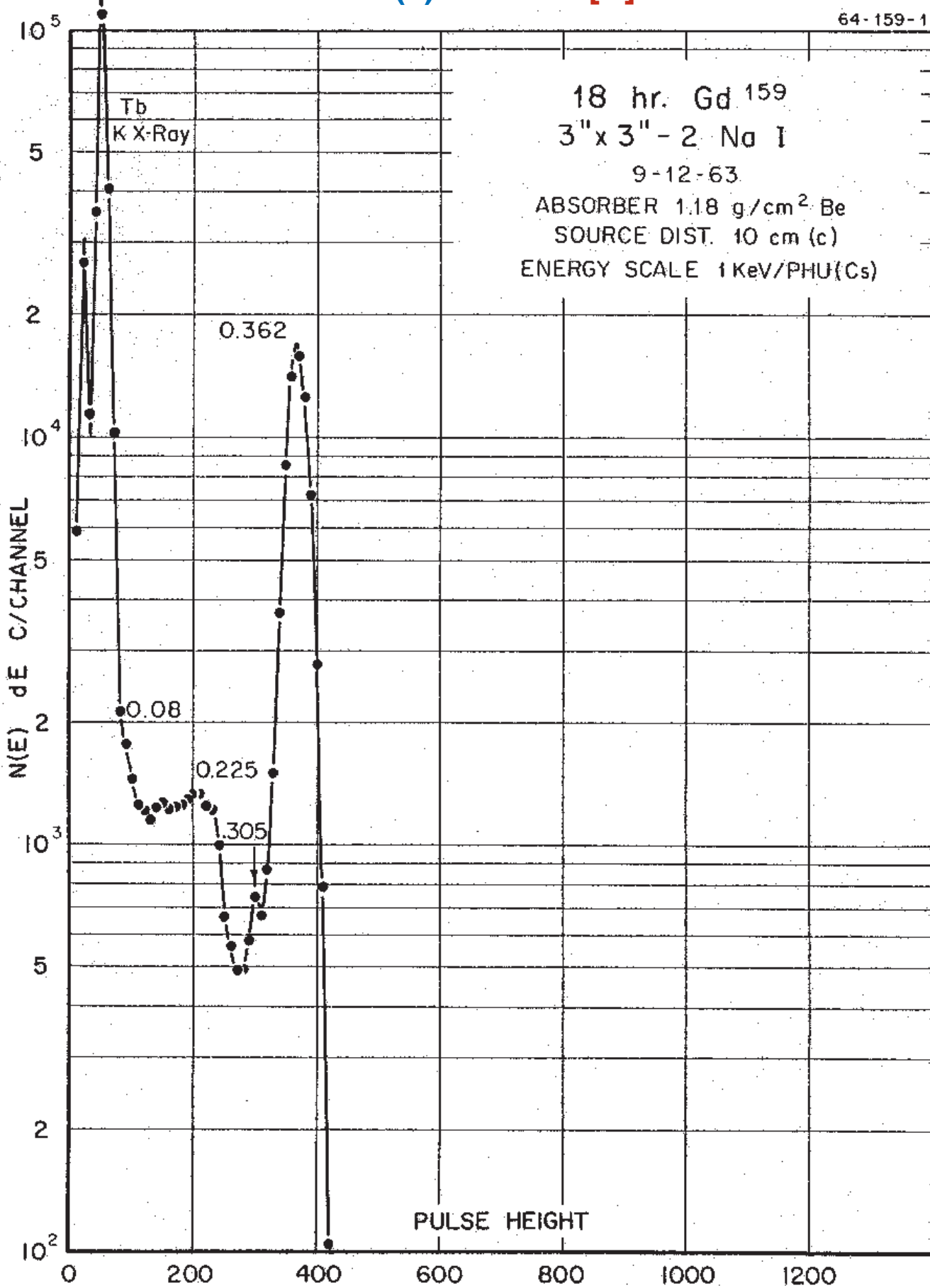
GAMMA-RAY ENERGIES AND INTENSITIES

Nuclide ^{153}Gd Half Life 241.6(2) day
 Detector 3" X 3" NaI-2 Method of Production: $^{152}\text{Gd}(n,\gamma)$

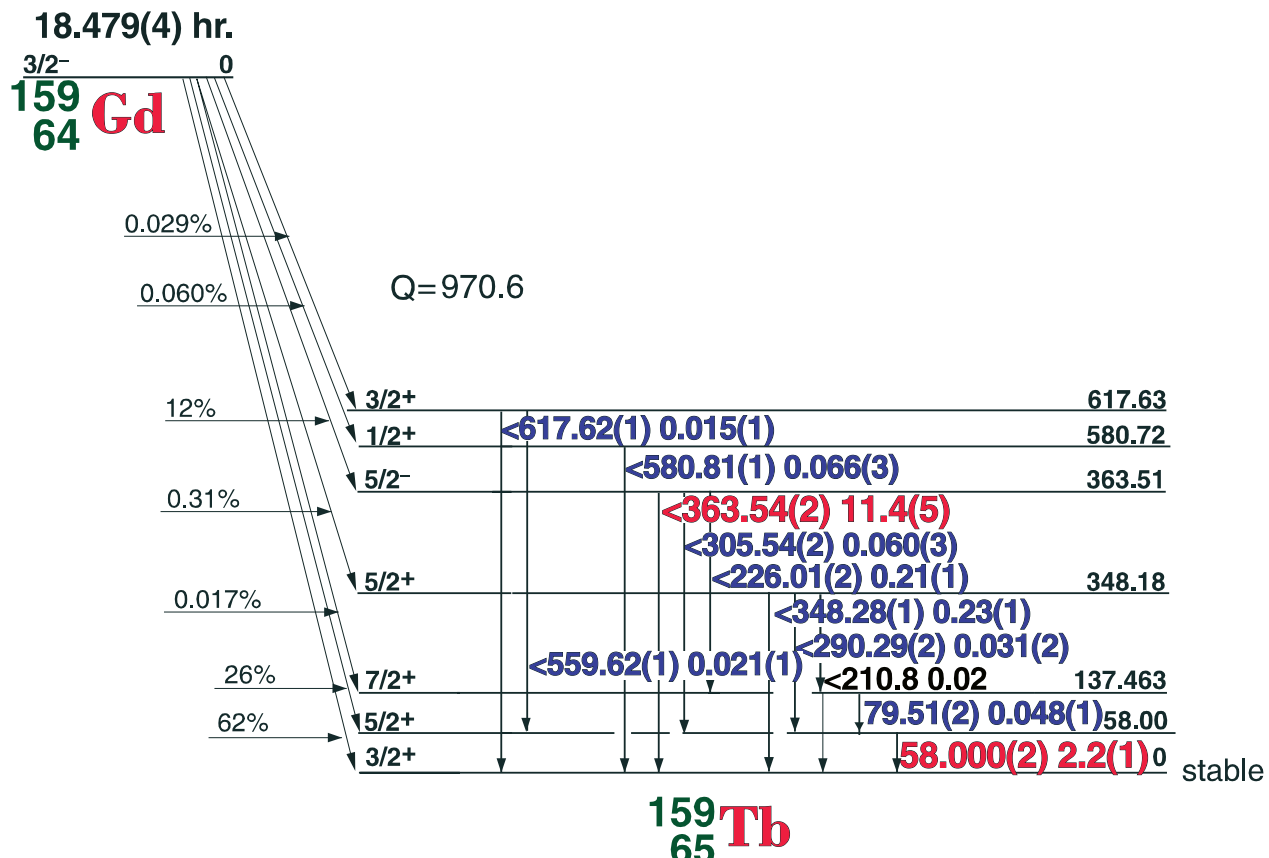
E_γ (KeV)[C]	ΔE_γ	I_γ (rel)	I_γ (%)[E]	ΔI_γ	S
Eu K x-ray					
69.676	± 0.002	7.8	2.54	± 0.06	2
75.42	± 0.01	0.30	0.079	± 0.004	4
83.37	± 0.01	0.80	0.21	± 0.02	4
89.48	± 0.01	0.30	0.069	± 0.003	4
97.432	± 0.005	100	30	± 1.0	1
103.180	± 0.002	73.5	21.4	± 0.4	1
151.62	± 0.01	0.0130	0.0033	± 0.0003	4
172.85	± 0.01	0.130	0.044	± 0.004	3

18.479(4) hr. ^{159}Gd [C]

64-159-1



18.479(4) hr. ^{159}Gd [C]



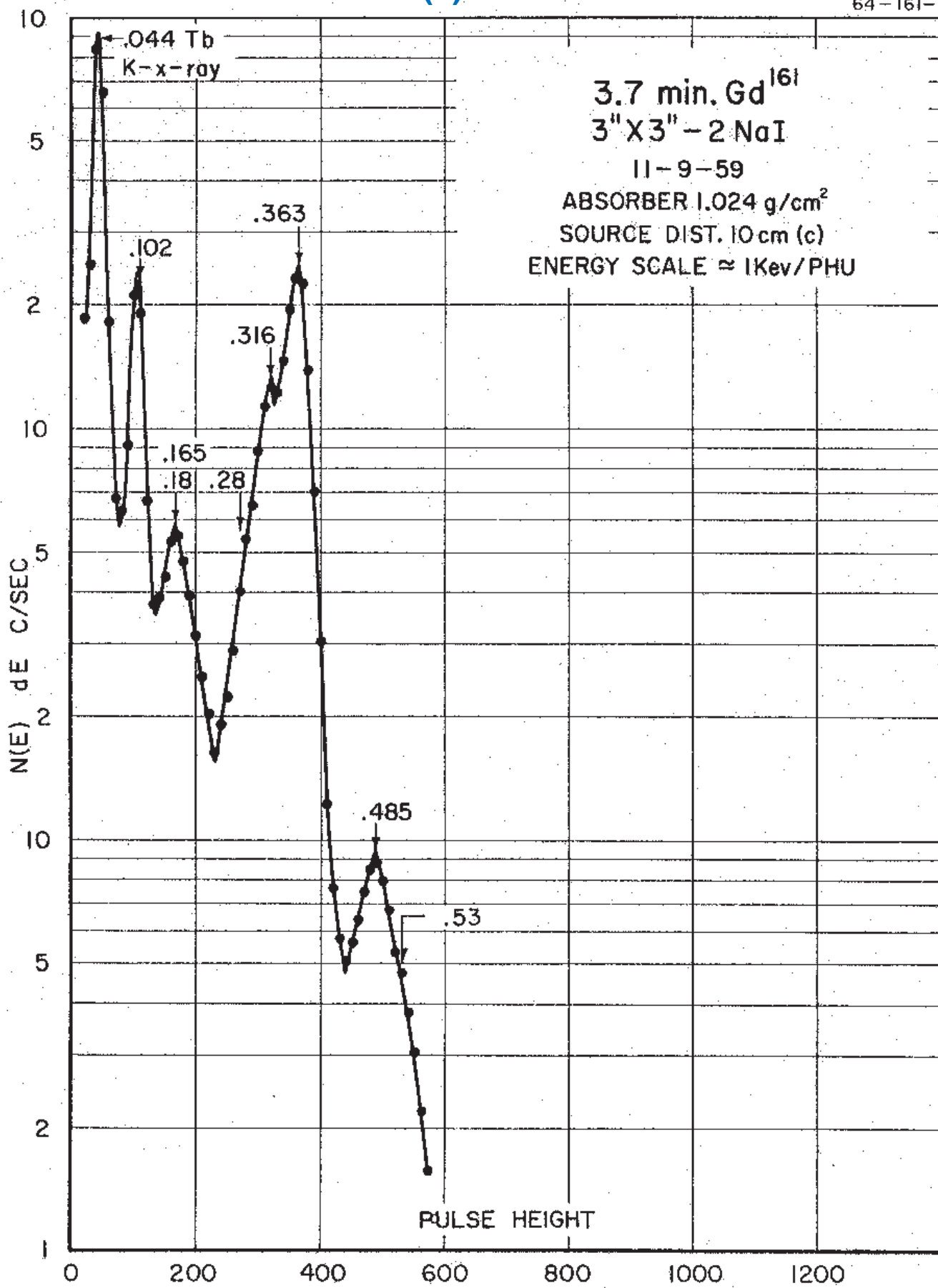
GAMMA-RAY ENERGIES AND INTENSITIES

Nuclide ^{159}Gd Half Life 18.479(4) hr.
 Detector 3" x 3" -2 NaI Method of Production: $^{158}\text{Gd}(n,\gamma)$

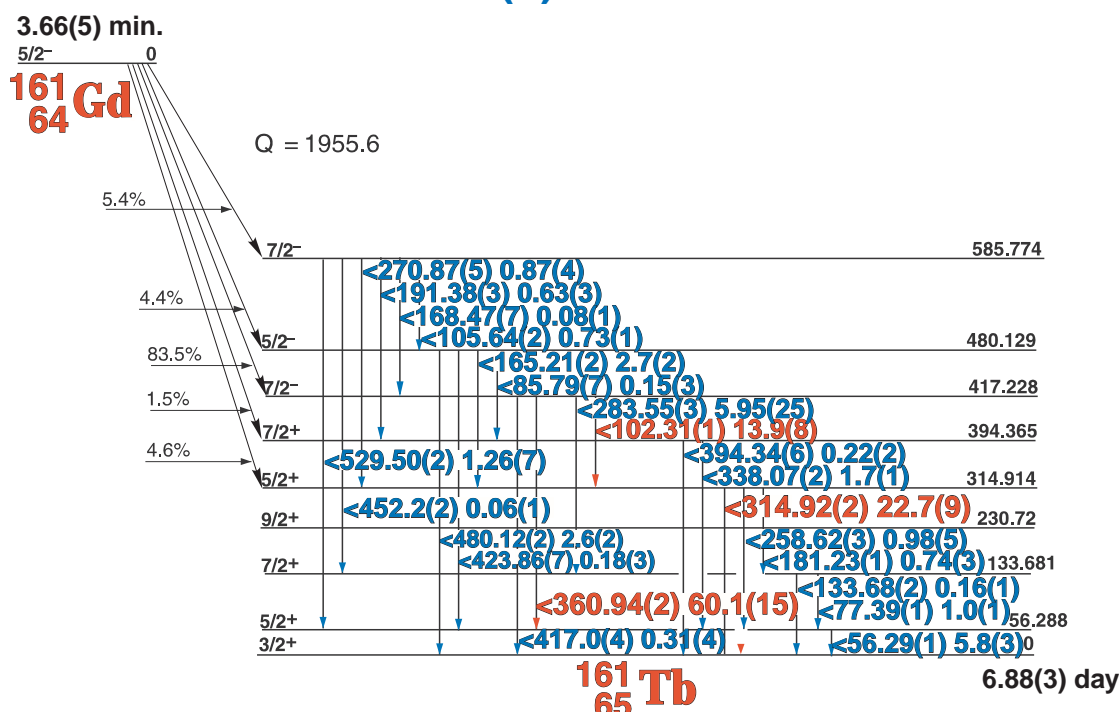
E_{γ} (KeV)[C]	ΔE_{γ}	I_{γ} (rel)	$I_{\gamma}(\%)$ [E]	ΔI_{γ}	S
Tb x- rays					
58.000	± 0.002	11.3	2.2	± 0.1	1
79.51	± 0.01	0.43	0.48	± 0.02	4
226.01	± 0.02	1.74	0.21	± 0.01	3
290.29	± 0.01	0.30	0.031	± 0.002	4
305.54	± 0.02	0.56	0.060	± 0.003	3
348.28	± 0.01	2.03	0.23	± 0.01	3
363.54	± 0.02	100	11.4	± 0.5	1
559.62	± 0.01	0.18	0.21	$+ 0.01$	3
580.81	± 0.01	0.59	0.066	$+ 0.003$	2
617.62	± 0.01	0.16	0.015	$+ 0.001$	3

3.66(5) min. ^{161}Gd

64-161-1



3.66(5) min. ^{161}Gd



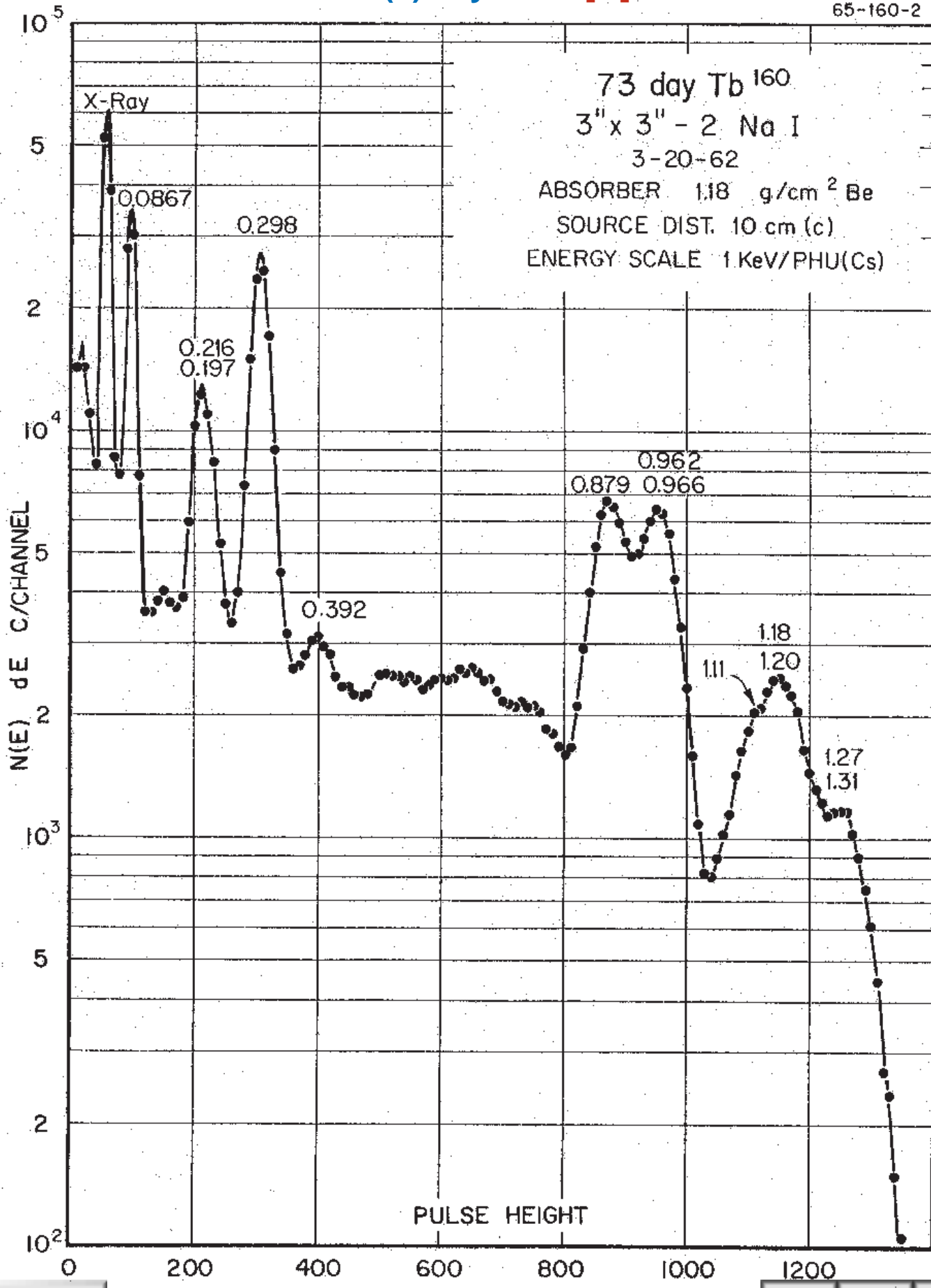
GAMMA-RAY ENERGIES AND INTENSITIES

Nuclide ^{161}Gd
Detector 3" x 3" -2 NaI
Half Life 3.66(5) min.
Method of Production: $^{160}\text{Gd}(n,\gamma)$

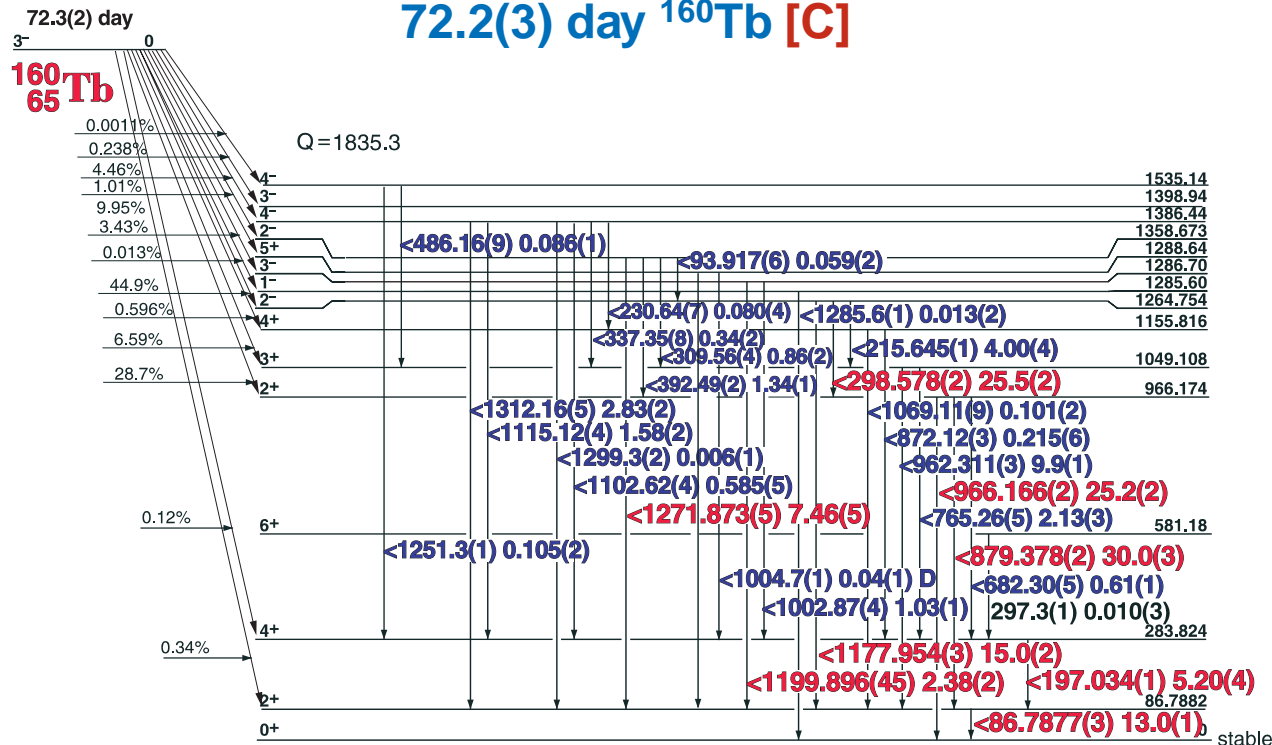
E_{γ} (KeV)[S]	ΔE_{γ}	$I_{\gamma}(\text{rel})$	$I_{\gamma}(\%)$ [E]	ΔI_{γ}	S
56.29	± 0.01		5.8	± 0.3	1
77.39	± 0.01	1.0	± 0.1	± 0.1	3
85.79	± 0.07	0.15	± 0.03	± 0.03	3
102.31	± 0.01	13.9	± 0.8	1	
105.64	± 0.02	0.73	± 0.01	± 0.01	3
133.68	± 0.02	0.16	± 0.01	± 0.01	3
165.21	± 0.02	2.7	± 0.2	± 0.2	2
168.47	± 0.07	0.08	± 0.01	± 0.01	4
181.23	± 0.01	0.74	± 0.03	± 0.03	3
191.38	± 0.03	0.63	± 0.03	± 0.03	3
258.62	± 0.03	0.98	± 0.05	± 0.05	3
270.87	± 0.05	0.87	± 0.04	± 0.04	3
283.55	± 0.03	5.95	± 0.25	2	
314.92	± 0.02	22.7	± 0.9	1	
338.07	± 0.02	1.7	± 0.1	± 0.1	3
360.94	± 0.02	60.1	± 1.5	1	
394.34	± 0.06	0.22	± 0.02	± 0.02	3
417.0	± 0.4	0.31	± 0.02	± 0.02	3
423.86	± 0.07	0.18	± 0.03	± 0.03	3
452.2	± 0.2	0.06	± 0.01	± 0.01	4
480.12	± 0.02	2.6	± 0.2	2	
529.50	± 0.02	1.26	± 0.07	2	

72.2(3) day ^{160}Tb [C]

65-160-2



72.2(3) day ^{160}Tb [C]



GAMMA-RAY ENERGIES AND INTENSITIES

Nuclide **^{160}Tb**
Detector 3" x 3" -2 NaI

Half Life 72.2(3) day
Method of Production: $^{159}\text{Tb}(\text{n},\gamma)$

E_{γ} (KeV)[C]	ΔE_{γ}	I_{γ} (rel)	$I_{\gamma}(\%)[E]$	ΔI_{γ}	S
86.7877	± 0.0003	46.80	13.0	± 0.1	1
93.917	± 0.006	0.12	0.059	± 0.002	4
197.034	± 0.001	17.20	5.20	± 0.04	1
215.645	± 0.001	13.05	4.00	± 0.04	1
230.641	± 0.07	0.20	0.080	± 0.004	4
298.578	± 0.002	88.89	25.5	± 0.2	1
309.564	± 0.044	2.73	0.86	± 0.02	3
337.347	± 0.085	1.14	0.34	± 0.02	4
392.493	± 0.023	4.34	1.34	± 0.01	3
486.16	± 0.09	0.32	0.086	± 0.001	
682.298	± 0.055	1.79	0.61	± 0.01	4
765.260	± 0.054	6.63	2.13	± 0.03	4
872.12	± 0.030	0.95	0.21	± 0.01	4
879.378	± 0.002	100	30.0	± 0.3	1
962.311	± 0.003	35.37	9.9	± 0.1	2
966.166	± 0.002	84.80	25.2	± 0.2	1
1002.87	± 0.04	3.47	1.03	± 0.01	3
1004.7	± 0.1		0.04	± 0.01	
1069.113	± 0.09	0.38	0.101	± 0.002	4
1102.62	± 0.04	2.05	0.585	± 0.005	3
1115.122	± 0.04	5.05	1.58	± 0.02	2
1177.954	± 0.001	52.1	15.0	± 0.2	1
1199.896	± 0.046	8.28	2.38	± 0.02	1
1251.34	± 0.10	0.32	0.105	± 0.002	3
1271.873	± 0.005	26.0	7.48	± 0.05	1

1.257(6) min. ^{165}mDy

66 - ^{165}mDy - 1

75 sec $\text{Dy}^{165\text{m}}$

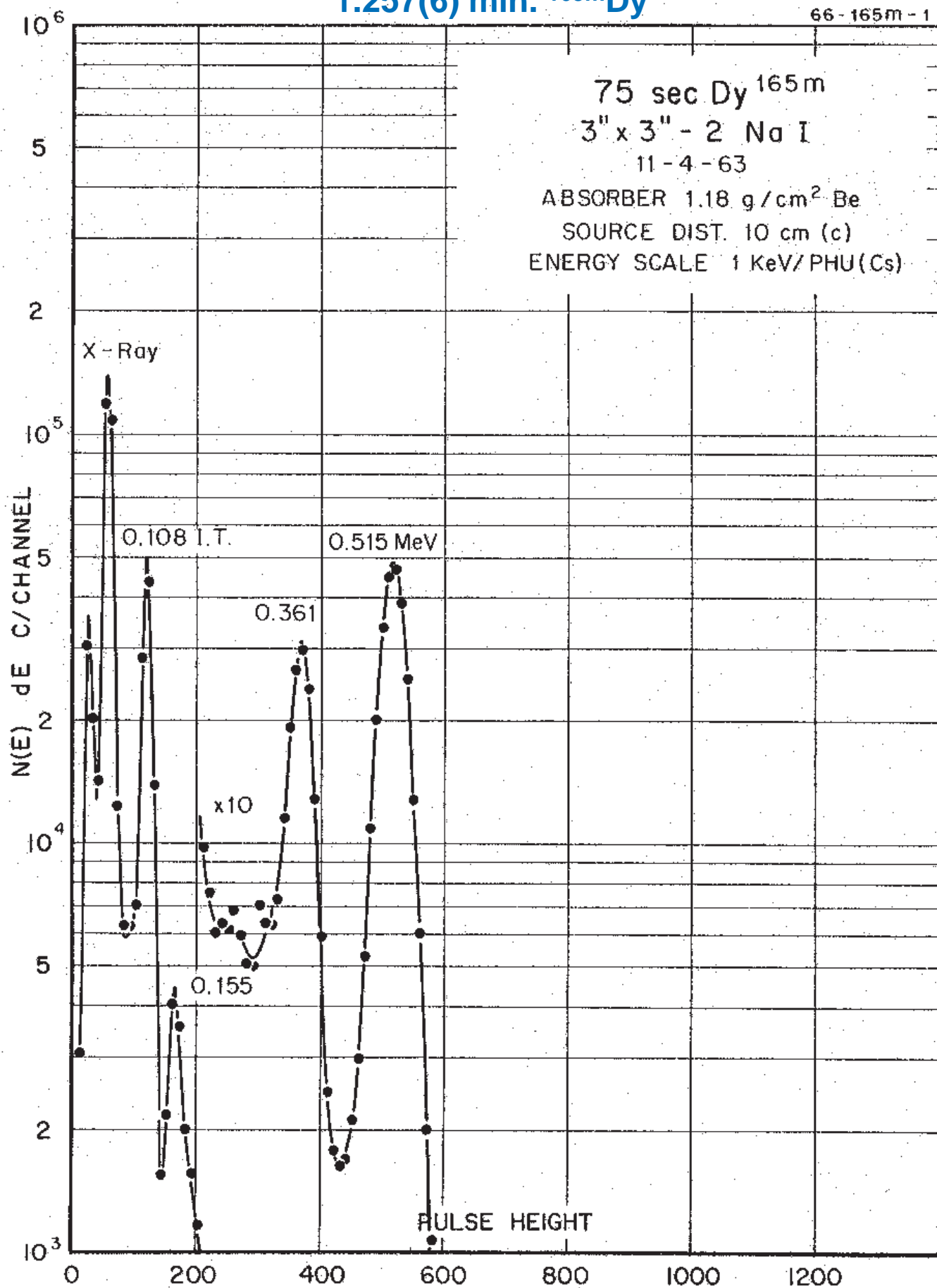
3" x 3" - 2 Na I

11 - 4 - 63

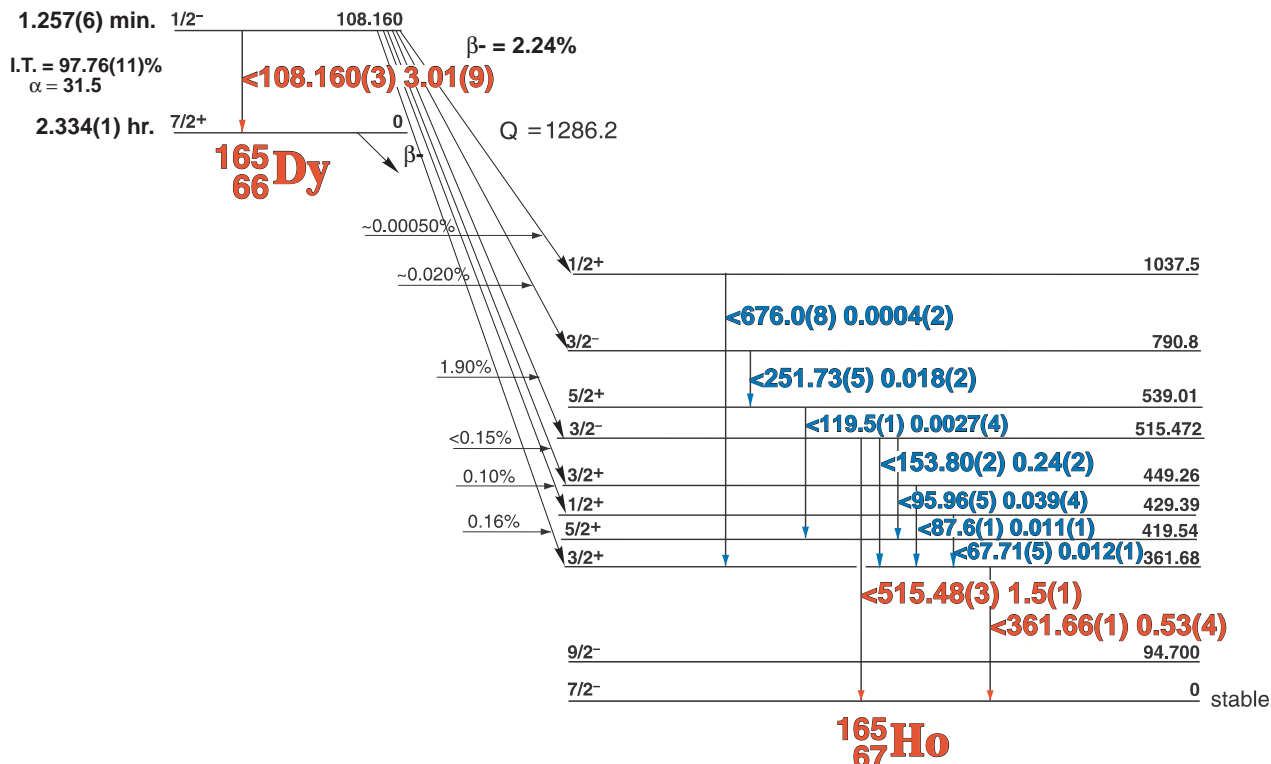
ABSORBER 1.18 g/cm² Be

SOURCE DIST. 10 cm (c)

ENERGY SCALE 1 KeV/PHU(Cs)



1.257(6) min. ^{165m}Dy

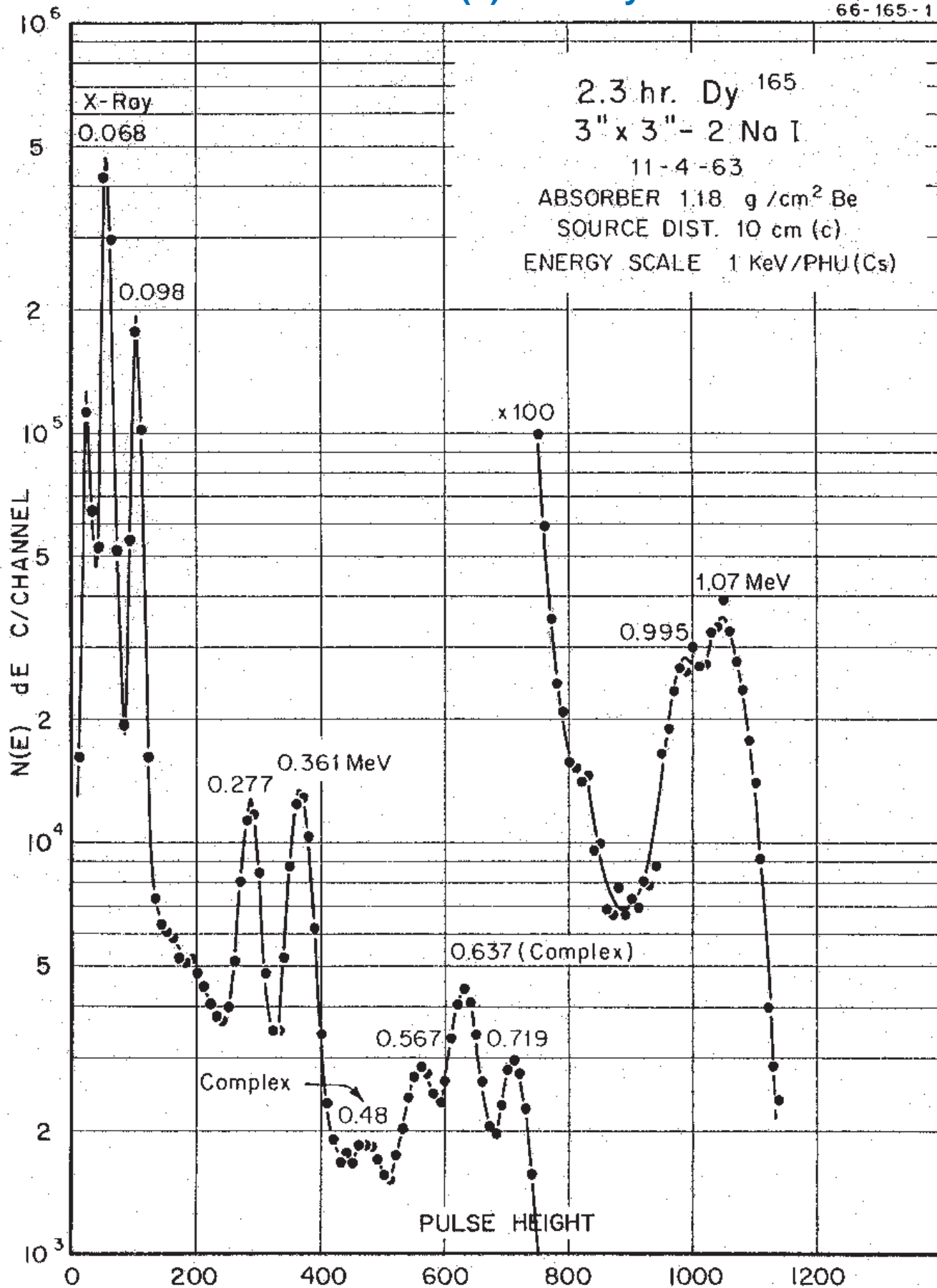


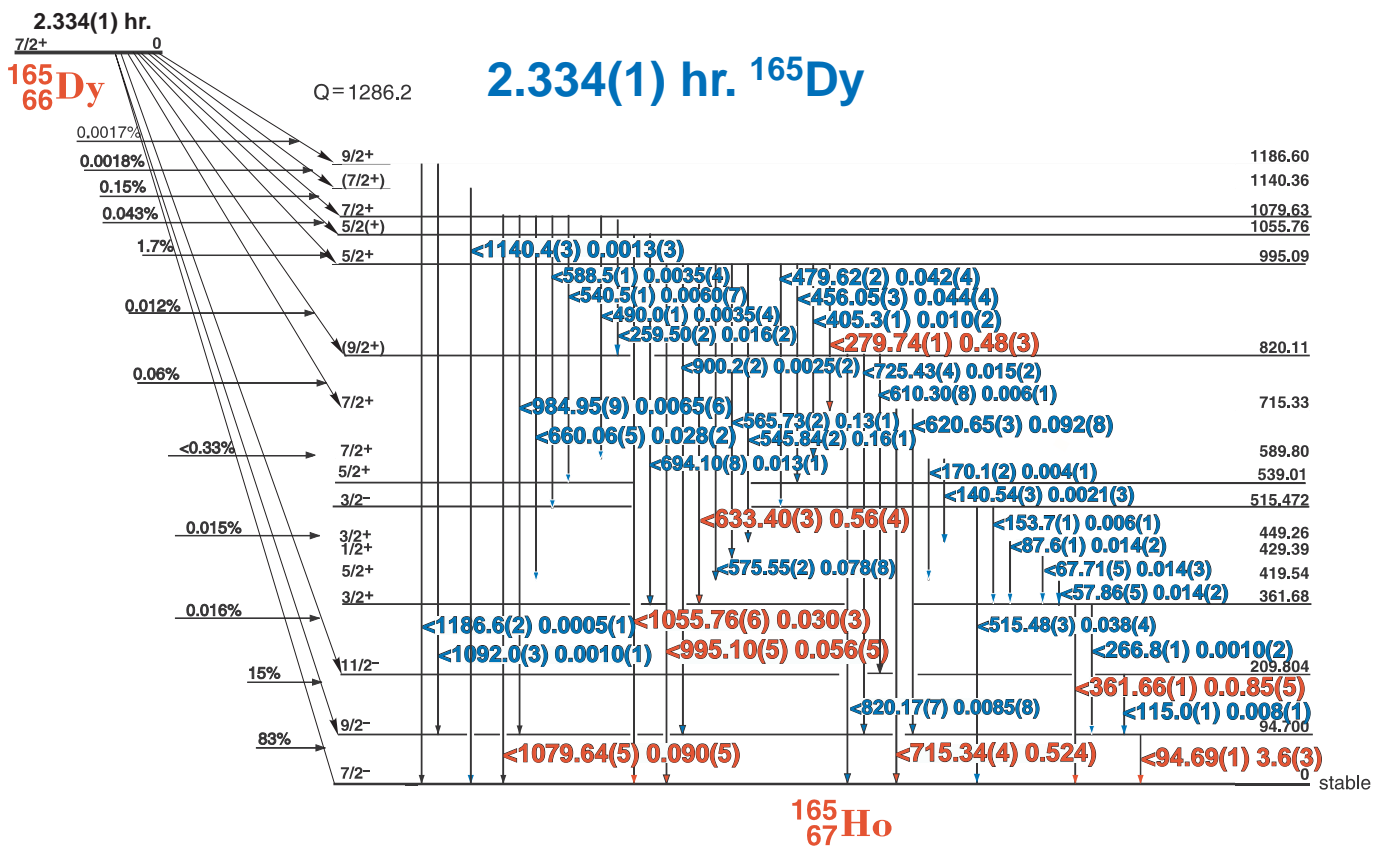
GAMMA-RAY ENERGIES AND INTENSITIES

Nuclide	^{165m}Dy	Half Life	1.257(6) min.		
Detector	3" x 3" -2 NaI	Method of Production:	$^{164}\text{Dy}(n,\gamma)$		
E_γ (KeV)[S]	ΔE_γ	I_γ (rel)	$I_\gamma(\%)$ [E]	ΔI_γ	S
Dy x-rays					
67.71	± 0.05		0.012	± 0.001	4
87.6	± 0.1		0.011	± 0.001	4
95.96	± 0.05		0.039	± 0.004	4
I.T.	108.160	± 0.003	3.01	± 0.09	1
119.5	± 0.1		0.0027	± 0.0004	4
153.80	± 0.02		0.24	± 0.02	3
251.73	± 0.05		0.018	± 0.002	4
361.66	± 0.01		0.53	± 0.04	2
515.48	± 0.03		1.5	± 0.1	1
676.0	± 0.8		0.0004	± 0.0002	4

2.334(1) hr. ^{165}Dy

66-165-1





GAMMA-RAY ENERGIES AND INTENSITIES

Nuclide ^{165}Dy
Detector 3" X 3" NaI-2

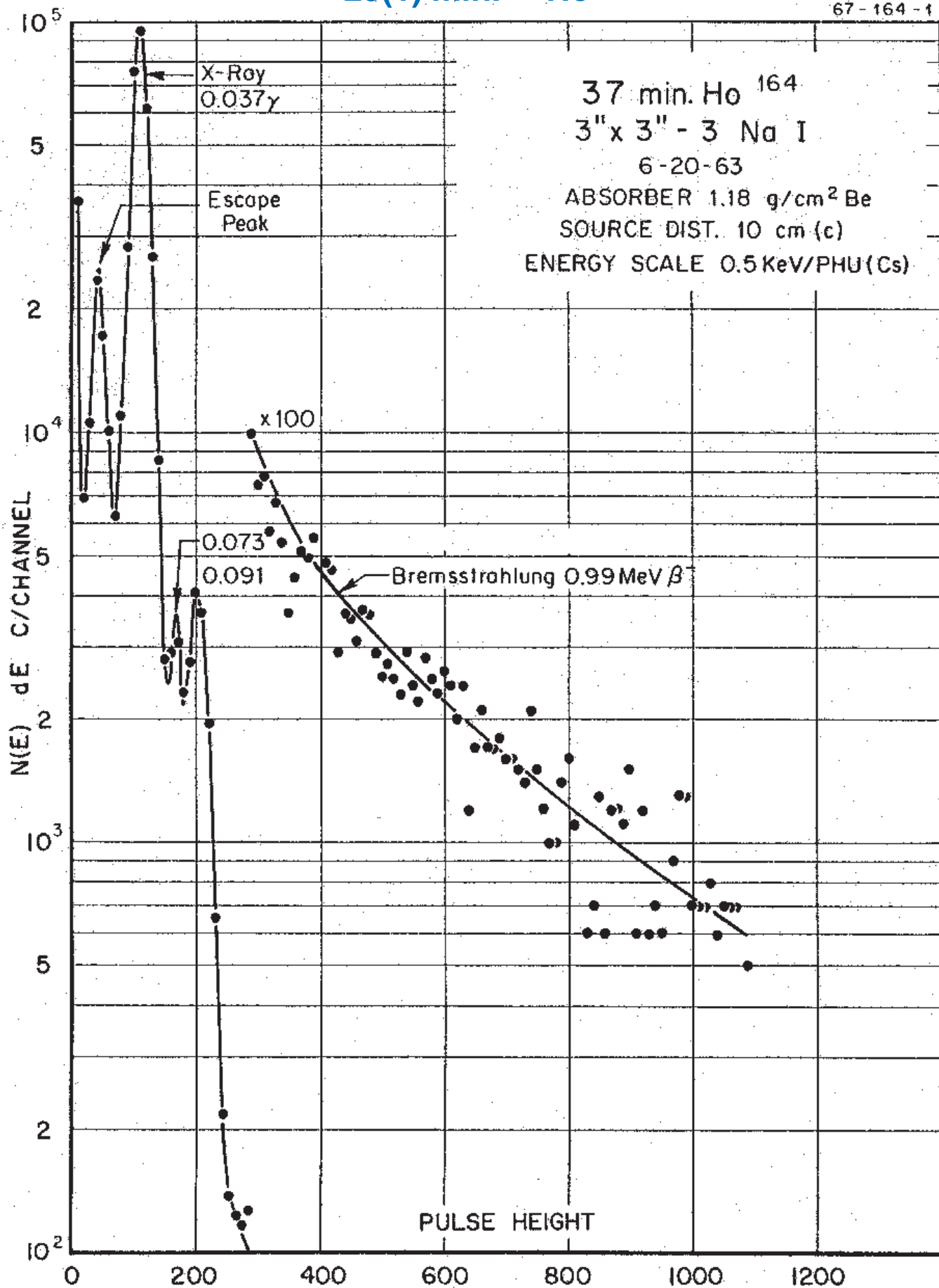
Half Life 2.334(1) hr.
Method of Production: $^{164}\text{Dy}(n,\gamma)$

E_{γ} (KeV)[S]	ΔE_{γ}	$I_{\gamma}(\text{rel})$	$I_{\gamma}(\%)[E]$	ΔI_{γ}	S
Ho x-rays					
57.86	± 0.05		0.014	± 0.002	1
87.76	± 0.05	1.21	0.014	± 0.002	5
94.69	± 0.015	100	3.6	± 0.3	1
115.0	± 0.10	0.63	0.008	± 0.001	4
119.5	± 0.10	0.52	0.007	± 0.001	4
140.52	± 0.03	1.4	0.0021	± 0.0003	4
153.7	± 0.08	0.56	0.006	± 0.001	4
170.1	± 0.10	0.34	0.004	± 0.001	4
259.498	± 0.025	0.52	0.016	± 0.002	4
266.8	± 0.2	0.09	0.0010	$\pm (2)$	4
279.736	± 0.012	15.2	0.48	± 0.03	1
361.662	± 0.015	26.2	0.85	± 0.05	1
405.37	± 0.1	0.49	0.010	± 0.002	4
456.054	± 0.032	1.51	0.044	± 0.004	3
479.619	± 0.020	1.40	0.041	± 0.004	3
490.0	± 0.1	0.07	0.0035	$\pm (4)$	4
515.484	± 0.035	1.45	0.038	± 0.004	3
540.51	± 0.10	0.41	0.0060	± 0.0007	4
545.840	± 0.025	5.05	0.16	± 0.01	2
565.729	± 0.025	3.97	0.13	± 0.01	2
575.549	± 0.025	2.48	0.078	± 0.008	2
588.50	± 0.15	0.175	0.0035	± 0.0004	4
610.30	± 0.08	0.219	0.006	± 0.001	4
620.649	± 0.030	2.89	0.092	± 0.008	2
633.40	± 0.030	17.4	0.56	± 0.04	1

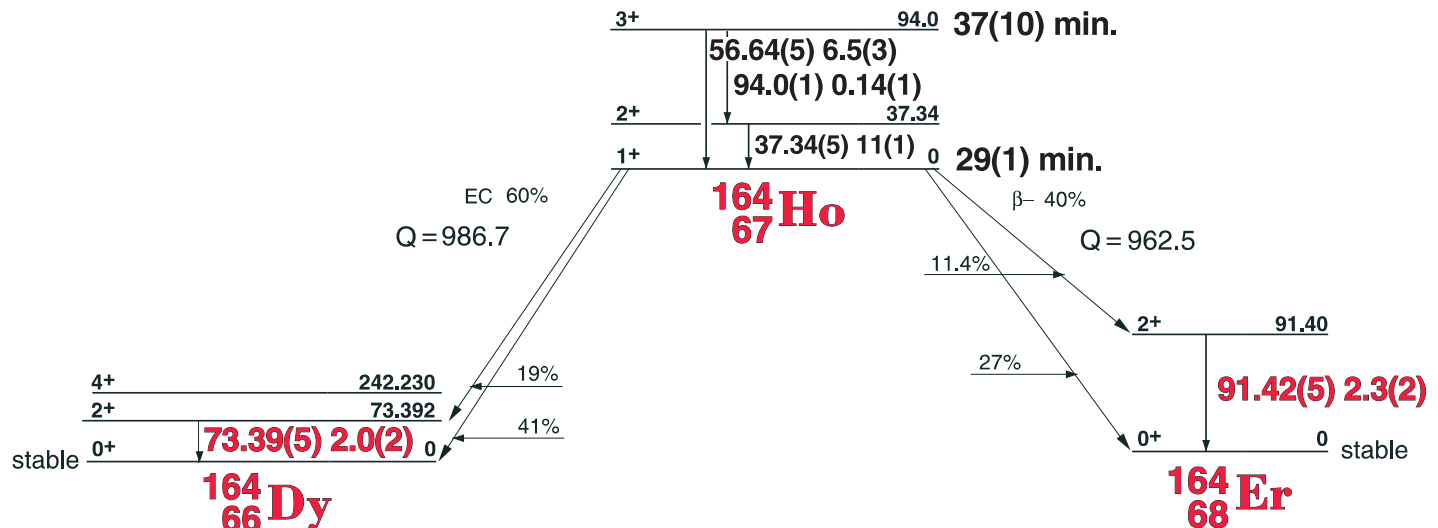
E_{γ} (KeV)[S]	ΔE_{γ}	$I_{\gamma}(\text{rel})$	$I_{\gamma}(\%)[E]$	ΔI_{γ}	S
660.06	± 0.05	0.88	0.028	± 0.002	3
694.10	± 0.08	0.40	0.013	± 0.001	3
715.337	± 0.040	16.3	0.52	± 0.04	1
725.431	± 0.040	0.48	0.015	± 0.002	3
820.17	± 0.07	0.26	0.0085	± 0.0008	4
900.20	± 0.15	0.16	0.0025	± 0.0002	4
984.95	± 0.09	0.18	0.0065	± 0.0006	3
995.10	± 0.05	1.71	0.056	± 0.005	1
1055.76	± 0.06	0.93	0.030	± 0.003	1
1079.64	± 0.05	2.76	0.090	± 0.005	1
1092.0	± 0.3	0.037	0.0010	± 0.0001	4
1140.4	± 0.3	0.044	0.0013	± 0.0003	4
1186.6	± 0.2	0.014	0.0005	± 0.0001	4

29(1) min. ^{164}Ho

67-164-1



29(1) min. ^{164}Ho



GAMMA-RAY ENERGIES AND INTENSITIES

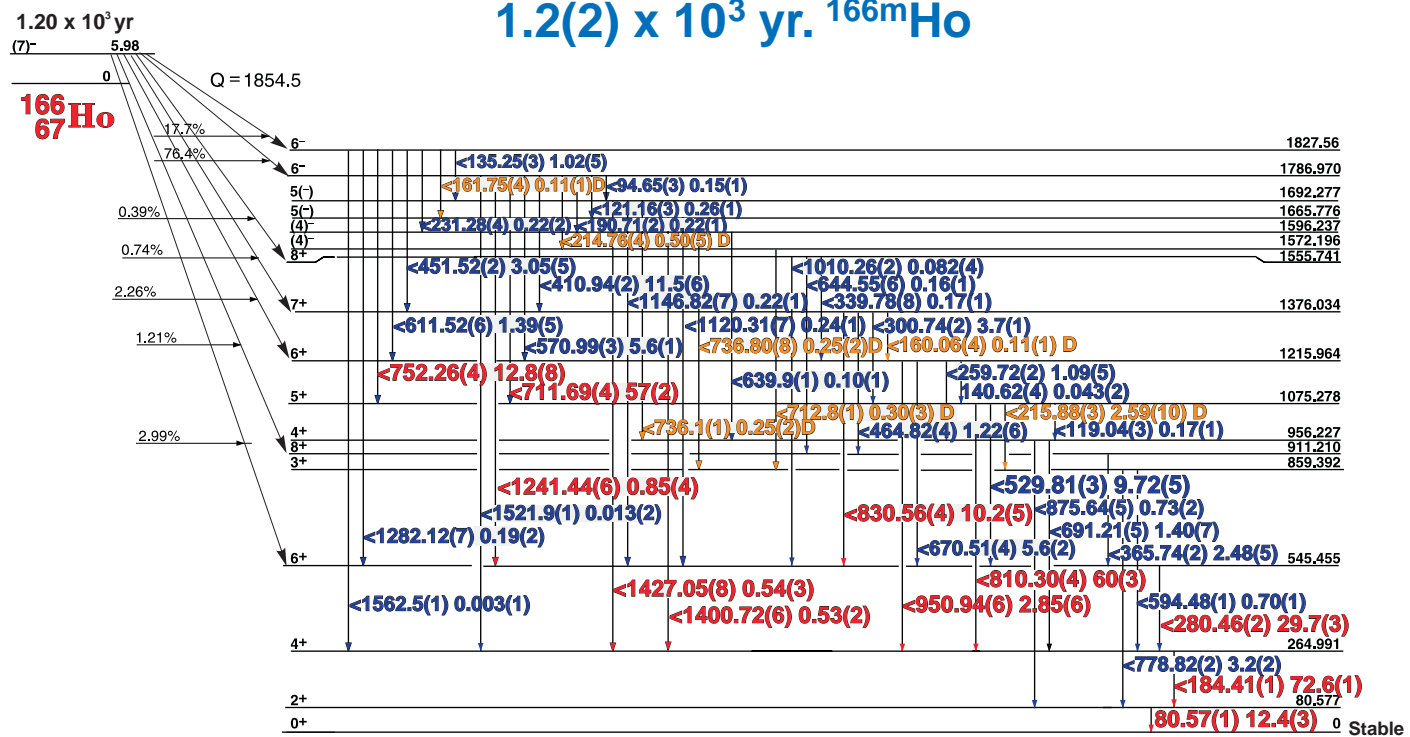
Nuclide
Detector

^{164}Ho
3" x 3" -2 NaI

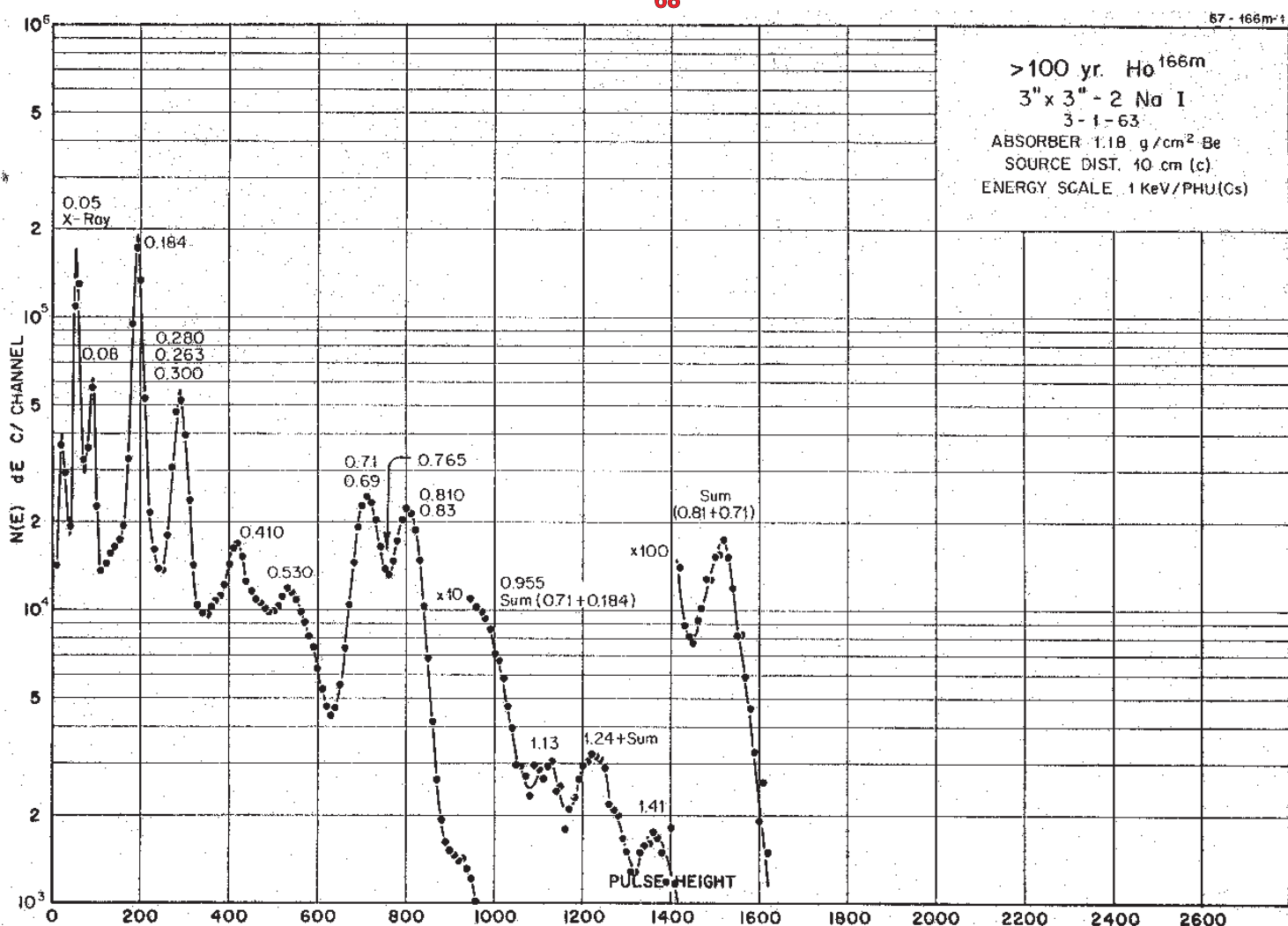
Half Life 29(1) min.
Method of Production: $^{165}\text{Ho}(\gamma, n)$

E_γ (KeV)[S]	ΔE_γ	I_γ (rel)	I_γ (%)[E]	ΔI_γ	S
Er K x-ray					
73.39	± 0.05	2.0	2.0	± 0.2	1
91.42	± 0.05	2.3	2.3	± 0.2	1

1.2(2) x 10³ yr. ^{166m}Ho



¹⁶⁶Er



1.2(2) x 10³ yr. ^{166m}Ho

GAMMA-RAY ENERGIES AND INTENSITIES

Nuclide
Detector

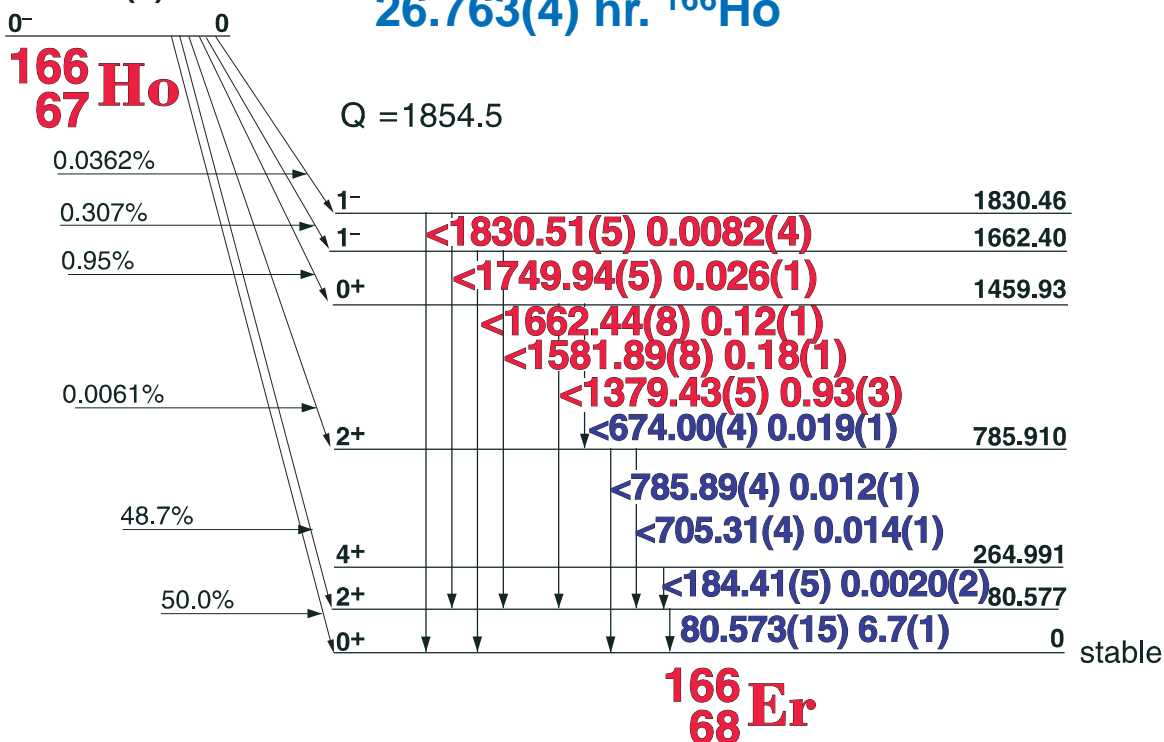
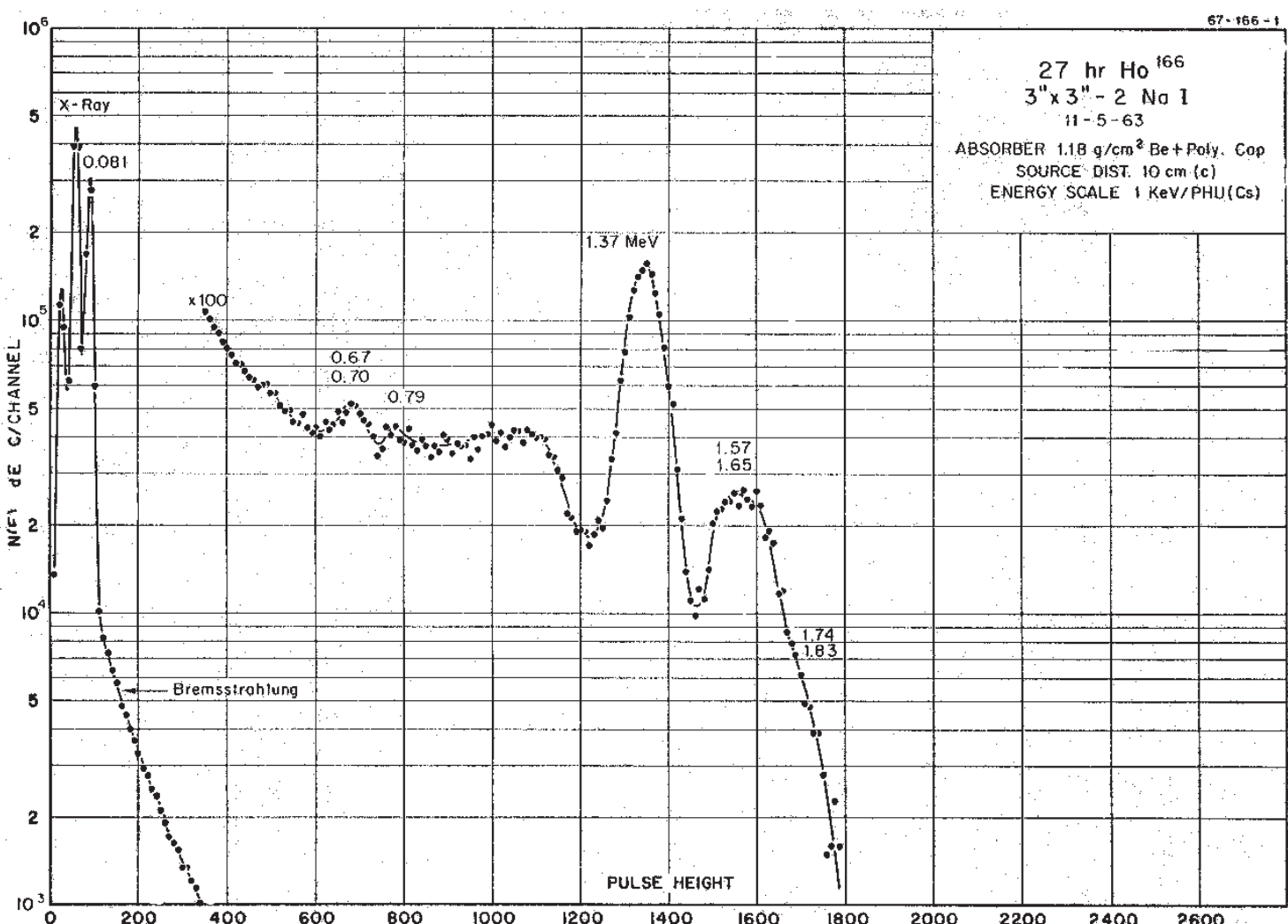
^{166m}Ho
3" x 3" -2 NaI

Half Life 1.2(2) x 10³ yr.
Method of Production: ¹⁶⁵Ho(n,γ)

E _γ (KeV)[S]	ΔE _γ	I _γ (rel)	I _γ (%)[E]	ΔI _γ	S
Er x-rays					
80.573	± 0.015	17.1	12.4	± 0.3	1
94.653	± 0.030	0.19	0.15	± 0.1	4
119.038	± 0.030	0.24	0.17	± 0.01	4
121.161	± 0.030	0.36	0.26	± 0.01	4
135.238	± 0.035	0.14	1.02	± 0.05	4
140.618	± 0.040	0.059	0.043	± 0.002	4
160.064	± 0.045	0.18	0.11	± 0.01	4
161.748	± 0.045	0.15	0.11	± 0.01	4
184.407	± 0.015	100	72.6	± 0.1	1
190.771	± 0.025	0.30	0.22	± 0.01	4
214.763	± 0.045	0.75	0.50	± 0.05	4
215.875	± 0.030	3.55	2.59	± 0.10	3
231.282	± 0.040	0.33	0.22	± 0.02	4
259.716	± 0.020	1.5	1.09	± 0.05	3
280.456	± 0.020	40.7	29.7	± 0.3	1
300.744	± 0.020	5.1	3.7	± 0.1	2
339.78	± 0.08	0.23	0.17	± 0.01	4
365.739	± 0.025	3.4	2.48	± 0.05	3
410.941	± 0.025	15.8	11.5	± 0.6	2
451.524	± 0.025	4.2	3.05	± 0.05	3
464.825	± 0.040	1.7	1.22	± 0.06	4
529.813	± 0.030	13.9	9.72	± 0.05	3
570.998	± 0.030	7.85	5.6	± 0.1	3
594.48	± 0.08	0.96	0.70	± 0.01	4

E _γ (KeV)[S]	ΔE _γ	I _γ (rel)	I _γ (%)[E]	ΔI _γ	S
611.522	± 0.065	1.89	1.39	± 0.05	4
639.770	± 0.060	0.22	0.10	± 0.01	4
644.55	± 0.10	0.24	0.16	± 0.02	4
670.509	± 0.040	7.88	5.6	± 0.2	2
691.211	± 0.50	2.09	1.40	± 0.07	3
711.693	± 0.040	80.2	56	± 1.0	1
736.1	± 0.1		0.25	± 0.03	4
736.8	± 0.1	0.14	0.25	± 0.02	3
752.265	± 0.040	17.9	12.8	± 0.8	1
778.817	± 0.040	4.5	3.2	± 0.2	2
810.309	± 0.040	85.6	59.0	± 0.8	1
830.560	± 0.040	14.5	10.2	± 0.5	1
875.64	± 0.05	1.08	0.73	± 0.02	2
950.94	± 0.06	4.15	2.85	± 0.06	1
1010.25	± 0.10	0.12	0.082	± 0.04	4
1120.31	± 0.07	0.31	0.24	± 0.01	3
1146.82	± 0.07	0.30	0.22	± 0.01	3
1241.44	± 0.06	1.37	0.85	± 0.04	1
1282.12	± 0.07	0.31	0.19	± 0.02	3
1400.72	+ 0.08	0.75	0.53	± 0.02	1
1427.05	± 0.08	0.80	0.54	± 0.03	1

26.763(4) hr.

26.763(4) hr. ^{166}Ho  ^{166}Er 

26.763(4) hr. ^{166}Ho

GAMMA-RAY ENERGIES AND INTENSITIES

Nuclide ^{166}Ho

Detector 3" x 3" -2 Nal

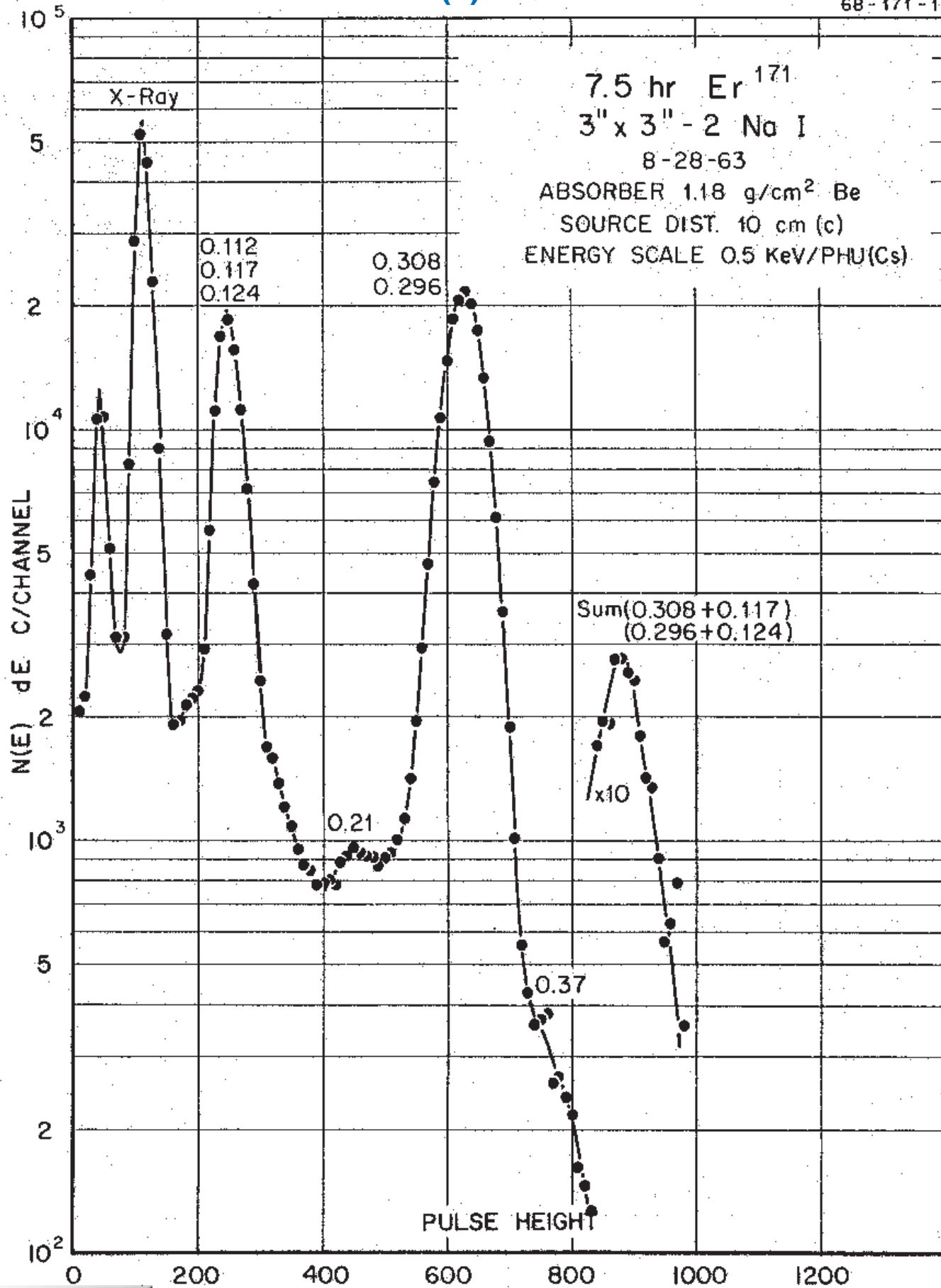
Half Life 26.763(4) hr.

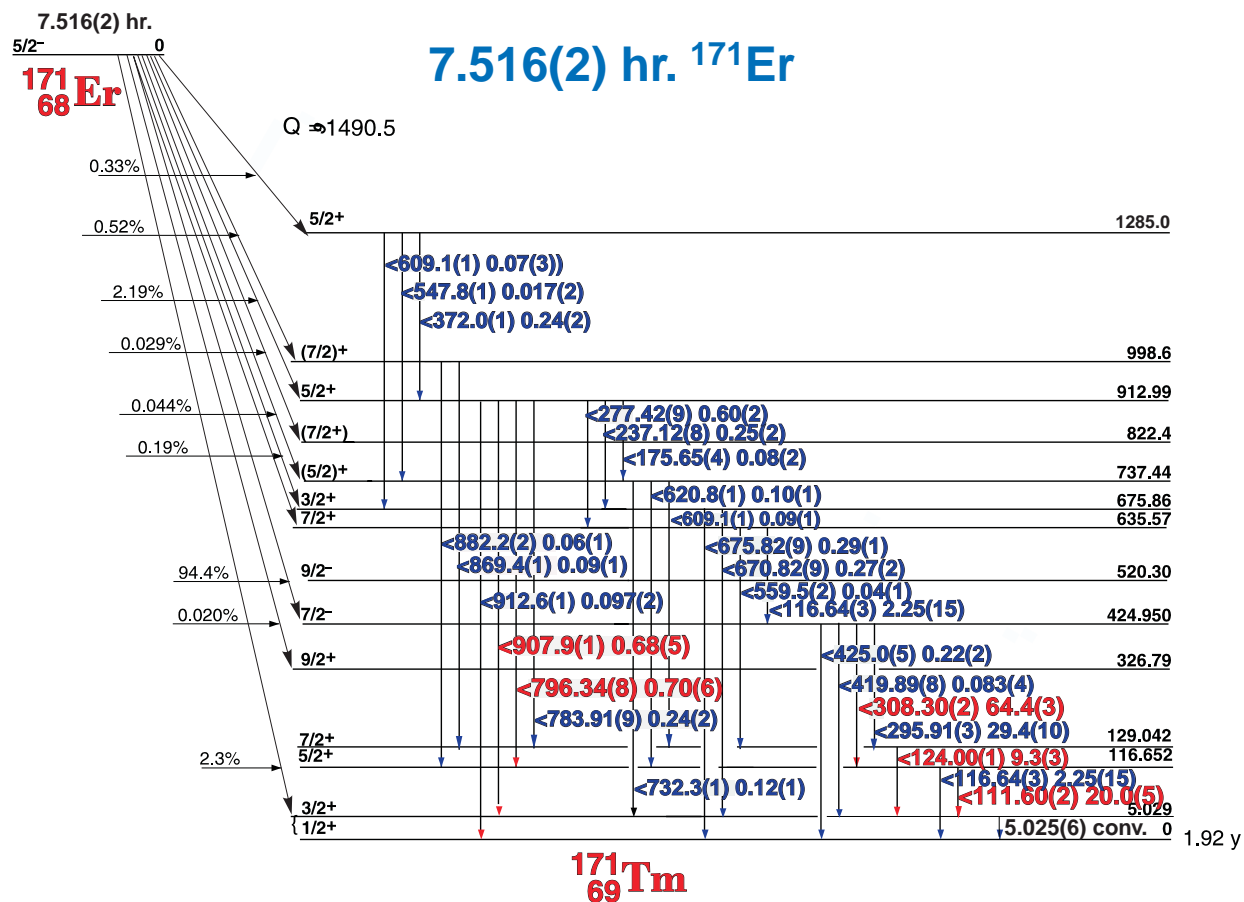
Method of Production: $^{165}\text{Ho}(n,\gamma)$

E_γ (KeV)[S]	ΔE_γ	I_γ (rel)	$I_\gamma(\%)$ [E]	ΔI_γ	S
Er x-ray	s				
80.573	± 0.015		6.7	± 0.1	2
184.41	± 0.05	0.215	0.0020	± 0.0002	4
674.00	± 0.04	2.1	0.019	± 0.001	3
705.31	± 0.04	1.61	0.014	± 0.001	3
785.89	± 0.04	1.4	0.012	± 0.001	3
1379.43	± 0.06	100	0.93	± 0.03	1
1581.89	± 0.08	19.5	0.18	± 0.01	1
1662.44	± 0.08	12.5	0.12	± 0.01	1
1749.94	± 0.10	2.68	0.026	± 0.001	1
1830.54	± 0.10	0.86	0.0082	± 0.0004	1

7.516(2) hr. ^{171}Er

68-171-1

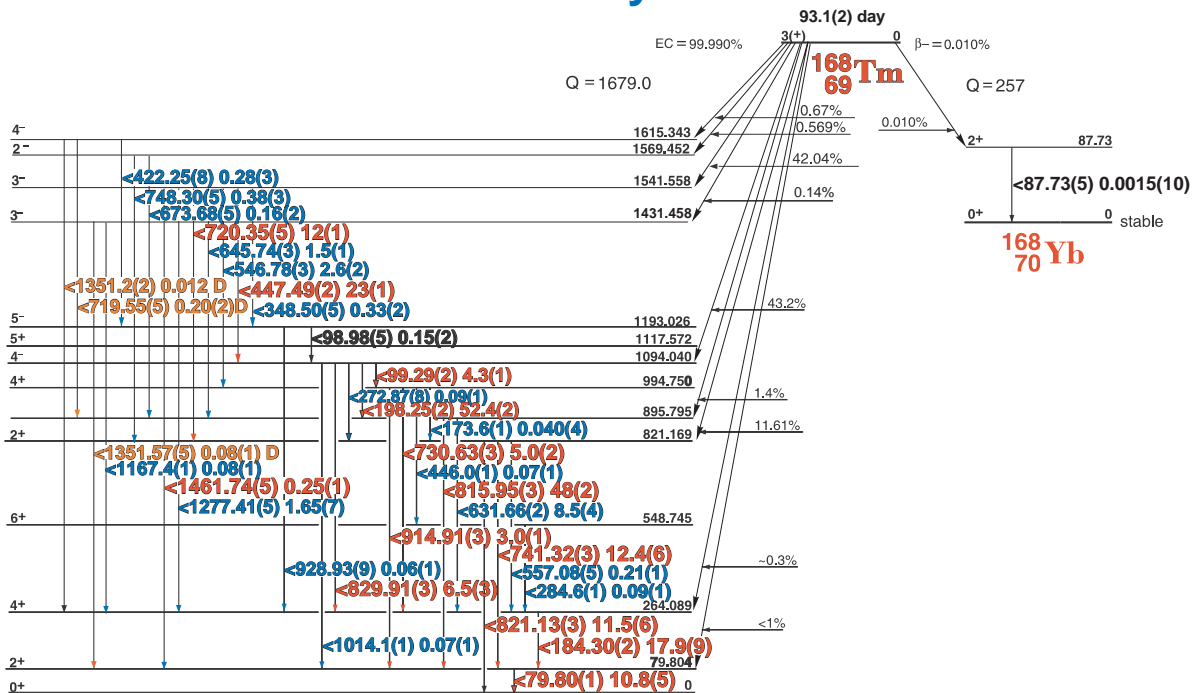




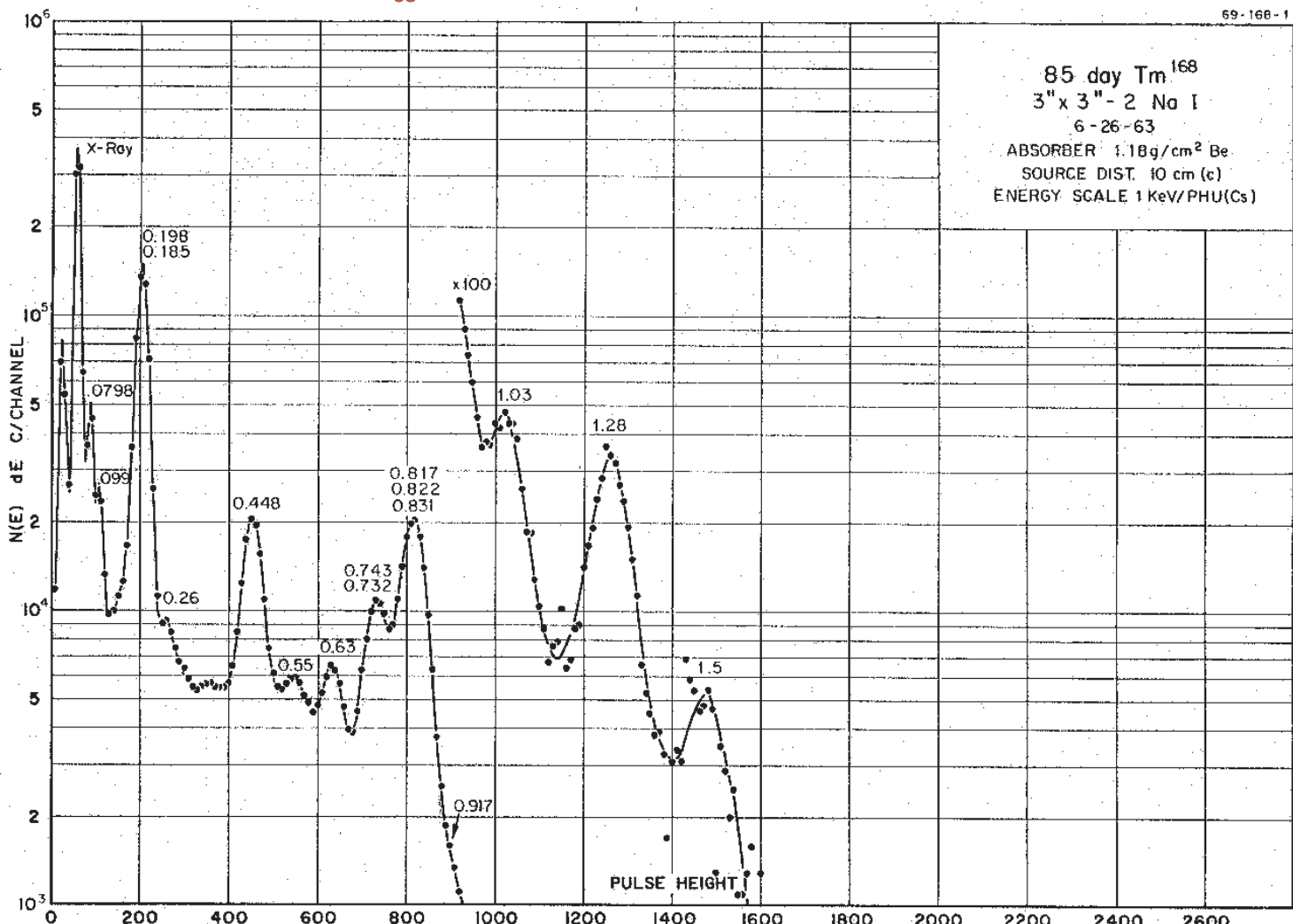
GAMMA-RAY ENERGIES AND INTENSITIES

Nuclide Detector	¹³⁷ Cs 3" x 3" NaI	Method of Production: ¹⁷⁰ Er(n, γ)	Half Life 30.07 Yr.		
E _{γ} (KeV)[S]	ΔE_{γ}	I _{γ} (rel)	I _{γ} (%)[E]	ΔI_{γ}	S
Tm x-rays					
111.598	± 0.020	30.44	20.0	± 0.5	1
116.640	± 0.035	3.55	2.25	± 0.15	3
124.00	± 0.015	14.39	9.3	± 0.3	1
175.65	± 0.04	0.09	0.08	± 0.02	4
210.52	± 0.04	1.12	0.72	± 0.06	3
237.12	± 0.08	0.56	0.25	± 0.02	3
277.42	± 0.09	0.99	0.60	± 0.02	3
295.91	± 0.03	45.7	29.4	± 1.0	1
308.303	± 0.018	100	64.4	± 0.3	1
372.04	± 0.10	0.37	0.24	± 0.02	3
419.89	± 0.08	0.51	0.083	± 0.004	3
425.0	± 0.2	0.06	0.22	± 0.02	4
609.1	± 0.15	0.13	0.09	± 0.01	4
620.8	± 0.1	0.15	0.10	± 0.01	4
670.82	± 0.09	0.42	0.27	± 0.02	3
675.82	± 0.09	0.47	0.29	± 0.01	3
732.30	± 0.10	0.18	0.12	± 0.01	3
783.91	± 0.09	0.37	0.24	± 0.02	2
796.344	± 0.08	1.09	0.70	± 0.06	1
869.44	± 0.12	0.14	0.09	± 0.01	3
882.2	± 0.2	0.08	0.06	± 0.01	4
907.95	± 0.10	1.06	0.68	± 0.05	1

93.1 day ^{168}Tm



^{168}Er



93.1(2) day ^{168}Tm

GAMMA-RAY ENERGIES AND INTENSITIES

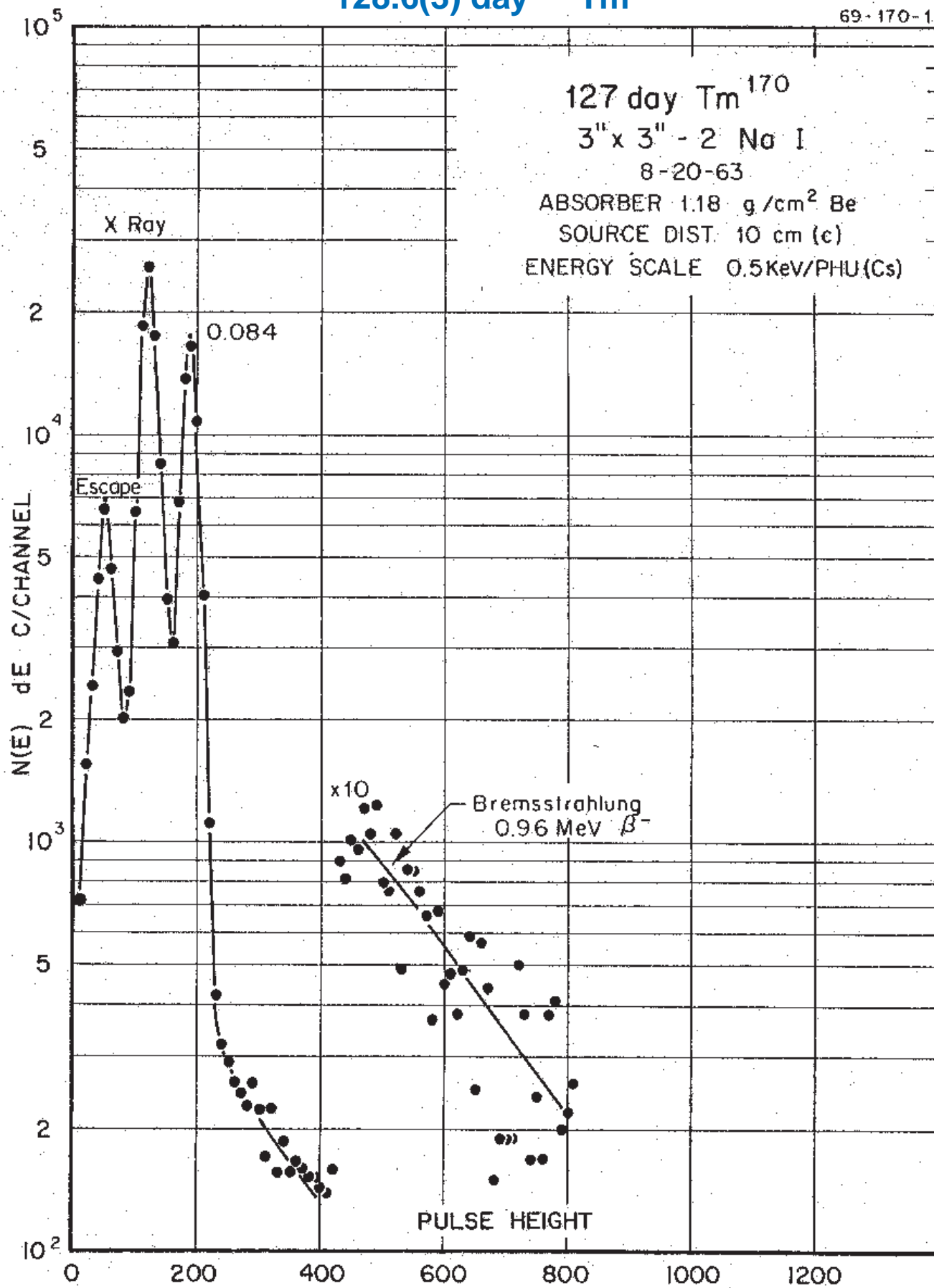
Nuclide ^{168}Tm
 Detector 3" x 3" NaI

Half Life 93.1(2) day
 Method of Production: $^{169}\text{Tm}(\gamma, n)$

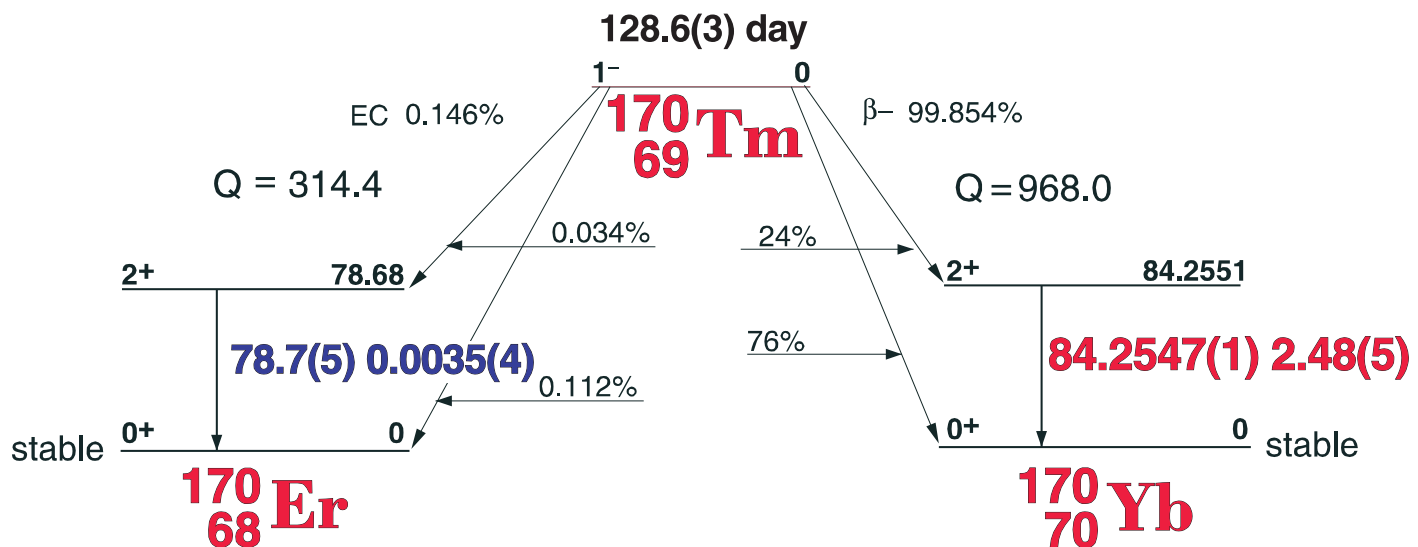
E_{γ} (KeV)[S]	ΔE_{γ}	I_{γ} (rel)	$I_{\gamma}(\%)[E]$	ΔI_{γ}	S
79.80	± 0.01	22.0	10.8	± 0.5	1
98.98	± 0.05	0.15	± 0.02	4	
99.29	± 0.02	8.7	4.3	± 0.1	1
173.6	± 0.1	0.18	0.040	± 0.004	4
184.30	± 0.02	33.0	17.9	± 0.9	1
198.25	± 0.02	-100	52.4	± 0.2	1
272.87	± 0.08	0.19	0.09	± 0.01	4
284.6	± 0.1	0.18	0.09	± 0.01	4
348.50	± 0.05	0.62	0.33	± 0.02	4
422.25	± 0.08	0.54	0.28	± 0.03	4
447.49	± 0.02	44.0	23	± 1.0	1
546.78	± 0.03	4.8	2.6	± 0.2	4
557.08	± 0.05	0.39	0.21	± 0.01	4
631.66	± 0.02	16.0	8.5	± 0.4	2
645.74	± 0.03	2.8	1.5	± 0.01	3
673.68	± 0.05	0.26	0.16	± 0.02	4
720.35	± 0.03	22.0	12	± 0.8	1
730.63	± 0.03	9.0	5.0	± 0.1	1
741.32	± 0.03	23.0	12.4	± 0.6	1
748.30	± 0.05	0.67	0.38	± 0.03	3
815.95	± 0.03	93.0	48	± 1.5	1
821.13	± 0.03	22.0	11.5	± 0.6	1
829.91	± 0.03	12.0	6.5	± 0.3	1
914.91	± 0.03	5.8	3.0	± 0.1	1
928.93	± 0.09	0.11	0.06	± 0.01	4
1014.1	± 0.1	0.13	0.07	± 0.01	3
1167.4	± 0.1	0.14	0.08	± 0.01	4
1277.41	± 0.05	3.2	1.65	± 0.07	1
D1351.2	± 0.1	0.03	0.012	± 0.001	4
D1351.57	± 0.05	0.16	0.08	± 0.01	2

128.6(3) day ^{170}Tm

69-170-1



128.6(3) day ^{170}Tm

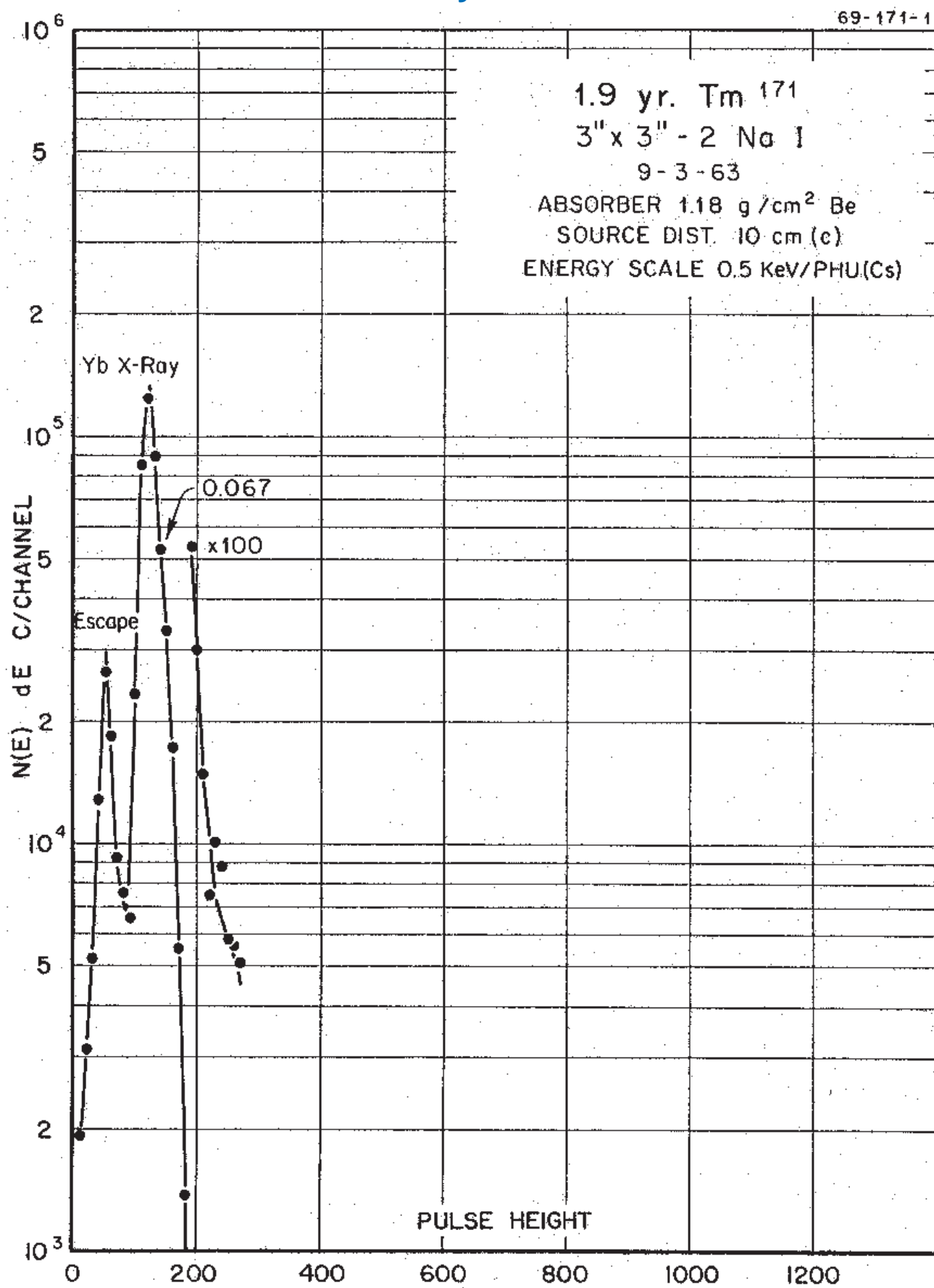


GAMMA-RAY ENERGIES AND INTENSITIES

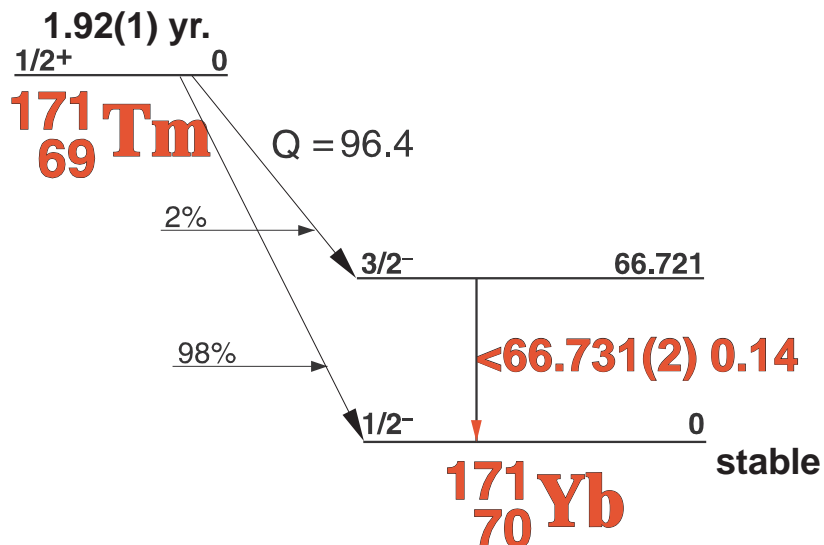
Nuclide ^{170}Tm Half Life 30.07 Yr.
 Detector 3" x 3" NaI Method of Production: $^{169}\text{Tm}(n,\gamma)$

E_γ (KeV)	ΔE_γ	I_γ (rel)	I_γ (%)	ΔI_γ	S
Yb K x-rays					
78.7	± 0.5	1	0.0035	$\pm 0.(4)$	4
84.2547	$\pm 0.(1)$	100	2.48	± 0.05	1

1.92 yr. ^{171}Tm



1.92(1) yr. ^{171}Tm



GAMMA-RAY ENERGIES AND INTENSITIES

Nuclide ^{171}Tm Half Life 1.92(1) yr.
Detector 3" x 3" NaI Method of Production: $^{169}\text{Tm}(n,\gamma,n,\gamma)$

E_γ (KeV)[S]	ΔE_γ	I_γ (rel)	$I_\gamma(\%)$ [E]	ΔI_γ	S
66.731	± 0.002		0.14		2

32.026 day ^{169}Yb

70-169-1

32 day Yb^{169}

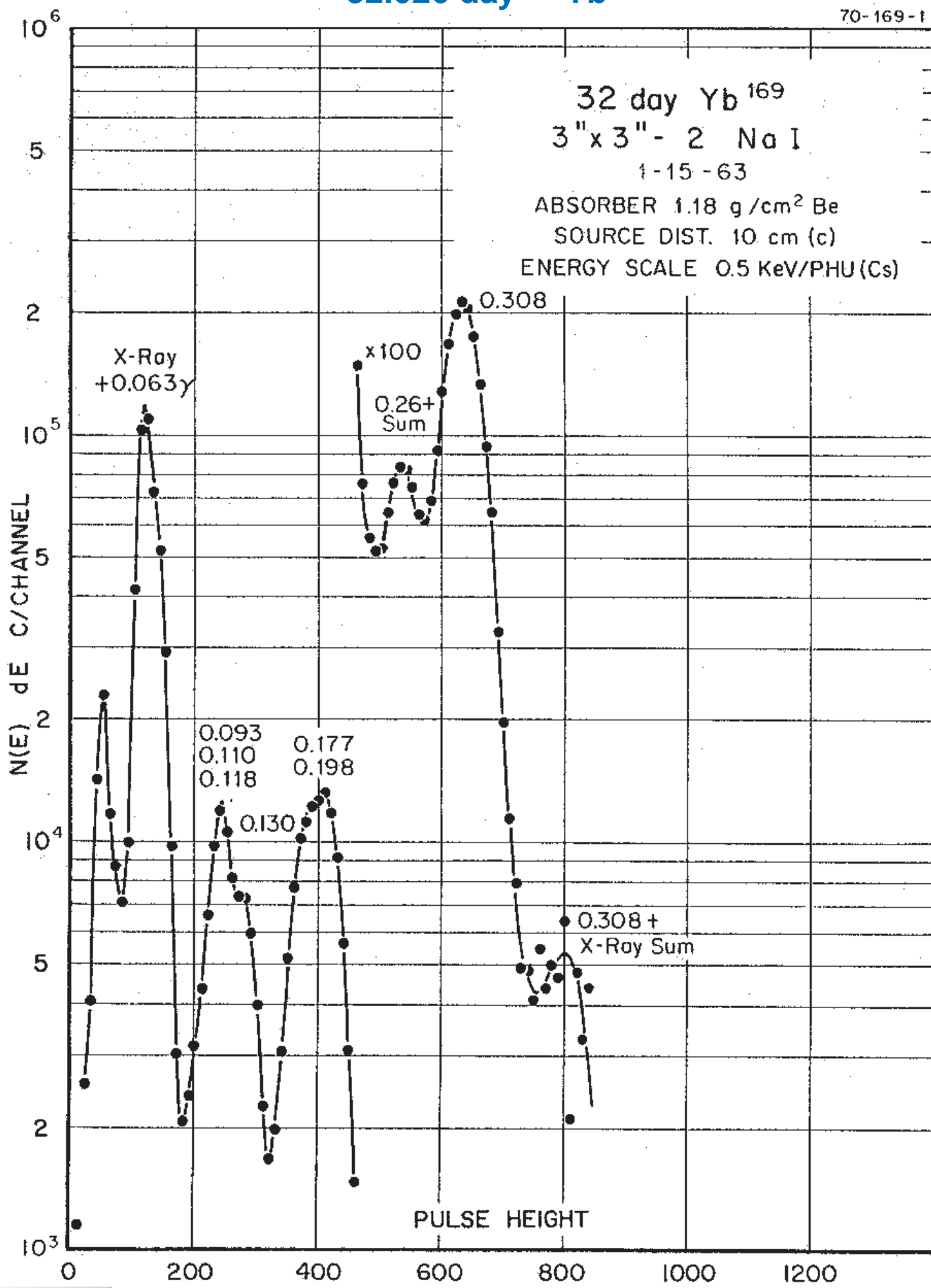
3" x 3" - 2 Na I

1-15-63

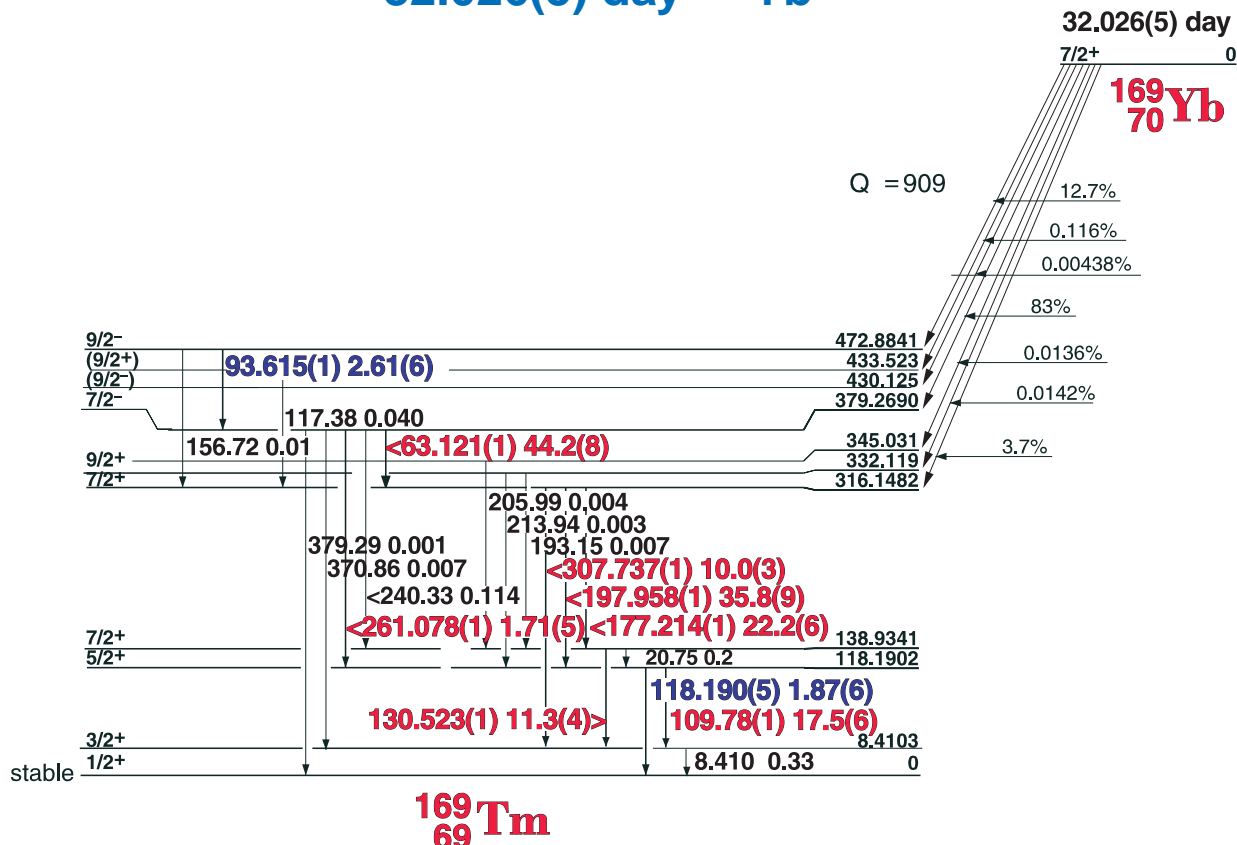
ABSORBER 1.18 g/cm² Be

SOURCE DIST. 10 cm (c)

ENERGY SCALE 0.5 KeV/PHU (Cs)



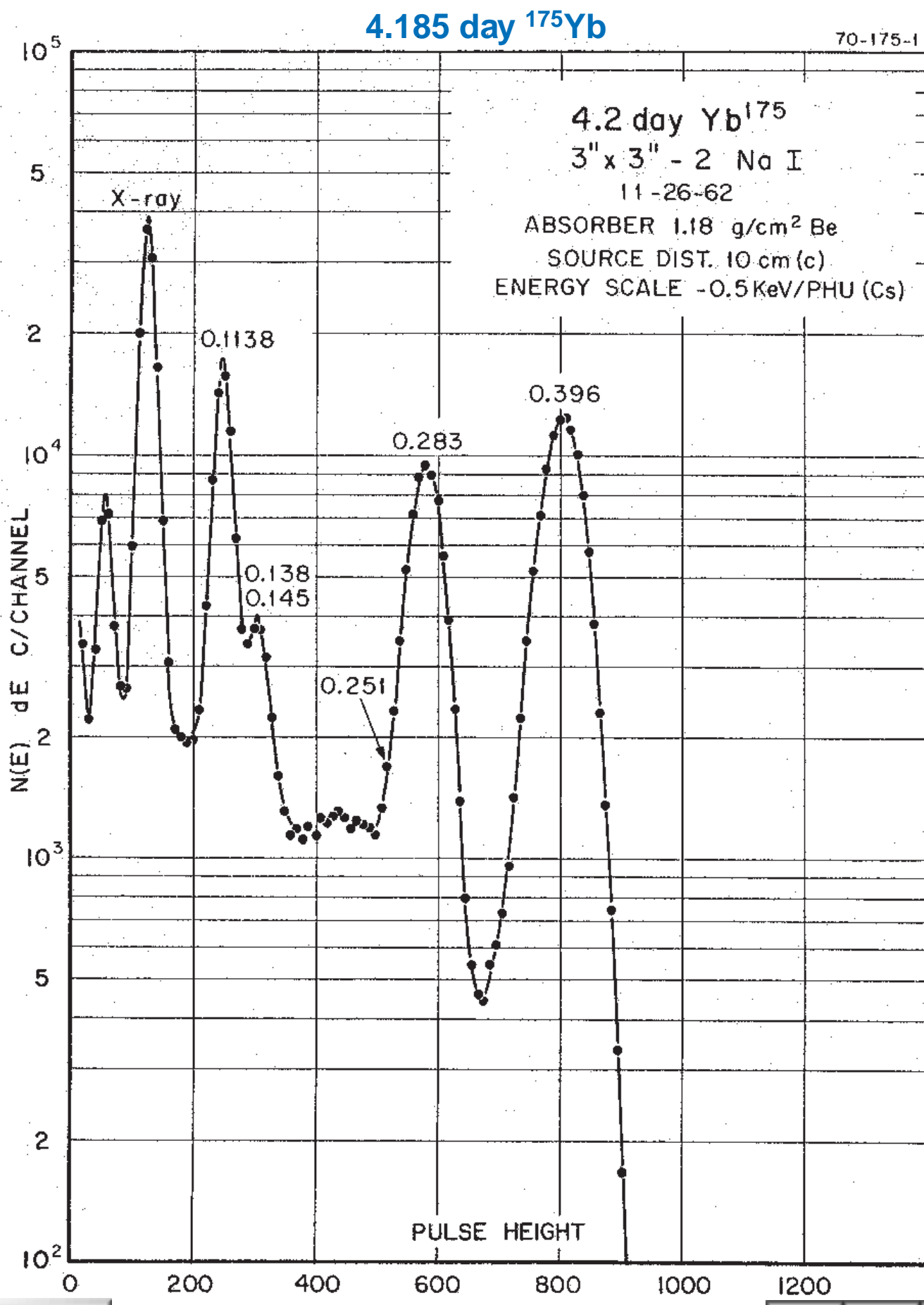
32.026(5) day ^{169}Yb



GAMMA-RAY ENERGIES AND INTENSITIES

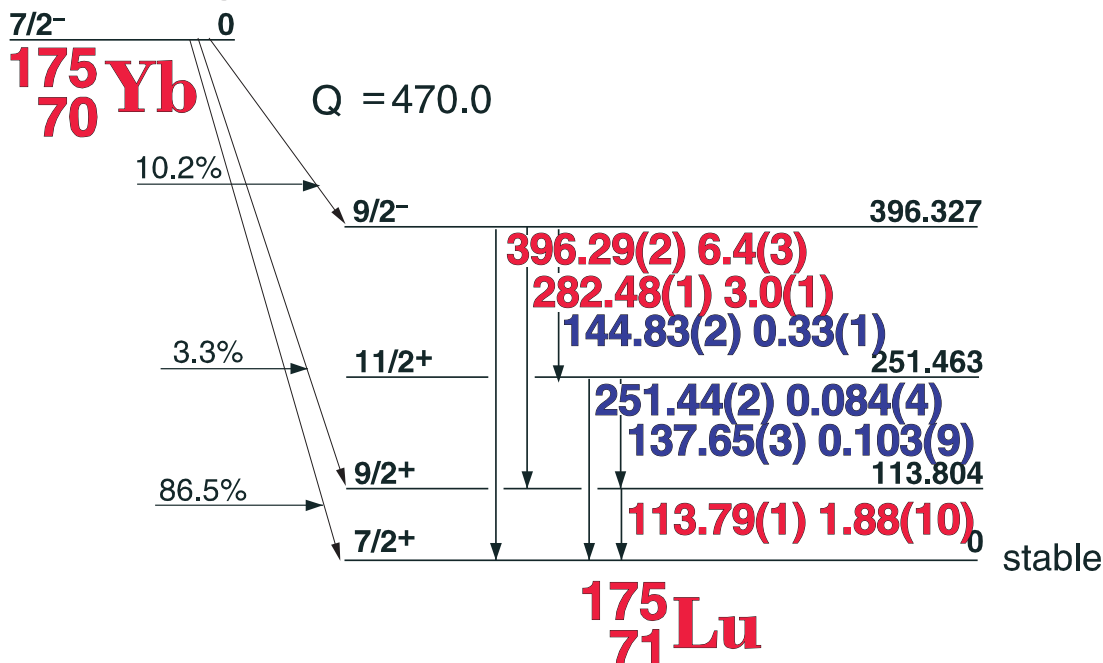
Nuclide ^{169}Yb Half Life 32.026(5) day
Detector 3" x 3" NaI Method of Production: $^{168}\text{Yb}(n,\gamma)$

E_γ (KeV)[S]	ΔE_γ	I_γ (rel)	I_γ (%) [E]	ΔI_γ	S
63.121	± 0.001	164	44.2	± 0.8	1
93.615	± 0.001	6.77	2.61	± 0.06	3
109.779	± 0.001	46.4	17.5	± 0.6	1
118.190	± 0.001	5.46	1.87	± 0.06	3
130.523	± 0.001	31.2	11.3	± 0.4	1
177.214	± 0.001	61.5	22.2	± 0.6	1
197.958	± 0.001	100	35.8	± 0.9	1
240.33	± 0.05	w	0.114	± 0.06	4
261.078	± 0.001	4.93	1.71	± 0.05	1
307.737	± 0.025	29.8	10.0	± 0.3	1
370.86	± 0.05		0.007	± 0.001	5



4.185(1) day ^{175}Yb

4.185(1) day



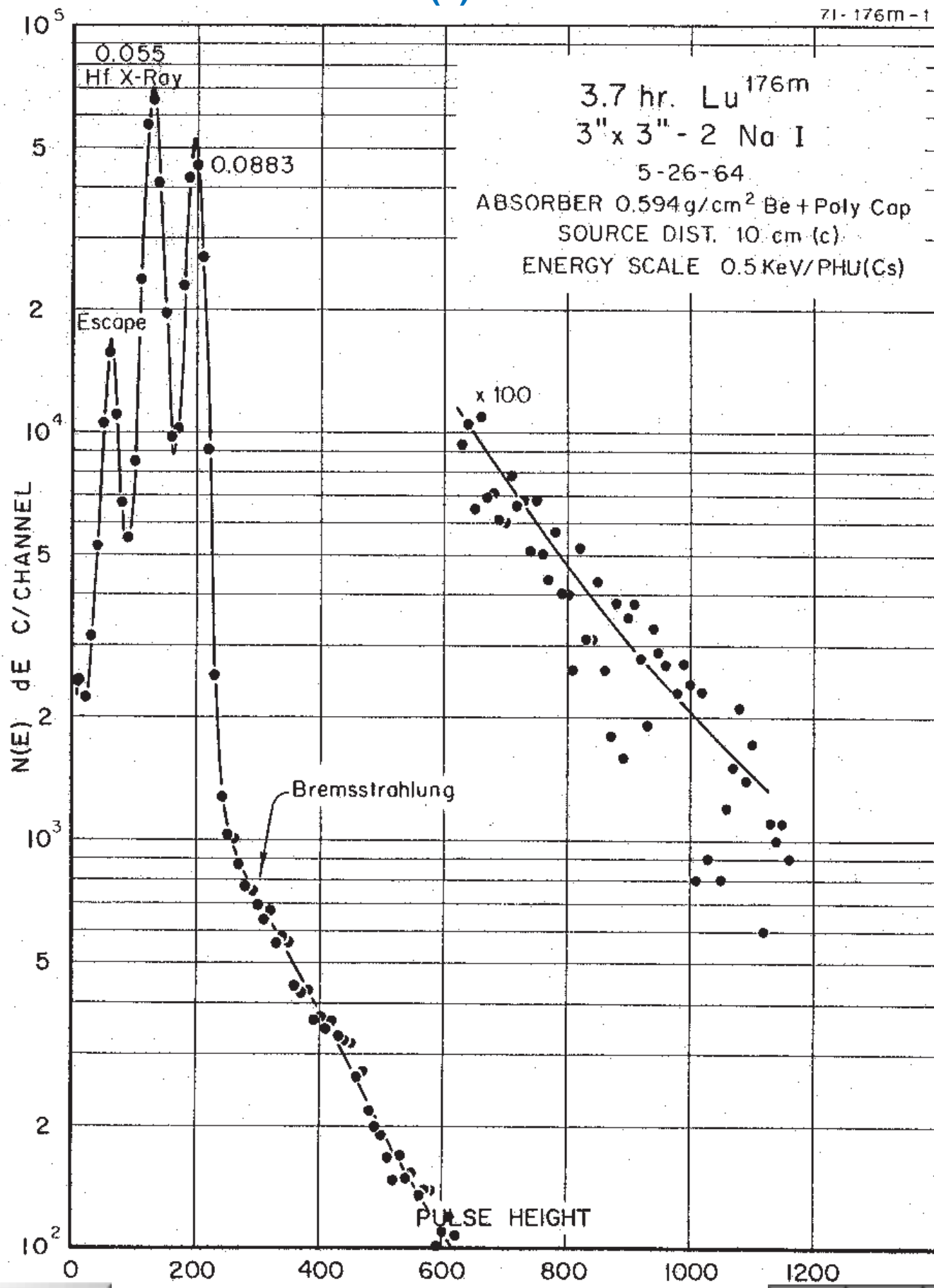
GAMMA-RAY ENERGIES AND INTENSITIES

Nuclide ^{175}Yb Half Life 4.185(1) day
Detector 3" x 3" NaI Method of Production: $^{174}\text{Yb}(n,\gamma)$

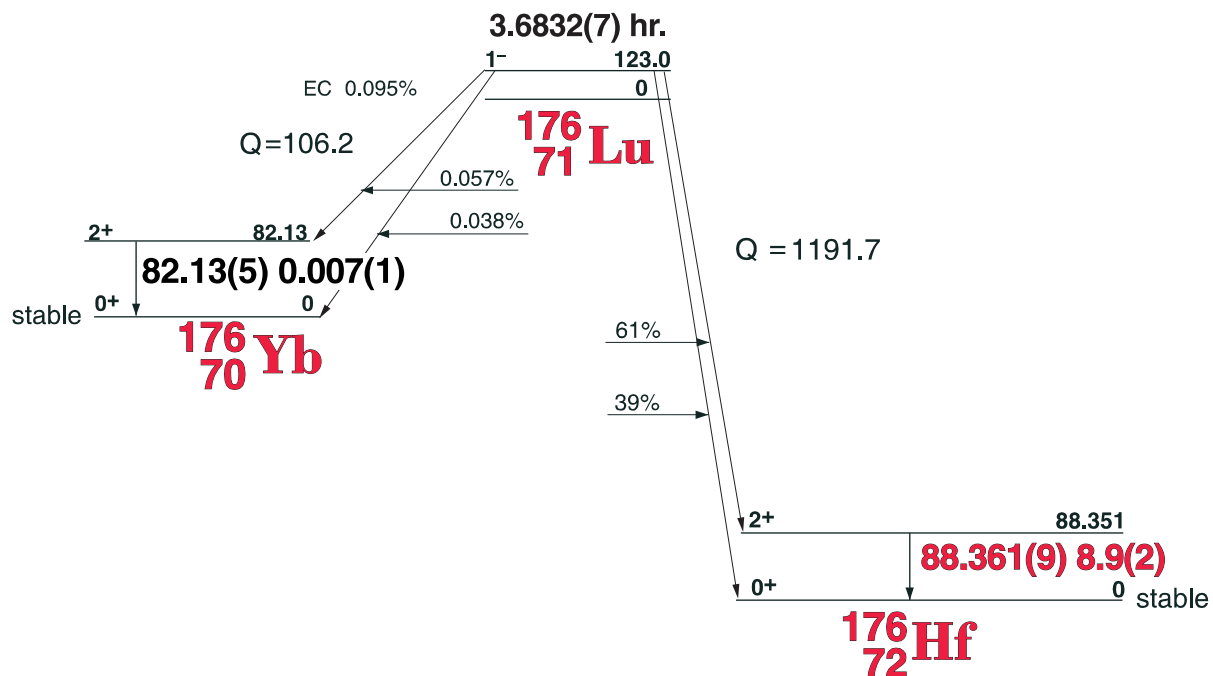
E_{γ} (KeV)[S]	ΔE_{γ}	$I_{\gamma}(\text{rel})$	$I_{\gamma}(\%)[E]$	ΔI_{γ}	S
113.786	± 0.010	25.0	1.88	± 0.10	1
137.65	± 0.03	2.1	0.103	± 0.009	3
144.827	± 0.020	5.1	0.33	± 0.01	2
251.439	± 0.020	1.7	0.084	± 0.004	3
282.484	± 0.015	47.0	3.0	± 0.1	1
396.286	± 0.020	100	6.4	± 0.3	1

3.6832(2) hr. ^{176m}Lu

ZI-176m-1



3.6832(7) hr. ^{176m}Lu



GAMMA-RAY ENERGIES AND INTENSITIES

Nuclide ^{176m}Lu Half Life 3.6832(7) hr.
Detector 3" x 3" NaI Method of Production: $^{175}\text{Lu}(\text{n},\gamma)$

E_{γ} (KeV)[S]	ΔE_{γ}	I_{γ} (rel)	$I_{\gamma}(\%)$ [E]	ΔI_{γ}	S
Hf L x-ray					1
Hf K x-ray					1
82.13	± 0.05		0.007	± 0.001	4
88.361	± 0.009		8.9	± 0.2	1

6.734 day ^{177}Lu

71-177-1

6.8 day Lu^{177}

3"X3" NaI

7-19-56

ABSORBER $\sim 750 \text{ mg/cm}^2$

SOURCE DIST. - 10cm

ENERGY SCALE $\approx .5 \text{ KeV/PHU}$

0.057 Hf Kx-ray

.071 Mev γ

0.115 Mev γ

0.208 Mev γ

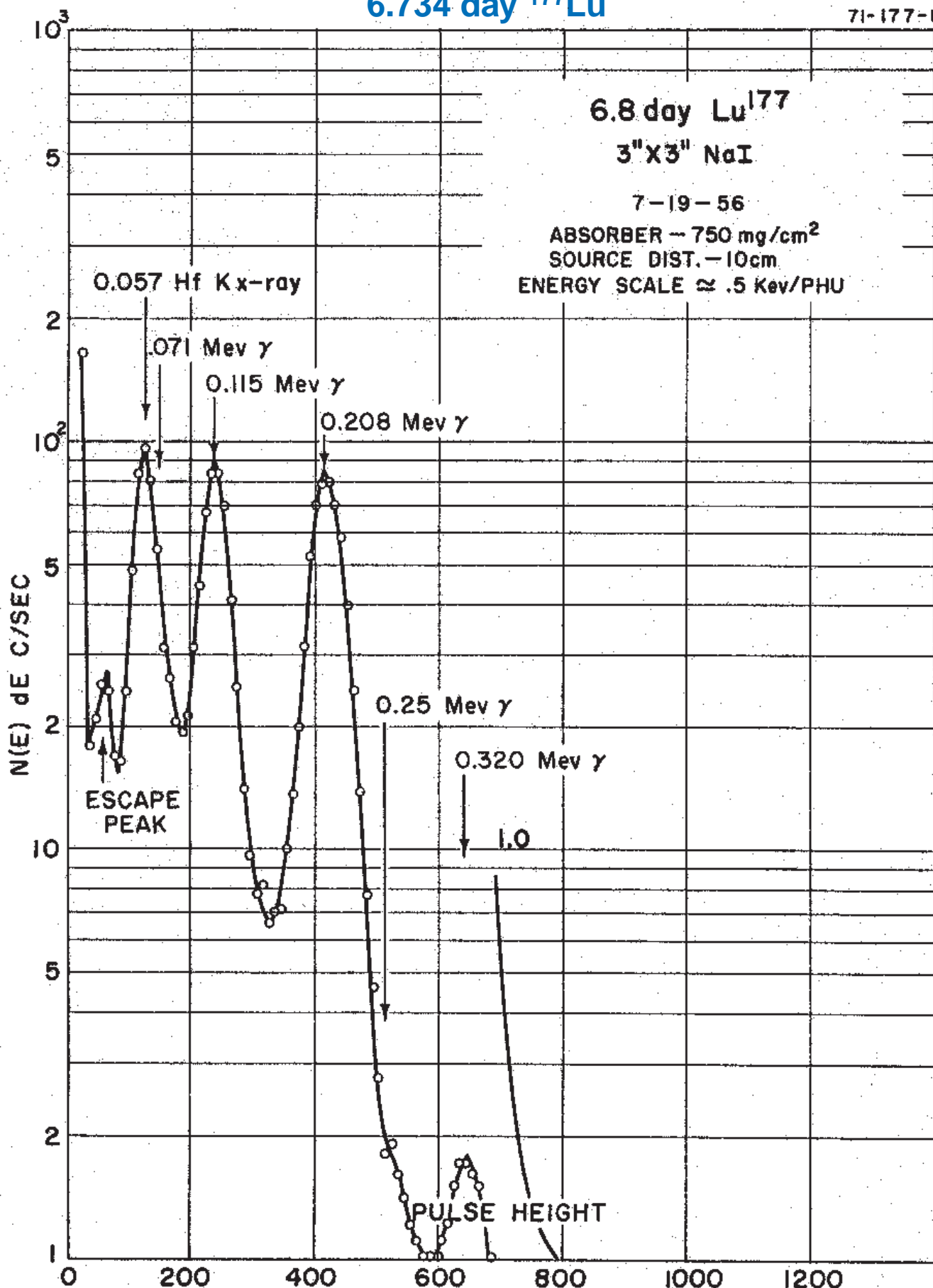
0.25 Mev γ

0.320 Mev γ

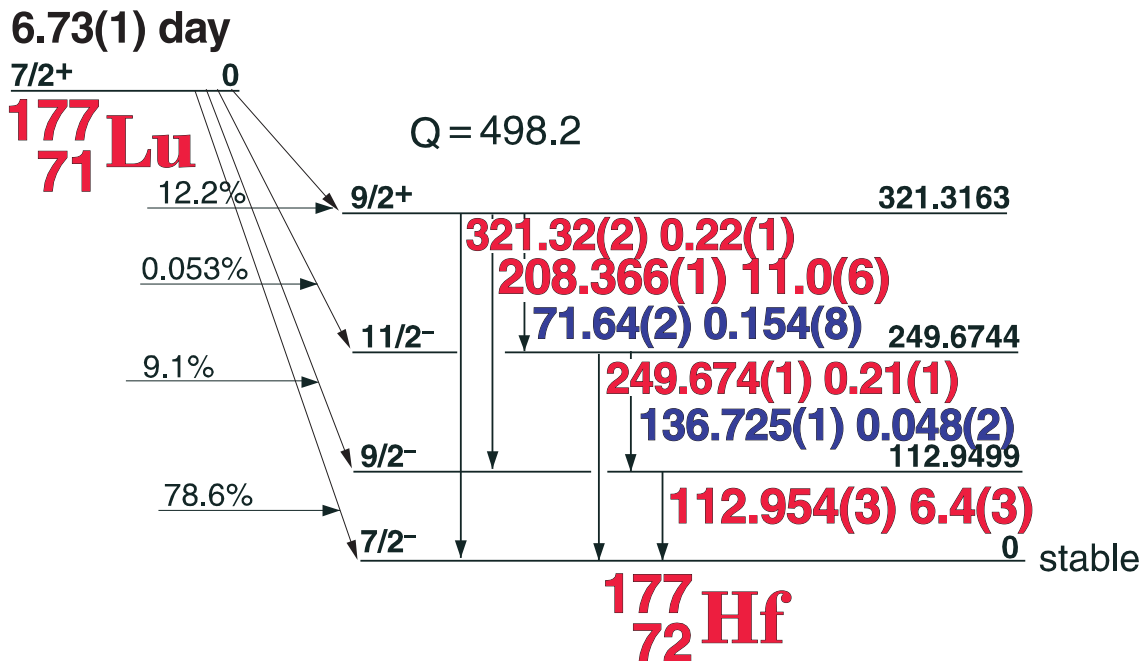
1.0

ESCAPE
PEAK

PULSE HEIGHT



6.73(1) day ^{177}Lu

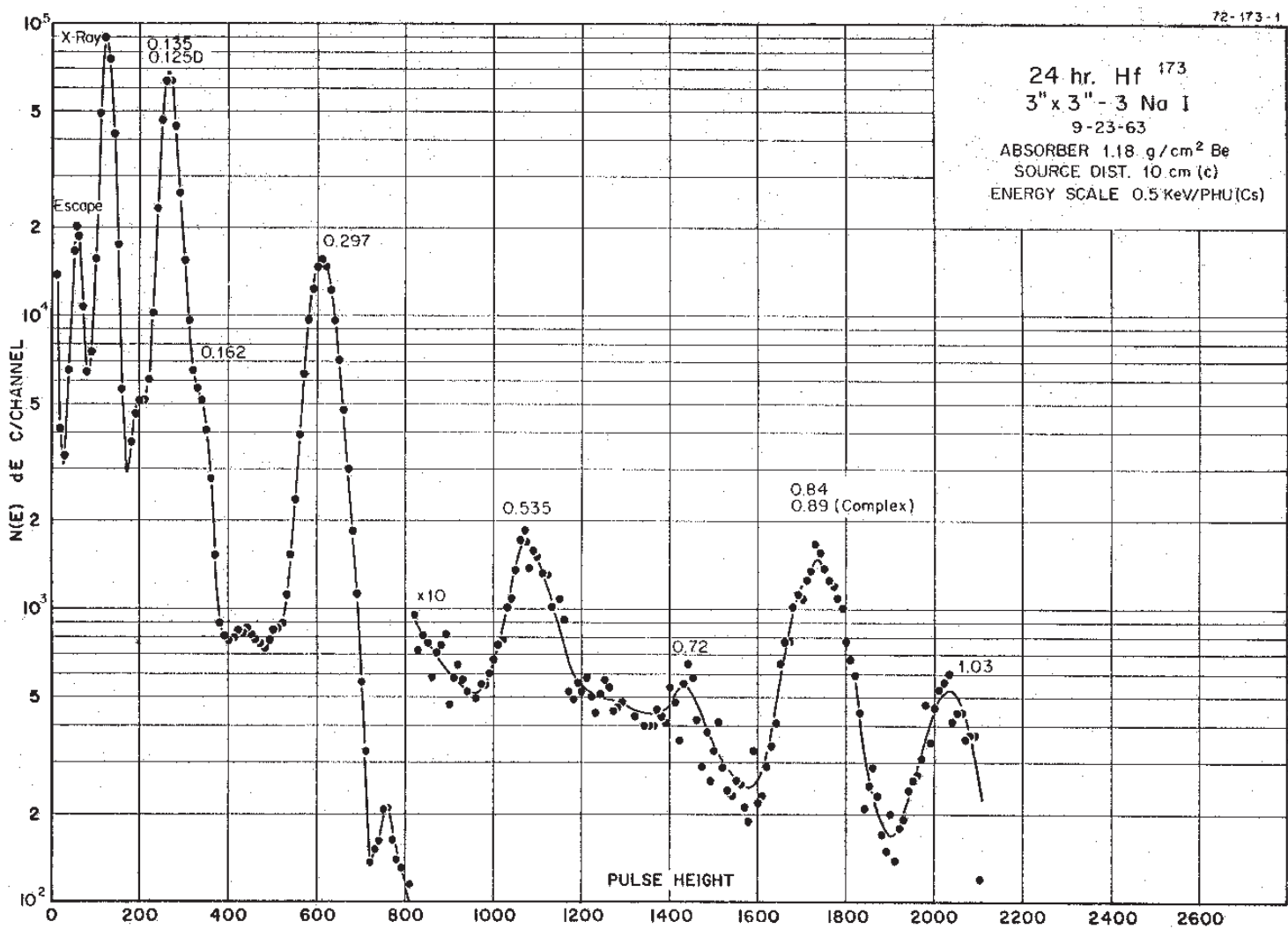


GAMMA-RAY ENERGIES AND INTENSITIES

Nuclide **^{177}Lu** Half Life 6.73(1) day
Detector 3" x 3" NaI Method of Production: $^{176}\text{Lu}(n,\gamma)$

E_{γ} (KeV)[S]	ΔE_{γ}	$I_{\gamma}(\text{rel})$	$I_{\gamma}(\%)[E]$	ΔI_{γ}	S
Hf K x-rays					
71.64	± 0.02	2.0	0.154	± 0.008	3
112.954	± 0.003	55.66	6.4	± 0.3	1
136.725	± 0.001	0.42	0.048	± 0.002	3
208.366	± 0.001	100	11.0	± 0.6	1
249.674	± 0.001	1.95	0.21	± 0.01	1
321.320	± 0.020	2.69	0.22	± 0.01	1

23.6 hr. ^{173}Hf



23.6(1) hr. ^{173}Hf

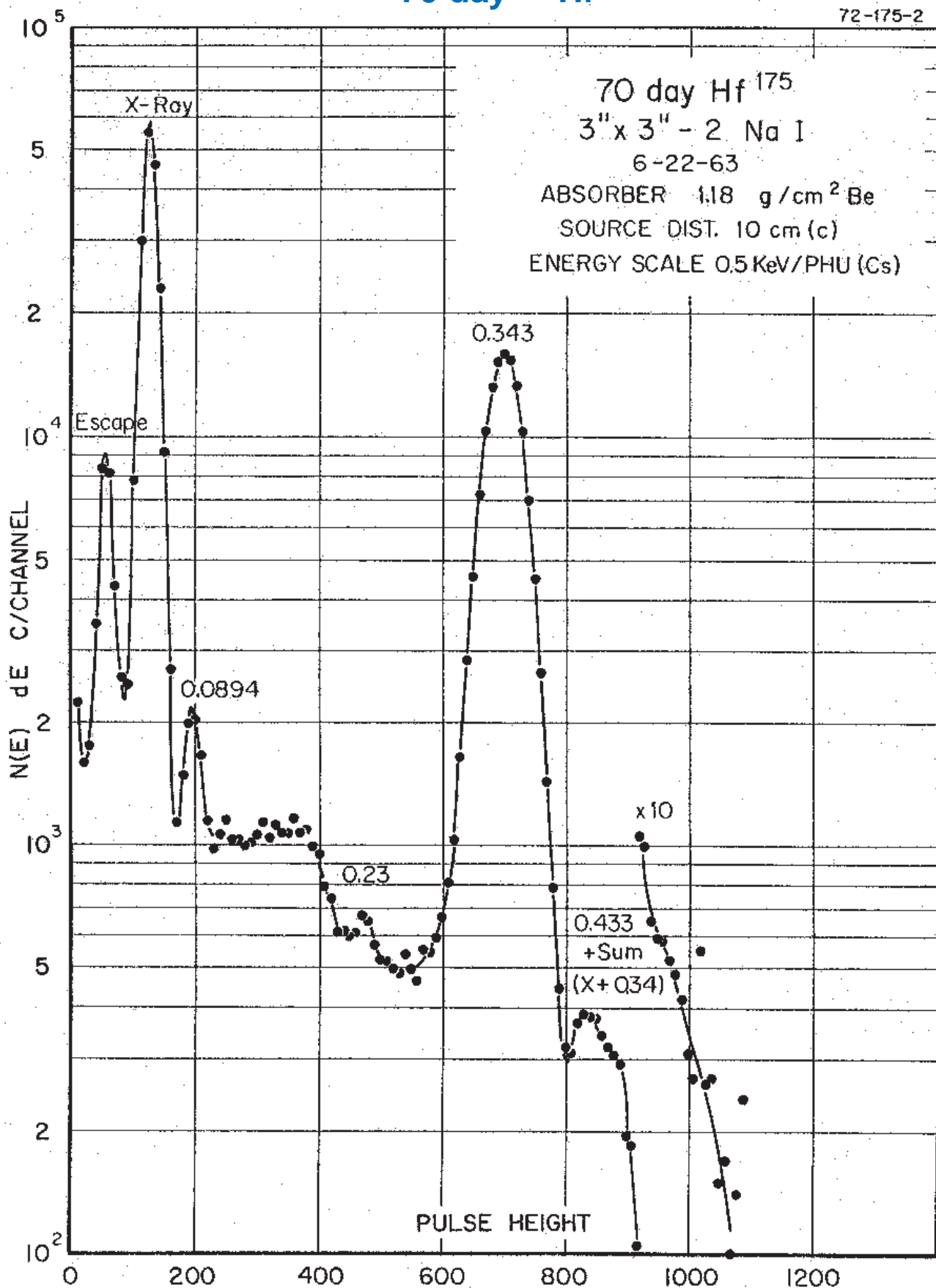
GAMMA-RAY ENERGIES AND INTENSITIES

Nuclide ^{173}Hf Half Life 23.6(1) hr.
Detector 3" x 3" NaI Method of Production: $^{174}\text{Hf}(\gamma, n)$

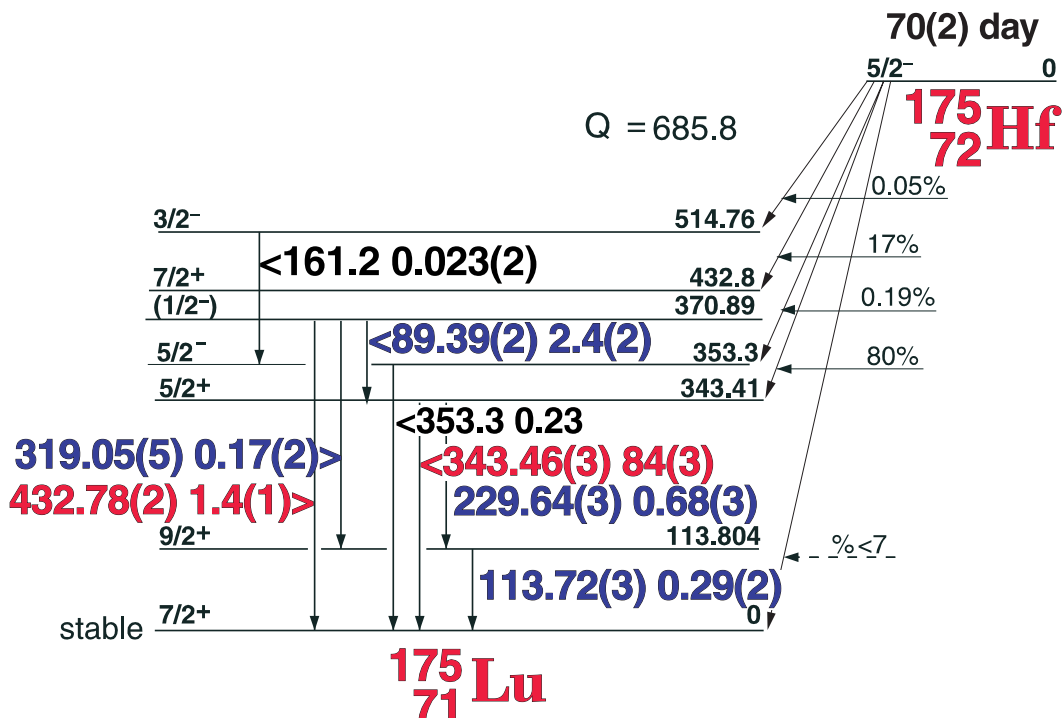
E_{γ} (KeV)[S]	ΔE_{γ}	I_{γ} (rel)	$I_{\gamma}(\%)$ [E]	ΔI_{γ}	S

70 day ^{175}Hf

72-175-2



70(2) day ^{175}Hf



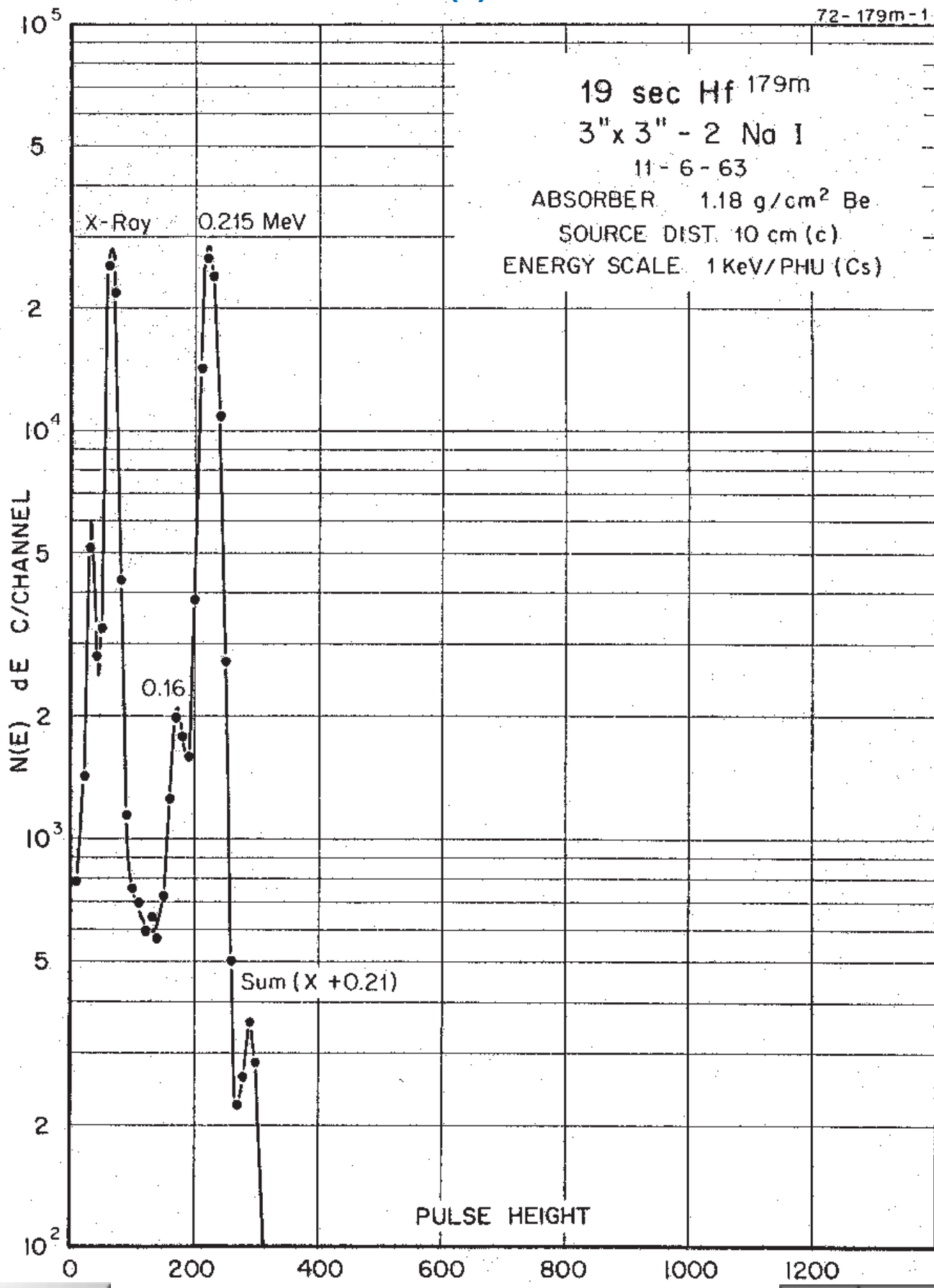
GAMMA-RAY ENERGIES AND INTENSITIES

Nuclide ^{175}Hf Half Life 70(2) day
Detector 3" x 3" NaI Method of Production: $^{174}\text{Hf}(n,\gamma)$

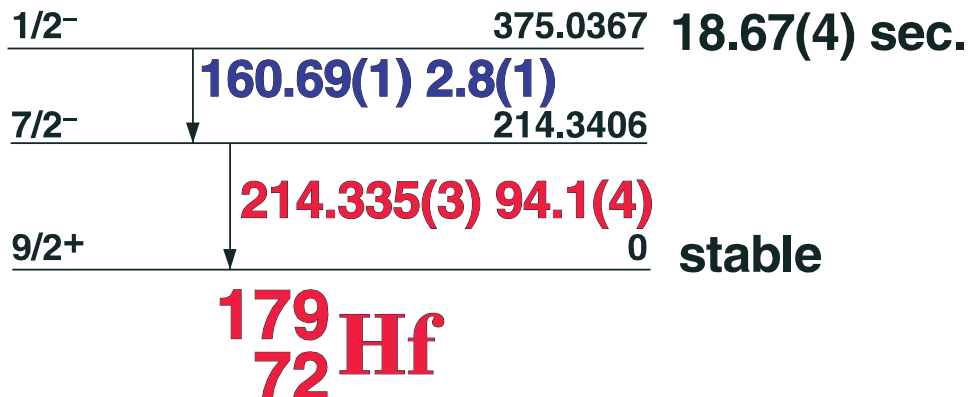
E_γ (KeV)[S]	ΔE_γ	I_γ (rel)	$I_\gamma(\%)$ [E]	ΔI_γ	S
Lu K x-rays		.			
89.395	± 0.015	2.02	2.4	± 0.20	2
113.77	± 0.03	0.369	0.29	± 0.02	4
229.64	± 0.03	0.896	0.68	± 0.03	3
319.05	± 0.05	0.240	0.17	± 0.025	4
343.460	± 0.030	100	84	± 3.0	1
432.782	± 0.020	1.72	1.4	± 0.12	1

26.763(4) hr. ^{179m}Hf

72-179m-1



18.67(4) sec. ^{179m}Hf



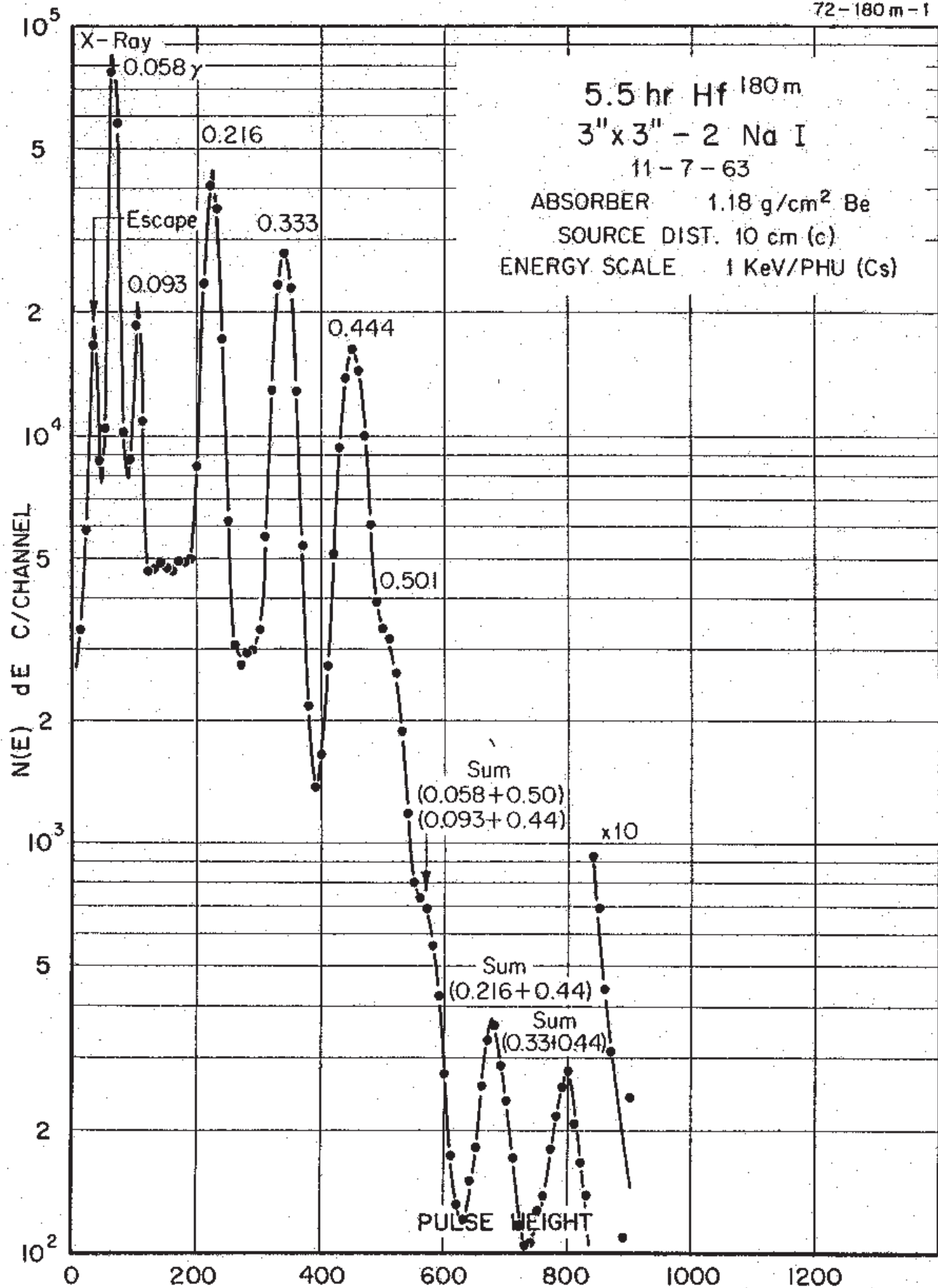
GAMMA-RAY ENERGIES AND INTENSITIES

Nuclide ^{179m}Hf Half Life 18.67(4) sec.
 Detector 3" x 3" NaI Method of Production: $^{178}\text{Hf}(n,\gamma)$

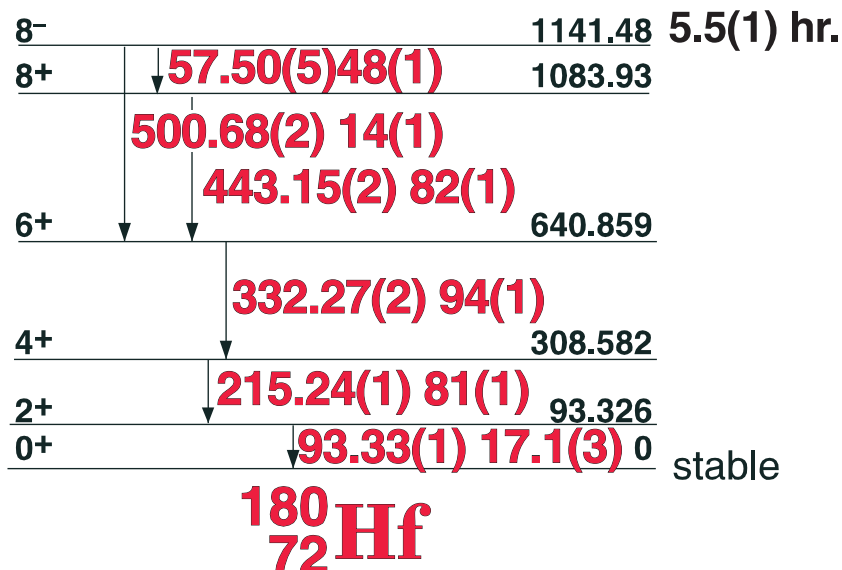
E_γ (KeV)[S]	ΔE_γ	I_γ (rel)	$I_\gamma(\%)$ [E]	ΔI_γ	S
160.69	± 0.01		2.8	± 0.1	2
214.335	± 0.003	100	94.1	± 0.4	1

5.5 hr. ^{180m}Hf

72-180 m-1



5.5(1) hr. ^{180}mHf



GAMMA-RAY ENERGIES AND INTENSITIES

Nuclide ^{180m}Hf **Half Life** 5.5(1) hr.
Detector 3" x 3" NaI **Method of Production:** $^{179}\text{Hf}(n,\gamma)$

E_{γ} (KeV)[S]	ΔE_{γ}	$I_{\gamma}(\text{rel})$	$I_{\gamma}(\%)[E]$	ΔI_{γ}	S
Hf K x-rays					1
57.44	± 0.05	49.0	48	± 1.0	1
93.328	± 0.015	15.5	17.1	± 0.3	1
215.243	± 0.015	86.2	81	± 1.0	1
332.269	± 0.018	100	94	± 1.2	1

42.39 day ^{181}Hf

72-181-1

43 day Hf^{181}

3" x 3" - 2 No 1

11-14-63

ABSORBER 1.18 g / cm² Be

SOURCE DIST. 10 cm (c)

ENERGY SCALE 1 KeV/PHU(Cs)

0.133
0.136

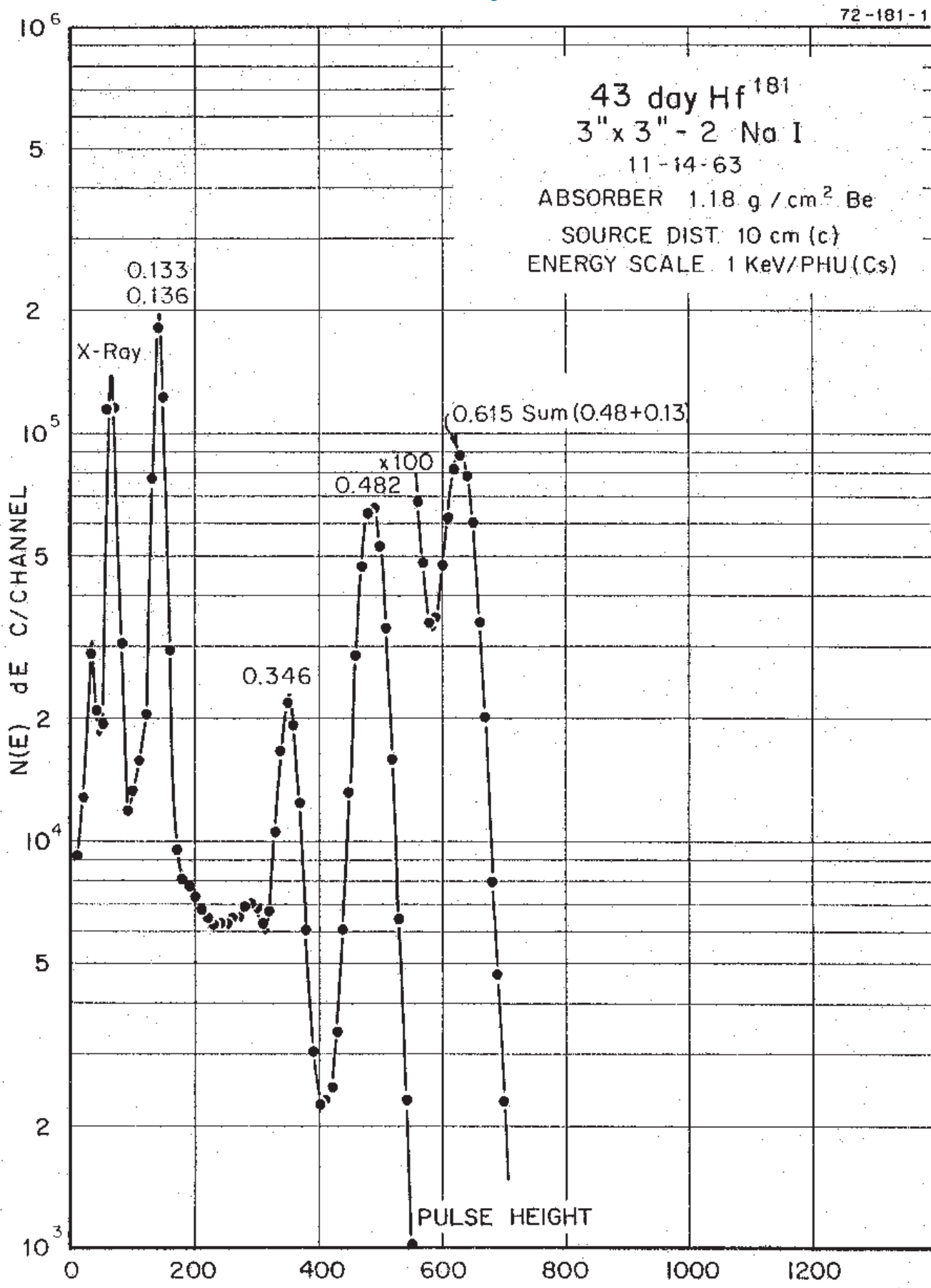
X-Ray

0.615 Sum (0.48+0.13)

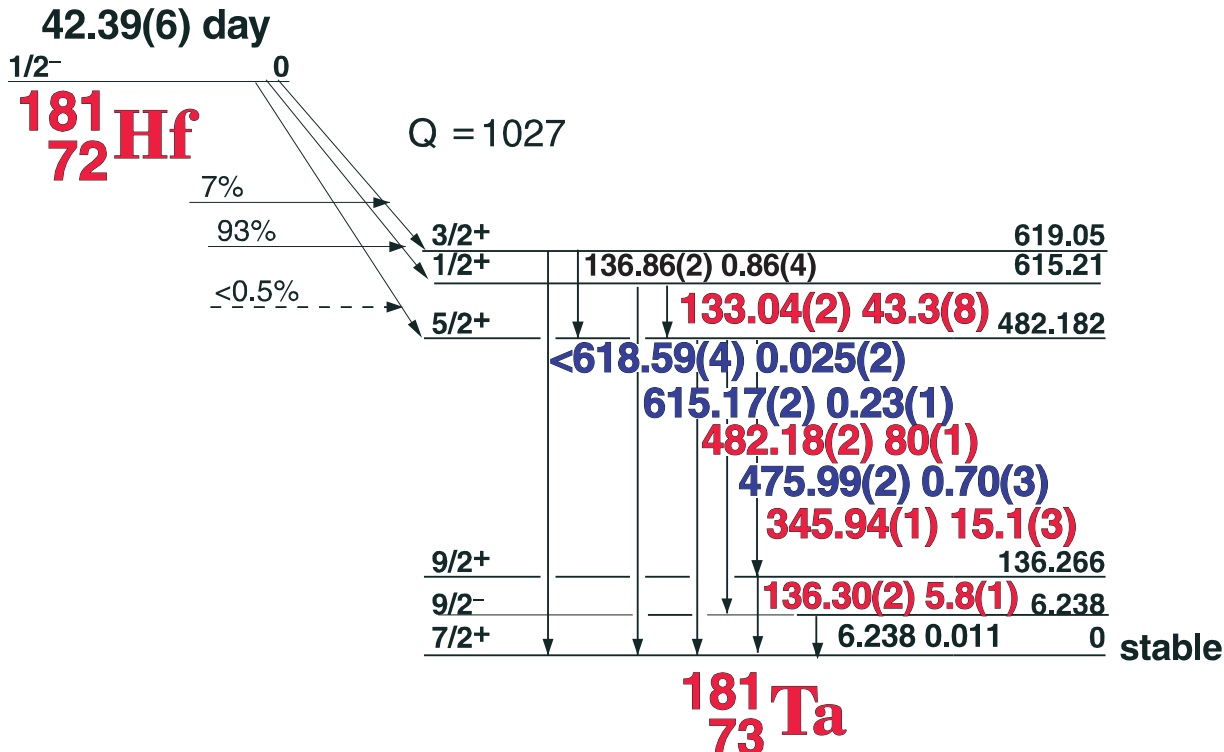
x100
0.482

0.346

PULSE HEIGHT



42.39 day ^{181}Hf



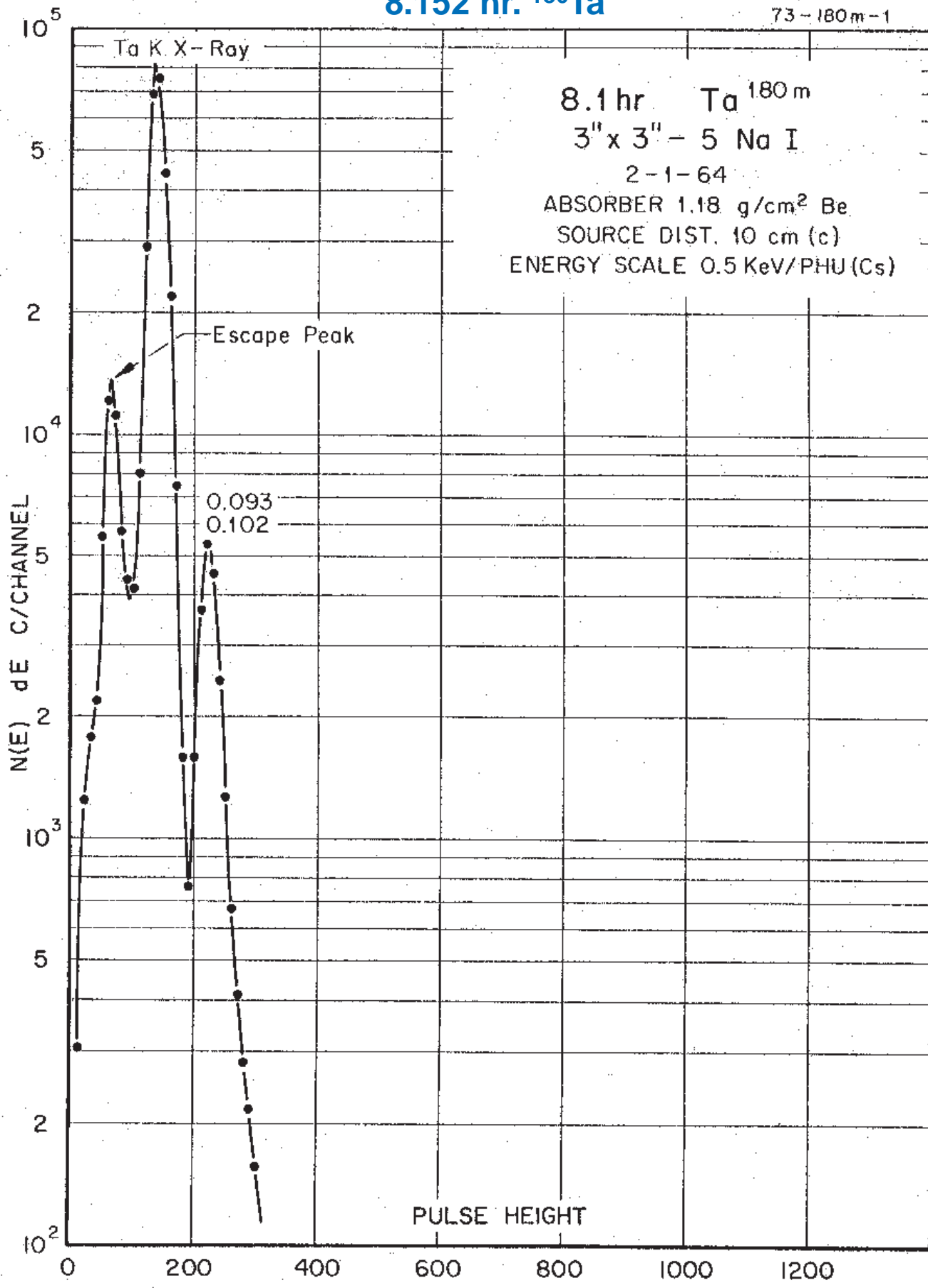
GAMMA-RAY ENERGIES AND INTENSITIES

Nuclide **^{181}Cs** Half Life 42.39(6) day
 Detector 3" x 3" NaI Method of Production: $^{180}\text{Hf}(n,\gamma)$

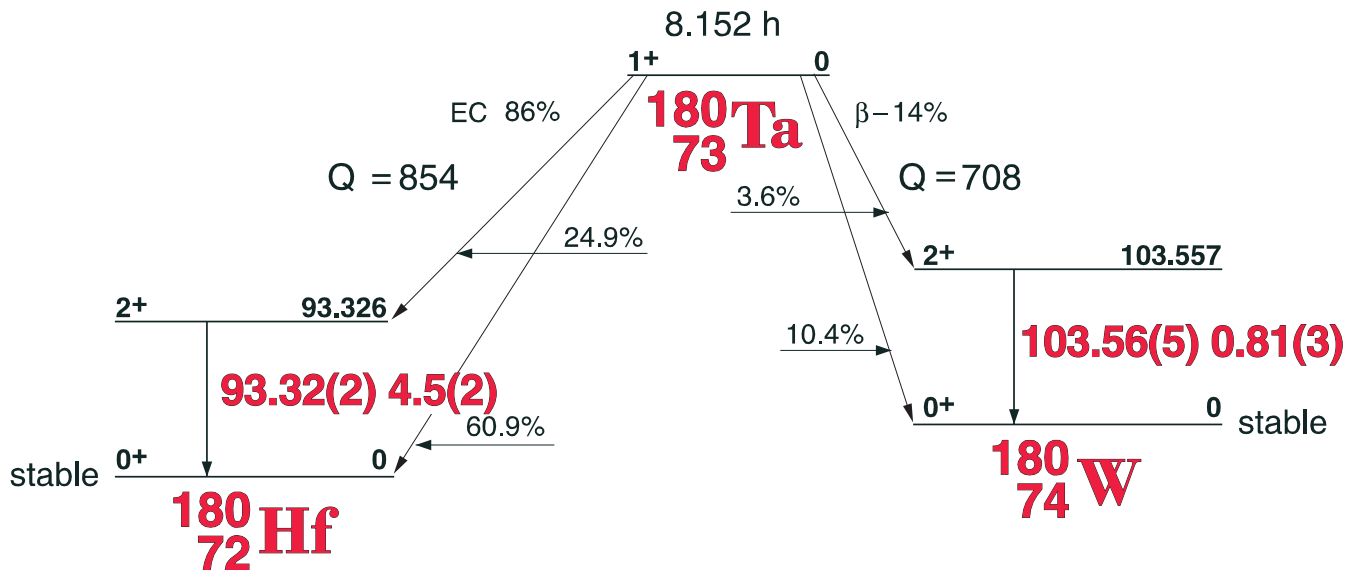
E_{γ} (KeV)[S]	ΔE_{γ}	I_{γ} (rel)	$I_{\gamma}(\%)$ [E]	ΔI_{γ}	S
Ta K x-rays					
133.039	± 0.020	44.51	43.3	± 0.8	1
136.306	± 0.020	7.24	5.8	± 0.1	1
324.08	± 0.08	0.25		± 0.1	4
345.940	± 0.015	18.71	15.1	± 0.3	1
475.997	± 0.025	1.45	0.70	± 0.03	3

8.152 hr. ^{180}Ta

73 → 180 m⁻¹



8.152(6) hr. ^{180}Ta



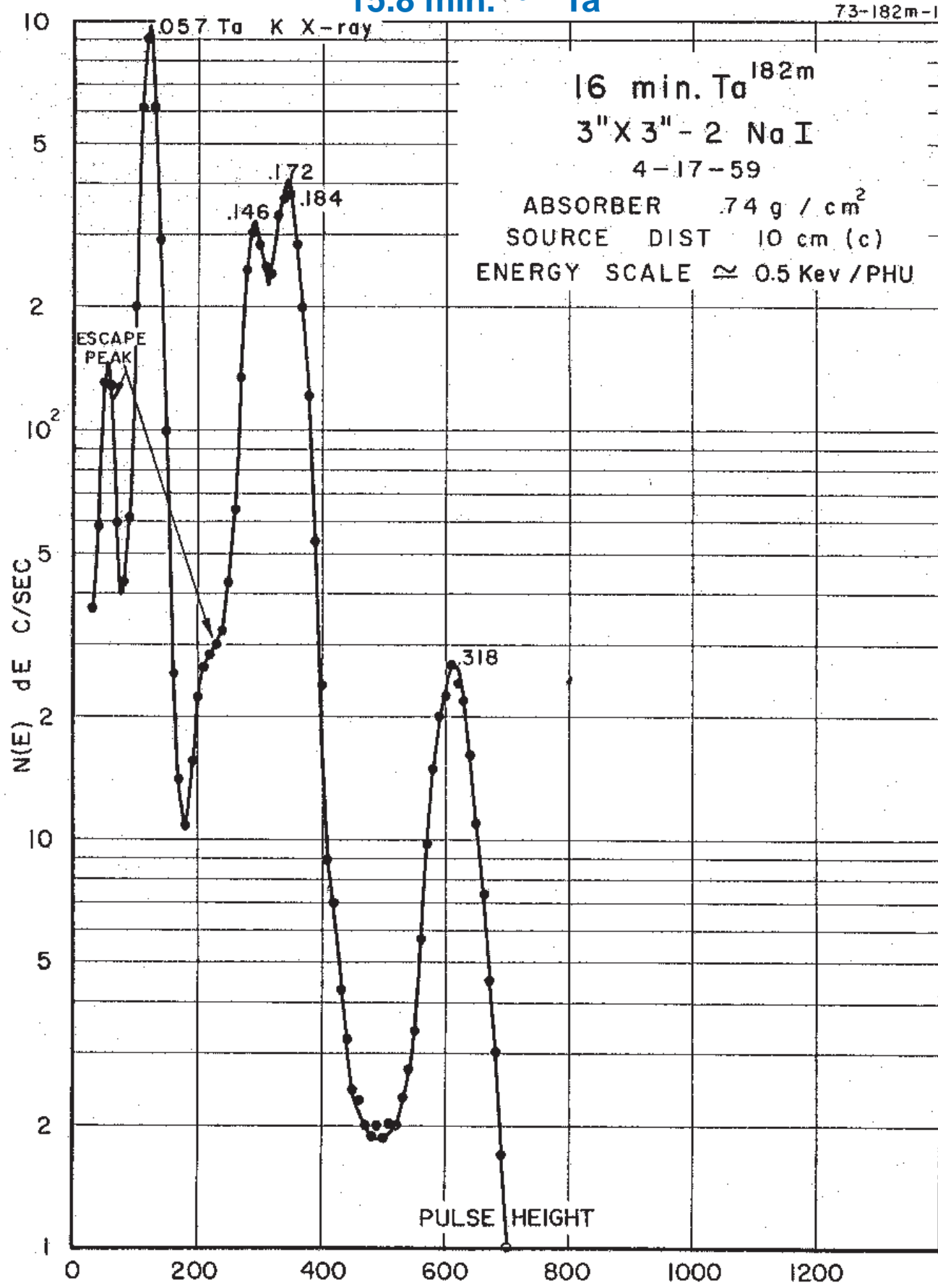
GAMMA-RAY ENERGIES AND INTENSITIES

Nuclide ^{180}Ta Half Life 8.152(60 hr.)
 Detector 3" x 3" NaI Method of Production: $^{181}\text{Ta}(\gamma, n)$

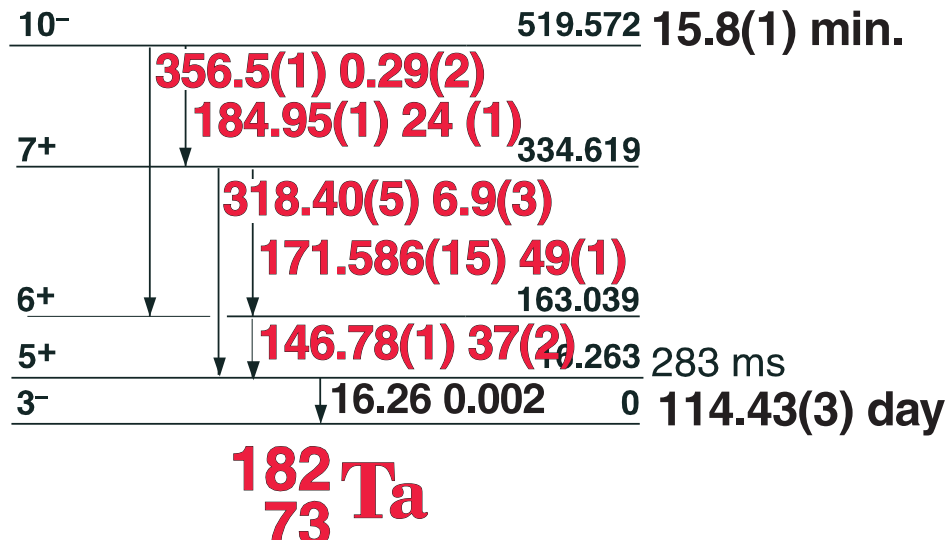
E_γ (KeV) [S]	ΔE_γ	I_γ (rel)	$I_\gamma (\%)$ [E]	ΔI_γ	S
Hf x-rays					
93.32	± 0.02	100	4.5	± 0.2	1
103.56	± 0.05	18.0	0.81	± 0.03	1

15.8 min. ^{182m}Ta

73-182m-1



15.8(1) min. ^{182m}Ta



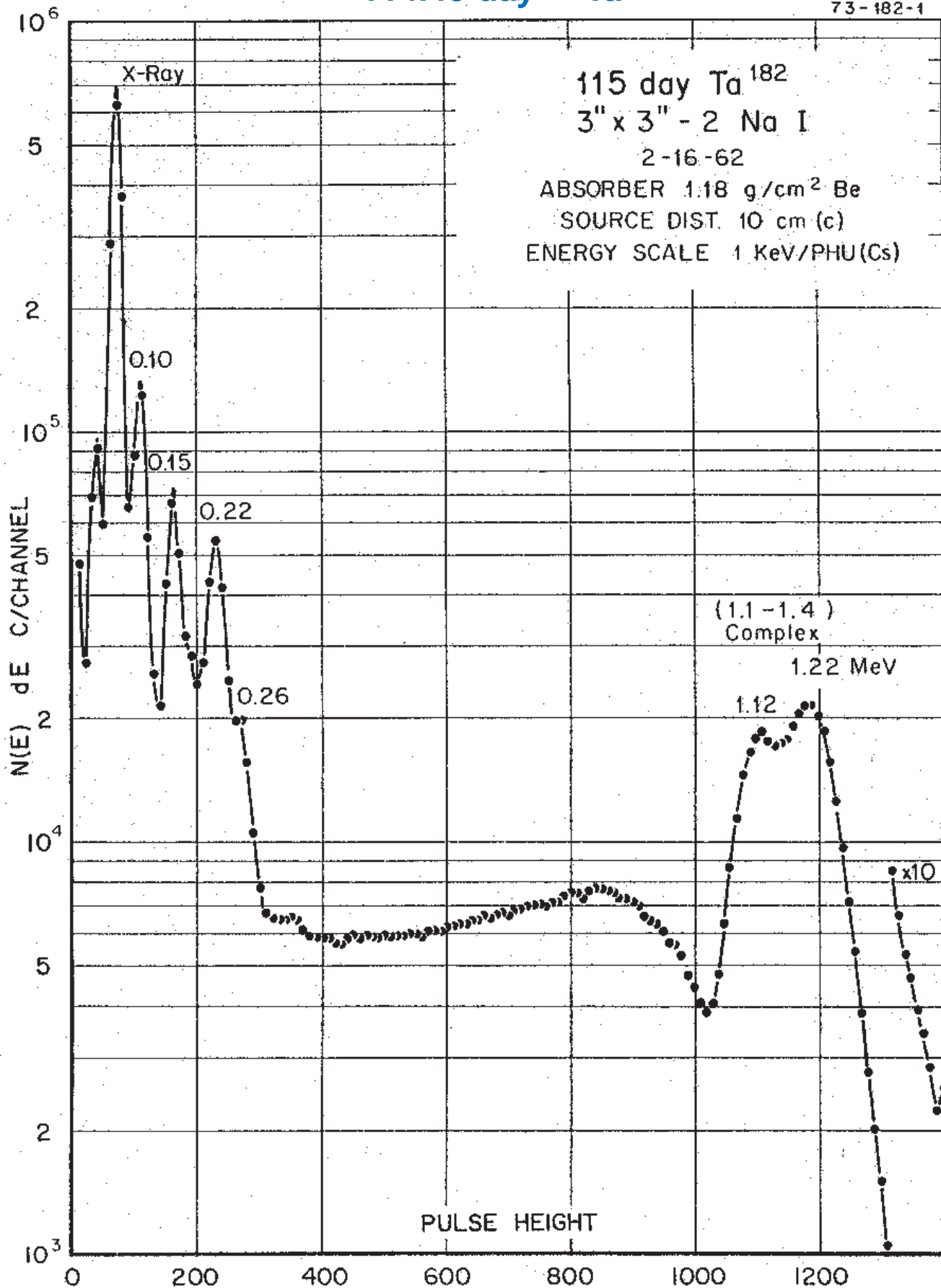
GAMMA-RAY ENERGIES AND INTENSITIES

Nuclide ^{182m}Ta Half Life 15.8(1) min.
Detector 3" x 3" NaI Method of Production: $^{181}\text{Ta}(n,\gamma)$

E_{γ} (KeV)[S]	ΔE_{γ}	I_{γ} (rel)	$I_{\gamma}(\%)$ [E]	ΔI_{γ}	S
146.785	± 0.015	76.0	37	± 2.0	1
171.586	± 0.015	100	49	± 2.0	1
184.951	± 0.015	50.0	24	± 1.0	1
318.40	± 0.05	14.0	6.9	± 0.3	1
356.47	± 0.10	0.6	0.29	± 0.02	3

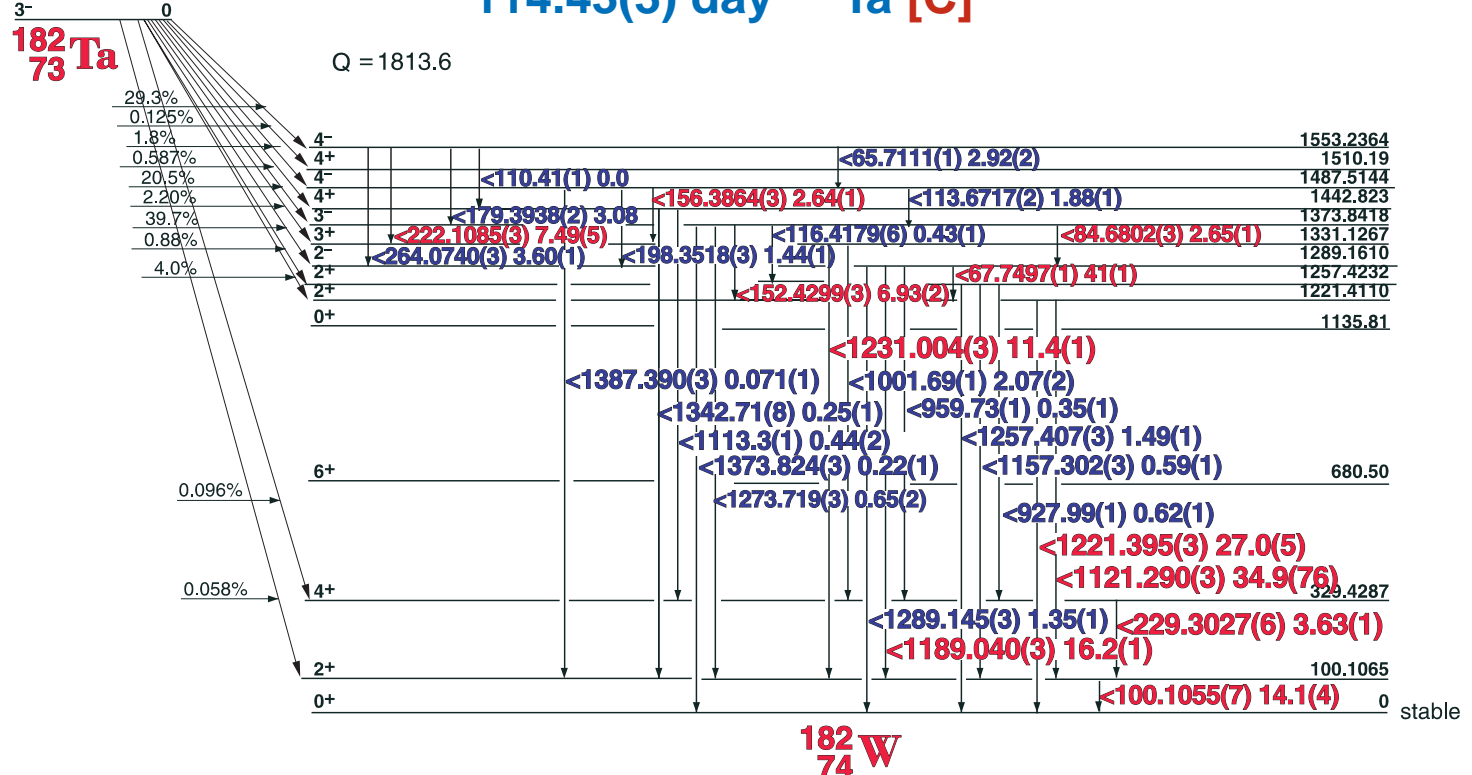
114.43 day ^{182}Ta

73-182-1



114.43(3) day

114.43(3) day ^{182}Ta [C]



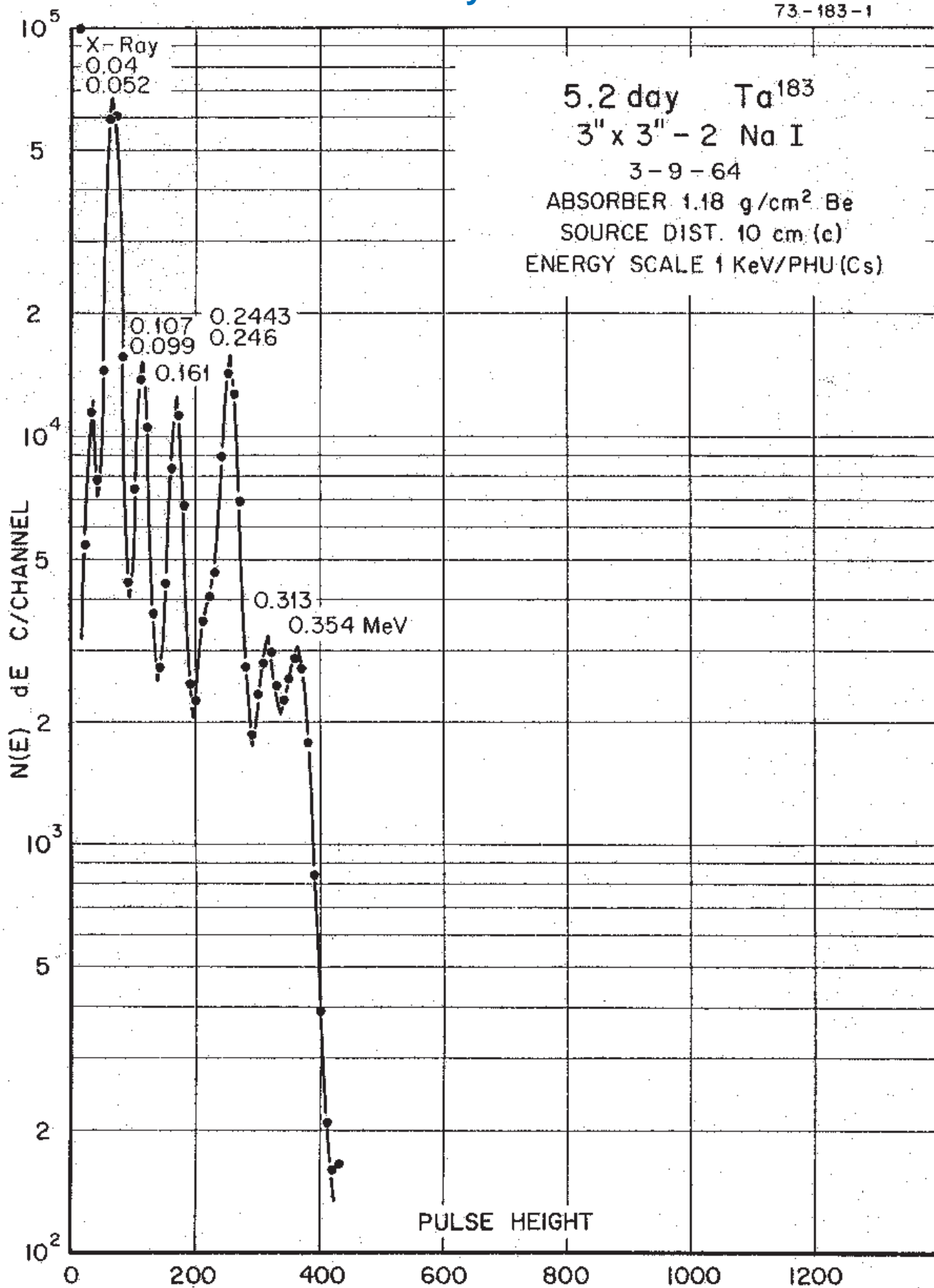
GAMMA-RAY ENERGIES AND INTENSITIES [C]

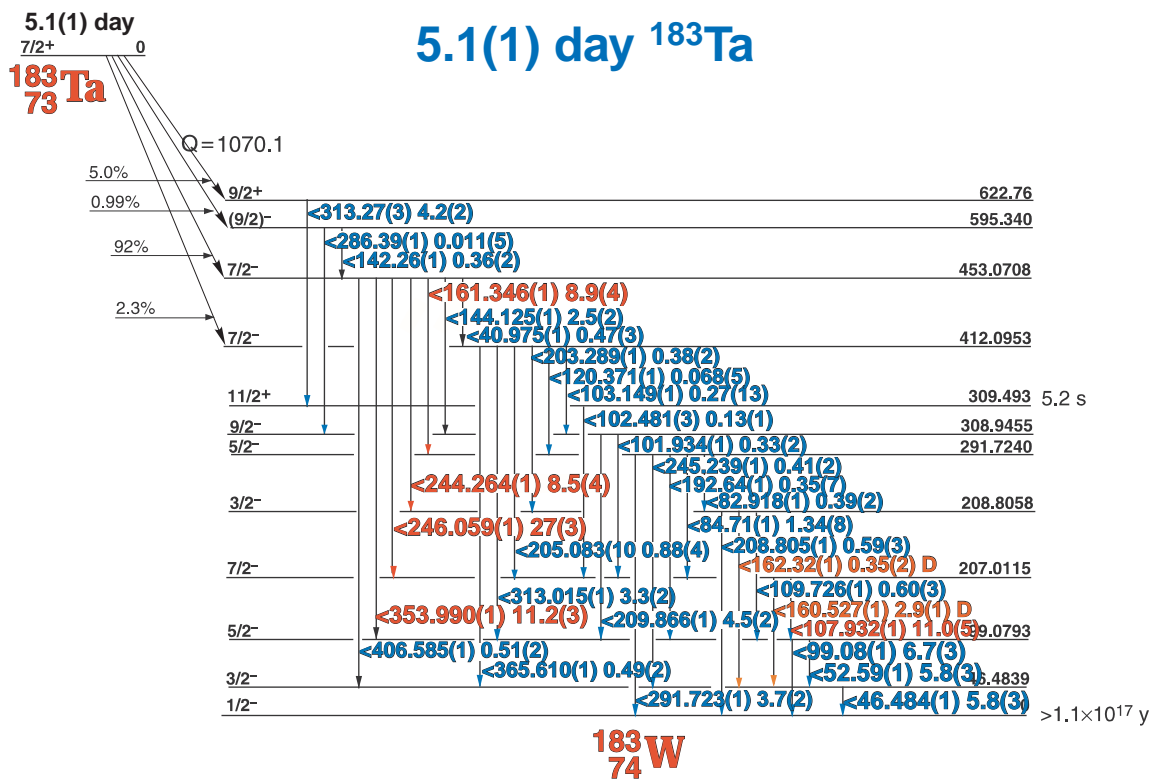
Nuclide ^{182}Ta Half Life 114.43(3) day
Detector 3" x 3" NaI Method of Production: $^{181}\text{Ta}(n,\gamma)$

E_{γ} (KeV) [C]	ΔE_{γ}	$I_{\gamma}(\text{rel})$	$I_{\gamma}(\%)$ [C]	ΔI_{γ}	S
65.7111	± 0.00001		2.92	± 0.02	4
67.7497	± 0.0001	100	41.0	± 0.1	1
84.6802	± 0.0003	6.04	2.65	± 0.01	2
100.1055	± 0.0007	30.40	14.1	± 0.4	1
110.41	± 0.05	0.27	0.087	± 0.01	4
113.6717	± 0.0002	3.93	1.88	± 0.01	2
116.4179	± 0.0006	0.90	0.43	± 0.01	3
152.4299	± 0.0003	15.62	6.93	± 0.02	1
156.3864	± 0.0003	6.01	2.64	± 0.01	1
179.3938	± 0.0002	7.04	3.08	± 0.01	1
198.3518	± 0.0003	3.40	1.44	± 0.01	2
222.1085	± 0.0003	17.05	7.49	± 0.05	1
229.3027	± 0.0006	8.42	3.63	± 0.03	1
264.0740	± 0.0003	8.40	3.60	± 0.02	1
927.99	± 0.01	1.50	0.62	± 0.01	4
1001.69	± 0.01	5.34	2.07	± 0.02	3
1113.3	± 0.1	0.83	0.44	± 0.02	3
1121.290	± 0.003	79.94	34.9	± 0.7	1
1157.302	± 0.003	2.22	0.59	± 0.01	3
1189.040	± 0.027	37.41	16.2	± 0.1	1
1221.395	± 0.003	62.10	27.0	± 0.5	1
1231.004	± 0.003	26.02	11.4	± 0.1	1
1257.407	± 0.003	3.50	1.49	± 0.01	1
1273.719	± 0.003	1.49	0.65	± 0.02	1
1289.145	± 0.003	3.24	1.35	± 0.01	1
1342.71	± 0.08	0.61	0.25	± 0.01	2
1373.824	± 0.003	0.51	0.22	± 0.01	2
1387.390	± 0.003	0.15	0.071	± 0.001	3

5.1 day ^{183}Ta

73-183-1





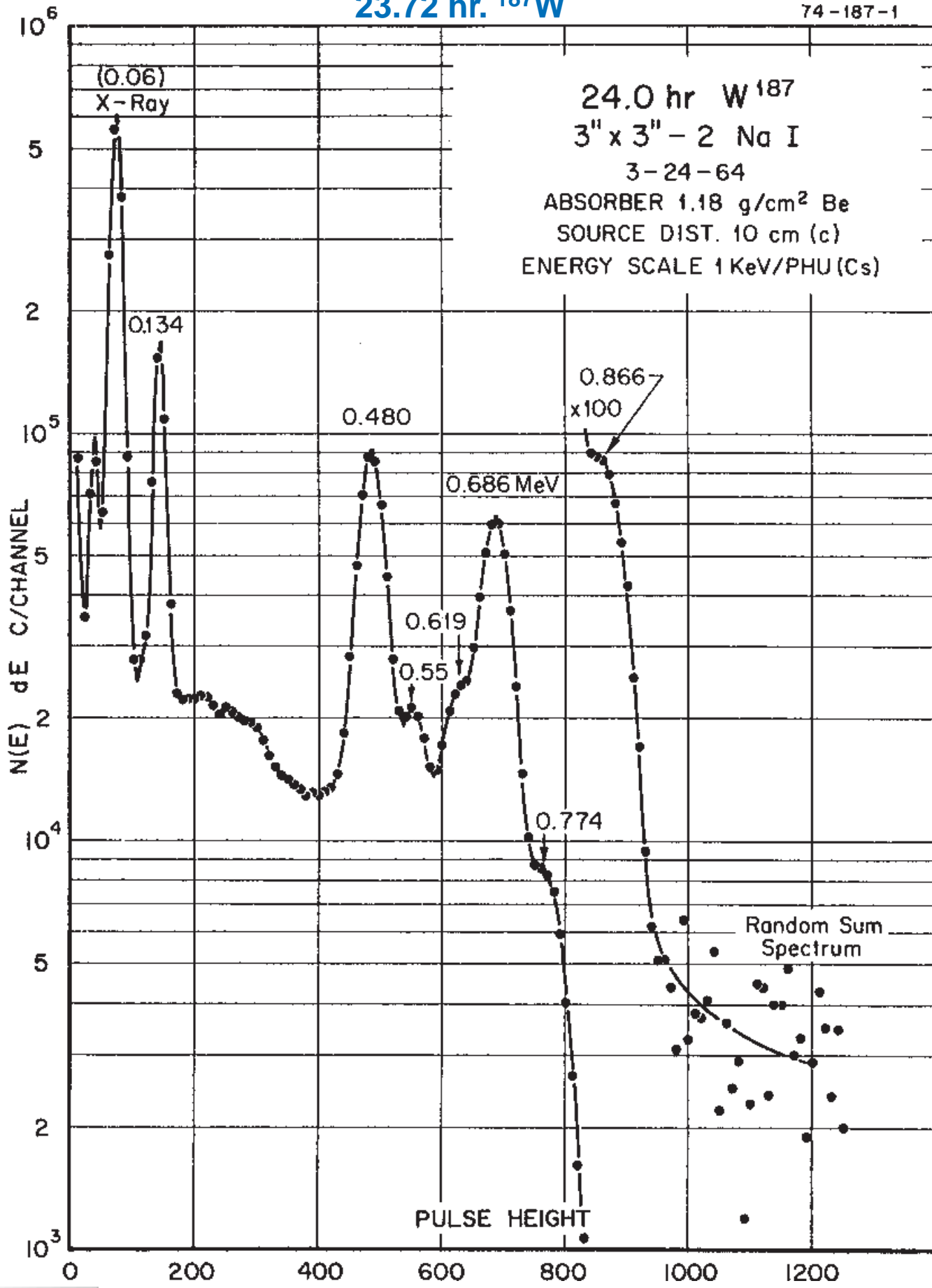
GAMMA-RAY ENERGIES AND INTENSITIES

Nuclide **^{183}Ta** Half Life 5.1(1) day
Detector 3" x 3" NaI Method of Production: $^{181}\text{Ta}(n,\gamma,n,\gamma)$

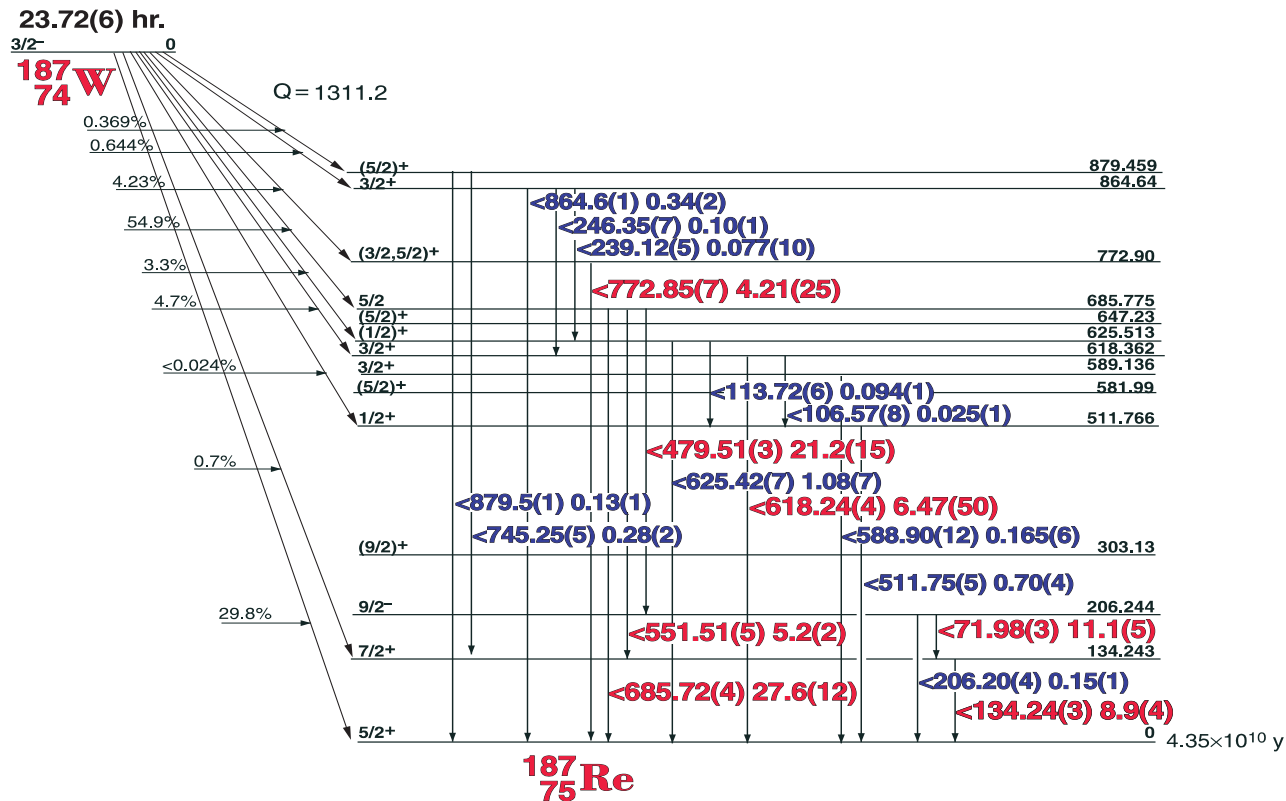
E_{γ} (KeV)	ΔE_{γ}	$I_{\gamma}(\text{rel})$	$I_{\gamma}(\%)$	ΔI_{γ}	S
W x-rays					
40.975	± 0.001		0.47	± 0.03	4
46.484	± 0.001		5.8	± 0.3	2
52.59	± 0.01		5.8	± 0.3	2
82.918	± 0.001		0.39	± 0.02	3
84.71	± 0.01		1.34	± 0.08	3
99.08	± 0.01		6.7	± 0.3	3
101.934	± 0.001		0.33	± 0.02	3
103.149	± 0.001		0.27	± 0.1	3
107.932	± 0.001		11.0	± 0.5	1
109.726	± 0.001		0.60	± 0.03	3
120.371	± 0.001		0.068	± 0.005	4
142.26	± 0.01		0.36	± 0.02	3
144.125	± 0.01		2.5	± 0.1	3
160.527	± 0.01		2.9	± 0.1	2
161.346	± 0.001		8.9	± 0.4	1
162.32	± 0.01		0.35	± 0.02	3
192.64	± 0.01		0.35	± 0.07	3
205.083	± 0.001		0.88	± 0.04	3
208.805	± 0.001		0.59	± 0.03	3
209.866	± 0.001		4.5	± 0.2	2
244.264	± 0.001		8.5	± 0.4	1
246.059	± 0.001		27	± 1.0	1
291.723	± 0.001		3.7	± 0.2	2
313.015	± 0.001		3.3	± 0.2	2
313.27	± 0.03		4.2	± 0.2	2
353.990	± 0.001		11.2	± 0.3	1
365.610	± 0.001		0.49	± 0.02	3
406.585	± 0.001		0.51	± 0.02	3

23.72 hr. ^{187}W

74-187-1



23.72 hr. ^{187}W



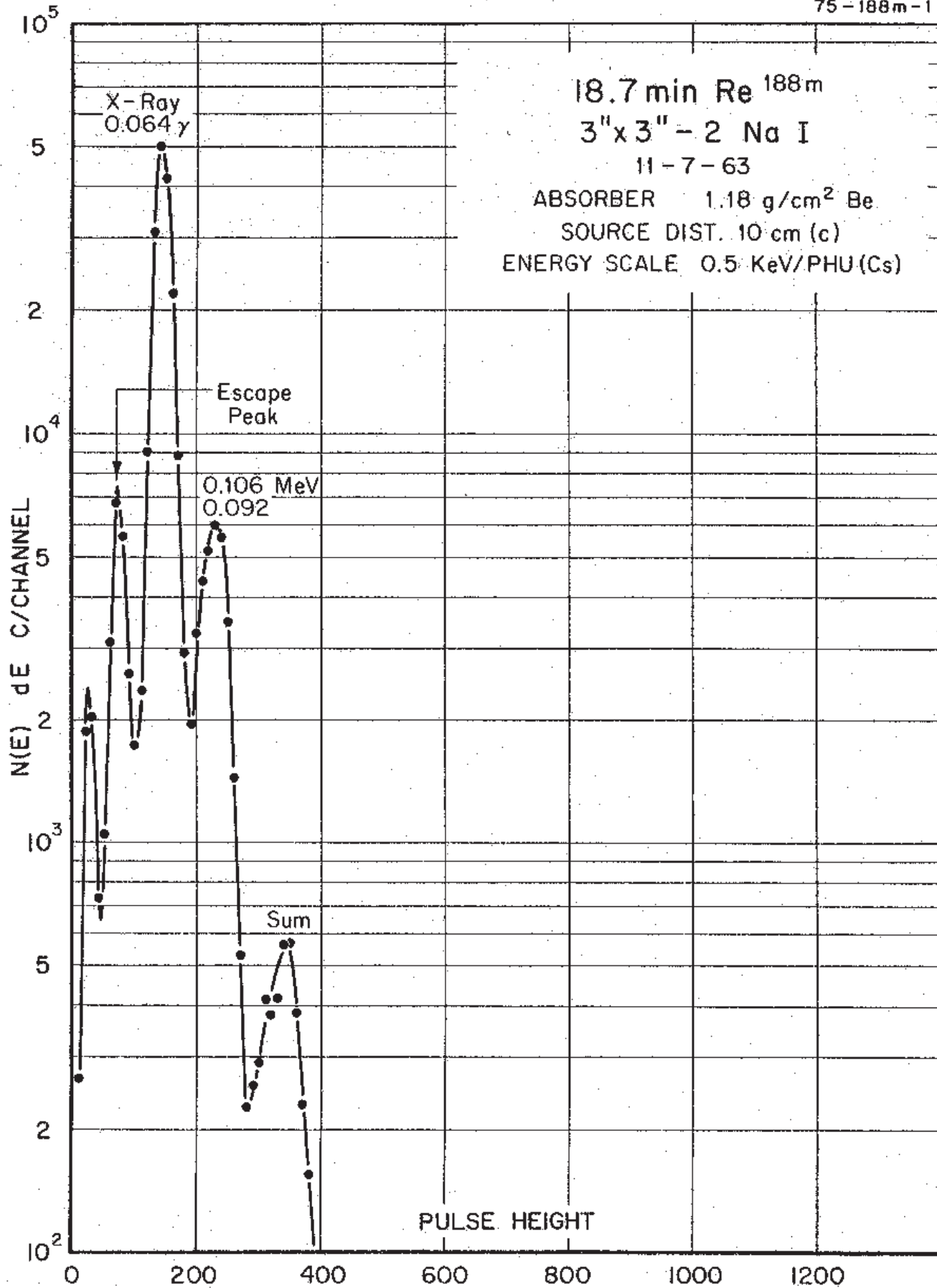
GAMMA-RAY ENERGIES AND INTENSITIES

Nuclide ^{187}W Half Life 23.72(6) hr.
Detector 3" x 3" NaI Method of Production: $^{186}\text{W}(n,\gamma)$

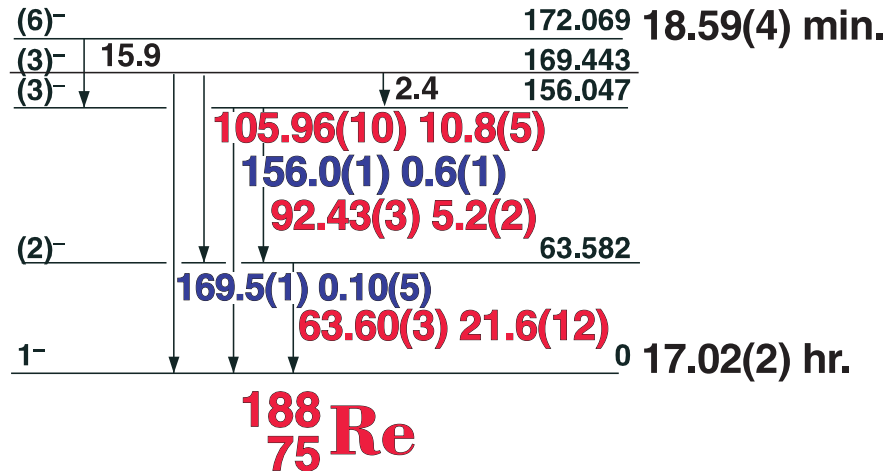
E_{γ} (KeV)[S]	ΔE_{γ}	I_{γ} (rel)	$I_{\gamma}(\%)[E]$	ΔI_{γ}	S
71.98	± 0.03	37.0	8.9	± 0.4	1
106.57	± 0.08	0.09	0.025	± 0.001	4
113.72	± 0.06	0.34	0.094	± 0.001	4
134.24	± 0.03	29.4	8.9	± 0.4	1
206.20	± 0.04	0.53	0.15	± 0.01	4
239.12	± 0.05	0.28	0.077	± 0.01	4
246.35	± 0.07	0.38	0.10	± 0.01	4
479.51	± 0.03	80.4	21.2	± 1.5	1
511.75	± 0.06	2.60	0.70	± 0.04	3
551.51	± 0.10	18.9	5.2	± 0.2	1
588.90	± 0.12	0.60	0.165	± 0.006	3
618.24	± 0.04	23.3	6.47	± 0.50	1
625.42	± 0.07	3.9	1.08	± 0.07	1
685.72	± 0.04	100	27.6	± 1.2	1
745.33	± 0.10	1.0	0.28	± 0.02	2
772.85	± 0.07	14.9	4.21	± 0.25	1
864.53	± 0.10	1.25	0.34	± 0.02	2
879.57	± 0.15	0.47	0.13	± 0.01	3

18.59 min. ^{188m}Re

75-188m-1



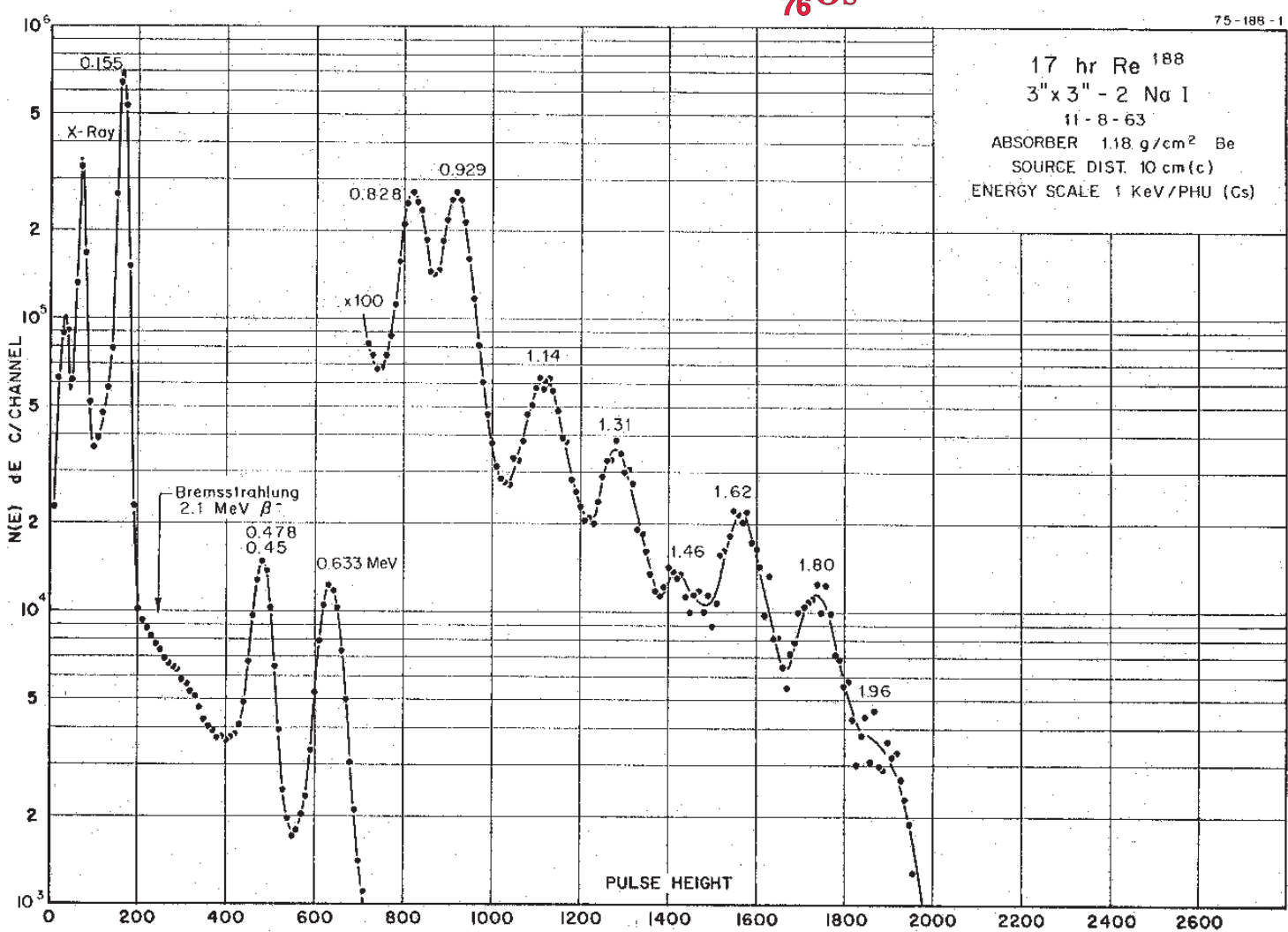
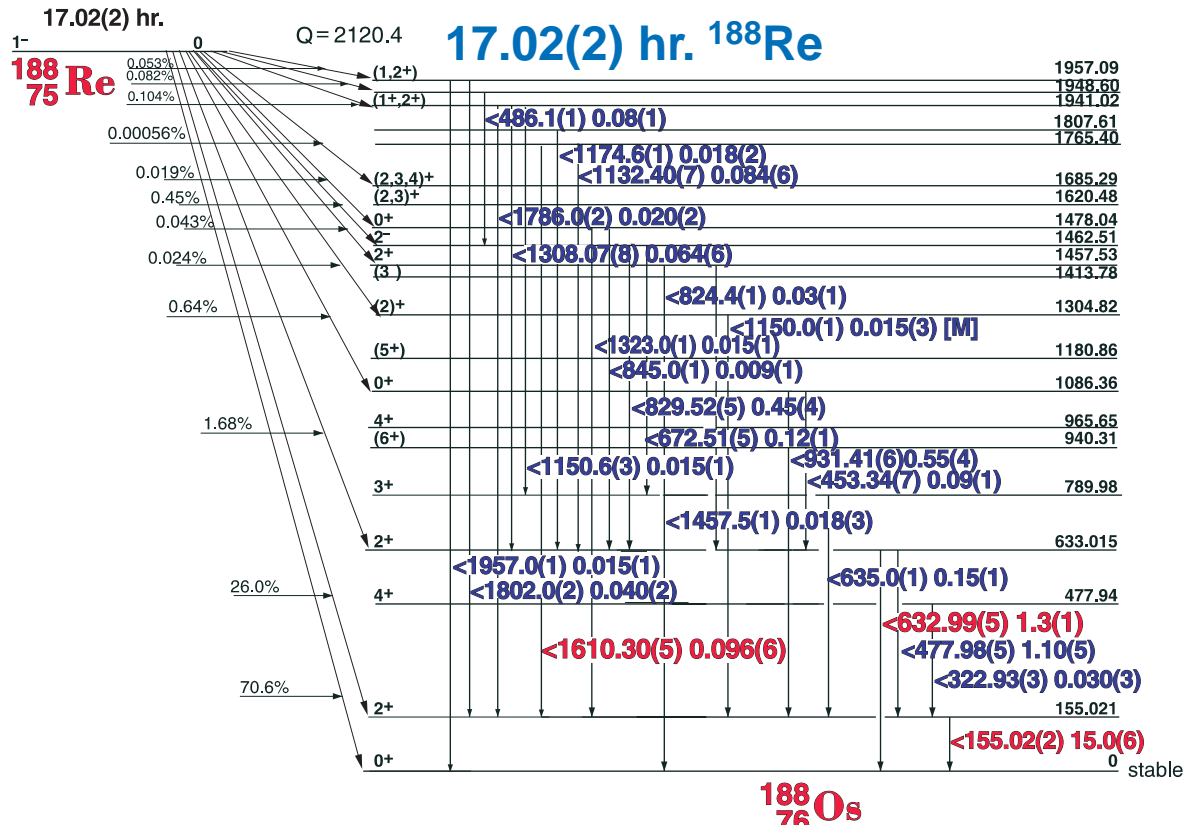
18.59(4) min. ^{188m}Re



GAMMA-RAY ENERGIES AND INTENSITIES

Nuclide ^{188m}Re Half Life 18.59(4) min.
 Detector 3" x 3" NaI Method of Production: $^{187}\text{Re}(n,\gamma)$

E_{γ} (KeV) [S]	ΔE_{γ}	$I_{\gamma}(\text{rel})$	$I_{\gamma}(\%) [E]$	ΔI_{γ}	S
63.60	± 0.03		21.6	± 1.2	1
92.43	± 0.03		5.2	± 0.2	1
105.96	± 0.10		10.8	± 0.5	1
156.0	± 0.1	0.60	± 0.10	3	
169.5	± 0.12	0.10	± 0.05	3	



17.02(2) hr. ^{188}Re

GAMMA-RAY ENERGIES AND INTENSITIES

Nuclide
Detector

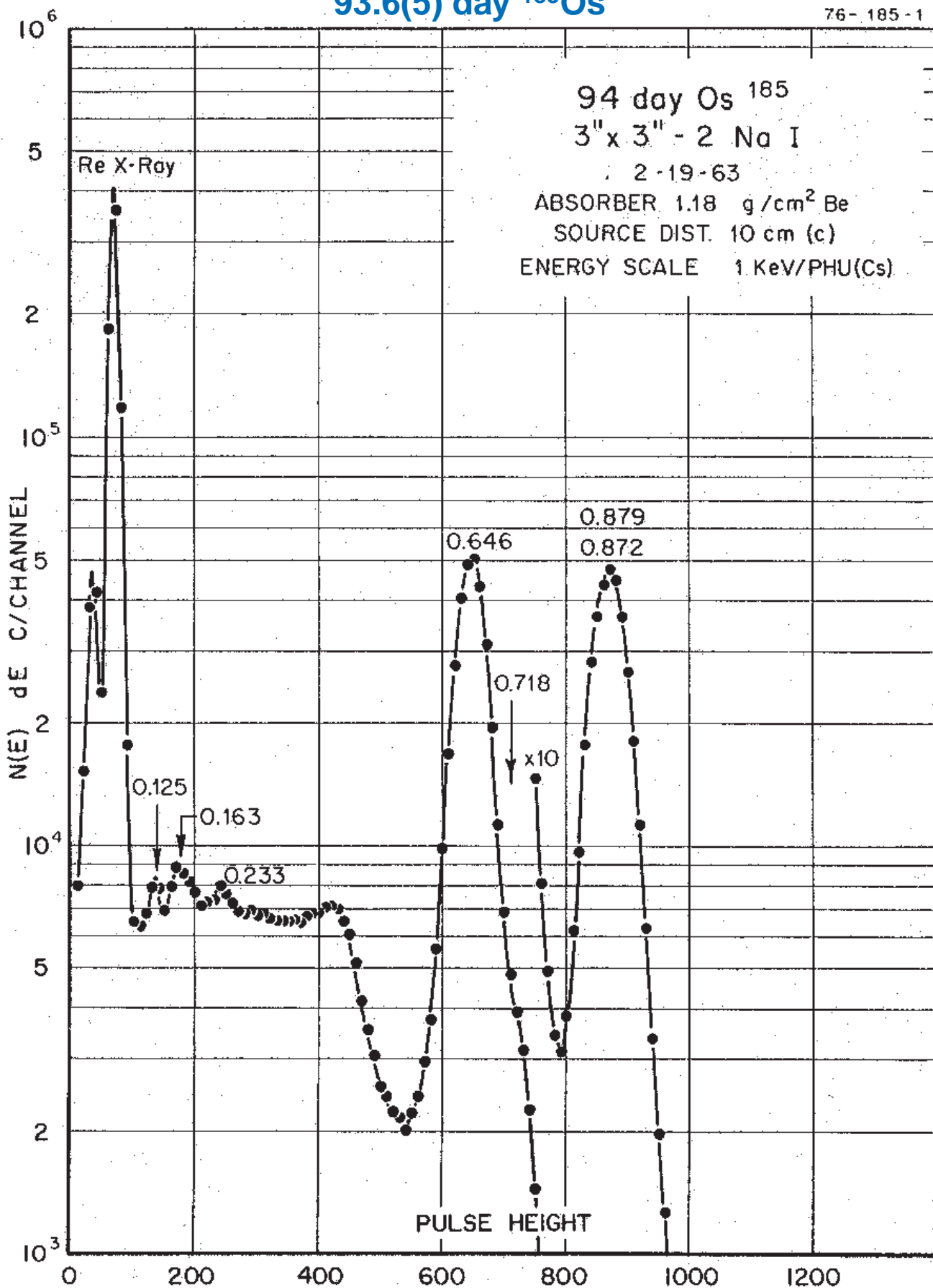
^{188}Re
3" x 3" Nal

Half Life 17.02(4) hr.
Method of Production: $^{187}\text{Re}(n,\gamma)$

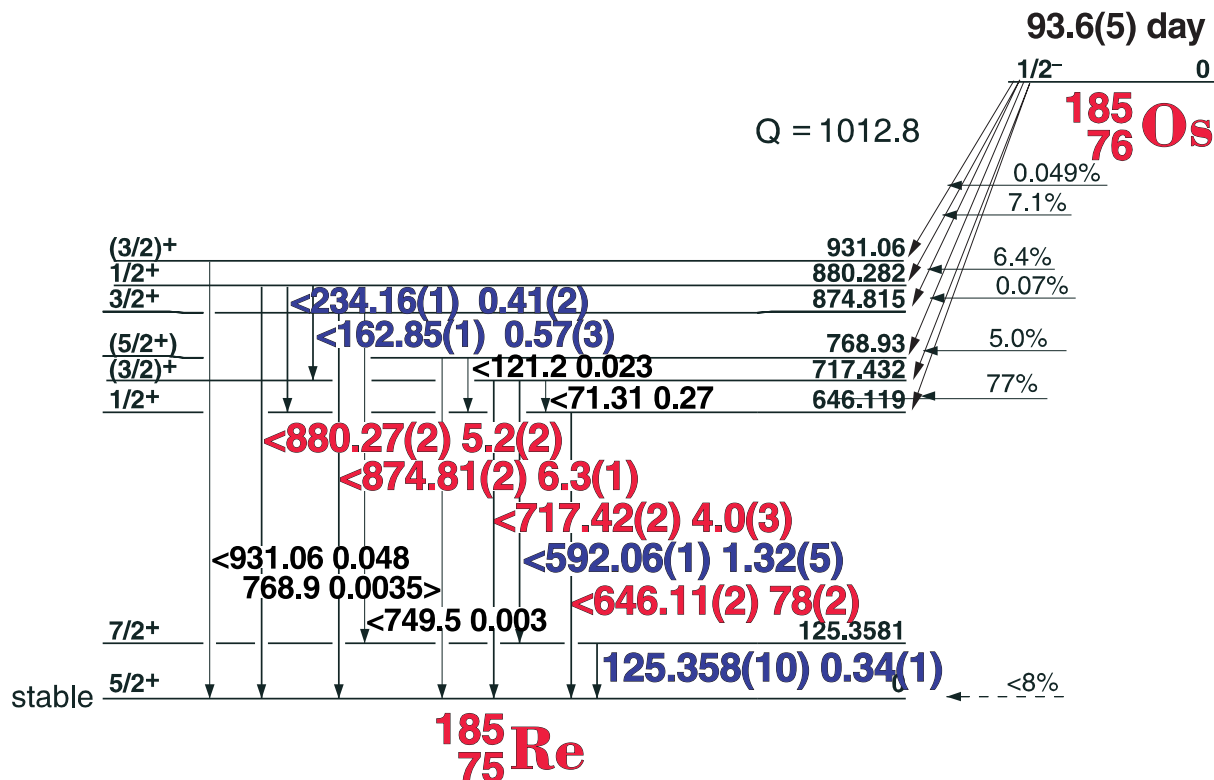
E_{γ} (KeV)[S]	ΔE_{γ}	I_{γ} (rel)	$I_{\gamma}(\%)[E]$	ΔI_{γ}	S
155.023	± 0.020	100	15.0	± 0.5	1
322.93	± 0.03	0.21	0.030	± 0.003	4
453.34	± 0.07	0.77	0.09	± 0.01	4
477.98	± 0.05	7.1	1.10	± 0.05	3
486.12	± 0.05	0.71	0.08	± 0.01	3
632.99	± 0.05	10.0	1.3	± 0.07	1
672.51	± 0.05	0.83	0.12	± 0.01	3
824.4	± 0.1	0.26	0.03	± 0.01	4
829.52	± 0.05	3.0	0.45	± 0.02	1
845.0	± 0.1	0.08	0.009	± 0.001	4
931.41	± 0.06	3.9	0.55	± 0.04	1
1132.40	± 0.07	0.59	0.084	± 0.006	3
1150.6	± 0.3	0.31	0.015	± 0.001	3
1174.6	± 0.1	0.13	0.018	± 0.002	4
1308.07	± 0.08	0.46	0.064	± 0.006	3
1323.0	± 0.1	0.10	0.015	± 0.001	4
1457.5	± 0.3	0.20	0.018	± 0.003	4
1610.28	± 0.05	0.66	0.096	± 0.006	1
1786.0	± 0.2	0.16	0.020	± 0.002	3
1802.0	± 0.2	0.24	0.040	± 0.002	2
1957.0	± 0.1	0.13	0.015	± 0.001	3

93.6(5) day ^{185}Os

76-185-1



93.6(5) day ^{185}Os



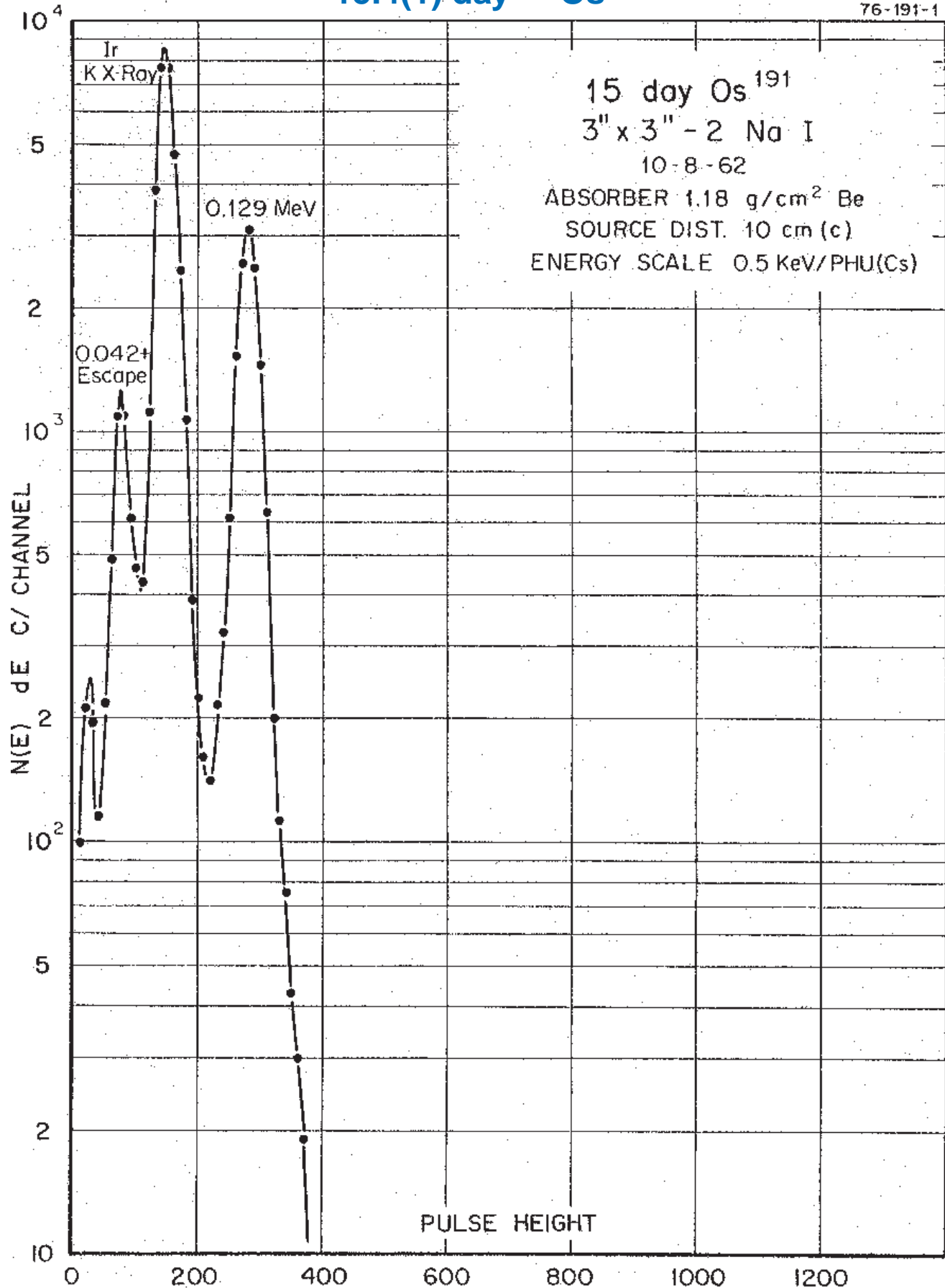
GAMMA-RAY ENERGIES AND INTENSITIES

Nuclide ^{186}Os Half Life 93.6(5) day
Detector 3" x 3" NaI Method of Production: $^{184}\text{Os}(n,\gamma)$

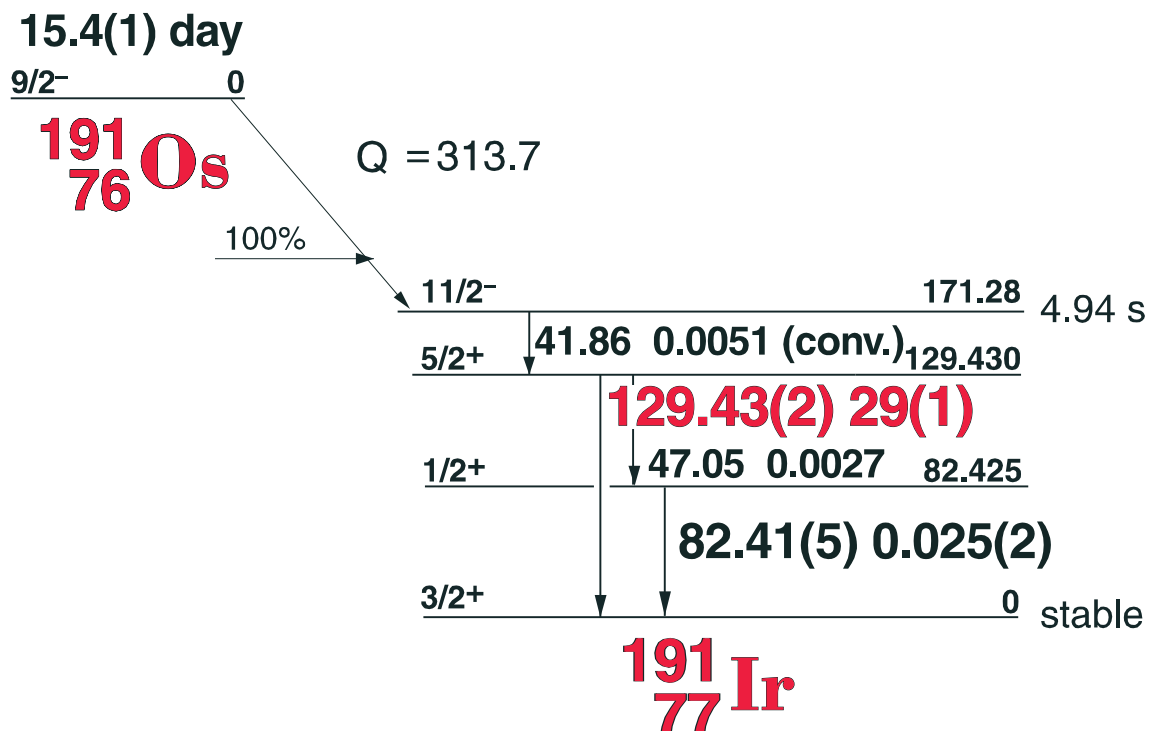
E_γ (KeV)[S]	ΔE_γ	I_γ (rel)	I_γ (%) [E]	ΔI_γ	S
Re x-rays					
125.358	± 0.010	0.42	0.34	± 0.01	1
162.854	± 0.010	0.69	0.57	± 0.03	3
234.160	± 0.010	0.51	0.41	± 0.02	4
592.061	± 0.014	1.61	1.32	± 0.05	3
646.115	± 0.020	100	78	± 2.0	1
717.419	± 0.018	5.32	4.0	± 0.30	1
874.814	± 0.023	8.24	6.3	± 0.10	1
880.272	± 0.022	6.69	5.2	± 0.20	1

15.4(1) day ^{191}Os

76-191-1



15.4(1) day ^{191}Os



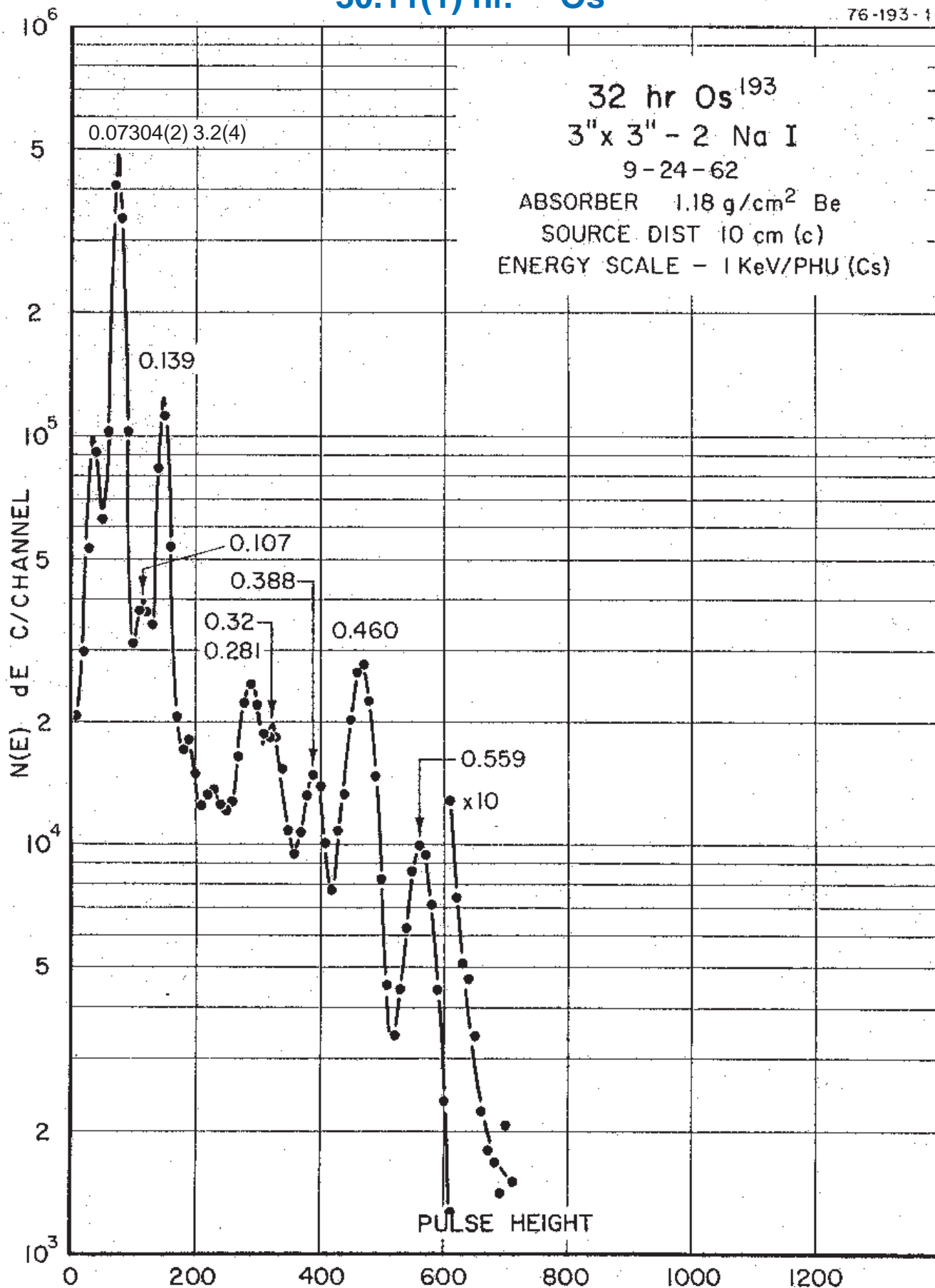
GAMMA-RAY ENERGIES AND INTENSITIES

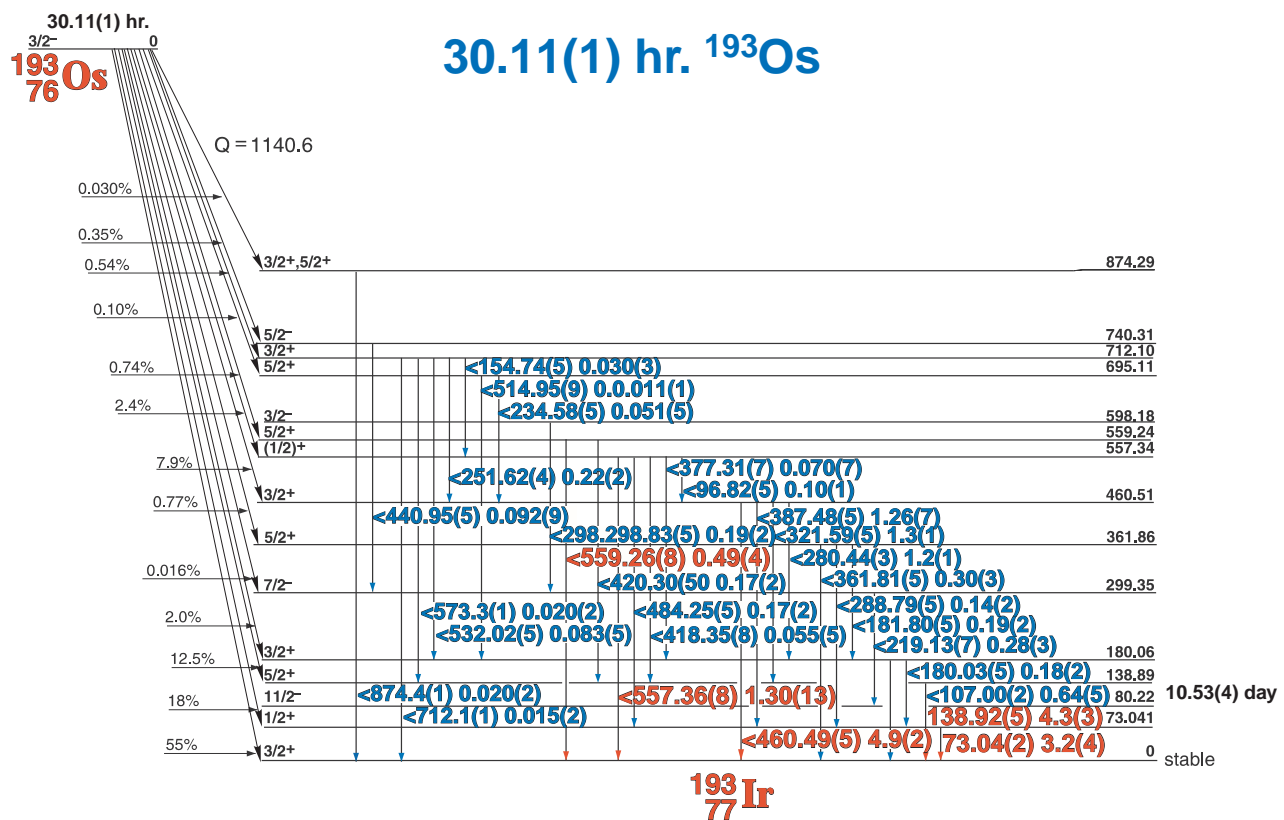
Nuclide ^{191}Os Half Life 15.4(1) day
 Detector 3" x 3" NaI Method of Production: $^{199}\text{Os}(n,\gamma)$

E_γ (KeV)[S]	ΔE_γ	I_γ (rel)	$I_\gamma(\%)$ [E]	ΔI_γ	S
Os & Ir	x-rays				
41.86	± 0.05		0.005	$\pm 0.(1)$	4
82.41	± 0.05		0.025	± 0.002	4
129.427	± 0.015		29	± 1.0	1

30.11(1) hr. ^{193}Os

76-193-1





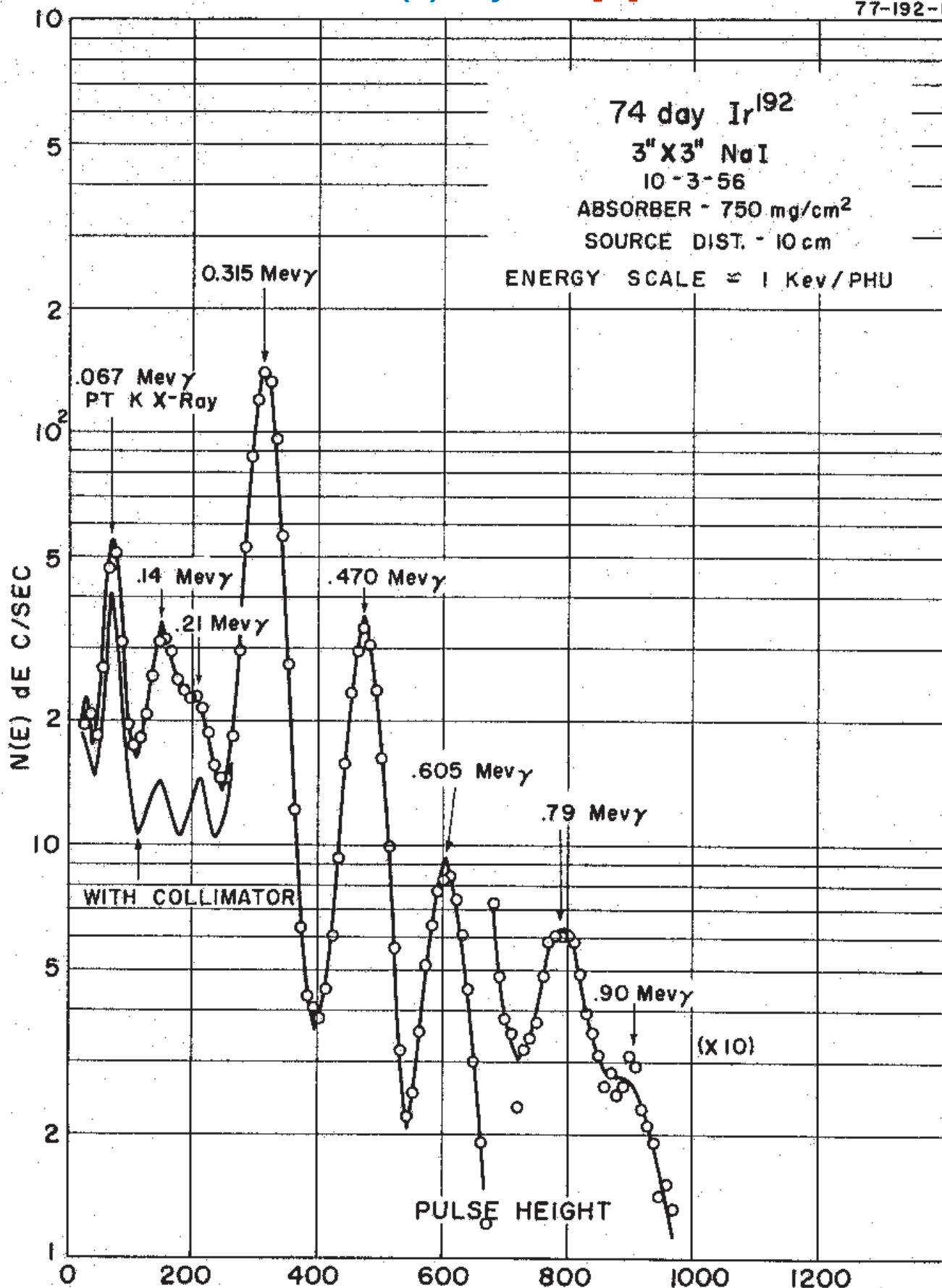
GAMMA-RAY ENERGIES AND INTENSITIES

Nuclide ^{193}Os Half Life 30.11(1) hr.
Detector 3" x 3" NaI Method of Production: $^{192}\text{Os}(n,\gamma)$

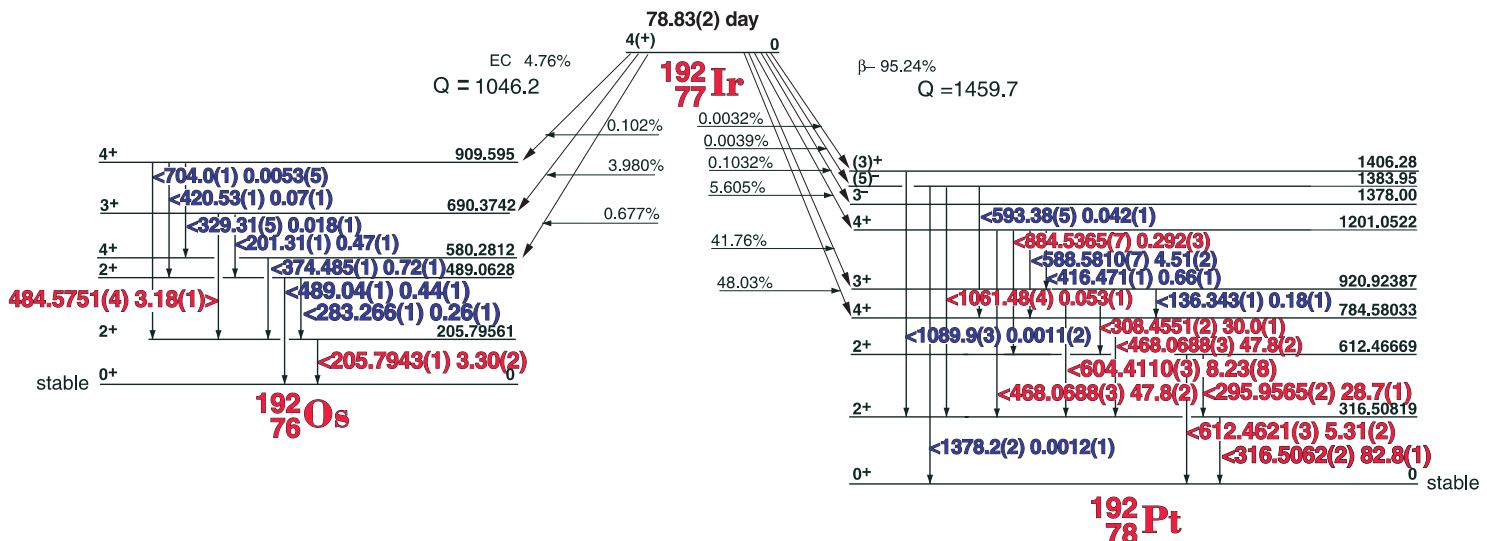
E_γ (KeV)[S]	ΔE_γ	I_γ (rel)	I_γ (%)[E]	ΔI_γ	S
Ir	x-rays				
73.04	± 0.03		3.2	± 0.04	1
96.82	± 0.05		0.10	± 0.01	4
107.00	± 0.02		0.64	± 0.05	3
138.92	± 0.05		4.3	± 0.3	1
180.03	± 0.05		0.18	± 0.02	3
181.80	± 0.05		0.19	± 0.02	3
219.13	± 0.07		0.028	± 0.03	3
280.44	± 0.03		1.2	± 0.1	2
288.79	± 0.05		0.14	± 0.02	3
298.83	± 0.05		0.19	± 0.02	3
361.81	± 0.05		0.30	± 0.03	3
377.31	± 0.07		0.070	± 0.007	3
387.48	± 0.05		1.26	± 0.07	2
418.35	± 0.05		0.055	± 0.005	4
420.30	± 0.05		0.17	± 0.02	3
298.83	± 0.05		0.19	± 0.02	3
440.95	± 0.05		0.092	± 0.09	4
460.49	± 0.05		4.9	± 0.2	1
484.25	± 0.05		0.17	± 0.02	3
514.95	± 0.09		0.11	± 0.01	3
532.02	± 0.05		0.083	± 0.005	4
557.36	± 0.08		1.30	± 0.13	1
559.26	± 0.08		0.49	± 0.13	1
573.3	± 0.1		0.020	± 0.002	4
712.1	± 0.1		0.015	± 0.002	4
874.4	± 0.1		0.020	± 0.002	3

73.83(2) day ^{192}Ir [C]

77-192-1



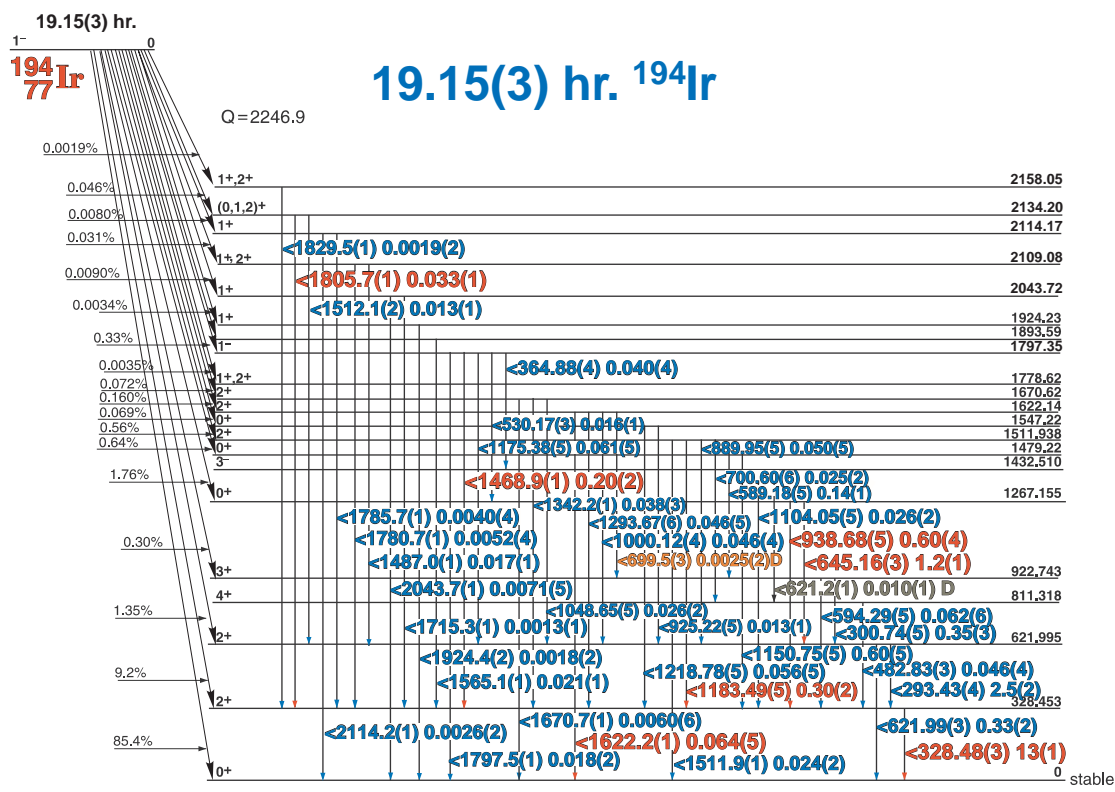
73.83(2) day ^{192}Ir [C]



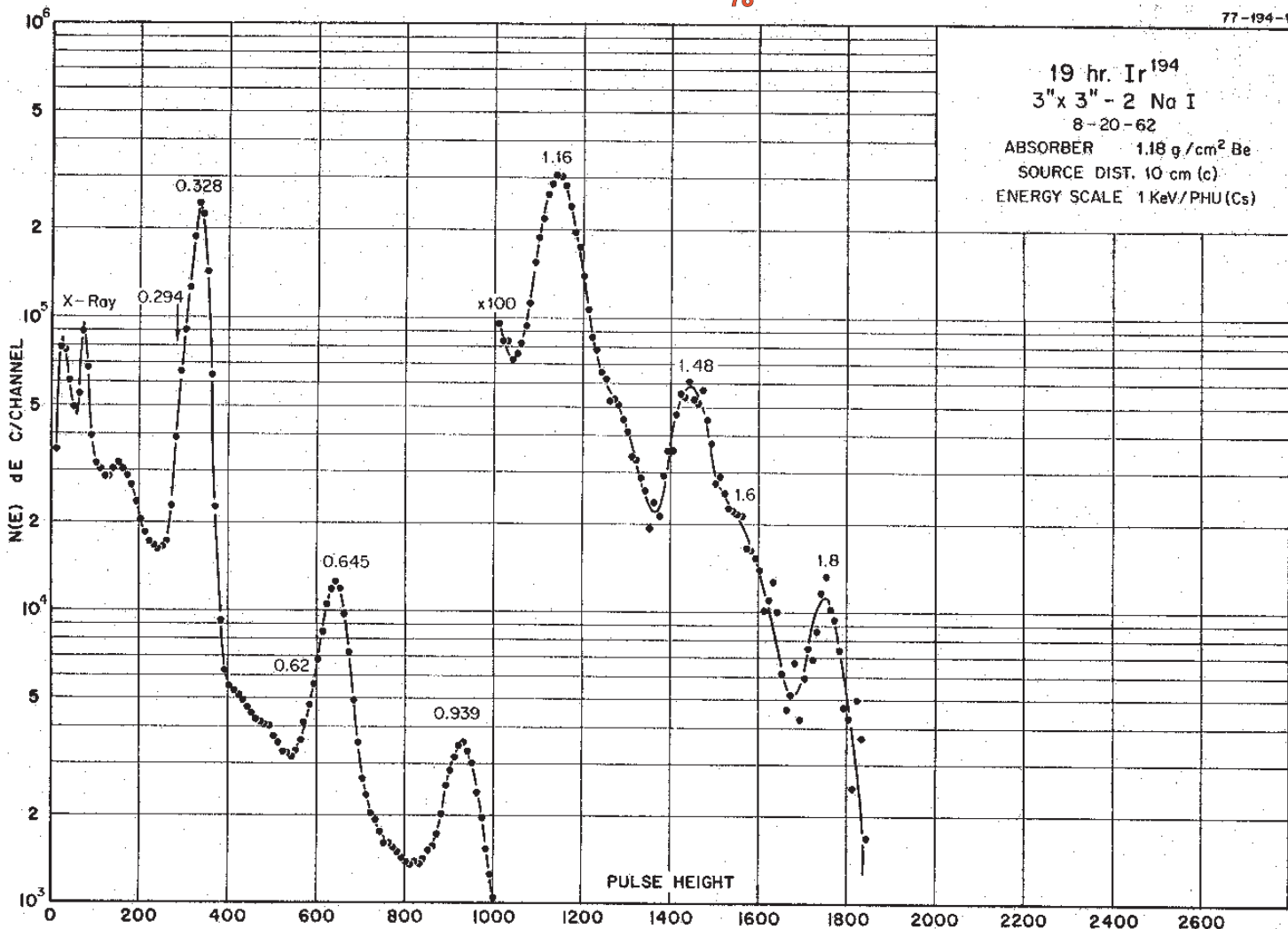
GAMMA-RAY ENERGIES AND INTENSITIES [C]

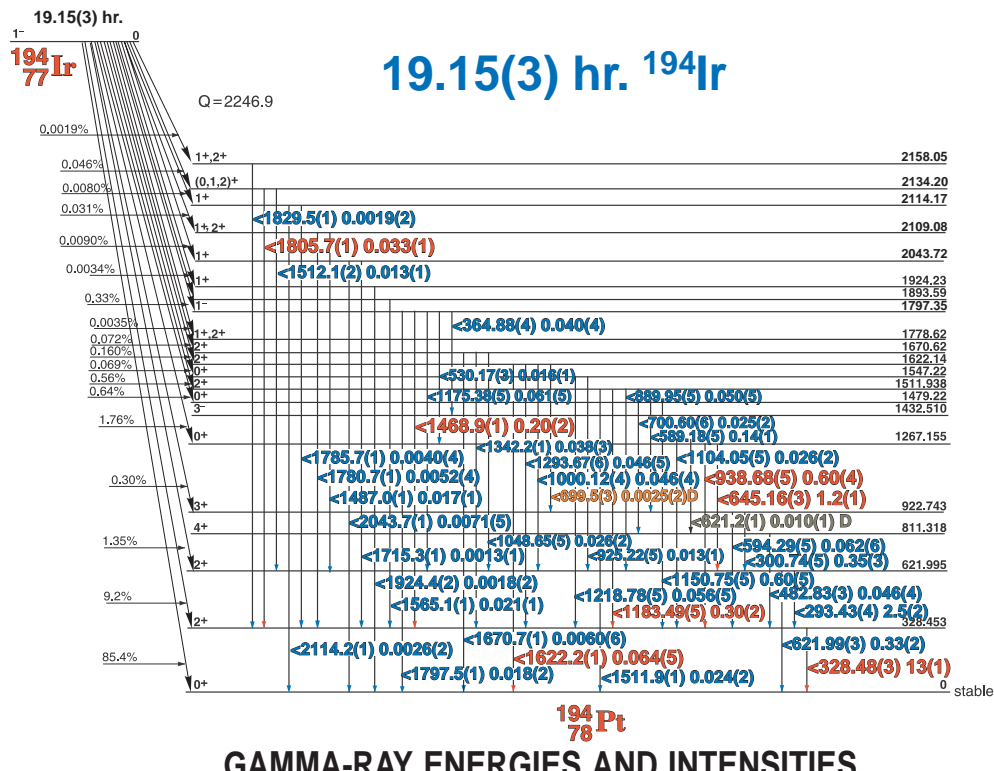
Nuclide ^{192}Ir Half Life 73.83(2) day
Detector 3" x 3" NaI Method of Production: $^{191}\text{Ir}(n,\gamma)$

E_{γ} (KeV) [C]	ΔE_{γ}	I_{γ} (rel)	$I_{\gamma}(\%)$ [C]	ΔI_{γ}	S
136.343	± 0.001	0.218	0.18	± 0.010	4
201.31	± 0.01	0.551	0.47	± 0.012	4
205.7943	± 0.001	3.86	3.30	± 0.02	2
283.266	± 0.001	0.320	0.26	± 0.008	4
295.9565	± 0.0002	34.64	28.7	± 0.1	1
308.4551	± 0.0001	35.77	30.0	± 0.1	1
316.5062	± 0.0002	100	82.8	± 0.1	1
329.31	± 0.05	0.019	0.018	± 0.001	4
374.485	± 0.001	0.875	0.72	± 0.01	3
416.471	± 0.001	0.802	0.66	± 0.01	3
420.53	± 0.01	0.070	0.07	± 0.006	4
468.0688	± 0.0003	58.0	47.8	± 0.2	1
484.5751	± 0.0001	3.81	3.18	± 0.01	1
489.04	± 0.04	0.480	0.44	± 0.010	3
588.5810	± 0.0007	5.52	4.51	± 0.02	1
593.38	± 0.05	0.045	0.042	± 0.001	4
604.4110	± 0.0003	10.04	8.23	± 0.08	1
612.4621	± 0.0003	6.55	5.31	± 0.02	1
704.0	± 0.1	0.007	0.0053	± 0.0005	4
884.5365	± 0.0007	0.364	0.293	± 0.002	1
1061.48	± 0.04	0.067	0.053	± 0.001	1
1089.9	± 0.3	0.002	0.0011	± 0.0002	4
1378.2	± 0.2	0.0015	0.0012	± 0.0001	3



^{194}Pt





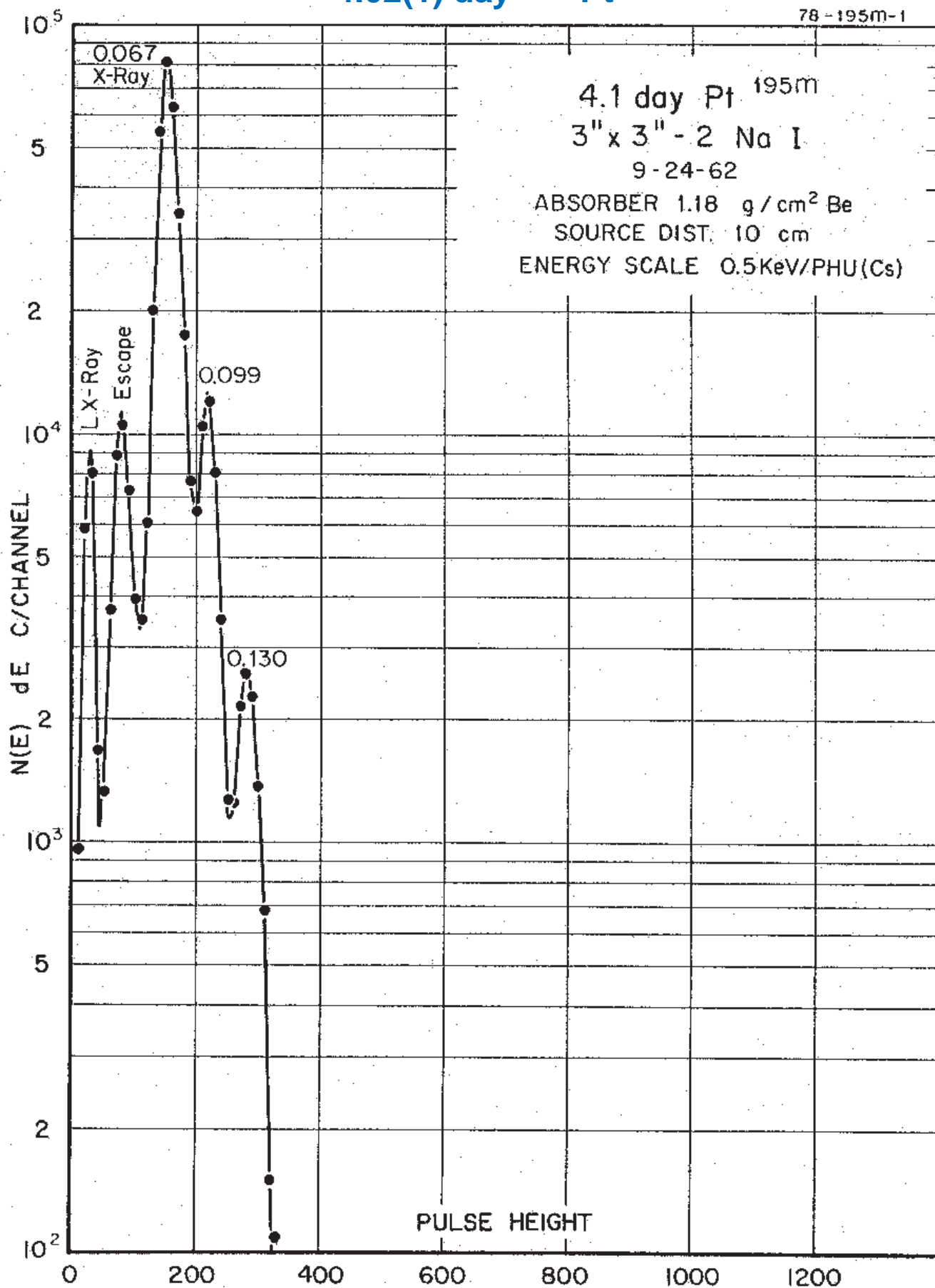
GAMMA-RAY ENERGIES AND INTENSITIES

Nuclide ^{194}Ir Half Life 19.15(3) hr.
 Detector 3" x 3" NaI Method of Production: $^{193}\text{Ir}(n,\gamma)$

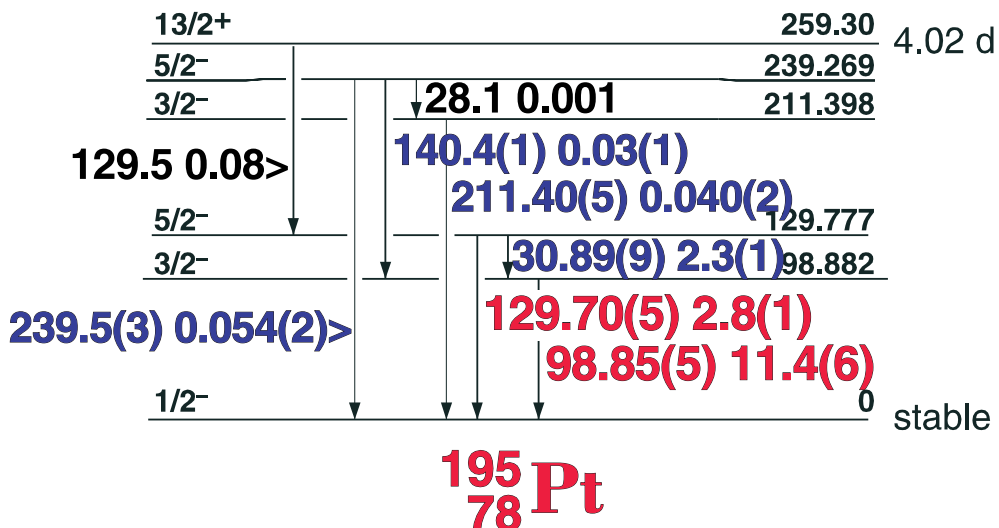
E_{γ} (KeV)[S]	ΔE_{γ}	$I_{\gamma}(\text{rel})$	$I_{\gamma}(\%)[E]$	ΔI_{γ}	S
293.435	± 0.040	18.1	2.5	± 0.2	3
300.74	± 0.05		0.35	± 0.04	4
328.501	± 0.030	100	13	± 1.0	1
364.88	± 0.04	0.32	0.04	± 0.04	4
530.17	± 0.04	0.15	0.016	± 0.002	4
621.2	± 0.1		0.010	± 0.001	4
621.99	± 0.035	2.52	0.33	± 0.02	3
645.162	± 0.030	9.14	1.2	± 0.1	1
700.60	± 0.06	0.21	0.025	± 0.002	4
889.95	± 0.05	0.39	0.050	± 0.005	4
925.22	± 0.05	0.08	0.013	± 0.001	4
938.68	± 0.05	4.56	0.60	± 0.05	1
1000.12	± 0.05	0.38	0.046	± 0.004	3
1048.65	± 0.05	0.20	0.026	± 0.002	4
1104.05	± 0.05	0.23	0.025	± 0.002	4
1150.75	± 0.05	4.69	0.60	± 0.05	1
1175.38	± 0.05	0.43	0.061	± 0.005	3
1183.49	± 0.05	2.42	0.30	± 0.02	1
1218.78	± 0.05	0.45	0.056	± 0.005	3
1293.67	± 0.05	0.34	0.046	± 0.005	3
1342.6	± 0.1	0.32	0.038	± 0.003	3
1468.9	± 0.1	1.53	0.20	± 0.02	1
1487.0	± 0.1	0.16	0.017	± 0.002	3
1511.9	± 0.1	0.31	0.024	± 0.002	2
1565.1	± 0.1	0.20	0.021	± 0.002	2
1622.2	± 0.1	0.50	0.064	± 0.005	1
1670.7	± 0.1	0.05	0.0060	± 0.0006	4
1715.3	± 0.1	0.010	0.0013	± 0.0001	4
1780.7	± 0.1	0.05	0.0052	± 0.0005	3
1785.7	± 0.1	0.04	0.0040	± 0.0004	4
1797.5	± 0.1	0.14	0.018	± 0.002	2
1805.7	± 0.1	0.24	0.033	± 0.002	1
1829.5	± 0.1	0.02	0.0019	± 0.0002	4
1924.4	± 0.2	0.02	0.0018	± 0.0002	4
2043.7	± 0.1	0.06	0.0071	± 0.0005	2

4.02(1) day ^{195m}Pt

78 - 195m-1



4.02(1) day ^{195m}Pt



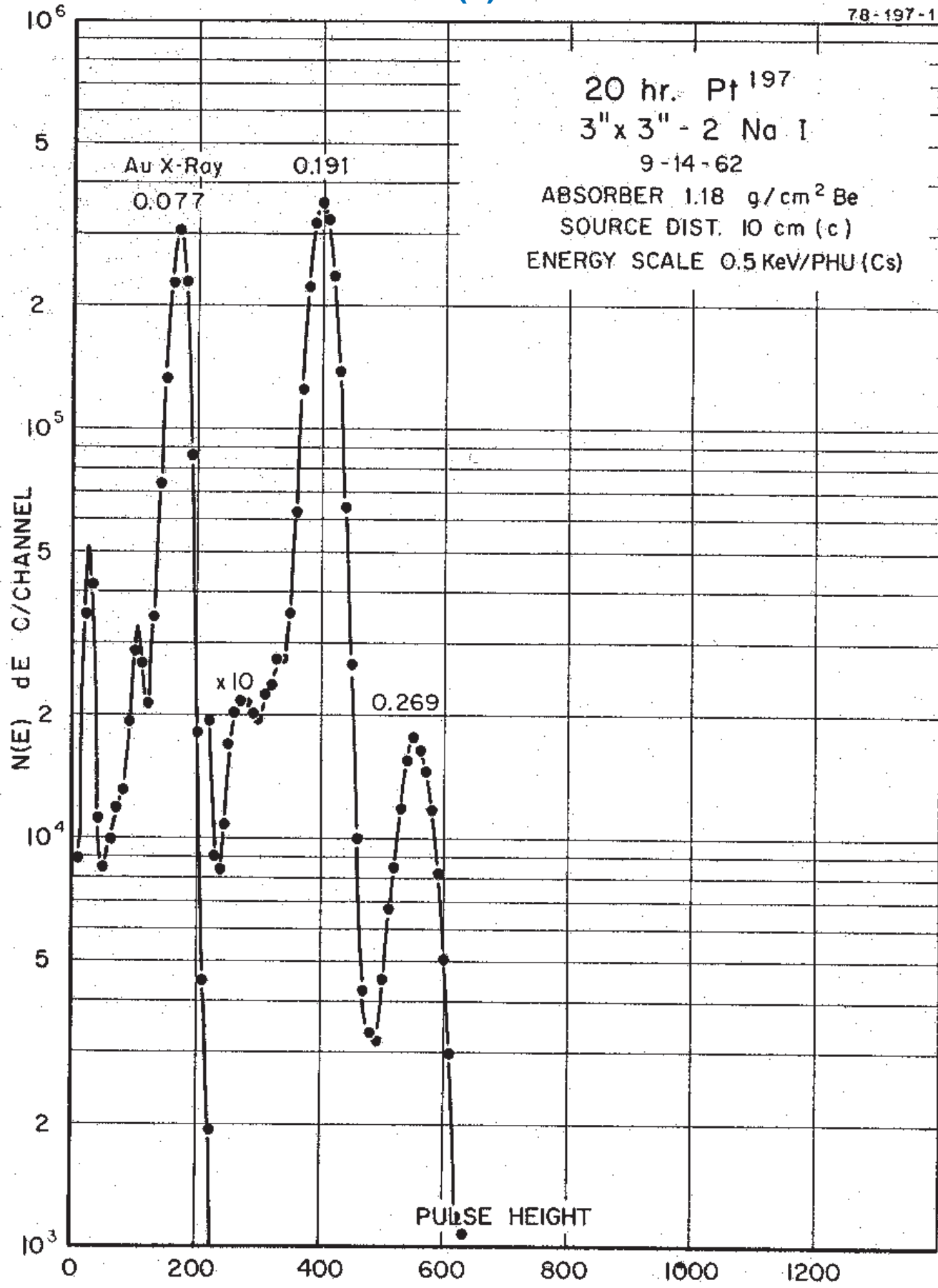
GAMMA-RAY ENERGIES AND INTENSITIES

Nuclide ^{195m}Pt Half Life 4.02(1) day
 Detector 3" x 3" NaI Method of Production: $^{194}\text{Pt}(n,\gamma)$

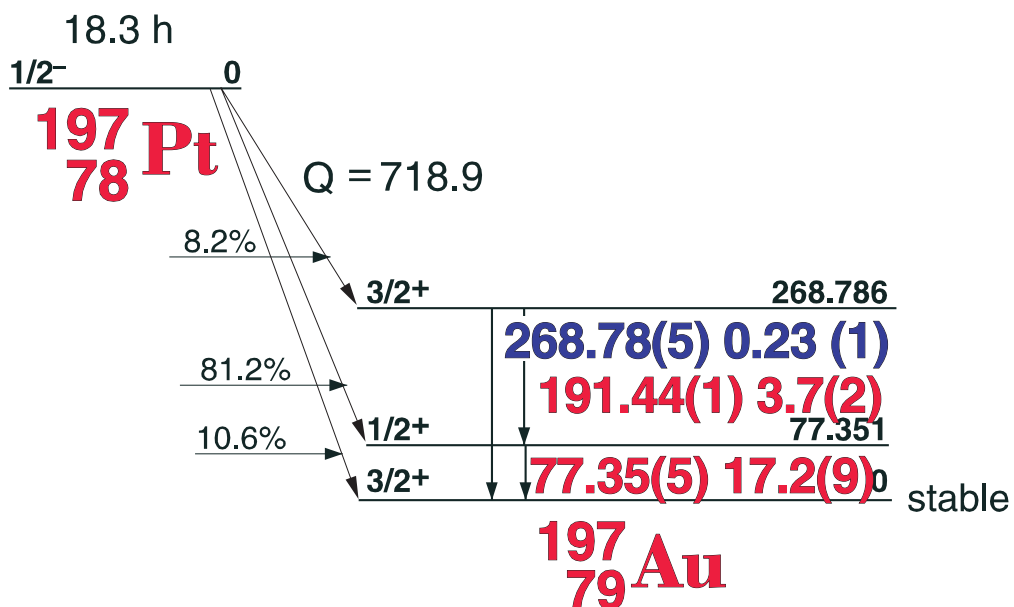
E_γ (KeV)[S]	ΔE_γ	I_γ (rel)	$I_\gamma(\%)$ [E]	ΔI_γ	S
195mPt					
98.85	± 0.10	100	11.4	± 0.6	1
129.427	± 0.05	38.25	2.8	± 0.1	1
140.4	± 0.1		0.03	± 0.01	3
211.40	± 0.05		0.040	± 0.02	4
239.5	± 0.3		0.054	± 0.002	4

19.891(2) hr. ^{197}Pt

78-197-1



19.891(2) hr. ^{197}Pt

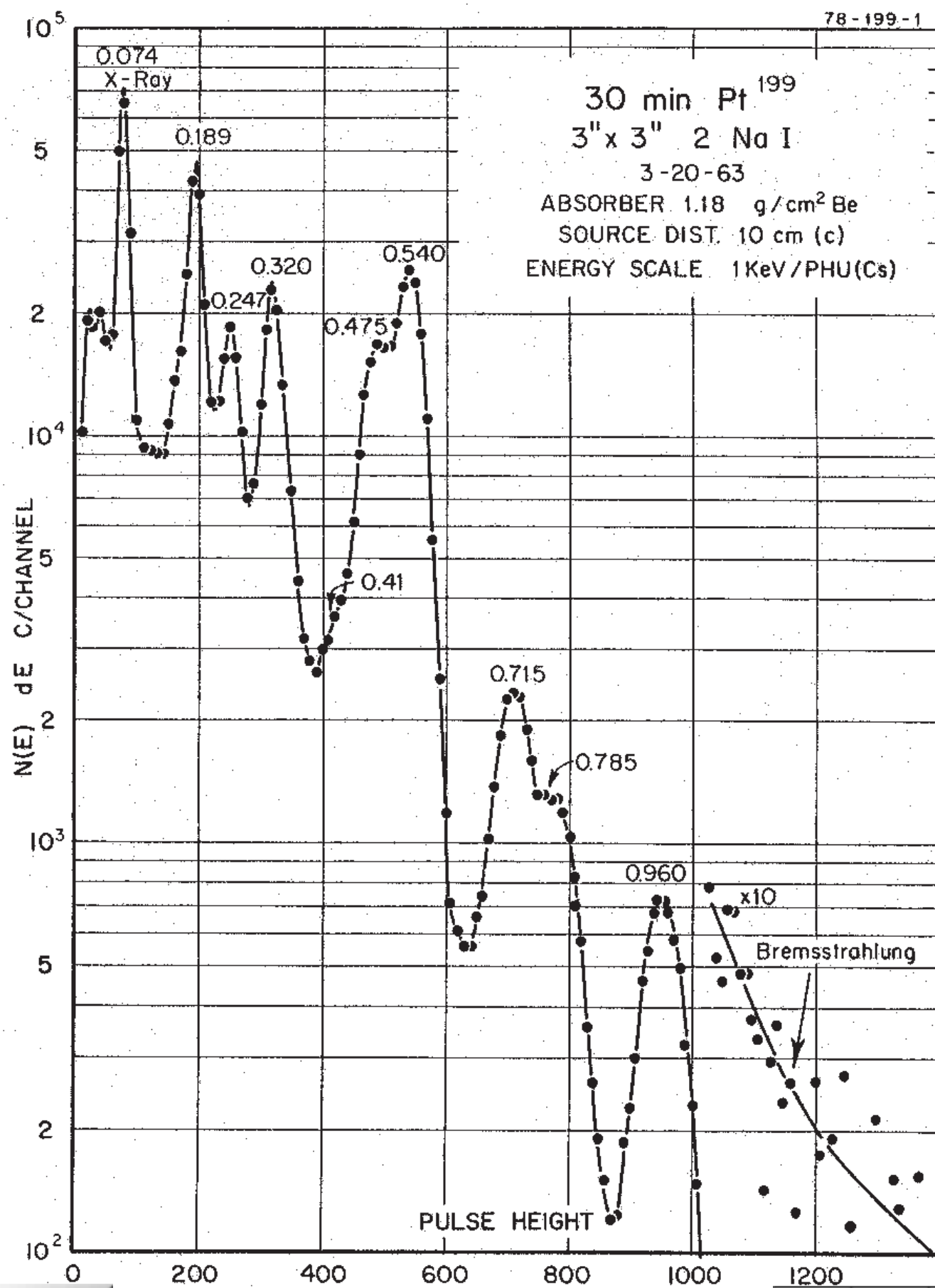


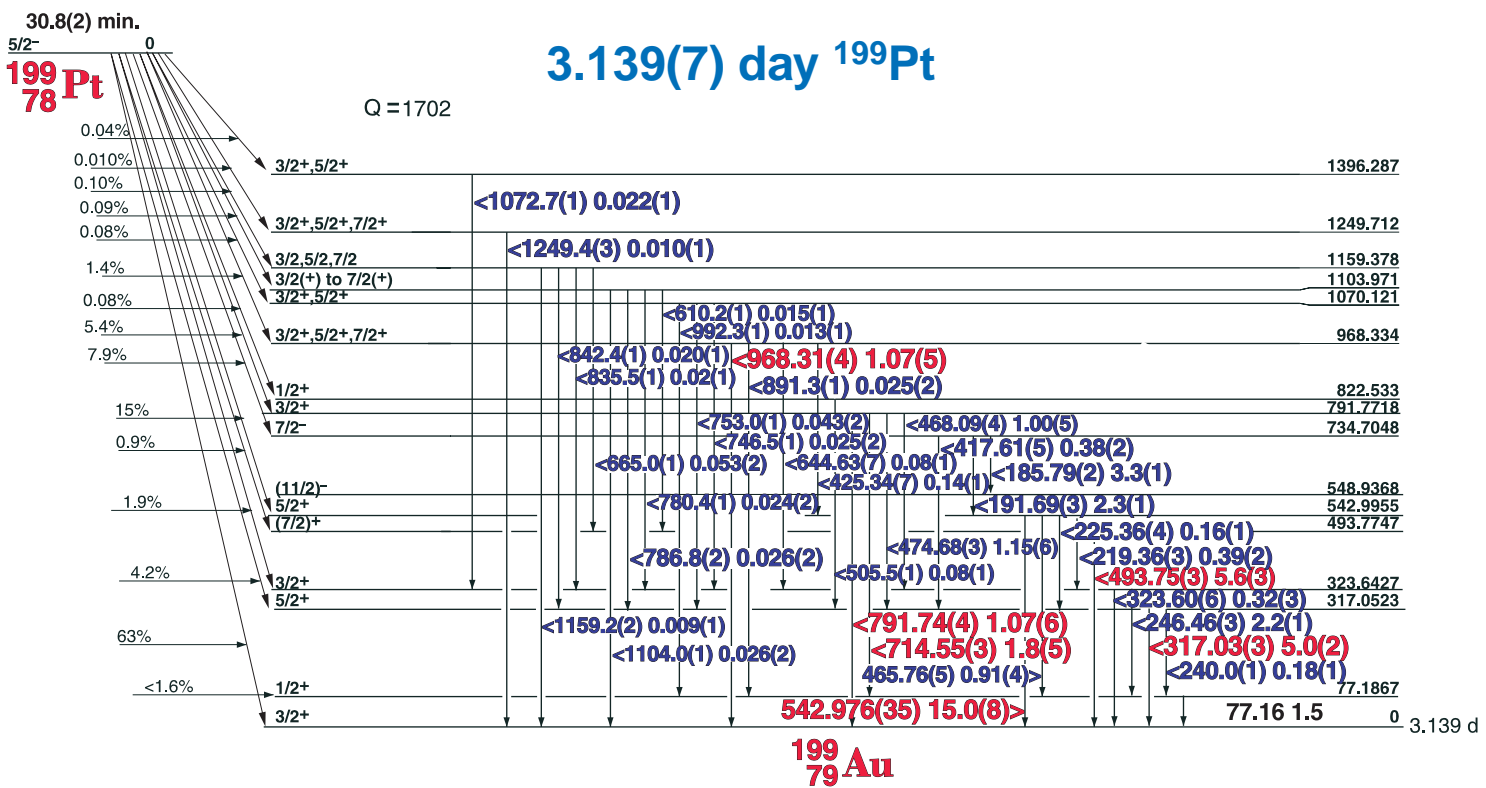
GAMMA-RAY ENERGIES AND INTENSITIES

Nuclide ^{195m}Pt Half Life 4.02(1) day
Detector 3" x 3" NaI Method of Production: $^{194}\text{Pt}(n,\gamma)$

E_γ (KeV)[S]	ΔE_γ	I_γ (rel)	$I_\gamma(\%)$ [E]	ΔI_γ	S
77.35	± 0.05	100	17.2	± 0.9	1
191.44	± 0.01	32	3.7	± 0.2	1
268.78	± 0.05		0.23	± 0.01	3

3.139(7) day ^{199}Pt





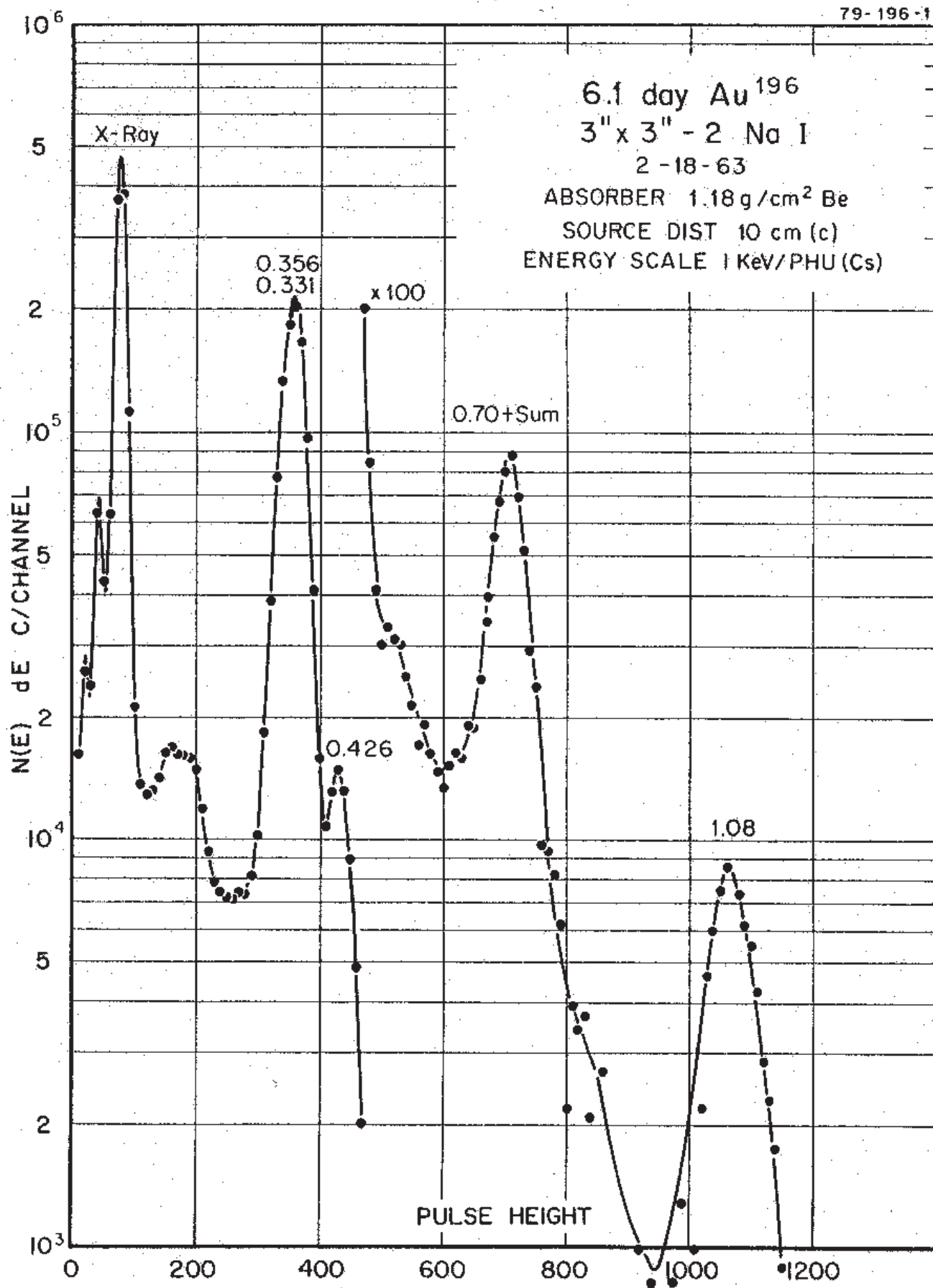
GAMMA-RAY ENERGIES AND INTENSITIES

199Pt Half Life 3.139(7) day
3" x 3" NaI Method of Production: $^{198}\text{Pt}(n,\gamma)$

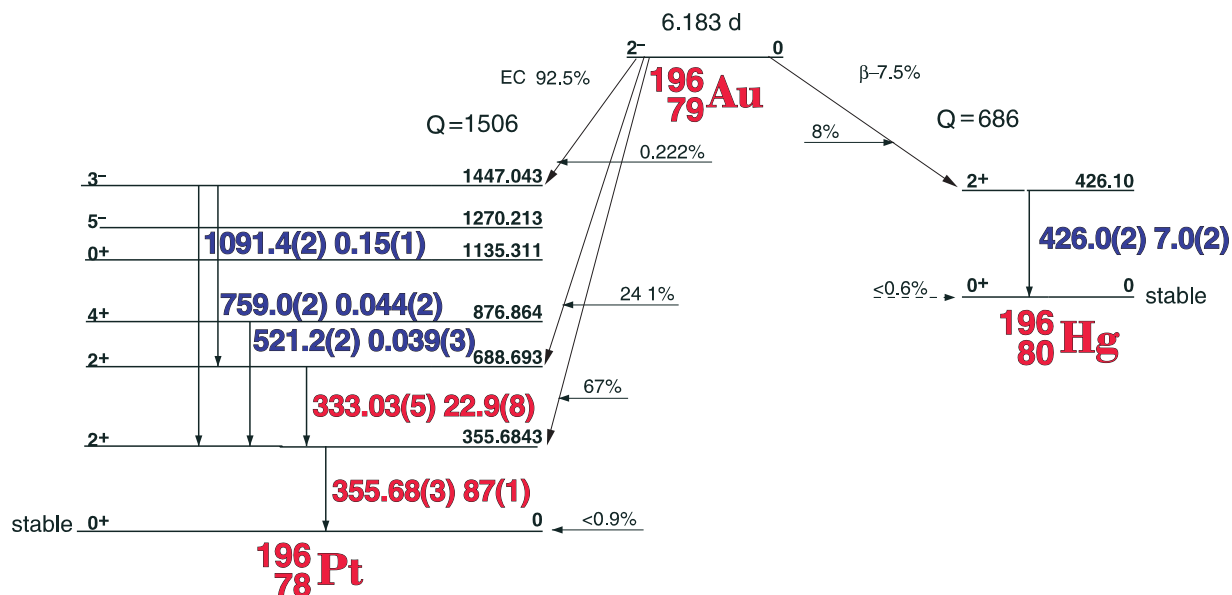
E_{γ} (KeV)[S]	ΔE_{γ}	$I_{\gamma}(\text{rel})$	$I_{\gamma}(\%)$ [E]	ΔI_{γ}	S
185.795	± 0.025	22.0	3.3	± 0.1	2
191.692	± 0.028	16.1	2.3	± 0.1	2
219.360	± 0.035	2.62	0.38	± 0.2	3
225.36	± 0.04	1.04	0.16	± 0.01	4
240.01	± 0.06	1.22	0.18	± 0.01	4
246.46	± 0.03	14.60	2.2	± 0.10	2
317.029	± 0.035	32.9	5.0	± 0.20	1
323.60	± 0.06	1.68	0.32	± 0.02	4
417.61	± 0.05	2.64	0.38	± 0.02	3
425.34	± 0.07	1.18	0.14	± 0.01	4
465.76	± 0.050	6.30	0.91	± 0.04	2
468.09	± 0.045	6.70	1.00	± 0.05	2
474.68	± 0.035	7.80	1.15	± 0.06	2
493.748	± 0.030	38.67	5.6	± 0.3	1
505.5	± 0.1		0.08	± 0.01	3
542.976	± 0.035	100	15.0	± 0.2	1
644.63	± 0.07	0.60	0.08	± 0.01	3
665.0	± 0.10	0.41	0.053	± 0.002	4
714.553	± 0.035	12.65	1.80	± 0.09	1
746.4	± 0.20	0.26	0.025	± 0.002	4
753.0	± 0.1	0.30	0.043	± 0.002	4
780.4	± 0.1	0.25	0.024	± 0.002	4
786.8	± 0.2	0.23	0.026	± 0.002	4
791.745	± 0.040	7.24	1.07	± 0.06	1
835.5	± 0.12	0.14	0.02	± 0.01	4
842.4	± 0.15	0.13	0.020	± 0.001	4
891.3	± 0.15	0.16	0.025	± 0.002	4
968.315	± 0.045	7.36	1.07	± 0.05	1
1072.7	± 0.15	0.12	0.022	± 0.001	3
1104.0	± 0.2	0.17	0.026	± 0.002	3
1159.23	± 0.5	0.05	0.009	± 0.001	4
1249.4	± 0.3	0.06	0.010	± 0.001	4

6.18(1) day ^{196}Au

79-196-1



6.18(1) day ^{196}Au



GAMMA-RAY ENERGIES AND INTENSITIES

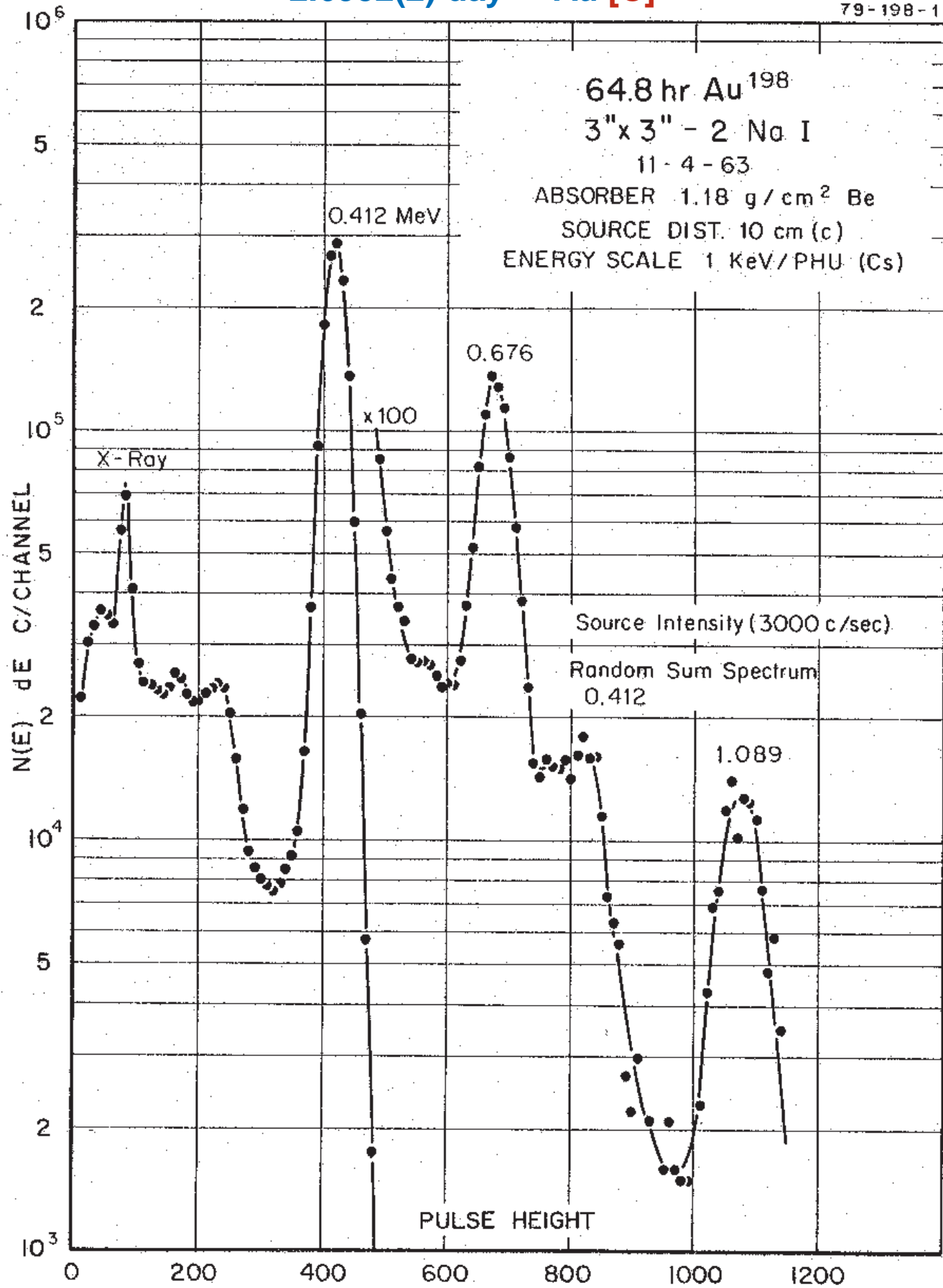
Nuclide ^{196}Au
Detector 3" x 3" NaI

Half Life 6.18(1) day
Method of Production: $^{197}\text{Au}(\gamma, n)$

E_γ (KeV)[S]	ΔE_γ	I_γ (rel)	$I_\gamma(\%)$ [E]	ΔI_γ	S
Pt K x-rays					
333.03	± 0.05		22.9	± 0.8	1
355.68	± 0.03		87	± 1.0	1
426.0	± 0.2		7.0	± 0.2	1
521.2	± 0.2		0.039	± 0.003	3
759.0	± 0.2		0.044	± 0.002	3
1091.4	± 0.2		0.15	± 0.01	2

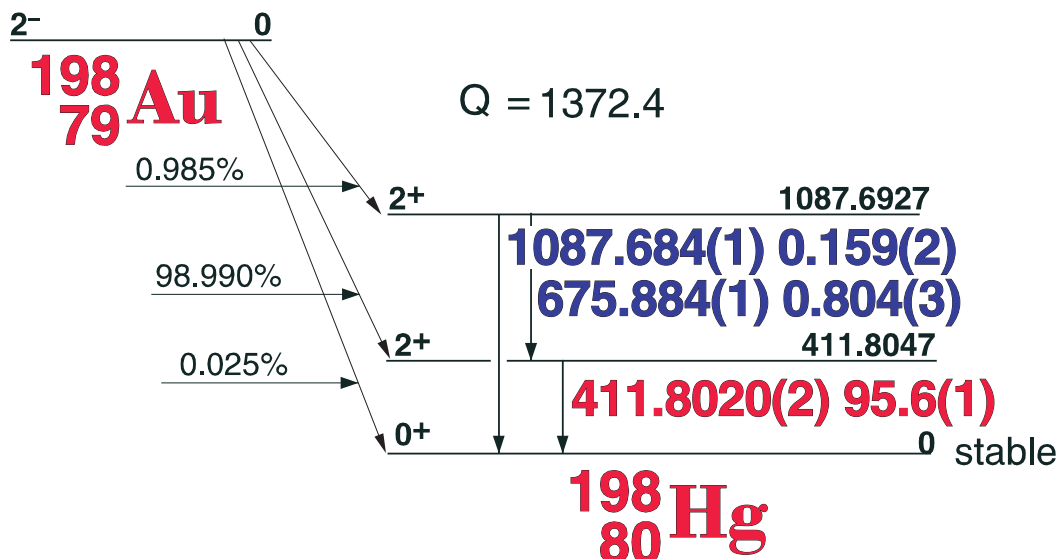
2.6952(2) day ^{198}Au [C]

79-198-1



2.6952(2) day ^{198}Au [C]

2.6952(2) day



GAMMA-RAY ENERGIES AND INTENSITIES [C]

Nuclide ^{198}Au Half Life 2.6952(2) day
Detector 3" x 3" NaI Method of Production: $^{197}\text{Au}(n,\gamma)$

E_γ (KeV) [C]	ΔE_γ	I_γ (rel)	I_γ (%) [C]	ΔI_γ	S
Hg K x-rays					
411.8020	± 0.0002	100	95.6	± 0.1	1
675.884	± 0.001		0.804	± 0.003	2
1087.684	± 0.001		0.159	± 0.002	2

3.139(7) day ^{199}Au

79-199-2

3.2 day Au 199

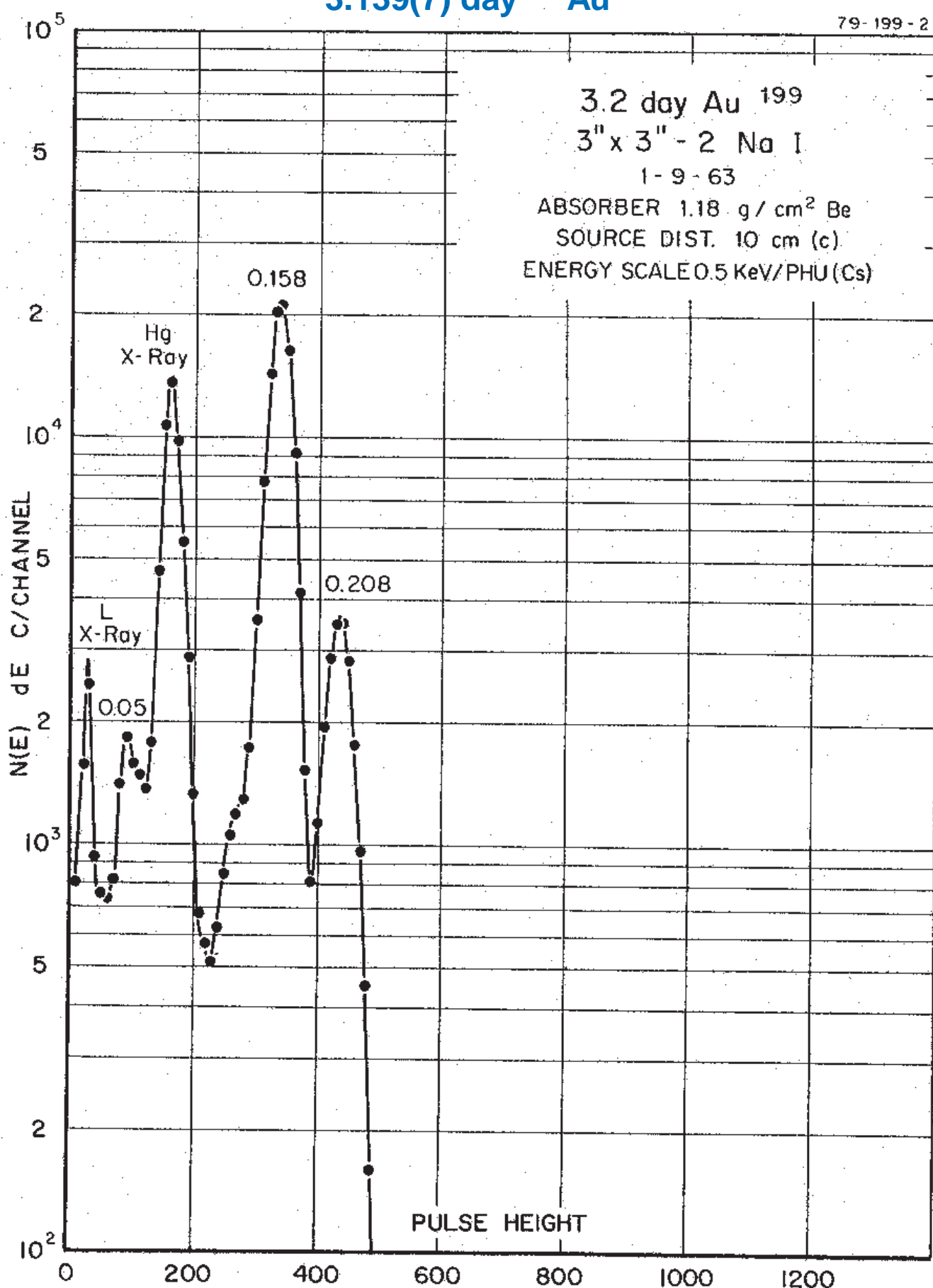
3" x 3" - 2 No I

1-9-63

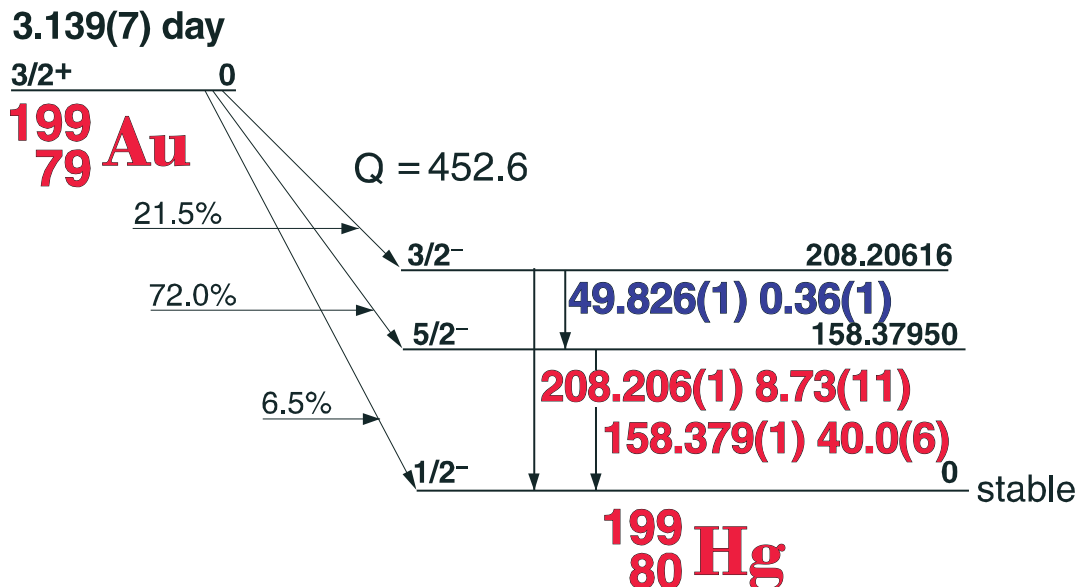
ABSORBER 1.18 g / cm² Be

SOURCE DIST. 10 cm (c)

ENERGY SCALE 0.5 KeV/PHU (Cs)



3.139(7) day ^{199}Au



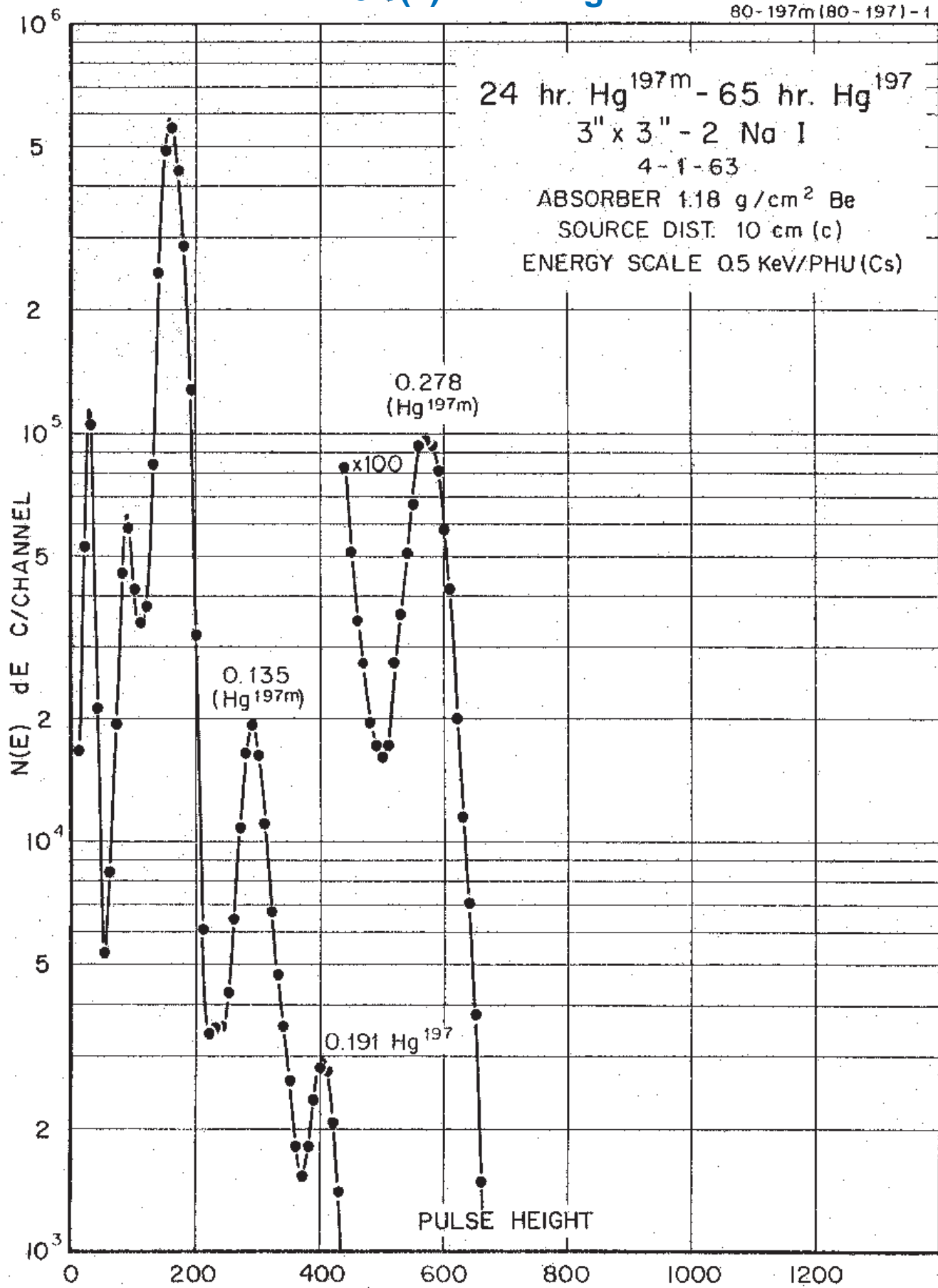
GAMMA-RAY ENERGIES AND INTENSITIES

Nuclide ^{199}Au Half Life 3.139(7) day
Detector 3" x 3" NaI Method of Production: $^{198}\text{Pt}(n,\gamma,\beta)$

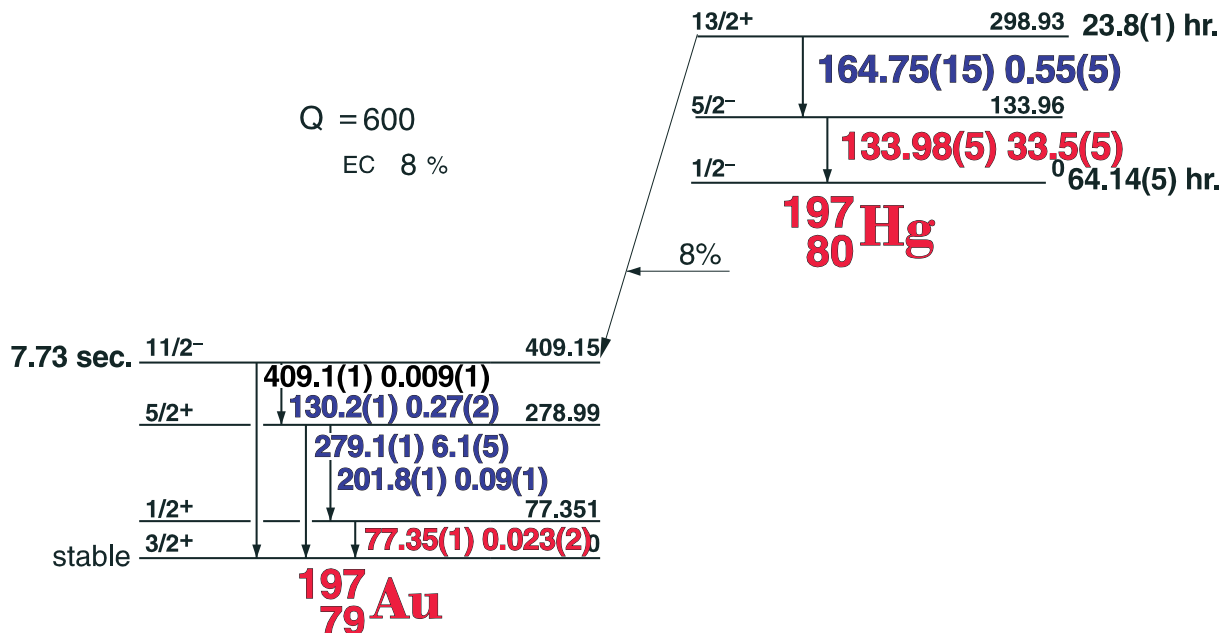
E_{γ} (KeV)[S]	ΔE_{γ}	$I_{\gamma}(\text{rel})$	$I_{\gamma}(\%)$ [E]	ΔI_{γ}	S
Hg x-rays					
49.826	± 0.001		0.36	± 0.01	3
158.379	± 0.001	100	40.0	± 0.6	1
208.206	± 0.001	23.42	8.73	± 0.11	1

23.8(1) hr. ^{197m}Hg

80-197m (80-197)-1



23.8(1) hr. ^{197m}Hg



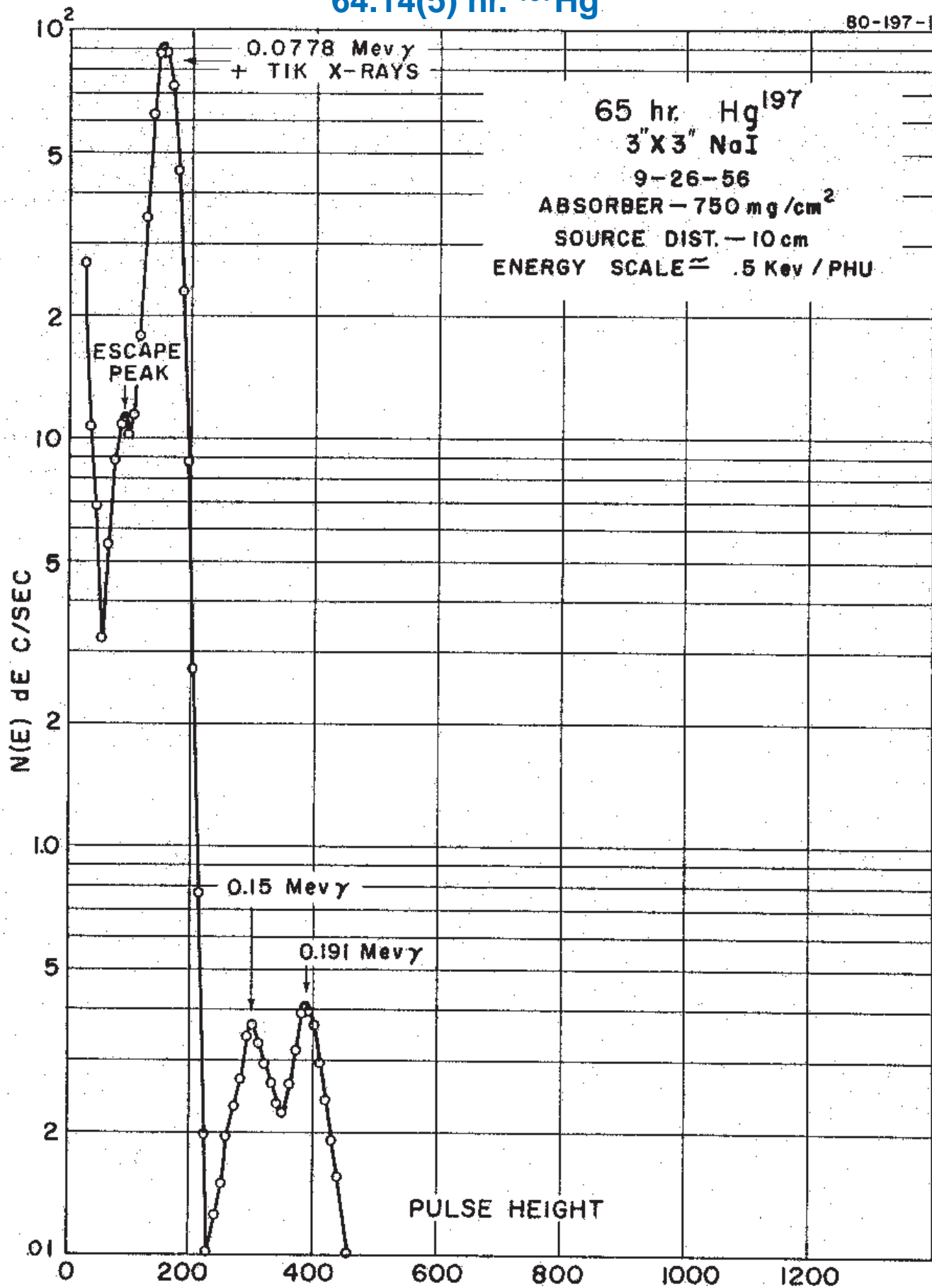
GAMMA-RAY ENERGIES AND INTENSITIES

Nuclide ^{197m}Hg Half Life 23.8(1) hr.
Detector 3" x 3" NaI Method of Production: $^{196}\text{Hg}(n,\gamma)$

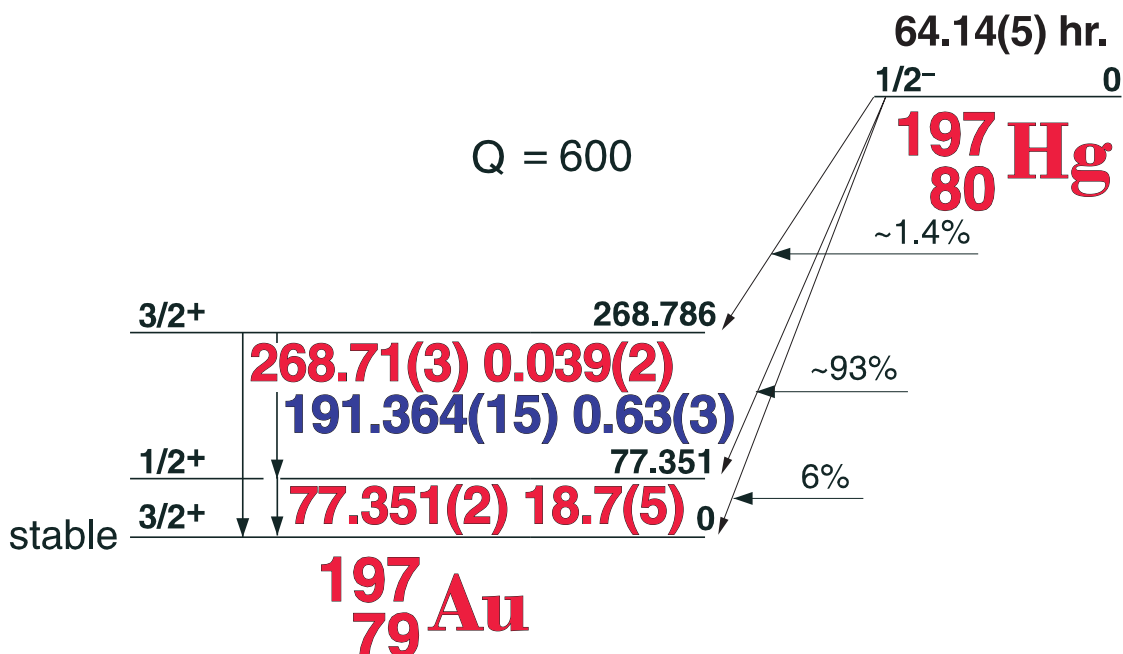
	E_γ (KeV)[S]	ΔE_γ	I_γ (rel)	$I_\gamma(\%)$ [E]	ΔI_γ	S
^{197m}Hg .						
I.T.	Hg K x-ray 133.98	± 0.05	100	33.5	± 5.0	1
	164.75	± 0.15	1.6	0.55	± 0.05	4
	279.17	± 0.1		6.1	± 0.6	3

64.14(5) hr. ^{197}Hg

80-197-1



64.14(5) hr. ^{197}Hg



GAMMA-RAY ENERGIES AND INTENSITIES

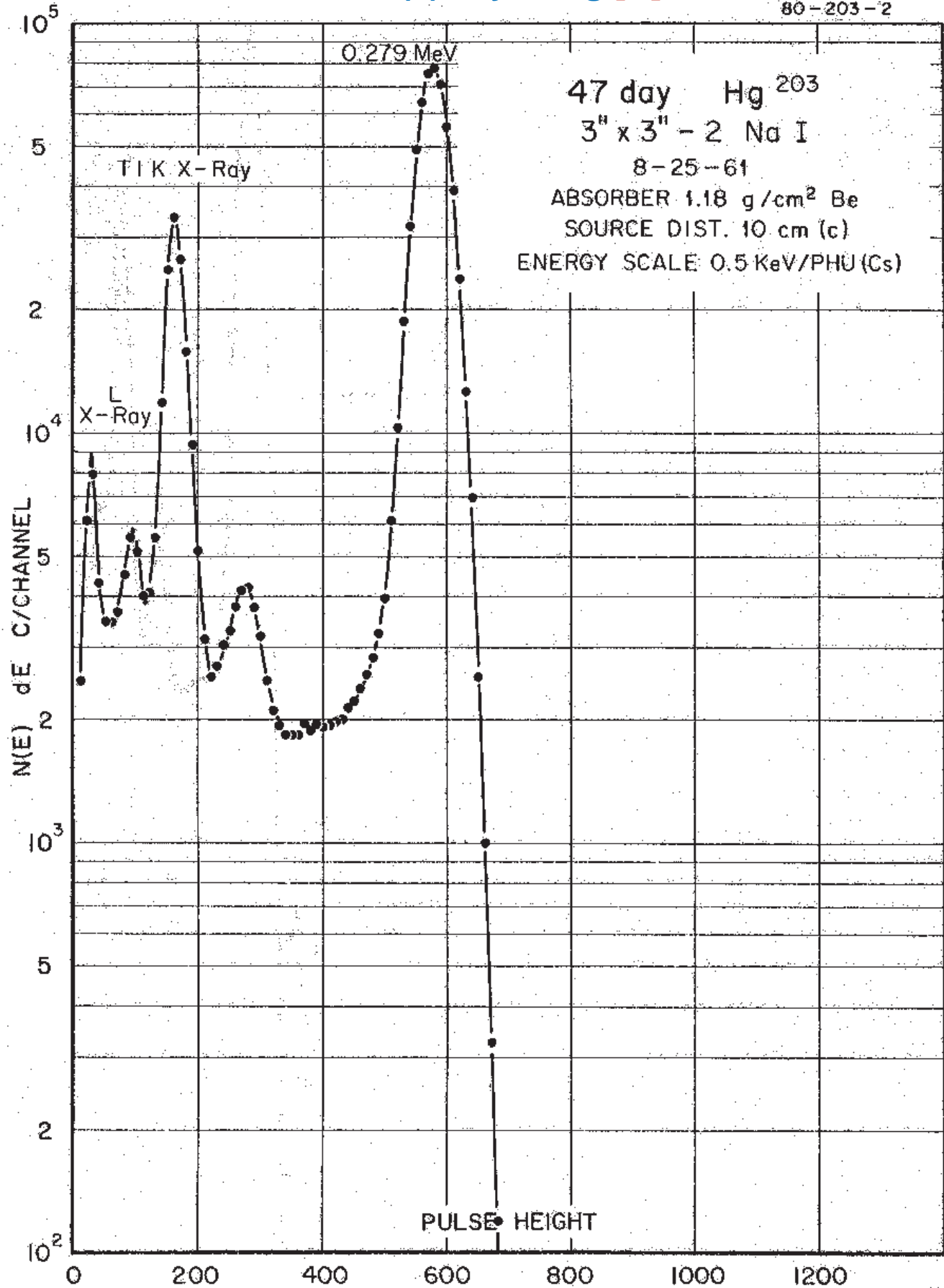
Nuclide ^{197}Hg
Detector 3" x 3" NaI

Half Life 64.14(5) hr.
Method of Production: $^{196}\text{Hg}(n,\gamma)$

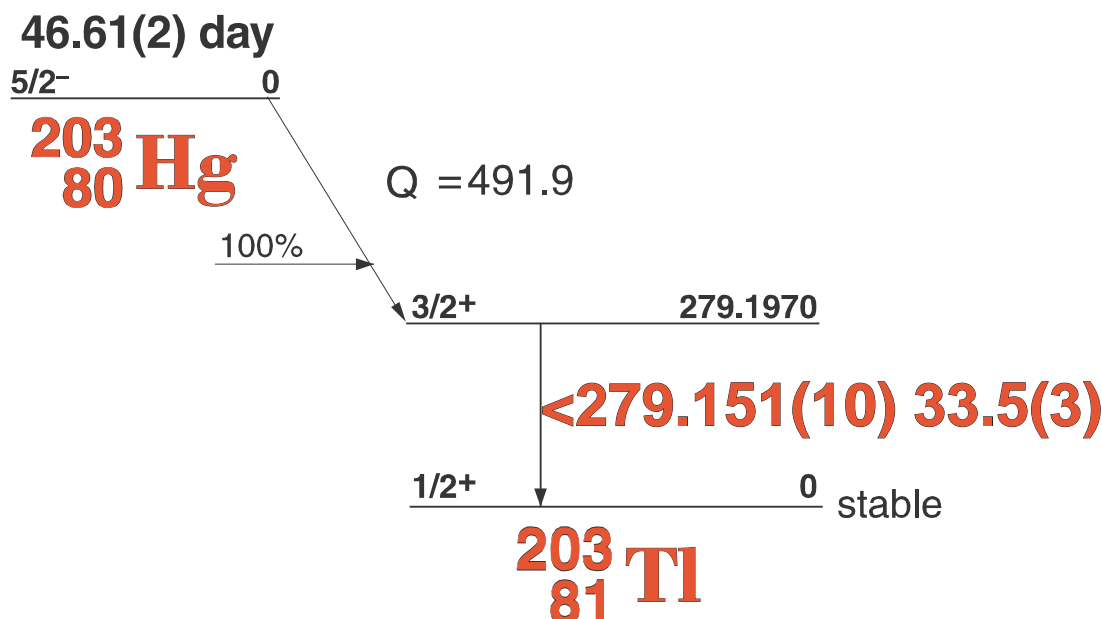
E_γ (KeV)[S]	ΔE_γ	I_γ (rel)	$I_\gamma(\%)$ [E]	ΔI_γ	S
77.351	± 0.002	100	18.7	± 0.5	1
191.364	± 0.015	2.69	0.63	± 0.03	3
268.71	± 0.03	0.21	0.039	± 0.002	3

46.61(2) day ^{203}Hg [C]

80-203-2



46.61(2) day ^{203}Hg [C]



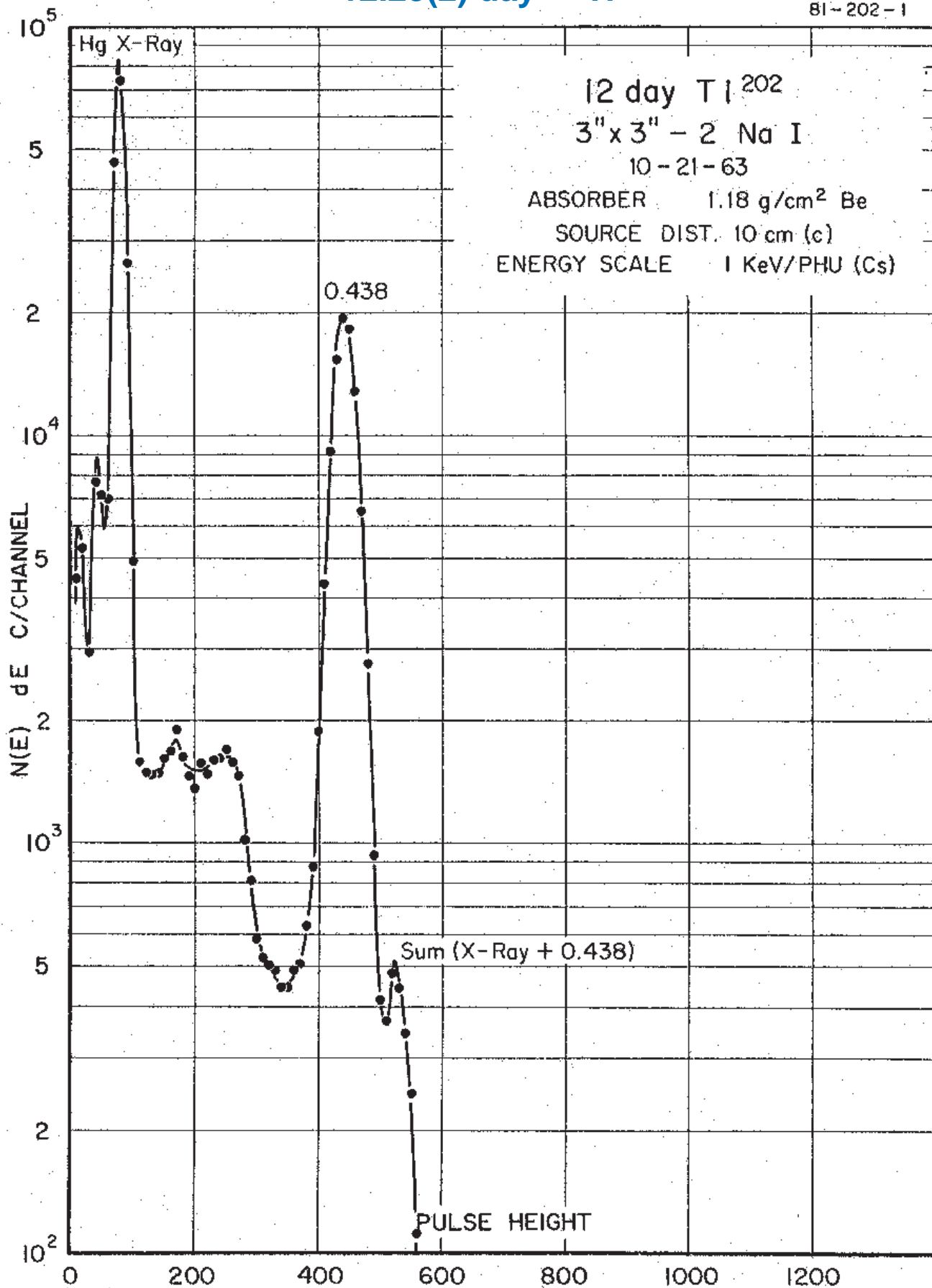
GAMMA-RAY ENERGIES AND INTENSITIES

Nuclide ^{203}Hg Half Life 46.61(2) day
Detector 3" x 3" NaI Method of Production: $^{194}\text{Pt}(n,\gamma)$

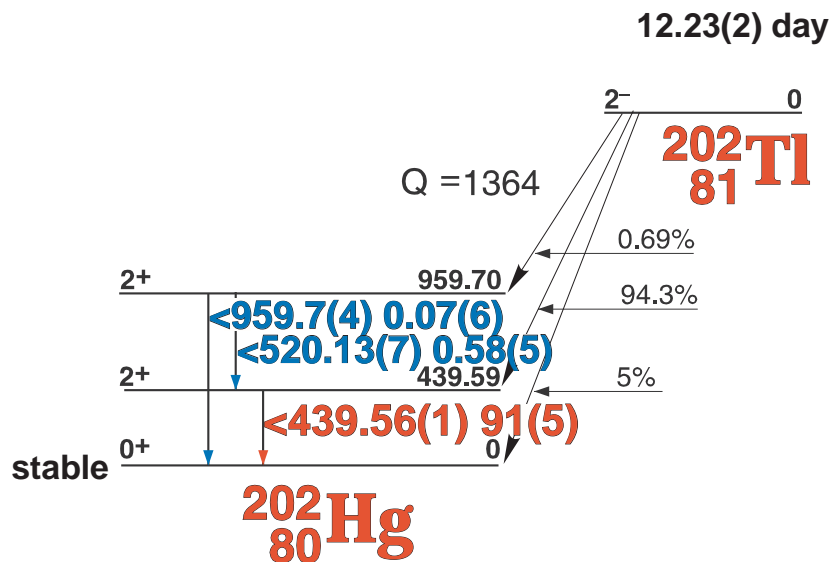
E_γ (KeV)[S]	ΔE_γ	$I_\gamma(\text{rel})$	$I_\gamma(\%)$ [E]	ΔI_γ	S
Tl K x-ray					
279.151	± 0.010	100	33.5	± 0.3	1

12.23(2) day ^{202}TI

81-202-1



12.23(2) day ^{202}Tl



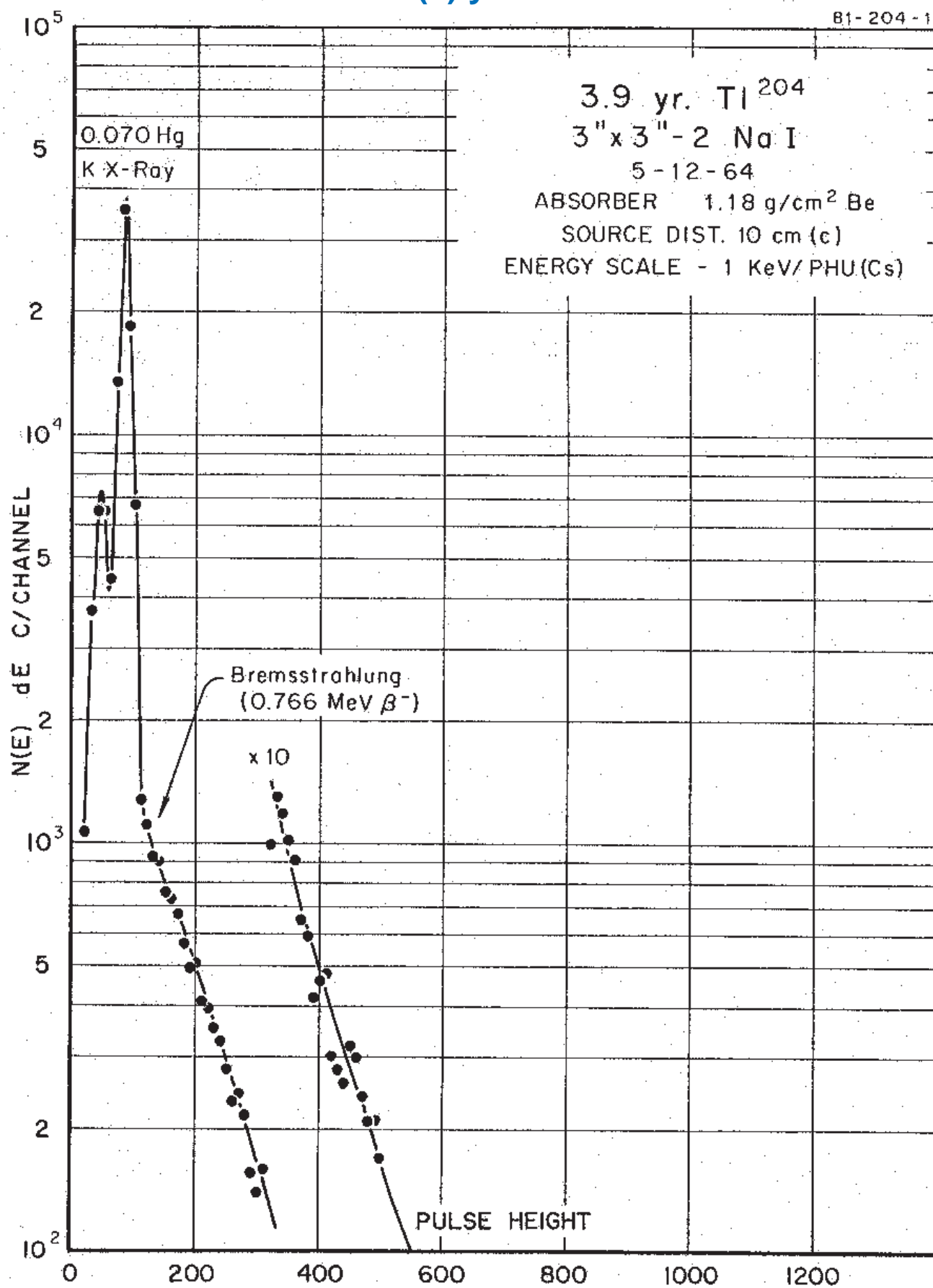
GAMMA-RAY ENERGIES AND INTENSITIES

Nuclide ^{202}Tl Half Life 12.23(2) day
 Detector 3" x 3" NaI Method of Production: $^{203}\text{Tl}(\gamma, n)$

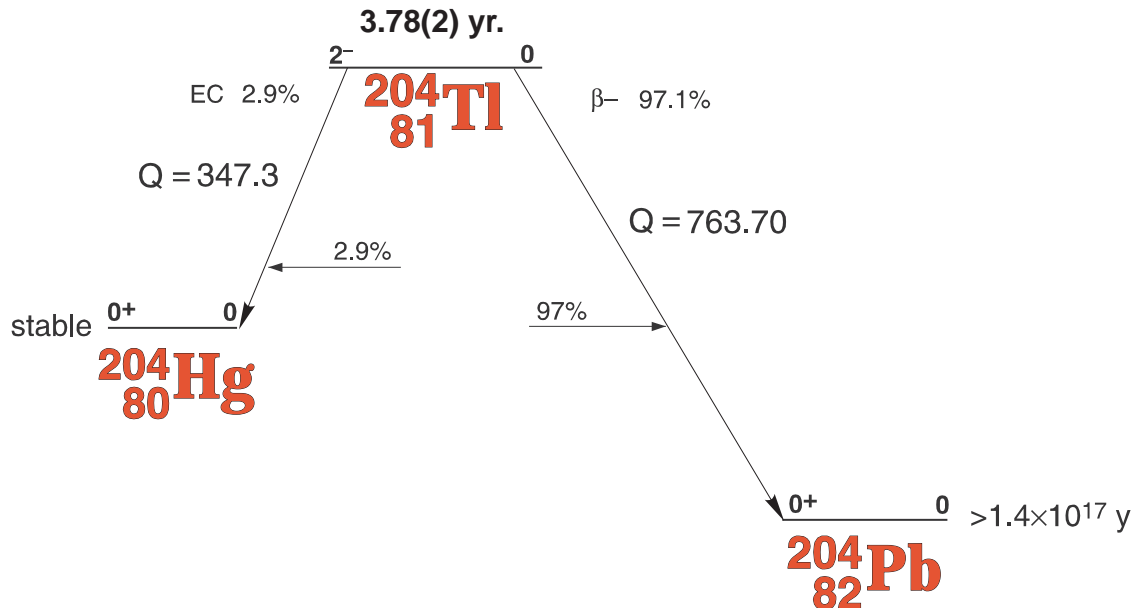
E_γ (KeV)[S]	ΔE_γ	I_γ (rel)	I_γ (%)[E]	ΔI_γ	S
Hg K x-ray					
439.58	± 0.01	100	91	± 5.0	1
520.13	± 0.07		0.58	± 0.05	4
959.7	± 0.4		0.07	± 0.006	4

3.78(2) yr. ^{204}TI

B1-204-1



3.78(2) yr. ^{204}TI

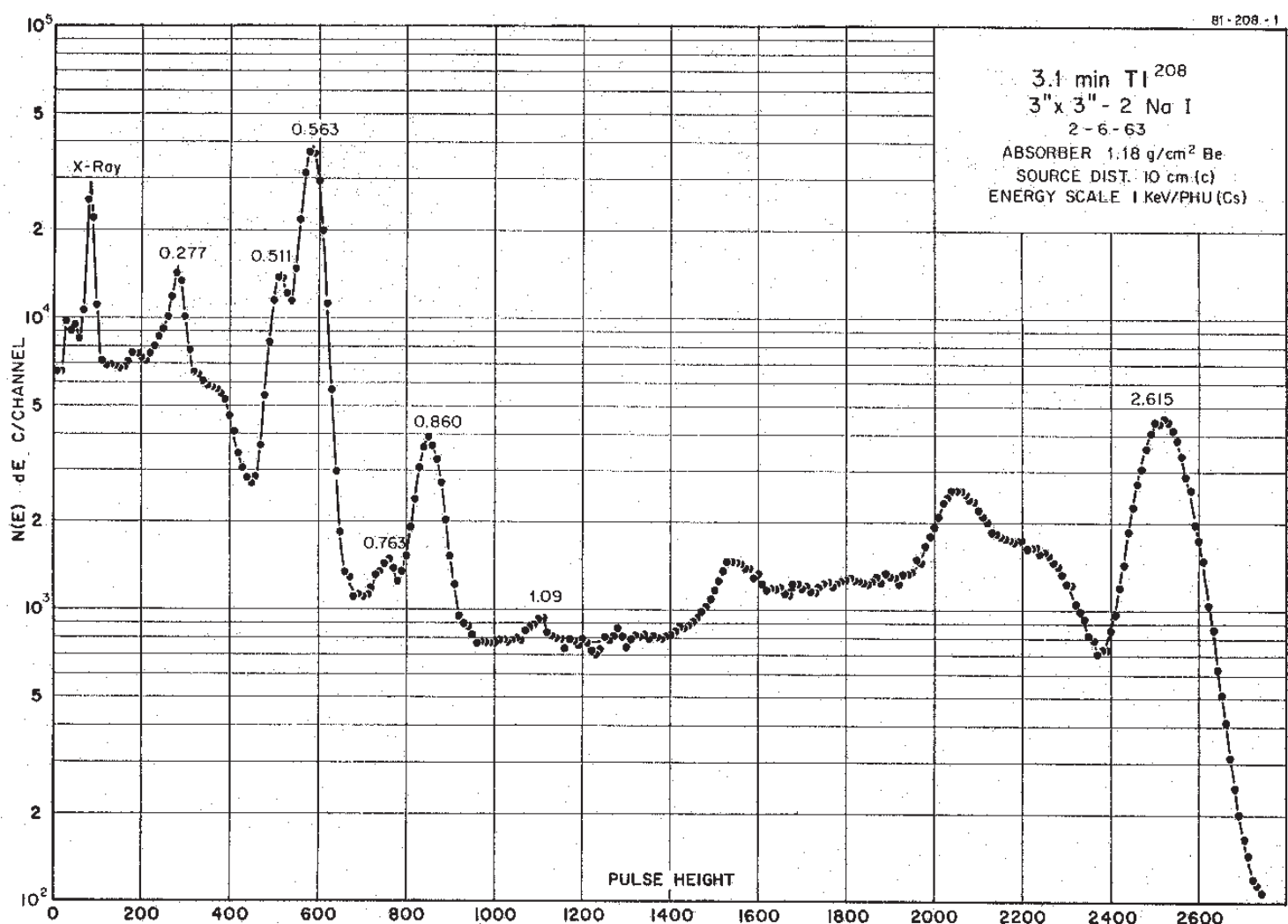


GAMMA-RAY ENERGIES AND INTENSITIES

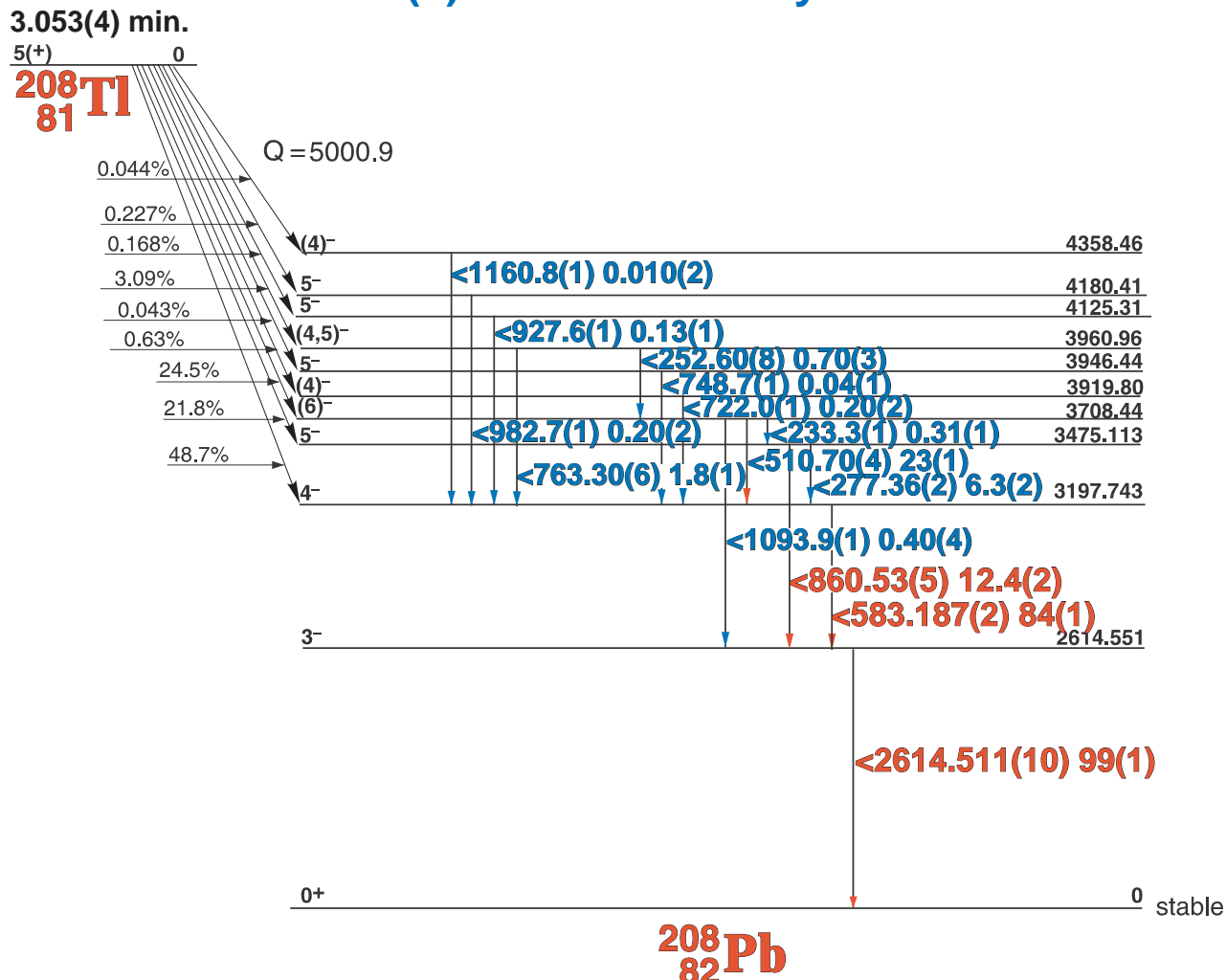
Nuclide ^{204}TI Half Life $3.78(2)$ yr.
Detector 3" x 3" NaI Method of Production: $^{203}\text{TI}(n,\gamma)$

E_γ (KeV)[S]	ΔE_γ	I_γ (rel)	$I_\gamma(\%)$ [E]	ΔI_γ	S

3.053(4) min. ^{208}TI



3.053(4) min. ^{208}TI Decay Scheme



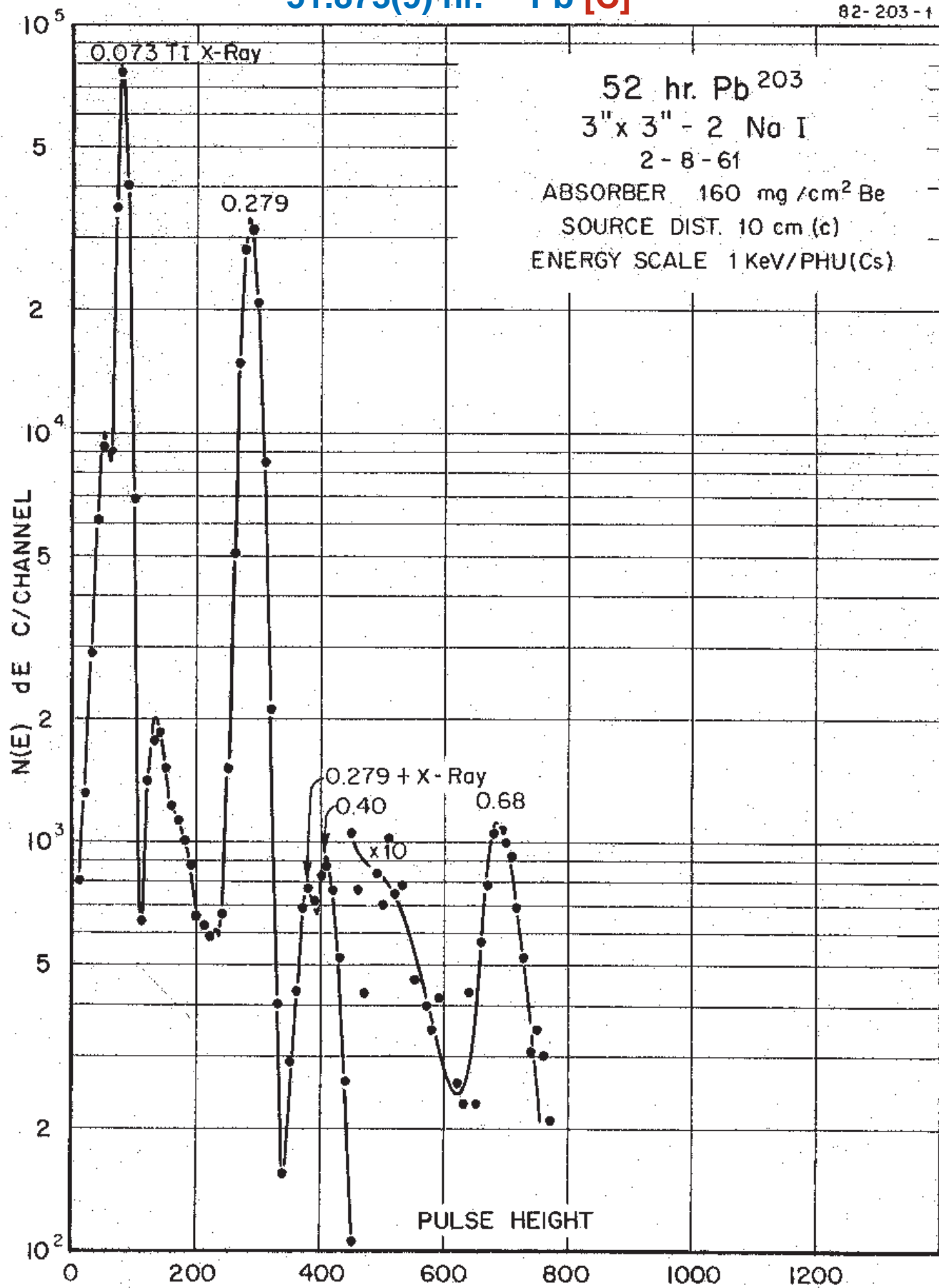
GAMMA-RAY ENERGIES AND INTENSITIES

Nuclide **^{208}TI** Half Life 3.053(4) min.
Detector 3" x 3" NaI Method of Production: ^{228}Th decay (chem.)

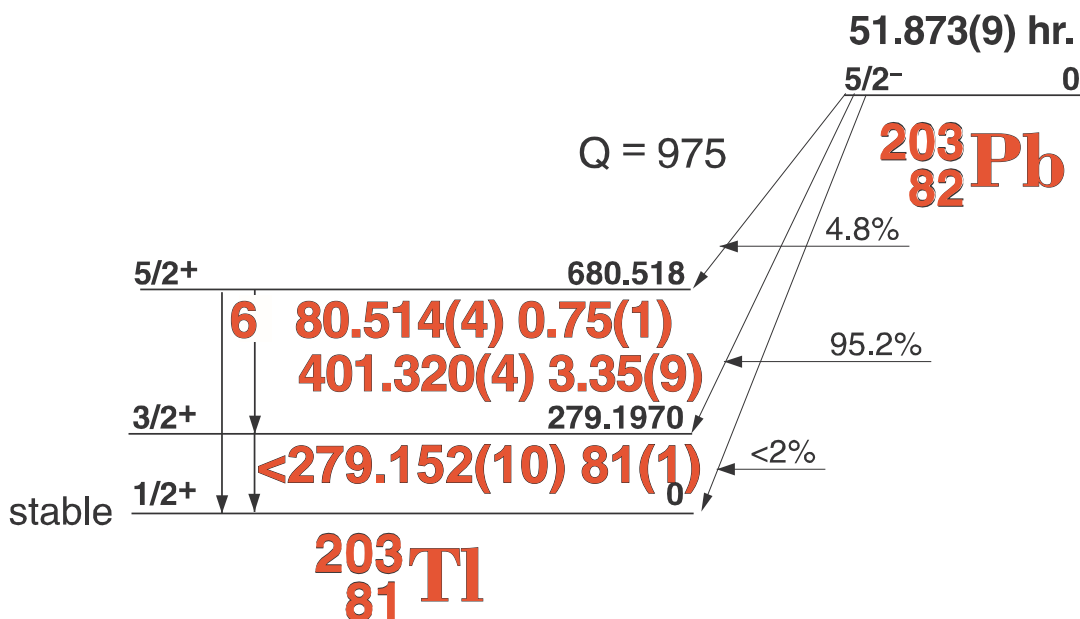
	E_{γ} (KeV) [S]	ΔE_{γ}	I_{γ} (rel)	I_{γ} (%) [E]	ΔI_{γ}	S
DE	233.3	± 0.1		0.31	± 0.1	4
SE	252.60	± 0.08	0.80	0.70	± 0.03	4
	277.36	± 0.02	6.34	6.3	± 0.2	2
	510.70	± 0.04	22.0	23	± 1.0	1
	583.187	± 0.002	83.2	84	± 1.0	1
	722.0	± 0.1	0.20	0.20	± 0.02	4
	763.30	± 0.06	1.68	1.8	± 0.1	2
	860.53	± 0.05	12.5	12.4	± 0.2	1
	927.6	± 0.1	0.15	0.13	± 0.01	4
	982.7	± 0.1	0.20	0.20	± 0.02	4
	1093.9	± 0.1	0.41	0.40	± 0.04	3
	1160.8	± 0.1		0.018	± 0.2	4
	1592.60	± 0.06				1
	2103.50	± 0.04				2
	2614.511	± 0.010	100	99	± 1.0	1

51.873(9) hr. ^{203}Pb [C]

82-203-1



51.873(9) hr. ^{203}Pb Decay Scheme [C]



GAMMA-RAY ENERGIES AND INTENSITIES

Nuclide ^{203}Pb Half Life $51.873(9)$ hr.
 Detector 3" x 3" NaI Method of Production: $^{204}\text{Pb}(\gamma, n)$

E_γ (KeV)[C]	ΔE_γ	I_γ (rel)	$I_\gamma(\%)$ [E]	ΔI_γ	S
TI K x-ray					1
279. 152	± 0.010	100	81	± 1.0	1
401.320	± 0.004	4.36	3.35	± 0.09	1
680. 514	± 0.004	0 .92	0.75	± 0.01	3

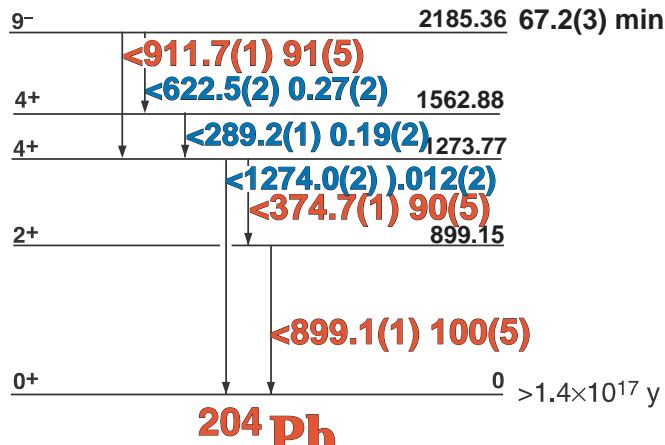
67.2(3) min. ^{204m}Pb

GAMMA-RAY ENERGIES AND INTENSITIES

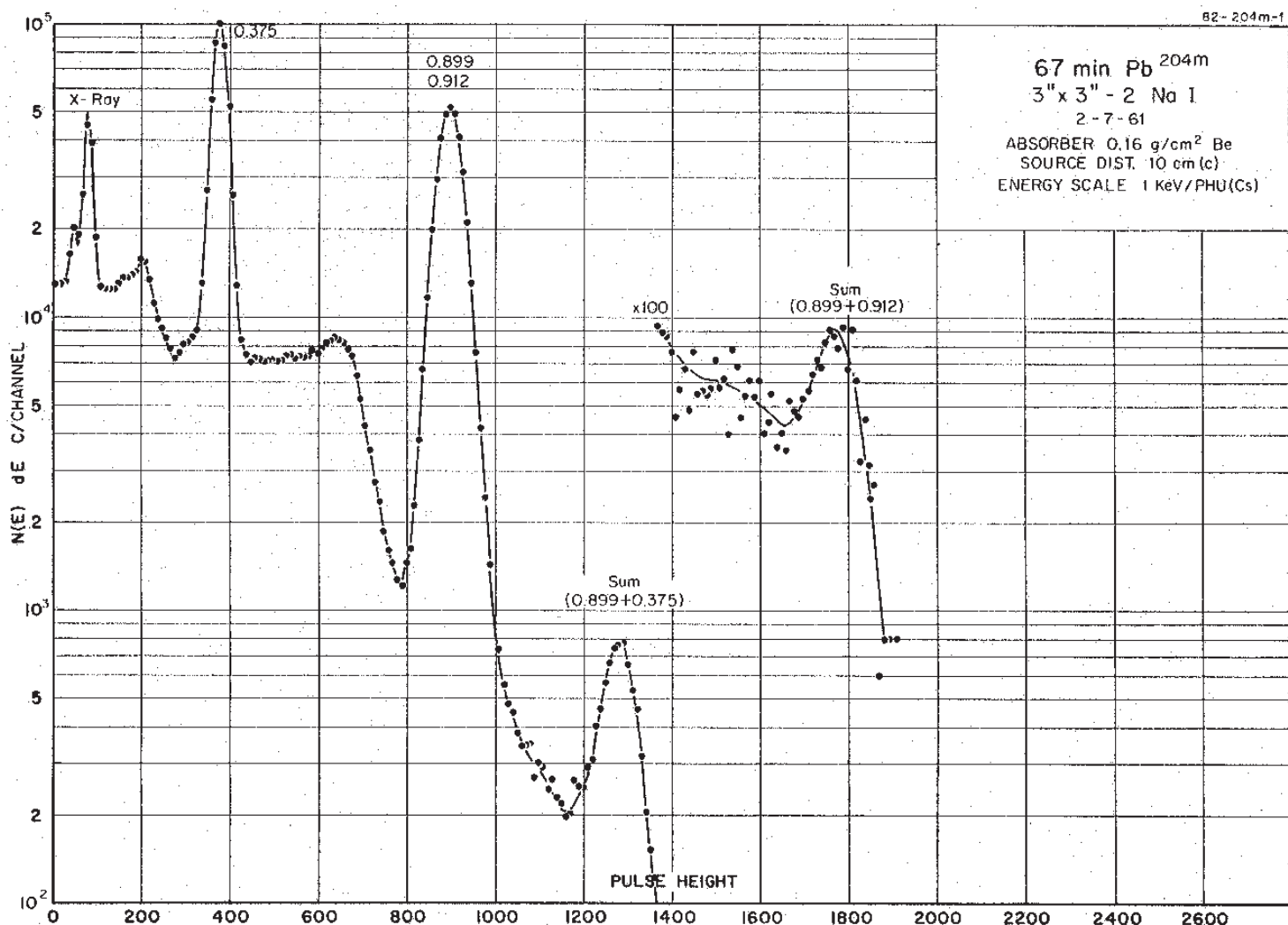
Nuclide
Detector

^{204m}Pb
3" x 3" NaI

Half Life 67.2(3) min.
Method of Production: $^{204}\text{Pb}(\gamma, \gamma)$



E_γ (KeV)[S]	ΔE_γ	I_γ (rel)	I_γ (%)[E]	ΔI_γ	S
289.2	± 0.1	0.20	0.19	± 0.02	4
374.7	± 0.1	90	90	± 5.0	1
622.5	± 0.2	0.27	0.27	± 0.02	4
899.1	± 0.1	100	100	± 5.0	1
911.7	± 0.1	91	91	± 5.0	1
1274.0	± 0.2		0.012	± 0.004	4



0.806(6) sec. ^{207m}Pb

13/2+

1633.368 0.806(6) sec.

5/2-

1063.662(4) 88.5(3)

569.703

1/2-

569.702(2) 97.9(1)

stable

207₈₂Pb

GAMMA-RAY ENERGIES AND INTENSITIES

Nuclide
Detector

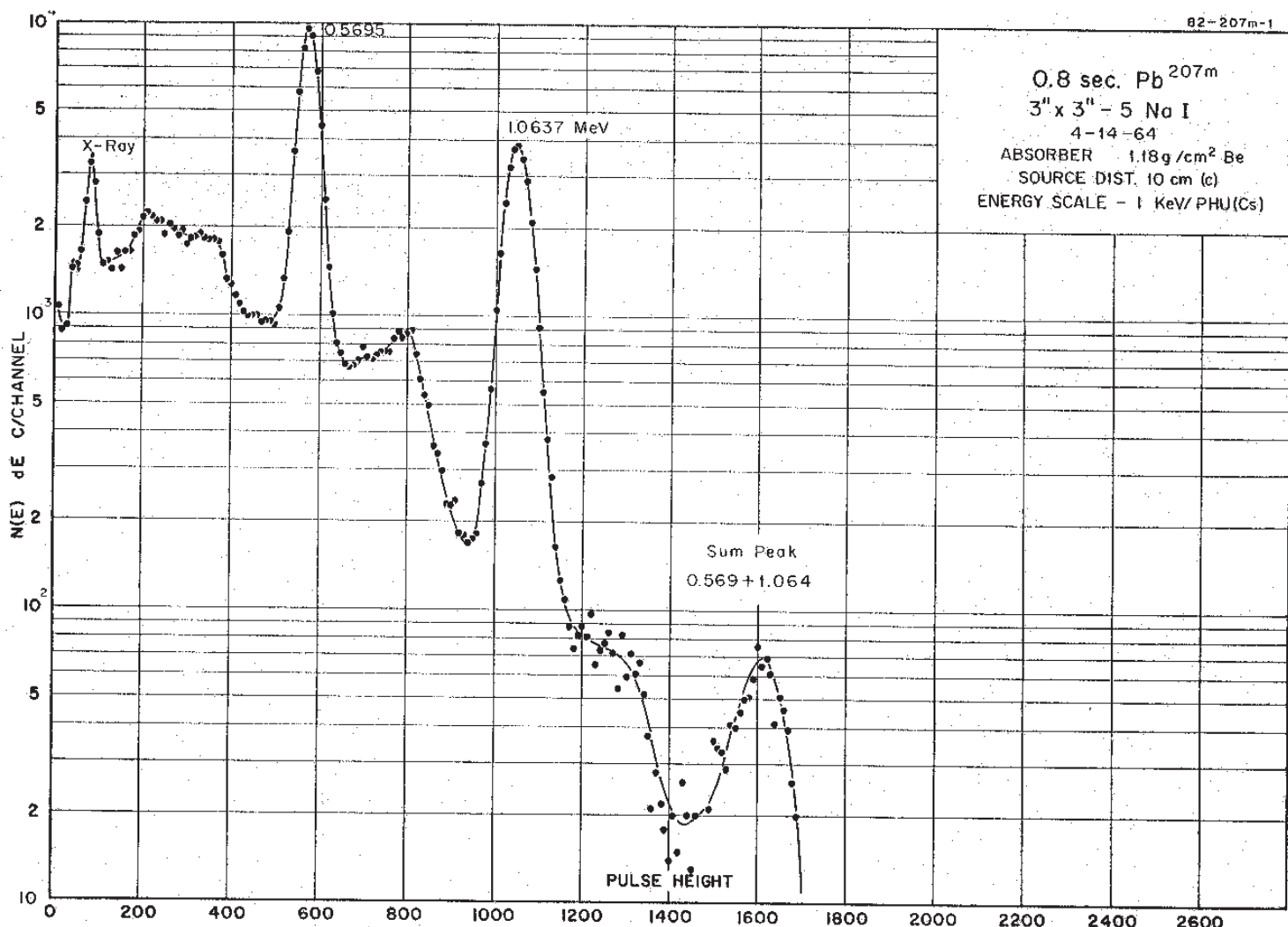
^{207m}Pb

3" x 3" NaI

Half Life 0.806(6) sec.

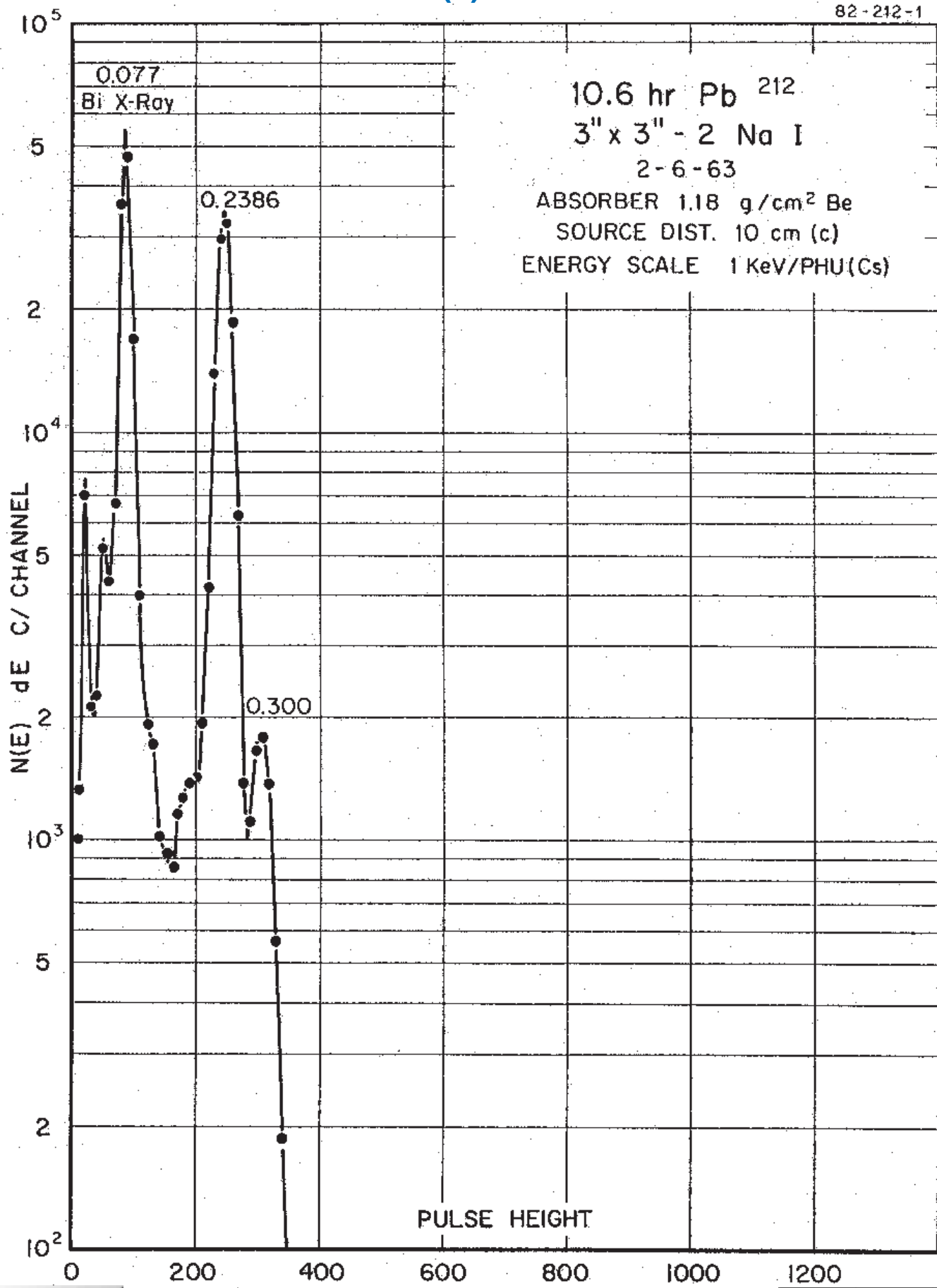
Method of Production: $^{208}\text{Pb}(\gamma, n)$

E_{γ} (KeV)[S]	ΔE_{γ}	I_{γ} (rel)	$I_{\gamma}(\%)$ [E]	ΔI_{γ}	S
569.702	± 0.002	100	97.9	± 0.1	1
1063.662	± 0.004	91	88.5	± 0.3	1

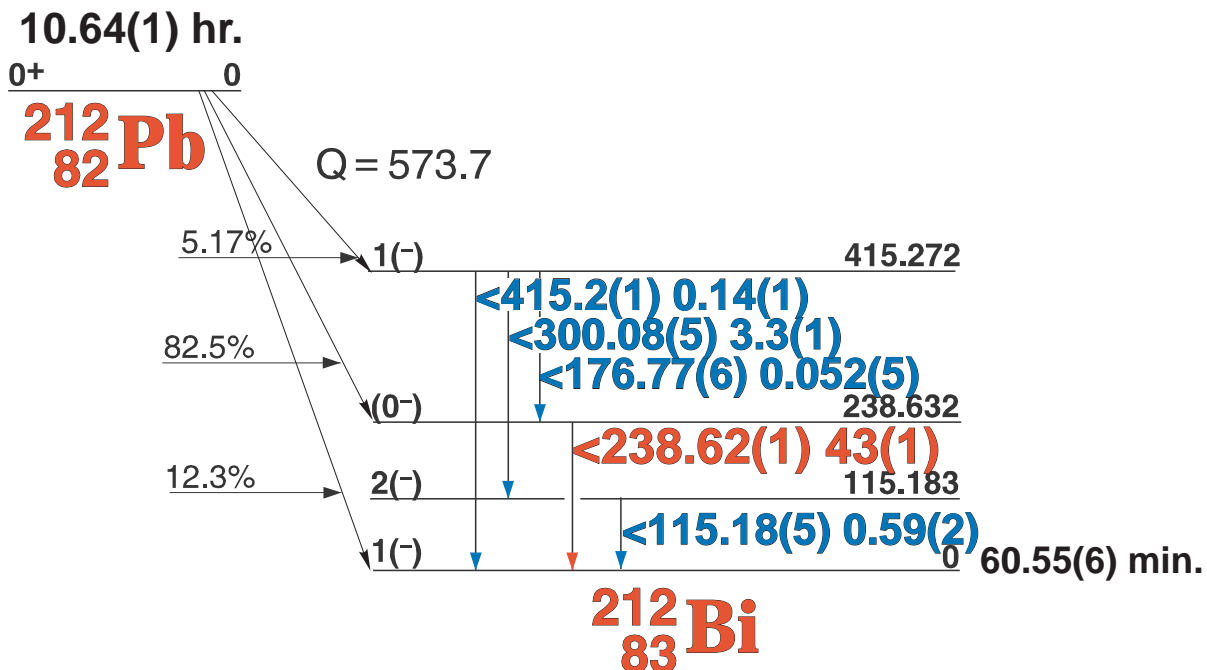


10.64(1) hr. ^{212}Pb

82-212-1



10.64(1) hr. ^{212}Pb

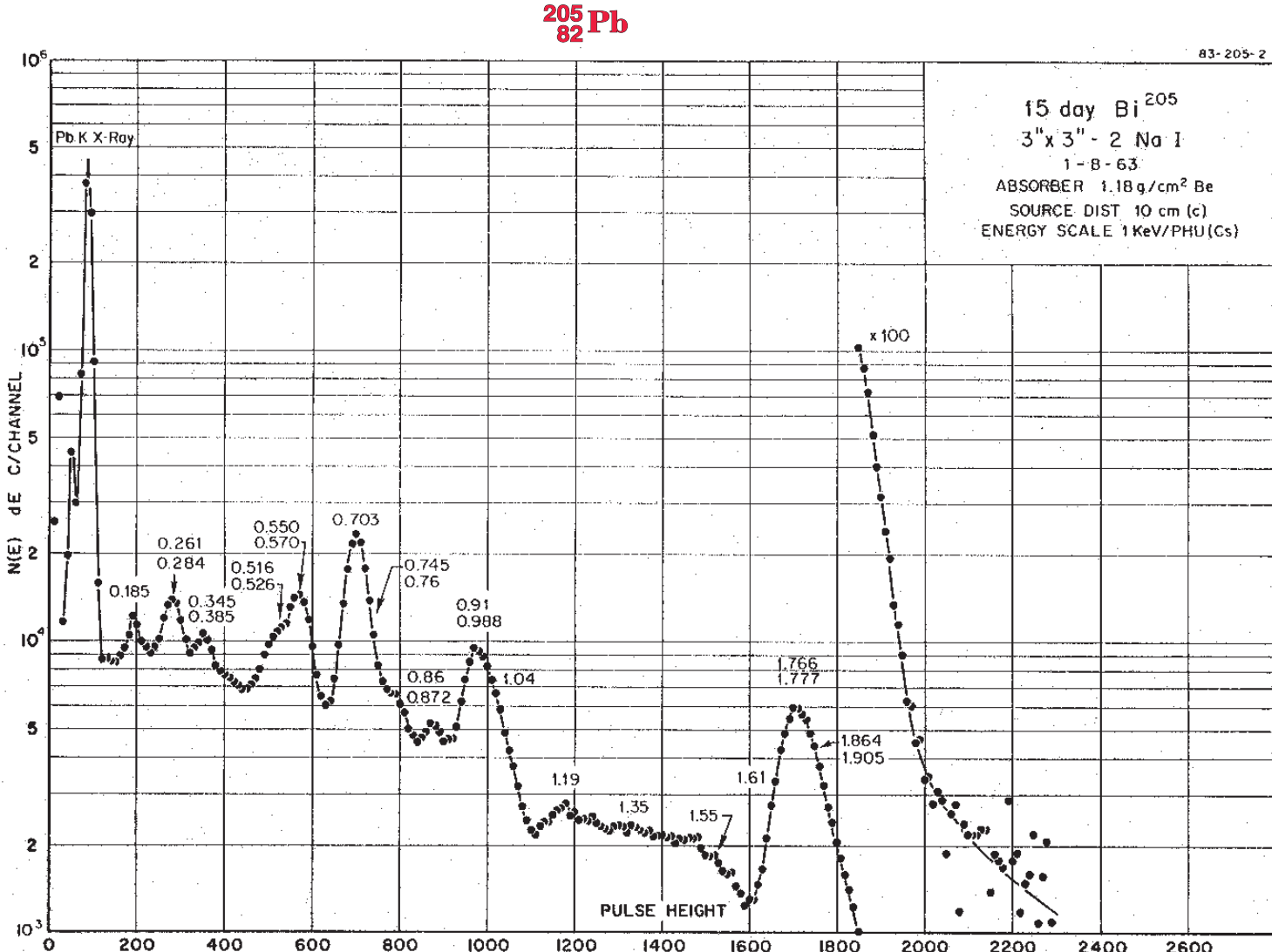
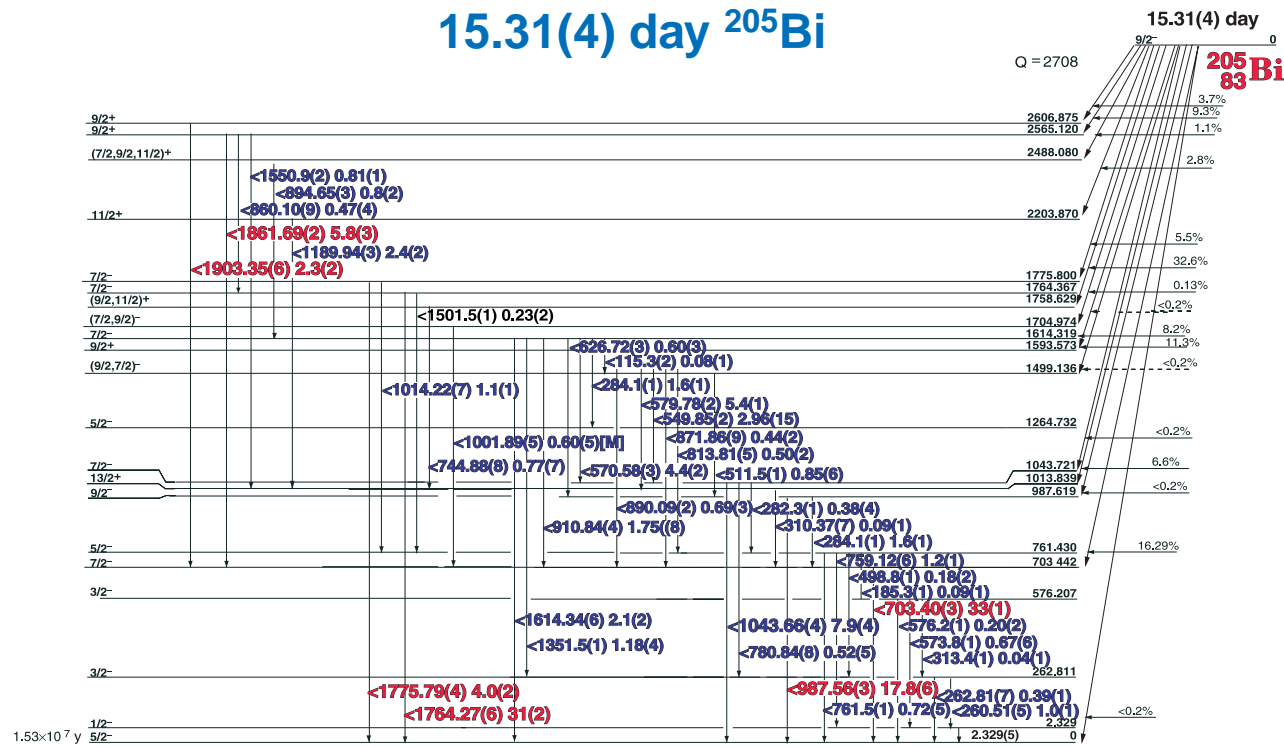


GAMMA-RAY ENERGIES AND INTENSITIES

Nuclide ^{212}Pb Half Life 10.64(1) hr.
Detector 3" x 3" NaI Method of Production: 228Tl decay

E_γ (KeV)[S]	ΔE_γ	I_γ (rel)	$I_\gamma(\%)$ [E]	ΔI_γ	S
115.18	± 0.05	1.59	0.59	± 0.02	3
176.77	± 0.06	0.15	0.052	± 0.005	4
238.624	± 0.009	120	43	± 1.0	1
300.08	± 0.05	8.76	3.3	± 0.06	2
415.2	± 0.1		0.14	± 0.01	3

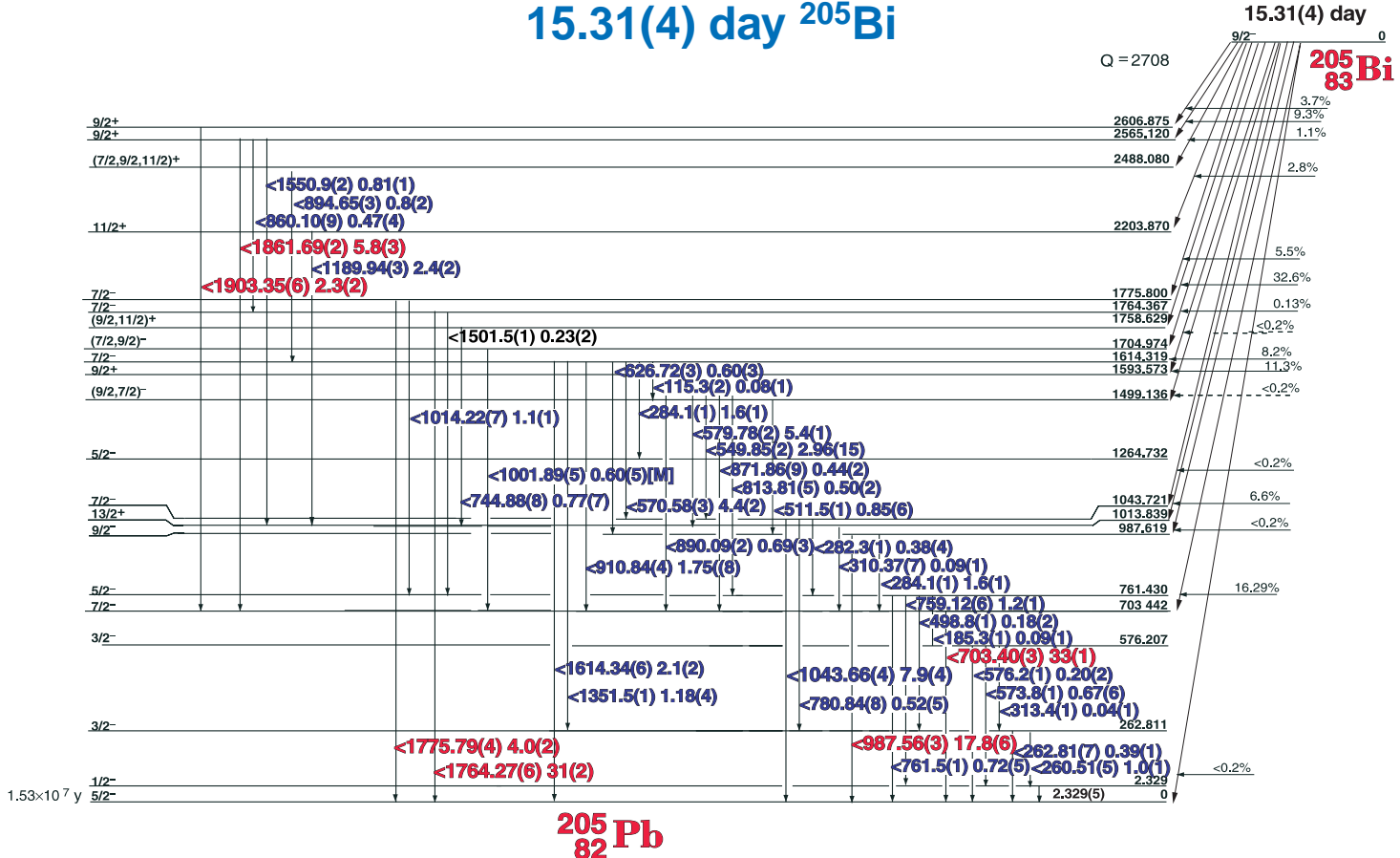
15.31(4) day ^{205}Bi



Decay Data



15.31(4) day ^{205}Bi



^{205}Pb

GAMMA-RAY ENERGIES AND INTENSITIES

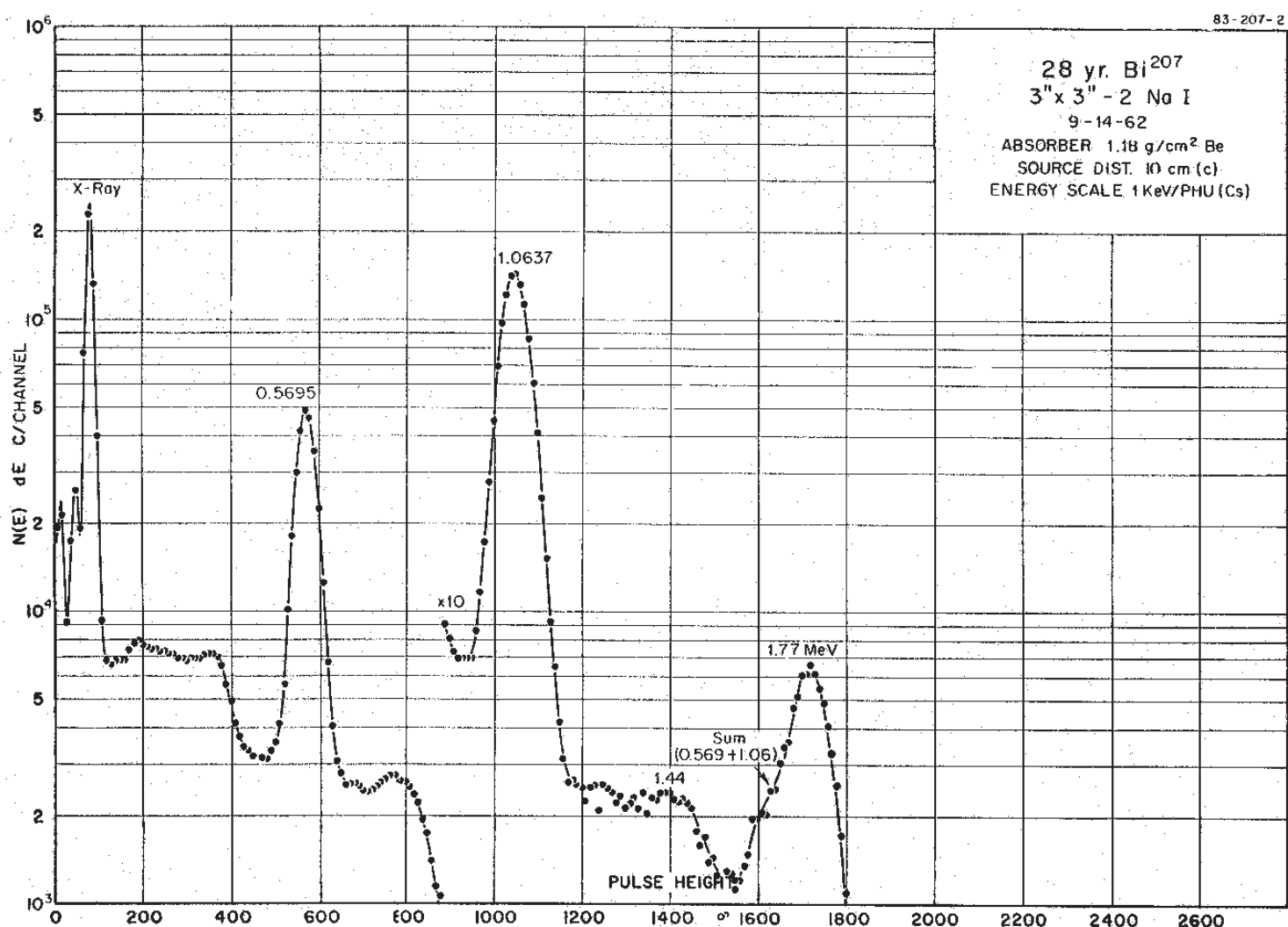
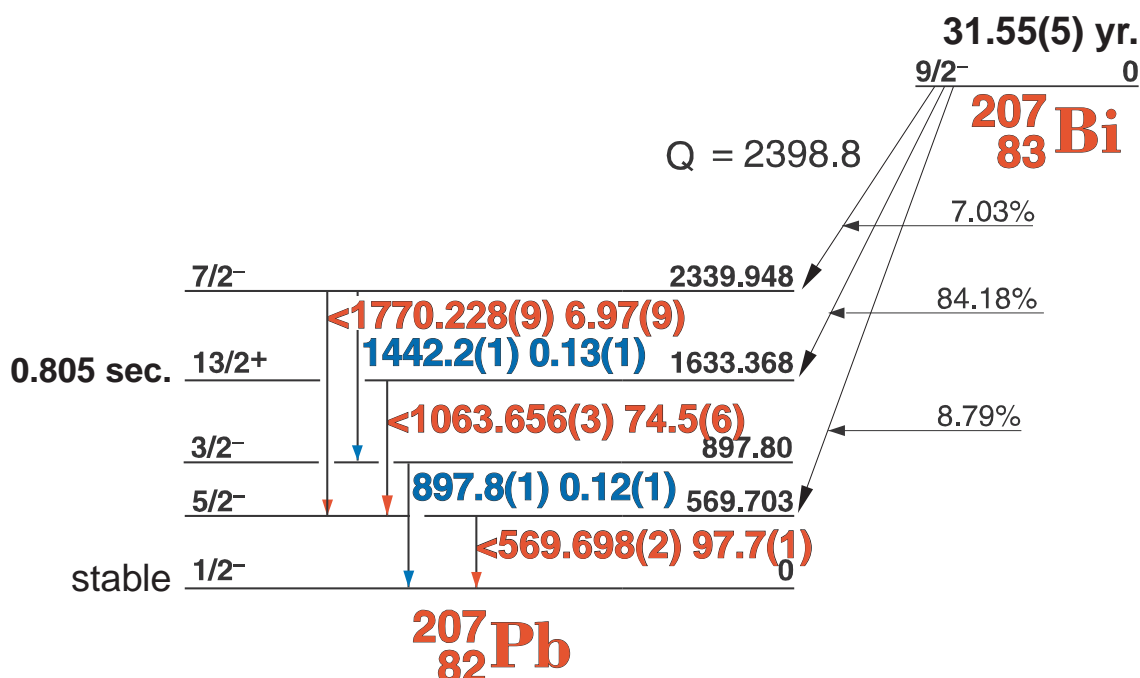
Nuclide ^{205}Bi
Detector 3" x 3" NaI

Half Life 15.31(4) day
Method of Production: $^{206}\text{Pb}(p,2n)$

E_{γ} (KeV)[S]	ΔE_{γ}	I_{γ} (rel)	$I_{\gamma}(\%)[E]$	ΔI_{γ}	S
115.409	± 0.18	0.23	0.08	± 0.01	4
129.62	± 0.02	0.03	0.006	± 0.002	4
185.29	± 0.11	0.28	0.09	± 0.01	4
260.511	± 0.05	3.10	1.0	± 0.11	3
262.81	± 0.07	1.19	0.39	± 0.02	4
282.26	± 0.10	1.14	0.38	± 0.02	4
284.12	± 0.10	4.80	1.6	± 0.1	3
310.37	± 0.07	0.27	0.09	± 0.01	4
313.4	± 0.1	0.18	0.04	± 0.01	4
349.55	± 0.05	1.48	0.50	± 0.03	4
493.70	± 0.035	0.97	0.35	± 0.02	4
498.84	± 0.15	0.55	0.18	± 0.02	4
511.5	± 0.1		0.85	± 0.06	3
549.855	± 0.02	8.88	2.96	± 0.15	3
570.581	± 0.035	13.22	4.4	± 0.20	2
579.78	± 0.020		5.4	± 0.1	3
626.72	± 0.03	1.78	0.60	± 0.03	4
703.401	± 0.028	100	33	± 1.0	1
744.88	± 0.08	2.33	0.77	± 0.06	4
759.12	± 0.06	3.73	1.2	± 0.10	4
761.47	± 0.10	2.16	0.72	± 0.05	4

E_{γ} (KeV)[S]	ΔE_{γ}	I_{γ} (rel)	$I_{\gamma}(\%)[E]$	ΔI_{γ}	S
780.84	± 0.08	1.56	0.52	± 0.05	4
813.81	± 0.05	1.49	0.50	± 0.02	4
860.10	± 0.09	1.40	0.47	± 0.04	4
871.86	± 0.09	1.32	0.44	± 0.02	4
890.09	± 0.025	2.05	0.69	± 0.03	4
894.65	± 0.03	2.69	0.80	± 0.09	4
910.84	± 0.04	5.25	1.75	± 0.08	3
950.76	± 0.07	1.27	0.41	± 0.03	4
987.557	± 0.030	53.46	17.8	± 0.6	
1001.89	± 0.05	1.78	0.60[M]	± 0.05	
1014.22	± 0.07	3.29	1.1	± 0.1	
1043.661	± 0.040	23.87	7.9	± 0.4	2
1189.94	± 0.030	7.34	2.4	± 0.2	3
1208.57	± 0.08	1.65	0.55	± 0.05	4
1351.47	± 0.10	3.51	1.18	± 0.05	4
1550.81	± 0.23	2.54	0.81	± 0.01	4
1614.34	± 0.06	6.36	2.1	± 0.2	3
1764.274	± 0.065	93.05	31	± 2.0	1
1775.795	± 0.040	11.10	4.0	± 0.2	1
1861.691	± 0.025	17.44	5.8	± 0.3	1
1903.346	± 0.060	6.71	2.3	± 0.1	1

31.55(5) yr. ^{207}Bi



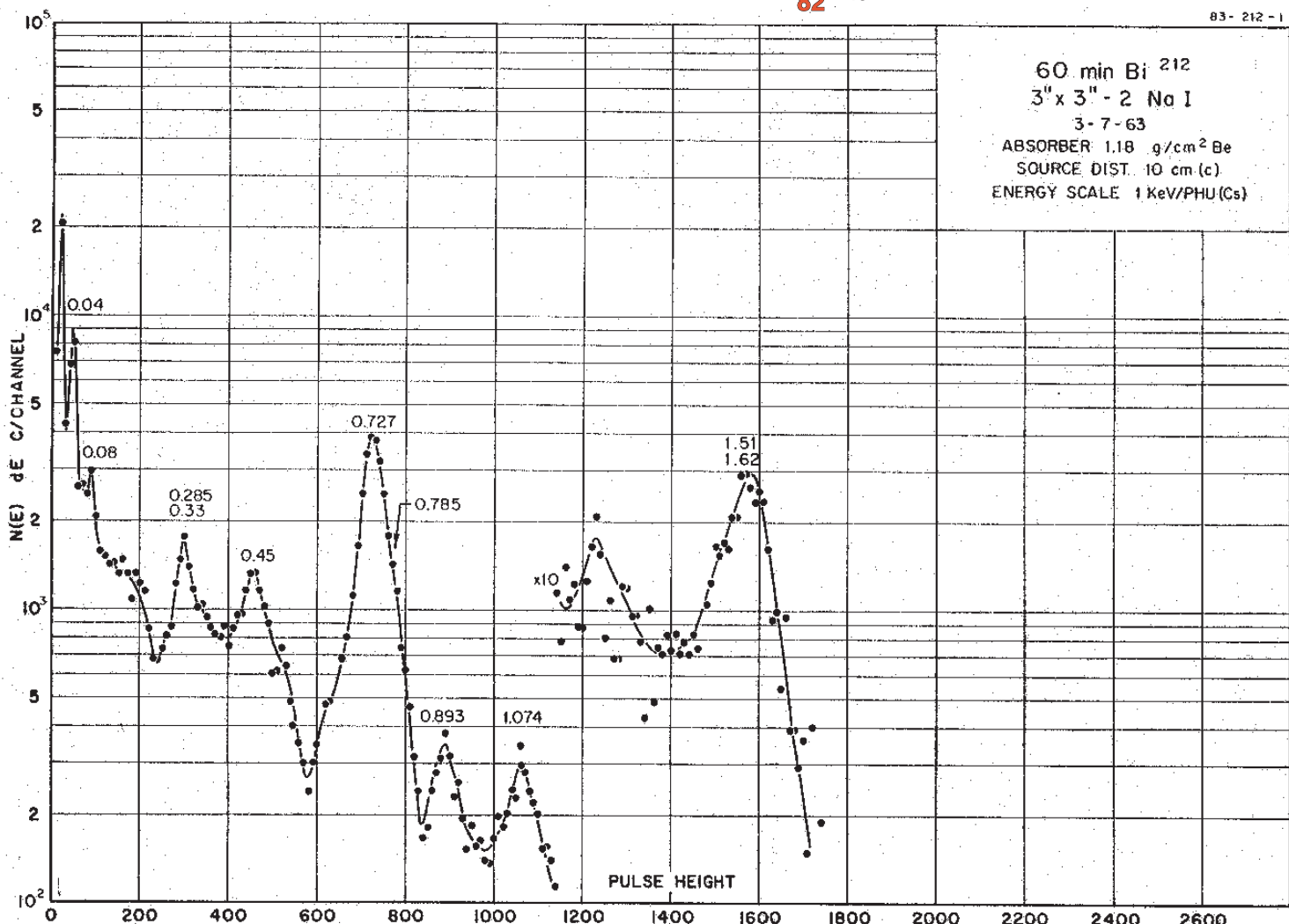
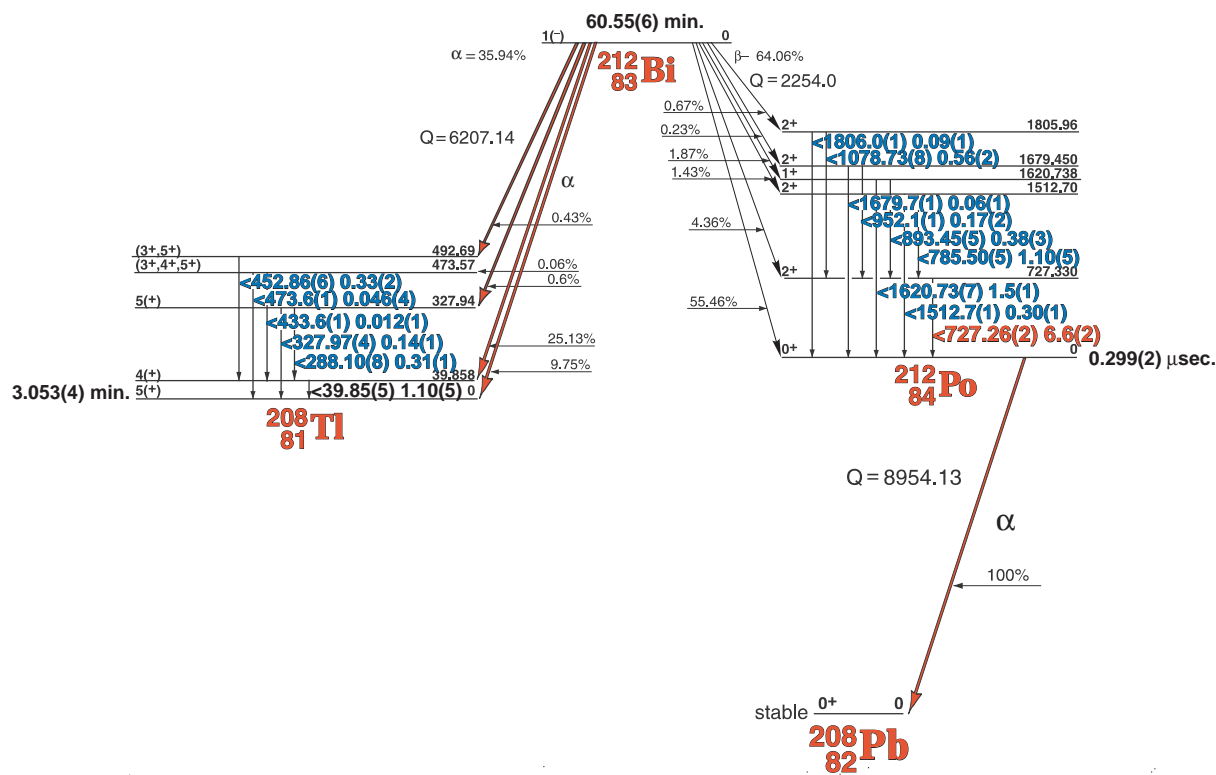
31.55(5) yr. ^{207}Bi

GAMMA-RAY ENERGIES AND INTENSITIES

Nuclide ^{207}Bi
 Detector 3" x 3" NaI Half Life 31.55(5) yr.
 Method of Production: $^{207}\text{Pb}(\text{p},\text{n})$

	E_{γ} (KeV)[S]	ΔE_{γ}	$I_{\gamma}(\text{rel})$	$I_{\gamma}(\%)[\text{E}]$	ΔI_{γ}	S
Pb K x-ray						
	569.698	± 0.002	100	97.7	± 0.1	1
	748.26	± 0.15	0.13		± 0.05	4
DE	897.81	± 0.12	0.25	0.12	± 0.01	4
	1063.656	± 0.003	77.0	74.5	± 0.6	1
	1259.3	± 0.1	0.14		± 0.05	4
SE	1442.27	± 1.0	0.13	0.13	± 0.01	4
	1770.228	± 0.009	7.39	6.97	± 0.09	1

60.55 min. ^{212}Bi



60.55(6) min. ^{212}Bi

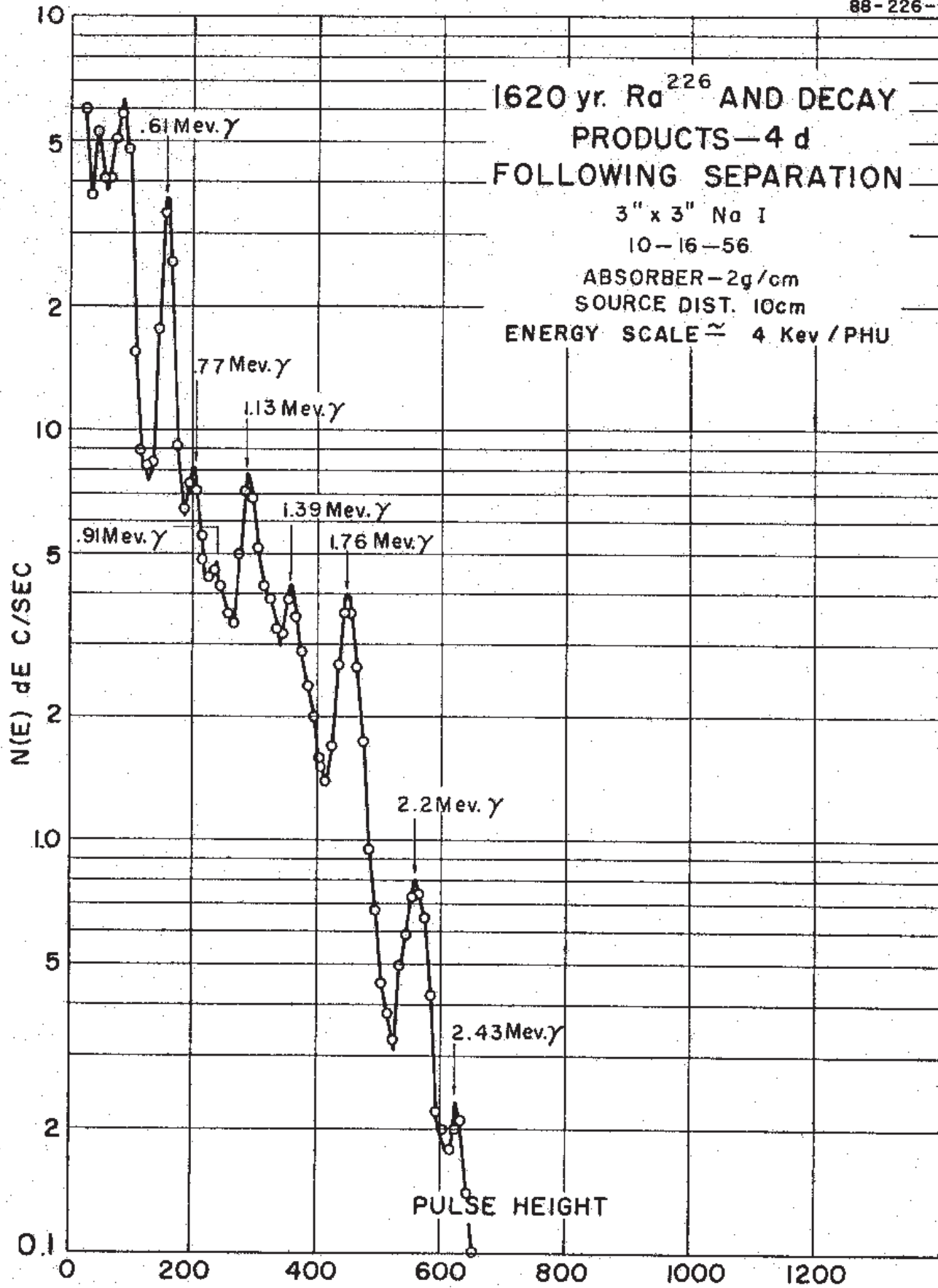
GAMMA-RAY ENERGIES AND INTENSITIES

Nuclide ^{212}Bi Half Life 60.55(60 min.
Detector 3" x 3" NaI Method of Production: ^{228}Th Decay

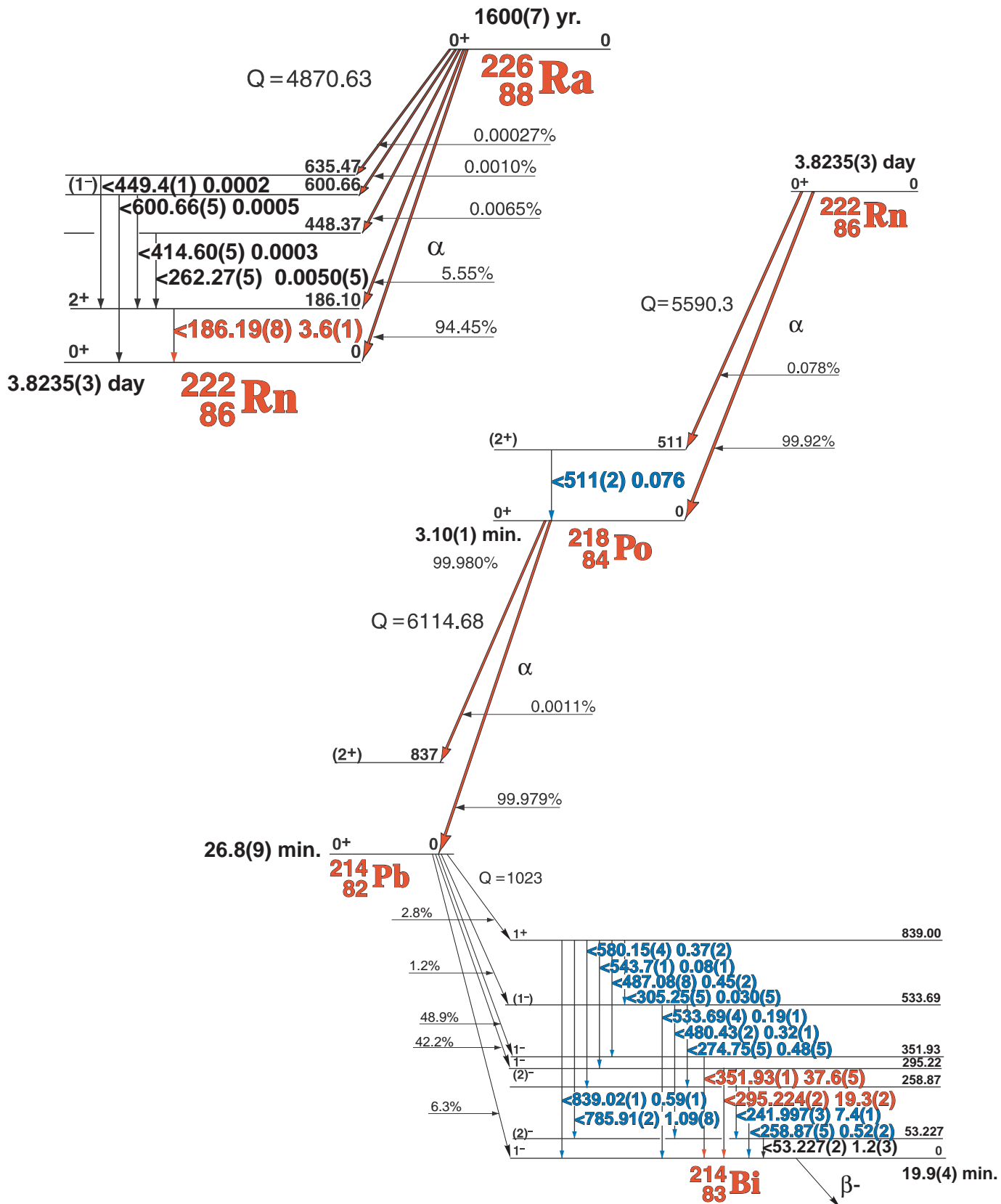
E_{γ} (KeV)[S]	ΔE_{γ}	$I_{\gamma}(\text{rel})$	$I_{\gamma}(\%)[E]$	ΔI_{γ}	S
288.10	± 0.08	0.92	0.31	± 0.01	4
327.97	± 0.04	0.36	0.14	± 0.01	4
452.86	± 0.06	1.06	0.33	± 0.02	3
727.264	± 0.025	18.4	6.6	± 0.2	1
785.50	± 0.05	2.95	1.10	± 0.05	2
893.45	± 0.05	0.94	0.38	± 0.03	3
952.0	± 0.15	0.65	0.17	± 0.02	4
1078.73	± 0.08	1.51	0.56	± 0.02	3
1512.7	± 0.1		0.30	± 0.01	4
1620.73	± 0.07	4.09	1.5	± 0.1	3
1679.7	± 0.1		0.06	± 0.01	4

1600(7) yr. ^{226}Ra with decay Products

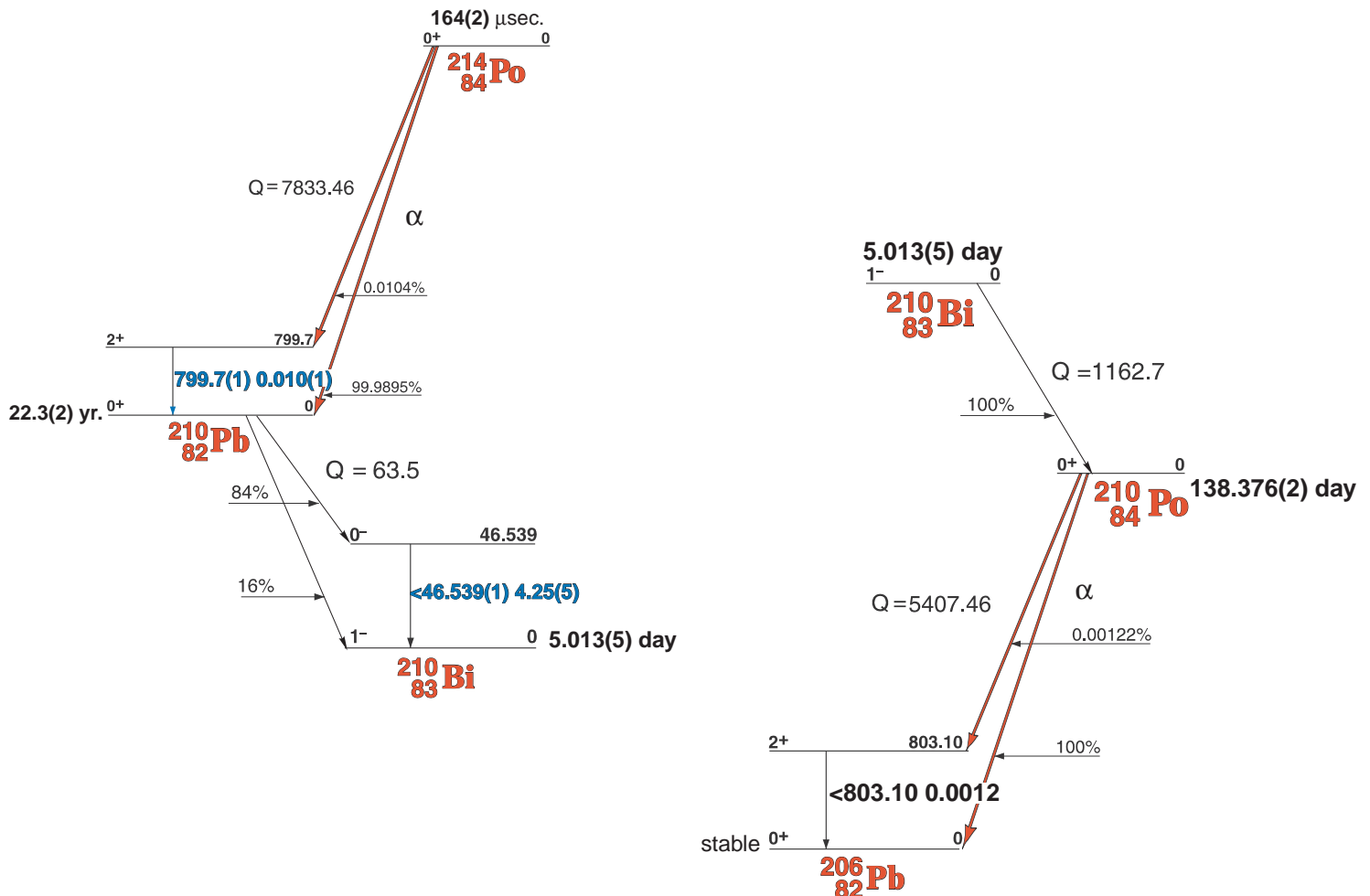
88-226-1



1600(7) yr. ^{226}Ra with decay Products



1600(7) yr. ^{226}Ra with decay Products



1600(7) yr. ^{226}Ra with decay Products

GAMMA-RAY ENERGIES AND INTENSITIES

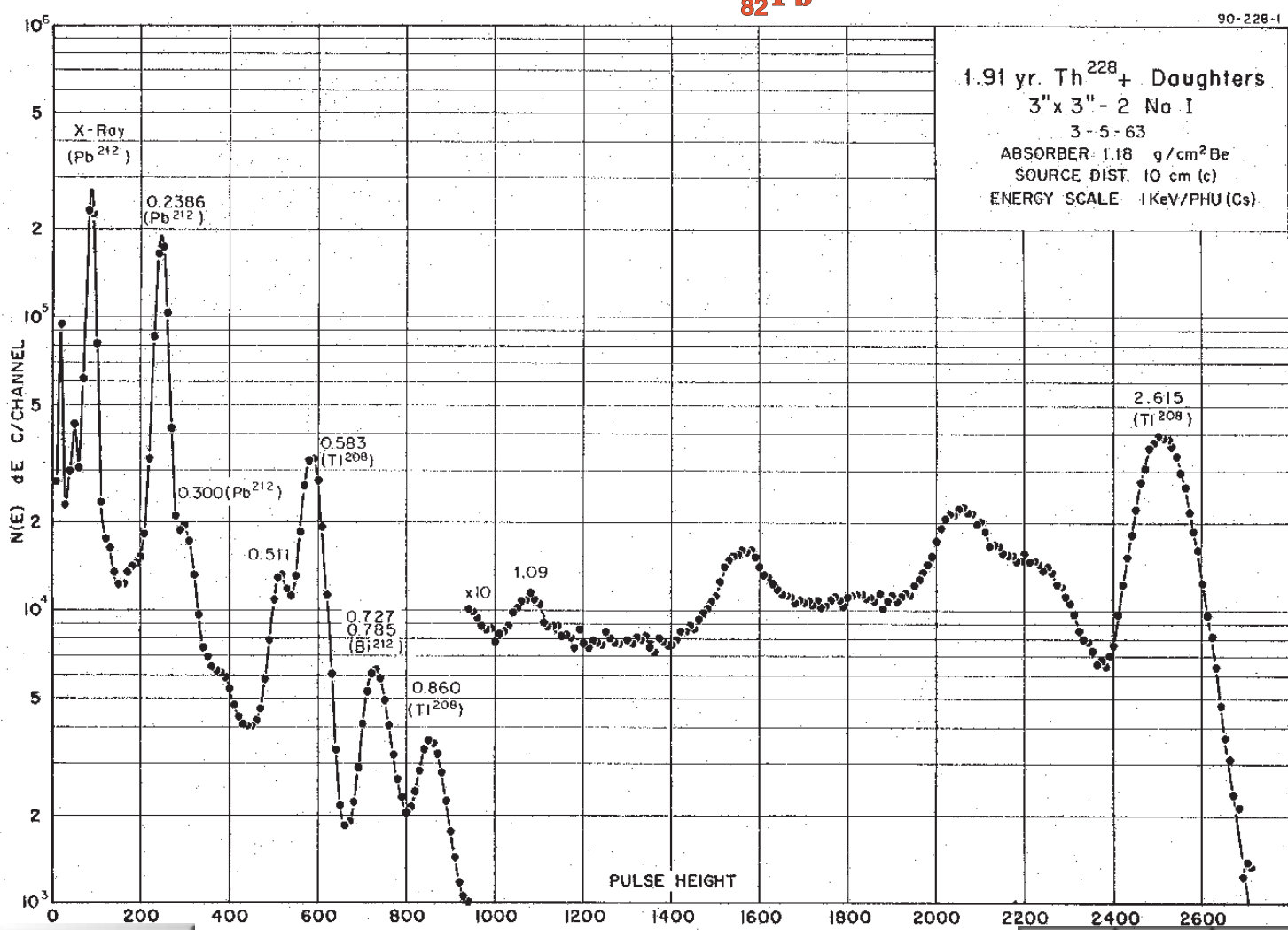
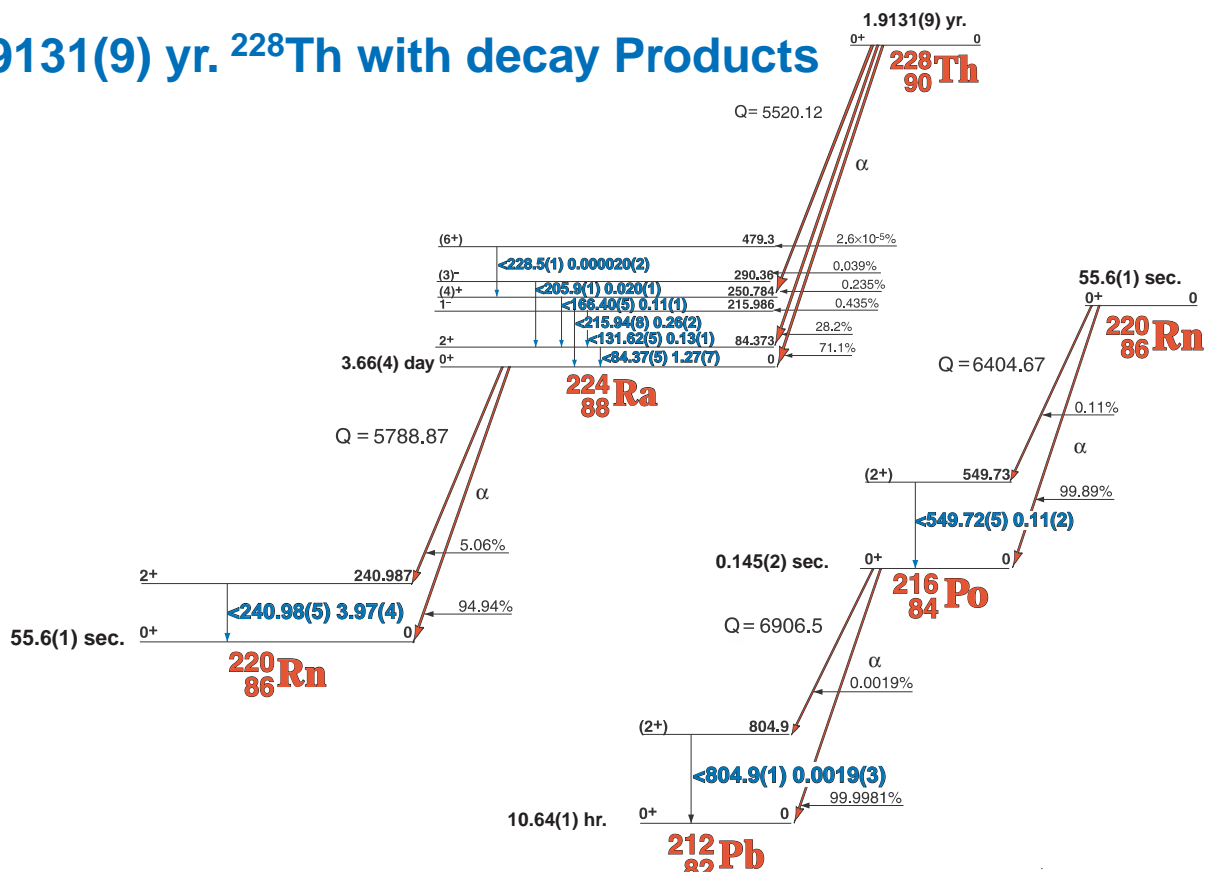
Nuclide: ^{226}Ra and daughters

Half Life: 1600 (7) yr

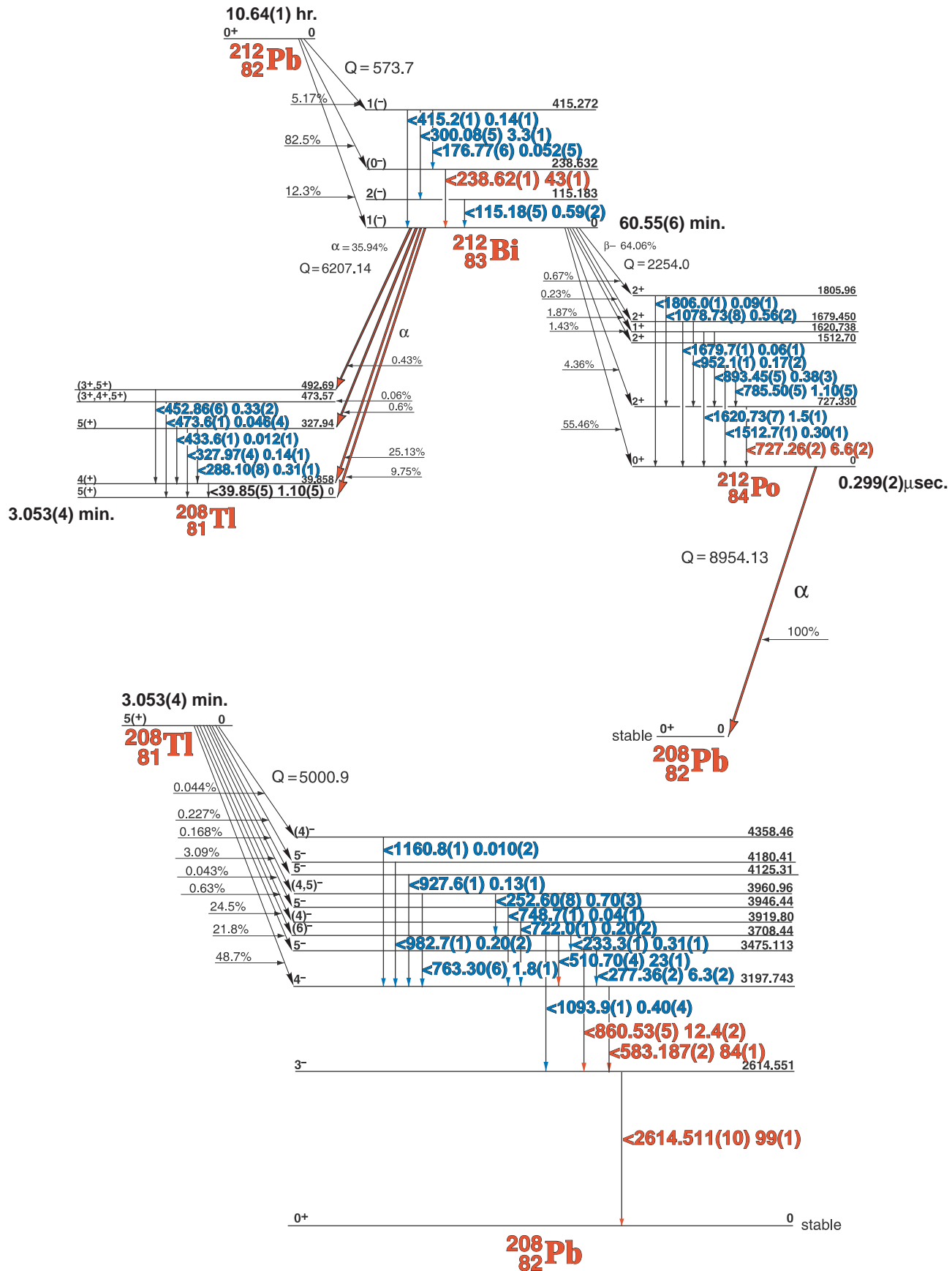
Detector: 55 Cm³ coaxial (c) Ge(Li) Method of Production: nat. (chem.)

	E_{γ} (KeV)[S]	ΔE_{γ}	I_{γ} (rel)[S]	$I_{\gamma}(\%)[E]$	ΔI_{γ}	S		E_{γ} (KeV)[S]	ΔE_{γ}	I_{γ} (rel)[S]	$I_{\gamma}(\%)[E]$	ΔI_{γ}	S
^{226}Ra	186.12	\pm 0.06	4.3	3.6	\pm 0.1	3	^{214}Bi	683.22	\pm 0.06	0.073	0.08	\pm 0.01	4
	195.67	\pm 0.12	w				^{214}Bi	697.90	\pm 0.25	0.035	0.035	\pm 0.005	4
^{214}Pb	241.99	\pm 0.03	9.0	7.4	\pm 0.1	2	^{214}Bi	703.11	\pm 0.04	0.45	0.47	\pm 0.01	3
^{214}Pb	258.87	\pm 0.06	0.47	0.52	\pm 0.02	4	^{214}Bi	710.6	\pm 0.1	0.077	0.075	\pm 0.002	4
^{214}Pb	274.75	\pm 0.05	0.55	0.48	\pm 0.05	4	^{214}Bi	719.86	\pm 0.03	0.39	0.38	\pm 0.01	3
	280.94	\pm 0.12	0.099		\pm 0.019	4		727.8	\pm 0.8	0.016		\pm 0.002	4
^{214}Pb	295.22	\pm 0.02	21.3	19.3	\pm 0.2	1	^{214}Bi	733.7	\pm 0.10	0.050	0.050	\pm 0.006	4
^{214}Bi	304.2	\pm 0.12	0.14	0.04	\pm 0.02	4	^{214}Bi	752.84	\pm 0.03	0.135	0.13	\pm 0.010	4
^{214}Bi	314.17	\pm 0.15	0.158	0.15	\pm 0.002	4	^{214}Bi	768.361	\pm 0.018	4.90	4.94	\pm 0.06	2
	323.62	\pm 0.10	0.055		\pm 0.014	4	^{214}Pb	785.910.	\pm 0.020	1.09	1.09	\pm 0.08	3
^{214}Bi	333.61	\pm 0.12	0.106	0.08	\pm 0.01	4	^{214}Po	799.76	\pm 0.15	0.044	0.010	\pm 0.004	4
^{214}Bi	348.92	\pm 0.06	0.061	0.12	\pm 0.04	4	^{214}Bi	806.174	\pm 0.018	1.26	1.22	\pm 0.02	3
^{214}Pb	351.93	\pm 0.01	40.0	37.6	\pm 0.5	1	^{214}Bi	815.10	\pm 0.08	0.046	0.038	\pm 0.005	4
^{214}Bi	386.77	\pm 0.05	0.56	0.31	\pm 0.03	4	^{214}Bi	821.18	\pm 0.03	0.141	0.16	\pm 0.01	4
^{214}Bi	388.88	\pm 0.05	0.61	0.37	\pm 0.04	4	^{214}Bi	826.12	\pm 0.03	0.010	0.11	\pm 0.02	4
^{214}Bi	396.01	\pm 0.12	0.033	0.033	\pm 0.006	4	^{214}Bi	832.35	\pm 0.08	0.020	0.028	\pm 0.003	4
^{214}Bi	405.74	\pm 0.03	0.18	0.18	\pm 0.02	4	^{214}Pb	839.025	\pm 0.015	0.59	0.59	\pm 0.01	3
^{214}Bi	454.77	\pm 0.12	0.35	0.30	\pm 0.02	4	^{214}Bi	904.25	\pm 0.1	0.124	0.10	\pm 0.02	4
^{214}Bi	+ 461.80	\pm 0.10	0.281	0.06	\pm 0.01	4	^{214}Bi	934.052	\pm 0.020	3.13	3.03	\pm 0.04	2
^{214}Bi	469.69	\pm 0.12	0.14	0.13	\pm 0.014	4	^{214}Bi	964.08	\pm 0.03	0.38	0.36	\pm 0.02	3
^{214}Bi	474.38	\pm 0.10	0.131	0.13	\pm 0.014	4	^{214}Bi	1032.37	\pm 0.08	0.10	0.08	\pm 0.02	4
^{214}Pb	480.42	\pm 0.08	0.40	0.32	\pm 0.01	4	^{214}Bi	1033.2	\pm 0.1	0.03	0.03	\pm 0.01	5
^{214}Pb	487.08	\pm 0.08	0.46	0.45	\pm 0.02	4	^{214}Bi	1051.961	\pm 0.028	0.33	0.31	\pm 0.01	4
^{222}Rn	- 511.5	\pm 0.2	0.37	0.08	\pm 0.08	4	^{214}Bi	1069.96	\pm 0.08	0.29	0.28	\pm 0.02	4
^{214}Pb	533.69	\pm 0.08	0.173	0.19	\pm 0.01	4	^{214}Bi	1103.8	\pm 0.1	0.183	0.10	\pm 0.01	4
^{214}Bi	536.80	\pm 0.05	0.074	0.070	\pm 0.009	4	^{214}Bi	1120.276	\pm 0.022	15.3	15.1	\pm 0.2	1
^{214}Pb	543.70	\pm 0.05	0.083	0.08	\pm 0.009	4	^{214}Bi	1133.66	\pm 0.03	0.26	0.25	\pm 0.012	4
^{214}Bi	572.83	\pm 0.08	0.091	0.08	\pm 0.008	4	^{214}Bi	1155.19	\pm 0.02	1.69	1.63	\pm 0.02	3
^{214}Pb	580.15	\pm 0.04	0.39	0.37	\pm 0.02	3	^{214}Bi	1173.00	\pm 0.05	0.070	0.06	\pm 0.01	4
^{214}Bi	609.318	\pm 0.020	46.1	46.1	\pm 0.5	1	^{214}Bi	1207.68	\pm 0.03	0.47	0.45	\pm 0.02	3
^{214}Bi	615.78	\pm 0.06	0.10	0.07	\pm 0.02	4	^{214}Bi	1238.11	\pm 0.03	6.0	5.8	\pm 0.1	1
^{214}Bi	633.14	\pm 0.10	0.064	0.055	\pm 0.006	4	^{214}Bi	1280.96	\pm 0.02	1.45	1.43	\pm 0.02	3
^{214}Bi	639.5	\pm 0.1	0.032	0.030	\pm 0.005	4	^{214}Bi	1303.76	\pm 0.08	0.118	0.112	\pm 0.007	4
^{214}Bi	649.18	\pm 0.07	0.061	0.060	\pm 0.008	4	^{214}Bi	1316.96	\pm 0.15	0.087	0.080	\pm 0.004	4
^{214}Bi	665.453	\pm 0.022	1.54	1.46	\pm 0.03	3							

1.9131(9) yr. ^{228}Th with decay Products



1.9131(9) yr. ^{228}Th with decay Products



1.9131(9) yr. ^{228}Th with decay Products

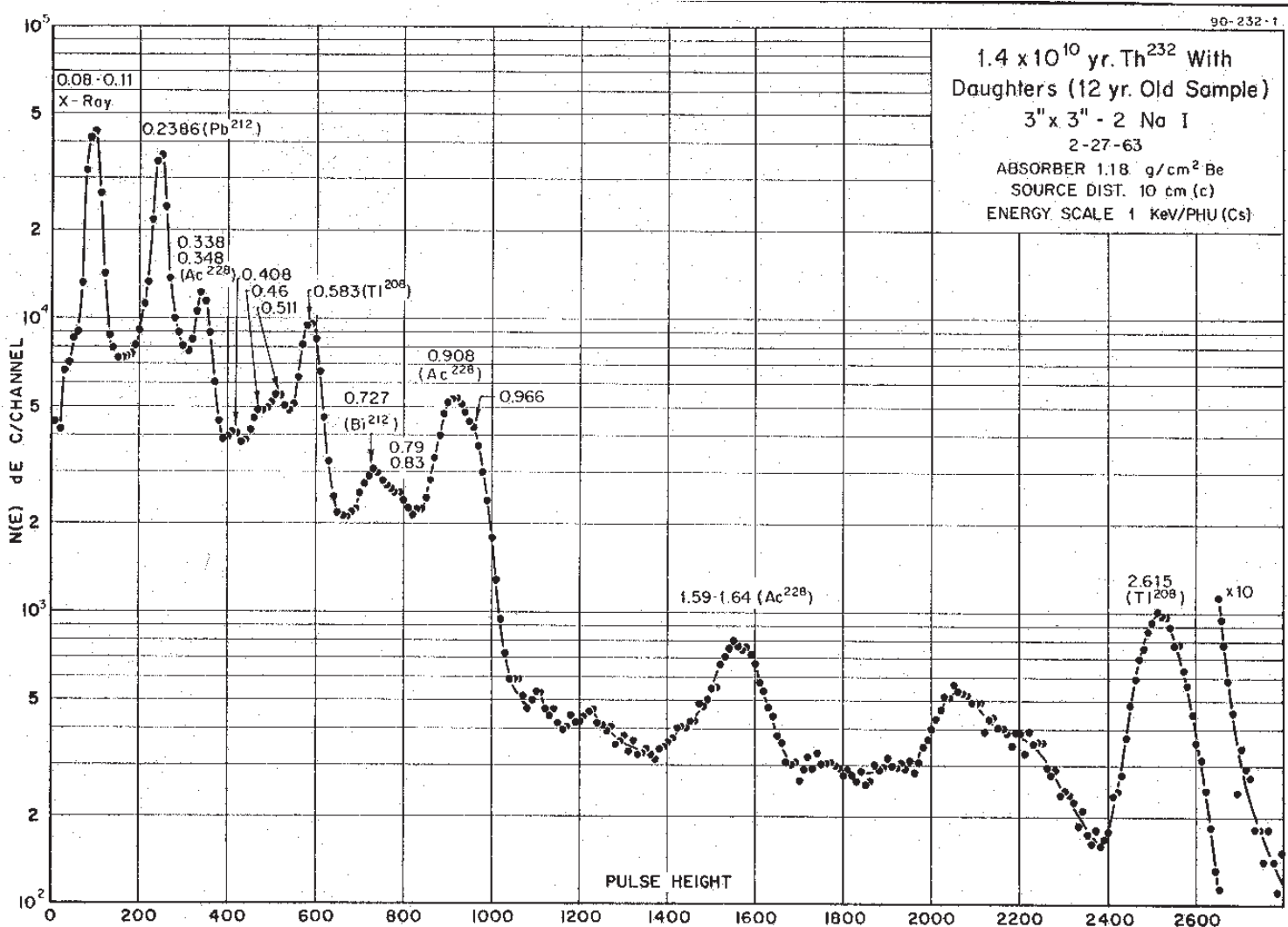
GAMMA-RAY ENERGIES AND INTENSITIES

Nuclide ^{228}Th (in equil. with daughters) Half Life 1.9131(9) yr.
 Detector 3" x 3" -2 Nal Method of Production: natural decay chain

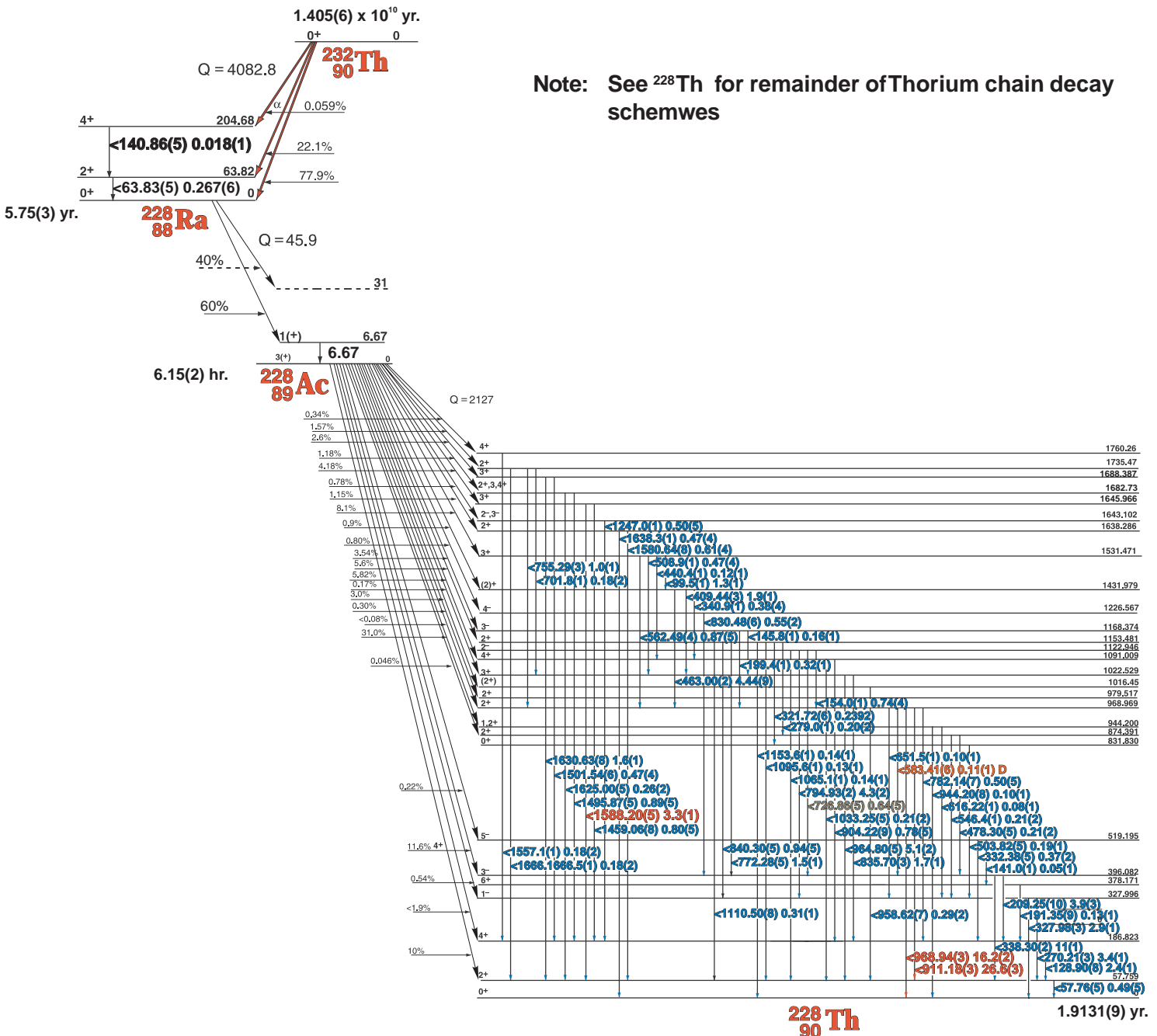
	E_γ (KeV)[S]	ΔE_γ	I_γ (rel)	$I_\gamma(\%)$ [E]	ΔI_γ	S
	K x-rays					
	84.37	± 0.05		1.27	± 0.07	3
212Pb	115.18	± 0.05	1.59	0.59	± 0.02	3
	131.62	± 0.05	0.32	0.13	± 0.01	4
	166.40	± 0.05	0.23	0.11	± 0.01	4
212Pb	176.80	± 0.05	0.15	0.052	± 0.005	4
	215.94	± 0.08	0.78	0.26	± 0.02	4
212Pb	238.624	± 0.009	120	43	± 1.0	1
224Ra	240.98	± 0.05	10	3.97	± 0.04	3
208Tl	252.60	± 0.08	0.80	0.70	± 0.03	4
208Tl	277.36	± 0.02	6.34	6.3	± 0.2	2
212Bi	288.10	± 0.08	0.92	0.31	± 0.01	4
212Pb	300.08	± 0.05	8.76	3.3	± 0.06	2
212Bi	327.97	± 0.04	0.36	0.14	± 0.01	4
212Bi	452.86	± 0.06	1.06	0.33	± 0.02	3
208Tl	510.70	± 0.04	22.0	23	± 1.0	1
220Rn	549.72	± 0.05	0.33	0.11	± 0.02	4
208Tl	583.174	± 0.013	83.2	84	± 1.0	1
208Tl	722.0	± 0.1	0.20	0.20	± 0.02	4
212Bi	727.264	± 0.025	18.4	6.6	± 0.2	1
208Tl	763.30	± 0.06	1.68	1.8	± 0.1	2
212 Bi	785.50	± 0.05	2.95	1.10	± 0.05	2
216 Po	804.9	± 0.1		0.0019	$\pm 0.(2)$	4
208Tl	860.53	± 0.05	12.5	12.4	± 0.2	1
212 Bi	893.45	± 0.05	0.94	0.38	± 0.03	3
208Tl	927.6	± 0.1	0.15	0.13	± 0.01	4
208Tl	982.7	± 0.1	0.20	0.20	± 0.02	4
212 Bi	952.0	± 0.15	0.65	0.17	± 0.02	4
212Bi	1078.73	± 0.08	1.51	0.56	± 0.02	3
208Tl	1093.9	± 0.1	0.41	0.40	± 0.04	3
212Bi	1512.7	± 0.1		0.30	± 0.01	4

	E_γ (KeV)[S]	ΔE_γ	I_γ (rel)	$I_\gamma(\%)$ [E]	ΔI_γ	S
DE	1592.60	± 0.06				
212Bi	1620.73	± 0.07	4.09	1.5	± 0.1	3
212Bi	1679.7	± 0.1		0.06	± 0.01	4
212Bi	1806.0	± 0.1		0.09	± 0.01	4
SE	2103.48	± 0.04				
208Tl	2614.476	± 0.055	100	99	± 1.0	1

$1.405(6) \times 10^{10}$ yr. ^{232}Th with decay Products

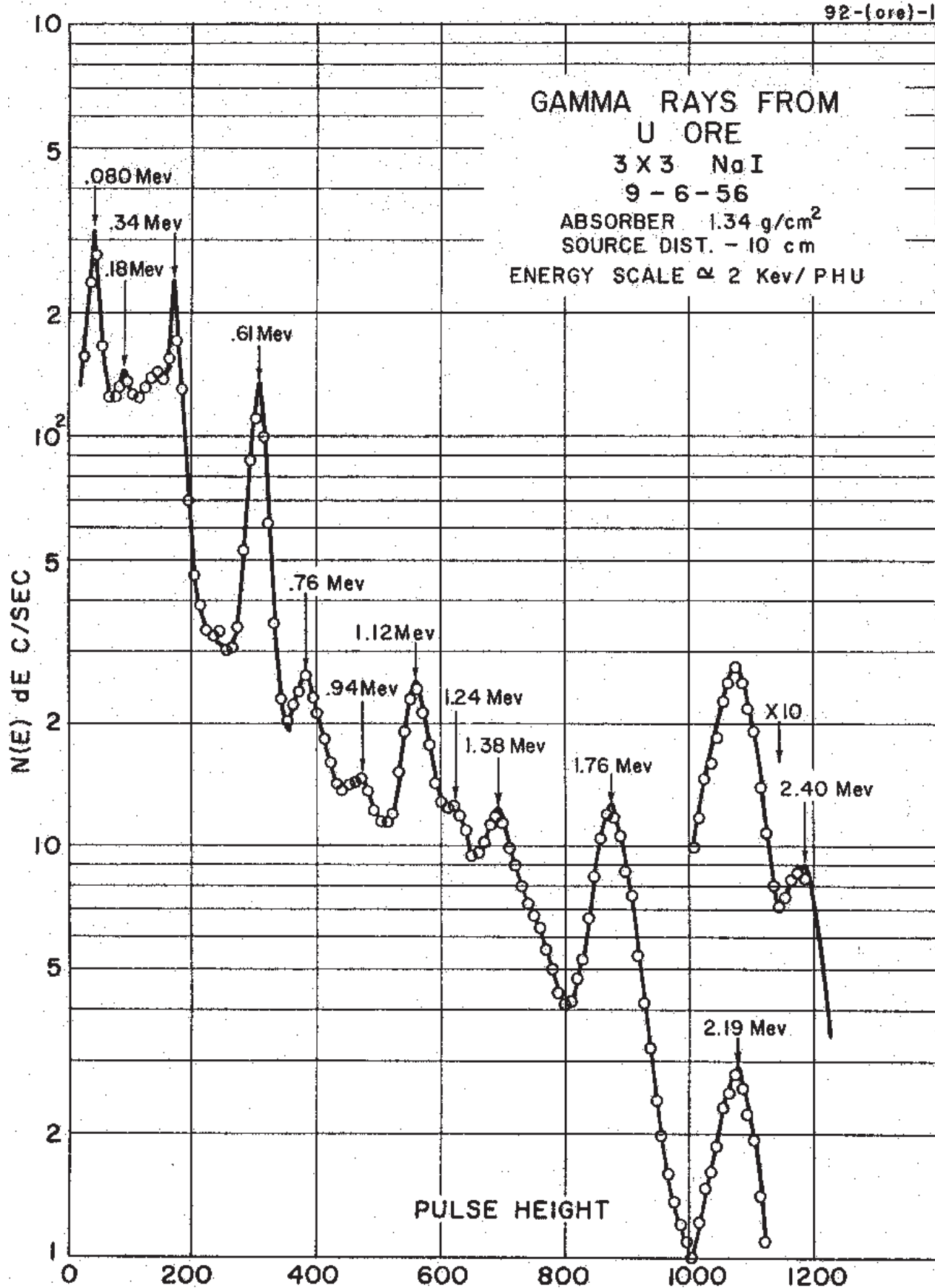


$1.405(6) \times 10^{10}$ yr. ^{232}Th with decay Products



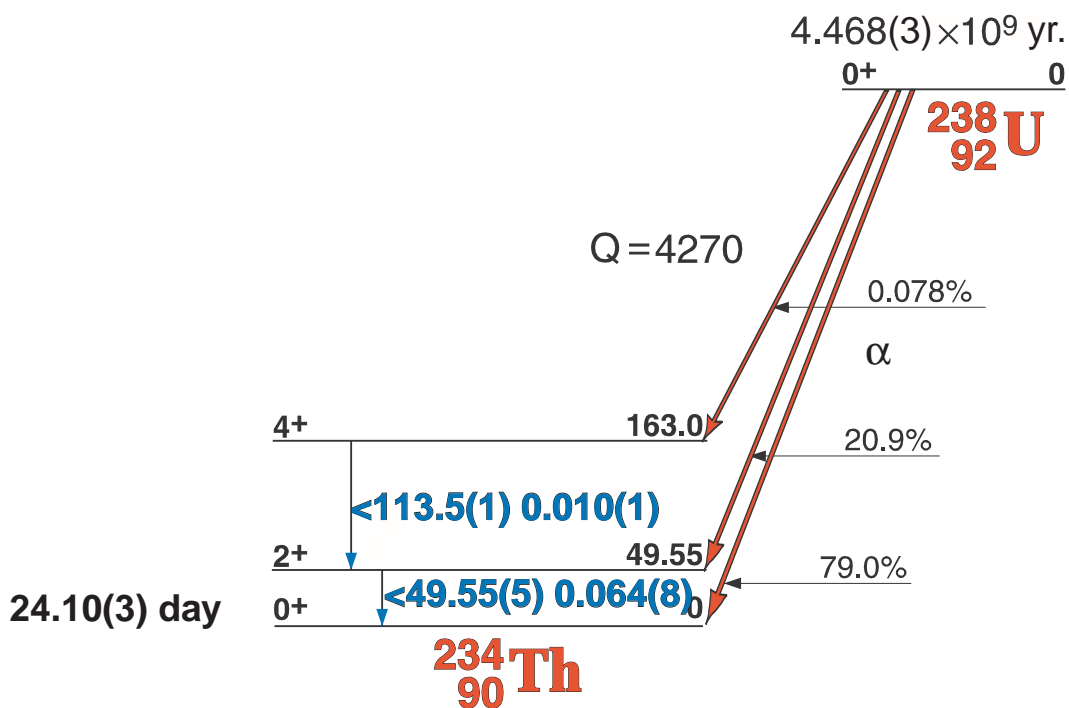
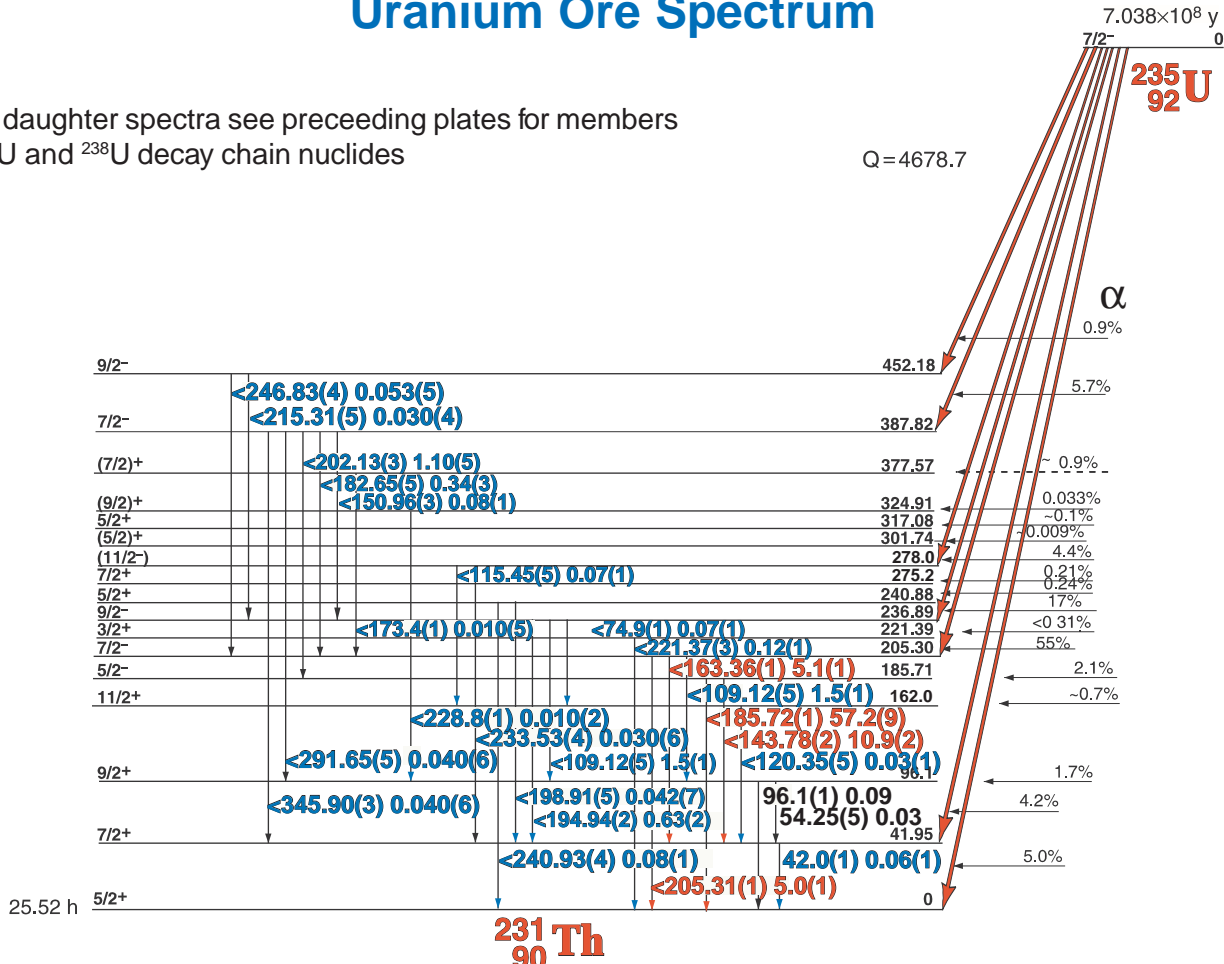
Uranium Ore Spectrum

92-(ore)-1



Uranium Ore Spectrum

Note: For daughter spectra see preceding plates for members of both ^{235}U and ^{238}U decay chain nuclides



**Converted to digital format
revised for CD-ROM
Publication
with expanded content**

